

RELATÓRIO FINAL

TCCE ICMBio/Vale (01/2018)

UNIVERSIDADE FEDERAL DE LAVRAS

Relatório final
TCCE ICMBio/Vale (01/2018)

Dispersão versus confinamento: análise composicional e de estrutura de habitat como subsídio à compreensão de mecanismos responsáveis pela identidade faunística subterrânea



Coordenador
Dr. Rodrigo Lopes Ferreira

LAVRAS – MG
Abril de 2024

RESUMO

Nas últimas décadas, o avanço de novas técnicas analíticas ampliou as perspectivas sobre os potenciais direcionadores dos padrões de biodiversidade subterrânea em diferentes escalas temporais e espaciais. Isso possibilitou o confrontamento de hipóteses estabelecidas no início do século passado, especialmente aquelas relacionadas à distribuição das espécies subterrâneas e seu nicho ecológico. Apesar destes avanços, certos processos responsáveis pelo isolamento de populações nos ambientes subterrâneos permanecem pouco esclarecidos. Neste sentido, a conectividade e permeabilidade destes relevos se mostra como um dos principais fatores que determinam a distribuição da fauna. Além disso, a hidrologia é fundamental para o aporte de recursos nestes ambientes oligotróficos. A compreensão do efetivo papel das bacias hidrográficas (em suas diferentes configurações) em processos de dispersão ou contenção de fauna subterrânea, no entanto, ainda depende de estudos abrangentes que a confrontem com outras hipóteses e que façam uso das comunidades biológicas subterrâneas como um todo. A falta de percepção da hidrologia cárstica como um dos pilares dos padrões de biodiversidade subterrânea tem se traduzido numa rápida depleção destes relevos, cruciais para a recarga de aquíferos. Deste modo, o objetivo principal deste projeto concentra-se na elucidação dos preditores dos padrões de riqueza e diversidade subterrânea em escala local e regional, testando hipóteses relacionadas à hidrologia em relevos cársticos e as suas feições geomorfológicas. Para isso, foram realizadas coletas em cavernas das regiões de Santana, Serra do Ramalho e Iuiú, no centro-sul da Bahia, regiões com elevado potencial de ocorrência de espécies endêmicas. Preditores de paisagem em escala regional e preditores de habitat em escala local foram confrontados com dados de riqueza e de composição utilizando diferentes famílias de modelos matemáticos. Além disso, novas espécies de alguns grupos taxonômicos alvo (Isopoda, Orthoptera e Psedoscorpiones) foram descritas ao longo do projeto. No total, foram produzidos 17 manuscritos, dos quais 9 focaram aspectos da ecologia subterrânea equanto 8 referiram-se a descrições de novas espécies. Destes 17 manuscritos, 9 já se encontram publicados, e os demais estão submetidos ou em fase de submissão. Os resultados obtidos neste projeto têm o potencial de subsidiar novos protocolos baseados em mecanismos responsáveis pelos padrões de distribuição das espécies subterrâneas, aperfeiçoando a legislação voltada a preservação do patrimônio espeleológico brasileiro e contribuindo para o maior conhecimento de três importantes áreas cársticas do país.

INTRODUÇÃO

INTRODUÇÃO

Há aproximadamente quatro décadas, as cavernas deixaram de ter o protagonismo absoluto no cenário dos estudos em biologia subterrânea, dividindo espaço com outros habitats subterrâneos adjacentes que por sua vez possuem enorme importância no contexto ecológico das comunidades biológicas subterrâneas (JUBERTHIE; DELAY; BOUILLON, 1980). Apesar destas ideias terem sido cunhadas em teorias que datam do início do século XX, elas somente se estabeleceram após o avanço de novas técnicas de amostragem que se desenvolveram no final do mesmo século (MAMMOLA et al., 2016). Graças a esses avanços teóricos (e agora, práticos), os mecanismos responsáveis pelos padrões de biodiversidade subterrânea começaram a ser desvendados, especialmente aqueles que descrevem seus preditores (RABELO et al., 2020) e que determinam a ocupação efetiva dos domínios subterrâneos (PAVLEK; MAMMOLA, 2020).

Hoje se sabe que certos atributos de habitats de superfície são determinantes para os padrões de distribuição das espécies subterrâneas, especialmente no que diz respeito ao "envelope" de condições ambientais onde essas espécies podem ocorrer (FICETOLA et al., 2018) e nos mecanismos responsáveis por sua dispersão (KONEC et al., 2016). Por exemplo, considerando as classificações biogeográficas mais robustas que existem para a ambientes de superfície (as ecoregiões) e as condições ambientais que as caracterizam (SMITH et al., 2018), há uma aparente dependência dos padrões de riqueza nos ambientes subterrâneos em relação aos externos, o que faz com que eles tendam a acompanhar essas delimitações (RABELO et al., 2020). Por sua vez, os padrões de composição dos taxa que ocorrem nestes ambientes também se mostram (pelo menos em parte) sobrepostos às delimitações das ecoregiões, refletindo o pool de espécies existente na superfície. Entretanto, alguns padrões de distribuição "desconexos" decorrem da relativa estabilidade ambiental dos ambientes subterrâneos, que os tornam propensos à manutenção de grupos cujos taxa aparentados existentes na superfície foram extintos (BRYSON et al., 2014) ou, onde as espécies acabam sendo tratadas como crípticas pois os mecanismos responsáveis por sua dispersão ainda não foram elucidados (BRESCOVIT et al., 2012).

Alguns estudos recentes têm indicado que os fluxos hídricos no relevo estão intimamente relacionados à dispersão e à distribuição espacial de muitos taxa, levando, por exemplo, a alterações na composição faunística após inundações (PACIOGLU et al., 2019) e atuando nos padrões de diversidade beta em escalas continentais de taxa aquáticos e terrestres. A dispersão ocasionada pelos fluxos de drenagem está diretamente ligada ao fluxo gênico entre populações de diferentes cavernas e consequentemente ao sucesso na colonização dos ambientes subterrâneos (POULSON; WHITE, 1969). Na fauna de macroinvertebrados aquáticos, estes processos são visíveis, por exemplo, nas distribuições confinadas de diferentes espécies de acordo com fluxos hídricos divergentes no relevo cárstico (KONEC et al., 2016). Além disso, os fluxos hídricos estão por trás de grande parte do aporte de recursos orgânicos para os ambientes subterrâneos (SOUZA-SILVA et al., 2012), que por sua vez são marcados pelas severas restrições tróficas (GIBERT; DEHARVENG, 2002). Especialmente em cavernas onde há pouca ou nenhuma presença de guano, os demais recursos tróficos de

origem alóctone se tornam cruciais para a manutenção das comunidades subterrâneas (SOUZA-SILVA et al., 2012). Desta forma, além do papel central na formação das paisagens cársticas (FORD; WILLIAMS, 2007), hoje é cada vez mais evidente a atuação da hidrologia na manutenção dos processos ecológicos nestes relevos.

Apesar dos enormes avanços teóricos e práticos que marcaram a biologia subterrânea nas últimas décadas, há certa defasagem nas práticas previstas pela legislação ambiental brasileira, especialmente no que diz respeito às normativas que orientam os estudos de biologia subterrânea (MMA, 2017). Muito embora existam prerrogativas legais para que as análises em enfoque local e regional levem em conta a "continuidade espacial" da unidade geomorfológica ou a "homogeneidade fisiográfica" da unidade espeleológica (MMA, 2017), as mesmas podem ser inadequadas para a definição de áreas de influência sob o contexto ecológico abordado anteriormente. Talvez o principal ponto que necessita de uma melhor exploração seja o papel da hidrologia cárstica como mecanismo de dispersão e/ou confinamento da fauna, confrontado com hipóteses que evidenciem, por exemplo, o papel das descontinuidades existentes entre unidades geomorfológicas.

Graças à sua elevada permeabilidade, as paisagens cársticas se apresentam como uma das principais fontes de recursos hídricos para as atividades humanas (GOLDSCHEIDER et al., 2020). Apesar disso, são notáveis os impactos ocasionados pelo uso insustentável destes recursos, especialmente a contaminação de aquíferos e o assoreamento completo de cavidades e sistemas subterrâneos que atuam como zonas de recarga de aquíferos (RABELO et al., 2020), processos estes, muitas vezes negligenciados. Especialmente em escalas locais, o papel das drenagens confrontado a interconectividade típica dos relevos cársticos permanece inexplorado na legislação ambiental brasileira. Neste sentido, a análise dos padrões de distribuição dos táxons frente a diferentes componentes da paisagem cárstica, especialmente as drenagens, tem grande potencial de subsídio à compreensão das áreas de influência de cavernas e outros habitats subterrâneos adjacentes. Em situações favoráveis, a conservação destes relevos de forma a garantir a manutenção dos processos hidrológicos (e consequentemente os processos ecológicos das comunidades biológicas subterrâneas) teria como principal consequência indireta a manutenção da segurança hídrica das populações humanas.

Considerando o anteriormente exposto, o principal objetivo deste projeto se concentra na exploração de diferentes componentes da paisagem cárstica como potenciais direcionadores dos padrões de riqueza e composição entre comunidades biológicas subterrâneas em escala regional. Para esta tarefa, além da avaliação de atributos de paisagem em nível regional e de atributos de habitat em nível local, utilizou-se um grande número de espécies no intuito de testar de forma mais eficiente as hipóteses propostas, especialmente no que diz respeito aos padrões de distribuição da fauna subterrânea. Acreditamos que os resultados têm o potencial de contribuir para tomadas de decisões que visem o aperfeiçoamento da legislação ambiental brasileira sob a ótica dos processos ecológicos que moldam as comunidades subterrâneas, permitindo sua preservação e atendendo as demandas do Programa Nacional de Conservação do Patrimônio Espeleológico – PNCPE.

OBJETIVOS

OBJETIVO PRINCIPAL

Analisar a composição faunística e estrutura de habitat em escala local e regional como subsídios à compreensão dos mecanismos responsáveis pela identidade faunística (composição) e riqueza de espécies subterrâneas nas regiões de Santana, Serra do Ramalho e Iuiú, estado da Bahia. Para cumprir este objetivo principal, a princípio serão consideradas as seguintes hipóteses:

Os padrões de diversidade podem estar diretamente relacionados aos padrões hidrológicos evidenciados pelas direções de fluxo, possibilitando formas de dispersão que intercomunicam feições cársticas isoladas e ampliando as áreas de ocorrências das espécies. Estas, por sua vez, evidenciaram distribuições que acompanhariam as delimitações das drenagens;

Os padrões de diversidade subterrânea podem estar relacionados às feições dos maciços cársticos graças a sua permeabilidade e interconectividade. Por sua vez, formas de dispersão entre feições descontínuas seriam inviáveis devido a impermeabilidade de outros relevos adjacentes, consequentemente confinando a distribuição das espécies;

Especialmente para as espécies subterrâneas estritamente terrestres, suas respectivas distribuições podem estar confinadas pelas delimitações das calhas dos rios. A atuação dos rios como barreira geográfica evidenciaria processos de especiação alopátrica, impedindo o fluxo gênico de populações de cavernas em margens opostas;

Os preditores de habitat em nível local (especialmente as condições altamente restritivas dos ambientes subterrâneos) seriam os principais determinantes da ausência ou presença das espécies nas cavernas, sobrepondo-se aos preditores em escala regional das hipóteses anteriores. Assim, os padrões de diversidade seriam explicados por processos baseado em nicho operando em microescala (e. g. ocupação de micro-habitats, dependência de recursos ou de condições microclimáticas).

Especificamente, pretendeu-se:

- Inventariar a fauna de invertebrados cavernícolas encontrados nos ambientes subterrâneos das regiões de Santana, Serra do Ramalho e Iuiú, Estado da Bahia;
- Identificar e descrever eventuais novos táxons de invertebrados cavernícolas terrestres e aquáticos encontrados nos ambientes subterrâneos estudados, de forma a subsidiar o teste das hipóteses com maior precisão;
- Avaliar possíveis variações na estrutura de comunidades de invertebrados cavernícolas terrestres influenciadas pela heterogeneidade de habitat em escala local e regional;
- Avaliar a similaridade da fauna cavernícola terrestre entre as cavernas das regiões de Santana, Serra do Ramalho e Iuiú, observando o possível papel dos componentes de paisagem como direcionadores destes padrões;
- Descrever de forma elucidativa e abrangente os processos responsáveis pelos padrões ecológicos avaliados, subsidiando meios teóricos e metodológicos para sua replicação e posterior aperfeiçoamento dos mecanismos legais referentes à legislação espeleológica brasileira.

METODOLOGIA



METODOLOGIA

Ecologia

Este projeto foi executado ao longo de uma diagonal SE-NW no estado da Bahia, nas regiões de Santana, Serra do Ramalho e Iuiú (Figura 1). Estas regiões encontram-se em áreas de transição da Caatinga e Florestas sazonalmente secas (DINERSTEIN et al., 2017) e destacam-se pelo alto potencial de ocorrência de espécies endêmicas. Tal potencial decorre das várias transformações paleoclimáticas enfrentadas pelo semiárido brasileiro, o qual esteve continuamente sujeito as expansões alternadas das florestas úmidas Atlântica e Amazônica (SOBRAL-SOUZA; LIMA-RIBEIRO; SOLFERINI, 2015). Estes eventos, por sua vez, podem ter permitido a colonização de habitats subterrâneos, bem como levado ao isolamento de populações nos ambientes subterrâneos e na consequente especiação de muitas linhagens.

É importante destacar que as três áreas contempladas nesse projeto são consideradas prioritárias para conservação do patrimônio Espeleológico Brasileiro, segundo o mapa publicado pelo CECAV (2018). As três áreas (Santana, Serra do Ramalho e Iuiú) são praticamente "tomadas" por polígonos inseridos em alguma categoria de prioridade, o que demonstra o elevado potencial deste projeto de vir a contribuir com ações diretas de conservação para estas áreas, indo, assim, de encontro às expectativas de conservação do patrimônio espeleológico nacional.

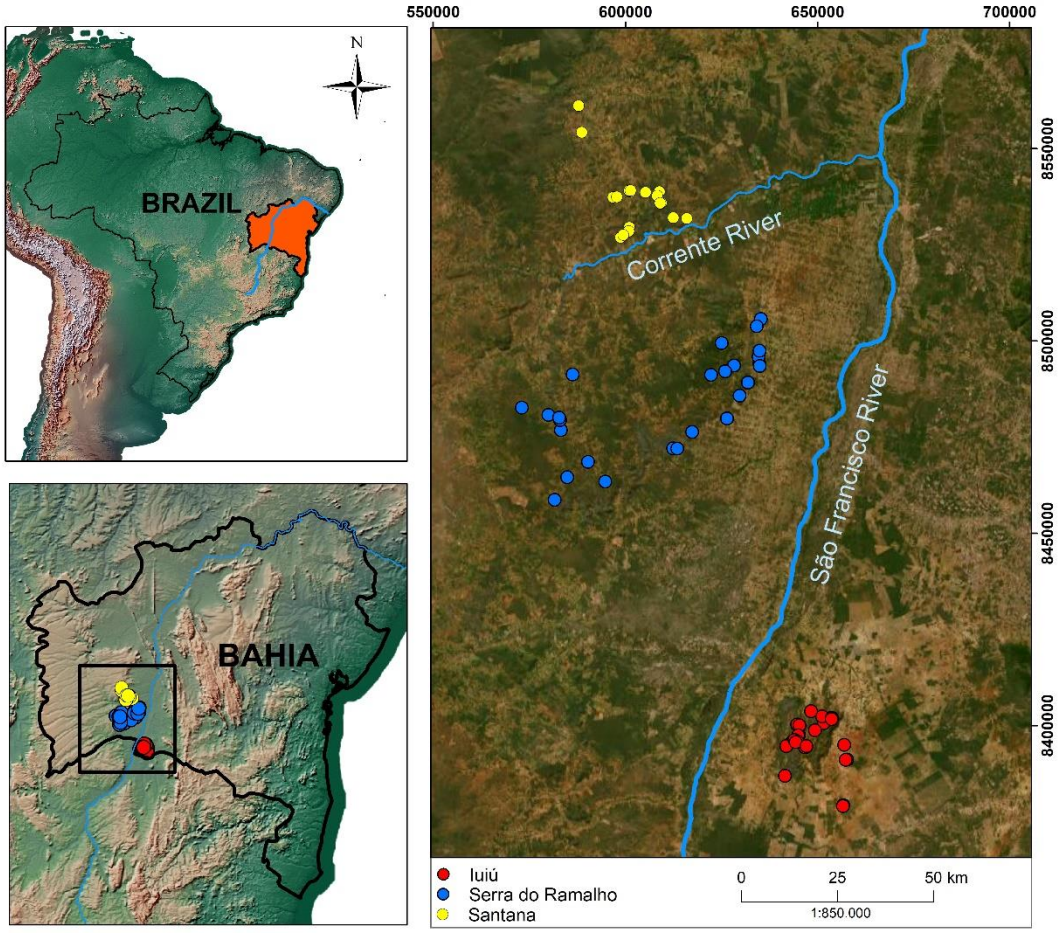


Figura 1: Área de estudo, destacando as cavernas amostrada nas regiões de Santana (círculos amarelos), Serra do Ramalho (círculos azuis) e Iuiú (círculos vermelhos)

As coletas foram realizadas em duas campanhas distintas em cada área, priorizando períodos secos por questões de segurança (muitas das cavernas nestas regiões possuem rios e amplas bacias de captação, o que faz com que visitas em períodos chuvosos sejam severamente desaconselháveis).

O número de cavernas amostradas (81 cavernas) variou entre as diferentes regiões abrangidas pelo projeto. Na região de Santana foram amostradas 24 cavernas; na região da Serra do Ramalho foram amostradas 26 cavernas e finalmente na região de Iuiú formam amostradas 31 cavernas. A escolha das cavidades a serem amostradas priorizou parâmetros como distanciamento geográfico mínimo e localização em afloramentos cásticos e microbacias hidrográficas distintas. Além disso, foi dada ênfase a cavernas com maiores desenvolvimentos lineares. É importante destacar que o número amostrado superou o planejamento inicial do projeto (que seria em torno de 20 cavernas por área, totalizando 60 cavernas). Assim, a expectativa inicial do projeto foi **superada em 21 cavernas**.

As amostragens de invertebrados foram realizadas em duas escalas espaciais (micro e mesoescala). Para essas coletas, setores medindo 3m por 10m foram posicionados ao nível do solo das cavernas. Estes setores compreenderam a mesoescala. Na parte interna de casa setor foram dispostos três quadrantes medindo 1m² cada, sendo estes considerados como microescala. Conforme o esquema a baixo, dois quadrantes foram posicionados nas extremidades de cada setor, e outro quadrante em sua região mediana (Figura 2).

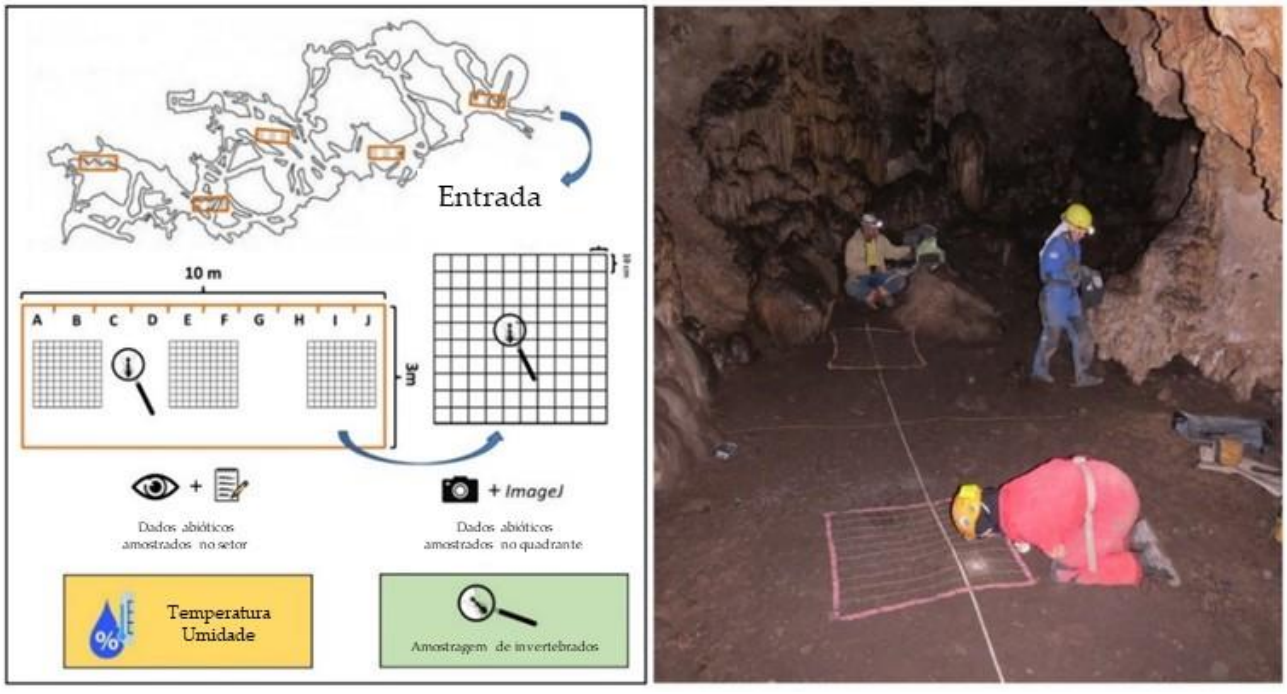


Figura 2: Esquema ilustrando o método de amostragem dos invertebrados a ser empregado no presente estudo. A numeração de 0 – 10 no setor amostral refere-se às seções (1m x 3m) utilizadas como referência para a caracterização do substrato.

Em escala local, os preditores abióticos considerados foram obtidos a partir dos quadrantes de 1m², delimitados no piso das cavidades, permitindo que o esforço amostral

fosse padronizado. Estes preditores serão: a) a distância de cada quadrante em relação a (às) entrada (s) das cavernas, aferida com trenas manuais ou a laser; b) A temperatura e umidade relativa imediatamente acima do solo e nos limites dos quadrantes, aferidas com termo higrômetro digital; c) As proporções de substratos orgânicos (guano, detritos animais, vegetais, fungos, entre outros) e inorgânicos (sedimento fino, cascalho, blocos, espeleotemas, rocha matriz, entre outros), cujas proporções serão obtidas em relação a área total dos quadrantes.

Em escala regional, os preditores abióticos considerados foram obtidos conforme a sobreposição das localizações geográficas das cavernas e seus respectivos setores e quadrantes. Estes preditores serão: a) a distância geográfica entre cavidades, obtidas em uma matriz de distância construída conforme suas coordenadas geográficas; b) As bacias de drenagem, direções dos fluxos hídricos e mananciais hídricos em suas diferentes ordens de grandeza, obtidos em arquivos SIG disponíveis na plataforma Hydrosheds (LEHNER; VERDIN; JARVIS, 2006, 2008); c) Dados referentes às unidades espeleológicas e maciços cársticos sobrepostos as coordenadas das cavidades, obtidos in loco e/ou em arquivos SIG disponibilizados pelo Centro Nacional de Pesquisa e Conservação de Cavernas – CECAV. Para fins metodológicos, serão consideradas "feições cársticas isoladas" aquelas que apresentarem descontinuidades físicas visíveis entre si.

Em ambas as escalas, as variáveis resposta consideradas foram a riqueza de invertebrados e a composição de espécies. Todas as análises consideraram, quando possível, o conjunto total de espécies, as espécies estritamente subterrâneas (troglóbias) e as não restritas às cavernas (troglófilas e troglóxenas), separadamente. Organismos sabidamente acidentais (espécies cujos ciclos de vida sejam notoriamente incompatíveis com as características de habitats subterrâneos) tenderam a ser desconsiderados das análises, evitando superestimavas de valores de riqueza.

As análises em ambas as escalas utilizaram duas abordagens distintas conforme a natureza dos dados, todas realizando testes de autocorrelação espacial (evidenciando, nos modelos, a parcela da variância explicada pela distância geográfica) (ZAGMAJSTER et al., 2018) e respeitando protocolos de tratamento preliminar dos preditores (e. g. outliers, normalidade, multicolinearidades, interações, independência) (ZUUR; IENO; ELPHICK, 2010). Na primeira abordagem os dados de riqueza foram cruzados com os preditores de escala local e regional a partir de Generalised linear models – GLM ou Generalized linear mixed models – GLMm (Caso tenha sido necessária a inserção de variáveis com efeito não controlado nos modelos) (PACHECO et al., 2020). Na segunda abordagem foram utilizados os dados de composição, que foram cruzados com os preditores em escala local e regional em Generalised dissimilarity models – GDM (FERRIER et al., 2007) ou em Distance-based linear models – DistLM (ANDERSON; GORLEY; CLARKE, 2008), dependendo da natureza dos dados.

Taxonomia

Os espécimes oriundos das coletas de campo foram depositados na Coleção de Invertebrados Subterrâneos no Centro de Estudos em Biologia Subterrânea (CEBS) da Universidade Federal de Lavras. Materiais adicionais pertencentes à Coleção foram eventualmente incorporados às descrições das novas espécies para fortalecer os trabalhos de taxonomia e ampliar dados de distribuição e ocorrência das espécies de interesse. O material preservado na Coleção é proveniente de diversos projetos realizados nos últimos anos pela equipe do CEBS e encontra-se preservado em microtubos contendo etanol 70%.

Para as descrições, inicialmente foram feitas análises morfológicas dos espécimes inteiros sob estereomicroscópio ZEISS Stemi 2000. Posteriormente os espécimes foram dissecados com auxílio de alfinetes entomológicos montados em uma haste, o que permite a separação de todos os apêndices. Os apêndices dissecados foram dispostos em uma lâmina contendo um meio de fixação e cobertos com lamínulas. Cada característica morfológica foi analisada detalhadamente sob microscópio óptico ZEISS Axio Lab.A1. Registros fotográficos foram feitos de cada apêndices para posterior ilustração destes com o auxílio do microscópio óptico ZEISS Primo Star com câmera acoplada. Além disso neste mesmo equipamento foram obtidas medidas através do software ZEN Blue edition.

A definição do número de novas espécies foi feita depois de analisar todas características morfológicas de importância taxonômica de representes das espécies alvo (de interesse). Destaca-se que, neste projeto, foi dada ênfase a três grupos taxonômicos: Orthoptera (Hexapoda), Isopoda (Crustacea) e Pseudoscorpiones (Arachnida). Assim, o número total de espécies novas descoberto ao longo do projeto supera, em muito, aquelas descritas. Os trabalhos de descrição das demais espécies serão objeto de diversos projetos a serem desenvolvidos nas próximas décadas.

Após as análises iniciais para a confirmação das novas espécies, um espécime representante de cada espécie foi ilustrado com auxílio de software apropriado para vetorização de imagens. Cada espécie teve suas características morfológicas detalhadamente descritas em forma de texto com base em artigos de táxons relacionados já descritos. Posteriormente foi feita uma revisão bibliográfica para então redigir as partes restantes dos manuscritos.

As ilustrações dos apêndices foram agrupadas em pranchas e as demais imagens incluídas nos manuscritos foram editadas e devidamente arranjadas ao longo do texto. Os manuscritos foram formatados e submetidos para revistas de alcance internacional da área de taxonomia.



RESULTADOS

RESULTADOS

Ecologia

Os trabalhos de ecologia produzidos ao longo do projeto referiram-se a cada uma das três áreas (Santana, Ramalho e Iuiú) bem como a uma análise macroecológica considerando todas elas conjuntamente. Para tal, foram criados bancos de dados específicos para cara uma das áreas, que foram posteriormente unificados para as análises macroecológicas do último trabalho. Para este fim, todas as espécies coletadas nas três áreas tiveram de ser comparadas para a criação de um banco de dados unificado sobre riqueza e composição dos táxons observados.

Região de Santana

Para a região de Santana, foram produzidos dois trabalhos. O primeiro deles teve como objetivo entender quais características do habitat influenciam a riqueza e composição das comunidades de invertebrados em 24 cavernas localizadas na região de Santana. Características físicas, tróficas, microclimáticas e da paisagem foram usadas como preditores. No total, foram encontradas 338 espécies de 37 ordens e pelo menos 93 famílias, sendo que 41 delas foram consideradas troglóbias. Os resultados mostraram que a distância da entrada mais próxima e as distâncias geográficas entre as cavernas foram importantes para a composição e riqueza das comunidades, juntamente com a heterogeneidade do habitat, representada por diferentes substratos usados como abrigos e recursos tróficos.

O segundo trabalho focou exclusivamente na gruta do Padre, a maior e mais expressiva caverna da região. Os objetivos deste trabalho foram compreender como os diferentes compartimentos da caverna se diferenciam em termos de composição faunística. Para tal, realizamos análises sobre a riqueza e composição das comunidades de invertebrados para avaliar como essas comunidades respondem às características do habitat, como variáveis físicas, tróficas e climáticas, diferentes substratos, presença de abrigos e recursos alimentares. Os resultados demonstram que a distância da entrada mais próxima e a Zonação do habitat dentro da caverna, são os principais fatores para a distribuição da fauna. Além disso, a heterogeneidade do habitat correlaciona-se com a riqueza e composição da fauna, com abrigo e disponibilidade de alimentos como características decisivas. Este trabalho também acabou revelando um número expressivo de espécies troglóbias anteriormente desconhecidas, fazendo com que a gruta do Padre emergisse como um novo Hotspot de Biodiversidade Subterrânea na América do Sul, com 25 espécies restritas a cavernas. Além da perspectiva ecológica, as informações obtidas aqui demonstram a grande importância biológica desta caverna e destacam a urgência de proteger esta caverna em toda sua complexidade, uma vez que se trata de uma caverna muito heterogênea.

Região da Serra do Ramalho

Para a região da Serra do Ramalho, foram produzidos quatro trabalhos. O primeiro deles teve como foco as cavernas do sistema Água Clara. Este sistema de Cavernas foi previamente reconhecido como um importante Hotspot de Biodiversidade Subterrânea na América do Sul, abrigando 31 espécies restritas a cavernas. No entanto, uma das expedições deste projeto, realizada em setembro de 2023, coincidindo com um período excepcionalmente

seco na região, proporcionou acesso a áreas previamente não exploradas. Portanto, o objetivo desta pesquisa foi o de ampliar os resultados de um artigo anterior sobre este Sistema publicado em junho de 2023, enfatizando sua importância como um dos mais ricos hotspots na região tropical. Esta pesquisa revelou mais 10 espécies, elevando o total de espécies restritas a cavernas dentro do sistema para impressionantes 41. Esta notável diversidade não apenas solidifica a posição do Sistema de Cavernas Água Clara como o mais rico em biodiversidade subterrânea nos trópicos, mas também serve como um forte alerta sobre os riscos iminentes enfrentados por essas espécies. As crescentes alterações induzidas pelo ser humano na região, especialmente o desmatamento, representam um risco significativo para a sobrevivência de muitas dessas espécies únicas e endêmicas.

O segundo trabalho teve como foco a gruta Pedro Cassiano. Nosso objetivo foi compreender como as características e condições do substrato podem contribuir para variações na composição e riqueza de invertebrados e sobreposição de nichos. Além disso, buscamos compreender os padrões de seleção de habitat e distribuição de algumas espécies troglóbias. Esta caverna abriga uma rica fauna restrita, com 20 espécies obrigatoriamente cavernícolas (19 invertebrados e 1 peixe), o que a posiciona como um novo Hotspot de Biodiversidade Subterrânea na América do Sul. A diversidade de substratos foi um fator fundamental na estruturação das comunidades de invertebrados. Nossas observações enfatizaram que invertebrados troglóbios e não troglóbios são influenciados por determinantes ambientais distintos. As espécies troglóbias são mais prevalentes nas áreas mais profundas da caverna do que as espécies não troglóbias, e exibem uma sobreposição mínima de nicho. Por fim, discutimos sobre a urgência de esforços de conservação para esta caverna importante.

O terceiro trabalho teve como foco a gruta Três Cobras. Este trabalho teve como objetivo avaliar os efeitos da localização espacial e da distância da entrada nas características dos micro-habitats e como essas variações afetam a fauna troglóbia e não troglóbia. Outras variáveis também foram coletadas, como temperatura, umidade, atributos tróficos e físicos, para avaliar se também influenciam a fauna de forma direta ou indireta. A distância da entrada produz variações nas condições e recursos, e como resultado, determina micro-habitats distintos que influenciam na composição e riqueza da fauna.

Finalmente, o quarto trabalho teve como objetivo entender quais características do habitat influenciam a riqueza e composição das comunidades de invertebrados em 26 cavernas localizadas na região da Serra do Ramalho. Assim, foram avaliadas as influências da heterogeneidade do habitat por meio de características físicas, tróficas, microclimáticas e de substrato na riqueza e composição de espécies em diferentes escalas de amostragem, e se os troglóbios respondem de maneira diferente da fauna não troglóbia a essas variáveis. Também foram utilizadas duas características paisagísticas: microbacias e zonas de descarga e recarga para avaliar seus efeitos sobre a composição subterrânea. Concluímos que as características físicas, tróficas, microclimáticas e de substrato são importantes para estruturar a fauna da caverna, tanto isoladamente quanto em conjunto, em diferentes escalas, e têm um efeito

distinto sobre espécies não troglóbias e troglóbias. A única variável paisagística que teve influência sobre a composição da fauna foram as zonas de recarga e descarga.

Região de Iuiú

Para a região de Iuiú, foram produzidos dois trabalhos. O primeiro deles teve como foco o gradiente de luminosidade entre regiões de entrada e profundas em cavernas. Esse gradiente estrutural do ambiente potencialmente exerce influências distintas sobre as comunidades de invertebrados que residem em diferentes zonas de luz da caverna. Para investigar esta questão, formulamos a hipótese de que comunidades dentro de diferentes zonas de luz da caverna respondem de maneira diferente à estrutura do habitat e às condições microclimáticas. Nossa abordagem envolveu uma amostragem de invertebrados em múltiplas escalas e a aplicação de análises estatísticas para contrastar as respostas das comunidades que habitam zonas fóticas e afóticas, em 31 cavernas na região de Iuiú. A riqueza da zona fótica é influenciada por fatores como umidade do ar, disponibilidade de recursos, presença de raízes e diversidade de abrigos. Por outro lado, a riqueza das comunidades nas zonas afóticas é moldada pela disponibilidade de recursos, presença de raízes, galhos e distância da entrada da caverna. Como esperado, a riqueza na zona fótica foi maior que a das regiões mais profundas. A composição de espécies das comunidades faunísticas variou da entrada para a zona afótica, e os três fatores mais importantes que impulsionaram essa variação foram distância geográfica entre as cavernas, umidade e distância da entrada. A composição entre essas zonas da caverna difere significativamente, principalmente devido ao grande número de espécies de cavernas obrigatórias que habitam predominantemente a região afótica. De fato, as comunidades associadas a diferentes zonas da caverna exibem respostas distintas a variáveis de recursos, microclimáticas e estruturais.

O segundo trabalho teve como foco as variações temporais nas comunidades de invertebrados em cavernas de Iuiú. O objetivo foi avaliar como a composição e diversidade de substratos influencia na estruturação espaço-temporal de comunidades de invertebrados subterrâneos. Para isso, comparamos comunidades amostradas em dois eventos amostrais independentes, com cinco anos entre os eventos de amostragem. Para tanto, formulamos três hipóteses: i) a riqueza média de espécies irá se manter constante entre as amostragens; ii) elementos do substrato influenciarão na estruturação espacial das comunidades de invertebrados e, iii) a resposta das comunidades quanto à estruturação do habitat permanecerão similares entre os períodos de amostragem. As análises indicaram não haver diferença significativa entre a riqueza de invertebrados coletada entre os dois períodos amostrais. Além disso, a presença de "rocha influenciou negativamente a riqueza de espécies, ao passo que "bloco" influenciou positivamente no primeiro evento, enquanto apenas "bloco" influenciou de maneira positiva a riqueza de invertebrados na segunda coleta.

Nas sessões seguintes, apresentamos cada um dos trabalhos supracitados, na íntegra. Para aqueles já publicados, mantivemos a formatação original da revista onde foi publicado.


SANTANA


ARE THERE CHOICES IN THE DARKNESS?

Are there choices in the darkness? Responses to habitat structure and conservation of cave invertebrates in a Brazilian semi-arid region

Vitor Gabriel Pereira Junta[1], Marconi Souza Silva[1], Rodrigo Lopes Ferreira[1]*

[1]Center of Studies in Subterranean Biology, Ecology and Conservation Department, Natural Sciences Institute, Federal University of Lavras, Lavras, MG, Brazil
*Corresponding Author
vitor.junta@outlook.com
marconisilva@ufla.br
drops@ufla.br

Abstract
Habitat characteristics are key factors for fauna distribution inside caves, as distinct species usually present different microhabitat requirements. Hence, this work aimed to understand which habitat traits influence the richness and composition of invertebrate communities in 24 caves located in southwestern Bahia state, in a semi-arid area. Landscape, physical, trophic, and microclimatic traits were used as predictors and were analyzed in both meso and microscale inside the caves. In total, 338 species from 37 orders and at least 93 families were found, with 41 of them considered troglobitic. The results showed that the distance from the nearest entrance and the geographic distances between caves were important for communities' composition and richness, along with habitat heterogeneity, represented by different substrates used as shelters and trophic resources.
Key-words

Introduction

Different environmental traits can lead to several responses from the associated biota, thus determining singular distribution patterns (Tews *et al.* 2004; Odum & Barret 2006). Habitat heterogeneity is one of the keys factors for the distribution patterns since a higher heterogeneity usually allows the coexistence of a higher number of species (Yang *et al*. 2015; Stein *et al*. 2015; Vargas-Mena *et al*. 2020; Pacheco *et al*. 2020; Souza-Silva *et al*. 2021).

In subterranean environments, habitat heterogeneity is also determinant for species distribution, even considering that the subterranean realm many times presents unique habitat characteristics (Pacheco *et al*. 2020; Souza-Silva *et al*. 2021). From theories proposed at the beginning of the XX century to advances in sampling techniques and analysis achieved at the end of the same period, important mechanisms for the definition of subterranean biodiversity started to be unraveled (Mammola *et al.* 2016; Rabelo *et al.* 2020).

Even though the subterranean environments are not limited to caves, they are amongst the most important subterranean habitats, and are the most studied subterranean habitats due to its dimensions (Juberthie *et al*. 1980; Mammola *et al.* 2016; Rabelo *et al.* 2020; Pacheco *et al*. 2020; Souza-Silva *et al*. 2021). These natural cavities are known for having peculiar characteristics, such the higher climatic stability when compared to the epigean surrounding environments, with stable temperature all over the year and high humidity (Howarth 1980, 1983). These habitats are also characterized by the absence of light and a tendency towards the oligotrophy (Culver & Pipan 2009).

Among the mechanisms determining the subterranean biodiversity, the distance from the caves´ entrances stands out (Ficetola *et al.* 2018; Mammola 2019; Souza-Silva *et al*. 2021; Furtado *et al.* 2022). Since most cave trophic resources come from the external habitats and are transported to caves through their entrances, a higher distance from the entrance limits the organic supply availability for the communities (Tobin *et al*. 2013; Moseley 2008; Ficetola *et al*. 2018; Mammola 2019). Moreover, regardless of the general stability, caves present a gradient of conditions from near-to-entrance (usually more unstable) to deep zones (Moseley 2009; Tobin *et al*. 2013; Lunghi *et al*. 2014; Prous *et al*. 2015; Mammola & Isaia 2018; Lunghi & Manenti 2020; Souza-Silva *et al*. 2021). This zonation creates distinct microhabitats for cave species, which vary regarding substrate types as well as climatic and photic properties (Moseley 2008; Souza-Silva *et al*. 2011b; Du Preez *et al*. 2015; Lunghi *et al*. 2017; Mammola & Isaia 2017; Mammola 2019; Lunghi & Manenti 2020; Mammola *et al*. 2020; Souza-Silva *et al*. 2021).

The uniqueness of the environmental traits found in caves usually selects pre-adapted species, which are the only capable to colonize these habitats. It also creates singular evolutive pressures that may lead to restricted subterranean species, called troglobitic, which can maintain viable populations exclusively in subterranean environments (Racovitza 1907; Sket 2008).

The evolution in subterranean habitats can produce, in the restricted species, adaptations. These adaptations can be morphological (named troglomorphisms), such as reduction in ocular structures, loss of melanic pigmentation, and appendage elongation. It also can be physiological, like metabolic rate reduction and K life strategy, and even behavioral (Romero & Green 2005). These animals are, in their majority, rare and endemic, being very sensitive to slight variations in their habitats, as in temperature and moisture content (Culver & Pipan 2009; Mammola *et al*. 2019).

Troglobitic species descend from epigean ancestors that migrate to subterranean environments as became isolated, for example by past climatic events, such as retractions of rain forests. Accordingly, caves can function as a refuge for fauna in moments of climate change, besides being a showcase of the fauna from the past (Culver & Sket 2000; Sobral-Souza *et al*. 2015).

The western Bahia state, located in the Brazilian northeast, is a semi-arid region that presents areas with high speleological potential. The region of the municipalities of Santana, Santa Maria da Vitória, and Canápolis, presents approximately 120 registered caves (CECAV 2022) and is home of important caves, such as the Gruta do Padre cave, with along two other

caves (Gruta do Cipó Cave and Gruta da Bananeira Cave) represent the longest hydrological subterranean system from Brazil. Considering the high potential and the few studies accomplished in this area, the main objective of this work was to identify habitat variables determining the richness and composition of cave invertebrates. Using landscape, physical, trophic, and microclimatic traits of the caves, these hypotheses were tested: *i)* species richness will reduce with the increase of distance from the entrance; *ii)* geographically closer caves will present more similar communities, and *iii)* invertebrates will respond to different habitat components and habitat heterogeneity on the cave floor. In addition, we discuss the importance of preserving this high-potential area for subterranean biodiversity.

Material and Methods

Study area

The sample campaigns occurred between August 23 and September 02 of 2021, and May 23 and June 02 of 2022 in the municipalities of Santana, Santa Maria da Vitória e Canápolis, Bahia State, Brazil. This transition zone between Seasonal Dry Forests and Caatinga is classified by Köppen (1936) as Aw, with dry winters and rainy summers, and has a high potential for endemic species (Dinerstein 2017). The high potential found in this area may be due to many paleoclimatic changes caused by expansions and retractions of the Amazonian and Atlantic rains forests (Sobral-Souza *et al*. 2015). The area is located within the limits of the Corrente River basin and its affluents which are an important tributary of the São Francisco River. For security reasons, the samples were conducted only in the dry season, since many caves in this region present subterranean rivers with wide capitation basins, which make the rainy season highly dangerous for those intending to visit such caves (Fig. 1; Table 5).

This area is inserted in the Bambuí Group, the largest carbonate formation in the country, with more than 145,000 Km², and more than 6,000 caves registered (Auler *et al*. 2019). It is important to highlight that this region represents a priority area for the Brazilian Speleological heritage conservation according to the map published by the Centro Nacional de Pesquisa e Conservação de Cavernas – CECAV.

Field procedures

Sampling design

The composition and richness of cave invertebrates, as well as the habitat structure traits, were determined along 122 transects (mesoscale sampling - 10 × 3 m each) distributed on the floor of 24 caves, from the entrances to their deeper regions. Quadrats (micro-scale sampling - 1 m²) were placed in triplicates inside the limits of each transect (Fig. 2), totalizing 366 quadrats (Souza-Silva *et al*. 2021). Invertebrate sampling was executed by visual search along the transects and quadrats (Souza-Silva *et al*. 2021). The sampling in the quadrats allowed the detection of small-size and low-mobility species, which could then be carefully searched in the remaining transect if discovered. The sampling was first conducted in the quadrats and later in the respective transect, always by three collectors, and was only finished when all the invertebrates had been sampled and/or accounted for. Since the several sampling

regions along the cave presented a significant structural distinction, the time spent searching for invertebrates in each transect was variable. Moreover, direct intuitive search approaches were used in different cave locations to increase the discovery of troglobitic and stygobitic species (Wynne et al. 2019). Invertebrates were preserved in labeled vials containing 70% ethanol. In laboratory, the specimens were sorted with a Stemi 508 (ZEISS) stereomicroscope, identified until the lowest possible taxonomic level, and separated into morphotypes (Oliver & Beattie, 1996). Potential troglobitic species were identified by the presence of troglomorphic characteristics, such as pigmentation and eye reduction, and appendage elongation, among others (Culver & Pipan 2009). Furthermore, experts in several taxa were contacted to help to identify particular troglomorphic characteristics (specialists are acknowledged further on). The voucher specimens were deposited in the Collection of Subterranean Invertebrates of Lavras (ISLA), linked to the Center of Studies on Subterranean Biology (CEBS) of the Federal University of Lavras (UFLA).

Environmental traits in different scales

The measurement of the habitat structure traits in the transects was carried out according to the methodology used by Souza-Silva *et al*. (2021). In order to visually quantify the surface area occupied by various organic and inorganic substrates, each transect was divided into 10 parts (1 x 3 m) (Fig. XX). The area occupied by each substrate along the whole transect was then calculated by sum. The same researcher characterized all transects to reduce observer error. The humidity and temperature were measured using a digital thermo-hygrometer that was set up on the ground in the center of each transect. Photographs (4000 x 3000 pixels) of each quadrat taken at the researcher's chest height with a Canon Powershot SX60HS camera at the closest possible angle to a 90° angle were used to calculate the percentage of each substrate in the quadrats. Posteriorly, Photographs were analyzed with the aid of *ImageJ 1.53K* software. The distances were obtained by a laser tape measure or by the plot of each transect on the map. For the definition of the Micro Drainage Basins, the function "Channel Network and Drainage Basins" from the SAGA Next Generation plugin was used with the aid of a Digital Elevation Model (DEM) in the QGIS 3.22.11 software. The DEM was also used to extract the altitude information for each sector. The sectors with 600m or higher in elevation were classified as Recharge Zones and those under this altitude were classified as Discharge Zones.

Data analysis

Pre-analysis routine

All the analyses were run in the R Studio 2022.07.02 Build 576 software. Prior to the analysis of invertebrate fauna composition and richness, the correlation between the variables was tested with the help of the *CHART.CORRELATION* function from the '*PerformanceAnalytics*' package and the variables with correlation value > 0.70 were excluded from the models. The functions *VIF* and *VIF.CCA* from the '*Car*' package was used to test the multicollinearity of variables, and the ones that present valor > 10 were discarded. A Shapiro-Wilk test was executed, to verify the normality of the data, using the *SHAPIRO.TEST* function

from the package '*Stats*'. A Mantel test was performed to try the spatial autocorrelation between the samples, in mesoscale, for all the fauna types.

Mesoscale abiotic features

All the substrates in each sector were evaluated and classified into the following classes: guano - GU; feces - FZ; carcass - CRC; roots - RZ; litter - SER; vegetal debris - DTV (< 10mm); fine branch - GALF (11 - 30 mm); medium branch - GALM (31 - 50 mm); coarse branch - GALG (65 - 250 mm); trunk - TRO (> 250mm); termite mounts - TM; water streams - ST; water pond - WP; drip water - DP; phanerogams - FG; actinomycetes - ACT; another organic substrate - OTO; concrete floor - RC; rough rock - RR; large rock - XB (1000 - 4000mm); medium rock - MB (500 - 1000mm); small rock - SB (250 - 500mm); cobbles - CB (64 - 250mm); coarse gravel - CAG (16 - 64mm); fine gravel - CAF (2 - 16mm); sand - ARE (0.06 - 2mm); silt - SEF (≤ 0.05 mm); hardpan - HP; speleothems - ES; calcite rafts - JNS; concreted calcite raft - JNC; stalactite - ESTC; stalagmite - EST; micro travertine - MTR; travertine - TRA; rough flowstone - ESR; flowstone - ESC; worm acorn - BM; retraction cracks - GRR; gastropod shell - COG.

Based on those classes and using a Shannon-Weaver Index (Buttigieg & Ramette 2014), were determined the Substrate Diversity (all classes), the Shelter Diversity (WP, DP, XB, MB, SB, CB, CAG, CAF, ES, ESTC, EST, MTR, TRA, BM, GRR, COG) and the Trophic Resources Diversity (GU, FZ, CRC, RZ, SER, DTV, GALF, GALM, GALG, TRO, FG, ACT, OTO) for each sector. The classes were also used to generate, by sum, the Shelter Availability (WP, DP, XB, MB, SB, CB, CAG, CAF, ES, ESTC, EST, MTR, TRA, BM, GRR, COG) and the Trophic Resources Availability (GU, FZ, CRC, RZ, SER, DTV, GALF, GALM, GALG, TRO, FG, ACT, OTO) for each sector.

For their use in analysis with individual substrate classes, a few categories were grouped in order to reduce variables. DTV, GALF, GALM, GALG, and TRO were grouped into **DTV**, while ES, JNS, JNC, EST, MTR, and TRA have grouped into the class **ES**.

The abiotic attributes were then divided into *Landscape features*, such as *Micro Drainage Basins*, *Water Zones*, and *Caves*; *Physical features*, which comprise the *Distance of each transect from the nearest entrance*, *Substrate Diversity*, *Shelter Diversity*, and *Shelter Availability*; *Trophic Resources* grouped *Trophic Resources Diversity* and *Trophic Resources Availability*; the *Microclimatic Variables* considered were *Temperature* and *Moisture*.

Micro-scale abiotic features

For the micro-scale, the same substrate classes were evaluated, and the same groupings were made. The diversities and availabilities were calculated equally for the sectors. The *Landscape, Physical* and *Trophic* features were also formed similarly to the mesoscale. For the quadrats, the microclimatic variables were not measured.

Habitat traits determining the communities' richness and composition

In order to understand the potential correlation between total, troglobitic, and non-troglobitic invertebrate richness with *physical*, *trophic*, and *microclimatic* traits, Generalized Linear Models (GLM) and Generalized Linear Mixed Models (GLMM) were performed, with sectors and quadrats as sample units, using two models for each fauna group. The first model (Succinct Model) used *Microclimatic Variables*, *Distance from the nearest entrance*, *Diversities*

(general substrate, shelter, and trophic resources), and *Availabilities* (shelter and trophic resources). The second model (Long Model) used *Microclimatic Variables*, *Distance from the nearest entrance*, *Diversities* (general substrate, shelter, and trophic resources), and each substrate class individually. For the micro-scale, the *Microclimatic Variables* were not used.
For those models, the Poisson family was adopted because it better fitted the data. For the evaluation of model overdispersion, the function *CHECK_OVERDISPERSION* from the package '*Performance*' was used. To obtain r^2 values of the GLMMs was used the function *r.squaredGLMM* from the '*MuMIn*' package, while the function *r.squaredLR* from the '*piecewiseSEM'* package was used to obtain r^2 values of the GLMs.

To evaluate the possible correlation between total, troglobitic, and non-troglobitic invertebrate composition with *landscape, physical*, *trophic*, and *microclimatic* variables a Distance-Based Redundancy Analysis (dbRDA) was performed (Clarke *et al*. 2014), with sectors and quadrants as sample units, using two models for each fauna group. The first model (Succinct Model) used *Landscape features*, *Microclimatic Variables*, *Cave*, *Distance from the nearest entrance*, *Diversities* (general substrate, shelter, and trophic resources), and *Availabilities* (shelter and trophic resources). The second model (Long Model) used *Landscape features, Microclimatic Variables*, *Cave*, *Distance from the nearest entrance*, *Diversities* (general substrate, shelter, and trophic resources), and each substrate class individually. For the micro-scale, the *Microclimatic Variables* were not used.

Results

Richness and composition of cave invertebrates

Considering all 24 caves (with samplings in the transects, quadrats, and other habitats) 2,754 specimens were found, totalizing 338 species from 37 orders and at least 93 families (Fig. 4). The most expressive group was Araneae, with 66 species distributed in 17 families, totalizing 1,062 individuals. The spiders were followed by Diptera and Coleoptera, with 49 and 37 species respectively.

Cave-restricted species

The sampled caves presented at least 41 cave-restricted species belonging to 8 higher taxa and 14 families (Fig. 5; Table 1). The eight higher taxa were Crustacea (11), Arachnida (11), Hexapoda (10 spp.), Myriapoda (5), Mollusca (1), Nemertea (1), Annelida (1) and Osteicthyes (1) (Table 1). The richness of the observed obligate cave fauna was Gastropoda (1), Nemertea (1), Oligochaeta (1), Isopoda (10), Amphipoda (1), Polydesmida (4), Symplyla (1), Blattodea (1), Collembola (4), Coleoptera (2), Hemiptera (1), Orthoptera (1), Pseudoscorpiones (2), Araneae (4), Opiliones (3), Palpigradi (2), and Siluriformes (1).

Is very important to highlight that from all 41 troglobitic species, 25 are found in the Gruta do Padre Cave, which represents more than 60% of the species. Furthermore, only 14% of the obligate cave species from this area are currently described. Such described species are *Coarazuphium tessai* (Godoy & Vanin 1990); *Phaneromerium cavernicolum* (Golovatch & Wytwer 2004), *Spelaeogammarus santanensis* (Koenemann & Holsinger 2000), *Eusarcus cf. cavernicola* (Hara & Pinto-da-Rocha 2010), *Pectenoniscus santanensis* (Cardoso *et al*. 2020) and *Chaimowiczia*

tatus (Cardoso *et al*. 2021). Although Hara & Pinto-da-Rocha (2010) considered that *E. cavernicola* may represent an assembly of species that cannot be identified by external and genital characteristics, herein we considered the population of the Gruta do Padre cave (and other related caves) as a troglobitic species, due to the strong troglomorphic traits they present.

Habitat traits determining the communities' richness and composition

On the mesoscale, the Mantel test revealed the existence of spatial autocorrelation for the general and non-troglobitic fauna (p=0.0004); therefore, the geographic distances between transects explain 20.43% and 20.17% respectively of the variation in the composition. For the troglobitic fauna, the geographic distances were not significant.

For the composition of communities, the *Distance from the nearest entrance* was significant for all models, both at the meso and micro-scale. The *Cave* itself was also an important variable, presenting significance except for the troglobitic fauna at the microscale. *Shelter Availability* was significant only for the general and troglobitic invertebrate fauna in the mesoscale. On the other hand, *Trophic Availability*, , was only related to the general and non-troglobitic fauna at the micro-scale. *Trophic Diversity* showed a significant correlation only with the non-troglobitic fauna on the micro-scale, for both long and succinct models. Concerning individualized substrates, guano (GU), vegetal debris (DTV), and course gravel (CAG) were important in some of the models. GU only was significant at the microscale for general and non-troglobitic fauna, while DTV was only important for the general fauna on the microscale. CAG was significant for both non-troglobitic fauna at the mesoscale, and troglobitic fauna at the micro-scale (Table 2).

For community richness, the *Distance from the nearest entrance* did not show significance only for the troglobitic fauna in the long model of the mesoscale. The correlation between *Distance from the nearest entrance* and Richness was positive for the troglobitic fauna and negative for general and non-troglobitic. The *Temperature* always presented a negative correlation and was significant for the general and non-troglobitic fauna of the succinct model, and general fauna of the long model. The *Trophic Availability* was only important for the general fauna at the micro-scale, presenting a positive correlation (Table 3).

For the individual substrates, GU had a negative correlation with the troglobitic fauna on the mesoscale, but showed a positive correlation with general and non-troglobitic fauna on the micro-scale, similar to DTV. Carcass (CRC), Phanerogams (FG), Sand (ARE), and Worm Acorn (BM) were also found to be positively significant, whereas Hardpan (HP) and Speleothems (ES) were negatively correlated, affecting general and non-troglobitic fauna at the mesoscale. On the mesoscale, Actinomycetes (ACT) were positively significant for the troglobitic fauna, while small rock (SB) and flowstone (ESC) were important for the general fauna, with negative and positive correlations, respectively. On the microscale, concrete floor (RC) showed a positive correlation with the non-troglobitic fauna, while rough rock (RR) and retraction cracks (GRR) had negative significance for general and troglobitic fauna, respectively.

Discussion

Distance from the entrance and its relationship with communities' traits

For all habitat traits analyzed, the *distance from the nearest entrance* stood out as the most important. In terms of community richness, only the troglobitic fauna from the long model at the mesoscale did not respond to the *distance*. In all other models, the general and non-troglobitic fauna responded negatively to an increase in the *distance from the nearest entrance*, while the troglobitic fauna showed a positive response. For species composition, the *Distance from the nearest entrance* was important for all types of fauna, models, and scales, demonstrating its strong relationship with the fauna distribution. It is important to note that most of the general fauna is composed of non-troglobitic species, which may bias the results towards this group.

The decrease observed in the richness of general and non-troglobitic fauna is the anticipated response for this trait, given that the distance from the cave entrance is a well-known limiting factor for species distribution. The restrictive influence of the distance from the entrance is linked to the reduction of trophic resources, as well as the habitat heterogeneity, which decreases from near-to-entrance to deep zones of the caves (Tobin *et al*. 2013; Moseley 2008; Ficetola *et al*. 2018; Mammola 2019; Souza-Silva *et al*. 2021).

In this way, greater distances limit the amount of accessible energy for the communities, as the majority of cave trophic resources are transported from the entrances (Tobin *et al*. 2013; Moseley 2008; Ficetola *et al*. 2018; Mammola 2019; Souza-Silva *et al*. 2021, Furtado *et al*. 2022). Additionally, since zones closer to the entrances present less stable climatic conditions, a gradient of temperature, moisture, and sunlight is created. This gradient can also be observed on the cave floor, leading to the simplification and homogenization of substrates in deeper zones (Prous *et al*. 2004; Prous *et al*. 2015; Souza-Silva *et al*. 2021; Furtado *et al*. 2022).

On the other hand, the restricted subterranean fauna richness shows a contrary response to that of the general and non-troglobitic fauna. The higher climatic stability found in the deeper zones of the caves favors the existence of troglobitic fauna due to their adaptations. These adaptations include reduced metabolic rates and cuticle thinning, which increase the risk of desiccation and may limit the distribution of these species to areas with minor temperature and moisture variations, often found in deeper areas (Tobin *et al*. 2013; Lunghi *et al*. 2014 and 2017; Kozel *et al*. 2019; Souza-Silva *et al*. 2021).

This preference of troglobitic organisms for stabler habitats can, on the other hand, be associated with a cave characteristic initially thought to limit the communities, the oligotrophy. However, as demonstrated by Hüppop (2005), the K-strategy life history adopted by these animals, combined with their reduced metabolic rates, enables troglobitic fauna to survive for extended periods without food. Thus, restricted fauna is commonly more prevalent in areas with fewer trophic resources, allowing them to avoid non-troglobitic competitors (Sket 1999; Deharveng & Bedos 2000; Souza-Silva *et al*. 2021). Is important to emphasize that an increase in organic matter in these oligotrophic zones can be detrimental

to troglobites, as it may attract more competitive and energetically needed non-troglobites (Sket 1999; Souza-Silva *et al*. 2021).

Similarity between caves thus geographic position

The Mantel test performed revealed that geographic distances between transects account for 20.43% of the variation in the composition of the general fauna and20.17% on the non-troglobitic fauna communities. This indicates that sampling units that are closer to each other exhibit a greater similarity in fauna than those that are farther apart.

As demonstrated in previous studies, spatial autocorrelation can imply that cave communities can affect the composition of adjacent subterranean habitats (Christman *et al*. 2015; Jaffé *et al*. 2016; Jaffé *et al*. 2018). The findings of this study support this notion, but only for the general and non-troglobitic fauna, as the troglobitic composition did not exhibit any spatial autocorrelation.

This lack of influence of geographic distance on the restricted fauna may suggest that, unlike in other studies, this region does not have a highly interconnected subterranean environment, or at least the troglobitic species are not utilizing these connections (Ferreira 2005; Souza-Silva *et al*. 2011; Auler *et al*. 2014; Christman *et al*. 2005; Jaffé *et al*. 2016; Jaffé *et al*. 2018).

On the other hand, the spatial autocorrelation observed in the composition of general and non-troglobitic fauna suggests that, despite the subterranean connections between caves being unused, non-restricted species may still disperse in epigean environments (Ribera *et al*. 2019). These surface movements by animals raise concerns for the overall conservation of the area, as degraded regions can obstruct the dispersal of fauna and negatively impact the subterranean diversity.

Is important to note that spatial autocorrelation, and thus the potential for epigean dispersal movements of fauna, can account for approximately 20% of the variation in composition. However, a higher explanatory value is attributed to the grouping of other analyzed variables, such as *physical*, *trophic*, and *climatic*.

Invertebrates' response to habitat heterogeneity

The *trophic* and *physical* attributes play a highly significant role in defining cave invertebrate communities in the semi-arid regions of Brazil. Since caves are naturally oligotrophic environments, they depend greatly on the surface, with the majority of the energy of the system originating from epigean zones (Tobin *et al*. 2013; Moseley 2008; Ficetola *et al*. 2018; Mammola 2019).

The presence and diversity of trophic resources are not only important for the existence of cave invertebrate communities, but they also affect their composition and richness. This suggests that different types of organic matter may provide a higher number of specific niches, allowing for greater richness and creating differences in composition. These findings align with previous research on non-troglobitic fauna (Schneider *et al*. 2011; Souza-Silva *et al*. 2011; Ladle *et al*. 2012; Ferreira 2019; Pacheco *et al*. 2020a; Furtado *et al*. 2022).

Among the different types of organic matter observed in the sampled caves, bat guano and vegetal debris were found to be the most significant. Bat guano serves as one of the primary

energy sources for invertebrate fauna, particularly in caves that are permanently dry (Ferreira & Martins 1999; Souza-Silva *et al*. 2011). However, the guano production in caves may vary seasonally due to external vegetation fluctuations and, as a result, food availability for bats (Faria 1996; Souza-Silva *et al*. 2011). The transport of guano into caves is crucial because the piles formed by bats can sustain entire invertebrate communities that vary depending on the age and composition of the deposit (Ferreira & Martins 1999; Ferreira 2019). Furthermore, guano deposits may be critical for establishing richer cave communities, as they attract colonizer species that initiate a complex process, resulting in more extensive trophic webs (Ferreira & Martins 1999; Ferreira 2019; Pacheco *et al*. 2020a).

Due to the prevalence of deciduous species in the limestone vegetation of this region, a significant amount of leaves and small branches accumulate in the litter during the dry season (Crowther 1987; Brina 1998; Souza-Silva et al. 2011). In turn, this accumulated vegetal debris frequently finds its way into caves via flood pulses during the rainy season. These floods typically carry substantial volumes of water downstream, transporting organic matter and other substrates into caves (Minshall et al. 1983; Carrling 1987; Downes & Street 2005). Therefore, as shown by Souza-Silva et al. (2011), the dependence of cave communities on external vegetal material causes the trophic dynamics of subterranean habitats to be influenced by seasonal changes outside the cave environment.

The positive correlation observed between cave invertebrate communities and organic matter is generally applicable to non-restricted fauna. However, when considering troglobitic species, this correlation may not hold. Restricted subterranean animals typically have reduced metabolic rates and K-strategy life history, enabling them to endure periods of starvation (Hüppop 2005; Souza-Silva et al. 2021). Consequently, due to the greater energetic demand and superior competitive ability of non-troglobitic species, troglobites tend to seek for locations with limited organic matter, thus avoiding competitors (Sket 1999; Deharveng & Bedos 2000; Souza-Silva et al. 2021).

It is essential to emphasize that the distribution of trophic resources inside caves is not uniform, with the majority concentrated near the entrance, creating an energy gradient that decreases towards deeper areas (Tobin et al. 2013; Moseley 2008; Ficetola et al. 2018; Mammola 2019; Souza-Silva et al. 2021, Furtado et al. 2022). This gradient encompasses not only trophic resources but also physical and microclimatic conditions (Prous et al. 2004; Prous et al. 2015; Souza-Silva et al. 2021; Furtado et al. 2022).

The data obtained from this study demonstrate that the presence of different types of substrates can have a positive effect on the composition and richness of cave invertebrate communities. This supports the notion that greater substrate diversity and variation in climatic traits generate more microhabitats, enabling a greater number of species to occupy the habitats by creating new niches (Prous et al. 2004; Prous et al. 2015; Souza-Silva et al. 2021; Furtado et al. 2022). However, troglobitic species respond differently from non-troglobitic fauna, displaying distinct responses to different substrates. This contrasting response may be attributed to the high level of specialization of restricted organisms, which seek specific conditions within subterranean habitats (Pacheco et al. 2020a; Souza-Silva et al. 2021).

Conservation of subterranean environments in Santana region

The Santana region lies in a transition zone between the Caatinga and Seasonal Dry Forests. While some caves have entrances that are covered by native vegetation, it is evident that the original forests surrounding the caves have been replaced by pastures and other monocultures. Deforestation in the caves'surroundings can have a direct and indirect impact on the energetic dynamics of subterranean invertebrate communities. The loss of vegetation in the cave surroundings can directly reduce the amount of litter available to be transported to hypogean environments. This litter, derived from vegetation, is one of the most significant food sources for cave invertebrates in the region, and its depletion can disrupt the entire subterranean trophic web (Crowther 1987; Brina 1998; Souza-Silva et al. 2011). Indirectly, deforestation can limit the availability of bat food, which may decrease the input of guano to the caves. Bat guano is one of the most critical energy sources for invertebrates in permanently dry caves, and its absence can pose a threat to entire communities (Faria 1996; Ferreira & Martins 1999; Souza-Silva et al. 2011; Ferreira 2019).

Despite the high speleological potential in the Santana region, many locals are unfamiliar with most of the caves, even the larger ones like the Gruta do Padre Cave. Fear or lack of opportunities may contribute to this lack of awareness, which is not unique to the region but extends to the Brazilian population as a whole. It is estimated that there are almost 23 thousand caves registered in the country, but this represents only a small fraction of the real potential, which is around 300 thousand caves (CECAV 2022). Similarly, in the Santana region, unexplored limestone outcrops are easy to find. This study alone identified nine previously unregistered caves out of 25 sampled, highlighting significant gaps and unprospected areas.

It is crucial to emphasize that the general lack of knowledge among the population, both nationally and in Santana, is also attributable to the research community as a whole, not just in Brazil but worldwide. Regrettably, many researchers overlook the local population when conducting their work, neglecting to communicate scientific findings in a more accessible manner, which is equally true for speleology.

Clearly, legislation plays a crucial role in protecting the speleological heritage. However, despite regulations and management controls, some damage to cave ecosystems is still caused by locals, and effective monitoring is a challenging task in a vast country like Brazil. Sometimes, due to lack of awareness or for basic survival needs, locals can inadvertently cause harm to subterranean environments and their surroundings. Therefore, it is imperative to provide accessible information about the legislation and the significance of cave habitats for the local communities in Santana's region. This could foster a sense of ownership and stewardship among locals, and they could become new and powerful allies in the conservation of the unique and fragile cave ecosystems of the Brazilian semi-arid region.

Acknowledgments

The authors would like to thank the Centro Nacional de Pesquisa e Conservação de Cavernas - CECAV and Instituto Brasileiro de Desenvolvimento e Sustentabilidade - IABS (n°.

006/2021. TCCE ICMBio/Vale (01/2018) for the financial support; CNPq (National Council for Scientific and Technological Development) for the productivity scholarship provided to RLF (CNPq n. 302925/2022-8); to the Vale Company and the team from the Center of Studies in Subterranean Biology (CEBS/UFLA) for the support in the field trips. VGPJ is grateful to Coordenação de Aperfeiçoamento de Pessoal de Nível Superior (CAPES) for the master's degree scholarship granted. We are also thankful to Giovanna Cardoso, Guilherme Prado, and Leopoldo Bernardi for their help in the identification of some taxa.

References

Auler A, Piló L, Parker C, Senko J, Sasowsky I, Barton H. 2014. Hypogene cave patterns in iron ore caves: convergence of forms or processes? In: Klimchouk A, Sasowsky ID, Mylroie J, Engel SA, Engel AS, eds. Hypogene cave morphologies. Leesburg: Karst Water Institute, 15–19

Auler AS, Rubbioli E, Menin D, Brandi R (2019) Cavernas. Atlas do Brasil Subterrâneo. Editora IABS, Brasília.

Brina A. E. 1998. Aspectos da dinâmica da vegetação associada a afloramentos calcários na APA carste de Lagoa Santa, MG. Dissertação de Mestrado em Ecologia Conservação e Manejo da Vida Silvestre, UFMG. 105pp

Buttigieg PL, Ramette A (2014) A Guide to Statistical Analysis in Microbial Ecology: a community-focused, living review of multivariate data analyses. FEMS Microbiol Ecol 90:543–550. https://doi. org/10.1111/1574-6941.12437

Carling PA (1987) Bed stability in gravel streams, with reference to stream regulation and ecology. In: Richards, K. (ed.) River Channels: Environment and Process. Blackwell, Oxford, pp. 321–347.

Centro Nacional de Pesquisa e Conservação de Cavernas – CECAV (2022) Cadastro Nacional de Informações Espeleológicas (CANIE)

Christman MC, Culver DC, Madden MK, White D (2005) Patterns of endemism of the eastern North American cave fauna. Journal of Biogeography 32:1441–1452 DOI 10.1111/j.1365-2699.2005.01263.x.

Clarke KR, Gorley RN, Somerfeld PJ, Warwick RM (2014) Change in marine communities: an approach to statistical analysis and interpretation, 3rd ed. PRIMER-E, Plymouth

Crowther J. 1987. Ecological Observations in Tropical Karst Terrain, West Malaysia. II. Rainfall Interception, Litterfall and Nutrient Cycling. Journal of Biogeography, 2, (14):145-155.

Culver DC, Sket B (2000). Hotspots of subterranean biodiversity in caves and wells. Journal of Cave and Karst Studies. 62:11–17

Culver DC, Pipan T (2009) Biology of Caves and Other Subterranean Habitats, 1st ed. Oxford, New York

Deharveng L, Bedos A (2000) The cave fauna of southeast Asia. In: Wilkens H, Culver DC, Humphries WF (eds) Origin, evolution and ecology—subterranean ecosystems. Elsevier, Amsterdam, pp 603–632.

Dinerstein E (2017) An Ecoregion-Based Approach to Protecting Half the Terrestrial Realm. BioScience, [s. l.], 67, 6, 534–545. https://doi.org/10.1093/biosci/bix014

Downes, B.J. and Street, J.L. 2005. Regrowth or dispersal? Recovery of a freshwater red alga following disturbance at the patch scale. Austral Ecology 30, 526–536.

Du Preez G, Forti P, Jacobs G, Jordaan A, Tiedt LR (2015) Hairy Stalagmites, a new biogenic root speleothem from Botswana. Int J Speleol 44(1):37–47. https://doi.org/10.5038/1827-806X.44.1.4

Ferreira RL, Martins RP (1999) Trophic structure and natural history of bat guano invertebrate communities with special reference to Brazilian caves. Tropical Zoology, 12:231-259. https://doi.org/10.1080/03946975.1999.10539391

Ferreira RL (2004). A medida da complexidade ecológica e suas aplicações na conservação e manejo de ecossistemas subterrâneos. Tese de doutorado, Universidade Federal de Minas Gerais, 158p.

Ferreira RL (2005) A vida subterrânea nos campos ferruginosos. O Carste 3:106–115.

Ficetola GF, Lunghi E, Canedoli C, Padoa-Schioppa E, Pennati R, Manenti R (2018) Diferences between microhabitat and broad-scale patterns of niche evolution in terrestrial salamanders. Sci Rep 8(1):1– 12. https://doi.org/10.1038/s41598-018-28796-x

Ferreira RL (2019) Guano Communities. In: Encyclopedia of Caves (Third Edition). Academic Press. 474-484. https://doi.org/10.1016/B978-0-12-814124-3.00057-1.

Furtado L, Ferreira RL, Fernández JIR, Souza-Silva M (2022) Recreational caving impact of visitors in a high-altitude cave in Bolivian Andes: Main effects on microhabitat structure and faunal distribution. International Journal of Speleology, 51(2), 93-103. https://doi.org/10.5038/1827-806X.51.2.2418

Howarth FG (1980) The zoogeography of specialized cave animals: a bioclimatic model. Evolution 394-406.

Howarth FG (1983) Ecology of cave arthropods. Annual Review of Entomology 28:365-389. https://doi.org/10.1111/j.2041-210X.2009.00001.x

Hüppop K (2005) Adaptation to low food. In: Culver D, White WB (ed) Encyclopedia of caves. Ensevier, Amsterdam, pp 4–10.

Jaffé R, Prous X, Zampaulo R, Giannini T, Imperatriz-Fonseca V, Maurity C, Oliveira G, Brandi I, Siqueira J (2016) Reconciling mining with the conservation of cave biodiversity: a quantitative baseline to help establish conservation priorities. PLOS ONE 11:e0168348 DOI 10.1371/journal.pone.0168348

Jaffé R, Prous X, Calux A, Gastauer M, Nicacio G, Zampaulo R, et al (2018) Conserving relics from ancient underground worlds: assessing the influence of cave and landscape features on obligate iron cave dwellers from the Eastern Amazon. Peer J 6:e4531; DOI 10.7717/peerj.4531

Juberthie C, Delay B, Bouillon M (1980) Sur l'existence d'un milieu souterrain superficiel en zone non calcaire. C. R. Acad. Sc. Paris. 1 (290) 49–52.

Koppen W (1936) Das geographische system der klimat. Handbuch der klimatologie. 46.

Kozel P, Pipan T, Mammola S, Culver DC, Novak T (2019) Distributional dynamics of a specialized subterranean community oppose the classical understanding of the preferred subterranean habitats. Invertebr Biol 138(3):e12254. https://doi.org/10.1111/ivb.12254

Ladle RJ, Firmino JV, Malhado AC, Rodriguez-Duran A (2012) Unexplored diversity and conservation potential of Neotropical hot caves. Conservation Biology, 26(6), 978-982.

Lunghi E, Manenti R, Ficetola GF (2014) Do cave features affect underground habitat exploitation by non-troglobite species? Acta Oecol 55:29–35. https://doi.org/10.1016/j.actao.2013.11.003

Lunghi E, Manenti R, Ficetola GF (2017) Cave features, seasonality, and subterranean distribution of non-obligate cave dwellers. PeerJ 5:e3169. https://doi.org/10.7717/peerj.3169

Lunghi E, Manenti R (2020) Cave communities: from the surface border to the deep darkness. Diversity 12(5):167. https://doi.org/10.3390/d12050167

Mammola S, Giachino PM, Piano E, Jones A, Barberis M, Badino G & Isaia M (2016) Ecology and sampling techniques of an understudied subterranean habitat: the Milieu Souterrain Superficiel (MSS). The Science of Nature, 103: 88. https://doi.org/10.1007/ s00114-572 016-1413-9

Mammola S, Isaia M (2017) Spiders in caves. Proc R Soc B. https://doi.org/10.1098/rspb.2017.0193

Mammola S, Isaia M (2018) Day-night and seasonal variations of a subterranean invertebrate community in the twilight zone. Subterr Biol 27:31–51. https://doi.org/10.3897/subtbiol.27.28909

Mammola S (2019) Finding answers in the dark: caves as models in ecology fifty years after Poulson and White. Ecography 42(7):1331–1351. https://doi.org/10.1111/ecog.03905

Mammola S, Piano E, Cardoso P, Vernon P, Domínguez-Villar D, Culver Dc, Pipan T, Isaia M (2019) Climate change going deep: The effects of global climatic alterations on cave ecosystems. The Anthropocene Review. 6 (1–2), 98–116. https://doi.org/10.1177%2F2053019619851594

Mammola S, Arnedo MA, Fišer C, Cardoso P et al (2020) Environmental filtering and convergent evolution determine the ecological specialization of subterranean spiders. Funct Ecol 35(5):1064–1077. https://doi.org/10.1111/1365-2435.13527

Minshall GW, Andrews DA, Manuel-Faler CY (1983) Application of island biogeographic theory to streams: macroinvertebrate recolonization of the Teton River, Idaho. In: Barnes, J.R. and Minshall, G.W. (eds) Stream Ecology: Application and Testing of General Ecological Theory. Plenum Press, New York, pp. 279–297.

Moseley M (2008) Size matters: scalar phenomena and a proposal for an ecological definition of 'cave'. Cave Karst Science 35(3):89–94

Moseley M (2009) Are all caves ecotones? Cave Karst Science 36(2):53–58

Odum EP, Barrett GW (2006) Fundamentals of Ecology. Brooks Cole, Thomson Learning. Inc., Bangalore, India.

Oliver I, Beattie AJ (1996) Invertebrate morphospecies as surrogates for species: a case study. Conservation Biology, 10(1):99–109

Pacheco GSM, Souza-Silva M, Cano E, Ferreira LF (2020) The role of microhabitats in structuring cave invertebrate communities in Guatemala. International Journal of Speleology, 49 (2), 161–169. https://doi.org/10.5038/1827-806X.49.2.2333

Prous X, Ferreira RL, Martins RP (2004) Ecotone delimitation: Epigean–hypogean transition in cave ecosystems. Austral Ecol 29(4):374–382. https://doi.org/10.1111/j.1442-9993.2004.01373.x

Prous X, Ferreira RL, Jacobi CM (2015) The entrance as a complex ecotone in a Neotropical cave. Int J Speleol 44:177–189. https://doi.org/10.5038/1827-806X.44.2.7

QGIS Development Team (2023) QGIS Geographic Information System. Open-Source Geospatial Foundation Project. http://qgis.osgeo.org

Rabelo LM, Souza-Silva M, Ferreira RL (2020) Epigean and hypogean drivers of Neotropical subterranean communities. Journal of Biogeography. 1 https://doi.org/10.1111/jbi.14031

Racovitza EG (1907) Essai sur les problèmes biospéologiques. Archives de Zoologie Expérimentale et Générale, 4(6):371–488.

Rasband WS (1997) Image, J., US National Institutes of Health. "ImageJ64," US National Institutes of Health, Bethesda, MD

R Core Team (2019) R: a language and environment for statistical computing. R Foundation for Statistical Computing, Vienna. https://www.R-project.org/

Romero A, Green SM (2005) The end of regressive evolution: examining and interpreting the evidence from cave fishes. Journal of fish biology. 67(1): 3–32.

Schneider K, Christman MC, Fagan WF (2011) The influence of resource subsidies on cave invertebrates: results from an ecosystem-level manipulation experiment. Ecology, 92, 765-776. https://doi.org/10.1890/10-0157.1

Sket B (1999) The nature of biodiversity in hypogean waters and how it is endangered. Biodivers Conserv 8:1319–1338. https://doi.org/10.1023/A:1008916601121

Sket B (2008) Can we agree on an ecological classifcation of subterranean animals? J Nat Hist 42:1549– 1563. https://doi.org/10.1080/00222930801995762

Sobral-Souza T, Lima-Ribeiro MS, Solferini VN (2015) Biogeography of Neotropical Rainforests: past connections between Amazon and Atlantic Forest detected by ecological niche modeling. Evolutionary Ecology. 29(5):643–655. https://doi.org/10.1007/s10682-015-9780-9

Souza-Silva M, Parentoni RM, Ferreira RL (2011b) Trophic dynamics in a neotropical limestone cave. Subterranean Biology 9:127–138. https://doi.org/10.3897/subtbiol.9.2515

Souza-Silva M, Cerqueira, RFV, Pellegrini TG, Ferreira RL (2021) Habitat selection of cave-restricted fauna in a new hotspot of subterranean biodiversity in Neotropics. Biodiversity and Conservation, 1–28. https://doi.org/10.1007/s10531-021-02302-8

Stein A, Beck J, Meyer C, Waldmann E, Weigelt P, Kreft H (2015) Differential effects of environmental heterogeneity on global mammal species richness. Global Ecol Biogeogr 24 (9), 1072–1083. https://doi.org/10.1111/geb.12337

Tews J, Brose U, Grimm V, Tielbörger K, Wichmann MC, Schwager M, Jeltsch F (2004) Animal species diversity driven by habitat heterogeneity/diversity: the importance of keystone structures. Journal of biogeography, 31(1), 79-92.

Tobin BW, Hutchins BT, Schwartz BF (2013) Spatial and temporal changes in invertebrate assemblage structure from the entrance to deep-cave zone of a temperate marble cave. International Journal of Speleology 42:203-214. https://doi.org/10.5038/1827-806X.42.3.4

Vargas-Mena JC, Cordero-Schmidt E, Rodriguez-Herrera B (2020) Inside or out? Cave size and landscape effects on cave-roosting bat assemblages in Brazilian Caatinga caves. J Mammal 101 (2), 464–475. https://doi.org/10.1093/jmammal/gyz206

Wynne JJ, Howarth FG, Sommer S, Dickson BG (2019) Fifty years of cave arthropod sampling: techniques and best practices. Int J Speleol 48(1):33–48. https://doi.org/10.5038/1827-806X.48.1.2231

Yang Z, Liu X, Zhou M, Ai D, Wang G (2015) The effect of environmental heterogeneity on species richness depends on community position along the environmental gradient. Sci Rep 5(1):1–7. https:// doi.org/10.1038/srep15723

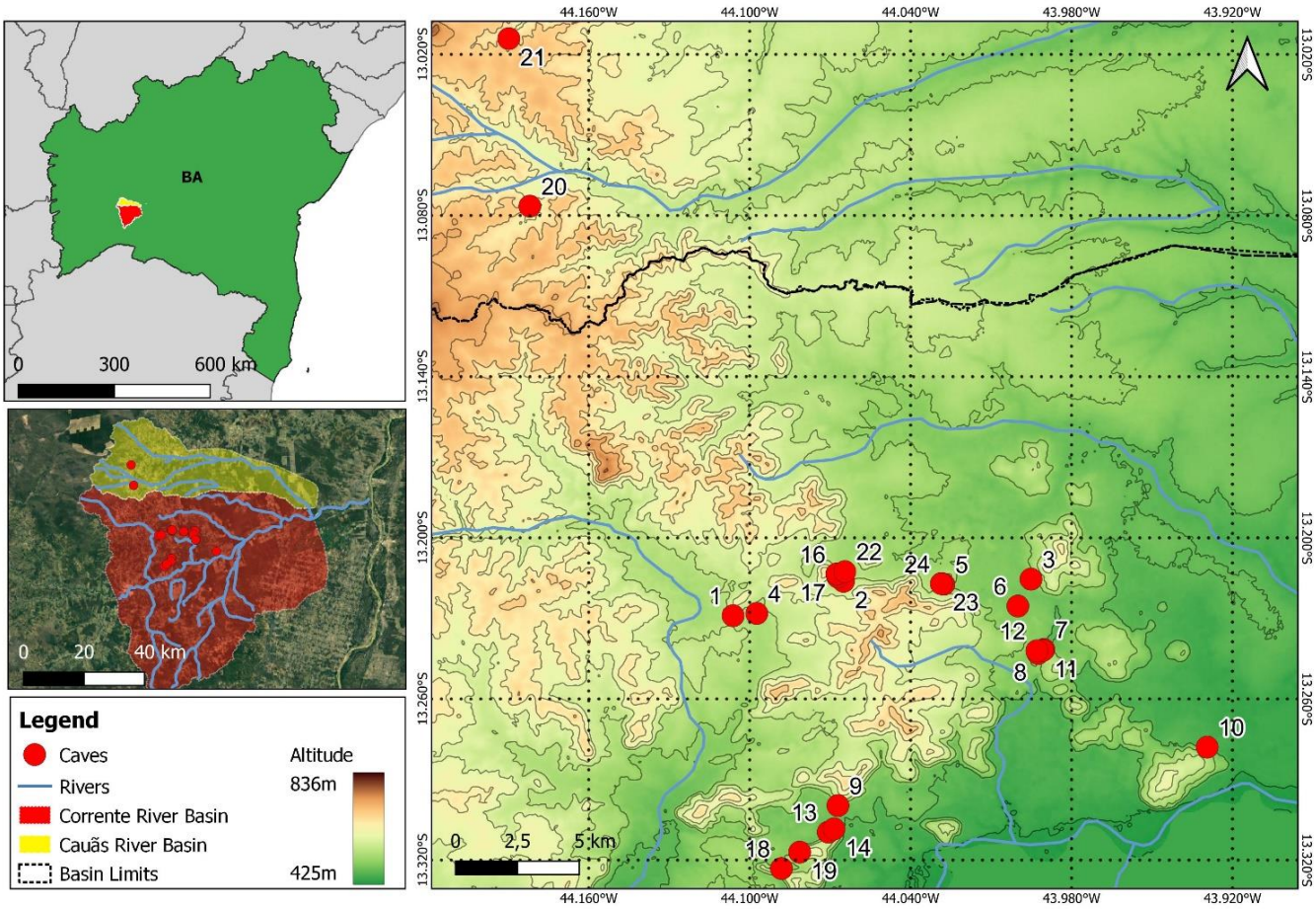


Figure 1. Location map of the caves sampled in Santana region. Caves identification are in table 5.

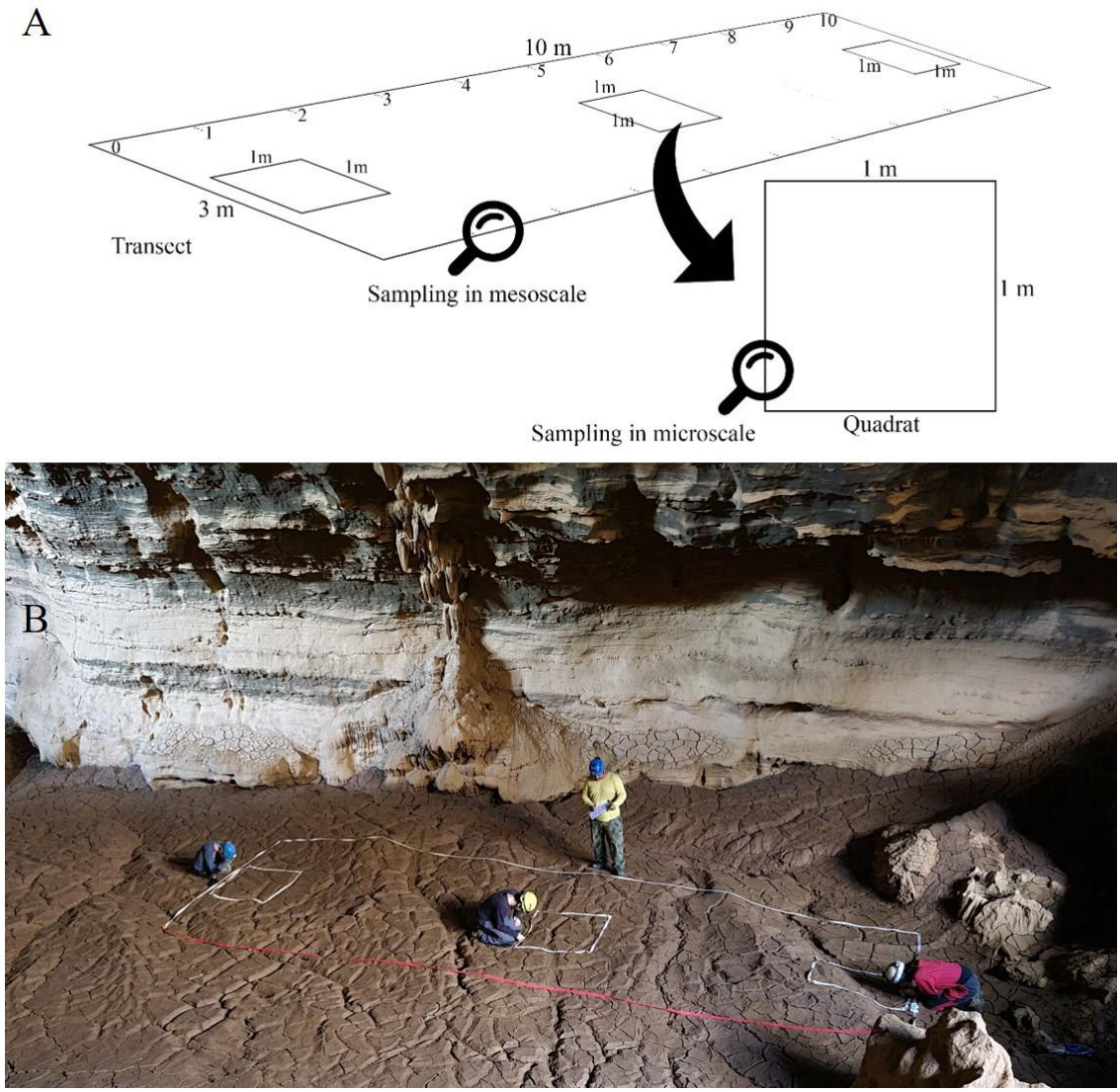


Figure 2. Sampling method. A–sampling method scheme showing both meso and microscale; B–sampling method being apply in one of the caves.



Figure 3. 20 of the 41 troglobitic species found in Santana region. A– *Pectenoniscus santanensis;* B– *Chaimowiczia tatus*; C– *Chaimowiczia tatus*; D– *Pseudochthonius* sp1; E– Ideoroncidae sp1; F– *Eukoenenia* sp2; G– Ochyroceratidae sp1; H– Caponidae sp1; I– Ochyroceratidae sp2; J– Escadabiidae sp1; K– *Endecous* sp1; L– Blattidae sp1; M– Arrhopalitidae sp1; N– *Phaneromerium cavernicolum*; O– *Coarazuphium tessai*.

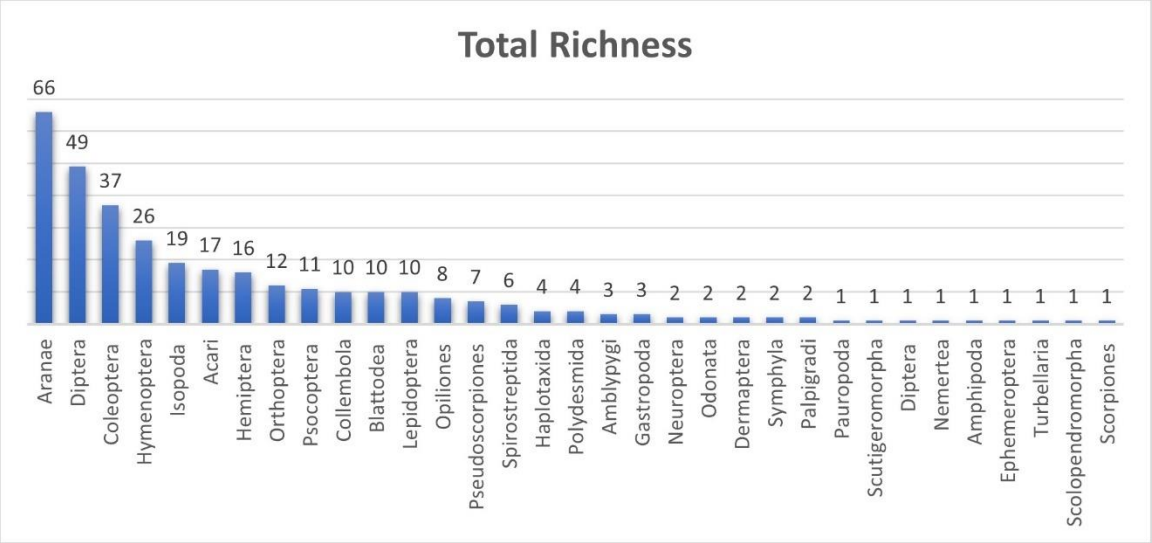


Figure 4. Main invertebrate groups richness of Santana region caves.

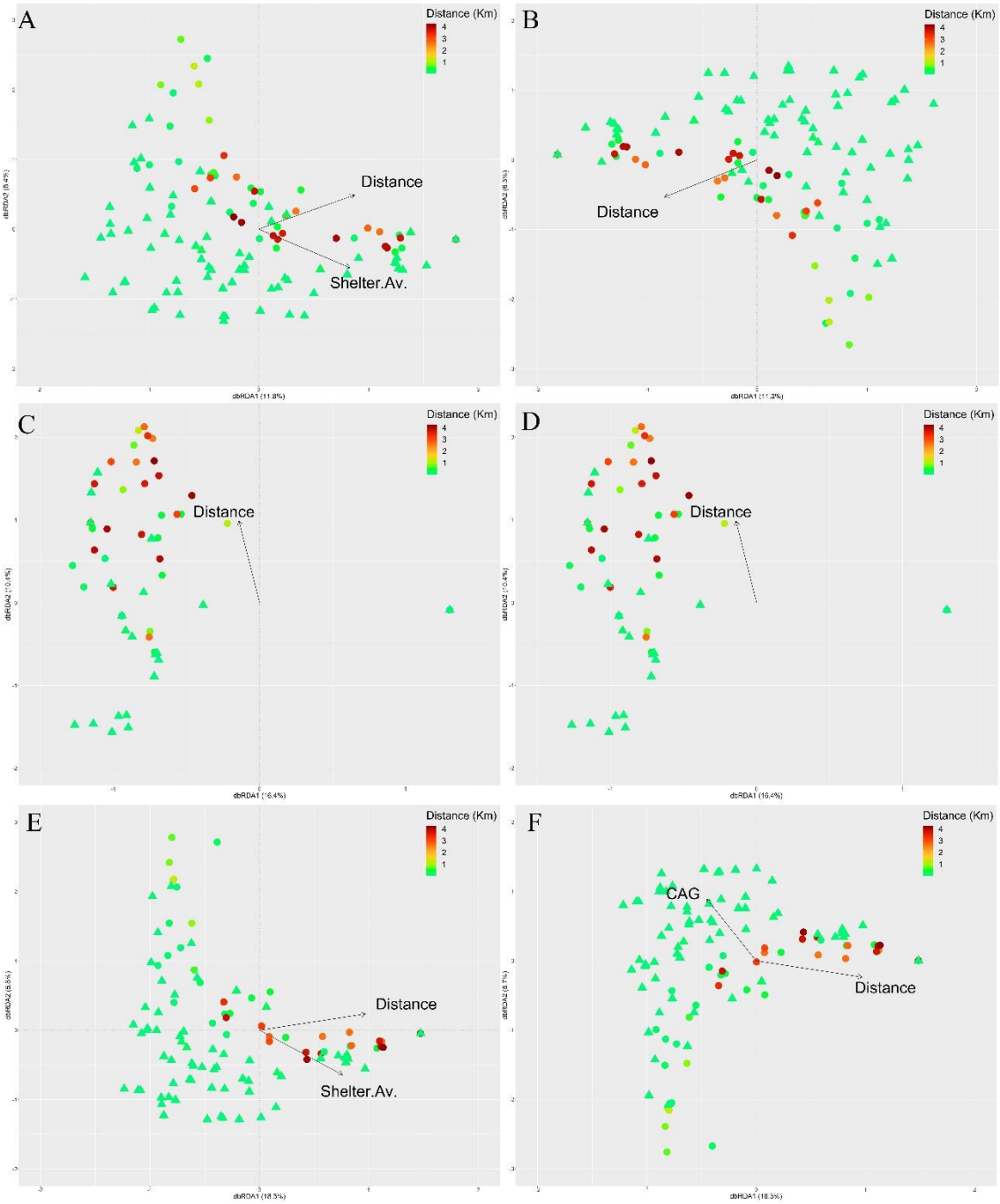


Figure 6. Distance-based Redundancy Analysis (dbRDA) on the mesoscale, succinct (A, C, E) and long (B, D, F) models. A and B–general fauna; C and D–troglobitic fauna; E and F–non-troglobitic fauna.

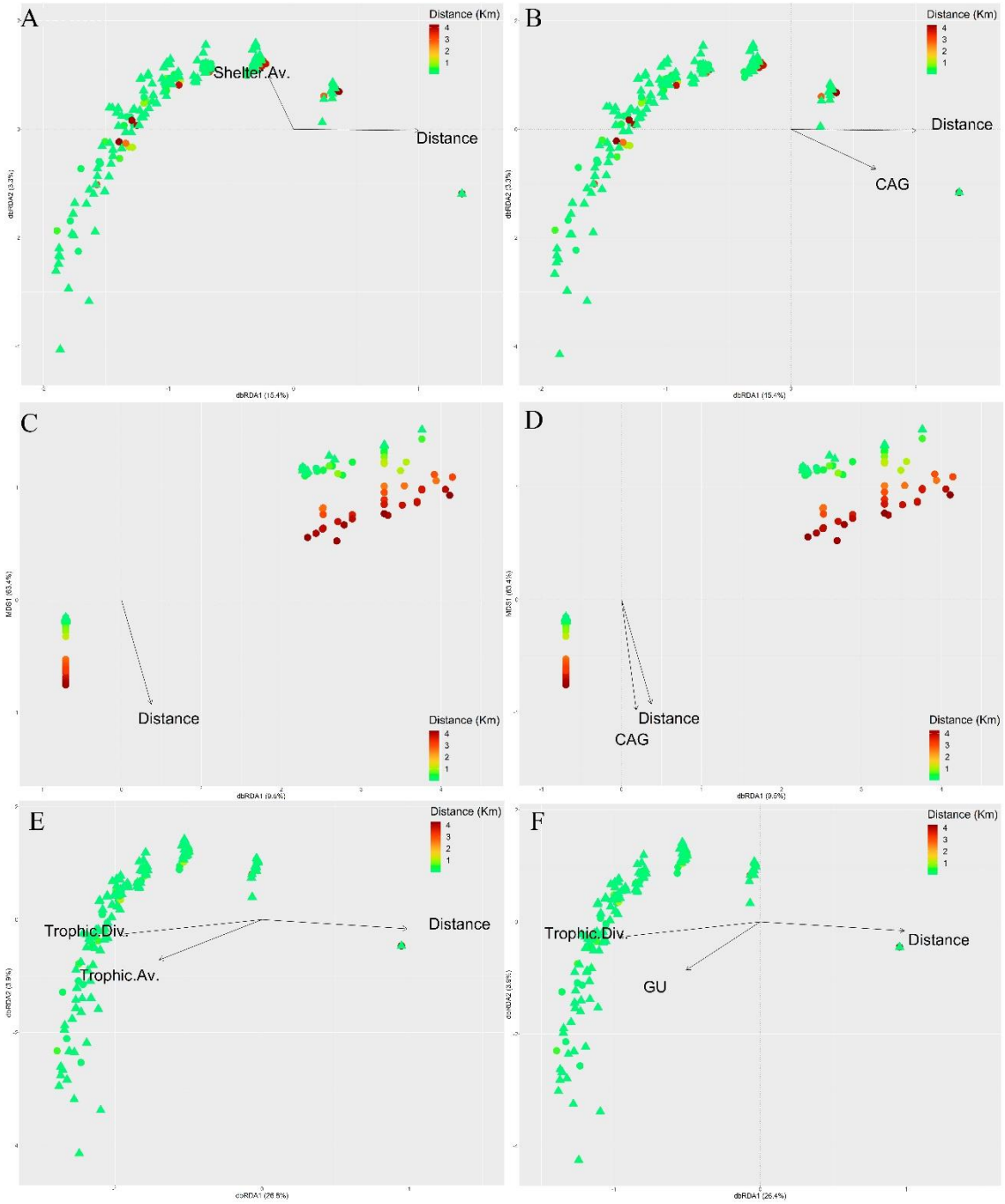


Figure 7. Distance-based Redundancy Analysis (dbRDA) on the microscale, succinct (A, C, E) and long (B, D, F) models. A and B–general fauna; C and D–troglobitic fauna; E and F–non-troglobitic fauna.

Table 1. Troglobitic species and the sample scale where they were found.

Taxons	Species and Morphotypes	Ca	Qu	Sec
Amphipoda	*Spelaeogammarus santanensis*	+		
Aranae	Ochyroceratidae sp1	+	+	+
	Ochyroceratidae sp2		+	+
	Ochyroceratidae sp3		+	+
	Prodidomidae sp2	+		
	Caponiidae sp1	+		
Blattodea	Blattidae sp1	+		
Coleoptera	*Clivina* sp1	+	+	
	Coarazuphium tessai	+		
Entomobryomorpha	Paronellidae sp2	+	+	+
Gastropoda	Gastropoda sp3	+		+
Oligochaeta	Lumbricina sp3	+		
Hemiptera	Kinnaridae sp1	+	+	+
Isopoda	*Chaimowiczia tatus*	+		
	Pectenoniscus santanensis	+	+	+
	Platyartridae sp1		+	+
	Styloniscidae sp1	+	+	+
	Styloniscidae sp2		+	+
	Pectenoniscus sp3			+
	Philosciidae sp1	+		
	Trichorhina sp2			+
	Calabozoidea sp1		+	
	Xangoniscus sp1	+		+
Nemertea	Nemertea sp1	+		
Opiliones	Escadabiidae sp1	+		+
	Escadabiidae sp2	+		
	Eusarcus aff. cavernicola	+	+	+
Orthoptera	*Endecous* sp1	+	+	+
Palpigradi	*Eukoenenia* sp1	+	+	
	Eukoenenia sp2	+	+	
Poduromorpha	Poduromorpha sp1			+
Pseudoscorpiones	*Pseudochthonius aware*	+	+	+
	Garypoidea *sp1*	+	+	+
Polydesmida	*Phaneromerium cavernicolum*	+	+	+
	Phaneromerium sp2			+
	Phaneromerium sp3	+	+	+
	Phaneromerium sp4	+		
Symphyla	Symphyla sp1	+		
Symphypleona	Arrhopalitidae sp1	+	+	+
	Arrhopalitidae sp2	+		
Siluriformes	*Pimelodella* sp1	+		

Table 2. P-values for Distance-based Redundancy Analysis (dbRDA).

Variables	Mesoscale						Microscale					
	Succinct Model			Long Model			Succinct Model			Long Model		
	General	T	n-T	General	T	n-T	General	T	n-T	General	T	n-T
Cave*	0.005	0.005	0.005	0.005	0.005	0.005	0.005		0.005	0.005		0.005
Distance*	0.005	0.005	0.005	0.005	0.005	0.005	0.005	0.005	0.005	0.005	0.005	0.005
Shelter Av.	0.045	0.050										
Trophic Av.							0.005		0.005			
Trophic Div.									0.035			0.005
GU										0.005		0.005
DTV										0.005		
CAG						0.025					0.050	
Explanation	**41.14%**	**33.51%**	**45.74%**	**39.75%**	**33.51%**	**45.75%**	**24.31%**	**9.52%**	**36.86%**	**24.66%**	**10.29%**	**36.63%**

Table 3. P-values and Estimate values for the GLM and GLMM on the mesoscale.

Varibles	Mesoscale											
	Succinct Model						Long Model					
	General		T		n-T		General		T		n-T	
	P	Est.	P	Est.	P	Est.	P	Est.	P	Est.	P	Est.
Distance*	1.61E-05	-0.273	0.003	0.265	1.79E-09	-0.553	1.73E-07	-0.350			3.09E-14	-0.671
Temperature	0.010	-0.156			0.007	-0.187	0.040	-0.130				
Trophic Av.												
GU									0.026	-3.349		
DTV												
CRC							0.020	0.070			0.033	0.065
FG							0.001	0.085			1.00E-04	0.095
ACT									0.041	1.895		
RC												
RR												
SB							0.049	-0.096				
ARE							1.028	0.111			0.021	0.134
HP							0.035	-0.107			0.038	-0.112
ES							0.015	-0.133			0.007	-0.156
ESC							0.022	0.113				
BM							0.027	0.114			0.013	0.155
GRR												
R^2/R^2M	**38.80%**		**15.74%**		**60.42%**		**56.05%**		**31.52%**		**79.38%**	
R^2C	**65.73%**				**80.71%**		**60.86%**					

Table 4. P-values and Estimate values for the GLM and GLMM on the microsocale

Varibles	Microscale											
	Succinct Model						Long Model					
	General		T		n-T		General		T		n-T	
	P	Est.	P	Est.	P	Est.	P	Est.	P	Est.	P	Est.
Distance*	8.44E-08	-0.390	2.79E-08	0.507	7.64E-13	-1.055	6.45E-09	-0.390	1.40E-06	0.475	1.85E-14	-1.091
Temperature												
Trophic Av.	0.001	0.120										
GU							0.015	0.075			0.003	0.092
DTV							0.001	0.119			3.00E-04	0.142
CRC												
FG												
ACT												
RC											0.029	0.121
RR							0.041	-0.116				
SB												
ARE												
HP												
ES												
ESC												
BM												
GRR									0.047	-0.471		
R^2/R^2M	**24.34%**		**10.55%**		**64.15%**		**28.82%**		**16.25%**		**48.00%**	
R^2C	**39.40%**				**72.21%**							

Table 5. The 24 sampled caves' coordinates. Sirgas 200; UTM 23S.

Map ID	Cave	Long. X	Lat. Y
1	Gruta Cânion da Baixa Verde Cave	596844	8537362
2	Gruta do Padre Cave	601311	8538762
3	Gruta Labirinto do Toxodon Cave	608884	8538822
4	Gruta do Boqueirao Cave	597800	8537451
5	Gruta da Pedra Escrevida I Cave	612496	8532062
6	Gruta das Duas Cobras Cave	608351	8537716
7	Gruta do Tunel II Cave	609390	8535922
8	Gruta São Geraldo Cave	609156	8535758
9	Olho D'água do Cumbra Cave	601050	8529525
10	Racha Bovina Cave	615975	8531872
11	Gruta do Tunel I Cave	609348	8535882
12	Gruta Couve-Flor Cave	609111	8535870
13	Gruta do Geraldo Cruz Cave	600656	8528434
14	Fenda Obliqua Cave	600891	8528568
15	Gruta do Cedro Cave	601082	8538937
16	Gruta do Cedrão Cave	601040	8539058
17	Gruta do Cedrículo Cave	601044	8539067
18	Gruta do Pajeú Cave	598760	8526941
19	Gruta Cristal Cave	599497	8527612
20	Gruta do Salobro Cave	588687	8554258
21	Gruta da Grota Cave	587858	8561161
22	Gruta do Leão Cave	601365	8539161
23	Gruta Cinquentona Cave	605268	8538657
24	Gruta da Pedra Escrevidinha Cave	605264	8538648

ONE CAVE, MULTIPLE WORLDS

One cave, multiple worlds: cave zonation, habitat selection and conservation of cave-dwelling fauna in a new hotspot of subterranean biodiversity in South America

Vitor Gabriel Pereira Junta[a,b], Marconi Souza Silva[a,b], Gabriel Augusto Silva Vaz[a,b], Rodrigo Lopes Ferreira[a,b]*

[a]Programa de Pós-graduação em Ecologia Aplicada, Universidade Federal de Lavras, Lavras, Minas Gerais, Brasil, CEP 37200-900.

[b]Centro de Estudos em Biologia Subterrânea, Departamento de Ecologia e Conservação, Instituto de Ciências Naturais, Universidade Federal de Lavras, Lavras, Minas Gerais, Brasil, CEP 37200-900.

*Corresponding author: Rodrigo Lopes Ferreira (drops@ufla.br)

Junta, V.G.P ORCID identifier is 0000-0001-8579-955X

Souza-Silva, M. ORCID identifier is 0000-0002-3184-5319

Vaz, G.A.S. ORCID identifier is 0000-0001-5813-435X

Ferreira, R.L. ORCID identifier is 0000-0003-3288-4405

Abstract

Despite the importance of understanding the factors influencing invertebrate communities inside caves worldwide, studies are scarce in this regard. To understand ecological aspects influencing the fauna associated with the Gruta do Padre cave, the fifty-largest cave in Brazil, we performed analysis regarding the richness and composition of invertebrate communities to assess how these communities respond to habitat characteristics, such as physical, trophic, and climatic variables, different substrates, presence of shelters, and food resources. The results demonstrate that the *Distance from the nearest entrance* and the habitat *Zonation* within the cave where the transects are placed are the main factors for fauna distribution. In addition, habitat heterogeneity correlates with the fauna richness and composition, with shelter and food availability as decisive traits. This study also revealed previously unregistered species, totaling 25 cave-restricted species, which makes the Gruta do Padre Cave a new hotspot of subterranean biodiversity in South America. Besides the ecological perspective, the information accomplished herein demonstrates the great biological importance of this cave under no protection and highlights the urge to protect the cave in all its complexity since this is a very heterogeneous cave with unique habitats within it.

Keywords: Invertebrates conservation, Habitat protection, Cave biodiversity, tropical karst

Introduction

Several studies have demonstrated that the cave linear development tends to be strongly related to the species richness in such environments (Simões et al. 2015; Souza-Silva et al. 2020; Souza-Silva et al. 2021; Rabelo et al. 2021). This relation is probably because bigger caves tend to present both greater areas and higher habitat heterogeneity. However, the large linear development can be limiting, especially in caves with few entrances. It is well known that caves rarely present primary production, excepting a few subterranean chemautotrophically based ecosystems (Sarbu andKane 1996; Porter et al. 2009; Barton et al. 2010; Galassi et al. 2017) and entrance zones (Souza-Silva et al. 2011; Prous et al. 2015). Thus, the main source of energy in caves comes from external environments, corresponding to the organic matter transported by physical and biological agents (Souza-Silva et al. 2011; Ferreira 2019). Hence, in large caves with few entrances, the organic matter hardly reaches deep areas, limiting the available energy for the communities (Tobin et al. 2013; Moseley 2008; Ficetola et al. 2018; Mammola 2019).

As well as the large extension of the caves, the presence of rivers also contributes to the maintenance of richer communities (Simões et al. 2015). Rivers and streams act as trophic resource carriers, especially in the case of allogenic drainages, taking energy from external habitats and bringing it to deeper cave zones (Venarsky et al. 2012) Additionally, microclimate traits, such as temperature and moisture, are usually linked to the presence of great water bodies (Souza-Silva et al. 2011; Lobo et al. 2015; Simões et al. 2015; Souza-Silva et al. 2020). Furthermore, despite the general stability observed in caves, a gradient of climate conditions is usually observed from near-to-entrance zones (which are more variable) to deeper areas (Moseley 2009; Tobin et al. 2013; Lunghi et al. 2014 Prous et al. 2015; Mammola and Isaia 2018; Lunghi and Manenti 2020; Souza-Silva et al. 2021). This zonation generates distinct microhabitats for cave fauna, which varies not only in climatic and photic characteristics but also in the types of substrates they present (Moseley 2008; Souza-Silva et al. 2011; Du Preez et al. 2015; Lunghi et al. 2017; Mammola and Isaia 2017; Mammola 2019; Lunghi and Manenti 2020; Mammola et al. 2020; Souza-Silva et al. 2021).

Cave-restricted species (troglobitic species) usually present adaptations to the cave environments, which can be morphological, physiological, reproductive, or even behavioral (Romero and Green 2005). Furthermore, those species are usually rare and endemic because of their long evolutive history in such stable environments, which makes them sensitive to changes in their ecosystems, such as slight variations of temperature and moisture (Culver and Pipan 2009; Mammola et al. 2019).

The troglobitic species are so unique that caves with many cave-restricted species are classified as Hotspots of Subterranean Biodiversity (HSB). According to Culver and Sket (2000), a cave or a cave system must have 20 or more cave-restricted species to be considered a hotspot. However, Culver et al. (2021) raised the cutoff to 25 species, arguing that the global list was too lengthy. It is important to consider, nevertheless, that 25 species is another arbitrary cutoff (as the originally purposed number of 20 species), that probably results from an analysis preferably considering temperate regions. Thus, it is important to mention that

caves located in tropical areas will rarely present up to 25 cave-restricted species. Hence, we herein opted to keep the original concept of HSB (Culver and Sket 2000).

Considering the original definition of Culver and Sket (2000), there are currently three HSB in Brazil: the Toca do Gonçalo cave (northeastern Brazil) with 22 troglobitic species; the Areias Cave System (southeastern Brazil) with 28 troglobitic species and the Água Clara Cave System (northeastern Brazil), with 30 troglobitic species (Souza-Silva and Ferreira 2016; Souza-Silva et al. 2021). Of those three HSBs, only one (Areias Cave System) is protected within the limits of a State Conservation Unit (Parque Estadual Turístico do Alto Ribeira). The two remaining are in unprotected areas and are currently exposed to several anthropogenic threats (Souza-Silva and Ferreira 2016; Souza-Silva et al. 2021).

Unfortunately, Brazilian speleological legislation does not protect these important areas. From 1990 onwards, Brazilian caves were fully protected, but in 2008, a decree determined that Brazilian caves should be classified according to their relevance degree, allowing some caves to be destroyed for mineral resources exploitation. Only those caves classified as presenting maximum cultural, geological, and/or biological value should be preserved (Decree nº 6.640). However, a new decree (Decree nº 10.935) from 2022, started to allow the destruction of even those caves with maximum relevance.

The Gruta do Padre Cave is one of the largest known caves in Brazil, with 16,400 meters of mapped galleries, representing the fifth longest cave in the country. Additionally, it is part of the most extensive subterranean hydrological system in Brazil (Rubbioli et al. 2019). Considering the uniqueness and high biological relevance of this Cave, the main goal of this study was to identify the variables determining the spatial distribution of invertebrates along with presenting the fourth hotspot of subterranean biodiversity in the Neotropical region. Furthermore, as this cave presents areas with highly distinct conditions (upper chambers near and far from entrances and river chambers near and far from entrances), variables describing the physical, trophic, and microclimatic attributes of the cave were used to test four hypotheses: *i*) upper and lower areas within the cave will present distinct communities regarding the species composition; *ii)* species richness will be reduced in areas far from the cave entrances; *iii)* invertebrates will respond to different habitat components and habitat heterogeneity on the cave floor in the distinct cave compartments and *iv)* niches from the most abundant species may vary along the different cave areas. In addition, we discuss the impacts over this cave and argue about the importance of preserving this unique new South American hotspot of subterranean biodiversity.

Material and Methods

Study area

The Gruta do Padre cave is located in the Santana municipality (Fig. 1), in southwestern Bahia state, and is inserted in the Bambuí Group, the largest carbonate region in Brazil, with 146,378 Km² of area and approximately 6,302 registered caves. The Santana municipality is placed in a transition zone between the Caatinga and Seasonal Dry Forests and has a high potential for endemic species (Dinerstein et al. 2017). This high potential

probably resulted from several paleoclimatic changes in the Brazilian semi-arid caused by the expansions and retreats of Atlantic and Amazonian humid forests (Sobral-Souza et al. 2015). The climate in the area is the Aw (Köppen 1936), with dry winters and rainy summers. Due to the strong tropical rains that occur in the region during the summer, safe access to the cave is only possible in dry periods (March to October).

The Padre Cave comprises the largest portion of the longest subterranean hydrologic system in the country, formed by a long subterranean stretch of the Santo Antônio River (Auler et al. 2019). This river flows through four caves before reaching the Corrente River. Firstly, the Santo Antônio River becomes underground in a small nameless cave, which siphons after the entrance. In a second moment, the river reappears in the Cipó Cave, with approximately 2.76 Km of extension, sinks again, and reappears in the Padre Cave. Into this cave, it flows through 6.2 Km of large conducts until sinks. Finally, the river reappears in the Bananeira Cave, the twenty-fifth longest cave in Brazil, with its 6.55 Km of waterlogged conducts, and then flows into Corrente River (Auler et al. 2019).

The Padre Cave has two entrances, located around 1.7 km from each other. The upstream entrance is also locally known as Lapa do Cedro Cave or Lapa D'água Cave (Fig. 2–B) and presents rupestrian paintings and archeological engravings indicating its past use by native populations. The downstream entrance, known as Padre Cave or Santo Antônio Cave, was used as a peregrination point for religious purposes in the 20th century. Although both entrances have a narrow area of dry forest protecting them (Fig. 2–A), pastures and monocultures are dominant in the surrounding landscape (Auler et al. 2019).

The cave can be divided into three distinct levels. The lower level (Fig. 2–D), where the Santo Antônio river flows, is the longest, with very deep areas and a high ceiling, reaching 40 meters. The second level is located around 45 meters above the river level and comprises giant galleries (Fig. 2–C), some of which are almost 50 meters in width. These galleries are composed of different kinds of substrates, such as downed blocks, sandy areas, and speleothems. The third and last level is smaller and can be found 53 meters above the Santo Antônio River (Auler et al. 2019).

Field procedures

Sampling design

The richness and composition of cave invertebrates, as well as the habitat structure traits, were determined along 53 transects (mesoscale sampling - 10 × 3 m each) distributed on the caves' floor (Fig. 3), from the entrances to the deeper regions of the cave, encompassing both the lower level (river conduit) and the upper level (upper dry galleries). Quadrats (micro-scale sampling - 1 m^2) were inserted in triplicates within the limits of each transect (Fig. 2), totalizing 159 quadrats (Souza-Silva et al. 2021). Invertebrate sampling was done by visual search along the transects and quadrats (Souza-Silva et al. 2021). The sampling in the quadrats allowed the detection of low mobility and small-size species, which could then be thoroughly searched in the remaining transect if detected. The sampling was first performed in the quadrats and later in the respective transect, always by three collectors, and was only completed when all the invertebrates had been sampled and/or accounted for. The search time

varied among each sampling unit since the different sampling areas presented a considerable structural distinction along the cave. Additionally, to maximize the detection of troglobitic and stygobitic species, direct intuitive search techniques were also applied in other cave areas (Wynne et al. 2019). Invertebrates were preserved in properly labeled jars containing 70% ethanol. In the laboratory, the specimens were sorted with a Stemi 508 (ZEISS) stereomicroscope, identified until the lowest possible taxonomic level, and separated into morphotypes (Oliver and Beattie 1996). Potential troglobitic species were identified by the presence of troglomorphic traits, such as eyes and pigmentation reduction, and appendage elongation, among others (Culver and Pipan 2009). Furthermore, specialists in different taxa were also consulted to assist in the detection of specific troglomorphic traits (specialists are acknowledged further on). The voucher specimens were deposited in the Collection of Subterranean Invertebrates of Lavras (ISLA), linked to the Center of Studies on Subterranean Biology (CEBS) of the Federal University of Lavras (UFLA).

Environmental traits in different scales

The survey of the habitat structure parameters in the transects was performed according to the methodology used by Souza-Silva et al. (2021). Each transect was subdivided into 10 sections (1 × 3 m) (Fig. 3), in which the surface area occupied by distinct organic and inorganic substrates was visually quantified. Then, a sum was made to obtain the area occupied by each substrate throughout the entire transect. To minimize observer error, all transects were characterized by the same researcher. A digital thermo-hygrometer positioned at the ground at the center of each transect was used to measure the temperature and humidity. The proportion of each substrate in the quadrats was determined through photographs (4000 × 3000 pixels) taken of each quadrat as close as possible to a 90º angle with a Canon Powershot SX60HS camera, at the researcher's chest high. Photographs were posteriorly analyzed with the aid of *ImageJ 1.53K* software. Each sector's position in the cave was plotted on its map and then the distances to the nearest entrance were obtained. The coordinates of each sector in the cave were obtained by the plot in the map with the aid of *QGis 3.22* software.

Data analysis

Pre-analysis routine

All analyses were conducted considering four distinct cave zones, determined by both the distance from the entrances and the cave level (upper or lower): the *Upper Chambers Near Entrances* (UCNE – transects 1-11 and 42-47), the *Upper Chambers Far from Entrances* (UCFE – transects 34-41), the *River chamber Near Entrances* (RCNE – transects 12-21) and the *River Chamber Far from Entrances* (RCFE – transects 22-33 and 48-53) (Fig. 1). These acronyms will be used henceforth throughout the text.

All the analyses were performed in the R Studio 2022.07.02 Build 576 software. Before running the analysis for invertebrate fauna composition and richness, the correlation between the variables was tested with the aid of the *CHART.CORRELATION* function from the '*PerformanceAnalytics*' package. Variables with correlation values higher than 0.70 were excluded from the models. Variables correlated with more than one other variable and with

less specificity were favorite to exclusion. Using the functions *VIF* and *VIF.CCA* from the '*Car*' package, the multicollinearity of variables was tested, and those presenting values higher than 10 were excluded. Firstly, the variable with the highest value was excluded, then the test was repeated, and the process continued until no higher than 10 value was found. A Shapiro-Wilk test was executed, to verify the normality of the data, using the *SHAPIRO.TEST* function from the package '*Stats*'. A Mantel test was performed to try the spatial autocorrelation between the samples, in both meso and microscales.

Mesoscale abiotic features

All the substrates in each sector were evaluated and classified into the following classes: vegetal debris - DTV (< 10mm); fine branch - GALF (11 - 30 mm); medium branch - GALM (31 - 50 mm); coarse branch - GALG (65 - 250 mm); trunk - TRO (> 250mm); water pond - WP; drip water - DP; coleoptiles - COL; smooth rock - RL; concrete floor - RC; large rock - XB (1000 - 4000mm); medium rock - MB (500 - 1000mm); small rock - SB (250 - 500mm); cobbles - CB (64 - 250mm); coarse gravel - CAG (16 - 64mm); fine gravel - CAF (2 - 16mm); sand - ARE (0.06 - 2mm); silt - SEF (≤ 0.05 mm); hardpan - HP; speleothems - ES; calcite rafts - JNS; concreted calcite raft - JNC; stalagmite - EST; micro travertine - MTR; travertine - TRA; rough flowstone - ESR; flowstone - ESC; worm acorn - BM; retraction cracks - GRR; owl acorn - BCO; pinnacle - PIN; another inorganic substrate - OTI.

Based on those classes and using a Shannon-Weaver Index (Buttigieg and Ramette 2014), the *Substrate Diversity* (all classes), the *Shelter Diversity* (WP, DP, XB, MB, SB, CB, CAG, CAF, ES, JNS, JNC, EST, MTR, TRA, ESR, ESC, BM, GRR, BCO) and the *Trophic Resources Diversity* (DTV, GALF, GALM, GALG, TRO) were calculated for each sector. The classes were also used to generate, by simple summation, the *Shelter Availability* (WP, DP, XB, MB, SB, CB, CAG, CAF, ES, JNS, JNC, EST, MTR, TRA, ESR, ESC, BM, GRR, BCO) and the *Trophic Resources Availability* (DTV, GALF, GALM, GALG, TRO) for each sector.

The abiotic attributes were then separated into *Physical features*, which comprise the *Distance of each transect from the nearest entrance*, the *Cave Zone* (UCNE, UCFE, RCNE, RCFE), *Substrate Diversity*, *Shelter Diversity*, and *Shelter Availability*. The *Trophic Resources* grouped *Trophic Resources Diversity* and *Trophic Resources Availability*. The *Microclimatic Variables* considered were *Temperature* and *Moisture*.

Microscale abiotic features

For the quadrats, the same substrate classes were evaluated, and the same groupings were formed. The diversities and availabilities were calculated in the same manner as for the sectors. The *Physical* and *Trophic* features were also formed similarly to the mesoscale. For the microscale, the microclimatic variables were not measured.

Habitat traits determining the communities' richness and composition

To understand the possible correlation between total richness, troglobitic, and non-troglobitic invertebrate richness with *physical*, *trophic*, and *microclimatic* variables, Generalized Linear Mixed Models (GLMM) were performed, with sectors and quadrats as sample units, for troglobitic and non-troglobitic fauna. The models used *Microclimatic Variables*, Distance,

Diversities (general substrate, shelter, and trophic resources), and Availabilities (shelter and trophic resources). For the microscale, the *Microclimatic Variables* were not used.

For those models, the Poisson family was adopted because it better fitted the data, and the cave zones were used as random variables. For the evaluation of model overdispersion, the function *CHECK_OVERDISPERSION* from the package '*Performance*' was used. To obtain r^2 values, the function *r.squaredGLMM* from the '*MuMIn*' package was used.

To evaluate the possible response between troglobitic and non-troglobitic invertebrate composition with *physical*, *trophic*, and *microclimatic* variables a Distance-Based Redundancy Analysis (dbRDA) was performed (Clarke et al. 2014), with sectors and quadrants as sample units. The models used *Microclimatic Variables*, Zones, Distance, Diversities (general substrate, shelter, and trophic resources), and Availabilities (shelter and trophic resources). For the microscale, the *Microclimatic Variables* were not used.

Distinction among the cave zones

To access the differences in the average habitat traits in each *Zone* of the Gruta do Padre Cave, a Kruskal-Wallis's test was used. For those significantly different variables, a Dunn Post Hoc test was used to understand which area differs from the others (Ostertagova et al. 2014).

Niche analysis

We investigated species' ecological niche in different cave zones through the Outlying Mean Index (OMI) analysis (Dolédec et al. 2000), using the 'ade4' package in the R software. The OMI analysis was conducted using an invertebrate abundance table (excluding species found in only one sample unit) and an environmental matrix comprising variables such as temperature, humidity, distance from the entrance, vegetal debris (DTV), guano (GU), substrate diversity, shelter diversity, and shelter availability. For a more in-depth understanding of the analysis, additional information is available in Dolédec et al. (2000).

The OMI analysis allowed the placement of each species within a two-dimensional Euclidean space, decomposing their distribution patterns in terms of marginality, tolerance, and residual tolerance. Marginality, in this context, represents the distance between the average environmental conditions utilized by a species and the overall average conditions. Species are positioned in relation to their deviation from a reference species, which is a ubiquitous species occurring across all available habitat conditions. Lower marginality values indicate a wider occurrence of the species within the studied environment. Tolerance quantifies the range of environmental conditions utilized by each species. Residual tolerance offers insights into the reliability of the identified niche (Dolédec et al. 2000).

To perform the OMI analysis, we commenced with a principal component analysis (PCA) using the components of mesoscale habitat structure. Following this, we determined and plotted the niche of each selected species within the environmental niche. Ultimately, we applied the Monte Carlo test, with 999 permutations, to assess the significance of the difference between the observed marginality of species and simulated values (Dolédec et al. 2000).

Changes in environmental conditions in different cave zones were detected by calculating Within Outlying Mean Indexes (WitOMI, 'subniche' package in R, Karasiewicz et

al. 2017). WitOMI indexes refine the OMI analysis using their properties in combination with the species marginality decomposition from the K-select analysis (Karasiewicz et al. 2017). This allows the division of niches into sub-niches linked to spatial or temporal subsets. The environmental subsets in this study were defined by the physical, trophic, and microclimatic characteristics of four cave zones (UCNE, UCFE, RCNE, and RCFE). This analysis enables an understanding of how a community responds to changes in environmental conditions on individual scales (Karasiewicz et al. 2017; Saccò et al. 2020). Subniche parameters for each species, compared by the average environmental condition from the OMI analysis (G), were calculated (WitOMI G) and additionally compared with the average environmental condition within a specific subset (GK) (WitOMIGK) (Karasiewicz et al. 2017; Saccò et al. 2019). Details about the analysis can be found in Karasiewicz et al. (2017) and Saccò et al. (2020).

Results

Richness and composition of cave invertebrates

Considering the whole Padre Cave (with samplings in the sectors, quadrants, and other habitats) 1,811 specimens were counted, totaling 115 species. These were grouped into 31 orders and at least 61 families (Fig. 4). The richest group was Araneae, with 22 species distributed in 11 families, totaling 277 individuals. The spiders were followed by Diptera and Coleoptera, with 15 and 14 species respectively.

Cave-restricted species

The Gruta do Padre Cave has at least 25 cave-restricted species belonging to 8 higher taxa and 14 families (Fig. 5 and 6). The eight higher taxa were Hexapoda (8 spp.), Arachnida (6), Crustacea (5), Myriapoda (2), Mollusca (1), Nemertea (1), Annelida (1) and Osteichthyes (1) (Table 1). It is important to emphasize that while this work primarily focused on invertebrates, a single fish species was considered due to its restriction to the cave environment, thereby contributing to the overall assessment of troglobitic fauna in the cave. The richness of the observed obligate cave fauna was Gastropoda (1), Nemertea (1), Oligochaeta (1), Isopoda (4), Amphipoda (1), Polydesmida (1), Symplyla (1), Blattodea (1), Collembola (4 spp.), Coleoptera (2), Orthoptera (1), Pseudoscorpiones (1), Araneae (1), Opiliones (2), Palpigradi (2), and Siluriformes (1). However, only 24% of the obligate cave species from the Gruta do Padre Cave are described. Such described species are *Coarazuphium tessai* (Godoy andVanin 1990); *Phaneromerium cavernicolum* (Golovatch & Wytwer, 2004), *Spelaeogammarus santanensis* (Koenemann and Holsinger 2000), *Eusarcus cf. cavernicola* (Hara and Pinto-da-Rocha 2010), *Pectenoniscus santanensis* (Cardoso et al. 2020) and *Chaimowiczia tatus* (Cardoso et al. 2021). It is important to note that although the type series of *E. cavernicola* presents specimens from Gruta do Padre cave, Hara and Pinto-da-Rocha (2010) attested that "it is possible that what we know as *E. cavernicola* is actually an assembly of species that cannot be recognized by external and genitalic features". Considering that the population observed in the Gruta do Padre Cave is strongly troglomorphic (much elongated and depigmented when compared to other populations), we are herein considering that it constitutes a troglobitic species.

Habitat traits determining the communities' richness and composition

For the communities' composition, the *Zone* of the cave where the samples were made was the most important factor, being significant for all models. The *Distance from the nearest entrance* was important for the troglobitic fauna. The *Shelter Diversity* was significant for both fauna groups, but only on the mesoscale. *Trophic Resources Diversity* and *Availability* were important to non-troglobitic fauna on both scales (Table 2, Fig. 5).

For the communities' richness, there was no significant response from the troglobitic fauna. For the non-troglobitic species, however, *Temperature* and *Substrate Diversity* were important on the mesoscale, while *Distance* and *Shelter Availability* were significant for the microscale (Table 3).

Differences between Zones of the Gruta do Padre Cave

The cave *Zones* (UCNE, RCNE, UCFE, RCFE) within Gruta do Padre Cave differed in Shelter Availability, Trophic Availability, Shelter Diversity, and Temperature. The Shelter Availability in Upper zones was significantly different from River Zones in both scales. In the case of Trophic Resources Availability and Temperature, UCNE and RCNE were different from UCFE and RCFE zones. The Shelter Diversity was contrasting only between RCNE and upper zones (UCNE, UCFE), in the mesoscale (Table 4).

Regarding the troglobitic average richness, both River zones are statistically different from the Upper zones (UCNE and UCFE). For the non-troglobitic fauna, regions near the entrance (UCNE and RCNE) differ from those far from the entrance (UCFE and RCFE). In the microscale, regions near the entrance and far entrance also are significantly different (Table 4).

Ecological niches

The combined explanation of the first two OMI axes accounts for 91.1% of the variability, where OMI axis 1 represents 53.1% and OMI axis 2 represents 38% of the variance. The significance of the average marginality for the theoretical ubiquitous species ($P < 0.05$; 999 Monte Carlo permutations) underscores the influence of environmental variables on the invertebrate community within the Padre Cave.

The subsets of environmental conditions associated with each cave zone (RCFE, RCNE, UCFE, UCNE) were not only statistically different from the origin (OMI mean (G)) but also significantly differed among themselves (RCFE: $p < 0.001$; RCNE: $p < 0.001$; UCFE: $p < 0.001$; UCNE $p < 0.001$; 999 Monte Carlo Permutations). This observation confirms that the four areas exhibit distinct habitat characteristics. Among the environmental variables, humidity and distance from the nearest entrance were identified as the most significant contributors to the differentiation in the average conditions of the cave zones (Fig. 6). Interestingly, the invertebrate community displayed less dispersed distributions in the UCFE zone (Fig. 6). This outcome is partly attributed to the sampling design of this study, characterized by fewer sample units in this specific area. Nonetheless, it underscores how certain locations can impose restrictions on the overall fauna.

Few species displayed low marginality values (OMI), defined by some authors as OMI values < 2, indicating taxa with a common habitat use (Karasiewicz et al., 2017; Sacco et al.,

2019). Out of 41 species, fifteen (36.5%) exhibited significant niche breadth (OMI, $p < 0.05$, 999 Monte Carlo permutations; Table X). *Leucauge* sp1 (Araneae: Tetragnathidae) (OMI = 17.672; Tol = 0.250), *Loxosceles* sp2 (Araneae: Sicariidae) (OMI = 16.090; Tol = 0.058), *Lutzomya* sp5 (Diptera: Psychodidae) (OMI = 15.219; Tol = 0.144), *Oecobius* sp1 (Araneae: Oecobiidae) (OMI = 16.318; Tol = 0.028), Sciaridae sp1 (Diptera) (OMI = 10.724; Tol = 0.847), Staphylinidae sp1 (Coleoptera) (OMI = 9.613; Tol = 0.416), and *Zelurus* sp1 (Hemiptera: Reduviidae) (OMI = 15.152; Tol = 0.048) exhibited high marginality values and low tolerance values. Among these species, *Loxosceles* sp2, *Oecobius* sp1, and *Zelurus* sp1 showed more similar niche dimensions. *Psyllipsocus* sp2 (Psocodea: Psyllipsocidae) also exhibited high marginality values (OMI = 15.206), but it had a broader niche (Tol = 1.386). Species such as *Charinus santanensis* (Amblypygi: Charinidae), *Isoctenus* sp3 (Araneae: Ctenidae), *Eusarcus* sp1 (Opiliones: Gonyleptidae), Lumbricina sp2 (Oligochaeta: Haplotaxida), and Paronellidae sp1 (Collembola: Entomobryomorpha) had intermediate marginality values (between 3 and 6). Among these species, *Eusarcus* sp1 and Paronellidae sp1 had the widest niche breadth (Tol = 2.283 and 2.575, respectively), while *Charinus santanensis* had the narrowest niche breadth (Tol = 0.453). *Endecous* sp1 (Orthoptera: Phalangopsidae) and *Pseudonannolene microzoporus* (Diplopoda: Spirostreptida) utilized average habitat conditions (OMI < 2) (Table S1, Supplementary Material 1).

All WitOMI values reached statistical significance (Table S2 and S3, Supplementary Material 1). Consequently, the observed changes in sub-niches occupations are associated with variations in the average environmental conditions of the subsets of cave zones (GK) (depicted as red dots in the Fig. 8).

The troglobitic cricket species *Endecous* sp1 exhibits a wide distribution, being observed across all zones of the cave and utilizing the most prevalent habitat conditions. However, the habitats used in the areas farther from the cave entrance (RCFE, UCFE) were more marginal compared to those in the areas closer to the entrances (RCNE, UCNE) (Table S2 and Fig. S1, Supplementary Material 1). Nevertheless, differences in marginality were noted when considering the areas distant from the entrance (WitOMIG RCFE = 4.4; WitOMIG UCFE = 7.2), differences that did not occur in the areas near the entrance (WitOMIG RCNE, UCNE = 3.2). The changes in niche occupancy regarding marginality and tolerance are attributed to variations in the average habitat conditions of the subsets (red dots in Fig. S1, Supplementary Material 1) and habitat condition constraints in the subsets (space between the fundamental niche and the realized niche in the subsets, referred to as SB, Fig. S1, Supplementary Material 1). When considering the habitat conditions of each zone separately (WitOMI GK), the lowest marginality value occurred in RCNE, where the highest tolerance value for this species was also observed (WitOMI GK RCNE < UCNE < RCFE < UCFE; Tol = RCNE > UCNE > RCFE > UCFE; Table S3, Supplementary Material 1), indicating a preference for areas near the entrance, specifically RCNE.

The species *Leucauge* sp1, *Loxosceles* sp2, *Lutzomya* sp5, *Oecobius* sp1, *Psyllipsocus* sp2, *Zelurus* sp1, and Sciaridae sp1 exclusively utilized the habitat conditions of the UCNE zone, exhibiting significant deviations from the origin (G) and demonstrating a lack of utilization of

the average habitat conditions of the cave (Table S2 and Fig. S2, Supplementary Material 1). Within this subset, these species also showed a preference for marginal conditions, indicating a high level of specialization in this specific zone of the cave. In contrast, *Isoctenus* sp3 exclusively utilized the habitat conditions of the RCNE zone, which, in relation to the origin (G), deviates its realized niche towards locations with greater availability of trophic resources (GU and DTV) (Fig S3, Supplementary Material 1). However, considering the marginality within its subset (Table S3), this species utilizes the average habitat conditions.

The remaining species occupied at least two zones of the cave. *Charinus santanensis* did not utilize the average conditions of the cave (OMI > 2), occupying areas near the entrances (RCNE, UCNE), and displaying higher marginality concerning the origin (G) in UCNE. Considering the habitat conditions of the subsets (WitOMI GK; Table S3, Supplementary Material 1), this species does not deviate significantly from the midpoint of RCNE, but its tolerance is minimal, indicating that in this location, the species faces greater restrictions than in UCNE (Fig. S4).

Another arachnid, the harvestman *Eusarcus* sp1, also avoids using the average habitat conditions of the cave and instead occupies areas near the entrances. The marginality concerning the origin (G) was higher in UCNE than in RCNE for this species (WitOMI G, Table S2, Supplementary Material 1). However, considering the midpoint of the subsets (GK), the most significant deviation occurred in RCNE (WitOMI GK, Table S3, Supplementary Material 1). Analyzing the breadth of the realized niche, *Eusarcus* sp1 exhibited a broader niche in UCNE, precisely in an area where greater biological restrictions prevail (SB, Fig. S5, Supplementary Material 1).

The earthworm species Lumbricina sp2 also avoids utilizing the average habitat conditions of the cave and was only absent in UCFE. Its marginality concerning the origin (G) was lower in RCFE than in areas near the entrances (RCNE, UCNE) (Table S2, Supplementary Material 1). Concerning the midpoint of each subset, its marginality was higher in UCNE than in the river areas (WitOMI GK RCNE and RCFE have similar values; Table S3, Supplementary Material 1). However, this species did not establish a broad niche in UCNE, showing a preference for areas at the river level, more precisely in RCNE. This is because, in RCFE, this earthworm faced more significant constraints of conditions (SB) and realized a niche with lower tolerance (Table S3, Fig. S6, Supplementary Material 1).

The springtail species Paronellidae sp1 displayed the broadest realized niche breadth among all the significant species in the OMI analysis, accompanied by intermediate marginality (Table S1, Supplementary Material 1). This springtail occupied areas near the entrance (UCNE, RCNE) and RCFE. The marginality concerning the origin (G) was higher in areas near the entrance (UCNE > RCNE) than in RCFE, but in this zone, the species exhibited a minimal realized niche breadth (Table S2, Supplementary Material 1). Considering the average conditions of the subsets (GK), in areas located by the river, this collembolan showed lower marginality values than in UCNE (Table S3, Supplementary Material 1). When comparing the areas with a prevalence of the species, it was observed that the realized niche breadth was greater in RCNE, a region where this species utilized its entire fundamental niche

(the fundamental niche in UCNE is characterized by greater biological constraints) (Fig. S7, Supplementary Material 1).

Finally, the millipede *Pseudonannolene microzoporus* utilized the average habitat conditions, occupying the same areas as the springtail Paronellidae sp1. The marginality concerning the origin (G) was also higher in areas near the entrance (UCNE, RCNE) than in RCFE, but in this zone, the species had a smaller realized niche breadth. Considering the average conditions of the subsets (GK), in areas at the river level, this millipede showed lower marginality values than in UCNE (Table S3, Supplementary Material 1). It was observed that the realized niche breadth was greater in RCNE, a region where the constraints represented a small area of the fundamental niche. In UCNE, despite this species having a broad realized niche breadth, a significant portion of its fundamental niche had areas of biological restriction (Fig. S8, Supplementary Material 1).

Discussion

Distance from the entrance and Cave Zones affecting the communities

Two habitat traits have emerged as crucial factors influencing the distribution of invertebrate species within the Gruta do Padre Cave. These are the *distance from the nearest entrance* and the *cave zones*. The distance from the entrance is a key determinant of community distribution, as demonstrated by various studies on cave communities. This is due to the limiting effect of long distances within the cave, which leads to a decrease in trophic resources and habitat diversity from the entrance to deeper regions of the cave (Tobin et al. 2013; Moseley 2008; Ficetola et al. 2018; Mammola 2019; Souza-Silva et al. 2021). Organic matter is one of the most significant inputs into caves, primarily transported from external habitats through the entrances. As a result, the availability of organic matter decreases in the deeper zones of the cave (Sarbu and Kane 1996; Moseley 2008; Souza-Silva et al. 2011; Tobin et al. 2013; Prous et al. 2015; Galassi et al. 2017; Ficetola et al. 2018; Mammola 2019).

The distance from the entrance also affects habitat heterogeneity, as caves exhibit a gradient of features from the entrance to the deeper regions. The proximity to the entrance is characterized by less stable climatic conditions, resulting in gradients of temperature, moisture, and sunlight. This gradient is also reflected in the cave floor, with the substrates becoming increasingly simpler and homogeneous as one moves towards deeper zones (Prous et al. 2004; Prous et al. 2015; Souza-Silva et al. 2021; Furtado et al. 2022). In the case of Gruta do Padre Cave, which is a vast cave (16.5 km) with only two entrances, these effects are particularly noticeable. As one moves from the entrances to deeper areas, there is a reduction in organic matter and habitat heterogeneity, which directly affects the cave fauna.

The richness of the non-troglobitic fauna decreases as one moves from near the entrance to the deeper zones of Gruta do Padre Cave, likely due to the decrease in food sources and habitat complexity (Prous et al. 2004; Prous et al. 2015; Souza-Silva et al. 2021; Furtado et al. 2022). Conversely, the troglobitic fauna responds differently, not being affected by the increase in the distance. Troglobitic species are highly adapted to living in areas with very limited resource availability, making them attracted to the greater climatic stability observed

in the deeper regions of the cave. Furthermore, many troglobitic species are vulnerable to fluctuations in microclimate conditions due to thin cuticles, which increase the risk of desiccation. Therefore, these species tend to occur in areas with minimal temperature and moisture fluctuations, which are typically found in deeper areas of caves (Tobin et al. 2013; Lunghi et al. 2014, 2017; Kozel et al. 2019; Souza-Silva et al. 2021). In Gruta do Padre Cave, this preference for stable locations is particularly evident at the River level. While the richness of non-troglobitic fauna significantly decreases towards deeper areas of the zone, the richness of troglobitic species remains relatively constant. This is likely due to the presence of large water bodies, such as the Santo Antônio River, which can maintain stable microclimatic conditions such as temperature and moisture, enabling the existence of troglobitic species throughout the entire river's length (Souza-Silva et al. 2011; Lobo et al. 2015; Simões et al. 2015; Souza-Silva et al. 2020).

However, despite their climatic stability, deeper zones are often characterized by a lack of food resources, as noted by Souza-Silva et al. (2011) and Prous et al. (2015). This scarcity of trophic resources can limit the presence of many species. However, unlike the non-troglobitic fauna, cave-adapted species usually exhibit K-strategy life histories and reduced metabolic rates, enabling them to flourish in oligotrophic environments (Hüppop, 2005). Therefore, troglobitic species can evade stronger and more energy-demanding competitors, typically non-troglobitic species, by inhabiting areas with limited food sources (Sket, 1999; Deharveng and Bedos 2000; Souza-Silva et al. 2021). This preference for resource-poor regions is evident in the Deep zone of Gruta do Padre Cave, where only troglobitic species are present.

Nevertheless, it is noteworthy that although the distance from the nearest entrance is a significant factor in determining the distribution of fauna inside Gruta do Padre Cave, the levels or cave zones where the communities reside also play a crucial role. Notably, the availability of food resources is relatively higher at the Santo Antônio River level, spanning both shallow and deep zones. This finding supports the notion that rivers can transport trophic resources through the cave, providing energy to communities in diverse locations (Simões et al. 2015).

The variation in habitat complexity also varies between the levels of Gruta do Padre Cave. In the upper dry level, the habitat heterogeneity decreases towards deeper zones, while in the stream level, the complexity increases. This is because the near-to-entrance stream zone consists mainly of sediment banks composed of silt, sand, and gravel, while the deep stream zone features more complex habitats, such as travertines, waterfalls, and a variety of speleothems. These distinctive features between the upper dry and stream levels also contribute to the unique characteristics of Gruta do Padre Cave, with each zone hosting a distinct community with unique species and habitat characteristics.

Habitat heterogeneity affecting communities

In the Gruta do Padre Cave, the diversity of habitats, characterized by both trophic and physical traits, plays a vital role in determining the distribution of invertebrate communities. It is well-established that in cave environments, greater habitat diversity can facilitate the coexistence of a larger number of species, by creating new niches in unique

microhabitats (Prous et al. 2004; Prous et al. 2015; Souza-Silva et al. 2021; Furtado et al. 2022). The Gruta do Padre Cave supports this notion by highlighting the importance of both shelter and substrate diversity for sustaining its communities. The environmental complexity, particularly of substrates, provides additional microhabitats, thereby reducing niche overlap and competition among species (Poulson and Culver 1969; Ferreira and Souza-Silva 2001; Tews et al. 2004; Stein et al. 2014; Pellegrini et al. 2016; Resende and Bichuette 2016; Pacheco et al. 2020).

However, the response of troglobitic species to habitat heterogeneity differs from that of non-troglobitic species. While an increase in shelter availability and habitat complexity may lead to a higher number of individuals, it does not necessarily result in higher species richness due to the high specialization of these animals (Pacheco et al. 2020). This suggests that cave-restricted species have specific preferences for the conditions inside Gruta do Padre Cave (Pacheco et al. 2020; Souza-Silva et al. 2021).

The composition and richness of invertebrate communities in Gruta do Padre Cave strongly depend on the availability and diversity of trophic resources. The different types of organic matter available provide a greater variety of niches, allowing for higher species richness and causing changes in community composition in different areas of the cave. This pattern is consistent with previous studies of non-troglobitic animals (Schneider et al. 2011; Souza-Silva et al. 2011; Ladle et al. 2012; Ferreira 2019; Pacheco et al. 2020; Furtado et al. 2022).

Among all the types of organic matter found in the Gruta do Padre Cave, vegetal debris (DTV) was the most prevalent. The vegetation around the cave consists mainly of deciduous species, which leads to an accumulation of leaves and small branches in the litter during the dry season (Crowther 1987; Brina 1998; Souza-Silva et al. 2011). During the rainy season, flood pulses transport large volumes of this stored vegetal debris and other substrates downstream into the cave (Minshall et al. 1983; Carrling 1987; Downes and Street 2005). Thus, external seasonal events affect the trophic dynamics of subterranean habitats, as cave populations rely on vegetal debris from the external environment (Souza-Silva et al. 2011).

Although the relationship between cave invertebrate populations and organic matter is relevant for non-restricted fauna, it varies for troglobitic species. Restricted subterranean fauna often has low metabolic rates and a K strategy life history, enabling them to tolerate periods of hunger (Hüppop 2005; Souza-Silva et al. 2021). Due to increased energetic needs and better competitive fit of non-troglobitic species, troglobites choose areas with minimal organic materials, avoiding competition with other species (Sket 1999; Deharveng and Bedos 2000; Souza-Silva et al. 2021). Therefore, the response to organic matter availability differs depending on the trophic specialization and ecological requirements of each species.

Ecological niches

The WitOMI analysis confirmed a significant shift in the ecological niche occupancy among cave zones (UCNE, RCNE, UCFE, RCFE) for certain taxa identified as significant in the OMI analysis. These regions displayed distinct physical, trophic, and microclimatic characteristics in the flooring of their respective conduits. This outcome emphasizes the existence of environmental gradients extending from entrance zones to the deeper cavern

areas, encompassing crucial factors influencing the changes in niche occupancy for these species.

We have observed that troglobitic species, such as the cricket *Endecous* sp1, may exhibit reduced dispersal in areas farther from the entrance. This suggests that even for groups confined to caves, there is a need for a balance between environments with more stable microclimates (to prevent desiccation) and those with greater trophic resource availability. From this perspective, the increased trophic resources in *River chamber Near Entrances* (RCNE) may contribute to decreased interspecific and intraspecific competition, supporting the findings of the comparison of niche breadth among the species *Endecous* sp1, *Paronellidae* sp1, and *Pseudonannolene microzoporus*.

Predatory species like *Oecobius* sp1 (invasive species), *Leucauge* sp1, *Loxosceles* sp2, and *Zelurus* sp1 displayed highly similar realized niches, utilizing marginal habitat conditions in the *Upper Chambers Near Entrances* (UCNE). This is characteristic of microhabitats in transition zones between epigean and hypogean environments, marked by low air humidity and high substrate diversity, as observed in this study, and distinguished by the presence of light. Prous et al. (2004, 2015) demonstrated the crucial role of these predatory species, typical of cave entrances in tropical regions, including spiders of the genera *Loxosceles* and *Isoctenus*, and bugs of the genus *Zelurus*, serving as significant biological filters in shaping communities within caves. The importance of predation by such species as a selective force becomes apparent when considering that *Lutzomya* sp5 and *Psyllipsocus* sp2, winged organisms, were the only significant species in the OMI analysis that successfully occupied these ecotonal regions. Given their ability to fly, these species can effectively evade the majority of predators present in these ecotonal areas.

Other predators, such as *Charinus santanensis* and *Eusarcus* sp1, also predominantly occupied microhabitats in the UCNE zone, but their realized niches did not overlap with those of other predatory species present in ecotonal areas. The degree of specialization to cave life may be the determining factor for niche differentiation in this case, with *Charinus santanensis* and *Eusarcus* sp1 preferring aphotic environments in the UCNE zone that are more stable or simply more humid. It is noteworthy that *Eusarcus* sp1 has a broader realized niche than *Charinus santanensis*, and they exhibit marginal overlap. However, in a more refined analysis, their realized niches do not overlap. The coexistence between these species may be mediated by spatial niche dynamics, as observed by Mammola et al. (2016), who studied the niche dynamics of two spiders in disused mines in Italy. However, other factors can also be determinants, such as differences in foraging strategy, preferred prey size, energy needs (*Charinus santanensis* is considerably larger than *Eusarcus*), and a preference for different microhabitats. Studies aiming to understand the niche dynamics among these predators may reveal more detailed insights into the factors responsible for their coexistence, using specific methodologies (considering that these genera are also commonly found on cave walls).

In contrast to predators in ecotonal areas, *Isoctenus* sp3 exclusively occupied RCNE, shifting its niche from the average cave conditions to areas with greater availability of organic resources where more potential prey may occur. It is noteworthy that the residual tolerance

values for all significant taxa in our analysis suggest the influence of other environmental variables on the species' niche. Similar findings have been recurrent in OMI analyses in underground environments (Saccò et al. 2019; Martins and Ferreira 2020; Souza-Silva et al. 2021; Pellegrini et al. 2022), indicating the challenges involved in determining ecological niches (Saccò et al. 2019).

Conservation of a new Hotspot of Subterranean Biodiversity

The Gruta do Padre Cave stands out as a unique cave in the Brazilian semiarid region, owing to its extensive linear development, voluminous conduits and chambers, and the presence of the Santo Antonio River, as well as the remarkable and exclusive fauna that inhabit the cave.

Out of the fauna surveyed in this cave, 25 species are cave-restricted, thereby designating the Gruta do Padre Cave as a Subterranean Biodiversity Hotspot, as per Culver and Sket (2000). This finding places the cave on the South American roster of subterranean hotspots, along with three other caves: the Toca do Gonçalo Cave in the Campo Formoso municipality (Bahia state) (Souza-Silva and Ferreira 2016); the Areia Cave System in the Iporanga municipality (São Paulo state) (Souza-Silva and Ferreira 2016), and the Água Clara Cave System in the Carinhanha municipality (Bahia state) (Souza-Silva et al. 2021; Ferreira et al. 2023; Ferreira and Souza-Silva 2023). The inclusion of the Gruta do Padre Cave in this elite list highlights the crucial importance of the semiarid region for subterranean biodiversity in Brazil since three of the four hotspots are situated in the Caatinga, the only semi-arid biome in Brazil.

The high biodiversity and endemism of troglobitic fauna in the Caatinga domain may be related to the climatic history of this dry region (Souza-Silva et al. 2021). During the Last Glacial Maximum, the area where these cave systems are located was covered by humid tropical forests (Collevatti et al. 2013). As these forests began to recede to their current locations, the ancestors of the current troglobitic species were likely "trapped" inside caves (Wang et al. 2004; Souza-Silva and Ferreira 2016; Polhemus and Ferreira 2018). However, the lack of hotspots in South America may also be related to the scarcity of well-studied areas or caves (Deharveng and Bedos 2012; Souza-Silva et al. 2021), as Brazil still has vast expanses of karst areas that have not undergone speleological surveys.

Many of the 25 troglobitic species are endemic to the Padre Cave, which highlights the need to protect this cave since it may be the only habitat for such species. Nonetheless, the differences between distinct zones of the cave underscore the importance of preserving the unique attributes of each zone.

It is crucial to emphasize that the Padre Cave constitutes just one component of a vast cave system that encompasses the largest subterranean hydrological system in Brazil (Auler et al. 2019). The conservation of both the Cipó and Bananeira Caves (which are also trespassed by the Santo Antônio River) is also vital for the preservation of the Santo Antônio River. This river, aside from being critical to the invertebrate communities of the Padre Cave, is a significant tributary of the Corrente River, which serves as the primary water source for the population of Santana municipality, Bahia State. Therefore, any negative impacts on this

critical cave system could have far-reaching consequences, not only for the troglobitic and non-troglobitic invertebrates but also for more than 26,000 residents living in the semiarid northeast of Brazil, an area that already experiences drought conditions (IBGE 2020).

It is essential to note that despite the native vegetation covering both entrances of the Gruta do Padre Cave, most of the surrounding areas have been deforested. The natural Caatinga and Dry Forests in the region have historically been replaced by pastures, resulting in a direct impact on the energetic dynamics of the subterranean invertebrate communities in the Gruta do Padre Cave. The reduction of native vegetation in the surrounding areas of the Gruta do Padre Cave could lead to a decline in the total organic resources available to be transported to subterranean environments. Since the organic matter of vegetal origin is the most crucial trophic source inside this cave, any decrease in its availability could jeopardize the entire subterranean trophic web of the Gruta do Padre Cave.

Despite being a Hotspot of Subterranean Biodiversity, the Gruta do Padre Cave unfortunately lacks protection under Brazilian speleological legislation. Since 2008, a decree has stipulated that Brazilian caves must be classified according to their level of importance. Only those caves classified as having maximum cultural, geological, and/or biological value are supposed to be preserved (Decree nº 6.640). However, a new decree (Decree nº 10.935) implemented in 2022 permits even the destruction of caves with maximum relevance (Ferreira et al. 2022). Consequently, since the Gruta do Padre Cave is not situated within any protected area, the entire speleological heritage within the cave is currently at risk.

Acknowledgments

The authors would like to thank the Centro Nacional de Pesquisa e Conservação de Cavernas - CECAV and Instituto Brasileiro de Desenvolvimento e Sustentabilidade - IABS (n°. 006/2021. TCCE ICMBio/Vale (01/2018) for the financial support; CNPq (National Council for Scientific and Technological Development) for the productivity scholarship provided to RLF (CNPq n. 302925/2022-8); to the Vale Company and the team from the Center of Studies in Subterranean Biology (CEBS/UFLA) for the support in the field trips. VGPJ is grateful to Coordenação de Aperfeiçoamento de Pessoal de Nível Superior (CAPES) for the master's degree scholarship granted. Also, thanks to Giovanna Cardoso, Guilherme Prado, and Leopoldo Benardi for the help in the identification of some animal groups.

References

Auler AS, Rubbioli E, Menin D, Brandi R (2019) Cavernas. Atlas do Brasil Subterrâneo. Editora IABS, Brasília.

Barton LL, Mandl M, Loy A (Eds) (2010) Geomicrobiology: Molecular and Environmental Perspective. Springer. https://doi.org/10.1007/978-90-481-9204-5

Buttigieg PL, Ramette A (2014) A Guide to Statistical Analysis in Microbial Ecology: a community-focused, living review of multivariate data analyses. FEMS Microbiol Ecol 90:543–550. https://doi. org/10.1111/1574-6941.12437

Cardoso GM, Bastos-Pereira R, Souza LA, Ferreira RL (2020) New cave species of Pectenoniscus Andersson, 1960 (Isopoda: Oniscidea: Styloniscidae) and an identification key for the genus. Nauplius, 28. https://doi.org/10.1590/2358-2936e2020039

Cardoso GM, Bastos-Pereira R, Souza LA, Ferreira RL (2021) Chaimowiczia: a new Iuiuniscinae genus from Brazil (Oniscidea, Synocheta, Styloniscidae) with the description of two new troglobitic species. Subterranean Biology, 39, 45-62. https://doi.org/10.3897/subtbiol.39.65305

Clarke KR, Gorley RN, Somerfeld PJ, Warwick RM (2014) Change in marine communities: an approach to statistical analysis and interpretation, 3rd edn. PRIMER-E, Plymouth

Collevatti RG, Terribile LC, de Oliveira G, Lima-Ribeiro MS, Nabout JC, Rangel TF, Diniz-Filho JAF (2013) Drawbacks to palaeodistribution modeling: the case of South American seasonally dry forests. J Biogeogr 40(2):345–358. https://doi.org/10.1111/jbi.12005

Culver DC, Sket B (2000) Hotspots of subterranean biodiversity in caves and wells. Journal of Cave and Karst Studies. 62:11–17

Culver DC, Pipan T (2009) Biology of Caves and Other Subterranean Habitats, 1st ed. Oxford, New York

Culver DC, Deharveng L, Pipan T, Bedos A (2021). An overview of subterranean biodiversity hotspots. Diversity. 13(10): 487. https://doi.org/10.3390/d13100487

Decreto nº 6.640, de 07 de novembro de 2008 (2008); www.planalto.gov.br/ccivil_03/_Ato2007-2010/2008/ Decreto/D6640.htm [in Portuguese].

Decreto nº 10.935, de 12 de janeiro de 2022 (2022); www.in.gov.br/en/web/dou/-/decreto-n-10.935-de-12- de-janeiro-de-2022-373591582 [in Portuguese].

Deharveng L, Bedos A (2012) Diversity patterns in the tropics. In: Culver DC, White WB (eds) Encyclopedia of Caves, 2nd edn. American University, Washington, pp 238–251

Dinerstein E (2017) An Ecoregion-Based Approach to Protecting Half the Terrestrial Realm. BioScience, 67(6):534–545. https://doi.org/10.1093/biosci/bix014

Dolédec S, Chessel D, Gimaret-Carpentier C (2000) Niche separation in community analysis: a new method. Ecology 81(10):2914-2927. https://doi.org/10.1890/0012-9658(2000)081[2914:NSICAA]2.0.CO;2

Du Preez G, Forti P, Jacobs G, Jordaan A, Tiedt LR (2015) Hairy Stalagmites, a new biogenic root speleothem from Botswana. Int J Speleol 44(1):37–47. https://doi.org/10.5038/1827-806X.44.1.4

Ferreira RL, Martins RP (1998) Diversity and Distribution of Spiders Associated with Bat Guano Piles in Morrinho Cave (Bahia State, Brazil). Diversity and Distributions 4(5): 235–241.

Ferreira RL (2004). A medida da complexidade ecológica e suas aplicações na conservação e manejo de ecossistemas subterrâneos. Tese de doutorado, Universidade Federal de Minas Gerais, 158p.

Ficetola GF, Lunghi E, Canedoli C, Padoa-Schioppa E, Pennati R, Manenti R (2018) Diferences between microhabitat and broad-scale patterns of niche evolution in terrestrial salamanders. Sci Rep 8(1):1–12. https://doi.org/10.1038/s41598-018-28796-x

Galassi DM, Fiasca B, Di Lorenzo T, Montanari A, Porfirio S, Fattorini S (2017) Groundwater biodiversity in a chemoautotrophic cave ecosystem: how geochemistry regulates microcrustacean community structure. Aquatic ecology 51:75-90. DOI 10.1007/s10452-016-9599-7

Hara MR, Pinto-Da-Rocha R (2010) Systematic review and cladistic analysis of the genus Eusarcus Perty 1833 (Arachnida, Opiliones, Gonyleptidae). Zootaxa 2698(1): 1-136. https://doi.org/10.11646/zootaxa.2698.1.1

Howarth FG (1983) Ecology of cave arthropods. Annual Review of Entomology 28:365–389.

IBGE – Instituto Brasileiro De Geografia E Estatística (2020) Censo Brasileiro de 2020. Rio de Janeiro: IBGE, 2020.

Karasiewicz S, Dolédec S, Lefebvre S (2017) Within outlying mean indexes: refining the OMI analysis for the realized niche decomposition. PeerJ 5:e3364. doi: 10.7717/peerj.3364

Koppen W (1936) Das geographische system der klimat. Handbuch der klimatologie. 46.

Sket B (2008) Can we agree on an ecological classifcation of subterranean animals? J Nat Hist 42:1549– 1563. https://doi.org/10.1080/00222930801995762

Lobo HAS, Boggiani PC, Perinotto JAJ (2015) Speleoclimate dynamics in Santana Cave (Petar, São Paulo State, Brazil): general characterization and implications for tourist management. Int J Speleol 44(1):61–73. https://doi.org/10.5038/1827-806X.44.1.6

Lunghi E, Manenti R, Ficetola GF (2014) Do cave features affect underground habitat exploitation by non-troglobite species? Acta Oecol 55:29–35. https://doi.org/10.1016/j.actao.2013.11.003

Lunghi E, Manenti R, Ficetola GF (2017) Cave features, seasonality, and subterranean distribution of non-obligate cave dwellers. PeerJ 5:e3169. https://doi.org/10.7717/peerj.3169

Lunghi E, Manenti R (2020) Cave communities: from the surface border to the deep darkness. Diversity 12(5):167. https://doi.org/10.3390/d12050167

Mammola S, Piano E, Isaia M (2016) Step back! Niche dynamics in cave-dwelling predators. Acta Oecologica 75:35-42. https://doi.org/10.1016/j.actao.2016.06.011

Mammola S, Isaia M (2017) Spiders in caves. Proc R Soc B. https://doi.org/10.1098/rspb.2017.0193

Mammola S, Isaia M (2018) Day-night and seasonal variations of a subterranean invertebrate community in the twilight zone. Subterr Biol 27:31–51. https://doi.org/10.3897/subtbiol.27.28909

Mammola S (2019) Finding answers in the dark: caves as models in ecology ffty years after Poulson and White. Ecography 42(7):1331–1351. https://doi.org/10.1111/ecog.03905

Mammola S, Arnedo MA, Fišer C, Cardoso P etal (2020) Environmental filtering and convergent evolution determine the ecological specialization of subterranean spiders. Funct Ecol 35(5):1064–1077. https://doi.org/10.1111/1365-2435.13527

Martins VM, Ferreira RL (2020) Limiting similarity in subterranean ecosystems: a case of niche differentiation in Elmidae (Coleoptera) from epigean and hypogean environments. Hydrobiologia 847:593-604. https://doi.org/10.1007/s10750-019-04123-x

Moseley M (2008) Size matters: scalar phenomena and a proposal for an ecological definition of 'cave'. Cave Karst Science 35(3):89–94.

Moseley M (2009) Are all caves ecotones? Cave Karst Science 36(2):53–58.

Novak T, Matjaž P, Saška L et al (2012) Duality of terrestrial subterranean fauna. Int J Speleol 41:181– 188. https://doi.org/10.5038/1827-806X.41.2.5

Oliver I, Beattie AJ (1996) Invertebrate morphospecies as surrogates for species: a case study. Conservation Biology 10(1):99–109.

Ostertagova E, Ostertag O, Kováč J (2014) Methodology and application of the Kruskal-Wallis test. Applied mechanics and materials 611, 115-120. https://doi.org/10.4028/www.scientific.net/AMM.611.115

Pacheco GSM, Souza-Silva M, Cano E, Ferreira RL (2020) The role of microhabitats in structuring cave invertebrate communities in Guatemala. International Journal of Speleology 49(2):161–169. https://doi.org/10.5038/1827-806X.49.2.2333

Pellegrini TG, Ferreira RL, Zampaulo RA, Vieira L (2022) Three new troglobitic Coarazuphium (Coleoptera, Carabidae, Zuphiini) species from a Brazilian hotspot of cave beetles: exploring how the environmental attributes of caves drive ground-beetle niches. Subterranean Biology 43:97-126. https://doi.org/10.3897//subtbiol.43.73185

Polhemus DA, Ferreira RL (2018) Two unusual new genera of cavernicolous Hydrometridae (Insecta: Heteroptera) from eastern Brazil. Tijdschr Entomol 161(1):25–38. https://doi.org/10.1163/22119 434-00002072

Polis GA, Anderson WB, Holt RD (1997) Towards an integration of landscape and food web ecology: the dynamics of spatially subsidized food webs. Annual Review of Ecology and Systematics 28:289–316.

Porter ML, Summers Engel A, Kane TC, Kinkle BK (2009) Productivity-Diversity Relationships from Chemolithoautotrophically Based Sulfidic Karst Systems. International Journal of Speleology 38(1):27-40. http://dx.doi.org/10.5038/1827-806X.38.1.4

Prous X, Ferreira RL, Martins RP (2004) Ecotone delimitation: Epigean–hypogean transition in cave ecosystems. Austral Ecol 29(4):374–382. https://doi.org/10.1111/j.1442-9993.2004.01373.x

Prous X, Ferreira RL, Jacobi CM (2015) The entrance as a complex ecotone in a Neotropical cave. Int J Speleol 44:177–189. https://doi.org/10.5038/1827-806X.44.2.7

QGIS Development Team (2023) QGIS Geographic Information System. Open-Source Geospatial Foundation Project. http://qgis.osgeo.org

Rabelo LM, Souza-Silva M, Ferreira RL (2021) Epigean and hypogean drivers of Neotropical subterranean communities. Journal of Biogeography, 48(3), 662-675. https://doi.org/10.1111/jbi.14031

Racovitza EG (1907) Essai sur les problèmes biospéologiques. Archives de Zoologie Expérimentale et Générale 4(6):371–488.

Rasband WS (1997) Image, J., US National Institutes of Health. "ImageJ64," US National Institutes of Health, Bethesda, MD

R Core Team (2019) R: a language and environment for statistical computing. R Foundation for Statistical Computing, Vienna. https://www.R-project.org/

Romero A, Green SM (2005) The end of regressive evolution: examining and interpreting the evidence from cave fishes. Journal of fish biology 67(1): 3–32. https://doi.org/10.1111/j.0022-1112.2005.00776.x

Saccò M, Blyth AJ, Humphreys WF, Karasiewicz S, Meredith KT, Laini A, Cooper SJB, Bateman PW, Grice K (2019) Stygofaunal community trends along varied rainfall conditions: deciphering ecological niche dynamics of a shallow calcrete in Western Australia. Ecohydrology 13(1):e2150. https://doi.org/10.1002/eco.2150

Sarbu SM, Kane TC, Kinkle BK (1996) A chemoautotrophically based cave ecosystem. Science, 272(5270), 1953-1955.

Simões MH, Souza-Silva M, Ferreira RL (2015) Cave physical attributes influencing the structure of terrestrial invertebrate communities in Neotropics. Subterranean Biology 16:103–121. https://doi.org/10.3897/subtb iol.16.5470

Simon KS, Pipan T, Culver DC (2007) A conceptual model of the flow and distribution of organic carbon in caves. Journal of Cave and Karst Studies 69 (2):279–284.

Sobral-Souza T, Lima-Ribeiro MS, Solferini VN (2015) Biogeography of Neotropical Rainforests: past connections between Amazon and Atlantic Forest detected by ecological niche modeling. Evolutionary Ecology 29(5):643–655. https://doi.org/10.1007/s10682-015-9780-9

Souza-Silva M, Parentoni RM, Ferreira RL (2011) Trophic dynamics in a neotropical limestone cave. Subterranean Biology 9:127–138. https://doi.org/10.3897/subtbiol.9.2515

Souza-Silva M, Ferreira RL (2016) The frst two hotspots of subterranean biodiversity in South America. Subterr Biol 19:1–21. https://doi.org/10.3897/subtbiol.19.8207

Souza-Silva M, Iniesta LFM, Ferreira RL (2020) Invertebrates diversity in mountain Neotropical quartzite caves: which factors can infuence the composition, richness, and distribution of the cave communities? Subterranean Biology 33:23–43. https://doi.org/10.1080/00222930801995762

Souza-Silva M, Cerqueira RFV, Pellegrini TG, Ferreira RL (2021) Habitat selection of cave-restricted fauna in a new hotspot of subterranean biodiversity in Neotropics. Biodiversity and Conservation 1–28. https://doi.org/10.1007/s10531-021-02302-8

Stein A, Gerstner K, Kreft H (2014) Environmental heterogeneity as a universal driver of species richness across taxa, biomes, and spatial scales. Ecology Letters 17:866–880. https://doi.org/10.1111/ele.12277

Tobin BW, Hutchins BT, Schwartz BF (2013) Spatial and temporal changes in invertebrate assemblage structure from the entrance to deep-cave zone of a temperate marble cave. Int J Speleol 42:203–214. https://doi.org/10.5038/1827-806X.42.3.4

Venarsky MP, Benstead JP, Huryn AD (2012) Effects of organic matter and season on leaf litter colonization and breakdown in cave streams. Freshwater Biology 57(4):773-786. https://doi.org/10.1111/j.1365-2427.2012.02742.x

Wang X, Auler AS, Edwards L, Cheng H, Cristalli PS et al (2004) Wet periods in northeastern Brazil over the past 210 kyr linked to distant climate anomalies. Letters to Nature 432(9):740–743. https://doi. org/10.1038/nature03067

Wynne JJ, Howarth FG, Sommer S, Dickson BG (2019) Fifty years of cave arthropod sampling: techniques and best practices. Int J Speleol 48(1):33–48. https://doi.org/10.5038/1827-806X.48.1.2231

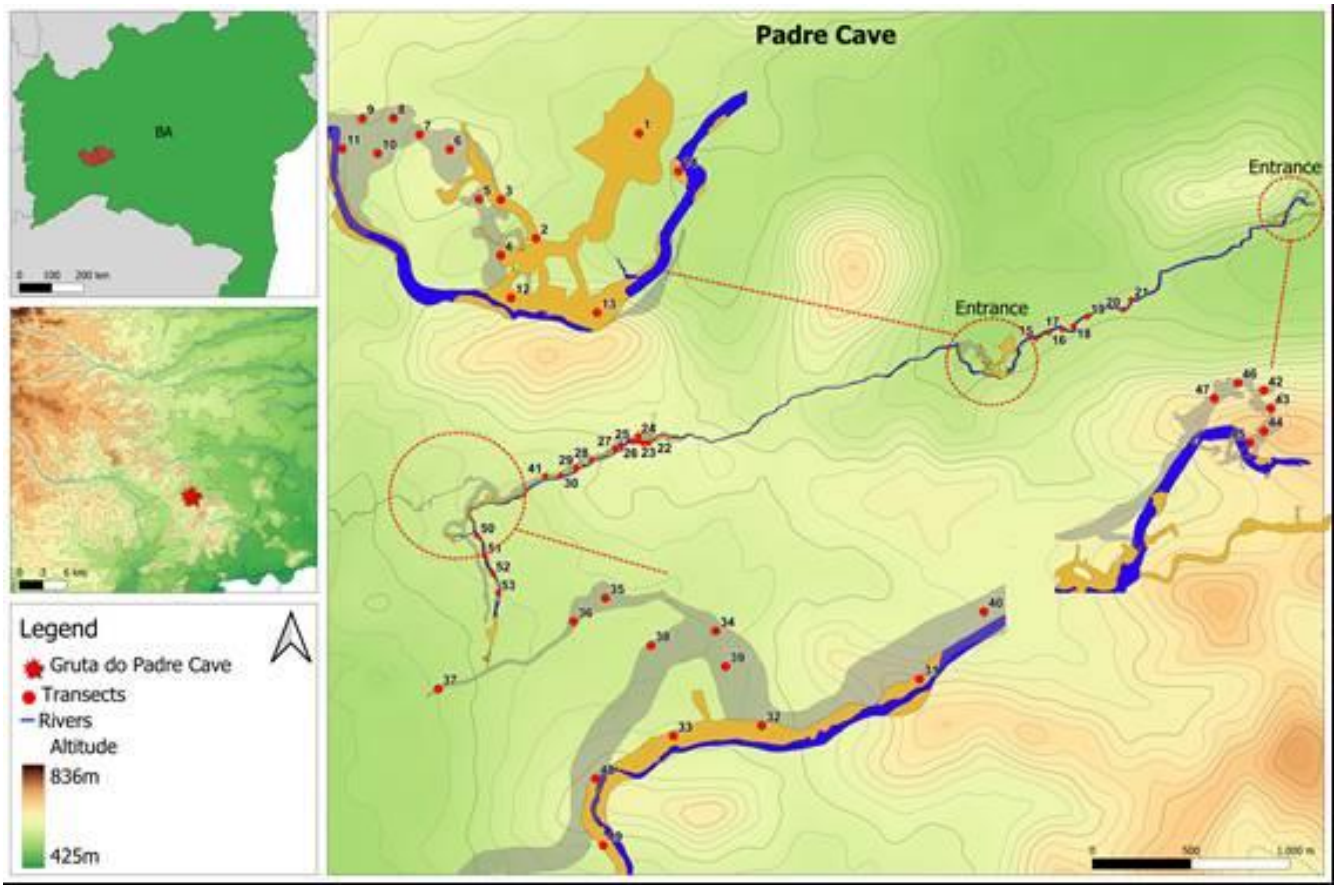


Fig 2. Location map of Gruta do Padre Cave (upper left) and the sampling transects plotted inside the cave system.

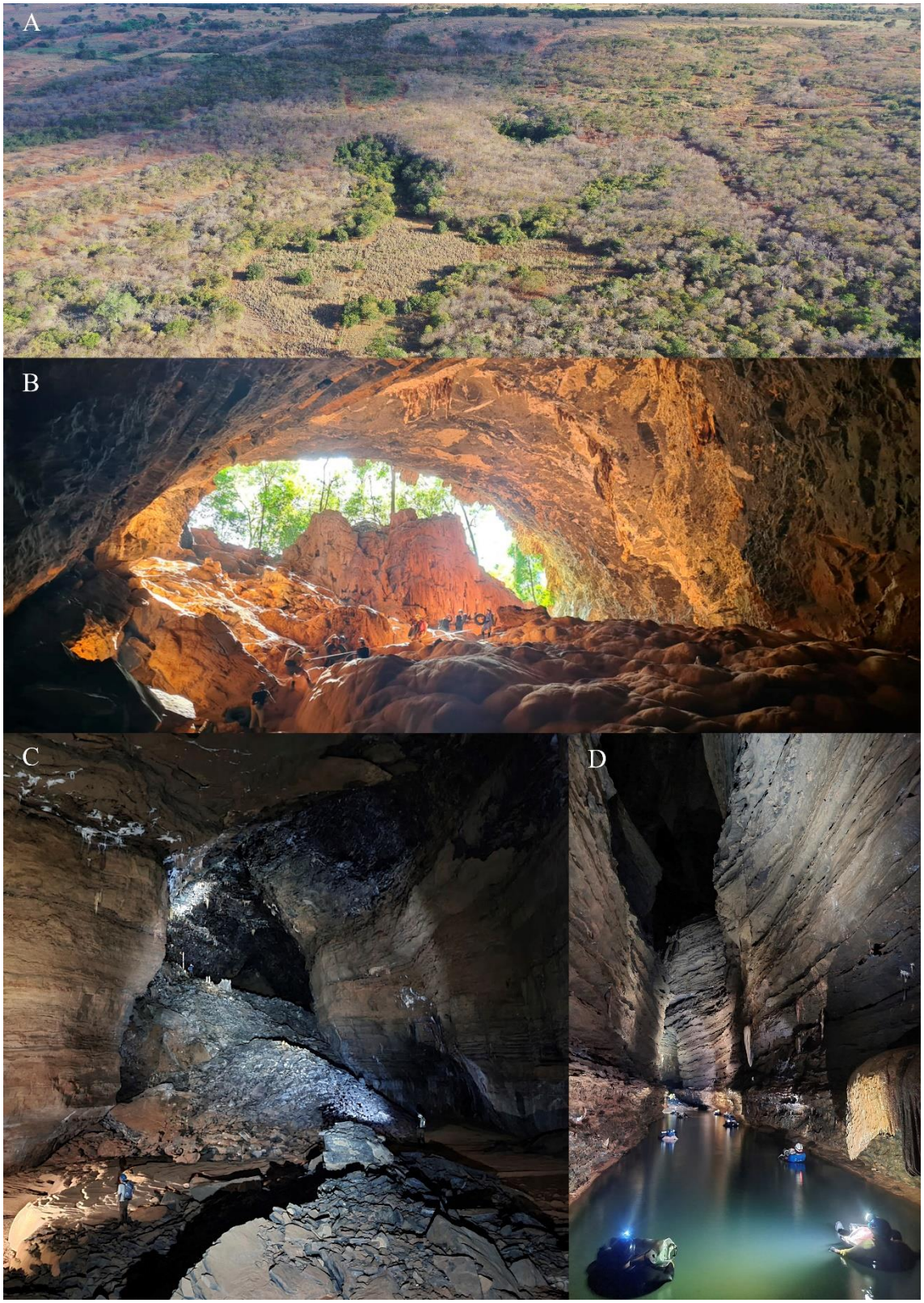


Fig 3. Gruta do Padre Cave. A- aerial view from the landscape and Gruta do Padre Cave's entrance area; B- entrance; C - upper dry gallery; Santo Antônio River level.

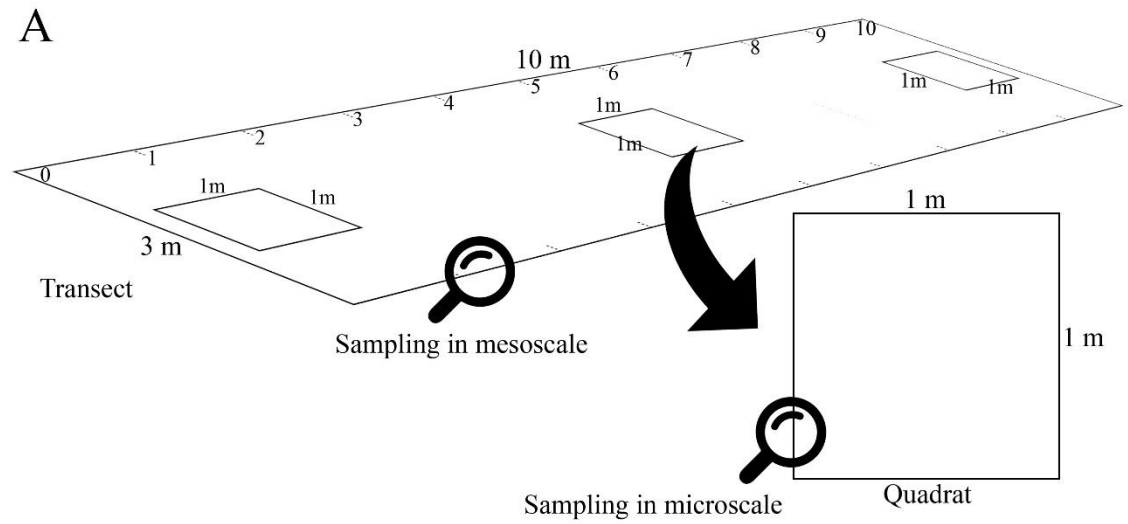




Fig 4. Sampling method. A–sampling method scheme showing both meso and microscale; B–sampling method being applied in Gruta do Padre Cave gallery.



Fig 5. Some troglobitic species found in the Gruta do Padre Cave. A) *Phaneromerium cavernicolum*; B) *Spiripockia* sp1; C) Copepoda sp1. D) *Chaimowiczia tatus*; E) *Xangoniscus* sp1.; F) *Pectenoniscus santanensis*; G) *Spelaeogammarus santanensis*; H) *Eukoenenia* sp1.; I) *Eukoenenia* sp2.; J) Escadabiidae sp1; K) *Eusarcus cff. cavernicola*; L) Ochyroceratidae sp1; M) *Pseudochthonius aware*; N) Arrhopalitidae sp1.; O) Blattidae sp1; P) *Endecous* sp1; Q) *Coarazuphium tessai;* R) Lumbricina sp3; S) *Pimelodella* sp1.

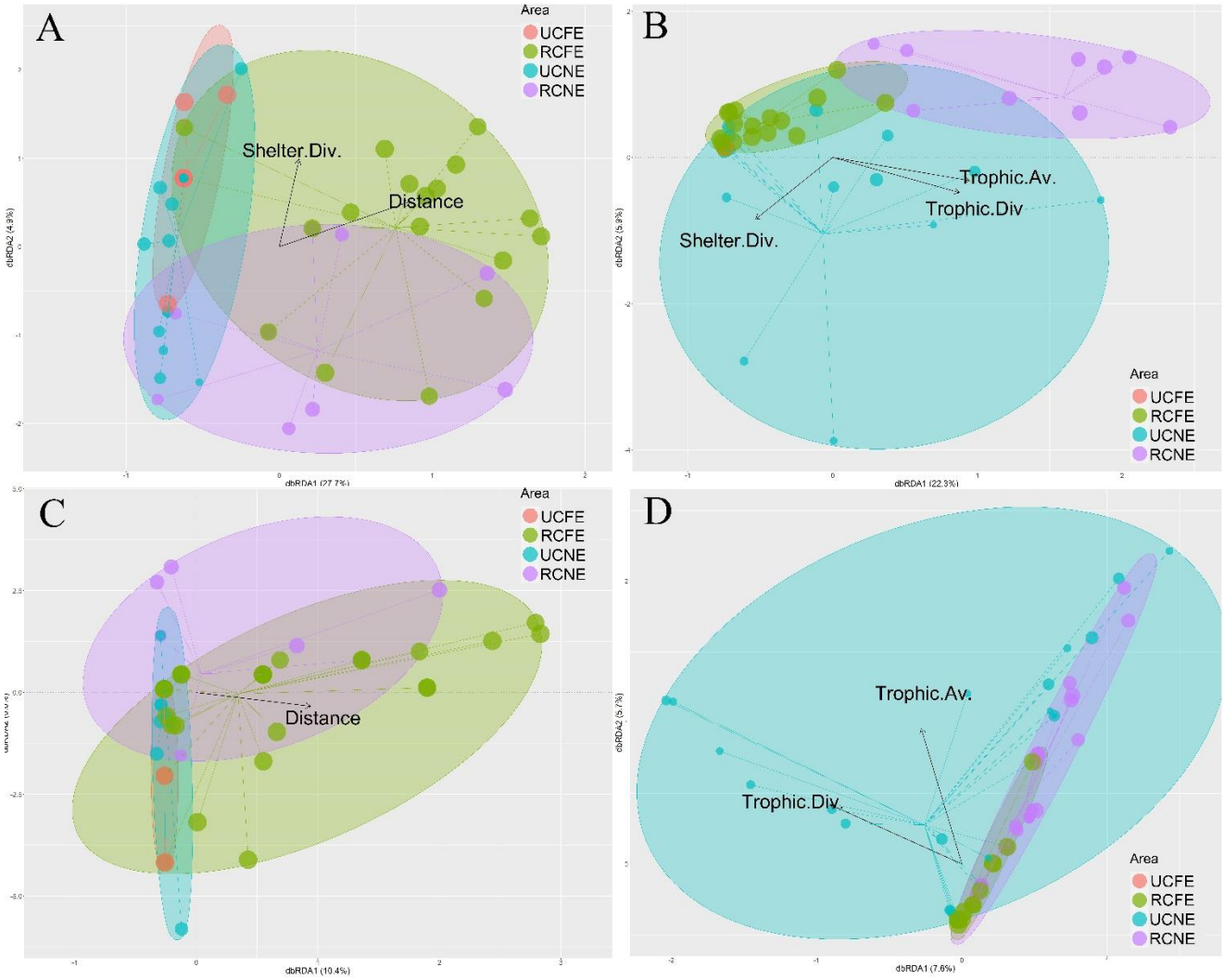


Fig 6. Distance-based Redundancy Analysis (dbRDA) on the mesoscale (A and B) and microscale (C and D). A and C–troglobitc fauna; B and D–non-troglobitic fauna. Diversity (Div), Availability (Av), distance from the entrance (distance), habitat zonation (Area).

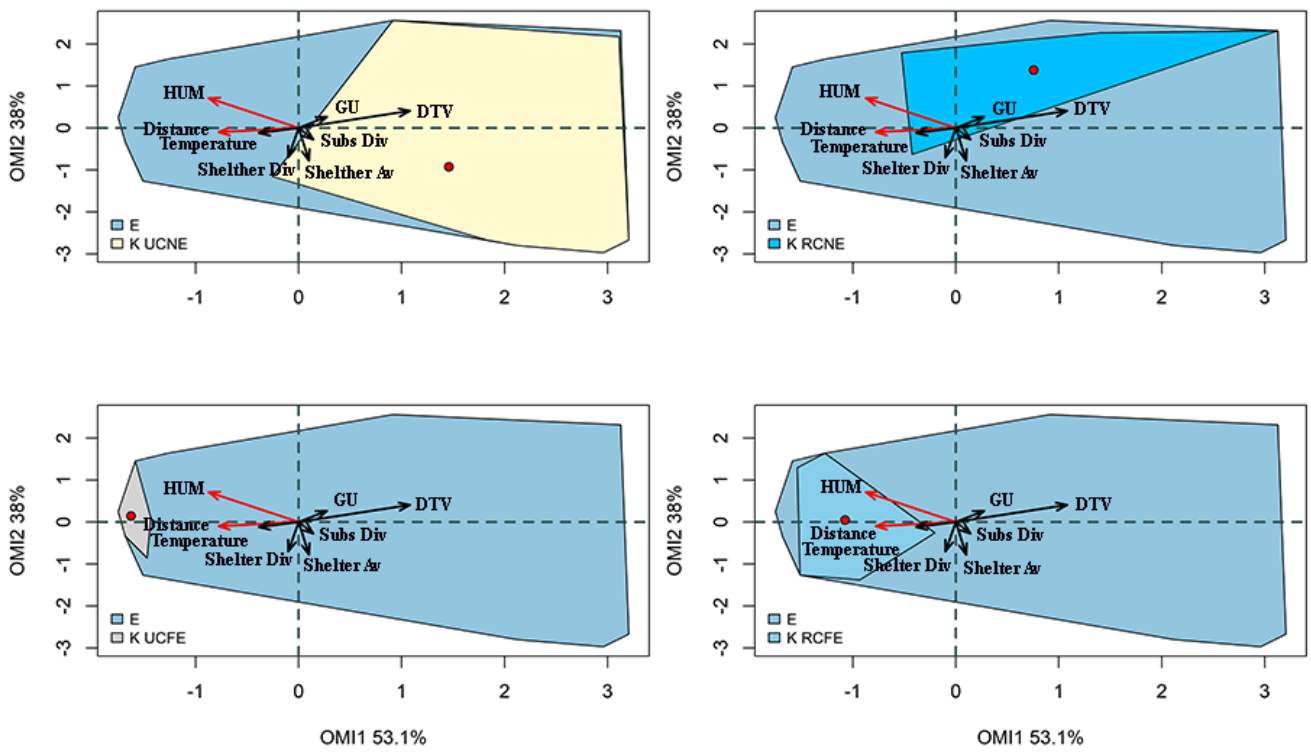


Fig 6 Cave areas subset's of habitat conditions found within the overall available habitat conditions (E). K subset realized environmental space. Red dots represent the suborigins (GK). Canonical weights of environmental variables. The red arrows highlight the variables tha most contribute to differentiation in the average conditions of the cave areas. HUM, Humidity; Distance, Distance from the nearest cave entrance; Shelter Div, Shelter diversity; Shelter Av, Shelter availability; Subs Div, Substrate diversity; DTV, vegetal debris; GU, guano (ex. Bat feces).

Table 1. Troglobitic species and the sample scale where they were found. **Sec**-Sector, mesoscale; **Qu**-Quadrat, microscale; **Ca**-Other cave microhabitats.

Taxons	Species and Morphotypes	Ca	Qu	Sec
Amphipoda	*Spelaeogammarus santanensis*	+		
Aranae	Ochyroceratidae sp1			
Blattodea	Blattidae sp1	+		
Coleoptera	*Clivina* sp1	+	+	
	Coarazuphium tessai	+		
Entomobryomorpha	Paronellidae sp2	+	+	+
Gastropoda	*Spiripockia* sp1	+		+
Oligochaeta	Lumbricina sp3	+		
Isopoda	*Chaimowiczia tatus*	+		
	Pectenoniscus santanensis	+	+	+
	Platyartridae sp1		+	+
	Styloniscidae sp1	+	+	+
	Xangoniscus sp1	+		+
Nemertea	Nemertea sp1	+		
Opiliones	Escadabiidae sp1	+		+
	Eusarcus cff. cavernicola	+	+	+
Orthoptera	*Endecous* sp1	+	+	+
Palpigradi	*Eukoenenia* sp1	+	+	
	Eukoenenia sp2	+		
Poduromorpha	Poduromorpha sp1			+
Pseudoscorpiones	*Pseudochthonius* sp1	+	+	+
Polydesmida	*Phanerомerium cavernicolum*	+	+	+
Symphyla	Symphyla sp1	+		
Symphypleona	Arrhopalitidae sp1	+	+	+
Siluriformes	*Pimelodella* sp1	+		

Table 2. P-values for Distance-based Redundancy Analysis (dbRDA). Diversity (Div), Availability (Av), distance from the entrance (distance), habitat zonation (Area)

	Troglobitic	**df**	**AIC**	**F**	**P**	**Explanation**
Mesoscale	Area	3	126.75	6.1779	0.005	35.25
	Shelter Div.	1	125.11	3.4074	0.005	
	Distance	1	124.71	2.1771	0.035	
Microscale	Area	3	12.075	5.4793	0.005	11.39
	Distance	1	10.877	3.1286	0.049	
	N-Troglobitic	**df**	**AIC**	**F**	**P**	**Explanation**
Mesoscale	Area	3	181.33	5.0266	0.005	36.93
	Trophic Av.	1	179.23	3.8574	0.005	
	Trophic Div.	1	177.33	3.5904	0.010	
	Shelter Div.	1	177.12	1.9591	0.025	
Microscale	Area	3	226.28	4.6746	0.005	15.69
	Trophic.Div.	1	219.53	8.7121	0.005	
	Trophic.Av.	1	216.92	4.5019	0.005	

Table 3. Results for the Generalized linear mixed models (GLMM) for troglobitic and non-troglobitic fauna at meso and microscale. Diversity (Div), Availability (Av), distance from the entrance (distance).

Mesoscale									
Troglobitic	*Estimate*	*Std Error*	*zvalue*	*P(z)*	**Non-Troglobitic**	*Estimate*	*Std Error*	*zvalue*	*P(z)*
Intercept	0.52662	0.31129	1.692	0.0907	*Intercept*	0.632987	0.6246	1.013	0.3109
Distance	0.33826	0.36109	0.937	0.3489	*Distance*	-0.56934	0.350742	-1.623	0.1045
Temperature	-0.11143	0.14432	-0.772	0.4401	***Temperature***	-0.17372	0.085493	-2.032	***0.0422***
Subs Div	0.15946	0.16404	0.972	0.3331	***Subs Div***	0.241048	0.120482	2.001	***0.0454***
Shelter Av	-0.1432	0.14576	-0.982	0.3259	*Shelter Av*	0.1353	0.097873	1.382	0.1668
Shelter Div	-0.11007	0.16634	-0.662	0.5082	*Shelter Div*	0.105078	0.130216	0.807	0.4197
Trophic Div	-0.2428	0.18245	-1.331	0.1833	*Trophic Div*	-0.00215	0.057545	-0.037	0.9701
Trophic Av	-0.05859	0.11939	-0.491	0.6236	*Trophic Av*	0.132895	0.070831	1.876	0.0606
AIC	**BIC**	**logLik**	**Deviance**	**df.resid**	**AIC**	**BIC**	**logLik**	**Deviance**	**df.resid**
197.8	215.6	-89.9	179.8	44	215.1	232.8	-98.5	197.1	44
Dispersion	**R^2m**		**R^2c**		**Dispersion**	**R^2m**		**R^2c**	
1.051395	0.1982586		0.5015627		0.9517778	0.3859331		0.9543016	
Microscale									
Troglobitic	*Estimate*	*Std Error*	*zvalue*	*P(z)*	**Non-Troglobitic**	*Estimate*	*Std Error*	*zvalue*	*P(z)*
Intercept	-1.19560	0.36810	-3.248	0.0012	*Intercept*	-1.1956	0.31098	-3.381	0.0007
Distance	0.42940	0.31890	1.347	0.1781	***Distance***	-1.34228	0.33003	-4.067	***4.76E-05***
Temperature	-0.29740	0.15350	-1.938	0.0526	*Temperature*	-0.07887	0.10671	-0.739	0.4598
Shelter Av	-0.27340	0.19780	-1.382	0.1670	***Shelter Av***	0.32059	0.11494	2.789	***0.0053***
Shelter Div	0.15240	0.19210	0.793	0.4276	*Shelter Div*	-0.26584	0.13853	-1.919	0.0550
Trophic Av	-0.15200	0.20200	-0.753	0.4516	*Trophic Av*	0.07895	0.07645	1.033	0.3018
AIC	**BIC**	**logLik**	**Deviance**	**df.resid**	**AIC**	**BIC**	**logLik**	**Deviance**	**df.resid**
285.5	280	-122.3	244.5	152	301.9	329.5	-141.9	283.9	150
Dispersion	**R^2m**		**R^2c**		**Dispersion**	**R^2m**		**R^2c**	
0.8711529	0.06762728		0.19321192		0.8619307	0.7284852		0.789012	

Table 4. Average values for variables in different zones of Gruta do Padre Cave. Diversity (Div), Availability (Av), distance from the entrance (distance)

	Mesoscale				**Microscale**			
	UCNE	**RCNE**	**RCFE**	UCFE	UCNE	**RCNE**	**RCFE**	UCFE
tal Richness	6.76	10.20	5.00	0.75	1.51	2.07	0.87	0.08
Richness	1.41	2.70	2.83	0.75	0.23	0.50	0.68	0.08
T Richness	5.35	7.50	2.17	0	1.27	1.57	0.18	0
mperature	24.3	24.6	25.5	26.0	-	-	-	-
elter Av.	70.8	14.0	40.8	30.6	38.43	14.76	23.11	27.97
ophic Av.	2.98	4.23	0.73	0	2.57	2.40	0.05	0
elter Div.	1.02	0.322	0.695	0.56	0.28	0.14	0.16	0.33
ophic. Div.	0.029	0.075	0	0	0.049	3.00E-04	0	0

RAMALHO



BEYOND EXPECTATIONS

diversity

MDPI

Interesting Images

Beyond Expectations: Recent Discovery of New Cave-Restricted Species Elevates the Água Clara Cave System to the Richest Hotspot of Subterranean Biodiversity in the Neotropics

Rodrigo Lopes Ferreira [1,2,*] and Marconi Souza-Silva [1,2]

[1] Centro de Estudos em Biologia Subterrânea, Departamento de Ecologia e Conservação, Instituto de Ciências Naturais, Universidade Federal de Lavras, Campus Universitário, P.O. Box 3037, Lavras CEP 37200-000, MG, Brazil; marconisilva@ufla.br
[2] Programa de Pós-Graduação em Ecologia Aplicada, Universidade Federal de Lavras, Lavras CEP 37200-000, MG, Brazil
* Correspondence: drops@ufla.br

Abstract: The Água Clara Cave System was previously recognized as a prominent hotspot of subterranean biodiversity in South America, harboring 31 cave-restricted species. However, a recent expedition conducted in September 2023, coinciding with an exceptionally dry period in the region, provided access to previously unexplored areas. Therefore, the objective of this research was to investigate the cave-restricted invertebrate species, extending the findings from a previous article on the Agua Clara Cave System published in June 2023, and emphasizing the significance of this system as one of the most crucial tropical biodiversity hotspots. This survey unveiled an additional 10 species, raising the count of cave-restricted species within the system to an impressive 41. This remarkable diversity not only solidifies the Água Clara Cave System's position as a paramount hotspot of subterranean biodiversity in the tropics but also serves as a stark warning about the imminent risks faced by these species. The escalating human-induced alterations in the region, notably deforestation, pose a significant risk to the survival of many of these unique and endemic species.

Keywords: obligate cave fauna; conservation; threats; species richness; stygobiont; troglobiont

check for updates

Citation: Ferreira, R.L.; Souza-Silva, M. Beyond Expectations: Recent Discovery of New Cave-Restricted Species Elevates the Água Clara Cave System to the Richest Hotspot of Subterranean Biodiversity in the Neotropics. *Diversity* **2023**, *15*, 1215. https://doi.org/10.3390/d15121215

Academic Editors: David C. Culver, Louis Deharveng, Tanja Pipan and Ana Sofia Reboleira

Received: 21 November 2023
Revised: 4 December 2023
Accepted: 12 December 2023
Published: 14 December 2023

Copyright: © 2023 by the authors. Licensee MDPI, Basel, Switzerland. This article is an open access article distributed under the terms and conditions of the Creative Commons Attribution (CC BY) license (https://creativecommons.org/licenses/by/4.0/).

The Água Clara Cave System (ACCS), situated in northeastern Brazil, has gained recognition as a "Hotspot of Subterranean Biodiversity" (HSB) due to its remarkable richness of cave-restricted fauna [1,2]. This cave system comprises a network of extensive subterranean conduits interconnected through one of the numerous fluvial outlets found on the eastern periphery of the Serra do Ramalho karst area in the western Bahia state. The system encopasses four caves: Gruna da Água Clara (13,880 m), Gruna dos Índios (510 m), Lapa dos Peixes I (9320 m), and Lapa dos Peixes II (2100 m) [1]. It is noteworthy that the cumulative length of all caves within the Agua Clara Cave System (ACCS) stands at 25,810 m. However, when accounting for the inaccessible and unexplored areas existing between the caves, it is plausible that the system might extend to more than 27 km.

The concept of HSB was originally introduced by Culver and Sket [3] to designate subterranean environments that host a minimum of 20 or more troglobitic/stygobitic species. More recently, there has been a movement to raise this threshold to a minimum of 25 cave-restricted species. However, this change has faced some criticism due to concerns about the arbitrary nature of the cutoff and the necessity to consider various parameters when defining subterranean hotspots [1]. These parameters encompass the need to consider different scales when identifying hotspots, the cave's latitudinal location, the lithology associated with the cave, the level of threat to subterranean habitats, and the number of cave-restricted species exclusive to that cave (or system) relative to the total number of troglobitic/stygobitic species it supports [1].

Most of the HSBs are situated in temperate regions, with only a smaller portion located in sub-tropical or tropical areas [4–11]. Additionally, it is noteworthy that most HSBs within these sub-tropical and tropical regions have only recently come to the forefront, signifying an upsurge in cave fauna research in these regions. For instance, the discovery of the first hotspots of subterranean biodiversity (HSB) in South America occurred only in recent years, following extensive sampling in the Areias cave system located in the southern São Paulo state (southeastern Brazil) and the Toca do Gonçalo cave in the northern Bahia state (northeastern Brazil) [11]. Presently, four recognized HSBs exist in South America: the Toca do Gonçalo cave, housing 22 cave-restricted species [11]; the Areias Cave System, hosting 31 cave-restricted species [9,11]; the ACCS, with a previously documented 31 cave-restricted species [2,11]; and the Igatu caves, harboring 37 cave-restricted species. It is important to note that the Igatu caves do not constitute a conventional, functionally interconnected "system" in the traditional sense. Instead, they comprise a collection of caves situated in a relatively small geographical area. Nevertheless, the significant number of cave-restricted species inhabiting these caves underscores their importance and emphasizes the urgency of conservation efforts [9].

Prior investigations conducted at the ACCS have identified a total of 31 cave-restricted species, spanning multiple taxonomic groups, including Hexapoda (9 species), Arachnida (7 species), Crustacea (6 species), Myriapoda (5 species), Gastropoda (2 species), Turbellaria (1 species), and Siluriformes (1 species) [1]. These species predominantly occupy terrestrial (22 species) habitats, with a smaller representation of semiaquatic (5 species) and aquatic species (3 species) [1]. Notably, only a fraction of this assemblage (11 species) has been formally described [12–22]. A recent expedition conducted in September 2023 coincided with an exceptionally dry period in the region, allowing access to previously unexplored sections of the system. This survey unveiled an additional 10 new species, increasing the tally of cave-restricted species within the system to an impressive 41 (Table 1). This number makes the ACCS the cave system with the highest richness of cave-restricted species in the Neotropical region. These newly documented species were encountered in Lapa dos Peixes I cave, within a conduit featuring a permanent water body (Figure 1A). The extreme drought conditions likely prompted many previously undocumented species to relocate from their original microhabitats, congregating near this subterranean "oasis", where they became observable. It is worth highlighting that this small, moisture-rich area of the cave hosted 24 cave-restricted species, which were found in a single day, using direct intuitive research. This observation suggests that during periods of severe external drought, this cave section plays a pivotal role in safeguarding several of the cave-restricted species found in the system. Furthermore, within this limited space, a substantial root mat system is present, serving as a consistent organic resource for the cave invertebrates (Figure 1B).

Table 1. Taxonomic diversity and distribution of 41 obligate cave species within the Águas Claras cave system, located in the northeastern region of Bahia state, Brazil (the newly recorded taxa in this study are highlighted in bold). The study includes observations from four specific caves within the cave system: Águas Claras cave (AC), Índios cave (IN), and Lapa dos Peixes (LP). Additionally, the study distinguishes fauna between terrestrial (T) and aquatic (A) or both habitats.

Phylum/Classis	Order	Family	Species and Morphotypes	AC	IN	LP II	LP I	Habitat
Platyhelminthes	Tricladida	Dugesiidae	*Girardia spelaea*			+	+	A
Arachnida	Acari	Rhagidiidae	Rhagidiidae sp.1	+			+	T
	Amblypygi	Charinidae	*Charinus troglobius*	+			+	T
	Araneae	Caponiidae	Caponiidae sp.1	+			+	T
		Ochyroceratidade	Ochyroceratidae sp.1	+		+	+	T
		Ochyroceratidade	**Ochyroceratidae sp.2**				+	T
		Palpimanidae	**Palpimanidae sp.1**				+	T
		Tetrablemmidae	**Tetrablemmidae sp.1**				+	T
	Opiliones	Gonyleptidae	*Giupponia chagasi*	+		+		T
	Palpigradi	Eukoeneniidae	*Eukoenenia* sp.1	+		+	+	T
	Pseudoscorpiones	Ctoniidae	*Pseudochthonius koinopoliteia*	+			+	T

Table 1. *Cont.*

Phylum/Classis	Order	Family	Species and Morphotypes	AC	IN	LP II	LP I	Habitat
Collembola	Symphypleona	Sminthuridae	*Troglobentosminthurus luridus*	+		+		T
		Sminthuridae	Sminthuridae sp.1				+	T
		unidentified	Symphypleona sp.1	+				T
	Entomobryomorpha		Entomobryomorpha sp.1	+			+	T
			Entomobryomorpha sp.2	+		+		T
Diplura		Projapygidae	**Projapygidae sp.1**				+	T
Insecta	Blattodea	unidentified	Blattodea sp.1	+		+	+	T
	Coleoptera	Carabidae	**Clivinina sp.1**			+	+	T
	Coleoptera	Carabidae	**Trechinae sp.1**				+	T
	Dermaptera	Diplatyidae	*Mesodiplatys falcifer*				+	T
	Ensifera	Phalangopsidae	*Endecous infernalis*	+	+	+	+	T
	Hemiptera	Delphacidae	**Delphacidae sp.1**				+	T
	Hemiptera	Hydrometridae	***Spelaeometra* sp.1**				+	T
	Hymenoptera	Formicidae	*Nylanderia* sp.1	+		+	+	T
Crustacea	Isopoda	Styloniscidae	*Pectenoniscus carinhanhensis*	+	+		+	T
		Styloniscidae	Styloniscidae sp.1	+			+	T/A
		Styloniscidae	Styloniscidae sp.2	+		+	+	T/A
		Styloniscidae	Styloniscidae sp.3			+	+	T/A
		Styloniscidae	*Xangoniscus aganju*	+		+	+	T/A
		Plathyarthridae	*Trichorhina* sp.1	+	+			T
Myriapoda	Geophilomorpha	unidentified	Geophilomorpha sp.1			+		T
	Polydesmida	Chelodesmidae	*Cayenniola* sp.1	+	+	+	+	T
		Trichopolidesmidae	*Phaneromerium* sp.1		+	+	+	T
		Trichopolidesmidae	**Trichopolidesmidae sp.1**				+	T
		Pyrgodesmidae	Pyrgodesmidae sp.1	+		+	+	T
		Oniscodesmidae	Oniscodesmidae sp.1				+	T
	Siphonophorida	Siphonophoridae	**Siphonophoridae sp.1**				+	T
Mollusca	Gastropoda	Pomatiopsidae	*Spiripockia punctata*			+	+	A
		unidentified	Eupulmonata sp.1	+			+	A
Osteichthyes	Siluriformes	Trichomycteridae	*Trichomycterus rubbioli*	+			+	A

The newly discovered species encompass a diverse array of taxa, all of which represent new taxa, with some already in the process of formal description. These include a palpimanid spider (Araneae: Palpimanidae—Figure 2A), an ochiroceratid spider (Araneae: Ochiroceratidae—Figure 2B), a tetrablemmid spider (Araneae: Tetrablemmidae: *Matta* sp.—Figure 2C), a siphonophorid millipede (Diplopoda: Siphonophorida: Siphonophoridae—Figure 2D), a trichopolydesmid millipede (Diplopoda: Polydesmida: Trichopolydesmidae), a delphacid planthopper (Hemiptera: Delphacidae—Figure 2E), two carabid beetles (Coleoptera: Carabidae: Clivinina—Figure 2F and Trechinae), a hydrometrid bug (Hemiptera: Hydrometridae: *Spelaeometra* sp.—Figure 2G), and a projapygid (Diplura: Projapygidae—Figure 2H).

All these species exhibited typical troglomorphic traits, including reduced or absent eyes and pigmentation. Additionally, specific troglomorphic characteristics were observed. The palpimanid spider displayed extremely reduced eyes and weak pigmentation, contrasting with the general morphology observed in the remaining species of this family. Similar traits were observed in the ochiroceratid and tetrablemmid spiders, which also exhibited an additional thickening of the cuticle and no eyes. Both the siphonophorid and the trichopolydesmid millipedes were completely unpigmented. They also showed an increase in sensory pits on the antennal segments and an unusually long tergal setae, considered troglomorphic traits in other millipede taxa [23–25]. The delphacid planthopper exhibited all the typical troglomorphic traits observed in other cave-restricted planthoppers, including the absence of eyes, pigment reduction, and wings reduction [26–30]. Both carabid beetles displayed typical troglomorphic traits, such as eye and pigment reduction, as well as wing reduction [31,32]. The hydrometrid bug (*Spelaeometra* sp.) exhibited all the troglomorphic traits observed in the other two known species of the genus. This included reduced eyes and pigmentation, along with elongated legs and antennae [33,34]. Finally,

the projapygid (Diplura) exhibited the most traditional troglomorphic traits among diplurans, such as appendage elongation and an increase in sensory setae at the antennal segments [35]. Unfortunately, the specimen lost both cerci when discovered above a rock on the cave floor (Figure 2H), but one cercus was later recovered, indicating considerable elongation.



Figure 1. Água Clara cave system: (**A**) spatial distribution of the caves Gruna da Água Clara (1), Gruna dos Índios (2), Lapa dos Peixes I (3), and Lapa dos Peixes II (4); the yellow arrow indicates the region where the newly discovered cave-restricted species were found; (**B**) conduit where the newly discovered species were found (notice the water pond on the floor of the conduit); (**C**) root mats covering the cave floor; (**D**) a close-up view of a root mat with a troglobitic isopod (*Xangoniscus* sp.).



Figure 2. Newly discovered cave-restricted species from the ACCS: (**A**) Palpimanidae (Araneae); (**B**) Ochiroceratidae (Araneae); (**C**) Tetrablemmidae (Araneae); (**D**) Siphonophoridae (Diplopoda: Siphonophorida); (**E**) Delphacidae (Hemiptera); (**F**) Clivinina (Coleoptera: Carabidae); (**G**) *Spelaeometra* sp. (Hemiptera: Hydrometridae); (**H**) Projapygidae (Diplura).

While troglomorphisms can serve as valuable indicators of the potential status of these species, their analysis should always consider the contexts of the external ecosystems surrounding the caves. For instance, if a species, completely depigmented, blind, and with a reduced cuticle, is discovered in a cave within a humid forest (like the Amazon rainforest), these traits may not necessarily signify its restriction to that cave. This is because the surrounding forest provides numerous shaded and humid microhabitats (such as spaces under logs, leaf litter, etc.) that could easily accommodate individuals of this species. On the contrary, if a species with similar characteristics were found in a cave located in an arid or semi-arid region, these morphological traits would strongly indicate its restriction to subterranean habitats. This is because, in the surrounding epigean environments, such organisms would rarely encounter suitable microhabitats for their survival.

Thus, considering the highly xeric epigean environment surrounding the ACCS (Figure 1A), it is unlikely that these species (as well as the other 31 troglomorphic species previously registered in the system) can maintain viable populations on the surface. Therefore, not only were troglomorphic traits instrumental in identifying these species as troglo-

bitic, but also the external surrounding conditions, which are highly restrictive, imposing physiological constraints and preventing the occurrence of these species in external habitats. Finally, it is noteworthy that some of the newly discovered species were examined by taxonomists who confirmed their status (as mentioned in the Acknowledgements section).

It is important to note that some of these newly discovered species hold particular significance, such as the palpimanid spider, which marks the first known troglobitic species within this family worldwide. Additionally, the presence of the delphacid planthopper in this region is noteworthy, as the three previously documented subterranean-restricted species from this family were exclusively recorded in New Caledonia [26,27].

Therefore, the Gruna da Água Clara cave, once recognized for harboring the highest troglobitic species richness among ACCS caves, with a total of 23 species, has now been surpassed by the Lapa dos Peixes I cave, which hosts 35 species. The Lapa dos Peixes II cave accommodates 17 species, whereas only 5 species have been found thus far in the Gruna dos Índios cave.

The recent discovery of ten additional species within the ACCS raises a red flag on two critical fronts. Firstly, it underscores the extraordinary diversity of this system, currently facing severe threats driven by an unprecedented increase in various anthropogenic impacts, particularly in recent decades [1]. Urgent actions, such as the establishment of a fully protected conservation unit, are imperative. Secondly, and perhaps more significantly, this discovery serves as a powerful reminder that limited samplings are insufficient when attempting to unveil the true extent of species richness within a cave or cave system. In Brazil, caves are increasingly at risk due to various industrial activities, such as mining and hydropower dam construction, among others. To assess which caves should be safeguarded, a mere two samplings are currently required to determine their relevance. Consequently, in Brazil, a cave may be deemed of low significance simply because of an inadequate sampling effort. Therefore, it is crucial to demand additional samplings during the environmental licensing processes to more accurately assess the relevance of a cave, especially given that Brazilian caves have never faced such high levels of threat as they do today [36].

Author Contributions: Conceptualization, R.L.F.; data acquisition, R.L.F. and M.S.-S.; original draft preparation, R.L.F.; review and editing, R.L.F. and M.S.-S. All authors have read and agreed to the published version of the manuscript.

Funding: The authors would like to thank the Centro Nacional de Pesquisa e Conservação de Cavernas (CECAV) and Instituto Brasileiro de Desenvolvimento e Sustentabilidade (IABS) for their financial support (TCCE ICMBio/Vale 01/2018). We are also thankful to the CNPq (National Council for Scientific and Technological Development, grant no. 302925/2022-8) for the productivity scholarship provided to R.L.F., and to the team from the Center of Studies in Subterranean Biology (CEBS/UFLA) for their support in the field trips.

Institutional Review Board Statement: Not applicable.

Informed Consent Statement: Not applicable.

Data Availability Statement: No new data were created or analyzed in this manuscript. Data sharing is not applicable for this manuscript.

Acknowledgments: The authors would like to thank the team from the Center of Studies in Subterranean Biology (CEBS/UFLA) for their support in the field trips. We also thank Gabriel Augusto Silva Vaz, Paulo César Reis Venâncio, and Priscila Emanuela Souza for their cooperation in field surveys. Finally, we would like to extend our sincere gratitude to the taxonomists who confirmed the cave-restricted status for some of the newly discovered species and who are currently describing some of them, including Leonardo Sousa Carvalho (Araneae), Leticia Vieira (Coleoptera), and Júlio César Do Carmo Vaz Santos (Auchenorrhynca).

Conflicts of Interest: The authors declare no conflict of interest.

References

1. Ferreira, R.L.; Berbert-Born, M.; Souza-Silva, M. The Água Clara Cave System in Northeastern Brazil: The Richest Hotspot of Subterranean Biodiversity in South America. *Diversity* **2023**, *15*, 761. [CrossRef]
2. Souza-Silva, M.; Cerqueira, R.F.V.; Pellegrini, T.G.; Ferreira, R.L. Habitat selection of cave-restricted fauna in a new hotspot of subterranean biodiversity in Neotropics. *Biodiv. Conserv.* **2021**, *30*, 4223–4250. [CrossRef]
3. Culver, D.C.; Sket, B. Hotspots of subterranean biodiversity in caves and wells. *J. Cave Karst Stud.* **2000**, *62*, 11–17.
4. Eberhard, S.M.; Howarth, F.G. Undara lava cave fauna in tropical Queensland with an annotated list of Australian subterranean biodiversity hotspots. *Diversity* **2021**, *13*, 326. [CrossRef]
5. Deharveng, L.; Le, C.K.; Bedos, A.; Judson, M.L.; Le, C.M.; Lukić, M.; Vermeulen, J. A hotspot of subterranean biodiversity on the brink: Mo So Cave and the Hon Chong Karst of Vietnam. *Diversity* **2023**, *15*, 1058. [CrossRef]
6. Francke, O.F.; Monjaraz-Ruedas, R.; Cruz-López, J.A. Biodiversity of the Huautla cave system, Oaxaca, Mexico. *Diversity* **2021**, *13*, 429. [CrossRef]
7. Deharveng, L.; Rahmadi, C.; Suhardjono, Y.R.; Bedos, A. The Towakkalak System, A hotspot of subterranean biodiversity in Sulawesi, Indonesia. *Diversity* **2021**, *13*, 392. [CrossRef]
8. Deharveng, L.; Ellis, M.; Bedos, A.; Jantarit, S. Tham Chiang Dao: A hotspot of subterranean biodiversity in Northern Thailand. *Diversity* **2023**, *15*, 1076. [CrossRef]
9. Gallão, J.E.; Ribeiro, D.B.; Gallo, J.S.; Bichuette, M.E. There and Back Again—The Igatu Hotspot Siliciclastic Caves: Expanding the data for subterranean fauna in Brazil, Chapada Diamantina Region. *Diversity* **2023**, *15*, 991. [CrossRef]
10. Clark, H.L.; Buzatto, B.A.; Halse, S.A. A hotspot of arid zone subterranean biodiversity: The Robe Valley in Western Australia. *Diversity* **2021**, *13*, 482. [CrossRef]
11. Silva, M.S.; Ferreira, R.L. The first two hotspots of subterranean biodiversity in South America. *Subterr. Biol.* **2016**, *19*, 1–21. [CrossRef]
12. Hellmann, L.; Ferreira, R.L.; Rabelo, L.; Leal-Zanchet, A.M. Enhancing the still scattered knowledge on the taxonomic diversity of freshwater triclads (Platyhelminthes: Dugesiidae) in caves from two Brazilian Biomes. *Stud. Neotrop. Fauna Envion.* **2022**, *57*, 148–163. [CrossRef]
13. Simone, L.R.L. A new genus and species of cavernicolous Pomatiopsidae (Mollusca, Caenogastropoda) in Bahia, Brazil. *Pap. Avulsos Zool.* **2012**, *52*, 515–524. [CrossRef]
14. Kury, A.B.; González, A.P. A new remarkable troglomorphic gonyleptid from Brazil (Arachnida, Opiliones, Laniatores). *Rev. Ibér. Arachnol.* **2002**, *246*, 43–50.
15. Baptista, R.L.C.; Giupponi, A.D.L. A new troglomorphic *Charinus* from Brazil (Arachnida: Amblypygi: Charinidae). *Rev. Ibér. Arac.* **2002**, *6*, 105–110.
16. Prado, G.C.; Ferreira, R.L. Three new troglobitic species of *Pseudochthonius* Balzan, 1892 (Pseudoscorpiones, Chthoniidae) from northeastern Brazil. *Zootaxa* **2023**, *5249*, 92–110. [CrossRef]
17. Campos-Filho, I.S.; Araujo, P.B.; Bichuette, M.E.; Trajano, E.; Taiti, S. Terrestrial isopods (Crustacea: Isopoda: Oniscidea) from Brazilian caves. *Zool. J. Linn. Soc.* **2014**, *172*, 360–425. [CrossRef]
18. Cardoso, G.M.; Bastos-Pereira, R.; Souza, L.A.; Ferreira, R.L. New cave species of *Pectenoniscus* Andersson, 1960 (Isopoda: Oniscidea: Styloniscidae) and an identification key for the genus. *Nauplius* **2020**, *28*, e2020039. [CrossRef]
19. Souza, P.G.C.; Medeiros, G.D.S.; Ferreira, R.L.; Souza-Silva, M.; Bellini, B.C. A highly troglomorphic new genus of Sminthuridae (Collembola, Symphypleona) from the Brazilian semiarid region. *Insects* **2022**, *13*, 650. [CrossRef]
20. Carvalho, P.H.M.; Junta, V.G.P.; Castro-Souza, R.A.; Ferreira, R.L. Three new cricket species and a new subgenus of *Endecous* Saussure, 1878 (Grylloidea: Phalangopsidae) from caves in northeastern Brazil. *Zootaxa* **2023**, *5263*, 001–039. [CrossRef]
21. Kamimura, Y.; Ferreira, R.L. Description of a second South American species in the Malagasy earwig genus *Mesodiplatys* from cave habitat, with notes on the definition of Haplodiplatyidae (Insecta, Dermaptera). *ZooKeys* **2018**, *790*, 87–100. [CrossRef] [PubMed]
22. Rizzato, P.P.; Bichuette, M.E. A new species of cave catfish from Brazil, *Trichomycterus rubbioli* sp. n., from Serra do Ramalho karstic area, São Francisco River basin, Bahia State (Silurifomes: Trichomycteridae). *Zootaxa* **2012**, *3480*, 48–66.
23. Iniesta, L.F.M.; Ferreira, R.L. The first troglobitic *Pseudonannolene* from Brazilian iron ore caves (Spirostreptida: Pseudonannolenidae). *Zootaxa* **2013**, *3669*, 85–95. [CrossRef] [PubMed]
24. Iniesta, L.F.M.; Ferreira, R.L. *Pseudonannolene lundi* n. sp., a new troglobitic millipede from a Brazilian limestone cave (Spirostreptida: Pseudonannolenidae). *Zootaxa* **2015**, *3949*, 123–128. [CrossRef] [PubMed]
25. Golovatch, S.I.; Wytwer, J. The South American millipede genus *Phaneromerium* Verhoeff, 1941, with the description of a new cavernicolous species from Brazil (Diplopoda: Polydesmida: Fuhrmannodesmidae). *Ann. Zool.* **2004**, *54*, 511–514.
26. Fennah, R.G. A cavernicolous new species of *Notuchus* from New Caledonia (Homoptera: Fulgoroidea: Delphacidae). *Rev. Suisse Zool.* **1980**, *87*, 757–759. [CrossRef]
27. Hoch, H.; Asche, M.; Burwell, C.; Monteith, G.M.; Wessel, A. Morphological alteration in response to endogeic habitat and ant association in two new planthopper species from New Caledonia (Hemiptera: Auchenorrhyncha: Fulgoromorpha: Delphacidae). *J. Nat. Hist.* **2006**, *40*, 1867–1886. [CrossRef]
28. Hoch, H.; Ferreira, R.L. *Ferricixius davidi* gen. n., sp. n.–the first cavernicolous planthopper from Brazil (Hemiptera, Fulgoromorpha, Cixiidae). *Dtsch. Entomol. Z.* **2012**, *59*, 201–206.

29. Hoch, H.; Ferreira, R.L. *Potiguara troglobia* gen. n., sp. n.–first record of a troglobitic Kinnaridae from Brazil (Hemiptera: Fulgoromorpha). *Dtsch. Entomol. Z.* **2013**, *60*, 33–40.
30. Hoch, H.; Ferreira, R.L. *Iuiuia caeca* gen. n., sp. n., a new troglobitic planthopper in the family Kinnaridae (Hemiptera, Fulgoromorpha) from Brazil. *Dtsch. Entomol. Z.* **2016**, *63*, 171–181. [CrossRef]
31. Balkenohl, M.; Pellegrini, T.G.; Zampaulo, R.D.A. A peculiar new beetle from Brazil associated with a cave habitat (Coleoptera, Carabidae, Clivinini). *Zootaxa* **2018**, *4497*, 398–410. [CrossRef] [PubMed]
32. Pellegrini, T.G.; Ferreira, R.L. Ultrastructural analysis and polymorphisms in *Coarazuphium caatinga* (Coleoptera: Carabidae, Zuphiini), a new Brazilian troglobitic beetle. *Zootaxa* **2014**, *3765*, 526–540. [CrossRef] [PubMed]
33. Polhemus, D.A.; Ferreira, R.L. Two unusual new genera of cavernicolous Hydrometridae (Insecta: Heteroptera) from eastern Brazil. *Tijdschr. Voor Entomol.* **2018**, *161*, 25–38. [CrossRef]
34. Cordeiro, I.R.; Bichuette, M.E.; Moreira, F.F. A New Species of *Spelaeometra* Polhemus & Ferreira, 2018 (Hemiptera: Heteroptera: Hydrometridae) from a Hotspot of Troglobites in Brazil, Serra do Ramalho Karst Area. *Animals* **2023**, *13*, 3199.
35. Sendra, A.; Yoshizawa, K.; Ferreira, R.L. New oversize troglobitic species of Campodeidae in Japan (Diplura). *Subterr. Biol.* **2018**, *27*, 53–73. [CrossRef]
36. Ferreira, R.L.; Bernard, E.; da Cruz Júnior, F.W.; Piló, L.B.; Calux, A.; Souza-Silva, M.; Barlow, J.; Pompeu, P.S.; Cardoso, P.; Mammola, S.; et al. Brazilian cave heritage under siege. *Science* **2022**, *375*, 1238–1239. [CrossRef]

Disclaimer/Publisher's Note: The statements, opinions and data contained in all publications are solely those of the individual author(s) and contributor(s) and not of MDPI and/or the editor(s). MDPI and/or the editor(s) disclaim responsibility for any injury to people or property resulting from any ideas, methods, instructions or products referred to in the content.

EXPLORING THE FACTORS SHAPING CAVE INVERTEBRATE COMMUNITIES

Exploring the factors shaping cave invertebrate communities and habitat selection in a new Hotspot of Subterranean Biodiversity in South America

Gabriel Augusto Silva Vaz[a], Marconi Souza-Silva[a,b], Alicia Helena Souza Rodrigues Ferreira[a,b], Rodrigo Lopes Ferreira[a,b*]

[a]*Centro de Estudos em Biologia Subterrânea, Departamento de Ecologia e Conservação, Instituto de Ciências Naturais, Universidade Federal de Lavras, Lavras, Minas Gerais, Brasil, CEP 37200-900.*
[b]Programa de P-os-graduação em Ecologia Aplicada, Universidade Federal de Lavras, Lavras, Minas Gerais, Brasil, CEP 37200-900.

Vaz, G.A.S. ORCID identifier is 0000-0001-5813-435X
Souza-Silva, M. ORCID identifier is 0000-0002-3184-5319
Rodrigues-Ferreira, A.H.S ORCID identifier is 0000-0002-9965-2265
Ferreira, R.L. ORCID identifier is 0000-0003-3288-4405

Abstract

Caves serve as exceptional ecological models for studying the environmental factors that shape biological communities. However, there has been limited exploration into understanding how these environmental factors affects communities within the same cave system. To address this gap, we employed standardized sampling methodologies across two scales within a limestone cave located in the Brazilian semi-arid region (Pedro Cassiano cave). Our objective was to uncover how substrate characteristics and conditions may contribute to variations in the composition and richness of invertebrates and niche overlapping. Furthermore, we aimed to comprehend the habitat selection and distribution patterns of some troglobitic species. This particular cave hosts a rich restricted fauna, with 20 obligate cave species (19 invertebrates and 1 fish), which positions it as new Hotspot of Subterranean Biodiversity in South America. The diversity of substrates, acting as a proxy for habitat heterogeneity, emerged as a pivotal environmental factor shaping invertebrate communities. Our observations emphasized that the factors structuring invertebrate communities depend on the analytical scale. Furthermore, troglobiotic and non-troglobiotic invertebrates are influenced by distinct environmental determinants. Troglobitic species are more prevalent in the cave's deeper areas than non-troglobitic species, and they exhibit minimal niche overlap. Finally, we deliberated on the urgency of conservation efforts for this important cave.
Key Words: Cave conservation; Habitat heterogeneity; Troglobites; Non-troglobites, Niche.

Introduction

Understanding the factors that shape biological communities and unraveling species distribution patterns at regional and local scales pose significant challenges in the field of community ecology. These challenges are compounded by the multifactorial nature of responses and the inherent difficulty in controlling variables in natural environments. In comparison to surface habitats, caves offer a simpler yet fascinating ecological setting, both in terms of their biological communities and their environmental conditions and characteristics (Poulson & White, 1969; Sánchez-Fernández et al., 2018a).

Despite their simplicity, caves exhibit a diverse array of microhabitats and organic resources (Souza-Silva et al., 2011b; Lunghi et al., 2017; Lunghi and Manenti, 2020; Mammola et al., 2020), which are distributed along gradients from the entrance to the deeper areas (Tobin et al., 2013; Prous et al., 2015; Mammola and Isaia, 2018; Lunghi and Manenti, 2020). These unique characteristics make caves an ideal "natural laboratory" for conducting ecological, biogeographical, and evolutionary studies (Poulson and White, 1969; Sánchez-Fernández et al., 2018; Mammola et al., 2019).

The richness and composition of cave communities are intricately shaped by various factors, including the presence of distinct zones with differing light conditions, availability of organic resources, temperature, and humidity (Tobin et al., 2013; Prous et al., 2004, 2015; Kozel et al., 2019; Mammola et al., 2017; Lunghi and Manenti, 2020). Cave entrances harbor communities that exhibit remarkable resilience to fluctuations in daily and seasonal environmental conditions. In contrast, deeper areas of caves experience relatively stable temperature and humidity, yet suffer from a scarcity of organic resources (Tobin et al., 2013; Mammola et al., 2019). Consequently, these deeper regions are typically inhabited by highly specialized species, which present adaptations to cope with nutrient limitations and challenging conditions (Novak et al., 2012; Kozel et al., 2019).

Pioneering researchers, including Schiner in 1854 and Racovitza in 1907, laid the groundwork for understanding the intricate relationships between species inhabiting caves and their environment. These early scholars classified organisms based on their ecological-evolutionary characteristics. Trogloxenes, for instance, utilize caves for specific purposes such as shelter, but depend of the aboveground environment to complete their life cycle. In contrast, Troglophiles are capable of establishing viable populations both inside and outside caves. Finally, Troglobites, highly specialized for life in perpetually dark and often nutrient-poor environments, are exclusively restricted to cave habitats.

Trogloxenes and troglophiles are occasionally grouped as non-troglobites due to the limited availability of practical criteria for distinguishing between these categories (Novak et al., 2012). In contrast, troglobites can be identified by their troglomorphic traits, characterized by features such as reduced or absent eyes, depigmentation, and the presence of elongated appendages (Cristiansen 1962). However, it is noteworthy that certain groups, such as Palpigradi, consistently exhibit depigmentation and blindness, necessitating the examination

of additional morphological characteristics for accurate classification (Souza and Ferreira, 2010).

The distribution patterns of non-troglobites and troglobites within cave systems are governed by spatial and temporal dynamics that are influenced by microclimatic, physical, and trophic variations occurring along the cave passages (Novak et al., 2012; Tobin et al., 2013; Bento et al., 2016; Lunghi et al., 2017; Kozel et al., 2019; Souza-Silva et al., 2021). Additionally, the occurrence of interspecific competition within this environment is closely linked to the eco-evolutionary categories, as troglobites and non-troglobites often display limited spatial overlap along the cave's extent. This is primarily due to the troglobitic species' preference for more stable and specialized environments, resulting in distinct ecological niches (Sket, 1999; Novak et al., 2012; Souza-Silva et al., 2021).

However, our understanding of subterranean biodiversity remains incomplete. The ecological factors that govern subterranean habitats and the characterization of species' ecological niches are still inadequately understood (Mammola and Isaia, 2016). Furthermore, patterns of subterranean diversity are subject to geographical biases (Sànchez-Fernández et al., 2018). For instance, in Neotropical regions, the diversity patterns and factors influencing the distribution of subterranean species are less explored compared to temperate regions (Niemiller et al., 2018; Mendes-Rabelo et al., 2018).

With the increase in the number of studies in the ecology of subterranean ecosystems in recent years, some ecological factors influencing the fauna have been described, such as cave extent, seasonal variation, landscape structure, cave lithology, habitat heterogeneity, among others (Souza-Silva et al., 2011a; Pellegrini et al., 2016a; Jaffé et al., 2018; Bento et al., 2016; Pacheco et al., 2020a). Some of these studies have focused on factors that affect troglobitic species, partly due to their importance for conservation, as well as on variations that occur between caves and regions.

The term "hotspots of subterranean biodiversity" (HSB) was initially introduced by Culver and Sket (2000) to designate subterranean habitats that harbor a minimum of twenty or more cave-obligate species. Subsequently, Culver and Pipan (2013) refined this threshold by suggesting that an HSB should encompass a minimum of 25 species restricted to cave environments. However, in a recent study, Ferreira et al., (2023) deliberated on the limitations of maintaining a fixed cutoff value, considering various factors such as geographic location, lithology, and biome, which directly influence the species richness of cave-restricted organisms within a specific cave. Consequently, they proposed a more flexible approach, suggesting that the determination of an HSB cutoff should be adaptable depending on the contextual factors associated with the cave's environment.

It is crucial to acknowledge that relying solely on species richness as a criterion for identifying hotspots may not fully capture the ecological significance of these habitats or their susceptibility to anthropogenic disturbances (Ferreira et al., 2023). Thus, it becomes essential to consider not only the biodiversity value but also the potential threats to the habitat when identifying and prioritizing conservation areas. Accordingly, it is paramount to comprehend the potential patterns of subterranean biodiversity at different scales to effectively implement

protective measures for this ecosystem amidst anthropogenic changes. Additionally, the detection of new hotspots of subterranean biodiversity is of significant importance as these areas often receive greater attention in conservation efforts. Thus, the primary objectives of this study were to investigate the environmental factors that govern the variation in richness and composition of invertebrate communities within a cave situated in the Brazilian semi-arid region, while considering two distinct sampling scales. Additionally, we aimed to elucidate the distribution patterns of troglobitic species and their habitat preferences within this cave. Notably, this study unveils a novel hotspot of subterranean biodiversity in South America.

We hypothesized that the diversity of substrates on the cave floor (a proxy for habitat heterogeneity), the trophic resource availability, the distance from the cave entrance, and microclimatic characteristics (temperature and humidity) would serve as pivotal factors influencing the variations in invertebrate composition and richness within the cave ecosystem. Furthermore, we anticipated that ecological-evolutionary categories would exhibit differential responses to these habitat components. Moreover, we expected that the influence of habitat components on invertebrates would exhibit variations contingent on the chosen sampling scale. Finally, we postulated that troglobitic species would demonstrate a greater occurrence in areas distanced from the cave entrance and that widely distributed troglobites would exhibit minimal niche overlap.

Material and Methods

Study site

The study was carried out in Pedro Cassiano Cave (UTM 23L: 617427 - 8474330), situated in the municipality of Carinhanha, within the western region of Bahia state in northeastern Brazil. The study area is located within the Serra do Ramalho karst region, which encompasses a remarkable expanse of karst terrain housing numerous known caves. This region is particularly notable for the presence of extensive subterranean hydrological systems that serve as habitats for numerous species that are restricted to cave environments (Ferreira et al., 2023). The local climate is classified as "Aw" according to the Köppen-Geiger climate classification system, characterized as tropical with a dry winter season spanning from March to October (Alvares et al., 2013). The region is part of the Caatinga biome, which represents the only semi-arid biome in Brazil (Fig. 1)

The Pedro Cassiano cave is situated within carbonate rock formations and spans a total length of 2,660 meters (Fig. 2A). It is characterized by the presence of two autogenic drainages that traverse the cave, each flowing through separate tributary branches in its final section (upstream) (Fig. 2C). These tributaries subsequently converge to form a unified drainage system, which emerges at the main cave entrance, which represent an intermittent resurgence (Fig. 2B).

Sampling design

The sampling of biotic and abiotic data was conducted at both the mesoscale (sectors) and microscale (quadrants) on the cave floor during a single visit to the cave. The sampling design involved dividing the cave floor into distinct sectors, each measuring 10x3 meters. Within each sector, three 1m² quadrants were established: two located at the extremities and one positioned in the center. A total of 15 sectors were sampled along the entire length of the cave, encompassing areas ranging from proximity to the cave entrance to deeper regions.

Invertebrate sampling and identification

The invertebrate survey was conducted using active visual search and manual collection techniques, as described by Wynne et al., (2019), using tweezers and brushes. The sampling of invertebrates followed a sequential approach, beginning with the quadrats and subsequently extending to the corresponding transects. Three collectors participated in the sampling process, ensuring thorough coverage, and the sampling effort continued until all invertebrates were accounted for. Due to the structural differences across various sampling areas within the cave (e.g., the presence or absence of crevices, rocks, and ledges), the time required for searching varied among each sampling unit (Souza-Silva et al., 2021). Additionally, to enhance the detection of cave-restricted species, direct and intuitive search techniques were employed beyond the designated sampling units. This approach aimed to ensure comprehensive coverage of all microhabitats within the cave (Wynne et al., 2019).

The collected specimens were carefully preserved in labeled vials filled with a 70% ethanol solution. Subsequently, they underwent sorting procedures under a stereomicroscope at the Center for Studies in Subterranean Biology (CEBS) of the Federal University of Lavras (UFLA). The specimens were then identified to the lowest taxonomic level achievable, employing identification keys, and subsequently categorized into distinct morphotypes (Oliver and Beattie, 1996). The identification of potentially troglobitic species was conducted by assessing the presence of troglomorphic traits, such as reduced or absent eyes, depigmentation, and elongated appendages (Christiansen 1962). Furthermore, the expertise of taxonomic specialists in various taxa was sought to aid in the recognition of specific troglomorphic characteristics (the contributions of these specialists are acknowledged). Finally, the specimens were deposited in the Collection of Subterranean Invertebrates of Lavras (ISLA), which is affiliated with the Center for Studies in Subterranean Biology at the Federal University of Lavras (www.biologiasubterranea.com.br).

Measuring habitat structure

Temperature and air humidity measurements were conducted in each sector using a thermo-hygrometer positioned near the cave floor. To ensure accurate readings, the device was allowed to stabilize for approximately 15 minutes within each sector. Each sector was further divided into 10 one-meter sections, and the percentage of different substrates and resources (such as guano, animal and plant debris, fungi, fine sediment, gravel, blocks, speleothems, matrix rock, among others) was visually estimated in each section, following the methodology employed by Souza-Silva et al. (2021). It is noteworthy that the same researcher conducted the characterization of all transects to minimize observer error.

In the laboratory, the proportions of each substrate were calculated by summing the direct measurements from each session, and the arithmetic average of substrate coverage was determined for the entire sector. At the microscale, digital photographs of each quadrant (4000 x 3000 pixels) were captured in the field, taken at the researcher's chest height, using a Canon Powershot SX60HS camera positioned as close as possible to a 90° angle. These photographs were later analyzed in the laboratory using ImageJ 1.53K software (Ferreira and Rasband, 2012) to characterize and measure the substrates present. The distances from each transect to the cave's entrance were obtained by plotting the position of each transect on the cave map, providing a quantitative assessment of their spatial relationship to the entrance.

Habitat traits surveyed in each sampling scale

The environmental parameters analyzed at the mesoscale (sectors) were: guano (GU), plant debris (PD), water (W) - which is a grouping of watercourses (WC) and water pools (WP), dripping (DP), actinomycetes (ACT), basidiomycetes (BAM), blocks (64-250 mm) (CB), coarse gravel (17-63 mm) (GRAC), fine gravel (2-16 mm) (GRAF), sand (SAN), silt (0.2 - 0.05 mm) (SIL), hardpan (HRP), speleothems (SPL), temperature (°C) (Temp), humidity (HUM), and distance from the cave entrance (m) (DE).

At the microscale, the analyzed parameters were guano, roots (ROO), water - which in this case refers to water pools (WP) - rough rocks (RR), small boulders (SB), blocks, coarse gravel, fine gravel, sand, silt, hardpan, speleothems, and distance from the cave entrance.

Habitat heterogeneity was assessed in both scales using the Shannon diversity index (H'). The calculations encompassed measures of substrate diversity (Subs H'), shelter diversity (Shelter H'), and resource diversity (Resource H') (Pellegrini et al., 2016; Pacheco et al., 2020; Furtado Oliveira et al., 2022; Cardoso et al., 2022). However, resource diversity was not considered in the microscale analyses as it consistently yielded a value of zero across almost all the quadrants.

To analyze the environmental parameters influencing variations in invertebrate richness, certain variables were grouped together to reduce the number of predictors and quantify resource and shelter availability at different scales. At the mesoscale, the variable "resource" was computed as the sum of proportions of guano, plant debris, actinomycetes, and basidiomycetes. The variable "shelter" was derived by summing the proportions of dripstones holes, boulders, coarse gravel, fine gravel, and speleothems. On the other hand, at the microscale, the variable "resource" was calculated as the sum of guano and roots, while the variable "shelter" was determined by summing rough rocks, small boulders, blocks, coarse gravel, fine gravel, and speleothems.

Lastly, we investigated the potential linear relationship between the environmental parameters and the distance from the cave entrance. This analysis aimed to provide insights into the arrangement of the physical, microclimatic, and trophic components within the Pedro Cassiano Cave along the surface-to-deeper areas gradient.

Data analysis

The richness and abundance of invertebrates were determined by quantifying the number of individuals and morphotypes in each sample unit, comprising 15 sectors and 45

quadrants. It is important to note that the sectors' richness encompassed the species found in both the sectors *per se* and their respective quadrants.

To investigate the key components of habitat structure influencing variations in overall species composition, troglobitic species composition, and non-troglobitic species composition, we employed a DistLM (distance-based linear model) analysis at both sampling scales. Prior to the analysis, the species abundance values were standardized through a square root transformation. Subsequently, a similarity analysis was conducted using the Bray-Curtis index to assess the resemblance between sampling points. Model selection was performed using the AICc (Akaike Information Criterion corrected for small sample size) with the Forward procedure, which identifies the best models based on the lowest criterion value (Anderson et al., 2008). The software Primer 7 & Permanova® was utilized for conducting these analyses.

We employed Generalized Linear Models (GLM) to investigate the components of habitat structure that contribute to variations in overall species richness, troglobitic species richness, and non-troglobitic species richness. Due to limited troglobitic species at the microscale, our focus was solely on overall species richness at this scale. To ensure the reliability of our analysis, we first examined collinearity among all predictor variables using the Spearman correlation index, via 'CHART.CORRELATION' function of the 'PERFORMANCEANALYTICS' package (Peterson and Carl, 2018). Predictor variables exhibiting correlation values exceeding 70% ($r \geq 0.7$) were assessed separately (Schober et al., 2018).

For each type of richness, we initially generated six GLM models with the Poisson distribution family at the mesoscale (whose models do not present variance inflation factors). Utilizing the forward stepwise procedure, we successively eliminated predictors with the highest p-value until only significant predictors remained within each of the six models. Finally, for each type of richness, we selected the model with the lowest Akaike information criterion (AIC). In each model, we assessed the presence of overdispersion using the 'SIMULATIONOUTPUT' function from the 'DHARMa' package (Hartig, 2022). In these cases, a change was made to the distribution for a better fit, which was the negative binomial distribution. At the microscale, none of the predictors exhibited collinearity, allowing the construction of a Poisson Generalized Linear Model (GLM) that incorporated all the measured environmental variables at this scale. However, the initial model displayed multicollinearity issues indicated by elevated variance inflation factors (VIF). To tackle this challenge, predictors surpassing a VIF threshold of 10 were eliminated from the model, and a fresh set of variables was introduced for reanalysis. As a result, three alternative Poisson GLM models were generated, effectively alleviating concerns of collinearity and multicollinearity. These refined models underwent the same procedure outlined for the mesoscale analysis.

To assess whether troglobitic species exhibit a greater prevalence in the deeper regions of the cave, a simple linear regression analysis was conducted. Prior to this analysis, we performed a Shapiro-Wilk test using the 'SHAPIRO.TEST' function from the 'STATS' package to confirm that the residuals followed a normal distribution.

In the regression analysis, the distance from the cave entrance was chosen as the predictor variable, while the proportion of troglobitic richness in relation to the invertebrate richness within each sector was considered as the response variable. It is important to highlight that, since certain sectors exclusively contained troglobitic species, we had to employ an alternative ratio instead of the troglobitic richness/non-troglobitic richness ratio utilized in the study by Souza-Silva et al., (2021).

The ecological niches of selected troglobitic species (those occurring in at least three sectors) were assessed using the Outlying Mean Index (OMI) analysis (Dolédec et al., 2000) conducted with the 'ade4' package (Dray and Dufour, 2007). The OMI analysis allowed us to position each species in a two-dimensional Euclidean space, decomposing their distribution patterns into marginality, tolerance, and residual tolerance. Species marginality represents the distance between the average environmental conditions used by the species and the overall average conditions. Species are positioned based on their deviation from a reference species (ubiquitous species occurring under all available habitat conditions). Lower values of marginality indicate a broader occurrence of the species within the studied environment. Tolerance reflects the variation in environmental conditions used, with higher values suggesting generalist species and lower values indicating specialist species. Residual tolerance provides insight into the reliability of the identified niche (Dolédec et al., 2000).
To execute the OMI analysis, we initially conducted a principal component analysis (PCA) using the mesoscale habitat structure components. Subsequently, we calculated and plotted the niche of each of the six selected species within the environmental niche. Finally, we employed the Monte Carlo test, employing 999 permutations, to evaluate the significance of the difference between the observed species' marginality and simulated values (Dolédec et al., 2000).

Results

Richness and composition of cave fauna

Through all sampling methods employed, a total of 972 invertebrate specimens and one vertebrate were documented within Pedro Cassiano cave (excluding bats, which were not included in the count). These organisms were identified as belonging to 56 species, spanning at least 40 families. Among these species, 20 exhibited troglomorphic traits, and were considered as cave-restricted. The troglobitic species encompassed various taxa, including Amblypygi (*Charinus troglobius* - Baptista and Giupponi, 2002), Araneae (Ochyroceratidae, Oonopidae and Pholcidae), Opiliones (*Giupponia chagasi* - Peréz-González and Kury, 2002), Palpigradi (*Eukoenenia* sp.), Pseudoscorpiones (*Pseudochthonius koinopolitea* - Prado and Ferreira, 2023), Blattodea, Coleoptera (Carabidae: Clivinina - 2 species), Entomobryomorpha (*Trogolaphysa* sp. - 2 species), Neelipleona, Orthoptera (*Endecous infernalis* - Carvalho et al., 2023), Symphypleona, Isopoda (*Xangoniscus* sp. and *Pectenoniscus* sp.), Polydesmida (Oniscodesmidae), Mollusca: (*Spiripockia* sp.) and Siluriformes (*Trichomycterus* sp.)(Figure 3).

Within the 15 sampled sectors, we documented a total of 41 invertebrate species, including 13 troglobitic species and 28 non-troglobitic species. In the quadrants, we recorded 15 invertebrate species, with 5 being troglobitic and 10 non-troglobitic (Appendix 1). Considering the significant number of cave-restricted species discovered in Pedro Cassiano cave (20 species), we propose that this cave be recognized as a new hotspot of subterranean biodiversity in South America (see discussion for further details).

Richness, composition, and distribution of cave invertebrates

At the mesoscale, substrate diversity emerged as a crucial environmental parameter influencing the variation in overall invertebrate composition (AICc = 121.48; R^2 = 0.1554; p = 0.014), troglobitic species composition (AICc = 118.15; R^2 = 0.1548; p = 0.032), and non-troglobitic species composition (AICc = 100.94; R^2 = 0.2012; p = 0.004). Additionally, at this sampling scale, sand was identified as the variable that best explained the variation in both overall invertebrate species richness and troglobitic richness (Table 1) (Fig. 4 A, B). Conversely, resource availability and shelter availability were found to be more effective in explaining the variation in non-troglobitic richness (Table 1) (Fig. 4 C, D).

The Pedro Cassiano Cave displayed gradients along its length. Notably, resource availability ($F_{1,13}$= 4.664; R= 0.455; p= 0.05), shelter availability ($F_{1,13}$= 48.846; R= 0.599; p= 0.01), and substrate diversity ($F_{1,13}$= 9.003; R= 0.603; p= 0.01) were observed to decrease as the cave extended into deeper zone (Fig. 5).

At the microscale, however, none of the predictor variables employed in this study were able to account for the variation in composition. It is plausible that other unexamined variables play a significant role in community structuring at this sampling scale. Nonetheless, water (puddles), sand, substrate diversity, and shelter were identified as effective in explaining the variation in total richness (Table 2) (Fig. 6).

The linear regression analysis revealed a clear trend indicating an increase in troglobitic species richness as non-troglobitic species richness decreased towards the deeper regions of Pedro Cassiano cave ($F_{1,13}$= 4.746; R= 0.517; p= 0.0483) (Fig. 7).

Habitat selection of some cave-restricted species

The OMI analysis encompassed six troglobitic species: *Xangoniscus* sp.1 (isopod), *Giupponia chagasi* (harvestman), Ochyroceratidae sp.1 (spider), *Trogolaphysa* sp.1 (springtail), *Eukoenenia* sp.1 (palpigrade), and *Charinus troglobius* (whip spider). Among these species, only *Xangoniscus* sp.1 exhibited a significant result in the permutation test (Table 3), indicating that it deviates from the average habitat conditions compared to the other species. Thus, it can be considered the most specialized species, showing a strong association with the presence of streams and water pools, high temperatures, and locations featuring a greater diversity of shelters (Fig. 8).

The remaining species, while utilizing average habitat conditions, displayed varying degrees of generalism. The species *Giupponia chagasi*, Ochyroceratidae sp.1, *Trogolaphysa* sp.1, and *Eukoenenia* sp.1 were more generalist than *Charinus troglobius*. The latter species exhibited a high marginality value and a low tolerance value, suggesting a potential preference for deeper locations characterized by high humidity and the presence of hardpan clay.

It is important to acknowledge that the interpretation of these results should consider the limited occurrence of *Giupponia chagasi* (found in four sectors: 2, 6, 9, and 10) and *Charinus troglobius* (found in three sectors: 8, 9, and 10), which may introduce some degree of uncertainty and susceptibility to random fluctuations. However, considering the overall conditions of the cave environment, where troglobitic species are typically scarce, these findings provide valuable insights into the habitat preferences of these species.

Discussion

The results of our study revealed that both habitat heterogeneity and the presence of specific substrates significantly influenced the community structure of invertebrates inhabiting the Pedro Cassiano cave. These findings are consistent with previous studies that have emphasized the importance of habitat heterogeneity in shaping the structure of invertebrate communities across different caves (Bregović and Zagmajster, 2016; Pacheco et al., 2020; Reis-Venâncio et al., 2022; Cardoso et al., 2022) and even within the same cave (Prous et al., 2015; Kozel et al., 2019; Furtado Oliveira et al., 2022).

Additionally, our study demonstrated that substrate diversity played a prominent role in explaining variations in invertebrate composition at the mesoscale within the Pedro Cassiano cave. Interestingly, even though the distance from the entrance did not significantly influence the invertebrate communities, sectors characterized by higher substrate diversity, which were found closer to the cave entrance displayed greater dissimilarity in comparison to sectors with lower substrate diversity, particularly in the deeper regions of the cave.

Habitat traits determining the richness and composition of cave invertebrates.

Caves exhibit various environmental gradients, including the widely recognized light availability zones such as the photic, disphotic, and aphotic zones. In the case of Pedro Cassiano cave, additional gradients are observed, with a decline in resource availability and habitat heterogeneity as one moves towards deeper areas. Concurrently, the microclimatic conditions, including temperature and humidity, demonstrate relative stability in the deeper regions compared to the entrance areas. Interestingly, these conditions appear to contribute to variations in the composition and richness of invertebrate communities, as already observed for other cave systems, in both tropical and temperate zones (Novak et al., 2012; Prous et al., 2015).

It is important to highlight that the distance from the entrance did not have a significant impact on the structuring of invertebrate communities in the Pedro Cassiano cave, which contradicts initial expectations. This can be attributed to two main factors. Firstly, the first sector sampled was located approximately 40 meters from the cave entrance, resulting in a reduced influence of epigean species and limited variation in species composition and richness along the distance gradient. Additionally, the cave's drainages are autogenic, originating from the end of the cave and flowing towards the entrance. Consequently, the availability of organic resources brought by these drainages is limited. Although there is a gradual decline in resource availability towards deeper areas, it is not as pronounced as in

caves with allogenic drainages, where there is a substantial reduction in organic resources from the entrance to deeper regions. Therefore, the relatively modest decrease in resource availability along the surface-to-deeper gradient may have contributed to the observed pattern in this cave. While these findings contradict some previous studies (Novak et al., 2012; Furtado-Oliveira et al., 2022), it is evident that the distance from the entrance still influences species distribution in most tropical caves, as trophic resource availability and habitat heterogeneity decrease from the entrance to deeper areas (Souza-Silva et al., 2021).

The influence of factors on species distribution and diversity is known to vary across different spatiotemporal scales (Bregovic & Zagmajster, 2016). However, there are certain factors that cannot be adequately assessed at specific scales, posing challenges in such studies (González-Magias et al., 2007). In subterranean environments, limited research has been conducted on the influence of spatial scale on terrestrial community structure (Pellegrini et al., 2016; Pacheco et al., 2020b; Furtado-Oliveira et al., 2022).

In our study, we examined variations in the structure of invertebrate communities using two sampling scales. Interestingly, substrate diversity was found to be a significant variable only at the mesoscale. This may be attributed to the low number of species encountered at the microscale, particularly troglobitic species. It is important to note that sampling bias can play a determinant role in results when investigating different scales, especially when dealing with highly spatially restricted scales. In cave environments, which are known to impose restrictive conditions on most species, understanding the effects of habitat structure on invertebrate communities at micro spatial scales can be challenging, primarily due to the limited availability of suitable specimens for analysis.

Nevertheless, certain variables proved to be influential in determining invertebrate richness at the microscale. Specifically, the percentage of areas occupied by water bodies (W) exhibited a significant positive relationship with richness. This finding aligns with the preferences of subterranean species for microhabitats characterized by high humidity (Tobin et al., 2013; Mammola et al., 2015, 2016). Water presence plays a crucial role in maintaining adequate humidity levels at this scale, thereby providing favorable conditions for a greater number of subterranean species, particularly troglobitic species with thinner cuticles that rely on moisture to prevent desiccation (Tobin et al., 2013; Kozel et al., 2019; Souza-Silva et al., 2021).

Few studies have investigated how habitat structure can affect troglobitic and non-troglobitic species separately (Pacheco et al., 2020b; Mammola et al. 2020b; Furtado Oliveira et al., 2022). Our analyses revealed that substrate diversity had a stronger influence on species composition variation for non-troglobitic species compared to troglobitic species, although the differences observed were subtle. Furthermore, only the species richness of non-troglobitic species was affected by shelter availability, an environmental parameter related to habitat heterogeneity (Reis-Venâncio et al., 2022). This suggests that the pronounced specializations of troglobitic species obviates the necessity for diverse sheltering strategies observed in non-troglobitic species. This divergence is potentially attributable to the heightened physiological adaptations of troglobitic species, affording them to thrive in several distinct cave

microclimatic conditions. Conversely, the physiological constraints of non-troglobitic species likely prompt them to seek out a range of sheltering options. This selection process appears to be contingent upon the prevailing microclimatic conditions specific to each distinct cave area.

Caves are recognized as oligotrophic environments, primarily relying on external inputs of resources (Souza-Silva et al., 2012). Guano deposits and plant debris carried by water are considered the primary energy sources in tropical caves (Ferreira et al., 2007; Souza-Silva et al., 2012). Furthermore, these organic inputs can also provide suitable habitats for certain species (Ferreira et al., 2007). Consequently, intense intra- and interspecific competition for these limited organic resources becomes a crucial factor in shaping cave communities (Culver et al., 1991; Schneider et al., 2011; Culver and Pipan, 2015).

In our study, we found a positive and significant relationship between resource availability and the richness only for the non-troglobitic species. Such species are generally less specialized compared to the cave-restricted species, and therefore, they have higher energy demands. Consequently, areas with greater resource availability are more likely to support a higher diversity of non-troglobitic species. On the other hand, cave-restricted species exhibit high specialization, including an enhanced tolerance to starvation (Kozel et al., 2023). This adaptability enables them to persist in highly oligotrophic areas, which may explain why we did not identify resource availability as a significant factor influencing the richness of troglobitic species. Furthermore, non-troglobitic species have a competitive advantage over troglobitic species (Sket, 1999), leading the latter to avoid resource-rich areas within the caves. Deharveng and Bedos, (2000) also observed that troglobitic invertebrates prefer areas farther away from trophic resources to minimize competition with non-troglobitic species. Studies focusing on guano communities in Neotropical caves have also demonstrated that the establishment of large populations of non-troglobitic species in guano piles can displace troglobitic species (Ferreira et al., 2007).

Substrate diversity exhibited a significant and positive correlation with invertebrate richness. Heterogeneous sites offer a variety of organic resources, refuges, shelters, and microclimatic conditions that promote niche differentiation and support a greater number of coexisting species (Poulson and Culver 1969; Bregovic and Zagmajster, 2016). Conversely, more homogeneous habitats tend to have the opposite effect on communities. For instance, the presence of a higher percentage of sand in the sectors had a negative impact on invertebrate richness, emphasizing the importance of habitat heterogeneity for the cave fauna in the Pedro Cassiano cave.

At both sampling scales, an increase in sand content led to a decrease in species richness, indicating a scale-invariant relationship. Specifically, we observed a decline in species richness with each 7.5% rise in sand content within the sectors. Fine substrates like sand create a more homogeneous environment that does not provide favorable conditions for supporting a diverse invertebrate community (Reis-Venâncio et al., 2022). Additionally, we found that troglobitic species richness also declined with increasing sand content in the sectors. This suggests that areas with diverse microhabitats, characterized by the overlapping

of rocks and sediments, can provide suitable microclimatic conditions for these specialized species (Mammola et al., 2016).

Finally, at the microscale, the availability of shelters exhibited an unexpected negative relationship with richness, contradicting previous studies that proposed a positive association between shelter availability and habitat heterogeneity (Reis-Venâncio et al., 2022). It is important to note, however, that despite the significant relationship observed in the model, the estimate value is quite low, thus indicating a very weak relation between such variables. It was observed that many quadrants within the Pedro Cassiano Cave lacked shelters entirely, and those that did contain shelters typically had a maximum of three distinct substrates. In this particular case, the limited diversity of available shelters represents a less varied microhabitat, incapable of supporting a greater number of species. This interpretation is reinforced by the relationship between shelter diversity and species richness, which was almost statistically significant, and displayed a positive estimate, suggesting a potential increase in species numbers within quadrants with higher shelter diversity index values.

Invertebrates' distribution

Areas closer to cave entrances typically harbor ecotonal fauna, which relies on an environment with diverse substrate types and a greater abundance of shelters and organic resources (Prous et al., 2015). These communities are typically composed of epigean edaphic, trogloxene, and troglophilic species, collectively referred to as "para-epigean" communities (Prous et al., 2004, 2015). However, as one moves away from the entrance, these characteristics and species composition change and only those species with a stronger affinity for subterranean habitats are able to establish themselves. Consequently, in the deeper areas of the cave, troglophilic and troglobitic species prevail (Kozel et al., 2019).

These characteristics of strictly subterranean species described so far limit their distribution to more stable areas within caves. Just as the scarcity of organic resources and the reduction of substrate diversity influence the distribution of non-troglobitic species (Sket, 1999), which decreases richness towards deeper zones (Souza-Silva et al., 2021). Thus, in many caves, there is a low spatial interspecific overlap between the eco-evolutionary categories (Sket, 1999; Novak et al., 2012; Souza-Silva et al., 2021). In areas closer to the entrance, when climatic stability occurs, troglobitic and non-troglobitic species can even coexist (Kozel et al., 2019), but in deeper zones, troglobites prevail. Through our analyses, we reinforce this hypothesis of invertebrate distribution in Neotropical caves.

Habitat selection

Souza-Silva et al. (2021) conducted a niche analysis of ten troglobitic species within the Água Clara cave system (ACCS), which is situated in the same geographical area as our present study. Many of the species investigated by them also inhabit the Pedro Cassiano cave, allowing for meaningful comparisons. Several predatory species, including Ochyroceratidae sp.1, *Eukoenenia* sp.1, and *Giupponia chagasi*, demonstrated a notable tolerance for the diverse environmental conditions present on the cave floor. This adaptability likely arises from their necessity to hunt for prey in oligotrophic environments. The whip spider species *Charinus troglobius* exhibited a lower degree of generalism compared to the other predators, showing a subtle preference for deeper locations (Baptista and Giupponi, 2002), with high humidity and the presence of hardpan.

However, it is important to highlight that certain distinctions emerged between the two cave systems. For instance, *Giupponia chagasi* displayed a niche that was more closely linked to factors such as moisture content and distance from the cave entrance in the ACCS. In contrast, in the Pedro Cassiano cave, this species' niche appeared to be more influenced by variables like shelter availability and resource availability, including guano. The palpigrade *Eukoenenia* sp.1 exhibited a niche determined by moisture content and distance from the cave entrance in the ACCS. Conversely, in the Pedro Cassiano cave, the species' niche leaned more towards shelter availability and substrate diversity. The springtail *Trogolaphysa* sp. 1 (referred to as Entomobryomorpha sp. 1 in the ACCS) displayed a niche defined by shelter availability and substrate diversity in the former cave. In the Pedro Cassiano cave, the species appeared to adopt a more generalized niche. The isopod *Xangoniscus* sp.1 had its niche largely determined by temperature and wood in both cave systems. However, in the Pedro Cassiano cave, additional factors like guano and the diversity of shelters also played significant roles in shaping its niche. Lastly, only the Ochiroceratidae sp.1 (the same species in both caves) presented similar niches, being generalist in both cave systems.

These disparities observed between the two cave systems underscore the fact that the same species can occupy distinct niches contingent upon the specific cave environment. It is important to highlight that this information not only represents an innovative contribution to the field but also holds significant implications for conservation efforts, particularly given the scarcity of studies pertaining to the niches of cave-restricted species.

Why Is Pedro Cassiano cave so rich in cave restricted species?

Ferreira et al. (2023) proposed that caves experiencing flood pulses during rainy periods could maintain a high diversity of species. The possible explanation for this pattern is based on the intermediate disturbance hypothesis (IDH) (Dial and Roughgarden, 1998). In this context, flood pulses seasonally alter the cave floor substrates, creating a type of disturbance that can be classified as intermediate. This disturbance prevents dominant species from establishing themselves by temporarily and partially modifying the microhabitats, allowing different stages of ecological succession to coexist after the flood pulse. This process fosters long-term coexistence and, consequently, biodiversity.

Pedro Cassiano Cave exhibits seasonal flood pulses and presents a high richness of troglobitic species, as observed in the Água Clara cave system. As argued by Ferreira et al. (2023), the theory of intermediate disturbance could also provide a potential explanation for the maintenance of a substantial number of troglobites in this particular cave. Furthermore, through OMI analysis, we revealed the presence of specialist troglobitic species and troglobitic species with varying degrees of generalism, which aligns with the findings of Souza-Silva et al., (2021), supporting our hypothesis that there is not a high niche overlap among them.

Lastly, it is worth emphasizing the significant overlap of cave-restricted species between the Pedro Cassiano cave and the Água Clara cave system (ACCS). Out of the 20 cave-restricted species identified in the Pedro Cassiano Cave, a remarkable 15 are also present in the ACCS. This finding underscores the likelihood that both systems have been subjected to similar ecological and evolutionary pressures and conditions, ultimately resulting in a notable abundance of cave-restricted taxa.

Conservation issues

It is crucial to underscore the impressive number of troglobites discovered within Pedro Cassiano Cave, especially when considering that this abundance was determined from a single collection effort. The number of species exclusive to the cave environment observed here aligns with the originally established threshold for designating a cave (or cave system) as a Hotspot of Subterranean Biodiversity (HSB) (20 troglobites/stygiobites) (Culver and Sket, 2000). However, it is worth noting that some researchers have questioned the arbitrariness of the 20-species criterion (Souza-Silva and Ferreira, 2016; Zeppelini et al., 2022; Ferreira et al., 2023). Ferreira et al., (2023) emphasizes the importance of incorporating additional parameters in defining an HSB. These parameters might encompass factors such as scale, latitude, lithology associated with caves, levels of endemism, and the degree of threat that the subterranean habitat faces, as proposed by Myers et al., (2000).

Therefore, especially when considering parameters as degree of threats to enhance the comprehension of subterranean hotspots, Pedro Cassiano Cave is certainly a new HSB in South America. Conducting additional samplings utilizing supplementary methodologies, like micro invertebrate sampling, undoubtedly holds the promise of revealing further species residing within this cave. It is equally crucial to highlight that endeavors directed towards species description play a pivotal role in conserving this potential priority area, currently facing escalated anthropogenic interventions, including deforestation (Ferreira et al., 2023).

It is important to note that this cave is threatened, especially when considering the strong anthropic alterations occurring in its surroundings. The deforestation around cave entrances disrupts the availability of organic resources and microhabitats crucial for hypogean fauna (Pellegrini et al., 2016; Cardoso et al., 2022). Furthermore, it exposes the soil to erosive processes capable of conveying fine sediments into the cavities, culminating in watercourse sedimentation and the uniformity of cave substrates. Within this context, Pedro Cassiano Cave could experience a substantial decline in its invertebrate diversity, as our study's findings emphasize the critical role of substrate diversity in sustaining this diversity. Another consequence of deforestation in karst landscapes is the reduction of preserved

vegetation corridors, which are essential for species movement between caves, particularly trogloxene and troglophile species (Cardoso et al., 2022). This population isolation contributes to reduced genetic diversity, heightening the vulnerability of species to extinction risks (Campbell Grant, 2011).

Lastly, it is important to highlight that the Pedro Cassiano Cave is located approximately 4 km in a straight line from the Água Clara Cave System (ACCS), recognized as the most diverse Hotspot of Subterranean Biodiversity (HSB) in South America (Souza-Silva et al., 2021; Ferreira et al., 2023). The ACCS comprises four functionally interconnected caves, all intersected by the same intermittent drainage. Ferreira et al. (2023) initially reported 31 cave-restricted species within this system. However, recent sampling efforts conducted in September 2023 revealed nine new and previously undocumented cave-restricted species. This discovery brings the total count of cave-restricted species within the system to 40, further emphasizing its significance in South America (Ferreira, unpublished data).

Moreover, the ACCS and the Pedro Cassiano Cave share a considerable number of species, as previously mentioned. This underscores the urgent need for collaborative conservation strategies that encompass both cave systems. Establishing comprehensive conservation measures, such as the creation of a protected area encompassing the hydrological basins that contribute to these cave networks, becomes imperative to safeguard the unique subterranean fauna of these remarkable Neotropical HSBs.

Conclusions

We have delved into the environmental factors that play a crucial role in shaping the richness and composition of invertebrates within a cave located in Brazil's semi-arid region. We want emphasize the pressing need for conservation efforts to safeguard this new Hotspot of Subterranean Biodiversity. We summarized the following points:

1) The Substrate heterogeneity turned out to be a key factor influencing the structure of invertebrate communities, confirming what previous literature has suggested;
2) Areas with a higher abundance of trophic resources housed a greater number of non-troglobitic species. However, this pattern might not hold true for troglobitic species;
3) The distance from the cave entrance was not a determining variable in community structuring, as initially expected. The reasons for this observation include the location of the first sampling sector (approximately 40 meters from the entrance), which minimized the contribution of epigean species, and the presence of autogenic drainage, which seems to prevent a significant decrease in resources towards the deeper areas of the cave;
4) As anticipated, environmental factors influencing the richness and composition of troglobitic and non-troglobitic invertebrates differed due to the specialized adaptations of these organisms to the cave environment;
5) It is worth noting that the environmental variables driving the variations in composition and richness of cave invertebrates are dependent on the scale of sampling;

6) Our study also supports the hypothesis that troglobitic species in tropical regions tend to be more prevalent in deep cave areas compared to non-troglobitic species. This preference is likely due to the climatic stability offered by these deeper areas, creating an ideal habitat for troglobitic species;
7) Our findings revel low niche overlap among widely distributed troglobitic species, suggesting that they select different habitat conditions;
8) Urgent collaborative conservation strategies are imperative to encompass both the Pedro Cassiano and Água Clara cave systems. A primary objective should be the establishment of a protected area that covers the hydrological basins contributing to these cave networks. This step is critical for safeguarding the exceptional subterranean fauna found in these remarkable Neotropical HSBs.

Author contributions

Rodrigo Lopes Ferreira and Marconi Souza-Silva formulated the idea, built the sample design and contributed to the literature review. Alicia Helena Souza Rodrigues Ferreira collected the data and sorted the invertebrates. Gabriel Augusto Silva Vaz performed the statistical analysis. Gabriel Augusto Silva Vaz wrote the manuscript with collaboration from Rodrigo Lopes Ferreira and Marconi Souza-Silva. Rodrigo Lopes Ferreira finalized the manuscript and contributed to the discussion of the results.

Acknowledgments

The authors would like to thank the Centro Nacional de Pesquisa e Conservação de Cavernas (CECAV) and Instituto Brasileiro de Desenvolvimento e Sustentabilidade (IABS) for the financial support (TCCE ICMBio/Vale 01/2018). We are also thankful to the CNPq (National Council for Scientific and Technological Development, grant n. 302925/2022-8) for the productivity scholarship provided to R.L.F., and to the team from the Center of Studies in Subterranean Biology (CEBS/UFLA) for the support in the field trips. Gabriel Augusto Silva Vaz was sponsored by FAPEMIG (Fundação de Amparo à Pesquisa do Estado de Minas Gerais) with a 12 month grant. This paper is part of his undergraduate thesis in Bachelor of Biology. We also thank Paulo Venâncio for his help with the map of the study area. Finally, we thank Joaquim Ferreira and family, residents, who provide accommodation in Agrovila 23.

References

Alvares, C.A., Stape, J.L., Sentelhas, P.C., De Moraes Gonçalves, J.L., Sparovek, G., 2013. Köppen's climate classification map for Brazil. Meteorologische Zeitschrift. 22, 711–728. https://doi.org/10.1127/0941-2948/2013/0507

Anderson, M.J., Gorley, R.N., Clarke, K.R., 2008. *PERMANOVA+ for PRIMER: Guide to Software and Statistical Methods*. Massey University, Albany Campus, Auckland: New Zealand.

Baptista, R.L.C., Guipponi, A.P. de L., 2002. A new troglomorphic Charinus from Brazil (Arachnida: Amblypygi: Charinidae). Ver Iber Aracnol. 6, 105–110.

Bento, D. de M., Ferreira, R.L., Prous, X., Souza-Silva, M., Bellini, B.C., Vasconcellos, A., 2016. Seasonal variations in cave invertebrate communities in the semiarid Caatinga, Brazil. Journal of Cave and Karst Studies. 78, 61–71. https://doi.org/10.4311/2015LSC0111

Bregović, P., Zagmajster, M., 2016. Understanding hotspots within a global hotspot – identifying the drivers of regional species richness patterns in terrestrial subterranean habitats. Insect. Conserv. Divers. 9, 268–281. https://doi.org/10.1111/icad.12164

Campbell Grant, E.H., 2011. Structural complexity, movement bias, and metapopulation extinction risk in dendritic ecological networks. J. North. Am. Benthol. Soc. 30, 252–258. https://doi.org/10.1899/09-120.1

Cardoso, R.C., Ferreira, R.L., Souza-Silva, M., 2022. Multi-spatial analysis on cave ecosystems to predict the diversity of subterranean invertebrates. Basic. Appl. Ecol. 65, 111–122. https://doi.org/10.1016/j.baae.2022.11.007

Carvalho, P.H.M.; Junta, V.G.P.; Castro-Souza, R.A.; Ferreira, R.L. Three new cricket species and a new subgenus of Endecous Saussure, 1878 (Grylloidea: Phalangopsidae) from caves in northeastern Brazil. Zootaxa 5263, 001–039. https://doi.org/10.11646/zootaxa.5263.1.1

Christiansen, K.A., 1962. Proposition pour la classification des animaux cavernicoles. Spelunca Mem 2, 76–78.

Culver, D.C., Fong, D.W., Jernigan, R.W., 1991. Species Interactions in Cave Stream Communities: Experimental Results and Microdistribution Effects, Source: The American Midland Naturalist.

Culver, D.C., Sket, B., 2000. Hotspots of subterranean biodiversity in caves and wells. Journal of Cave and Karst Studies 62, 11–17.

Culver DC., Pipan T., 2013. Subterranean Ecosystems. In: Levin SA (ed) Encyclopedia of Biodiversity, 2nd edn. Academic Press, Waltham, pp 49–62.

Culver, D.C., Pipan, T., 2015. Shifting paradigms of the evolution of cave life. Acta Carsologica 44, 415–425. https://doi.org/10.3986/ac.v44i3.1688

Deharveng, L., Bedos, A., 2000. The cave fauna of southeast Asia. In: Wilkens H, Culver DC, Humphries WF (eds) Origin, evolution and ecology—subterranean ecosystems. Elsevier, Amsterdam, pp 603–632.

Dial, R., Roughgarden, J., 1998. Theory of Marine Communities: The Intermediate Disturbance Hypothesis. Ecology 79, 1412. https://doi.org/10.2307/176752

Dolédec, S., Chessel, D., Gimaret-Carpentier, C., 2000. Niche Separation in Community Analysis: A New Method. Ecology 81, 2914. https://doi.org/10.2307/177351

Dray, S., Dufour, A.-B., 2007. The ade4 Package: Implementing the Duality Diagram for Ecologists. https://doi.org/10.18637/jss.v022.i04

Ferreira, T., Rasband, W., 2012. ImageJ user guide. *ImageJ/Fiji*, *1*, 155-161.

Ferreira, R.L., Prous, X., Martins, R.P., 2007. Structure of bat guano communities in a dry Brazilian cave. Tropical Zoology 20, 55–74.

Ferreira, R.L., Berbert-Born, M., Souza-Silva, M., 2023. The Água Clara Cave System in Northeastern Brazil: The Richest Hotspot of Subterranean Biodiversity in South America. Diversity (Basel) 15, 761. https://doi.org/10.3390/d15060761

Furtado-Oliveira, L., Ferreira, R.L., Rodríguez Fernández, J.I., Souza-Silva, M., 2022. Recreational caving impacts of visitors in a high-altitude cave in Bolivian Andes: main effects on microhabitat structure and faunal distribution. Int. J. Speleol. 51, 93–103. https://doi.org/10.5038/1827-806X.51.2.2418

González-Megías, A., María Gómez, J., Sánchez-Piñero, F., 2007. Diversity-habitat heterogeneity relationship at different spatial and temporal scales. Ecography 30, 31–41. https://doi.org/10.1111/j.2006.0906-7590.04867.x

Hartig, F., 2022. DHARMa: Residual Diagnostics for Hierarchical (Multi-Level/Mixed) Regression Models (Version 0.4.6). R package. https://CRAN.Rproject.org/package=DHARMa

Jaffé, R., Prous, X., Calux, A., Gastauer, M., Nicacio, G., Zampaulo, R., Souza-Filho, P.W.M., Oliveira, G., Brandi, I. V., Siqueira, J.O., 2018. Conserving relics from ancient underground worlds: Assessing the influence of cave and landscape features on obligate iron cave dwellers from the Eastern Amazon. PeerJ 2018. https://doi.org/10.7717/peerj.4531

Kozel, P., Novak, T., Janžekovič, F., Lipovšek, S., 2023. Starvation hardiness as preadaptation for life in subterranean habitats. Sci. Rep. 13. https://doi.org/10.1038/s41598-023-36556-9

Kozel, P., Pipan, T., Mammola, S., Culver, D.C., Novak, T., 2019. Distributional dynamics of a specialized subterranean community oppose the classical understanding of the preferred subterranean habitats. Invertebrate Biology 138. https://doi.org/10.1111/ivb.12254

Lunghi, E., Manenti, R., Ficetola, G.F., 2017. Cave features, seasonality and subterranean distribution of non-obligate cave dwellers. PeerJ. https://doi.org/10.7717/peerj.3169

Lunghi, E., Manenti, R., 2020. Cave communities: From the surface border to the deep darkness. Diversity (Basel) 12, 167. https://doi.org/10.3390/D12050167

Mammola, S., Piano, E., Giachino, P.M., Isaia, M., 2015. Seasonal dynamics and micro-climatic preference of two alpine endemic hypogean beetles. Int. J. Speleol. 44, 239–249. https://doi.org/10.5038/1827-806X.44.3.3

Mammola, S., Piano, E., Isaia, M., 2016. Step back! Niche dynamics in cave-dwelling predators. Acta Oecologica 75, 35–42. https://doi.org/10.1016/j.actao.2016.06.011

Mammola, S., Piano, E., Giachino, P.M., Isaia, M., 2017. An ecological survey of the invertebrate community at the epigean/hypogean interface. Subterr. Biol. 24, 27–52. https://doi.org/10.3897/subtbiol.24.21585

Mammola, S., Isaia, M., 2018. Day-night and seasonal variations of a subterranean invertebrate community in the twilight zone. Subterr. Biol. 27, 31–51. https://doi.org/10.3897/SUBTBIOL.27.28909

Mammola, S., 2019. Finding answers in the dark: caves as models in ecology fifty years after Poulson and White. Ecography 42, 1331-1351. https://doi.org/10.1111/ecog.03905

Mammola, S., Arnedo, M.A., Fišer, C., Cardoso, P., Dejanaz, A.J., Isaia, M., 2020a. Environmental filtering and convergent evolution determine the ecological specialization of subterranean spiders. Funct. Ecol. 34, 1064–1077. https://doi.org/10.1111/1365-2435.13527

Mammola, S., Chiappetta, N., Giachino, P.M., Antić, D., Zapparoli, M., Isaia, M., 2020b. Exploring the homogeneity of terrestrial subterranean communities at a local spatial scale. Ecol. Entomol. 45, 1053–1062. https://doi.org/10.1111/een.12883

Myers, N., Mittermeier[2], R.A., Mittermeier[2], C.G., Da Fonseca[3], G.A.B., Kent, J., 2000. Biodiversity hotspots for conservation priorities, NATURE 403(6772), 853-8.

Niemiller, M.L., Taylor, S.J., Bichuette, M.E., 2018. Conservation of Cave Fauna, with an Emphasis on Europe and the Americas. pp. 451–478. https://doi.org/10.1007/978-3-319-98852-8_22

Novak, T., Perc, M., Lipovšek, S., Janžekovič, F., 2012. Duality of terrestrial subterranean fauna. Int. J. Speleol. 41, 181–188. https://doi.org/10.5038/1827-806X.41.2.5

Oliver, I., Beattie, A.J., 1996. Invertebrate morphospecies as surrogates for species: A case study. Conservation Biology 10, 99–109. https://doi.org/10.1046/j.1523-1739.1996.10010099.x

Pacheco, G.S.M., de Oliveira, M.P.A., Cano, E., Souza-Silva, M., Ferreira, R.L., 2020. Tourism effects on the subterranean fauna in a Central American cave. Insect. Conserv. Divers 14, 294–306. https://doi.org/10.1111/icad.12451

Pacheco, G.S.M., Souza-Silva, M., Cano, E., Ferreira, R.L., 2020. The role of microhabitats in structuring cave invertebrate communities in Guatemala. Int J Speleol 49, 161–169. https://doi.org/10.5038/1827-806X.49.2.2333

Pellegrini, T.G., Sales, L.P., Aguiar, P., Ferreira, R.L., 2016. Linking spatial scale dependence of land-use descriptors and invertebrate cave community composition. Subterr. Biol. 18, 17-38. https://doi.org/10.3897/SUBTBIOL.18.8335

Pérez-González, A., Kury, A.B., 2002. A new remarkable troglomorphic Gonyleptid from Brazil (Aracnida, Opiliones, Laniatores). Revista Ibérica de Aracnología 5, 43–50.

Peterson, B.G., Carl, P., 2020. _PerformanceAnalytics: Econometric Tools for Performance and Risk Analysis_. R package version 2.0.4.

Prado, G.C.; Ferreira, R.L., 2023. Three new troglobitic species of Pseudochthonius Balzan, 1892 (Pseudoscorpiones, Chthoniidae) from northeastern Brazil. Zootaxa 5249, 92–110. https://doi.org/10.11646/zootaxa.5249.1.5

Prous, X., Ferreira, R.L., Jacobi, C.M., 2015. The entrance as a complex ecotone in a Neotropical cave. Int. J. Speleol. 44, 177–189. https://doi.org/10.5038/1827-806X.44.2.7

Prous, X., Lopes Ferreira, R., Parentoni Martins, R., 2004. Ecotone delimitation: Epigean-hypogean transition in cave ecosystems. Austral. Ecol. 29, 374–382. https://doi.org/10.1111/j.1442-9993.2004.01373.x

Rabelo, L.M., Souza-Silva, M., Ferreira, R.L., 2018. Priority caves for biodiversity conservation in a key karst area of Brazil: comparing the applicability of cave

conservation indices. Biodivers. Conserv. 27, 2097-2129. https://doi.org/10.1007/s10531-018-1554-6

Reis-Venâncio, P.C., Rabelo, L.M., Pellegrini, T.G., Ferreira, R.L., 2022. From light to darkness: the duality of influence of habitat heterogeneity on Neotropical terrestrial cave invertebrate communities. Stud. Neotrop. Fauna. Environ. 1-10. https://doi.org/10.1080/01650521.2022.2095832

Sánchez-Fernández, D., Rizzo, V., Bourdeau, C., Cieslak, A., Comas, J., Faille, A., Fresneda, J., Lleopart, E., Millán, A., Montes, A., Pallarés, S., Ribera, I., 2018a. The deep subterranean environment as a potential model system in ecological, biogeographical and evolutionary research. Subterr Biol 25, 1–7. https://doi.org/10.3897/subtbiol.25.23530

Schneider, K., Christman, M.C., Fagan, W.F., 2011. The influence of resource subsidies on cave invertebrates: results from an ecosystem-level manipulation experiment, Ecology 92, 765-776.

Schober, P., Boer, C., Schwarte, L. A., 2018. Correlation coefficients: appropriate use and interpretation. Anesthesia & analgesia, 126(5), 1763-1768. https://doi.org/10.1213/ANE.0000000000002864

Sket, B., 1999. The nature of biodiversity in hypogean waters and how it is endangered, Biodiversity and Conservation 8, 1319-1338.

Souza, M.V.R., Ferreira, R.L., 2010. Eukoenenia (Palpigradi: Eukoeneniidae) in Brazilian caves with the first troglobiotic palpigrade from South America. J Arachnol 38, 415–424. https://doi.org/10.1636/Ha09-112.1

Souza-Silva, M., Martins, R.P., Ferreira, R.L., 2011a. Trophic dynamics in a neotropical limestone cave. Subterr. Biol. 9, 127–138. https://doi.org/10.3897/subtbiol.9.2515

Souza-Silva, M., Martins, R.P., Ferreira, R.L., 2011b. Cave lithology determining the structure of the invertebrate communities in the Brazilian Atlantic Rain Forest. Biodivers. Conserv. 20, 1713–1729. https://doi.org/10.1007/s10531-011-0057-5

Souza-Silva, M., Bernardi, L.F.O., Martins, R.P., Ferreira, R.L., 2012. Transport and consumption of organic detritos in a neotropical limestone cave. Acta Carsologica 41, 139–150. https://doi.org/10.3986/ac.v41i1.54

Souza-Silva, M., Ferreira, R.L., 2016. The first two hotspots of subterranean biodiversity in South America. Subterr. Biol. 19, 1–21. https://doi.org/10.3897/subtbiol.19.8207

Souza-Silva, M., Cerqueira, R.F.V., Pellegrini, T.G., Ferreira, R.L., 2021. Habitat selection of cave-restricted fauna in a new hotspot of subterranean biodiversity in Neotropics. Biodivers. Conserv. 30, 4223–4250. https://doi.org/10.1007/s10531-021-02302-8

Tobin, B.W., Hutchins, B.T., Schwartz, B.F., 2013. Spatial and temporal changes in invertebrate assemblage structure from the entrance to deep-cave zone of a temperate marble cave. Int J Speleol 42, 203–214. https://doi.org/10.5038/1827-806X.42.3.4

Wynne, J.J., Howarth, F.G., Sommer, S., Dickson, B.G., 2019. Fifty years of cave arthropod sampling: Techniques and best practices. Int J Speleol 48, 33–48. https://doi.org/10.5038/1827-806X.48.1.2231

Zeppelini, D., Oliveira, J.V.L.C., de Lima, E.C.A., Brito, R.A., Ferreira, A.S., Stievano, L.C., Brito, N.P., Oliveira-Neto, M.A., Lopes, B.C.H., 2022. Hotspot in ferruginous rock may have serious implications in Brazilian conservation policy. Sci Rep 12. https://doi.org/10.1038/s41598-022-18798-1

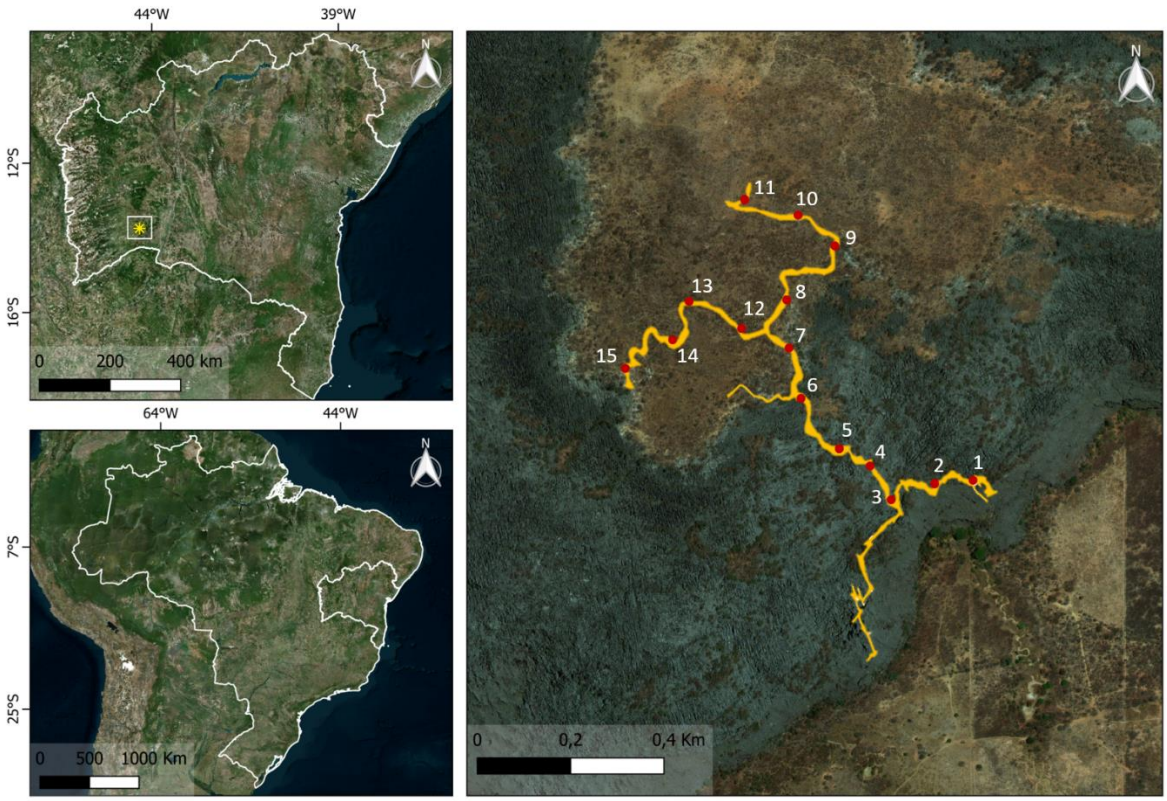


Figure 1. Location of the study site in the municipality of Carinhanha (yellow star, within the white square), Bahia state, Brazil. The cave map was modified from the original survey produced by the team from the Bambui Speleological group (http://www.gsbm.fr/publications/gsbm/2001_bahia99/2001_OCarste13_94_Rubbioli.pdf), and the red dots represent the sampling areas (quadrants and sectors) within the cave



Figure 2. Pedro Cassiano cave and its surroundings: A) Limestone outcrop were the cave is located (the yellow arrow indicates the main entrance of the cave); B) Main cave entrance; C) Cave inner conduit.



Figure 3. Some troglobites species from the Gruna do Pedro Cassiano cave: A) *Giupponia chagasi* (Opiliones: Gonyleptidae); B) *Charinus troglobius* (Amblypygi: Charinidae); C) Araneae sp4 (Araneae: Oonopidae); D) *Eukoenenia* sp. (Palpigradi: Eukoeneniidae).; E) *Pseudochthonius koinopoliteia* (Pseudoscorpiones: Chthoniidae); F) Ochyroceratidae (Araneae); G) Metagonia sp. (Araneae: Pholcidae); H) Clivinina sp1 (Coleoptera); I) Clivinina sp2 (Coleoptera); J) *Endecous infernalis* (Ensifera, Phalangopsidae); K) Blattidae (Blattodea); L) *Trogolaphysa* sp1 (Collembola: Paronellidae); M) Neelipleona (Collembola); N) Oniscodesmidae sp1 (Polydesmida); O) *Xangoniscus* sp. (Isopoda: Styloniscidae); P) *Pectenoniscus* sp. (Isopoda: Styloniscidae); Q) *Trychomycterus* sp. (Silurifomes: Trichomycteridae).

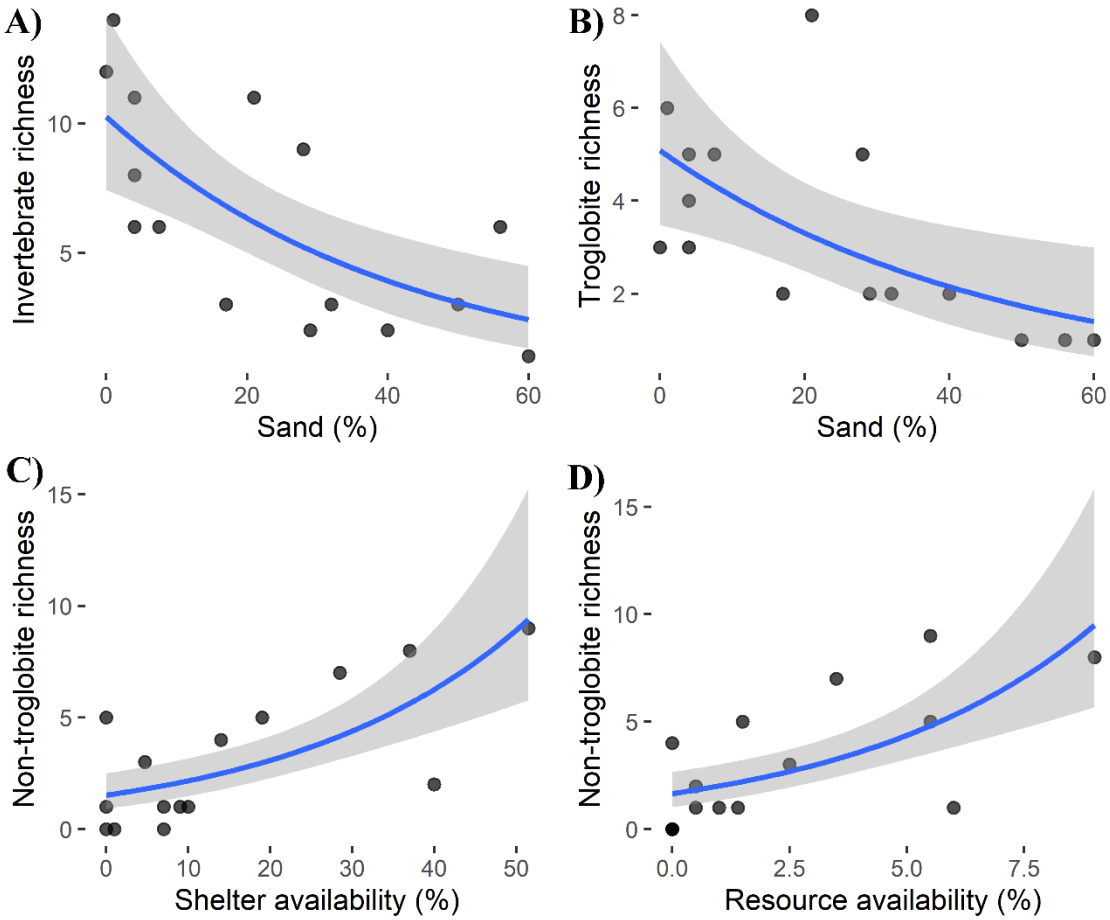


Figure 4. Relationship between the invertebrate richness with the percentage of sand on the mesoscale (**A**), the relationship between the troglobitic species richness with the percentage of sand on the mesoscale (**B**), the relationship between the non-troglobitic species richness with the shelter availability (**C**) and percentage of food resource at the mesoscale (**D**).

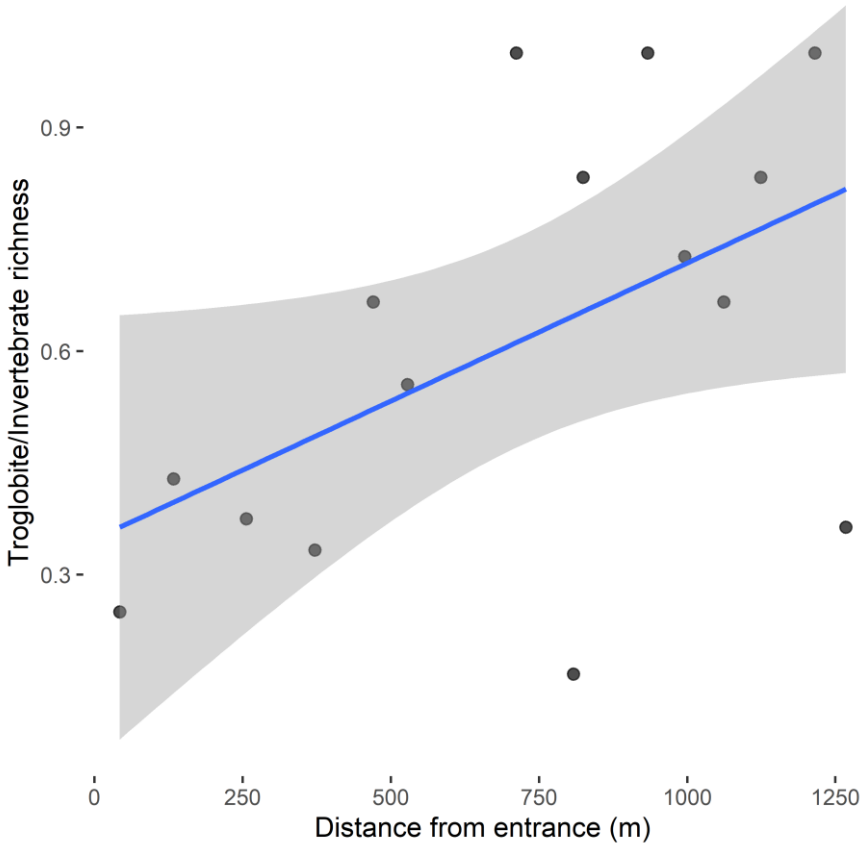


Figure 7. The relationship between cave entrance distance and troglobitic species richness/total invertebrate richness ratio.

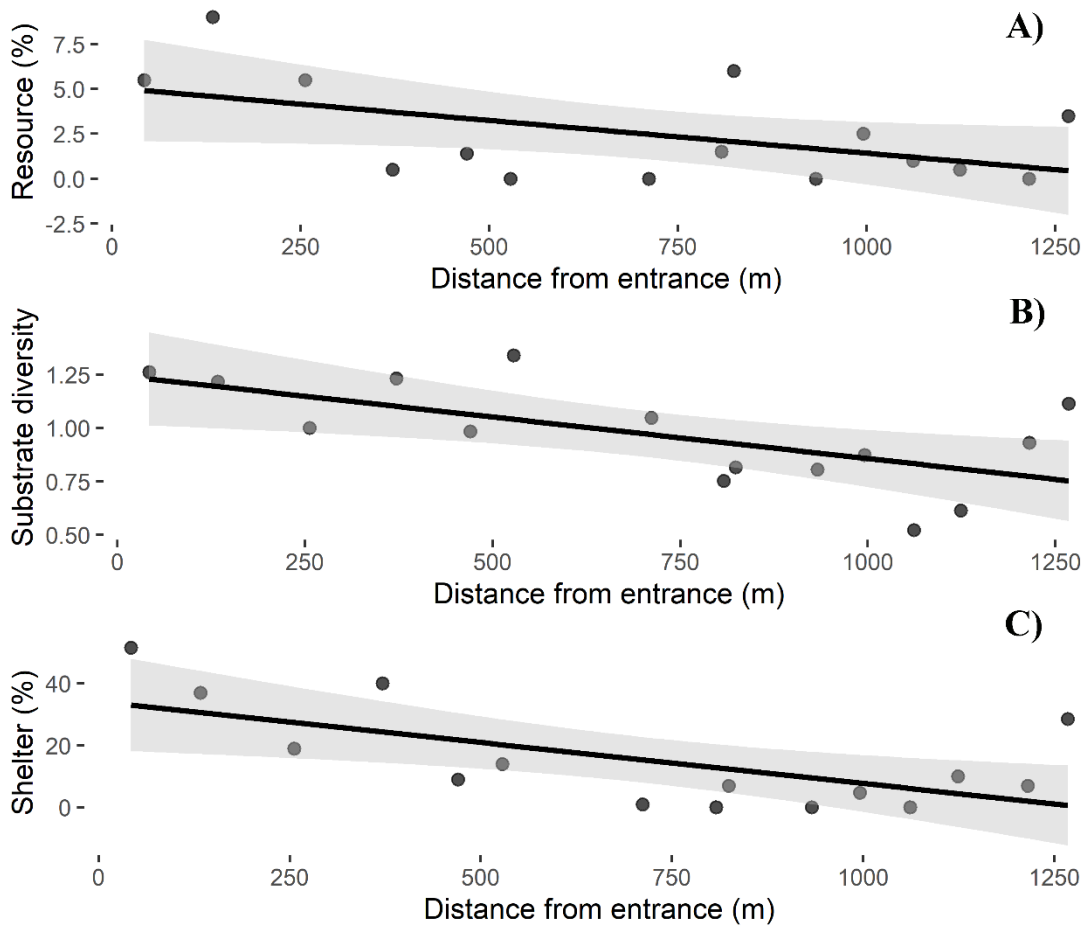


Figure 5. Relationship between percentage of resource availability (**A**), Substrate diversity (**B**), and percentage of Shelter (**C**), with distance from the cave entrance (m).

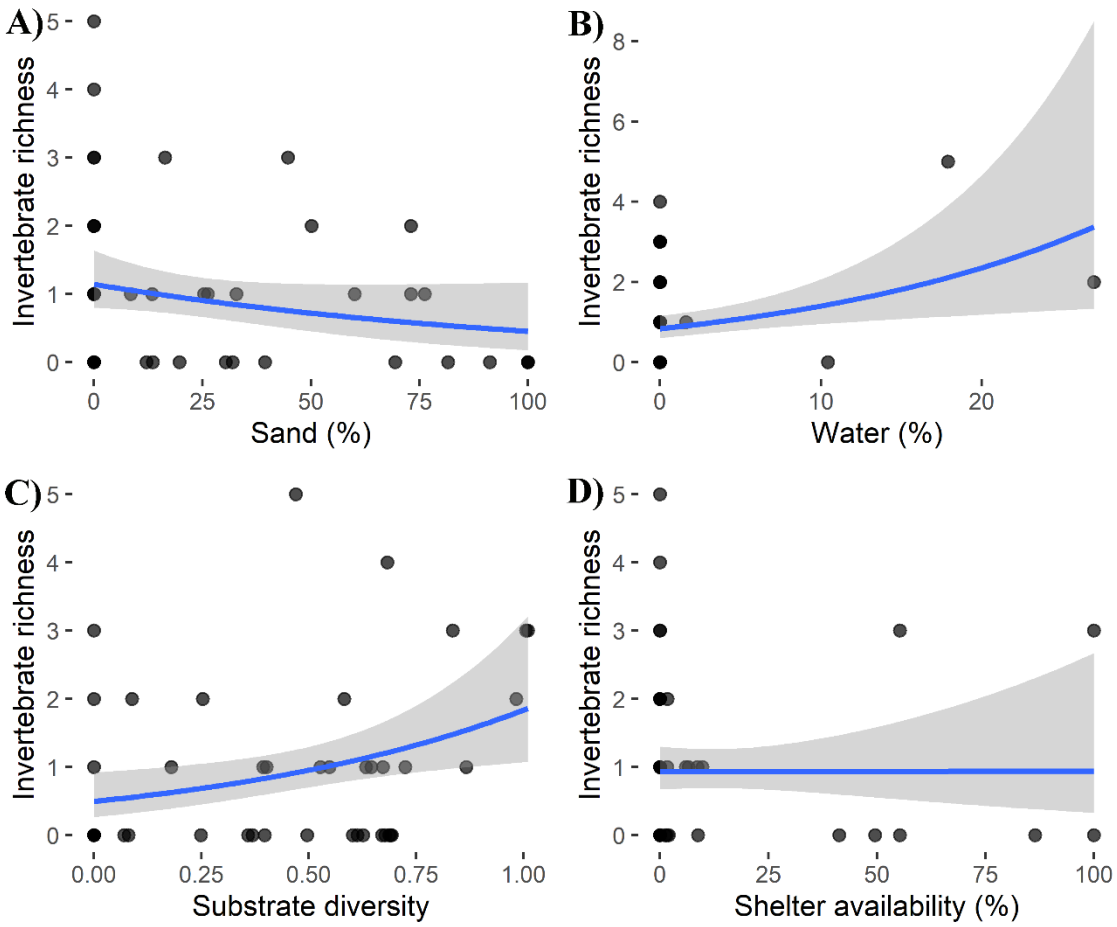


Figure 6. Relationship between the invertebrate richness with the percentage of sand **(A)**, percentage of area with water bodies (**B**), diversity of substrates (**C**), and percentage of shelter (**D**) at the microscale.

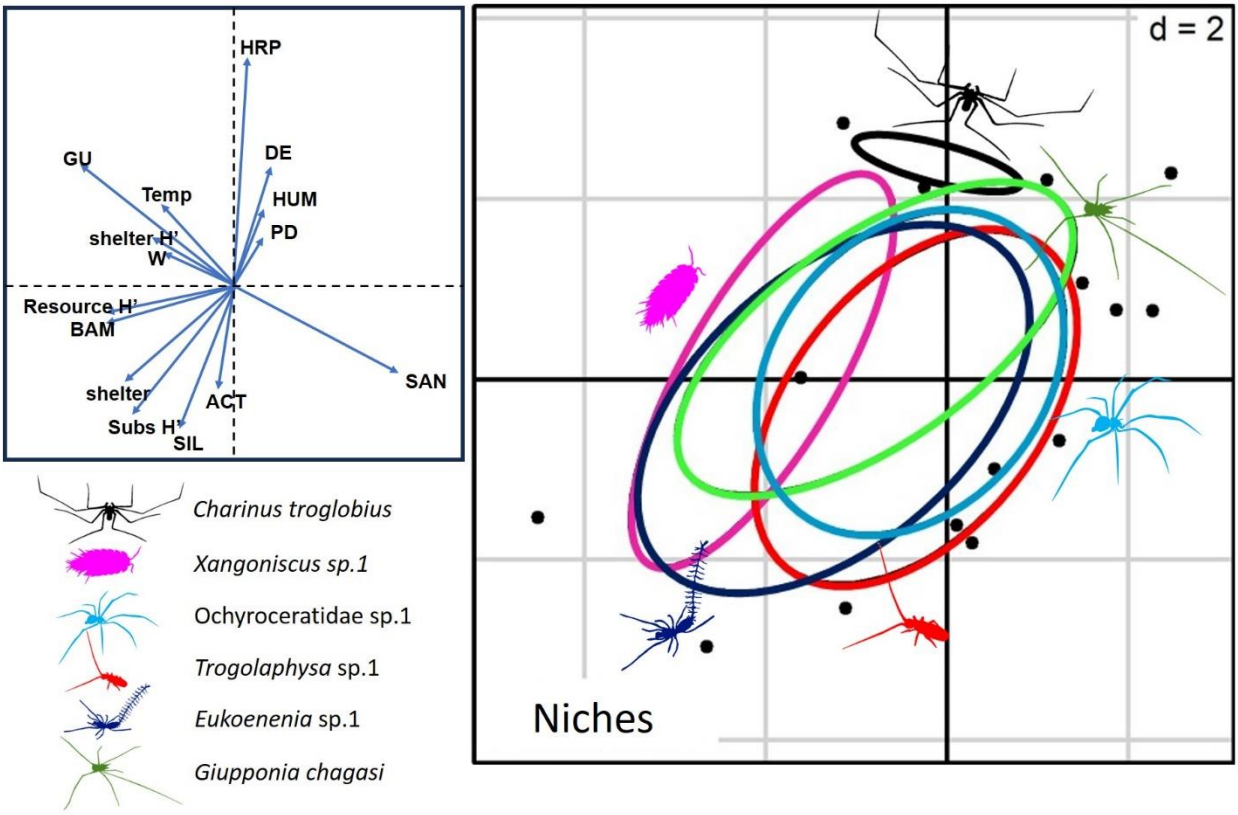


Figure 8. Outlying Marginality Index (OMI) showing species habitat selecting according to habitat components of cave floor. Hardpan (HRP), distance for entrance (DE), humidity (HUM), plant debris (PD), sand (SAN), Actinomycetes (ACT), Silt (SIL), substrate diversity (Subs H'), Basidiomycetes (BAM), resource diversity (Resource H'), water body (W), shelter diversity (shelter H'), guano (GU), temperature (temp).

Table 1. GLM models selected to explain the variation of richness in the mesoescale. S (invertebrate richness), S-t (troglobite richness), S-nt (non-troglobite richness), SAN (% sand), subs H' (diversity of substrate), HRP (% hardpan), shelter H' (diversity of shelter), W (% of areas with bodies of water), HUM (humidity), PseudoR² (percentage of explanation of models)

Model: S ~ SAN + subs H' + shelter H', family = negative binomial PseudoR² = 0,6630				
Variables	Estimate	Std.Error	Zvalue	Pr(>|z|)
Intercept	1,258443	0,528028	2,383	0,017159
SAN	-0,02088	0,6143	-3,399	0,000676*
subs H'	0,822354	0,48044	1,712	0,086957
shelter H'	0,438641	0,25902	1,693	0,090368

Model: S-t ~ HRP + SAN + shelter H', family = negative binomial PseudoR² = 0,6695				
Variables	Estimate	Std.Error	Zvalue	Pr(>|z|)
Intercept	1,14254	0,303031	3,77	0,000163
HRP	0,006742	0,004127	1,634	0,102339
SAN	-0,02203	0,008909	-2,473	0,013408*
shelter H'	0,05683	0,308535	1,842	0,065485

Model: S-nt ~ resource + HUM + shelter + W, family = poisson PseudoR² = 0,6428				
Variables	Estimate	Std.Error	Zvalue	Pr(>|z|)
Intercept	-9,21993	5,71600	-1,613	0,10674
resource	0,19486	0,07464	2,611	0,00904*
HUM'	0,09686	0,05763	1,681	0,09285
Shelter	0,04177	0,01368	3,053	0,00226*
W	-0,15305	0,09342	-1,638	0,10139

Table 2. GLM model selected to explain the variation of invertebrate richness in microscale. SAN (% sand), subs H' (diversity of substrate), HRP (% hardpan), shelter H' (diversity of shelter), W (% of areas with bodies of water), PseudoR² (percentage of explanation of models).

Model: S ~ W + SAN + subs H' + shelter + shelter H', family = poisson PseudoR² = 0,3728				
Variables	Estimate	Std.Error	Zvalue	Pr(>|z|)
Intercept	-0,52589	0,330073	-1,593	0,1111
W	0,065152	0,020709	3,146	0,00166*
SAN	-0,02322	0,007063	-3,288	0,00101*
subs H'	1,945431	0,60503	3,215	0,0013*
shelter	-0,02601	0,012641	-2,058	0,03962*
shelter H'	2,326601	1,19245	1,951	0,05104

Table 3. Results of Outlying Mean Index (OMI) analysis for the most widespread troglobitic species in cave Pedro Cassiano.

Troglobitic species	Inertia	OMI	Tol	Rtol	P value
Charinus troglobius	14, 71	5,93	0,35	8,41	0,15
Giupponia chagassi	16,08	2,28	2,45	11,34	0,657
Ochyroceratidae sp.1	14,48	0,41	1,22	12,83	0,678
Eukoenenia sp.1	18,56	2,16	4,14	12,26	0,406
Trogolaphysa sp.1	16,35	0,32	4,78	11,24	0,175
Xangoniscus sp.1	21,52	4,38	1,29	15,84	0,02*
OMI mean		2,58			0,109

COMMUNITY STRUCTURE THROUGHOUT A SINGLE CAVE



DETERMING FACTORS OF MICROHBAITST AND INVERTEBRATE COMMUNITY STRUCTURE THROUGHOUT A SINGLE CAVE: THE ROLE OF SPATIAL LOCATION AND DISTANCE OF THE MAIN ENTRANCES

Alicia Helena Souza Rodrigues Ferreira, Marconi Souza-Silva, Rodrigo Lopes Ferreira.
Universidade Federal de Lavras, Instituto de Ciências Naturais, Departamento Ecologia e Conservação, Centro de Estudos em Biologia Subterrânea, Caixa Postal 3037, CEP 37200-900, Lavras, MG, Brasil.

* Corresponding author: aliciahsrferreira@gmail.com
Ferreira, R.L. ORCID identifier is 0000-0003-3288-4405
Souza-Silva, M. ORCID identifier is 0000-0002-3184-531
Rodrigues-Ferreira, A.H.S ORCID identifier is 0000-0002-9965-2265

Abstract:
Even though the effects of location and distance from the entrance are known for a few decades, however, the effects of these variations along a single cave and on cave fauna are still quite unknown. Therefore, this work has the objective of evaluating the effects of spatial location and distance from the entrance in the microhabitats traits and how these variations affect the troglobitic and non-troglobitic fauna. Other variables were also collected such as temperature, humidity, trophic, and physical attributes to assess whether they also influence the fauna indirectly or directly. The invertebrate fauna was sampled using sectors (10x3m) and quadrats (1x1m), displayed on the cave floor. The distance from the entrance produces variations in conditions and resources, and as a result, forms distinct microhabitats that determine variations in the composition and richness of troglobitic fauna.
Keywords: Troglobitic, distance, entrance, microhabitats, cave.

INTRODUCTION

It is known that distance from the surface is an important environmental factor that influences cave features such as temperature, humidity, substrate heterogeneity, shelter and resource diversity, and availability, among others (Souza-Silva et al., 2021; Pacheco et al., 2020). Based on that, it is expected to observe a gradient of resources and conditions that consequently can promote distinct microhabitats and allow different species to co-exist (Culver & Pipan 2010; Pacheco et al., 2020; Souza-Silva et al., 2021). However, such gradient can also work by filtering and limiting species distribution, for non-troglobitic species, once as far from the entrance, the more homogeneous the habitat, are fewer resources available when compared to the amount of resources near the entrance, less shelter availability, and stabler values of temperature and humidity (Souza-Silva et al., 2021), which creates an unsuited environment for them. Therefore, the richness of non-troglobitic reduces as it enters the cave.

On the other hand, the richness of troglobitic species increase as it enters the cave, once at deepest parts of the cave possess stabler conditions of temperature and humidity. So, these microclimatic features are one of the main determinants of their distribution since they are not able to tolerate microclimatic fluctuations. Another peculiarity of deeper zones of the cave that allows the presence of troglobitic species, is the scarcity of food resources since they are resistant to starvation and also reduces the competition with other invertebrates (Novak et al., 2012; Tobin et al., 2013, Souza-Silva et al., 2021).

The maintenance of specific or representative habitats inside the caves can be an important strategy to protect populations and/or cave communities, mainly because the habitat requirements are different at different scales, ranging from macro to microhabitats, and habitat specialization is primarily driven by those environmental filtering (Pellegrini & Ferreira, 2012; Mammola et al., 2020a; Nicolosi et al., 2021). For example, Ferreira & Martins (2001) argued that the spatial distribution of terrestrial invertebrate communities in caves is strongly influenced by the distribution of food resources and habitat requirements (resource-space-dependent, resource-space independent, and para-epigean communities). The resource-space-dependent communities are those formed by generally small organisms (smaller than 5 mm) with low mobility, with populations preferentially observed within the limits of the organic resources (e.g. guano communities). The resource-space-independent communities are those in which organisms are not spatially restricted to the piles of organic resources, thus actively moving among distinct organic patches inside caves. Para-epigean communities are those occurring near the cave entrance, composed of epigean and hypogean organisms with low or moderate mobility (Ferreira & Martins, 2001; Prous et al., 2004). In addition, low-adapted species of spiders have a distribution primarily associated with external or cave entrance microhabitats, intermediate-adapted species live in shallow cave microhabitats, and highly-adapted species use deep cave microhabitats (Mammola et al., 2019; Cuff et al., 2021). Furthermore, micro and meso habitats can be defined not only regarding the different zonation of the cave (photic, twilight zone, transition zone, and deep zone) but also concerning different compartments within these zones (terrestrial, aquatic habitats, streams, puddles and water table) (Eberhard, 2001; Prous et al., 2004, 2015). Cave species, in turn, can be restricted to a certain type of habitat (Nicolosi et al., 2021, Souza-Silva et al., 2021) or they can present a wide distributional inside the cave, occurring in several habitat types (Peck, 1975; Eberhard, 2001; Ferreira & Martins, 2001).

Therefore, studies regarding space-scale dependence over cave invertebrates are indispensable to identify and understand the patterns for conservation (Pellegrini et al., 2016a). Thus, the main purpose of this study is to assess the response of the invertebrate species richness and composition against variations in some physical, trophic, and microclimate features inside a cave. It was also tested if the responses are different at distinct spatial scales. More specifically, it was evaluated the role of the spatial distribution of entrances and distance from the cave entrance on the microhabitats characteristics and how such variations can affect troglobitic and non-troglobitic distribution It was hypothesized that troglobitic species will respond to variations in cave environmental features choosing stable

and oligotrophic places far from the entrance. On the other hand, non-troglobitic distribution inside the cave will be limited by the true cave characteristic (high humidity and oligotrophy).

MATERIALS AND METHODS

Study area

This study was carried out at "Três Cobras" limestone Cave (13°37'6.63"S 43°45'9.87"O), located in the karst area of Serra do Ramalho, southwestern Bahia (Figure 1). This region is formed by large limestone areas, belonging to the Jacaré formation, Bambuí group. It is inserted in Caatinga domain and in the middle of São Francisco River basin. According to Köppen's climate classification system, the local climate type is "Aw", with a dry winter and an average annual precipitation rate between 800 and 1000 mm (Gonçalves et al., 2018)

The Três Cobras Cave has 5620m of horizontal projection and a slope of 32m. The cave is composed of labyrinthine conduits, presenting seven entrances (Figure 1). This region differs from the rest by presenting lower outcrops and isolated outcrops eminences. Entrances A, B and C of the cave face to pasture, an area with few/ almost no trees near, while entrance D faced an area with a dry forest with scattered trees. Finally, the entrances E, F and G, are faced to a densest dry forest.

Fields procedures

Sampling invertebrates along the Três Cobras cave floor

To evaluate variations on invertebrate species composition and richness along the cave sectors (3 x 10m) containing 3 quadrats (1 x 1m) were placed on the cave floor at least 100m apart from each other. Sectors and quadrants were considered "mesoscale' and "microscale", respectively. Distance from the entrances and sample unit positions were taken using a laser tape measure.

The invertebrate fauna was recorded in the sectors and quadrats through detailed visual search and hand sampling using tweezers and brushes (Souza-Silva et al., 2021; Oliveira Furtado et al., 2022). Sampled invertebrates were stored in plastic tubes with alcohol 70% aiming for the preservation of the material for identification in the laboratory. In order to minimize the impact on cave fauna, some specimens were collected, and their abundance where accounted (Pacheco et al., 2020; Souza-Silva et al., 2021; Oliveira Furtado et al., 2022).

The specimen's identification was made through taxonomic keys at the lowest taxonomic level accessible. Identifying troglobitic species considered troglomorphisms, which are traits that represent their evolution and adaptability to subterranean environments. The troglomorphisms observed were a lack or reduction in ocular structure and pigmentation, and elongation of appendices and sensorial structures (Culver & Pipan, 2009). When specialists were available, they were consulted for the following orders Isopoda, Pseudoscorpiones, Orthoptera, Acari, Entomobryomorpha and Diplopoda. All the collected specimens are deposited in the Lavras Subterranean Invertebrates Collection (ISLA), affined to the Center of Studies on Subterranean Biology at the Federal University of Lavras, Minas Gerais, Brazil (http://www.biologiasubterranea.com.br/en/about-the-group/).

Abiotic attributes of the cave floor

The temperature and humidity were taken with a thermohygrometer device inside every sampling sector (accuracy ± 1°C for temperature and ±5% for relative humidity). The device was placed on the cave floor and the values were obtain after its stabilization. To avoid the interference/alter the values, the presence of people prevents (Souza-Silva et al., 2021; Oliveira Furtado et al., 2022).

To measure abiotic attributes in mesoscale, the sectors were fractionated into 10 sections of 1 meter each and were made a visual estimate of the percentual of substrate and resources available on the cave floor, as proposed by Pellegrini et al., (2016a), and Souza-Silva et al., (2021). To measure the abiotic in a microscale/quadrat, photographs were taken before the collection occurred. To take the photographs were used a Canon Powershot SX50, HS (4000 x 3000 pixels). Posteriorly, the photos were analyzed with the aid of ImageJ software (Rasband, 1997), and finally, the arithmetic average of every abiotic attribute was made (Souza-Silva et al., 2021; Oliveira Furtado et al., 2022).

Data analysis

Biotic attributes of the caves

The abundance and richness of non-troglobitic and troglobitic were obtained by counting individuals and morphotypes of each sample unit (22 sectors and 66 quadrats).

Abiotic attributes on the cave floor regarding the sectors

All the *physical*, *trophic,* and *microclimatic* characteristics of the sectors were classified in the following classes: guano GU, hematophagous guano-GH, other mammals feces-FZM, carcass-CRC, litter-SER, plants debris-DTV (> 10mm), rock-RR, concrete-like floor-RC, medium rock -MB(500-1000mm), small rock -SB(250-500mm), cobbles-CB (64-250mm), coarse gravel-CAG (16-64mm), fine gravel-CAF (2-16mm), sand-ARE (0.06-2mm), silt-SEF (≤ 0.05 mm), hardpan-HP, stalagmite-EG, speleothems-ES, retraction cracks-GR, cave-wall-PA, hardpan pinnacle-PHP, speleothems- ES, another inorganic substrate-OTI.

Based on such classes we obtained the *physical features* that included distance from the entrance, the substrate diversity (calculated considering all classes above), the shelter diversity (calculated considering RR, RC, MB, SB, CB, CAG, CAF, ES, EG, GR, PA, and PHP) and trophic resources diversity (calculated considering GU, GH, FZM, CRC, SER and DTV). All diversities were calculated using the Shannon-Weaver Index (Buttigieg & Ramette, 2014).

The availabilities of each *Abiotic attribute* were also included as *physical*, *trophic* and *microclimatic* characteristics. The shelter availability was calculated by the sum of SER, DTV, GALF, GALM, GALG, TRO, RR, RC, XB, MB, RR, RC, MB, SB, CB, CAG, CAF, ES, EG, GR, PA, and PHP in each sector. On the other side, the trophic resource availability was calculated by the sum of considering GU, GH, FZM, CRC, SER, and DTV in each sector, and are also the same for the *trophic resources.* Finally, the *microclimatic variables* considered were temperature and humidity.

Abiotic attributes on the cave floor regarding the quadrats

On the other hand, *physical* and *trophic* characteristics of the quadrats were evaluated and classified into the following classes: guano—GU, roots—RZ, plants debris-DTV (>10mm),

fine branch -GRAF (11-30 mm), drip water-DP, another organic substrate—OTO, smooth rock—RL, rough rock—RR, wide rock—XB (1000-4000mm), medium rock-MB (500-1000mm), a small rock-SB(250-500mm), cobbles-CB (64-250mm), coarse gravel-CAG (16-64mm), fine gravel-CAF (2-16mm), sand-ARE (0.06-2mm), silt-SEF (0.2 < diameter ≤ 0.05 mm), hardpan-HP, speleothems-ES and retraction cracks-GR.

Based on such classes we obtained the *physical features* that included distance from the entrance, the substrate diversity (calculated considering all classes above), the shelter diversity (calculated considering RR, XB, MB, SB, CB, CAG, CAF, and GR), and trophic resources diversity (calculated considering GU, RZ, DTV, GALF, and OTO). All diversities were calculated using the Shannon-Weaver Index (Buttigieg & Ramette, 2014).

The availabilities are also included in *physical*, *trophic,* and *microclimatic* characteristics. The shelter availability was calculated by the sum of DTV, GALF, RR, XB, MB, SB, CB, CAG, CAF, and GR in each quadrat. On the other side, the trophic resource availability was calculated by the sum of GU, RZ, DTV, GALF, and OTO in each quadrat, and are also the same for the *trophic resources*.

Relationship between habitat structure of the sectors and quadrats with cave fauna

To predict the influence of local abiotic variables on total species richness, species richness of non-troglobitic and species richness of troglobitic (response variables), using sectors as sample units was performed a *General Linear Models* (GLM) and temperature (ºC), humidity (%), distance from the cave entrance, diversity of shelter, diversity of substrate, diversity of resources, availability of shelter and availability of resources as response variables. The same was made using the quadrats as sample units, however, temperature and humidity were not included in the model, since their values were not taken in each quadrat.

The Poisson family was chosen to be part of the GLM's, since it is used when models depend on the counting of events in space or time. To compare the model results with the null models, the ANOVA function from 'Vegan' package was performed. To assess the overdispersion the function CHECK_OVERDISPERSION from the package 'Performance' was applied. Were used function r.squaredLR from the 'piecewiseSEM' package in order to obtain r^2 values of the GLM's. The correlation of all variables was tested before running the models, for that, CHART. CORRELATION from the 'PerformanceAnalytics' package. Variables with high correlation values (>0.65) were excluded from the model as proposed by Zuur et al., (2010). To test if exist multicollinearity, the function VIF from 'Car' package was used, however, none of them were presented.

It was performed a Distance-based redundancy analysis (dbRDA) based on the Bray-Curtis similarity matrix in order to explain the possible relationships, s strength, and direction (- or +) between +) between overall fauna, non-troglobitic and troglobitic species composition with the *physical*, *trophic*, and *microclimatic* variables (Clarke et al., 2014).

Variations on habitat structure

The possible differences between temperature, humidity, substrate diversity, shelter diversity, resource diversity, availability of resources, and availability of shelter among the seven entrances, sectors, and quadrats (here temperature and humidity were not used since it

was not measure in this scale) using KRUSKAL.TEST function from the 'Stats' package in RStudio. To compare all-pairs for Kruskall-Wallis ranked data, we used the function KWALLPAIRSNEMENYITEST from the 'PCMCRplus' package. To test if *trophic*, *microclimatic,* and *physical* attributes varied depending on the distance from the entrance using the sectors, it was made a *Linear Regression.* The same analysis was performed using the quadrats as sample unit. All regressions were performed using the function LM from 'Stats' package in RStudio.

RESULTS

Biotic attributes of the cave

A total of 571 individuals were recorded, distributed in 26 orders and 55 families, and 126 morphospecies. From the total 15 were considered troglobitic (11.9 %). The richest order considering overall fauna was Araneae (31 ssp.), followed by Coleoptera (19 ssp.) and Diptera (12 ssp.). The richest order of non-troglobitic species was Araneae (28 ssp.), followed by Coleoptera (19 ssp.) and Diptera (12 spp.). Lastly, the richest orders of troglobitic species were Isopoda (5 ssp.), Collembola (3 ssp.), Polydesmida, and Araneae (2 ssp., each) (Figure 2A, B). The relationship between non-troglobitic and troglobitic fauna is shown in Figure 2C. Some of the troglobitic species found in Three Cobras Caves are shown in Figure 3.

Relationship between habitat structure inside the sectors with cave fauna

For the overall fauna, the non-troglobitic (nTB) and the troglobitic (TB), none of the variables here used explained its species richness variations. Regarding the dbRDA, for the overall fauna and troglobitic only distance from the entrance was the best predictor, explaining 8.0% and 11% of the variation in species composition (p=0.03 and 0.05, respectively), (Figure 4). None of the used variables explained the variation in the composition of the troglobitic species.

For the troglobitic species, variation in species richness was best explained only by resource availability (R^2= 0.19, p=0.0007). Regarding the overall fauna and non-troglobitic none of the variables here used explained species richness variations. Regarding the dbRDA, for the troglobitic only resource availability was the best predictor, explaining 12% of the variation in species composition (p=0.005). Regarding the overall fauna and non-troglobitic none of the variables here collected explained variation in species composition (Figure 5).

Variations in habitat structure

The values of temperature, humidity, substrate diversity, resource diversity, shelter diversity, availability of resources, and availability of shelter of the sectors and quadrats are shown in Material Supplementary I and II. When using the data of the sector, none of the variables showed any differences in the averages among the entrances, while using the quadrats data, the distance from the entrance (B≠C, p=0.004; C≠G, P= 0.01), resource availability (A≠ C, p=0.052; B ≠ C, p=0.056; C≠G, P= 0.04) and shelter availability (C≠E, p=0.03) showed differences in the averages among the entrances. Lastly, the remaining predictor variables did not show differences in averages when using sectors and quadrats as variable responses.

Regarding the sectors, only the humidity indicated a negative relationship with the distance from the entrance ($R^2 = 0.36$, $p = 0.002$), While regarding the quadrats, only the resource availability ($R^2 = 0.77$, $p = 2^{-16}$) showed a positive relationship with the distance from the entrance and shelter availability ($R^2 = 0.17$, $p = 0.0003$) showed a negative relationship with the distance from the entrance.

DISCUSSION

The study calls attention to the usage of different sampling scales and different abiotic and biotic features in only one cave. These features showed to be more influential over troglobitic species than non-troglobitic species, in both mesoscale (sector) and microscale (quadrat). Besides that, distance from the entrance had an effect in decreasing humidity and shelter availability, while resource availability had an effect in increasing it as far from the entrance. Therefore, the distance from the entrance is an important factor in structuring the subterranean cave communities.

Relationship between habitat structure of the sectors and quadrats with cave fauna

Our findings corroborate with our hypothesis that troglobitic species respond differently than non-troglobitic to the variables and at the two-sampling scales and that their distribution along the cave is different. There were expected troglobitic to live in deeper zones of the cave and non-troglobitic in parts nearest the entrance.

The troglobitic species richness and composition responded to resource availability and distance from the entrance, while non-troglobitic did not respond to the variables here explored, while the overall fauna responded to distance from the entrance.

Plant debris and litter are the main food resource for the cave invertebrate communities in Três Cobras Cave (3CC). Vegetation in outcrop limestone in Caatinga accumulates plenty of leaves in the soil during the dry season, which later in the rainy season is taken to inside the cave by rains or through river input. The input of these resources that are not washed off can accumulate in the sediment bank (Souza-Silva et al., 2011). Therefore, supplying constant food to these environments. The input of resources can also be given through percolation and surface runoff (Ferreira et al., 2010).

In contrast, the other resource available in Três Cobras Cave is guano which is supplied by bats as they enter the cave. This resource is essential in the structure of cavernicolous invertebrate communities once the guano can maintain many species. On the other hand, guano deposited in places far from the water bodies cannot be exported, therefore being available for longer periods (Faria, 1996; Souza-Silva et al., 2011 trophic). The low guano availability can be due to a part of the 3CC surroundings being covered by pasture and the other part by vegetation, meaning that caves surrounded by vegetation can potentially be colonized by a bigger diversity of bats, therefore, preserving caves' surroundings can affect its invertebrate communities (Cardoso et. al. 2022).

The species richness decreased further from the entrances of the cave which can be related to the habitat homogeneity and scarcity of food resource availability, found in the deepest parts. These environments can be suitable for troglobitic species since they present

morphological adaptations to live under extreme conditions, such as eye size reduction, appendage elongation, thin coticule, and resistance to starvation, among others (Romero & Green, 2005). These adaptations/specializations were developed through selective pressures or the lack of them at the parts of the cave (Culver, 1982). As a result, troglobitic species are rare and endemic, having a low population rate, and low tolerance to environmental changes.

Variations in habitat structure

The abiotic data set sampled inside the quadrats indicated that resource availability from the entrances A and C, B and C, C and G are different (p=0.052, p=0.056 and 0.04, respectively). The differences noted between these features can be related to the vegetation near the entrances, the distribution, size, and inclination of entrances of Três Cobras Cave, and the type of substrate available. However, is not possible to affirm for sure since not all entrances were accessed, and size and inclination were not measured. On the other hand, some studies showed the importance of the land cover and land use surrounding the cave entrances over cave fauna (Souza-Silva et al., 2015; Jaffé et al., 2018; Canedoli et al., 2022, Cardoso et al 2022), since these underground environments are connected to external one. Therefore, in areas bordering caves with deforestation, soil erosion is common, which might be carried inside the cave and silt up the water bodies present (Bárány-Kevei, 1999).

Furthermore, when considering the physical and microclimatic characteristics within subterranean environments at distinct sampling scales, they may increase/decrease as you move farther from the entrance. About the sectors, only the humidity varied, while for the quadrats only resource availability and shelter availability varied. Resource availability was the only variable positively influenced by the distance from the entrance, which means as far from the entrance higher its value, this can be probably explained due to that half of the sectors were collected at least 1 km from the entrance. On the other hand, the humidity and shelter availability showed a negative relationship with the distance from the entrance, which means as far from the entrance its values were reduced. Regarding the humidity, is the opposite of expected, since it is expected the humidity gets stabler as far from the entrance, however in 3CC, eleven sectors were sampled at least one kilometer from the entrance, so probably is due to the places the sectors were placed. The shelter, availability was expected since the cave was extremely dry and presented a heterogeneity of substrates that can be used as shelters along the cave. An elevated number of substrates can provide different types of shelter and consequently attend to different species, increasing both species richness and composition (Poulson & Kane, 1977; Pacheco et al., 2020). These results are supported by Holsinger & Culver (1988), that geological structure affects the subterranean fauna and its ecological complexity.

In conclusion, the distance from the entrance can create filters over conditions and resources that further affect the subterranean invertebrate fauna by the formation of microhabitats along the caves, permitting the co-existence of several species without niche overlapping. The presence of several entrances is another factor that can influence conditions and resources; however, it was not evaluated in this paper, therefore needing more studies to

check the relationship between several entrances and their external environment such as forest/pasture and the distance from the entrance.

Acknowledgments: The authors would like to thank the Programa de Pós-Graduação in Applied Ecology (UFLA), Center of Study in Subterranean Biology (CEBS/UFLA) for providing structure for the development of the study; to Paulo, Guilherme, Giovanna, Gabrielle, Leandro for helping with the collections; to Giovanna Cardoso, Guilherme Prado, Leopoldo Benardi, Vitor Gabriel, Ivan, Danielle, Paola, Rodrigo (diplópodes) and Vinicius for helping with invertebrate identification. We also thank Joaquim Lopes for receiving us in his house during our stay in Agrovila 23, and Lózin, Vanuza, Duzinho, for welcoming us and accompanying in the field.

Funding: This work was supported by Termo Aditivo de Compromisso de Compensação Espeleológica nº 1/2018, firmado entre o Instituto Chico Mendes de Conservação e Biodiversidade (ICMBio-Vale S.A.) regarding the implementation of compensation for the irreversible negative impacts of natural underground cavities with a high degree of relevance, through the project: " Dispersion versus confinement: compositional analysis and habitat structure as a subsidy to the understanding of mechanisms responsible for subterranean fauna identity". Author Alicia Ferreira has received research support from Cnpq (Conselho Nacional de Pesquisa).
Competing Interests: The authors have no relevant financial or non-financial interests to disclose.

REFERENCES

Bàràny-Kevei, I.,1999. Impact of agricultural land use on some Hungarian karst regions. International Journal of Speleology, 28(1):6.

Buttigieg, P.L., Ramette A., 2014. A Guide to Statistical Analysis in Microbial Ecology: a communityfocused, living review of multivariate data analyses. FEMS Microbiol Ecol 90:543–550. https://doi. org/10.1111/1574-6941.12437.

Canedoli, C., Ficetola, G. F., Corengia, D., Tognini, P., Ferrario, A., Padoa-Schioppa, E., 2022. Integrating landscape ecology and the assessment of ecosystem services in the study of karst areas. Landscape Ecology, 37(1):347–365. doi:10.1007/s10980-021-01351-2.

Cardoso, R. C., Ferreira, R. L., & Souza-Silva, M. (2022). Multi-spatial analysis on cave ecosystems to predict the diversity of subterranean invertebrates. Basic and Applied Ecology, 65, 111-122.

Cuff, J.P., Aharon, S., Armiach Steinpress, I., Seifan, M., Lubin, Y., Gavish-Regev, E., 2021. It's All about the Zone: Spider Assemblages in Different Ecological Zones of Levantine Caves. Diversity, 13:576.

Culver D.C., Pipan, T., 2010. Climate, abiotic factors, and the evolution of subterranean life. Acta carsologica, 39.3.

Culver, D., 1982. Cave life. Harvard University Press.

Culver, D.C., Pipan, T., 2009. Biology of Caves and Other Subterranean Habitats, 1st edn. Oxford, New York.

Eberhard, S., 2001. Cave fauna monitoring and management at Ida Bay, Tasmania. Records of the Western Australia Museum Supplement, 64:97-104.

Ferreira R.L., Prous X., Bernardi L.F.O., Souza-Silva M., 2010. Fauna subterrânea do Estado do Rio Grande do Norte: Caracterização e impactos. Rev Bras Espeleol 1:25–51.

Ferreira, R.L. & Martins, R.P. (2001) Cavernas em risco de 'extinção'. Ciência Hoje, 29, 20-28.

Holsinger, J.R., Culver D.C., 1988. The invertebrate cave fauna of Virginia and a part of eastern Tennessee: Zoogeography and Ecology. Brimleyana 14: 1-162.

Jaffe, R., Prous, X., Calux, A., Gastauer, M., Nicacio, G., Zampaulo, R., Souza-Filho, P. W. M., Oliveira, G., Brandi, I. V., Siqueira, J. O., 2018. Conserving relics from ancient underground worlds: Assessing the influence of cave and landscape features on obligate iron cave dwellers from the Eastern Amazon. PeerJ, 6: e4531. doi:10.7717/peerj.4531.

Juberthie, C., Delay, B., Bouillon, M., 1980. Extension du Milieu Souterrain en zone non-Calcaire. Mem. Biospeol. 7, 19-52.

Mammola, S., Arnedo, M.A., Fišer, C., Cardoso, P., Dejanaz, A.J., Isaia, M., 2020. Environmental filtering and convergent evolution determine the ecological specialization of subterranean spiders. Functional Ecology, 34:1064–1077.

Mammola, S., Piano, E., Malard, F., Vernon, P., Isaia, M., 2019. Extending Janzen's hypothesis to temperate regions: A test using subterranean ecosystems. Functional Ecology, 33:1638–1650.

Nicolosi, G., Mammola, S., Costanzo, S., Sabella, G., Cirrincione, R., Signorello, G., Isaia M., 2021. Microhabitat selection of a Sicilian subterranean woodlouse and its implications for cave management. International Journal of Speleology, 50 (1):53-63.

Oliveira, L.F., et al., 2022. Recreational caving impacts of visitors in a high-altitude cave in Bolivian Andes: main effects on microhabitat structure and faunal distribution. International Journal of Speleology 51.2:2.

Pacheco, G.S.M., Souza-Silva, M., Cano, E., Ferreira R.L., 2020. The role of microhabitats in structuring cave invertebrate communities in Guatemala. International Journal of Speleology, 49 (2):161-169. Tampa, FL (USA) ISSN 0392-6672.

Peck, S.B., 1975 A population study of the cave beetle *Ptomaphagus loedingi* (Coleoptera; Leiodidae; Catopinae). International Journal of Speleology, 7(1):3.

Pellegrini, T.G., & Ferreira, R.L., 2016. Are inner cave communities more stable than entrance communities in Lapa Nova show cave? Subterranean Biology, 20:15–37.

Poulson, T.L., Kane, T.C., 1977. Ecological diversity and stability: Principles and management. In Proceedings 1976 National Cave Management Symposium: Albuquerque, NM, Speleobooks (pp. 18-21).

Prous, X., Ferreira R.L., Jacobi, C.M., 2015. The entrance as a complex ecotone in a Neotropical cave. International Journal of Speleology, 44 (2):177-189.

Prous, X., Ferreira, R.L., Martins, R.P., 2004. Ecotone delimitation: Epigean–hypogean transition in cave ecosystems. Austral Ecology, 29(4):374-382.

Rasband, W.S., 1997. Image, J., US National Institutes of Health. "ImageJ64," US National Institutes of Health, Bethesda, MD.

Romero, A., Green, S.M., 2005. The end of regressive evolution: examining and interpreting the evidence from cave fishes. Journal of fish biology, 67(1): 3-32.

Souza-Silva, M., Cerqueira, R.F.V., Pellegrini T.G. et al., 2021. Habitat selection of cave-restricted fauna in a new hotspot of subterranean biodiversity in Neotropics. Biodivers Conserv 30:4223–4250. https://doi.org/10.1007/s10531-021-02302-8.

Souza-Silva, M., Martins, R. P., Ferreira, R.L., 2015. Cave conservation priority index to adopt a rapid protection strategy: A case study in Brazilian Atlantic rain forest. Environmental Management, 55(2):279–295. doi:10.1007/s00267-014-0414-8.

Souza-Silva, M., Martins, R.P., Ferreira, R.L., 2011. Trophic Dynamics in a Neotropical Limestone Cave. Subterranean Biology 9: 127–138. doi: 10.3897/subtbiol.9.2515.

Tobin, B.W., Hutchins, B.T., Schwartz, B.F., 2013. Spatial and temporal changes in invertebrate assemblage structure from the entrance to deep-cave zone of a temperate marble cave. International Journal of Speleology, 42 (3):203-214. https://doi.org/10.5038/1827-806X.42.3.4.

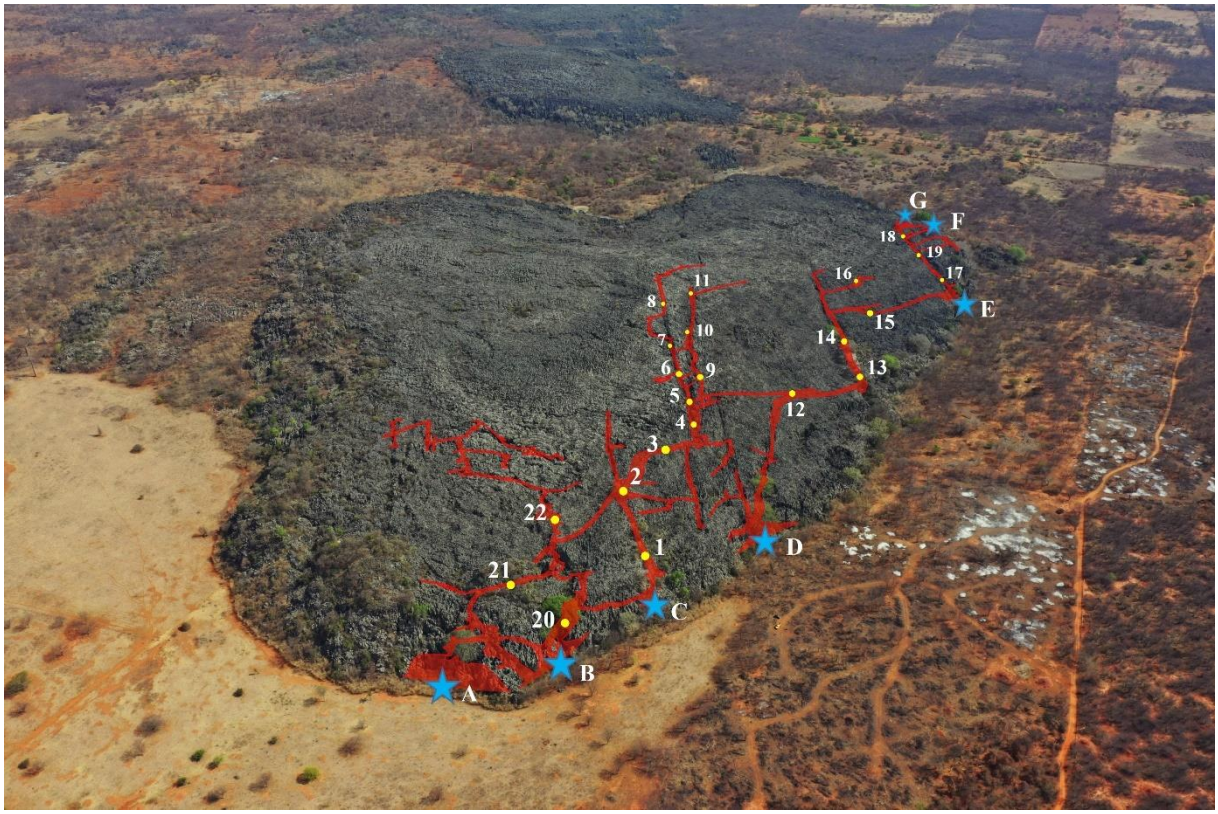


Figure 1. Map showing the outcrop where Three Cobras Cave is inserted, as showing the mapped area of the cave, the seven main entrances (marked with a blue star and white letters A-F) and the places where the sectors were placed (number from 1 to 22).

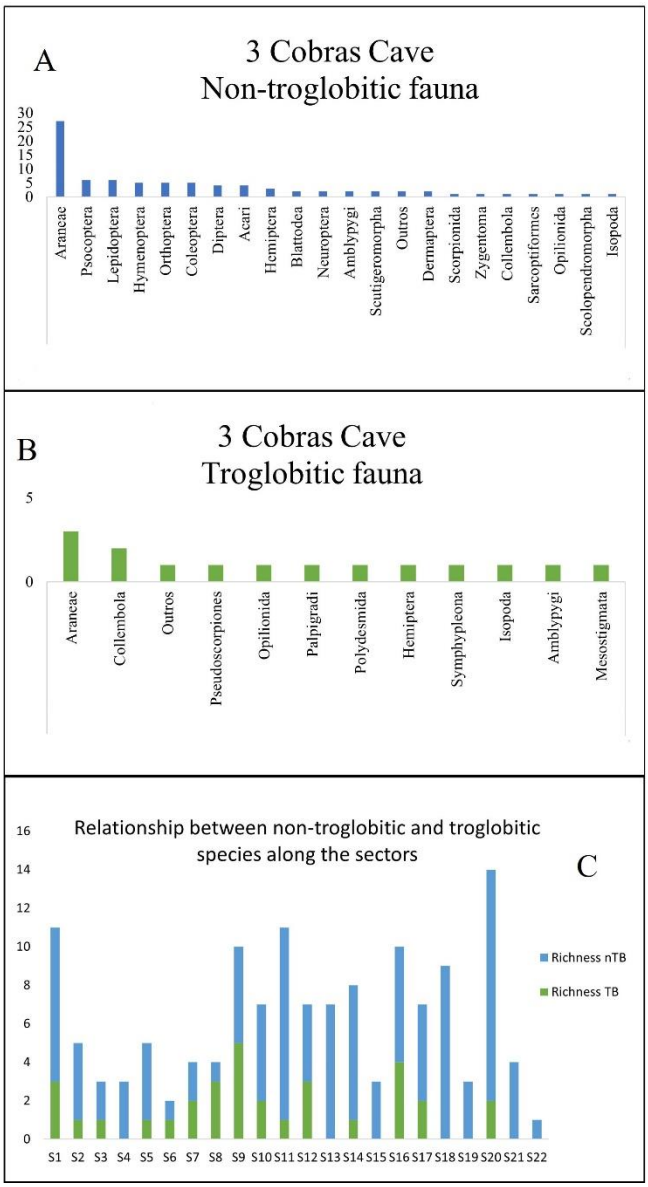


Figure 2. The richness of non-troglobitic species in different taxa observed in Three Cobras Cave (A); The richness of troglobitic species in different taxa observed in Three Cobras Cave (B); The relationship of non-troglobitic and troglobitic species along the sectors. nTB means non-troglobitic and TB means troglobitic.



Figure 3. Some of the troglobitic species found in Three Cobras Cave: *Charinus* (A); Araneae (B, D, F); *Pseudochthonius* (C); Palpigradi (E); Isopoda (G, H); Trichopolidesmidae (I); Blattodea (J); *Troglobentosminthurus* (K); and Kinnaridae (L).

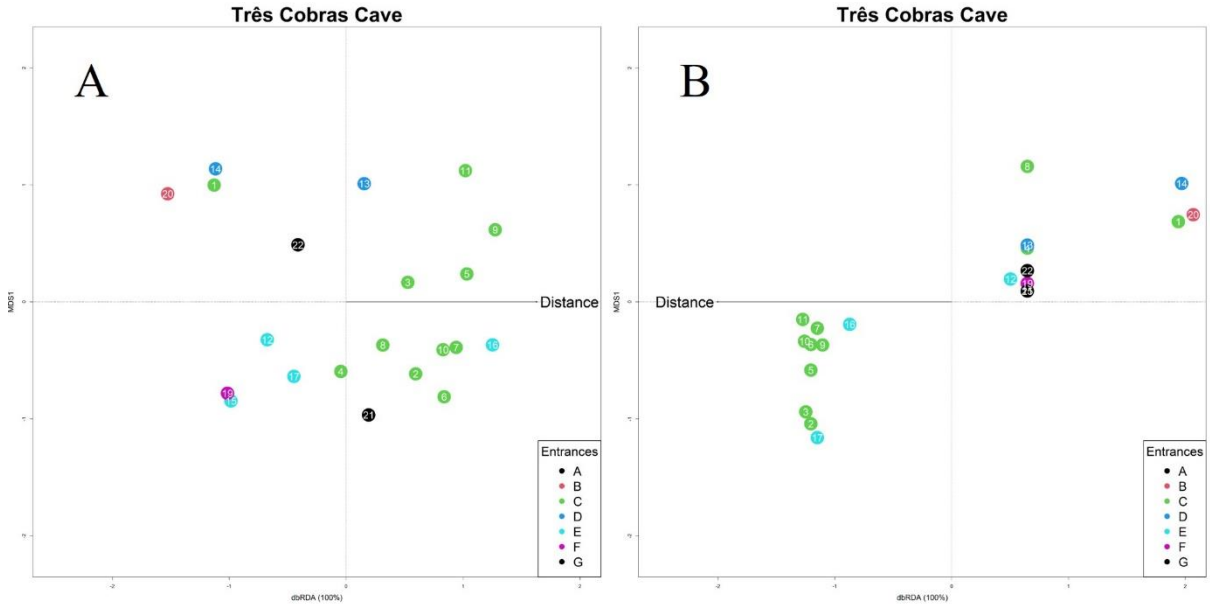


Figure 4. dbRDA shows the spatial variation in overall and troglobitic composition. Distance from the entrance explained 8.0% and 11% of spatial variation in species composition (A and B, respectively). The colored dots are representing the closest entrance from the sector.

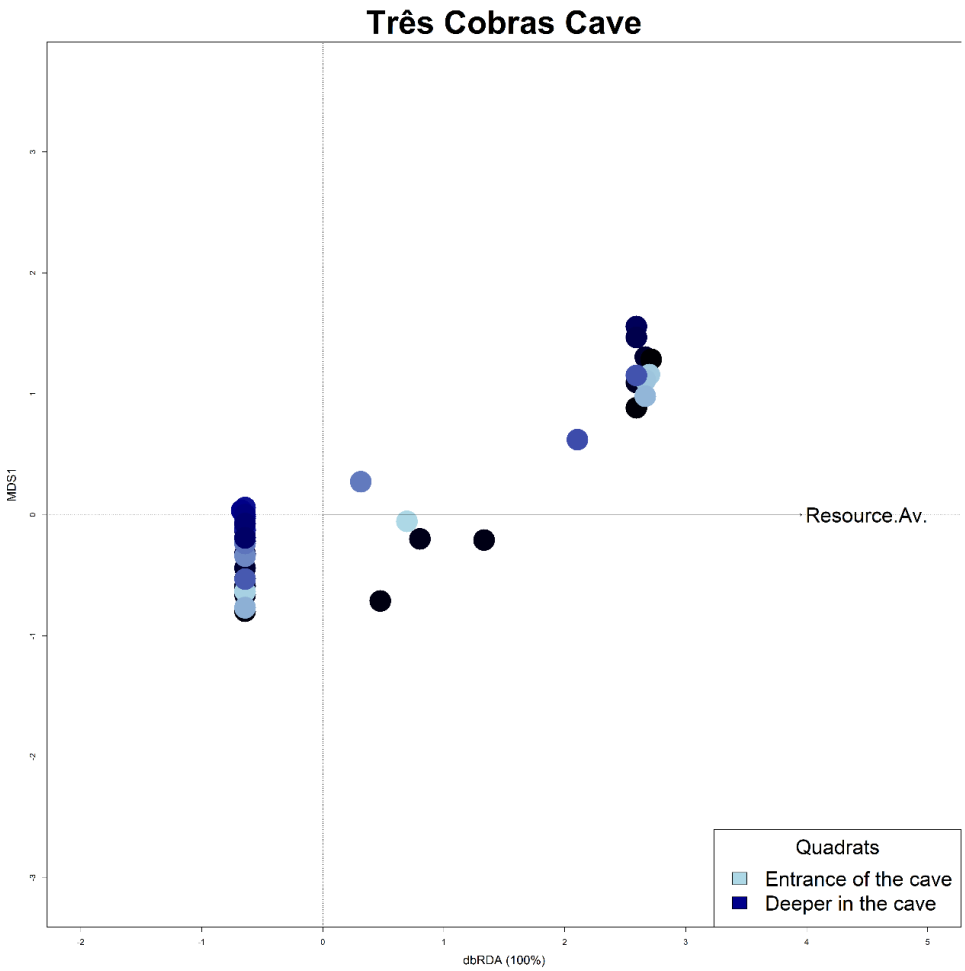


Figure 5. dbRDA showing the spatial variation in troglobitic composition. Resource Availability explained 12% spatial variation in species composition. The dots are representing the closest entrance from the quadrat, the darker the dot the deeper in the cave the quadrat is located.



FROM MICRO-HABITATS TO LANDSCAPES

LOCAL AND REGIONAL INFLUENCES OF THE HABITAT CHARACTERISTICS ON CAVE INVERTEBRATES' ASSEMBLAGE: FROM MICRO-HABITATS HETEROGENEITY TO LANDSCAPE FEATURES

Alicia Helena Souza Rodrigues Ferreira, Marconi Souza-Silva, Rodrigo Lopes Ferreira.

Universidade Federal de Lavras, Instituto de Ciências Naturais, Departamento Ecologia e Conservação, Centro de Estudos em Biologia Subterrânea, Caixa Postal 3037, CEP 37200-900, Lavras, MG, Brasil.

* Corresponding author: aliciahsrferreira@gmail.com
Ferreira, R.L. ORCID identifier is 0000-0003-3288-4405
Souza-Silva, M. ORCID identifier is 0000-0002-3184-531
Rodrigues-Ferreira, A.H.S ORCID identifier is 0000-0002-9965-2265

ABSTRACT

The knowledge of Serra do Ramalho karst still poorly studied and the previous study showed that this area possesses an endemic fauna and threat of extinction. In this sense, this work was developed with the aim of contributing to the ecology and conservation of the subterranean fauna. So, it was evaluated the influences of habitat heterogeneity through physical, trophic, microclimatic and substrate features on the species richness and composition at distinct sampling scales and if the troglobitic respond differently than non-troglobitic fauna to those variables cited above. Two samples were made in 2021 and 2022 in 26 caves distributed in three municipalities in Serra do Ramalho. The invertebrate fauna was sampled using sectors (10x3m) and quadrats (1x1m), displayed along the floor of the cave. Were also used two landscapes features: micro basins (São Francisco River basin and Corrente River basin) and water zones (discharge and recharge) to evaluated their effects on the subterranean composition. Finally, it was concluded that the physical, trophic, microclimatic and substrates feature are important for structuring the cave fauna together and/or isolated, at different scales and have a distinct effect over non-troglobitic and troglobitic species. And the only landscape variable that had an influence on composition was the recharge and discharge zones.

Keywords: Serra do Ramalho, caves, fauna, troglobitic, scales, richness.

INTRODUCTION

Subterranean environments, for a long time, were considered unable to support a diverse fauna in the function of the absence of light, low productivity, and oligotrophic characteristics, however, it is now known that caves can maintain high invertebrate diversity in function of the high temporal and spatial heterogeneity in resources and conditions (Gilbert and Deharveng 2002; Simon et al. 2007; Culver and Pipan 2009). Once subterranean environments present spatial variations and gradients of resources and conditions, it allows

the existence of different microhabitats between and along caves, with a potential reduction in competition and niche overlapping, (Culver and Pipan 2010; Pacheco et al. 2020; Souza-Silva et al. 2021; Simões et al. 2022).

In that sense, to understand local and regional patterns of distribution in subterranean communities, not only abiotic and biotic factors should be taken into consideration, but also the spatial scales of analysis. Among the local scale abiotic factors can be enhanced temperature, relative humidity, type of substrate, availability of resources, and the number of shelters, among others (Dunson and Travis 1991; Pacheco et al. 2020). While the regional scale abiotic factors can be highlighted such as rock type, altitude, productivity, vegetation types, drainage basins, and water recharge zones, etc. Besides that, can be enhanced resource availability and intra and interspecific interactions such as predation and competition (Danks 1991; Dunson and Travis 1991). Temperature and humidity are one of the mains factors that have influenced the obligate cave fauna distribution (troglobitic), since they tend to choose microhabitats with higher and stabler temperature and humidity, as their sensibility even to small variations in these factors (Pacheco et al. 2020; Howarth 1980; Pallarés et al. 2019, 2020).

On the other side, non-obligate cave fauna (troglophiles) living near the entrance can experience more microclimate fluctuations, hence, being capable to tolerate these fluctuations more than the troglobitic species living at the deepest parts of the cave (Prous et al. 2004; Lunghi et al. 2014; Prous et al. 2015; Mammola et al. 2017; Mammola and Isaia 2017). So, understanding the microhabitat selection is equally important as understanding patterns of distribution on a local and regional scale. Recently, microhabitats have been implied as one of the most fundamental factors that drive species diversity, since the existence of microhabitats attracts different species to the cave including those seeking refuge (Caruso 1994). Such preferences in using different types of microhabitats are linked to the coexistence of several species with different degrees of morphological, behavioral, reproductive, and physiological specializations (Souza-Silva et al. 2021; Gibert e Deharveng 2002; Tobin et al. 2013). To end, a considerable point to highlight is that studies regarding microhabitats selection also must contain biotic factors (Dunks 1991).

In contrast, the landscape context can also cause influences biodiversity (MacDonald et al. 2000), since caves present no or little light and photoautotrophs are also not found, leading the subterranean fauna to be dependent on allochthonous resources and on roots (Howarth 1983; Ferreira et al. 2007; Schneider et al. 2011). Therefore, changes in the landscape can affect nutrient input, and microhabitats availabilities (Pellegrini et al. 2016a).

In this sense habitat heterogeneity can be considered another good predictor of animal diversity and abundance, being an important factor that has been studied by many authors in searching for answers regarding species distribution patterns (Amarasekare and Nisbet 2001; Cornell 2010; Yang et al. 2015; Stein et al. 2015; Vargas-Mena et al. 2020; Souza-Silva et al. 2021). Despite that, the relationship between habitat heterogeneity and diversity relies on the spatial and temporal scale (González-Megías et al. 2007; Mehrabi et al. 2014). Moreover, historical factors, geographic position, and regional hydrology combined with those cited above (e.g., habitat heterogeneity e availability) can also explain the distribution of

subterranean species (Christman et al. 2016). As an example, environmental differences between micro basins and hydrological zones (recharge and discharge) explain the faunistic identities of the subterranean fauna at a broad scale (Alvarenga et al. 2020; Stein et al. 2012; Iannella et al. 2020).

There are few studies evaluating the space-scale dependence on communities for cave invertebrates (Pellegrini et al. 2016a; Bento et al. 2021; Oliveira Furtado et al. 2022). Such studies are essential to identify and understand the characteristics and patterns for futures management and conservation, since models get more accurate at larger scales once it is possible to incorporate variables that are not present in smaller scales (Pellegrini et al. 2016a), however, the combination of different scales can explicate more precisely the invertebrate's fauna and its structure. Thus, the main purpose of this paper is to elucidate the responses of the cave invertebrate fauna (composition and richness) against *physical*, *trophic*, and *microclimatic* variations, substrate heterogeneity/diversity, and substrate features within the caves at different scales, such as microscale (1 m^2 quadrats), mesoscale (30 m^2 sectors) and landscape features (micro basin and water zones). To that end, (i) we hypothesized that higher substrate diversity higher invertebrate species richness in the sectors and quadrats; (ii) troglobitic species tend to respond differently to these variables than non-troglobitic species because of their preference for stabler environment and higher levels of specialization to subterranean habitats; (iii) to investigate the relationship between the invertebrates community and the water zones and micro basins in which the caves are inserted as they function as geographical barriers, limiting the dispersion of cave fauna.

MATERIALS AND METHODS

Studied caves and surroundings areas

The study was conducted in 26 caves in the municipalities of Carinhanha, Coribe, and Serra do Ramanho (BA) (Figure 1, Table 1). The Serra do Ramalho karst is in Rio São Francisco basin and possesses a variety of limestone outcrops formed by the Bambuí Group. The region comprehends important cave systems, some obtaining several kilometers in extent, therefore, having a high subterranean diversity. This region is in the Caatinga biome and experiences a tropical dry climate, the "Aw" type characterized by dry winter by the classification of Köeppen (Alvares et al. 2013). Due to tropical rains that occur in the region, it is safe to access these caves only in dry periods (March to October). Caves extension varies from 12m to 8400m (sd= 708.3), and caves altitudes varies from 473.5 to 742.19 (sd= 102.2).

Fields procedures

Invertebrate quantitative sampling on the cave floor

To evaluate the composition and richness of invertebrate communities 145 sectors were established in the 26 sampled caves, where each sector (3 x 10m) contains 3 quadrats (1 x 1m), here considered "mesoscale' and "microscale", respectively. All transects were placed on the cave floor at least 100m apart from each other (when possible).

The invertebrate fauna was recorded into the sectors and quadrats through detailed visual search and hand sampling (Souza-Silva et al. 2021; Oliveira Furtado et al. 2022). The

sampling method was exhaustive, and the invertebrates were collected with aid of tweezers and brushes and placed in vials with alcohol 70% in order to preserve the material for further identification in the laboratory. To minimize the impact of the sampling on the invertebrate communities some specimens were collected and their abundance where accounted.

All specimens were identified at the lowest taxonomic level possible with the assistance of taxonomic keys. The troglobitic species were separated by traits that indicate their evolution and adaptability in subterranean environments. The troglomorphisms observed were a lack or reduction in ocular structure and pigmentation, and elongation of appendices and sensorial structures (Culver and Pipan 2009). Experts reviewed species from the following orders Isopoda, Pseudoscorpiones, Orthoptera, Acari, Entomobryomorpha and Diplopoda. All the collected specimens are deposited in the Lavras Subterranean Invertebrates Collection (ISLA), affined to the Center of Studies on Subterranean Biology at the Federal University of Lavras, Minas Gerais, Brazil.

Abiotic attributes of the cave floor

The temperature and humidity were measured with the aid of a thermohydrometer device in each sector. The device was set on the cave floor and its values were taken after its stabilization. The presence of people was avoided to not interfere with or alter the measures (Souza-Silva et al. 2021; Oliveira-Furtado et al. 2022).

The measurement of abiotic attributes in mesoscale (sectors) was made through the methodology proposed by Pellegrini et al. (2016a), and Souza-Silva et al. (2021). The sectors were divided into 10 sections of 1 meter each and were made a visual estimate of the percentual of substrate and resources available on the cave floor. In the laboratory were made a sum of these proportions and the arithmetic average of every substrate and resource proportion in the sector and finally, the Shannon-diversity Index (H') was calculated for each sector. On the other hand, the measurement of abiotic attributes on a microscale (quadrats) was evaluated using photographs. Digital photographs (4000 x 3000 pixels) were taken in the field in a vertical position (camera positioned at 90º relative to the cave floor) using the Canon Powershot SX50, HS. In the laboratory, the photos were analyzed through ImageJ software (Rasband 1997), and finally, the arithmetic average of every abiotic attribute was made (Souza-Silva et al 2021, Oliveira-Furtado et al. 2022).

The definition of hydrological zone-recharge and discharge was made based on terrain elevation after getting caves entrance geographic position and plotted in a map. Altitudes values higher than 550 meters were considered recharge zones and altitudes lower than 550 meters were considered discharge zones (Figure 1). The altitudes were taken in QGis software based on a Digital Elevation Model (DEM) of the area. To define the micro basins were used the function CHANNEL NETWORK AND DRAINAGE BASINS from the 'Saga Next Generation' plugin based on a Digital Elevation Model (DEM) of the area, using the software QGis version 3.22.11.

Data analysis

Biotic attributes of the caves

The abundance and richness of overall fauna, non-troglobitic and troglobitic were obtained by counting individuals and morphotypes of each sample unit (26 caves, 145 transects, and 435 quadrats).

Abiotic attributes on the cave floor regarding the sectors

All the *physical*, *trophic* and *microclimatic* characteristics of the sectors were evaluated and classified in the following classes: guano—GU, insectivorous guano —GI, hematophagous guano—GH, bird feces—FZA, others mammals feces—FZM, mocó feces—FZMO, tamanduá feces—FZT, feces—FZ, carcass—CRC, roots—RZ, litter—SER, plants debris—DTV (> 10mm), fine branch —GALF (11-30 mm), medium branch —GALM (31-50 mm), coarse branch—GALG (65-250 mm), trunk—TRO (>250mm of width), river—R, river pond—PR, water pond—WP, stalactite—EL, drip water—DP, hyphae—HI, actinomycetes biofilms—ACT, basidiomycetes—BAM, shell—CO, seedlings—PL, another organic substrate—OTO, smooth rock—RL, rough rock—RR, concrete like floor—RC, wide rock—XB (1000-4000mm), medium rock —MB(500-1000mm), small rock —SB(250-500mm), cobbles—CB (64-250mm), coarse gravel—CAG (16-64mm), fine gravel—CAF (2-16mm), sand—ARE (0.06-2mm), silt—SEF (≤ 0.05 mm), hardpan—HP, travertine—TV, flowstone—EC, cauliflower-like speleothem—CF, rough stalagmite—ER, stalagmite—EG, calcite rafts—JS, *megalobolimus* shell—CM, gastropod shell—CG, speleothems—ES, worm acorns —BM, retraction cracks—GR, cave-wall—PA, water pipe—CA, hardpan pinnacle—PHP, another inorganic substrate—OTI.

Based on such classes we obtained the *physical features* that included distance from the entrance, the substrate diversity (calculated considering all classes above), the shelter diversity (calculated considering RR, RC, XB, MB, SB, CB, CAG, CAF, TV, CF, ES, EG, CM, CG, BM, GR and CA) and trophic resources diversity (calculated considering GU, GI, GH, FZM, FZMO, FZT, FZ, CRC, RZ, SER, DTV, GALF, GALM, GALG, TRO, CR, FG, AL, HI, ACT, BAM and PL). All diversities were calculated using Shannon-Weaver Index (Buttigieg and Ramette 2014).

The availabilities of each *Abiotic attribute* were also included as *physical*, *trophic* and *microclimatic* characteristics. The shelter availability was calculated by the sum of RR, RC, XB, MB, SB, CB, CAG, CAF, TV, CF, ES, EG, CM, CG, BM, GR, CO and CA in each sector. On the other side, the trophic resources availability was calculated by the sum of GU, GI, GH, FZM, FZMO, FZT, FZ, CRC, RZ, SER, DTV, GALF, GALM, GALG, TRO, CR, HI, ACT, BAM and PL in each transect, and are also the same for the *trophic resources.* Finally, the *microclimatic variables* considered were temperature and humidity.

When using the analysis with individual classes, some classes were set to minimized variables. GH, GU, GI, and GU were grouped into GU. The classes ES, CF, EL, EG, ER, TV, and JS were grouped into ES. The classes CO, CM, and CG were grouped into CO. Lastly, R, WP, and PR were grouped into W.

Abiotic attributes on the cave floor regarding the quadrats

On the other hand, *physical* and *trophic* characteristics of the quadrats were evaluated and classified into the following classes: guano—GU, feces—FZ, carcass—CRC, roots—RZ,

plants debris—DTV (> 10mm), fine branch —GALF (11-30 mm), medium branch —GALM (31-50 mm), coarse branch—GALG (65-250 mm), trunk—TRO (>250mm of width), water pond—WP, drip water—DP, another organic substrate—OTO, shell—CO, cow bone—CN, smooth rock—RL, rough rock—RR, concrete floor—RC, wide rock—XB (1000-4000mm), medium rock—MB(500-1000mm), a small rock—SB (250-500mm), cobbles—CB (64-250mm), coarse gravel—CAG (16-64mm), fine gravel—CAF (2-16mm), sand—ARE (0.06-2mm), silt—SEF (0.2 < diameter ≤ 0.05 mm), hardpan—HP, speleothems—ES, worm acorns —BM, flowstone—EC, water pipe—CA, card burn—CU and retraction cracks—GR.

Based on such classes we obtained the *physical features* that included distance from the entrance, the substrate diversity (calculated considering all classes above), the shelter diversity (calculated considering DTV, GALF, GALM, GALG, TRO, CO, RR, RC, XB, MB, SB, CB, CAG, CAF, TV, EG, BM, CA, CU and GR), and trophic resources diversity (calculated considering GU, FZ, CRC, RZ, DTV, GALF, GALM, GALG, TRO and OTO). All diversities were calculated using Shannon-Weaver Index (Buttigieg and Ramette 2014).

The availabilities are also included in *physical*, *trophic,* and *microclimatic* characteristics. The shelter availability was calculated by the sum of CO, RR, RC, XB, MB, SB, CB, CAG, CAF, TV, EG, BM, CA, CU and GR in each quadrat. On the other side, the trophic resources availability was calculated by the sum of GU, FZ, CRC, RZ, DTV, GALF, GALM, GALG, TRO and OTO in each quadrat, and are also the same for the *trophic resources*. For the quadrats, some classes were set to minimized variables, where the same groups were formed when using the analysis with individual classes.

Spatial variations on habitat Structure

To compare the existence of differences in the average in temperature, humidity, substrate diversity, resource diversity, shelter diversity, availability of resources, and shelter among all 26 caves sampled it was performed the Kruskal-Wallis test, using a KRUSKAL.TEST function from the 'Stats' package in RStudio. About the sectors, it was tested if such trophic, microclimatic and physical attributes varied depending on the distance from the entrance using *Linear Regression*. It also was tested about the quadrats if such trophic, microclimatic, and physical attributes varied depending on the distance from the entrance using *Linear Regression*. All regressions were calculated using the function LM from 'Stats' package in RStudio.

Relationship between habitat structure of the sectors and quadrats with cave fauna

Linear models (GLM e GLMM) were performed to predict the influence of local abiotic variables on total species richness, species richness of non-troglobitic and species richness of troglobitic (response variables), using transects and quadrats as sample units, performed in RStudio. We used two different models to evaluate the influence of the substrate on the response variables. The variables included in the first model were temperature (^{0}C), humidity (%), distance from the cave entrance, diversity of shelter, diversity of substrate, and diversity of resources, and availability of shelter and availability of resources. The variables included in the second model were temperature (^{0}C), humidity (%), distance from cave entrance, diversity of shelter, diversity of substrate, and diversity of resource and the components of

the substrate in their single version (for the sectors: guano, insectivorous guano, hematophagous guano, bird feces, Others mammals feces, mocó feces, tamanduá feces, other feces, carcass, roots, litter, plants debris, fine branch, medium branch, coarse branch, trunk, river, river pond, water pond, stalactite, drip water, hyphae, actinomycetes biofilms, basidiomycetes, shell, seedlings, another organic substrate, smooth rock, rough rock, concrete floor, wide rock, medium rock, small rock, cobbles, coarse gravel, fine gravel, sand, silt, hardpan, travertine, flowstone, cauliflower-like speleothem, rough stalagmite, stalagmite, calcite rafts, *megalobolimus* shell, gastropod shell, speleothems, word acorn, retraction cracks, cave-wall, water pipe, hardpan and pinnacles, another inorganic substrate; Inside quadrats: guano, feces, carcass, roots, plants debris, fine, medium branch, coarse branch, trunk, water pond, drip water, another organic substrate, shell, cow bone, smooth rock, rough rock, concrete floor, wide rock, medium rock, small rock, cobbles, coarse gravel, fine gravel, sand, silt, hardpan, speleothems, word acorn, flowstone, pipe, card burn and retraction crack). For that, the Poisson family was adopted, since is often used in models that count of occurrences given in time or space. To compare the model results with the null models, the ANOVA function from 'Vegan' package was made. To evaluate the overdispersion were used the function CHECK_OVERDISPERSION from the package 'Performance'. To obtain r^2 values of the GLMMs, we used the function r.squaredGLMM from the 'MuMIn' package, while to obtain r^2 values of the GLM's, we used the function r.squaredLR from the 'piecewiseSEM' package. Before running the GLM's and GLMM's, we tested the correlation of all variables included in their respective model through the function CHART. CORRELATION from the 'PerformanceAnalytics' package. Variable with high correlation values (>0.65) were excluded from the model (Zuur et al. 2010). The multicollinearity was also tested before running the models through function VIF from 'Car' package. The variables that presented multicollinearity higher than 10 were excluded from the model, one by one (Zuur et al. 2010).

To explain the possible relationship, strength, and direction (- or +) between overall fauna, non-troglobitic and troglobitic species composition with the *physical*, *trophic*, and *microclimatic* variables, it was performed a Distance-based redundancy analysis (dbRDA) based on Bray-Curtis similarity matrix (Clarke et al. 2014). To perform this analysis, were used the two models as explained above.

Relationship between landscape features, cave habitat structure and cave fauna

To access the relationship between landscape features and invertebrates' composition (overall fauna, TB and nTB) a similarity analysis (ANOSIM) was performed using micro basins (São Francisco River and Corrente River), and hydro zones (water zone of recharge and water zone of discharge) as factors. The similarity was based on a Bray-Curtis similarity matrix, using the transects as sampling units. Species abundance was square root transformed before running a resemblance analysis (Clarke 1993). This analysis was performed using Primer-e7 software (https://www.primer-e.com/our-software/primer-version-7/).

To access the relationship between landscape features and abiotic attributes of the caves was also performed an ANOSIM using micro basins (São Francisco River and Corrente River), and hydro zones (water zone of recharge and water zone of discharge) as factors. For

that it was performed a Euclidean-distance matrix, using the transects as sampling units. Before running the ANOSIM was performed a square root transformation of the data was and created a resemblance matrix (Clarke 1993). This analysis was performed using Primer-e7 software (https://www.primer-e.com/our-software/primer-version-7/).

RESULTS

Biotic attributes of the cave

A total of 9178 individuals were recorded, distributed in 43 orders and 123 families, and 416 morphospecies. From the total 72 was considered troglobitic (17,3 %). The richest order considering overall fauna was Araneae (116 ssp.), followed by Coleoptera (73 ssp.) and Diptera (62 ssp.), (Figure 2a). The richest order of non-troglobitic species was Araneae (104 ssp.), followed by Coleoptera (73 ssp.) and Diptera (61 spp.) (Figure 2b). Lastly, the richest orders of troglobitic species were Araneae (12 ssp.), Polydesmida (9 ssp.) and Isopoda, Palpigradi and Pseudoscorpiones (6 ssp. Each) (Figure 2c). Some of the troglobitic found among the 26 caves are shown in Figure 3.

Relationship between habitat structure of the sectors with cave fauna

For the overall fauna (troglobitic and non-troglobitic), in the first model showed that the variation in morphospecies richness was best explained by temperature and resource availability (R^2= 0.22), while in the second model the variation on morphospecies richness was best explained by temperature, DTV, GALF, GALM, TRO, DP, OTO, SEF, FZA, FZMO, BAM and PHP (R^2: 0.80). For the non-troglobitic (nTB), the first model showed that the variation in morphospecies richness was best explained by temperature, distance from the entrance and resource availability (R^2= 0.31), while the second model showed that the variation in morphospecies richness was best explained by temperature, distance from the entrance, humidity, FZMO, DTV, GALF, GALM, TRO, ACT, OTO, CAF and SEF (R^2= 87). Finally, for the troglobitic fauna (TB), the first model showed that the variation in morphospecies richness was best explained by temperature and humidity (R^2=0.20), while on the second model showed that the variation in morphospecies richness was best explained by temperature, humidity, FZA, RZ, DP, ACT and BAM (R^2= 0.43). The p-values are in Table 2.

For the overall fauna, the first dbRDA model showed that distance, resource availability, humidity and temperature were the best predictors, explaining 9.99% of the variation in species composition (p-value: 0.005 for all) (Figure 4a), while the second model showed that distance, humidity, temperature, DTV, SEF, GU, GALM, TRO, FZMO, RZ were the best predictors, explaining 19% of the variation in species composition), (Figure 4b). For the non-troglobitic (nTB), the first dbRDA model showed that distance from the entrance, resource availability, temperature and humidity were the best predictors, explaining 9% of the variation in species composition (Figure 4c), while the second model showed that distance, temperature, humidity, resource div., DTV, SEF, GU, FZT, TRO, ARE and RZ were best predictors, explaining 18% of the variation in species composition (Figure 4d). Finally, for the troglobitic fauna (TB), the first dbRDA model showed that distance from the entrance and humidity were the best predictors, explaining 6% of the variation in species composition (p-

value: 0.005 for both) (Figure 4e), while the second model showed that distance, temperature, humidity, GALM, RZ, FZMO, ES, SEF, TRO and OTO were best predictors, explaining 20% of the variation in species composition (Figure 4f). The p-values are shown in Table 3.

Relationship between habitat structure of the quadrats with cave fauna

For the overall fauna (troglobitic and non-troglobitic), the first model showed that the variation in morphospecies richness was best explained by distance and resource availability (R^2: 0.12), while in the second model, the variation in morphospecies richness was best explained by distance, resource div., substrate div., shelter div., GU, DTV, WP, OTO, SEF and BM (R^2: 0.12). For the non-troglobitic (nTB), the first model showed that the variation in morphospecies richness was best explained by distance from the entrance and substrate diversity (R^2= 0.25), while in the second model, the variation in morphospecies richness was best explained by distance, substrate div., GU, DTV, GALF, OTO, MB, SB, CAG, ARE, SEF, and HP (R^2= 0.85). Finally, for the troglobitic fauna (TB), the first model showed that the variation in morphospecies richness was best explained by distance from the entrance and resource availability (R^2 = 0.12), while in the second model the variation on morphospecies richness was best explained by distance, resource div., shelter div., substrate div., GU, DTV, OTO, SEF and BM (R^2= 0.79). The p-values are in Table 4.

For the overall fauna, the first dbRDA model showed that resource availability and substrate diversity were the best predictors, explaining 11% of the variation in species composition (p-value: 0.005 for all) (Figure 5a), while the second model showed that distance, resource diversity, substrate diversity, GU, DTV, SEF, BM, OTO, TRO were best predictors, explaining 17% of the variation in species composition (Figure 5b). For the non-troglobitic (nTB), the first dbRDA model showed that distance from the entrance and substrate diversity were the best predictors, explaining 13% of the variation in species composition (p-value: 0.005, for all) (Figure 5c), while the second model showed that distance, substrate div., OTO, GR, WP, GU, SEF, and RC were best predictors, explaining 18% of the variation in species composition (Figure 5d). Finally, for the troglobitic (TB), the first dbRDA model showed that distance, resource availability, and resource diversity were the best predictors, explaining 14% of the variation in species composition (Figure 5e), while the second model showed that distance, GR, SEF and OTO were best predictors, explaining 16% of the variation in species composition (Figure 5f). The p-values are shown in Table 3.

Spatial variations on habitat structure

The values of temperature, humidity, substrate diversity, resource diversity, shelter diversity, availability of resources, and shelter of the sectors and quadrats are presented in Material Supplementary I and II. Temperature, humidity, shelter and resources diversity, and resource availability showed differences in the averages among all 26 caves. Regarding the sectors, the humidity indicated a positive relationship with the distance from the entrance (R^2 = 0.08, p = 0.0003), while the substrate diversity (R^2 = 0.07, p = 0.001), shelter diversity (R^2 = 0.05, p = 0.006), resource availability (R^2 = 0.06, p = 0.003) and shelter availability (R^2 = 0.04, p = 0.01), showed a negative relationship with the distance from the entrance (R^2 = 0.07, p = 0.001). Additionally, regarding the quadrats, the resource diversity (R^2 = 0.02, p = 0.001), shelter diversity (R^2 = 0.01,

p = 0.006), and resource availability (R^2 = 0.01, p = 0.003), indicated a negative relationship with the distance from the entrance.

Relationship between landscape features and cave fauna

The ANOSIM revealed significant differences in overall fauna, the non-troglobitic and troglobitic composition in the sectors among hydro zones (Global R= 0.14, p= 0.001; Global R- 0.082, p= 0.001; Global R= 0.099, p= 0.001, respectively). It also revealed significant differences in substrates composition among hydro zones (Global R= 0.14, p= 0.021). Lastly, the fauna also varied among caves (Global R: 0.39, p= 0.001).

DISCUSSION

Our study highlights the importance of different environmental factors, including spatial scales to explain local and regional variations in the composition of substrate components and in the number of species and composition of the invertebrate fauna on the cave floor. Both biotic and abiotic attributes of the caves were extremely heterogeneous in micro (between quadrats of $1m^2$), meso (sectors of $30m^2$), and macro-scale (caves and recharge zones). That spatial habitat and microhabitats differentiation driven by changes in substrate components on the cave floor might be promoting replacement in species richness and similarity at the local and regional scale and permitting the occurrence of distinct faunistic identities in a narrow geographic area. Distance from the entrance showed a strong influence in reducing substrate diversity, shelter diversity, resource availability and shelter availability, but increasing moisture content in the microhabitats. Then we can assign high heterogeneity in microhabitats spatial distribution even inside a single cave.

Relationship between habitat structure of the sectors and quadrats with cave fauna

The results referent to substrate heterogeneity/diversity showed that the first and second model did totally corroborate our hypothesis, that higher substrate diversity can promote increases in invertebrate species richness in caves. Only the results of the first model corroborate our second hypothesis that troglobitic species tend to be differently influenced by the cave variables than non-troglobitic species.

Being more specific the non-troglobitic richness and composition responded to temperature, humidity, distance from the entrance, resource availability, substrate diversity, mocó feces, plants debris, medium and fine branch, trunk, actinomycetes, fine gravel, silt and other organics substrates. While the troglobitic richness and composition responded to temperature, humidity, distance from the entrance, resource availability and resource diversity.

The influence of temperature and humidity on cave fauna is known, once temperature at deepest parts of the cave is almost the same as the annual average of the external surrounding of the cave where its located, while for the humidity, it tends to saturation as far from the entrance of the cave. When compared to temperate areas, tropical areas possess less differentiation between inside the cave and external areas (Tobin et al. 2013). The zone connecting these two environments (internal and external) are called ecotones (Prous et al. 2015). These ecotones possess both hypogean and epigean fauna transitioning, seeking for

shelter and/or refuge, as a result the patterns of distribution and composition of species tend to be different when compared to the fauna at deepest parts of the cave.

Temperature also produces distinct types of habitats, one near the entrance and one at the deepest parts of the cave, therefore influencing on species richness, which decreases as far from the entrance of the cave. However, the humidity increases as far as the entrance and consequently increases the richness, but in this case, the richness of troglobitic species, since the distance from the entrance affect species composition and limits species richness of non-troglobitic, therefore, remaining only the species more adapted to even more oligotrophic and humid environments. This same pattern was observed by Souza-Silva et al. (2021) and Deharveng and Bedos (2000), where troglobitic species were found in cave areas far from entrance, since they manage to keep away from drier areas and competitors, in this case being the non-troglobitic species.

The resource diversity and resource availability, and the number of classes of organic matter such as plants debris, branches and trunk were expected since the subterranean invertebrates are on dependent of organic resources input (Culver and White 2005), which can occur from surface runoff and percolation (Ferreira et al. 2010) and through rivers importation (Souza-Siva et al. 2011), that act as distribution agents, supporting a regular food supply (Hawes 1939). One of the possible interpretations is that forests in limestone areas produce more leaf during dry periods (Brina 1998), which during rainfall periods can be imported, including fallen trunks, however it only moves inside the caves in rainy periods with high velocity and high-water flux. That creates an almost dependence on organic matter importation (Bento et al. 2016). Although, the distinction between the use of microhabitats and food resources not only depends on their availability but also on the competition for it between species (Souza-Siva et al 2021).

About the resources such guano and feces, they are provided to the caves by bats and by other mammals there enter seeking for shelter or food, therefore, playing an important role in community structure. Concerning the types of guano, there are three mains: frugivorous, hematophagous and insectivorous. They are related to their feeding habitats, which varies from seeds, blood of mammals and insects or arthropods. Their feeding habits are also influenced by variations in seasonality where in beginning of the rainy season there is an thrive in flowering and fructification, leading to increase food availability to bats and consequently intensifying guano deposition inside caves, and if they are deposited where is not accessible to water, being available for longer time (Faria 1996; Wolda 1988; Souza-Silva et al. 2011). Since most caves are an oligotrophic environment, places having such resources can present higher diversity of invertebrate fauna and act as the main food font, as shown for some authors (Decu 1986; Gnaspini 1989; Ferreira and Martins 1998; Ferreira and Martins 1999; Ferreira et al. 2000). Although these variables work together, they can behave in different ways and level over the subterranean fauna (Simões et al. 2015).

The troglobitic fauna are more specialized to live in these oligotrophic environments. One of the specializations is the resistance to starvation. In contrast, the non-troglobitic fauna showed that is needed a wider range of food resources. These corroborate strongly to our

findings once the TB species were found mostly at the deepest parts of the caves and nTB species reduces as far from the entrance. These indicate that there is no or low competition for food resources and shelter. A similar pattern was found in Águas Claras Cave System (ACCS), where the microclimatic variables were the most important influencing the structure and distribution of troglobitic and not the organic resources and habitat physical structure (Souza-Silva 2021). On the opposite, non-troglobitic-fauna can support variations in microclimatic features.

Variations in Habitat Structure

The difference observed in temperature, humidity, shelter and resource diversity, and resource availability among caves was expected because the studied caves present differences in features relating to the form or surface interactions that can facilitate or difficult environmental dynamics. Some of the features are the distance between cave, altitude, number, distribution and size of the entrances and cave extension. Besides that, morphology of the relief and position in recharge or discharge areas, water course presence and vegetation near the entrances can affect the internal cave dynamic (Souza-Silva et al. 2020; Cardoso et al. 2022). Recharge areas with different external features capture and transmit the surface waters to subterranean compartments, and are indispensable in the movement, transport and deposition of organic and inorganic sediment inside caves (Bonacci et al. 2009, Souza-Silva et al. 2011). Different openings and water courses, such as skylights, horizontal entrances, rivers and runoffs and waters that percolate the rock through pores or fractures, represent the particulate or dissolved organic matter form of transport to the caves (Bonacci et al. 2009, Culver and Pipan 2019).

In addition to it, *physical* and *microclimatic* features can also change inside caves at meso and micro scale when related to the distance from the entrance. Regarding the sectors, the variables that varied along the sectors are humidity, substrate diversity, resource diversity, shelter availability and resource availability, while for the quadrats the variables that varied along the quadrats are shelter diversity, resource diversity and resource availability. Humidity was the only one that presented a positive relationship, meaning that as far from the entrance higher its value, this can be explained by the size of the caves, whereas far from the entrance the higher environmental stability (Pellegrini et al. 2016b). The remaining variables presented a negative effect with the distance from the entrance, meaning that as far from the entrance, the smaller their presence, which can be related to the importation of organic matter inside the caves, since the hydrological chances is a factor that influences not only the cave fauna but the input of organic matter, therefore, being one of the determinants for resources availability. The other determinant of resource availability is the width of the entrances of the cave, since bigger the entrance, higher the chance of importation of organic matter and increasing the number of species from hypogean environment to the cave (Simões et al. 2015, Cardoso et al 2022).

Relationship between landscape features and cave fauna

Our findings showed that the overall fauna varied significantly between caves and between hydro zones, while the nTB, TB fauna and substrate features (including organic and

rocky susbtrate) only varied between hydro zones. These results may indicate that presence of rivers can isolate terrestrial communities, limiting their dispersion. On the hand, the presence of aquifers and/or subterranean water can be an important element that contributes to enhance the richness of cavernicolous fauna (Culver and Piper 2009). The presence of river/water bodies can also carry rocky substrates that also contribute to increase the richness of invertebrates, functioning as shelter. As said by Bento et al. (2016), the existence of groundwater is more determining in semiarid conditions, since it permit maintenance and colonization of stygobites, and also benefit the terrestrial troglobitic since it provides appropriate conditions such as carrying organic matter and aid in keeping humidity.

Some studies regarding invertebrate taxa showed a positive relationship between population size and rainfall (Vasconcellos et al. 2010; Araújo et al. 2010; Hernández 2007). Given that, the presence of water bodies/rivers inputting organic matter increase the availability of resources and shelter, therefore, increasing the number of species and microhabitat available (Ferreira et al. 2016). However, the amount of organic matter entering the cave depends on the season, since in the dry season the leaves fall and form a little that posteriorly on the rainy season are carried into the cave, along with substrates of different sizes (Souza-Silva et al. 2011, 2012). Opposition to that, the intensive floods can also interfere over the fauna, especially in the appearance strict fauna in small caves, but when considering caves with large linear extensions may be an exception, since some species might be able to escape from de river and flood area (Simões et al. 2015).

Regarding the sampling scale, the present study imply that microhabitats influence the diversification on subterranean fauna. Eberle et al. (2018), suggest that microhabitats make possible to the coexistence of several spider species on a local scale (micro and meso scale), however these may be able not only for spiders, but for many other species inhabiting caves.

Regarding the landscape features studied here, showed that the recharge and discharge zones are important to determinate the identity of the caves faunistic, while the micro basins were not. These can happen since the presence of rivers can carry on some species, species in larvae stages, where some species that are found in recharge zones will also be found in discharge zones, and also by the inputting of organic matter and substrate as said above. Therefore, when using larger scales such landscape features is possible to access variables that are nonexistence at smaller scales, that way accessing greater structural. For that reason, the usage of different scales can improve the explaining the species composition in subterranean environments complexity (Pellegrini et al. 2016a).

In both models performed, it was found habitat heterogeneity, indicating that of non-troglobitic fauna responding differently from the troglobitic, where the first possess a wider range of food and shelter resources and more tolerance to microclimatic features, while the second needs more specific conditions and are starvation tolerance. However, the micro basins did not show an important feature to cave fauna community while the hydro zones showed an importance in cave fauna community, however further studies are needed to understand how this relationship works specifically. Finally, these changes in habitat structure can impact subterranean fauna at different sampling scales.

Deforestation around cave entrances can affect epigean fauna in a way that decrease their movement in search of shelter/food resources in caves, therefore reducing the composition and richness of species of these environments and make future colonization difficult, since these environments function as corridors. In addition, they can affect the existing cave fauna, since the deforestation also affects the temperature and humidity conditions, which consequently can affect the troglobitic fauna, since they are sensitive to even small microclimatic changes, in this way, the preservation of these surroundings can help to stabilize these conditions and help with water retention.

Lastly, we emphasize the importance of biological research for comprehension on cave biodiversity and offer insight and how the biodiversity might be dispersed inside a cave. Besides, it provides a biological dataset for future use or creates new parameters for management and conservation of caves in Serra do Ramalho/Bahia.

Funding: This work was supported by Termo Aditivo de Compromisso de Compensação Espeleológica nº 1/2018, firmado entre o Instituto Chico Mendes de Conservação e Biodiversidade (ICMBio-Vale S.A.) regarding the implementation of compensation for the irreversible negative impacts of natural underground cavities with a high degree of relevance, through the project: " Dispersion versus confinement: compositional analysis and habitat structure as a subsidy to the understanding of mechanisms responsible for subterranean fauna identity". Author Alicia Ferreira has received research support from Cnpq (Conselho Nacional de Pesquisa).

Competing Interests: The authors have no relevant financial or non-financial interests to disclose.

Acknowledgments: The authors would like to thank the Programa de Pós-Graduação in Applied Ecology (UFLA), Center of Study in Subterranean Biology (CEBS/UFLA) for providing structure for the development of the study; to Paulo, Guilherme, Pedro H., Priscilla, Giovanna, Gabrielle, Leandro, Lucas and Vitor for helping with the collections; to Giovanna Cardoso, Guilherme Prado, Leopoldo Benardi, Vitor Gabriel, Ivan, Danielle, Paola, Rodrigo (diplópodes) and Vinicius for helping with invertebrate identification. We also thank Joaquim Lopes for receiving us in his house during our stay in Agrovila 23, and Lózin, Vanuza, Duzinho, for welcoming us and accompanying in the field.

REFERENCES

Alvarenga D, Silva M, & Ferreira R (2020) Trogloregions: Delimiting subterranean faunistic identities in Afrotropics and Neotropics.

Alvares CA, Stape JL, Sentelhas PC, Moraes-Gonçalves JL, Sparovek G (2013) Köppen's climate classifcation map for Brazil. Meteorol Z 22:711–728. https://doi.org/10.1127/0941-2948/2013/0507

Amarasekare P, Nisbet R (2001) Spatial heterogeneity, source-sink dynamics and the local coexistence of competing species. Am Nat 158:572–584. https://doi.org/10.1086/323586

Araújo CS, Candido DM, Araújo HFP, Dias SC, Vasconcellos A (2010a), Seasonal variations in scorpion activities (Arachnida: Scorpiones) in an area of Caatinga vegetation in northeastern Brazil: Zoologia, 3:372–376.

Bento DDM, Ferreira RL, Prous X, Souza-Silva M, Bellini BC, Vasconcellos A (2016) Seasonal Variations in Cave Invertebrate Communities in the Semiarid Caatinga, Brazil. J Caves Karst Stud 78:61–71. https://doi.org/10.4311/2015LSC0111

Bento DDM, Ferreira RL, Prous X, Souza-Silva M, Bellini BC, Vasconcellos A (2016) Seasonal Variations in Cave Invertebrate Communities in the Semiarid Caatinga, Brazil. J Caves Karst Stud 78:61–71. https://doi.org/10.4311/2015LSC0111

Bento DM et al (2016) Seasonal variations in cave invertebrate communities in the semiarid Caatinga, Brazil. *Journal of Cave and Karst Studies* 78.2:61-71.

Bento DM, Diego et al (2021) Subterranean "oasis" in the Brazilian semiarid region: neglected sources of biodiversity. *Biodiversity and Conservation* 30:3837-3857.

Bonacci O, Pipan T, Culver D C (2009). A framework for karst ecohydrology. Environmental Geology 56:891-900.

Brina AE, (1998) Aspectos da dinâmica da vegetação associada a afloramentos calcários na APA Carste de Lagoa Santa. Dissertation. Universidade Federal de Minas Gerais.

Buttigieg PL, Ramette A (2014) A Guide to Statistical Analysis in Microbial Ecology: a communityfocused, living review of multivariate data analyses. FEMS Microbiol Ecol 90:543–550. https://doi. org/10.1111/1574-6941.12437.

Cardoso RC, Ferreira RL, Souza-Silva M (2022) Multi-spatial analysis on cave ecosystems to predict the diversity of subterranean invertebrates. *Basic and Applied Ecology* 65:111-122.

Caruso D (1994) La fauna della grotta Monello. Atti e Memorie dell'Ente Fauna Siciliana 2: 87-21

Christman MC et al (2005) Patterns of endemism of the eastern North American cave fauna. *Journal of Biogeography* 32.8:1441-1452.

Christman MC, Doctor DH, Niemiller ML, Weary DJ, Young JA, Zigler KS, Culver DC (2016) Predicting the occurrence of cave-inhabiting fauna based on features of the earth surface environment. PLoS ONE, 11:e0160408.

Cornell HW (2010) Niche overlaping. In: Hastings A, Gross LJ (ed) Encyclopedia of theoretical ecology. University of California Press, Oakland

Culver DC, Pipan T (2009) Biology of Caves and Other Subterranean Habitats, 1st edn. Oxford, New York

Culver DC, Pipan T (2010) Climate, abiotic factors, and the evolution of subterranean life. Acta carsologica

Culver DC, Pipan T (2019) The biology of caves and other subterranean habitats. Oxford University Press.

Danks HV (1991) Winter habitats and ecological adaptations for winter survival." *Insects at low temperature* 231-259.

Decu V (1986) Some considerations on the bat guano synusia. Travaux de L'Institut de Spéologie "Emile Racovitza" 25:41-51. doi:10.1590/S1984-46702010000300008.

Dunson WA, Travis J (1991) The role of abiotic factors in community organization. The American Naturalist, 138:1067-1091. https://doi.org/10.1086/285270

Eberle J, Dimitrov D, Valdez-Mondragón A, Huber, BA (2018). Microhabitat change drives diversification in pholcid spiders. BMC Evolutionary Biology 18:141.

Ferreira R.L, Prous X, Martins RP (2007) Structure of bat guano communities in a dry Brazilian cave. Tropical Zoology, 20:55-74.

Ferreira RL, Cardoso RC, Souza-Silva M (2016) Composição, riqueza e diversidade de invertebrados em cavernas de Dianópolis (TO). Revista Brasileira de Espeleologia 01-18

Ferreira RL, Martins RP (1998) Diversity and distribution of spiders associated with bat guano piles in Morrinho cave (Bahia State, Brazil). Diversity and Distributions 4:235-241. https://www.jstor.org/stable/2999829

Ferreira RL, Martins RP (1999) Trophic structure and natural history of bat guano invertebrate communities with special reference to Brazilian caves. Tropical Zoology, 12:231-259. https://doi.org/10.1080/03946975.1999.10539391

Ferreira RL, Martins RP, Yanega D (2000) Ecology of bat guano arthropod communities in a Brazilian dry cave. Ecotropica, 6:105-116.

Ferreira RL, Prous X, Bernardi LFO, Souza-Silva M (2010) Fauna subterrânea do Estado do Rio Grande do Norte: Caracterização e impactos. Rev Bras Espeleol 1:25–51.

Gibert J, Deharveng L (2002) Subterranean ecosystems: a truncated functional biodiversity. American Institute of Biological Sciences Bulletin, 52:473-481.

Gnaspini P (1989) Análise comparativa da fauna associada a depósitos de guano de morcegos cavernícolas no Brasil: primeira aproximação. Revista Brasileira de Entomologia, 33:183-192.

Goldsbrough CL, Hochuli DF, Shine R (2003) Invertebrate biodiversity under hot rocks: habitat use by the fauna of sandstone outcrops in the Sydney region. *Biological Conservation* 109.1:85-93.

González-Megías A, Gómez JM, Sánchez-Piñero F (2007) Diversity-habitat heterogeneity relationship at diferent spatial and temporal scales. Ecography 30:31–41. https://doi.org/10.1111/j.0906-7590.2007. 04867.x

Hawes RS (1939) The flood factor in the ecology of caves. *The Journal of Animal Ecology* 1-5.

Hernández MIM (2007) Besouros escarabeíneos (Coleoptera: Scarabaeidae) da caatinga paraibana, Brasil: Oecologia Brasiliensis 356–364.

Howarth FG (1980) The zoogeography of specialized cave animals: a bioclimatic model. *Evolution* 394-406.

Howarth FG (1983) Ecology of cave arthropods. Annual Review of Entomology 28:365-389.
https://doi.org/10.1111/j.2041-210X.2009.00001.x

Hüppop K (2005) Adaptation to low food. In: Culver D, White WB (ed) Encyclopediaof caves. Ensevier, Amsterdam, pp 4–10.

Iannella M, Fiasca B, Di Lorenzo T, Biondi M, Di Cicco M, Galassi DM (2020) Spatial distribution of stygobitic crustacean harpacticoids at the boundaries of groundwater habitat types in Europe. Scientific Reports, 10: 1-10.

Lobo HAS, Boggiani PC, Perinotto JAJ (2015) Speleoclimate dynamics in Santana Cave (Petar, São Paulo State, Brazil): general characterization and implications for tourist management. Int J Speleol 44(1):61–73. https://doi.org/10.5038/1827-806X.44.1.6

Lunghi E, Raoul M, Ficetola GF (2014) Do cave features affect underground habitat exploitation by non-troglobite species?.*Acta Oecologica* 55:29-35.

MacArthur RH, Levins R (1967) The limiting similarity, convergence, and divergence of coexisting species. Am Nat 101:377–385. https://doi.org/10.1086/282505

Mammola S, Leroy B 2017) Applying species distribution models to caves and other subterranean habitats. Ecography 41:1194-1208. https://doi.org/10.1111/ecog.03464

Mammola S, Marco I (2017) Spiders in caves. *Proceedings of the Royal Society B: Biological Sciences* 284.1853: 20170193.

Mehrabi Z, Slade EM, Solis A, Mann DJ (2014) The Importance of microhabitat for biodiversity sampling. PLoS ONE 9(12):E114015. https://doi.org/10.1371/journal.pone.0114015

Novak T et al (2014) Cold tolerance in terrestrial invertebrates inhabiting subterranean habitats. *Int. J. Speleol*. 43: 265– 272.

Oliveira, LF et al (2022) Recreational caving impacts of visitors in a high-altitude cave in Bolivian Andes: main effects on microhabitat structure and faunal distribution." *International Journal of Speleology* 51.2:2.

Pacheco GSM, Souza-Silva M, Cano E, Ferreira RL (2020) The role of microhabitats in structuring cave invertebrate communities in Guatemala. International Journal of Speleology 49:161-169.

Pallarés S et al (2019) Heat tolerance and acclimation capacity in subterranean arthropods living under common and stable thermal conditions. *Ecology and Evolution* 9.24: 13731-13739.

Pallarés S et al (2020) Beyond survival experiments: using biomarkers of oxidative stress and neurotoxicity to assess vulnerability of subterranean fauna to climate change. *Conservation Physiology* 8.1: coaa067.

Pellegrini TG, et al. (2016a) Linking spatial scale dependence of land-use descriptors and invertebrate cave community composition. Subterranean Biology 18:17-38.

Pellegrini TG, Ferreira RL (2012) Sampling effort in mite communities associated with cave bat guano. Speleobiology Notes 4:10-16.

Pellegrini TG, Ferreira RL (2013) Structure and interactions in a cave guano–soil continuum community. European Journal of Soil Biology 57:19-26. https://doi.org/10.1016/j.ejsobi.2013.03.003

Pellegrini TG, Ferreira RL (2016b) Are inner cave communities more stable than entrance communities in Lapa Nova show cave?. Subterranean Biology 20:15-37.

Poulson TL, Culver DC (1969) Diversity in terrestrial cave communities. Ecology 50:153-158.

Prous X, Ferreira RL, Jacobi CM (2015) The entrance as a complex ecotone in a Neotropical cave. International Journal of Speleology 44: 177-189. https://doi.org/10.5038/1827-806X.44.2.7

Prous X, Ferreira RL, Martins RP (2004) Ecotone delimitation: epigean–hypogean transition in cave ecosystems. Austral Ecology 29:374-382.

Rasband WS (1997) Image, J., US National Institutes of Health. "ImageJ64," US National Institutes of Health, Bethesda, MD.

Romero A (2009) Cave biology: life in darkness. Cambridge University Press, New York.

Schneider K, Christman MC, Fagan WF (2011) The influence of resource subsidies on cave invertebrates: results from an ecosystem-level manipulation experiment. Ecology 92:765-776. https://doi.org/10.1890/10-0157.1

Simões MH, Souza-Silva M, Ferreira RL (2015) Cave physical attributes influencing the structure of terrestrial invertebrate communities in Neotropics. Subterranean Biology 16:103-121. https://doi.org/10.3897/subtbiol.16.5470

Simões MH, Souza-Silva M, Lopes RF (2002) Species-area relationship and richness persistence as a proxy of environmental carrying capacity: A case study in a neotropical show cave. *Acta Oecologica* 116: 103848.

Simon KS, Pipan T, Culver DC (2007) A conceptual model of the flow and distribution of organic carbon in caves. *Journal of Cave and Karst Studies* 69.2: 279-284.

Souza-Silva M, Bernardi LFO, Martins RP, Ferreira RL (2012) Transport and consumption of organic detritus in a neotropical limestone cave. Acta Carsologica 41: 139–150. doi: 10.3986/ac.v41i1.54

Souza-Silva M, Cerqueira RFV, Pellegrini TG et al (2021) Habitat selection of cave-restricted fauna in a new hotspot of subterranean biodiversity in Neotropics. Biodivers Conserv 30:4223–4250 (2021). https://doi.org/10.1007/s10531-021-02302-8

Souza-Silva M, Iniesta LFM, Ferreira R (2020) Cave lithology effect on subterranean biodiversity: A case study in quartzite and granitoid caves. *Acta Oecologica* 108: 103-645.

Souza-Silva M, Martins RP, Ferreira RL (2011) Trophic Dynamics in a Neotropical Limestone Cave. Subterranean Biology 9:127–138. doi: 10.3897/subtbiol.9.2515

Stein A, Beck J, Meyer C, Waldmann E, Weigelt P, Kreft H (2015) Diferential efects of environmental heterogeneity on global mammal species richness. Global Ecol Biogeogr 24(9):1072–1083. https:// doi.org/10.1111/geb.12337

Stein H, Griebler C, Berkhoff S, Matzke D, Fuchs A, Hahn HJ, (2012) Stygoregions–a promising approach to a bioregional classification of groundwater systems. Scientific reports.

Tobin BW, Hutchins BT, Schwartz BF (2013). Spatial and temporal changes in invertebrate assemblage structure from the entrance to deep-cave zone of a temperate marble cave. International Journal of Speleology 42:203-214. https://doi.org/10.5038/1827-806X.42.3.4

Vargas-Mena JC, Cordero-Schmidt E, Rodriguez-Herrera B et al (2020) Inside or out? Cave size and landscape effects on cave-roosting bat assemblages in Brazilian Caatinga caves. J Mammal 101(2):464– 475. https://doi.org/10.1093/jmammal/gyz206

Vasconcellos A, Andreazze R, Almeida AM, Araujo HFP, Oliveira ES, Oliveira U (2010) Seasonality of insects in the semi-arid Caatinga of northeastern Brazil: Revista Brasileira de Entomologia 54: 471–476. doi:10.1590/S0085-56262010000300019.

Wolda H (1988) Insect seasonality: why? Ann. Review. Ecol. Syst. 19:1-18.

Yang Z, Liu X, Zhou M, Ai D, Wang G et al (2015) The efect of environmental heterogeneity on species richness depends on community position along the environmental gradient. Sci Rep 5(1):1–7. https:// doi.org/10.1038/srep15723

Zuur AF, Ieno EN, Elphick CS (2010) A protocol for data exploration to avoid common statistical problems. Methods in Ecology and Evolution 1:3-14.

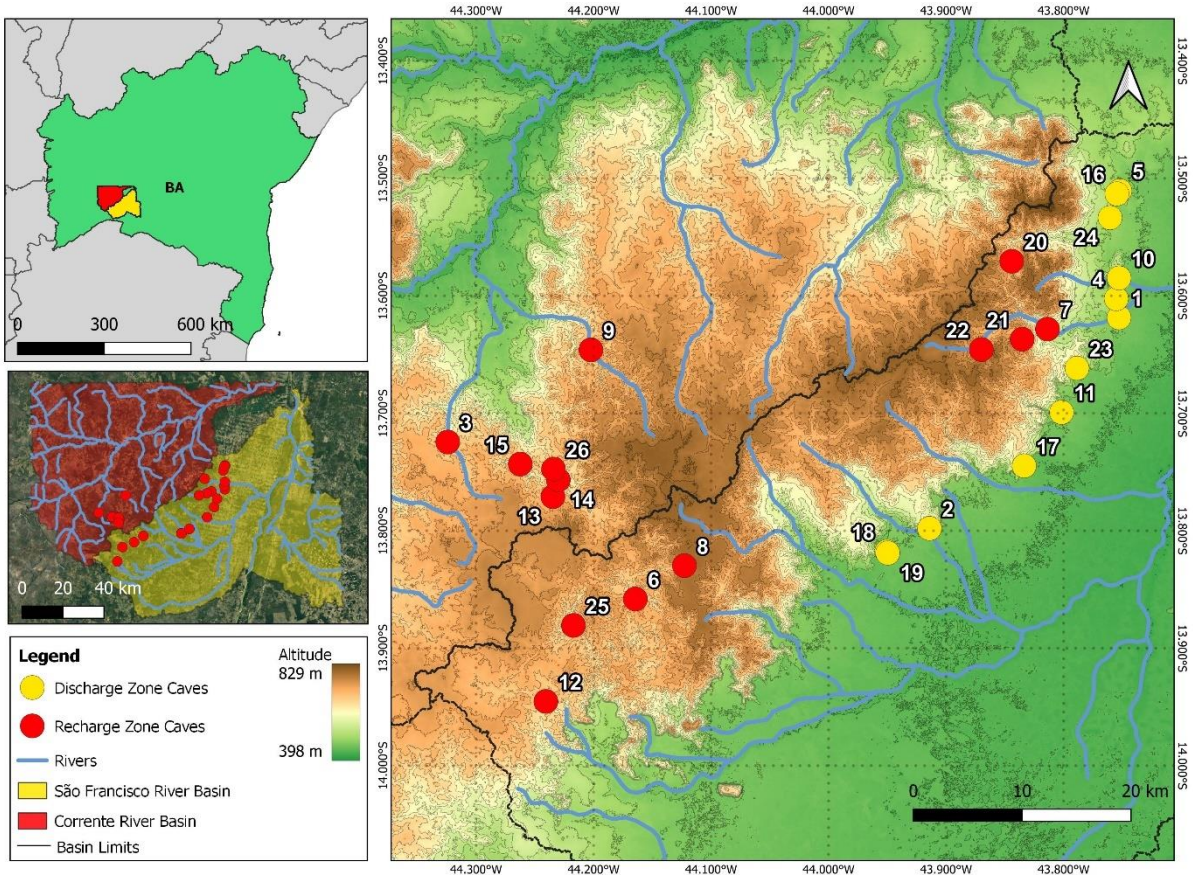


Figure 1: Map of caves location, which micro basins the caves are insert and if the cave are at discharge or recharge zone. The numbers represent the caves:1- Três Cobras Cave; 2- Pedro Cassiano Cave; 3- Serra Verde Cave; 4- Grande Cave; 5- Serra Solta II Cave; 6- Baixão da Canoa Cave; 7- Google Cave; 8- Pingueira do João Nonato; 9- Enfurnado Cave; 10- Riacho do Floriano Cave; 11- Três Bocas Cave; 12- Govi Cave; 13- Zeferini Cave; 14- Lagoa do Meio Cave; 15- Ventilador Cave; 16- Serra Solta III Cave; 17- Domingão Cave; 18- Água Escura I Cave; 19- Água Escura II Cave; 20- Zoológico Cave; 21- Vandecir Cave; 22- Tocas II Cave; 23- Pé de Serra Cave; 24- Mandiaçu Cave; 25- Dedê Cave; 26- Quatro Cabras Cave. The yellow dots are representing discharge zones, while the red dots are representing recharge zones. The fade yellow represents the São Francisco River Basin, while the fade red represents the Corrent River Basin. Lastly, the rivers are represented by the lines in blue.

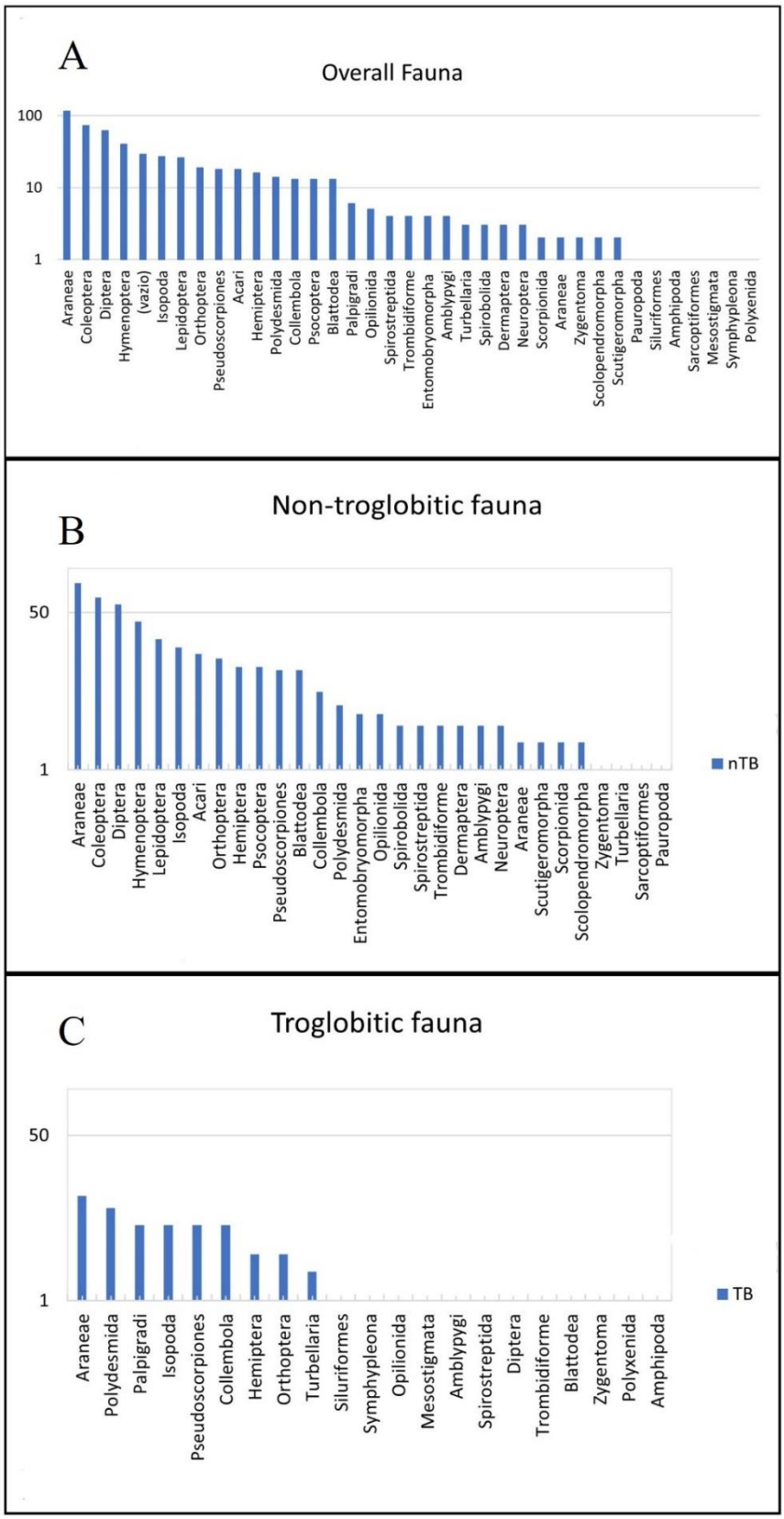


Figure 2. The richness of Overall Fauna (A); The richness of Non-troglobitic Fauna (B); The richness of Troglobitic Fauna (C); nTB means non-troglobitic, while TB means troglobitic.



Figure 3. Some of the troglomorphic species found in Três Cobras Cave. Isopoda (A-E); *Speleaeogammarus* (F); Diplopoda (G-K); Araneae (L, R); *Eukoenenia* (M); *Pseudochthonius* (N); Acari (O); Opiliones (P); *Charinus* (Q); Pseudoscorpiones (S); *Troglobentosminthurus* (T); *Endecous* (U); Blattodea (V); Carabidae (W, X); Gastropoda (Y,Z); Planária (A'); Siluriformes (B'-D').

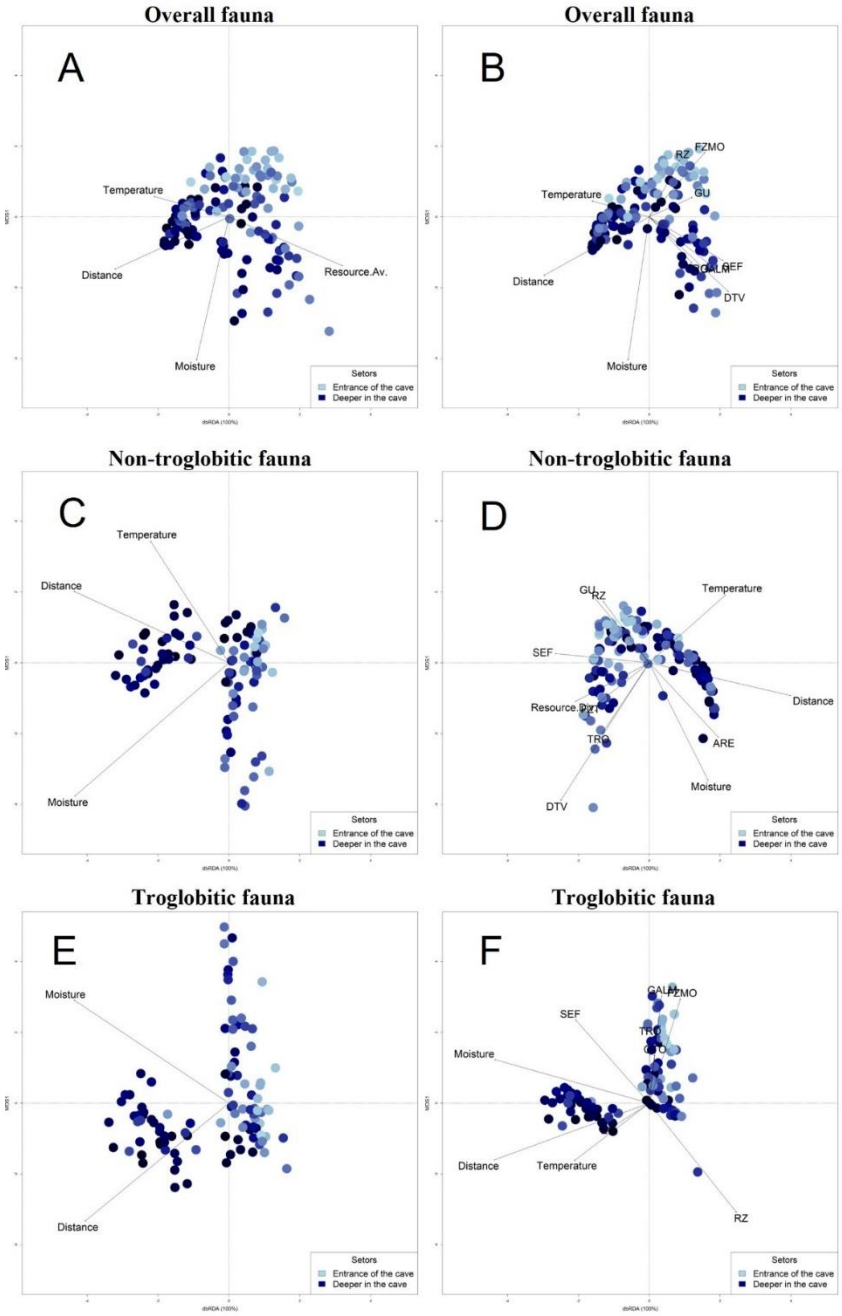


Figure 4. Metric multidimensional scaling (MDS) to show variations of the first model on temperature, moisture, distance from the entrance and resource availability for the overall fauna in the sectors (A); MDS showing variations of the second model on temperature, moisture, distance from the entrance, roots (RZ), Mocó feces (FZMO), guano (GU), trunks (TRO), silt (SEF), medium branch (GALM) and plants debris (DTV) for the overall fauna in the sectors (B); MDS showing variations of the first model on temperature, moisture and distance from the entrance for the non-troglobitic fauna in the sectors (C); MDS showing variations of the second model on temperature, moisture, distance from the entrance, resource diversity, roots (RZ), Tamanduá feces (FZT), guano (GU), trunks (TRO), silt (SEF), sand (ARE) and plants debris (DTV) for the non-troglobitic fauna in the sectors (D); MDS showing variations of the first model on moisture and distance from the entrance for the troglobitic fauna in the sectors (E); MDS showing variations of the second model on temperature, moisture, distance from the entrance, roots (RZ), Mocó feces (FZMO), medium branch (GALM), trunk (TRO), other organic substrate (OTO) and silt (SEF) for the troglobitic fauna in the sectors (F). The colors one the dots represent the distance from the cave entrance to bottom of the cave, so as lighter the dot the closer from the entrance, and the darker the dot the deeper is the sector.

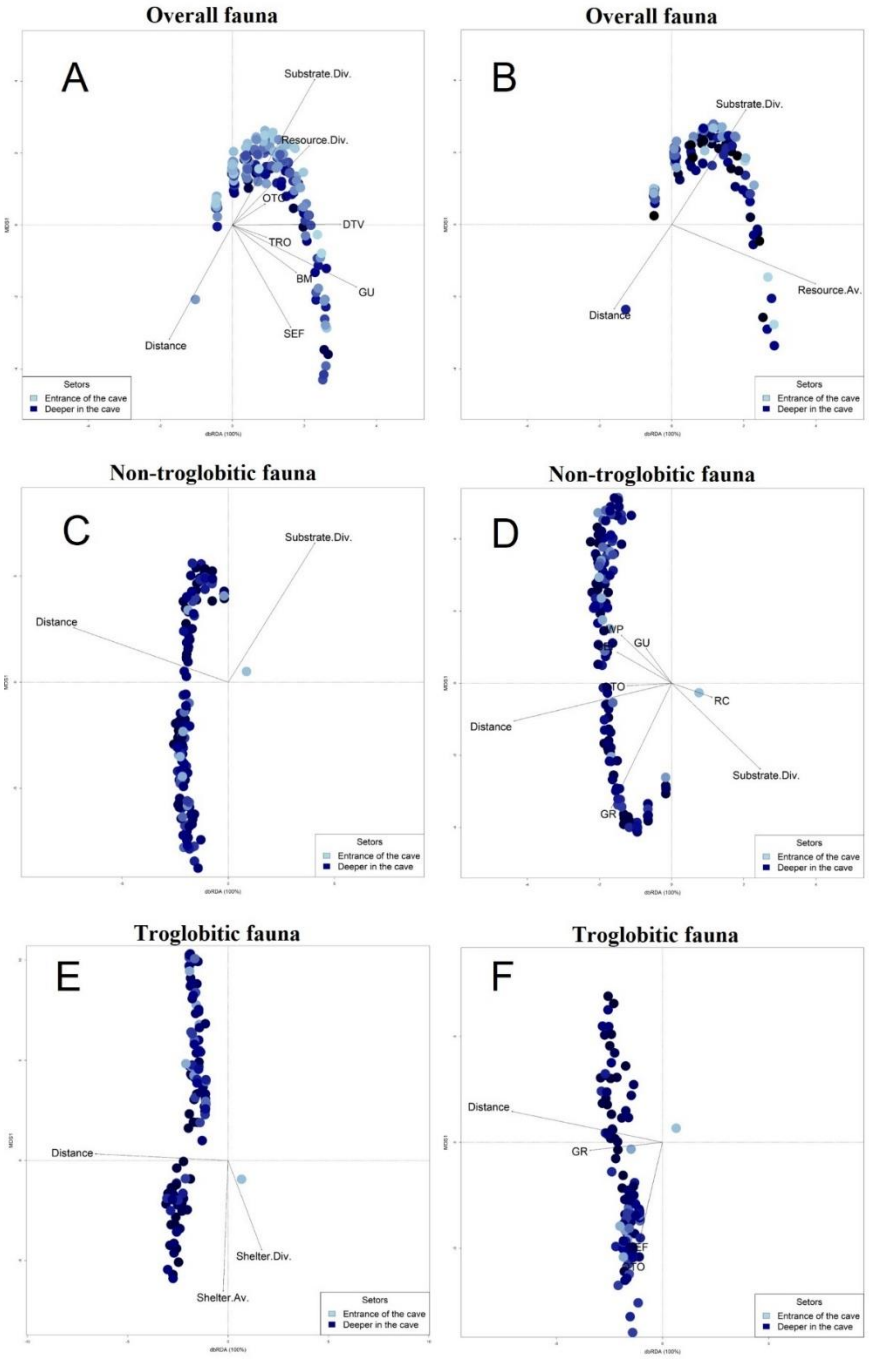


Figure 5. Metric multidimensional scaling (MDS) to show variations of the first model on substrate diversity, resource diversity, distance from the entrance, guano (GU), trunks (TRO), silt (SEF), plants debris (DTV), word acorn (BM) and other organic substrate (OTO) for the overall fauna in the quadrats (A); MDS showing variations of the second model on substrate diversity, resource availability and distance from the entrance for the overall fauna in the quadrats (B); MDS showing variations of the first model on substrate diversity and distance from the entrance for the non-troglobitic fauna in the quadrats (C); MDS showing variations of the second model on substrate diversity, distance from the entrance, guano (GU), water pond (WP), silt (SEF), concrete like floor (RC), retraction cracks (GR) and other organic substrate (OTO) for the non-troglobitic fauna in the quadrats (D); MDS showing variations of the first model on distance from the entrance, shelter availability and diversity for the troglobitic fauna in the sectors (E); MDS showing variations of the second model on distance from the entrance, retraction cracks (GR), silt (SEF) and other organic substrate (OTO) for the troglobitic fauna in the sectors (F). The colors one the dots represent the distance from the cave entrance to bottom of the cave, so as lighter the dot the closer from the entrance, and the darker the dot the deeper is the quadrat.

TABLES

Table 1. Information regarding the caves coordinates (UTM), municipality, altitudes, the number of sectors that were collected, total richness and troglobitic richness of the cave, the microbasin and hydro zone that the cave is insert. TB: troglobitic; SF: São Francisco River Basin; CR: Corrente River Basin; R: Recharge zone; D: Water zone;

Caves	Municipality	nº sectors	Lat	Long	Total Richness	TB Richness	Altitude	Micro basins	Hydro zones (R/D)
Três Cobras Cave	Serra do Ramalho	22	-13.618507	-43.7527	67	14	486.475	SF	D
Pedro Cassiano Cave	Carinhanha	15	-13.798	-43.914	39	5	473.538	SF	D
Serra Verde Cave	Coribe	10	-13.724455	-44.3241	29	2	663.924	CR	D
Grande Cave	Serra do Ramalho	9	-13.602472	-43.7551	41	3	486.443	SF	D
Serra Solta 2 Cave	Serra do Ramalho	9	-13.510601	-43.7521	20	3	500.781	SF	D
Baixão da Canoa Cave	Coribe	8	-13.858135	-44.1644	27	3	654.786	SF	R
Google Cave	Serra do Ramalho	7	-13.628315	-43.8136	32	3	565.711	SF	R
Pingueira do João Nogueira Cave	Coribe	6	-13.829726	-44.1226	15	4	742.194	SF	R
Enfurnado Cave	Coribe	6	-13.646025	-44.2022	12	3	637.067	CR	D
Riacho do Floriano Cave	Serra do Ramalho	6	-13.584813	-43.7527	19	2	486.809	SF	D
Três Bocas Cave	Serra do Ramalho	5	-13.699167	-43.8016	12	1	486.513	SF	D
Govi Cave	Coribe	5	-13.945361	-44.2405	42	12	682.335	SF	R
Zeferini Cave	Coribe	5	-13.771024	-44.2346	26	2	698.921	CR	D
Lagoa do Meio Cave	Coribe	4	-13.756661	-44.23	39	3	691.703	CR	D
Ventilador Cave	Coribe	4	-13.743252	-44.2624	16	1	629.643	CR	D
Serra Solta 3 Cave	Serra do Ramalho	4	-13.513154	-43.7545	19	1	497.387	SF	D
Domingão Cave	Carinhanha	3	-13.744734	-43.8335	8	1	473.96	SF	D
Água Escura 1 Cave	Carinhanha	3	-13.817694	-43.9504	11	1	477.839	SF	D
Água Escura 2 Cave	Carinhanha	3	-13.818957	-43.9496	12	2	476.769	SF	D
Zoológico Cave	Serra do Ramalho	2	-13.57058	-43.844	31	5	698.2	SF	R
Vandecir Cave	Serra do Ramalho	2	-13.636943	-43.8352	48	8	738.202	SF	R
Tocas 2 Cave	Serra do Ramalho	2	-13.645741	-43.8699	37	8	734.591	SF	R
Pé de Serra Cave	Serra do Ramalho	2	-13.661617	-43.7885	50	7	526.655	SF	D
Mandiaçu Cave	Serra do Ramalho	1	-13.533514	-43.7603	59	9	499.485	SF	D
Dedê Cave	Coribe	1	-13.880596	-44.2171	39	5	681.085	SF	R
4 Cabras Cave	Coribe	1	-13.747524	-44.2341	43	3	669.033	CR	D

Table 2. Relationship between habitat structure of the sectors with species richness.

Variables	Mesoscale/Sector											
	Model 1						Model 2					
	Overall		T		n-T		Overall		T		n-T	
	P	Est.	P	Est.	P	Est.	P	Est.	P	Est.	P	Est.
Distance					1.0E⁻1	-0.180					3.0E⁻1	-0.150
Temperature	0.020	-0.1100	0.0300	0.150	0.006	-0.140	0.003		0.030	0.220	8.37 E⁻5	-0.160
Humidity			0.0004	0.300					0.010	0.270	0.010	-0.090
Resource Av.	2.00E-04	0.1600			5.00E-04	0.160						
DTV							1.09E⁻8	-0.110			1.33E-08	0.130
GALF							2.00E-04	0.080			0.001	0.070
GALM							0.010	0.070			0.020	0.070
TRO							7.75E⁻6	0.090			2.33E-06	0.110
DP							0.004	0.070	0.010	0.090		
OTO							0.001	0.060			7.00E-04	0.070
SEF							1.02E⁻5	0.160			4.11E-05	0.170
FZA							0.020	0.040	0.010	0.120		
FZMO							0.009	0.060			0.012	0.060
BAM							0.040	0.040	0.002	0.120		
PHP							0.030	0.050				
ACT									0.004	0.200	0.040	
CAF											0.020	0.080
RZ									0.020	-0.390		
R^2/R^2M	**22.48%**		**20.00%**		**31.62%**		**80.07%**		**43.69%**		**87.14%**	
R^2C	**68.99%**				**72.92%**		**80.13%**					

Table 3. Relationship between habitat structure of the sectors and quadrats with species composition. dbRDA 1: refers to model number one; dbRDA 2: refers to model number two.

Variables	Mesoscales/Sector						Microscale/Quadrat					
	dbRDA 1			dbRDA 2			dbRDA 1			dbRDA 2		
	Overalll	T	n-T	General	T	n-T	Overall	T	n-T	General	T	n-T
Distance	0.005	0.005	0.005	0.005	0.005	0.005		0.005	0.005	0.015	0.005	0.005
Humidity	0.005	0.005	0.005	0.010	0.005	0.005						
Temperature	0.005	0.005		0.005	0.04	0.005						
Resource av.	0.005	0.005					0.005					
Resource div.						0.050		0.045		0.010		
Substrate div.							0.005		0.005	0.005		0.005
DTV				0.005		0.005				0.005		
SEF				0.005	0.05	0.010				0.005	0.030	0.010
GU				0.005		0.010				0.005		0.010
GALM				0.005	0.005							
TRO				0.010	0.02	0.005				0.050		
FZMO				0.010	0.005							
RZ				0.040	0.005	0.030						
FZT						0.020						
ARE						0.040						
ES					0.010							
OTO					0.040					0.020	0.040	0.005
BAM										0.005		
GR											0.005	0.010
WP												0.005
CR												0.030
Explanation	**9.99%**	**6.00%**	**9.00%**	**19.00%**	**20.00%**	**18.00%**	**11.00%**	**14.00%**	**13.00%**	**17.00%**	**16.00%**	**18.00%**

Table 4. Relationship between habitat structure of the quadrats with species richness.

Variables	Microscale/Quadrat											
	Model 1						Model 2					
	Overall		T		n-T		Overall		T		n-T	
	P	Est.	P	Est.	P	Est.	P	Est.	P	Est.	P	Est.
Distance	1.00E-02	-0.140	1.00E-02	-0.140	1.06E⁻10	1.120	1.00E-03	-0.170	1.00E-03	-0.170	3.17E⁻15	0.190
Resource Av.	7.84E⁻9	0.240	7.85E⁻9	0.240								
Resource div.							0.020	0.080	0.020	0.080		
Substrate div.					0.008	-0.58	0.040	0.110	0.040	0.110	2.20E⁻15	-3.43E-01
Shelter div.							0.010	0.140	0.010	0.140		
DTV							9.49E⁻11	0.180	6.55E⁻10	0.150	1.00E-04	-4.210
GALF											1.00E-02	-9.56E-10
OTO							3.41E⁻7	0.110	2.65E⁻7	0.110	1.03E⁻9	1.04E-01
SEF							4.00E-04	0.210	4.00E-04	0.140		
BAM									8.06E⁻10	0.090		
MB											0.003	-2.98E-01
SB											0.030	1.06E-01
CAG											2.00E-04	-2.73E-01
HP											0.010	1.14E-01
ARE											1.54E⁻5	1.66E-01
GU							3.71E⁻6	0.120	1.75E⁻5	0.110	0.020	6.34E-02
BM							2.37E⁻10	0.100				
WP							0.020	0.060				
R^2/R^2M	**12.08%**		**12.08%**		**25.49%**		**41.89%**		**79.47%**		**85.00%**	
R^2C	**47.92%**		**47.92%**		**99.79%**							

IUIÚ


FROM THE FRONT DOOR
TO THE BASEMENT

From the front door to the basement: invertebrate communities' structure as a proxy for determining cave zonation in Neotropics.

Paulo C. Reis-Venâncio[1,2], Rodrigo L. Ferreira[1,2], Marconi Souza-Silva[1,2]
[1] Universidade Federal de Lavras, Instituto de Ciências Naturais, Departamento de Ecologia e Conservação, Centro de Estudos em Biologia Subterrânea, Caixa postal 3037, CEP 372000-900, Lavras, MG, Brasil.
[2] PPG- Ecologia Aplicada, Departamento de Ecologia e Conservação (DEC), Universidade Federal de Lavras, Minas Gerais, Brazil.

Reis-Venâncio, P. C. ORCID identifier is 0000-0002-5655-8703
Ferreira, R.L. ORCID identifier is 0000-0003-3288-4405
Souza-Silva, M. ORCID identifier is 0000-0002-3184-5319

Abstract:
In caves, the absence of natural light in deeper regions starkly contrasts with the entrance areas, which still exhibit a light gradient extending into the cave interior. This interplay with the structural gradient of the environment potentially exerts distinct influences on invertebrate communities residing in different cave light zones. To investigate this, we formulated a hypothesis positing that communities within distinct cave light zones respond differently to habitat structure and microclimatic conditions. Our approach involved a spatial multi-scale sampling of invertebrates and the application of statistical analyses to contrast the responses of communities inhabiting photic and aphotic zones. Photic zone richness is influenced by factors such as air moisture, resource availability, root presence, and shelter diversity. In contrast, the richness of communities in aphotic zones is shaped by resource availability, the presence of roots, branches, and distance from the cave entrance. As expected, the richness in the photic zone surpasses that of the deeper regions, highlighting the challenges faced by invertebrates attempting to establish themselves in the aphotic zone. The species composition of faunal communities varied predictably from the entrance to the aphotic zone, and the three most important factors driving this variation were geographic distance, humidity, and distance from the entrance. The composition between these cave zones differs significantly, primarily due to the high number of obligate cave species predominantly inhabiting the aphotic region. Indeed, communities associated with different cave zones exhibit distinct responses to resource, microclimatic, and structural variables.
Keywords: Brazil, habitat structure, niche overlap, light gradient, structural gradient, limestone caves, Caatinga

INTRODUCTION

Since the initial description of the first cave-dwelling organism in 1768, interest in this scientific field has surged significantly in Europe and the USA, and more recently, in tropical regions (Polak, 2005; Mammola, 2019). Substantial efforts have been directed towards enhancing our comprehension of the biogeographical, ecological, and evolutionary processes that govern subterranean ecosystems (Lienhard & Ferreira, 2013; Mammola et al., 2019, 2020; Souza-Silva et al., 2021; Recknagel & Trontelj, 2022).

These studies not only aim to comprehend the cave environment itself but also utilize it as a natural laboratory to gain deeper insights into the dynamics of more complex systems and environments. Caves present stringent environmental constraints and harbor simple communities, making them valuable models for ecological research (Poulson & White, 1969; Howarth, 1983; Culver & Pipan, 2015, 2019; Mammola, 2019; Mammola et al., 2020). However, despite the significant progress made, many questions about the ecological processes behind cave organisms remain unanswered, and well-established patterns are only just beginning to be unveiled (Mammola et al., 2020). This knowledge gap directly impacts our understanding of these unique environments and limits their effective conservation and management.

Subterranean environments, in general, possess a set of ecological and physical attributes that function as biological filters, determining which species are capable of colonizing and establishing populations in the subterranean environment (Poulson & White, 1969; Howarth, 1983; Prous et al., 2004, 2015; Mammola, 2019). Among the primary characteristics of the subterranean environment, which include climatic stability and food scarcity, the most prominent is the complete absence of natural light (Poulson & White, 1969; Culver & Pipan, 2019; Mammola, 2019; Reis-Venâncio et al., 2022).

Natural caves are commonly divided into three zones based on the presence/absence of light and its variability along their extension: the photic zone (with direct light incidence near entrances and skylights, and variable climate), the twilight zone (experiencing indirect light incidence with characteristics intermediate to adjacent zones), and the aphotic zone (completely devoid of light, with a tendency to high climatic stability and high humidity) (Badino, 2010; Tobin et al., 2013).

Along with the light gradient, a structural gradient can be observed, wherein regions closer to the entrances harbor a greater diversity and quantity of organic substrates. In contrast, these attributes decrease towards regions farther from the entrances, resulting in, most cases, a more uniform and energetically limited environment (Poulson & White, 1969; Moseley, 2009; Mammola, 2019; Souza-Silva et al., 2021), although there are exceptions (Iskali & Zhang, 2015).

The variable conditions within caves directly influence the invertebrate fauna due to their habitat and microhabitat preferences, physiological constraints, ecological interactions, and ecological niche breadth (Tobin et al., 2013; Culver & Pipan, 2019;

Mammola et al., 2020; Pacheco et al., 2020; Furtado-Oliveira, 2021; Souza-Silva et al., 2021; Cardoso et al., 2022; Reis-Venâncio et al., 2022). Researchers have investigated the factors responsible for the spatial structuring of cave communities, particularly in tropical caves. For instance, species diversity increases with the presence of water bodies, cave extension (Simões et al., 2015), resource availability (Ferreira & Martins, 1999; Ferreira et al., 2007; Souza-Silva et al., 2011, 2021), and substrate diversity. Additionally, habitat heterogeneity, a global driver of diversity in a diversity of ecosystems (Tews et al., 2004), also plays a critical role in structuring cave communities (Pacheco et al., 2020; Souza-Silva, 2021; Furtado-Oliveira et al., 2022; Reis-Venâncio et al., 2022).

The conditions and resources vary along the gradient, spanning from the cave entrance to its deepest regions (Moseley, 2009; Cuff et al., 2021; Souza-Silva et al., 2021). In this sense, cave fauna communities tend to be microhabitat specialists, consequently, there should be a quantitative association between this environmental gradient and faunal community structure.

The principal goal of this study was to quantify variation in conditions, resources, and faunal community structure along the gradient from the entrance to the aphotic zone of caves in Brazil. We predicted that: i) communities within the photic zones demonstrate elevated compositional dissimilarity and higher species richness than those in the aphotic zones; and ii) communities associated with distinct zones exhibit differing responses to substrate, microclimatic conditions, and resource diversity.

METHODS

Study area

To evaluate our proposed hypothesis, we conducted the study in 31 caves located in the Iuiú and Malhada municipalities, located in the Southwestern Bahia state, Brazil (**Erro! Fonte de referência não encontrada.**, Appendix S1). These caves are distributed across four distinct and non-contiguous carbonate massifs. All of these massifs are part of the Bambuí geological group, dating back to the Neoproterozoic era, approximately 750 to 600 million years ago.

The region is located on the right bank of the São Francisco River, at an altitude of approximately 794 meters above sea level. It falls within the Caatinga domain, characterized by seasonally dry tropical forests as the predominant vegetation (Apgaua et al., 2014). According to the Köppen-Geiger climate classification system (Alvares et al., 2013), the area experiences a hot semi-arid tropical climate (Bsh), with an average temperature of 24°C and an annual average precipitation of 788 mm (Fick & Hijmans, 2017). For each cave, the geographical coordinates were recorded near its main entrance using a GPS device.

Sampling design

Habitat structure, along with invertebrate richness and composition, was assessed during two field expeditions conducted in October 2021 and July 2022, during the dry

season. These assessments were carried out using sectors (3x10m) and quadrants (1x1m) (e.g., Pacheco et al., 2020; Souza-Silva et al., 2021; Furtado-Oliveira et al., 2022).

Data encompassing the richness, composition, and abundance of terrestrial cave invertebrates, alongside physical, microclimatic, and substrate parameters, were collected within each sampling unit. The 30 m² sectors were uniformly positioned across the entire accessible length of the cave, spanning from the entrance to the deepest reaches, and encompassing the cave floor. This comprehensive approach resulted in a total of 114 sectors being sampled across all investigated caves.

Within each sector, a set of three 1m² quadrants were positioned: two at opposing ends of the sector and one situated in its midpoint. This arrangement led to a total of 342 quadrants being examined. Considering the dimensions of each sampling unit, the sector was defined as a mesoscale, while the quadrants constituted the microscale. The species collected within the quadrants were incorporated and accounted for within the mesoscale analysis. Given their varying sizes and volumes, the allocation of quadrants and sectors in each cave was not uniform (see Appendix S1).

Measuring microhabitat structure

The quantification of both organic and inorganic substrates constituting the cave floor within each sample unit was conducted at both the mesoscale and microscale (Appendix S2). At the mesoscale, each sector was subdivided into ten perpendicular sections spanning 3 m² each. Within each section, the occupied area by different organic and inorganic substrates was estimated through visual assessment. To determine the cumulative area occupied by each substrate along the sector, the summation of occupied substrate areas across all ten sections was calculated, subsequently leading to the calculation of their respective percentages per sector (Pacheco et al., 2020; Souza-Silva et al., 2021; Furtado-Oliveira et al., 2022).

At the microscale, the quantification within each quadrant was conducted through the analysis of pre-sampling photographs (Pacheco et al., 2020; Souza-Silva et al., 2021; Furtado-Oliveira et al., 2022). These photographs were captured as parallel as possible to encompass all boundaries of the quadrant. Subsequent substrate quantification occurred using ImageJ software within the laboratory setting, where we determined the proportional representation of each organic and inorganic substrate within the quadrant's 1 m² area.

Measuring physical and microclimatic predictors

Temperature and humidity variables were assessed using a digital thermo-hygrometer (model Akso – AK625) positioned within the central portion of the sector at floor level. This setup was maintained for a minimum of 15 minutes to ensure accuracy. To establish the light exposure within each sector, a digital lux meter (Incoterm PLUX1000) was positioned in the central area of the sector to gauge the incident light intensity. Sectors registering non-zero values were categorized as photic, while values equivalent to zero were designated as aphotic. The light values recorded for the sectors were subsequently applied to their corresponding triads of quadrants. Temperature and

humidity measurements were taken for each individual quadrant. Lastly, the proximity of each sector and quadrant to the nearest entrance was determined from the midpoint of the sampling unit to the edge of the entrance or skylight, employing laser tapes and cave maps.

Invertebrate sampling

We conducted the sampling of terrestrial invertebrates across all sectors and quadrants using the Direct Intuitive Search (DIS) method and manual collection techniques (Wynne et al., 2019). Tweezers and brushes were employed to facilitate this process. The sampling procedures were executed by a team of at least four seasoned professionals skilled in subterranean fauna collection.

The collection of invertebrates within each sampling unit was deemed complete only when all the invertebrates present had been captured and/or accounted for. Moreover, to ensure comprehensive coverage of invertebrate diversity, particularly species exclusive to cave environments, all potential habitats were thoroughly examined throughout the accessible cave length, extending beyond the designated sampling units (Ferreira, 2004; Wynne et al., 2018, 2019). All collected specimens were preserved in vials containing 70% ethanol.

It is worth noting that, to avoid excessive sampling impacts from sensitive populations, we collected a few individuals and estimated the total abundance of the non-sampled invertebrates with low densities. (Mammola et al 2020).

Invertebrate identification

In the laboratory, the collected invertebrates underwent identification up to the feasible taxonomic level. Subsequently, they were categorized into morphospecies (Oliver & Beattie, 1996a, 1996b). Taxonomists confirmed species identities or morphospecies assignments for selected groups (Isopoda, Orthoptera, Polydesmida, Palpigradi, Coleoptera, Acari, Araneae, Pseudoscorpiones, Hemiptera, Eupulmonata, Entomobryomorpha, Symphypleona, and Poduromorpha).

We identified potential troglobitic species by referencing available literature specific to the studied region and considering the presence of troglomorphic characteristics, including elongated appendages, anophthalmia, and depigmentation (Christiansen, 1962; Culver & Pipan, 2019). To ensure accurate determinations of these traits, we sought input from specialists in each taxon.

All collected individuals have been deposited in the Coleção de Invertebrados Subterrâneos de Lavras (ISLA, acronym in Portuguese), which is associated with the Centro de Estudos em Biologia Subterrânea at Universidade Federal de Lavras (http://www.biologiasubterranea.com.br).

Data analysis

Substrate measures

We employed the Shannon Diversity index (H') to obtain substrate, shelter and resource diversities values for each sampling unit (Cardoso et al., 2022; Pellegrini et al., 2016; Souza-Silva et al., 2021; Oliveira-Furtado et al., 2022). To obtain the substrate

diversity, we applied the Shannon Diversity index across all substrate classes within each sampling unit. For the assessment of resource diversity, we considered all classes of the cave floor organic substrates (guano, feces, roots, leaf litter, plant debris, branches, wood, fungi, algae, and undetermined organic matter). On the other hand, the diversity of shelters was calculated based on the proportions of large, medium, and small boulders, branches, wood, leaf litter, coarse and fine gravel, speleothems, cracks, and cobble.

Additionally, we calculated the resource and shelter availability by summing up the values of the substrate classes (Reis-Venâncio et al., 2022; Souza-Silva et al., 2021). For shelter availability, the included substrate classes comprising large boulders, medium boulders, small boulders, cobblestones, coarse gravel, fine gravel, speleothems, and retraction cracks. The availability of resources was calculated by summing up the values associated with guano, feces, roots, leaf litter, plant debris, branches, wood, algae, fungi, and undetermined organic matter.

Differences in habitat structure along a luminosity gradient

We used a Principal Component Analysis (PCA) to assess the variation in physical structure concerning the cave zone, for both scales. The analysis and its graphical representation were generated using the factoextra package (Kassambara and Mundt, 2020).

We conducted a Distance-based Linear Model (DistLM) analysis to explore the relationship between physical factors (shelter diversity and availability), organic resources (resource diversity and availability), and microclimatic variables (temperature and humidity) with the entrance distance. Each environmental variable was considered a response variable in relation to entrance distance. To achieve this, we developed distinct models using a Euclidean distance-based matrix and employed a stepwise approach in conjunction with the AICc model selection criterion (Anderson et al., 2008).

Faunal differences between photic and aphotic zones

Richness data were not normally distributed (Shapiro-Wilk test), thus we used a Mann-Whitney U-test to compare faunal species richness between photic and aphotic zones.

To examine differences in faunal composition between the different cave zones, we first standardized the data using the Hellinger method. We then constructed a Bray-Curtis dissimilarity matrix and used it in a non-Metric Multidimensional Scaling (nMDS) to visualize the data and look for eventual group formation (Zuur et al., 2007; Legendre & Legendre, 2012; Borcard et al., 2011). To determine if the composition varied significantly between photic and aphotic zones, we performed a Permutational Multivariate Analysis of Variance (Permanova) with the caves´ zones as factors using the 'adonis2' function from the *vegan* package (Oksanen et al., 2022).

To visualize the contribution of each morphospecies to the fauna similarity between the different caves´ zones, we conducted a Similarity Percentages Breakdown (SIMPER), calculated from a Bray-Curtis dissimilarity matrix (Anderson et al., 2008). This analysis

was performed in the Plymouth routine in Multivariate ecological research - Primer 7 (http://www.primer-e.com).

Habitat structure and invertebrate communities between aphotic and photic zones

Prior to conducting the regression analyzes, we assessed multicollinearity among all predictors using Spearman correlation with the 'chart.correlation' function from the *PerformanceAnalytics* package (Peterson and Carl, 2020). Variables with correlation values exceeding $\hat{r} \geq 0.7$ were analyzed separately to mitigate potential collinearity issues (Schober et al., 2018). As the Spearman coefficient only shows paired correlations (Zuur et al., 2009), we also used variance inflation factors (VIF) in the initial model, which includes all predictors. Predictors with values exceeding 3 were removed from the models and then, reanalyzed.

To analyze the effects of all substrate variables, resource and microclimatic features on morphospecies richness at the mesoscale, we constructed four independent Generalized Linear Models (GLMs). We used the negative binomial distribution of errors for all models, as the Poisson distribution showed overdispersion in all the constructed models. Using the Poisson distribution under these conditions can lead to an enhanced type I error, where explanatory variables that have no real effect may appear significant (Zuur et al., 2009).

The first model investigates the response of the aphotic zone fauna to microclimatic predictors (temperature and humidity), the components of the substrate diversity (total substrate diversity, resource diversity, and shelter diversity), as well as the availability of shelter and resources. The second model also considers the aphotic zone as the response variable and uses microclimate and components of the substrate diversity (total substrate diversity, resource diversity, and shelter diversity) as predictors. However, instead of using the availability of shelter and of resources, it includes each component of the substrate separately (as presented in Appendix S2). Models three and four maintained the same configuration as models one and two but used the richness of the photic zone as the response variable.

To analyze the effects of all substrate variables, resource and microclimatic features on morphospecies richness on the microscale, we performed four generalized linear mixing models (GLMM), assuming the sector as the random effect. The predictors and response variables included in each model were consistent with the mesoscale models. We assumed the negative binomial distribution family for the models with the photic groups as response variables. However, for the models considering the aphotic group as the response variable, the Poisson distribution family provided the best fit. We assessed model fit by visually inspecting the spatial distribution of residuals and using the 'simulateResiduals' function from the DHARMa package (Hartig, 2022). The model with the lowest Akaike Information Criterion (AIC) value was selected.

We followed three steps to construct the GLM and GLMM models: (i) we first created the full model with all predictors; (ii) we then ran the model, excluded the predictor with the highest p-value, and reanalyzed the model; (iii) we repeated this step

until the final model included only significant predictors or showed the lowest AIC value. To calculate the pseudo adjusted R^2 values we used the 'r.squaredGLMM' and 'r.squaredLR' function from the *MuMIn* package (Bartoń, 2022).

To investigate the relation of the morphospecies composition in the different cave zones with the substrate components, resource diversity, and microclimatic predictors, we performed a Distance-based linear model (DistLM) using a Bray-Curtis matrix, while excluding units without morphospecies. We employed a forward selection procedure and the adjusted R^2 as model selection criteria, with 999 permutations (Anderson et al., 2008). All analyses were conducted in R (R Core Team 2022) unless otherwise noted.

RESULTS

Invertebrate composition and richness

We recorded a total of 449 morphospecies in the 31 sampled caves, including 381 at the mesoscale (234 in the aphotic zone and 263 in the photic zone) and 240 at the microscale (140 in the aphotic zone and 163 in the photic zone). Our sampling methods enabled us to detect 36 orders of invertebrates (Figure 2), distributed across at least 99 families. Araneae emerged as the most diverse taxon, succeeded by Coleoptera and Acari. Within the aphotic zone, Araneae maintained its richness, trailed by Coleoptera, while Acari and Diptera each accounted for 16 morphospecies. Within the photic zone, Araneae retained its dominance, followed by Coleoptera, while Hemiptera and Hymenoptera tied with 21 morphospecies each.

The Mann-Whitney analysis revealed a significant distinction in morphospecies richness between the aphotic and photic zones (Figure 3). Regardless of the spatial scale analyzed, we consistently observed higher average richness in the photic zone.

The Permanova analysis unveiled a significant dissimilarity in faunal composition across distinct cave zones ($F= 7.0118$; $R^2= 0.05942$; $p= 0.001$). The ordination techniques, revealed a pattern wherein the communities within the photic zone exhibited greater similarity, while those within the aphotic zone displayed heightened dissimilarity (Figure 4).

The morphospecies that contributed to at least 50% of the dissimilarity between the cave zones are listed in the Appendix S3. From the taxa listed, the two troglobitic species, *Iuiuia caeca* and *Trogolaphysa* sp.1, were primarily found in the aphotic zone.

Troglobitic species richness

Across all of our sampling methods, we documented 56 morphospecies displaying troglomorphic traits. These morphospecies span 13 orders, with all troglobiont morphotypes detailed in Appendix S4, while select representatives are depicted in Figure 5.

Regarding the cave zones, we found that 52.56% of the sectors in the aphotic zone contained troglobitic morphospecies (41 sectors out of 78), whereas, in the photic zone, only 36.11% of the sectors presents troglobitic morphospecies (13 sectors out of 36).

Habitat physical structure

The Principal Components Analysis revealed that there is a distinction in the habitat structure between photic and aphotic zones (Appendix S5), regardless of the spatial scale analyzed. As expected, the photic zone presented a more complex physical structure and lower humidity compared to the aphotic zone.

At the mesoscale, several variables play a crucial role, including resource diversity and availability, substrate diversity, shelter diversity and availability, humidity, and coarse gravel. On the other hand, at the microscale, the key variables are resource diversity and availability, substrate diversity, shelter diversity, small boulder, cobble, hardpan, humidity, and distance from the cave entrance.

The humidity presented a positive relationship with distance from the entrance (AICc= -17.806, R^2= 0.16894, p= 0.001), while the shelter diversity exhibited a negative relationship with distance from the entrance (AICc= -6.4514, R^2= 0.0811, p= 0.004).

Furthermore, the average humidity in the aphotic zone was 82.31% (SD= 11.58), which is higher than the 75.21% (SD= 12.146) observed in the photic zone. Additionally, despite temperature differences, the average temperature in the aphotic zone was only slightly lower (24.14ºC, SD= 1.426) than that in the photic zone (24.65ºC, SD= 1.795).

Relationship between habitat structure and invertebrate richness in aphotic and photic zones

Invertebrates´ richness in the aphotic zone increases with the rise in the availability of organic resources and decreased with the distance from the cave entrance (Appendix S6, Figures 6-a, b). Considering the fauna in the photic zone, the models indicated that morphospecies richness increased in response to the rise of the humidity, availability of organic resources, and plant debris, while it decreases with distance from the entrance and rough rock percentage (Appendix S6, Figures 6-c, d).

Based on the models used to investigate the response of the morphospecies richness in the aphotic zone at the microscale, we found that the distance from the entrance continued to negatively affect this community component. Nevertheless, we also observed that the predictors such as resource availability, plant debris, branches, and silt are important in increasing morphospecies richness in this zone (Appendix S7, Figures 7-a, b, c). Finally, the models used to investigate the response of morphospecies richness at the microscale associated with the photic zone, showed a positive relationship with humidity, shelter diversity, resource availability, roots, leaf litter, and branches (Appendix S7, Figures 7-d, e, f).

In summary, our observations reveal that humidity, rough rock terrain, shelter diversity, root presence, and leaf litter density significantly influence morphospecies richness within the photic zone. However, these factors do not demonstrate a discernible effect on morphospecies richness within the aphotic zone. Conversely, we found that the

amount of silt was the sole predictor that exclusively influenced the richness of the aphotic zone.

Relationship between habitat structure and invertebrate composition in different cave zones

Considering the models at the mesoscale, the aphotic zone composition is influenced by the geographic distance, microclimatic variables, organic matter (fish carcass and coconut), and cracks. On the other hand, in the photic zone, only geographic distance and microclimatic variables explained the composition (Appendix S8).

Furthermore, the models using microscale variables revealed that the composition of the aphotic zone, was influenced by the combination of humidity, temperature, geographic distance, distance from entrances and some of the habitat elements. Similarly, for the photic zone, the faunal composition was also influenced by geographic distance, distance from entrances, humidity, temperature, and another habitat elements (Appendix S8).

DISCUSSION

Our study has unveiled consistent differences in habitat structure across the examined cave zones, coupled with distinctions in their resource and microclimatic conditions. In this senesce, photic regions exhibit heightened environmental heterogeneity and as the distance from the cave entrances expands, this heterogeneity gradually diminishes, leading to the development of more homogeneous environments in the deeper cave areas. In this regard, the gradient of environmental, microclimatic, and resource heterogeneity exerts a direct influence on the spatial configuration of subterranean communities (Figure 8).

Effects of habitat structure on the richness

The photic zones are intricately linked with entrance regions, serving as ecotone zones - transitional environments situated at the boundary between surface and subterranean realms (Prous et al., 2004, 2015; Moseley, 2009). This environmental trait culminates in fostering communities that are more abundant and diverse compared to those found in the deeper sections of caves (Prous et al., 2004). Our study lends support to this premise, as it aligns with the notion that photic regions inherently exhibit greater species diversity in contrast to the aphotic regions.

Cave entrances serve as conduits for resource influx from the surface environment into the subterranean realm (Peck, 1976; Prous et al., 2004, 2015; Mammola, 2019; Mendes-Rabelo et al., 2021). Consequently, entrance regions are recognized for their pronounced environmental heterogeneity, standing in stark contrast to the deeper cave areas (Poulson & White, 1969; Mammola, 2018; Souza-Silva et al., 2021). This environmental heterogeneity results from irregularities, recesses, porosities, and discontinuities in the cave floor, as well as from micro and macro spaces formed by

varying sizes, roughness, and configurations of gravel and blocks (Ferreira & Souza-Silva, 2001; Ferreira et al., 2019; Souza-Silva et al., 2021; Reis-Venâncio et al., 2022).

These sites furnish a greater spectrum of potential habitats, ready for colonization by fauna, culminating in elevated richness of non-troglomorphic species. Additionally, this heightened habitat availability may lead to a reduction in niche overlap and antagonistic ecological interactions, thereby fostering the coexistence of species that might otherwise be potential competitors (Tews et al., 2004; Arellano et al., 2016; Ferreira & Pellegrini, 2019; Souza-Silva et al., 2021; Reis-Venâncio et al., 2022). As underscored by Mammola et al. (2016), niche-driven dynamics are significantly more prevalent within cave environments than previously perceived, and they are now recognized as expected rather than exceptional occurrences in such settings.

Additionally, harsh surface environmental conditions, exacerbated by rising deforestation rates (Souza-Silva et al., 2015; Cardoso et al., 2021, 2022), may prompt certain epigean species from the regional pool (Medes-Rabelo et al., 2021) to migrate toward entrance regions, forming what's known as the para-epigean community (Prous et al., 2004), driven by resource availability and stable climatic conditions. This migration could potentially enhance local species richness (Mendes-Rabelo et al., 2021). Notably, our study took place in a semi-arid region with a documented history of deforestation, which may amplify these effects (Salazar et al., 2007; Lessa et al., 2018; Antongiovanni et al., 2020; Cardoso et al., 2021, 2022; Bento et al., 2021).

Conversely, aphotic regions exhibit a lower richness. This disparity can be attributed to the restrictive conditions commonly characteristic of deep subterranean habitats, including the perpetual absence of light, elevated humidity, and the scarcity of organic resources. Such conditions prevent the establishment of numerous external species not adapted to subterranean life, consequently leading to environments characterized by reduced diversity (Poulson & White, 1969; Souza-Silva et al., 2011, 2021; White & Culver, 2011; Mammola, 2018; Moldovan et al., 2018). On the contrary, species capable of thriving within these environments generally exhibit physiological, morphological, and behavioral attributes that enhance their efficiency in exploiting the available resources (Howarth, 1983, 1993; Hüppop, 2005; Culver & Pipan, 2015).

Although invertebrate richness is lower in deeper aphotic regions, our findings underscore a positive correlation between invertebrate richness in these areas and the abundance of organic resources, such as plant debris and branches. This observation underscores that even within environments known for their oligotrophic conditions, the resource availability plays a pivotal role in shaping communities, probably by reducing competition and increasing local richness. It is important to note that large accumulations of organic resources within subterranean environments are frequently sparse and dispersed. Even so, these resources also can act as "attractors" for cave fauna (Ferreira and Martins, 1999; Schneider et al., 2011; Ferreira et al., 2019). This characteristic favors the presence of predators searching for potential prey attracted by the available resource (Ferreira and Martins, 1999; Schneider et al., 2011). Furthermore, in an

ecosystem point of view, organic resources also provide shelter for fauna, in addition to exhibiting favorable microclimatic conditions for reproduction (Ferreira et al., 2019; Souza-Silva et al., 2011; Souza-Silva & Ferreira, 2022).

Effects of habitat structure on species composition

Species in subterranean environments often exhibit high habitat specificity, resulting in notable endemism. Many are exclusive to single caves or cave systems (Mammola et al., 2019; Cuff et al., 2021; Nicolosi et al., 2021; Souza-Silva et al., 2021). Souza-Silva et al. (2021) noted decreasing overlap between troglobitic and non-troglobitic species deeper in caves. Troglobitic species are more common in resource-limited deep areas, while non-troglobitic species prevail near entrances with higher resource availability. This contrast favors species with distinct traits, contributing to divergent community compositions.

The faunal dissimilarity between the photic and aphotic zones primarily results from divergent physical and resource attributes. A microclimatic gradient exists from the cave entrance to the innermost areas (Badino, 2010; Mammola, 2019), fostering species community diversification due to unique physiological and ecological requirements (Figure 8). In this sense, microclimatic conditions serve as modulating factors influencing the spatial distribution of species (Mammola et al., 2018; Mammola et al., 2020; Ferreira et al., 2015).

When focusing solely on the communities within the photic zones, several factors exert influence over the species composition, including temperature, humidity, geographical distance, distance from the cave entrance, and the presence of mocó feces (*Kerodon rupestris*, Caviidae, Rodentia). As previously mentioned, cave entrances typically offer microclimatic conditions more conducive than those on the surface, as well as a more diverse array of organic resources, leading to an increase in species richness and diversity.

It is important to note that geographic distance between caves plays an important role in determining the faunal composition, especially in photic zones, since the regional species pool is important for maintaining such communities. The regional species pool includes pre-adapted transient species that establish themselves in photic areas within caves (Prous et al., 2004, 2015; Mendes-Rabelo et al., 2021). These species not only colonize these regions but, owing to their capacity to traverse the epigean environment, actively contribute to enhancing the similarity observed between photic zones within different caves, in addition to acting as potential colonizers. As a result, the communities associated with different cave entrances exhibit greater faunal similarity (Souza-Silva et al. 2020; Mendes-Rabelo et al. 2021; Reis-Venâncio et al. 2022). On the other hand, within aphotic zones, we discerned a pronounced faunistic divergence across distinct caves (Mammola et al., 2020; Souza-Silva et al., 2020; Reis-Venâncio et al., 2022). Despite caves being regarded as components of a network intricately threaded with fissures and subsurface passages within the karst system, they retain an essential characteristic of semi-isolated environments (Pipan & Culver, 2007; Mammola, 2019; Souza-Silva et al.,

2020). This condition allows the dispersal of troglobitic species, which occurs exclusively underground, even among nearby caves, resulting in limited species sharing. Caves located nearby display distinct faunal identities within their aphotic zones, while areas near entrances show a greater faunal similarity (Reis-Venâncio et al., 2022).

The consistently high humidity present throughout the year constitutes an important structuring factor for the fauna inhabiting aphotic zones. This persistent high humidity renders these areas conducive to troglobitic species (Howarth, 1983; Mammola, 2019; Mammola et al., 2020; Souza-Silva et al., 2021). However, it is worth noting that humidity also acts as a limiting factor for communities within the photic regions. Given the heightened humidity levels in these zones compared to the epigean environment, they become preferred habitats for epigean fauna.

Lastly, the role of organic resources cannot be understated, as their broader variety is explored and consumed by species possessing distinct specializations and dietary preferences. Notably, plant-derived resources wield a substantial influence on species richness, underscoring the significance of these allochthonous resources in shaping the spatial organization of subterranean fauna (Cardoso et al., 2022). Consequently, the influence of these resources and habitat components merits recognition and ought to be treated as pivotal elements within subterranean environments. They are essential in fostering heightened richness and diversity within these unique ecosystems.

Conservation issues

Cardoso et al. (2021) conducted a study focused on caves within the Iuiú and Malhada karstic landscape, shedding light on the imminent need for conservation interventions. Their findings underscored the area's elevated diversity encompassing both troglobitic and non-troglobitic species, as well as the range of impacts that have beset the region. These impacts encompass diverse anthropogenic activities such as agro-pastoral practices, mining, road construction, and notably, deforestation.

The cumulative effects of these activities exert a substantial impact on the entrance zones of caves. The removal of vegetation in proximity to cave entrances can profoundly disrupt the microclimatic conditions and energy dynamics that are central to the maintenance and organization of the resident fauna (Prous et al., 2015).

The conversion of native forests can precipitate rapid disturbances within subterranean environments, culminating in the extinction of troglobitic species, known for their heightened vulnerability to environmental changes (Reboleira et al., 2011). Consequently, the loss of habitat, both on the surface and in subterranean realms, can trigger cascading repercussions throughout the subterranean ecosystem (Cardoso et al., 2022).

Conclusions

It is crucial for researchers and managers to deeply consider the variations in habitat structure, microclimate conditions, and resource diversity present in subterranean environments. These considerations are essential when developing and improving management methods that promote the conservation of a wide variety of

organisms, ecological processes, and endangered species. Moreover, understanding these gradients is essential when seeking to enhance knowledge about the ecology, evolution, and prevailing processes in the subterranean ecosystem.

It is noteworthy that communities inhabiting distinct cave areas exhibit heterogeneous responses to habitat structure, microclimatic conditions, and resource availability. Consequently, this intricate variability mandates careful consideration in forthcoming investigations and the formulation of comprehensive management strategies.

ACKNOWLEDGMENTS

We express our sincere gratitude to Professor Dr. Reuber Albuquerque Brandão and Dr. Diego de Medeiros Bento for their invaluable contributions in reviewing and refining this manuscript. We extend our heartfelt thanks to the dedicated taxonomists who assisted with taxa identification (Cardoso G.M., Bernardi L., Prado G.C., Brescovit A., Bouzan R., Castro R., Vilelva M., Pellegrini T.G., Benjumea D., Medeiro G., de Souza P.G.C., Michelly N., Magalhães I.L.F., Vaz J., Vaz-de-Melo F. and Simone L.R.); the team from the Center of Studies in Subterranean Biology (CEBS/UFLA) for the support in the field trips; the citizens of Iuiú who helped guide and accompany us while finding the cave sites (Belarmino, Tiãozinho, Joãozinho, Sr. Mathias, Jovino, Edson Pagani, Sr. Honorato and families); the Centro Nacional de Pesquisa e Conservação de Cavernas - CECAV and Instituto Brasileiro de Desenvolvimento e Sustentabilidade - IABS for the financial support (TCCE ICMBio/Vale 01/2018); CNPq (National Council for Scientific and Technological Development, grant n. 302925/2022-8) for the productivity scholarship provided to RLF, Coordination for the Improvement of Higher Education Personnel (CAPES) under Grant 88887.816191/2023-00, which supported PCRV's research. This paper represents a part of PCRV's master's thesis in Applied Ecology at Universidade Federal de Lavras, Minas Gerais state, Brazil. The samples were collected according to the authorization for activities with scientific purpose SISBIO nº78415-3.

REFERENCES

Alvares, C. A., Stape, J. L., Sentelhas, P. C., de Moraes, J. L. G., & Sparovek, G. (2013). Köppen's climate classification map for Brazil. Meteorologische Zeitschrift, 22(6), 711–728. https://doi.org/10.1127/0941-2948/2013/0507

Anderson, M. J. (2014). Permutational multivariate analysis of variance (PERMANOVA). Wiley statsref: statistics reference online, 1-15. https://doi.org/10.1002/9781118445112.stat07841

Antongiovanni, M., Venticinque, E. M., Matsumoto M., & Fonseca, C. R. (2020). Chronic anthropogenic disturbance on Caatinga dry forest fragments. Journal of Applied Ecology, 57(10), 2064-2074. https://doi.org/10.1111/1365-2664.13686

Apgaua, D. M. G., dos Santos, R. M., Pereira, D. G. S., de Oliveira Menino, G. C., Pires, G. G., Fontes, M. A. L., & Tng, D. Y. P. (2014). Beta-diversity in seasonally dry tropical forests (SDTF) in the Caatinga Biogeographic Domain, Brazil, and its implications for conservation. Biodiversity and Conservation, 23(1), 217–232. https://doi.org/10.1007/s10531-013-0599-9

Arellano, G., Umaña, M. N., Macía, M. J., Loza, M. I., Fuentes, A., Cala, V., & Jørgensen, P. M. (2017). The role of niche overlap, environmental heterogeneity, landscape roughness and productivity in shaping species abundance distributions along the Amazon–Andes gradient. Global Ecology and Biogeography, 26(2), 191-202. https://doi.org/10.1111/geb.12531

Badino, G. (2010). Underground meteorology—"What's the weather underground?" Acta Carsologica, 39(3), 427–448. https://doi.org/10.3986/ac.v39i3.74

Bartoń, K. (2022). MuMIn: Multi-Model Inference. R package version 1.47.1. https://CRAN.R-project.org/package=MuMIn

Bento, D. M., Souza-Silva, M., Vasconcellos, A. C., Bellini, B. C., Prous, X., & Ferreira, R. L. (2021). Subterranean "oasis" in the Brazilian semiarid region: neglected sources of biodiversity. Biodiversity and Conservation, 30, 3837–3857. https://doi.org/10.1007/s10531-021-02277-6

Borcard, D., Gillet, F., & Legendre, P. (2011). Numerical ecology with R. Biotropica, 688p.

Cardoso, R. C., Ferreira, R. L., & Souza-Silva, M. (2021). Priorities for cave fauna conservation in the Iuiú karst landscape, northeastern Brazil: a threatened spot of troglobitic species diversity. Biodiversity and Conservation, 30(5), 1433–1455. https://doi.org/10.1007/s10531-021-02151-5

Cardoso, R. C., Ferreira, R. L., & Souza-Silva, M. (2022). Multi-spatial analysis on cave ecosystems to predict the diversity of subterranean invertebrates. Basic and Applied Ecology, 65, 111–122. https://doi.org/10.1016/j.baae.2022.11.007

Christiansen, K. A. (1962). Proposition pour la classification des animaux cavernicoles. Biotropica Mem. 2, 76-78.

Cuff, J. P., Aharon, S., Armiach Steinpress, I., Seifan, M., Lubin, Y., & Gavish-Regev, E. (2021). It's all about the zone: spider assemblages in different ecological zones of Levantine caves. Diversity, 13(11), 576. https://doi.org/10.3390/d13110576

Culver D., Pipan, T. (2019). The biology of caves and other subterranean habitats (2nd ed.). Oxford University Press, 272 pp..

Culver, D., & Pipan, T. (2015). Shifting paradigms of the evolution of cave life. Acta Carsologica, 44(3), 353–367. https://doi.org/10.3986/ac.v44i3.1688

Ferreira, R. L. (2004). A medida da complexidade ecológica e suas aplicações na conservação e manejo de ecossistemas subterrâneos. Ph.D. thesis, Universidade Federal de Minas Gerais, 158pp.

Ferreira, R. L. (2019). Guano communities. In: Encyclopedia of caves. Academic Press, 474-484.

Ferreira, R. L., & Martins, R. P. (1999). Trophic structure and natural history of bat guano invertebrate communities, with special reference to Brazilian caves. Tropical Zoology, 12(2), 231–252. https://doi.org/10.1080/03946975.1999.10539391

Ferreira, R. L., & Pellegrini, T. G. (2019). Species-area model predicting diversity loss in an artificially flooded cave in Brazil. International Journal of Speleology, 56(1), 230–240. https://doi.org/10.5038/1827-806X.48.2.2244

Ferreira, R. L., & Souza-Silva, M. (2001). Biodiversity under rocks: the role of microhabitats in structuring invertebrate communities in Brazilian outcrops. Biodiversity & Conservation, 10, 1171-1183.

Ferreira, R. L., Martins, V. M., Paixão, E. A., & Silva, M. S. (2015). Spatial and temporal fluctuations of the abundance of Neotropical cave-dwelling moth Hypena sp.(Noctuidae, Lepidoptera) influenced by temperature and humidity. Subterranean Biology, 16, 47-60.

Ferreira, R. L., Prous, X., & Martins, R. P. (2007). Structure of bat guano communities in a dry Brazilian cave. Tropical Zoology, 20(1), 55-74.

Fick, S. E., & Hijmans, R. J. (2017). WorldClim 2: new 1-km spatial resolution climate surfaces for global land areas. International Journal of Climatology, 37(12), 4302–4315. https://doi.org/10.1002/joc.5086

Furtado-Oliveira, L., Ferreira, R. L., Fernández, R. J. I., & Souza-Silva, M. (2022). Recreational caving impacts of visitors in a high-altitude cave in Bolivian Andes: main effects on microhabitat structure and faunal distribution. International Journal of Speleology, 51(2), 93–103. https://doi.org/10.5038/1827-806X.51.2.2418

Hartig, F. (2022). DHARMa: Residual Diagnostics for Hierarchical (Multi-Level/Mixed) Regression Models (Version 0.4.6). R package. https://CRAN.R-project.org/package=DHARMa

Howarth, F. G. (1983). Ecology of cave arthropods. Annual Review of Entomology, 28(1), 365-389.

Howarth, F. G. (1993). High-stress subterranean habitats and evolutionary change in cave-inhabiting arthropods. The American Naturalist, 142, 65-77. https://doi.org/10.1086/285523

Hüppop, K. (2005). Adaptation to low food. In: D. Culver & W. B. White (Eds.) Encyclopedia of caves. Elsevier, Amsterdam, 4:10.

Iskali, G., & Zhang, Y. (2015). Guano subsidy and the invertebrate community in Bracken cave: the world's largest colony of bats. Journal of Cave & Karst Studies, 77(1), 28-36.

Kassambara, A., & Mundt, F. (2020). factoextra: Extract and Visualize the Results of Multivariate Data Analyses (Version 1.0.7). R package. https://CRAN.R-project.org/package=factoextra.

Legendre, P., & Legendre, L. (2012). Numerical ecology. 2nd ed. Elsevier.

Lessa, T., Dos Santos, J. W., Correia, R. A., Ladle, R. J., & Malhado, A. C. (2019). Known unknowns: Filling the gaps in scientific knowledge production in the Caatinga. PlosOne, 14(7), e0219359. https://doi.org/10.1371/journal.pone.0219359

Lienhard, C., & Ferreira, R. L. (2013). A new species of Neotrogla from Brazilian caves (Psocodea: 'Psocoptera': Prionoglarididae). Revue Suisse de Zoologie, 120(1), 3-12.
Mammola S, Piano E, Malard F, Vernon P, Isaia M (2019). Extending Janzen's hypothesis to temperate regions: a test using subterranean ecosystems. *Functional Ecology, 33(9),* 1638-1650. https://doi.org/10.1111/1365-2435.13396
Mammola, S. (2019). Finding answers in the dark: caves as models in ecology fifty years after Poulson and White. Ecography, 42(7), 1331-1351. https://doi.org/10.1111/ecog.03905
Mammola, S., & Isaia, M. (2018). Day–night and seasonal variations of a subterranean invertebrate community in the twilight zone. Subterranean Biology, 27, 31-51. https://doi.org/10.3897/subtbiol.27.28909
Mammola, S., Amorim, I. R., et al. (2020). Fundamental research questions in subterranean biology. Biological Reviews, 95(6), 1855-1872. https://doi.org/10.1111/brv.12642
Mammola, S., Cardoso, P., et al. (2019). Local-versus broad-scale environmental drivers of continental β-diversity patterns in subterranean spider communities across Europe. Proceedings of the Royal Society B, 286(1914), 20191579. https://doi.org/10.1098/rspb.2019.1579
Mammola, S., Piano, E., & Isaia, M. (2016). Step back! Niche dynamics in cave-dwelling predators. Acta Oecologica, 75, 35-42. https://doi.org/10.1016/j.actao.2016.06.011
Mendes-Rabelo, L., Souza-Silva, M., & Ferreira, R. L. (2018). Priority caves for biodiversity conservation in a key karst area of Brazil: comparing the applicability of cave conservation indices. Biodiversity and Conservation, 27, 2097-2129. https://doi.org/10.1007/s10531-018-1554-6
Mendes-Rabelo, L., Souza-Silva, M., & Ferreira, R. L. (2021). Epigean and hypogean drivers of Neotropical subterranean communities. Journal of Biogeography, 48(3), 662-675. https://doi.org/10.1111/jbi.14031
Moldovan, O. T., Kovac, L., Halse, S. (2018). Cave ecology. Basel, Switzerland: Springer International Publishing. https://doi.org/10.1007/978-3-319-98852-8.
Moseley, M. (2009). Are all caves ecotones?. Cave and Karst Science, 36(2), 53-58.
Nicolosi, G., Mammola, S., Costanzo, S., Sabella, G., Cirrincione, R., Signorello, G., & Isaia, M. (2021). Microhabitat selection of a Sicilian subterranean woodlouse and its implications for cave management. International Journal of Speleology, 50(1), 53-63. https://doi.org/10.5038/1827-806X.50.1.2370
Oksanen, J., Simpson, G., et al. (2022). *vegan: Community Ecology Package*. R package version 2.6-4. https://CRAN.R-project.org/package=vegan.
Oliver, I., & Beattie, A. J. (1996a). Invertebrate morphospecies as surrogates for species: a case study. Conservation Biology, 10(1), 99-109. https://doi.org/10.1046/j.1523-1739.1996.10010099.x
Oliver, I., & Beattie, A. J. (1996b). Designing a cost-effective invertebrate survey: a test of methods for rapid assessment of biodiversity. Ecological Applications, 6(2), 594-607. https://doi.org/10.2307/2269394

Pacheco, G. S., Souza-Silva, M., Cano, E., & Ferreira, R. L. (2020). The role of microhabitats in structuring cave invertebrate communities in Guatemala. International Journal of Speleology, 49(2), 8.

Peck, S. B. (1976). The effect of cave entrances on the distribution of cave-inhabiting terrestrial arthropods. International Journal of Speleology, 8(4), 309-321. http://dx.doi.org/10.5038/1827-806X.8.4.1

Pellegrini, T. G., Sales, L. P., Aguiar, P., & Ferreira, R. L. (2016). Linking spatial scale dependence of land-use descriptors and invertebrate cave community composition. Subterranean Biology, (18), 17–38. https://doi.org/10.3897/SUBTBIOL.18.8335

Peterson, B. G., & Carl, P. (2020). *PerformanceAnalytics: Econometric Tools for Performance and Risk Analysis*. R package version 2.0.4, https://CRAN.R-project.org/package=PerformanceAnalytics.

Pipan, T., & Culver, D. C. (2007). Copepod distribution as an indicator of epikarst system connectivity. Hydrogeology Journal, 15, 817-822. https://doi.org/10.1007/s10040-006-0114-4

Polak, S. (2005). Importance of discovery of the first cave beetle Leptodirus hochenwartii Schmidt, 1832. Endins: publicació d'espeleologia, 71-80.

Poulson, T. L., & White, W. B. (1969). The Cave Environment: Limestone caves provide unique natural laboratories for studying biological and geological processes. Science, 165(3897), 971-981.

Prous, X., Ferreira, R. L., & Jacobi, C. M. (2015). The entrance as a complex ecotone in a Neotropical cave. Journal of Applied Ecology, 44(2), 177-189. http://dx.doi.org/10.5038/1827-806X.44.2.7

Prous, X., Ferreira, R. L., & Martins, R. P. (2004). Ecotone delimitation: Epigean–hypogean transition in cave ecosystems. Austral Ecology, 29(4), 374-382. https://doi.org/10.1111/j.1442-9993.2004.01373.x

R Core Team (2022). R: A language and environment for statistical computing. R Foundation for Statistical Computing, Vienna, Austria. URL https://www.R-project.org/

Reboleira, A. S., Borges, P. A., Gonçalves, F., Serrano, A. R., & Oromí, P. (2011). The subterranean fauna of a biodiversity hotspot region-Portugal: an overview and its conservation. International Jounal of Speleology, 40(1), 23-37. http://dx.doi.org/10.5038/1827-806X.40.1.4

Recknagel, H., & Trontelj, P. (2022). From cave dragons to genomics: advancements in the study of subterranean tetrapods. Bioscience, 72(3), 254-266. https://doi.org/10.1093/biosci/biab117

Reis-Venâncio, P. C., Mendes-Rabelo, L., Pellegrini, T. G., & Ferreira, R. L. (2022). From light to darkness: the duality of influence of habitat heterogeneity on Neotropical terrestrial cave invertebrate communities. Studies on Neotropical Fauna and Environment, 1-10. https://doi.org/10.1080/01650521.2022.2095832

Salazar, L. F., Nobre, C. A., & Oyama, M. D. (2007). Climate change consequences on the biome distribution in tropical South America. Geophysical Research Letters, 34(9), 1-6. https://doi.org/10.1029/2007GL029695

Schneider, K., Christman, M. C., & Fagan, W. F. (2011). The influence of resource subsidies on cave invertebrates: results from an ecosystem-level manipulation experiment. Ecology, 92(3), 765-776. https://doi.org/10.1890/10-0157.1

Schober, P., Boer, C., & Schwarte, L. A. (2018). Correlation coefficients: appropriate use and interpretation. Anesthesia & Analgesia, 126(5), 1763-1768. https://doi.org/10.1213/ANE.0000000000002864

Simões, M. H., Souza-Silva, M., & Ferreira, R. L. (2015). Cave physical attributes influencing the structure of terrestrial invertebrate communities in Neotropics. Subterranean Biology, 16, 103-121. https://doi.org/10.3897/subtbiol.16.5470

Souza-Silva, M., & Ferreira, R. L. (2022). Dinâmica trófica em Ambientes de Cavernas. In: Zampaulo, R. A., & Prous, X. (Eds.), *Fauna cavernícola do Brasil*. Belo Horizonte: Editora Rupestre, pp. 58-81.

Souza-Silva, M., Cerqueira, R. F. V., Pellegrini, T. G., & Ferreira, R. L. (2021). Habitat selection of cave-restricted fauna in a new hotspot of subterranean biodiversity in Neotropics. Biodiversity and Conservation, 30(14), 4223–4250. https://doi.org/10.1007/s10531-021-02302-8

Souza-Silva, M., Iniesta, L. F. M., & Ferreira, R. L. (2020). Cave lithology effect on subterranean biodiversity: A case study in quartzite and granitoid caves. Acta Oecologica, 108(103645), 1-10. https://doi.org/10.1016/j.actao.2020.103645

Souza-Silva, M., Martins, R. P., & Ferreira, R. L. (2011). Trophic dynamics in a neotropical limestone cave. Subterranean Biology, 9, 127-138. doi:10.3897/subtbiol.9.2515

Souza-Silva, M., Martins, R. P., & Ferreira, R. L. (2015). Cave conservation priority index to adopt a rapid protection strategy: A case study in Brazilian Atlantic rainforest. Environmental Management, 55, 279-295. https://doi.org/10.1007/s00267-014-0414-8

Tews, J., Brose, U., Grimm, V., Tielbörger, K., Wichmann, M. C., Schwager, M., & Jeltsch, F. (2004). Animal species diversity driven by habitat heterogeneity/diversity: The importance of keystone structures. Journal of Biogeography, 31(1), 79-92. https://doi.org/10.1046/j.0305-0270.2003.00994.x

Tobin, B. W., Hutchins, B. T., & Schwartz, B. F. (2013). Spatial and temporal changes in invertebrate assemblage structure from the entrance to deep-cave zone of a temperate marble cave. International Journal of Speleology, 42(3), 203-214. https://doi.org/10.5038/1827-806X.42.3.4

White, W. B., & Culver, D. C. (Eds.) (2011). *Encyclopedia of Caves*. Academic Press.

Wynne, J. J., Howarth, F. G., Sommer, S., & Dickson, B. G. (2019). Fifty years of cave arthropod sampling: Techniques and best *practices. International Journal of Speleology*, 48(1), 33–48. https://doi.org/10.5038/1827-806X.48.1.2231

Wynne, J. J., Sommer, S., Howarth, F. G., Dickson, B. G., & Voyles, K. D. (2018). Capturing arthropod diversity in complex cave systems. Diversity and Distributions, 24(10), 1478-1491. https://doi.org/10.1111/ddi.12772

Zuur, A. F., Ieno, E. N., & Smith, G. M. (2007). Analyzing ecological data. Springer Science & Business Media.

Zuur, A. F., Ieno, E. N., Walker, N. J., Saveliev, A. A., & Smith, G. M. (2009). Mixed effects models and extensions in ecology with R. Springer, New York.

Appendix S1: Some characteristics of the studied caves in the carbonate massifs of Iuiú and Malhada, Bahia state, Brazil. The number of sectors (Sect.) and quadrants (Quad.) within each cave, average temperature (T) in degree centigrade, average humidity (U) in percentage, and morphospecies richness (S) for each cave. Each cave is identified by a name and a subscribed number corresponding to its location on the map shown in figure 1.

Cave	Latitude	Longitude	Sect.	Quad.	T (sd)	U (sd)	S
Tabocas[1]	14º35′13.16"S	43º41′9.64"W	15	45	24.09 (1.25)	90.34 (7.2)	42
Toca Fria[2]	14º32′52.86"S	43º32′8.99"W	10	30	23.82 (1.2)	90.92 (4.23)	50
Toca Cavala[3]	14°27'18.49"S	43°35'33.92"W	1	3	27 (-)	54 (-)	19
Pau D'árco ll[4]	14°30'27.30"S	43°39'20.78"W	1	3	22.3 (-)	69 (-)	21
Pau D'árco l[5]	14°30'27.13"S	43°39'21.21"W	1	3	22 (-)	71 (-)	32
Olho D'água do Coitezeiro[6]	14°27'58.76"S	43°39'26.24"W	2	6	24.15 (0.21)	96.65 (1.34)	50
Olho D'água do Aylton[7]	14°27'0.98"S	43°34'31.59"W	1	3	26.7 (-)	88.5 (-)	18
Loca da Serra[8]	14°26'51.53"S	43°35'45.42"W	1	3	23.7 (-)	58.6 (-)	24
Urubu-Jatobá[9]	14°32'55.40"S	43°32'22.10"W	13	39	24.83 (0.8)	66.64 (3.71)	74
Toca Valada[10]	14°29'27.75"S	43°39'8.80"W	8	24	25.26 (0.38)	86.46 (2.5)	88
Morro do Aurélio[11]	14°30'49.34"S	43°32'35.56"W	8	24	27.19 (1.3)	75.5 (4.81)	74
Sepultamento[12]	14°39'19.85"S	43°32'40.28"W	4	12	24.3 (0.45)	89.07 (4.92)	71
Joãozinho[13]	14°27'8.51"S	43°34'27.29"W	1	3	24.6 (-)	63.5 (-)	07
Esqueleto[14]	14°31'10.69"S	43°38'17.34"W	1	3	22.8 (-)	54.3 (-)	07
Belarmino[15]	14°28'5.38"S	43°39'5.19"W	1	3	25.4 (-)	85.2 (-)	21
Duas Gazelas[16]	14°39'28.23"S	43°32'43.29"W	6	18	24.78 (1.04)	70.15 (8.93)	33
Brilhante[17]	14°27'8.74"S	43°34'26.81"W	1	3	24.1 (-)	79.9 (-)	19
Bacupari[18]	14°30'26.27"S	43°40'10.14"W	1	3	23.6 (-)	62.4 (-)	20
Tapera D'água[19]	14°31'2.17"S	43°40'58.23"W	3	9	25.73 (0.8)	94.57 (1.25)	20
Lapa do Honorato[20]	14°27'46.36"S	43°35'33.60"W	4	12	22.22 (1.11)	92.52 (0.33)	74
Vaca Ausente[21]	14°31'11.88"S	43°38'15.33"W	1	3	25.4 (-)	82.4 (-)	16
do Matias[22]	14°28'46.97"S	43°36'50.72"W	3	9	23.63 (0.45)	83.33 (2.3)	23
Licuri[23]	14°26'50.09"S	43°35'47.18"W	2	6	24.35 (0.35)	61.2 (11.45)	24
Imbé[24]	14°29'30.02"S	43°39'16.00"W	10	30	22.84 (1.01)	70.94 (7.39)	83
Gustavo[25]	14°30'10.28"S	43°39'48.75"W	2	6	21.5 (0.56)	82.95 (7.84)	48
Caquinho[26]	14°30'22.92"S	43°39'20.59"W	1	3	21.6 (-)	75.4 (-)	17
Boi Perdido[27]	14°27'1.65"S	43°34'24.25"W	2	6	23.7 (1.41)	67 (7.49)	21
Barriguda[28]	14°27'11.46"S	43°34'27.44"W	2	6	24.55 (0.5)	69.1 (1.41)	23
Baixão[29]	14°26'6.61"S	43°37'25.23"W	6	18	24.1 (1.65)	92.23 (3.23)	54
Dente de Cão[30]	14°30'27.95"S	43°39'36.93"W	1	3	23.6 (-)	73.3 (-)	23
Buraco da Aroeira[31]	14°31'1.63"S	43°38'3.74"W	1	3	22.8 (-)	86.7 (-)	38

Appendix S2: Components of the substrate included in the analysis, in each spatial scale. Variables considered in fauna of aphotic (Az) and fauna of photic (Pz) zone analysis.

Spatial scale	Substrate components on the cave floor	
Mesoscale (cave sectors)	Guano (flying animal feces) Az, Pz	Large Boulder (1000-4000 mm) Pz
	Terrestrial animal feces Az, Pz	Medium Boulder (500-1000mm) Az, Pz
	Roots Az, Pz	Small Boulder (250-500mm) Az, Pz
	Leaf Litter (pile of leaves) Az, Pz	Cobble (64-250mm) Az, Pz
	Plant Debris (fragmented leaves and branches) Az, Pz	Coarse Gravel (16-64mm) Az, Pz
	Branch (< 250 mm) Az, Pz	Fine Gravel (2-16mm) Az, Pz
	Wood (≥ 250 mm) Pz	Sand Az, Pz
	Smooth Rock Pz	Silt Az, Pz
	Rough Rock Az, Pz	Organic Matter Az, Pz
	Speleothem Az, Pz	Hardpan Az, Pz
	Retraction Crack Az, Pz	Flowstone Pz
	Fungi Az	Water Bodies Az, Pz
	Algae Pz	
Microscale (cave quadrants)	Guano (flying animal feces) Az, Pz	Large Boulder (1000-4000 mm) Az
	Terrestrial animal feces Az, Pz	Medium Boulder (500-1000mm) Az, Pz
	Roots Az, Pz	Small Boulder (250-500mm) Az, Pz
	Leaf Litter (pile of leaves) Az, Pz	Cobble (64-250mm) Az, Pz
	Plant Debris (fragmented leaves and braches) Az, Pz	Coarse Gravel (16-64mm) Az, Pz
	Branch (< 250 mm) Az, Pz	Fine Gravel (2-16mm) Az, Pz
	Smooth Rock Az, Pz	Sand Az, Pz
	Rough Rock Az, Pz	Silt Az, Pz
	Speleothem Az, Pz	Hardpan Az, Pz
	Retraction Crack Az, Pz	Flowstone Pz
	Fungi Pz	Water Bodies Az, Pz
	Phanerogam Pz	

Appendix S3: Key species contributing to the fauna dissimilarity between the photic and aphotic zones. Troglobitic species (*).

Morphospecies/ species	Av. abundance photic zone	Av. abundance aphotic zone	Contribution (%)
Loxosceles ericsoni	0.89	0.59	3.98
Trogolaphysa sp1*	0.75	0.95	3.89
Neotrogla sp1	0.82	0.40	3.11
Loxosceles karstica	0.80	0.45	2.92
Venezillo sp1	0.68	0.42	2.51
Iuiuia sp1	0.66	0.43	2.27
Nesticodes rufipes	0.66	0.41	2.23
Cardiocondyla sp1	0.79	0.18	2.03
Zelurus sp1	0.58	0.27	2.00
Endecous sp1	0.20	0.44	1.91
Brachymyrmex sp1	0.75	0.34	1.90
Hesperolpiidae sp1	0.47	0.29	1.86
Solenopsis sp2	0.42	0.40	1.69
Mogoplistidae sp1	0.54	0.28	1.65
Pikelinia sp1	0.33	0.24	1.61
Cixiidae sp1	0.27	0.35	1.49
Lygaeidae sp1	0.34	0.37	1.46
Charinus iuiu	0.26	0.31	1.36
Mesabolivar sp1	0.26	0.29	1.28
Cixiidae sp2	0.36	0.08	1.20
Veliidae sp1	0.22	0.11	1.03
*Iuiuia caeca**	0.03	0.26	0.89
Pholcidae sp	0.12	0.21	0.88
Leucauge sp1	0.24	0.12	0.87
Pseudonannolene sp1	0.11	0.19	0.87
Lepidocyrtinus sp1	0.09	0.26	0.84
Zelurus sp2	0.27	0.12	0.83
Pholcidae sp2	0.18	0.20	0.80

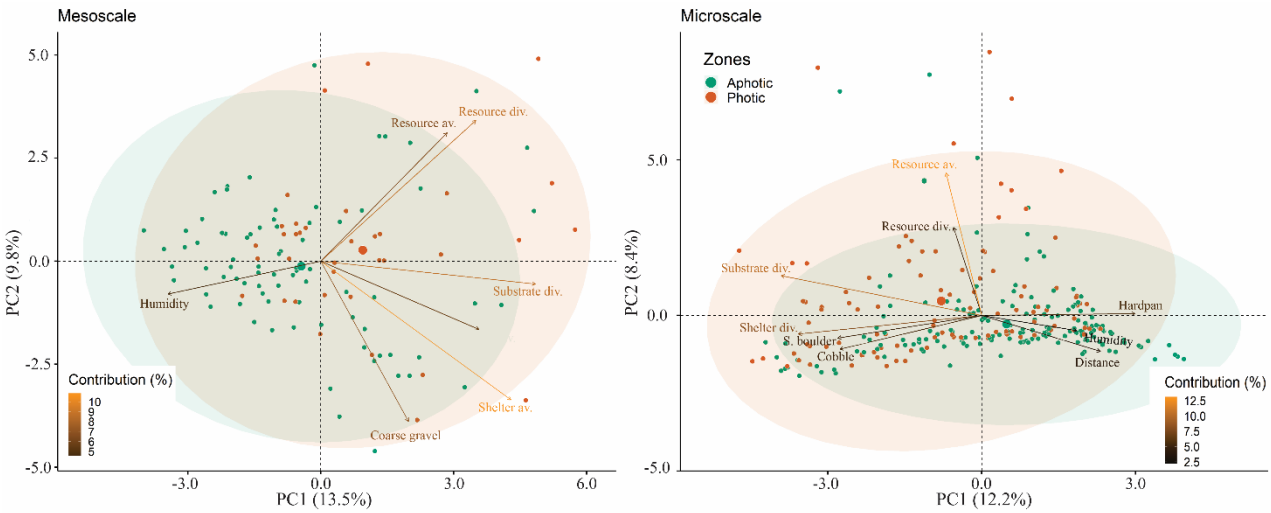
Appendix S4: The list enumerates troglobitic species sampled from the caves of Iuiú, Bahia, along with the habit of each one. (UJ) Caverna Urubu-Jatobá, (Ta) Caverna Tabocas, (Ba) Baixão, (DG) Caverna Duas Gazelas, (Mat) Lapa do Senhor Mathias, (BP) Boi Perdido, (Bar) Caverna da Barriguda, (Gus) Caverna do Gustavo, (LS) Loca da Serra, (Li) Licuri, (DC) Dente de Cão, (Caq) Gruta do Caquinho, (Imb) Imbé, (BAro) Buraco da Aroeira, (LH) Lapa do Honorato, (Co) Coitezeiro, (MA) Morro do Aurélio, (TV) Toca Valada, (Sep) Sepultamento, (TF) Toca Fria, (TA) Tapera D'água; ([T]) Terrestrial habit, ([a]) aquatic habit.

Taxa	Morphospecies/ especies	UJ	Ta	Ba	DG	Mat	BP	Bar	Gus	LS	Li	DC	Caq	Imb	BAro	LH	Co	MA	TV	Sep	TF	TA
Acari	Erythraeidae sp2[T]	x																				
Araneae	Ochyroceratidae sp2 [T]																x					
	Lygromma sp1 [T]																x	x				x
	Loxosceles troglobia [T]		x			x						x										x
	Matta sp1 [T]																			x		
	Lygromma sp2 [T]													x								
	Matta sp2 [T]								x													
	Lygromma sp3 [T]							x														
	Ochyroceratidae sp3 [T]		x																			
	Ochyroceratidae sp4 [T]		x																			
	Ochyroceratidae sp5 [T]	x																				
	Prodidomidae troglo sp1 [T]	x																				
	Ochyroceratidae sp6 [T]																			x		
Blattodea	Blattodea troglo sp1 [T]		x																			
	Eucnemidae sp1 [T]																	x	x	x		
	Anillina sp1 [T]																	x				

| | | |

| | | |

| | | |



Appendix S5: Principal components analysis (PCA) in both scales, showing variations in caves habitat attributes between aphotic and photic zones. Arrow colors represent the contribution of each abiotic variable on component axes.

Appendix S6: Results of the selected generalized linear models (GLM) investigating the effects of the predictors on the species richness in mesoscale. (A) The best model including the available classes for aphotic ($adjR^2$ = 0.3707. AIC = 447.05). and photic ($adjR^2$ = 0.46. AIC = 231.79); (B) the best models including the substrate elements for aphotic ($adjR^2$ = 0.3305. AIC = 449.86) and photic ($adjR^2$ = 0.5354. AIC = 230.41) zones. Distance from the entrance (Entr. dist.). Humidity (Humid.). resource (Res.).

Species richness	Predictor variables	Estimate	SE	z	P
a) *Model with resource and shelter availability*					
Aphotic zone	Entr. Dist.	-0.0024	0.0004	-6.068	1.3^{-09}
	Res. Availability	0.014	0.0062	2.239	0.025
Photic zone	Humid.	0.025	0.005	4.929	8.25^{-07}
	Res. Availability	0.02	0.006	3.05	2^{-03}
b) *Model with substrate elements*					
Aphotic zone	Entr. Dist.	-0.0023	0.0004	-5.652	1.58^{-08}
Photic zone	Entr. Dist.	-0.029	0.012	-2.486	0.013
	Humid.	0.0229	0.0046	5.0	5.74^{-07}
	Plant Debris	0.0291	0.009	3.237	1.2^{-03}
	Rough Rock	-0.0135	0.0068	-1.992	0.0464

Appendix S7: Results of the selected generalized linear mixed models (GLM) of the effects of the predictors variables on the species richness in microscale. (A) The best model including the classes of resource and shelter availability for aphotic ($cR^2 = 0.095$. AIC = 586.6). and photic ($cR^2 = 0.281$. AIC = 433.1); (B) the best models including the elements of the substrate for aphotic ($cR^2 = 0.1193$. AIC = 585) and photic zones ($cR^2 = 0.3426$. AIC = 424.3). Distance from the entrance (Entr. dist.). Humidity (Humid.). Shelter (Sh.). resource (Res.). Substrate (Sub.).

Species richness	Predictor variables	Estimates	SE	z	P
a) *Model with resource and shelter availability*					
Aphotic zone	Entr. Distance	-0.0011	0.0004	-2.415	0.016
	Res. Availability	0.0115	0.0037	3.075	2.11^{-03}
Photic zone	Humid.	0.0205	0.005	3.999	6.36^{-05}
	Sh. Diversity	0.506	0.148	3.415	6.38^{-04}
	Res. Availability	0.014	0.0033	4.156	3.24^{-05}
b) *Model with substrate elements*					
Aphotic zone	Entr. Distance	-0.0011	0.000	-2.360	0.0183
	Plant debris	0.024	0.0098	2.482	0.0131
	Branch	0.019	0.0085	2.206	0.0274
	Silt	0.0028	0.0014	2.075	0.0380
Photic zone	Humid.	0.0197	0.0048	4.126	3.70^{-05}
	Sh. Diversity	0.535	0.138	3.869	1.09^{-04}
	Roots	0.032	0.007	4.683	2.83^{-06}
	Leaf Litter	0.0222	0.007	3.108	1.883^{-03}
	Branch	0.055	0.019	2.959	3.09^{-03}

Appendix S8: The selected predictors of the species composition variations in the different cave zones. (E.D) Distance from the entrance. (G.D) geographic distance. (Hu.) humidity. (T.) temperature. (Cr.) cracks. (O.M.) organic matter. (Sil.) silt. (S.D.) substrate diversity. (R.A.) resource availability. (Fe) feces. (P.D.) plant debris. (Sp.) speleothems. (F.G.) fine gravel. (S.B.) small boulder. (S.A.) shelter availability. (S.D.) substrate diversity. (R.R.) rough rock. (Br.) branches.

Spatial scale	Group	Predictor	$_{adj}R^2$	R^2	P
Mesoscale	Photic zone	G.D.+ Hu. + T.	0.1218	0.222	0.0001
	Aphotic zone	G.D.+ E.D.+ O.M.+ Hu. + T+ Cr.	0.1258	0.2064	0.0001
Microscale	Aphotic zone	G.D.+ Hu. + E.D.+ Cr.+ Sil+ T+ P.D.+ Sp.+ F.G.+ S.B.+ S.A.+ S.D.+ R.R.+ Br.	0.1123	0.192	0.0001
	Photic zone	Hu. + G.D.+T.+ Sil. + E.D.+ Fe.	6.54^{-02}	0.13	0.0001

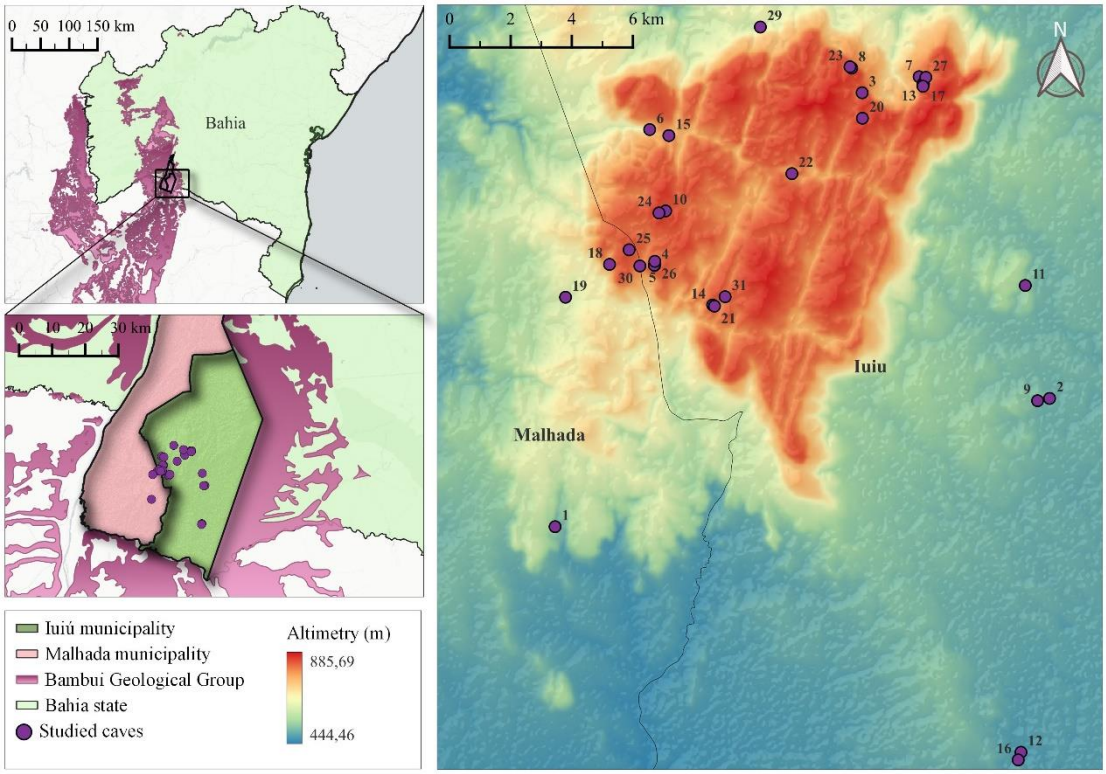


Figure 1: Location of the study area and caves in the municipalities of Iuiú and Malhada, Bahia state, Brazil. The extent of the Bambuí Geological Group and the spatial distribution of the caves included in the study are shown on the topographic map. The names of the caves are listed in Appendix S1 along with their corresponding numbers.

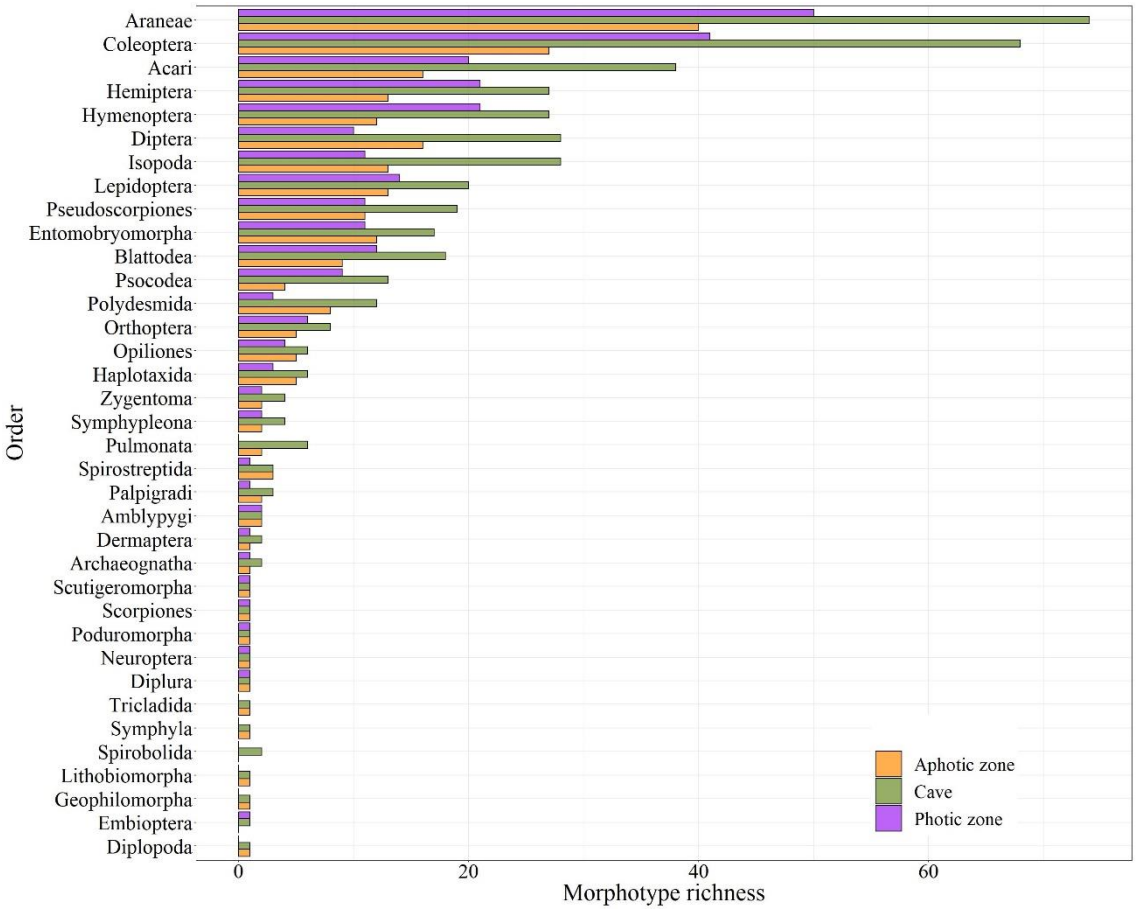


Figure 2: Morphospecies richness sampled in the 31 studied caves. The morphospecies richness is differentiated by cave zone and overall cave richness.

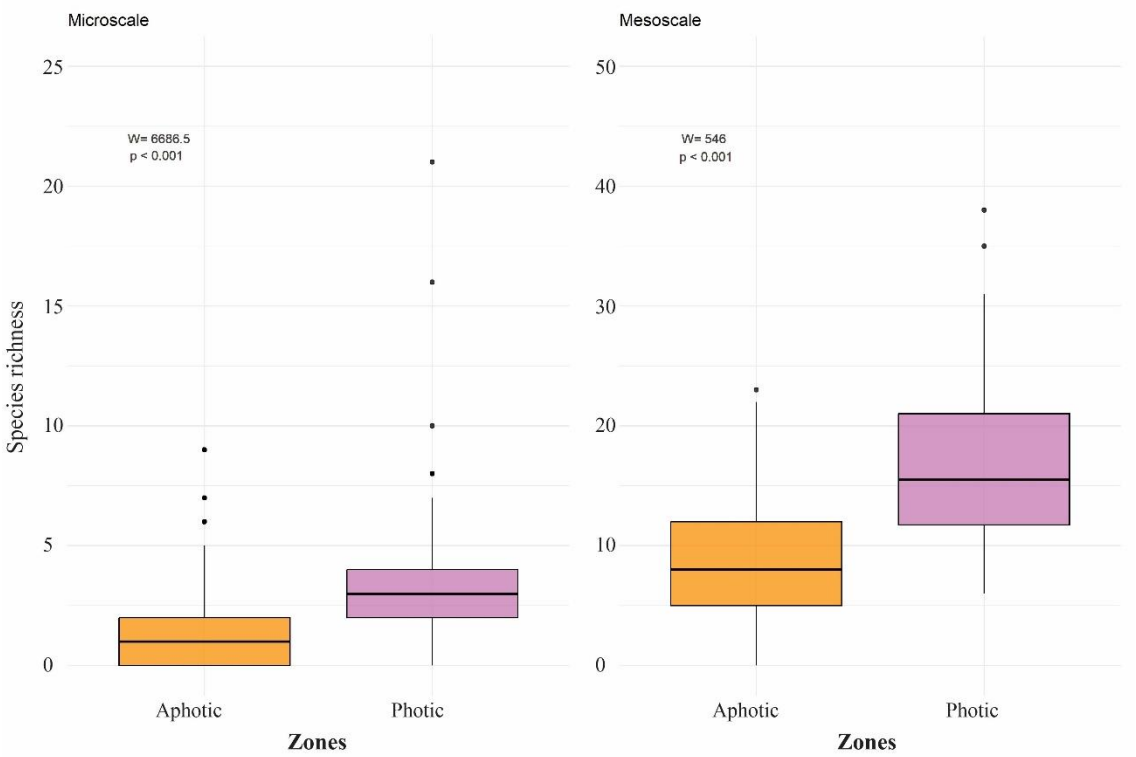


Figure 3: Box-plot illustrating differences in species richness between the aphotic and photic zones, with the photic zone consistently exhibiting higher average richness across all analyzed scales. The statistical significance of these results is indicated by the values of W statistics and p-values, which are displayed in the top-left corner of each graphic.

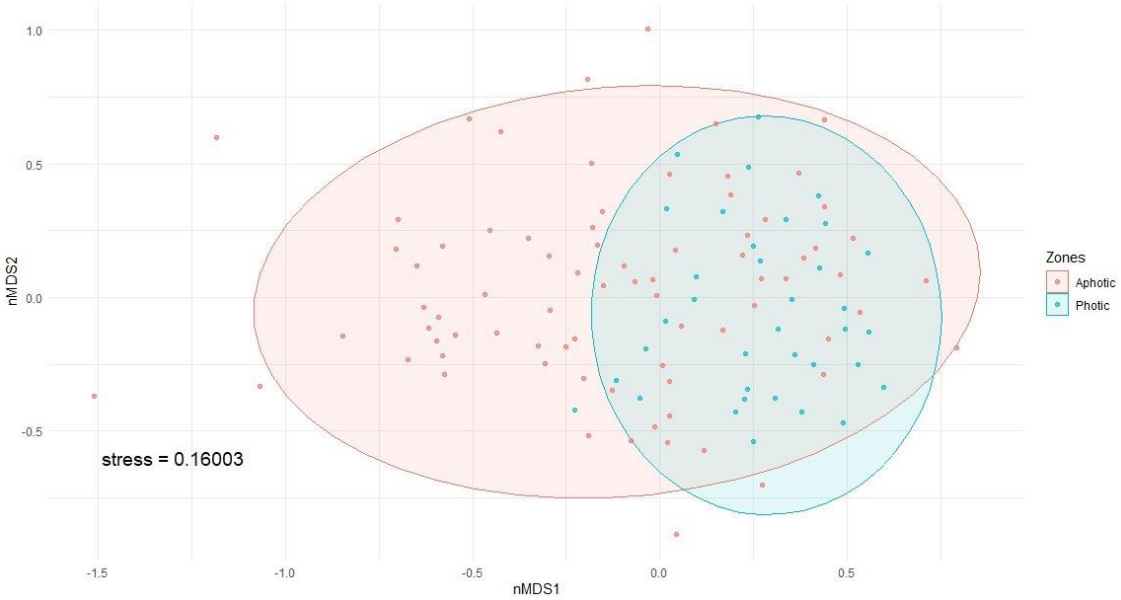


Figure 4: Non-metric multidimensional scaling (nMDS) ordination plot of the sampling units and orbits formed by the cave zones. The stress model value is provided in the lower-left corner of the plot.

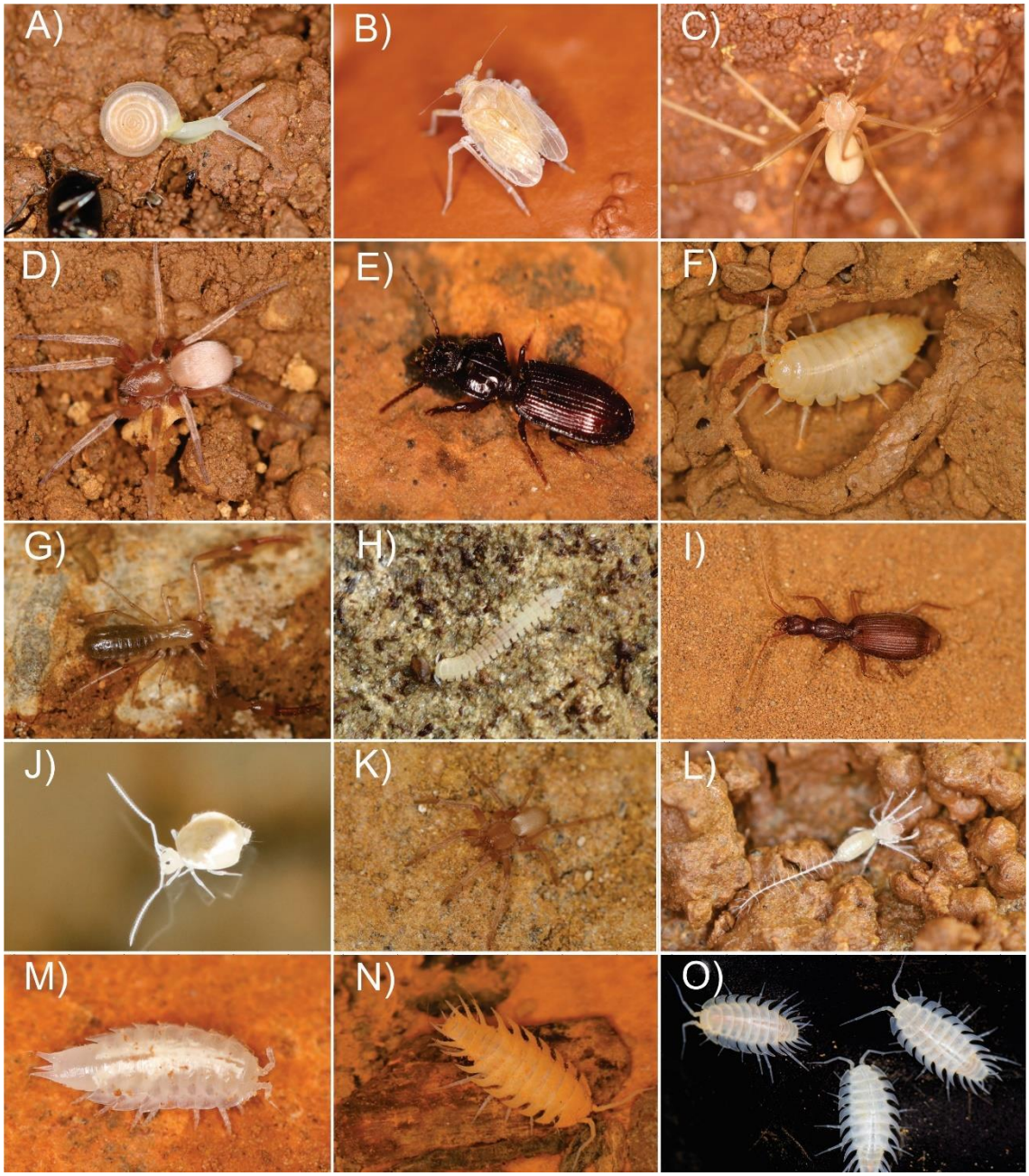


Figure 5: Some troglobitic species sampled during the study. (A) Eupulmonata (Gastropoda), (B) Iuiuia caeca (Hemiptera: Kinnaridae), (C) Loxosceles troglobia (Araneae: Sicariidae), (D) Lygromma (Araneae: Prodidomidae), (E) Schizogenius (Coleoptera: Carabidae: Scaritini), (F) Styloniscidae (Isopoda), (G) Spelaeobochica iuiu (Pseudoscorpiones: Bochicidae), (H) Pyrgodesmidae (Polydesmida), (I) Thalpius (Coleoptera: Carabidae), (J) Disparrhopalites (Symphypleona: Sminthuridae), (K) Lygromma (Araneae: Prodidomidae), (L) Eukoenenia (Paplpigradi: Eukoeneniidae), (M) Pectenoniscus (Isopoda: Styloniscidae), (N, O) Iuiuniscus iuiuensis (Isopoda: Styloniscidae). Photos: Ferreira, R. L..

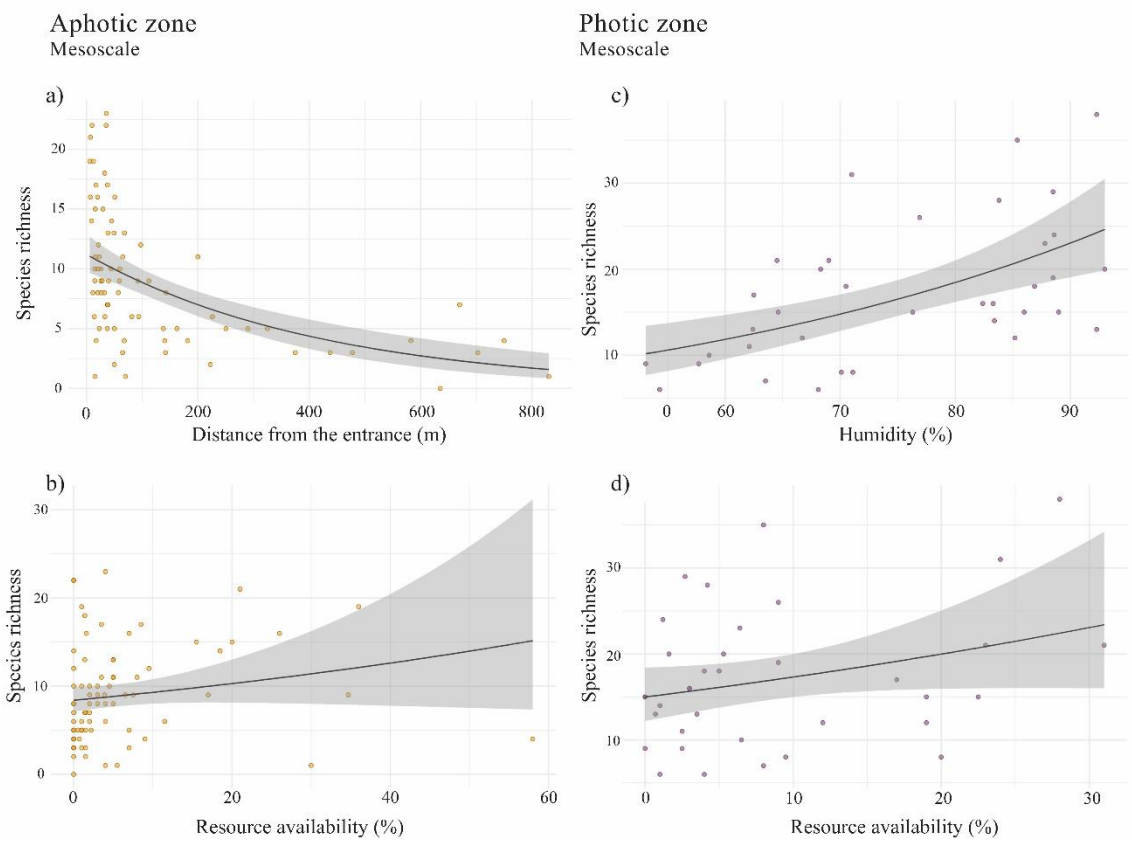


Figure 6: Relationship between the species richness with distance from nearest entrance (a) and resource availability (b) in the aphotic zone. The effects of humidity (c) and resource availability (d) on photic zone richness.

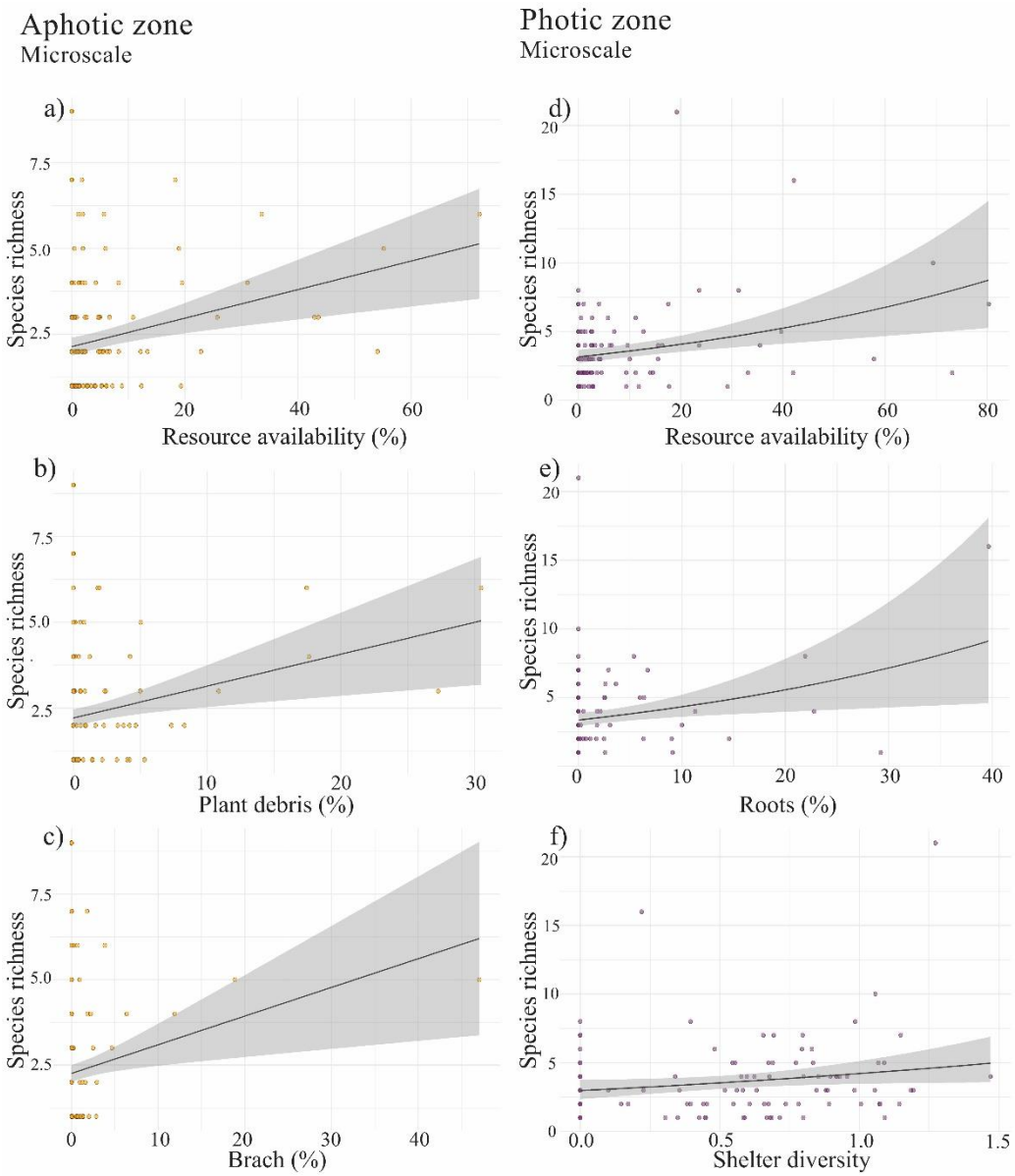


Figure 7: Relationship between the species richness with resource availability (a), plant debris (b) and branch percentage (c) in the aphotic zone. The effects of resource availability (d), roots percentage (e) and shelter diversity on photic zone richness (f).

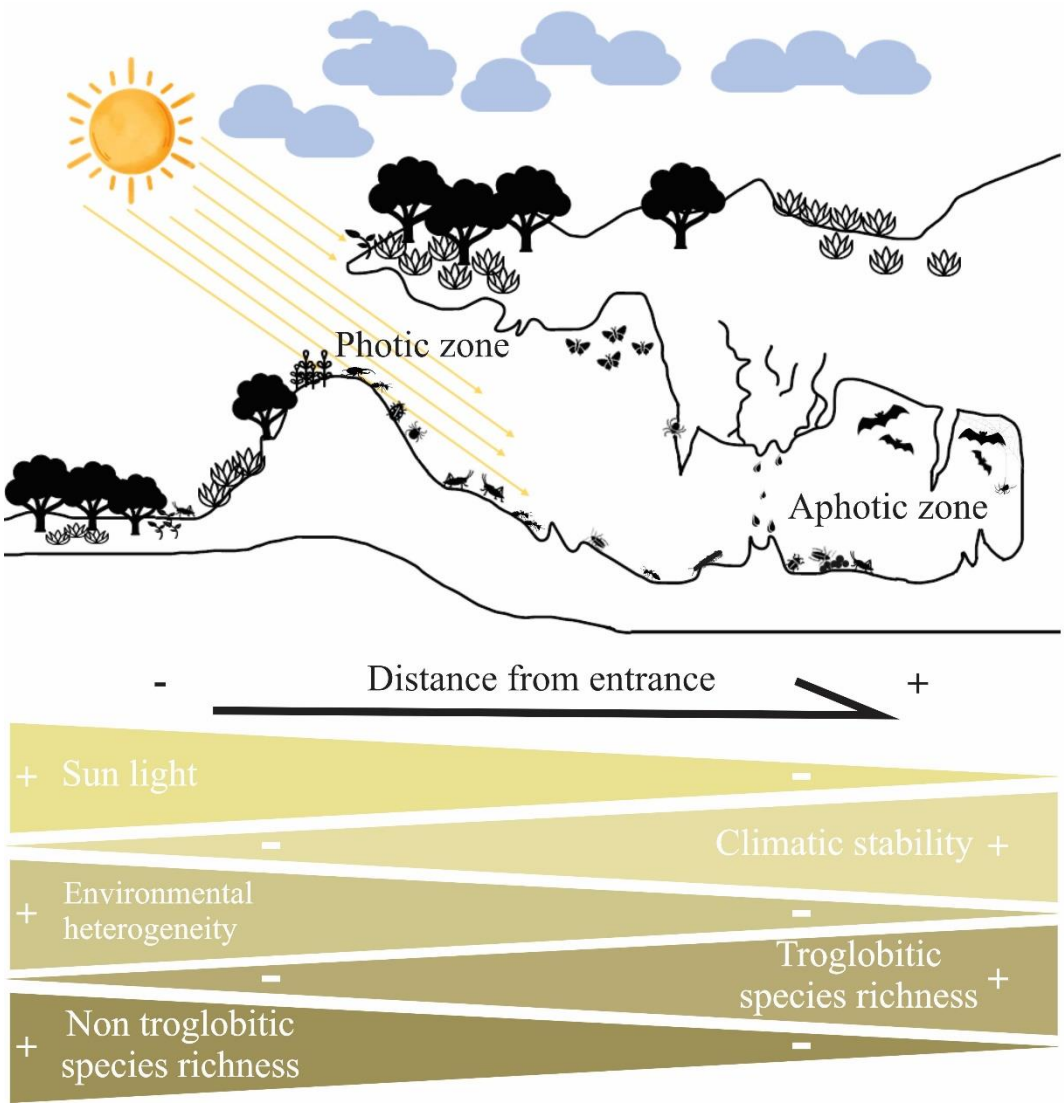


Figure 8: This infographic visually depicts the environmental gradients present within a typical tropical cave ecosystem concerning their proximity to the cave entrance and their influence on the diversity of both troglobitic and non-troglobitic species.

INVERTEBRATE COMMUNITIES OVER TIME



Direcionadores da estruturação de comunidades de invertebrados subterrâneos: uma perspectiva temporal

Paulo C. Reis-Venâncio[1,2], Rodrigo L. Ferreira[1,2], Marconi Souza-Silva[1,2]

[1] Universidade Federal de Lavras, Instituto de Ciências Naturais, Departamento de Ecologia e Conservação, Centro de Estudos em Biologia Subterrânea, Caixa postal 3037, CEP 372000-900, Lavras, MG, Brasil.

[2] PPG- Ecologia Aplicada, Departamento de Ecologia e Conservação (DEC), Universidade Federal de Lavras, Minas Gerais, Brazil.

Reis-Venâncio, P. C. ORCID identifier is 0000-0002-5655-8703
Ferreira, R.L. ORCID identifier is 0000-0003-3288-4405
Souza-Silva, M. ORCID identifier is 0000-0002-3184-5319

Introdução

Os sistemas cársticos ao redor do mundo enfrentam inúmeras ameaças antrópicas, incluindo o desmatamento, a perda de habitat, a exploração mineral e a alteração do uso do solo, entre outras. (Van Beynen & Towsend 2005, Sugai et al. 2015, Cardoso et al. 2021,2022). Essas atividades podem afetar de maneira direta e indireta todo o ecossistema subterrâneo, considerado frágil, alterando dinâmicas tróficas e clásticas, levando à perda de habitats, a disponibilidade e qualidade de recursos orgânicos carreados para seu interior, impactar populações epígeas, quais são consideradas potenciais colonizadores desse ambientes, além de ocasionar sua homogeneização estrutural (Furtado-Oliveira et al. 2022, Rabelo et al. 2021, Souza-Silva et al. 2021, Cardoso et al. 2022, Souza-Silva & Ferreira 2022). Entender como características físicas, tróficas e climáticas do ambiente influenciam na estruturação espacial e temporal de comunidades subterrâneas tem sido uma das questões norteadoras em estudos recentes (Simões et al. 2015, Mammola et al. 2020a, Pacheco et al. 2020, Souza-Silva et al. 2021, Cardoso et a. 2022, Furtado-Oliveira et al. 2022, Reis-Venâncio et al. 2022). Esse conhecimento pode gerar subsídios para elaboração e aperfeiçoamento de ações de conservação, além de aprimorar o entendimento sobre os processos ecológicos predominantes nos ecossistemas subterrâneos.

Os ambientes subterrâneos possuem uma série de características distintas em relação aos ambientes de superfície, tais como a ausência permanente de luz, tendência à oligotrofia, comunidades biológicas funcionalmente truncadas e apresentam uma simplificação da complexidade estrutural (Poulson & White 1969, Badino 2010, Mammola 2019, Simões et al. 2015, Souza-Silva & Ferreira 2022). Paralelamente a essas características, cavernas são consideradas semi-isoladas da superfície, permitindo seu uso como "laboratórios naturais", facilitando o estudo de processos ecológicos e evolutivos (Poulson & White 1969, Mammola 2019). Fatores externos que podem prejudicar e enviesar os estudos acabam sendo amenizados e até mesmo controláveis no interior das cavernas.

No entanto, mesmo apresentando comunidades relativamente simples, sua caracterização e a descoberta dos processos predominantes nesse ecossistema ainda se mostram como desafios ecológicos bem interessantes. Esses sistemas apresentam uma ampla diversidade de microhabitats e recursos orgânicos, como clastos de variados tamanhos e formas, rachaduras, cascalhos, detritos vegetais, guano, dentre outros (Souza-Silva et al. 2011, Pacheco et al. 2020, Souza-Silva et al. 2021, Furtado-Oliveira et al. 2022, Reis-Venâncio et al. 2022) e mesmo relativamente isoladas da superfície, respondem às variações sazonais e diárias (Ferreira et al. 2015, Bento et al. 2016, Simões et al. 2022). Essas variações refletem significativamente na maneira em que os invertebrados estão estruturados espacialmente.

Estudos que buscam entender a influência das características do habitat sobre a estruturação de comunidades em ambientes cavernícolas, têm demonstrado a forte relação da disponibilidade e diversidade de microhabitats e recursos orgânicos, da extensão da caverna e da presença de cursos d'água (Simões et al. 2015,2022, Pacheco et al. 2020, Souza-Silva et al. 2021, Cardoso et al. 2022, Furtado-Oliveira et al. 2022, Reis-Venâncio et al. 2022). A partir disso, a heterogeneidade ambiental, entendida como um dos direcionadores globais da biodiversidade (Tews et al. 2004, Tonetti et al. 2023), exerce papel fundamental na estruturação de comunidades subterrâneas, sendo recentemente investigada por pesquisadores da área (Pacheco et al. 2020, Souza-Silva et al. 2021, Cardoso et al. 2022, Furtado-Oliveira et al. 2022, Reis-Venâncio et al. 2022).

A diversidade e a disponibilidade de microhabitats e recursos têm uma influência positiva na composição e riqueza de invertebrados subterrâneos. No entanto, concentram-se exclusivamente na influência espacial, não considerando a influência temporal das relações ecológicas, ou seja, se tais relações sem mantêm ou variam com o passar do tempo. Entender os traços temporais por trás dessas relações ecológicas possui fortes implicações na maneira em que entendemos a ecologia de ecossistemas subterrâneos, caminhando para o aprimoramento de técnicas e meios de conservação efetivos desse ambiente.

Nesse contexto, o presente trabalho objetivou avaliar como a composição e diversidade de substratos influencia na estruturação espaço-temporal de comunidades de invertebrados subterrâneos. Para isso, comparamos comunidades amostradas em dois eventos amostrais independentes, com cinco anos entre os eventos de amostragem. Para tanto, formulamos três hipóteses: i) a riqueza média de espécies irá se manter constante entre as amostragens; ii) elementos do substrato influenciarão na estruturação espacial das comunidades de invertebrados e, iii) a resposta das comunidades quanto à estruturação do habitat permanecerão similares entre os períodos de amostragem.

Metodologia

Área de estudo

O presente estudo foi realizado em sete cavernas distribuídas em quatro maciços de calcário não contíguos na região cárstica de Iuiú e Malhada, situada na porção sudoeste do estado da Bahia, Brasil. Esses maciços estão localizados na margem direita do rio São

Francisco. A formação de calcário na região pertence ao grupo geológico Bambuí, datando da era Neoproterozoica, aproximadamente 750-600 milhões de anos atrás. Quatro cavernas (Baixão, Tapera D'água, Toca Valada e Lapa do Honorato) estão situadas no maciço chamado "Serra de Iuiú", duas (Urubú-Jatobá e Toca Fria) estão localizadas no maciço "Serrinha", e uma caverna, com o mesmo nome do maciço ao qual pertence, "Sepultamento", está situada na parte mais ao sul (Fig. 1).

A região está inserida no domínio da Caatinga, caracterizada predominantemente por florestas tropicais sazonalmente secas (Apgaua et al., 2014). O clima, classificado de acordo com o sistema Köppen-Geiger, é tropical semiárido quente, designado como "Bsh", apresentando verões quentes e secos, com uma temperatura média de 24ºC e uma precipitação média anual de 788 mm (Köppen, 1923; Alvares et al., 2013). A região está a uma altitude média de 794 metros acima do nível do mar. A estação chuvosa ocorre entre março e outubro, enquanto a estação seca se estende de novembro a fevereiro (Hijmans et al., 2005). As coordenadas geográficas de cada caverna foram obtidas na entrada principal de cada cavidade usando GPS.

Coleta de dados bióticos e abióticos

Os eventos de amostragem foram realizados durante duas expedições à área estudada: a primeira na estação seca de 2016 e a segunda na estação seca de 2021. Quadrantes medindo 1m² foram utilizados tanto para avaliar a estrutura do habitat quanto para amostrar invertebrados terrestres subterrâneos (Souza-Silva et al., 2021; Cardoso et al., 2022; Furtado Oliveira et al., 2022).

Durante cada evento de amostragem, um número igual de quadrantes foi posicionado em cada cavidade amostrada. Esses quadrantes foram distribuídos ao nível do solo, desde a entrada até as regiões mais profundas da caverna. Devido às extensões e morfologias únicas de cada cavidade, a disposição e espaçamento dos quadrantes variaram de acordo com as cavernas (ver Tabela 1).

Medindo os componentes de substrato

Em cada unidade de amostragem, qualificamos e quantificamos componentes inorgânicos e orgânicos do solo através da análise de fotografias pré-amostragem capturadas digitalmente (Pacheco et al., 2020; Souza-Silva et al., 2021; Furtado-Oliveira et al., 2022; Reis-Venâncio et al., 2022). Para aumentar a precisão, as fotografias foram tiradas com o enquadramento o mais paralelo possível ao solo, abrangendo toda a área do quadrante.

Em laboratório, selecionamos as melhores imagens e, usando o software ImageJ, identificamos e quantificamos os tipos de substrato. Para este propósito, atribuímos um valor de 100% à área total do quadrante e determinamos assim a porcentagem de cada componente de substrato dentro dele (Pacheco et al., 2020; Souza-Silva et al., 2021; Furtado-Oliveira et al., 2022, Reis-Venâncio et al., 2022). As classes de substrato obtidas durante as análises fotográficas incluem sedimento (areia (0,06-2 mm) e pavimento consolidado), silte (silte e argila), cascalho (2-64 mm), rachaduras de retração, seixo (64-1000 mm), matéria orgânica (fezes de Kerodon rupestris, serapilheira, detritos vegetais e galhos), raízes, guano de morcego, rocha exposta e corpos d'água.

Amostragem e identificação de invertebrados terrestres

Os invertebrados foram coletados manualmente dentro dos quadrantes utilizando o método de Busca Direta Intuitiva (BDI) (Wynne et al., 2019), empregando pinças e pincéis umedecidos com álcool (Fig. 2). A coleta dentro de cada quadrante foi realizada por pelo menos um profissional com experiência em amostragem de fauna de cavernas. Imediatamente após a coleta, todos os invertebrados amostrados foram colocados em recipientes plásticos contendo álcool a 70% e posteriormente transportados para o laboratório para identificação taxonômica.

No laboratório, com o auxílio de microscópios ópticos e estereomicroscópios, os indivíduos coletados foram identificados até o menor nível taxonômico possível e posteriormente agrupados em morfotipos (Oliver & Beattie, 1996a, 1996b). Para garantir maior precisão na identificação, pesquisadores especializados em grupos específicos foram consultados para refinamento taxonômico (Isopoda, Orthoptera, Polydesmida, Palpigradi, Coleoptera, Acari, Araneae, Pseudoscorpiones, Hemiptera, Pulmonata, Entomobryomorpha, Symphypleona e Poduromorpha).

Para a determinação de espécies potencialmente troglóbias, consultamos a literatura disponível sobre a fauna da região, identificando a presença de características troglomórficas, como anoftalmia, alongamento de apêndices, redução de pigmentação, entre outros específicos de cada grupo (Cristiansen 1962; Culver & Pipan 2019). Além disso, consultamos especialistas em determinados grupos taxonômicos para uma maior precisão na identificação desses troglomorfismos.

Após a conclusão do processo de identificação dos invertebrados, todos os indivíduos amostrados foram depositados na Coleção de Invertebrados Subterrâneos de Lavras (ISLA - sigla em português), vinculada ao Centro de Estudos em Biologia Subterrânea da Universidade Federal de Lavras. (http://www.biologiasubterranea.com.br).

Análises estatísticas

Medidas de substratos

Para acessar a diversidade de substrato, abrangendo todas as variáveis de substrato medidas, aplicamos o índice de diversidade de Shannon, considerando todas as classes de substrato obtidas para cada quadrante (Cardoso et al., 2022; Pellegrini et al., 2016; Souza-Silva et al., 2021; Furtado et al., 2022). Além dessa métrica, também utilizamos o índice de Shannon para calcular a diversidade de abrigos e a diversidade de recursos.

Para a determinação da diversidade de abrigos, consideramos as seguintes classes: "cascalho", "greta de retração" e "blocos". No que diz respeito à diversidade de recursos, o cálculo incluiu as classes: matéria orgânica (fezes de *K. rupestris*, serapilheira, detritos vegetais e galhos), raízes e guano de morcego.

Os valores de riqueza foram derivados da soma do número de morfotipos amostrados por quadrante. Para explorar variações na riqueza média do quadrante entre o primeiro e o segundo evento de amostragem, examinamos a distribuição dos dados por meio de visualização gráfica. Posteriormente, avaliamos a normalidade dos dados usando o teste de Shapiro-Wilk, revelando uma falta de normalidade.

Consequentemente, optamos pelo teste não paramétrico de Mann-Whitney. Os mesmos passos e análises foram aplicados para avaliar variações nos valores de riqueza de espécies por caverna entre os eventos de amostragem.

Similaridade na composição faunística ao longo do tempo

Para investigar se a variação temporal na composição entre diferentes períodos de amostragem está associada à perda ou substituição de espécies, empregamos o cálculo da diversidade Beta total. Posteriormente, realizamos uma análise da partição de seus componentes (Brep. e Bnest.) (Legendre, 2019; Magurran et al., 2019). Os cálculos foram realizados utilizando a função "beta.pair" do pacote betapart (Baselga et al., 2023), comparando os dados de composição do primeiro evento de amostragem com os do segundo.

Para compreender a similaridade dos níveis taxonômicos entre os eventos de amostragem, conduzimos uma análise da distinção taxonômica média (Δ+) no software Primer 7 - Plymouth routine in Multivariate ecological research – (http://www.primer-e.com), utilizando 111 morfotipos identificados até o nível de família. Níveis taxonômicos como Filo (peso 100), Classe (peso 80), Ordem (peso 60), Família (peso 40) e Morfotipo/Espécie (peso 20) foram utilizados como variáveis incluídas em uma matriz de distribuição dos morfotipos pelos quadrantes. Posteriormente, os dois eventos de amostragem foram contrastados (Clarke & Warwick 1998; Anderson et al. 2008; Souza-Silva et al. 2020). Em seguida, aplicamos o teste não paramétrico de Mann-Whitney para avaliar se a magnitude da variação nos níveis taxonômicos entre os eventos de amostragem divergiu significativamente.

Influência do substrato na estruturação das comunidades

Para compreender como a influência das variáveis do substrato na riqueza de invertebrados, foram construídos dois Modelos Lineares Generalizados Mistos (GLMMs, na sigla em inglês). Para ambos os modelos, os quadrantes foram considerados como um efeito aleatório, e a riqueza de espécies foi considerada como a variável de resposta. A distribuição de erro de Poisson apresentou o melhor ajuste em todos os modelos. Avaliamos a superdispersão nos modelos, reconhecendo que essa condição pode levar a inferências errôneas, onde preditores sem um efeito verdadeiro aparecem como significantes (Zuur et al. 2009).

Para explorar potenciais combinações de preditores, utilizamos o comando 'dredge' do pacote MuMIn (Bartoń 2022). Posteriormente, empregamos uma abordagem de modelo múltiplo para identificar modelos com maior poder explicativo. Em seguida, calculamos a média dos parâmetros dos modelos com valores do Critério de Seleção de Akaike (ΔAICc) menores que 4 (Burnham & Anderson 2002; Carrara et al. 2015; Solar et al. 2016; Coelho et al. 2020). Além disso, apresentamos o modelo com o menor AIC, escolhido como o mais parcimonioso entre todas as combinações testadas. O coeficiente de determinação (pseudoR^2 ajustado) para cada modelo foi obtido usando o comando 'r.squaredGLMM' do pacote MuMIn.

Resultados

Riqueza e composição dos invertebrados cavernícolas

Durante o primeiro evento de amostragem, foram identificados 63 morfotipos distribuídos em 16 ordens taxonômicas, enquanto o segundo evento de amostragem revelou um total de 94 morfotipos pertencentes a 25 ordens de invertebrados (Fig. 3). Vale ressaltar que os grupos Isopoda, Haplotaxida, Spirostreptida, Scutigeromorpha, Poduromorpha, Opiliones, Diplura e Archaeognatha foram exclusivamente amostrados no segundo evento utilizando o método do quadrante (Fig. 3).

As análises não-paramétricas indicaram não haver diferença significativa entre a riqueza de invertebrados coletada entre os dois eventos amostrais, nem quando comparada a riqueza entre cavernas (Fig. 4A), nem para a riqueza por quadrante (Fig. 4B).

O teste não-paramétrico revelou que os valores médios de distinção taxonômica (Δ+) não variaram entre os dois eventos amostrais (W= 1997; p = 0.641). Os valores de Δ+ para a primeira amostragem variaram de 0 a 83.33, com média de 36.332; ao passo que, os valores para a segunda amostragem variaram entre 0 e 83.33, com média de 35.29, sendo que a maioria dos pontos (quadrantes amostrados) está inclusa no intervalo de confiança de 0.95 (Fig. 5).

Diversidade de invertebrados troglóbios

Ao todo, com a método de coleta por quadrantes, conseguimos acessar o total de nove espécies troglóbias. As espécies estão distribuídas em cinco ordens: Araneae (5 spp.), Entomobryomorpha (2 spp.), Hemiptera (2 spp.) Isopoda (1 sp.) e Polydesmida (1 sp.).

No primeiro evento amostral, foram coletadas apenas duas espécies troglóbias, *Loxosceles troglobia* (Araneae: Sicaridae) (Souza & Ferreira 2018) na caverna Tapera D'água e um Polydesmida na caverna Baixão. No entanto, durante o segundo evento amostral, acessamos sete espécies, sendo *L. troglobia* na Tapera D'água, *Matta* sp. (Araneae: Tretrablemmidae) na Caverna Sepultamento, Ochyroceratidae (Araneae) na Urubu-Jatobá, *Trogolaphysa* (Entomobryomorpha: Entomobryidae) na Tapera D'água, *Pseudosinella* (Entomobryomorpha: Entomobryidae) na Toca Fria, Styloniscidae (Isopoda) na Lapa do Honorato, *Iuiuia caeca* (Hemiptera: Kinnaridae) (Hoch & Ferreira 2016) na Tapera D'água e Urubu Jatobá e uma nova espécie de *Spelaeometra* (Hemiptera: Hydrometridae) encontrada na Toca Fria. Algumas das espécies amostradas já se encontram formalmente descritas, em quanto outras estão em processo de descrição. Algumas das espécies troglóbias amostradas são mostradas na Figura 6.

Relação entre estruturação de habitat e riqueza de espécies

Nenhuma das variáveis apresentou correlação para o primeiro evento amostral, no entanto, as variáveis "silte" e "diversidade de recursos" foram correlacionados com "sedimento" ($r\hat{} = -0.7062$) e "raiz" ($r\hat{} = 0.802467$), respectivamente na segunda amostragem. Devido a esses altos valores de correlação, eliminamos "sedimento" e "raiz" dos modelos lineares generalizados mistos.

O melhor modelo explicou cerca de 49% da variação dos dados ($cR^2 = 0.494$; AIC = 304.5) no primeiro evento amostral, indicando relação positiva entre a riqueza invertebrados e a

porcentagem de bloco (Fig. 7A), onde a riqueza diminui em função da quantidade de rocha exposta (Fig. 7B). O segundo modelo selecionado, com dados obtidos no segundo evento amostral, explicou 42% ($cR^2 = 0.42$; AIC = 315.6) da variação, incluindo as variáveis matéria orgânica e bloco. No entanto, somente bloco exerceu influência significativa e positiva na riqueza de espécies (Fig. 7-c).

Os valores estimados para a classe "bloco" são similares entre os dois eventos, sendo para o primeiro evento, 1.1374, enquanto para o segundo evento fora 1.0279. As variáveis preditoras inclusas em cada modelo selecionado encontram-se dispostas na Tabela 2.

As mesmas variáveis preditoras inclusas no melhor modelo foram selecionadas a partir dos resultados obtidos pela média dos melhores modelos ($\Delta AICc < 4$), em ambas as amostragens. "Rocha" influenciou negativamente a riqueza de espécies amostradas no primeiro evento, ao passo que "bloco" influenciou positivamente (Figura 6A), e apenas bloco influenciou de maneira positiva a riqueza de invertebrados no segundo evento (Figura 6B). A variável "bloco" foi a única variável significativa para ambos os modelos.

Discussão

Compreender a estruturação espacial de comunidades biológicas e sua variação ao longo do tempo é essencial, uma vez que suas respostas podem ser um reflexo de distúrbios ambientais ou fatores naturais (White & Jentsch 2001; Fraterrigo & Rusak 2008). O monitoramento sistemático efetivo dessas comunidades ao longo do tempo permite identificar se as variações observadas são decorrentes de distúrbios ou fatores antrópicos negativos, além de avaliar possíveis variações naturais na composição e dinâmica das comunidades. O monitoramento dessas respostas ao longo do tempo surge como uma ferramenta fundamental na elaboração e estabelecimento de padrões ecológicos (Hoffmann 2010), uma vez que relações ecológicas devem perdurar no tempo e serem detectáveis em diferentes escalas, para que sejam verdadeiros.

O conhecimento dos padrões ecológicos das comunidades pode ser usado como base para estudos comparativos, permitindo avaliar se determinada comunidade está em um estado natural ou se já sofreu influências antrópicas significativas. Dessa forma, entender como comunidades encontram-se estruturadas ao longo do tempo se configura um valioso conhecimento para a gestão e conservação da biodiversidade e dos ecossistemas em geral.

Encontramos que a riqueza de invertebrados não variou entre os eventos amostrais, nem ao avaliarmos a riqueza total por caverna, nem a riqueza por quadrante. Essa constância no número de espécies é consistente com estudos que demonstram que habitats subterrâneos suportam um número limitado de espécies, apresentando, assim, uma capacidade de carga ecológica (Simões et al. 2022). Apesar de valores elevados de substituição de espécies em comunidades subterrâneas poderem ser encontrados quando eventos são comparados, a riqueza de espécies pode sofrer baixa variação, onde maiores variações são encontradas apenas entre períodos úmidos e períodos seco (Simões et al. 2022). A disponibilidade de recursos e de microhabitats, juntamente às interações ecológicas, são os principais fatores que

regulam e estabilizam a capacidade de suporte de um dado ambiente (Chesson 2000; Simões et al. 2022). Esses mecanismos regulatórios são fundamentais para a coexistência das espécies em um determinado habitat, especialmente de espécies que apresentam ecologias e preferências similares. O número de espécies presente em habitats subterrâneos está intimamente ligado à capacidade de carga do sistema (Mammola & Isaia 2018).

Em ecossistemas subterrâneos, uma maior riqueza de espécies é esperada durante o período chuvoso, em virtude de fatores limitantes, como condições climáticas favoráveis aos invertebrados e maior disponibilidade de recursos ao fim do período (Souza-Silva et al. 2011, 2013; Bento et al. 2016, Simões et al. 2022; Souza-Silva & Ferreira 2022). O presente estudo foi inteiramente realizado durante o período seco, quando a disponibilidade de recursos para a fauna era baixa, e as condições climáticas desfavoráveis prevalecem. Consequentemente, observamos uma riqueza de espécies baixa, ao contrário do esperado para períodos chuvosos. Períodos secos são rigorosos para as espécies, levando à diminuição na riqueza de espécies. Esse fator acaba influenciando também na baixa variação na diversidade de espécies encontrada entre os eventos amostrais.

Estudos que buscam compreender variações composicionais em ambientes subterrâneos costumam comparar comunidades em diferentes períodos do ano, como o período chuvoso e o período seco (Lunghi et al. 2015, Bento et al. 2016, Mammola et al. 2020b), ou são executados em curto período (Tobin et al. 2013), evidenciando variações consistentes em relação à composição faunística em virtude da sazonalidade. Nesse sentido, nossos resultados corroboram com estudos que investigaram a variação nas comunidades entre sucessivos períodos de seca (Di Russo et al. 1997, Salvidio et al. 2020, Simões et al. 2022), demonstrando relativa constância temporal na composição faunística. Portanto, baseado nos estudos citados e em nossos resultados, é correto afirmar que a composição faunística varia entre os diferentes períodos do ano, mas se mantem relativamente constante quando comunidades de mesmo período são comparadas.

Com relação às variáveis de estruturação de habitat e a riqueza de invertebrados coletados na primeira campanha, observamos efeitos das classes "bloco" e "rocha nua". Como esperado, a presença de rochas nuas tem efeito negativo na riqueza de espécies, resultando em menor diversidade de invertebrados em áreas onde esse tipo de substrato é predominante. Essa relação ocorre porque superfícies lisas e sem muitas reentrâncias, porosidades e espaços disponíveis, reduzem o número de microhabitats e, consequente, diminuem a heterogeneidade espacial e a disponibilidade de potenciais abrigos. Isso pode ocasionar em elevadas taxas competição inter/intraespecíficicas e taxas de predação, favorecendo a diminuição da riqueza local (Tews et al. 2004, Pacheco et al. 2020, Brothers & Blakeslee 2021, Souza-Silva et al. 2021, Furtado-Oliveira et al. 2022, Reis-Venâncio et al. 2022). Em suma, ambientes estruturalmente mais simples, mais homogêneos, tendem a comunidades biológicas menos ricas e diversas (Tews et al. 2004, Loke et al. 2015, Chang & Todd 2023).

Em contrapartida, a presença de "bloco" favorece o aumento da heterogeneidade ambiental, elevando a complexidade estrutural do ambiente (Loke et al. 2015, Tosseti et al. 2023). Os inúmeros macro e micro espaços criados pela presença e a sobreposição desses

clastos de distintos tamanhos, formatos e porosidades levam à maior disponibilidade de microhabitats, que poderão ser utilizados pela fauna como abrigo, local de reprodução, além de espaços com condições microclimáticas (em relação à temperatura e umidade) mais favoráveis às espécies de invertebrados (Ferreira & Souza-Silva 2001, Ferreira et al. 2009, Cardoso et al. 2022, Reis-Venâncio et al. 2022). Essa série de benefícios gerada pela presença desses clastos promove aumento no estabelecimento das espécies, resultando em ambientes mais ricos (Souza-Silva et al. 2021). De maneira complementar, o maior número de habitats potenciais permite um maior número de nichos disponíveis, além de levar à redução na sobreposição de nichos (Tews et al. 2004, Souza-Silva et al. 2021, Reis-Venâncio et al. 2022). Esses fatores possibilitam que espécies potencialmente competidoras, com preferências e restrições ecológicas similares, co-existam em um mesmo sistema. As taxas de predação também podem ser reduzidas em ambientes de elevada heterogeneidade, o que pode gerar um aumento na riqueza de espécies (Brothers & Blakeslee 2021).

A relação entre disponibilidade de matacões e riqueza de espécies perdurou ao longo do tempo, sendo a mesma relação visualizada para ambos os eventos amostrais e, de maneira complementar, a magnitude do efeito da variável sobre a riqueza apresentou valores bem similares (Tabela 2). Frente a isso, é plausível considerarmos esses elementos do ecossistema subterrâneo como "elementos-chave", afetando a estruturação espaço-temporal de comunidades subterrâneas. Estrutura-chave pode ser definida, nesse caso, como certa característica física do ambiente que fornece abrigo e condições especiais para as espécies, sendo essencial para a manutenção da estrutura e funcionamento de comunidades biológicas (Tews et al. 2004). A identificação desses elementos-chave se dá, geralmente, através de aumentos significativos na riqueza de espécies, como é o caso da relação aqui estabelecida, que persiste ao longo dos anos. O estudo e a identificação desses elementos-chave é crucial quando o objetivo final é a manutenção da biodiversidade subterrânea e a conservação efetiva dos ecossistemas.

A perda de habitat por meio de atividades humanas está entre as principais ameaças aos ambientes cársticos (Van Beynen & Townsend 2005), não sendo diferente para a região de estudo. A região de Iuiú vem sofrendo fortemente com atividades agropastoris e mineração, além de apresentar um longo histórico de desmatamento (Cardoso et al. 2021, 2022), sendo atualmente entendida como uma região prioritária para conservação. Ambientes subterrâneos são intimamente ligados à processos no ambiente superficial (Prous et al. 2004, 2015, Souza-Silva et al. 2015, Rabelo et al. 2018, 2021, Cardoso et al. 2022). Áreas em torno de entradas de cavernas com elevadas taxas de desmatamento podem sofrer com a exposição do solo e subsequentes processos erosivos, resultando no transporte de sedimento fino para o interior das cavernas (Cardoso et al. 2022). Esse sedimento carreado pode ser depositado em camadas e se acumular nos espaços entre as rochas, inviabilizando esses possíveis habitats e tornando-os inacessíveis a fauna terrestre. Esse processo de assoreamento no interior das cavidades acaba afetando a sobrevivência das espécies locais, refletindo na diminuição da riqueza de espécies (Cardoso et al. 2022). Portanto, destacamos a importância do monitoramento das atividades que ocorrem no ambiente epígeo visando aperfeiçoar os meios de conservação e

manutenção das comunidades subterrâneas. A preservação dos elementos-chave pode garantir a viabilidade e o equilíbrio dos ecossistemas subterrâneos, e sua estruturação tanto no espaço como no tempo.

Referência bibliográficas

Alvares, C. A., Stape, J. L., Sentelhas, P. C., de Moraes Gonçalves, J. L., & Sparovek, G. (2013). Köppen's climate classification map for Brazil. *Meteorologische Zeitschrift*, *22*(6), 711–728. https://doi.org/10.1127/0941-2948/2013/0507

Anderson, M.J., Gorley, R.N., Clarke, K.R., 2008. PERMANOVA+ for PRIMER: Guide to software and statistical methods. Massey University, Albany Campus, Auckland: New Zealand.

Apgaua, D. M. G., dos Santos, R. M., Pereira, D. G. S., de Oliveira Menino, G. C., Pires, G. G., Fontes, M. A. L., & Tng, D. Y. P. (2014). Beta-diversity in seasonally dry tropical forests (SDTF) in the Caatinga Biogeographic Domain, Brazil, and its implications for conservation. *Biodiversity and Conservation, 23(1),* 217–232. https://doi.org/10.1007/s10531-013-0599-9

Badino, G. (2010). Underground meteorology-"What's the weather underground?". *Acta carsologica*, *39*(3), 427-448.

Bartoń K (2022). _MuMIn: Multi-Model Inference_. R package version 1.47.1. https://CRAN.R-project.org/package=MuMIn.

Bento, D. D. M., Ferreira, R. L., Prous, X., Souza-Silva, M., Bellini, B. C., & Vasconcellos, A. (2016). Seasonal variations in cave invertebrate communities in the semiarid Caatinga, Brazil. *Journal of Cave and Karst Studies*, *78*(2), 61-71. DOI: 10.4311/2015LSC0111

Brothers, C. A., & Blakeslee, A. M. (2021). Alien vs predator play hide and seek: How habitat complexity alters parasite mediated host survival. *Journal of Experimental Marine Biology and Ecology*, *535*, 151488. https://doi.org/10.1016/j.jembe.2020.151488

Burnham, K. P., Anderson, D. R. (2002). Model selection and multimodel inference: a practical informationtheoretic approach. J Wildl Manag 67:677

Cardoso, R. C. (2017). Ecologia e conservação de cavernas na região cárstica de Iuiú – BA. Dissertação, Universidade Federal de São João del-Rei, São João del-Rei, 117 p..

Cardoso, R. C., Ferreira, R. L., & Souza-Silva, M. (2021). Priorities for cave fauna conservation in the Iuiú karst landscape, northeastern Brazil: a threatened spot of troglobitic species diversity. *Biodiversity and Conservation*, *30*(5), 1433-1455.

Cardoso, R. C., Ferreira, R. L., & Souza-Silva, M. (2022). Multi-spatial analysis on cave ecosystems to predict the diversity of subterranean invertebrates. *Basic and Applied Ecology*, *65*, 111–122. https://doi.org/10.1016/j.baae.2022.11.007

Carrara, E., Arroyo-Rodríguez, V., Vega-Rivera, J. H., Schondube, J. E., de Freitas, S. M., & Fahrig, L. (2015). Impact of landscape composition and configuration on forest specialist and generalist bird species in the fragmented Lacandona rainforest, Mexico. *Biological Conservation*, *184*, 117-126. https://doi.org/10.1016/j.biocon.2015.01.014

Chang, C. C., & Todd, P. A. (2023). Reduced predation pressure as a potential driver of prey diversity and abundance in complex habitats. *npj Biodiversity*, *2*(1), 1. https://doi.org/10.1038/s44185-022-00007-x

Chesson, P. (2000). Mechanisms of maintenance of species diversity. *Annual review of Ecology and Systematics*, *31*(1), 343-366.

Christiansen, K. A. (1962). Proposition pour la classification des animaux cavernicoles. Spelunca Mem. 2, 76-78.

Clarke, K. R., & Warwick, R. M. (1998). A taxonomic distinctness index and its statistical properties. *Journal of applied ecology*, *35*(4), 523-531. https://doi.org/10.1046/j.1365-2664.1998.3540523.x

Coelho, A. J. P., Magnago, L. F. S., Matos, F. A. R., Mota, N. M., Diniz, É. S., & Meira-Neto, J. A. A. (2020). Effects of anthropogenic disturbances on biodiversity and biomass stock of Cerrado, the Brazilian savanna. *Biodiversity and Conservation*, *29*, 3151-3168.

Culver, D. C., & Pipan, T. (2019). *The Biology of Caves and Other Subterranean Habitats (Second edi)*. Oxford University Press, https://doi.org/10.1093/oso/97801 98820 765.001.0001

Culver, D. C., & Pipan, T. (2019). The biology of caves and other subterranean habitats (2nd ed.). Oxford University Press, 272 pp..

Di Russo, C., Carchini, G., Rampini, M., Lucarelli, M., & Sbordoni, V. (1997). Long term stability of a terrestrial cave community. *International Journal of Speleology*, *26*(1), 75-88. http://dx.doi.org/10.5038/1827-806X.26.1.7

Ferreira, R. L., Martins, V. M., Paixão, E. A., & Silva, M. S. (2015). Spatial and temporal fluctuations of the abundance of Neotropical cave-dwelling moth Hypena sp.(Noctuidae, Lepidoptera) influenced by temperature and humidity. *Subterranean Biology*, *16*, 47-60.

Fraterrigo, J. M., & Rusak, J. A. (2008). Disturbance-driven changes in the variability of ecological patterns and processes. *Ecology letters*, *11*(7), 756-770. https://doi.org/10.1111/j.1461-0248.2008.01191.x

Furtado-Oliveira, L., Lopes Ferreira, R., Rodríguez Fernández, J. I., & Souza Silva, M. (2022). Recreational caving impacts of visitors in a high-altitude cave in Bolivian Andes: main effects on microhabitat structure and faunal distribution. *International Journal of Speleology*, *51*(2), 93–103. https://doi.org/10.5038/1827-806X.51.2.2418

Hijmans, R.J., Cameron, S.E., Parra, J.L., Jones, P.G., Jarvis, A., 2005 - Very high resolution interpolated climate surfaces for global land areas. International journal of climatology, 25(15): 1965-1978.

Hoch, H., & Ferreira, R. (2016). Iuiuia caeca gen. n., sp. n., a new troglobitic planthopper in the family Kinnaridae (Hemiptera, Fulgoromorpha) from Brazil. *Deutsche Entomologische Zeitschrift*, *63*(2), 171-181.

Hoffmann, B. D. (2010). Using ants for rangeland monitoring: global patterns in the responses of ant communities to grazing. *Ecological Indicators*, *10*(2), 105-111. https://doi.org/10.1016/j.ecolind.2009.04.016

Köppen, W. P. (1923). Die klimate der erde: Grundriss der klimakunde. Walter de Gruyter 46pp.

Loke, L. H., Ladle, R. J., Bouma, T. J., & Todd, P. A. (2015). Creating complex habitats for restoration and reconciliation. *Ecological Engineering*, *77*, 307-313. https://doi.org/10.1016/j.ecoleng.2015.01.037

Lunghi, E., Manenti, R., & Ficetola, G. F. (2015). Seasonal variation in microhabitat of salamanders: environmental variation or shift of habitat selection?. *PeerJ*, *3*, e1122. https://doi.org/10.7717/peerj.1122

Mammola, S. (2019). Finding answers in the dark: caves as models in ecology fifty years after Poulson and White. *Ecography, 42(7),* 1331-1351. 10.1111/ecog.03905

Mammola, S., Amorim, I.R., Bichuette, M.E., Borges, P.A.V., Cheeptham, N., Cooper, S.J.B., Culver, D.C., Deharveng, L., Eme, D., Ferreira, R.L., Fišer, C., Fišer, Ž., Fong, D.W., Griebler, C., Jeffery, W.R., Jugovic, J., Kowalko, J.E., Lilley, T.M., Malard, F., Manenti, R., Martínez, A., Meierhofer, M.B., Niemiller, M.L., Northup, D.E., Pellegrini, T.G., Pipan, T., Protas, M., Reboleira, A.S.P.S., Venarsky, M.P., Wynne, J.J., Zagmajster, M. and Cardoso, P. (2020a). Fundamental research questions in subterranean biology. Biol Rev, 95: 1855-1872. https://doi.org/10.1111/brv.12642

Mammola, S., Chiappetta, N., Giachino, P. M., Antić, D., Zapparoli, M., & Isaia, M. (2020b). Exploring the homogeneity of terrestrial subterranean communities at a local spatial scale. *Ecological Entomology*, *45*(5), 1053–1062. https://doi.org/10.1111/een.12883

Mammola, S., Isaia, M. (2018) Cave communities and species interactions. In Cave Ecology; Ecological Studies 235; Moldovan, O.T., Kováˇc, L., Halse, S., Eds.; Springer Nature: Cham, Switzerland pp. 255–267.

Oliver, I., Beattie, A. J. (1996a) Invertebrate morphospecies as surrogates for species: a case study. Conservation Biology, 10(1): 99-109. https://doi.org/10.1046/j.1523-1739.1996.10010099.x

Oliver, I., Beattie, A. J. (1996b) Designing a cost-effective invertebrate survey: a test of methods for rapid assessment of biodiversity. Ecological applications 6(2): 594-607. https://doi.org/10.2307/2269394

Pacheco, G. S. M., Souza-Silva, M., Cano, E., Ferreira, R. L. (2020). The role of microhabitats in structuring cave invertebrate communities in Guatemala. International Journal of Speleology, 49(2): 161-169. https://doi.org/10.5038/1827-806X.49.2.2333

Pellegrini, T. G., Sales, L. P., Aguiar, P., & Ferreira, R. L. (2016). Linking spatial scale dependence of land-use descriptors and invertebrate cave community composition. In *Subterranean Biology* (Vol. 18, pp. 17–38). Pensoft Publishers. https://doi.org/10.3897/SUBTBIOL.18.8335

Peterson, B.G. & Carl, P. (2020). _PerformanceAnalytics: Econometric Tools for Performance and Risk Analysis_. R package version 2.0.4, <https://CRAN.R-project.org/package=PerformanceAnalytics>.

Poulson, T. L., & White, W. B. (1969). The Cave Environment: Limestone caves provide unique natural laboratories for studying biological and geological processes. *Science, 165(3897),* 971-981.

Prous, X., Ferreira, R. L., & Jacobi, C. M. (2015). The entrance as a complex ecotone in a Neotropical cave. *International Journal of Speleology, 44(2),* 177-189. http://dx.doi.org/10.5038/1827-806X.44.2.7

Prous, X., Ferreira, R. L., & Martins, R. P. (2004). Ecotone delimitation: Epigean–hypogean transition in cave ecosystems. *Austral Ecology, 29(4),* 374-382. https://doi.org/10.1111/j.1442-9993.2004.01373.x

R Core Team (2022). R: A language and environment for statistical computing. R Foundation for Statistical Computing, Vienna, Austria. URL https://www.R-project.org/

Rabelo, L. M., Souza-Silva, M., & Ferreira, R. L. (2018). Priority caves for biodiversity conservation in a key karst area of Brazil: comparing the applicability of cave conservation indices. *Biodiversity and conservation, 27,* 2097-2129. https://doi.org/10.1007/s10531-018-1554-6

Rabelo, L. M., Souza-Silva, M., & Ferreira, R. L. (2021). Epigean and hypogean drivers of Neotropical subterranean communities. *Journal of Biogeography*, *48*(3), 662-675. https://doi.org/10.1111/jbi.14031

Reis-Venâncio, P. C., Rabelo, L. M., Pellegrini, T. G., & Ferreira, R. L. (2022). From light to darkness: the duality of influence of habitat heterogeneity on Neotropical terrestrial cave invertebrate communities. *Studies on Neotropical Fauna and Environment*. https://doi.org/10.1080/01650521.2022.2095832

Salvidio, S., Costa, A., Oneto, F., & Pastorino, M. V. (2019). Variability of a subterranean prey-predator community in space and time. *Diversity*, *12*(1), 17.

Schober, P., Boer, C., & Schwarte, L. A. (2018). Correlation coefficients: appropriate use and interpretation. *Anesthesia & analgesia*, *126*(5), 1763-1768.

Simões, M. H., Souza-Silva, M., & Ferreira, R. L. (2015). Cave physical attributes influencing the structure of terrestrial invertebrate communities in Neotropics. *Subterranean Biology*, *16*, 103-121. https://doi.org/10.3897/subtbiol.16.5470

Simões, M. H., Souza-Silva, M., & Ferreira, R. L. (2022). Species-area relationship and richness persistence as a proxy of environmental carrying capacity: A case study in a neotropical show cave. *Acta Oecologica*, *116*, 103848. https://doi.org/10.1016/j.actao.2022.103848

Solar, R. R. de C., Barlow, J., Andersen, A. N., Schoereder, J. H., Berenguer, E., Ferreira, J. N., & Gardner, T. A. (2016). Biodiversity consequences of land-use change and forest disturbance in the Amazon: A multi-scale assessment using ant communities. *Biological Conservation*, *197*, 98-107.

Souza, M. F., & Ferreira, R. L. (2018). A new highly troglomorphic Loxosceles (Araneae: Sicariidae) from Brazil. *Zootaxa*, *4438*(3), 575-587.

Souza-Silva, M., & Ferreira, R. L. (2022). Dinâmica trófica em Ambientes de Cavernas. In: Zampaulo, R. A., & Prous, X. (Eds.), *Fauna cavernícola do Brasil.* Belo Horizonte: Editora Rupestre, pp. 58-81.

Souza-Silva, M., Cerqueira, R. F. V., Pellegrini, T. G., & Ferreira, R. L. (2021). Habitat selection of cave-restricted fauna in a new hotspot of subterranean biodiversity in Neotropics. *Biodiversity and Conservation*, *30*(14), 4223–4250. https://doi.org/10.1007/s10531-021-02302-8

Souza-Silva, M., Iniesta, L. F. M., & Ferreira, R. L. (2020). Invertebrates diversity in mountain Neotropical quartzite caves: which factors can influence the composition, richness, and distribution of the cave communities?. *Subterranean Biology*, *33*, 23-43.

Souza-Silva, M., Júnior, A. S., & Ferreira, R. L. (2013). Food resource availability in a quartzite cave in the Brazilian montane Atlantic Forest. *Journal of Cave & Karst Studies*, *75*(3), 177-188.

Souza-Silva, M., Martins, R. P., & Ferreira, R. L. (2011). Trophic dynamics in a neotropical limestone cave. *Subterranean Biology*, *9*, 127-138. doi: 10.3897/subtbiol.9.2515

Souza-Silva, M., Martins, R. P., & Ferreira, R. L. (2015). Cave conservation priority index to adopt a rapid protection strategy: a case study in Brazilian Atlantic rain forest. *Environmental Management*, *55*, 279-295. https://doi.org/10.1007/s00267-014-0414-8

Sugai, L. S. M., Ochoa-Quintero, J. M., Costa-Pereira, R., & Roque, F. O. (2015). Beyond aboveground. *Biodiversity and Conservation*, *24*, 2109-2112.

Tews, J., Brose, U., Grimm, V., Tielbörger, K., Wichmann, M. C., Schwager, M., & Jeltsch, F. (2004). Animal species diversity driven by habitat heterogeneity/diversity: the importance of keystone structures. *Journal of Biogeography*, *31(1)*, 79-92. https://doi.org/10.1046/j.0305-0270.2003.00994.x

Tobin, B. W., Hutchins, B. T., & Schwartz, B. F. (2013). Spatial and temporal changes in invertebrate assemblage structure from the entrance to deep-cave zone of a temperate marble cave. *International Journal of Speleology*, *42*(3), 4.

Tonetti, V., Pena, J. C., Scarpelli, M. D., Sugai, L. S., Barros, F. M., Anunciação, P. R., ... & Ribeiro, M. C. (2023). Landscape heterogeneity: concepts, quantification, challenges and future perspectives. *Environmental Conservation*, 1-10. https://doi.org/10.1017/S0376892923000097

Van Beynen, P., & Townsend, K. (2005). A disturbance index for karst environments. *Environmental Management*, *36*, 101-116. https://doi.org/10.1007/s00267-004-0265-9.

White, P. S., & Jentsch, A. (2001). The search for generality in studies of disturbance and ecosystem dynamics. *Progress in botany: Genetics physiology systematics ecology*, 399-450.

Wynne, J. J., Howarth, F. G., Sommer, S., & Dickson, B. G. (2019). Fifty years of cave arthropod sampling: Techniques and best practices. *International Journal of Speleology*, *48(1)*, 33–48. https://doi.org/10.5038/1827-806X.48.1.2231

Zuur, A. F., Ieno, E. N., & Smith, G. M. (2007). Analyzing ecological data. Springer Science & Business Media.

Zuur, A. F., Ieno, E. N., Walker, N. J., Saveliev, A. A., & Smith, G. M. (2009). Mixed effects models and extensions in Ecology with R. New York: Springer, 574 p..

Baselga A, Orme D, Villeger S, De Bortoli J, Leprieur F, Logez M, Martinez-Santalla S, Martin-Devasa R, Gomez-Rodriguez C, Crujeiras R (2023). _betapart: Partitioning Beta Diversity into Turnover and Nestedness Components_. R package version 1.6, <https://CRAN.R-project.org/package=betapart>.

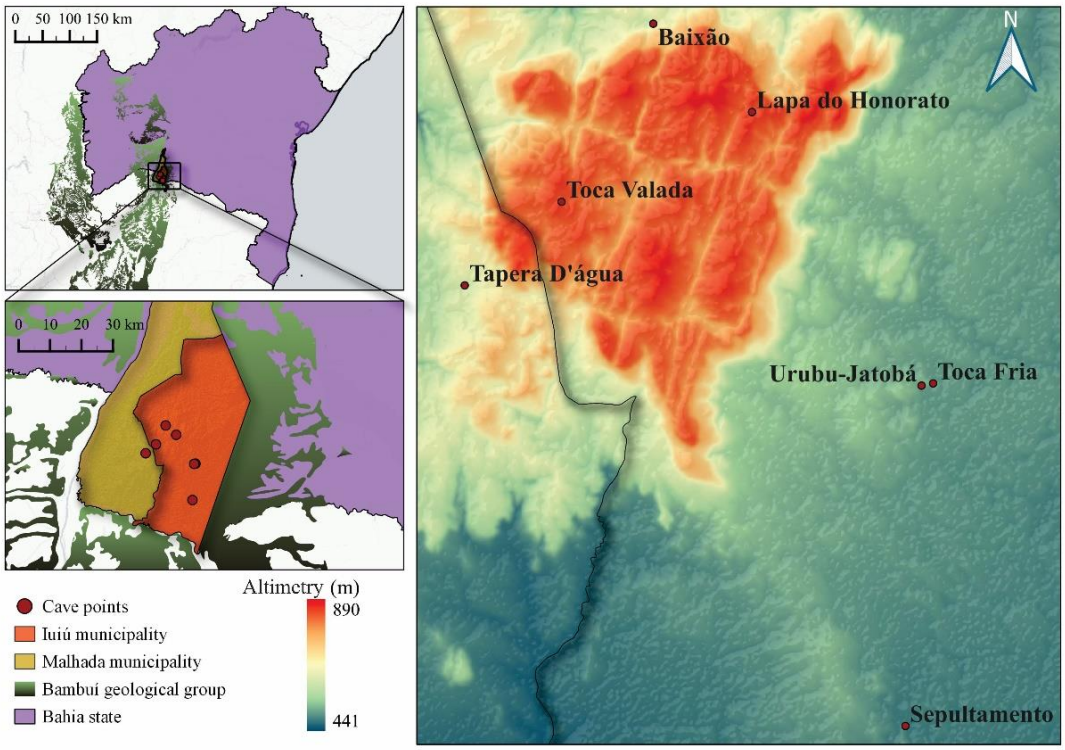


Figura 1. Localização da áreas de estudos, nos municípios de Iuiú e Malhada, porção Sudoeste do estado da Bahia. Localização e extensão do grupo geológico Bambuí em destaque e a distribuição espacial das cavernas amostradas no estudo no mapa altimétrico.



Figura 2. Método de amostragem por quadrante (1m²) utilizado em ambos os eventos de amostragem, mostrando o uso de pincéis e pinças para coleta de invertebrados. A coleta de dados abióticos foi realizada na mesma área da coleta de invertebrados. Fotos: Lucas Mendes Rabelo e Paulo C. Reis-Venâncio.

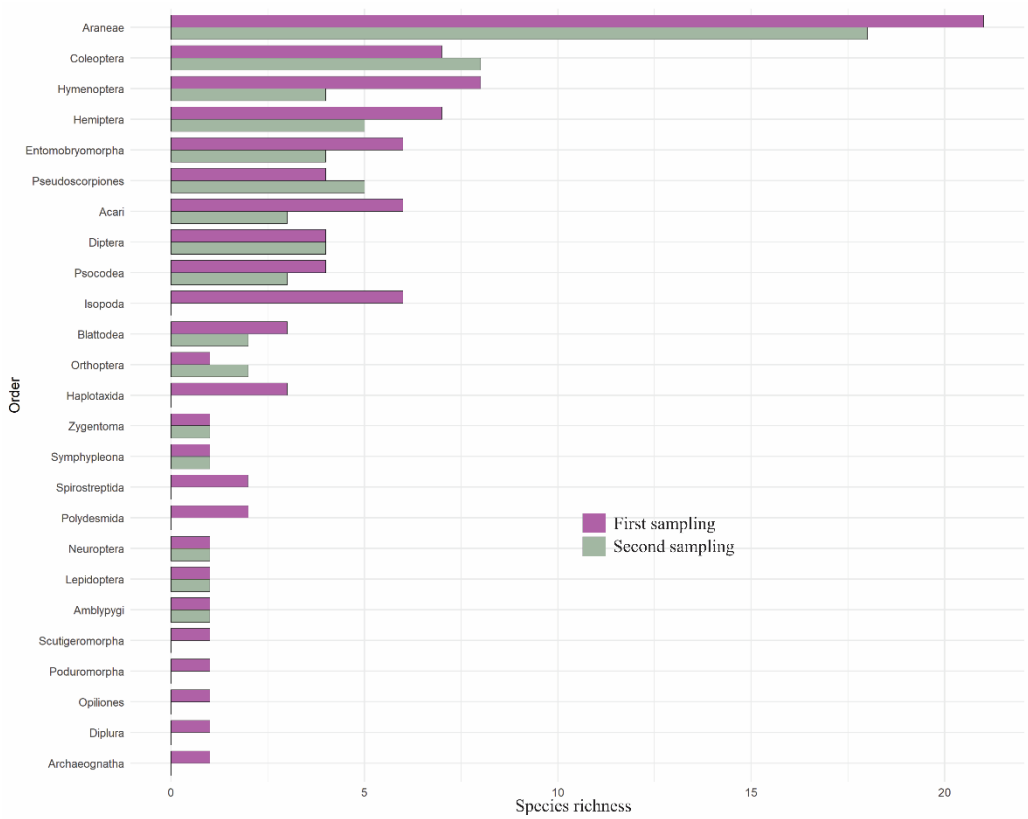


Figura 3: Riqueza total de espécies por ordem amostrada nas 7 cavernas estudadas, separada de acordo com os eventos de amostragem.

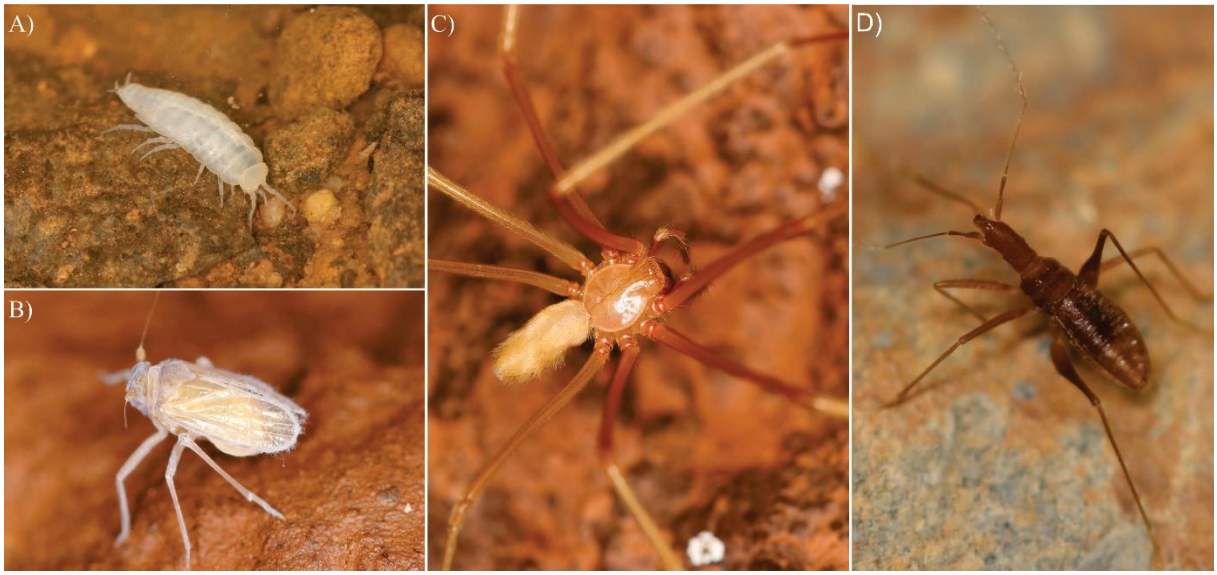


Figura 4. Algumas das espécies troglóbias amostradas durante os dois eventos amostrais em Iuií, Ba. (A) Styloniscidae sp. (Isopoda) da Lapa do Honorato; (B) *Iuiuia caeca* (Hemiptera: Kinnaridae) encontrado na caverna Tapera D'água; (C) *Loxosceles troglobia* (Araneae: Sicaridae) espécie amostrada durante ambas as coletas, na Tapera D'água; e, (D) *Spelaeometra* sp. (Hemiptera: Hydrometridae), amostrada na caverna Toca Fria. Fotos: Rodrigo Lopes Ferreira.

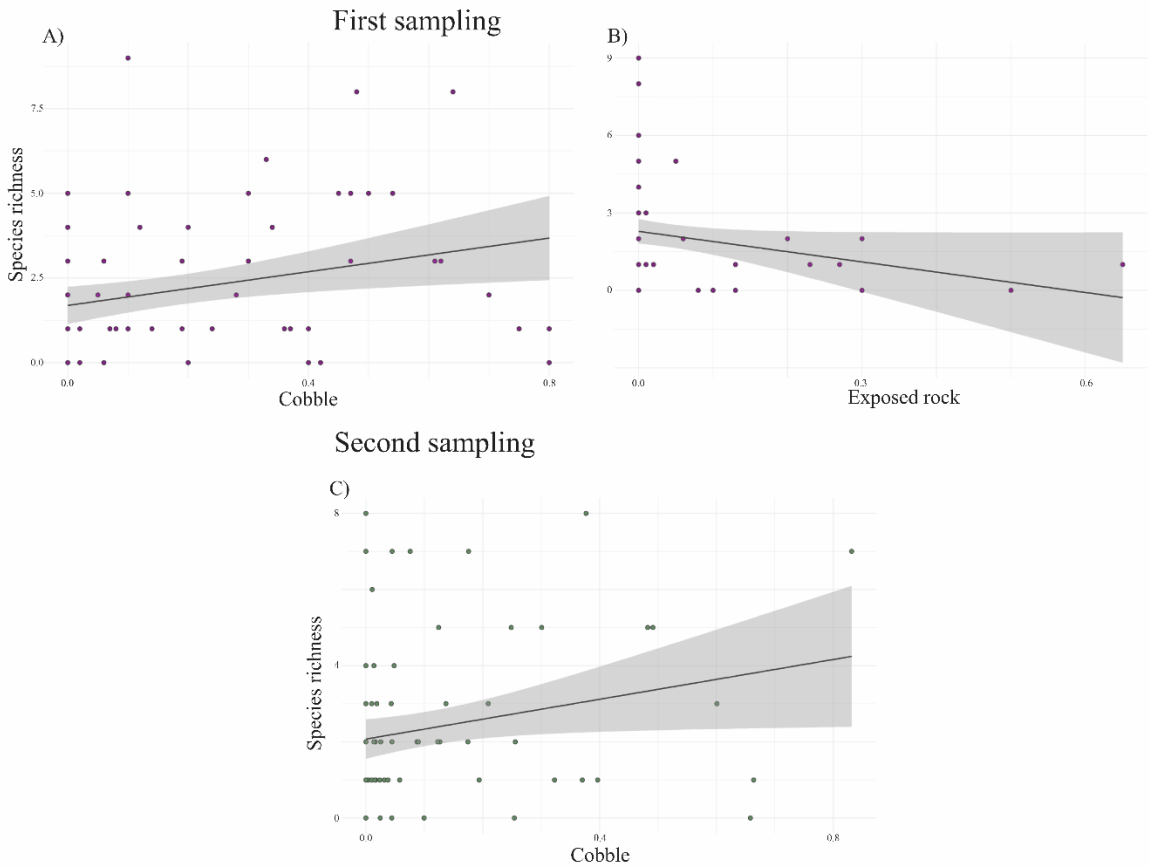


Figura 5. Relação encontrada entre a riqueza de invertebrados e as variáveis selecionadas pelo melhor modelo, para cada evento de amostragem. (A) Efeito positivo da porcentagem de bloco sobre a riqueza de espécies amostradas ao longo do primeiro evento; (B) Efeito negativo da porcentagem de rocha nua sobre a riqueza de espécies amostradas durante o primeiro evento; (C) Relação positiva entre a porcentagem de bloco e a riqueza de espécies amostradas durante o segundo evento amostral.

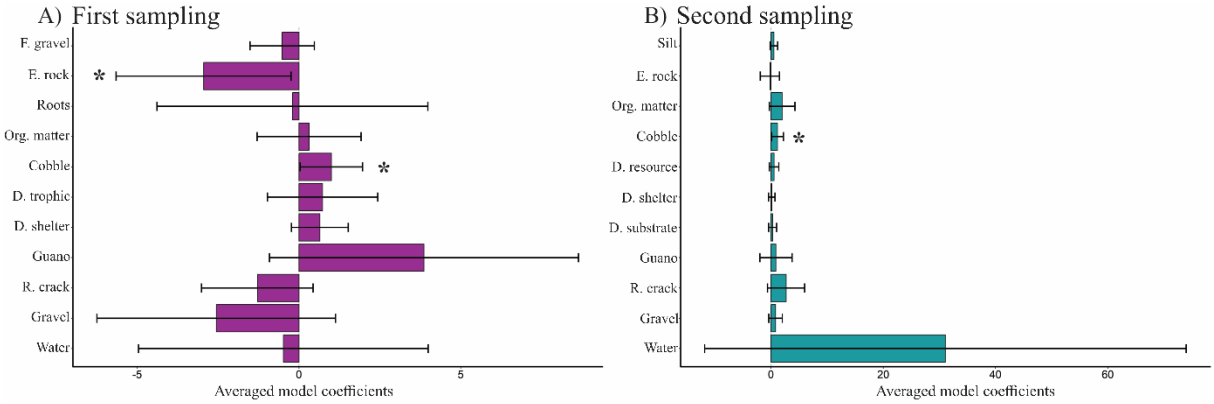


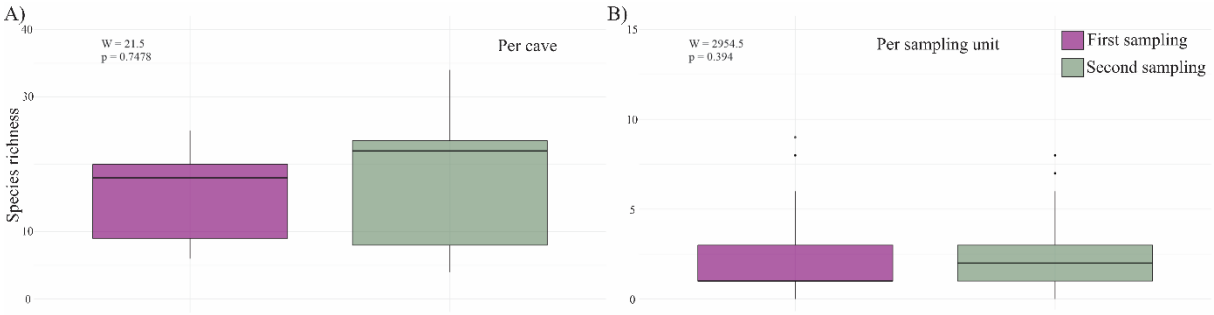
Figura 6: Média dos modelos selecionados com o recorte de ΔAICc < 4. (A) Média do modelo para a riqueza de espécies coletada no primeiro evento amostral; (B) média do modelo para a riqueza de espécies coletada no segundo evento amostral. Variáveis inclusas nos modelos: (sed) sedimento, (silt) silte, rocha, raiz, (matorg) matéria orgânica, (cobble) bloco, (htrof) diversidade de recursos, (habri) diversidade de abrigos, (h) diversidade de substratos, (guan) guano, (greta) greta de retração, (casc) cascalho e água. * Sinaliza as variáveis estatisticamente significativas, com $p < 0.05$.

Tabela 1. Cavernas de calcário amostradas na região de Iuiú e Malhada, Bahia. (Quad.) Número de quadrantes posicionados durante os levantamentos; (S1) riqueza total de invertebrados amostrados durante o primeiro evento de amostragem; (S2) riqueza total de invertebrados amostrados durante o segundo evento de amostragem; (D.L.) desenvolvimento linear estimado, em metros.

Caverna	Latitude	Longitude	Quad.	S^1	S^2	D.L.
Urubu-Jatobá	-14.548723	-43.539471	30	18	34	4600
Toca Fria	-14.548017	-43.535831	20	25	22	2500
Sepultamento	-14.655515	-43.544522	10	18	24	400
Toca Valada	-14.491043	-43.652444	5	8	8	700
Tapera D'água	-14.51727	-43.682842	5	22	4	150
Toca Baixão	-14.435169	-43.623675	5	6	8	150
Lapa do Honorato	-14.462879	-43.592667	5	10	23	30

Tabela 4: Resultado dos modelos lineares generalizados mistos selecionados a partir do menor valor de AIC. (A) modelo selecionado para os dados obtidos durante a primeira amostragem (2016); (B) modelo selecionado para os dados obtidos durante a segunda amostragem (2021), com os respectivos valores de AIC e R^2 condicional mostrados na frente. Nível de significância de $\alpha = 0.05$.

Preditora	**Estimate**	**Erro padrão**	**Z**	**p**
a) *Primeiro evento amostral (AIC = 304.5, cR^2 = 0.494)*				
Guano	3.8795	2.2670	1.711	0.08702
Bloco	1.1374	0.4066	2.798	0.00515**
Rocha	-2.9132	1.3782	-2.114	0.03454*
b) *Segundo evento amostral (AIC = 315.6, cR^2 = 0.42)*				
Bloco	1.0279	0.4842	2.123	0.0338*
Matéria orgânica	1.89094	1.1448	1.581	0.1140



S1. Boxplot exibindo a distribuição dos valores de riqueza de invertebrados entre os eventos amostrais, apresentando valores do teste de Mann-Whitney (W) e as probabilidades (p). (A) Diferença da riqueza de invertebrados entre cavernas; (B) diferença da riqueza de invertebrados por quadrantes.

EXPLORING THE CONNECTIONS

AMONG CAVE INVERTEBRATE COMMUNITIES

Landscape components determining cave invertebrate similarity patterns among karst units of southwestern Bahia state, Brazil

Lais Furtado Oliveira[1], Tássia Rayane Ferreira Chagas[1], Marconi Souza Silva[1] & Rodrigo Lopes Ferreira[1]*

[1]Centro de Estudos em Biologia Subterrânea, Departamento de Ecologia e Conservação, Instituto de Ciências Naturais, Universidade Federal de Lavras, Lavras, Minas Gerais, Brasil. Av. Dr. Sylvio Meniccucci, Caixa Postal 3037, CEP 37200-900.
*Corresponding author

INTRODUCTION

Karst regions encompass approximately 20% of the Earth's surface, making them one of the most diverse environments globally in terms of hydrology. They are intricately linked to biological and physical processes, as well as human history and development (Goldscheider et al., 2020). Karst aquifers contribute to 13% of the total global groundwater withdrawal (Stevanovic, 2019), with 16.5% of the world's population residing in karst areas (Goldscheider et al., 2020). Brazil, boasting the highest proportion of karst landscapes in South America, is home to numerous cave-restricted species within these areas (Souza-Silva & Ferreira, 2016; Ferreira et al., 2018; Bento et al., 2021). These environments offer various ecosystem functions and services owing to their diverse hydrological conditions, including the provision of potable water from aquifers for human consumption and agricultural irrigation (Bakalowicz, 2005). However, the exploitation of natural resources and human-induced alterations in karst regions have detrimental effects on the diversity of subterranean fauna, crucial components of groundwater-dependent ecosystems within karst landscapes (Niemiller et al., 2018; Mendes-Rabelo et al., 2018).

Subterranean environments host extraordinary life forms that have evolved to thrive under challenging conditions, including limited food resources and stable environmental parameters (Fišer et al., 2014; Culver et al., 2019). Moreover, these environments support diverse species crucial for maintaining groundwater quality (Griebler et al., 2014), making them essential for conservation efforts (Mammola et al., 2019). Despite their significance, subterranean habitats remain among the most unique, isolated, and least studied ecosystems on Earth, and the factors influencing the diversity patterns of subterranean fauna are still poorly understood. While the permeability and connectivity between subterranean and surface environments and responses to environmental conditions within ecoregions play key roles, other factors like land use in cave surroundings and karst hydrology are also critical considerations.

The dynamics of land use near caves can significantly affect subterranean diversity, as the aboveground areas serve as the primary source of organic resources crucial for sustaining these habitats. Conversion of forested areas to agricultural land can disrupt nutrient patterns and alter the availability of underground resources, thereby affecting the connectivity between different areas and ultimately influencing the distribution and diversity of cave-dwelling species. Besides land use, abiotic factors like precipitation play a pivotal role in determining cave fauna diversity, particularly in arid ecosystems where water resources are limited. Precipitation not only affects the amount of organic matter transported to underground systems but also influences the distribution and diversity of species. The hydrology of karst landscapes governs various ecological and evolutionary processes, including species dispersal and distribution, gene flow that facilitates colonization of subterranean environments, and the input of external resources. Consequently, karst hydrology can profoundly influence species distribution by acting as a mechanism for both dispersal and confinement of fauna.

Despite the theoretical and practical advancements in subterranean biology studies in recent decades, there remains a gap in the implementation of practices outlined by Brazilian environmental legislation, particularly regarding regulations governing studies on subterranean biology (MMA, 2017). While there are legal requirements for local and regional analyses to consider the "spatial continuity" of geomorphological units or the "physiographic homogeneity" of speleological units (MMA, 2017), these may prove inadequate in defining areas of influence given our understanding of patterns of subterranean fauna diversity. This is especially true when considering the significance of karst relief hydrology and landscape metrics as determining factors for the isolation or connectivity of communities.

From this perspective, this study aims to: *i)* assess landscape variables affecting the richness and composition of cave invertebrates in three regions of southwestern Bahia state, and *ii)* explore the similarity between these areas based on regional variables. As hypotheses, we anticipate that richness will be positively influenced by variables associated with precipitation, considering its role as an indirect measure of productivity supporting greater species diversity, especially in dryland ecosystems. Additionally, we expect composition to be influenced by the distance between caves and variables related to land use. We also anticipate differences in similarity between regions, potentially attributed to the São Francisco River's role as a dispersal barrier, with caves in the Iuiú region showing lower similarity compared to those in Santana and Ramalho.

METHODOLOGY

Study area and sampling design

Invertebrate sampling was conducted in 79 caves situated in southwestern Bahia across three distinct regions: Serra de Iuiú, Santana, and Serra do Ramalho (Figure 1). These areas are all within the Rio São Francisco basin and feature a variety of limestone outcrops formed by the Bambuí Group, dating back to the Neoproterozoic (between 750 and 600 million years ago).

The caves in the Serra de Iuiú region are distributed across four non-contiguous carbonate massifs named "Serra de Iuiú," "Morro do Aurélio," "Serrinha," and "Sepultamento." This region is situated on the right bank of the São Francisco River and has an altitude of approximately 794 meters above sea level. It falls within the Atlantic dry forest ecoregion (https://ecoregions.appspot.com/). According to the Köppen-Geiger climate classification system (Alvares et al., 2013), the area experiences a hot semi-arid tropical climate (Bsh), with an average temperature of 24°C and an average annual precipitation of 788 mm (Fick & Hijmans, 2017). Sampling took place in 31 caves located in the municipalities of Iuiú and Malhada during two field expeditions in October 2021 and July 2022.

The karst formations in the Serra do Ramalho region boast significant cave systems, some spanning several kilometers, thereby hosting a rich diversity of subterranean life. Situated within the Caatinga biome, the area experiences a tropical dry climate classified as "Aw" according to the Köppen system (Alvares et al., 2013). Our study was conducted across 26 caves located in the municipalities of Carinhanha, Coribe, and Serra do Ramalho, Bahia, Brazil. Sampling occurred in September 2021 and August 2022. It is worth noting that this region is designated as a priority area for the conservation of Brazil's speleological heritage, as indicated by the map published by the National Center for Cave Research and Conservation (CECAV).

The Santana region lies within a transition zone between Dry Seasonal Forests and the Caatinga, classified as Aw according to Köppen (1936), characterized by dry winters and rainy summers. It exhibits a high potential for endemic species (Dinerstein, 2017), with caves situated amidst the Cerrado and Brazilian Atlantic dry ecoregion forests. This area's remarkable potential can be attributed to numerous paleoclimatic changes resulting from the expansions and contractions of Amazonian and Atlantic rainforests (Sobral-Souza et al., 2015). Positioned on the boundaries of the Corrente River basin and its tributaries, crucial to the São Francisco River, the region presents significant ecological importance. Due to safety concerns, sampling was exclusively conducted during the dry season, as some caves feature subterranean drainages with extensive catchment basins, rendering the rainy season perilous for cave exploration. Sampling campaigns occurred between August 23 and September 2, 2021, and May 23 and June 2, 2022, in the municipalities of Santana, Santa Maria da Vitória, and Canápolis, Bahia, Brazil.

The geographic coordinates and altitude of the caves were determined near their main entrances using a GPS device. Sampling of both biotic and abiotic data was conducted on the cave floor. The sampling methodology entailed dividing the cave floor into discrete sectors, each spanning 10x3 meters. Within each sector, three 1m² quadrants were established: two positioned at the ends and one centrally located. The allocation of sectors and quadrants within each cave varied based on the cave's size and dimensions (refer to Table 1). Invertebrates collected across sectors and quadrants were aggregated, with caves serving as the primary sampling units.

Invertebrate sampling and identification

The survey of invertebrates was conducted through active visual search and manual collection techniques, as outlined by Wyanne et al. (2019), employing tweezers and brushes. Collected specimens were preserved in 70% ethanol. Subsequently, they were identified to the lowest taxonomic level possible at the laboratory using identification keys and classified into morphotypes following the methodology described by Oliver and Beattie (1996). Identification of potentially troglobitic species involved evaluating the presence of troglomorphic traits, such as reduced or absent eyes, depigmentation, and elongated appendages, following Christiansen's criteria (1962). Specimens were deposited in the Collection of Subterranean Invertebrates of Lavras (ISLA) at the Federal University of Lavras, Brazil.

Environmental variables

We gathered environmental data, including altitude, ecoregion, distance between caves, bioclimatic data, and land cover occupation in the vicinity of the caves. These data were acquired by overlaying the geographical coordinates of the cave entrances onto georeferenced values available in 'raster' or 'shapefile' files on digital platforms. Altitude information was retrieved using Google Earth Pro© software (Google LLC 2019). Ecoregion data was sourced from the map proposed by Olson and collaborators (2001). Climate data were obtained from the WorldClim version 2 database (Fick and Hijmans 2017).

At each sampling point, we settled buffers with a radius of 200 meters. Landscape variables were measured within these buffers to assess whether landscape metrics affect species richness (i.e., which landscape metric better explains the variation in the observed data). We collected land use classes and their percentage on the buffer using 30mx30m resolution satellite imagery available at a multi-disciplinary network called MapBiomas (MapBiomas, 2022). These images were processed using ArcGIS® software by Esri and landscape variables were measured using FRAGSTAT software (McGarigal et al., 2012).

Data analysis

Abundance and richness values were determined by counting individuals and morphospecies. Species categorized as 'uniques' and singletons, referring to those with either a single occurrence or occurrence in a solitary cave, were excluded from the

analysis due to their limited representation and occurrence within our datasets. The presence of these species in small numbers complicates drawing robust conclusions about their distribution and their influence on observed patterns. By excluding them, we focused on analyzing shared and more "common" species, which have a more significant impact on revealing similarity patterns and potential connections between the areas under investigation, while also reducing data dispersion.

Species richness at each site was estimated using rarefaction curves and extrapolation of Hill numbers to incidence data, following the procedures and functions outlined by Chao et al. (2014). For these analyses, we utilized the iNEXT package within the R software environment (Hsieh & Chao, 2016; R Development Core Team, 2016).

Influence of environmental variables on fauna richness and composition

We employed Generalized Linear Models (GLMs) to examine the impact of variables on species richness, considering the normality of the residuals of the response variables. To assess the effect of variables on species richness across different regions, we constructed models using all sampling units. These models utilized the negative binomial distribution, taking into account the dispersion of residuals through normal Q-Q plots and histograms (Crawley, 2007; Bates et al., 2014).

Following tests for normality, we conducted a Spearman correlation analysis using the 'chart.correlation' function from the PerformanceAnalytics package (Peterson and Carl, 2020). Variables with correlation coefficients exceeding 70% ($r\hat{} \geq 0.7$) were excluded from the models (Schober et al., 2018). Pseudo-adjusted R2 values were calculated, and the best models were selected using the 'r.squaredLR' and 'dredge' functions from the MuMIn package (Bartoń, 2022). GLM analyses were conducted using R software (R Core Team, 2022).

Subsequently, to explore the influence of variables on species composition, we performed linear model-based analyses using individual (marginal tests) and joint (sequential tests) distance-based redundancy analysis (DistLM). A similarity matrix based on the Bray-Curtis index, with abundance transformed into a square root, was employed (Clarke et al., 2014). All environmental variables were considered in the DistLM analysis, as the default mode already excludes correlated variables. We employed the Forward procedure and the Akaike Information Criterion corrected for small samples (AICc) for model selection, with models exhibiting smaller AICc values deemed preferable, after 999 permutations (Anderson et al., 2008).

We investigated similarity in community composition between regions and watersheds using the Bray-Curtis Index and Analysis of Similarity (ANOSIM), which uses a dissimilarity matrix to evaluate how dissimilar the groups are (values close to "1.0" suggests dissimilarity between groups while values close to "0" suggests an even distribution within and between groups). Abundance values were square root transformed (Clarke et al. 2014). Non-metric multidimensional scaling (MDS) was performed to visualize the dispersion of caves between regions and drainage basins and

was also associated with the similarity profile test (SIMPROF) (Clark et al. 2014) (http://www.primer-e.com).

Hierarchical agglomerative clustering (CLUSTER) was employed to illustrate the formation of groups based on fauna similarity, considering: I) Regions, II) Caves with perennial or intermittent rivers, III) Massifs, and also associating with IV) Similarity profiles to identify species that tend to co-occur in samples and group samples with similar taxonomic compositions. These analyses were conducted using Primer 7 software with the Permanova expansion.

RESULTS

Examining each of the three areas separately, the Iuiú region emerged with the highest species richness, boasting 449 species, followed by the Serra do Ramalho region with 416 species, and finally, the Santana region with 338 species. It is worth noting that both the number and extent of caves varied across these regions. The comparison of species across the three regions revealed an overlap in some species, totaling 596 species. The richest orders were Araneae, Coleoptera, Diptera, and Acari. After removing the uniques and singletons, the richest region was Serra do Ramalho with 143 species, followed by Iuiú with 134, and Santana with 80 species.

The species richness accumulation curves have reached a level of sample sufficiency across all three areas (Figure 2). Notably, the graph illustrates distinct species richness among the locations, evident from the non-overlapping confidence intervals. Additionally, alongside the rarefaction curves (solid lines), the graph includes extrapolation lines (dashed lines), offering estimations of potential species numbers with increased collection efforts.

Regarding the influence of variables on species richness, 17 models were selected (delta AICc < 2) (Table 1, Figures 3 and 4). The overall model demonstrated an explanatory power of $R^2 = 0.33$. The most influential model highlighted a positive correlation between water availability in the surroundings and the annual temperature range (BIO7). The second-best model indicated a negative correlation with altitude and the seasonality of precipitation (BIO15) and precipitation levels during the driest quarter (BIO17) while showing positive correlations with water availability and precipitation during the wettest month (BIO13). Similarly, the third-best model illustrated a negative correlation with altitude, agriculture (agro), seasonality of precipitation (BIO15), and precipitation levels during the driest quarter (BIO17), coupled with positive correlations with water availability and precipitation during the wettest month (BIO13).

Furthermore, the DistLM analysis, through sequential tests, revealed significant determinants of cave fauna composition, including the distance between caves (DIST), the Atlantic Dry Forest ecoregion (ADF), and variables such as seasonality of temperature (BIO4) and annual precipitation (BIO12) (Table 2).

Through Multidimensional Scaling Analysis (MDS), spatial groupings for species composition data between the regions of Iuiú, Santana, and S. Ramalho were identified

(Figure 5A). These groupings were confirmed by Similarity Analysis (ANOSIM: Rglobal = 0.778; $p < 0.01$). Furthermore, the MDS revealed the formation of groups with different factors; for example, subdivision into subgroups based on composition was observed using SIMPROF (Rglobal = 0.779; $p < 0.01$) (Figure 5C). Additionally, clusters associated with factors such as drainage basins (Rglobal = 0.653; $p < 0.01$) (Figure 5B) and massifs (Rglobal = 0.69; $p \leq 0.01$) (Figure 5D) were identified, which are considered barriers to the dispersal of species, with all these results corroborated by the ANOSIM analysis.

In the Cluster analysis, we observed the formation of significantly different groups in terms of composition. Three main clusters were identified, corresponding to the different regions studied: Iuiú, Serra do Ramalho, and Santana. By associating the cluster with the SIMPROF test, we identified 21 statistically distinct sample groups, with certain caves, notably Buraco da Aroeira, Tapera d'água, and Mandiaçu, showing a 100% dissimilarity compared to the other groups. These findings were also evident concerning the fauna similarity between the massifs (Figure 6).

DISCUSSION

This study provides valuable insights into the diverse array of variables shaping the richness and composition of species inhabiting caves across the Iuiú, Santana, and Serra do Ramalho regions. Despite Serra do Ramalho exhibiting the highest absolute regional species richness across all caves, it was Iuiú that boasted the highest local richness, calculated as the average richness per cave. This disparity arises from the extensive caves found in Ramalho, contributing to its elevated regional richness, while Iuiú, characterized by its topographic heterogeneity, hosts caves in better-preserved conditions, fostering greater species turnover.

The prominence of caves in the Iuiú region underscores their pivotal role in harboring a species richness, highlighting concerns regarding potential species loss due to cave suppression or improper land use in surrounding areas. Moreover, our findings underscore the positive influence of landscape factors, such as the presence of water bodies and forest cover, on species richness in these regions. This suggests that landscape features play a crucial role in determining the distribution of cave-dwelling species within the study area.

Surface variables, including temperature and precipitation, emerged as key determinants shaping community structure, alongside specific cave attributes such as inter-cave distance and altitude. These findings shed light on the intricate interplay between environmental factors and cave characteristics in shaping the biodiversity patterns observed in these regions.

Richness patterns

The findings from this study support the hypothesis that precipitation significantly influences species richness. Variables associated with higher precipitation rates and water availability positively affect richness, whereas those linked to low precipitation have a negative effect. Precipitation variables often serve as indicators of

surface productivity (Weiss et al., 2001), a factor directly correlated with food availability in caves, as noted by Souza Silva et al. (2011) and Venarsky et al. (2017). This relationship primarily involves increased availability of organic resources originating from the surface and transported to the subsurface through various pathways (Gers 1998, Poulson and Lavoie 2000; see Table 3). Consequently, a hypothesis emerges that higher surface productivity correlates with richer underground communities due to the greater availability of resources, a trend observed in our study and previous research (Culver et al., 2006; Eme et al., 2015).

Moreover, productivity is recognized as a key driver of species richness in surface terrestrial ecosystems (Whittaker, Willis, & Field, 2001), a trend that extends to subterranean environments due to their interconnectedness through topography and hydrology (Culver et al., 2006; Bregović and Zagmajster, 2016).

Soil characteristics such as water storage capacity, permeability, thickness, and percentage of organic matter, allied to vegetation cover emerge as potential predictors for the distribution of subterranean species. Despite limited studies exploring how land use and land cover affect cave communities in tropical regions (Souza-Silva, Martins & Ferreira, 2015; Pellegrini, Sales, Aguiar & Ferreira, 2016; Jaffé et al., 2018; Cardoso, Ferreira & Souza-Silva, 2021), our findings demonstrate that variables related to land use, such as water and forest cover, positively influence richness.

Water serves as a primary carrier of organic matter to subterranean environments, augmenting available resources and thereby supporting a greater diversity of species, consequently enhancing richness. Forested areas, known for their abundant organic matter, play a crucial role in this regard. As previously mentioned, epigean and hypogean environments are intricately connected, meaning that the greater availability of organic resources on the surface extends to caves and other subterranean habitats. The presence of forests significantly contributes to the richness of subterranean species by offering shelter, food, and favorable conditions for their survival and persistence.

On the other hand, the variable "agro," representing regions converted to agricultural land uses, exerts a negative influence on species richness. Across many karst regions globally, including Brazil, deforestation for agricultural purposes poses a significant threat to fauna (Souza-Silva et al., 2015; Jaffé et al., 2018; Canedoli et al., 2022). Degradation of cave surroundings can lead to erosive processes, exposing soil and allowing sediments to accumulate in watercourses (Cardoso et al. 2022). These sediments may also infiltrate cavities, homogenizing the environment and affecting microhabitats, thereby reducing available shelters and diminishing the number of species dependent on this resource.

Moreover, deforestation for agricultural systems significantly diminishes the availability of trophic resources in the external environment, consequently affecting the cave ecosystem. The repercussions from external areas also extend to the climate near cave entrances. Preserved external environments play a crucial role in maintaining the

stability of underground microclimatic conditions, influencing airflow patterns and temperatures.

Our findings indicate that temperature seasonality also positively influences species richness. Underground temperatures generally mirror the average annual surface temperature (Badino, 2010), with subterranean habitats relying on surface ecosystems for organic matter and colonization (Schneider et al., 2011; Souza-Silva et al., 2011; Culver and Pipan, 2019; Cardoso et al., 2022). Changes in external temperature can adversely affect fauna, particularly species associated with subterranean environments, which demonstrate sensitivity to environmental fluctuations.

Preserved environments have the capacity to retain water, and alterations in temperature can adversely affect fauna. Studies, such as that conducted by Jaffe et al. (2018), have identified detrimental effects on terrestrial troglobitic communities in ferruginous caves in Brazil due to agricultural activities nearby. Additionally, research like that of Pellegrini et al. (2016) underscores the importance of preserving external environments at various distances (between 50 and 250 meters), as they positively influence subterranean cavity characteristics. Understanding these impacts is pivotal for formulating effective conservation strategies aimed at maintaining biodiversity and the integrity of subterranean ecosystems amidst mounting pressures from agricultural expansion.

Among the landscape factors, altitude also negatively influenced species richness. Just as in surface environments, caves situated at higher altitudes contend with more severe conditions compared to those at lower elevations (Souza-Silva et al., 2020). Typically, caves at higher altitudes experience greater environmental challenges such as fluctuations in sunlight exposure, temperature, humidity, and winds, which can negatively affect species richness (Souza-Silva et al., 2020).

Composition patterns

Our results partially support the hypothesis that composition is influenced by the distance between caves, as well as variables related to eco-region, seasonality, and precipitation. Surprisingly, we did not observe any significant influence of variables associated with land use on the variation in species composition. These findings underscore the complexity of the subterranean environment and the importance of considering various factors when investigating composition dynamics in caves. The distance between caves can affect dispersal and, consequently, the colonization of invertebrate species, as closer caves tend to have greater species exchange, resulting in a more similar fauna composition. Conversely, distant caves may exhibit a more distinct fauna composition due to the geographical isolation of different dispersal routes. Jaffe et al. (2018) emphasized that geographical distance plays a crucial role as the primary determinant of similarity between communities in iron ore caves in the Amazon region.

Furthermore, a diverse range of geological and climatic factors have molded the landscape over millions of years, resulting in areas characterized by varied landscapes (Bramblett et al., 2012). These landscape disparities can create barriers that restrict the

dispersal of invertebrate species and shape the species pool in different regions. Furthermore, this assembly of species present on the surface, which represents potential colonizers of these environments, may influence the species composition within a cave (Mendes-Rabelo et al., 2021).

Another significant landscape feature influencing cave species composition is the eco-region. Although initially conceptualized based on surface communities (Olson et al., 2001), research has demonstrated their impact on the structure of cave species assemblages in both temperate and tropical regions (Niemiller & Zigler, 2013; Alvarenga et al., 2020). Therefore, eco-regions can also shape the composition of subterranean fauna, as factors directly linked to surface habitats can impact subterranean conditions, particularly on broader scales. As previously mentioned, many cave-dwelling species originate from surface environments, seeking food resources, shelter, and optimal conditions for growth within caves (Mendes-Rabelo et al., 2021). By revealing that caves represent only a fraction of the biodiversity found in surface ecosystems, variations in the composition patterns of subterranean communities can be significant, resulting in distinct faunal compositions. Such variations are influenced by various attributes of the external environment, including eco-regions, which possess a unique set of characteristics.

The composition was also affected by bioclimatic variables, such as temperature seasonality (BIO4) and annual precipitation (BIO12). These factors are recognized as climatic barriers that exert a pivotal role in species distribution and survival, representing significant limitations for their geographical range. Shifts in temperature and precipitation patterns can lead to substantial modifications in species distribution, directly impacting community composition.

Similarity patterns

In the present study, notable differences in community composition were observed among the surveyed regions. We noted that the cave fauna in Iuiú exhibited lower similarity compared to those in Serra do Ramalho and Santana, a contrast likely attributed to the significant geographical distance between these regions. As expected, the isolation imposed by the São Francisco River further accentuates this disparity. The impact of distance between caves proves pivotal in dispersal dynamics and consequently in the colonization patterns of invertebrate species. The proximity between caves tends to facilitate more pronounced species exchange, resulting in a more homogeneous faunal composition. This finding aligns with prior research where greater dissimilarity was observed among more distantly located caves, underscoring the limited dispersal capacity of organisms (Silva et al., 2017; Mammola et al., 2020).

Moreover, a multitude of biological, climatic, and physical barriers contribute to the environmental complexity of the landscape, some of which impede the dispersal of invertebrate species, thereby influencing species composition across different areas. These factors gain particular significance when assessed comprehensively (Mammola et al., 2020; Souza-Silva et al., 2020; Savie et al., 2022). Particularly noteworthy is the faunal

dissimilarity observed in Iuiú compared to the Santana and Ramalho regions. The presence of the São Francisco River between these areas can act as a dispersal barrier, as hydrological flows play a crucial role in impeding species movement, thereby contributing to the observed lower similarity.

Final remarks

Understanding the regional and local environmental factors influencing fauna is crucial for grasping the ecological processes that sustain and promote biodiversity conservation, particularly amidst significant anthropogenic environmental changes. Our findings highlight the detrimental impact of land use for agricultural activities on subterranean communities, leading to a reduction in species richness. Conversely, the preservation of water sources and conservation of forested areas emerge as indispensable elements for maintaining subterranean species richness and ensuring the vitality of these environments. Our research underscores the importance of a holistic understanding that considers both external landscapes and intricate subterranean processes as drivers of diversity patterns.

As demonstrated in this study, the presence of large water bodies between regions enhances biological dissimilarity to caves in each area, emphasizing the heightened significance of preserving these ecosystems in regions isolated by water bodies. Effective management of these ecosystems requires a multidimensional approach that goes beyond surface-level interventions, incorporating an understanding of processes occurring below the surface. Integrating such environmental management practices is essential to address contemporary challenges and safeguard the long-term health of these underground ecosystems.

ACKNOWLEDGMENTS

We express our sincere gratitude to the dedicated taxonomists who assisted with taxa identification (Cardoso G.M., Bernardi L., Prado G.C., Brescovit A., Bouzan R., Castro R., Vilelva M., Pellegrini T.G., Benjumea D., Medeiro G., de Souza P.G.C., Michelly N., Magalhães I.L.F., Vaz J., Vaz-de-Melo F. and Simone L.R.); the team from the Center of Studies in Subterranean Biology (CEBS/UFLA) for the support in the field trips; the citizens of Iuiú, Santana and Carinhanha who helped guide and accompany us while finding the cave sites; the Centro Nacional de Pesquisa e Conservação de Cavernas - CECAV and Instituto Brasileiro de Desenvolvimento e Sustentabilidade - IABS for the financial support (TCCE ICMBio/Vale 01/2018); CNPq (National Council for Scientific and Technological Development, grant n. 302925/2022-8) for the productivity scholarship provided to RLF.

REFERENCES

Bakalowicz, M. Karst groundwater: a challenge for new resources. Hydrogeology Journal, [s. l.], **13**(1):148–160, 2005.

Bento, M.D.; Souza-Silva, M.; Vasconcellos, A.C.; Bellini, B.C.; Prous, X.; Ferreira, R.L. Subterranean "oasis" in the Brazilian semiarid region: Neglected sources of biodiversity. Biodiversity Conservation, [s. l.], **30**:3837–3857, 2021.

Cardoso, R. C., Ferreira, R. L., & Souza-Silva, M. (2022). Multi-spatial analysis on cave ecosystems to predict the diversity of subterranean invertebrates. Basic and Applied Ecology, 65, 111-122.

Culver, D.C.; Pipan, T. The Biology of Caves and Other Subterranean Habitats; Oxford University Press: Oxford, UK, 2019.

Ferreira, R.L.; de Oliveira, M.P.A.; Souza-Silva, M. Subterranean biodiversity in ferruginous landscapes. In Cave Ecology; White, W.B., Culver, D.C., Eds.; Academic Press: Cambridge, MA, USA, 2018; pp. 435–447.

Fišer, C.; Pipan, T.; Culver, D.C. 2014. The vertical extent of groundwater metazoans: An ecological and evolutionary perspective. BioScience **64**: 971–979.

Goldscheider, N.; Chen, Z.; Auler, A.S. et al. Global distribution of carbonate rocks and karst water resources. Hydrogeology Journal **28**:1661–1677, 2020.

Griebler, C.; Malard, F.; Lefébure, T. Current developments in groundwater ecology—from biodiversity to ecosystem function and services, Current Opinion in Biotechnology, **27**:159-167, 2014.

Mammola, S.; Cardoso, P.; Culver, D.C.; Deharveng, L.; Ferreira, R. L.; Fisˇer, C.; Galassi, D. M. P.; Griebler, C.; Halse, S.; Humphreys, W. F.; Isaia, M.; Malard, F.; Martinez, A.; Moldovan, O. T.; Niemiller, M. L. et al. Scientists'warning on the conservation of subterranean ecosystems. Bioscience, **69**:641–650, 2019.

Mendes-Rabelo, L.; Souza-Silva, M.; Ferreira, R.L. Priority caves for biodiversity conservation in a key karst area of Brazil: Comparing the applicability of cave conservation indices. Biodiversity Conservation, **27**:2097–2129, 2018.

MMA, Ministério do Meio Ambiente, Instrução Normativa N°2, Brasil: [s. n.], 2017. p. 1.

Nakagawa, S.; Schielzeth, H. A general and simple method for obtaining R^2 from Generalized Linear Mixed-effects Models. Methods in Ecology and Evolution **4**:133-142, 2013.

Niemiller, M.L.; Taylor, S.J.; Bichuette, M.E. Conservation of cave fauna, with an emphasis on Europe and the Americas. In Cave Ecology; White, W.B., Culver, D.C., Eds.; Academic Press: Cambridge, MA, USA, 451– 478, 2018.

Stevanovic, Z. Karst waters in potable water supply: a global scale overview. Environmenal Earth Sciences **78**(23):662, 2019.

Souza-Silva, M.; Ferreira, R.L. The first two hotspots of subterranean biodiversity in South American Subterranean Biology, **19**:1–21, 2016.

Weiss, E., Marsh, S. E., & Pfirman, E. S. (2001). Application of NOAA-AVHRR NDVI time-series data to assess changes in Saudi Arabia's rangelands. *International Journal of Remote Sensing*, *22*(6), 1005-1027.

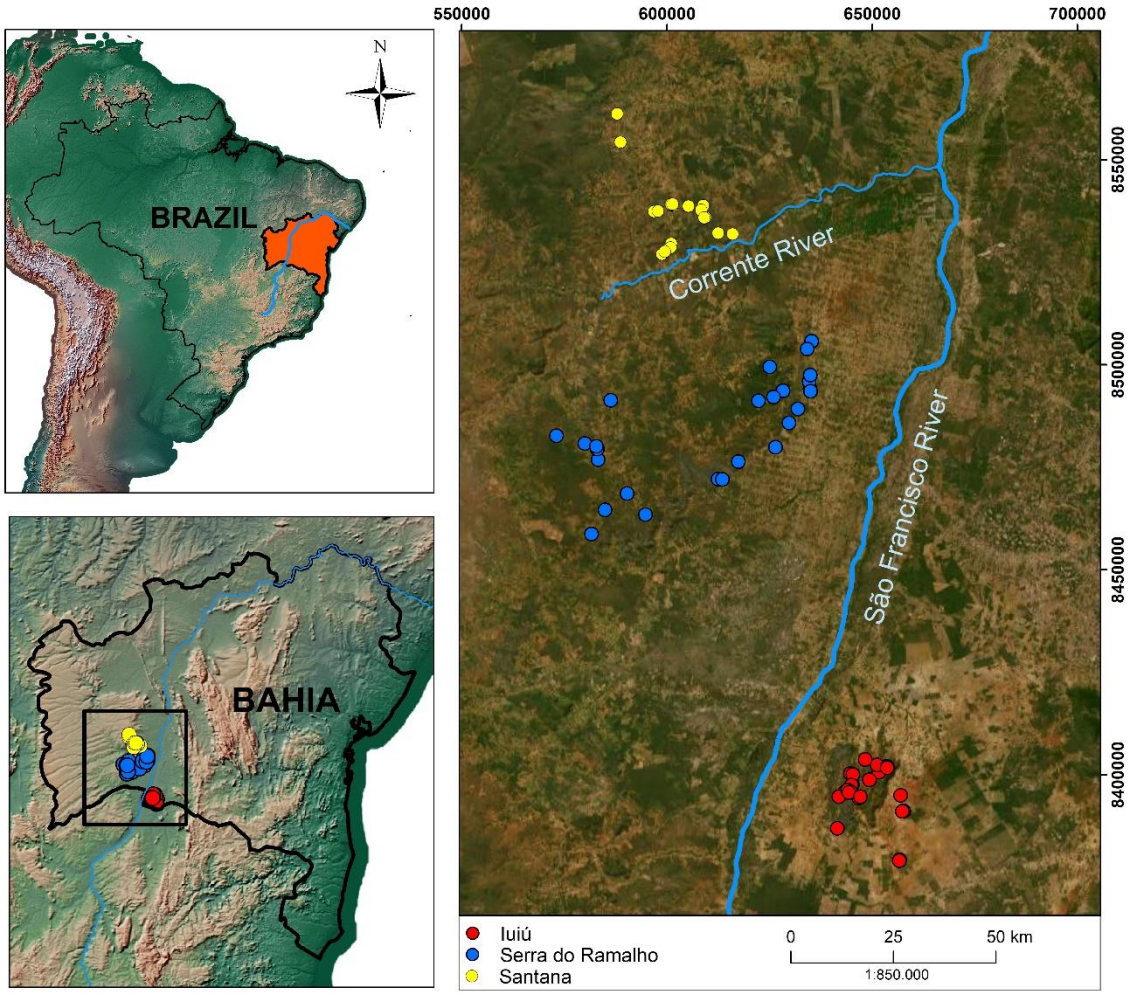


Figure 1: Study area including the three regions sampled. A) Priority conservation areas for the conservation of the Brazilian Speleological Heritage (CECAV), highlighting the sampled areas; B) Regions of Santana (1), Serra do Ramalho (2) and Serra de Iuiú (3), state of Bahia.

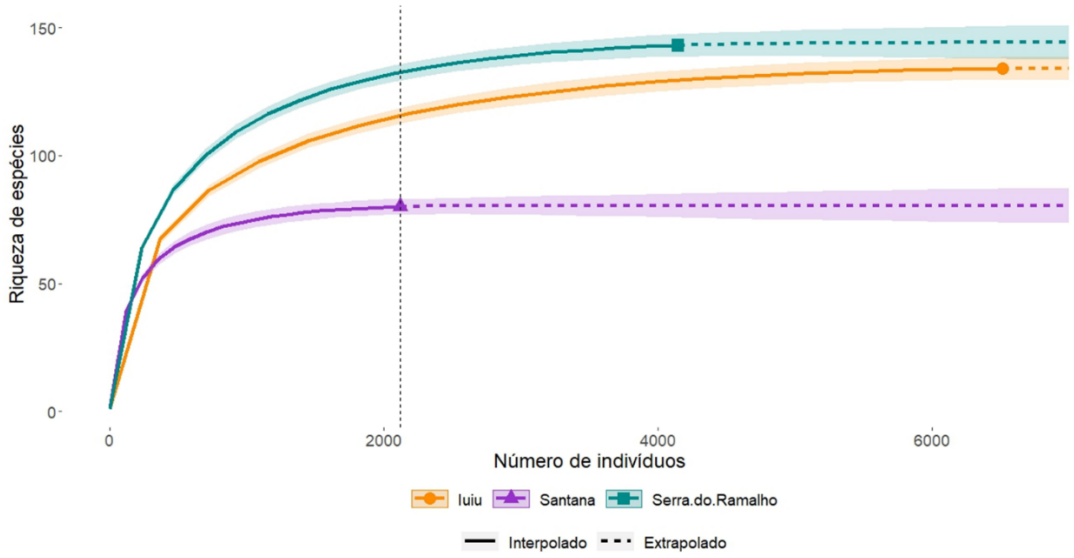


Figure 2: Rarefaction curves (solid lines) based on individuals and extrapolation (dashed lines) with 95% confidence intervals. Reference samples are indicated by colored solid points.

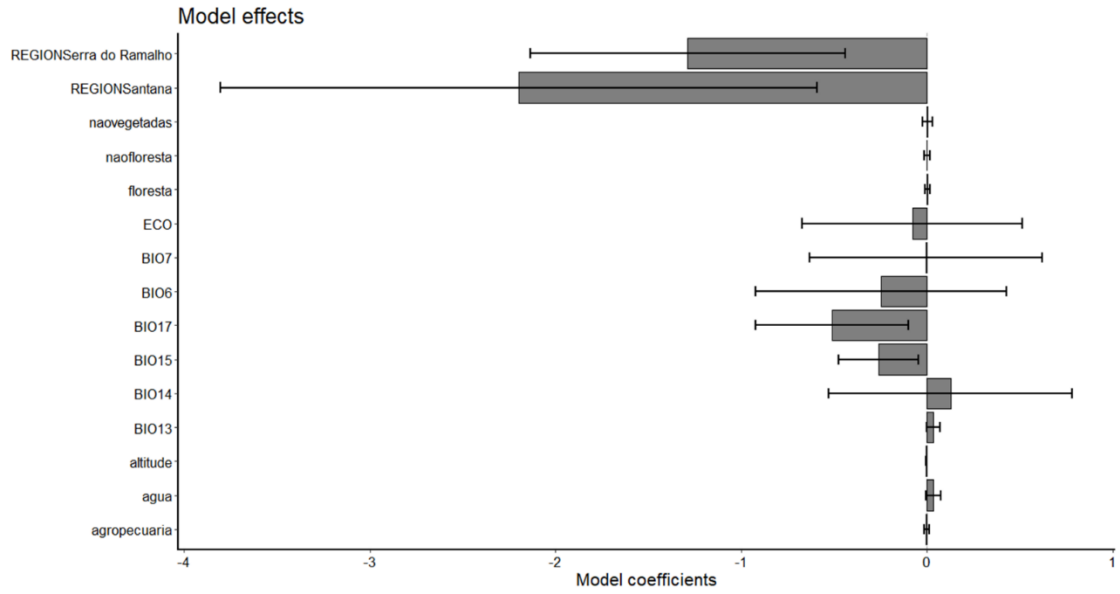


Figure 3: General Linear Models effects of the regions, land use, ecoregion and environmental variables on species richness. Ramalho and Santana regions effects on richness shown are obtained in comparison with Iuiú effect. Confidence interval = 0.95.

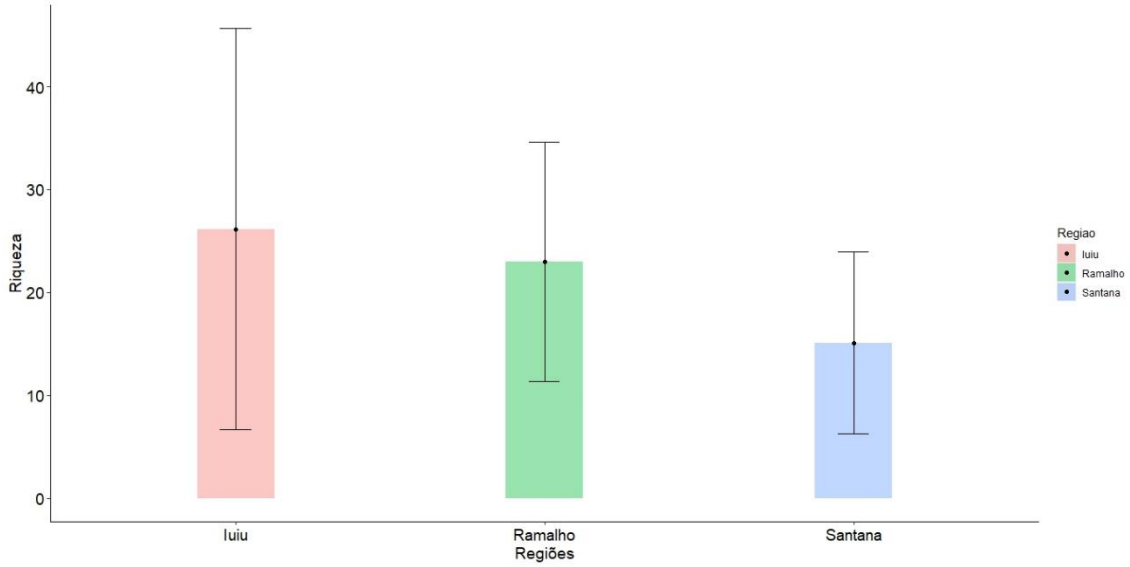


Figure 4. Effects and confidence interval of each studied region on the subterranean fauna richness.

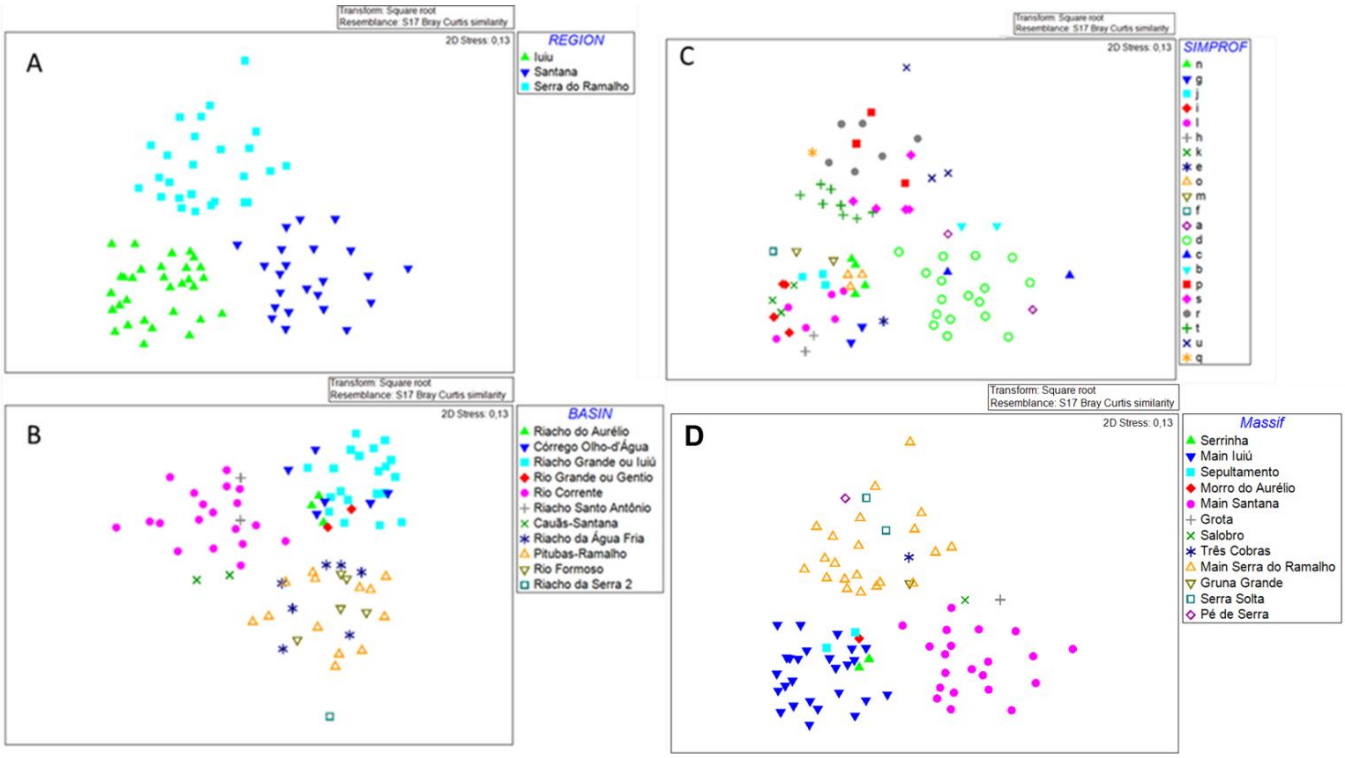


Figure 5: Multidimensional scaling of invertebrate samples, illustrating the similarity between a) different regions, b) different drainage basins, c) associated with SIMPROF and d) different massif.

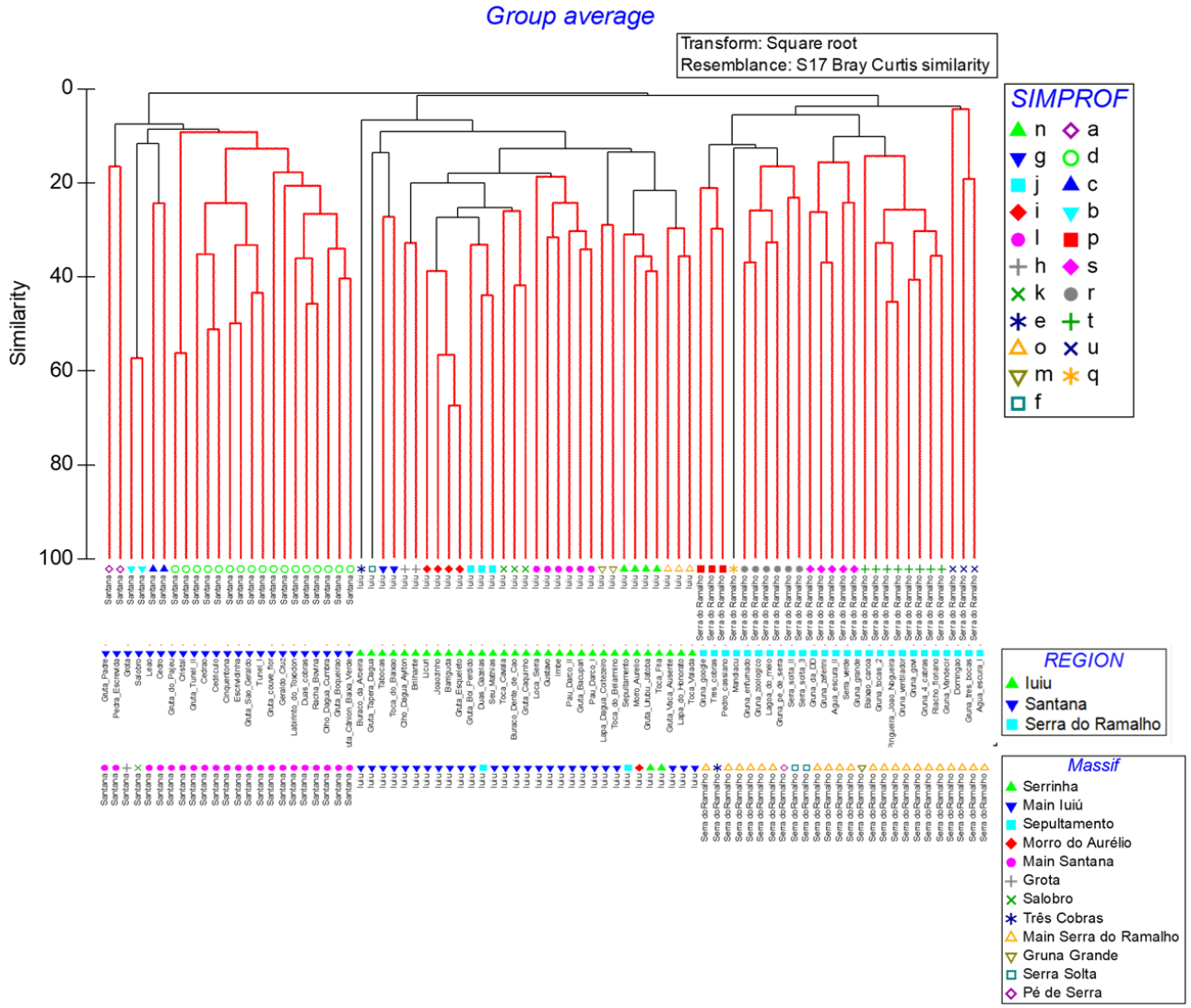


Figure 6: Cluster analysis (CLUSTER) highlighted the top three sets of samples based on their geographic regions. Combining this approach with the SIMPROF test, we identified 21 statistically different sample groups (represented by black lines), the caves, in particular Buraco da Aroeira, Tapera d'água and Mandiaçu, showed a 100% dissimilarity in relation to other groups. This result was also observed in relation to the similarity between the massif.

Table 1: Best Generalized Linear Models on the richness of the cave invertebrate community in Bahia, region: Santana, Ramalho, Iuiú; agro, water, forest, nforest, nonveg: land use classes at each sampling point; BIO13: Precipitation of the wettest month; BIO14: Precipitation of the driest month; BIO 15: Seasonality of Precipitation; BIO17: Precipitation from the driest quarter; BIO6: Minimum temperature of the coldest month; BIO7: Annual temperature range; ECO: ecoregions (Dry Atlantic Forest and Cerrado).

Modelo	região	altitude	agro	agua	floresta	nfloresta	naoveg	BIO13	BIO14	BIO15	BI
1	+	na	na	0.0410366	na	na	na	Na	na	na	
2	+	-1,80E+03	na	0.0337306	na	na	na	3,68E+04	na	-2,44E+05	-4,2
3	+	-1,72E+03	-4,87E+03	0.0311321	na	na	na	3,72E+04	na	-2,64E+05	-4,9
4	+	na	na	0.0416036	na	na	na	Na	na	na	-1,0
5	+	-1,88E+03	na	0.0374058	4,02E+03	na	na	3,89E+04	na	-2,67E+05	-4,6
6	+	-1,84E+03	-5,41E+03	na	na	na	na	3,99E+04	na	-3,07E+05	-5,3
7	na	-3,65E+03	na	0.0529184	na	na	na	-1,11E+04	na	na	
8	+	na	-4,62E+03	0.0404945	na	na	na	Na	na	na	-1,5
9	+	na	na	0.043925	na	na	na	Na	-2,10E+05	na	
10	+	na	-5,12E+03	0.033297	na	na	na	2,41E+04	na	-1,99E+05	-4,5
11	+	-3,10E+03	na	0.0490957	na	na	na	Na	na	na	
12	+	-1,94E+03	na	na	na	na	na	3,96E+04	na	-2,89E+05	-4,6
13	+	na	na	0.036035	na	na	na	2,33E+04	na	-1,77E+05	-3,8
14	na	-3,55E+03	-3,97E+03	0.0504732	na	na	na	-1,09E+04	na	na	
15	+	na	-2,30E+03	0.040333	na	na	na	Na	na	na	
17	+	na	na	0.0436489	2,16E+03	na	na	Na	na	na	

TAXONOMIA



Taxonomia

As expedições de campo possibilitaram o descobrimento de inúmeras espécies ainda não descritas pela ciência. Alguns desses invertebrados, como os isópodos, os grilos e os pseudoescorpiões, foram alvos de estudos taxonômicos vinculados a esse projeto. Cabe destacar, no entanto, que dezenas de novas espécies foram descobertas ao longo das amostragens, e suas respectivas descrições demandarão muitos anos de pesquisas. Nesta perspectiva, um especial destaque deve ser dado às espécies troglóbas. No total, foram descobertas **169 espécis troglóbias**, das quais somente uma pequena fração encontra-se formalmente descrita. Assim, é nítida a importância de projetos como este que, mesmo tendo como foco primordial responder à quetões ecológicas, abaca por revelar uma miríade de espécies novas, muitas das quais endêmicas e altamente ameaçadas. É importante destacar que talvez um dos mecanismos mais eficazes de conservação de cavernas no Brasil na atualidade é a descrição de espécies, em especial as troglóbias. Como boa parte destas espécies acaba se enquadrando em algum grau de ameaça segundo os critérios da IUCN, a descoberta e respectiva descrição destas espécies permite com que elas sejam avaliadas e passem a materializar a conservação das cavernas que representam seus habitats.

No total, 33 novas espécies foram descritas (incluindo algumas de outras regiões do Brasil, mas que foram incorporadas nos manuscritos). Destas, 22 novas espécies correspondem a isópodos dos gêneros *Chaimowiczia*, *Diploexochus*, *Pectenoniscus*, *Benthana*, *Benthanoides* e *Ctenorillo.* Seis novas espécies compreendem grilos do gênero *Endecous,* e cinco novas espécies compreendem pseudoescorpiões do gênero *Pseudochthonius.* É importante destacar que novas espécies de dois grupos originalmente não contemplados neste projeto (Diplopoda e Collembola) foram descritas a partir de exemplares coletados durante nossas campanhas de campo. Assim, optamos por também apresentar suas respectivas descrições neste relatório, já que elas decorrem das coletas realizadas durante este projeto.

Estas espécies, em conjunto, foram descritas em 10 manuscritos, nove dos quais já se encontram publicados em revistas internacionais. Destacamos novamente que o número de novas espécies encontrado no projeto é muito maior que somente estas aqui apresentadas. Muitas espécies descobertas em cada uma destas áreas abrangidas pelo projeto continuam a ser descritas, de modo que dezenas de novas espécies emergião nos próximos anos, fruto dos esforços empreendidos neste projeto. Assim, destacamos que investimentos em projetos desta natureza agregam um enorme valor ao patrimônio espeleológico nacional.

Nas sessões seguintes, apresentamos cada um dos trabalhos de descrição ralizados durante o projeto, na íntegra. Para aqueles já publicados, mantivemos a formatação original da revista onde foi publicado.

PSEUDOSCORPIONES



Zootaxa 5249 (1): 092–110
https://www.mapress.com/zt/
Copyright © 2023 Magnolia Press
ISSN 1175-5326 (print edition)
Article
ISSN 1175-5334 (online edition)
https://doi.org/10.11646/zootaxa.5249.1.5
http://zoobank.org/urn:lsid:zoobank.org:pub:FE36A1C1-8F8C-4B27-A35E-C4FCF35473FA

ZOOTAXA

Three new troglobitic species of *Pseudochthonius* Balzan, 1892 (Pseudoscorpiones, Chthoniidae) from northeastern Brazil

GUILHERME C. PRADO[1] & RODRIGO L. FERREIRA[1,2*]
[1]*Centro de Estudos em Biologia Subterrânea, Departamento de Ecologia e Conservação, Universidade Federal de Lavras, Lavras, MG. CEP 37200-900, Brazil.* *prado.gpc.99@gmail.com;* *https://orcid.org/0000-0001-9612-9906*
[2] *https://orcid.org/0000-0003-3288-4405*
[*]*Corresponding author.* *drops@ufla.br*

Abstract

Three new pseudoscorpion species, *Pseudochthonius pali* **sp. nov.**, *Pseudochthonius diamachi* **sp. nov.,** and *Pseudochthonius koinopoliteia* **sp. nov.,** are herein described from caves of Bahia state, Brazil. They can be distinguished from congeners mainly by the absence of eyes or eyespots, chelal and cheliceral dentition, coxal chaetotaxy and body size. Some ecological remarks on each species, possible threats, recommendations for future research and a key to the *Pseudochthonius* species from Brazil are provided.

Key words: Cave-dwelling, pseudoscorpion, taxonomy

Introduction

Pseudoscorpions (Arachnida: Pseudoscorpiones) are small predatory arthropods distributed throughout terrestrial habitats and commonly found across six continents (except for Antarctica). They occur in a diversity of habitats including leaf litter, beneath bark or stones, as well as bird nests or animal burrows. Several species are also known from caves and have subterranean-adapted traits (Chamberlin 1931; Harms 2018; Harvey 1988). Pseudoscorpions are quite diverse with 26 families (including an extinct one) and 473 extant genera (Harvey 2013; Benavides *et al.* 2019; World Pseudoscorpiones Catalog 2022).

Chthoniidae is the most specious pseudoscorpion family, with more than 800 species in 51 different genera, of which 11 genera are found in Brazil. This family has been recorded from nine Brazilian states, and the genus *Pseudochthonius* has been recorded from six states within four different regions. Apart from Brazil, this genus also occurs in Africa, Asia, Europe, Central America and other South American countries (World Pseudoscorpiones Catalog 2022; Assis *et al.* 2021; Schimonsky *et al.* 2022). *Pseudochthonius* is defined by the presence of plumose coxal spines on coxae I and II (Fig. 2F), the absence of intercoxal tubercle, and the sigmoid shape of the chelae (except for *Pseudochthonius orthodactylus* Muchmore, 1970) (Chamberlin 1929).

Considering the wide areas containing caves that remain unexplored in Brazil, there may be several species within this genus awaiting to be discovered. As an example, Brazil potentially has 300,000 caves (Auler 2019) from which only nearly 23,000 are officially registered, and an even smaller number have been sampled for fauna. Recent cave surveys in the Serra do Ramalho region (southwestern Bahia state) revealed three new species of *Pseudochthonius* that are described below. Additionally, we provide some notes on their habitat and potential threats, a brief discussion about their troglomorphisms, comparison and key to the Brazilian *Pseudochthonius* species.

Materials and methods

Study area

All the caves from which the new species come are located in a region known as “Serra do Ramalho”, situated

in southwestern Bahia state, northeastern Brazil. This region includes many subterranean river systems, which, in some cases, can reach tens of kilometers. Such systems have a dynamic hydrology, presenting high power of flow that results in substantial sedimentary movement in both surface and subterranean environments (Silva *et al.* 2019). The local climate is "Aw", according to Köppen's climate classification system, with dry winter and an average annual rainfall of 640 mm^3 (Alvares *et al.* 2013). The Serra do Ramalho region is inserted in the Caatinga domain (the only Brazilian semiarid biome), with transitional areas to the Cerrado (Brazilian Savanna) (Cole 1960). Detailed description of the habitats of each species will be provided further (see *Ecological remarks* for each species).

Field sampling

Fieldwork was carried out in October 2017, September 2021, and September 2022. Those trips stem from a project that aims to analyse the influence of habitat structure on the richness and composition of cave communities in Bahia. Throughout the Serra do Ramalho region, 26 caves were investigated as part of the project, using untimed direct intuitive searches (*sensu* Wynne *et al.* 2019) within several 10x3 m transects. The number of sampled transects was proportional to the size of the caves explored. Microhabitats and organic deposits were prioritized for general sampling carried out within the caves. All invertebrates were collected with a fine brush and stored in 70% ethanol.

Analysis and preparation

Specimens were examined using a Zeiss Axio Scope A1 optical microscope with software ZEN 2012 and a Leica M25 stereomicroscope along with Leica software Application Suite auto-handling. Illustrations of coxae and male genitalia were made with a drawing tube on a Olympus BX40 optical microscope equipped with phase contrast; kaiser's glycerol gelatine was used as a medium to stabilize those structures for observations and drawings. The paratypes were examined using a Hitachi TM4000 scanning electron microscope (SEM). Other structures and appendices were photographed using a Zeiss Axio Zoom V16 with its software ZEN 2.1. Images were vectorized using the Inkscape 1.1 software package (Montesanto 2015; inkscape.org). The holotype and paratypes are deposited in the Coleção de Invertebrados Subterrâneos de Lavras (ISLA).

Terminology

Terminology follows Chamberlin (1931), Harvey (1992), Judson (2007) and Zaragoza (2017). Abbreviations for the trichobothria: *b* = basal; *sb* = sub-basal; *st* = sub-terminal; *t* = terminal; *ib* = interior basal; *isb* = interior sub- basal; *ist* = interior sub-terminal; *it* = interior terminal; *eb* = exterior basal; *esb* = exterior sub-basal; *est* = exterior sub-terminal; *et* = exterior terminal. Abbreviations for the carapace: *al* = anterolateral setae of carapace; *ame* = anteromedial setae of carapace; *an* = anterior setae row of carapace; *il* = intermedian lateral setae of carapace; *in* = intermedian setae row of carapace; *me* = median setae row of carapace; *ml* = median lateral setae of carapace; *mm* = median medial setae of carapace; *oc* = ocular setae of carapace; *ol* = lateral oclar setae of carapace; *om* = medial ocular setae of carapace; *osl* = sublateral ocular setae of carapace; *pl* = posterolateral setae of carapace; *pm* = posteromedial setae of carapace; *po* = posterior setae row of carapace. Abbreviation for repository: ISLA.

Results

http://zoobank.org/urn:lsid:zoobank.org:act:600E59E5-EF18-4DAD-AEEE-B706E14D886A

Family Chthoniidae Daday, 1888 Genus

Pseudochthonius Balzan, 1892

Pseudochthonius diamachi sp. nov.

Material examined. ***Holotype*** female (ISLA 100994), preserved in ethanol: Brazil, Serra do Ramalho, Bahia, Gruna das Três Cobras Cave (13º37'6.63"S, 43º45'9.87"W), 15 September 2021, leg. R.L Ferreira. ***Paratype*** female (ISLA 100995), same data as holotype.

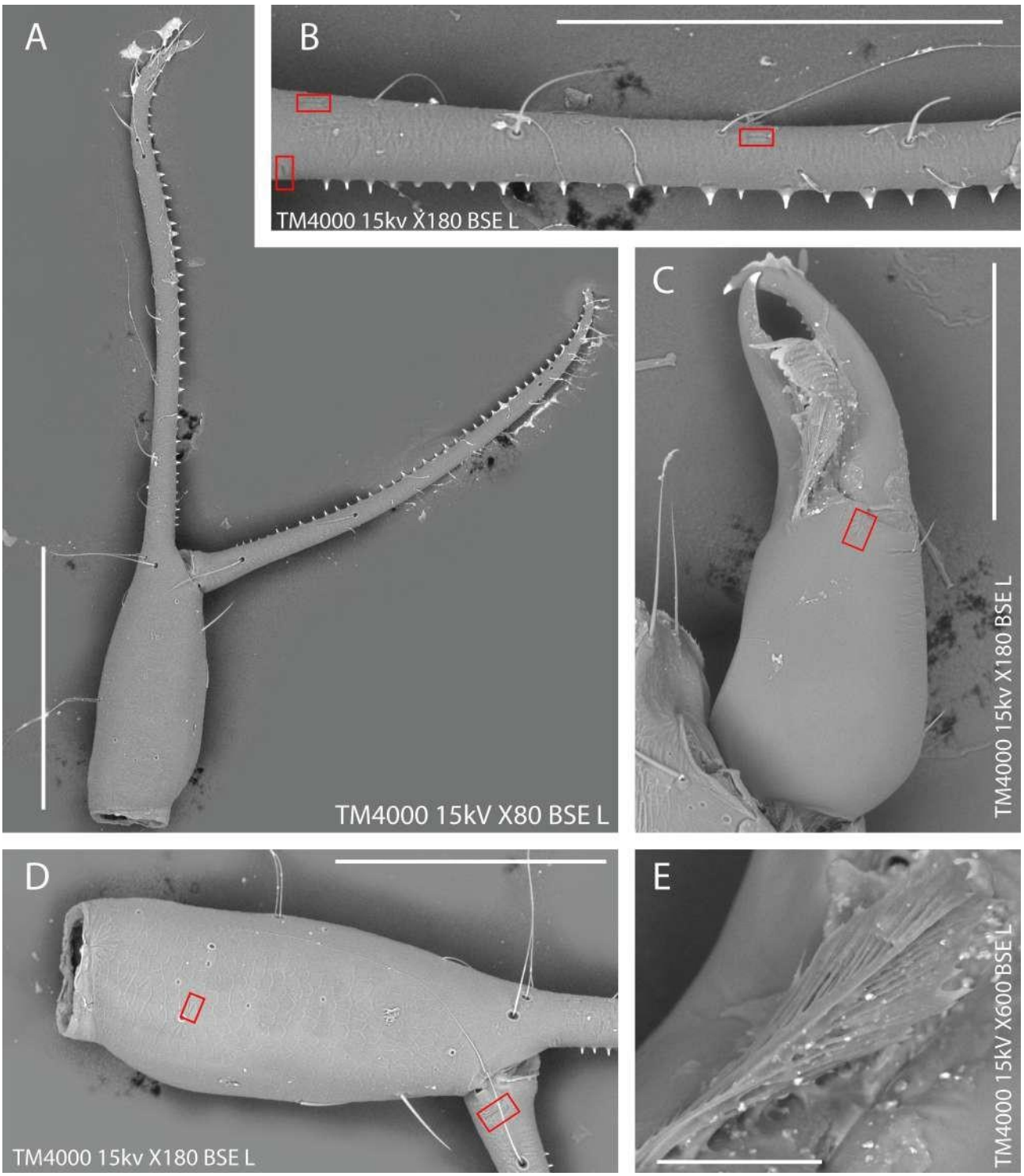


FIGURE 1. *Pseudochthonius diamachi* **sp. nov**. SEM images of the paratype **A** Right chela general aspect, antiaxial view **B** Basal region of chelal fixed finger **C** Left chelicera, showing rallum, exterior serrula and lyrifissure, ventral view. **D** Detail of the hand, showing lyrifussures and trichobothria arrangement **E** Rallum, showing detailed blades. Scale bars: 0.5 mm (**A**); 0.3 mm (**B–D**); 0.05 mm (**E**).

Etymology. Diamáchi ("διαμαχη") is a Greek word meaning "dispute". The epithet *diamachi* is an allusion to the unfortunate disputes over the region's caves and it intends to register our repudiation of any people or groups that consider themselves owners of Brazilian caves. This noun should be treated as noun in apposition.

Diagnosis. Differing from the other members of the genus by the following combination of characters: Absence of eyes or eyespots; carapace with a strong posterior constriction (confirmed by the difference between ocular width

and posterior width); *ist–est/ist–esb* trichobothria ratio of 1.02 (1.11); chelal fixed finger with 41 acute teeth with alternate heterodonty, chelal movable finger with 42 acute and well-defined teeth; movable and fixed finger of chelicera with poorly defined and constricted teeth, and with a small distal isolated tooth in both fingers; presence of two and four setae on the first and second tergite, respectively; trichobothrium *et* proximad to *dx* and distad to *it*; body length of 2.02 (2.33) mm; chela 7.7 to 7.8 times as long as broad.

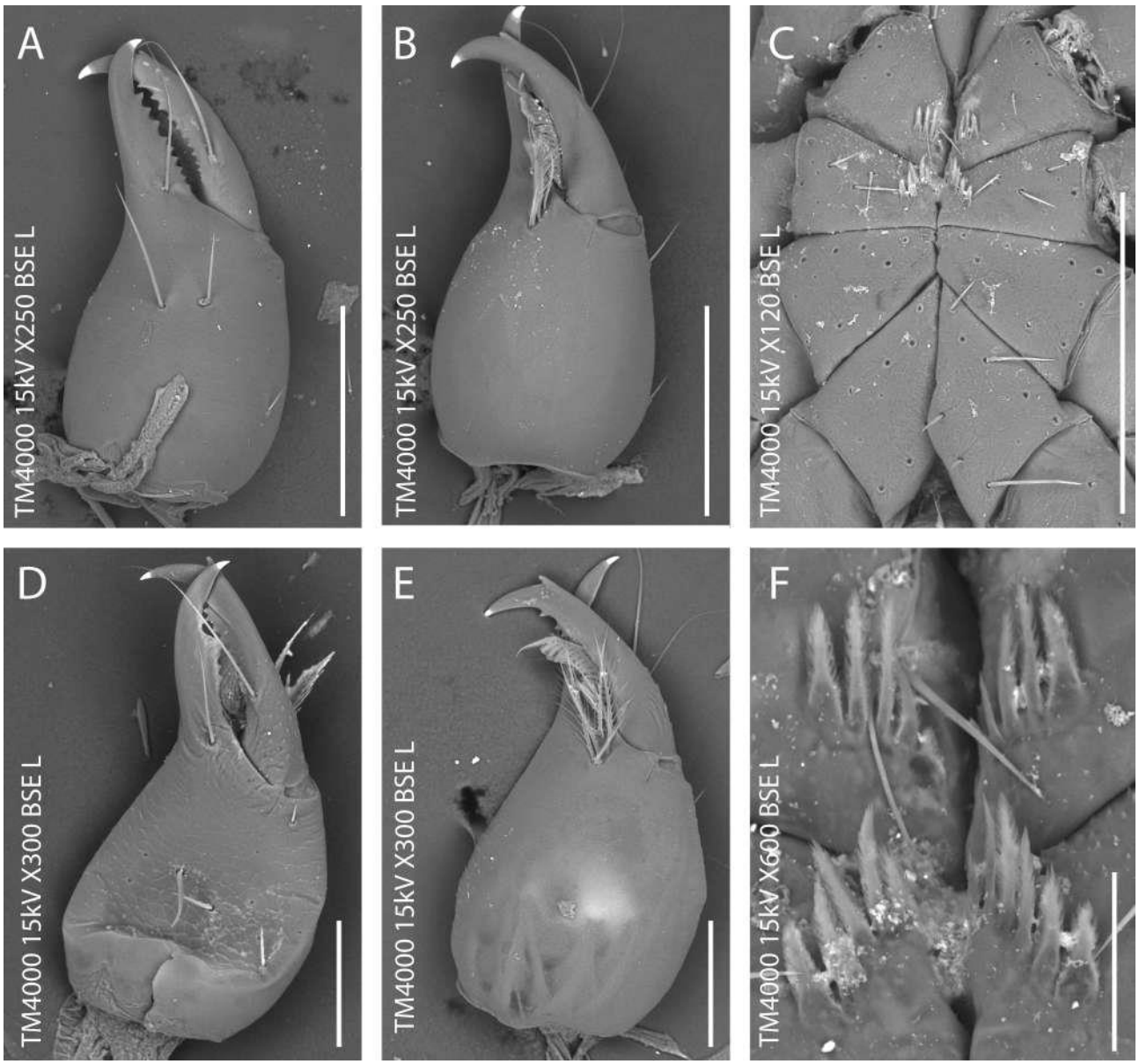


FIGURE 2. SEM images of the new species **A** *P. pali* **sp. nov.** right chelicera of the paratype, dorsal view **B** *P. pali* **sp. nov**. left chelicera of the paratype, ventral view **C** *P. diamachi* **sp. nov**. coxae region of the paratype **D** *P. koinopoliteia* **sp. nov**. right chelicera of the paratype, dorsal view **E** *P. koinopoliteia* **sp. nov**. left chelicera of the paratype, ventral view **F** *P. diamachi* **sp. nov**. detail of coxal spines of the paratype. Scale bars: 0.2 mm (**A–B**); 0.4 mm (**C**); 0.1 mm (**D–E**); 0.05 mm (**F**).

Description (Figs 4C–D, 11A). Body pale yellowish, very translucent; chelicerae slightly orange, abdomen beige. Some parts of the body scaly. Vestitural setae thin and anteriorly projected on prosoma and posteriorly projected on opisthosoma.

Carapace (Fig. 3E). 1.04 (1.07) times longer than broad, strongly constricted posteriorly showing a difference between ocular width and posterior width of 0.14 mm (Fig. 3E); anterior margin smooth (except for the epistome); no eyes or eyespots; epistome strongly dentate and serrated (ranging to seta *ame*); posterior margin of carapace smooth; chaetotaxy 4+2: 4: 4: 2: 2 (18).

Chelicera (Figs 1C, E, 3H). Hand with 5 setae; movable finger with 1 subdistal seta; galea present as a tubercle;

fixed finger with 9 constricted teeth, of which the distal one just isolated; movable finger with 10 constricted teeth, of which the distal one is isolated; rallum with 7 blades; serrula exterior and interior with 15 and 12 blades, respectively.

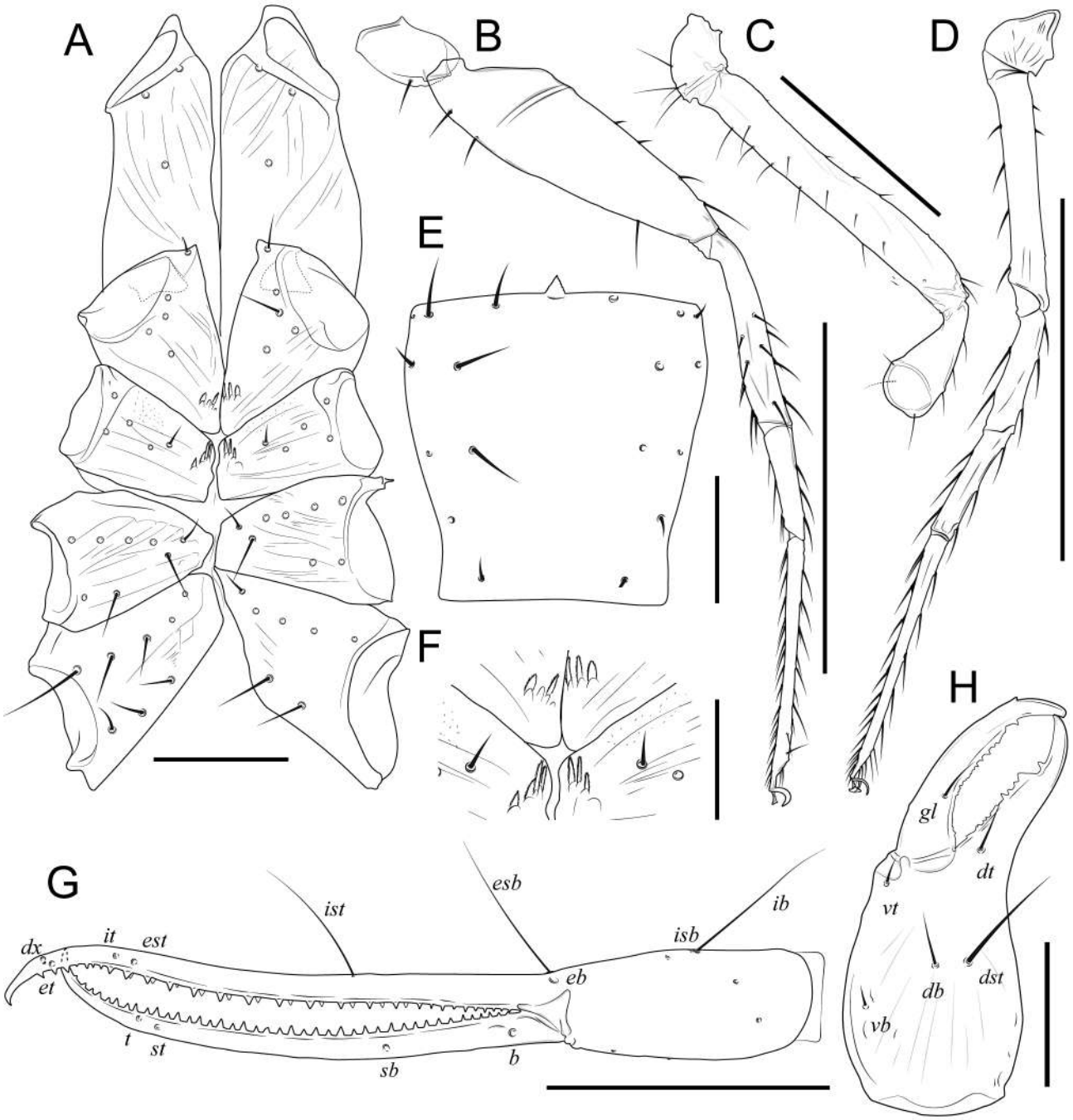


FIGURE 3. *Pseudochthonius diamachi* **sp. nov. A** Female holotype palp and pedal coxae **B** Leg IV of female holotype **C** Pedipalp femur of female holotype, dorsal view **D** Leg I of female holotype **E** Carapace of female holotype **F** Detail of female holotype coxae I and II, showing arrangement of coxal spines **G** Left Chela of female paratype, antiaxial view **H** Left Chelicera of female holotype, showing trichobothrial pattern, antiaxial view. Scale bars: 0.2 mm (**A, H**); 1.0 mm (**B, D**); 0.5 mm (**C, G**); 0.25 mm (**E**); 0.1 mm (**F**).

Tergites. Not divided; surface smooth; chaetotaxy uniseriate, I–XI 2: 4: 4: 4: 6: 6: 6: 4: 6: 2: 2 + 2 sensory setae. Pleural membranes striate.

Coxae (Figs 2C, F, 3A, F). Manducatory process with two apical setae; rest of palpal coxae with 3 setae arranged in a triangle; delicate lamellae outlined by 8(9) small spines. Pedal (Figs 2C, 3A): coxal spines plumose, arranged in a single transverse row in coxae I (3–5) and II (4) (Figs 2F, 3F), chaetotaxy: I 4+1, II 5, III 8, IV 7–8(9); intercoxal tubercle absent.

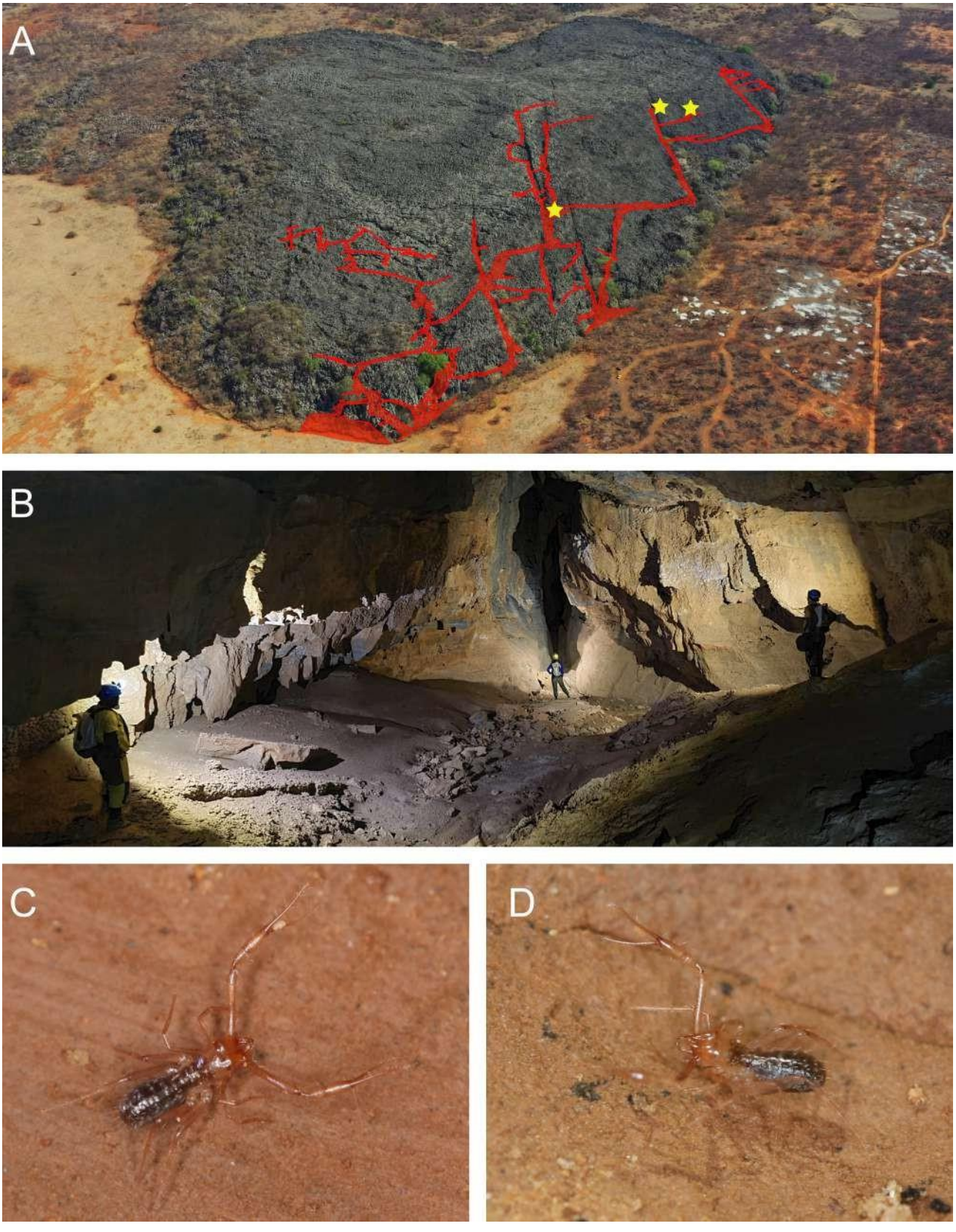


FIGURE 4. *Pseudochthonius diamachi* **sp. nov. A** Três Cobras cave and karst landscape with an overlapped map **B** Três cobras cave entrance **C** Três Cobras cave general aspect **D** Live female holotype **E** Live female paraype.

Genital operculum of female: 8–9 setae distributed in three transversal rows: 2: 4: 2–3, genital opening not bifurcated. Sternites: chaetotaxy IV–XI: 10: 8: 8: 8: 8: 6: 4: 2. Anal operculum with 2 ventral setae.

Palp (Figs 1A–B, D, 3C, G). Trochanter 1.78 (1.62) times longer than wide, patella two times longer than wide, femur 6.84 times longer than wide. Femoral chaetotaxy 5: 6: 3(5): 5(6): 1(2). Trichobothrial pattern: *ib* and *isb* located at the half portion of the hand, adjacent to each other and slightly dislocated to the paraxial face of the chela, *eb* proximad to *esb*, *ist* distad to *esb*, *it* distad to *est*, *et* proximad to *dx*; *ist* halfway between *esb* and *est* (ratio distance *ist-est/ist-esb* = 1.02 [1.11]). Fixed finger slightly bent; movable finger slightly curved (Figs 1A, 3G). Chelal fixed finger with 41 acute, triangular, and widely spaced teeth, with heterodonty starting proximally from the 8th teeth. Movable finger with 42 acute, triangular, and widely spaced teeth.

Leg IV (Fig. 3B). Arolia almost same length as claws; a tiny protuberance near end of telotarsus.

Measurements (length/width or depth in mm and ratios in parenthesis calculated by using three significant digits): Female holotype (female paratype in brackets). Body length 2.02 [2.334]. Carapace 0.59/0.56 (1.0) [0.60/0.56 (1.1)]. Palps: trochanter 0.33/0.18 (1.8) [0.28–0.17 (1.6)], femur 0.98/0.16 (6.8) [1.08/0.15 (6.8)], patella 0.37/0.18 (2.0) [0.37/0.18 (2.0)], chela 1.59/0.21 (7.7) [1.43/0.18 (7.8)], movable finger length1.02 [1.00]. Leg I: trochanter 0.22/0.16 (1.4) [0.18/0.14 (1.3)], femur 0.60/0.10 (5.9) [0.54/0.09 (6.2)], patella 0.31/0.08 (4.0) [0.30/0.07 (4.0)], femur/patella 1.93 [1.82], tibia 0.32/0.06 (5.6) [0.29/0.06 (5.0)], tarsus 0.64/0.05 (13.0) [0.57/0.05 (11.3)]. Leg IV: Trochanter: 0.28/0.16 (1.7) [0.27/0.15 (1.3)], femur + patella 0.95/0.28 (3.4) [0.89/0.26 (3.4)], tibia 0.58/0.10 (5.8) [0.53/0.10 (5.5)], basitarsus 0.33/0.09 (3.7) [0.29/0.08 (3.8), telotarsus 0.69/0.05 (13.9) [0.65/0.05 (13.4)].

Ecological Remarks. Specimens of *Pseudochthonius diamachi* **sp. nov**. were found in the Três Cobras cave, located in Serra do Ramalho municipality, in the southwest of Bahia state, Brazil. This cave has 5.620 meters of horizontal projection, presenting a labyrinth of internal conduits and chambers (Figs 4A–B). The cave has many entrances (Fig. 4A) that are situated mostly at the base of the limestone outcrop. Accordingly, the cave atmosphere is influenced by airflow from the entrances, which dries out several conduits during the dry season (Fig. 4B). However, inner chambers and conduits remain moist even during the dry season. In such moist and environmentally stable areas, most of the cave-restricted fauna is encountered, which includes specimens of *P. diamachi* **sp. nov**., usually observed walking on the cave floor (Figs 4C–D) a phenomenon that is not observed in non-troglobitic cave-dwelling species of *Pseudochthonius*, generally spotted underneath rocks on the cave floor, even in moist areas. The reduction of cryptobiotic behavior is commonly observed in multiple troglobitic invertebrates, including arachnids, such as palpigrades (Souza & Ferreira 2010), amblypygids (Vasconcelos & Ferreira 2017) and even pseudoscorpions from other families (Viana *et al.* 2018).

The main organic resources occurring in the cave are plant debris from the epigean vegetation (which is mainly concentrated near entrances) and bat guano. The latter is most common in deeper regions of the cave where the pseudoscorpions were observed. Such piles attract many springtails and other small invertebrates, such as barklice and immature crickets, which may represent the main prey for the pseudoscorpions.

The cave receives no human visitors, except for a few speleologists that sporadically enter the cave for research. However, the external area is highly damaged (Fig. 10A). During our visit to the area, drone images revealed the extensive tree logging in the cave surroundings. Most areas surrounding the cave were converted to pastures or have had the vegetation cleared and burned, probably for pasture expansion. We suggest reforestation as a means to preserve the cave and its fauna.

Pseudochthonius koinopoliteia sp. nov.

Material examined. ***Holotype*** male (ISLA 100996), preserved in ethanol: Brazil, Carinhanha, Bahia, Gruna da Água Clara Cave (13º48’4.26”S, 43º57’6.24”W), 11 October 2017, leg. R.L Ferreira. ***Allotype*** female (ISLA 100997), preserved in ethanol: Brazil, Carinhanha, Bahia, Pedro Cassiano Cave (13º47’52.80”S, 43º54’50.40”W), 14 September 2021, leg. R.L Ferreira. ***Paratype*** female (ISLA 103872), preserved in ethanol: same local and coordinates as holotype, 3 September 2022, leg. R.L Ferreira.

Etymology. Koinopoliteía (from Greek “κοινοπολιτεία”) can be translated as commonwealth. As previously mentioned, Brazilian caves are a public good, with no possibility of ownership by individuals or entities. This noun should be treated as a noun in apposition.

Diagnosis. Differing from the other members of the genus by the following combination of characters: Absence

of eyes or eyespots; carapace rectangular with almost no posterior constriction; *ist–est/ist–esb* trichobothria ratio of 0.68 (0.73–0.85); chelal fixed finger with 38 acute teeth with heterodonty starting from the 10th proximal tooth, chelal movable finger with 38 acute and well-defined teeth; cheliceral fixed finger with 7 teeth, exhibiting a constriction between the second and 5th proximal ones, movable finger of the chelicera with 8 (13) teeth, the second and third ones constricted, with a distal isolated tooth; presence of two setae on the first and second tergites; trichobothrium *et* proximad to *dx* and distad to *it*; body length of 1.69 (1.71–1.95) mm; chela 7.2 to 7.7 times as long as broad.

Description (Figs 6D, 8C). Body pale yellowish, very translucent; chelicerae slightly orange, abdomen beige. Some parts of the body scaly. Vestitural setae thin and anteriorly projected on prosoma and posteriorly projected on opisthosoma.

Carapace (Fig. 5D). 1.18 (1.12–1.21) times longer than broad, posteriorly slightly constricted showing a difference between ocular width and posterior width of 0.03 (0.06) mm (Fig. 5D); anterior margin partially serrated; no eyes or eyespots; epistome small and strongly dentate and serrated (ranging to seta *ame*); posterior margin of carapace smooth; chaetotaxy 4+2: 4: 4: 2: 2 (18).

Chelicera (Figs 2D–E, 5H). Hand with 5 setae; movable finger with 1 subdistal seta; galea present as a tubercle; fixed finger with 7 acute teeth highly constricted between 2nd and 5th (including a small slightly distal one); movable finger with 9(13) acute teeth (including a small distal one) with 2nd and 3rd teeth highly constricted (Figs 2D, 10H); rallum with 7 blades; serrula exterior with 15 blades, serrula interior with 9 blades.

Tergites. Not divided; surface smooth; chaetotaxy uniseriate, I–XI 2: 2: 4: 4: 4: 6: 6: 6: 6: 2: 2. Anal operculum without dorsal setae. Pleural membranes slightly striate.

Coxae (Figs 5A, F). Manducatory process with two apical setae; rest of palp coxae with 3 setae arranged in a triangle; delicate lamellae outlined by 10(11) small spines. Pedal (Figs 5A, F): coxal spines plumose, arranged in a single transverse row in coxae I (5–6) and II (4–5) (Fig. 5F), chaetotaxy: I 4+1, II 5– 6, III 8, IV 7–8 (9); intercoxal tubercle absent.

Genital operculum of female: 8 setae distributed in three transversal rows: 2: 4: 2, genital opening not bifurcated, 3rd tergite with 16 linear setae.

Genital operculum of male (Fig. 5G): Anterior genital operculum with 8 discal setae, 6 valvular genital setae and 4 setae along the sternite, with 2 microlateral setae on each side.

Sternites: chaetotaxy IV–XI: 10+4–6m: 8+2m: 8+2m: 9 (10): 8 (9): 6: 2(3: 4 + 2 sensory setae. Anal operculum with 2 ventral setae.

Palp (Figs 5C, I). Trochanter 1.66 (1.27–1.65) times longer than wide, femur 6.76 (6.63–6.85) times longer than wide, patella 2.16 (2.13–2.26) times longer than wide. Femoral chaetotaxy 5: 5 (6): 3 (5): 6: 2. Trichobothrial pattern: *ib* and *isb* located at the half portion of the hand, adjacent to each other, slightly dislocated to the paraxial face of the chela, *eb* proximad to *esb*, *it* proximad to *est*, *et* distad from *it* and proximad to *dx*; *ist* closer to *est* than *esb* (ratio distance *ist-est/ist-esb* = 0.68 (0.73–0.85). Fixed finger slightly sigmoid; movable finger slightly curved (Fig. 5I). Chelal fixed finger with 38 (39) acute, triangular, and widely spaced teeth, with heterodonty starting proximally from the 10th teeth. Movable finger with 38 acute, triangular, and widely spaced teeth, alternated in size.

Leg IV (Fig. 5B). Arolia almost with the same length as claws; a soft hump near end of telotarsus.

Measurements (length/width or depth in mm and ratios in parenthesis calculated by using three significant digits): Male holotype (female paratypes in brackets). Body length 1.69 [1.71–1.95]. Carapace 0.46/0.39 (1.2) [0.49–0.50/0.40–0.42 (1.2)]. Palps: trochanter 0.21/0.13 (1.7) [0.17–0.23/0.13–0.14 (1.3–1.6)], femur 0.74/0.11 (6.8) [0.78–0.82/0.11–0.12 (6.8–6.9)], patella 0.28/0.13 (2.2) [0.28–0.31/0.13–0.15 (2.3)], chela 1.04/0.15 (7.2) [1.04–1.16/0.14–0.17 (7.6–7.7)], movable finger length 0.66 [0.70–0.71]. Leg I: trochanter 0.14/0.11 (1.2) [0.13–0.15/0.11–0.13 (1.2)], femur 0.43/0.07 (6.1) [0.46/0.07–0.08 (6.2–6.5)], patella 0.22/0.06 (4.0) [0.23–0.24/0.06 (4.0–4.1)], femur/patella 1.95 [1.93–2.00], tibia 0.23/0.05 (4.8) [0.23–0.24/0.05 (4.8–4.9)], tarsus 0.45/0.05 (10.0) [0.48–0.49/0.04–0.05 (9.8–11.6)]. Leg IV: Trochanter: 0.27/0.14 (1.9) [0.17–0.24/0.13 (1.3–1.8)], femur + patella 0.72/0.21 (3.3) [0.73–0.75/0.21–0.23 (3.5)], tibia 0.45/0.08 (5.4) [0.45–0.48/0.07–0.09 (5.5–6.1)], basitarsus 0.25/0.07 (3.4) [0.25–0.26/0.06–0.07 (3.9–4.1)], telotarsus 0.54/0.04 (13.8) [0.58/–0.04 (16.5)].

Ecological Remarks. Specimens of *Pseudochthonius koinopoliteia* **sp. nov**. were found in two caves: Gruna da Água Clara cave (Figs 6A–C) and Gruna do Pedro Cassiano cave (Figs 7A–D), both located in Carinhanha municipality, southwestern Bahia state, Brazil. The Gruna da Água Clara cave has 13.880 meters of horizontal projection and belongs to a set of functionally interconnected caves known as the Água Clara cave system (ACCS). This system has approximately 24 km of extension, composed of four limestone caves traversed by an intermittent stream,

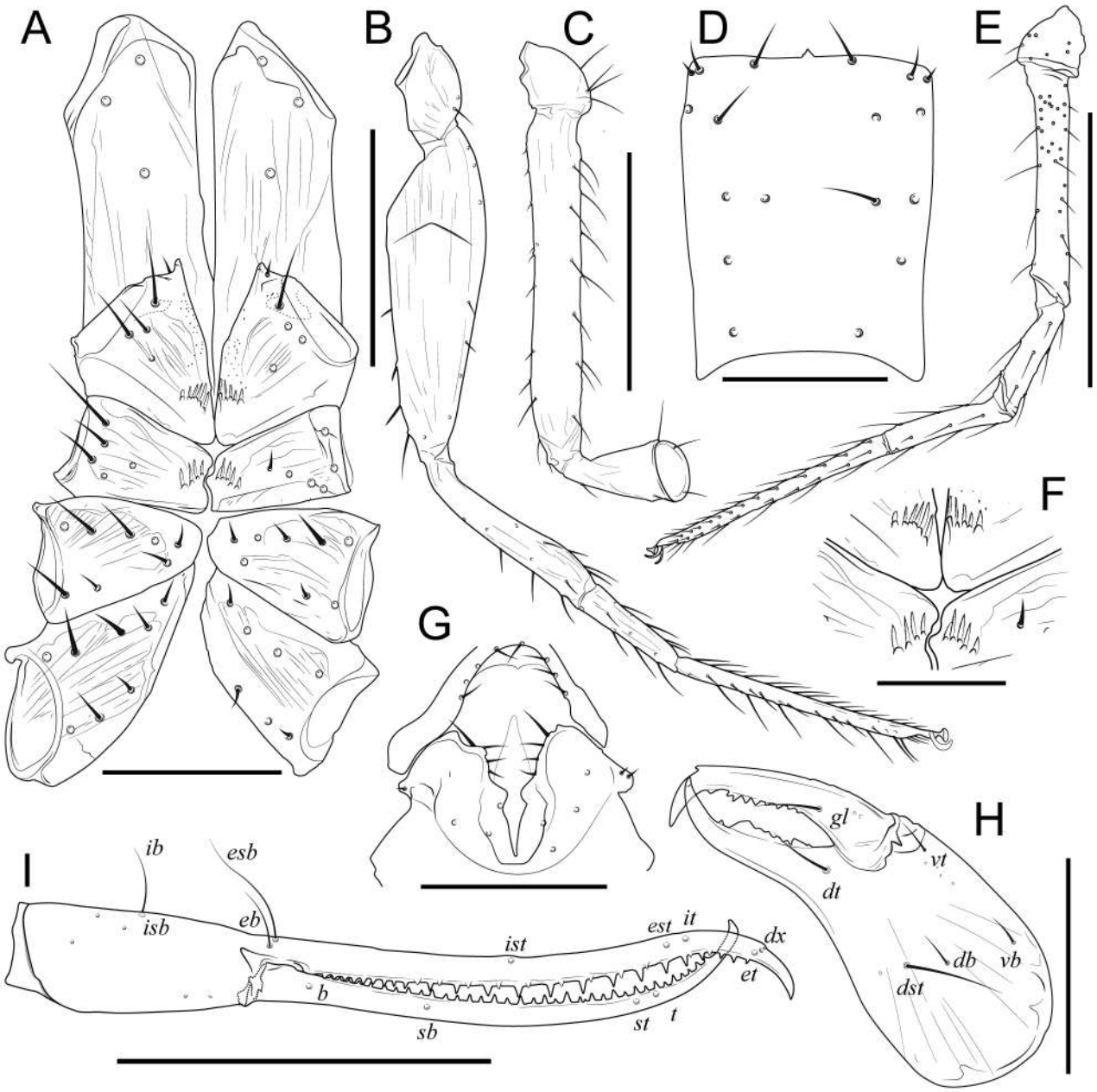


FIGURE 5. *Pseudochthonius koinopoliteia* **sp. nov**. **A** Male holotype palp and pedal coxae **B** Leg IV of male holotype **C** Pedipalp femur of male holotype, dorsal view **D** Carapace of male holotype **E** Leg I of male holotype **F** Detail of coxae I and II, showing arrangement of coxal spines **G** Male holotype genitalia **H** Left chelicera of male holotype, antiaxial view **I** Right chela of male holotype, showing trichobothrial pattern, antiaxial view. Scale bars: 0.2 mm (**A**); 0.5 mm (**B–C, E, I**); 0.25 mm (**D**); 0.1 mm (**F**); 0.2 mm (**G–H**).

active during the austral summer (October to March) (Souza-Silva *et al.* 2021). On the other hand, the Gruna do Pedro Cassiano cave presents 2.660 meters of horizontal projection and does not belong to the ACCS, even located near the system (about 4 km in straight line).

Although Gruna do Pedro Cassiano cave receives local visitors sporadically, the water flow trespassing the cave during the rainy periods (Figs 7C–D) seasonally "erases" eventual impacts caused by the visitors (such as trampling on cave sediments). Furthermore, local visitors do not reach the deepest regions of the cave–where the only specimen was found–since visitors tend to stay closer to the entrance. On the other hand, only speleologists visit the Gruna da Água Clara cave during technical/scientific expeditions, which seldom occurs. Such activities apparently do not represent a threat to the species. Most of the original forests have been removed and replaced by pastures or other monocultures, severely altering the surrounding external environment (Fig. 7A).

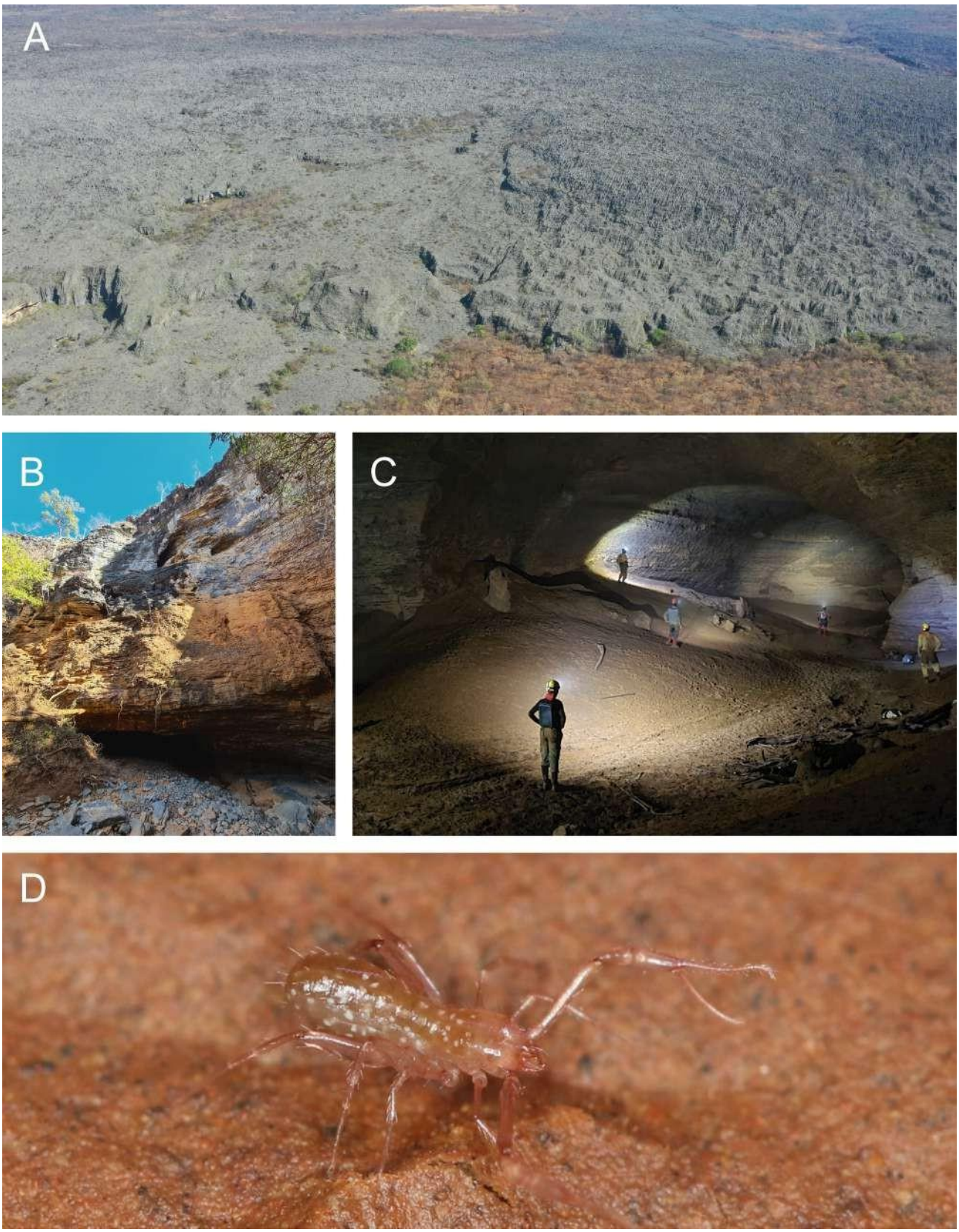


FIGURE 6. *Pseudochthonius koinopoliteia* **sp. nov**. holotype type locality and habitat **A** Água Clara cave karst landscape **B** Água Clara cave entrance **C** Água Clara cave general aspect **D** Live female paratype.

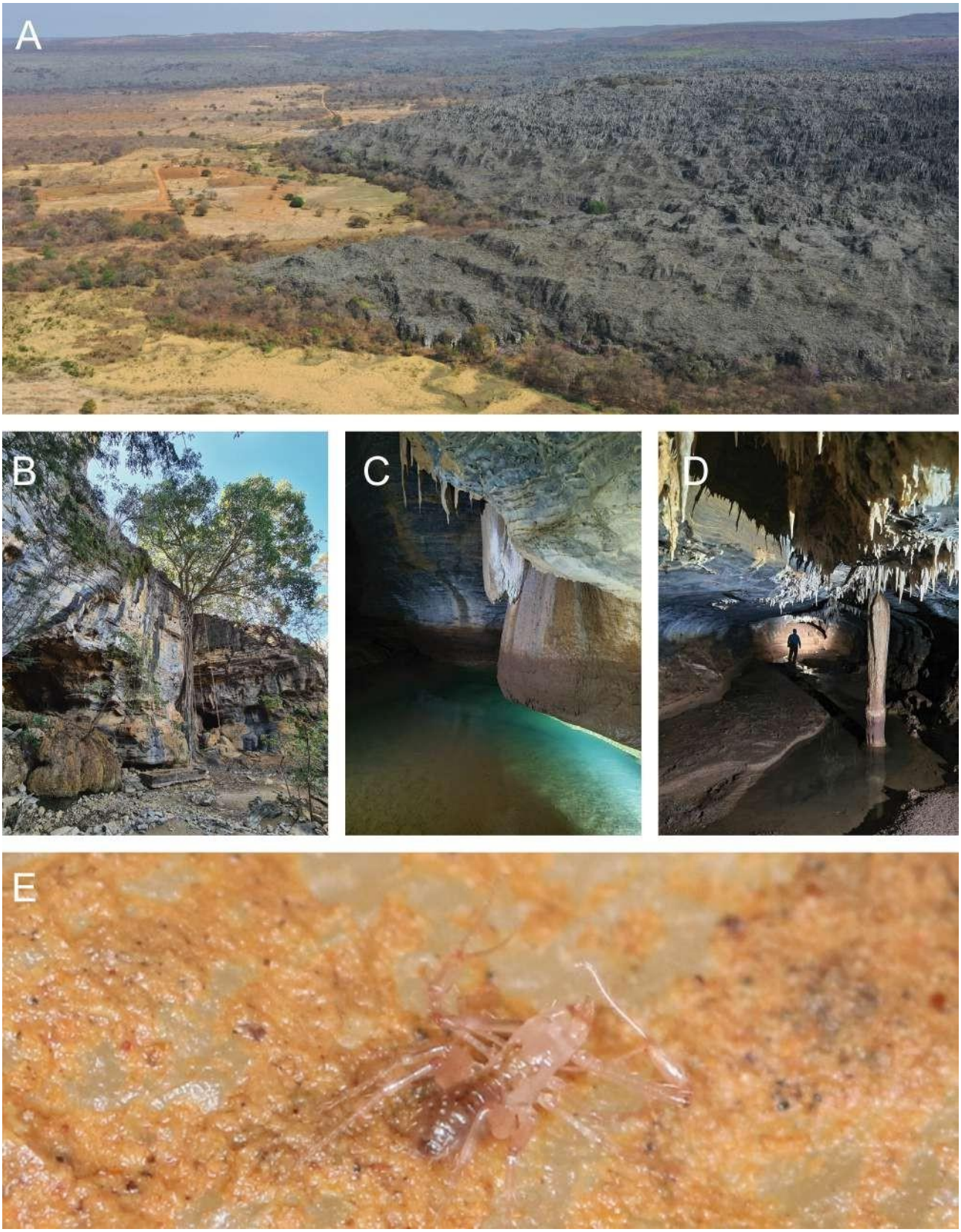


FIGURE 7. *Pseudochthonius koinopoliteia* **sp. nov**. paratype type locality and habitat **A** Karst landscape of Pedro Cassiano cave **B** Pedro Cassiano cave entrance **C** Pedro Cassiano cave interior **D** Pedro Cassiano general aspect **E** Live female paratype

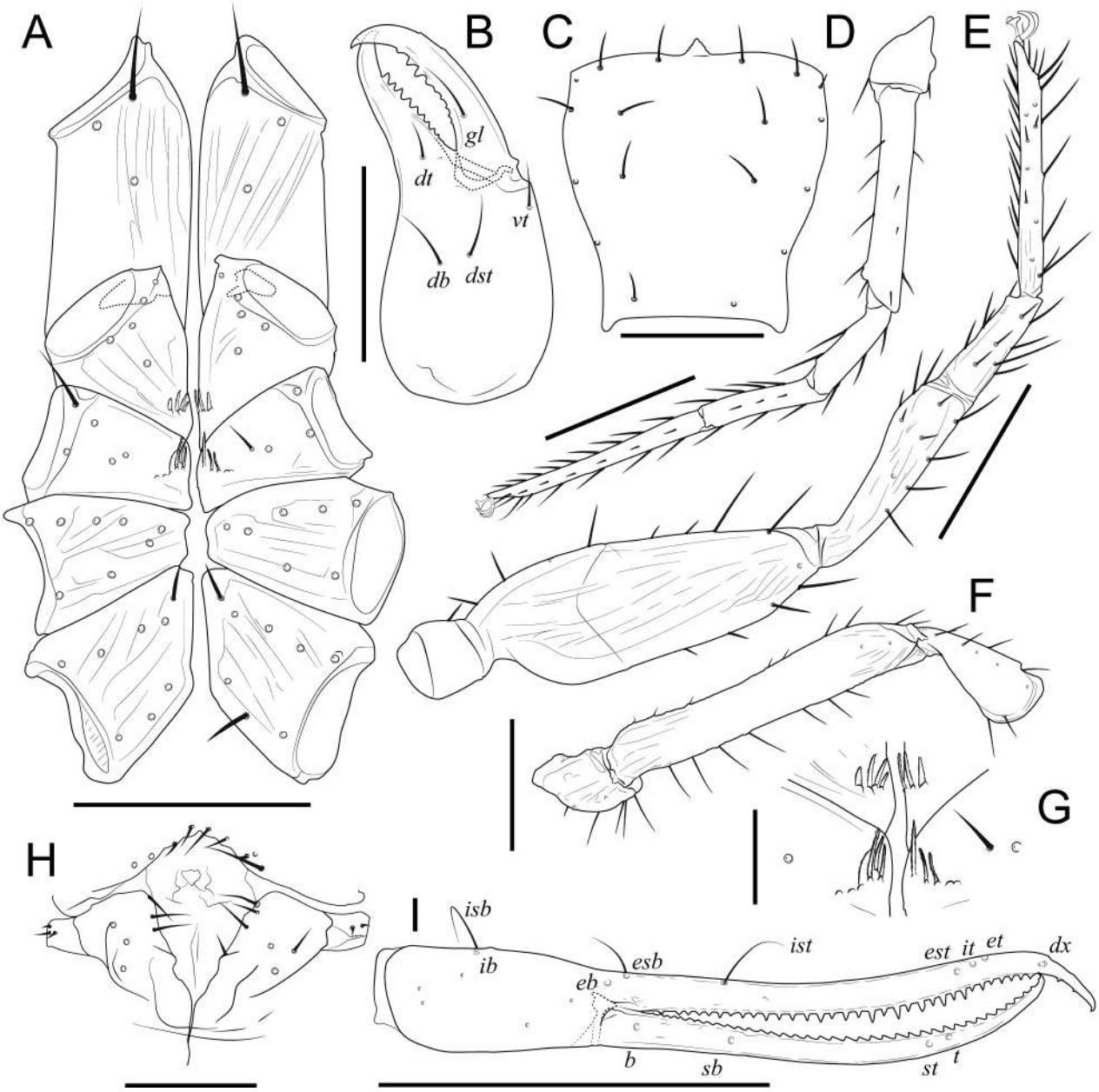


FIGURE 8. *Pseudochthonius pali* **sp. nov**. **A** Male holotype palp and pedal coxae **B** Left chelicera of male holotype, antiaxial view **C** Carapace of male holotype **D** Leg I of male holotype **E** Leg IV of male holotype **F** Pedipalp femur of male holotype, dorsal view **G** Detail of coxae I and II, showing arrangement of coxal spines **H** Male holotype genitalia **I** Right Chela of holotype, showing trichobothrial pattern, antiaxial view. Scale bars: 0.2 mm (**A–B**); 0.25 mm (**C–F**); 0.1 mm (**G–H**); 0.5 mm (**I**).

Pseudochthonius pali sp. nov.

Material examined. ***Holotype*** male (ISLA 100992), preserved in ethanol: Brazil, Serra do Ramalho, Bahia, Gruna do Google Cave (13º37'41.93"S, 43º48'49.04"W), 22 September 2021, leg. R.L Ferreira. ***Allotype*** female (ISLA 100993), same data as holotype.

Etymology. Páli (from Greek "πάλη") can be translated as "fight, battle", and represents the recent fight of the Brazilian speleology community in favor of cave preservation and against the recent presidential decree that allowed the destruction of maximum relevance caves in Brazil. This noun should be treated as noun in apposition.

Diagnosis. Differing from the other members of the genus by the following combination of characters: Absence of eyes or eyespots; carapace with a strong posterior constriction; *ist–est/ist–esb* trichobothria ratio of 2.46 (2.77);

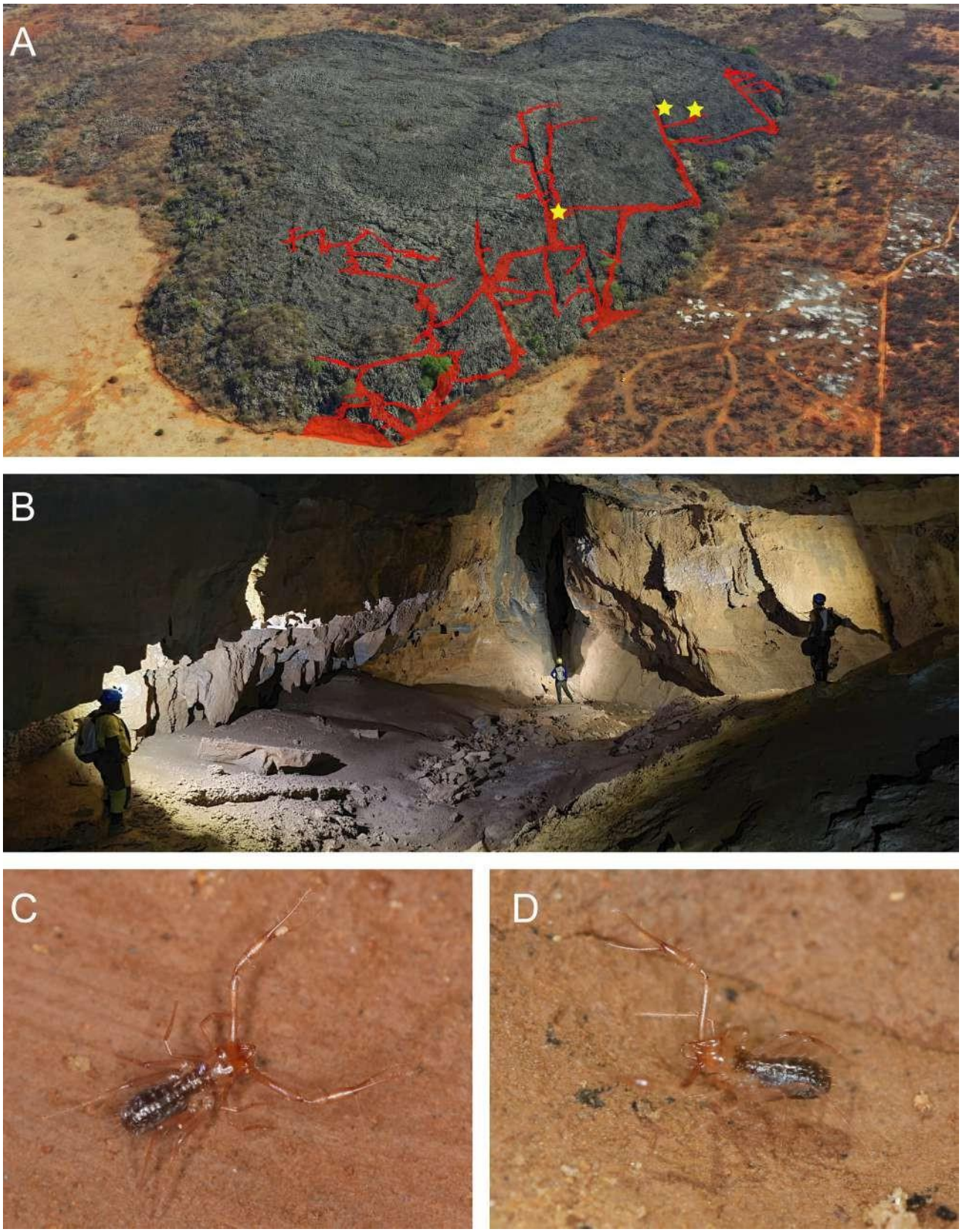


FIGURE 9. *Pseudochthonius pali* **sp. nov. A** Google cave region. Satellite view **B** Google cave general aspect **C** Live male holotype **D** Live female paratype.

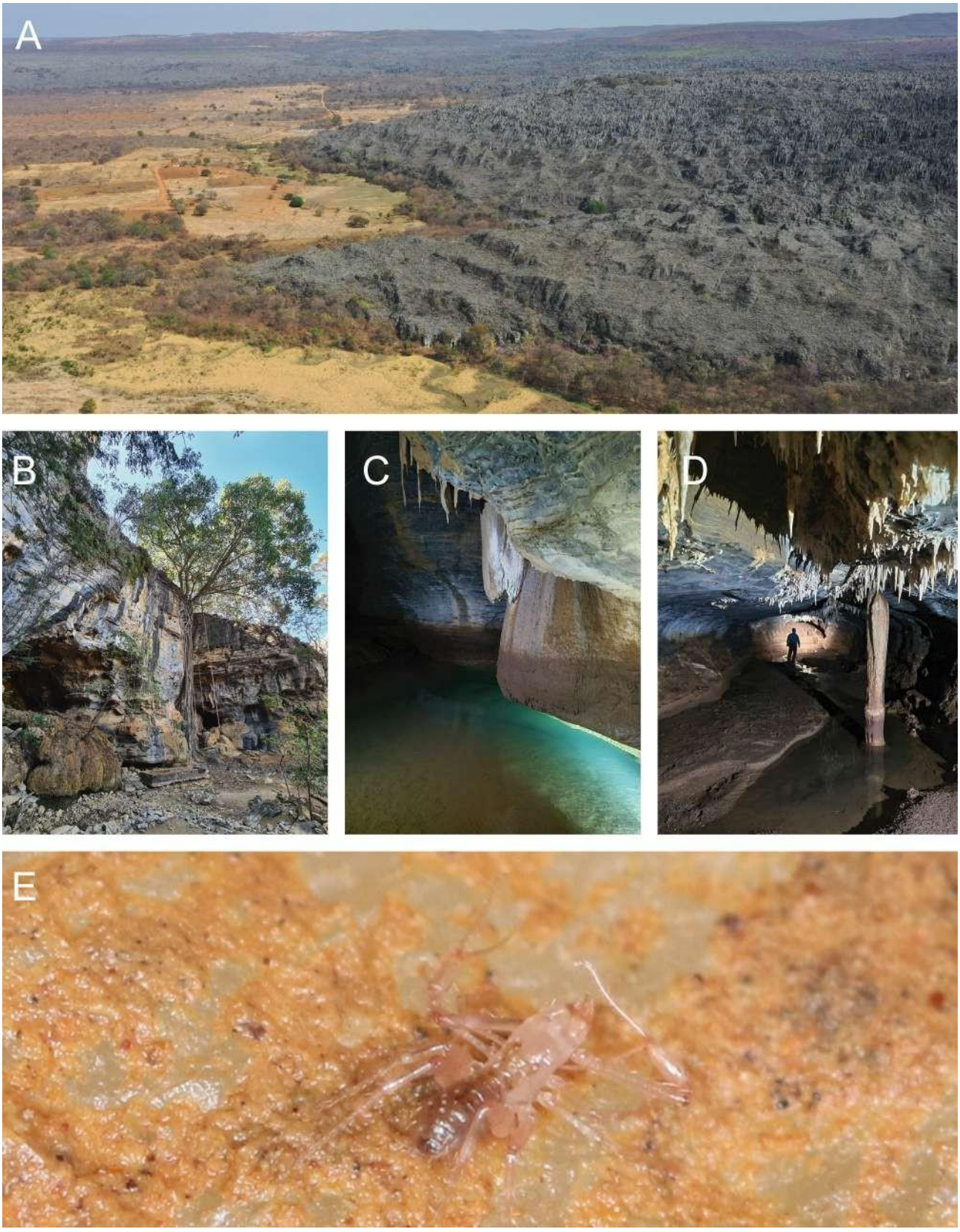


FIGURE 10. Ecological impacts to the subterranean habitat **A** Deforestation near cave entrance **B** Vegetal coal furnace.

chelal fixed finger with 34 (39) acute teeth with heterodonty starting from the 10th proximal tooth, chelal movable finger with 36 (38) small and retrorse teeth; cheliceral fixed finger with 9 (11) spaced and regular teeth, movable

finger with 9 (12) teeth, with no constrictions or distal isolated teeth; presence of two and four setae on the first and second tergites, respectively; trichobothria *est*, *it* and *et* grouped; body length of 1.33 (1.70) mm; chela 5.9 to 6.5 times as long as broad.

Description (Figs 9C–D, 11B). Body pale yellowish, very translucent; chelicerae slightly orange, abdomen beige. Vestitural setae thin and anteriorly projected on prosoma and posteriorly projected on opisthosoma.

Carapace (Fig. 8C). 1.09 (1.05) times longer than broad, strongly constricted posteriorly showing a difference between ocular width and posterior width of 0.11 (0.15) mm (Fig. 8C); anterior margin all serrated; no eyes or eyespots; epistome strongly dentate and saw-like (ranging to lateral setae); posterior margin of carapace smooth; chaetotaxy 4+2: 4: 4: 2: 2 (18).

Chelicera (Figs 2A–B, 8B). Hand with 5 setae; movable finger with 1 subdistal seta and fixed finger; galea present as a smooth hump; fixed finger with 9 (11) well-defined acute teeth; movable finger with 9 (12) well-defined acute teeth; rallum with 7 blades, serrula exterior with 14 blades, serrula interior with 10 blades.

Tergites. Not divided; surface smooth; chaetotaxy uniseriate, I–XI 2: 4: 4: 4: 6: 6: 6: 4: 6: 2: 2 + 2 sensory setae.

Anal operculum without dorsal setae. Pleural membranes striate.

Coxae (Figs 8A–G). Manducatory process with two apical setae, lateral ones slightly smaller than medial; rest of palp coxae with 3 setae arranged in a triangle; delicate lamellae outlined by 9 small spines. Pedal (Fig. 8A): coxal spines plumose (highly dentated), arranged in a single transverse row in coxae I (3–5) and II (5–6) ((Fig. 8G), chaetotaxy: I 4+1, II 4 (5), III 7–8, IV 8 (9); intercoxal tubercle absent.

Genital operculum of female: 9 setae distributed in three horizontal rows: 2: 3: 4, genital opening not clearly bifurcated. Genital operculum of male (Fig. 8H): anterior margin of operculum with 8 discal setae distributed marginally;
six valvular setae on each side of the opening; 4 surrounding setae and 3-2(5) microlateral setae (Fig. 8H).

Sternites: chaetotaxy IV–XI: 10: 8: 8: 8: 8: 6: 4: 2. Anal operculum with two ventral setae.

Palp (Figs 8F, I). Trochanter 1.67 times longer than wide, femur 5.65 (5.71) times longer than wide, patella 2.22 (2.23) times longer than wide. Femoral chaetotaxy 5: 6: 3: 5: 2. Trichobothrial pattern: *ib* and *isb* located at the half portion of the hand proximad to a tiny hump (Fig. 8I), adjacent to each other, *eb* proximad to *esb*, *ist* distad to *esb*, *it* between *est* and *et*, *et* proximad from *dx* and distad to *it*; *ist* closer to *esb* than to *est* (ratio distance *ist-est/ist-esb* = 2.46 [2.77]). Fixed finger slightly sigmoid; movable finger slightly curved (Fig. 8I). Chelal fixed finger with 34 (39) acute, triangular, and widely spaced teeth, with heterodonty starting from the 10th teeth. Movable finger with 36 (38) small and projected backwards teeth.

Leg IV (Fig. 8E). Arolia slightly smaller than claws.

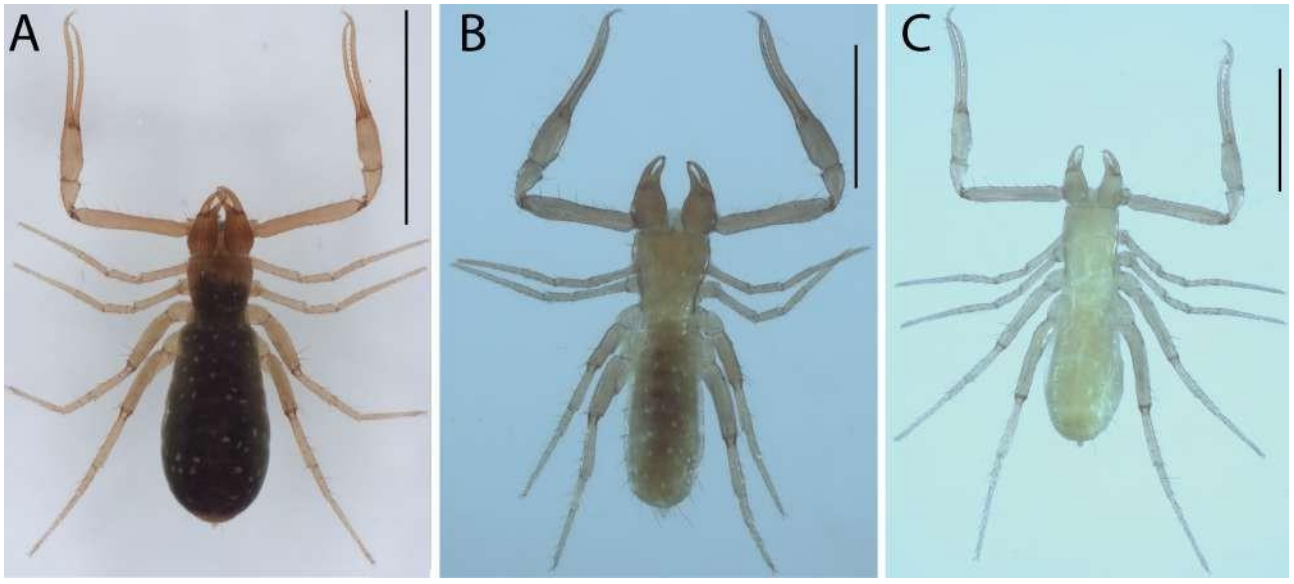


FIGURE 11. New species habitus. **A** *Pseudochthonius diamachi* **sp. nov**. paratype habitus. **B** *Pseudochthonius pali* **sp. nov**. paratype habitus **C** *Pseudochthonius koinopoliteia* **sp. nov**. holotype habitus. Scale bars: 2.0 mm (**A**); 1.0 mm (**B–C**).

Measurements (length/width or depth in mm and ratios in parenthesis calculated by using three significant digits): Male holotype (female paratypes in brackets). Body length 1.33 [1.70]. Carapace 0.42/0.39 (1.1) [0.49/0.46

(1.1)]. Palps: trochanter 0.20/0.12 (1.7) [0.22/0.13 (1.7)], femur 0.63/0.11 (5.7) [0.74/0.13 (5.7)], patella 0.28/0.13 (2.2) [0.31/0.14 (2.2)], chela 0.87/0.13 (6.5) [0.98/0.17 (5.9)], movable finger length 0.58 [0.64]. Leg I: trochanter 0.14/0.10 (1.4) [0.15/0.11 (1.4)], femur 0.34/0.07 (5.2) [0.39/0.07 (5.5)], patella 0.18/0.05 (3.6) [0.2/0.06 (3.6)], femur/patella 1.9 [2.0], tibia 0.19/0.04 (4.7) [0.22/0.04 (5.0)], tarsus 0.35/0.03 (10.2) [0.41/0.04 (10.2)]. Leg IV: Trochanter: 0.12/0.11 (1.2) [0.16/0.12 (1.3)], femur + patella 0.5/0.19 (2.7) [0.6/0.21 (2.8)], tibia 0.31/0.08 (3.9) [0.37/0.09 (4.2)], basitarsus 0.17/0.06 (2.9) [0.22/0.06 (3.6)], telotarsus 0.36/0.04 (9.9) [0.42/0.04 (10.6)].

Ecological Remarks. Specimens of *Pseudochthonius pali* **sp. nov.** were found in the Gruna do Google cave, located in Serra do Ramalho municipality, southwestern Bahia state, Brazil. This cave has 1.230 meters of horizontal projection, with a single entrance, which represents a sinkhole (Fig. 9A). There is an intermittent drainage in the external landscape, which drains to the cave entrance. Hence, a huge amount of sediment and organic matter are seasonally carried to the cave demanding periodic debris removal in order to access inner conduits. The conduits are predominantly wide, and moistened sediments cover the floor (Fig. 9B). The majority of the main conduit is seasonally flooded, and the main organic resource observed is plant-decaying material. The specimens of *P. pali* **sp. nov**. were found walking freely on the floor (Figs 9C–D) situated in an upper chamber located laterally in relation to the main cave conduit, at about 600 meters from the entrance.

This cave has only been visited by speleologists since its discovery, due to the difficult access to its inner portions, which leads to a quite preserved interior. Nonetheless, since it receives a huge contribution of external sediments brought by water, an apparent silting was observed along the main conduit of the cave. However, contrary to the observations for the other two caves herein described, the external landscape surrounding the cave (especially upstream) is slightly modified, and a secondary forest predominates along the area.

Discussion

The first Brazilian *Pseudochthonius* species, *Pseudocthonius strinatii* Beier, 1969 was registered for Gruta das Areias cave, Iporanga municipality, São Paulo state, and defined as a troglobiont. Since then, eleven additional species have been described that are distributed in the Atlantic and Amazonian rainforests, Cerrado (Brazilian savannah) and Caatinga (semi-arid) biomes. The last *Pseudochthonius* species described for northeast of Brazil (*Pseudochthonius ramalho* Assis *et al.*, 2021) is a cave-dwelling species also found in the Serra do Ramalho region, in Bahia state (World Pseudoscorpiones Catalog 2021; Assis *et al.* 2021).

Regarding the troglomorphic traits on species from this genus, we highlight the proportions of the appendages, which are not only important to differ the new species but also to emphasize their status as troglobionts. *Pseudochthonius diamachi* **sp. nov.** is described as the largest pseudoscorpion of the genus, however its appendices ratio resembles to *P. koinopoliteia* **sp. nov.** (see *measurements* of each species). It is important to note that the accentuated difference between ocular breadth and posterior breadth observed in *P. pali* **sp. nov.** and *P. diamachi* **sp. nov.** is not present in *P. koinopoliteia* **sp. nov**. (which shows almost no constriction of the carapace), although, the latter seems to have the same proportion of the anterior margin length in relation to the body size as the constricted carapace species.

Assis *et al.* (2021) assumed that some troglobitic species of *Pseudochthonius* (*P. ramalho*, *P. strinatii* and *Pseudochthonius Biseriatus* Mahnert, 2001) present a narrowing from the anterior to the posterior margin of the carapace. According to those authors, this could represent a troglomorphic trait. However, it is important to note that what they interpreted as a narrowing of the posterior portion of the carapace, in fact probably comprises an enlargement of the anterior portion. Biologically, there are no selective mechanisms that would lead to posterior narrowing of the carapace. On the other hand, the widening of the anterior portion certainly allows the insertion of larger and more voluminous chelicerae. These larger and stronger chelicerae certainly represent selective advantages in oligotrophic environments (such as caves), as they allow pseudoscorpions to prey upon a greater variety of invertebrates. Thus, even though Assis *et al.* (2021) correctly suggested a new troglomorphism for the genus (and eventually for the family), their proposed interpretation is challenged here.

Assis *et al.* (2021) also assumed that *P. ramalho* could be classified by the IUCN (International Union of Conservation of Nature) criteria as Critically Endangered (CR) according to criteria B1ab (iii) + B2ab (iii). According to those authors, the species has a restricted geographical distribution, with an estimated occurrence of less than 100 km² (B1) and 10 km² (B2), and the severely fragmented population (a) lives in a few locations with the continued

decline (b) in area, extension, and quality of habitat (iii). However, while attesting *P. ramalho* is endemic to a single cave (what fits on the distributional range criteria), the authors did not provide any data which could attest a continued decline in area, extension, and quality of habitat. Such information would certainly require a monitoring of the species population. Considering that only a single visit to the cave is mentioned in the species description (carried out in May 2012), and no references of any additional visits to the cave were provided, it is premature to propose any classification for the species at this moment. Additionally, there are hundreds of caves in the Serra do Ramalho region, and only a few of them were sampled; therefore, it is of paramount importance to sample other caves in the region before the species range can be esrablished with certainty.

Finally, it is important to highlight the increasing threats to the Brazilian speleological heritage, especially in recent years. Subterranean habitats in the country are under unprecedented threat due to recent changes in laws regarding cave protection (Ferreira *et al.* 2022). Thus, although little is known about the actual distribution and population densities of the new species described herein, it is possible that they are already threatened.

Key to Brazilian *Pseudochthonius* species

Eyes absent 2
Presence of a pair of eyes or eyespots in one or both gender 3
Trichobothrium *ist* closer to *est* than to *esb* ..... *Pseudochthonius koinopoliteia* **sp. nov.**
Trichobothrium *ist* closer to *esb* than to *est* or *ist* halfway from *esb* and *est* 4
Chelal fixed finger with heterodonty (off-set saw-like) 5
Chelal fixed finger without heterodonty (simple row of teeth) 6
Body length with at least 2.0 mm ..... *Pseudochthonius diamachi* **sp. nov.**
Body length less than 2.0 mm 7
Carapace 1.0–1.1 times longer than wide, chelal fixed finger teeth with microteeth on 15th and 29th teeth, endemic to Gruta do Vandercir, Serra do Ramalho, BA ..... *Pseudochthonius ramalho*
Carapace > 1.1 times longer than wide, chelal fixed finger without microteeth 8
Chelal morphology typically sigmoid with a small apodeme, with flattened teeth on movable finger . . . . *Pseudochthonius homodentatus* Chamberlin, 1929
Chelal morphology highly straight, large and well-developed apodeme, bearing rounded basal teeth in both fingers. . . . . *Pseudochthonius orthodactylus*
Epistome acute and smooth, endemic to Lapa Zé de Sidinei, Presidente Olegário, MG. . . . . *Pseudochthonius olegario* Schimonsky, 2022
Epistome acute and highly serrated 9
Chelal fixed finger bearing more than 26 teeth 10
Chelal fixed finger bearing less than 26 teeth 11
Heterodonty on fixed chelal finger present only after the 10th teeth from basal to distal one, trichobothrium *et* proximad to *it* and distad to *dx* *Pseudochthonius pali* **sp. nov.**
Heterodonty present on almost the whole dentition of chelal fixed finger, endemic to Gruta dos Olhos d'Água, Itacarambi, Minas Gerais *Pseudochthonius biseriatus*
Epistome small and highly dentate, *ist–est/ist–esb* ratio near 2.0, chelal movable finger with less teeth than chelal fixed finger (24 on movable and 35 on fixed) where the latter presents a distal isolated tooth ..... *Pseudochthonius tuxeni* Mahnert, 1979
Chelal movable finger with more teeth than chelal fixed finger, with occurrence in São Paulo state 12
Chelal movable finger with heterodonty dentition ..... *Pseudochthonius gracilimanus* Mahnert, 2001
Chelal movable finger partially or fully retroprojected homodont teeth 13
Epistome acute and prominent, with the anterior margin serrated from the epistome ranging to *ame* carapacal setae, coxa I and coxae II bearing two coxal spines ..... *Pseudochthonius strinatii*
Epistome acute and highly dentate only in female, lateral portion of the anterior margin of the carapace wrinkled, presence of six setae on the last seven tergite plates (from anterior to posterior), *ist–est/ist–esb* ratio of 2.5 . . . . *Pseudochthonius brasiliensis* Beier, 1970
Movable finger with 40 or more teeth, distally retrorse and basally rounded teeth ..... *Pseudochthonius ricardoi* Mahnert, 2001
Movable finger with about 30 retrorse tee ..... *Pseudochthonius heterodentatus* Hoff, 1946

Acknowledgements

We thank Dr. Marconi Souza Silva (Lavras) and all the team from the Center of studies on subterranean biology from the Federal University of Lavras for field assistance. We also thank the institutions that supported the study with funding for scholarships and infrastructure (FAPEMIG, VALE) also IABS and CECAV for the subsidized project n. 0.17/2021. RLF is grateful to the CNPq (National Council for Scientific and Technological Development) for the grant provided (CNPq n. 302925/2022-8). We also thank the reviewers, Dr. Mark Havey, Dr. Giulio Gardini, and the editor Dr. Danilo Harms, whose thoughtful comments and suggestions helped to improve the quality of this paper.

References

Alvares, C.A., Stape, J.L., Sentelhas, P.C., Gonçalves, J.L.M. & Sparovek, G. (2013) Köppen's climate classification map for Brazil. *Meteorologische Zeitschrift*, 22 (6), 711–728.
https://doi.org/10.1127/0941-2948/2013/0507

Assis, L.D., Schimonsky, D.M.V. & Bichuette, M.E. (2021) The first troglobitic *Pseudochthonius* Balzan, 1892 (Pseudoscorpiones, Chthoniidae) from the karst area of Serra do Ramalho, Brazil: a threatened species. *Subterranean Biology*, 40, 109–128.
https://doi.org/10.3897/subtbiol.40.77451

Auler, A. (2019) Histórico, ocorrência e potencial de cavernas no Brasil. *In*: Rubbioli, E., Auler, A., Menin, D. & Brandi, R., *Cavernas: Atlas do Brasil Subterrâneo*. ICMBio, Brasília, pp. 290.

Beier, M. (1969) Ein wahrscheinlich troglobionter *Pseudochthonius* (Pseudoscorp.) aus Brasilien. *Revue Suisse de Zoologie*, 76 (1) 1–2.
https://doi.org/10.5962/bhl.part.97044

Beier, M. (1970) Myrmecophile Pseudoskorpione aus Brasilien. *Annalen des naturhistorischen Museums in Wien*, 74, 51–56.

Benavides, L.R., Cosgrove, J.G., Harvey, M.S. & Gonzalo, G. (2019) Phylogenomic interrogation resolves the backbone of the Pseudoscorpiones tree of life. *Molecular Phylogenetics and Evolution*, 139, 106509. https://doi.org/10.1016/j.ympev.2019.05.023

Chamberlin, J.C. (1929) The genus *Pseudochthonius* Balzan (Arachnida—Chelonethida). *Bulletin de la Société Zoologique de France*, 54, 173–179.

Chamberlin, J.C. (1931) The arachnid order Chelonethida. Stanford University Publications. *Biological Sciences*, 7, 1–284.

Ferreira, R.L., Bernard, E., Júnior, F.W.C., Piló, L.B., Calux, A., Souza-Silva, M., Barlow, J., Pompeu, P.S., Cardoso, P., Mammola, S., García, A.M., Jeffery, W.R., Shear, W., Medellín, R.A., Wynne, J.J., Borges, P.A.V., Kamimura, Y., Pipan, T., Hajna, N.Z., Sendra, A., Peck, S., Onac, B.P., Culve, D.C., Hoch, H., Flot, J., Stoch, F., Pavlek, M., Niemiller, M.L., Manchi, S., Deharveng, L., Fenolio, D., Calaforra, J., Yager, J., Griebler, C., Nader, F.H., Humphreys, W.F., Hughes, A.C., Fenton, B., Forti, P., Sauro, F., Veni, G., Frumkin, A., Gavish-Regev, E., Fišer, C., Trontelj, P., Zagmajster, M., Delic, Teo., Galassi, D.M.P,. Vaccarelli, I., Komnenov, M., Gainett, G., Tavares, V.C., Kováč, L., Miller, A.Z., Yoshizawa, K., Di Lorenzo, T., Moldovan, O.T., Sánchez- Fernández, D., Moutaouakil, S., Howarth, F., Bilandžija, H., Dražina, T., Kuharić, N., Butorac, V., Lienhard, C., Cooper, S.J.B., Eme, D., Strauss, A.M., Saccò, M., Zhao, Y., Williams, P., Tian, M., Tanalgo, K., Woo, K., Barjakovic, M., Mccracken,
G.F., Simmons, N.B., Racey, P.A., Ford, D., Labegalini, J.A., Colzato, N., Pereira, M.J.R., Aguiar, L.M.S., Moratelli, R., Du Preez, G., Pérez-González, A., Reboleira, A.S.P.S., Gunn, J., Mc Cartney, A., Bobrowiec, P.E.D., Milko, D., Kinuthia, W., Fischer, E., Meierhofer, M.B. & Frick, W.F. (2022) Brazilian cave heritage under siege. *Science*, 375, 1238–1239.
https://doi.org/10.1126/science.abo1973

Cole, M.M. (1960) Cerrado, caatinga and pantanal: the distribution and origin of the savanna vegetation of Brazil. *The Geographical Journal*, 126 (2), 168–179.
https://doi.org/10.2307/1793957

Harms, D. (2018) The origins of diversity in ancient landscapes: deep phylogeographic structuring in a pseudoscorpion (Pseudotyrannochthoniidae: *Pseudotyrannochthonius*) reflects Plio-Pleistocene climate fluctuations. *Zoologischer Anzeiger*, 273, 112–123.
https://doi.org/10.1016/j.jcz.2018.01.001

Harvey, M.S. (1988) The systematics and biology of pseudoscorpions & N. W. Heather. *Australian Arachnology*. Australian Entomological Society, Brisbane, pp. 75–85.

Harvey, M.S. (1992) The phylogeny and classification of the Pseudoscorpionida (Chelicerata: Arachnida). *Invertebrate Taxonomy*, 6, 1373–1435.
https://doi.org/10.1071/IT9921373

Harvey, M.S. (2013) Pseudoscorpions of the World. Version 3.0. Western Australian Museum. Perth. Available from: http://www.museum.wa.gov.au/catalogues/pseudoscorpions (accessed 26 November 2021)

Hoff, C.C. (1946) Three new species of heterosphyronid pseudoscorpions from Trinidad. *American Museum Novitates*, 1322, 1–13.

IUCN (2017) Guidelines for using the IUCN Red List categories and criteria. Version 13. Available from: https://iucnredlist. org/resources/redlistguidelines (accessed 26 January 2023)
Mahnert, V. (2001) Cave-dwelling pseudoscorpions (Arachnida, Pseudoscorpiones) from Brazil. *Revue Suisse de Zoologie*, 108 (1), 95–148. https://doi.org/10.5962/bhl.part.79622
Montesanto, G. (2015) A fast GNU method to draw accurate scientific illustrations for taxonomy. *ZooKeys*, 515, 191–206. https://doi.org/10.3897/zookeys.515.9459
Muchmore, W.B. (1970) An unusual *Pseudochthonius* from Brazil (Arachnida, Pseudoscorpionida, Chthoniidae). *Entomological News*, 81, 221–223.
Schimonsky, D.M.V., Gallão, J.E. & Bichette, M.E. (2022) A new troglobitic *Pseudochthonius* (Pseudoscorpiones: Chthoniidae) from Minas Gerais State, south-east Brazil. *Arachnology*, 19 (1), 38–46. https://doi.org/10.13156/arac.2022.19.1.38
Souza, M.F.V.R. & Ferreira, R.L. (2010) *Eukoenenia* (Palpigradi: Eukoeneniidae) in Brazilian caves with the first troglobiotic palpigrade from South America. *Journal of Arachnology*, 38, 415–424. https://doi.org/10.1636/Ha09-112.1
Souza-Silva, M., Cerqueira, R.F.V., Pellegrini, T.G. & Ferreira, R.L. (2021) Habitat selection of cave-restricted fauna in a new hotspot of subterranean biodiversity in Neotropics. *Biodiversity and Conservation*, 30, 4223–4250. https://doi.org/10.1007/s10531-021-02302-8
Vasconcelos, A.C.O. & Ferreira, R.L. (2017) Two new species of cave-dwelling *Charinus* Simon, 1892 from Brazil (Arachnida: Amblypygi: Charinidae). *Zootaxa*, 4312 (2), 277–292. https://doi.org/10.11646/zootaxa.4312.2.4
Viana, A.C.M., Souza, M.F.V.R. & Ferreira, R.L. (2018) *Spelaeobochicha goliath* (Arachnida: Pseudoscorpiones: Bochicidae), a new troglobitic pseudoscorpion from Brazil. *Zootaxa*, 4402 (3), 585–594. https://doi.org/10.11646/zootaxa.4402.3.11
World Pseudoscorpiones Catalog (2022) World Pseudoscorpiones Catalog. Natural History Museum Bern. Available from: http/wac.nmbe.ch (accessed 7 December 2022)
Wynne, J.J., Francis, G.H., Stefan, S. & Brett, G. (2019) Fifty years of cave arthropod sampling: techniques and best practices. *International Journal of Speleology*, 48, 33–48. https://doi.org/10.5038/1827-806X.48.1.2231

Zootaxa 5256 (6): 597–600
https://www.mapress.com/zt/
Copyright © 2023 Magnolia Press
ISSN 1175-5326 (print edition)
Erratum
ISSN 1175-5334 (online edition)
https://doi.org/10.11646/zootaxa.5256.6.8
http://zoobank.org/urn:lsid:zoobank.org:pub:15095F43-5F7F-4D1A-B919-61693417032C

ZOOTAXA

GUILHERME C. PRADO & RODRIGO L. FERREIRA (2023) Three new troglobitic species of Pseudochthonius Balzan, 1892 (Pseudoscorpiones, Chthoniidae) from northeastern Brazil *Zootaxa,* 5249 (1), 092–110.

During the publication of the paper, two figures (plates) were inadvertently omitted and replaced by two other figures that had been mentioned in the text previously. Specifically, the affected figures are Fig. 9 and Fig. 10, and although their legends are correct, the figures themselves are incorrect.

WRONG CONFIGURATION:

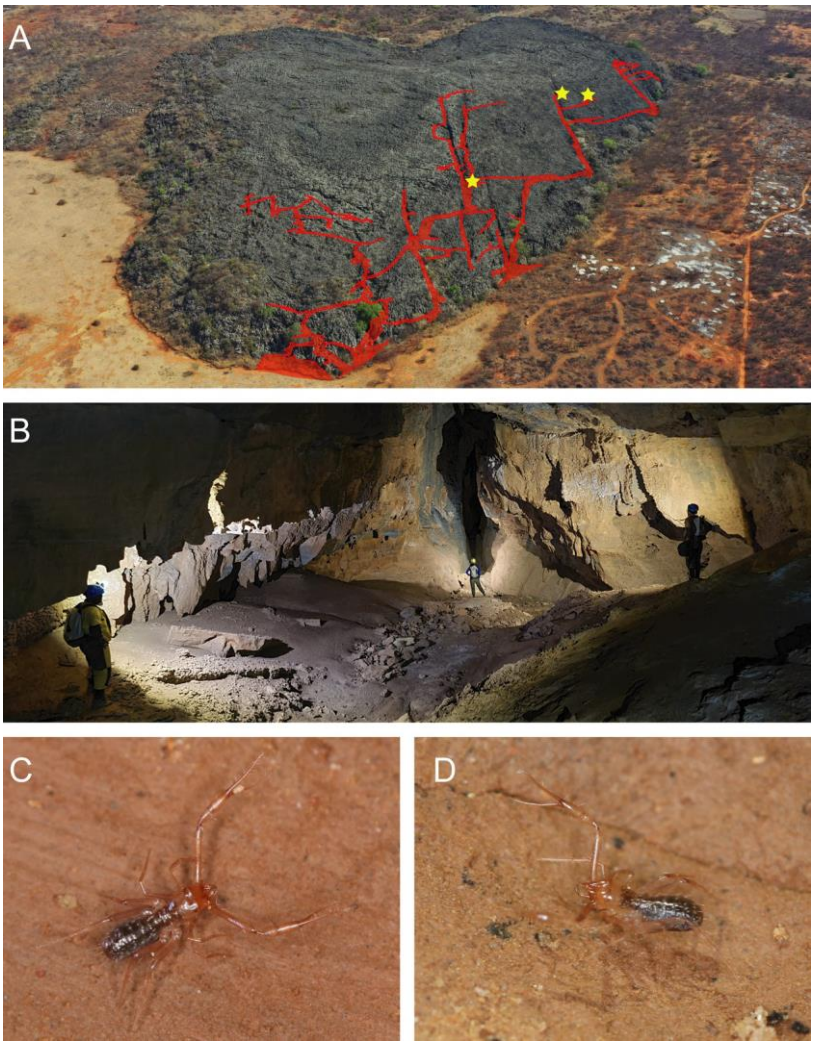


FIGURE 9. *Pseudochthonius pali* sp. nov. A Google cave region. Satellite view B Google cave general aspect C Live male holotype D Live female paratype.

Accepted by D. Harms: 26 Jan. 2023; published: 23 Mar. 2023

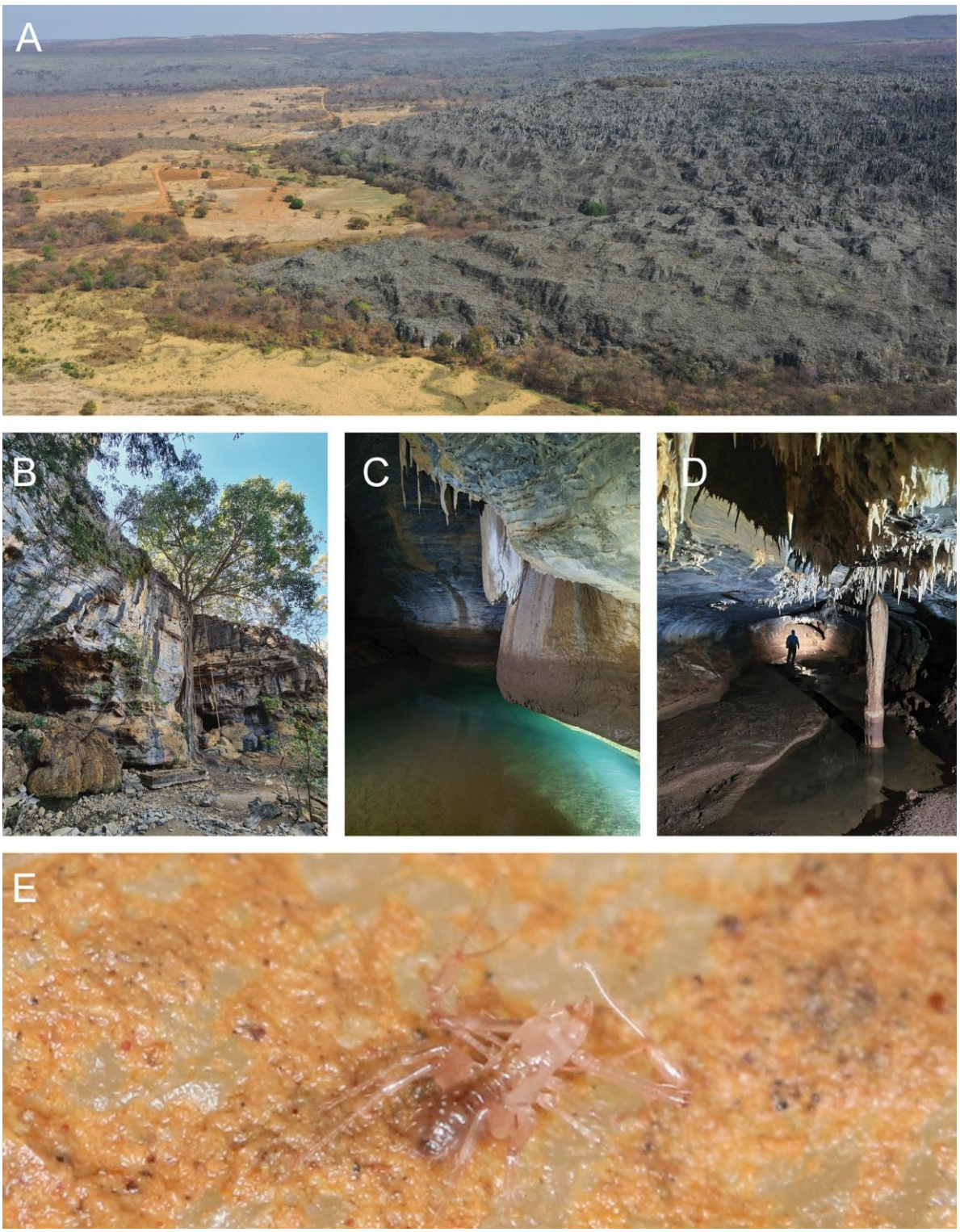


FIGURE 10. Ecological impacts to the subterranean habitat A Deforestation near cave entrance B Vegetal coal furnace.

THREE NEW TROGLOBITIC SPECIES FROM

RIGHT CONFIGURATION

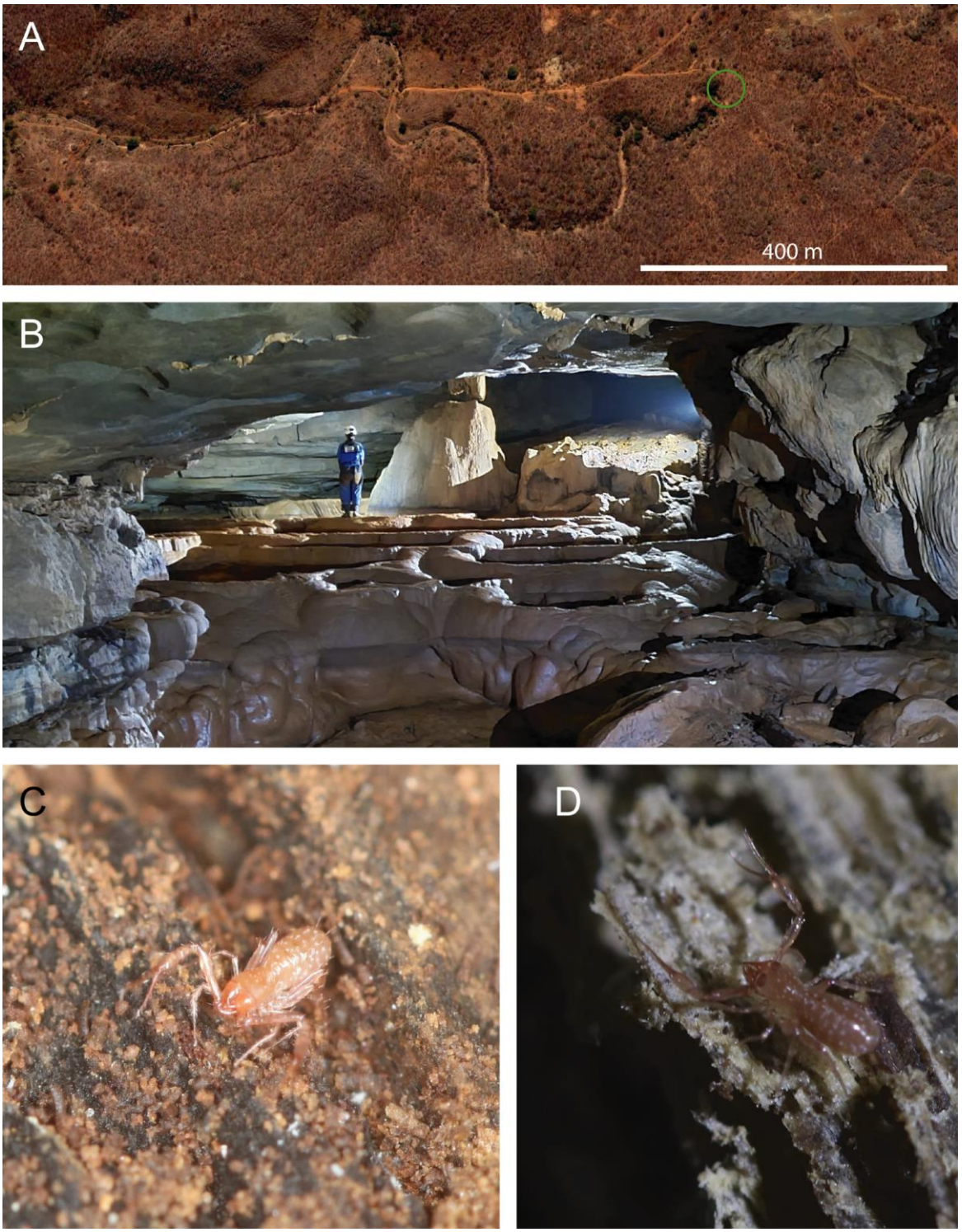


FIGURE 9. *Pseudochthonius pali* sp. nov. A Google cave region. Satellite view B Google cave general aspect C Live male holotype D Live female paratype.

THREE NEW TROGLOBITIC PSEUDOSCORPIONS FROM BRAZIL *Zootaxa* 5256 (1) © 2023 Magnolia Press 559



FIGURE 10. Ecological impacts to the subterranean habitat A Deforestation near cave entrance B Vegetal coal furnace.

Two new species of cave-dwelling pseudoscorpions *Pseudochthonius* Balzan, 1892 (Pseudoscorpiones, Chthoniidae) from northeastern Brazil: shedding light on the troglobitic status of some Brazilian species.

GUILHERME C. PRADO[1*] & RODRIGO L. FERREIRA[1]

[1]*Centro de Estudos em Biologia Subterrânea, Departamento de Ecologia e Conservação, Universidade Federal de Lavras, Lavras, MG. CEP 37200-900, Brazil.*
[1]*Email adresses: Guilherme C. Prado (prado.gcp.99@gmail.com) & Rodrigo L. Ferreira (drops@ufla.br)*

Date of submission: 09/06/2023

Abstract
Two new pseudoscorpion species, *Pseudochthonius aware* **sp. nov.** and *Pseudochthonius itakuatiara* **sp. nov.** are herein described. These species exhibit distinct characteristics that differentiate them from other congeneric species, including variations in chelal and cheliceral dentition, coxal chaetotaxy, and measurements. In addition to the taxonomic details, we provide ecological observations for each species, identify potential threats, propose avenues for future research, and offer a key for distinguishing the *Pseudochthonius* species found in Brazil.

Keywords: Cave-dwelling, pseudoscorpion, subterranean biology, taxonomy, troglomorphism

Correspondence: prado.gcp.99@gmail.com

Background
Pseudoscorpions (Arachnida: Pseudoscorpiones) are small predatory arthropods with a wide global distribution across terrestrial habitats in six continents, excluding Antarctica. They can be found in a variety of habitats such as leaf litter, under bark or stones, bird nests or animal burrows. Some species are adapted to the subterranean environment and are known to exhibit troglomorphic traits (Červená et al. 2021; Chamberlin 1931; Harms 2018; Harvey 1988). This diverse group of arachnids consists of 26 families (including an extinct one) and 473 extant genera (Benavides et al. 2019; Lin et al. 2022; World Pseudoscorpiones Catalog 2023).

The family Chthoniidae is recognized for its remarkable species diversity, comprising over 800 species distributed among 51 genera worldwide. In Brazil, 11 genera from this family have been identified, with the genus *Pseudochthonius* being the most prevalent. The distribution of this genus in Brazil spans six states across four different regions, in addition to its occurrence in other countries in Africa, Asia, Europe, Central America, and South America (World Pseudoscorpiones Catalog 2023). They can be distinguished by the presence of plumose coxal spines on coxae I and II (Figs 1G, 4G), the absence of an intercoxal tubercle, and the characteristic sigmoid shape of the chelae, with the exception of *Pseudochthonius orthodactylus* Muchmore 1970, which lacks this trait (Chamberlin 1929).

Recently, five new species of *Pseudochthonius* have been described for northeastern Brazil, *Pseudochthonius ramalho* Schimonsky et al. 2022, *Pseudochthonius pali* Prado and Ferreira 2023, *Pseudochthonius diamachi* Prado and Ferreira 2023, *Pseudochthonius koinopoliteia* Prado and Ferreira 2023 and *Pseudochthonius lubueno* Assis et al. 2023. Notably, *Pseudochthonius biseriatus* Mahnert 2001, previously regarded as troglobiont and restricted to a single cave in southeastern Brazil (Gruta Olhos d'Agua cave, Itacarambi municipality, Minas Gerais State) had its distribution extended to Pernambuco state, located in northeastern of Brazil (Schimonsky 2022; Prado and Ferreira 2023; Bedoya-Roqueme et al. 2023). These significant findings underscore the potential for further discoveries in recent surveys conducted within the northeast region and invite reconsideration regarding the cave-restricted distribution of certain species within the genus.

Cave surveys carried out in the Santa Maria da Vitória region (southwestern Bahia state, Brazil) have yielded to the discovery of two newly identified species of *Pseudochthonius*, which are described in this study. Additionally, we provide ecological observations for each species, assess potential threats to their habitats, propose directions for future research, and offer a comprehensive key to distinguish the *Pseudochthonius* species found in Brazil.

Materials and methods

Study area

The species herein described were found within two distinct cave environments located in the municipality of Santa Maria da Vitória, situated in the southwestern part of Bahia state, in the northeastern Brazil. The first cave, Gruta do Padre, is a karstic limestone formation extending over 16,400 meters, making it one of Brazil's most extensive cave systems as documented by Rubbioli et al. (2019). This cave is characterized by its intersection with the Santo Antônio river, and it is divided into three distinct stratigraphic levels. Additionally, the river's course runs through the cave's lowest stratum, situated approximately 120 meters beneath the surface (Figs 1A, C, 3D).

The second site, Gruta da Pedra Escrevida, also a limestone cave, covers a horizontal distance of approximately 470 meters. Its single entrance is positioned at the bottom of a sinkhole (doline) and lies roughly 4 km from Gruta do Padre's primary entrance and about 2.5 km from its secondary (downstream) entrance. The entrance leads to an upper disphotic chamber, predominantly arid throughout the year, beside which a vertical fissure opens into a large hall decorated with an array of speleothems (Figs 1A–B, 6A–B).

The climate of this region falls under the "Aw" category according to the Köppen's climate classification, characterized by a dry winter and an average annual precipitation of 640 mm^3 (Alvares et al. 2013). This area resides within the Caatinga biome, a semi-arid region in Brazil, and features transitional zones to the Cerrado biome, also known as the Brazilian Savannah (Cole 1960). Further sections will provide an in-depth ecological description of each species discovered within these caves, elucidating their habitat preferences and ecological adaptations (see the sections on *Ecological remarks* of each species).

Field sampling

Fieldwork was carried out in August and September 2021, as well as in May 2022, as part of a research project aiming to analyse the influence of habitat structure on the richness and composition of cave

communities in Bahia State. In the Santa Maria da Vitória region, a total of 26 caves were sampled using untimed direct intuitive searches (following the approach outlined by Wynne et al. 2019) along multiple 10x3 m transects. The number of transects sampled was proportional to the size of each cave. Special attention was given to microhabitats and organic deposits during opportunistic sampling throughout the caves. All invertebrates encountered were collected using a fine brush and preserved in 70% ethanol for further analysis.

Analysis and preparation

The specimens were examined using optical microscopes. General observations were made using a Zeiss Axio Scope A1 optical microscope, equipped with ZEN 2012 software. Illustrations of coxae and male genitalia were produced using a drawing tube attached to an Olympus BX40 optical microscope with phase contrast. To stabilize structures for observation and drawings, kaiser's glycerol gelatine medium was employed. Other structures and appendages were photographed using a Zeiss Axio Zoom V16 microscope with ZEN 2.1 software. The images were then vectorized using the Inkscape 1.1 software package (Montesanto 2015; available at inkscape.org). The holotype and paratypes have been deposited in the Coleção de Invertebrados Subterrâneos de Lavras (ISLA).

Terminology

Terminology follows Chamberlin (1931), Harvey (1992), Judson (2007) and Zaragoza (2017). (See *List of abbreviations* for details).

Results

urn:lsid:zoobank.org:pub:20A047C8-0D5D-47ED-AB5C-252BA0F3839E

Family Chthoniidae Daday, 1888

Genus *Pseudochthonius* Balzan, 1892

***Pseudochthonius aware* sp. nov.**

(Figs 1–3)

Material examined. ISLA 106129 (Holotype), male (Fig. 3B), collected 24 August 2021, preserved in 70% ethanol: Brazil, Santa Maria da Vitória, Bahia, Gruta do Padre Cave (13º12'58.8"S, 44º03'54.7"W), 24 August 2021, leg. R.L Ferreira. ISLA 106130, 106809–106817 (Paratypes): adult, one individual each, same sampling location as holotype, ISLA 106130 (female, Fig. 3C), ISLA 106809 (female), ISLA 106810 (female), ISLA 106811 (female), ISLA 106812 (female), ISLA 106813 (male), ISLA 106814 (male), ISLA 106815 (female), ISLA 106816 (female), ISLA 106817 (female). ISLA 106805–106808 (Tritonymphs), one individual each, same location as holotype. ISLA 106130, 106809–106812 collected on 28 May 2022, leg. R.L. Ferreira, ISLA 106813–106817 collected on 24 August 2021, leg. R.L. Ferreira.

Etymology. The specific epithet, "aware", is derived from the Tupi-guarani language, where it means "priest". This name is in reference to the Gruta do Padre cave, which translates to "priest's cave", location where the new species was discovered. The name is to be treated as a noun in apposition.

Diagnosis. The new species most closely resembles to *P. olegario* and *P. pali*. in the following combination of character states: Absence of eyes or eyespots; carapace with a strong posterior constriction (confirmed by the difference between ocular width and posterior width), small projected backwards dentition on the movable chelal finger and rallum with 7 blades. *Pseudochthonius aware* **sp. nov.** differs from *P. olegario* by the presence of 36–40 small and projected backwards teeth (*P. olegario* presents 26 small and projected backwards teeth) and by the *ist–est*/*ist–esb* trichobothria ratio of 2.34–2.61 (*P. olegario* with 3.3). The new species also differs from *P. pali* by the arrangement of the trichobothrium *et*, located proximal to tricobothrium *dx* (*P. pali* with trichobothrium *et* grouped with trichobothria *est* and *it*) and by the presence of 4 setae on tergite I (*P. pali* with 2 setae on tergite I).

Description (Figs 4B–C). *Adults:* Body pale yellowish, very translucent; chelicerae slightly orange, abdomen beige. Some parts of the body scaly. Vestitural setae sharp and anteriorly projected.

Carapace (Fig. 2A). 1.05–1.06 times longer than wide, strongly constricted posteriorly showing a difference between ocular width and posterior width of 0.12–0.13 mm (Fig. 2A); anterior margin fully serrated; absence of eyes or eyespots; epistome strongly dentate and saw-like (ranging to seta *al*); posterior margin of carapace smooth; chaetotaxy 4(2): 4: 4: 2: 2 (18).

Chelicera (Figs 2H). Hand with 5 setae; movable finger with 1 subdistal seta; galea present as a tubercle; fixed finger with 11 well separate and homogeneous teeth, absence of isolated tooth; movable finger with 11 well separate and homogeneous teeth, distal one slightly isolated; rallum with 7 blades; serrula exterior with 14 blades, serrula interior with 12 blades.

Tergites. Not divided; surface smooth; chaetotaxy uniseriate, I–XI 4: 4: 4: 4: 4: 6: 6: 6: 4: 2: 2. Pleural membranes striate.

Coxae (Figs 2D, G). Manducatory process with two apical setae; rest of palp coxae with 3 setae arranged in a triangle; delicate lamellae outlined by 12 small spines. Pedal (Fig. 1D, H): coxal spines plumose, arranged in a single transverse row in coxae I (3) and II (5) (Fig. 1H), coxae I-IV chaetotaxy 4(1):4–5:7:7–8.

Genital operculum of male (Fig. 2E). 8 discal setae, 6 marginal setae on each side of the opening, 10 setae on the third tergite.

Genital operculum of female. 8 setae distributed in two horizontal rows: 2: 2: 4. Opening not bifurcated.

Sternites. Chaetotaxy IV–XI: (2–3)10–11(2–3): 7–8: 8–10: 8: 6–8: 6: 4–5: 2. Anal operculum with 2 ventral setae.

Palp (Figs 2F, I). Trochanter 1.36–1.57 times longer than wide, patella 1.7 times longer than wide, femur 5.13 times longer than wide. Femoral chaetotaxy 5: 6: 4: 6: 2. Trichobothrial pattern: *ib* and *isb* located at the half portion of the hand, adjacent to each other and slightly dislocated to the paraxial face of the chela, *eb* proximal to *esb*, *ist* distal to *esb*, *it* proximal to *est*, *et* proximal to *dx*; *ist* almost exactly between *esb* and *est* (ratio distance *ist-est*/*ist-esb* = 2.34–2.61). Fixed finger slightly bent; movable finger slightly bent (Fig. 2I). Chelal fixed finger with 35–38 acute and paired teeth, except for the two rounded most basal teeth. Movable finger with 36–40 small and projected backwards teeth.

Leg IV (Fig. 2C). Arolia slightly smaller than claws; absence of protuberance or hump near end of tarsus. (Fig. 2C).

Measurements (length/width or depth in mm; ratios in parenthesis calculated by using three significant digits): Male holotype and female paratype range. Body length 1.236–1.459. Carapace 0.43–0.45/0.41–0.43 (1.1). Palps: trochanter 0.16–0.20/0.12–0.13 (1.4–1.6), femur 0.61–0.62/0.11–0.12 (5.1–5.4),

patella 0.26–0.21/0.12–0.13 (1.7–2.1), chela 0.87–0.88/0.13–0.15 (5.9–6.5), movable finger length 0.57. Leg I: trochanter 0.11–0.12/0.18–0.20 (1.0–1.1), femur 0.34–0.35/0.07 (5.1–5.4), patella 0.18–0.19/0.05 (3.3–3.7), femur/patella 1.81–1.98, tibia 0.19–0.20/0.04 (4.8–5.0), tarsus 0.33/0.03–0.04 (8.9–9.6). Leg IV: Trochanter: 0.13–0.15/0.11 (1.3–1.4), femur + patella 0.49–0.51/0.18–0.20 (2.5–2.8), tibia 0.33/0.07 (4.2–4.4), basitarsus 0.18–0.19/0.06 (3.1–3.3), telotarsus 0.34/0.04 (9.1–9.6).

Tritonymph: Body pale, mostly depigmented, chelicerae and chelae dark beige, abdomen pale mostly dyspigmented. Vestitural setae sharp, anteriorly projected on carapace and posteriorly projected in opisthosoma.

Chelicera. With 5 setae and 1 on movable finger; galea present as a tubercle; rallum with 6 blades.

Palp. Trochanter 1.63, femur 5.18, patella 1.86, chela 6.33, hand 1.92 times long than broad, and movable finger 2.85 times longer than hand. Fixed chelal finger with 6 trichobothria (*eb, esb, ist, est, it, et*), movable chelal finger with 3 trichobothria (*b, st, t*) and hand with 1 trichobothria (*ib*). Fixed chelal finger with 28 acute and paired and movable chelal finger with 27 projected backwards teeth (the 4 most basal rounded), *ist*–est/*ist–esb* ratio of 2.64.

Carapace. 1.08 times longer than broad; without eyes or eyespots.

Legs. much as in adults.

Abdomen. tergal chaetotaxy (I–XI): 4: 4: 4: 4: 4: 6: 6: 6: 2: 2: 2. Sternal chaetotaxy I–XI: 2: (0) 7 (0): (0) 3 (0): 4: 4: 4: 5: 6: 4: 2: 2. Anal opening without setae.

Measurements. Body length 1.151. Palps: trochanter 0.147/0.090, femur 0.440/0.085, patella 0.173/0.093, chela 0.658/0.104. hand length 0.2, movable finger length 0.417. Carapace 0.371/0.344.

Ecological Remarks

Gruta do Padre Cave, spanning an impressive length of 16,400 meters, is one of the largest caves in Brazil, ranking as the country's fifth longest cave (Rubbioli et al. 2019). Furthermore, it constitutes an integral component of Brazil's extensive subterranean hydrological system, encompassing the largest section traversed by the Santo Antônio river. The cave encompasses three distinct levels, with the lowest level accommodating the river watercourse at approximately 120 meters below the surface (Fig. 3D). Accessible through the main cave entrance (Figs 3B, 4A), the upper level is characterized by expansive galleries, many of which have been enlarged through the occurrence of collapsing processes (Fig. 3C). These galleries are disjointed throughout the system, divided into three sets along the cave's course. Two sets are linked to entrances, while the largest set is situated upstream in a deeper section of the cave, resulting in limited direct interaction with external environments. Consequently, this section houses most of the oligotrophic areas within the cave.

Specimens of *Pseudochthonius aware* sp. nov. were only found in the aforementioned cave, despite extensive sampling efforts in 23 other caves within the region. These pseudoscorpions exhibit a wide distribution throughout the cave, occupying both the upper chambers and the cave stream conduit. Their presence becomes apparent approximately 300 meters from the main entrance, where they can be observed along the lower-level conduit, in association with sediments deposited along the riverbank, as well as in the upper galleries located in the deeper sections of the cave.

Notably, in the lower cave level, characterized by a higher abundance of organic matter, individuals of *P. aware* sp. nov. were often found near organic debris, such as decomposing plant material carried by water. They exhibited associations with other invertebrates, particularly

springtails, suggesting a potential attraction to these areas in search of prey. Conversely, in the oligotrophic upper galleries, where organic resources are scarce, the few specimens observed were observed walking on the cave floor, often far from visible organic sources. This apparent shift in foraging strategy between the distinct cave levels could be attributed to differences in prey availability. Areas abundant in prey may facilitate a sit-and-wait strategy, while areas lacking other invertebrates, such as the oligotrophic upper chambers, may necessitate a more active search for prey. It is important to note that these observations were made during limited visits to the cave, conducted in different years. Therefore, further studies are warranted to better elucidate potential changes in the species' behavior and provide a more comprehensive understanding of its ecological dynamics.

The troglomorphic traits exhibited by *P. aware* sp. nov. are of significant importance. In addition to the absence of eyes and reduced pigmentation, this species displays an expansion of the anterior portion of the carapace. Prado and Ferreira (2023) have recently proposed this characteristic as a notable troglomorphic trait within the genus. Therefore, based on these observations, *P. aware* sp. nov. can be confidently classified as a troglobitic species.

In addition to the newly described species presented in this study, the Gruta do Padre cave is known to host a diverse array of troglobitic organisms. These include the amphipod *Spelaeogammarus santanensis* (Koenemann and Holsinger 2000), the beetle *Coarazuphium tessai* (Godoy and Vanin 1990), the isopods *Pectenoniscus santanensis* (Cardoso et al. 2020) and *Chaimowiczia tatus* (Cardoso et al. 2021), and the millipede *Phaneromerium cavernicolum* (Golovatch and Wytwer 2004). Furthermore, recent explorations have led to the discovery of several other troglobitic species within the cave, indicating that Gruta do Padre will likely emerge as a significant hotspot of subterranean biodiversity in Latin America in the near future.

The external environment surrounding the cave has undergone significant alterations, particularly due to the conversion of native vegetation into pastures (Fig. 3A). It is worth noting, however, that the vast extent of the cave and its limited accessibility to speleologists have contributed to the preservation of its inner sections. Nevertheless, the deforested areas in close proximity to the cave are susceptible to soil erosion during heavy rainfall, leading to the transportation of sediments into the cave system and resulting in the silting of the lower chamber. This silting process is evident in the upstream sections of the cave, where fine sediments have been gradually deposited over the past few decades. As a significant portion of the habitat of this species comprises the riverbanks in the lower cave level, changes in sedimentation rates can both disrupt their available microhabitats and hinder the transport of organic matter from external environments. These alterations pose concerns for the future of not only this species but also other endemic species within this unique cave ecosystem.

***Pseudochthonius itakuatiara* sp. nov.**

(Figs 4–5)

Material examined. ***Holotype*** female (ISLA 106131), preserved in 70% ethanol: Brazil, Santana, Bahia, Gruna da Pedra Escrevida Cave (13º16’33.6”S, 43º57’40.3”W), 02 September 2021, leg. R.L Ferreira.

Etymology. The specific epithet “itakuatiara” is derived from the Tupi-Guarani language where it means “written stone”. This name is in reference to the Gruta da Pedra Escrevida cave (in English, “written stone cave”), where the new species was discovered. The name is to be treated as a noun in apposition.

Diagnosis. The new species most closely resembles to *Pseudochthonius gracilimanus* Mahnert, 2001 in the following combination of character states: presence of 2 eyes; carapace with a posterior constriction (confirmed by the difference between ocular width and posterior width), small projected backwards dentition on the movable chelal finger and rallum with 7 blades. *Pseudochthonius itakuatiara* **sp. nov.** differs from *P. gracilimanus* by the presence of a distal microlateral tooth on the tip of the fixed finger (*P. gracilimanus* lacks the structure), by the presence of 36 acute teeth on the fixed chelal finger, whereas the medial teeth are alternated with heterodonty (*P. gracilimanus* with 23–26 acute and heterodont teeth on fixed chelal finger), by the presence of heterodonty only in fixed chelal finger (*P. gracilimanus* with heterodonty in both fingers) and by the *ist–est*/*ist–esb* trichobothria ratio of 2.21 (*P. gracilimanus* presents *ist* halfway between trichobothria *est* and *esb*).

Description. Body pale yellowish; chelicerae slightly orange, abdomen beige. Some parts of the body scaly. Vestitural setae sharp, anteriorly projected on prosoma and posteriorly projected on opisthosoma.

Carapace (Fig. 5A). 1.03 times longer than wider, slightly constricted posteriorly showing a difference between ocular width and posterior width of 0.062 mm (Fig. 5A); anterior margin partially serrated; presence of a pair of eyes; epistome small and strongly dentate (ranging to seta *ame*); posterior margin of carapace smooth; chaetotaxy 4(2): 4: 4: 2: 2 (18).

Chelicera (Figs 5C). Hand with 5 setae; movable finger with 1 subdistal seta; galea present as a tubercle; fixed finger with 8 acute teeth (2nd and 3rd grouped) (Fig. 5C); movable finger with 11 acute teeth (including a large distal one) with 2nd to 4th grouped (Fig. 5C); rallum with 7 blades; serrula exterior with 14 blades, serrula interior with 10 blades.

Tergites. Not divided; surface smooth; chaetotaxy uniseriate, I–XI 4: 4: 4: 4: 6: 6: 6: 6: 6: 4: 4. Anal operculum without dorsal setae. Pleural membranes slightly striate.

Coxae (Figs 5D). Manducatory process with two apical setae; rest of palp coxae with 3 setae arranged in a triangle; delicate lamellae outlined by 12 small spines. Pedal (Figs 5D, 5G): coxal spines plumose, arranged in a single transverse row in coxae I (3) and II (4) (Fig. 5F), coxae I-IV chaetotaxy 4(1):4:7:8.

Genital operculum (Fig. 5H). 8 setae distributed in three horizontal rows: 4: 2: 2, genital opening not bifurcated, 3rd tergite with 4 marginal setae.

Sternites. chaetotaxy IV–XI: (2)10(2): (2)8(2): 6: 6: 6: 6: 4: 2 + 2 sensory setae. Anal operculum without any ventral setae.

Palp (Figs 5E–F). Trochanter 1.71 times longer than wide, patella 1.95 times longer than wide, femur 4.7 times longer than wide. Femoral chaetotaxy 5: 4: 2: 5: 1. Trichobothrial pattern: *ib* and *isb* located at the half portion of the hand, adjacent to each other, slightly dislocated to the paraxial face of the chela, *eb* proximal to *esb*, *ist* distal to *esb*, *it* proximal to *est*, *et* distal from *it* and proximal to *dx*; *ist* closer to *est* than *esb* (ratio distance *ist-est*/*ist-esb* = 2.21). Fixed finger slightly bent; movable finger slightly bent (Fig. 5F). Chelal fixed finger with 36 teeth, the 19 more basal rounded and uniseriate, 9 medial teeth biseriate, 8 distal acute uniseriate teeth and a lateral micro denticule at the end of the chelae. Movable finger with 32 tiny projected backwards teeth (Fig. 5F).

Leg IV (Fig. 5B). Arolia almost with the same length as claws; end of the tarsus thin and long.

Measurements of the Holotype (length/width or depth in mm; ratios in parenthesis calculated by using three significant digits). Body length 1.24. Carapace 0.36/0.35 (1.0). Palps: trochanter 0.16/0.09 (1.7), femur 0.46/0.10 (4.7), patella 0.20/0.10 (2.0), chela 0.67/0.11 (6.1), movable finger length 0.45. Leg

I: trochanter 0.11/0.08 (1.4), femur 0.23/0.06 (4.1), patella 0.13/0.04 (3.1), femur/patella 1.72, tibia 0.14/0.04 (3.8), tarsus 0.25/0.03 (8.2). Leg IV: Trochanter: 0.11/0.10 (1.2), femur + patella 0.41/0.16 (2.6), tibia 0.25/0.07 (3.7), basitarsus 0.15/0.05 (3.0), telotarsus 0.27/0.03 (9.3).

Ecological Remarks

The specimen of *Pseudochthonius itakuatiara* sp. nov. was found in the Gruna da Pedra Escrevida cave. Despite conducting invertebrate sampling in 23 other caves within the region, no additional specimens were encoutered. This limestone cave spans approximately 470 meters horizontally and features a single entrance situated at the base of a sinkhole (doline) (Figs 6A–B). It is located approximately 4 km from the main entrance of the Gruta do Padre cave and approximately 2.5 km from its secondary (downstream) entrance. The cave entrance leads to an upper disphotic chamber, which remains dry for the majority of the year. Adjacent to this chamber is a vertically oriented fissure that grants access to a spacious hall adorned with abundant speleothems. The floor of this hall, consistently humid throughout the year, is entirely covered by travertine pools (Fig. 6D). Within the lowermost part of this chamber, amidst rock blocks, a narrow oblique crevice provides entry to the third and final chamber of the cave (Fig. 6C). This segment represents the deepest region of the cave, situated at least 40 meters below the surface. The area is characterized by high moisture levels, seemingly receiving water during periods of rainfall. Organic matter in this section is limited to a few piles of bat guano and scattered plant debris. The specimen of *P. itakuatiara* sp. nov. was discovered in this deepest chamber, observed traversing the damp cave floor.

In contrast to the wide distribution observed for *P. aware* sp. nov. within the Gruta do Padre cave, the presence of a single specimen of *P. itakuatiara* sp. nov. in the Pedra Escrevida cave, despite two sampling events, indicates its relative rarity. It should be noted that two other caves located within the same collapsed doline were also sampled, but no specimens of this species were found. However, these caves exhibit predominantly dry conditions, lacking the moist habitats observed where the specimen of *P. itakuatiara* sp. nov. was encountered.

Key to Brazilian *Pseudochthonius* species

1 Eyes absent 2
- Presence of a pair of eyes or eyespots in one or both gender 3
2 Trichobothrium *ist* closer to *est* than to *esb* ..... *Pseudochthonius koinopoliteia*
- Trichobothrium *ist* closer to *esb* than to *est* or *ist* halfway from *esb* and *est* 4
3 Chelal fixed finger with heterodonty (off-set sawlike) 5
- Chelal fixed finger without heterodonty (simple row of teeth) 6
4 Body length with at least 2.0mm ..... *Pseudochthonius diamachi*
- Body length less than 2.0mm 7
5 Carapace 1.0–1.1 times longer than wide, chelal fixed finger teeth with microteeth on 15th and 29th teeth, endemic to Gruta do Vandercir, Serra do Ramalho, BA .....*Pseudochthonius ramalho*
- Carapace > 1.1 times longer than wide, chelal fixed finger without microteeth between chelal fixed finger dentition 8
6 Chelal morphology typically sigmoid with a small apodeme, with flattened teeth on movable finger ..... *Pseudochthonius homodentatus* Chamberlin, 1929

- Chelal morphology highly straight, large and well-developed apodeme, bearing rounded basal teeth in both fingers..... *Pseudochthonius orthodactylus*

7 Epistome acute and smooth, endemic to Lapa Zé de Sidinei, Presidente Olegário, MG ..... *Pseudochthonius olegario* Assis et al. 2021

- Epistome acute and highly serrated..... 9

8 Chelal fixed finger bearing more than 26 teeth 10

- Chelal fixed finger bearing less than 26 teeth..... 11

9 Heterodonty on fixed chelal finger present only after the 10th teeth from basal to distal one.. 12

- Heterodonty present on almost the whole dentition of chelal fixed finger 16

10 Epistome small and highly dentate, *ist–est*/*ist–esb* ratio near 2.0, chelal movable finger with less teeth than chelal fixed finger..... 13

- Chelal movable finger with more teeth than chelal fixed finger, with occurrence in São Paulo state..... 14

11 Chelal movable finger with heterodonty dentition *Pseudochthonius gracilimanus* Mahnert, 2001

- Chelal movable finger partially or fully projected backwards homodont teeth 15

12 Trichobothrium *et* proximad to *it* and distad to *dx*..... *Pseudochthonius pali*

- Trichobothrium *et* distad to *it* and proximad to *dx* ..... *Pseudochthonius aware* **sp. nov.**

13 Carapace with two weak eyespots, fixed chelal teeth row with a distal isolated tooth, chelae 5.2 times longer than broad..... *Pseudochthonius tuxeni* Mahnert, 1979

- Carapace with two strong eyes, fixed chelal finger with a micro lateral denticle, chelae 6.1 times longer than broad..... *Pseudochthonius itakuatiara* **sp. nov.**

14 Epistome acute and prominent, with the anterior margin serrated from the epistome ranging to *ame* carapacal setae, coxa I and coxae II bearing two coxal spines..... *Pseudochthonius strinatii*

- Epistome acute and highly dentate only in female, lateral portion of the anterior margin of the carapace wrinkled, presence of six setae on the last seven tergite plates (from anterior to posterior), *ist–est*/*ist–esb* ratio of 2.5..... *Pseudochthonius brasiliensis* Beier, 1970

15 Movable finger with 40 or more teeth, distally projected backwards and basally rounded teeth ..... *Pseudochthonius ricardoi* Mahnert, 2001

- Movable finger with about 30 projected backwards teeth *Pseudochthonius heterodentatus* Hoff, 1946

16 Rallum with 9 blades..... *Pseudochthonius biseriatus*

- Rallum with 5 blades..... *Pseudochthonius lubueno*

Discussion

This work describes the 15th and the 16th (*P. aware* **sp. nov.** and *P. itakuatiara* **sp. nov.**) species of *Pseudochthonius* from Brazil (World Pseudoscorpiones Catalog 2023). Among the known species within this genus, seven are recognized as troglobitic due to the absence of eyes or eyespots in one or both genders, elongated appendages, sigmoid shape of the chelae, and the anterior part of the carapace being enlarged (Beier 1969; Mahnert 2001; Assis et al. 2021; Schimonsky et al. 2022; Prado and Ferreira 2023).

Pseudochthonius aware **sp. nov.** exhibits a limited geographical range, elongated appendages (see measurements), lack of eyes or eyespots, and a marked distinction between the anterior and posterior

sections of the carapace. These characteristics are consistent with typical adaptations observed in subterranean environments (Viana and Ferreira 2018). Consequently, we consider the presence of troglomorphic traits and the species' restricted geographic distribution as compelling evidence supporting its troglobitic status.

In contrast, *P. itakuatiara* **sp. nov.** presents two well-developed eyes, relatively robust appendages (see measurements), and a less pronounced distinction between the anterior and posterior margins of the carapace compared to other blind hypogean members of the genus. These features make it challenging to ascertain this species as troglobitic. Therefore, we have chosen to classify the species as cave dwelling, but we strongly encourage further investigations into the external environment surrounding the cave to ascertain the possibility of it being a troglobitic species.

Mahnert (2001) classified two species of Brazilian *Pseudochthonius* as troglobitic: *Pseudochthonius strinatii* Beier, 1969 and *P. biseriatus*. However, the recent expansion in the distribution of *P. biseriatus* as well as the observed disjunct distribution of *P. strinatii* highlight the necessity to reconsider this classification (Bedoya-Roqueme et al. 2023).

The original occurrence of *P. strinatii*, as documented by Beier (1969), was in the Gruta das Areias cave, located in the municipality of Iporanga, São Paulo state. Additional individuals were examined by Manhert (2001) in the same region, specifically in Morro Preto cave in the municipality of Iporanga, São Paulo, and Tapagem cave in the municipality of Eldorado, São Paulo. Furthermore, individuals from other states were identified as belonging to the same species, with reports from caves in Minas Gerais state (Buraco do Medo cave in Sete Lagoas municipality and Lapa Vermelha I cave in Confins municipality) and Paraná state (Gruta do Rocha cave in Adrianópolis municipality).

For *P. biseriatus*, the initial documented occurrence was recorded by Mahnert (2001) in Gruta Olhos d'Água cave, located in the municipality of Itacarambi, Minas Gerais state. Subsequent investigations by Schimonsky and Bichuette (2019) revealed additional specimens from Lapa do Cipó cave, which is located in the same region, indicating a possible connection between these caves, thus supporting the troglobitic status of *P. biseriatus*. However, recently, Bedoya-Roqueme et al. (2023) expanded the known distribution of *P. biseriatus* to Furna do Morcego cave, located in Catimbau National Park in Pernambuco state, northeastern region of Brazil. This new occurrence is noteworthy due to its considerable distance from previous occurrences (more than 1,000 km in a straight line) and the fact that the cave is inserted in sandstone, a distinct rock type compared to the initial occurrences in limestone caves. Therefore, the significant distance between these caves and their association with different lithologies strongly suggests the absence of subterranean connections between them.

Therefore, in the case of both species, the disjunct distribution observed, along with the absence of subsurface connections between the caves where populations are found, could suggest that these species may not be strictly confined to cave habitats. However, disregarding the troglobitic status of these species challenges the previously discussed troglomorphic traits attributed to the genus since Beier (1969). These troglomorphic traits include elongated appendages, absence of eyes or eyespots, enlargement of the anterior portion of the carapace, and body size (Beier 1969; Mahnert 2001; Schimonsky et al. 2022; Prado and Ferreira 2023).

To resolve this impasse, we propose two hypotheses: *i)* the troglomorphic traits alone may not be sufficient to support their troglobitic status, as their distribution is sparse and isolated, lacking any communication between caves, which would make it impossible to account for their observed distributional pattern, or *ii) P. biseriatus* and *P. strinatii* actually represent at least five cryptic species

distributed in different regions. Specifically, *P. strinatii* in the Iporanga region of São Paulo (Gruta Areias de Cima cave, Morro Preto cave, and Tapagem cave), *P. aff. strinatii* sp.1 in the Pedro Leopoldo region of Minas Gerais (Lapa Vermelha I cave and Buraco do Medo cave), *P. aff. strinatii* sp.2 in the Adrianópolis region of Paraná (Gruta do Rocha cave), *P. biseriatus* in the Itacarambi region of Minas Gerais (Gruta Olhos d'Água cave and Lapa do Cipó cave), and *P. aff. biseriatus* sp.1 in Catimbau National Park, Pernambuco (Furna do Morcego cave).

Given the complexities associated with the troglobitic status and distribution of *Pseudochthonius* species, the second hypothesis presents stronger support, considering that troglomorphic traits have been predominantly observed in hypogean species and are either completely absent or significantly reduced in epigean counterparts. Therefore, it is highly recommended to conduct further studies, particularly in less-explored regions, to potentially discover additional species that could shed light on these distributional patterns. Additionally, molecular investigations are necessary to determine the species identities within each population of *P. biseriatus* and *P. strinatii*, as well as to assess the level of population structure, which would contribute to understanding potential connections among distinct populations. Consequently, prioritizing comprehensive phylogenetic analyses of the genus is crucial to determine whether *P. biseriatus* and *P. strinatii* represent distinct cryptic species.

Conclusion

In conclusion, the study of *Pseudochthonius* species in Brazil has revealed intriguing patterns regarding their troglobitic status and distribution. The presence of troglomorphic traits, such as elongated appendages, absence of eyes or eyespots, and enlarged anterior margin of carapace, has been strongly associated with subterranean adaptations. However, the disjunct distribution observed in *P. biseriatus* and *P. strinatii*, along with the absence of subsurface connections between caves, challenges the strict confinement of these species to cave habitats. Two hypotheses have been proposed to address this impasse. The first, suggests that these troglomorphic traits alone may not be sufficient to support their troglobitic status, given the isolated distribution of these species. The second and more suggestive, proposes that *P. biseriatus* and *P. strinatii* represent at least five cryptic species distributed in different regions.

To further elucidate the troglobitic status and distributional patterns of *Pseudochthonius* species, it is crucial to conduct additional studies, particularly in less-explored regions. Comprehensive phylogenetic analyses, along with molecular investigations are necessary to determine the species identities within each population. These studies will contribute to a better understanding of potential connections among distinct populations and shed light on the complexities associated with the troglobitic status of *Pseudochthonius* species in Brazil.

List of abbreviations

Abbreviations for the trichobothria: *b* = basal; *sb* = sub-basal; *st* = sub-terminal; *t* = terminal; *ib* = interior basal; *isb* = interior sub-basal; *ist* = interior sub-terminal; *it* = interior terminal; *eb* = exterior basal; *esb* = exterior sub-basal; *est* = exterior sub-terminal; *et* = exterior terminal. Abbreviations for the carapace: *al* = anterolateral setae of carapace; *ame* = anteromedial setae of carapace; *an* = anterior setae row of carapace; *il* = intermedian lateral setae of carapace; *in* = intermedian setae row of carapace; *me* = median setae row of carapace; *ml* = median lateral setae of carapace; *mm* = median medial setae of carapace; *oc* = ocular setae of carapace; *ol* = lateral oclar setae of carapace; *om* = medial ocular setae of

carapace; *osl* = sublateral ocular setae of carapace; *pl* = posterolateral setae of carapace; *pm* = posteromedial setae of carapace; *po* = posterior setae row of carapace. Abbreviation for repository: ISLA, Coleção de Invertebrados Subterrâneos de Lavras.

Acknowledgements

We thank Dr. Marconi Souza Silva (Lavras) and all the team from the Center of studies on subterranean biology from the Federal University of Lavras for their assistance on the field trips in Bahia state. We also thank to Daniel Menin, whose great pictures from the Gruta do padre cave helped to improve the quality of the paper. We would also like to thank the institutions that supported the study with funding for scholarships and infrastructure (FAPEMIG, VALE) also IABS and CECAV for the subsidized project n. 0.17/2021. RLF is grateful to the CNPq (National Council for Scientific and Technological Development) for the grant provided (CNPq n. 302925/2022-8). We also thank the anonymous reviewers and the Editor in Chief, Dr. Benny Chan, whose thoughtful comments and suggestions helped to improve the quality of this paper.

Authors' contributions

All authors contributed equally to the manuscript.

Competing interest

The authors declare that they have no competing interests.

Availability of data and materials

The type specimen was deposited into the ISLA, Lavras, Minas Gerais, Brazil.

Consent for publication

GCP and RLF declare that they have no conflict of interests.

Ethics approval consent to participate

Not applicable.

References

Alvares CA, Stape JL, Sentelhas PC, Gonçalves JLM, Sparovek G. 2013. Köppen's climate classification map for Brazil. Met Zeit **22(6):**711–728. doi.org/10.11277/0941-2948/2013/0507.

Assis LD, Schimonsky DMV, Bichuette ME. 2021. The first troglobitic Pseudochthonius Balzan, 1892 (Pseudoscorpiones, Chthoniidae) from the karst area of Serra do Ramalho, Brazil: a threatened species. Sub Biol **40:**109–128. doi.org/10.3897/subtbiol.40.77451.

Assis LD, Schimonsky DMV, Bichuette ME. 2023. Contribution to the knowledge of Brazilian troglobitic Pseudoscorpiones (Arachnida): Description of Pseudochthonius lubueno sp. nov. (Chthoniidae) from Serra do Ramalho Karst area. Zoologia **40:** e22048. doi.org/10.1590/S1984-4689.v40.e22048.

Bedoya-Roqueme E, Tizo-Pedroso E, Barbier E, Lira AFA. 2023. Two new cave-dwelling pseudoscorpion species (Arachnida: Pseudoscorpiones) from Northeastern Brazil. Zootaxa **5293(2):**317–332. doi.org/10.11646/zootaxa.5293.2.6

Beier M. 1969. Ein wahrscheinlich troglobionter Pseudochthonius (Pseudoscorp.) aus Brasilien. Rev Suisse de Zool **76(1):**1–2.

Beier M. 1970. Myrmecophile Pseudoskorpione aus Brasilien. An des Nat Mus in Wien **74:**51–56.

Benavides LR, Cosgrove JG, Harvey M.S, Gonzalo G. 2019. Phylogenomic interrogation resolves the backbone of the Pseudoscorpiones tree of life. Mol Phylogen and Evol **139:**106509. doi.org/10.1016/j.ympev.2019.05.023

Cardoso GM, Bastos-Pereira R, Souza LA, Ferreira RL. 2020. New cave species of Pectenoniscus Andersson, 1960 (Isopoda: Oniscidea: Styloniscidae) and an identification key for the genus. Nauplius **28:**e2020039, 30p.

Cardoso GM, Bastos-Pereira R, Souza LA, Ferreira RL. 2021. Chaimowiczia: a new Iuiuniscinae genus from Brazil (Oniscidea, Synocheta, Styloniscidae) with the description of two new troglobitic species. Sub Biol **39:**45–62.

Červená M, Gardini G, Jablonski D, Christophoryová J. 2021. Checklist of pseudoscorpions (Arachnida, Pseudoscorpiones) of Albania. Zool Stud **60:**17. doi.org/10.6620/ZS.2021.60-17

Chamberlin JC. 1929. The genus Pseudochthonius Balzan (Arachnida – Chelonethida). Bulletin de la Soc Zool de France **54:**173–179.

Chamberlin JC. 1931. The arachnid order Chelonethida. Stanford University Publications. Biol Sci **7:**284 pp.

Cole MM. 1960. Cerrado, caatinga and pantanal: the distribution and origin of the savanna vegetation of Brazil. The Geo J **126(2):**168–179. doi.org/10.2307/1793957.

Godoy NM, Vanin SA. 1990. Parazuphium tessai, a new cavernicolous beetle from Bahia, Brazil (Coleoptera, Carabidae, Zuphiini). Rev Brasileira de Ent **34:**795–799.

Golovatch S, Wytwer J. 2004. The South American genus Phaneromerium Verhoeff, 1941, with the description of a new cavernicolous species from Brazil (Diplopoda: Polydesmida: Fuhrmannodesmidae). An Zool **54(3):**511–514.

Harms D. 2018. The origins of diversity in ancient landscapes: deep phylogeographic structuring in a pseudoscorpion (Pseudotyrannochthoniidae: Pseudotyrannochthonius) reflects Plio-Pleistocene climate fluctuations. Zool A **273:**112–123. doi.org./10.1016/j.jcz.2018.01.001

Harvey MS. 1988. The systematics and biology of pseudoscorpions. *In:* Heather NW (ed) Australian Arachnology. Australian Entomological Society, Brisbane.

Harvey MS. 1992. The phylogeny and classification of the Pseudoscorpionida (Chelicerata: Arachnida). Invert Tax **6:**1373–1435. doi.org/10.1071/IT9921373

Hoff CC. 1946. Three new species of heterosphyronid pseudoscorpions from Trinidad. American Mus Nov **1322:**1–13.

Lin HY, Huang JX, Liu HH, Chang CH. 2022. Two new pseudoscorpion species of the coastal genus Garypus L. Koch, 1873 (Garypidae) and an updated checklist of the Pseudoscorpiones of Taiwan. Zool Stud **61:** 24. doi.org/10.6620/ZS.2022.61-24

Judson MLI. 2007. A new and endangered species of the pseudoscorpion genus of Lagynochthonius from a cave in Vietnam, with notes on chelal morphology and the composition of the

tyrannochthoniini (Arachnida, Chelonethi, Chthoniidae). Zootaxa **1627:**53–68. doi.org/10.11646/zootaxa.162.1.4

Koenemann S, Holsinger JR. 2000. Revision of the subterranean amphipod genus Spelaeogammarus (Bogidellidae) from Brazil, including descriptions of three new species and considerations of their phylogeny and biogeography. P of the Biol Soc of Washington **113(1):**104–123

Mahnert V. 1979. Pseudoskorpione (Arachnida) aus dem Amazonas-Gebiet (Brasilien). Rev Suisse de Zool **86:**719–810.

Mahnert V. 2001. Cave-dwelling pseudoscorpions (Arachnida, Pseudoscorpiones) from Brazil. Rev Suisse de Zool **108(1):** 95–148.

Montesanto G. 2015. A fast GNU method to draw accurate scientific illustrations for taxonomy. ZooKeys **515:**191–206. doi.org/10.3897/zookeys.515.9459

Muchmore WB. 1970. An unusual Pseudochthonius from Brazil (Arachnida, Pseudoscorpionida, Chthoniidae). Ent News **81:**221–223.

Prado GC, Ferreira RL. 2023. Three new troglobitic species of Pseudochthonius Balzan, 1892 (Pseudoscorpiones, Chthoniidae) from northeastern Brazil. Zootaxa **5249(1):**092–110. doi.org/10.11646/zootaxa.5249.1.5.

Rubbioli E, Auler A, Menim D, Brandi R. 2019. Cavernas – Atlas do Brasil Subterrâneo. Brasília, ICMBio/Cecav, 370 pp.

Schimonsky DMV, Bichuette ME. 2019. Distribution of cave-dwelling pseudoscorpion (Arachnida) in Brazil. J of Arach **47:**110–123. doi.org/10.1636/0161-8202-47.1.110.

Schimonsky DMV, Gallão JE, Bichuette ME. 2022. A new troglobitic Pseudochthonius (Pseudoscorpiones: Chthoniidae) from Minas Gerais State, south-east Brazil. Arachnology **19(1):** 38–46. doi.org/10.13156/arac.2022.19.1.38.

Vasconcelos ACO, Ferreira RL. 2017 Two new species of cave-dwelling Charinus Simon, 1892 from Brazil (Arachnida: Amblypygi: Charinidae). Zootaxa **4312:**277–292. doi.org/10.11646/zootaxa.4312.2.4.

Viana ACM, Souza MFVR, Ferreira RL. 2018. Spelaeobochicha goliath (Arachnida: Pseudoscorpiones: Bochicidae), a new troglobitic pseudoscorpion from Brazil. Zootaxa **4402(3):**585–594. doi.org/10.11646/zootaxa.4402.3.11.

World Pseudoscorpiones Catalog. 2021. World Pseudoscorpiones Catalog. Nat Hist Mus Bern. http/wac.nmbe.ch. Accessed 29 Apr. 2023.

Wynne JJ, Francis GH, Stefan S, Brett G. 2019. Fifty years of cave arthropod sampling: tecehniques and best practices. Int J of Speleo **48:**33–48. doi.org/10.5038/1827-806X.48.1.2231

Zaragoza JA. 2017. Revision of the Ephippiochthonius complex (Pseudoscorpiones, Cthoniidae) in the Iberian Peninsula, Balearic Islands and Macaronesia, with proposed changes to the status of the Chthonius subgenera. Zootaxa **4246:**1–221. doi.org/10.11646/zootaxa.4246.1.1.

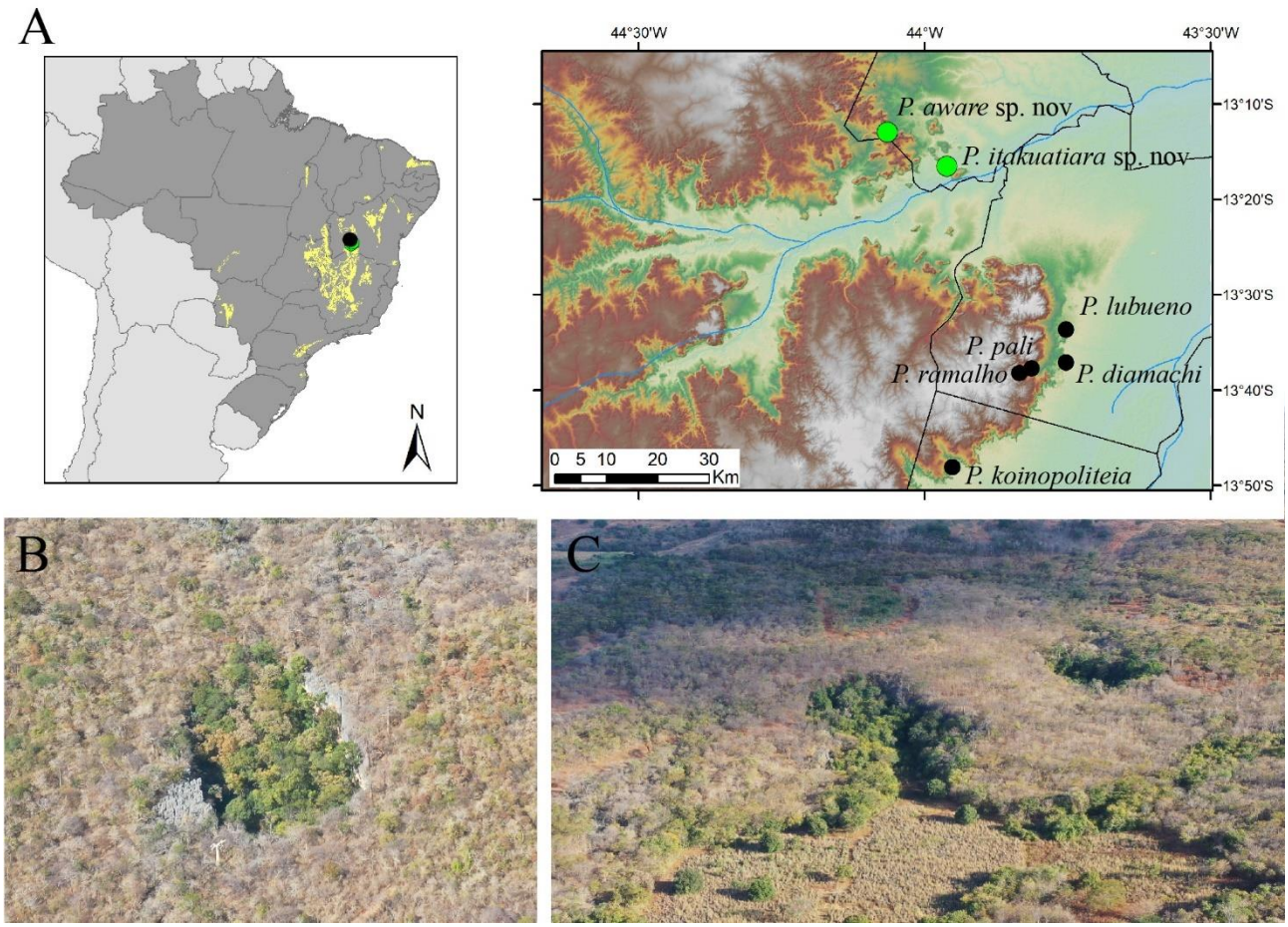


Fig. 1. (A) Brazilian karst areas, highlighting Santana's region in Bahia state, showing the type location of some Brazilian *Pseudochthonius* species, including the new ones; (B) Gruta Pedra Escrevida cave main entrance; (C) Gruta do Padre cave main entrance.

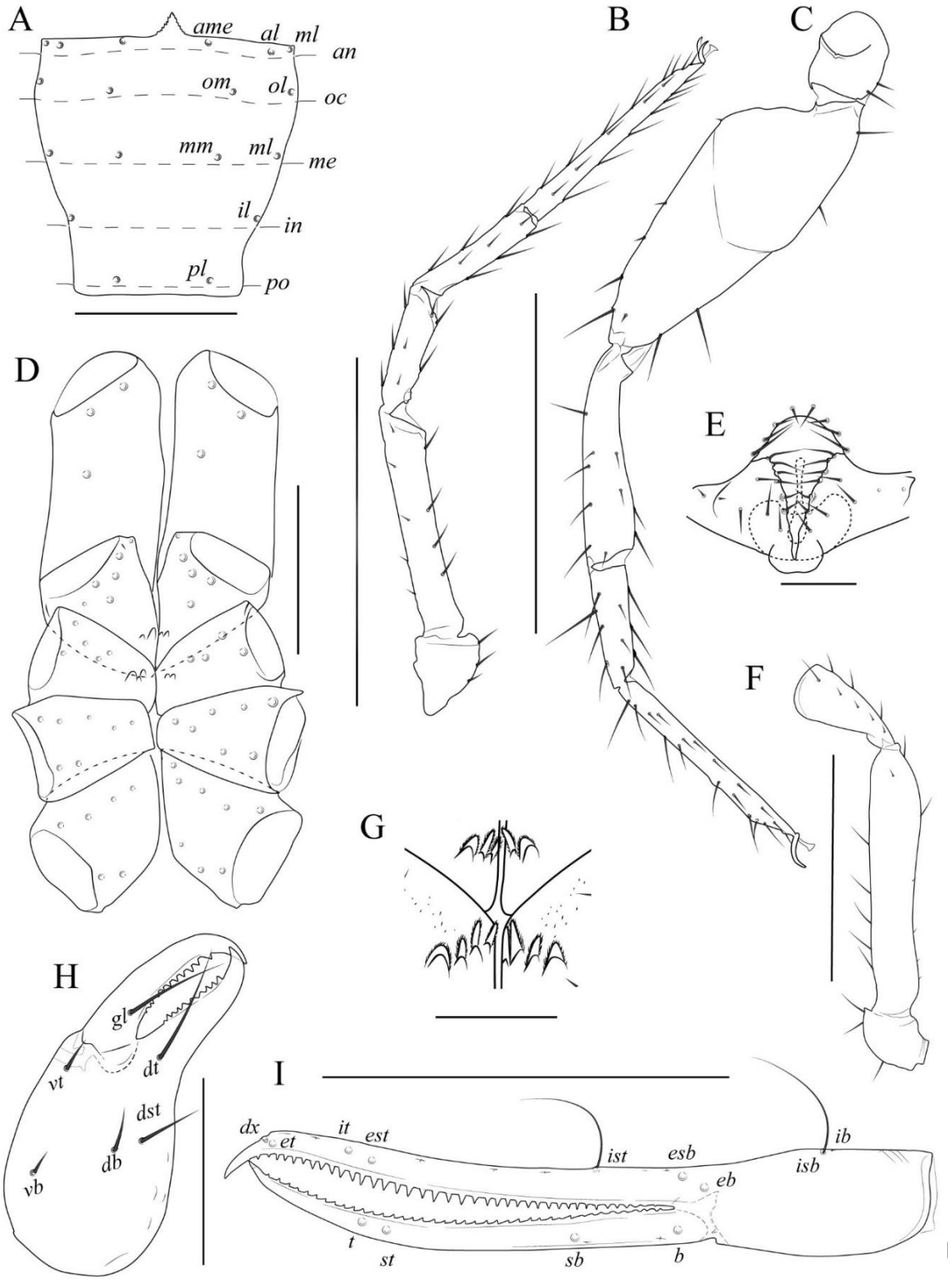


Fig. 2. *Pseudochthonius aware* **sp. nov.** male holotype. (A) Carapace, dorsal view; (B) Right leg I, antiaxial view; (C) Left leg IV, antiaxial view; (D) Palpal and pedal coxae; (E) Genitalia; (F) Left pedipalp, dorsal view; (G) Detail of coxal spines on coxae I and II; (H) Left chelicera, dorsal view; (I) Left chela showing trichobothrial pattern. Scale bars: 0.5 mm (A–C, F, I), 0.4 mm (D), 0.2 mm (H), 0.1 mm (E), 0.05 mm (G).

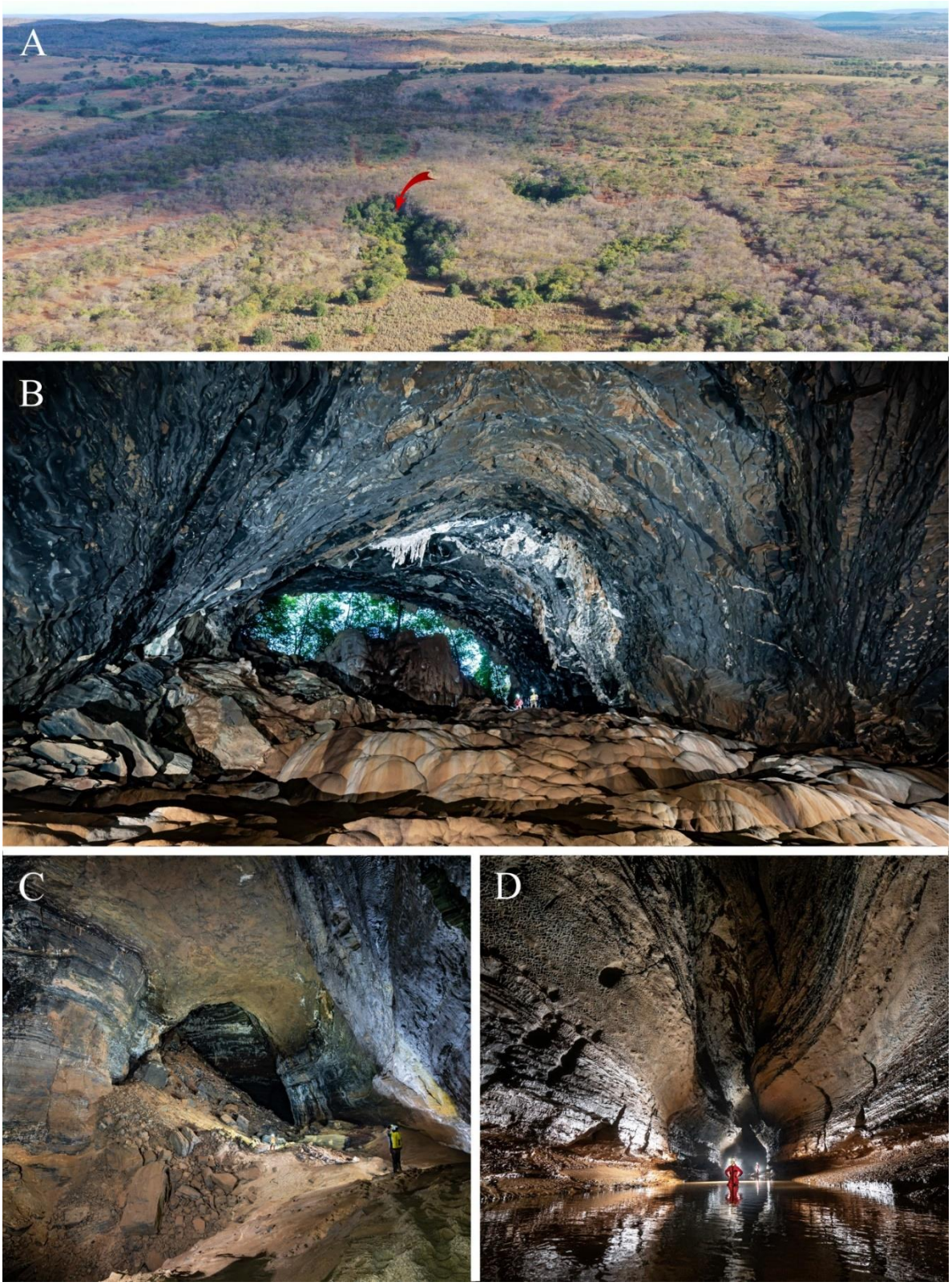


Fig. 3. Gruta do Padre cave region. (A) Cave surroundings and external landscape, showing main entrance location; (B) Main entrance; (C) Upper chamber; (D) Lower chamber, showing the Santo Antônio river.

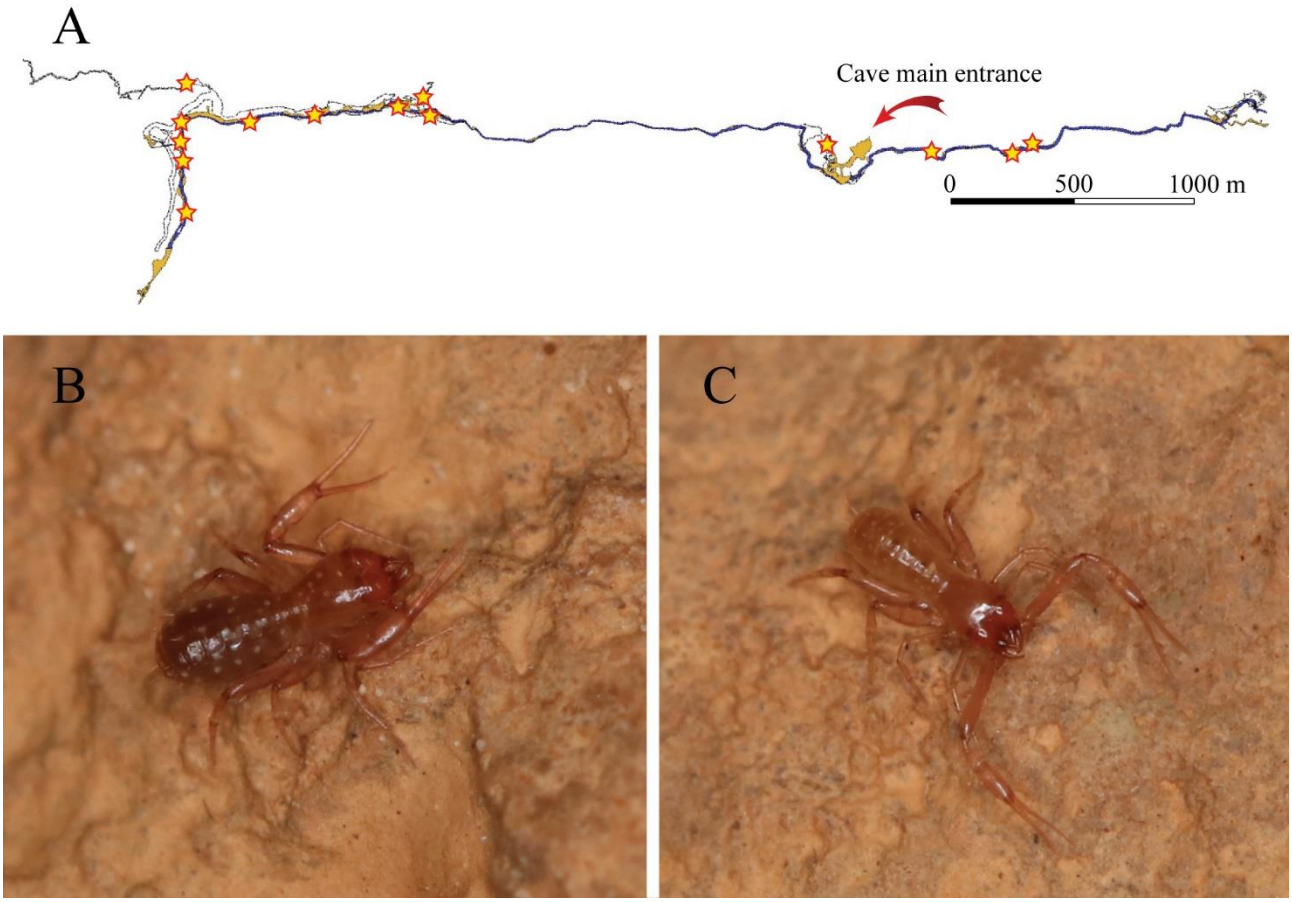


Fig. 4. (A) Gruta do Padre cave map, showing *Pseudochthonius* collection locations (yellow stars) and main entrance; (B) *Pseudochthonius aware* **sp. nov** holotype live habitus; (C) *Pseudochthonius aware* **sp. nov** paratype live habitus.

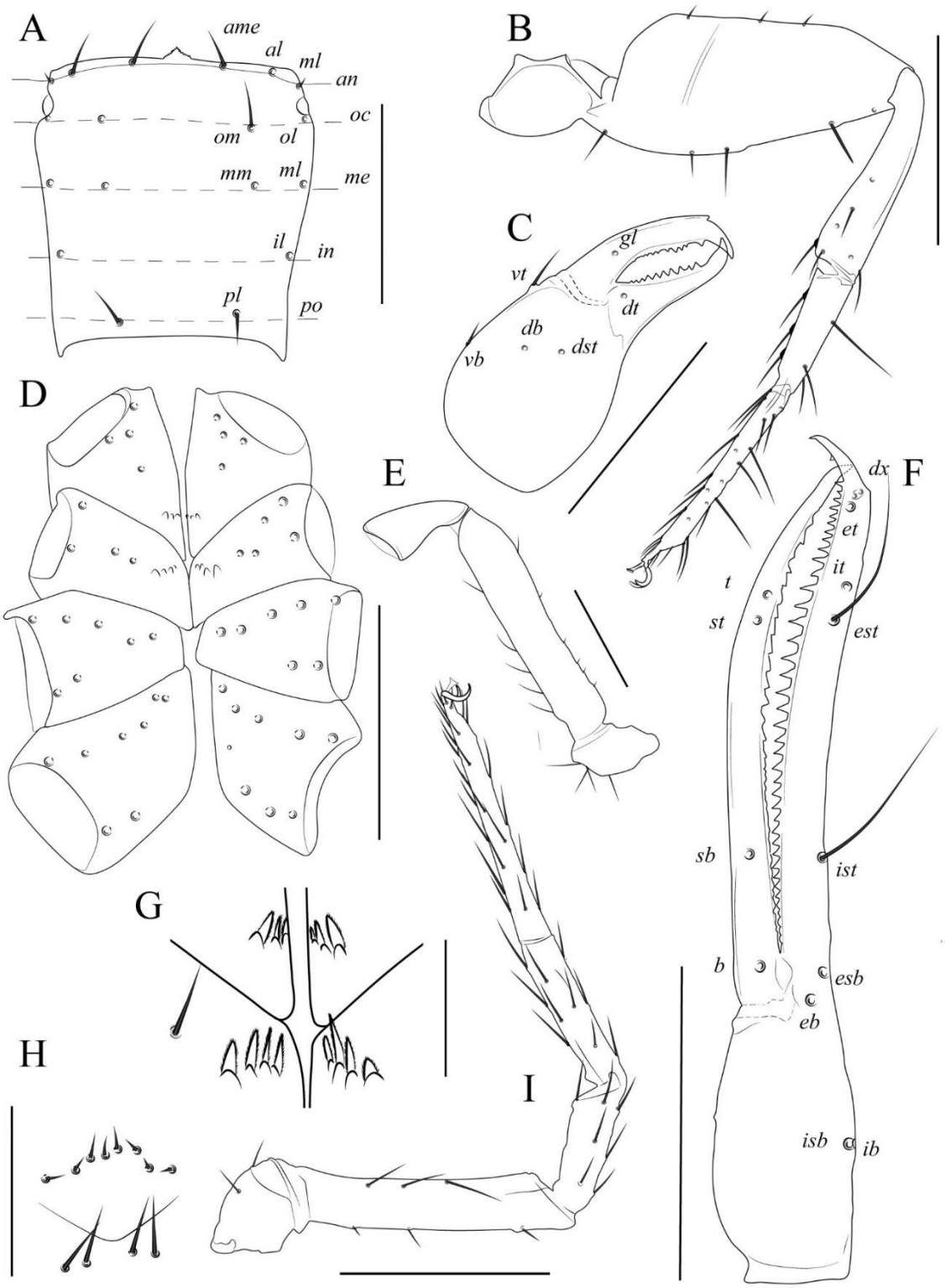


Fig. 5. *Pseudochthonius itakuatiara* **sp. nov.** female holotype. (A) Carapace, dorsal view; (B) Right leg IV, antiaxial view; (C) Left chelicera, dorsal view, antiaxial view; (D) Pedal coxae; (E) Right pedipalp, dorsal view; (F) Left chela showing trichobothrial pattern; (G) Detail of coxal spines on coxae I and II; (H) Genitalia; (I) Right Leg I, paraxial view. Scale bars: 0.5 mm (B, F), 0.25 mm (A), 0.2 mm (C–E, I), 0.1 mm (H), 0.05 mm (G).

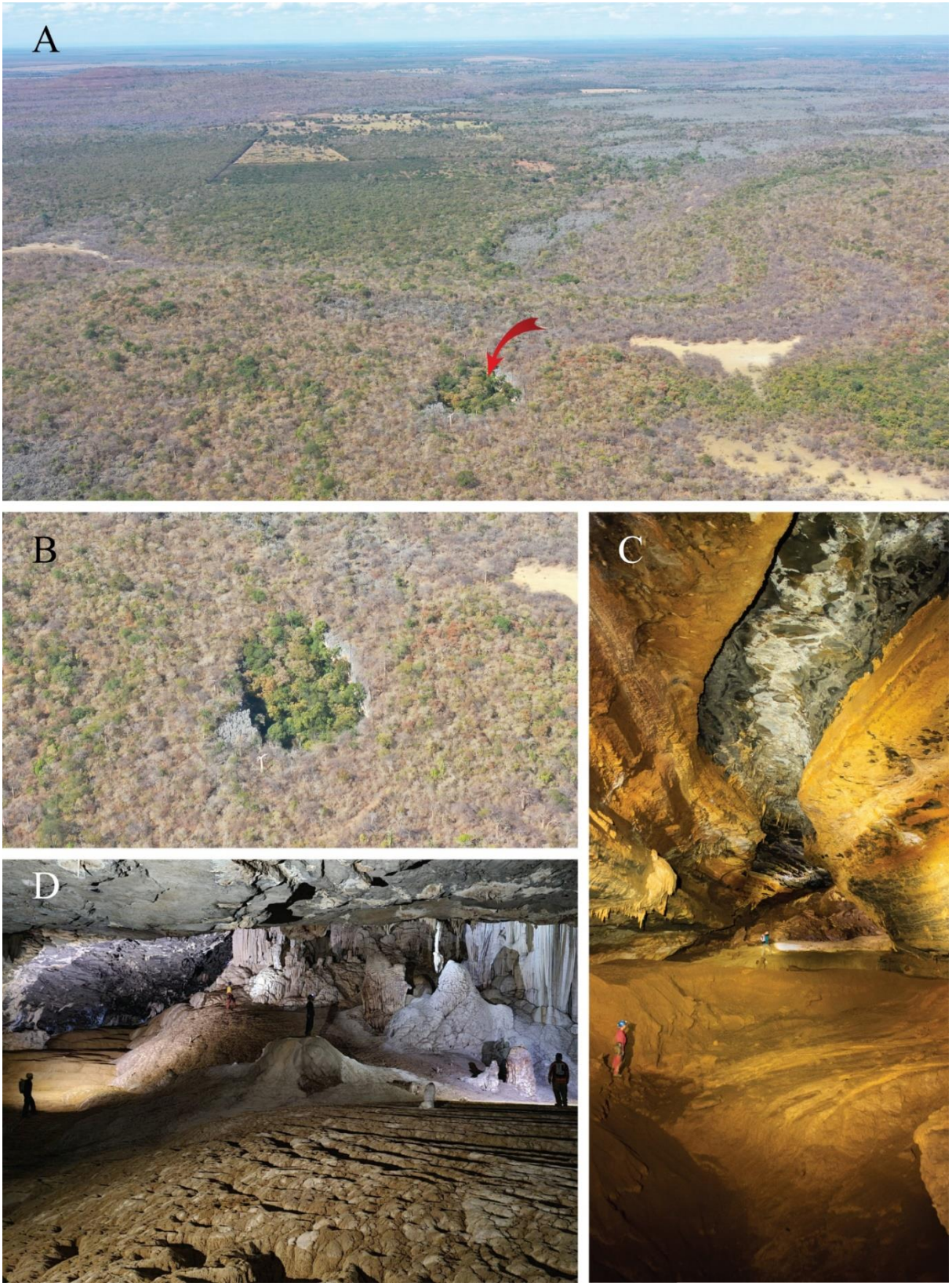


Fig. 6. Pedra Escrevida Cave. (A) Cave surroundings and external landscape, showing main entrance; (B) Main entrance external area; (C) Last chamber of the cave; (D) cave main hall.

ISOPODA



Subterranean Biology 42: 139–149 (2022)
doi: 10.3897/subtbiol.42.80274
https://subtbiol.pensoft.net

RESEARCH ARTICLE

Subterranean Biology
A peer-reviewed open-access journal
Published by The International Society for Subterranean Biology

A new species of *Chaimowiczia* from the karstic Serra do Ramalho plateau, Brazil (Oniscidea, Synocheta, Styloniscidae)

Giovanna Monticelli Cardoso[1], Rafaela Bastos-Pereira[1], Rodrigo Lopes Ferreira[1]

1 *Universidade Federal de Lavras (UFLA), Centro de Estudos em Biologia Subterrânea, Departamento de Biologia, Programa de Pós-graduação em Ecologia Aplicada, Lavras, Minas Gerais, Brazil*

Corresponding author: Giovanna Monticelli Cardoso (gmcardoso.bio@gmail.com)

Academic editor: José G. Palacios-Vargas | Received 8 January 2022 | Accepted 15 March 2022 | Published 29 March 2022

http://zoobank.org/638C7911-552F-4027-8238-13848DA132BC

Citation: Monticelli Cardoso G, Bastos-Pereira R, Lopes Ferreira R (2022) A new species of *Chaimowiczia* from the karstic Serra do Ramalho plateau, Brazil (Oniscidea, Synocheta, Styloniscidae). Subterranean Biology 42: 139–149. https://doi.org/10.3897/subtbiol.42.80274

Abstract

Chaimowiczia belongs to the subfamily Iuiuniscinae, family Styloniscidae, and is currently composed of two troglobitic species: *C. tatus* and *C. uai*, both occurring in Brazil. A new species of Styloniscidae found in Brazil (Bahia state, Serra do Ramalho, Serra Verde cave) was allocated into this genus by the antenna flagellum with three articles; rectangular-shaped lateral pereonites epimera not apically acute and apex of pleopod 2 endopod with an acute tip and an acute or rounded lobe directed outwards. The new species, *C. obybytyra* **sp. nov.**, is here described and rises to 25 the number of troglobitic styloniscidean species known for Brazilian caves.

Keywords

amphibious isopods, Bahia state, Isopoda, troglobite, Neotropics, São Francisco basin

Introduction

Chaimowiczia Cardoso, Bastos-Pereira, Souza & Ferreira, 2021 consists in a recently described genus for the subfamily Iuiuniscinae (Styloniscidae) (Cardoso et al. 2021). The species allocated into the new genus presented the antenna flagellum with three articles; rectangular-shaped lateral pereonites epimera not apically acute and apex of pleopod 2 endopod with an acute tip and an acute or rounded lobe directed outwards (Cardoso et al. 2021).

Copyright *Giovanna Monticelli Cardoso et al.* This is an open access article distributed under the terms of the Creative Commons Attribution License (CC BY 4.0), which permits unrestricted use, distribution, and reproduction in any medium, provided the original author and source are credited.

Chaimowiczia is currently composed of two species: *C. tatus*, Cardoso, Bastos-Pereira, Souza & Ferreira, 2021 found in Gruta do Padre (Bahia state), and *C. uai*, Cardoso, Bastos-Pereira, Souza & Ferreira, 2021, found in Lapa d'Água do Zezé cave (Minas Gerais state), both in Brazil. Here another species of *Chaimowiczia* is described for a cave in the Bahia state, which consists in a troglobite, as well as most of the styloniscids found in Brazil (Cardoso et al. 2021). Such description rises to 25 the number of troglobitic styloniscidean species known for Brazilian caves (Cardoso et al. 2020a, b, 2021; Campos-Filho et al. 2022).

Materials and methods

Study area

The region of Serra do Ramalho, where Serra Verde cave is located, is one of the most important karstic areas in Brazil (Auler et al. 2001), represented by a huge carbonate plateau with more than 70 km (in the N-S direction) between Corrente river (North) and Carinhanha river (South), in the left bank of the São Francisco River. The carbonate outcrops rise between 550 and 780 m above sea level. The region is inserted in the Caatinga domain (the only Brazilian semiarid biome), with transitional areas to the Cerrado (Brazilian Savanna) (Cole 1960). The local climate is "Aw", according to Köppen's climate classification system, with dry winter and an average annual rainfall of 640 mmS (Alvares et al. 2013). The local karst presents a strongly undulating relief, with epigean drainages typically ephemeral, forming deep-steep incisions (da Silva et al. 2019). The area presents more than 180 known caves, some of them among the biggest caves recorded for Brazil, many with more than 5 km in extension (Auler et al. 2001).

Laboratory procedures

The specimens were manually collected with the aid of a hand net and fixed in 70% ethanol. The studied individuals were measured and photographed with a ZEISS Axio ZoomV16 stereomicroscope coupled with an Axio Cam 506 Color camera, dissected and mounted in slides using Hoyer's medium in the Center of Studies on Subterranean Biology of the Federal University of Lavras (**CEBS-UFLA**, Lavras, Brazil). Drawings were made either from photographs or from dissected specimens mounted in slides with the aid of a camera lucida coupled with the microscope Leica DM750. Later the illustrations were prepared in the software GIMP (v. 2.8) (Montesanto 2015, 2016) with a Cintiq Drawing Pad (Wacom). Some specimens were put into an ultrasonic bath (L200 Schuster) to clean the sediment adhered to the cuticle and mounted in stubs for posterior observation of dorsal cuticular structures under the scanning electron microscope Hitachi TM4000. Holotype and paratypes of the new species were deposited in the Subterranean Invertebrate Collection of Lavras (**ISLA-UFLA**) in the Center of Studies on Subterranean Biology of the Federal University of Lavras (CEBS-UFLA, Lavras, Brazil).

Taxonomy

Family Styloniscidae Vandel, 1952
Genus *Chaimowiczia* Cardoso, Bastos-Pereira, Souza & Ferreira, 2021

***Chaimowiczia obybytyra* sp. nov.**
http://zoobank.org/E1EDC0BF-A3B5-48A7-B0D0-873DA3D7EC80

Type species. *Chaimowiczia tatus* Cardoso, Bastos-Pereira, Souza & Ferreira, 2021.
Material examined. *Holotype*: BRAZIL • Male; Bahia state, municipality of Cor- ibe, Serra Verde cave; 13°43'26.03"S, 44°19'24.46"W; 20 Sep. 2021; G.M. Cardoso and R.L. Ferreira leg.; ISLA 95829. ***Paratypes*:** • 4 males; same data as for holotype; ISLA 95830 • 17 females, same data as for holotype; ISLA 95831.
Description. Maximum length: 12 mm. Colorless, eyes absent (Figs 1A, 6C, D). Dorsal surface smooth with sparse scale setae with short triangular base, long sensory sheathed hair and plaques with serrated distal margin (Fig. 1B). Cephalon (Fig. 1C, D) suprantennal line well defined, directed downwards and truncated in middle; round antennal lobes. Body (Figs 1A, 2A) convex, pereonites 1–7 epimera quadrangular, widely separated and outwardly extended, pereonites postero-lateral corners progressively directed backwards; pleon epimera 3–5 well developed, pleonite 5 distal margin as long as telson. Telson (Fig. 1E) distal half subtriangular, depressed with round apex. Antennula (Fig. 2B) with three articles divided by thin suture, covered with thin setae, distal article with one lateral and two apical aesthetascs. Antenna (Figs 1F, 2C) reaches pereonite 2 when extended backwards, fifth article of peduncle longer than flagellum; flagellum with three articles, first article longest. Mandibles as in Fig. 2D, E. Maxillula (Fig. 2F) outer ramus with 5 + 5 teeth, apically entire, and two thick plumose stalks; inner ramus with three slender penicils. Maxilla (Fig. 2G) bilobate, inner lobe wider than outer, covered by setae. Maxilliped (Fig. 2H) basis trapezoidal, distal portion wider than basal; palp apex with tufts of setae; endite shorter than palp, setose, apex with one conic penicil between two strong teeth. Pereopod 1 (Figs 1G, 3A) antennal groom- ing brush longitudinally on frontal face of carpus and propodus, dactylus with one claw; pereopod 7 with water conducting scale rows. Uropod (Fig. 1E) protopod surpasses distal margin of telson; exopod slightly longer than endopod, inserted at the same level, covered with pectinate scales.
Male. Pereopods 1, 6 and 7 (Figs 1G, 3F, 4A) covered with setae; merus sternal margin with proximal tuft of setae. Genital papilla triangular (Fig. 4B). Pleopod 1 (Fig. 4B) protopod trapezoid, sinuous margin, apex tapering; exopod covered with setae, triangular with sinuous external margin; endopod as long as exopod, flagel- liform distal article. Pleopod 2 (Fig. 4C) exopod semi-oval, round distal margin, covered with setae; endopod of two articles, basal article quadrangular, shorter than exopod, distal article stout, apex with acute lobe (perpendicular) directed outwards. Pleopod 3 exopod (Fig. 4D) trapezoid, margin covered with thin setae, ventral face with lobe to hook pleopod 2. Pleopod 4 exopod (Fig. 4E) rhomboid, wider than

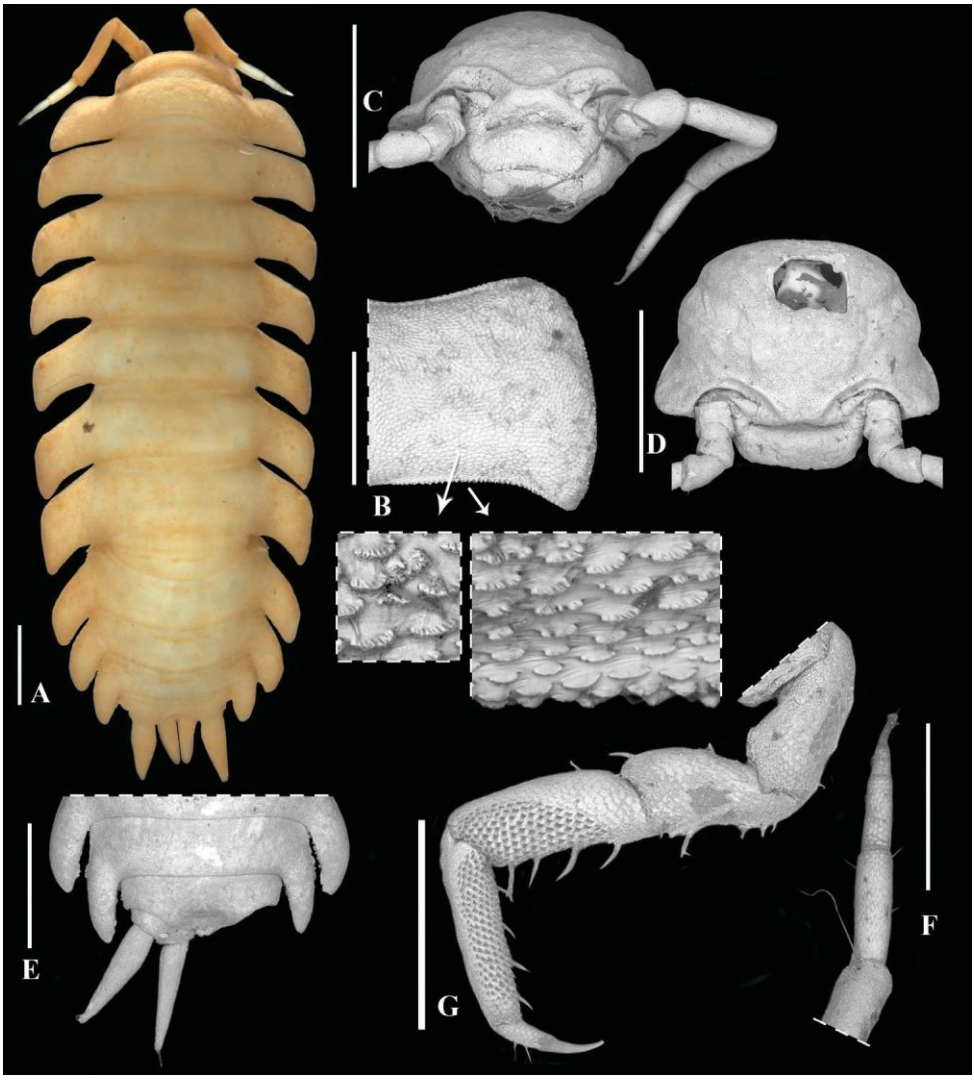


Figure 1. *Chaimowiczia obybytyra* sp. nov. Female paratype **A** habitus dorsal view **B** epimeron 1, dorsal view **C** cephalon, frontal view **D** cephalon, dorsal view **E** pleonites 4 and 5, uropod and telson, dorsal view **F** antennal flagellum **G** pereopod 1. Scale bar: 1mm (**A, C-E**); 500 µm (**B, G, F**).

long, covered with thin setae. Pleopod 5 exopod (Fig. 4F) ovoid, wider than long, covered with thin setae.

Etymology. The epithet "*obybytyra*" was given in reference to the name of the cave Serra Verde (in English, Green Mountain), that in the local Indian language "tupi- guarani" means: oby = green and ybytyra = mountain.

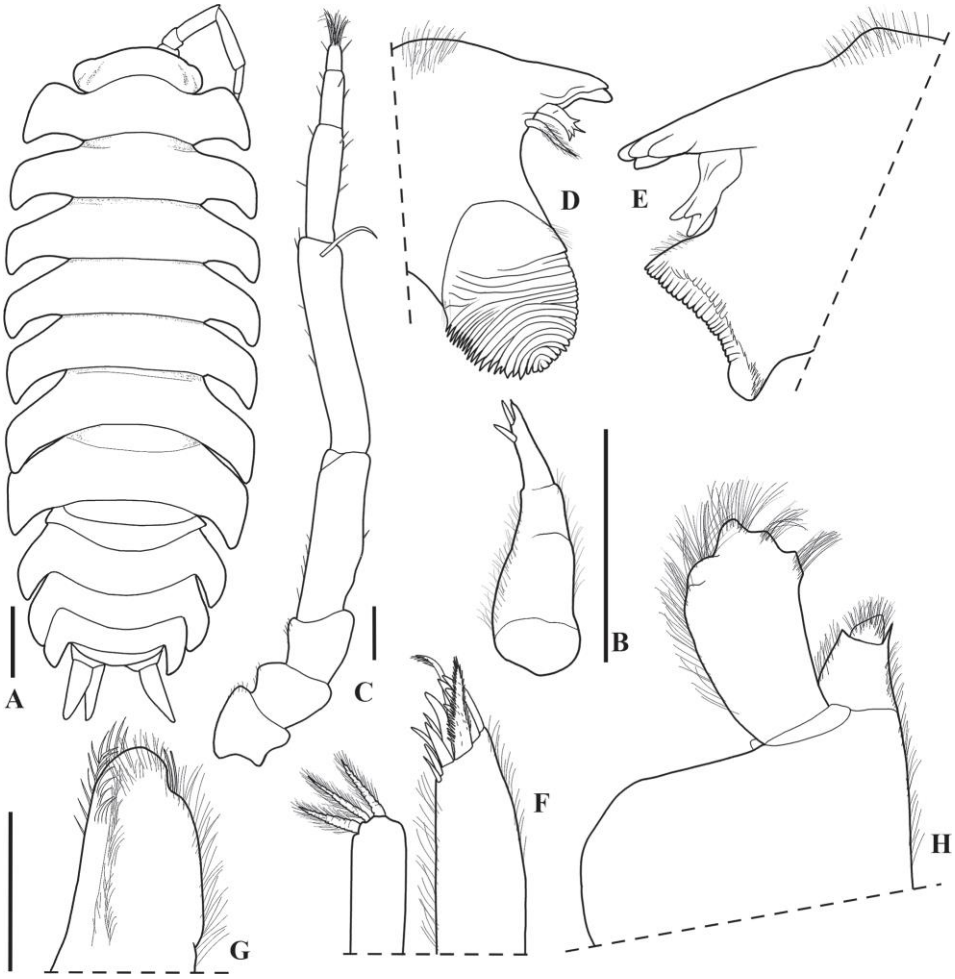


Figure 2. *Chaimowiczia obybytyra* sp. nov. Female paratype **A** habitus, dorsal view. Male paratype **B** antennula **C** antenna **D** right mandible **E** left mandible **F** maxilla **G** maxillula **H** maxilliped. Scale bars: 1 mm (**A**); 0.2 mm (**B-I**).

Discussion

Chaimowiczia obybytyra sp. nov. is larger than the other two species of the genus. The new species is similar to *C. uai* due to the antennal lobes and shape of pereonite 1 epimera, while the similarity with *C. tatus* is in the pleopod 2 endopod apex. A comparison among the morphology of the three species is presented on Table 1.

Chaimowiczia tatus and *C. obybytyra* sp. nov. inhabit caves situated around 63 km far from each other, while *C. uai* represents the southernmost record of the genus until the present (around 143 km far from *C. obybytyra* sp. nov.) (Fig. 5). Besides the distance, geographical barriers exist among the three species, since Corrente River separates the

Table 1. Comparative morphological characters for the three species of *Chaimowiczia*.

Characters	***C. tatus***	***C. uai***	***C. obybytyra* sp. nov.**
Body size (mm)	9	8	12
Antennula distal article: number/ position of aesthetascs	two apical	two apical	one lateral, two apical
Antennal lobes	quadrangular	rounded	rounded
Anterior portion of pereonite 1: epimera directed	outward	frontward	frontward
Pleonite 5 posterior margin telson	shorter than distal margin of telson	surpassing distal margin of telson	as long as telson

Uropod endopod ___ exopod endopod longer than exopod endopod as long as exopod endopod slightly shorter than exopod

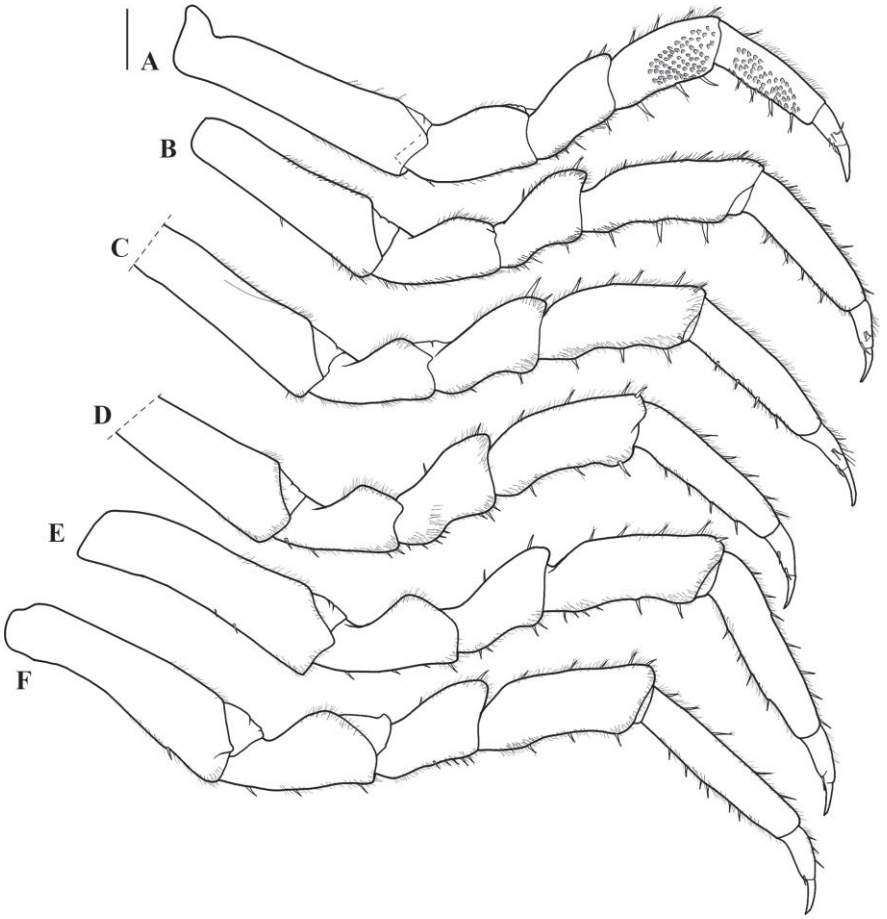


Figure 3. *Chaimowiczia obybytyra* sp. nov. Male paratype **A** pereopod 1 **B** pereopod 2 **C** pereopod 3 **D** pereopod 4 **E** pereopod 5 **F** pereopod 6. Scale bar: 0.2mm.

region of Santana, where *C. tatus* occur, from Serra do Ramalho, where *C. obybytyra* sp. nov. was found. *Chaimowiczia obybytyra* sp. nov. and *C. uai* are also separated by Carinhanha River. These rivers may have represented vicariant events that separated the species along the speciation process within such genus of Styloniscidae in those Brazilian caves.

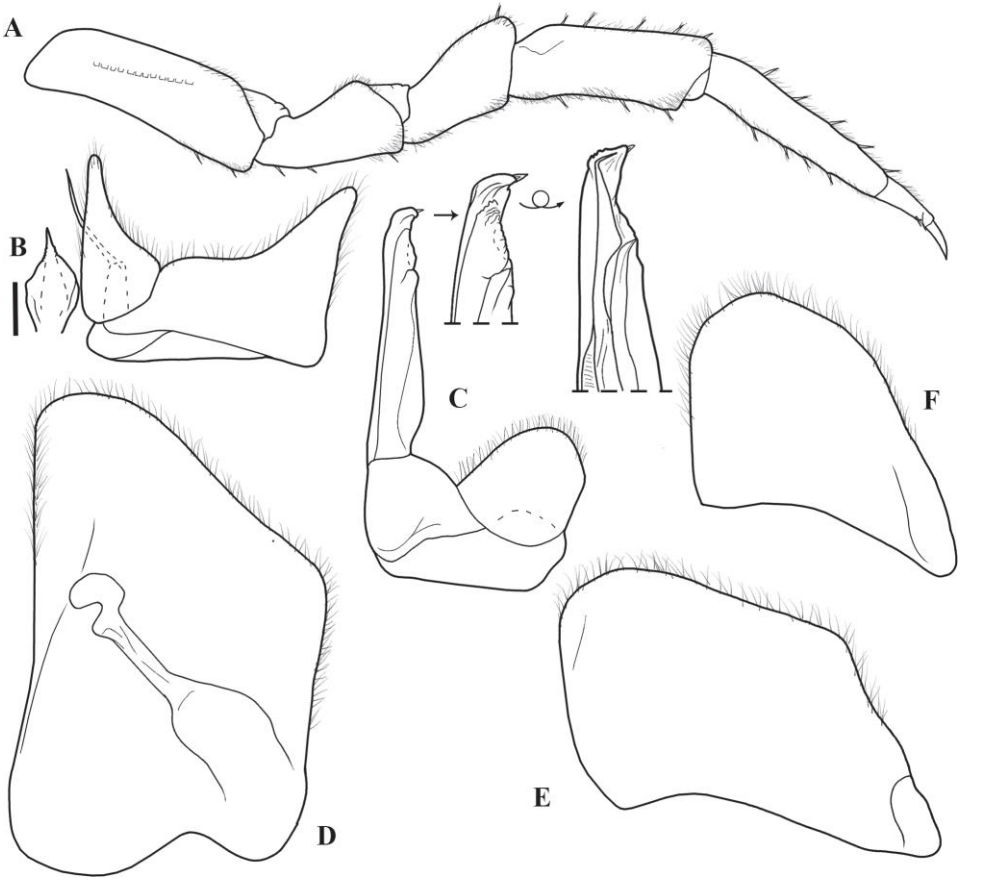


Figure 4. *Chaimowiczia obybytyra* sp. nov. Male paratype **A** pereopod 7 **B** genital papilla and pleopod 1 **C** pleopod 2 **D** pleopod 3 exopod, ventral view **E** pleopod 4 exopod, dorsal view **F** pleopod 5 exopod, dorsal view. Scale bar: 0.2mm.

Habitat and ecological remarks

Specimens of *Chaimowiczia obybytyra* sp. nov. were only observed in the Serra Verde cave. Such cave has at least 1,730 meters of horizontal projection, presenting the main conduit from which secondary passages develop. It is important to note that the cave is still under exploration, and the area where the specimens were collected was not mapped, since it remains flooded along the rainy period. Although the cave presents a wide entrance (Fig. 6A), there is a constriction on the cave conduit (20 meters from the entrance), which is quite long, thus preventing the general public to access the interior of the cave. The conduit that follows this constriction is relatively dry, although there are signs that the runoff water penetrates the cave in rainy periods. Since our team visited the cave during the dry period, the substrates were predominantly dry (near the entrance), however, as entering into the cave, its galleries become progressively wetter, and the conduits in the final portion were quite wet (Fig. 6B). Specimens of

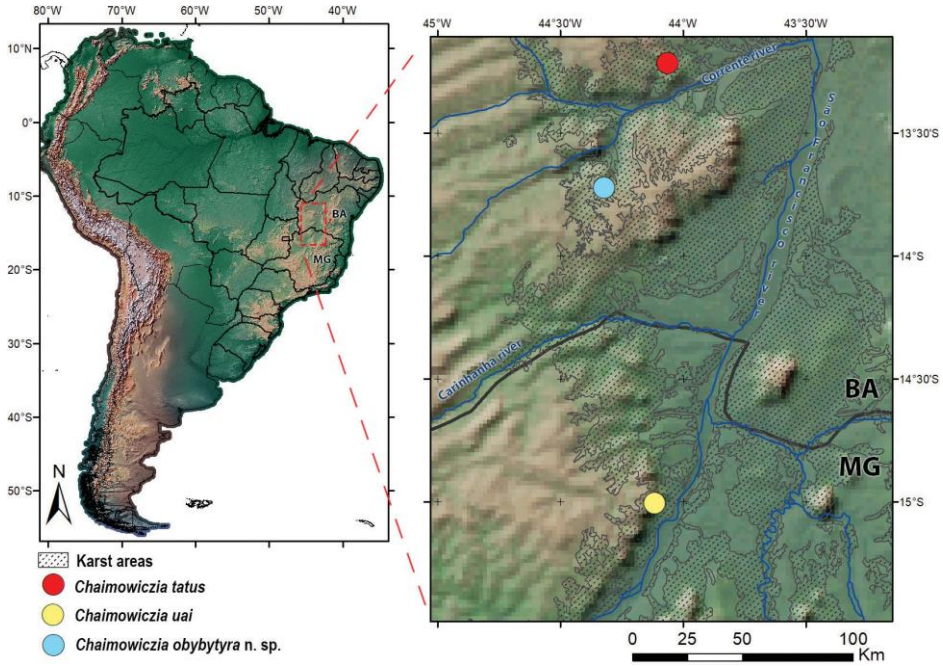


Figure 5. Map with the distribution of *Chaimowiczia* species in the Brazilian states of Bahia and Minas Gerais.

Chaimowiczia obybytyra sp. nov. (Fig. 6C) was found in small ponds in a lower-level conduit, which still maintained these small water collections, even at the height of the drought season. An expedition accomplished by speleologists during the rainy season revealed the inner conduits partially flooded, thus indicating the wide variation in the water table between dry and rainy seasons.

Chaimowiczia obybytyra sp. nov. also exhibits well-developed epimera on the pere- onites and pleonites 3–5, as on the other two congeneric species *C. uai* and *C. tatus*. Cardoso et al. (2021) hypothesized that such morphology could be related to a "ghost predation in the past" in a period when the ancestor populations could be under a predator selective pressure. However, this hypothesis still needs further studies in order to be confirmed (or refuted). It is interesting to highlight, however, the co-occurrence of *Chaimowiczia* species with amphipod species of the genus *Spelaeogammarus* (Amphipoda: Artesiidae). All the known species of *Chaimowiczia* share their habitat with such amphipods: *C. uai* co-occur with *S. uai* Bastos-Pereira & Ferreira, 2017; *C. tatus* co-occur with *S. santanensis* Koenemann & Holsinger, 2000; and *C. obybytyra* sp. nov. co-occur with an undescribed species of *Spelaeogammarus* (Fig. 6D) (Bastos-Pereira & Ferreira 2017; Cardoso et al. 2021). Although it is very unlikely that the amphipods could act as predator of adult isopods, it is interesting to consider at least an eventual competition for the scarce food resources occurring inside the caves. Furthermore, while adults of both isopod and amphipod are comparable in size, predation (which was already observed for *Spelaeogammarus* species – RLF personal observations) could

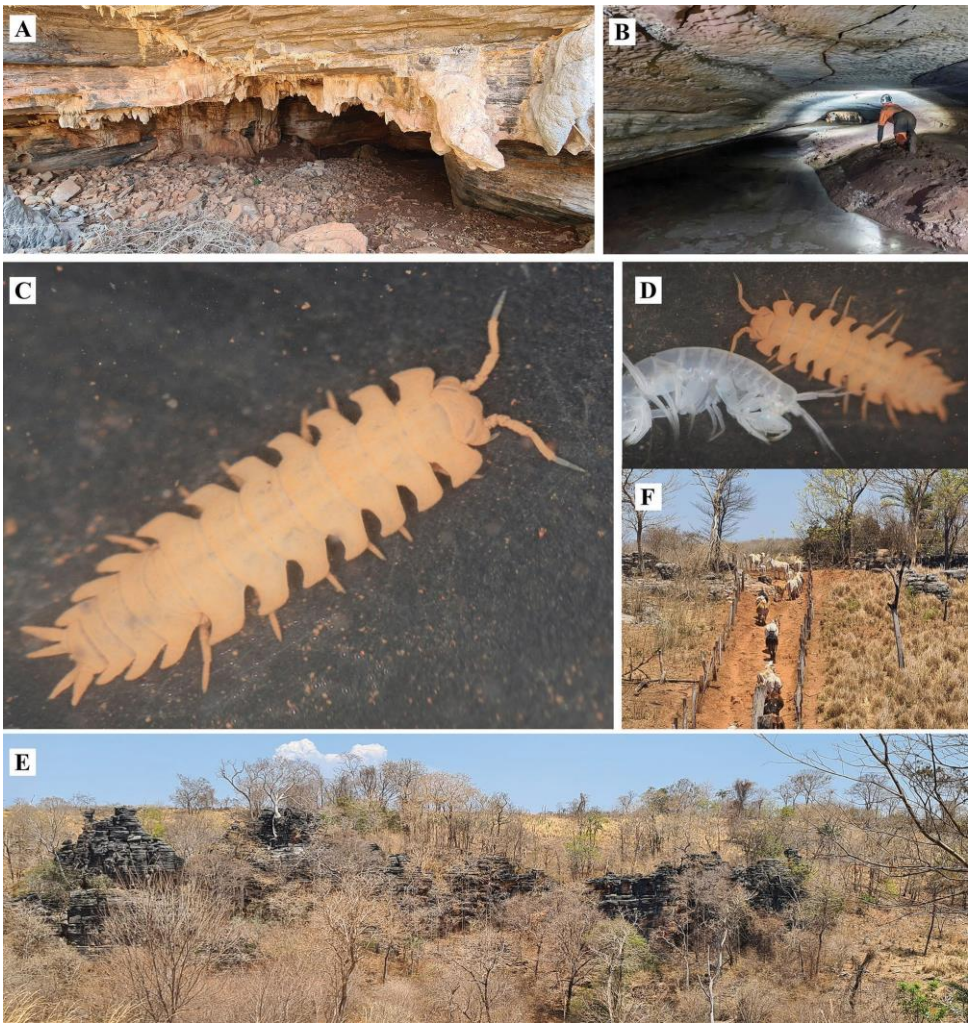


Figure 6. A Serra Verde cave's entrance **B** main conduit in rainy season **C** specimen of *Chaimowiczia obybytyra* sp. nov., *in situ* **D** specimen of *Chaimowiczia obybytyra* sp. nov. and *Spelaeogammarus* sp., *in situ* **E** pastures and livestock in the vicinity of the cave **F** Karst outcrop where the cave is located (Photo by Daniel Menin).

eventually occur between adult amphipods and juvenile isopods, though this is still speculative. In that case, the predation could be also acting currently, not only in the past, as hypothesized by Cardoso et al. (2021).

Two other aspects are also worth mentioning in this context: the first is the fact that all *Chaimowiczia* species have the body surface covered by sediment (which gives the species a brownish color, Fig. 6C). Such sediment adheres to the dorsal modi- fied scales. Hence, living specimens of *Chaimowiczia* present the body surface quite similar in texture to the sediment with which they are associated. This may eventually

represent a texture camouflage, in the case that adult *Spelaeogammarus* sp. feed on juvenile *Chaimowiczia*. The second fact is related to apparent niche segregation between *Chaimowiczia* and *Spelaeogammarus* species. While the former is benthic, frequently found digging the sediment and burying themselves, *Spelaeogammarus* sp. is an active swimming species (RLF personal observation). Again, further studies are highly advisable in order to address such hypothesis, not only based on observations *in situ* but also under laboratory conditions.

Conservation issues

As previously mentioned, the constriction on the conduit close to the entrance prevents residents to access the cave's inner portion. Hence, the cave is quite preserved. However, the external landscape surrounding the cave is severely altered. Only remnants of the original vegetation remain, especially close to the limestone outcrops (Fig. 6E). Most of the pristine forests were removed for pastures. During our visit, cattle were observed in the cave surroundings (Fig. 6F), compacting the exposed soil, which is highly vulnerable to erosional processes. Furthermore, the topography of the external area surrounding the cave entrance (which is located at the bottom of a valley) certainly contributes to the input of external sediments to the cave during rainy periods. Thus, the denudation of external soils can intensify erosive processes and, consequently, increase the sediment input to the cave, silting up microhabitats. It is important to note that other cave-restricted species were observed in this cave, as the undescribed species of *Spelaeogammarus*, millipedes, springtails, among others, which shows the biological relevance of this cave. Accordingly, it is highly recommendable that the cave surrounding be protected, especially by the reforestation of the immediate external landscape, to protect the cave and consequently the unique species it presents.

Acknowledgements

The authors would like to thank the Centro Nacional de Pesquisa e Conservação de Cavernas - CECAV and Instituto Brasileiro de Desenvolvimento e Sustentabilidade - IABS (nº. 006/2021. TCCE ICMBio/Vale (01/2018) for the financial support and scholarship provided to GMC; CNPq (National Council for Scientific and Technological Development) for the productivity scholarship provided to RLF (CNPq n. 308334/2018-3); we would like to thank Joaquim de Souza for the hospitality and logistic support in Agrovila 23 during the fieldwork. We would also like to thank the team from the Center of Studies in Subterranean Biology (CEBS/UFLA) for the support in the field trips; and Daniel Menin for the photograph of the cave in the rainy season in Fig. 6B. And Dr. Leila Aparecida Souza for her valuable contribution on the revision of this manuscript.

References

Alvares CA, Stape JL, Sentelhas PC, Moraes-Gonçalves JL, Sparovek G (2013) Köppen's cli- mate classification map for Brazil. Meteorologische Zeitschrift 22: 711–728. https://doi. org/10.1127/0941-2948/2013/0507

Auler A, Rubbioli E, Brandi R (2001) As Grandes Cavernas Do Brasil. Grupo Bambuí de Pes- quisas Espeleológicas, Belo Horizonte 228 pp.

Bastos-Pereira R, Ferreira RL (2017) *Spelaeogammarus uai* (Bogidielloidea: Artesiidae): a new troglobitic amphipod from Brazil. Zootaxa 4231(1): 38–50. https://doi.org/10.11646/ zootaxa.4231.1.2

Campos-Filho IS, Gallo JS, Gallão JE, Torres DF, Horta L, Carpio-Díaz YM, López-Orozco CM, Borja-Arrieta R, Aguiar JO, Bichuette ME (2022) Unique and fragile diversity emerges from Brazilian caves-two new amphibious species of *Xangoniscus* Campos-Filho, Araujo & Taiti, 2014 (Oniscidea, Stylioniscidae) from Serra do Ramalho karst area, state of Bahia, Brazil. Subterranean Biology 42: 1–22. https://doi.org/10.3897/subtbiol.42.75725 Cardoso GM, Bastos-Pereira R, Souza LA Ferreira RL (2020a) New troglobitic species of *Xan- goniscus* (Isopoda: Stylioniscidae) from Brazil, with notes on their habitats and threats.Zootaxa 4819(1): 84–108. https://doi.org/10.11646/zootaxa.4819.1.4

Cardoso GM, Bastos-Pereira R, Souza LA Ferreira RL (2020b) New cave species of *Pectenonis- cus* Andersson, 1960 (Isopoda: Oniscidea: Stylioniscidae) and an identification key for the genus. Nauplius 28: 1–30. https://doi.org/10.1590/2358-2936e2020039

Cardoso GM, Bastos-Pereira R, Souza LA Ferreira RL (2021) *Chaimowiczia*: a new Iuiunisci- nae genus from Brazil (Oniscidea, Synocheta, Stylioniscidae) with the description of two new troglobitic species. Subterranean Biology 39: 45–62. https://doi.org/10.3897/subt- biol.39.65305

Cole MM (1960) Cerrado, Caatinga and Pantanal: The Distribution and Origin of the Sa- vanna Vegetation of Brazil. The Geographical Journal 126:168–179. https://doi. org/10.2307/1793957

da Silva RC, Berbert-Born M, Bustamante DEF, Santoro TN, Sedor F, dos Santos Avilla L (2019) Diversity and preservation of Pleistocene tetrapods from caves of southwest- ern Bahia, Brazil. Journal of South American Earth Sciences 90: 233–254. https://doi. org/10.1016/j.jsames.2018.12.004

Koenemann S, Holsinger JR (2000) Revision of the subterranean amphipod genus *Spelae- ogammarus* (Bogidiellidae) from Brazil, including descriptions of three new species and considerations of their phylogeny and biogeography. Proceedings of the Biological Society of Washington: 113(1): 104–123.

Montesanto G (2015) A fast GNU method to draw accurate scientific illustrations for tax- onomy. ZooKeys 515: 191–206. https://doi.org/10.3897/zookeys.515.9459

Montesanto G (2016) Drawing setae: a GNU way for digital scientific illustrations. Nauplius 24: e2016017. [1–6] https://doi.org/10.1590/2358-2936e2016017

Vandel A (1952) Les trichoniscides (crustaces – isopodes) de l'hemisphere austral. Museum National d'Histoire Naturelle Serie A (6): 1–116.

Two new troglobitic species of *Iansaoniscus* from Brazilian caves (Crustacea, Isopoda, Pudeoniscidae)

Giovanna Monticelli Cardoso[1], Rafaela Bastos-Pereira[1], Rodrigo Lopes Ferreira[1]

1 *Universidade Federal de Lavras (UFLA), Centro de Estudos em Biologia Subterrânea, Departamento de Ecologia e Conservação, Programa de Pós-graduação em Ecologia Aplicada. Lavras, Minas Gerais, Brazil*

Corresponding author: Giovanna Monticelli Cardoso (gmcardoso.bio@gmail.com)

Academic editor: Matthew L. Niemiller | Received 27 January 2022 | Accepted 19 May 2022 | Published 14 June 2022

http://zoobank.org/AAF4E607-B43C-4797-9903-05BD241F9CF1

Citation: Cardoso GM, Bastos-Pereira R, Ferreira RL (2022) Two new troglobitic species of *Iansaoniscus* from Brazilian caves (Crustacea, Isopoda, Pudeoniscidae). Subterranean Biology 43: 127–143. https://doi.org/10.3897/subtbiol.43.81308

Abstract

Iansaoniscus species are troglobitic terrestrial isopods of the Pudeoniscidae family. In this work two new species are described from caves in the Bahia state, northeastern Brazil; *I. leilae* **sp. nov.** from Toca do Gonçalo cave, in the municipality of Campo Formoso; and *I. paulae* **sp. nov.** from Lapa do Bode cave in the municipality of Itaeté. Additionally, ecological notes and conservation status are provided for both new species.

Keywords

Cave fauna, Neotropics, Oniscidea, terrestrial isopods, troglobites

Introduction

Brazil currently shelters 36 described species of troglobitic oniscidean isopods, and this number has highly enhanced in the last few years (Cardoso et al. 2021, 2022; Campos-Filho et al. 2022). New species have continuously been discovered as new karstic areas are sampled. Styloniscidae stands out among the families with cave-restricted taxa, with 25 species (Fernandes et al. 2019; Cardoso et al. 2021, 2022; Campos-Filho et al. 2022); followed by Scleropactidae with five species (Campos-Filho and Araujo 2011; Campos-Filho et al. 2014, 2020), Philosciidae with four species (Campos-Filho et al. 2019, 2020), and Pudeoniscidae with two species (Campos-Filho et al. 2017).

Copyright *Giovanna Monticelli Cardoso et al*. This is an open access article distributed under the terms of the Creative Commons Attribution License (CC BY 4.0), which permits unrestricted use, distribution, and reproduction in any medium, provided the original author and source are credited.

Pudeoniscidae present nine species in four genera: *Brasiloniscus* Lemos de Castro, 1973, *Pudeoniscus* Vandel, 1963, *Iansaoniscus* Campos-Filho, Araujo & Taiti, 2017, and *Oxossioniscus* Campos-Filho, Lisboa & Cardoso, 2018 (Vandel 1963; Lemos de Castro 1973; Campos-Filho et al. 2017, 2018). Most species of this family occur in the Brazilian Atlantic Forest, with representatives found associated with leaf litter of cocoa, bromeliads, canopy of *Erythrina fusca* Lour., termite nests, and caves (Campos-Filho et al. 2017, 2018). To date, *Iansaoniscus* is the only genus of this family with troglobitic species (Campos-Filho et al. 2017). The genus comprises two species: *Iansaoniscus georginae* Campos-Filho, Araujo & Taiti, 2017 from Borboletas cave, municipality of Paripiranga and *Iansaoniscus iraquara* Campos-Filho, Araujo & Taiti, 2017 from Buraco do Cão cave, municipality of Iraquara, both in Bahia state.

The genus is distinguished by the unique shape of cephalon with well-developed antennary lobes and the triangular frontal shield, that is laterally interrupted by antennal grooves; pereonite 1 epimeron with dorsolateral furrow reduced or absent; pleon outline continuous with pereon; telson triangular; uropod protopod subquadrangular; and pleopod exopods with no respiratory structures (Campos-Filho et al. 2017).

In the present work, two new troglobitic species of *Iansaoniscus* are described, both from limestone caves in the Bahia state. Furthermore, ecological notes and conserva- tion status are provided for both new species.

Materials and methods

The new species were manually collected, fixed in 70% ethanol, and taken to the Center of Studies on Subterranean Biology of the Federal University of Lavras (CEBS, UFLA), Lavras, Brazil. Photographs and measurements were taken with ZEISS Axio ZoomV16 stereomicroscope coupled with an Axio Cam 506 Color camera. The specimens were dissected and mounted with Hoyer's medium (Anderson 1954). Illustrations were based on photographs or taken with the aid of a camera lucida on a microscope Leica DM750, and digitally drawn using the software GIMP (v. 2.8) (Montesanto 2015, 2016). Some specimens were dried in alcoholic series for the analysis of dorsal cuticular structures using the scanning electron microscope Hitachi TM4000. The material is deposited in the Collection of Subterranean Invertebrates of Lavras (ISLA), UFLA.

Taxonomy

Family Pudeoniscidae Lemos de Castro, 1973

Genus *Iansaoniscus* Campos-Filho, Araujo & Taiti, 2017

Type species. *Iansaoniscus iraquara* Campos-Filho, Araujo & Taiti, 2017, by original designation.

***Iansaoniscus leilae* sp. nov.**
http://zoobank.org/4F20CBD9-585B-48BF-9C18-019EFF7B5EEF
Figs 1–4

Sclreropactidae sp. nov. [sic!] – Souza-Silva and Ferreira 2016: 9, fig. 3F.

Diagnosis. Cephalon lateral lobes with straight distal margin; frontal shield triangular with frontal margin directed upwards with antennal socket depressed, vertex margin depressed; pereonite 1 epimeron without dorsolateral furrow; pereonite 1 grooved on ventral margin for two thirds of its length, pereonite 2 with well-developed ventral lobe; telson with acute apex; antennula distal article with two lateral and two apical aesthetascs; uropod exopod slightly shorter than endopod, as long as distal margin of telson.
Material examined. ***Holotype*:** BRAZIL • 1 male; Bahia state, municipality of Campo Formoso, Toca do Gonçalo cave (WGS84 -10.510992, -40.894659); 10th De- cember 2018; RL Ferreira leg.; ISLA 95911. ***Paratypes*:** • 1 male (mounted in slide), 2 females (1 mounted in slide); same data as holotype; ISLA 95912. • 1 male, 1 female; 05th January 2008; same location as holotype; ISLA 95913. • 6 females; 05th January 2008; same location as holotype; ISLA 95914. • 1 male (mounted in slide), 1 female; municipality of Campo Formoso, Toca da Tiquara cave (-10.458611, -40.542222); RL Ferreira leg.; ISLA 95917.
Etymology. The new species is named after Dr. Leila Aparecida Souza, UECE, for her contributions on the systematics of Brazilian subterranean Oniscidea.
Description. Maximum length: male and female, 6 mm. Body outline in lateral view as in Fig. 1A, colorless, eyes absent (Fig. 1A–C). Cephalon lateral lobes with straight distal margin; frontal shield triangular with frontal margin directed upward with antennal socket depressed, vertex margin depressed (Fig. 1B, C). Pereonite 1 epimeron without dorsolateral furrow; pereonite 1 grooved on ventral margin for two thirds of its length, pereonite 2 with well-developed ventral lobe (Fig. 1D–F); pereonites 3–7 with sub-quadrangular epimera. Pleonites 3–5 with epimera sub-quadrangular and directed backwards (Figs 1A, G, 2A). Telson (Figs 1G, 2A) slightly wider than long with concave sides, apex acute. Antennula (Fig. 2B) with three articles, distal article longer than second article bearing two lateral and two apical aesthetascs. Antenna (Fig. 2C) surpassing pereonite 3 when extended backwards, fifth article of peduncle as long as flagellum; flagellum with three articles; second and third articles subequal in length, third article with lateral aesthetascs (Fig. 1H). Mandibles (Fig. 2D, E) molar penicil with 7–8 branches, left mandible with 2+1 penicils, right with 1+1 penicils. Maxillula (Fig. 2F) outer branch with 4 + 5 teeth (two apically cleft); inner branch with two penicils. Maxilla (Fig. 2G) with bilobate apex, outer lobe wider than inner lobe, round, covered with thin setae; inner lobe bearing thick setae. Maxilliped (Fig. 2H) basis rectangular; palp basal article with two setae distinct in length; endite sub-rectangular, long medial seta, distal margin with two teeth. Pereopods 1–7 (Fig. 3A, B) merus and carpus with sparse setae on sternal margin; carpus 1 with longitudinal antennal grooming brush, distal seta apically cleft; dactylus with dactylar organ and

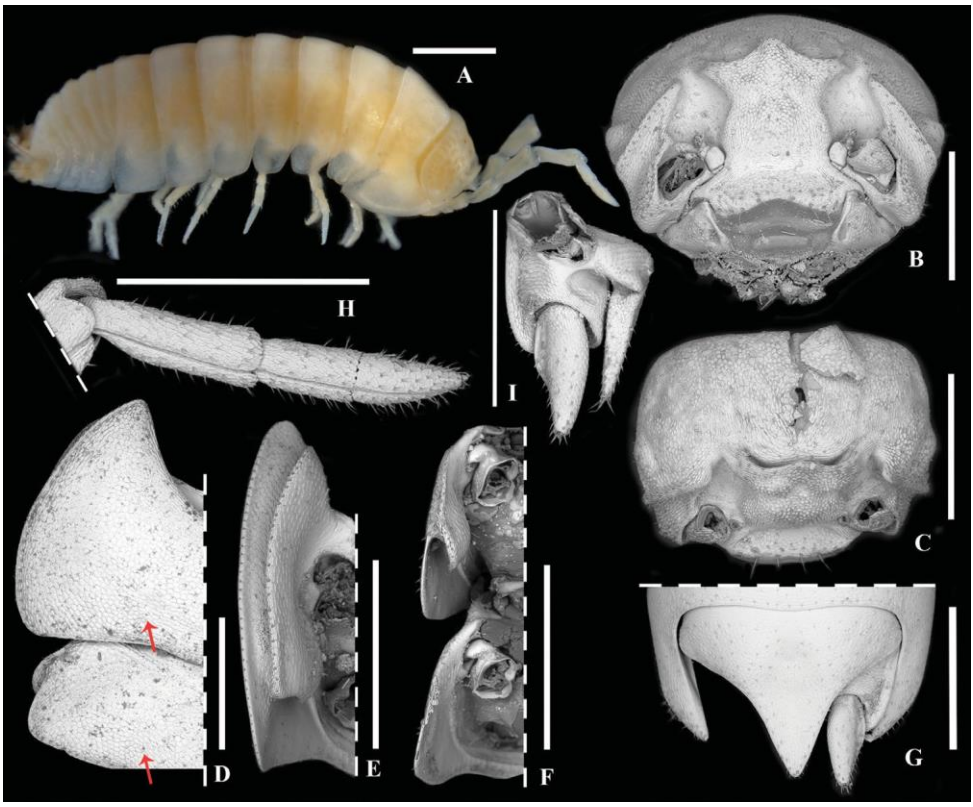


Figure 1. *Iansaoniscus leilae* sp. nov. **A** male holotype, lateral view. Female paratype **B** cephalon, frontal view **C** cephalon, dorsal view **D** pereonites 1 and 2, dorsal view, arrow indicating the *noduli laterales* **E** pereonite 1, ventral view **F** pereonites 2 and 3, ventral view **G** pleonite 5, telson and uropod, dorsal view **H** antennal flagellum **I** uropod. Scale bars: 1 mm (**A**); 500 μm (**B-I**).

ungual setae simple not surpassing outer claw. Uropod (Figs 1G, 2A) protopod longer than wide, with lateral groove; endopod inserted proximally, exopod slightly shorter than endopod, exopod slightly longer than distal margin of telson; proximal margin with lateral groove

Male: Genital papilla (Fig. 3C) with triangular ventral shield and subapical ori- fices. Pleopod 1 (Fig. 3C) exopod ovoid, margin straight, almost three times wider than long; endopod four times as long as exopod, distal portion slightly bent outwards, apex with small setae. Pleopod 2 exopod (Fig. 3D) triangular bearing one seta on outer margin, endopod flagelliform, almost three times as long as exopod. Pleopod 3–5 exo- pods as in Fig. 3E–G.

Habitat and conservation issues. The Toca do Gonçalo cave presents ca. 500 me- ters of mapped conduits. It is inserted at the Una geological group of carbonate rocks from the Caatinga Formation, which comprises relatively young rocks depos- ited around 600 million years ago (Auler 2019). It is located in the Campo Formoso

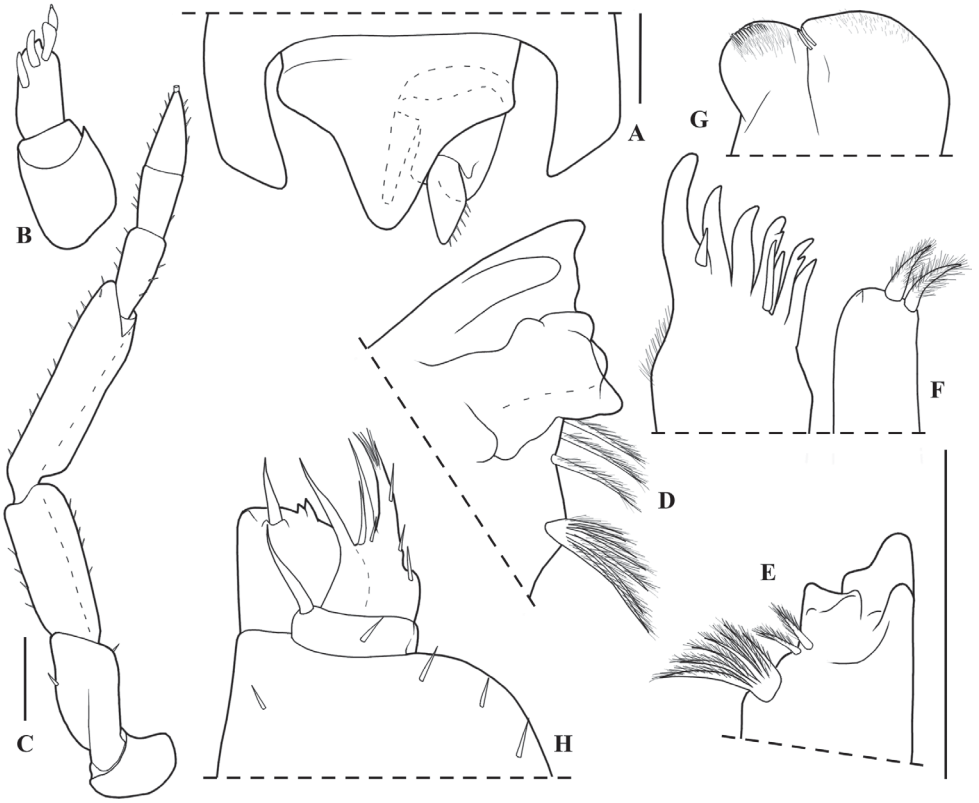


Figure 2. *Iansaoniscus leilae* sp. nov. Male holotype **A** telson and uropod, dorsal view **B** antennula **C** antenna **D** left mandible **E** right mandible **F** maxillula **G** maxilla **H** maxilliped. Scale bars: 0.2 mm.

municipality, Bahia state, Northeastern Brazil, within the Caatinga (a semiarid biome) (Fig. 9). The cave presents a single horizontal lenticular-shaped entrance, 2 m high and 8 m wide (Fig. 4A). It has two distinct levels: while the upper level is predominantly dry, the lower level used to be frequently filled with phreatic water (Fig. 4B, C). How- ever, as will be discussed further on, several changes (at both local and regional scales) led to a massive reduction in the water table level, thus, exposing several conduits that used to be inaccessible to men in the past decades (Fig. 4C). The main food sources for both the terrestrial and aquatic fauna seem to be particulate organic matter from the surface, although there are some root mats in the water table level and small guano piles in some areas within the cave.

Culver and Sket (2000) defined hotspots of subterranean biodiversity as caves (or cave systems) with 20 or more cave-restricted species. The Toca do Gonçalo cave shelters 22 troglobitic species and represents one of the three hotspots of subterranean biodiversity known for South America (Souza-Silva and Ferreira 2016; Souza-Silva et al. 2021). Most troglobitic species occurring in this cave remain undescribed, with descriptions already known for only seven of them: the beetle *Coarazuphium caatinga*

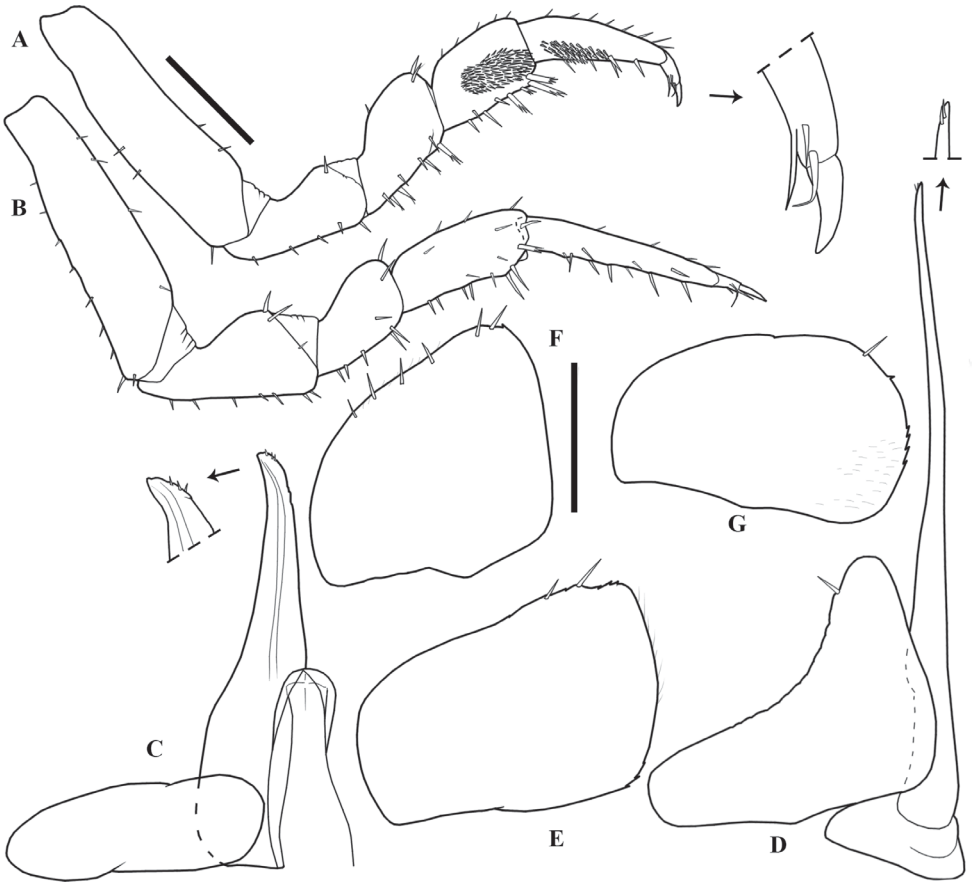


Figure 3. *Iansaoniscus leilae* sp. nov. Male holotype **A** pereopod 1 **B** pereopod 7 **C** pleopod 1 **D** pleopod 2 **E** pleopod 3 exopod **F** pleopod 4 exopod **G** pleopod 5 exopod. Scale bars: 0.2 mm.

(Pellegrini & Ferreira, 2014); the cricket *Erebonyx catacumbae* (Mello & Ferreira, 2021); the palpigrade *Allokoenenia canhembora* (Souza & Ferreira, 2022); the centipedes *Cryptops spelaeoraptor* (Ázara & Ferreira, 2014a) and *Newportia spelaea* (Ázara & Ferreira, 2014b); the amphipod *Spelaeogammarus trajanoae* (Koenemann & Holsinger, 2000); and the isopod *Pongycarcinia xyphidiorus* (Messana et al. 2002).

Specimens of *I. leilae* sp. nov. (Fig. 4D, E) were observed at the upper level in the first cave surveys, in the late 1990s. Several specimens were observed, especially near some old bat guano piles. At that moment, most of the lower level was filled with water. Hence, even the upper level was moist due to the influence of the high phreatic level on the whole cave atmosphere. However, local inhabitants use to draw water from the cave (as the region is quite dry) and this practice occurred for decades. This removal occurred manually at the beginning, but a diesel pump (Fig. 4F) was installed inside the cave in the 1980s, drying out previously flooded areas (Prevorčnik et al. 2012; Souza-Silva and Ferreira 2016). It is important to mention that the locals

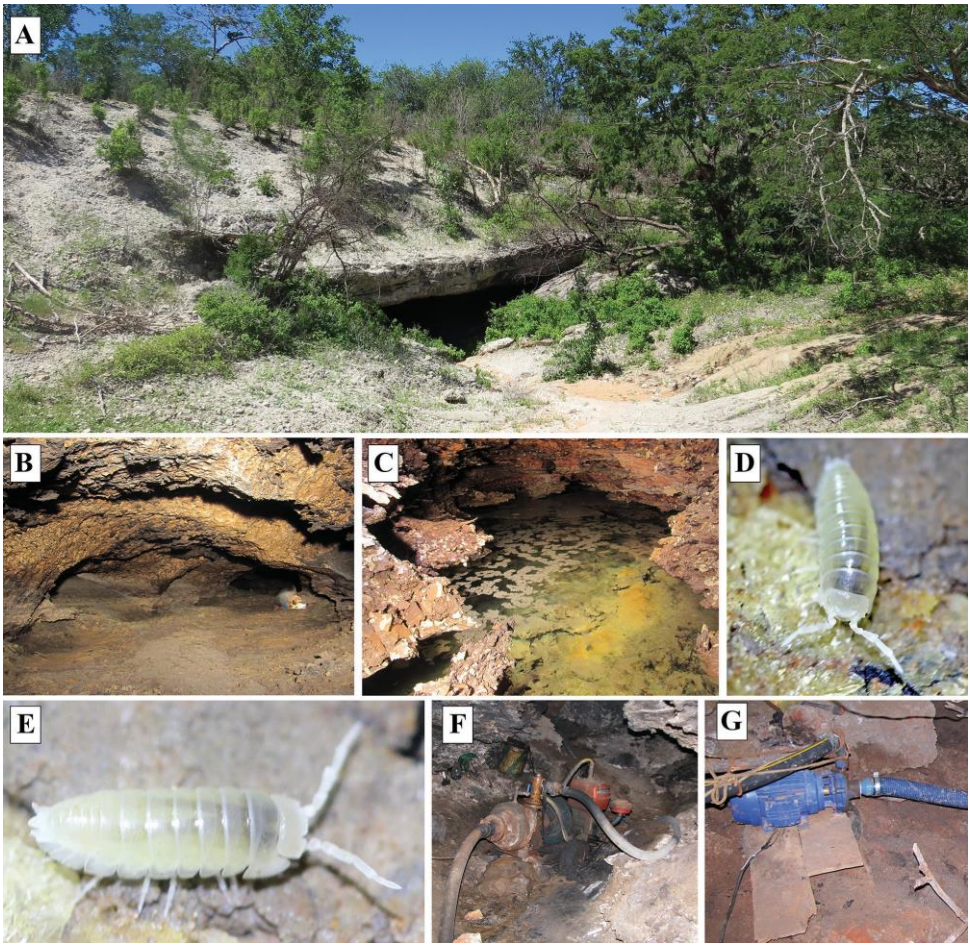


Figure 4. *Iansaoniscus leilae* sp. nov. habitat **A** Toca do Gonçalo cave entrance **B** cave floor in the inner portion of the cave, where specimens were found **C** water table at the cave lower level **D** adult specimen inside the cave, frontal view **E** adult specimen inside the cave, lateral view **F** diesel pump installed inside the cave in the 70's **G** electric pump installed inside the cave in 2010.

used to remove water from the cave once a week to fill up an external reservoir, hence the water table was persistent. However, in 2010, an electric pump employed by a local farmer for irrigation was installed in the cave (Fig. 4G), leading to a pronounced reduction of at least two meters in the water table inside the cave. Even after the removal of this electric pump (in 2012) the water table reduction continued, since artesian wells were built up outside the cave, so the water demand persisted. During a visit to the cave in August 2013, a major reduction in the water level was observed (approximately 3 m compared to the "pristine" level – observed in the 1990s). In 2013, specimens of *I. leilae* sp. nov. were no longer found in the upper level of the cave (that was extremely dry), being only observed on the moist substrates of the lower

level, even though, in lower densities when compared to the first observations. In December 2018, in a visit to the cave, the whole water table was no longer observed, so previously inaccessible areas were explored, revealing the cave to be much longer than previously thought, and only a few cave-restricted species were observed. From the 22 previously observed troglobitic species, only two (one specimen of *I. leilae* sp. nov., and one springtail) were observed in some moist areas located deep inside the cave in previously flooded areas. The single individual of *I. leilae* sp. nov. was found in a small piece of wood, apparently attracted by the organic compounds. It is important to mention that this species may be seriously threatened, as other cave-restricted species from the Toca do Gonçalo cave. Urgent intervention by the competent environmental agency is needed to ensure the protection of this hotspot of subterranean biodiversity in South America, especially considering that even the most relevant caves can now be destroyed in Brazil (Brasil 2022).

***Iansaoniscus paulae* sp. nov.**

http://zoobank.org/4B0755B7-18B1-404D-B6F0-A6F7A86A4EF4 Figs 5–8

Diagnosis. Cephalon with well-developed lateral lobes with round distal margin; frontal shield rounded, weakly developed; pereonite 1 epimeron without dorsolateral furrow; pereonite 1 and 2 without ventral lobes; antennula distal article with two lateral and one apical aesthetascs; third article longer than second; uropod exopod longer than endopod, longer than distal margin of telson.

Material examined. ***Holotype*:** BRAZIL • 1 male (mounted in slide); Bahia state, municipality of Itaeté, Lapa do Bode cave (WGS84 -12.938889, -41.062222); 26th July 2007; RL Ferreira leg.; ISLA 95915. ***Paratypes*:** • 5 females; same data as holotype; ISLA 95916.

Etymology. The new species is named after Dr. Paula Beatriz Araujo, UFRGS, for her contribution to the knowledge of Brazilian terrestrial isopods.

Description. Maximum length: male, 3 mm; female 5 mm. Body outline as in Fig. 5A, colorless, vestigial eyes (Fig. 5A, B). Cephalon with well-developed lat- eral lobes, round distal margin; frontal shield rounded, weakly developed (Fig. 5B). Pereonite 1 epimeron without dorsolateral furrow; pereonites 1 and 2 without ventral lobes (Fig. 5C, D); pereonite 3–7 with subquadrangular epimera. Pleonites 3–5 with epimera subquadrangular and directed backwards (Fig. 5A). Telson (Fig. 6A) slightly wider than long with concave sides, acute apex. Antennula (Fig. 5E) with three articles, distal article longer than second article, with two lateral and one apical aesthetascs. Antenna (Fig. 5F, 6B) surpassing pereonite 3 when extended backwards, fifth article of peduncle as long as flagellum, flagellum with three articles; faint suture between second and third, third article longest, aesthetascs on second and third articles. Mandibles (Fig. 6C, D) with molar penicil of 4 branches, left mandible with 2+1 penicils, right with 1+1 penicils. Maxillula (Fig. 6E) outer branch with 4 + 5 teeth (two apically

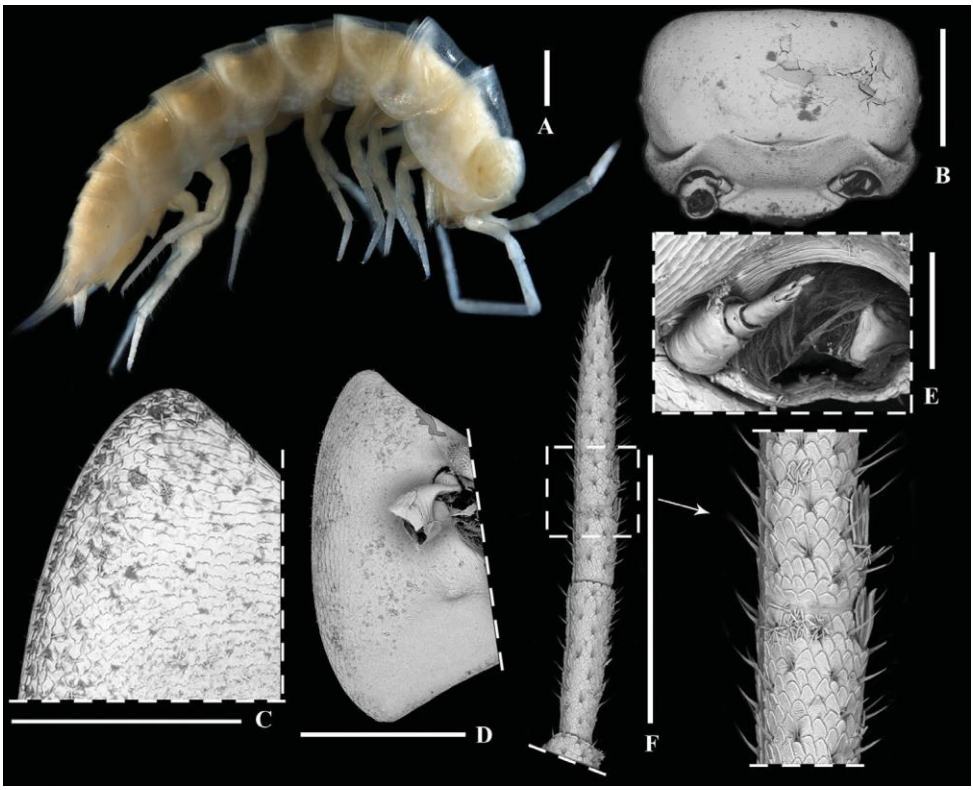


Figure 5. *Iansaoniscus paulae* sp. nov. Female paratype **A** lateral view **B** cephalon, dorsal view **C** pereonite 1, dorsal view **D** pereonite 1, ventral view **E** antennula **F** antennal flagellum. Scale bars: 0.5 mm (**A, B, D, E**); 0.3 mm (**C**); 0.1 mm (**E**).

cleft); inner branch with two penicils. Maxilla (Fig. 6F) with bilobate apex, outer lobe wider than inner lobe, rounded and covered with thin setae; inner lobe bearing thick setae. Maxilliped (Fig. 6G) basis rectangular; palp basal article with two setae distinct in length; endite rectangular, long medial seta, distal margin with two teeth. Pereopods 1–7 (Fig. 7A, B) merus and carpus with sparse setae on sternal margin; carpus 1 with longitudinal antennal grooming brush, distal setae cleft; dactylar organ and ungual seta simple not surpassing outer claw. Uropod (Fig. 7C) protopod distal margin and exopod proximal margin with lateral groove; endopod inserted proximally, exopod 1.4× longer than endopod and distinctly surpassing distal margin of telson.

Male: Pleopod 1 (Fig. 7D) exopod ovoid, twice wider than long; endopod almost four times longer than exopod, distal portion slightly bent outwards, apex with small setae. Pleopod 2 exopod (Fig. 7E) triangular bearing one seta on outer margin, endopod flagel- liform, almost three times longer than exopod. Pleopod 3–5 exopods as in Fig. 7F–H.

Habitat and conservation issues. The Lapa do Bode cave consists of a dolomite cave with 1,430 meters of horizontal projection, with conduits of labyrinthine pattern. It is inserted in an upper unit of the Una geological group of carbonate rocks from the

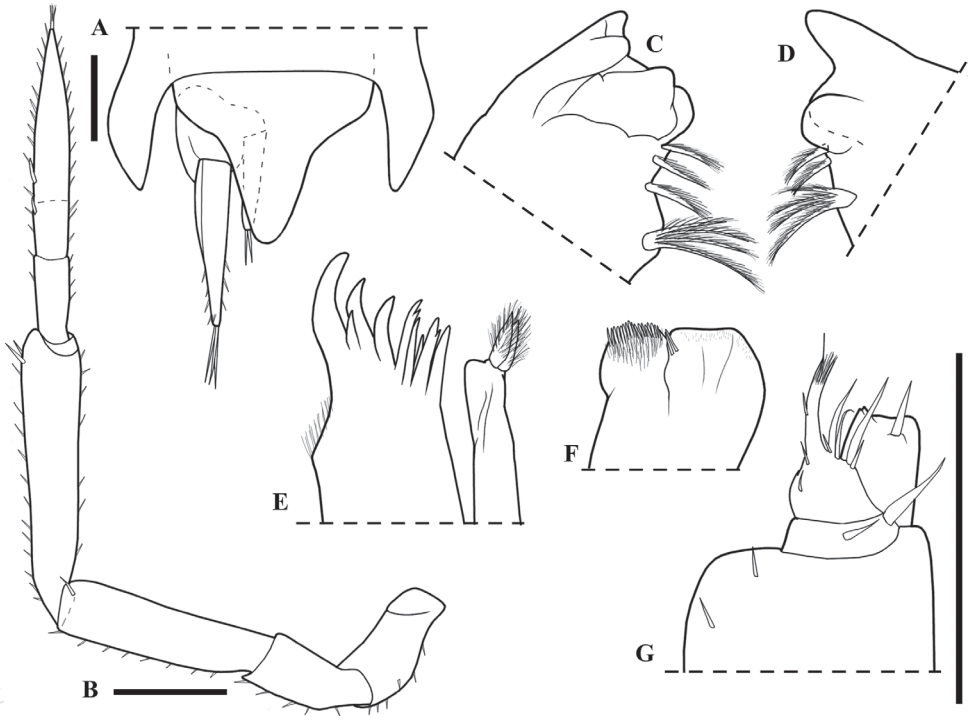


Figure 6. *Iansaoniscus paulae* sp. nov. Male holotype **A** telson and uropod, dorsal view **B** antenna **C** left mandible **D** right mandible **E** maxillula **F** maxilla **G** maxilliped. Scale bars: 0.2 mm.

Salitre Formation (Fig. 9) (Auler 2019). This cave presents five entrances (Fig. 8B, C) inserted in a rock wall parallel to the Una River, which flows close to the entrances (Fig. 8A). Although most of the cave is dry, the cave atmosphere is considerably moist due to water ponds in some inner areas. The temperature inside the cave is around 24.5 °C. The cave has been used for touristic purposes for the last decades, and the areas where individuals of *I. paulae* sp. nov. were found (inner portions of the cave, quite distant from the entrances) are also visited by tourists. They were observed walking on moist soil (Fig. 8D) and in some bat guano piles. Although the touristic activities apparently have not been altering intensively the cave features, there is concern that it could impact the species, especially by trampling (by visitors) due to the reduced size of the specimens and absence of structures guiding visitors to walk in specific pathways. The main available food resource is bat guano, that are concentrated in the inner chambers of the cave. It is worth mentioning that the Lapa do Bode cave presents ten cave-restricted species, among springtails, harvestmen, spiders, a beetle, a millipede, a silverfish, a palpigrade and a fish. However, only three of those species are currently described: the carabid beetle *Coarazuphium cessaima* (Gnaspini, Vanin & Godoy, 1998); the pholcid spider *Metagonia diamantina* (Machado, Ferreira & Brescovit, 2011)*;* and the catfish *Rhamdiopsis krugi* (Bockmann & Castro, 2010).

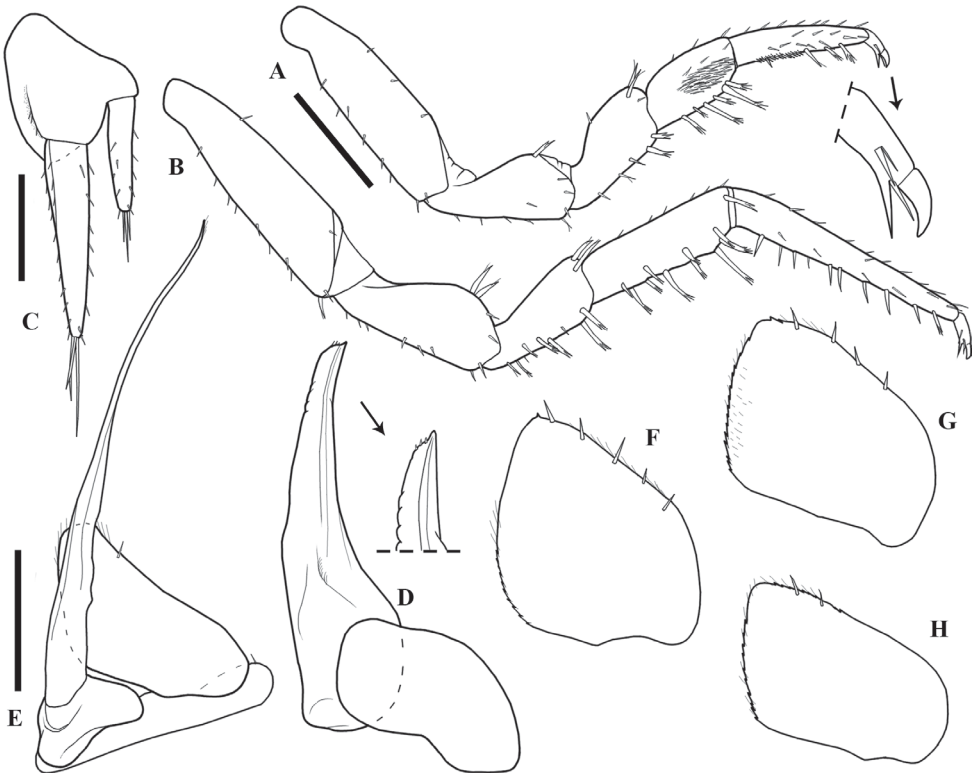


Figure 7. *Iansaoniscus paulae* sp. nov. Male holotype **A** pereopod 1 **B** pereopod 7 **C** uropod **D** pleopod 1 **E** pleopod 2 **F** pleopod 3 exopod **G** pleopod 4 exopod **H** pleopod 5 exopod. Scale bars: 0.2 mm.

Discussion

Taxonomy

The shape of cephalon is a unique feature in *Iansaoniscus* species, however it presents great phenotypic plasticity. *Iansaoniscus leilae* sp. nov. and *I. georginae* show similar patterns such as the frontal shield triangular with frontal margin directed upwards, lateral lobes weakly developed and antennal sockets depressed; while *I. paulae* sp. nov. and *I. iraquara* show well-developed lateral lobes with round margins and frontal shield rounded, weakly developed. The two new species are similar to *I. iraquara* due to pereonites 3 to 7 with subquadrangular epimera, maxillulae outer endite with 4+5 teeth (2 of them apically cleft) and absence of dorsolateral furrow on pereonite 1 epimera. However, while *I. iraquara* and *I. leilae* sp. nov. present ventral lobes on pereonites 1 and 2, such structures are absent in *I. paulae* sp. nov. In *I. georginae* the dorsolat- eral furrow and lobes are present, but weakly developed, while the maxillulae outer endite presents 4+6 teeth (2 apically cleft). Differently from the other three species, *I. georginae* presents subquadrangular epimera from pereonite 2. Regarding the telson shape, *I. iraquara*, *I. georginae* and *I. paulae* sp. nov. share the condition of a narrowly

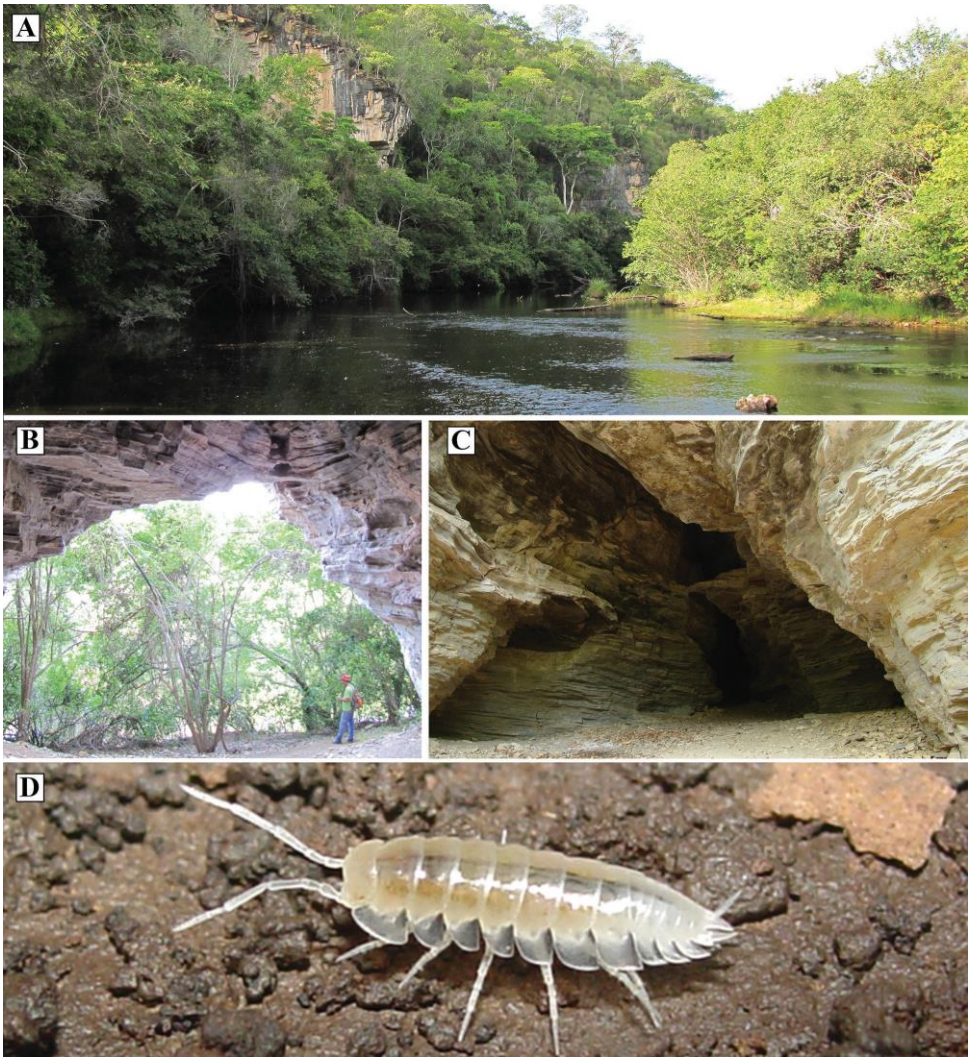


Figure 8. *Iansaoniscus paulae* sp. nov. habitat **A** limestone bordering the Paraguaçu river, where the Lapa do Bode cave's entrance is located **B** one of the entrances of Lapa do Bode cave **C** a secondary entrance of Lapa do Bode cave **D** adult specimen inside the cave.

rounded apex, which is acute in *I. leilae* sp. nov. Another difference among the species is that pleopod 1 exopod may present two conditions: ovoid (*I. iraquara*, *I. leilae* sp. nov. and *I. paulae* sp. nov.), and subquadrangular (*I. georginae*). In relation to eyes, such structures are absent in *I. iraquara*, *I. georginae* and *I. leilae* sp. nov., but present and vestigial in *I. paulae* sp. nov. Moreover, the *Iansaoniscus* species present distinct patterns of aesthetascs in the antennula distal article: *I. georginae* (four lateral plus one apical pair), *I. leilae* sp. nov. (two lateral plus two apical), *I. paulae* sp. nov. (two lateral plus one apical) and *I. iraquara* (missing antennule in the description). Additionally,

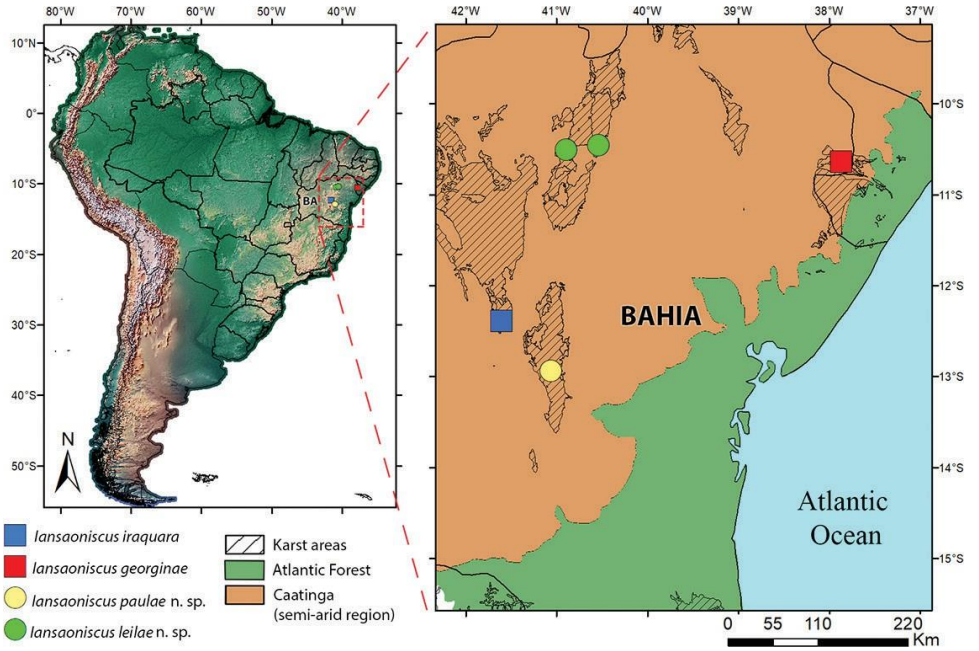


Figure 9. Geographical distribution of *Iansaoniscus* species, with Brazilian biomes and the karst areas delimited in the state of Bahia.

distinct patterns are observed regarding the number of branches in the mandible molar penicil: *I. iraquara* (5 to 7), *I. georginae* (6 to 7), *I. leilae* sp. nov. (7 to 8), *I. paulae* sp. nov. (4). The proportion of uropods exopod and endopod also varies among the species, with exopod as long as endopod in *I. iraquara*; exopod shorter than endopod in *I. leilae* sp. nov.; and exopod longer than endopod in *I. georginae* and *I. paulae* sp. nov. (being longer in *I. paulae* sp. nov. 1.4×).

Ecology and distribution

Until the discovery of *Iansaoniscus* species in the Caatinga biome (semi-arid region) (Fig. 9), the family was believed to be restricted to the Atlantic Forest (Campos-Filho et al. 2018; Cardoso et al. 2018). The other three genera occur in forests along the coast of Brazil, mainly associated with vegetation and/or leaf litter (Vandel 1963; Lemos de Castro 1973; Campos-Filho et al. 2017). Until then, few collection efforts had been made in more arid areas of Brazil, which conditions are not very suitable for the occurrence of isopods in general. In this sense, *Iansaoniscus*, which are restricted to caves in the only Brazilian semi-arid biome (Caatinga), are supposed to represent a geographical relict.

The xeric conditions of Caatinga currently act as a limiting barrier to the dis- persion of many hygrophilic components of fauna, such as isopods (Fernandes et al.

2016). However, Wang et al. (2004) dated speleothems and travertine deposits from the Bahia state and estimated 210,000 years of record of wet periods in northeastern Brazil caused by the displacement of the Intertropical Convergence Zone to the south. The rainforest distribution was affected during these wet periods, which formed a corridor between Amazonian and Atlantic Forests (Por 1992; Behling et al. 2000). Posteriorly, Cruz et al. (2009) observed an anti-phased relationship between precipitation in northeastern Brazil and the rest of tropical South America during the Holocene. The authors analyzed oxygen isotopic records from a speleothem in northeastern Brazil from the last 26,000 years and concluded that a predominantly wet climate dominated the currently semi-arid Caatinga. In this sense, the called south-eastern/north-western route (Bigarella et al. 1975), or the route across the Caatinga formation of eastern Brazil (Ledo and Colli 2017), seem to have favored many biotic exchanges in the past. Along this pathway and under climatic changes, some species or groups of species may have been isolated in moister areas, such as the subterranean conditions of many caves in Caatinga (Polhemus and Ferreira 2018), culminating in current geographical relicts, such as *Allokoenenia* (Palpigradi) (Souza & Ferreira, 2022) and *Iansaoniscus* species.

Acknowledgements

The authors would like to thank the Centro Nacional de Pesquisa e Conservação de Cavernas - CECAV and Instituto Brasileiro de Desenvolvimento e Sustentabilidade - IABS (n°. 006/2021. TCCE ICMBio/Vale (01/2018) for the financial support and scholarship provided to GMC; CNPq (National Council for Scientific and Technological Development) for the productivity scholarship provided to RLF (CNPq n. 308334/2018-3); and the team from the Center of Studies in Subterranean Biology (CEBS/UFLA) for the support in the field trips.

References

Anderson LE (1954) Hoyer's Solution as a Rapid Permanent Mounting Medium for Bryophytes. The Bryologist 57: e242. https://doi.org/10.2307/3240091

Auler AS (2019) Histórico, ocorrência e potencial de cavernas no Brasil. In: Rubbioli E, Menin D, Brandi R (Eds) Cavernas. Atlas do Brasil Subterrâneo. Instituto Chico Mendes de Con- servação da Biodiversidade, Brasília 14–51.

Ázara LN, Ferreira RL (2014a) *Cryptops* (Cryptops) *spelaeoraptor* n. sp. a remarkable troglobitic species (Chilopoda: Scolopendromorpha) from Brazil. Zootaxa 826(1): 291–300. https://doi.org/10.11646/zootaxa.3826.1.10

Ázara LN, Ferreira RL (2014b) Two new troglobitic *Newportia* (*Newportia*) from Brazil (Chilopoda: Scolopendromorpha). Zootaxa 3881(3): 267–278. https://doi.org/10.11646/zootaxa.3881.3.5

Behling H, Arz HW, Pätzold J, Wefer G (2000) Late Quaternary vegetational and climate dynamics in northeastern Brazil, inferences from marine core GeoB 3104-1. Quaternary Science Reviews 19: 981–994. https://doi.org/10.1016/S0277-3791(99)00046-3

Bigarella JJ, Andrade-Lima D, Riehs PJ (1975) Considerações a respeito das mudanças paleoambientais na distribuição de algumas espécies vegetais e animais do Brasil. Anais do Simpósio Internacional sobre o Quaternário, 411–464.

Bockmann FA, Castro R (2010) The blind catfish from the caves of Chapada Diamantina, Bahia, Brazil (Siluriformes: Heptapteridae): description, anatomy, phylogenetic relationships, natural history, and biogeography. Neotropical Ichthyology 8: 673–706. https://doi.org/10.1590/S1679-62252010000400001

Brasil (2022) Decreto N° 10.935, de 12 de janeiro de 2022. Dispõe sobre a proteção das cavidades naturais subterrâneas existentes no território nacional. Brasília: Diário Oficial da República Federativa do Brasil. https://www.in.gov.br/web/dou/-/decreto-n-10.935-de- 12-de-janeiro-de-2022-373591582 [accessed: 24 january 2022]

Campos-Filho IS, Araujo PB (2011) Two new troglobitic species of Scleropactidae (Crustacea: Isopoda: Oniscidea) from Pará, Brazil. Nauplius 19: 27–39. https://doi.org/10.1590/S0104-64972011000100004

Campos-Filho IS, Araujo PB, Bichuette ME, Trajano E, Taiti S (2014) Terrestrial isopods (Crustacea: Isopoda: Oniscidea) from Brazilian caves. Zoological Journal of the Linnean Society 172(2): 360–425. https://doi.org/10.1111/zoj.12172

Campos-Filho IS, Bichuette ME, Montesanto G, Araujo PB, Taiti S (2017) The first troglobiotic species of the family Pudeoniscidae (Crustacea, Isopoda, Oniscidea), with descriptions of a new genus and two new species. Subterranean Biology 23: 69–84. https://doi.org/10.3897/subtbiol.23.20963

Campos-Filho IS, Lisboa JT, Cardoso GM (2018) A new genus and two new species of Pudeoniscidae Lemos de Castro, 1973 (Crustacea: Isopoda: Oniscidea) from Brazil. Journal of Natural History 52(7–8): 457–482. https://doi.org/10.1080/00222933.2018.1437229

Campos-Filho IS, Fernandes CS, Cardoso GM, Bichuette ME, Aguiar JO, Taiti S (2019) Two new species and new records of terrestrial isopods (Crustacea, Isopoda, Oniscidea) from Brazilian caves. Zootaxa 4564 (2): 422–448. https://doi.org/10.11646/zootaxa.4564.2.6

Campos-Filho IS, Fernandes CS, Cardoso GM, Bichuette ME, Aguiar JO, Taiti S (2020) New species and new records of terrestrial isopods (Crustacea, Isopoda, Oniscidea) of the fami- lies Philosciidae and Scleropactidae from Brazilian caves. European Journal of Taxonomy 606: 1–38. https://doi.org/10.5852/ejt.2020.606

Campos-Filho IS, Gallo JS, Gallão JE, Torres DF, Horta L, Carpio-Díaz YM, López-Orozco CM, Borja-Arrieta R, Aguiar JO, Bichuette ME (2022) Unique and fragile diversity emerges from Brazilian caves – two new amphibious species of *Xangoniscus* Campos-Filho, Araujo & Taiti, 2014 (Oniscidea, Styloniscidae) from Serra do Ramalho karst area, state of Bahia, Brazil. Subterranean Biology 42: 1–22. https://doi.org/10.3897/subtbiol.42.75725

Cardoso GM, Campos-Filho IS, Araujo PB (2018) Taxonomic revision of *Brasiloniscus* (Oniscidea, Pudeoniscidae) with description of a new species. European Journal of Taxonomy 434: 1–16. https://doi.org/10.5852/ejt.2018.434

Cardoso GM, Bastos-Pereira R, Souza LA, Ferreira RL (2021) *Chaimowiczia*: a new Iuiuniscinae genus from Brazil (Oniscidea, Synocheta, Styloniscidae) with the description of two new troglobitic species. Subterranean Biology 39: 45–62. https://doi.org/10.3897/subtbiol.39.65305

Cardoso GM, Bastos-Pereira R, Ferreira RL (2022) A new species of *Chaimowiczia* from the karstic Serra do Ramalho plateau, Brazil (Oniscidea, Synocheta, Styloniscidae). Subterra- nean Biology 42: 139–149. https://doi.org/10.3897/subtbiol.42.80274

Cruz FW, Vuille M, Burn SJ, Wang X, Cheng H, Werners M, Edwards RL, Karmann I, Auler AS, Nguyen H (2009) Orbitally driven east–west antiphasing of South American precipi- tation. Nature Geoscience 2: 210–214. https://doi.org/10.1038/ngeo444

Culver DC, Sket B (2000) Hotspots of subterranean biodiversity in caves and wells. Journal of Cave and Karst Studies 62: 11–17.

Fernandes CS, Batalha MA, Bichuette ME (2016) Does the cave environment reduce functional diversity? PLoS ONE 11(3): e0151958. https://doi.org/10.1371/journal.pone.0151958

Fernandes CS, Campos-Filho IS, Araujo PB, Bichuette ME (2019) Synopsis of terrestrial isopods (Crustacea: Isopoda: Oniscidea) from Brazilian caves, with emphasis on new records from north, midwest, northeast and southeast regions. Journal of Natural History 53 (17–18): 1095–1129. https://doi.org/10.1080/00222933.2019.1634225

Gnaspini P, Vanin SA, Godoy NM (1998) A new genus of troglobitic carabid beetles from Brazil (Coleoptera, Carabidae, Zuphiini). Papéis Avulsos de Zoologia 40: 297–309.

Koenemann S, Holsinger JR (2000) Revision of the subterranean amphipod genus *Spelaeogammarus* (Bogidiellidae) from Brazil, including descriptions of three new species and considerations of their phylogeny and biogeography. Proceedings of The Biological Society of Washington 113: 104–123.

Ledo RMD, Colli GR (2017) The historical connections between the Amazon and the Atlantic Forest revisited. Journal of Biogeography 44: 2551–2563. https://doi.org/10.1111/jbi.13049

Lemos de Castro A (1973) Pudeoniscidae, família nova, com descrição de um gênero novo e três espécies novas de isópodos terrestres (Isopoda, Oniscoidea). Boletim do Museu Na- cional, Nova Serie, Zoologia 287: 1–10.

Machado EO, Ferreira RL, Brescovit AD (2011) A new troglomorphic *Metagonia* Simon, 1893 (Araneae, Pholcidae) from Brazil. Zootaxa 3135(1): 59–62. https://doi.org/10.11646/zootaxa.3135.1.4

Mello FDAG, Ferreira RL (2021) *Erebonyx catacumbae*, n. gen. et sp.: a blind, troglobitic cricket from Brazil (Orthoptera, Grylloidea, Phalangopsidae). Zootaxa 4975(2): 343–356. https://doi.org/10.11646/zootaxa.4975.2.5

Messana G, Baratti M, Benvenuti D (2002) *Pongycarcinia xiphidiourus* n. gen. n. sp., a new Brazilian Calabozoidae (Crustacea Isopoda). Tropical Zoology 15(2): 243–252. http://doi.org/10.1080/03946975.2002.10531178

Montesanto G (2015) A fast GNU method to draw accurate scientific illustrations for taxonomy. Zookeys 515: 191–206. https://doi.org/10.3897/zookeys.515.9459

Montesanto G (2016) Drawing setae: a GNU way for digital scientific illustrations. Nauplius 24: e2016017. https://doi.org/10.1590/2358-2936e2016017

Pellegrini TG, Ferreira RL (2014) Ultrastructural analysis and polymorphisms in *Coarazuphium caatinga* (Coleoptera: Carabidae, Zuphiini), a new Brazilian troglobitic beetle. Zootaxa 3765(6): 526–540. https://doi.org/10.11646/zootaxa.3765.6.2

Polhemus DA, Ferreira RL (2018) Two unusual new genera of cavernicolous Hydrometridae (Insecta: Heteroptera) from eastern Brazil. Tijdschrift voor Entomologie 161(1): 25–38. https://doi.org/10.1163/22119434-00002072

Por FD (1992) Sooretama: The Atlantic Rain Forest of Brazil. The Hague, SPB Academic Publishing, 130 pp.

Prevorčnik S, Ferreira LF, Sket B (2012) Brasileirinidae, a new isopod family (Crustacea: Isopoda) from the cave in Bahia (Brazil) with a discussion on its taxonomic position. Zootaxa 3452: 47–65. https://doi.org/10.11646/zootaxa.3452.1.2

Souza MFVR, Ferreira RL (2022) Two extraordinary troglobitic species of *Allokoenenia* (Eukoeneniidae: Palpigradi) from Brazil: first records of this initially monotypic genus more than a century after its description. European Journal of Taxonomy 789: 11–48. https://doi.org/10.5852/ejt.2022.789.1627

Souza-Silva M, Ferreira RL (2016) The first two hotspots of subterranean biodiversity in South America. Subterranean Biology 19: 1–21. https://doi.org/10.3897/subtbiol.19.8207

Souza-Silva M, Cerqueira RFV, Pellegrini TG, Ferreira RL (2021) Habitat selection of cave- restricted fauna in a new hotspot of subterranean biodiversity in Neotropics. Biodiversity and Conservation 30(14): 4223–4250. http://doi.org/10.1007/s10531-021-02302-8

Vandel A (1963) Isopodes terrestres recueillis en Amérique du Sud par Claude Delamare Deboutteville. In: Debouteville CD, Rapoport EH (Eds) Biologie de l'Amérique Austral, Paris 2: 63–100.

Wang X, Auler AS, Edwards L, Cheng H, Cristalli PS, Smart P, Richards DA, Shen C (2004) Wet periods in northeastern Brazil over the past 210 kyr linked to distant climate anomalies. Letters to Nature 432(9): 740–743. https://doi.org/10.1038/nature03067

ISSN 1175-5326 (print edition)
Article
ISSN 1175-5334 (online edition)
https://doi.org/10.11646/zootaxa.5319.4.5

ZOOTAXA

Zootaxa 5319 (4): 548–562
https://www.mapress.com/zt/
Copyright © 2023 Magnolia Press

http://zoobank.org/urn:lsid:zoobank.org:pub:3B5E09A6-21B3-4346-8CB4-D95DCC0B6C88

New troglobitic species of *Benthana* Budde-Lund, 1908 and *Benthanoides* Lemos de Castro, 1958 from iron-ore caves and their important record in the Amazon biome (Crustacea: Isopoda: Philosciidae)

GIOVANNA MONTICELLI CARDOSO[1]* & RODRIGO LOPES FERREIRA[1]
[1] *Universidade Federal de Lavras (UFLA), Centro de Estudos em Biologia Subterrânea, Departamento de Ecologia e Conservação. Programa de Pós-graduação em Ecologia Aplicada. Lavras, Minas Gerais, Brasil*
gmcardoso.bio@gmail.com; https://orcid.org/0000-0003-2682-1643
drops@ufla.br; https://orcid.org/0000-0003-3288-4405
**Corresponding author*

Abstract

A new cave-restricted species of *Benthana* and two cave-restricted species of *Benthanoides* are described from iron-ore caves located in the Serra dos Carajás complex, Pará state, in the Amazon biome. *Benthana alba* n. sp. occurs only in one cave in the south of Serra Norte, in the plateau N5 (cave N5SM2_0077); *Benthanoides amazonicus* n. sp. occurs in several caves in the north of Serra Norte, in the plateau N1; and *Benthanoides tarzan* n. sp. occurs in several caves in the Serra do Tarzan. This record represents an important distribution data for *Benthana* that typically occurs in the Brazilian Atlantic Forest, indicating that such species may represent a relict lineage of this genus. Additionally, efforts must be directed towards the conservation of these species, all of which are associated with caves occurring in areas of intense mining activity.

Key words: Crinocheta, woodlice, troglobitic species, relicts, Neotropics

Introduction

The family Philosciidae Kinahan, 1857 encompasses approximately 114 genera that exhibit a wide distribution across Europe, Africa, southern Asia, Australia, and the Americas (Leistikow 2001; Schmalfuss 2003; Boyko *et al*. 2008a onwards). Within South America, there are two taxonomically closely related taxa, *Benthana* Budde-Lund, 1908 and *Benthanoides* Lemos de Castro, 1958, which exhibit a seemingly disjunct distribution. *Benthana* is found in the Brazilian Atlantic Forest, while *Benthanoides* occurs in the Andean temperate region (Leistikow 2001).
To date, *Benthana* comprises 29 species (Campos-Filho *et al*. 2019; Boyko *et al*. 2008b onwards), distributed in the Southern (15 records) and Southeastern regions (23 records) of Brazil. Additionally, there are few records in the Central-Western region (2 records in the states of Mato Grosso do Sul and Distrito Federal); and in the Northeastern region (2 records in the state of Bahia) (Campos-Filho *et al*. 2018). The genus and its diagnostic characters were recently revised by Campos-Filho *et al*. (2015). Among the most notable features, we can mention the *noduli laterales* position with the d/c coordinates showing a maximum on pereonite 4; mandible with molar penicil dicothomized, dense cushion of coniform setae; maxillula outer endite with pectinate teeth; pereopod 1 carpus with distal seta with hand-like apex; and male pleopod 1 exopod heart-shaped with dentiform protrusion on outer margin. Currently, only two *Benthana* species that were found in caves are considered as troglobites: *B. iporangensis* Lima & Serejo, 1993 from São Paulo state (Ressurgência das Areias de Água Quente cave; Areias de Cima cave; and Gruta do Tatu cave); and *B. xiquinhoi* Campos-Filho, Bichuette & Taiti, 2019 from Bahia state (Gruna Parede Vermelha cave; Gruna Veio do Aurélio cave; and Gruna Lava Pé cave) (Campos-Filho *et al*. 2019). Both species present some troglomorphic traits, such as the reduction on the number of ommatidia, the enlarged appendages (such as pereopods and antennae) and the reduced pigmentation (Lima & Serejo 1993; Campos-Filho *et al*. 2015, 2019).

 Accepted by T. Riehl: 11 Jul. 2023; published: 27 Jul. 2023

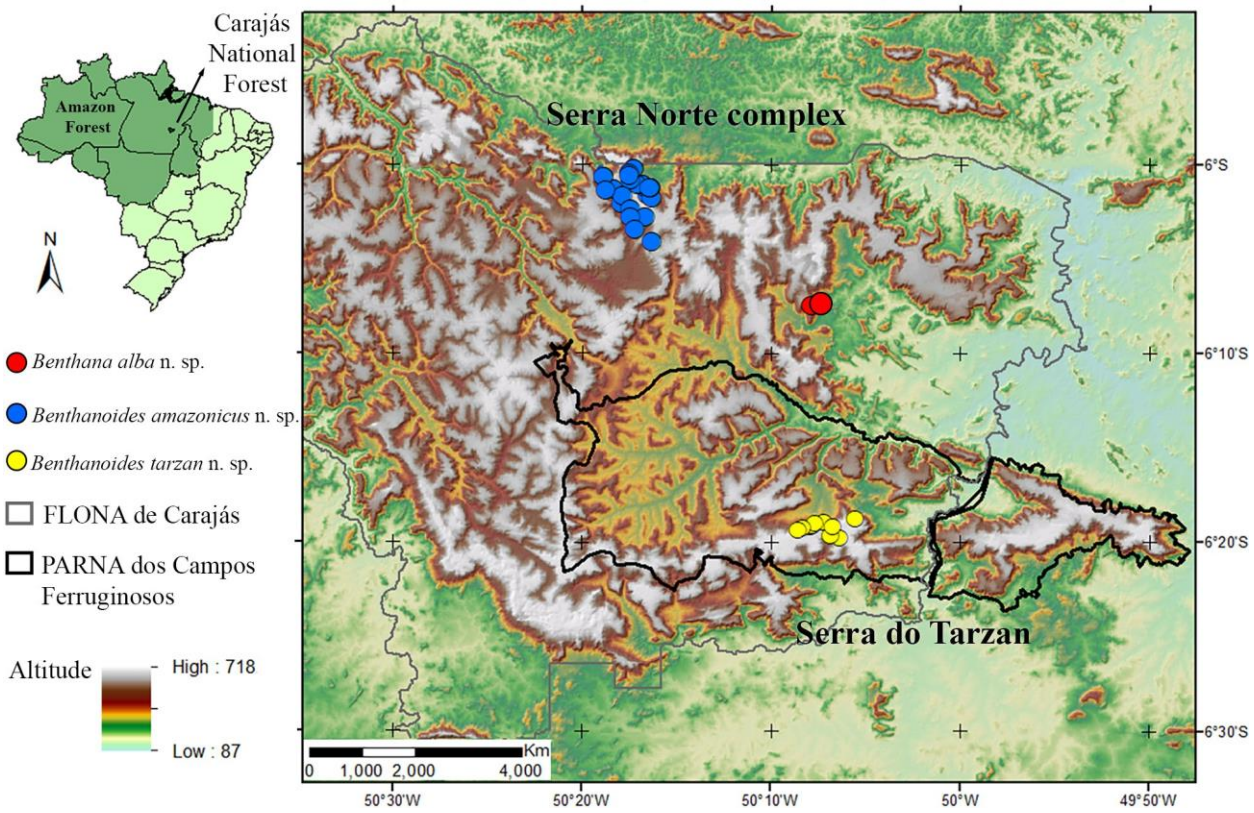


FIGURE 1. Map of Brazil with the Brazilian legal Amazon and the Carajás National Forest (FLONA) delimited in green.

Benthanoides comprises three species: *Be. pauper* (Jackson, 1926) from Chile; and *Be. peruensis* (Gruner, 1955) and *Be. villosus* (Jackson, 1926) from Peru (Schmalfuss 2003). The validity of the *Benthanoides* genus has been subject to uncertainty, with suggestions that it may represent a basal form of *Benthana* (Leistikow 2001; Leistikow & Araujo 2006). However, to date, no comprehensive study has been conducted to provide substantial evidence in support of this hypothesis.

In this work, one new species of *Benthana* and two new species of *Benthanoides* are described from the National Forest of Carajás, Pará State, in Northern Brazil. They represent the first records of *Benthana* in the Amazonian domain and the first record of *Benthanoides* for Brazil. Additionally, we provide some ecological notes and conservation status for the new species herein described.

Material and methods

The specimens are deposited at the Subterranean Invertebrate Collection of Lavras (ISLA) in the Center of Studies on Subterranean Biology (CEBS) of Federal University of Lavras (UFLA, Lavras, Brazil). They were measured and photographed with a ZEISS Axio ZoomV16 stereomicroscope coupled with an Axio Cam 506 Color camera. The illustrations were made with a *camera lucida* mounted on a microscope (Leica DM750). The final illustrations were made with the software GIMP (v. 2.8) (Montesanto 2015, 2016). The terminology used in the descriptions is based on Campos-Filho *et al.* (2014, 2015, 2016, 2019). The noduli laterales were measured and illustrated according to Vandel (1960). In the male pleopod 1 exopod the z:y ratio was defined according to Araujo & Lopes (2003) and the indentation level of the protrusion was defined according to Campos-Filho *et al.* (2013).

Study area

Specimens from the three species herein described were found in iron-ore caves inserted in the Carajás Mineral

Province in the Carajás National Forest (Floresta Nacional de Carajás or FLONA de Carajás), located in the Amazon biome in southeastern Pará state, Brazil (Figs 1 and 2). This region is worldwide recognized due to the expressive deposits of iron, nickel, copper, and gold, which represent around 49% of the Brazilian mineral production (ANM, 2020). The species were found in two distinct regions: in the Serra Norte complex area, which is under intense exploitation of iron ore, and in the Serra do Tarzan, which is protected by the Campos Ferruginosos National Park (Parque Nacional dos Campos Ferruginosos or PARNA dos Campos Ferruginosos). It is important to mention that the Carajás region comprises an important spot of subterranean biodiversity, presenting dozens of cave-restricted species, from which only part is formally described (Ferreira *et al*. 2018). The climate is characterized as continental equatorial (at altitudes lower than 350 m a.s.l.) or equatorial mesothermal (at altitudes higher than 700 m a.s.l.), with average temperature between 23 and 25 °C (Piló *et al*. 2015). The rainfall presents strong seasonal variations, with dry period between June and September (~10 to 90 mm per month) and the rainy period between October and April (~160 to 340 mm per month) (Sahoo *et al.* 2016). The average annual precipitation reaches 2,400 mm (Piló *et al.* 2015). Details on the habitat of each species will be provided further on.

Systematics

Family Philosciidae Kinahan, 1857 Genus

Benthana Budde-Lund, 1908

Type species. *Philoscia picta* Brandt, 1833 by subsequent designation (Van Name 1936).

Benthana iporangensis Lima & Serejo, 1993

(Figures 2F and 3A)

Material examined. 2 males, 3 females (ISLA 96769), Brazil, São Paulo state, municipality of Iporanga, cave Areias de Baixo (-24.583795º -48.700457º), 13.ii.2014, leg. R. L. Ferreira.
Remarks. *Benthana iporangensis* lacks pigmentation, as mentioned by Lima & Serejo (1993). A photograph of a live specimen is provided in Fig. 2F.

Benthana alba n. sp.

(Figures 3B, 4 and 5)

Type material. Holotype: male (ISLA 96766 in slide), Brazil, Pará state, municipality of Parauapebas, cave N5SM2_0077: GEM1762 (-6.124548º -50.131116º), 12.iii.2011, leg. M. P. A. Oliveira. Paratypes: 2 males, 1 juvenile (ISLA 96767), same data as holotype.
Diagnosis. Pleonites 3–5 with well-developed posterior point; eyes with seven ommatidia; antennula with 19+2 aesthetascs; male pleopod 1 exopod rounded with lateral protrusion prominent acute and lobe on inner distal margin.
Description. Maximum body length: male 9.5 mm. Colorless in ethanol. Body convex, outline as in Fig. 4A. Dorsal surface smooth bearing few long triangular scale-setae (Fig. 4B); *noduli laterales* long, one line per side with d/c coordinates reaching maximum on pereonite 4; b/c coordinates gradually decreasing (Fig. 4C, D). Cephalon (Fig. 4E) with suprantennal line bent downwards in middle, no frontal line and lateral lobes; eyes composed of seven small ommatidia arranged in two rows. Pereonites 5–7 with postero-lateral corners gradually more acute; pleon narrower than pereon, pleonites 3–5 with well-developed posterior point acute (Fig. 4A). Telson (Fig. 4F) triangular, lateral sides straight. Antennula (Fig. 4G) of three articles, distal article longest bearing 17 lateral aesthetascs in five rows, plus apical pair. Antenna (Fig. 4H) long, reaching pereonite 4 when extended backwards, distal article of peduncle longer than flagellum; flagellum of three articles, distal article longest, apical organ short. Mandibles with molar penicil of 11–13 branches, left mandible (Fig. 4I) with 2+1 penicils, and right mandible (Fig. 4J) with 1+1 penicils. Maxillula (Fig. 4K) inner endite with two penicils; outer endite with 4+5 teeth (5 pectinate), plus one

short and simple. Maxilla (Fig. 4L) inner lobe wider than outer lobe, covered with thick setae; outer lobe distal margin sinuous, covered with thin setae. Maxilliped (Fig. 4M) with rectangular basis; endite rectangular, medial seta surpassing distal margin, two hooks on distal margin, dorsal face with longitudinal ridge bearing dense setae plus one short triangular seta; proximal article of palp with two setae, one longer. Pereopods slender; carpus 1 with transverse antennal grooming brush, distal seta with hand-like apex; dactylus inner claw shorter than outer claw, dactylar and ungual setae simple, not surpassing outer claw. Uropod (Fig. 4F) protopod subquadrangular, protopod and exopod grooved on outer margin bearing glandular pores; exopod longer than endopod; endopod inserted at same level.

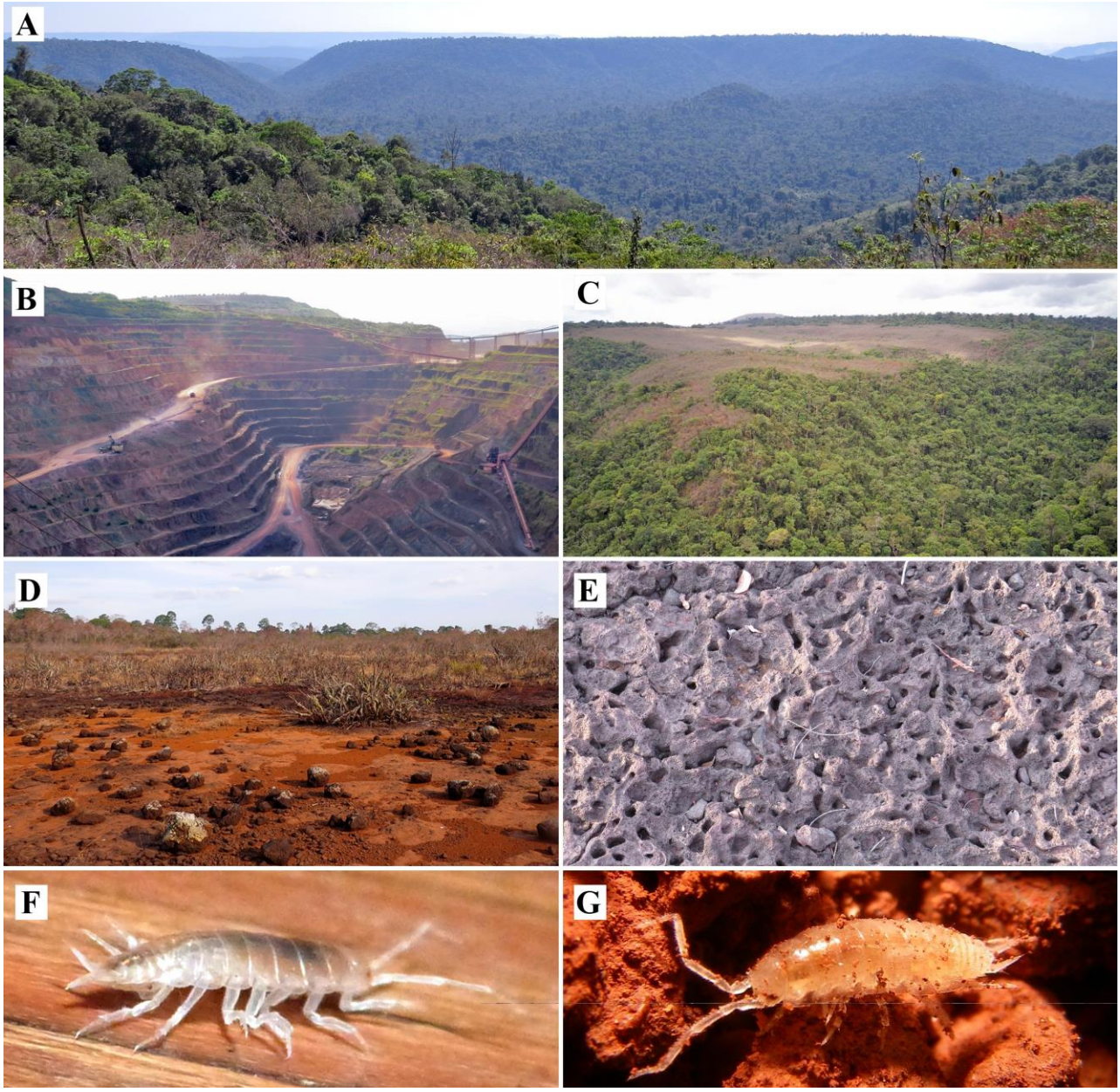


FIGURE 2. A, Plateaus in the Carajás National Forest; B, mining activities in the Serra Norte complex (Photo by Allan Calux); C, upperview of a canga formation; D, canga typical vegetation; E, canaliculi on canga; F, live specimen of *Benthana iporangensis*; G, live specimen of *Benthanoides tarzan* n. sp.

Male. Pereopods 1–3 (Fig. 5A, B) merus and carpus with brushes of setae on sternal margin. Pereopod 7 (Fig. 5C) without sexual dimorphism. Genital papilla (Fig. 5D) with triangular ventral shield and two subapical orifices. Pleopod 1 (Fig. 5D, E) exopod rounded (ratio z:y= 1.7) lateral protrusion prominent acute, lobe on inner margin; endopod longer than exopod, stout and straight, distal portion with line of short setae. Pleopod 2 (Fig. 5F) exopod

triangular, outer margin concave with three setae; endopod slender, longer than exopod. Pleopods 3 and 4 exopods as in Fig. 3G, H, respectively. Pleopod 5 exopod (Fig. 5I) triangular, outer margin sinuous with three setae and transverse plumose fringe.

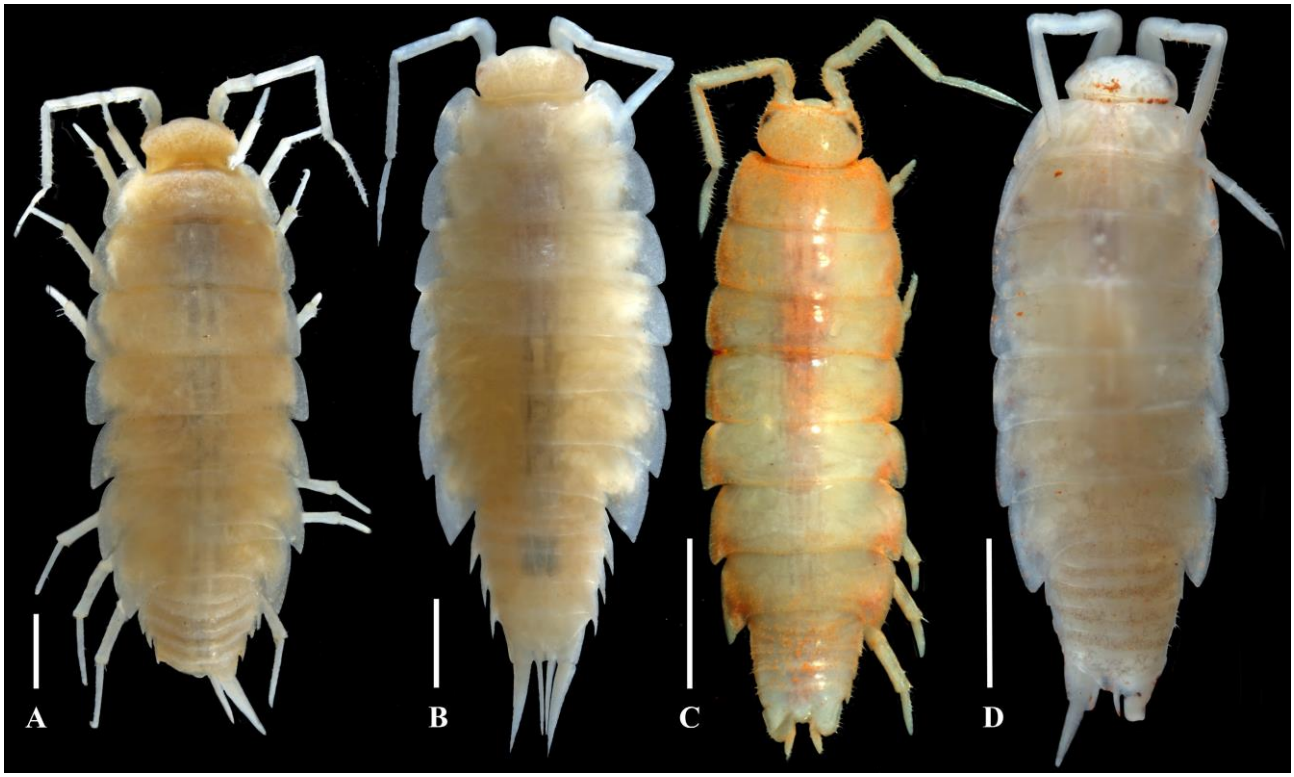


FIGURE 3. A, *Benthana iporangensis*; B, *Benthana alba* n. sp.; C, *Benthanoides amazonicus* n. sp.; D, *Benthanoides tarzan* n. sp. Scale bar: 1 mm.

Etymology. From the latin: *alba* = white. The name refers to the lack of pigmentation in the new species.

Morphological remarks. *Benthana alba* n. sp. presents some troglomorphic traits such as the lack of pigmentation and the reduction in the number of ommatidia. *Benthana alba* n. sp. is similar to *B. iporangensis* in the lack of pigmentation, in the shape of male pleopod 1 exopod, but it differs by the number of ommatidia (7 vs. 18 in *B. iporangensis*); by the number of aesthetascs on the antennula (19+2 vs. 11+2); and the articles proportion on the antenna (distal article longest vs. first article longest).

Ecological remarks. Specimens of *Benthana alba* n. sp. were only found in the N5SM2_0077 cave (also known as cave GEM-1762), in the plateau N5 (Serra Norte complex) (Fig. 1). This cave comprises a small cavity with 13,5 meters of horizontal projection. It is inserted on the "canga" formation (a topmost ferruginous breccia) with its entrance located inside the forest. The external area surrounding the cave features large trees and sparse understory, in addition to abundant undergrowth. The cave is, in general, a shelter under a high external environmental influence and without completely aphotic zones. The entrance is wide (around 3.5 x 8 m) and presents a large amount of organic matter; the floor (composed of many collapsed blocks) descends through the internal wings after an abrupt drop. Inside the cave, the floor is predominantly flat and composed of granulated sediment with some pebbles and sparse boulders, and a small pile of hematophagous bat guano was observed. In the iron-ore outcrop where the N5SM2_0077 cave is located there are several other caves that were also sampled (at least twice, in both dry and rainy periods) but specimens of *B. alba* n. sp. were only recorded in this cave. However, in the ferruginous subterranean systems this fact does not mean that it is restricted or rare, since many invertebrate species associated with the ferruginous subterranean systems use the interstitial voids such as the canaliculi network (Ferreira *et al.* 2018) (Fig. 2E). Therefore, specimens of *Benthana alba* n. sp. may be randomly found in macrocaverns, and this is at least partially reinforced by the small size of this cave (and consequently low environmental stability) where the specimens were found. On the other hand, one could think that the species is not restricted to subterranean habitats; however, external surveys for soil invertebrates accomplished in the Carajás region never revealed this species, thus

indicating it should be considered as troglobitic. It is worth mentioning that the canaliculi network is usually very superficial, what causes such habitats to become highly vulnerable to the mining processes that advance over the region. Therefore, even considering the lack of information about the real distribution and population density of this species, it is plausible to consider it as highly threatened due to its specific habitat, and effective loss of habitat caused by activities related to the iron ore exploitation on its occurrence area.

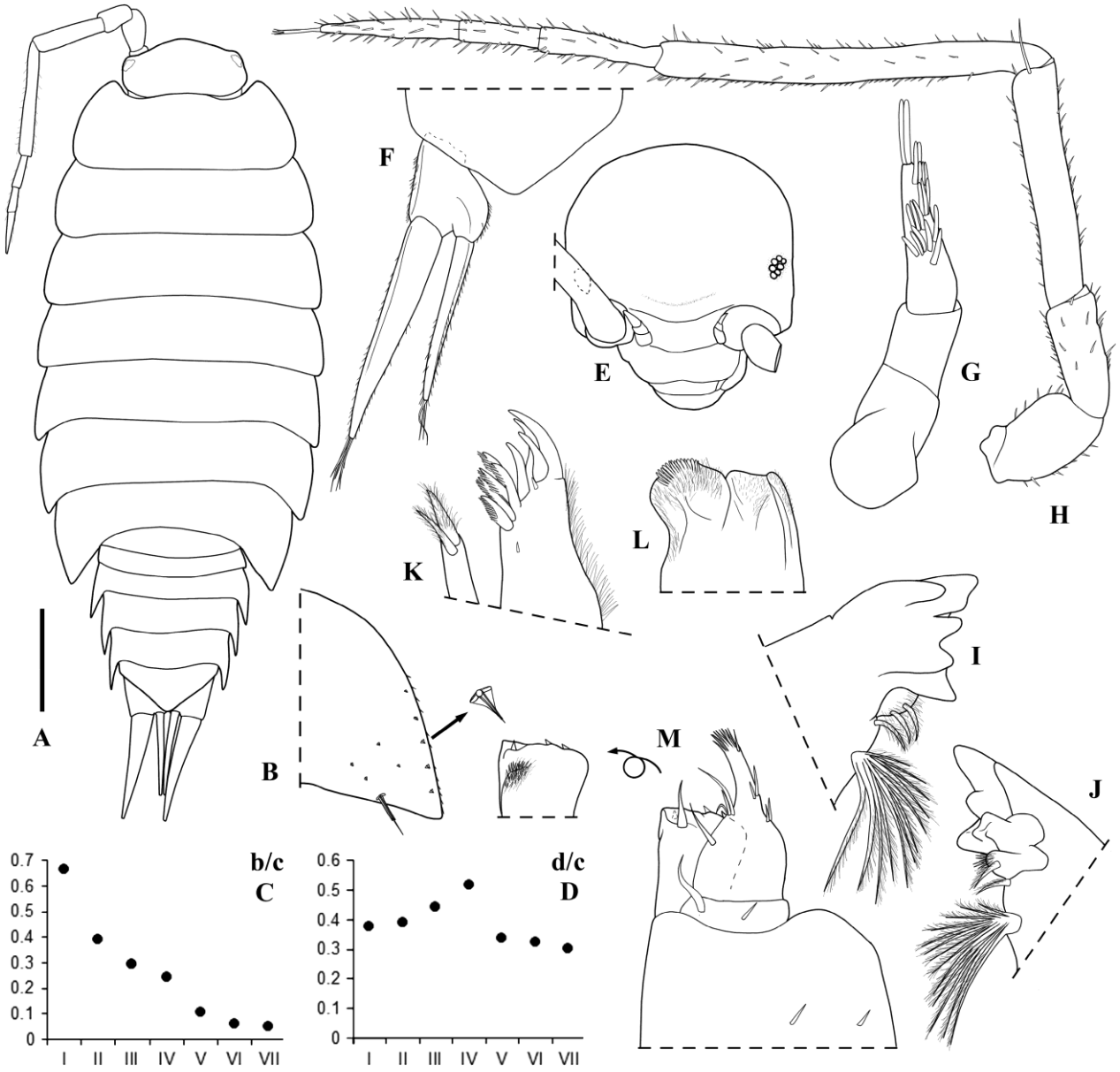


FIGURE 4. *Benthana alba* n. sp., male holotype (ISLA 96766). A, habitus, dorsal view; B, epimeron 7 with *nodulus lateralis* and tricorn scale-seta; C, *noduli laterales* b/c coordinates; D, *noduli laterales* d/c coordinates; E, cephalon, frontal view; F, pleotelson and uropod; G, antennula; H, antenna, I, left mandible; J, right mandible; K, maxillula; L, maxilla; M, maxilliped. Scale bar: 1 mm.

Genus *Benthanoides* Lemos de Castro, 1958

Type species. *Benthanoides pauper* (Jackson, 1926)

***Benthanoides amazonicus* n. sp.**
(Figures 3C, 6 and 7)

Type material. Holotype: male (ISLA 30597), Brazil, Pará state, municipality of Parauapebas, cave N1_0118 (-6.011570° -50.315151°), 17.vii–4.viii.2014, leg. Carste *et al*. Paratypes: 1 female (ISLA 30825), 7–28.i.2015; 1 female (ISLA 30824), 7–28.i.2015, same location as holotype.

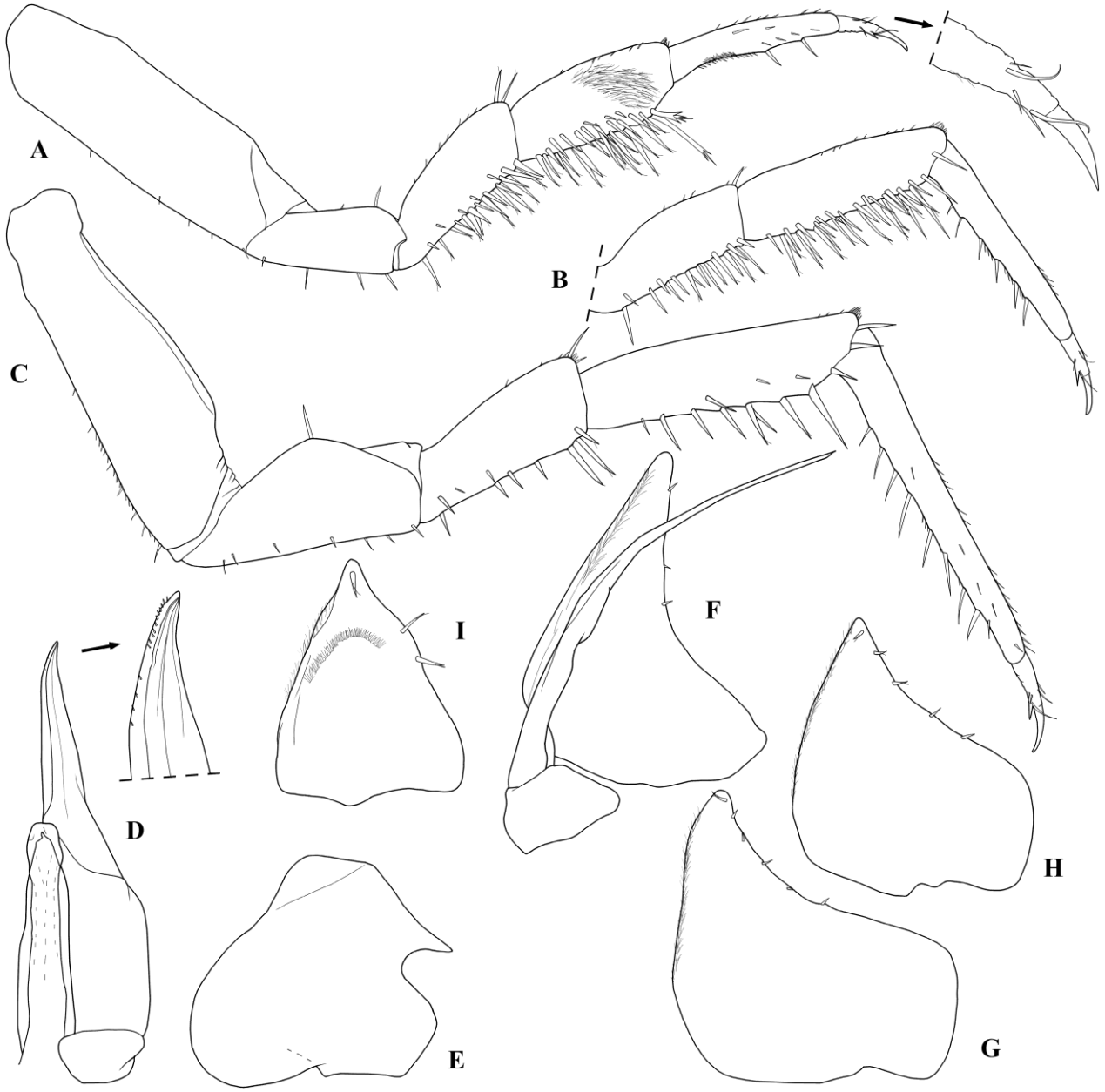


FIGURE 5. *Benthana alba* n. sp., male holotype (ISLA 96766). A, pereopod 1; B, pereopod 2; C, pereopod 7; D. genital papilla and pleopod 1 endopod; E, pleopod 1 exopod; F, pleopod 2; G, pleopod 3 exopod; H, pleopod 4 exopod; I, pleopod 5 exopod.

Additional material: Brazil, Pará state, municipality of Parauapebas, leg. Carste *et al*.: Cave N1_0052 (-6.027133° -50.276070°): 1 female (ISLA 30753), 4.ix–6.x.2014. Cave N1_0054 (-6.020486° -50.277299°): 1 female (ISLA 30598), 11.vi–2.vii.2014. Cave N1_0061 (-6.029507° -50.272607°): 1 female (ISLA 30456), 24.ii–13.iii.2015. Cave N1_0065 (-6.018455° -50.280455°): 1 female (ISLA 30742), 4.ix–6.x.2014. Cave N1_0088 (-6.017547° -50.284983°): 2 males (one in slide), 1 female (ISLA 30696). N1_0102 (-6.014371° -50.291041°): 1 female (ISLA 30458), 4.ix–6.x.2014; 1 male 1 female (ISLA 30461), 2–29.iv.2015; 2 females (ISLA 30472), 2–29.iv.2015; 1 male (ISLA 30724), 4.ix–6.x.2014; 2 males 1 female (ISLA 30730), 4.ix–6.x.2014. Cave N1_0106 (-6.022007° -50.306292°): 1 male (ISLA 30804 in slide), 7–28.i.2015; 1 female (ISLA 30585), 11.vi–2.vii.2014. Cave N1_0112 (-6.007904° -50.291736°): 1 female (ISLA 30438), 2–29.iv.2015. Cave N1_0117 (-6.011362° -50.314673°): 1 female (ISLA 30797), 7–28.i.2015. Cave N1_0121 (-6.034508° -50.299373°): 2 females (ISLA

30471), 2–29.iv.2015; 3 females (ISLA 30748), 4.ix–6.x.2014. Cave N1_0124 (-6.004271° -50.287711°): 1 female (ISLA 30807), 7–28.i.2015. Cave N1_0125 (-6.004525° -50.287964°): 1 female (ISLA 30811), 7–28.i.2015. Cave N1_0128 (-6.008184° -50.291799°): 2 females (ISLA 30436), 2–29.iv.2015. Cave N1_0129 (-6.010355° -50.291733°): 1 female (ISLA 30467), 2–29.iv.2015. Cave N1_0177 (-6.027469° -50.297973°): 1 male (ISLA 30726 part in slide), 4.ix–6.x.2014; 2 males (ISLA 30741); 1 female (ISLA 30697); 1 female (ISLA 30725), 2 males 1 female (ISLA 30473), 2–29.iv.2015. Cave N1_0178 (-6.040079° -50.291387°): 1 female (ISLA 30457), 24.ii–13.iii.2015. Cave N1_0191 (-6.046511° -50.277978°): 2 females (ISLA 30442), 2–29.iv.2015. Cave N1_0198 (-6.046546° -50.290927°): 1 female (ISLA 30747), 4.ix–6.x.2014. Cave N1_0207 (-6.057847° -50.286629°): 2 males 3 females (ISLA 30684), 4.ix–6.x.2014. Cave N1_0229 (-6.022811° -50.312824°): 1 male 1 female (ISLA 30459), 2–29.iv.2015; 1 male (ISLA 30740), 4.ix–6.x.2014. Cave N1_0231 (-6.020842° -50.272916°): 2 males 3 females (ISLA 30808), 3–17.xii.2014; 2 females (ISLA 30595), 11.vi–2.vii.2014. Cave N1_0232 (-6.020969° -50.273115°): 1 male (ISLA 30815), 3–17.xii.2014. Cave N1_0238 (-6.021051° -50.273964°): 1 juv (ISLA 30690), 11.vi–2.vii.2014; 1 female (ISLA 30602), 11.vi–2.vii.2014; 1 female (ISLA 30592), 11.vi–2.vii.2014. Cave N1_0248 (-6.068783° -50.272464°): 3 females (ISLA 30447), 2–29.iv.2015.

Diagnosis. Eyes with seven ommatidia; antennula with 13+2 aesthetascs; male pleopod 1 exopod elongated, longer than wide, distal part prominent acute, uropod exopod twice longer than endopod.

Description. Maximum body length: male 4 mm, female 5 mm. Colorless. Body convex, outline as in Fig. 6A. Dorsal surface smooth bearing long triangular scale-setae (Fig. 6B); *noduli laterales* long, one line per side with d/c coordinates reaching maximum on pereonite 4; b/c coordinates gradually decreasing (Fig. 6C, D). Cephalon (Fig. 6E) with suprantennal line bent downwards in middle, no frontal line and lateral lobes; eyes composed of seven small ommatidia arranged in two rows. Pereonites 5–7 with postero-lateral corners gradually more acute; pleon narrower than pereon (Fig. 6A). Telson (Fig. 6F) triangular, lateral sides straight, apex acute. Antennula (Fig. 6G) of three articles, distal article longest bearing 13 lateral aesthetascs in four rows, plus apical pair. Antenna (Fig. 6H) long, reaching pereonite 3 when extended backwards, distal article of peduncle longer than flagellum; flagellum of three articles, first and second articles subequal in length, distal article longest, second article with one aesthetasc, third article with two aesthetascs; apical organ short. Mandibles with molar penicil of 8 branches, left mandible (Fig. 6I) with 2+1 penicils, and right mandible (Fig. 6J) with 1+1 penicils. Maxillula (Fig. K) inner endite with two penicils; outer endite with 4+5 teeth (5 pectinate). Maxilla (Fig. 6L) outer as wide as inner lobe, covered with thick setae; outer lobe with sinuous distal margin, covered with thin setae. Maxilliped (Fig. 6M) with rectangular basis; endite rectangular, medial seta surpassing distal margin, two hooks on distal margin, dorsal face with longitudinal ridge bearing dense setae; proximal article of palp with two setae, one longer. Pereopods slender; carpus 1 with transverse antennal grooming brush, distal seta with hand-like apex; dactylus inner claw shorter than outer claw, dactylar and ungual setae simple, not surpassing outer claw. Uropod (Fig. 6F) protopod subquadrangular, protopod and exopod grooved on outer margin bearing glandular pores, exopod 2 times longer than endopod, endopod inserted proximally.

Male. Pereopods 1–3 (Fig. 7A) merus and carpus with brushes of setae on sternal margin. Pereopod 7 (Fig. 7B) ischium lateral margin grooved; merus with proximal lobe and thick setae near sternal margin. Genital papilla (Fig. 7C) with triangular ventral shield. Pleopod 1 (Fig. 7C) exopod elongated, longer than wide, distal part prominent acute, straight apex; endopod longer than exopod, stout and straight, distal portion tapering with line of short setae. Pleopod 2 (Fig. 7D) exopod triangular, outer margin concave with two setae; endopod slender, slightly longer than exopod. Pleopods 3 and 4 exopods as in Fig. 7E, F, respectively. Pleopod 5 exopod (Fig. 7G) triangular, outer margin sinuous with four setae and transverse plumose fringe.

Etymology. The name of the species refers to the locality of collection of the species, Amazon rainforest.

Morphological remarks. Considering the absence of the autapomorphic state of the male pleopod 1 exopod with a lateral dentiform protrusion of *Benthana* (Leistikow 2001), this new species was placed in *Benthanoides*, a close related taxon which lacks this protrusion. Unfortunately, the descriptions of *Benthanoides* species lack important taxonomic information regarding the position of *noduli laterales*, the number and disposition of aesthetascs on antennula, and the shape of male pleopods (Jackson 1926, Van Name 1936, Gruner 1955). However, *Benthanoides amazonicus* n. sp. presents the shape of male pleopod 1 exopod similar to the pattern for the genus, without a dentiform protrusion.

Ecological remarks. Specimens of *Benthanoides amazonicus* n. sp. were found in 25 caves in the N1 plateau (Serra Norte complex). Since the specimens were collected by consulting company, unfortunately, no data were

provided about the caves or the surrounding region. However, two aspects deserve to be highlighted: the first is the presence of large iron ore quarries in the N1 region, which certainly represents a great risk for this species, especially concerning habitat loss and potential disconnection between populations (or sub-populations) that can become isolated and thus even more threatened. The second refers to the very small size of the specimens (about 4 mm), which demonstrates the access of these organisms to the canga's canaliculi. Accordingly, such canaliculi may not only allow the dispersion of individuals between caves but also eventually comprise a significant portion of their habitat. In this perspective, the existing quarries in the region (in full expansion) certainly have the potential to fragment the populations of this species, increasing its risks of extinction.

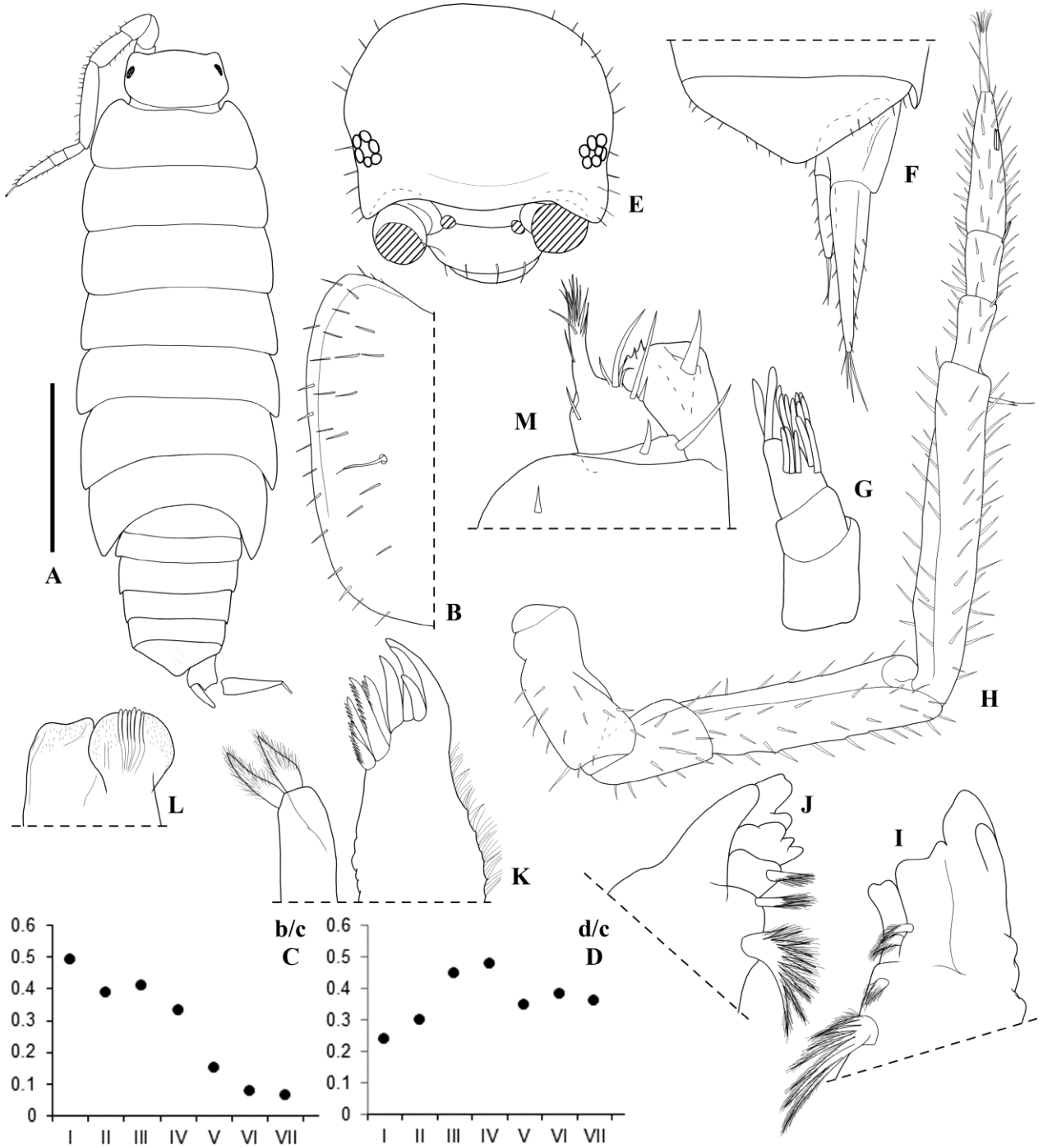


FIGURE 6. *Benthanoides amazonicus* n. sp., male paratype (ISLA 30726). A, habitus, dorsal view; B, epimeron 1 with *nodulus lateralis* and tricorn scale-setae; C, noduli laterales b/c coordinates; D, *noduli laterales* d/c coordinates; E, cephalon, frontal view; F, pleonite 5, pleotelson and uropod; G, antennula; H, antenna, I, left mandible; J, right mandible; K, maxillula; L, maxilla; M, maxilliped. Scale bar: 1 mm.



FIGURE 7. *Benthanoides amazonicus* n. sp., male paratype (ISLA 30726). A, pereopod 1; B, pereopod 7; C, genital papilla and pleopod 1; D, pleopod 2; E, pleopod 3 exopod; F, pleopod 4 exopod; G, pleopod 5 exopod.

***Benthanoides tarzan* n. sp.**
(Figures 2G, 3D, 8 and 9)

Type material. Holotype: male (ISLA 96768 in slide), Brazil, Pará state, municipality of Parauapebas, cave ST_ 0005 (-6.3297º -50.1067º), 11.viii.2016, leg. F.M.B Silva. Paratypes: 2 males, 3 juvenile (ISLA 96407), same data as holotype; 1 male (ISLA 96452), same data as holotype; 1 male (ISLA 96371), 21.i.2016, same data as holotype; 1 female (ISLA 44237), 21.i.2016, same location as holotype, leg. R.B. Pereira.

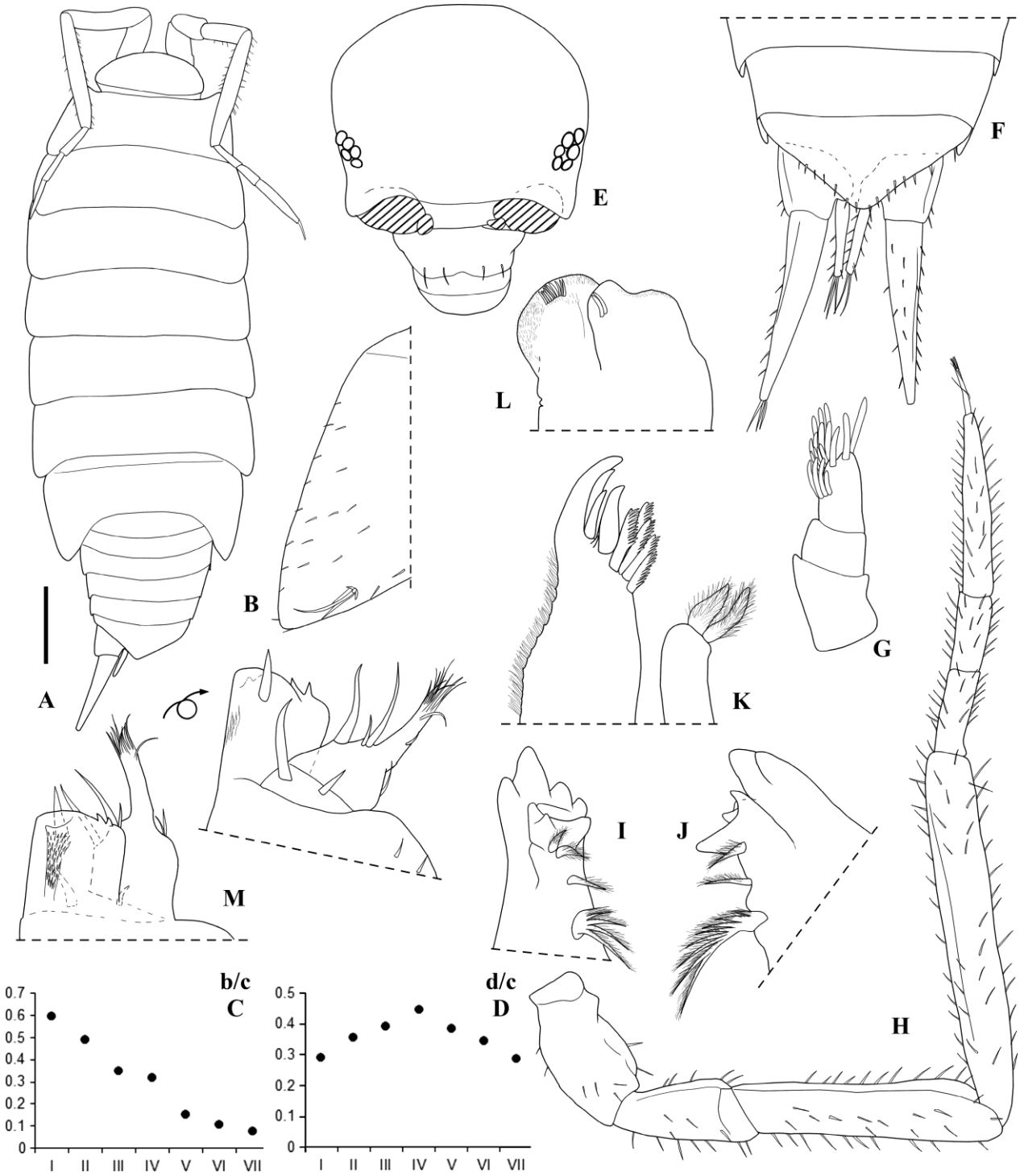


FIGURE 8. *Benthanoides tarzan* n. sp., male holotype (ISLA 96768). A, habitus, dorsal view; B, epimeron 7 with *nodulus lateralis* and tricorn scale-setae; C, *noduli laterales* b/c coordinates; D, *noduli laterales* d/c coordinates; E, cephalon, frontal view; F, pleonites 4 and 5, pleotelson and uropods; G, antennula; H, antenna, I, left mandible; J, right mandible; K, maxillula; L, maxilla; M, maxilliped. Scale bar: 0.5 mm.

Additional material: Brazil, Pará state, municipality of Parauapebas. Cave ST_0003 (-6.327461° -50.114125°): 1 female (ISLA 96370), 28.i.2016, leg. F.M.B Silva. Cave ST_0022 (-6.319868° -50.132135°): 1 female (ISLA 44236), 10.viii.2016, R.B. Pereira leg.; 1 male (ISLA 96367), 2.ii.2016, leg. F.M.B Silva; 2 males (ISLA 96443), 10.viii.2016, F.M.B Silva leg.; 1 male, 2 females (ISLA 96429), 10.viii.2016, leg. F.M.B Silva. Cave ST_0023 (-6.319160° -50.130079°): 2 females (ISLA 96451), 09.viii.2016, F.M.B Silva leg.; 2 females (ISLA 96461), 26.i.2016,

leg. F.M.B Silva. Cave ST_0030 (-6.3164º -50.1205º): 2 females (ISLA 96432), 04.ii.2016, leg. F.M.B Silva; 1 female (ISLA 96379), 04.ii.2016, leg. F.M.B Silva. Cave ST_0034 (-6.3201º -50.1128º): 1 female (ISLA 96428), 18.viii.2016, leg. F.M.B Silva. Cave ST_0043 (-6.3131º -50.0927º): 1 male, 1 female (ISLA 96389), 19.vii.2016, leg. F.M.B Silva. Cave ST_0050 (-6.3174º -50.1284º): 1 female (ISLA 96454), 26.i.2016, leg. F.M.B Silva. 1 female (ISLA 96459), 26.i.2016, leg. F.M.B Silva; 2 females (ISLA 96347), 26.i.2016, leg. F.M.B Silva. Cave ST_0054 (-6.3213º -50.1392º): 4 females (ISLA 96383), 20.viii.2016, leg. F.M.B Silva; 6 females (ISLA 96396), 29.i.2016, leg. F.M.B Silva; 1 male (ISLA 96414), 20.viii.2016, leg. F.M.B Silva; 1 male (ISLA 96444), 20.viii.2016, leg. F.M.B Silva. Cave ST_0062 (-6.3232º -50.1428º): 2 males, 1 female (ISLA 96416), 05.viii.2016, leg. F.M.B Silva; 1 male (ISLA 96447), 5.i.2016, leg. F.M.B Silva.

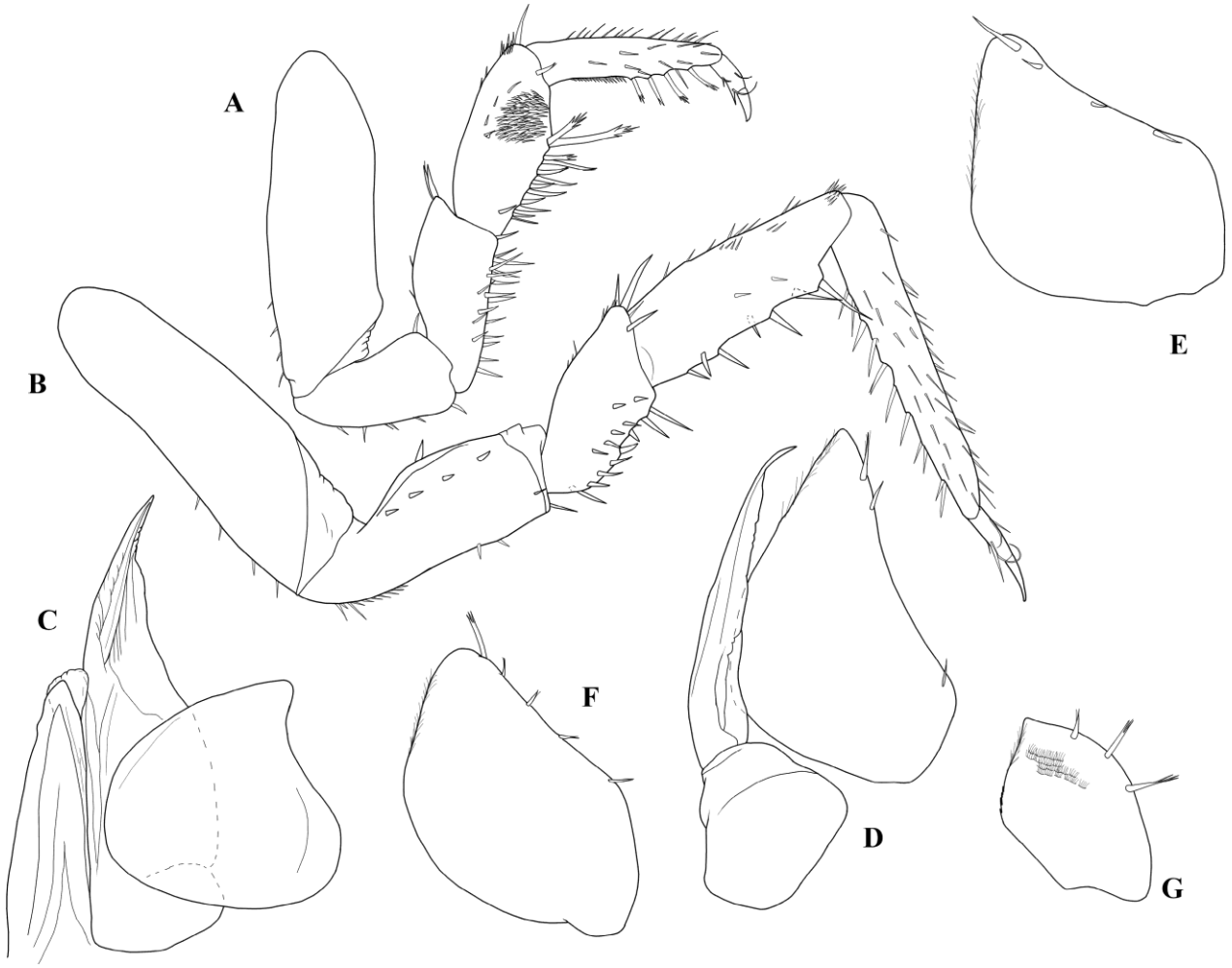


FIGURE 9. *Benthanoides tarzan* n. sp., male holotype (ISLA 96768). A, pereopod 1; B, pereopod 7; C, genital papilla and pleopod 1; D, pleopod 2; E, pleopod 3 exopod; F, pleopod 4 exopod; G, pleopod 5 exopod.

Diagnosis. Eyes with 5–6 ommatidia; antennula with 12+2 aesthetascs; male pleopod 1 exopod as long as wide, distal part triangular slightly developed; uropod exopod twice longer than endopod.

Description. Maximum body length: male and female with 4 mm. Colourless, some specimens with dots of pigmentation. Body convex, outline as in Fig. 8A. Dorsal surface smooth bearing long triangular scale-setae (Fig. 8B); noduli laterales long, one line per side with d/c coordinates reaching maximum on pereonite 4; b/c coordinates gradually decreasing (Fig. 8C, D). Cephalon (Fig. 8E) with suprantennal line straight, no frontal line and lateral lobes; eyes composed of 5–6 ommatidia arranged in two rows. Pereonites 5–7 with postero-lateral corners gradually more acute; pleon narrower than pereon, pleonites 3–5 with posterior point not developed (Fig. 8A). Telson (Fig. 8F) triangular, lateral sides straight. Antennula (Fig. 8G) of three articles, distal article longest bearing 12 lateral aesthetascs in four rows plus apical pair. Antenna (Fig. 8H) long, reaching pereonite 4 when extended backwards, distal article of peduncle longer than flagellum; flagellum of three articles, first and second articles subequal in

length, distal article longest, apical organ short. Mandibles with molar penicil of 8 branches, left mandible (Fig. 8I) with 2+1 penicils, and right mandible (Fig. 8J) with 1+1 penicils. Maxillula (Fig. 8K) inner endite with two penicils; outer endite with 4+5 teeth (5 pectinate). Maxilla (Fig. 8L) outer lobe wider than inner lobe, covered with thick setae; outer lobe distal margin sinuous, covered with thin setae. Maxilliped (Fig. 8M) with rectangular basis; endite rectangular, medial seta surpassing distal margin, two hooks on distal margin, dorsal face with longitudinal ridge bearing dense setae plus one short triangular seta; proximal article of palp with two setae, one longer. Pereopods slender; carpus 1 with transverse antennal grooming brush, distal seta with hand-like apex; dactylus inner claw shorter than outer claw, dactylar and ungual setae simple, not surpassing outer claw. Uropod (Fig. 8F) protopod subquadrangular, protopod and exopod grooved on outer margin, with glandular pores, exopod longer than endopod, endopod inserted proximally.

Male. Pereopod 1 (Fig. 9A) merus and carpus with brushes of setae on sternal margin. Pereopod 7 (Fig. 9B) ischium proximal margin setose; merus with proximal lobe and thick setae on lateral margin. Genital papilla (Fig. 9C) with triangular ventral shield and two subapical orifices. Pleopod 1 (Fig. 9C) exopod rounded, as long as wide, distal part triangular slightly developed; endopod longer than exopod, stout and straight, distal portion tapering with line of short setae. Pleopod 2 (Fig. 9D) exopod triangular, outer margin concave with three setae; endopod slender, slightly longer than exopod. Pleopods 3 and 4 exopods as in Fig. 9E, F, respectively. Pleopod 5 exopod (Fig. 9G) as wide as long, outer margin with three setae and transverse plumose fringe.

Etymology. The epithet name refers to the location where the species was found, Serra do Tarzan.

Morphological remarks. *Benthanoides tarzan* n. sp. is similar to *Benthanoides amazonicus* n. sp. in the disposition of the aesthetascs on antennula, in the modifications on merus on pereopod 7, in the shape of male 1 endopod, and in the shape of male pleopod 2. They can be distinguished from each other by the shape of male pleopod 1 exopod, that is as wide as long in *Benthanoides tarzan* n. sp., and longer than wide in *Benthanoides amazonicus* n. sp.

Ecological remarks. Specimens of *Benthanoides tarzan* n. sp. were observed in some caves located in "Serra do Tarzan" (ST). This area presents 69 caves, distributed along the whole extension of the ferruginous outcrop. Individuals of *Benthanoides tarzan* n. sp. were found in 10 caves (Fig. 1), thus indicating the species is widely distributed along the outcrop. Differently from *Benthana alba* n. sp., which may eventually inhabit voids in the ferruginous outcrop, the distribution of *Benthanoides tarzan* n. sp. indicates that this species seems to be also closely related to the macrocave itself. However, as the caves in which the species was observed are widely distributed throughout the iron ore formation, along with the specimens' small body size, it is plausible to assume that migrations between caves through the canaliculi network occur. Furthermore, *Be. tarzan* n. sp. has a lower number of ommatidia among all known species of *Benthanoides*, and may indicate an important troglomorphic trait, and that the species is troglobitic. However, unlike *B. alba* n. sp., which seems to be highly threatened, *Be. tarzan* n. sp. occurs in a region inserted within the limit of a conservation unit (Campos Ferruginosos National Park), which fully protects the caves and their surrounding area, preventing touristic and exploratory activities; in addition, the geographic isolation protects the area in its pristine state. Therefore, this species seems not to be currently under any threat.

Discussion

Most species of *Benthana*, as other Philosciidae species, are typically epigean and found in the leaf litter of the Atlantic Forest (Campos-Filho *et al.* 2015). However, the discovery of *Benthana alba* n. sp. in the Amazon biome represents the first recorded occurrence of the genus in this region, suggesting a potential relict lineage. The species of *Benthana* are usually well pigmented and the pattern of pigmentation may be used to distinguish species. Notably, troglobitic and endogean species often exhibit reduced or absent pigmentation, providing valuable evidence of their subterranean (endogean/cave) lifestyle (Fig. 3). The eyes also showed a reduction in the number of ommatidia, since most species of *Benthana* presented up to 20 ommatidia (27 species, with an average number of ommatidia corresponding to 22.48). There are only seven species with less than 20 ommatidia: *B. taeniata* Araujo & Buckup, 1994 (17–19 ommatidia), *B. schubarti* Lemos de Castro, 1958 (16 ommatidia), *B. canastraensis* Campos-Filho, Taiti & Araujo, 2015 (16 ommatidia), *B. aimores* Campos-Filho, Taiti & Araujo, 2015 (12–15 ommatidia), *B. tupinamba* Campos-Filho, Taiti & Araujo, 2015 (12 ommatidia), *B. iporangensis* (18 ommatidia) and *B. xiquinhoi* (10–12

ommatidia) (Campos-Filho *et al.* 2015, 2019). With the exception of *B. aimores*, which is classified as an endogean species, and lacks pigmentation, and presents a significantly lower number of ommatidia, *B. alba* n. sp. possesses the lowest recorded number of ommatidia among all known *Benthana* species.

Regarding the number of ommatidia between *Benthanoides* species: *Be amazonicus* n. sp. has 7 ommatidia and *Be. tarzan* n. sp. 5–6 ommatidia, while *Be. pauper* has 14 ommatidia; *Be. villosus* has 16–17 ommatidia; and *Be. peruensis* has 16–18 ommatidia. Consequently, the reduced number of ommatidia in both new species, coupled with their depigmented integument, suggests their adaptation to cave environments. Moreover, the elongation of appendages is often regarded as a significant trait associated with cave-restricted lifestyle. However, as previously mentioned, the new *Benthanoides* species are strongly associated not only with caves themselves but also with the interstitial voids (canaliculi) that occur between caves. Consequently, the ferruginous subterranean void system may serve as the primary habitat for them, rendering elongated appendages unsuitable for movement in such spatially restricted environments. Thus, appendage elongation appears to be dependent on the specific type of subterranean habitat preferred by the species, as observed in other groups such as amphipods (Trontelj *et al*. 2012) and beetles (Pellegrini & Ferreira 2017). As mentioned earlier, a revision of the *Benthanoides* genus and its species is necessary (Pérez-Schultheiss 2009; Pérez-Schultheiss & Urra 2020). These two newly described species from Brazil represents the first records of *Benthanoides* in the country and the first records of troglobitic species within the genus.

Acknowledgments

The authors would like to thank the Centro Nacional de Pesquisa e Conservação de Cavernas—CECAV and Instituto Brasileiro de Desenvolvimento e Sustentabilidade—IABS for the financial support and scholarship provided to GMC (n°. 006/2021. TCCE ICMBio/Vale 01/2018); CNPq (National Council for Scientific and Technological Development) for the productivity scholarship provided to RLF (n. 302925/2022-8). We would also like to thank the institutions that supported the study with funding for infrastructure (CNPq, FAPEMIG, VALE), Allan Calux for the photograph in Fig. 2B; and Marcos Oliveira for the photographs of Serra do Tarzan.

References

ANM (2020) Agência Nacional de Mineração-Brazilian Mineral Yearbook. Available from: https://www.gov.br/anm/pt-br/centrais-de-conteudo/publicacoes/serie-estatisticas-e-economia-mineral/anuario-mineral/anuario-mineral-brasileiro (26 January 2023)

Araujo, P.B. & Buckup, L. (1994) Two new species of terrestrial Isopoda from southern Brazil (Crustacea, Isopoda, Oniscidea). *Spixiana*, 17, 269–274.

Araujo, P.B. & Lopes, E.R.C. (2003) Three new species of *Benthana* Budde-Lund (Isopoda, 'Philosciidae') from Brazil. *Journal of Natural History*, 37 (20), 2425–2439.
https://doi.org/10.1080/00222930210154513

Brandt, J.F. (1833) Conspectus Monographiae Crustaceorum Oniscodorum Latreillii. *Byulleten Moskovskogo Obshchestva Ispŷtateleĭ Prirodŷ*, 6, 171–193.

Boyko, C.B., Bruce, N.L., Hadfield, K.A., Merrin, K.L., Ota, Y., Poore, G.C.B. & Taiti, S. (Eds.) (2008a onwards) World Marine, Freshwater and Terrestrial Isopod Crustaceans database. Philosciidae Kinahan, 1857. Available from: https://www.marinespecies.org/aphia.php?p=taxdetails&id=246825 (accessed 31 May 2023)

Boyko, C.B., Bruce, N.L., Hadfield, K.A., Merrin, K.L., Ota, Y., Poore, G.C.B. & Taiti, S. (Eds) (2008b onwards). World Marine, Freshwater and Terrestrial Isopod Crustaceans database. *Benthana* Budde-Lund, 1908. Available from: https://www.marinespecies.org/aphia.php?p=taxdetails&id=248513 (accessed 31 May 2023)

Budde-Lund, G. (1908) Isopoda von Madagaskar und Ostafrika mit Diagnosen verwandter Arten. *In*: Voeltzkow, A. (Ed.), *Reise in Ostafrika in den Jahren 1903–1905*. Wissenschaftliche Ergebnisse, Stuttgart, pp. 265–308.
https://doi.org/10.5962/bhl.title.12989

Campos-Filho, I.S., Costa, S.L.N. & Araujo, P.B. (2013) Two new species of *Benthana* Budde-Lund, (Crustacea: Isopoda: Philosciidae) from Brazil. *Tropical Zoology*, 26 (1), 1–14.
https://doi.org/10.1080/03946975.2013.773220

Campos-Filho, I. S., Araujo, P. B., Bichuette, M. E., Trajano, E. & Taiti, S. (2014) Terrestrial isopods (Crustacea: Isopoda: Oniscidea) from Brazilian caves. *Zoological Journal of the Linnean Society*, 172, 360–425. https://doi.org/10.1111/zoj.12172

Campos-Filho, I.S., Taiti, S. & Araujo, P. B. (2015) Taxonomic revision of the genus Benthana Budde-Lund, 1908 (Isopoda: Oniscidea: Philosciidae). *Zootaxa*, 4022 (1), 1–73.

https://doi.org/10.11646/zootaxa.4022.1.1
Campos-Filho, I.S., Bichuette, M.E. & Taiti, S. (2016) Three new species of terrestrial isopods (Crustacea, Isopoda, Oniscidea) from Brazilian caves. *Nauplius*, 24, e2016001.
https://doi.org/10.1590/2358-2936e2016001
Campos-Filho, I.S., Cardoso, G.M. & Aguiar, J.O. (2018) Catalogue of terrestrial isopods (Crustacea, Isopoda, Oniscidea) from Brazil: an update with some considerations. *Nauplius*, 26, 1–40.
https://doi.org/10.1590/2358-2936e2018038
Campos-Filho, I.S., Fernandes, C.S., Cardoso, G.M., Bichuette, M.E., Aguiar, J.O. & Taiti, S. (2019) Two new species and new records of terrestrial isopods (Crustacea, Isopoda, Oniscidea) from Brazilian caves. *Zootaxa*, 4564 (2), 422–448. https://doi.org/10.11646/zootaxa.4564.2.6
Ferreira, R.L., de Oliveira, M.P.A. & Silva, M.S. (2018) Subterranean Biodiversity in Ferruginous Landscapes. In: Moldovan, O., Kováč, Ľ. & Halse, S. (Eds.), Cave Ecology. Ecological Studies. Springer, Cham. 235, 435–447.
https://doi.org/10.1007/978-3-319-98852-8_21
Gruner, H.E. (1955) Die Gattung *Benthana* Budde-Lund, 1908 (Isopoda, Oniscoidea). Zoologische Jahrbücher, Abteilung für Systematik, Ökologie und Geographie der Tiere, 83, 441–452.
Jackson, H.G. (1926) Woodlice from Spain and Portugal, with an Account of Benthana, a Sub-genus of *Philoscia*–Crustacea.
Proceedings of the Zoological Society of London, 1926, 183–201.
Kinahan, J. (1857) Analysis of certain allied genera of terrestrial isopods; with description of a new genus, and a detailed list of the British species of *Ligia*, *Philougria*, *Philoscia*, *Porcellio*, *Oniscus* and *Armadillium* [sic]. *Natural History Review*, 4, 258–282.
Leistikow, A. (2001) Phylogeny and biogeography of South American Crinocheta, traditionally placed in the family "Philosciidae" (Crustacea: Isopoda: Oniscidea). *Organisms Diversity & Evolution*, 1 (3), 239–240.
https://doi.org/10.1078/1439-6092-00020
Leistikow, A. & Araujo, P.B. (2006) The systematic position of *Benthanoscia longicaudata* Lemos de Castro, 1958 (Isopoda: Oniscidea: Crinocheta). *Systematics and Biodiversity*, 4 (3), 243–254.
https://doi.org/10.1017/S1477200006001939
Lemos de Castro, A. (1958) Revisão do gênero *Benthana* Budde-Lund, 1908 (Isopoda, Oniscidae). *Arquivos do Museu Nacional*, 44, 85–118.
Lima, M.I. & Serejo, C.S. (1993) A new species of *Benthana* Budde-Lund from Brazilian caves (Crustacea; Isopoda; Oniscoidea).
Proceedings of the Biological Society of Washington, 106, 490–496.
Montesanto, G. (2015) A fast GNU method to draw accurate scientific illustrations for taxonomy. ZooKeys, 515, 191–206. https://doi.org/10.3897/zookeys.515.9459
Montesanto, G. (2016) Drawing setae: a GNU way for digital scientific illustrations.
Nauplius, 24, 1–6. https://doi.org/10.1590/2358-2936e2016017
Pellegrini, T.G. & Ferreira, R.L. (2017) Two new troglobitic *Coarazuphium* Gnaspini, Godoy & Vanin 1998 species of ground beetles from iron ore Brazilian caves (Coleoptera: Carabidae: Zuphiini). *Zootaxa*, 4306 (4), 551–566.
https://doi.org/10.11646/zootaxa.4306.4.6
Pérez-Schultheiss, J. (2009) State of knowledge on terrestrial isopods (Crustacea: Isopoda: Oniscidea) of Chile, with a species checklist. Boletín Museo Nacional de Historia Natural, 58, 51–66.
https://doi.org/10.54830/bmnhn.v58.2009.233
Pérez-Schultheiss, J. & Urra, F. (2020) Isópodos terrestres (Crustacea: Isopoda: Oniscidea) del Parque Nacional Bosque Fray Jorge, Región de Coquimbo, Chile. *Boletín Museo Nacional de Historia Natural*, 69 (2), 29–54.
https://doi.org/10.54830/bmnhn.v69.n2.2020.4
Piló, L.B., Auler, A.S. & Martins, F. (2015) Carajás National Forest: Iron ore plateaus and caves in southeastern Amazon. *In*: Vieira, B.C., Salgado, A.A.R., Santos, L.J.C. Landscapes and landforms of Brazil. Springer, Dordrecht, pp. 273–283. https://doi.org/10.1007/978-94-017-8023-0
Sahoo, P.K., Guimaraes, J.T., Souza-Filho, P.W., Silva, M.S., Silva Jr., R.O., Pessim, G., Morae, B.C, Pessoa, P.F.P., Rodrigues, T.M., Costa, M. & Dall'agnol, R. (2016) Influence of seasonal variation on the hydro-biogeochemical characteristics of two upland lakes in the Southeastern Amazon, Brazil. *Anais da Academia Brasileira de Ciências*, 88 (4), 2211–2227. https://doi.org/10.1590/0001-3765201620160354
Schmalfuss, H. (2003) World catalog of terrestrial isopods (Isopoda: Oniscidea). Stuttgarter Beiträge zur Naturkunde, Serie A, 654, 1–341.
Trontelj, P., Blejec, A. & Fišer, C. (2012) Ecomorphological convergence of cave communities. *Evolution: International Journal of Organic Evolution*, 66 (12), 3852–3865.
https://doi.org/10.1111/j.1558-5646.2012.01734.x
Van Name, W. (1936) The American land and freshwater isopod Crustacea. *Bulletin of the American Museum of Natural History*, 71, 1–535.
Vandel, A. (1960) *Faune de France. Vol. 64. Isopodes terrestres. Première Partie*. Lechevalier, Paris, 416 pp.

Nauplius
The Journal of The Brazilian Crustacean Society

e-ISSN 2358-2936
www.scielo.br/nau
www.crustacea.org.br

Cave-dwellers *Diploexochus* (Isopoda, Armadillidae): new species and new records of the genus from Brazil

Giovanna Monticelli Cardoso
Rafaela Bastos-Pereira
Rodrigo Lopes Ferreira

Universidade Federal de Lavras (UFLA), Centro de Estudos em Biologia Subterrânea, Departamento de Biologia, Programa de Pós-Graduação em Ecologia Aplicada. Lavras, Minas Gerais, Brasil.
GMC E-mail: gmcardoso.bio@gmail.com
RB-P E-mail: rafaelabastospereira@gmail.com
RLF E-mail: drops@ufla.br

ZOOBANK: https://zoobank.org/urn:lsid:zoobank.org:pub:88BC9632-9146-4B75-B62F-59480ABB3E24

ABSTRACT

Two new species of *Diploexochus* are described. *Diploexochus spinatus* sp. nov. from Lapa do Honorato cave, located in the municipality of Iuiu, and *Diploexochus obscurus* sp. nov. from Água Escura I cave, located in the municipality of Carinhanha, both in the southwest of Bahia State, northeastern Brazil. Both species are likely to occur in caves due to anthropogenic impacts in the surrounding area (such as deforestation) and/or looking for the stable microclimatic conditions found in the subterranean realm. Additionally, *D. echinatus* is recorded in a cave in the municipality of Rurópolis, Pará State, northern Brazil. These represent the first records of the genus for subterranean environments.

KEYWORDS

Bahia, cave species, Neotropics, terrestrial isopods, Woodlice

Editor-in-chief Christopher Tudge

Associate Editor
Spyros Sfenthourakis

Corresponding Author Giovanna Cardoso
gmcardoso.bio@gmail.com

Submitted 28 April 2022
Accepted 01 August 2022
Published 23 January 2023

DOI 10.1590/2358-2936e2023008

All content of the journal, except where identified, is licensed under a Creative Commons attribution-type BY.

INTRODUCTION

Although described in 1833 by Brandt, the genus *Diploexochus* Brandt, 1833 currently has only one valid taxon, the type species *Diploexochus echinatus* (Schmalfuss, 2003). Most species originally described as belonging to *Diploexochus* had been relocated into other armadillid genera, namely: *Venezillo* Verhoeff, 1928, *Lobodillo* Taiti, Paoli and Ferrara, 1998, *Pseudodiploexochus* Lewis, 1998, *Parasphaerillo* Arcangeli, 1934, *Sphaerillodillo* Taiti, Paoli and Ferrara, 1998, *Spherillo* Dana, 1853, *Ctenorillo*

Verhoeff, 1942, *Myrmecodillo* Arcangeli, 1934, *Armadillo* Latreille, 1802, *Pachydillo* Taiti, Paoli and Ferrara, 1998, and *Aulacodillo* Verhoeff, 1942 (Bokyo et al., 2022). This scenario reveals how diffuse and poorly explored the diagnoses are within Armadillidae Brandt, 1831, reinforcing the urgent need for revisional studies.

Endemic to Central America and northern South America, *Diploexochus* was already recorded from Brazil, French Guiana, Guyana, and Trinidad (Schmalfuss, 2003). Campos-Filho et al. (2017) redescribed *D. echinatus*, recording the species from Floresta Nacional Caxiuanã in the state of Pará, northern Brazil. The present work reports a new occurrence of this species, the first in the subterranean realm, also in the state of Pará. Moreover, two new species from caves in the state of Bahia, northeastern Brazil, are described. Additionally, ecological notes and conservation status are provided for the new species and *D. echinatus*.

MATERIAL AND METHODS

In the field, specimens were manually collected with the aid of brushes and fixed in 70% ethanol. In the laboratory, they were measured and photographed with a ZEISS Axio ZoomV16 stereomicroscope with an Axio Cam 506 Color camera, dissected and mounted on slides using Hoyer's medium. Drawings were made either from photographs or from dissected mounted specimens with the aid of a camera lucida on a Leica DM750 microscope. Final illustrations were prepared in the software GIMP (v. 2.8) (Montesanto 2015; 2016) with a Cintiq Drawing Pad (Wacom). Some specimens were analyzed under an Hitachi TM4000 scanning electron microscope. For this purpose, the specimens were dissected and their parts were glued onto an aluminum support stub with double-sided adhesive carbon tape. Specimens were not sputter-coated with gold, since this SEM operates at low vacuum. Holotype and paratypes of the new species were deposited in the Subterranean Invertebrate Collection of Lavras (ISLA - UFLA) in the Center of Studies on Subterranean Biology of the Federal University of Lavras (CEBS/UFLA, Lavras, Brazil).

SYSTEMATICS

Family Armadillidae Brandt, 1831 Genus

Diploexochus Brandt, 1833

Diploexochus echinatus Brandt, 1833

(Figs. 1, 2)

Diploexochus echinatus Brandt, 1833: 192, pl. IV, figs. 20, 21; H. Milne-Edwards, 1840: 180; Budde-Lund, 1909: 54; Richardson, 1912: 479; Arcangeli, 1934: 92, 1957: 101; Van Name, 1936: 398, figs. 241–243; Lemos de Castro, 1967: 322; Souza-Kury, 1998: 6532; Leistikow and Wägele, 1999: 44; Schmalfuss, 2003: 90; Campos-Filho et al., 2017: 22, figs. 98–122; Campos-Filho et al., 2018: 27.

Armadillo echinatus — Budde-Lund, 1879: 7; Budde-Lund, 1885: 26; Budde-Lund, 1904: 104, pl. IX figs. 35–37.

Cubaris echinatus — Pearse, 1917: 3.

Cubaris gaigei — Pearse, 1917: 2, fig. 1; Van Name, 1925: 467.

Material examined. 2 males (ISLA 77541), Brazil, Pará State, municipality of Rurópolis, Lucas cave (-4.139791º -55.071947º), 09 October 2020, R.L. Ferreira coll.

Previous records. French Guiana, Guyana, Trinidad (Schmalfuss, 2003, Campos-Filho et al., 2017), and Brazil, Pará State: Acará and Belém (Ilha do Marajó) (Lemos de Castro, 1967), and Caxiuanã (Floresta Nacional Caxiuanã) (Campos-Filho et al., 2017).

Habitat and ecological remarks. Two specimens of *D. echinatus* (Fig. 1) were found in a sandstone cave (Lucas cave – Fig. 2) located in the municipality of Rurópolis, Pará State, northern Brazil. Paleozoic rocks covered by a dense Amazon ombrophilous rainforest represent the regional geology. The area is located in the hot tropical climate domain with annual dry period of 2 to 3 months. The annual average temperatures are above 20 ºC and the annual precipitation is around 1,754 mm (Tereso et al., 1975). Lucas cave presents a single entrance (Fig. 2A) leading to the main cave conduit (Fig. 2B, C), which presents 365 m of horizontal projection.

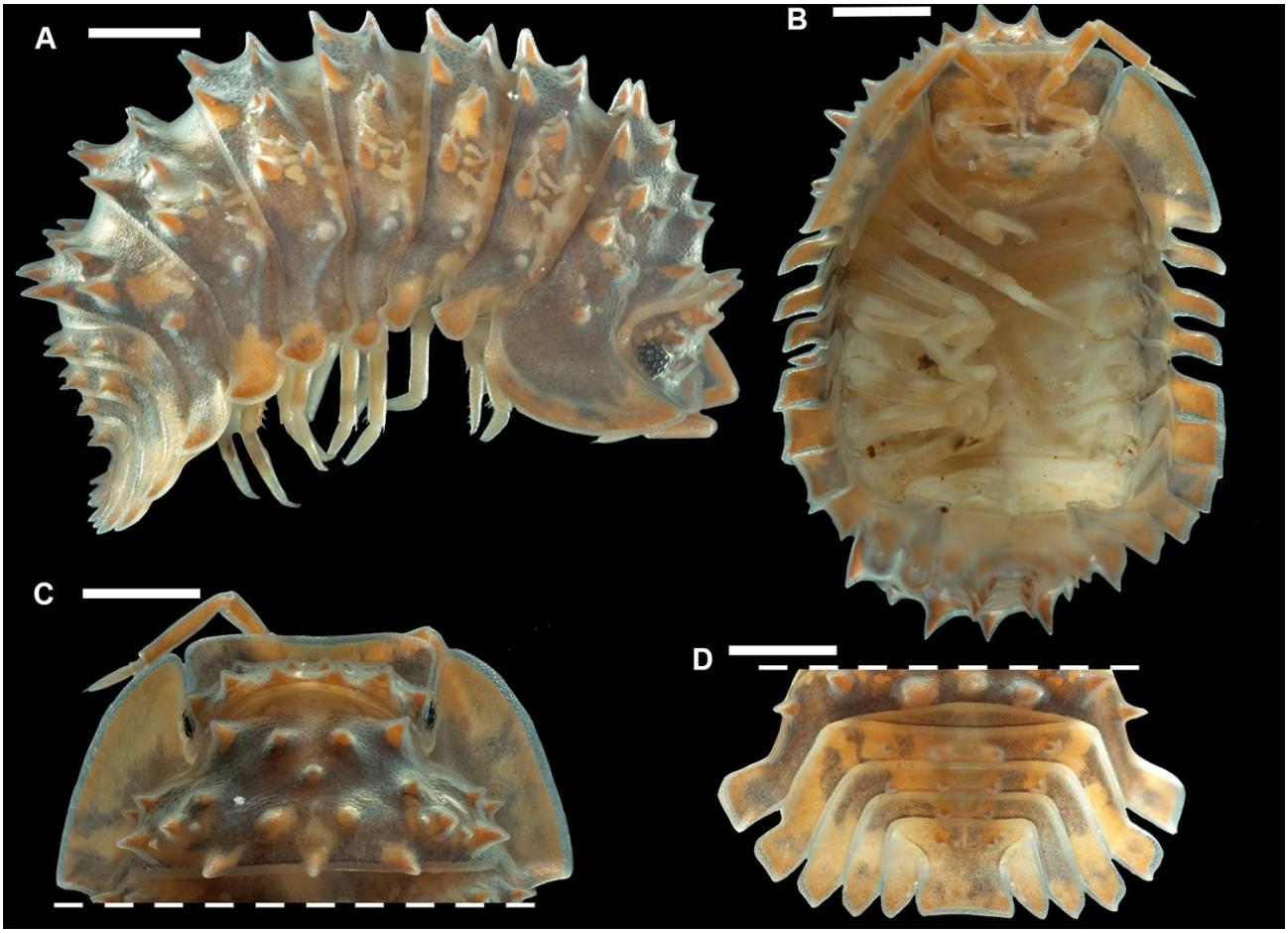


Figure 1. *Diploexochus echinatus*, female. **A**, Habitus, lateral view; **B**, epimera of pereonites 1-7, ventral view; **C**, cephalon and pereonite 1, dorsal view; **D**, pereonite 7, pleonites and telson, dorsal view. Scale bars: 1 mm.

The cave does not present any drainage, although the atmosphere is moist due to the external forest and climate. A big bat colony inhabits the cave, producing massive amounts of guano, which covers a considerable portion of the floor. Both specimens of *D. echinatus* were found in a region close to the entrance, though already aphotic, around 25 m from the entrance on a pile of stones made by ancient inhabitants of the region (unknown reason) (Fig. 2D). These organisms are quite sensitive, curling up at the slightest touch, like other armadillids (Fig. 2E). Even though the cave was meticulously inspected looking for invertebrates, only these two specimens of *Diploexochus* were found. In addition, other caves sampled in the region did not reveal the presence of this species. It is important to mention that this represents the first record of this species from cave environments.

***Diploexochus spinatus* sp. nov.**

(Figs. 3 – 6)

Zoobank: urn:lsid:zoobank.org:act:7A394BCA- F660-4424-A8A3-5AE58475F71C

Type material. Holotype: male (ISLA 77536), Brazil, Bahia State, municipality of Iuiu, Lapa do Honorato cave (-14.4628º -43.5931º), 19 October 2021, R.L. Ferreira coll. Paratypes: 2 males (1 in slide), 7 females (ISLA 77537), same data as holotype.

Additional material. 1 female (ISLA 77537), Brazil, Bahia State, municipality of Malhada, Tapera d'Água cave (-14.517270º -43.682842º), 18 October 2021, R.L. Ferreira coll.

Diagnosis. Dorsal surface covered with acute and rectangular tubercles; pleonites 3–5 with 2 paramedian tubercles, telson with 2 tubercles or smooth; pereonites epimera f lattened directed backwards; pleonites epimera quadrangular with round distal corner.

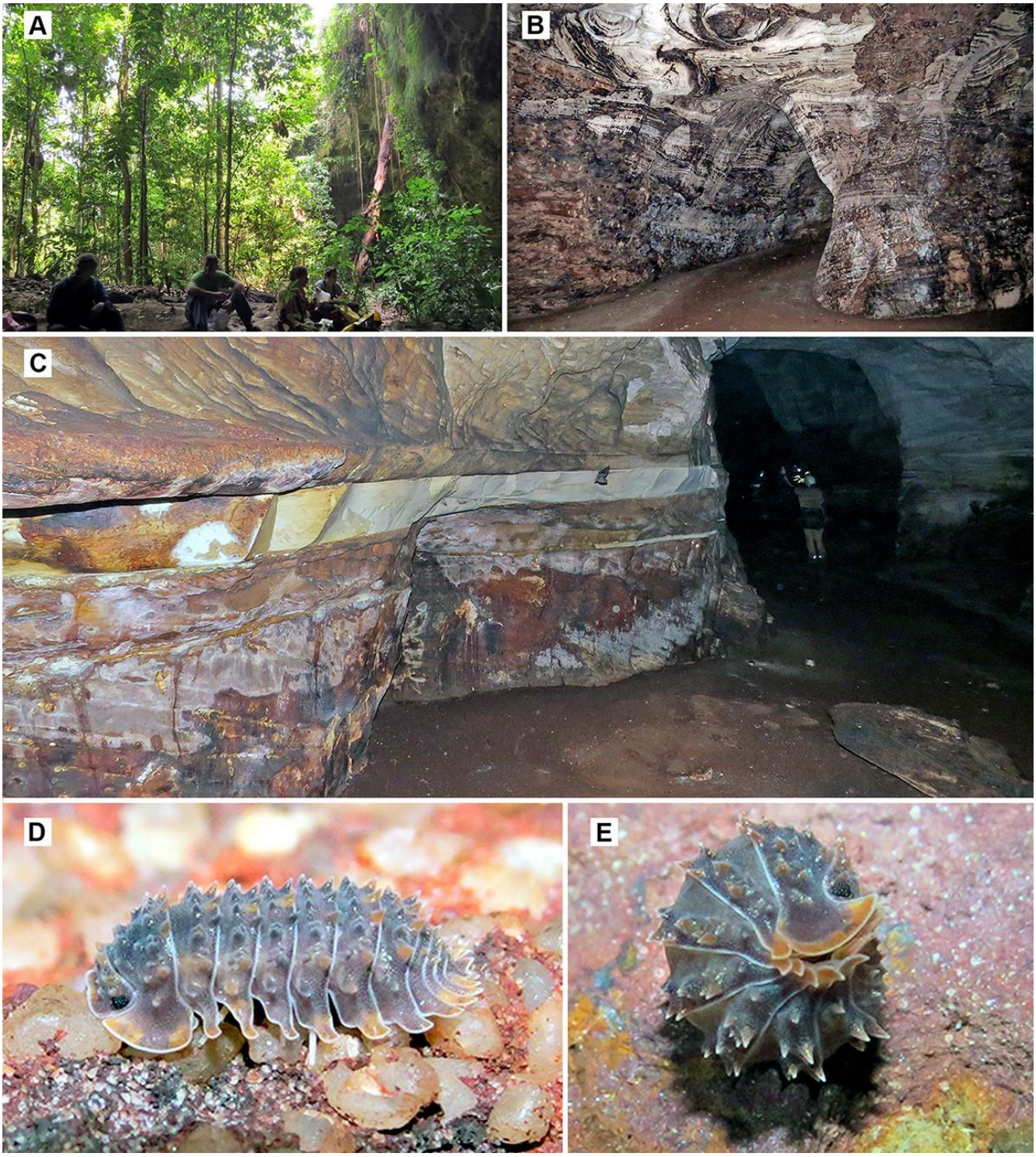


Figure 2. Lucas cave, Rurópolis, Pará State, Brazil. **A**, Surrounding area; **B**, main cave conduit; **C**, cave conduit; **D**, live specimen of *Diploexochus echinatus* in lateral view; **E**, live specimen of *Diploexochus echinatus* showing the ability to roll into a ball.

Description. Body length: ♂ 10 mm, ♀ 12 mm. Body dark gray with depigmented spots, antenna yellowish (Fig. 3A). Endoantennal conglobation (Fig. 4A, B). Dorsal surface covered with acute and rectangular tubercles disposed as follows (Fig. 4B): cephalon with 11 tubercles in 3 rows; pereonite 1 with 21 tubercles in 3 rows; pereonites 2–6 with 13 tubercles in 2 rows; pereonite 7 with 11 tubercles in 2 rows; pleonites 3–5 with 1 row of 2 paramedian tubercles each, telson smooth (holotype) or with 2 small tubercles. Dorsal surface with short semi-circular scale-setae, one nodulus lateralis on the second line of tubercles far from lateral margin, on outer distal margin (Fig. 3B). Cephalon with frontal shield prominent, distal margin

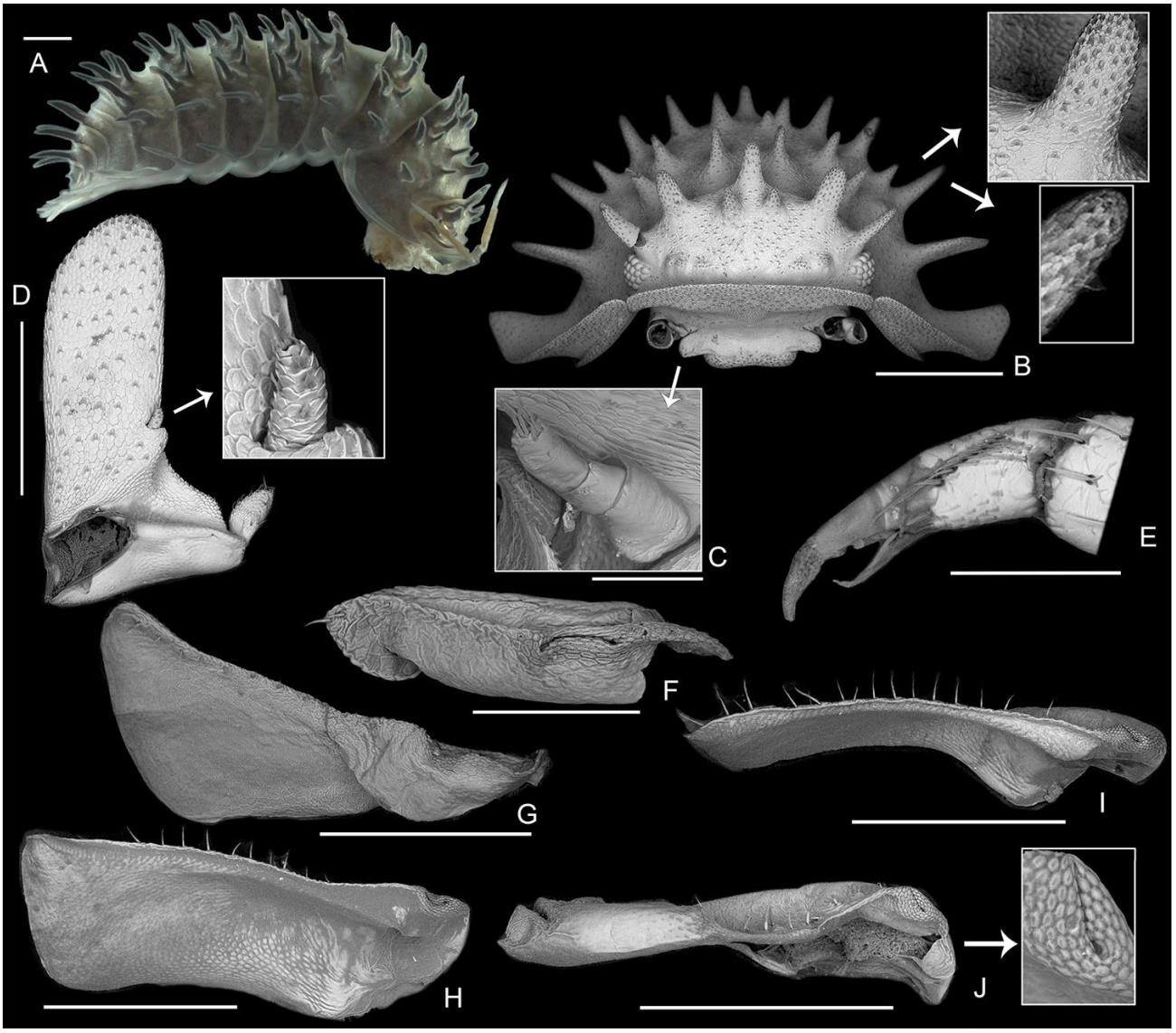


Figure 3. *Diploexochus spinatus* sp. nov., female paratype. **A**, Habitus, lateral view; **B**, cephalon and pereonite 1, frontal view; **C**, antennula; **D**, pereopod 7 dactylus; **E**, pleopod 1 exopod; **F**, pleopod 2 exopod; **G**, pleopod 3 exopod; **H**, pleopod 4 exopod; **I**, pleopod 5 exopod; **J**, uropod, dorsal view. Scale bars: **A, B**: 1 mm; **C, E**: 100µm; **F**: 200µm; **D, G–J**: 500µm.

slightly curved, protruding above vertex; eye with about 20 ommatidia (Figs. 3B; 4C, D). Pereonites with distal epimera flattened and directed backwards; pereonite 2 with triangular ventral lobe; pereonites 5–7 with oblique ventral ridge (Fig. 4E). Pleonites 3–5 with well-developed epimera, quadrangular with round distal corner slightly directed outwards (Fig. 4F). Telson hourglass-shaped, base broader than distal part, distal margin straight (Fig. 4F). Antennula (Figs. 3C, 4G) with 3 articles, proximal and distal articles subequal in length, distal article with 9 apical aesthetascs. Antenna (Fig. 4H) short, not surpassing distal margin of pereonite 1; flagellum with 2 articles, 1 article about 2 times longer than first, with 1 row of strongly grooved on lateral margin, inner lobe of aesthetascs. Mandibles (Fig. 4I, J) molar penicil simple, schisma rounded (Figs. 3B, 4C–E), pereonite 2 with right mandible with 1 + 1, left mandible with 2 + 1 free penicils. Maxillula (Fig. 4K) outer branch with 4 + 5 simple teeth; inner branch with 2 long penicils. Maxilla (Fig. 4L) bilobate, outer lobe twice wider than inner lobe, covered with thin setae. Maxilliped (Fig. 4M) endite with medial seta surpassing distal margin, distal margin slightly rounded with 2 short triangular setae; palp with 2 setae on basal article. Pereopod 1 with longitudinal antennal grooming

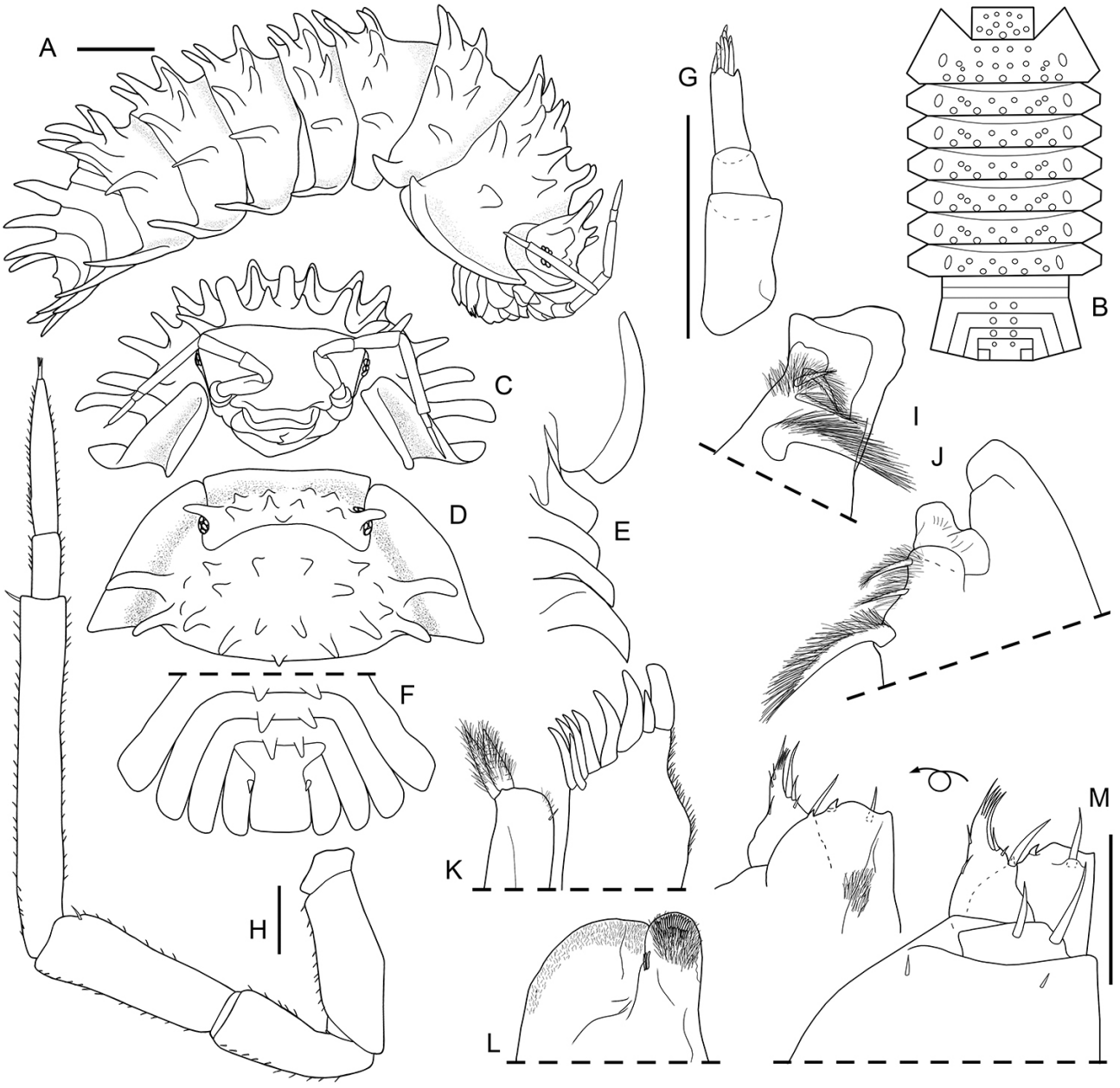


Figure 4. *Diploexochus spinatus* sp. nov., female paratype. **A**, Habitus, lateral view; **B**, disposition of dorsal tubercles; **C**, cephalon and pereonite 1, frontal view; **D**, cephalon and pereonite 1, dorsal view; **E**, epimera 1–5 ventral view; **F**, pleonites 3–5, uropods and telson, dorsal view. Male paratype: **G**, antennula; **H**, antenna; **I**, right mandible; **J**, left mandible; **K**, maxillula; **L**, maxilla; **M**, maxilliped. Scale bars: **A**: 1 mm; **C**–**M**: 0.2 mm.

brush (Fig. 5A), dactylus inner claw not surpassing *Male:* pereopods 1 and 7 (Figs. 3D; 5A, B) with no outer claw, dactylar organ and ungual seta simple, with particular modifications. Genital papilla with longitudinal scale-field (Fig. 3E). Pleopods 1–5 with triangular ventral shield, papilla slightly surpassing monospiracular lungs (Fig. 3E–I). Uropod (Fig. 3J) ventral shield with apical orifices (Fig. 5C). Pleopod 1 protopod flattened, distal part subrectangular with (Fig. 5C) exopod small, triangular, wider than long; round apex, exopod short inserted medially; endopod endopod about threefold longer than exopod, distal stout, short, not reaching the insertion of exopod, part slightly bent outwards. Pleopod 2 (Fig. 5D) around 2 times exopod length. exopod triangular, outer margin strongly concave

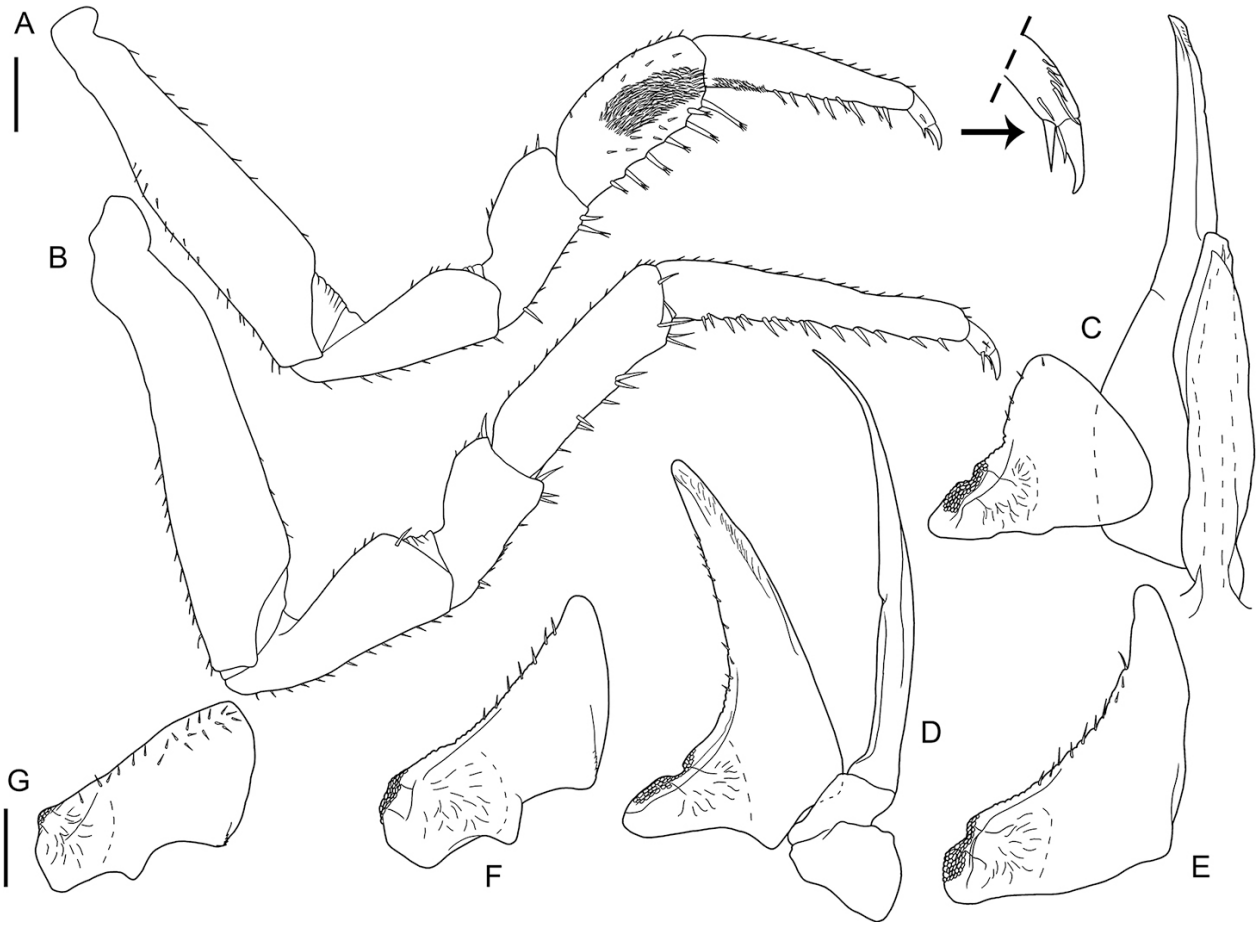


Figure 5. *Diploexochus spinatus* sp. nov., male paratype. **A**, Pereopod 1; **B**, pereopod 7; **C**, pleopod 1 and genital papilla; **D**, pleopod 2; **E**, pleopod 3 exopod; **F**, pleopod 4 exopod; **G**, pleopod 5 exopod. Scale bars: 0.2 mm.

bearing setae; endopod longer than exopod. Pleopods 3–5 exopods as in Fig. 5E–G.

Etymology. The specific epithet "*spinatus*" refers to the morphology of the dorsal tubercles, which in this species are like spines.

Morphological remarks. The specimens from Honorato cave showed variations in the tubercle development on the telson, being very reduced in relation to the tubercles on pleonites (in 4 specimens) or absent (in 5 specimens); while on the female from Tapera D'água cave these tubercles are as long as those on pleonites 3–5 (Fig. 6D, E). Furthermore, the female from Tapera D'água cave presents the cephalon with seven tubercles and pereonites and pleonite epimera with posterior points well-developed, curved and directed outwards, in a pattern similar to *D. echinatus* (Fig. 6E).

Habitat and ecological remarks. Specimens of *D. spinatus* sp. nov. were found in two caves in the municipality of Iuiú, a region with several caves and cave-restricted endemic species (Souza et al., 2015; Souza and Ferreira, 2018; Cardoso et al., 2020; 2021). Other caves in the area were also inventoried, however specimens of *D. spinatus* sp. nov. were only found in these two caves. This area is located in the Caatinga domain, the only xeric biome of Brazil with xeromorphic and deciduous vegetation (Fig. 6A). Several specimens of *D. spinatus* sp. nov. were found in Honorato cave, a limestone cave with 150 meters of horizontal projection. This cave has a single entrance leading to a wide chamber (Fig. 6B), partially trespassed by an intermittent stream that occurs in the cave main conduit. During dry periods, only a few ponds are observed inside the cave, while during rainy periods the stream can flow, especially after strong rains. Several specimens were found from the middle

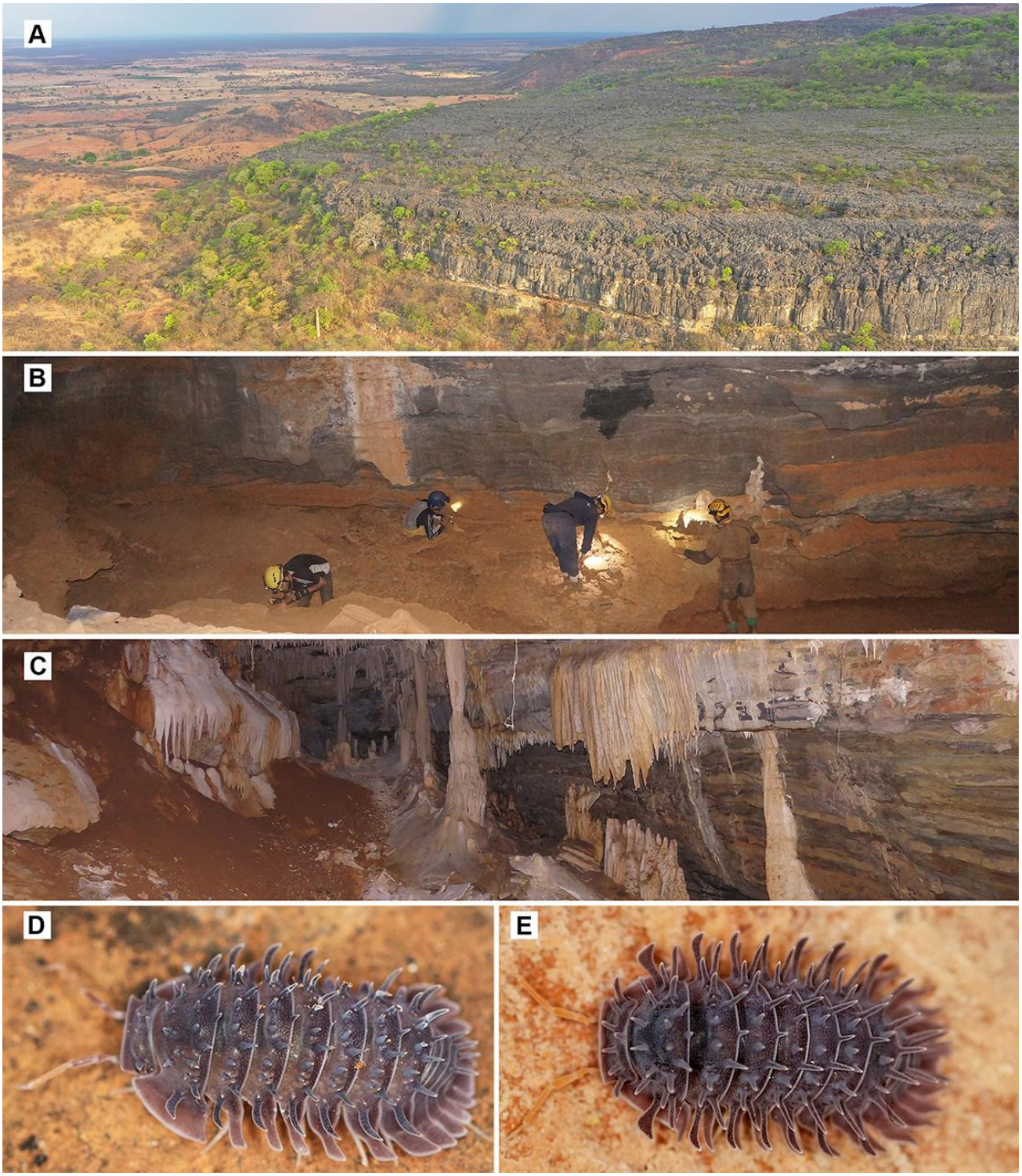


Figure 6. **A**, Karstic area surrounding Honorato cave; **B**, Honorato cave; **C**, Tapera D'água cave; **D**, *Diploexochus spinatus* sp. nov. from Honorato cave; **E**, *Diploexochus spinatus* sp. nov. from Tapera D'água cave.

portion of the cave to the deepest chamber (Fig. 6D). In all cases, they were sheltered under rocks on the cave floor distant from the potentially flooded areas. Although three samplings have been performed in this cave (in 2008, 2012, and 2021), specimens of *D. spinatus* sp. nov. were only found in the last sampling event, although body remnants potentially belonging to this species were observed in 2008. It is worth mentioning that in the first two samplings, there was a forested area surrounding the cave. In the last sampling, however, this forest was no longer present, and a considerable area of exposed soil was observed.

The presence of living specimens of *D. spinatus* sp. nov. only in the last sampling may have occurred due to their migration from the external area to the cave environment, seeking more suitable habitat. Considering that the species lacks any troglomorphic traits, it is likely that it exhibits external populations and their occurrence in caves may be related to the presence of impacts (such as deforestation) in the epigean environments. A single specimen was observed in Tapera D'água cave, located around 11.5 km away from Honorato cave. This cave presents around 300 meters of horizontal projection, trespassed by a stream. The single specimen (Fig. 6E) was also found under a rock on the cave floor, in a chamber located in the deep portion of the cave (Fig. 6C), far from the potentially flooded areas. The surrounding area of this cave is more preserved, although there are signs of human impacts in the past (like deforested areas and some abandoned water reservoirs). In this sense, several suitable habitats seem to exist for the species in the cave surroundings.

***Diploexochus obscurus* sp. nov.**

(Figs. 7 – 10)

Zoobank: urn:lsid:zoobank.org:act:E2B21901- 1FE9-4731-B8B0-B00C3FA56987

Type material. Holotype: male (ISLA 77539, part in slide), Brazil, Bahia State, municipality of Carinhanha, Água Escura I cave (-13.817694º -43.950366º), 17 September 2021, G.M. Cardoso and R.L. Ferreira coll. Paratypes: 3 females (1 in slide) (ISLA 77540), same data as holotype.

Diagnosis. Dorsal surface covered with acute and rectangular tubercles; pereonites 2–7 with 11 tubercles in 2 rows; pleonite 3 with 4 tubercles, pleonites 4, 5 and telson with 2 paramedian tubercles; uropod exopod inserted medially, endopod around threefold exopod length.

Description. Body length: ♂ 7.5 mm, ♀ 6 mm. Body gray with depigmented spots; antenna 5th article and flagellum yellowish (Fig. 7A). Endoantennal conglobation. Dorsal surface covered with acute and rectangular tubercles disposed as follows (Fig. 8A, B): cephalon with 12 tubercles in 3 rows; pereonite 1 with 21 tubercles in 3 rows; pereonite 2 with 13 tubercles in 2 rows; pereonites 3–7 with 11 tubercles in 2 rows; pleonite 3 with 4 tubercles, pleonites 4 and 5 with 2 paramedian tubercles, telson with 2 tubercles. Dorsal surface with short semi-circular scale-setae (Fig. 7C). Cephalon (Figs. 7B, 8C, D) with frontal shield prominent, protruding above vertex, distal margin straight; eye with about 16 ommatidia. Pereonites with epimera flattened and directed backwards; pereonite 1 strongly grooved on lateral margin, inner lobe of schisma rounded (Fig. 8C, E); pereonite 2 with triangular ventral lobe; pereonites 5–7 with oblique ventral ridge. Pleonites 3–5 (Fig. 8F) with epimera well developed, quadrangular with round distal margin, slightly directed outwards. Telson hourglass-shaped, base wider than distal part, distal margin straight. Antennula (Fig. 7D) of 3 articles, proximal and distal articles subequal in length, distal article with 2 lateral and 5 apical aesthetascs. Antenna (Fig. 8G) short, not surpassing distal margin of pereonite 1; flagellum of 2 articles, distal article about fourfold longer than first, with 1 row of aesthetascs. Mandible (Fig. 8H, I) molar penicil simple; left mandible with 2 + 1 and right mandible with 1 + 1 free penicils. Maxillula (Fig. 8J) outer branch with 4 + 5 simple teeth. Maxilla (Fig. 8K) bilobate, outer lobe twice wider than inner lobe, covered with thin setae. Maxilliped (Fig. 8L) endite with medial seta surpassing distal margin, distal margin slightly rounded with 2 short triangular setae; palp with 2 setae on basal article. Pereopod 1 with longitudinal antennal grooming brush, dactylus inner claw not surpassing outer claw, dactylar organ and ungual seta simple, with longitudinal scale-field (Fig. 9A). Pleopods 1–5 with monospiracular lungs. Uropod (Fig. 7D) protopod flattened, distal part subrectangular, exopod short inserted medially, endopod stout, short, not reaching the insertion of exopod, around threefold exopod length.

Male: pereopods 1 and 7 (Fig. 9A, B) with no particular modifications. Genital papilla with triangular ventral shield, papilla slightly surpassing ventral shield with apical orifices (Fig. 9C). Pleopod 1 (Fig. 9C) exopod small, triangular, wider than long; endopod about 4 times longer than exopod, distal part straight. Pleopod 2 (Fig. 9D) exopod triangular, outer margin strongly concave bearing setae; endopod longer than exopod. Pleopods 3 and 4 exopods as in Fig. 9E, F.

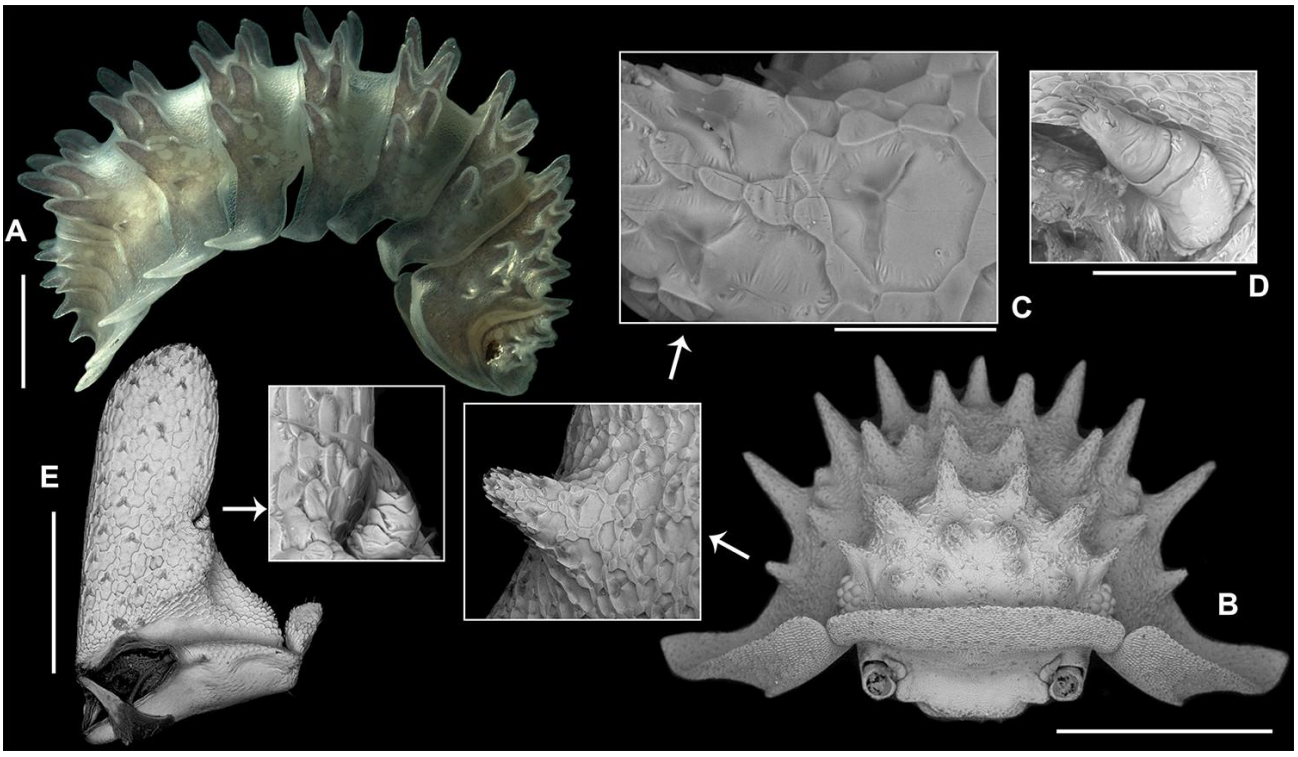


Figure 7. *Diploexochus obscurus* sp. nov., female paratype. **A**, Habitus, lateral view; **B**, cephalon and pereonite 1, frontal view; **C**, scale setae; **D**, antennula; **E**, uropod. Scale bars: **A, B**: 1 mm; **C**: 50µm; **D**: 100µm; **E**: 300µm.

Etymology. The specific epithet *"obscurus"* refers to the cave where the species was collected, Água Escura (that in Portuguese means dark water).

Habitat and ecological remarks. Specimens of *D. obscurus* sp. nov. were found in a limestone cave (Água Escura I cave) located in the region of "Serra do Ramalho", northeastern Brazil. This area has hundreds of caves and several cave-restricted species (e.g., Baptista and Giupponi, 2002; Kamimura and Ferreira, 2018; Hellmann et al., 2020). Although many other caves in the area were also inventoried, specimens of *D. obscurus* sp. nov. were only found in this cave. Although this cave is peripheral to the main subterranean drainage in the area, it can be considered part of the Água Clara cave system, which comprises the richest hotspot of subterranean biodiversity in South America (Souza-Silva et al., 2021). The Água Escura I cave presents a single entrance, located at the base of a limestone outcrop (Fig. 10A). The cave presents two main conduits (one intercepting the other), which were extremely dry during the samplings (Fig. 10C). However, the cave conduits are located at a lower level when compared to the surface, so that the water from floods can enter the cave, submerging part of its chambers during strong rains (Fig. 10B). According to Köppen's climate classification system, the local climate is "Aw", with dry winter and an average annual rainfall of 640 mm^3 (Alvares et al., 2013). Only four specimens of *D. obscurus* sp. nov. were found in the cave (Fig. 10D, E), all sheltered under big rocks, in which microhabitats still retained some moist content on the subjacent floor (Fig. 10C). The cave surroundings are severely impacted (Fig. 10A), mainly by deforestation and fires, although cattle and goat breeding were also observed. As mentioned for *D. spinatus* sp. nov., the cave is likely being used by *D. obscurus* sp. nov. as a refuge, considering the highly impacted area surrounding the cave.

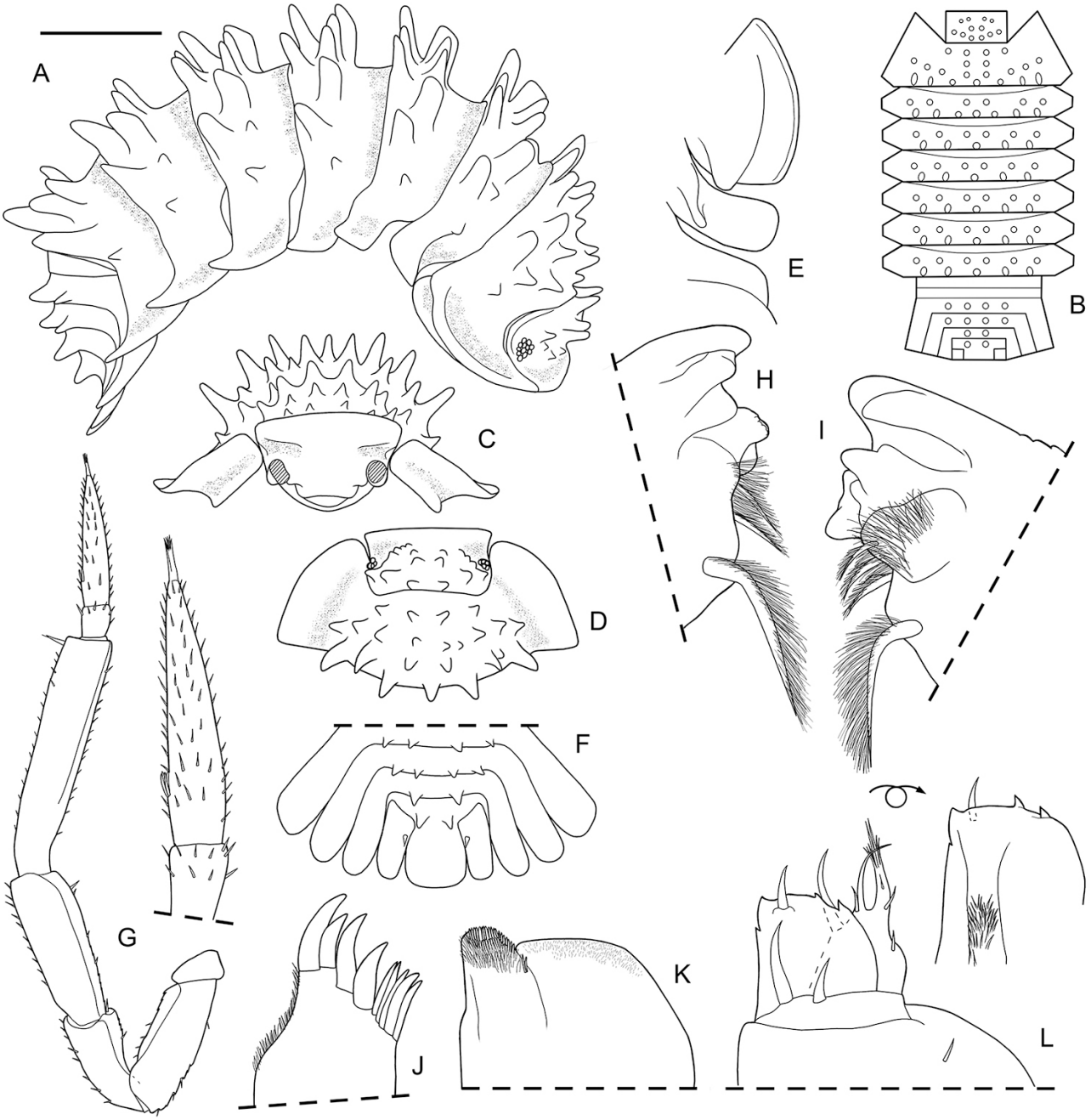


Figure 8. *Diploexochus obscurus* sp. nov., female paratype. **A**, Habitus, lateral view; **B**, disposition of dorsal tubercles; **C**, cephalon and pereonite 1, frontal view; **D**, cephalon and pereonite 1, dorsal view; **E**, epimera 1–4 ventral view; **F**, pleonites 3-5, uropods and telson, dorsal view. Male paratype: **G**, antenna; **H**, right mandible; **I**, left mandible; **J**, maxillula; **K**, maxilla; **L**, maxilliped. Scale bars: **A**: 1 mm; **C–L**: 0.2 mm.

DISCUSSION

The disposition of tubercles has shown to be a strong character that varies among *Diploexochus* species, along with the shape of the male pleopod exopod, the proportion of the uropod exopod, and the shape of the telson. The number and topology of pereonite tubercles differ in the new species in relation to *D. echinatus*, which shows 15 tubercles on pereonites 2–6; and 13 tubercles on pereonite 7. *Diploexochus spinatus* sp. nov. presents 13 tubercles in two rows on pereonites 2–6 and 11 tubercles on pereonite 7; while *D. obscurus* sp. nov. presents 13 tubercles on pereonite 2, and 11 tubercles on pereonites 3–7. Regarding the pleonites, each species shows a different pattern. In

D. echinatus there are four tubercles on pleonites 3 and 4 and two paramedian tubercles on pleonite 5 and telson; in *D. spinatus* sp. nov. there are two paramedian tubercles on pleonites 3–5, with some species showing tubercles on the telson; and in *D. obscurus* sp. nov. there are four tubercles on pleonite 3, and two paramedian tubercles on pleonites 4 and 5 and telson.

The shape of the male pleopod 1 exopod in *D. spinatus* sp. nov. is similar to *D. echinatus*. In comparison with *D. echinatus*, the uropod exopods and endopods in *D. spinatus* sp. nov. and *D. obscurus* sp. nov. are minute. In proportion, in *D. spinatus* sp. nov. the endopod is around twice as long as the exopod, similar to *D. echinatus*, while in *D. obscurus* sp. nov. the endopod is around threefold longer than the exopod. Lastly, the distal part of the telson in *D. echinatus* is quadrangular with the dorsum slightly depressed, and the distal margin concave, while in both new species it is rectangular with the distal margin straight.

Although several species have been described as belonging to the genus *Diploexochus*, all of them ended up being reallocated into other genera. Accordingly, almost two centuries after the description of the genus, two new species are described, which not only contributes to the taxonomy of this group but also points to potential discoveries. Furthermore, the occurrence of the herein described species in a semi- arid biome, quite distinct from the moist Amazon region where *D. echinatus* is found, demonstrates the great adaptive plasticity of the species in this genus.

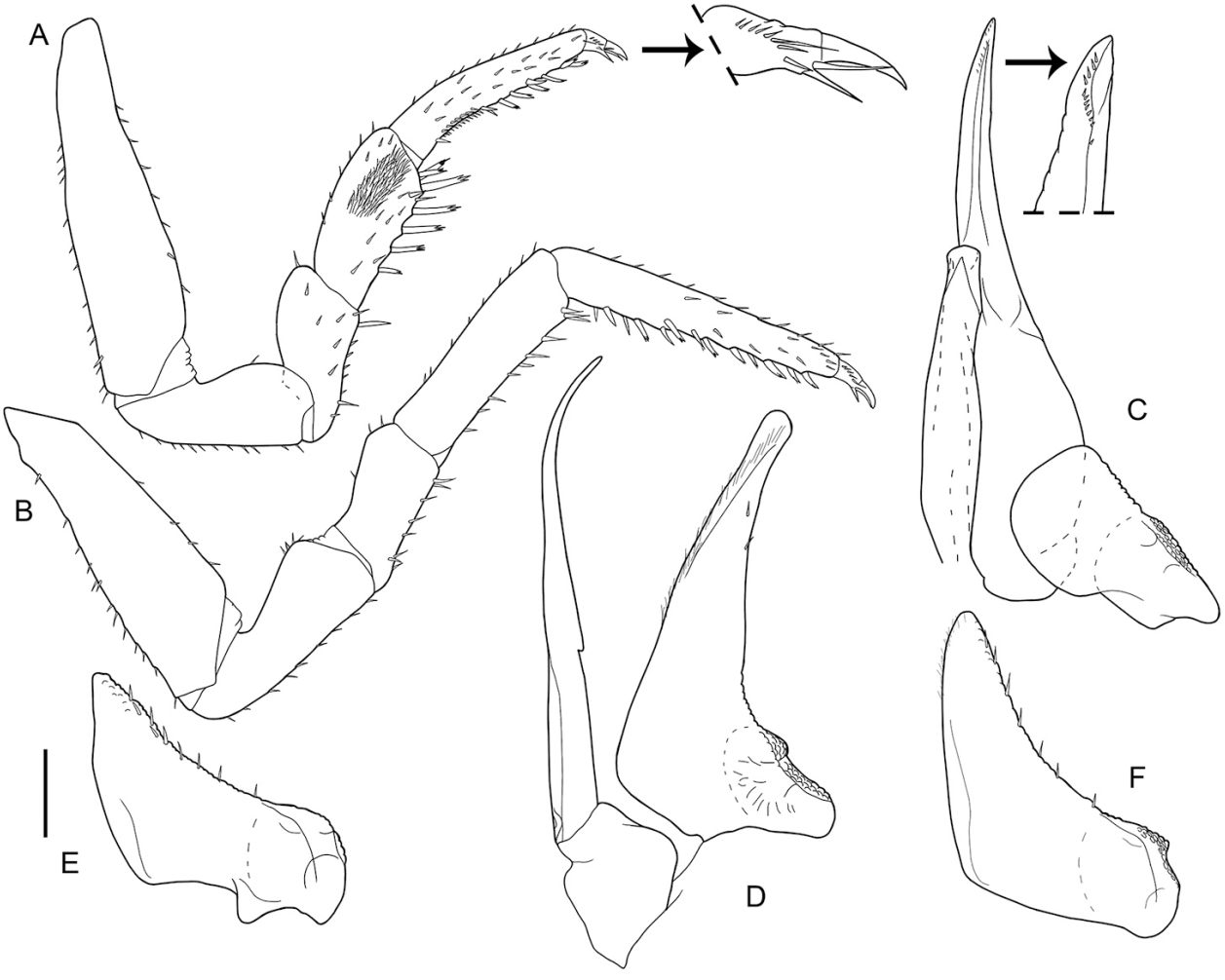


Figure 9. *Diploexochus obscurus* sp. nov., male paratype. **A**, Pereopod 1; **B**, pereopod 7; **C**, pleopod 1 and genital papilla; **D**, pleopod 2; **E**, pleopod 3 exopod; **F**, pleopod 4 exopod. Scale bar: 0.2 mm.

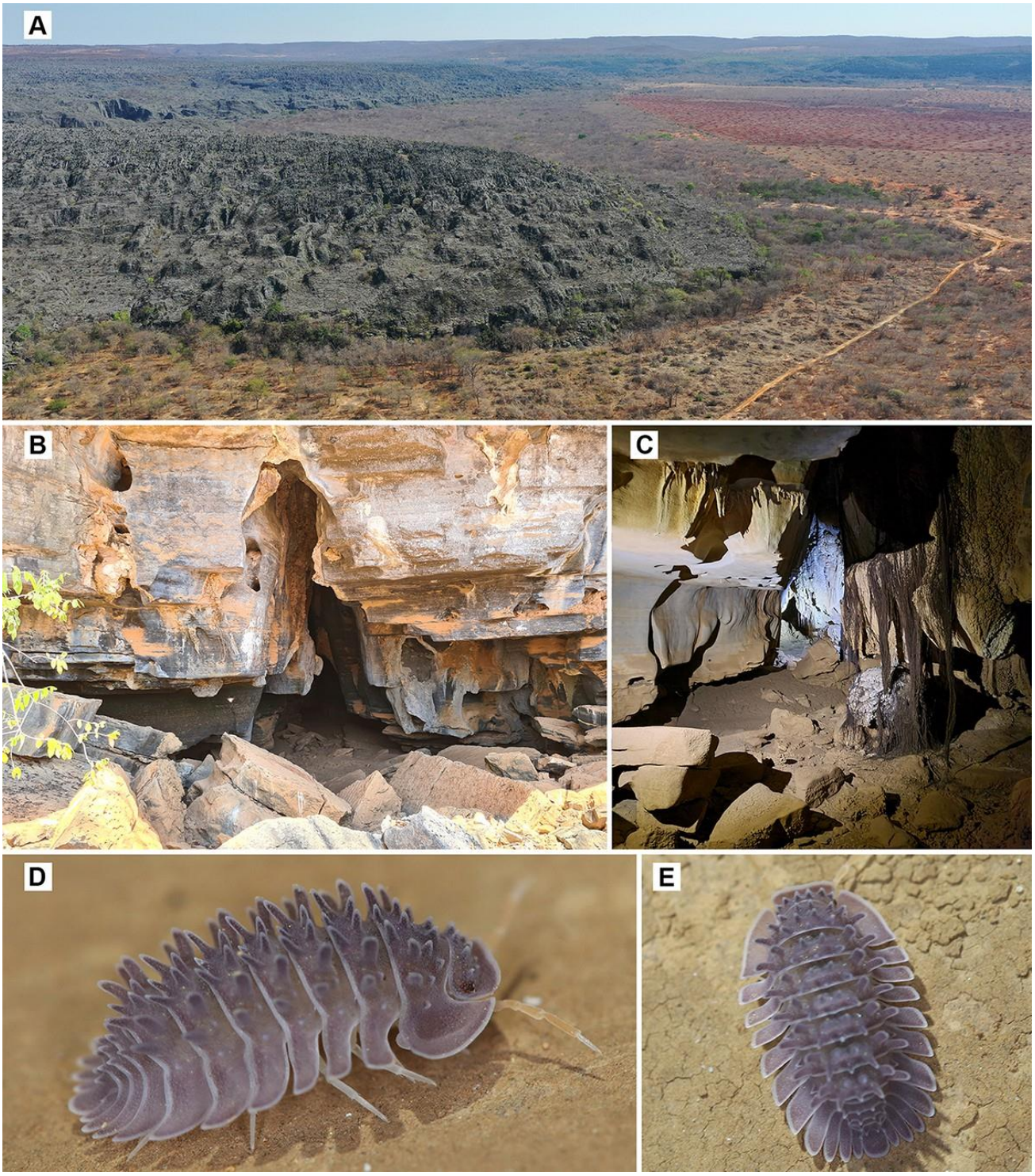


Figure 10. **A**, Karstic area surrounding Água Escura I cave; **B**, entrance of Água Escura I cave; **C**, conduit where the specimens were found; **D**, live specimen of *Diploexochus obscurus* sp. nov. in lateral view; **E**, live specimen of *Diploexochus obscurus* sp. nov. in dorsal view.

Finally, it is important to highlight the increase in threats to Brazilian speleological heritage. Even considering caves as possible peripheral habitats of the herein described species, the high degree of alterations in the external environments may have forced their populations to migrate into the caves. In turn, such subterranean habitats are under unprecedented threat due to recent changes in laws regarding the protection of Brazilian speleological heritage (Ferreira et al., 2022). Thus, although little is known about the real distribution of these new species, it is worrying that they may already be threatened.

ACKNOWLEDGMENTS

We would like to thank Joaquim de Souza for the hospitality and logistic support; the team from the Center of Studies in Subterranean Biology (CEBS/UFLA) for their support on the field trips; and Leda Zogbi for the invitation and support in the expedition to Rurópolis.

REFERENCES

Alvares CA; Stape JL; Sentelhas PC; Moraes-Gonçalves JL and Sparovek G 2013. Köppen's climate classification map for Brazil. *Meteorologische Zeitschrift*, 22: 711–728. DOI: https://www.doi.org/10.1127/0941-2948/2013/0507

Arcangeli A 1934. Note di revisione sulla famiglia Armadillidae. *Bollettino dei Musei di Zoologia ed Anatomia Comparata della Reale Università di Torino*, 44: 83–119.

Baptista RLC; Giupponi ADL 2002. A new troglomorphic *Charinus* from Brazil (Arachnida: Amblypygi: Charinidae). *Revista Ibérica de Aracnología*, 6(31): 105–110. https://sea-entomologia.org/PDF/RIA_6/R06-010-105.pdf

Boyko CB; Bruce NL; Hadfield KA; Merrin KL; Ota Y; Poore GCB; Taiti S; Schotte M and Wilson GDF (Eds.) 2022. World Marine, Freshwater and Terrestrial Isopod Crustaceans database. *Diploexochus* Brandt, 1833. Available at: https://www.marinespecies.org/aphia.php?p=taxdetails&id=248694. Accessed on 05 April 2022.

Brandt I 1833. Conspectus Monographiae Crustaceorum Oniscodorum Latreillii. *Byulleten Moskovskogo Obshchestva Ispytatelei Prirody*, 6: 171–193.

Budde-Lund G 1879. Prospectus generum specierumque Crustaceorum Isopodum Terrestrium. Copenhagen, Imprimerie de Jørgensen & Knudtzon, 10p.

Budde-Lund G 1885. Crustacea Isopoda Terrestria per Familias et Genera et Species Descripta. Nielsen and Lydiche, Hauniae [Copenhagen], 319p. https://decapoda.nhm.org/pdfs/14338/14338.pdf

Budde-Lund G 1904. A revision of Crustacea Isopoda terrestria, with additions and illustrations. Copenhagen, H. Hagerup: 33–144. DOI: https://www.doi.org/10.5962/bhl.title.9883

Budde-Lund G 1909. Zoologische und anthropologische Ergebnisse im westlichen und zentralen Südafrika, vol. 2, IX. Isopoden (I), *Land-Isopoden. Denkschriften der medizinisch-naturwissenschaftlichen Gesellschaft zu Jena*, 14: 53–70.

Campos-Filho IS; Montesanto G; Araujo PB and Taiti S 2017. New species and new records of terrestrial isopods (Crustacea, Isopoda, Oniscidea) from Brazil. *Iheringia, Série Zoologia*, 107: 1–30. DOI: https://www.doi.org/10.1590/1678- 4766e2017034

Campos-Filho IS; Cardoso GM and Aguiar JO 2018. Catalogue of terrestrial isopods (Crustacea, Isopoda, Oniscidea) from Brazil: an update with some considerations. *Nauplius*, 26: 1–40. DOI: https://www.doi.org/10.1590/2358-2936e2018038

Cardoso GM; Bastos-Pereira R; Souza LA and Ferreira RL 2020. New cave species of *Pectenoniscus* Andersson, 1960 (Isopoda: Oniscidea: Styloniscidae) and an identification key for the genus. *Nauplius*, 28: 1–30. DOI:10.1590/2358-2936e2020039

Cardoso RC; Ferreira RL and Souza-Silva M 2021. Priorities for cave fauna conservation in the Iuiú karst landscape, northeastern Brazil: a threatened spot of troglobitic species diversity. *Biodiversity and Conservation*, 30(5): 1433–1455. DOI: https://www.doi.org/10.1007/s10531-021-02151-5

Dana J 1853. Crustacea. Part II. United States Exploring Expedition. During the years 1838, 1839, 1840, 1841, 1842. Under the command of Charles Wilkes, U.S.N. Vol. 14. Philadelphia, C. Sherman, p. 689–1618. https://www.biodiversitylibrary.org/item/124951

Ferreira RL; Bernard E; da Cruz Júnior FW; Piló LB; Calux A; Souza-Silva M; ... and Frick WF 2022. Brazilian cave heritage under siege. *Science*, 375(6586): 1238–1239. DOI: https://www.doi.org/10.1126/science.abo1973

Hellmann L; Ferreira RL; Rabelo L and Leal-Zanchet AM 2020. Enhancing the still scattered knowledge on the taxonomic diversity of freshwater triclads (Platyhelminthes: Dugesiidae) in caves from two Brazilian Biomes. *Studies on Neotropical Fauna and Environment*, 55: 1–16. DOI: https://www.doi.org/10.1080/01650521.2020.1829901

Kamimura Y and Ferreira RL 2018. Description of a second South American species in the Malagasy earwig genus *Mesodiplatys* from a cave habitat, with notes on the definition of Haplodiplatyidae (Insecta, Dermaptera). *ZooKeys*, 790: 87–100. DOI: https://www.doi.org/10.3897/ zookeys.790.27193

Latreille PA 1802. Histoire naturelle, générale et particulière des Crustacés et des Insectes. Ouvrage faisant suite à l'histoire naturelle générale et particulière, composée par Leclerc de Buffon, et rédigée par CS Sonnini, membre de plusieurs Sociétés savantes. F. Dufart, Paris, Vol. 3, 476p. https://www.biodiversitylibrary.org/item/80064 - page/5/mode/1up

Leistikow A and Wägele JW 1999. Checklist of terrestrial isopods of the New World (Crustacea, Isopoda, Oniscidea). *Revista brasileira de Zoologia*, 16(1): 1–72. DOI: https://www.doi.org/10.1590/S0101-81751999000100001

Lemos de Castro A 1967. Isópodos terrestres da Amazônia brasileira. *Atas do Simpósio sobre a Biota Amazônica*, 5: 311–336.

Lewis F 1998. Oniscidea (Isopoda) from Lord Howe Island. Crustaceana, 71: 743–777. https://www.jstor.org/stable/20106052

Milne-Edwards, H. 1840. Ordre des isopodes. p. 115–283. In: Histoire Naturelle des Crustacés, comprenant l'anatomie, la physiologie et la classficiation de ces animaux. Vol. 3. Paris, Librairie Encyclopédique de Roret. https://www.biodiversitylibrary.org/item/54604 - page/11/mode/1up

Montesanto G 2015. A fast GNU method to draw accurate scientific illustrations for taxonomy. *Zookeys*, 515: 191–206. DOI: https://www.doi.org/10.3897/zookeys.515.9459

Montesanto G 2016. Drawing setae: a GNU way for digital scientific illustrations. *Nauplius*, 24: 1–6. DOI: https://www.doi.org/10.1590/2358-2936e2016017

Pearse A 1917. Isopoda collected by the Bryant Walker Expedition to British Guiana, with notes on Crustacea from other localities. *Occasional Papers of the Museum of Zoology of University of Michigan*, 46: 1–8. https://www.biodiversitylibrary.org/ item/49289 - page/119/mode/1up

Richardson H 1912. Description of a new terrestrial isopod belonging to the genus *Cubaris* from Panama. *Proceedings of the United States National Museum*, 42: 477–479. DOI: https://www.doi.org/10.5479/si.00963801.42-1911.477

Schmalfuss H 2003. World catalog of terrestrial isopods (Isopoda: Oniscidea). *Stuttgarter Beiträge zur Naturkunde*, *Serie A* (*Biologie*), 654: 1–341. https://www.zobodat.at/pdf/ Stuttgarter-Beitraege-Naturkunde_654_A_0001-0341.pdf

Souza-Kury LA 1998. Malacostraca. Peracarida. Isopoda. Oniscidea. p. 653–674. In: Young P (Ed.), Catalogue of Crustacea of Brazil. Rio de Janeiro, Museu Nacional. Série Livros, 6.

Souza LA; Ferreira RL and Senna AR 2015. Amphibious shelter-builder Oniscidea species from the New World with description of a new subfamily, a new genus and a new species from Brazilian Cave (Isopoda, Synocheta, Styloniscidae). *PloS one*, 10(5): 1–18. DOI: https://www.doi.org/10.1371/ journal.pone.0115021

Souza MF and Ferreira RL 2018. A new highly troglomorphic *Loxosceles* (Araneae: Sicariidae) from Brazil. *Zootaxa*, 4438(3): 575–587. DOI: https://www.doi.org/10.11646/ zootaxa.4438.3.9

Souza-Silva M; Cerqueira RFV; Pellegrini TG and Ferreira RL 2021. Habitat selection of cave-restricted fauna in a new hotspot of subterranean biodiversity in Neotropics. *Biodiversity and Conservation*, 30: 4223–4250. DOI: https:// www.doi.org/10.1007/s10531-021-02302-8

Taiti S; Paoli P and Ferrara F 1998. Morphology, Biogeography, and Ecology of the family Armadillidae (Crustacea, Oniscidea). *Israel Journal of Zoology*, 44(3–4): 291–301. https://www.tandfonline.com/doi/pdf/10.1080/00212210.1998.106 88952

Tereso EFM; Góes Filho L; Ferreira HC; Veloso HP; Fonseca WN and Silva SB 1975. As Regiões Fitoecológicas, sua Natureza e seus Recursos Econômicos, Estudo Fitogeográfico. In: Projeto Radam, Folha SB-21 Tapajós. Rio de Janeiro: DNPM, Departamento Nacional de Produção Mineral: 287–384.

Van Name WG 1925. The isopods of Kartabo, Bartica District, British Guiana. *Zoologica*, 6: 461–503. DOI: https://www.doi.org/10.5962/p.190325

Van Name WG 1936. The American land and freshwater isopod Crustacea. *Bulletin of the American Museum of Natural History*, 71: 1–535. http://hdl.handle.net/2246/1185

Verhoeff KW 1928. Über einige Isopoden der Zoologischen Staatssammlung in München. *Zoologischer Anzeiger*, 76: 25- 36, 113–123.

Verhoeff KW 1942. Äthiopische Isopoda terrestria der Hamburger Zoologischen Museums. *Zoologischer Anzeiger*, 140: 1–163.

ADDITIONAL INFORMATION AND DECLARATIONS

Author Contributions

Illustrations and figures: GM; preparation, editing and review of the manuscript: GMC, RBP, RFL.

Consent for publication

All authors declare that they have reviewed the content of the manuscript and gave their consent to submit the document.

Data availability

All data are archived within the Universidade Federal de Lavras (UFLA) in the Subterranean Invertebrate Collection of Lavras (ISLA – UFLA) at the Center of Studies on Subterranean Biology of the Federal University of Lavras (CEBS/UFLA, Lavras, Brazil), and available on request from RLF.

Funding and grant disclosures

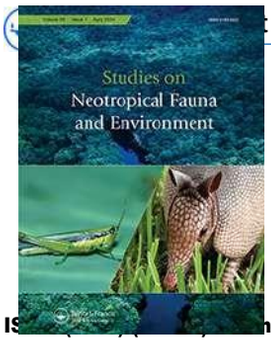
The authors would like to thank the Centro Nacional de Pesquisa e Conservação de Cavernas – CECAV and Instituto Brasileiro de Desenvolvimento e Sustentabilidade – IABS (nº. 006/2021. TCCE ICMBio/Vale 01/2018) for the financial support and scholarship provided to GMC and CNPq (National Council for Scientific and Technological Development) for the productivity scholarship provided to RFL (CNPq n. 302925/2022-8).

Study association

This work is part of the Post Doctoral research of GMC in the Programa de Pós-graduação em Ecologia Aplicada, at the Universidade Federal de Lavras (UFLA) Lavras, Minas Gerais, Brazil.

Study permits

Field collection and transportation of specimens were made under the SISBIO permit number 78415-3/2021 issued to RLF.



Studies on Neotropical Fauna and Environment

ISSN (print), (online) Journal homepage: www.tandfonline.com/journals/nnfe20

New troglobitic species of *Pectenoniscus* Andersson, 1960 (Isopoda: Oniscidea: Styloniscidae) from Bahia state, Brazil

Giovanna Monticelli Cardoso & Rodrigo Lopes Ferreira

To cite this article: Giovanna Monticelli Cardoso & Rodrigo Lopes Ferreira (2024) New troglobitic species of *Pectenoniscus* Andersson, 1960 (Isopoda: Oniscidea: Styloniscidae) from Bahia state, Brazil, Studies on Neotropical Fauna and Environment, 59:1, 202-223, DOI: 10.1080/01650521.2023.2230735

To link to this article: https://doi.org/10.1080/01650521.2023.2230735

Published online: 18 Jul 2023.

Submit your article to this journal

Article views: 35

View related articles View Crossmark

data

Citing articles: 1 View citing articles

Full Terms & Conditions of access and use can be found at https://www.tandfonline.com/action/journalInformation?journalCode=nnfe20

STUDIES ON NEOTROPICAL FAUNA AND ENVIRONMENT
2024, VOL. 59, NO. 1, 202–223
https://doi.org/10.1080/01650521.2023.2230735

Taylor & Francis
Taylor & Francis Group

ORIGINAL ARTICLE

Check for updates

New troglobitic species of *Pectenoniscus* Andersson, 1960 (Isopoda: Oniscidea: Styloniscidae) from Bahia state, Brazil

Giovanna Monticelli Cardoso and Rodrigo Lopes Ferreira

Departamento de Biologia, Programa de Pós-graduação em Ecologia Aplicada, Universidade Federal de Lavras (UFLA), Centro de Estudos em Biologia Subterrânea, Lavras, Brazil

ARTI
Rece
Acce
KEY
Sync

ABSTRACT

Five new species of *Pectenoniscus* are described from Bahia state: *Pectenoniscus monsviridis* n. sp. and *Pectenoniscus revelatus* n. sp. from Serra do Ramalho Karst area; *Pectenoniscus archaeos* n. sp. and *Pectenoniscus sepultus* n. sp. from Serra de Iuiú Karst area; and *Pectenoniscus caesarius* n. sp. from Campo Formoso Karst area. Additional notes are provided on their habitats and threats.

http://www.zoobank.org/urn:lsid:zoobank.org:pub:1C9A1DD9-D1C0-454A-9157-098A14FA739B

Introduction

Recently, research carried out in underexplored areas of Brazil led to the discovery of new species of terrestrial isopods. Among the isopods found, the species of the genera *Iansaoniscus* Campos-Filho, Araujo & Taiti, 2017, *Pectenoniscus* Andersson, 1960, *Spelunconiscus* Campos-Filho, Araujo & Taiti, 2014, and *Xangoniscus* Campos-Filho, Araujo & Taiti, 2014 stood out (Andersson 1960; Campos-Filho et al. 2014, 2017; Cardoso et al. 2021). Furthermore, species belonging to new genera such as *Chaimowiczia* Cardoso, Bastos-Pereira, Souza & Ferreira, 2021 were discovered (Cardoso et al. 2021).

The genus *Pectenoniscus* is composed of 10 known species, among which nine occur in caves. With the excep- tion of *Pectenoniscus angulatus* Andersson, 1960, which is an epigean isopod from Santa Catarina state (southern Brazil), most of the species occur in northeastern Brazil. Two species occur in Minas Gerais state (*P. juveniliensis* Cardoso, Bastos-Pereira, Souza & Ferreira, 2020 and *P. montalvaniensis* Cardoso, Bastos-Pereira, Souza & Ferreira, 2020); six species occur in Bahia state (*P. carinhanhensis* Cardoso, Bastos-Pereira, Souza & Ferreira, 2020; *P. iuiuensis* Cardoso, Bastos-Pereira, Souza & Ferreira, 2020; *P. liliae* Campo-Filho, Bichuette & Taiti, 2019; *P. morrensis* Cardoso, Bastos-Pereira, Souza & Ferreira, 2020, *P. pankaru* Campos-Filho, Torres & Bichuette, 2022; *P. santanensis* Cardoso, Bastos-Pereira, Souza & Ferreira, 2020); and one species occurs in Piaui state (*P. fervens* Campos-Filho, Taiti & Bichuette, 2022), which, to date, represents the northernmost occurrence for the genus (Campos-Filho et al. 2019; Cardoso et al. 2020, 2022).

Despite the recent description of *Pectenoniscus* species (Cardoso et al. 2020), new troglobitic species were found in the regions of Serra do Ramalho and Serra de Iuiú (southwestern Bahia state) and Campo Formoso (north- ern Bahia state). Such species are described in this manu- script, with additional notes on their habitats and threats.

Material and methods

Specimens were collected during field expeditions in Bahia state, for a project related to cave invertebrate communities from the Serra do Ramalho and Iuiú regions. Additionally, one species from a cave located in Campo Formoso muni- cipality, that was deposited in the Subterranean Invertebrate Collection of Lavras (ISLA, UFLA), was ana- lyzed and incorporated to the manuscript. The specimens were collected by hand with the aid of brushes and fixed in 70% ethanol. At the Center of Studies on Subterranean Biology (CEBS) of the Federal University of Lavras (UFLA, Lavras, Brazil) the specimens were dissected, mea- sured and photographed with a ZEISS Axio ZoomV16 stereomicroscope (Göttingen, Germany) coupled with an Axio Cam 506 Color camera (Göttingen, Germany). Additionally, some individuals were mounted onto stubs with a carbon tape and analyzed under a scanning electron microscope (Hitachi TM4000, Chiyoda, Japan). The illus- trations were obtained with the aid of a camera lucida mounted on a stereomicroscope (Leica DM750, China).

CONTACT Giovanna Monticelli Cardoso gmcardoso.bio@gmail.com
© 2023 Informa UK Limited, trading as Taylor & Francis Group

Published online 18 Jul 2023

The final illustrations were made with the software GIMP (v. 2.8) (Montesanto 2015, 2016). The type-material is deposited at ISLA.

Study area

The new species described herein were found in caves located in Bahia state, northeastern Brazil (Figure 1). Some caves are located in southwestern Bahia state, in the regions known as Serra do Ramalho and Serra de Iuiú, both inserted in the Bambuí geological formation. According to the Köppen's climate classification system, the climate is classified as 'Aw,' with dry winter and an average annual rainfall of 640 mm^3 (Alvares et al. 2013). These two areas are within the Caatinga domain (the Brazilian semiarid biome), with transi- tional areas to the Cerrado (Brazilian Savanna) (Cole 1960). The other area is located in northeastern Bahia state, in Campo Formoso municipality. According to the Köppen's climate classification system, the climate is classified as 'BSh,' which is a hot semi-arid climate (Alvares et al. 2013). Detailed description of the habi- tats of each species will be provided later (see the Ecological remarks sections of each species).

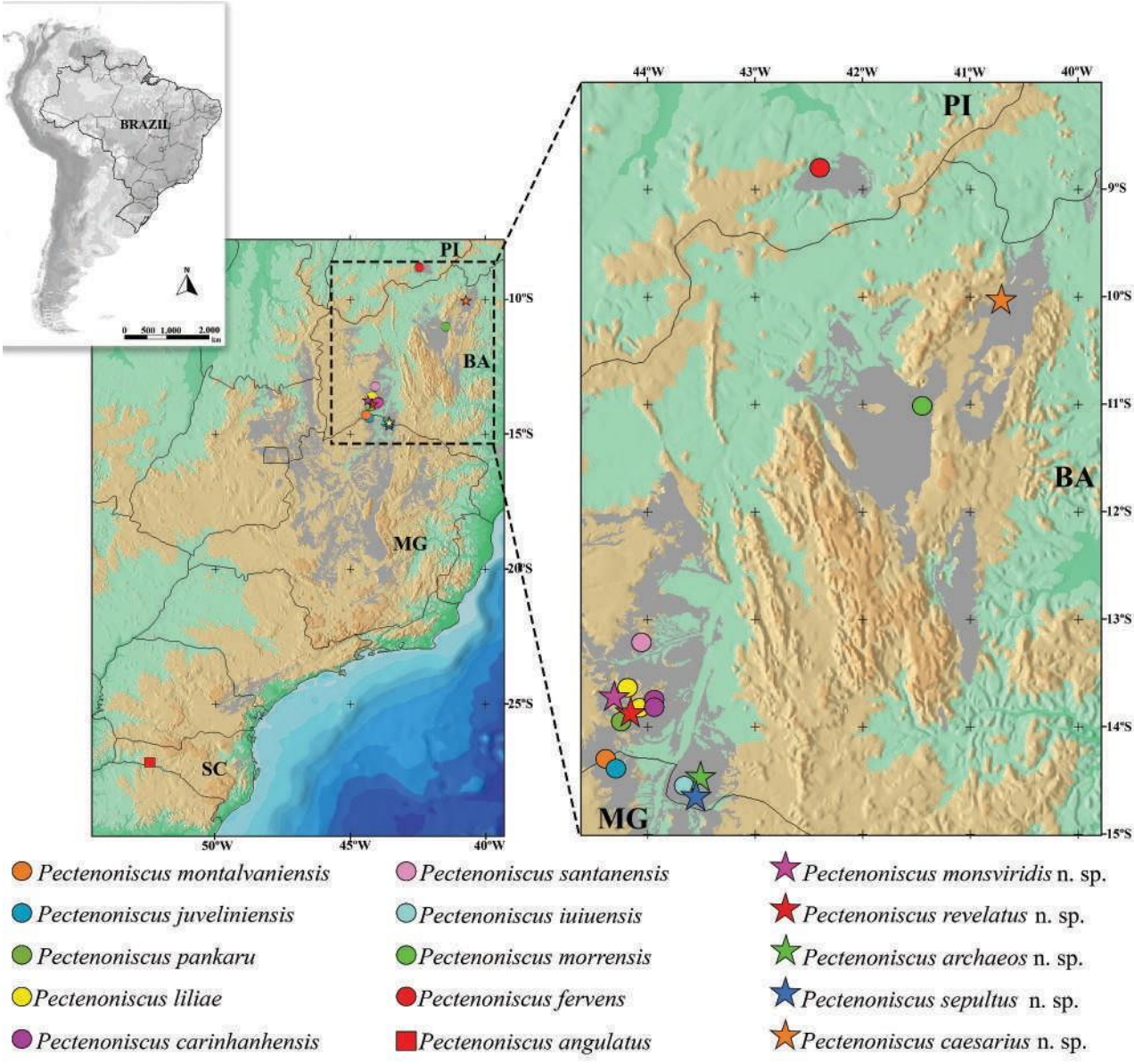


Figure 1. Distribution map of *Pectenoniscus* species in Brazil. Records in the states of Santa Catarina (SC); Minas Gerais (MG); Bahia (BA); and Piaui (PI). The colors indicate the elevation of the terrain, with brown for higher levels, green for lower levels; and gray indicates karstic areas.

Systematics

Family Styloniscidae Vandel, 1952 Genus

Pectenoniscus Andersson, 1960

Pectenoniscus monsviridis n. sp.

(Figures 2–5)

Type material

Holotype. male (ISLA 96634 in slide), Brazil, Bahia state, municipality of Coribe, Serra Verde cave (−13.723897° −44.323461°); 20 September 2021; G.M. Cardoso and R.L. Ferreira leg. Paratypes: 1 male (ISLA 96770 in slide), 1 female (ISLA 96770), 2 males, 6 females (ISLA 96635), same data as holotype.

Diagnosis

Antennula with nine aesthetascs; pleopod 1 exopod trapezoid, apex round; pleopod 2 exopod sub-triangular, endopod distal article thickset, twisted, apex with inner lobe, transverse pointed process directed outward.

Description

Maximum length: male, 4 mm. Colorless, eyes absent (Figures 2A, 3A,C). Dorsum (Figures 2A, 3A) with tricorn-shaped scale-setae (Figure 3B); granulations disposed in five rows on cephalon, in three rows on pereonite 1, two rows on pereonites 2–7 (Figure 3A). Cephalon with round antennal lobes; supra-antennal line bent in middle (Figures 2B, 3C). Pereonite 1 with margin projected for- ward, not surpassing median portion of cephalon; pereo- nites 4–7 posterior margin progressively more concave; pleonites 3–5 epimera posterior points slightly developed, pleon narrower than pereon (Figures 2A, 3A). Telson with concave sides and round apex (Figure 2C). Antennula with three articles, distal article with nine aesthetascs with apical point (Figures 2D, 3D). Antenna fifth article of peduncle longer than flagellum, with one seta longer than first flagellum article; flagellum with three articles (Figure 2E). Left mandible with two penicils (Figure 2F); right mand- ible with one penicil (Figure 2G). Maxillula outer branch with 4 + 4 teeth, apically entire, and one plumose seta; inner branch with three penicils (Figure 2H). Maxilla with bilobate apex, inner lobe wider than outer lobe covered by setae (Figure 2I). Maxilliped palp with two setae; endite triangular, apex with one triangular penicil and two lateral spines (Figure 2J). Pereopod 1 antennal grooming brush composed of serrated scale setae longitudinally on propo- dus and on sternal margin of carpus (Figure 4A); dactylar seta bifid with thin setulae. Water conducting system on ischium, merus, carpus and propodus of pereopod 6 and in pereopod 7. Uropod protopod longer than wide, longer than distal margin of telson; exopod longer than endopod, inserted distally (Figure 4D).

Male

Pereopods 6 and 7 (Figure 4B,C) propodus with tufts of setae on tergal margin. Genital papilla (Figure 4E) enlarged on medial portion, apically narrow. Pleopod 1 (Figure 4E) protopod rectangular, three times wider than long; exopod trapezoid, apex round, lateral margin straight; endopod twice longer than exopod. Pleopod 2 (Figure 4F) protopod rectangular; exopod sub-triangular, wider than long; endopod distal article almost three times longer than proximal article, thickset, twisted, apex with inner lobe, transverse pointed process directed outward. Pleopod 3 exopod (Figure 4G) trapezoidal, distal margin straight. Pleopods 4 and 5 exopod as in Figure 4H,I.

Etymology

The epithet '*monsviridis*' was given in reference to the name of the cave, Serra Verde (in English, Green Mountain). In Latin this translates to *mons* = mountain and *viridis* = green. This term should be treated as a noun in apposition.

Morphological remarks

Pectenoniscus monsviridis n. sp. is one of the largest species of *Pectenoniscus*, with 4 mm long, followed by *P. juveniliensis*, *P. carinhanhensis* and *P. pankaru*. Regarding the number of aesthetascs, *Pectenoniscus monsviridis* n. sp. resembles *P. lilae* and *P. juveniliensis*. Moreover, the shape of male pleopod 1 exopod resembles *P. pankaru*. However, *Pectenoniscus monsviridis* n. sp. is distinct by the shape of male pleopod 2 endopod with a thickset, twisted apex with inner lobe and transverse pointed process directed outward.

Ecological remarks

Specimens of *Pectenoniscus monsviridis* n. sp. were only found in Serra Verde cave. However, since many other caves occur in the area (which were not sampled), other populations may eventually exist. Serra Verde cave has at least 1.7 km of horizontal projection, but there are several unexplored conduits and galleries, as the topography is on course. The cave presents a relatively wide entrance (Figure 5A), with a constriction around 20 meters from the entrance. The main conduit, following this constric- tion, was dry during our survey (in the dry season), but there are signs that runoff water penetrates the cave in rainy periods. As mentioned, our team visited the cave during the dry period; hence, the substrates were predo- minantly dry close to the entrance. On the other hand,

deeper galleries became progressively wetter, and the final portion was extremely humid (Figure 5B).

Specimens of *Pectenoniscus monsviridis* n. sp. were observed in the innermost humid galleries, far from the entrance. The few observed specimens were found in the cave walls, walking on moistened cave deposits of mud (Figure 5C). The main resources observed in the cave were bat guano (especially pro- duced by vampire bats – *Desmodus rotundus* (É. Geoffroy, 1810)) and plant debris brought by the water. However, the area where the specimens occurred presented only bat guano as a visible organic resource (even so, only a few small piles). An expedi- tion accomplished by other speleologists in the rainy season revealed the inner conduits partially flooded, indicating the wide variation in the water table between dry and rainy seasons. Hence, individuals of *Pectenoniscus monsviridis* n. sp. probably migrate to other cave regions (or other subterranean habitats con- nected to the cave) in the rainy periods.

It is important to note that the small dimensions of the conduit close to the entrance prevent locals

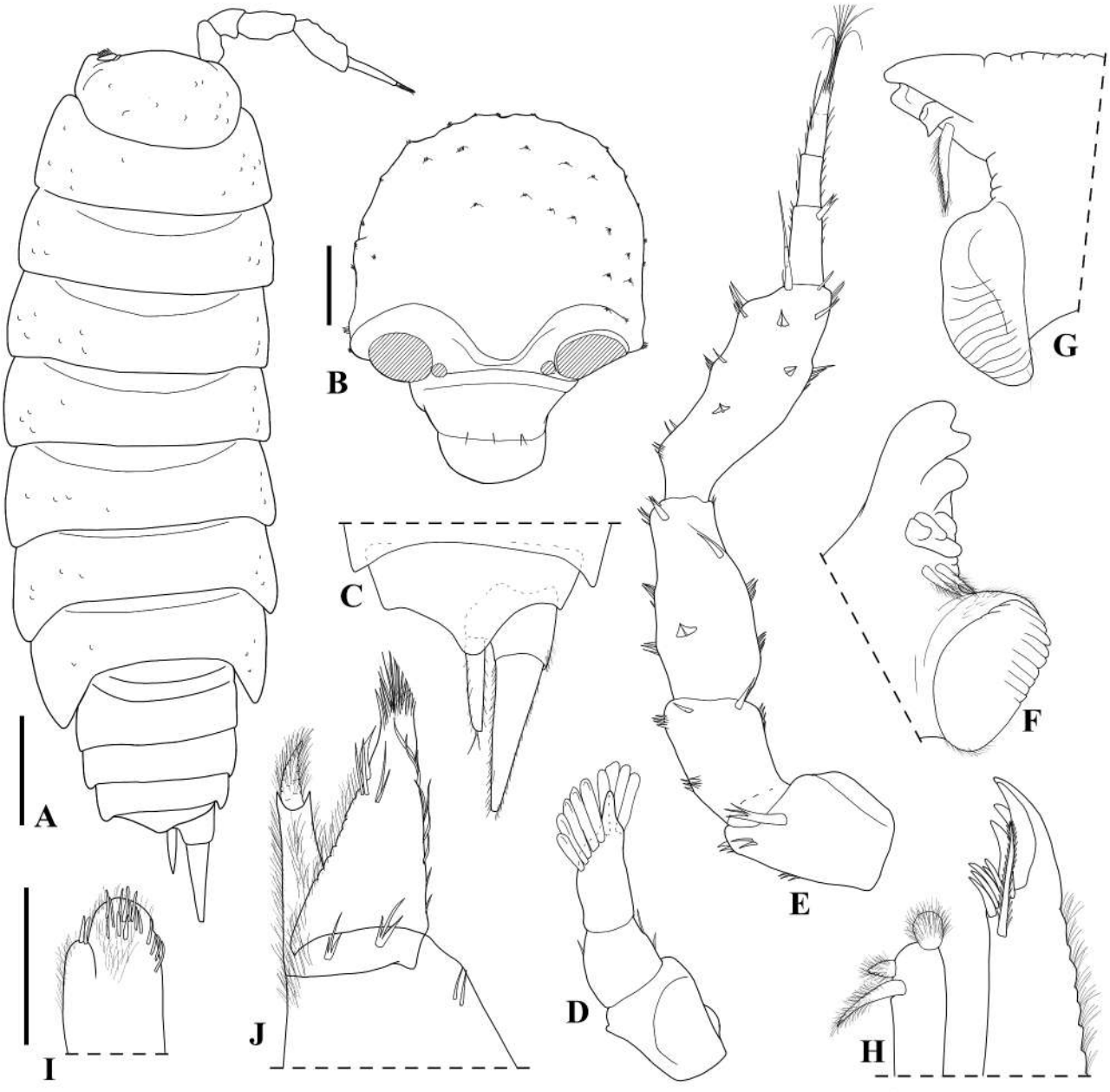


Figure 2. *Pectenoniscus monsviridis* n. sp. Male paratype (ISLA 96770): A, habitus, dorsal view; B, cephalon, frontal view; C, pleonite 5, telson and uropod, dorsal view; D, antennula; E, antenna; F, left mandible; G, right mandible; H, maxillula; I, maxilla; J, maxilliped. Scale bars: A: 0.5 mm; B–J: 0.2 mm.

from accessing the cave's inner portions, thus pro- tecting the cave interior from vandalism. However, the external landscape is severely altered, only patches of the original vegetation close to the lime- stone outcrops are currently observed and the sur- roundings of the cave were replaced by pastures with cattle compacting the exposed soil (Figure 5D,E), which is highly vulnerable to erosional processes. Furthermore, the external topography contributes to the input of sediments to the cave during rainy periods, since the cave entrance is located at the bottom of a valley (Figure 5E). Therefore, erosive processes acting over the exposed soils can intensify the sediment input to the cave, silting up microha- bitats. Hence, it is highly recommended to protect the cave surroundings, especially by the reforestation of the immediate external landscape.

Pectenoniscus revelatus n. sp.

(Figures 6–8)

Type material

Holotype: male (ISLA 96636), Brazil, Bahia state, municipality of Coribe, Baixão da Canoa cave (−13.857692° −44.163986°); 20 August 2022; R.L. Ferreira leg. Paratypes: 1 male (ISLA 96772 in slide) 4 males, 5 females (ISLA 96637), same data as holotype.

Diagnosis

Male pleopod 1 exopod trapezoid with sinuous margin; male pleopod 2 exopod triangular, endopod straight, apex with two lobes, one lobe directed inward and one directed outward.

Description

Maximum length: male, 2 mm. Colorless, eyes absent (Figures 6A, 8D). Dorsum (Figure 6A, B) with tricorn-shaped scale-setae; granulations disposed in five rows on cephalon, three rows on pereonite 1 and two rows on pereonites 1–7. Cephalon with round antennal lobes; supra-antennal line bent in middle (Figure 6B). Pereonite 1 with margin slightly projected forward; pereonites 4–7 posterior margin progressively more concave; pleonites 3– 5 epimera posterior points slightly developed, pleon nar- rower than pereon (Figure 6A). Telson with concave sides and round apex (Figure 6C). Antennula with three articles, distal article with seven aesthetascs (Figure 6D). Antenna fifth article of peduncle longer than flagellum, with one seta longer than first flagellum article; flagellum with three

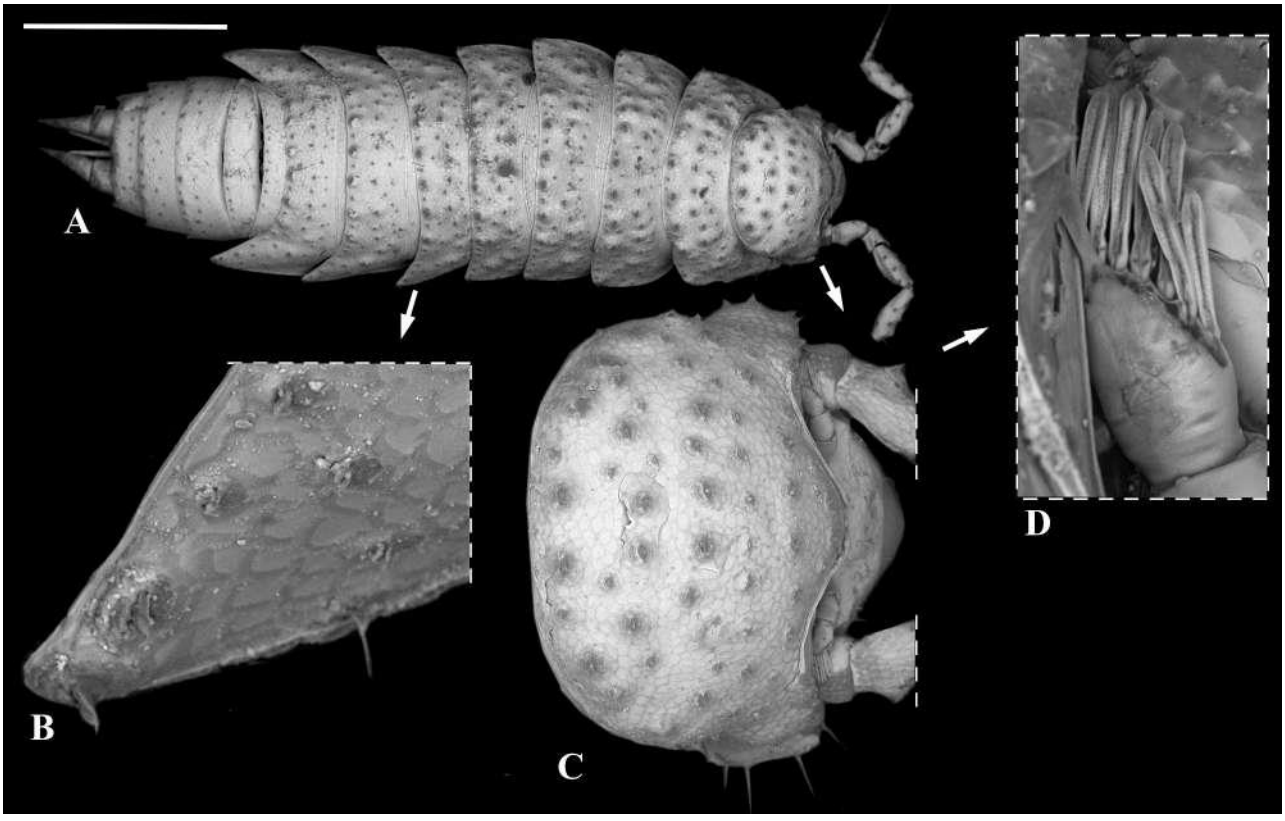


Figure 3. *Pectenoniscus monsviridis* n. sp. Female paratype (ISLA 96771): A, habitus, dorsal view; B, epimeron 5, scale-setae; C, cephalon, dorsal view; D, aesthetascs on antennula. Scale bar: 1 mm.

articles (Figure 6E). Buccal pieces as *Pectenoniscus monsviridis* n. sp. (Figure 6F–J), except maxillula outer branch with 4 + 5 teeth, apically entire. Pereopod 1 antennal grooming brush composed of serrated scale setae longitudinally on propodus and on sternal margin of carpus (Figure 7A); dactylar seta bifid with thin setulae. Water conducting system on ischium, merus, carpus and propodus of pereopod 6 and in pereopod 7. Uropod protopod

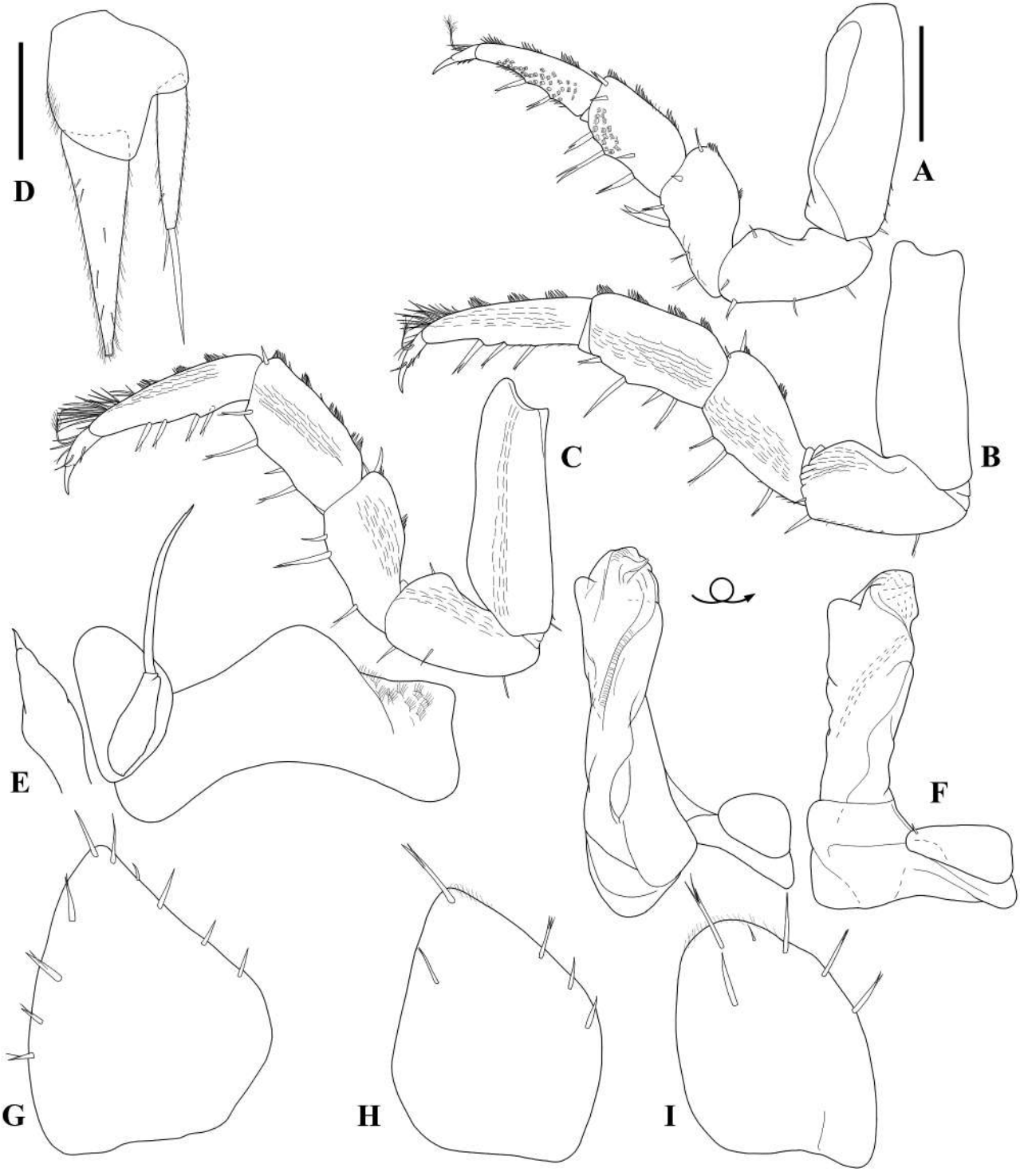


Figure 4. *Pectenoniscus monsviridis* n. sp. Male paratype (ISLA 96770): A, pereopod 1; B, pereopod 6; C, pereopod 7; D, uropod; E, genital papilla and pleopod 1; F, pleopod 2; G, pleopod 3 exopod; H, pleopod 4 exopod; I, pleopod 5 exopod. Scale bars: 0.2 mm.

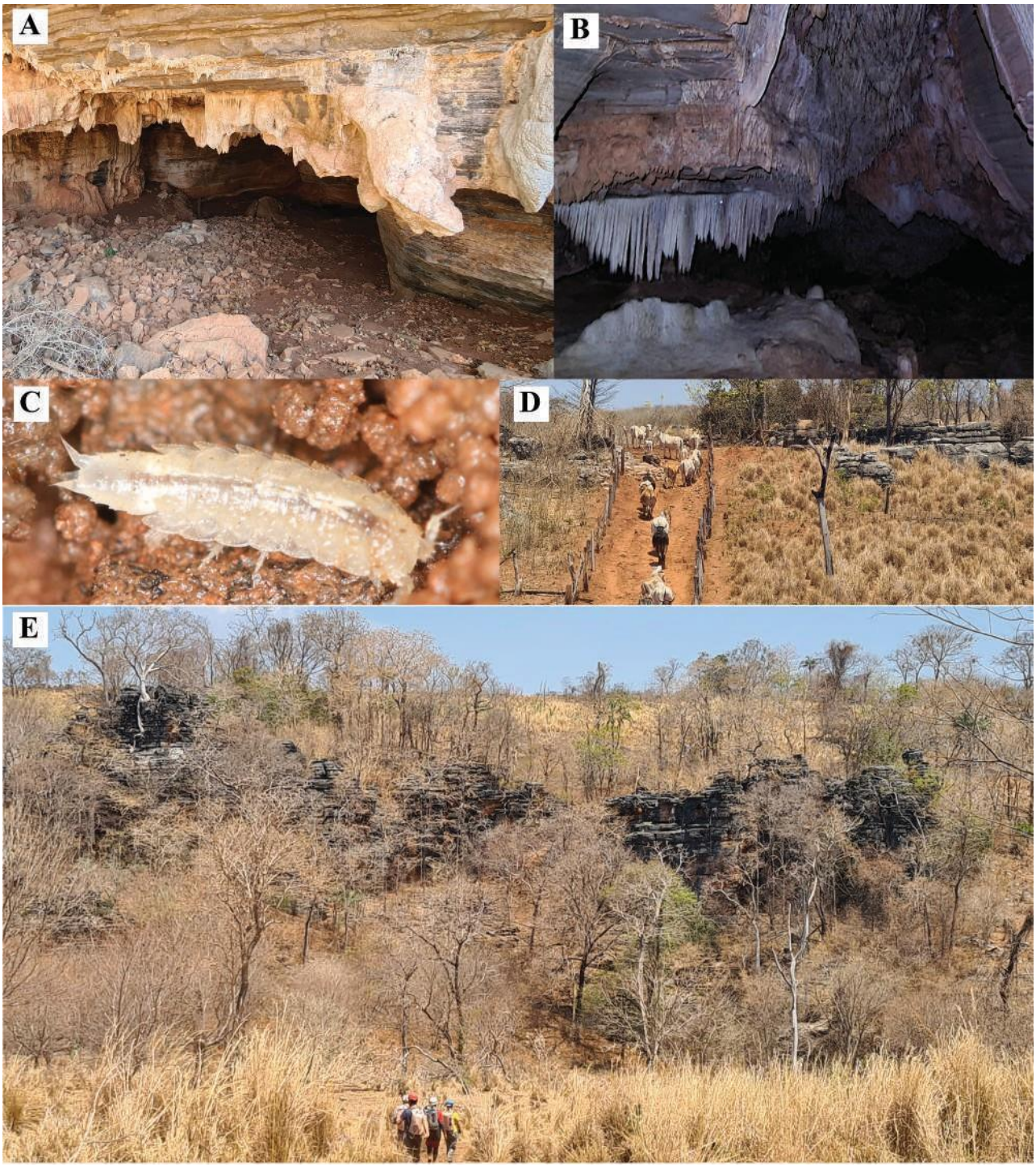


Figure 5. Habitat of *Pectenoniscus monsviridis* n. sp. A, Serra Verde cave's entrance; B, cave interior; C, living specimen of *Pectenoniscus monsviridis* n. sp. inside the cave; D, pastures and livestock in the vicinity of the cave; E, karst outcrop where the cave is located.

longer than wide, longer than distal margin of telson; exopod longer than endopod, inserted distally (Figure 6C).

Male

Pereopods 6 and 7 (Figure 7B,C) propodus with tufts of setae on tergal margin. Genital papilla (Figure 7D) enlarged on medial portion, apically narrow. Pleopod 1 (Figure 7D) exopod trapezoid, apex acute and sinuous lateral margin; endopod twice longer than exopod. Pleopod 2 (Figure 7E) exopod triangular, twice wider than long; endopod distal article almost three times longer than proximal article, straight, apex with two lobes, one

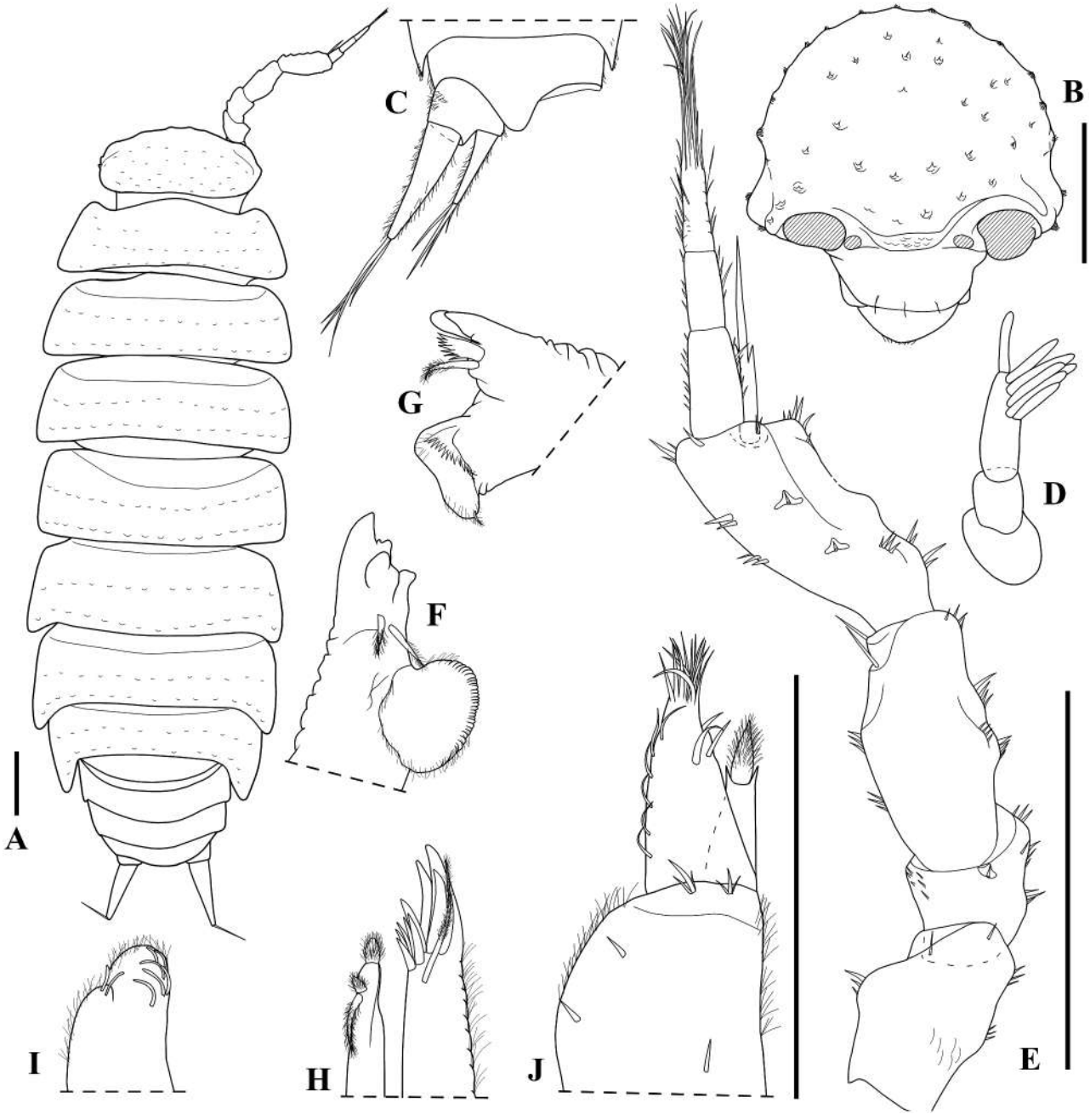


Figure 6. *Pectenoniscus revelatus* n. sp. Male paratype (ISLA 96772): A, habitus, dorsal view; B, cephalon, frontal view; C, pleonite 5, telson and uropod, dorsal view; D, antennula; E, antenna; F, left mandible; G, right mandible; H, maxillula; I, maxilla; J, maxilliped. Scale bars: 0.2 mm.

lobe directed inward and one directed outward. Pleopods 3–5 exopods (Figure 7F–H) subquadrangular.

Etymology

The epithet '*revelatus*' was given in reference to the fact that Baixão da Canoa cave was only recently discovered despite the long years of speleological exploration on the Serra do Ramalho karst area by distinct speleologists. *Revelatus* is a Latin word meaning revealed.

Morphological remarks

By the shape of male pleopod 1 exopod *Pectenoniscus revelatus* n. sp. resembles *Pectenoniscus monsviridis* n. sp., but the apex is distinct (round versus acute with sinuous lateral margin in *Pectenoniscus revelatus* n. sp.). The shape of male pleopod 2 exopod is distinct from all species since it is triangular.

Ecological remarks

Specimens of *Pectenoniscus revelatus* n. sp. were only observed in the Baixão da Canoa cave. This cave was

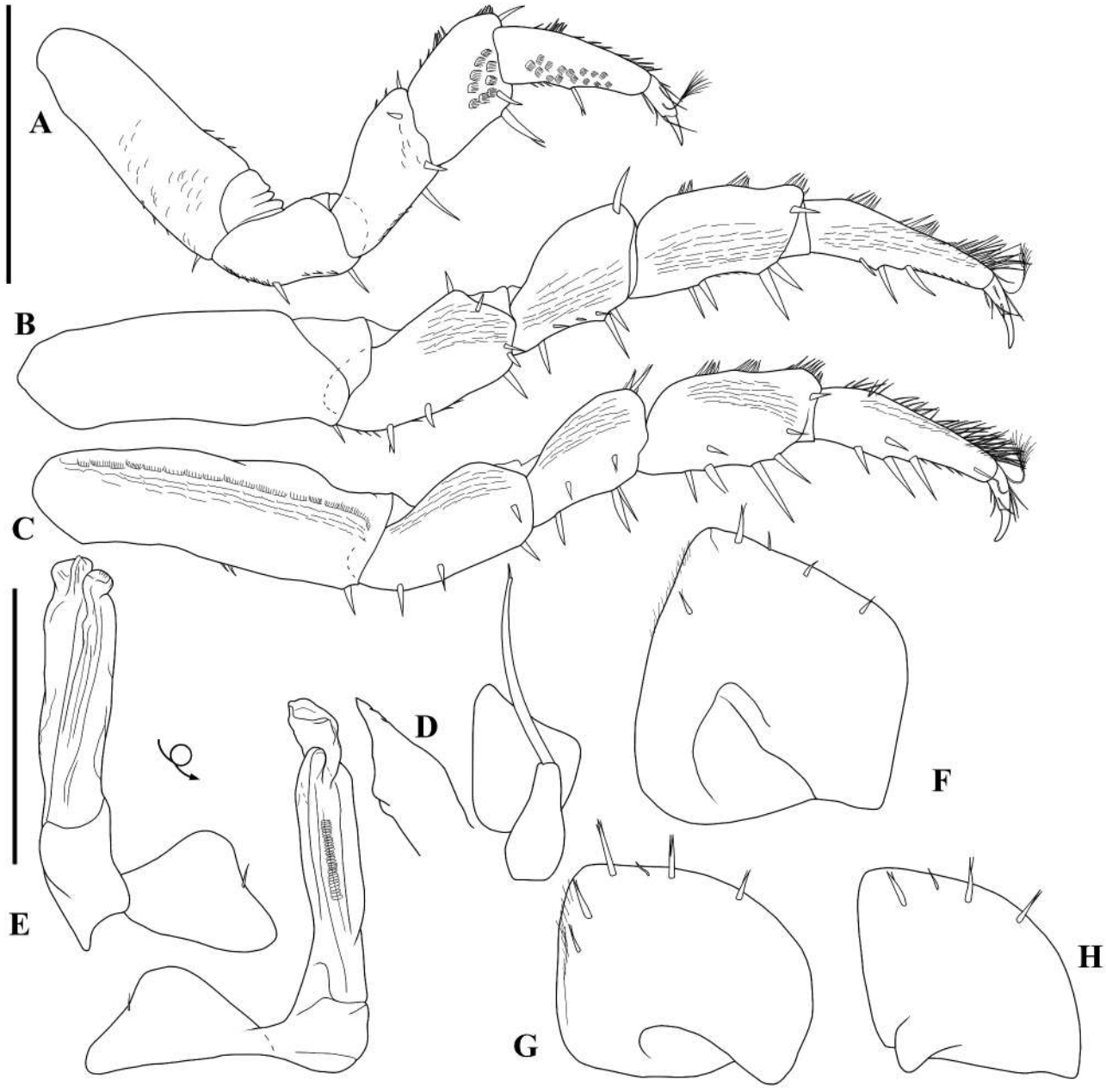


Figure 7. *Pectenoniscus revelatus* n. sp. Male paratype (ISLA 96772): A, pereopod 1; B, pereopod 6; C, pereopod 7; D, genital papilla and pleopod 1; E, pleopod 2; F, pleopod 3 exopod; G, pleopod 4 exopod; H, pleopod 5 exopod. Scale bars: 0.2 mm.

recently discovered and was not totally explored, although it presents at least 1.5 km of extension. It has a single known entrance that gives access to a crawling conduit and connects to the main conduit, which presents an intermittent drainage (Figure 8A). Following the downstream direction, the conduit leads to a voluminous chamber that connects to a lower level (around 20 m below the upper level) which also presents a drainage (this part of the cave was not explored). The conduit upstream splits and both conduits follow distinct directions with one flooded and the other dry, although with clear signs of water flow that probably occur during rainy periods (Figure 8B). Although the drainage seems to be active only during the rainy season (our visit occurred during the dry season), several areas seem to remain flooded throughout the year. Specimens of *Pectenoniscus revelatus* n. sp. were observed far from the entrance, on moist conduits. They were walking on clayish sediments along the riverbanks. Some specimens were found near small bat guano patches, suggesting they could be feeding on this organic resource. The digestive tube seen by transparency (Figure 8C) reveals a blackish content, which could be bat guano. Considering that most

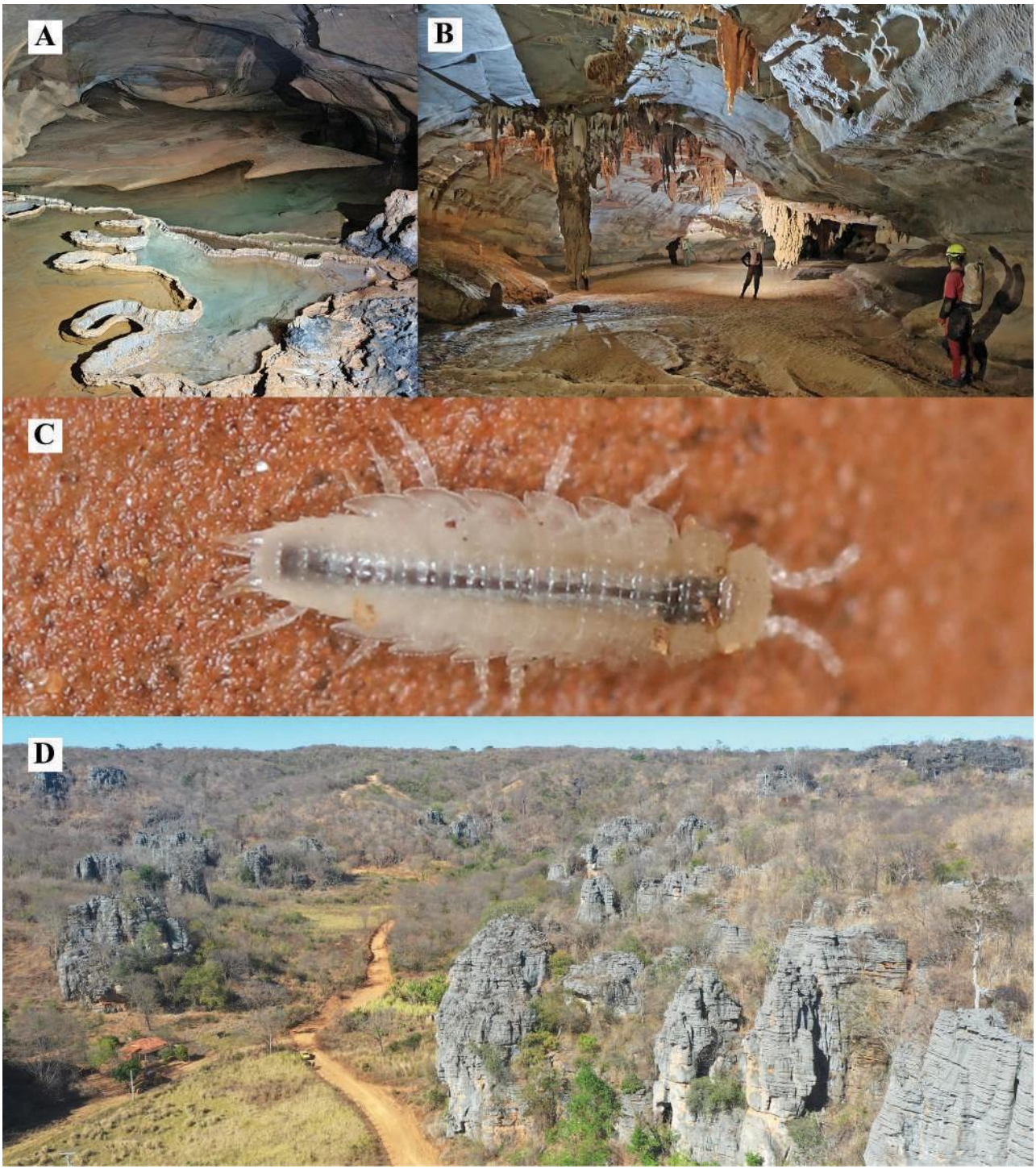


Figure 8. Habitat of *Pectenoniscus revelatus* n. sp. A, cave main conduit; B, cave interior in the upstream direction; C, living specimen of *P. revelatus* n. sp. inside the cave; D, external landscape on the Karst area surrounding the cave.

parts of the cave were not explored, the distribution of this species inside the cave remains unknown. Furthermore, many other caves in the area were biologically surveyed, and specimens of *P. revelatus* n. sp. were not found.

As previously mentioned, the cave was recently discovered, so most of its sediments were in pristine condition, being only seasonally (and naturally) altered by floods. On the other hand, the external environment surrounding the cave is altered, presenting unpaved roads and monocultures, although forests are still observed especially on the tops of the limestone out- crops (Figure 8D).

Pectenoniscus archaeos n. sp.

(Figures 9–11)

Type material

Holotype: male (ISLA 96638 in slide), Brazil, Bahia state, municipality of Iuiú, Morro do Aurélio cave (−14.513705° −43.543210°); 20 October 2021; R.L. Ferreira leg. Paratypes: 2 females (ISLA 96639), same data as holotype.

Diagnosis

Antennula with four aesthetascs; pleopod 1 exopod triangular with acute apex and lateral margin concave;

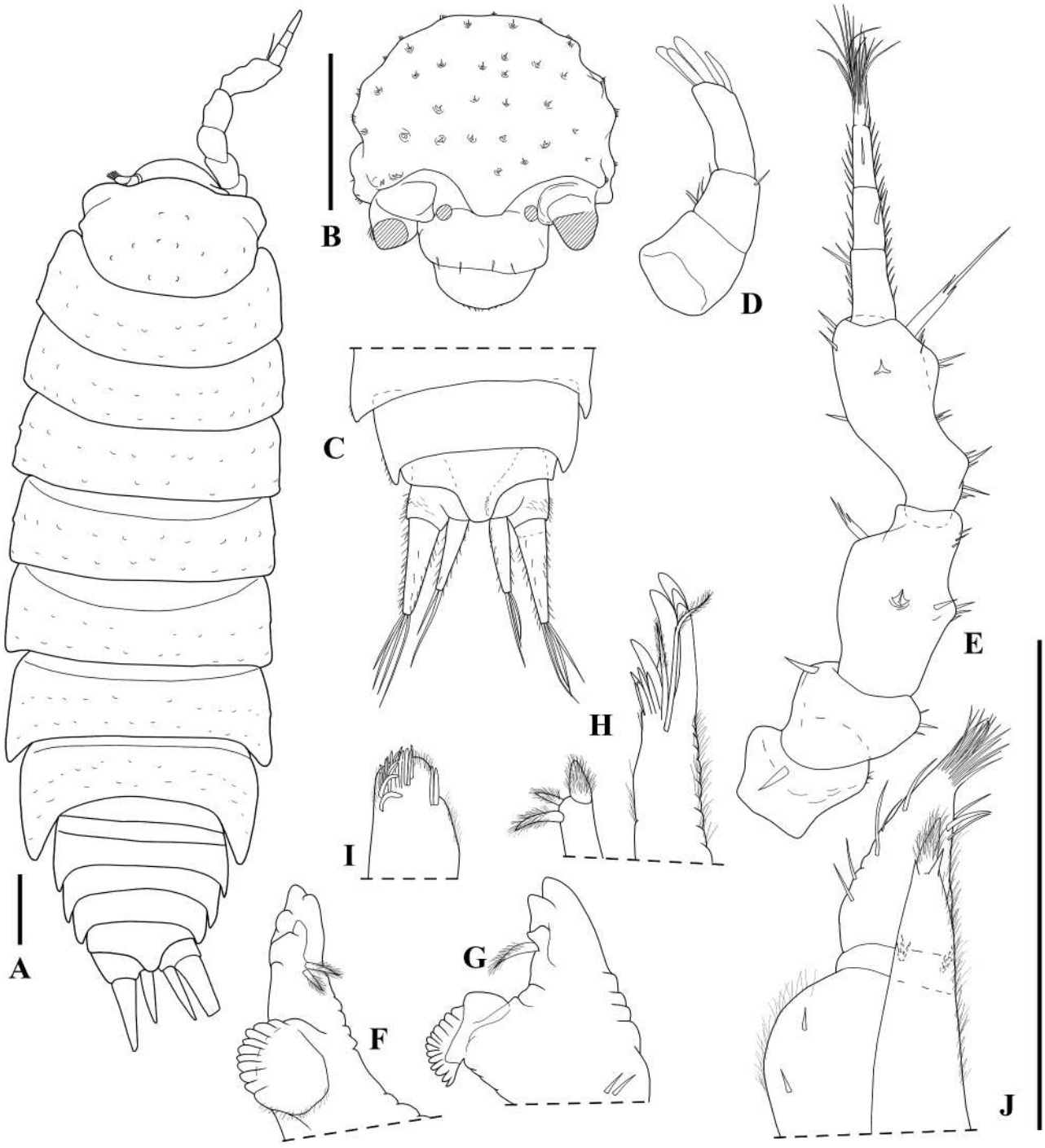


Figure 9. *Pectenoniscus archaeos* n. sp. Male holotype (ISLA 96638): A, habitus, dorsal view; B, cephalon, frontal view; C, pleonites 4 and 5, telson and uropod, dorsal view; D, antennula; E, antenna; F, left mandible; G, right mandible; H, maxillula; I, maxilla; J, maxilliped. Scale bars: 0.2 mm.

male pleopod 2 endopod thickset with apex twisted, distal projection and robust outer lobe.

Description

Maximum length: male, 2.5 mm. Colorless, eyes absent (Figures 9A, 11E). Dorsum (Figure 9A) with tricorn- shaped scale-setae with granulations in five rows on cephalon, and two rows on pereonites 1–7, smooth pleon. Cephalon with round antennal lobes; supra-antennal line bent in middle (Figure 9B). Pereonite 1 with margin projected forward, not surpassing median portion of cephalon; pereonites 3–7 posterior margin progressively more concave; pleonites 3–5 epimera pos- terior points developed; pleon narrower than pereon (Figure 9C). Telson with concave sides and round apex (Figure 9C). Antennula with three articles, distal article with four aesthetascs (Figure 9D). Antenna fifth article of peduncle longer than flagellum, with one seta longer than

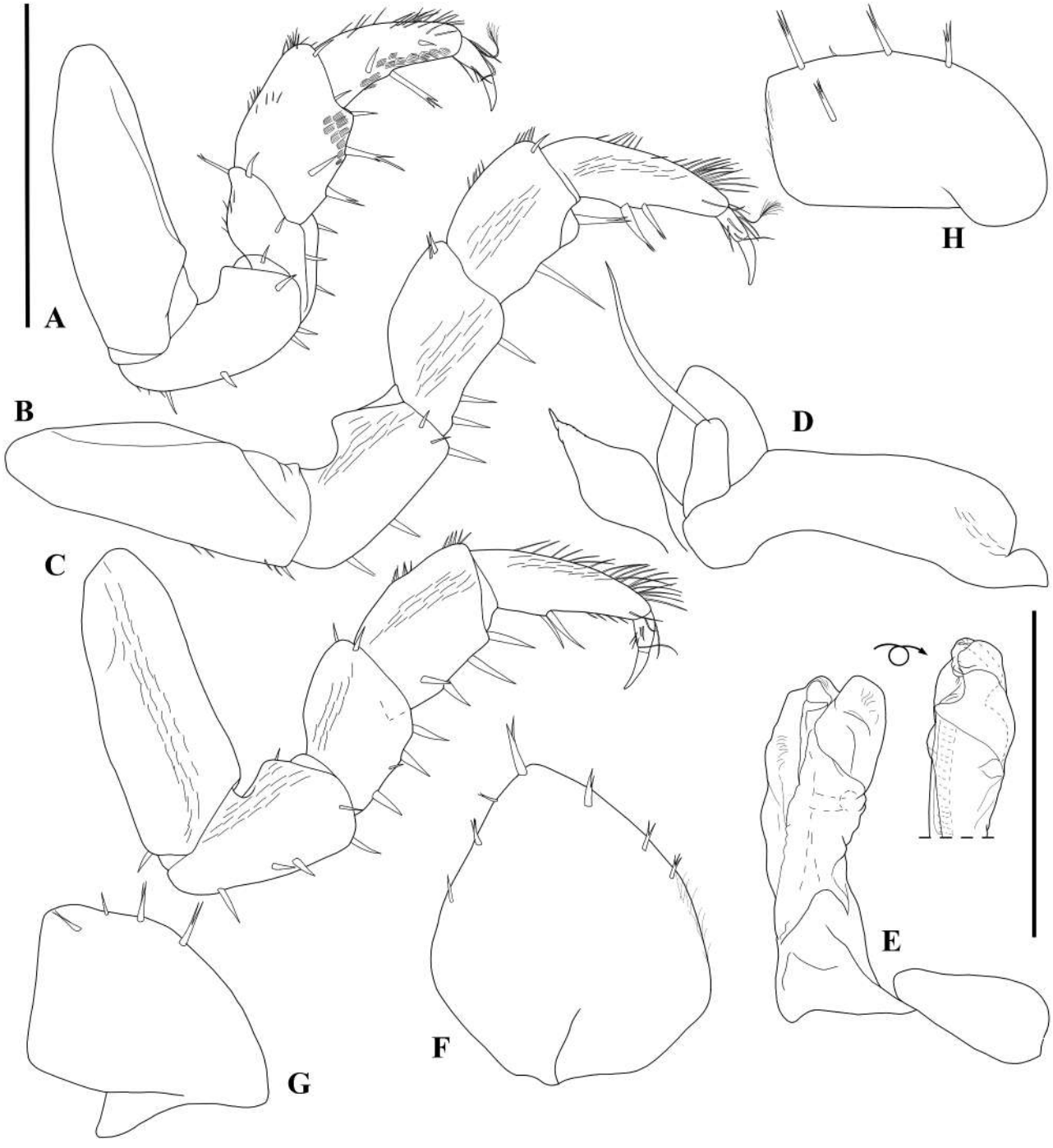


Figure 10. *Pectenoniscus archaeos* n. sp. Male holotype (ISLA 96638): A, pereopod 1; B, pereopod 6; C, pereopod 7; D, genital papilla and pleopod 1; E, pleopod 2; F, pleopod 3 exopod; G, pleopod 4 exopod; H, pleopod 5 exopod. Scale bars: 0.2 mm.

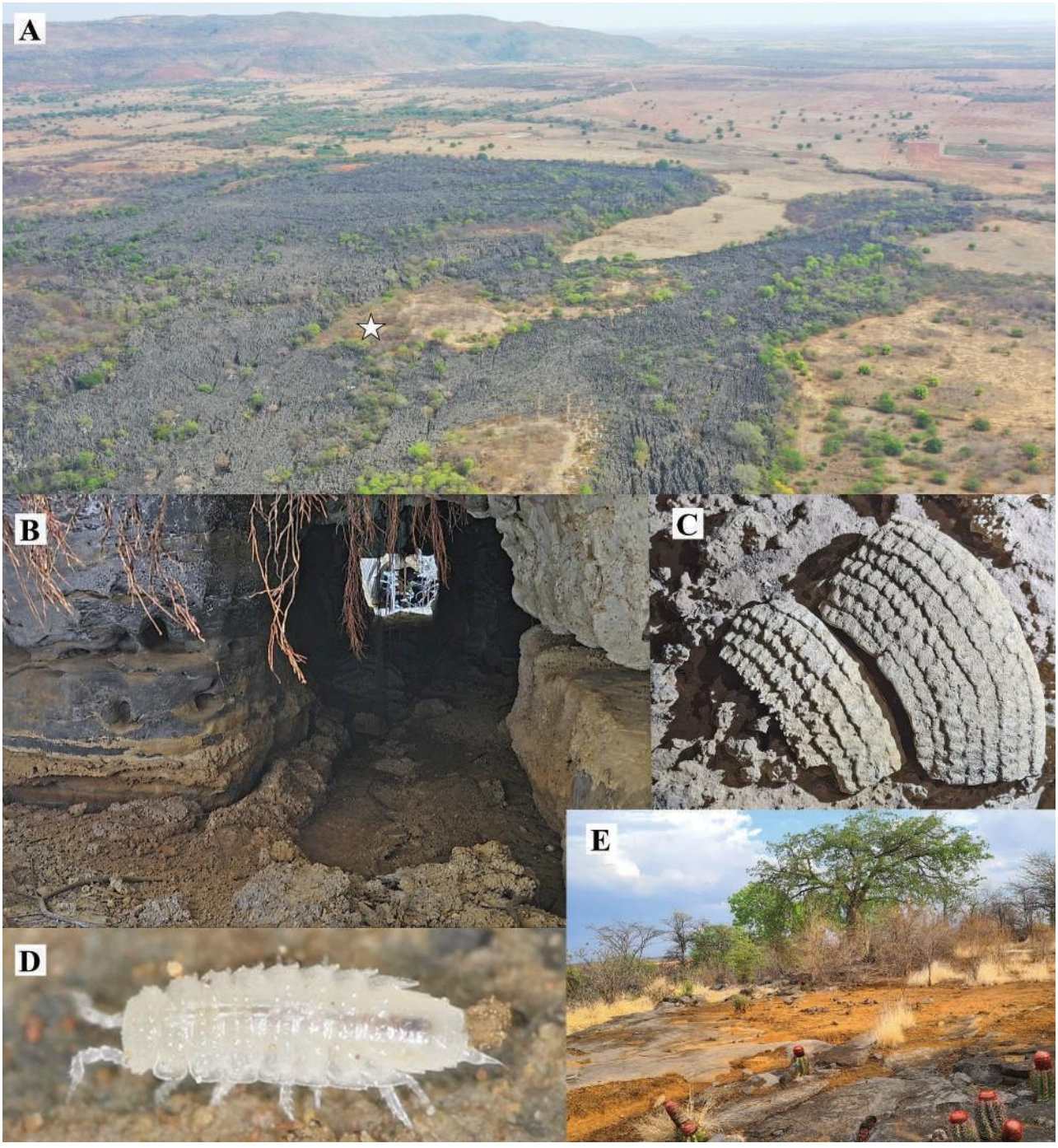


Figure 11. Habitat of *Pectenoniscus archaeos* n. sp. A, outcrop where Morro do Aurélio Cave is located (star indicates the main cave entrance); B, a conduit inside the cave; C, archeological fragmented of a ceramic pot; D, specimen of *P. archaeos* n. sp. inside the cave; E, external landscape surrounding the cave.

first flagellum article; flagellum with three articles (Figure 9E). Buccal pieces as *Pectenoniscus monsviridis* n. sp. (Figure 9F–J), except maxillula outer branch with 5 + 5 teeth. Pereopod 1 antennal grooming brush longitudinally on propodus and on sternal margin of carpus (Figure 10A); dactylar seta bifid with thin setulae. Water conducting system on ischium, merus, carpus and propodus of pereopod 6 and in pereopod 7. Uropod protopod longer than wide, longer than distal margin of telson; exopod longer than endopod, inserted distally (Figure 9C).

Male

Pereopods 6 and 7 (Figure 10B,C) propodus with tufts of setae on tergal margin. Genital papilla (Figure 10D) enlarged on medial portion, apically narrow. Pleopod 1

(Figure 10D) protopod rectangular, three times wider than long; exopod triangular, acute apex, lateral margin concave; endopod longer than exopod. Pleopod 2 (Figure 10E) exopod trapezoidal, wider than long; endo- pod robust, distal article almost three times longer than proximal article, apex twisted, distal projection and robust outer lobe. Pleopod 3 exopod (Figure 10F) trape- zoidal, distal margin concave; pleopods 4 and 5 exopod (Figure 10G,H) subrectangular.

Etymology

The epithet '*archaeos*' was given in reference to the archeological remains observed in the Morro do Aurélio cave.

Morphological remarks

By the triangular shape of male pleopod 1 exopod with acute apex *Pectenoniscus archaeos* n. sp. resembles *P. juveniliensis*. By the trapezoidal shape of male pleopod 2 exopod, *Pectenoniscus archaeos* n. sp. is simi- lar to *P. montalvaniensis*. However, *Pectenoniscus archaeos* n. sp. differs by the shape of male pleopod 2 endopod.

Ecological remarks

Specimens of *Pectenoniscus archaeos* n. sp. were only observed in the Morro do Aurélio cave. This cave is associated with a limestone outcrop close to the Serra de Iuiú (about 2.5 km in a straight line). The Morro do Aurélio outcrop (Figure 11A) is relatively small (2.2 km long and 1.5 km wide) and the cave is labyrinthine Figure 11B), with 1.380 meters of extension and several entrances, most located at the top of the outcrop (sky- lights). This cave presents several archeological remains, which include lithic materials and pottery shards (Figure 11C), and demonstrates the use of this cave by ancient South American cultures. As the cave has several entrances, both vertical and horizontal, there is considerable wind flow inside, as well as exten- sive illuminated areas. Thus, much of the cave has very dry substrates, especially during the dry seasons. The specimens of *P. archaeos* n. sp. were found in an aphotic zone far from entrances, which still retained some moisture. The specimens were found walking on wet sediments under limestone blocks (Figure 11D). This area receives runoff water in rainy periods, which also transport plant organic materials that are deposited on the floor. Apparently, these organic remains constitute trophic resources for isopods. The cave does not receive local visitors, hence the innermost portions are well preserved. Although the top of the outcrop presents well-preserved vege- tation (Figure 11E), the external environment sur- rounding the cave is quite altered, as observed for other areas in the Iuiú region. Pastures and mono- cultures replace most of the original vegetation (Figure 11A). However, in contrast to the other caves previously described, the Morro do Aurélio cave will probably not be directly affected by such changes in the surroundings, as it is located at the top of the outcrop.

Pectenoniscus sepultus n. sp.

(Figures 12–14)

Type material

Holotype. male (ISLA 96640 in slide), Brazil, Bahia state, municipality of Iuiú, Gruta do Sepultamento cave (−14.655515° −43.544522°); 24 October 2021; R.L. Ferreira leg. Paratypes: 5 males (ISLA 96641), same data as holotype.

Diagnosis

Male pleopod 1 exopod triangular shaped with apex round; pleopod 2 exopod ovoid; endopod apex thick- set, inner margin with lateral lobe with wrinkle margin, apex with transverse pointed process directed outward toward one outer lobe.

Description

Maximum length: male, 2.5 mm. Colorless, eyes absent (Figures 12A, 14D). Dorsum with tricorn- shaped scale-setae with granulations in five rows on cephalon, two rows on pereonite 1–6, one row on pereonite 7, pleon smooth (Figure 12A). Cephalon with triangular antennal lobes; supra-antennal line bent in middle (Figure 12B). Pereonite 1 with margin slightly projected forward; pleonites 3–5 epimera posterior points slightly developed, pleon narrower than pereon. Telson with concave sides, round apex (Figure 12C). Antennula with three articles, distal article with six aesthetascs (Figure 12D). Antenna fifth article of peduncle longer than flagellum, with one seta longer than second flagellum article; flagel- lum with three articles (Figure 12E). Buccal pieces as *Pectenoniscus monsviridis* n. sp. (Figure 12F–J). Pereopod 1 antennal grooming brush composed of serrated scale-setae longitudinally on propodus and on sternal margin of carpus (Figure 13A); dactylar seta bifid with thin setulae. Water conducting system on ischium, merus, carpus and propodus of pereopod 6 and on pereopod 7. Uropod protopod longer than wide, longer than distal margin of telson; exo- pod longer than endopod, inserted distally (Figure 12C).

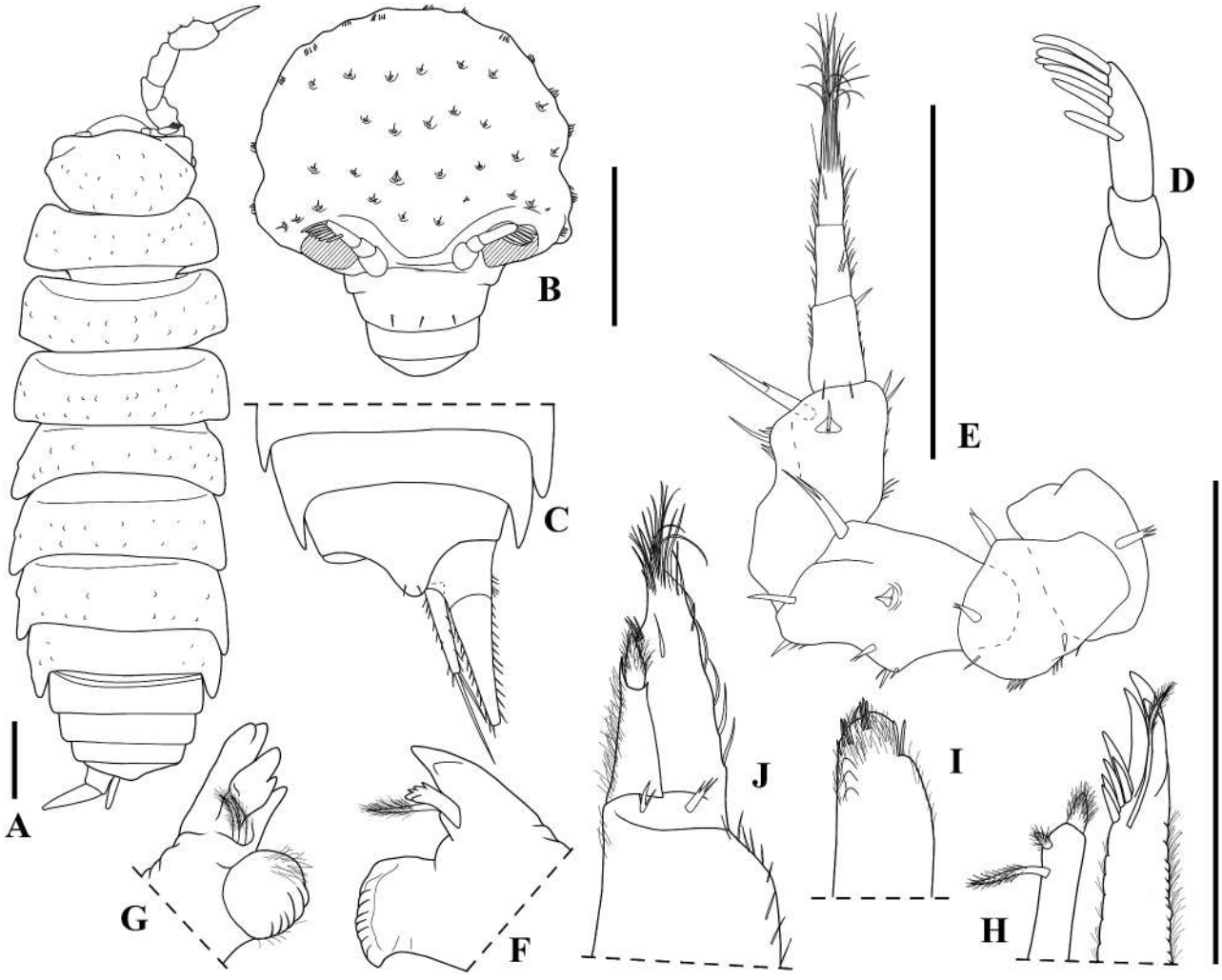


Figure 12. *Pectenoniscus sepultus* n. sp. Male holotype (ISLA 96640): A, habitus, dorsal view; B, cephalon, frontal view; C, pleonites 4 and 5, telson and uropod, dorsal view; D, antennula; E, antenna; F, left mandible; G, right mandible; H, maxillula; I, maxilla; J, maxilliped. Scale bars: 0.2 mm.

Male

Pereopods 6 and 7 (Figure 13B,C) propodus with tufts of setae on tergal margin. Pleopod 1 (Figure 13D) pro- topod subrectangular, wider than long, distal margin straight; exopod triangular shaped, as long as wide, apex round; endopod twice longer than exopod. Pleopod 2 (Figure 13E) exopod ovoid, wider than long; endopod with distal article almost three times longer than proximal article, apex thickset, wider than base, inner margin with lateral lobe with wrinkle mar- gin, apex with transverse pointed process directed out- ward toward one outer lobe. Pleopod 3 exopod (Figure 13F) trapezoidal, straight distal margin; pleo- pod 4 as in Figure 13G.

Etymology

The epithet '*sepultus*' is a Latin noun that means bur- ied, thus referring to the name of the cave where the specimens were found. In Portuguese 'sepultamento' means burial.

Morphological remarks

By the number of aesthetascs *Pectenoniscus sepultus* n. sp. resembles *P. santanensis*, *P. morrensis* and *P. fervens*. By the shape of male pleopod 1 exopod *Pectenoniscus sepultus* n. sp. resembles *P. liliae*, *P. montalvaniensis*, *P. santanensis*, and *P. morrensis*. However, the species differ from others by the shape of male pleopod 1 endopod.

Ecological remarks

Specimens of *Pectenoniscus sepultus* n. sp. were found in Gruta do Sepultamento cave. However, since many other caves occur in the same outcrop (which were not sampled), other populations may eventually exist. This cave is also

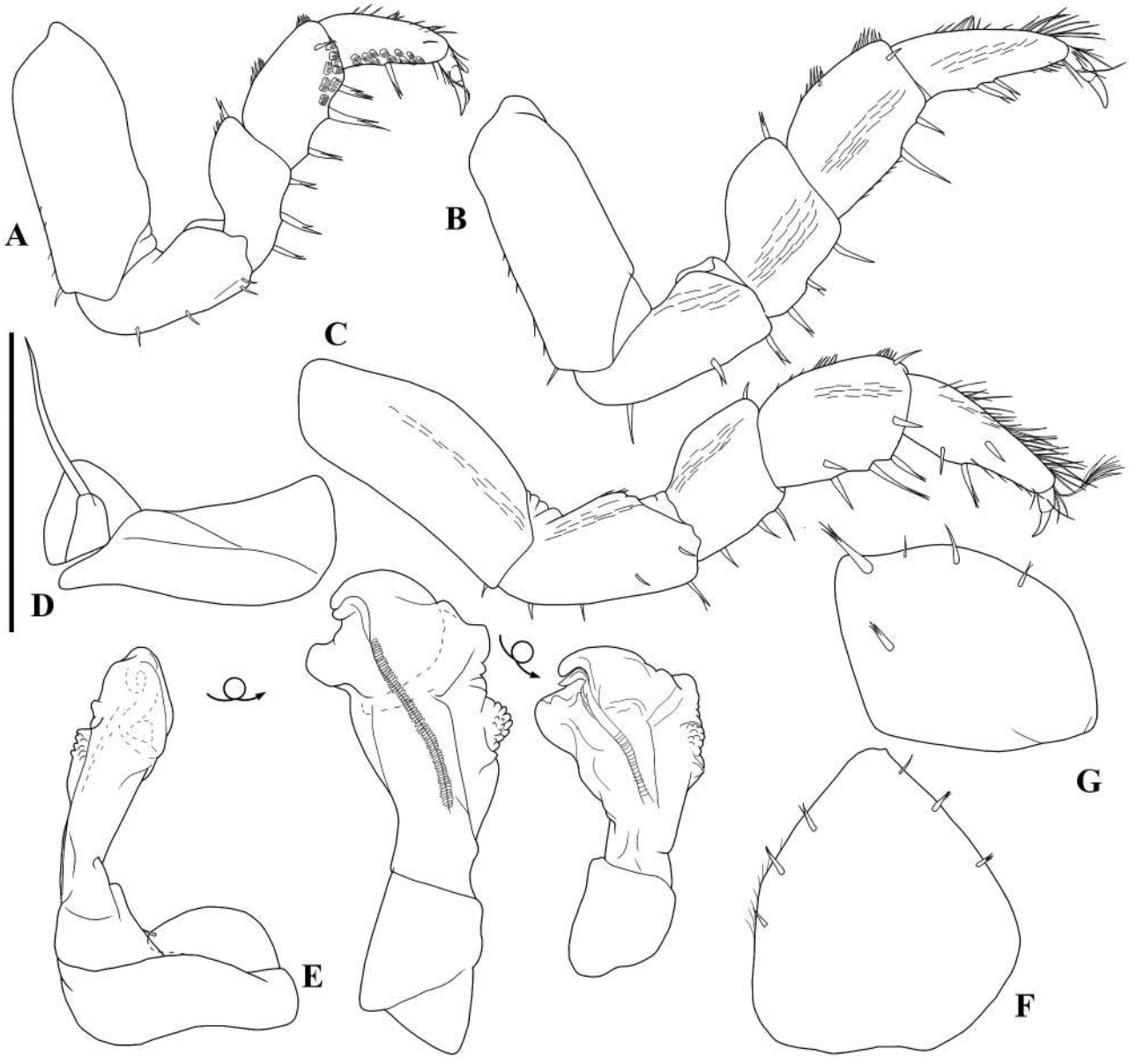


Figure 13. *Pectenoniscus sepultus* n. sp. Male holotype (ISLA 96640): A, pereopod 1; B, pereopod 6; C, pereopod 7; D, pleopod 1; E, pleopod 2; F, pleopod 3 exopod; G, pleopod 4 exopod. Scale bars: 0.2 mm.

located close to the Serra de Iuiú outcrop (about 10 km apart in a straight line). The Sepultamento outcrop is relatively small (1.4 km long by 0.5 km wide) when com- pared to the Serra de Iuiú, which is much more extensive (20 km long by 14 km wide) (Figure 14A). The Gruta do Sepultamento cave has several conduits forming a labyrinth of passages that interconnect larger galleries (Figure 14B). There are several entrances, both horizontal and vertical (skylights that open at the top of the massif). Almost all horizontal entrances lead to very narrow con- duits that connect the entrances to the large galleries located in the innermost portion of the cave. This cave represents an important archeological site, which has started to be studied. Several traces of past human presence are observed along the cave. Among these remains, there are ceramics fragments, lithic materials and even human bones associated with funerary urns, some of which are exposed and fragmented on the cave floor (Figure 14C). Although the practice of looting archeological and paleon- tological sites in Brazil is quite frequent, the difficulty of accessing the cave interior apparently prevented residents from entering the cave and eventually looting or altering these archeological sites.

An important aspect that deserves mention is the pronounced seasonality of the external environment and its important influence on the cave. As the cave is located in a topographically lower area, most of its conduits are flooded in the rainy periods, remaining

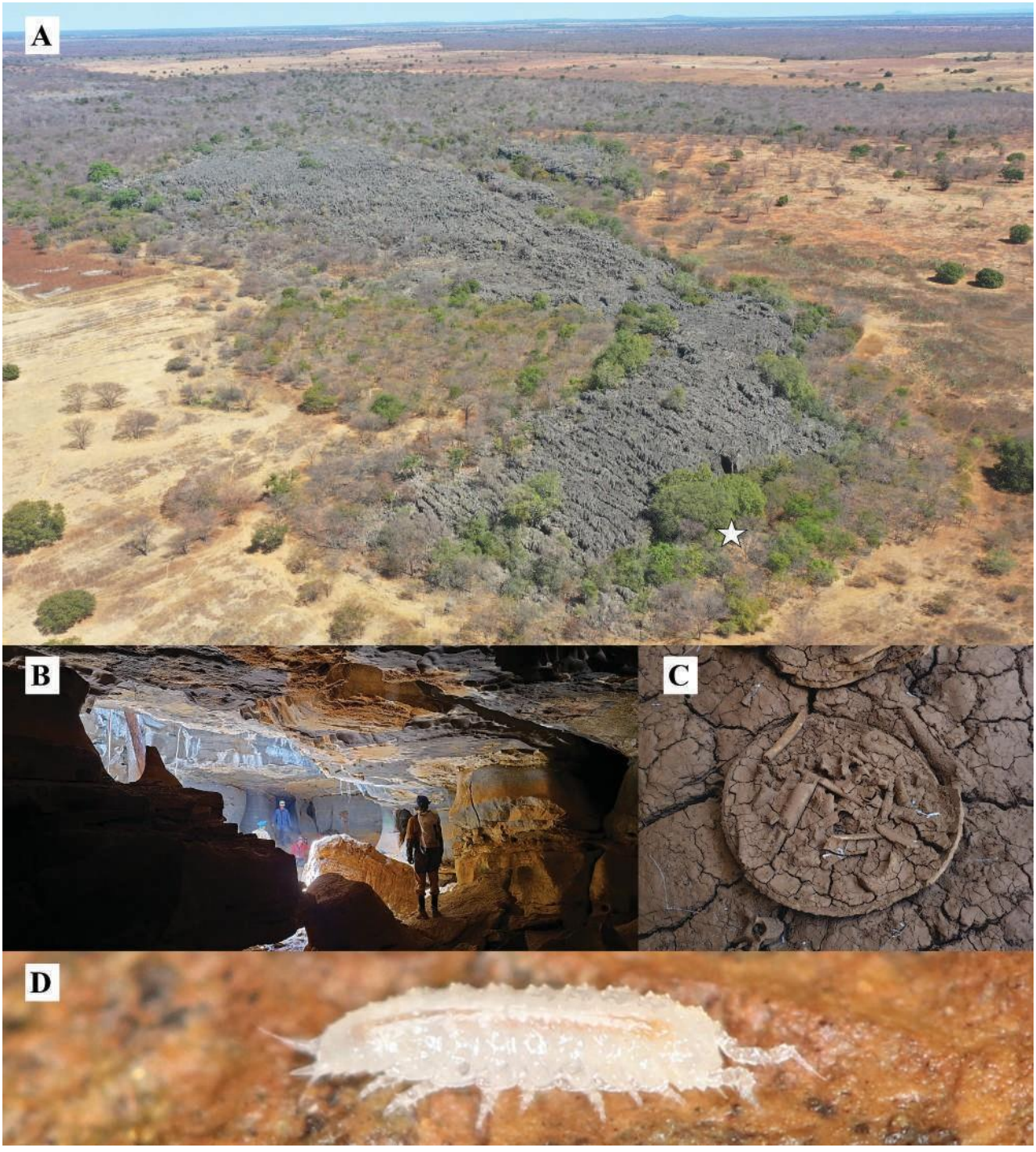


Figure 14. Habitat of *Pectenoniscus sepultus* n. sp. A, outcrop where the Gruta do Sepultamento cave is located (star indicates the main cave entrance); B, one chamber inside the cave; C, human archeological remains inside a fragmented ceramic pot; D, specimen of *Pectenoniscus sepultus* n. sp. inside the cave.

submerged. Conversely, during the dry season, almost the entire length of the cave becomes extremely dry, with the exception of a few deeper and isolated con- duits. Therefore, most of the substrates on the cave floor are covered by a cracked clayey sediment, which results from the drying of the floor after the end of the rainy season.

Specimens of *Pectenoniscus sepultus* n. sp. were found under rocks located at moistened areas inside the cave (Figure 14D). The same areas surveyed in drier periods failed in finding specimens, as all sub- strates (even under rocks) were dry. It is likely that during such periods, the individuals might migrate to moistened areas, which may be inaccessible to

humans, as there are deep cracks on the cave floor. The organic resources observed inside the cave were plant debris brought by water, bat guano piles (quite uncommon in this cave) and roots from the external vegetation.

The external environment surrounding the cave is severely altered, since most of the original vegeta- tion was replaced by pastures or other monocultures (Figure 14A). Additionally, there are extensive bare land areas, which can increase silting inside the cave during rainy periods. Such impacts may act in both reducing the organic input to the cave ecosystems and in altering several microhabitats of this species.

Pectenoniscus caesarius n. sp.

(Figures 15–17)

Type material

Holotype. male (ISLA 96642 in slide), Brazil, Bahia state, municipality of Campo Formoso, Toca do Cesário cave

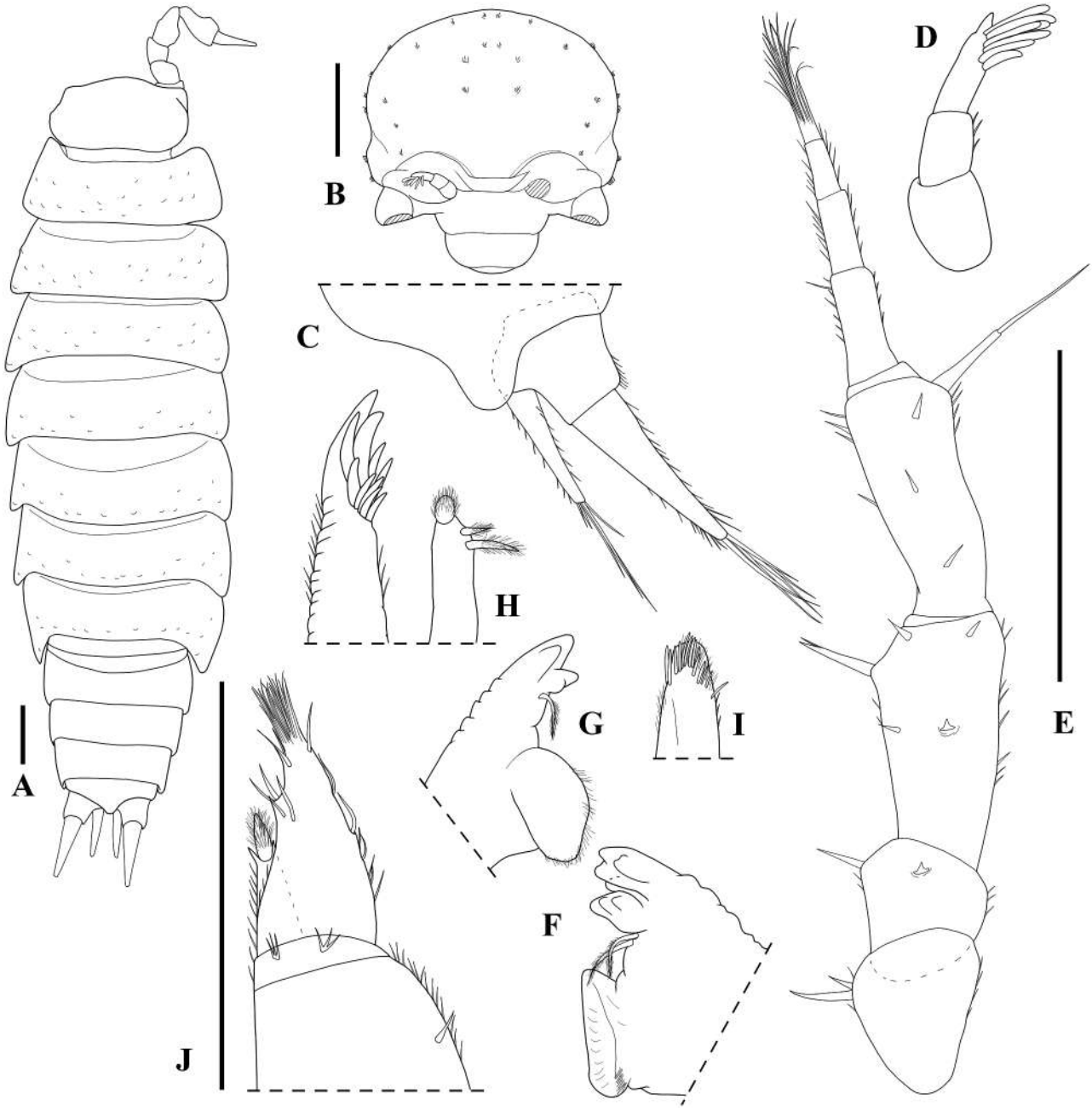


Figure 15. *Pectenoniscus caesarius* n. sp. Male holotype (ISLA 96642): A, habitus, dorsal view; B, cephalon, frontal view; C, telson and uropod, dorsal view; D, antennula; E, antenna; F, left mandible; G, right mandible; H, maxillula; I, maxilla; J, maxilliped. Scale bars: 0.2 mm.

(−10.017393° −40.701007°), 12 January 2013, R.L. Ferreira leg. Paratype: 3 females (ISLA 96643), same data as holotype.

Diagnosis

Male pleopod 1 exopod ovoid, pleopod 2 exopod sub-triangular, endopod apex thickset, with three lobes distally, one round lobe directed inward, one in middle, and another outward.

Description

Maximum length: male, 2.5 mm. Colorless, eyes absent (Figure 15A, 17D). Dorsum (Figure 15A) with tricorn-shaped scale-setae with granulations in five rows on cephalon, in two rows on pereonite 1–6, one row on pereonite 7, pleon smooth. Cephalon with triangular antennal lobes obliquely directed and grooved dorsally; supra-antennal line bent in middle (Figure 15B). Pereonite 1 with margin slightly projected forward;

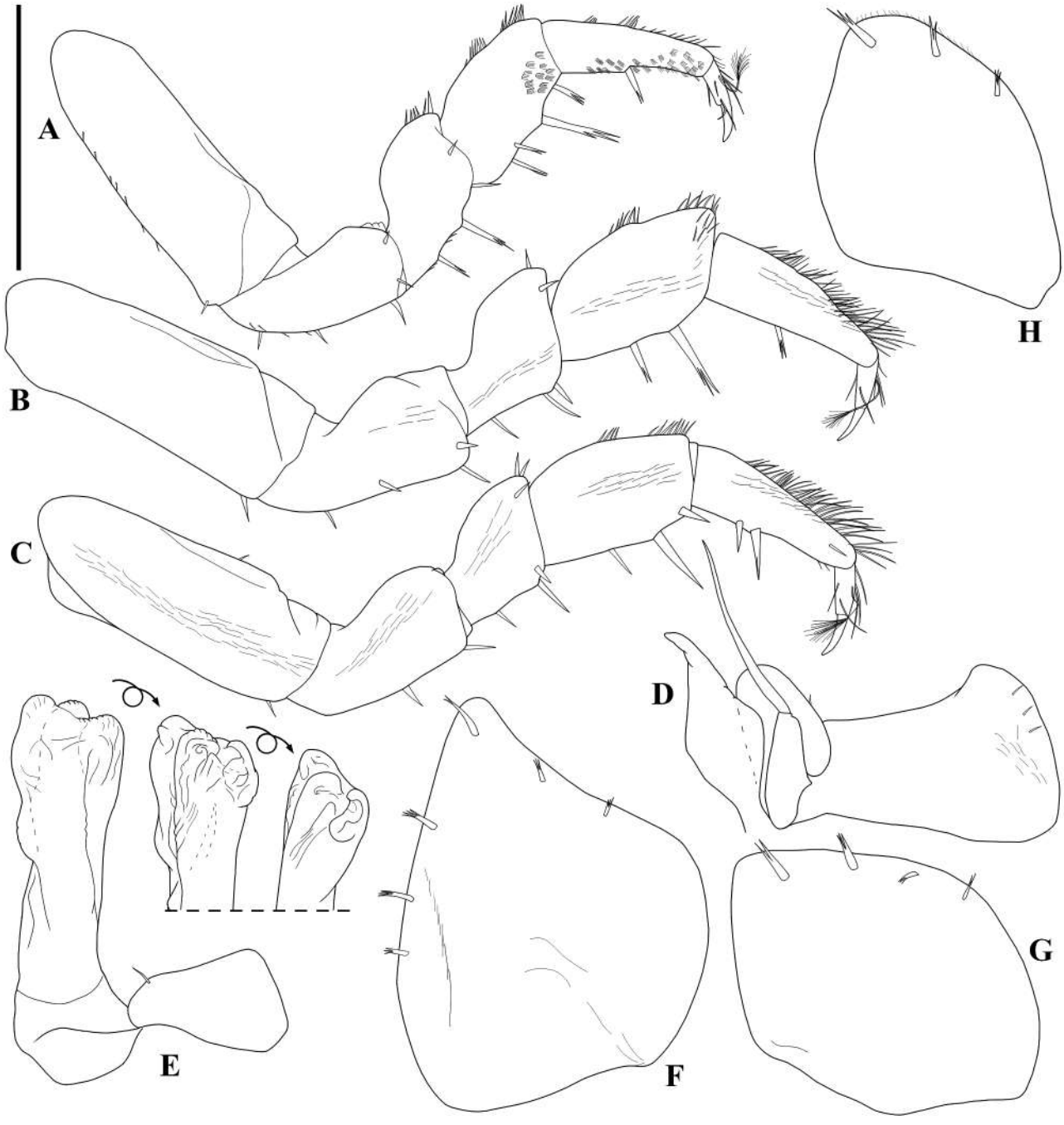


Figure 16. *Pectenoniscus caesarius* n. sp. Male holotype (ISLA 96642): A, pereopod 1; B, pereopod 6; C, pereopod 7; D, pleopod 1; E, pleopod 2; F, pleopod 3 exopod; G, pleopod 4 exopod; H, pleopod 5 exopod. Scale bars: 0.2 mm.

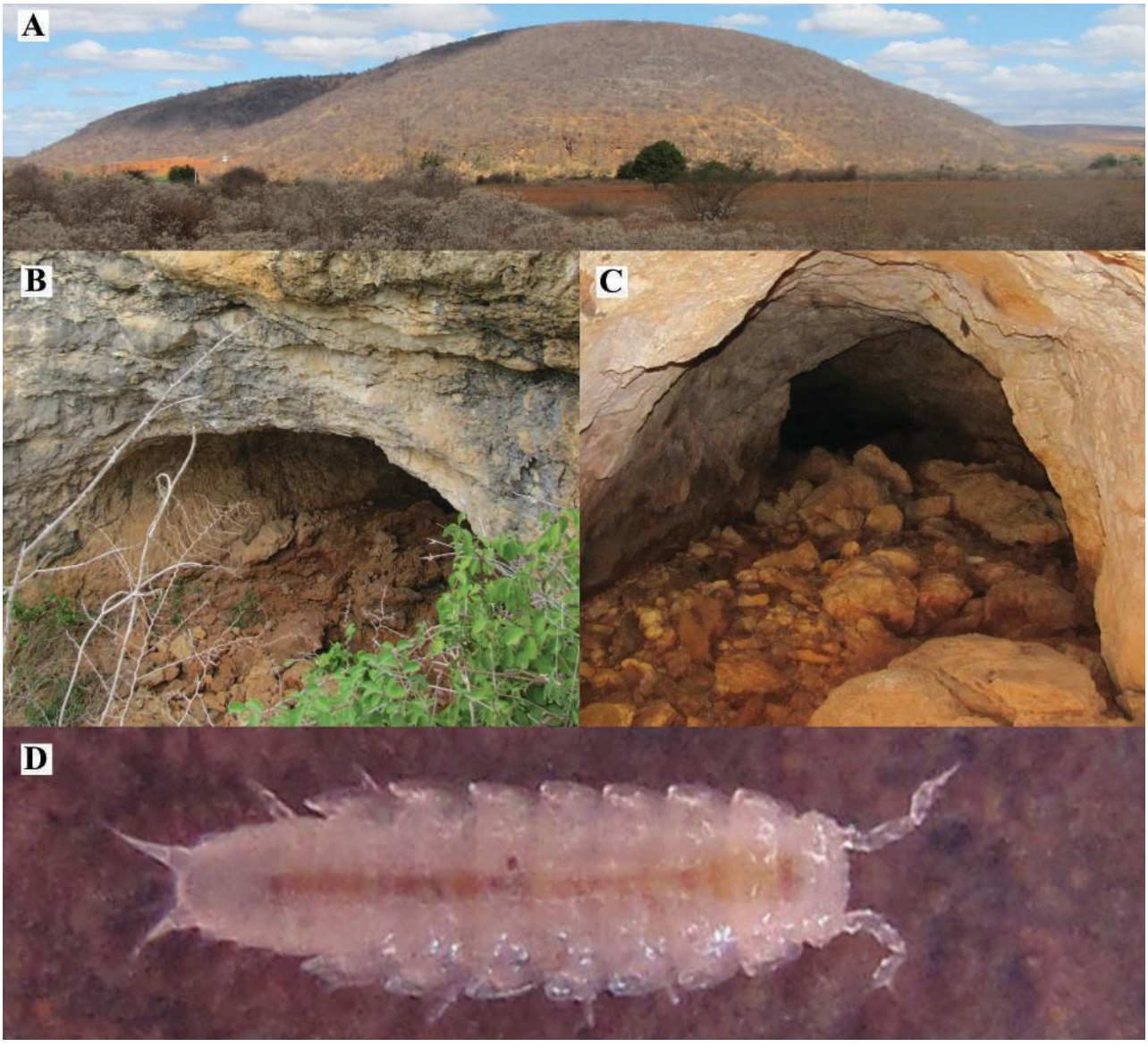


Figure 17. Habitat of *Pectenoniscus caesarius* n. sp. A, external landscape on the Karst area of Campo Formoso municipality; B, Toca do Cesário cave's entrance; C, cave interior; D, living specimen of *P. caesarius* n. sp. inside the cave.

pereonites posterior margin progressively more con- cave; pleonites 3–5 epimera posterior points slightly developed, pleon narrower than pereon (Figure 15A). Telson with concave sides, round apex (Figure 15C). Antennula with three articles, distal article with seven aesthetascs (Figure 15D). Antenna fifth article of ped- uncle as long as flagellum, with one seta longer than first flagellum article; flagellum with four articles (Figure 15E). Buccal pieces as *Pectenoniscus monsvir- idis* n. sp. (Figure 15F–J), except maxillula outer branch with 4 + 6 teeth, apically entire. Pereopod 1 antennal grooming brush composed of serrated scale- setae longitudinally on propodus and on sternal mar- gin of carpus (Figure 16A); dactylar seta bifid with thin setulae. Water conducting system on ischium, merus, carpus and propodus of pereopod 6 and in pereopod 7. Uropod protopod longer than wide, longer than distal margin of telson; exopod longer than endopod, inserted distally (Figure 15C).

Male

Pereopods 6 and 7 (Figure 16B,C) propodus with tufts of setae on tergal margin. Genital papilla (Figure 16D) enlarged on medial portion, apically narrow. Pleopod 1 (Figure 16D) protopod subrectan- gular, wider than long, distal margin sinuous; exo- pod ovoid, longer than wide, apex round; endopod twice longer than exopod. Pleopod 2 (Figure 16E)

exopod sub-triangular, wider than long; endopod with distal article almost four times longer than proximal article, apex thickset, wider than base, with three lobes distally, one round lobe directed inward, one in middle, and another outward. Pleopod 3 exopod (Figure 16F) trapezoidal, convex distal margin; pleopods 4 and 5 exopod as in Figure 16G,H.

Etymology

The epithet '*caesarius*' was given in reference to the name of the cave where the specimens were found (Toca do Cesário cave).

Morphological remarks

By the number of aesthetascs *Pectenoniscus caesarius* n. sp. resembles *P. revelatus* n. sp. By the shape of male pleopod 1 exopod *Pectenoniscus caesarius* n. sp. resem- bles *P. fervens*. However, the species differ from others by the shape of male pleopod 1 endopod.

Ecological remarks

Specimens of *Pectenoniscus caesarius* n. sp. were only observed in the Toca do Cesário cave. This cave pre- sents around 2 km of topographed conduits, being traversed by intermittent drainage. The only entrance comprises the resurgence of this drainage (Figure 17B). Although the drainage is active only during the rainy season in the region, several substrates remain moist along the cave throughout the year. The organic resources are mainly represented by bat guano, espe- cially produced by common vampire bats (*Desmodus rotundus*). Specimens of *Pectenoniscus caesarius* n. sp. were observed far from the entrance, in moist conduits (Figure 17C). They were walking on muddy substrates, which covered the cave walls. The few observed speci- mens were close to small bat guano patches, thus suggesting they could be feeding on this organic resource. However, the digestive tube, observed by transparency, was composed by a brownish content (Figure 17D), suggesting that they can eventually feed on the muddy substrate, which may be rich in microbes or dissolved organic matter. It is important to mention that most parts of the cave were not explored, so that the actual distribution of this species inside the cave remains unknown. Furthermore, many other caves in the area (most of which are dry) were surveyed, but specimens of *P. caesarius* n. sp. were not observed.

Although the cave receives local visitors, most remain close to the entrance. Accordingly, the inner- most portions of the cave are well preserved. The external environment surrounding the cave is extremely dry, since the area is located within the Caatinga domains (Figure 17A). Furthermore, the cave surroundings are altered, presenting settle- ments, unpaved roads and monocultures.

Discussion

Although studies on Brazilian cave fauna have been established since the 1980s, they mainly consisted of species surveys, especially concerning invertebrates (Pinto-da-Rocha 1995). However, from the 2000s onwards, studies on Brazilian subterranean fauna have intensified, many of which address aspects related to the ecology of subterranean populations or commu- nities (e.g. Ferreira et al. 2007; Souza-Silva et al. 2011). Throughout this period, cave species were described, but quite sporadically.

The Brazilian rules regarding the protection of the national speleological heritage are historically governed by decrees, with no laws imposing formal protection for caves. In 1990, the decree no. 99,556 gave full protection to caves in the country. However, in prac- tice, there was an unrestricted (and uncontrolled) destruction of caves throughout the country, especially due to the lack of adequate surveillance. In 2008, a new decree (no. 6640) allowed the destruction of caves in Brazil, but established that the caves needed to be analyzed under different criteria (e.g. geological, biological, and historical) to determine the level of relevance. Only the caves considered to be of maximum relevance were fully protected. From this decree onwards, speleological studies in the country intensified, and not only several previously unexplored areas started to be sampled, but also several new spe- cies started to be described, especially due to the need for this knowledge for decision makers.

As many unexplored or poorly prospected areas began to be studied, the number of species discovered and described increased substantially. As an example, 73% of the cave-restricted species in the country were described from 2009 onwards.

Among the groups commonly found in caves, isopods are quite diverse and present several species preadapted to subterranean environments. Thus, even with the growing number of publications describing new cave isopods in Brazil, there is still a huge number of species deposited in collections awaiting formal description as well as an even greater number of species awaiting discovery.

However, it is important to highlight the increasing threats to the Brazilian speleological heritage, especially in recent years. Recent changes in decrees regarding cave protection are exposing the subterranean habitats in the country to an unprecedented threat (Ferreira et al. 2022).

Thus, although little is known about the actual distribution and population densities of these new species herein described, it is likely that they may eventually be already threatened, and emergency protective measures need to be taken to ensure that these species do not become extinct in the near future.

Acknowledgments

The authors would like to thank the Centro Nacional de Pesquisa e Conservação de Cavernas – CECAV and Instituto Brasileiro de Desenvolvimento e Sustentabilidade – IABS for the financial support and scholarship provided to GMC; CNPq (National Council for Scientific and Technological Development) for the productivity scholarship provided to RLF; and the team from the Center of Studies in Subterranean Biology (CEBS/UFLA) for the support in the field trips.

Disclosure statement

Field collection and transportation of specimens were made under the SISBIO permit number 78,415-3/2021 issued to RLF.

Funding

This work was supported by Centro Nacional de Pesquisa e Conservação de Cavernas – CECAV and Instituto Brasileiro de Desenvolvimento e Sustentabilidade – IABS [grant no. 006/2021. TCCE ICMBio/Vale 01/2018]; and by CNPq (National Council for Scientific and Technological Development, productivity scholarship CNPq [grant no. 302925/2022-8 to RLF].

ORCID

Giovanna Monticelli Cardoso http://orcid.org/0000- 0003-2682-1643
Rodrigo Lopes Ferreira http://orcid.org/0000-0003-3288- 4405

References

Alvares CA, Stape JL, Sentelhas PC, de Moraes Gonçalves JL, Sparovek G. 2013. Köppen's climate classification map for Brazil. Meteorol Z. 22(6):711–728.
Andersson Å. 1960. South American terrestrial isopods in the collection of the Swedish State Museum of Natural History. Arkiv För Zoologi. 12:537–570.
Campos-Filho IS, Araujo PB, Bichuette ME, Trajano E, Taiti S. 2014. Terrestrial isopods (Crustacea: Isopoda:

Oniscidea) from Brazilian caves. Zool J Linn Soc 172:360–425. doi:10.1111/zoj.12172
Campos-Filho IS, Bichuette ME, Araujo PB, Taiti S. 2017. Description of a new species of *Cylindroniscus* Arcangeli, 1929 (Isopoda: Oniscidea) from Brazil, with considerations on the family placement of the genus. North-West J Zool. 13:e161305. Available from: https:// biozoojournals.ro/nwjz/content/v13n2/nwjz_e161305_ Campos.pdf
Campos-Filho IS, Fernandes CS, Cardoso GM, Bichuette ME, Aguiar JO, Taiti S. 2019. Two new species and new records of terrestrial isopods (Crustacea, Isopoda, Oniscidea) from Brazilian caves. Zootaxa. 4564:422–448. doi:10.11646/zootaxa.4564.2.6
Campos-Filho IS, Gallo JS, Gallão JE, Torres DF, Carpio- Díaz YM, López-Orozco CM, Borja-Arrieta R, Taiti S, Bichuette ME. 2022. Expanding the knowledge on the diversity of the cavernicolous Styloniscidae Vandel, 1952 (Oniscidea, Synocheta) from Brazil, with descriptions of two new species from the semiarid karst regions. ZooKeys. 1101:35–55. doi:10.3897/zookeys.1101.79043
Cardoso GM, Bastos-Pereira R, Souza LA, Ferreira RL. 2020. New cave species of *Pectenoniscus* Andersson, 1960 (Isopoda: Oniscidea: Styloniscidae) and an identification key for the genus. Nauplius. 28:e2020039. doi:10.1590/2358-2936e2020039
Cardoso GM, Bastos-Pereira R, Souza LA, Ferreira RL. 2021. *Chaimowiczia*: a new Iuiuniscinae genus from Brazil (Oniscidea, Synocheta, Styloniscidae) with the description of two new troglobitic species. Subterr Biol. 39:45–62. doi:10.3897/subtbiol.39.65305
Cole MM. 1960. Cerrado, Caatinga and Pantanal: the distribution and origin of the Savanna Vegetation of Brazil. Geog J. 126:168–179. doi:10.2307/1793957
Ferreira RL, Bernard E, da Cruz Júnior FW, Piló LB, Calux A, Souza-Silva M, Barlow J, Pompeu PS, Cardoso P, Mammola S, et al. 2022. Brazilian cave heritage under siege. Science. 375(6586):1238–1239.
Ferreira RL, Prous X, Martins RP. 2007. Structure of bat guano communities in a dry Brazilian cave. Tropical Zoology. 20(1):55–74.
Montesanto G. 2015. A fast GNU method to draw accurate scientific illustrations for taxonomy. ZooKeys. 515:191–206. doi:10.3897/zookeys.515.9459
Montesanto G. 2016. Drawing setae: a GNU way for digital scientific illustrations. Nauplius 24:e2016017. doi:10.1590/ 2358-2936e2016017
Pinto-da-Rocha R. 1995. Sinopse da fauna cavernícola do Brasil (1907-1994). Papéis avulsos de Zoologia. 39 (6):61–173.
Souza-Silva M, Martins RP, Ferreira RL. 2011. Trophic dynamics in a neotropical limestone cave. Subterr Biol. 9:127–138. doi:10.3897/subtbiol.9.2515

zoosystema

2024 • 46 • 5

Unveiling a hidden diversity: descriptions of nine new species of *Ctenorillo* Verhoeff, 1942 (Isopoda, Armadillidae) discovered in Brazilian caves and their importance for conservation

Giovanna Monticelli CARDOSO,
Diego Medeiros BENTO & Rodrigo Lopes FERREIRA



art. 46 (5) — Published on 5 March 2024
www.zoosystema.com

PUBLICATIONS SCIENTIFIQUES

MUSÉUM NAL HIST NATURELLE

DIRECTEUR DE LA PUBLICATION / *PUBLICATION DIRECTOR* : Gilles Bloch
Président du Muséum national d'Histoire naturelle

RÉDACTRICE EN CHEF / *EDITOR-IN-CHIEF* : Laure Desutter-Grandcolas ASSISTANTE

DE RÉDACTION / *ASSISTANT EDITOR* : Anne Mabille (zoosyst@mnhn.fr) MISE EN PAGE

/ *PAGE LAYOUT* : Anne Mabille

COMITÉ SCIENTIFIQUE / *SCIENTIFIC BOARD* :

Nesrine Akkari (Naturhistorisches Museum, Vienne, Autriche)
Maria Marta Cigliano (Museo de La Plata, La Plata, Argentine)
Serge Gofas (Universidad de Málaga, Málaga, Espagne)
Sylvain Hugel (CNRS, Université de Strasbourg, France) Marco
Isaia (Università degli Studi di Torino, Turin, Italie) Rafael
Marquez (CSIC, Madrid, Espagne)
Jose Christopher E. Mendoza (Lee Kong Chian Natural History Museum, Singapour) Annemarie
Ohler (MNHN, Paris, France)
Jean-Yves Rasplus (INRA, Montferrier-sur-Lez, France)
Wanda M. Weiner (Polish Academy of Sciences, Cracovie, Pologne)

COUVERTURE / *COVER* :
Habitus of the species of the genus *Ctenorillo* Verhoeff, 1942 discussed in the present paper.

Zoosystema est indexé dans / Zoosystema *is indexed in:*
Science Citation Index Expanded (SciSearch®)
ISI Alerting Services®
Current Contents® / Agriculture, Biology, and Environmental Sciences®
Scopus®

Zoosystema est distribué en version électronique par / Zoosystema *is distributed electronically by:*
BioOne® (http://www.bioone.org)

Les articles ainsi que les nouveautés nomenclaturales publiés dans *Zoosystema* sont référencés par / *Articles and nomenclatural novelties published in* Zoosystema *are referenced by:*
ZooBank® (http://zoobank.org)

Zoosystema est une revue en flux continu publiée par les Publications scientifiques du Muséum, Paris / **Zoosystema** *is a fast track journal published by the Museum Science Press, Paris*

Les Publications scientifiques du Muséum publient aussi / *The Museum Science Press also publish:*
Adansonia, ***Geodiversitas***, ***Anthropozoologica***, ***European Journal of Taxonomy***, ***Naturae***, ***Cryptogamie*** **sous-sections** ***Algologie***, ***Bryologie***, ***Mycologie***, ***Comptes Rendus Palevol***.

Diffusion – Publications scientifiques Muséum national d'Histoire naturelle
CP 41 – 57 rue Cuvier F-75231 Paris cedex 05 (France)
Tél. : 33 (0)1 40 79 48 05 / Fax : 33 (0)1 40 79 38 40
diff.pub@mnhn.fr / https://sciencepress.mnhn.fr

© Publications scientifiques du Muséum national d'Histoire naturelle, Paris, 2024 ISSN (imprimé / *print*) : 1280-9551/ ISSN (électronique / *electronic*) : 1638-9387

Unveiling a hidden diversity: descriptions of nine new species of *Ctenorillo* Verhoeff, 1942 (Isopoda, Armadillidae) discovered in Brazilian caves and their importance for conservation

Giovanna Monticelli CARDOSO Universidade Federal de Lavras (UFLA), Centro de Estudos em Biologia Subterrânea, Departamento de Biologia, programa de Pós-graduação em Ecologia Aplicada, Campus Universitário, CP 3037, 37200-000 Lavras, Minas Gerais (Brasil)
gmcardoso.bio@gmail.com (corresponding author)

Diego de Medeiros BENTO Instituto Chico Mendes de Conservação da Biodiversidade (ICMBio), Centro Nacional de Pesquisa e Conservação de Cavernas (CECAV),
Base Avançada no Rio Grande do Norte, avenida Alexandrino de Alencar 1399, Tirol, Natal, Rio Grande do Norte (Brasil)
diego.bento@icmbio.gov.br.

Rodrigo Lopes FERREIRA Universidade Federal de Lavras (UFLA), Centro de Estudos em Biologia Subterrânea, Departamento de Biologia, programa de Pós-graduação em Ecologia Aplicada, Campus Universitário, CP 3037, 37200-000 Lavras, Minas Gerais (Brasil)
drops@ufla.br

Submitted on 28 April 2023 | Accepted on 25 October 2023 | Published on 5 March 2024

urn:lsid:zoobank.org:pub:1B0779F3-FAE4-4105-8130-A26DE519721E

Cardoso G. M., Bento D. de M. & Ferreira R. L. 2024. — Unveiling a hidden diversity: descriptions of nine new species of *Ctenorillo* Verhoeff, 1942 (Isopoda, Armadillidae) discovered in Brazilian caves and their importance for conservation. *Zoosystema* 46 (5): 95-132. https://doi.org/10.5252/zoosystema2024v46a5. http://zoosystema.com/46/5

ABSTRACT
Nine species of *Ctenorillo* Verhoeff, 1942 are described from Brazil, revealing a great diversity of the genus in South America. *Ctenorillo pelado* Cardoso & Ferreira, n. sp., and *C. araguaia* Cardoso & Ferreira, n. sp. are described, and *C. ferrarai* Campos-Filho, Araujo & Taiti, 2014 has the knowledge of its distribution expanded from the state of Pará (north of Brazil); *Ctenorillo intertidalis* Cardoso & Ferreira n. sp., *C. ubajarensis* Cardoso & Ferreira, n. sp., *C. cearensis* Cardoso & Ferreira, n. sp. and *C. quiteriensis* Cardoso & Ferreira, n. sp. are described from the state of Ceará (northeast Brazil); *C. potiguar* Cardoso & Ferreira, n. sp. from the state of Rio Grande do Norte (northeast Brazil); *C. iuiuensis* Cardoso & Ferreira, n. sp. from the state of Bahia (northeast Brazil); and *C. jequitinhonha* Cardoso & Ferreira, n. sp. from the state of Minas Gerais (southeast Brazil). Most of the newly iden- tified species are found in protected conservation areas and are therefore legally protected. However, special attention should be paid to *C. iuiuensis* Cardoso & Ferreira, n. sp., a troglobitic species, due to its distinctive ecological features and its habitat being limited to a single cave, which is currently not protected.

KEY WORDS
Woodlice, terrestrial isopods, cave species, Brazil, Neotropics, troglobitic, new species.

RÉSUMÉ

Une diversité cachée dévoilée : description de neuf nouvelles espèces de Ctenorillo *Verhoeff, 1942 (Isopoda, Armadillidae) découvertes dans des grottes brésiliennes et leur importance pour la conservation.*

Neuf espèces de *Ctenorillo* Verhoeff, 1942 sont décrites du Brésil, révélant une grande diversité du genre en Amérique du Sud. *Ctenorillo pelado* Cardoso & Ferreira, n. sp. et *C. araguaia* Cardoso & Ferreira, n. sp. sont décrites, et *C. ferrarai* Campos-Filho, Araujo & Taiti, 2014 voit la connaissance de sa distribution étendue à l'État de Pará (nord du Brésil) ; *Ctenorillo intertidalis* Cardoso & Ferreira, n. sp., *C. ubajarensis* Cardoso & Ferreira, n. sp., *C. cearensis* Cardoso & Ferreira n. sp. et *C. quiter- iensis* Cardoso & Ferreira, n. sp. sont décrites dans l'État de Ceará (nord-est du Brésil) ; *C. potiguar* Cardoso & Ferreira, n. sp. dans l'État de Rio Grande do Norte (nord-est du Brésil) ; *C. iuiuensis* Cardoso & Ferreira, n. sp. dans l'État de Bahia (nord-est du Brésil) ; et *C. jequitinhonha* Cardoso & Ferreira, n. sp. dans l'État de Minas Gerais (sud-est du Brésil). La plupart des espèces nouvellement identifiées se trouvent dans des zones de conservation protégées et sont donc légalement protégées. Toutefois, une attention particulière devrait être accordée à *C. iuiuensis* Cardoso & Ferreira, n. sp., une espèce troglobie, en raison de ses caractéristiques écologiques originales et de son habitat limité à une seule grotte, qui n'est pas protégée à l'heure actuelle.

MOTS CLÉS

Cloporte, isopodes terrestres, espèces cavernicoles, Brésil, néotropiques, troglobie, espèces nouvelles.

BACKGROUND

The genus *Ctenorillo* Verhoeff, 1942 is distributed across Africa and South America (Taiti *et al.* 1998; Schmalfuss 2003; Boyko *et al.* 2008; Campos-Filho *et al.* 2014, 2017; Cifuentes & Da Silva 2023; Carpio-Díaz *et al.* 2023). In Brazil, three species are known: *C. mineri* (Van Name, 1936) from Brazil, Guyana and Venezuela; *C. ferrarai* Campos-Filho, Araujo & Taiti, 2014 from Brazil; and *C. tuberosus* (Budde-Lund, 1904) from Brazil, Haiti and Germany (introduced) (Campos-Filho *et al.* 2018).

Ctenorillo is distinguished by its diminutive size and strongly convex body shape, endoantennal conglobation and dorsal surface featuring more or less developed ribs and/or tubercles; cephalon with a subquadrangular frontal shield, and the pereonite 1 epimera with a schisma; pereonites 1 and 2 with ventral lobes, the latter bearing a triangular lobe; telson with hour-glass shape; antenna with two articles on flagellum, with the distal article longer than the proximal one; subquadran- gular uropod with flattened protopod, with a concave medial margin and a tiny exopod inserted near the medial margin; and pleopod 1-5 exopods with monospiracular-covered lungs (Carpio-Díaz *et al.* 2018). As previously noted by Schmalfuss & Ferrara (1983), Campos-Filho *et al.* (2014, 2017) and Taiti (2018), species of *Ctenorillo* are often similar and can be distinguished by the shape, number, and disposition of dorsal tubercles.

This manuscript presents the taxonomic descriptions of nine newly discovered species (Figs 1-27), expanding the known diversity of the genus and its distribution within the Neotropical Region. Of these newly described species, two were found in Northern Brazil (Pará state), six in northeastern Brazil (Ceará, Rio Grande do Norte and Bahia states), and one in southeastern Brazil (Minas Gerais state). A notable finding is the discovery of the first troglobitic species within the genus, which was found in a cave located in Iuiu municipality, Bahia state. Additionally, this manuscript provides new occurrences of *C. ferrarai* and offers notes on the habitats along with a discussion on the conservation status of each new species herein described.

MATERIAL AND METHODS

Specimens were collected using brushes and fixed in 70% ethanol. In the Center of Studies on Subterranean Biology at the Federal University of Lavras (CEBS/UFLA), located in Lavras, Brazil, the specimens were measured and photographed with a ZEISS Axio ZoomV16 stereomicroscope equipped with an Axio Cam 506 Color camera. After dissection, they were mounted on slides using Hoyer's medium. Drawings were produced through a combination of photographic and dissected specimens with the aid of a camera lucida fitted to a Leica DM750 microscope. Final illustrations were created in GIMP software (v. 2.8) (Montesanto 2015, 2016) using a Wacom Cintiq drawing tablet. A subset of specimens (from some species) were investigated further using a Hitachi TM4000 scanning electron microscope. The utilization of low vacuum imaging technology allowed the examination of non-conductive samples without the need for a metal coating. All material is deposited in the Collection of Subterranean Invertebrates of Lavras (ISLA), some were collected by consulting companies that collects the material to evaluate the significance of caves, as mandated by Brazilian environmental agencies in their review of potentially environmentally impactful projects. The holotype and paratypes are deposited at ISLA. In this study, we have employed the cave fauna classification system proposed by Sket (2008).

ABBREVIATION

ISLA Collection of Subterranean Invertebrates of Lavras (ISLA), at the Ecology and Conservation Department of the Federal University of Lavras, Lavras, Minas Gerais, Brazil.

SYSTEMATIC ACCOUNT

Family Armadillidae Brandt, 1831 Genus *Ctenorillo* Verhoeff, 1942

Ctenorillo ferrarai Campos-Filho, Araujo & Taiti, 2014 (Figs 1; 27A)

Ctenorillo ferrarai Campos-Filho, Araujo & Taiti *in* Campos-Filho *et al.*, 2014: 412, figs 37-40. — Campos-Filho *et al.* 2017: 20; 2018: 27. — Fernandes *et al.* 2019: 1119, table 1.

nec *Ctenorillo ferrarai* – Campos-Filho *et al.* 2023: 560, figs 22, 23.

Material examined. — **Brazil.** Pará state, Parauapebas municipality, Serra Norte plateau • 1 ♀; N1_0002 cave; GEM_578; 6°0’14”S, 50°17’56”W; 24.II-13.III.2015; ISLA 30422 • 1 ♀; N1_0002 cave; GEM_805; 11.VI-2.VII.2014; ISLA 30636 • 1 ♂; N1_0002 cave; GEM_818; 11.VI-2.VII.2014; ISLA 30644 • 1 ♂; N1_0004 cave; GEM_812; 6°0’48”S, 50°18’24”W; 17.VII-4.VIII.2014; ISLA 30638 • 2 ♀; N1_0004 cave; GEM_817; 11.VI-2.VII.2014; ISLA 30643 • 1 ♀; N1_0004 cave; GEM_824; 17.VII-4.VIII.2014; ISLA 30649 • 1 ♀; N1_0004 cave; GEM_1032; 7-28.I.2015; ISLA 30840 • 1 ♂; N1_0004 cave; GEM_1049; 7-28.I.2015; ISLA 30857 • 2 ♀; N1_0005 cave; GEM_589; 6°0’44”S, 50°18’52”W; 24.II-13.III.2015; ISLA 30432 • 4 ♀; N1_0007 cave; GEM_555; 6°6’30”S, 50°8’0”W; 2-29.IV.2015; ISLA 30399 • 1 ♀; N1_0007 cave; GEM_820; 11.VI-2.VII.2014; ISLA 30646 • 1 ♀; N1_0009 cave; GEM_558; 6°0’40”S, 50°18’51”W; 24.II-13.III.2015; ISLA 30402 • 1 ♀; N1_0009 cave; GEM_591; 24.II-13.III.2015; ISLA 30434 • 1 ♂; N1_0012 cave; GEM_588; 6°6’23”S, 50°8’7”W; 24.II-13.III.2015; ISLA 30431 • 1 ♀; N1_0013 cave; GEM_1027; 6°6’23”S, 50°8’7”W; 7-28.I.2015; ISLA 30835 • 1 juv.; N1_0030 cave; GEM_551; 6°2’4”S, 50°16’19”W; 24.II-13.III.2015; ISLA 30395 • 1 ♀; N1_0033 cave; GEM_514; 6°1’9”S, 50°16’46”W; 24.II-13.III.2015; ISLA 30388 • 1 ♂; N1_0044 cave; GEM_915; 6°2’3”S, 50°16’16”W; 4.IX-6.X.2014; ISLA 30735 • 1 ♂; N1_0050 cave; GEM_911; 6°1’37”S, 50°17’28”W; 4.IX-6.X.2014; ISLA 30731 • 1 ♀; N1_0056 cave; GEM_1030; 6°2’33”S, 50°16’27”W; 7-28.I.2015; ISLA 30838 • 1 ♀; N1_0056 cave; GEM_1045; 7-28.I.2015; ISLA 30853 • 1 ♀; N1_0060 cave; GEM_816; 6°2’32”S, 50°16’28”W; 4.IX-6.X.2014; ISLA 30742 • 1 ♀; N1_0060 cave; GEM_1005; 7-28.I.2015; ISLA 30813 • 1 juv.; N1_0062 cave; GEM_559; 6°2’39”S, 50°16’24”W; 2-29.IV.2015; ISLA 30403 • 1 ♂, 1 ♀; N1_0062 cave; GEM_919; 4.IX-6.X.2014; ISLA 30739 • 1 ♀; N1_0063 cave; GEM_547; 6°7’41”S, 50°8’5”W; 24.II-13.III.2015; ISLA 30391 • 1 ♀; N1_0063 cave; GEM_550; 24.II-13.III.2015; ISLA 30394 • 1 ♂; N1_0063 cave; GEM_584; 24.II-13.III.2015; ISLA 30428 • 1 juv.; N1_0064 cave; GEM_537; 6°7’42”S, 50°8’7”W; 24.II-13.III.2015; ISLA 30381 • 1 ♂; N1_0067 cave; GEM_564; 6°1’17”S, 50°18’5”W; 2-29.IV.2015; ISLA 30408 1 ♀; N1_0074 cave; GEM_789; 6°1’24”S, 50°17’59”W; 11.VI-2.VII.2014; ISLA 30620 • 2 ♀; N1_0074 cave; GEM_833; 11.VI-2.VII.2014; ISLA 30658 • 1 ♂, 1 ♀; N1_0078 cave; GEM_548; 6°7’23”S, 50°7’48”W; 24.II-13.III.2015; ISLA 30392 • 1 ♀; N1_0092 cave; GEM_570; 6°1’28”S, 50°17’56”W; 2-29.IV.2015; ISLA 30414 1 ♀; N1_0096 cave; GEM_569; 6°1’28”S, 50°17’55”W; 2-29.IV.2015; ISLA 30413 • 1 ♂, 1 ♀; N1_0096 cave; GEM_1033; 7-28.I.2015; ISLA 30841 • 2 ♀; N1_0103 cave; GEM_774; 6°1’29”S, 50°17’54”W; 11.VI-2.VII.2014; ISLA 30605 • 1 ♀; N1_0106 cave; GEM_790; 6°2’36”S, 50°16’34”W; 11.VI-2.VII.2014; ISLA 30621 2 ♀; N1_0106 cave; GEM_1019; 7-28.I.2015; ISLA 30827 • 1 ♀; N1_0108 cave; GEM_778; 6°2’25”S, 50°16’13”W; 17.VII-4.VIII.2014; ISLA 30609 • 1 ♂; N1_0108 cave; GEM_796; 17.VII-4.VIII.2014; ISLA 30627 • 1 ♀; N1_0108 cave; GEM_1018; 7-28.I.2015; ISLA 30826 • 2 ♀; N1_0113 cave; GEM_562; 6°2’24”S, 50°17’38”W; 2-29.IV.2015; ISLA 30407 • 1 ♀; N1_0116 cave; GEM_823; 6°2’14”S, 50°16’1”W; 11.VI-2.VII.2014; ISLA 30648 1 ♀; N1_0116 cave; GEM_1035; 7-28.I.2015; ISLA 30843 • 1 ♀; N1_0117 cave; GEM_1013; 6°1’22”S, 50°18’45”W; 7-28.I.2015; ISLA 30821 • 1 ♀; N1_0119 cave; GEM_592; 6°1’15”S, 50°18’6”W; 2-29.IV.2015; ISLA 30435 • 1 ♂, 2 juv.; N1_0123 cave; GEM_566; 6°1’9”S, 50°16’46”W; 24.II-13.III.2015; ISLA 30410 • 2 ♀; N1_0142 cave; GEM_543; 6°1’37”S, 50°17’29”W; 2-29.IV.2015; ISLA 30387 1 ♀; N1_0148 cave; GEM_581; 6°1’20”S, 50°16’27”W; 2-29.IV.2015; ISLA 30425 • 1 ♂; N1_0150 cave; GEM_527; 6°0’25”S, 50°18’17”W; 24.II-13.III.2015; ISLA 30380 • 1 ♀; N1_0158 cave; GEM_787; 6°0’31”S, 50°18’7”W; 11.VI-2.VII.2014; ISLA 30618 2 ♀; N1_0166 cave; GEM_795; 6°1’47”S, 50°16’24”W; 17.VII-4.VIII.2014; ISLA 30626 • 3 ♀; N1_0166 cave; GEM_1037; 3-17.XII.2014; ISLA 30845 • 1 ♂; N1_0167 cave; GEM_1050; 6°1’51”S, 50°16’29”W; 3-17.XII.2014; ISLA 30858 • 1 ♂; N1_0168 cave; GEM_819; 6°2’24”S, 50°16’13”W; 17.VII-4.VIII.2014; ISLA 30645 • 1 ♀; N1_0168 cave; GEM_840; 17.VII-4.VIII.2014; ISLA 30665 • 1 ♀; N1_0168 cave; GEM_1029; 3-17.XII.2014; ISLA 30837 • 1 ♂; N1_0169 cave; GEM_837; 6°1’24”S, 50°17’59”W; 17.VII-4.VIII.2014; ISLA 30662 • 1 ♀; N1_0170 cave; GEM_1034; 6°1’14”S, 50°16’42”W; 3-17.XII.2014; ISLA 30842 • 1 ♂, 1 ♀; N1_0172 cave; GEM_1023; 6°2’24”S, 50°16’12”W; 7-28.I.2015; ISLA 30831 • 1 ♂; N1_0173 cave; GEM_777; 6°1’28”S, 50°17’56”W; 17.VII-4.VIII.2014; ISLA 30608 • 1 ♀; N1_0174 cave; GEM_776; 6°1’12”S, 50°16’45”W; 17.VII-4.VIII.2014; ISLA 30607 • 1 ♂, 1 ♀; N1_0174 cave; GEM_781; 17.VII-4.VIII.2014; ISLA 30612 3 ♀; N1_0174 cave; GEM_782; 17.VII-4.VIII.2014; ISLA 30613 2 juv.; N1_0174 cave; GEM_784; 17.VII-4.VIII.2014; ISLA 30615 • 1 ♂, 1 ♀; N1_0174 cave; GEM_785; 17.VII-4.VIII.2014; ISLA 30616 • 2 ♂; N1_0174 cave; GEM_786; 17.VII-4.VIII.2014; ISLA 30617 • 1 ♀; N1_0174 cave; GEM_791; 17.VII-4.VIII.2014; ISLA 30622 • 1 ♂, 2 ♀; N1_0174 cave; GEM_793; 17.VII-4.VIII.2014; ISLA 30624 • 2 ♀; N1_0174 cave; GEM_800; 17.VII-4.VIII.2014; ISLA 30631 • 4 ♂; N1_0174 cave; GEM_801; 17.VII-4.VIII.2014; ISLA 30632 • 1 ♂, 1 ♀; N1_0174 cave; GEM_803; 17.VII-4.VIII.2014; ISLA 30634 • 1 ♀; N1_0174 cave; GEM_829; 17.VII-4.VIII.2014; ISLA 30654 • 1 ♂; N1_0174 cave; GEM_830; 17.VII-4.VIII.2014; ISLA 30656 • 1 juv.; N1_0174 cave; GEM_834; 17.VII-4.VIII.2014; ISLA 30659 • 1 ♂; N1_0174 cave; GEM_834; 17.VII-4.VIII.2014; ISLA 30660 • 1 juv.; N1_0174 cave; GEM_834; 17.VII-4.VIII.2014; ISLA 30661 • 1 ♂, 1 ♀; N1_0174 cave; GEM_841; 17.VII-4.VIII.2014; ISLA 30666 • 1 ♀; N1_0174 cave; GEM_842; 17.VII-4.VIII.2014; ISLA 30667 • 1 ♂; N1_0174 cave; GEM_1022; 17.VII-4.VIII.2014; ISLA 30830 • 1 ♂; N1_0174 cave; GEM_1026; 17.VII-4.VIII.2014; ISLA 30834 • 1 ♂, 1 ♀ ; N1_0174 cave; GEM_1028; 17.VII-4.VIII.2014; ISLA 30836 • 2 ♂; N1_0174 cave; GEM_1040; 7-28.I.2015; ISLA 30848 • 2 ♂; N1_0174 cave; GEM_1041; 7-28.I.2015; ISLA 30849 • 2 ♂; N1_0174 cave; GEM_1042; 7-28.I.2015; ISLA 30850 • 1 ♀; N1_0174 cave; GEM_1043; 7-28.I.2015; ISLA 30851 • 1 ♀; N1_0174 cave; GEM_1046; 7-28.I.2015; ISLA 30854 • 2 ♂, 2 ♀; N1_0174 cave; GEM_1047; 7-28.I.2015; ISLA 30855 • 1 ♀; N1_0174 cave; GEM_1048; 7-28.I.2015; ISLA 30856 • 1 ♀; N1_0174 cave; GEM_1051; 7-28.I.2015; ISLA 30859 • 1 ♂, 1 ♀; N1_0174 cave; 17-14.VIII.2014; ISLA 37900 • 1 juv.; N1_0175 cave; GEM_828; 6°1’13”S, 50°16’42”W; 17.VII-4.VIII.2014; ISLA 30653 • 2 ♀; N1_0185 cave; GEM_1036; 6°1’10”S, 50°16’45”W; 7-28.I.2015; ISLA 30844 • 1 ♀; N1_0200 cave; GEM_587; 6°1’8”S, 50°16’46”W; 2-29.IV.2015; ISLA 30430 • 1 ♂ ; N1_0227 cave; GEM_565; 6°2’14”S, 50°16’1”W; 2-29.IV.2015; ISLA 30409 • 1 ♂; N1_0229 cave; GEM_930; 6°1’43”S, 50°17’21”W; 4.IX-6.X.2014; ISLA 30750 • 1 ♀; N1_0231 cave; GEM_811; 6°2’23”S, 50°16’13”W; 11.VI-2.VII.2014; ISLA 30637 • 1 ♀; N1_0235 cave; GEM_571; 6°1’17”S, 50°16’50”W; 2-29.IV.2015; ISLA 30415 • 1 ♀; N1_0236 cave; GEM_1031; 6°1’16”S, 50°16’53”W; 3-17.XII.2014; ISLA 30839 • 1 ♀; N1_0236 cave; GEM_1044; 3-17.XII.2014; ISLA 30852 • 1 ♀; N1_0239 cave; GEM_788; 6°2’21”S, 50°16’14”W; 11.VI-2.VII.2014; ISLA 30619 • 1 ♀; N1_0244 cave;

GEM_783; 6°0’43”S, 50°18’15”W; 11.VI-2.VII.2014; ISLA 30614 1 ♂; N1_0246 cave; GEM_557; 6°1’10”S, 50°16’59”W; 2-29.IV.2015; ISLA 30401 • 1 ♀; N1_0246 cave; GEM_557; 2-29.IV.2015; ISLA 30433 • 1 ♂; N1_0246 cave; GEM_792; 11.VI-2.VII.2014; ISLA 30623 • 1 ♂; N1_0246 cave; GEM_838; 11.VI-2.VII.2014; ISLA 30663 • 2 ♀; N5S_0002 cave; 6°5’33”S, 50°7’32”W; 10-17.IV.2017; ISLA 95925 • 1 juv.; N5S_0023 cave; 6°5’30”S, 50°7’34”W; 10-17.IV.2016; ISLA 95921 • 3 ♀; N5S_0072 cave; RESCUE; 6°6’3”S, 50°8’7”W; 11.I.18; ISLA 48885 • 1 ♂, 2 ♀; N5SM1_0005 cave; GEM_1178; 6°6’26”S, 50°8’2”W; 18.II.2011; ISLA 96759 • 1 ♀; N5SM1_0007 cave; GEM_1180; 6°6’26”S, 50°8’7”W; 26.II.2010; ISLA 96760 • 1 ♂, 2 ♀, 3 juv.; N5SM1_0008 cave; GEM_1181; 6°6’23”S, 50°8’8”W; 31.VIII.2010; ISLA 96758 2 ♂, 5 ♀ ; N5SM1_0008 cave; GEM_1181; 1.II.2011; ISLA 96765 • 1 ♀; N5SM1_0011 cave; GEM_1184; 6°6’22”S, 50°8’7”W; 24.II.2011; ISLA 6266 • 1 ♀; N5SM1_0014 cave; GEM_1187; 6°6’20”S, 50°8’16”W; 23.VIII.2010; ISLA 6273 • 1 ♀; N5SM1_0015 cave; GEM_1188; 6°6’21”S, 50°8’8”W; 21.VIII.2010; ISLA 6279 1 ♀; N5SM1_0016 cave; GEM_1189; 6°6’21”S, 50°8’13”W; 21.VIII.2010; ISLA 6285 • 1 ♂; N5SM1_0018 cave; GEM_1191; 6°6’21”S, 50°8’12”W; 19.VIII.2010; ISLA 6287 • 1 ♂; N5SM1_0020 cave; GEM_1193; 6°6’34”S, 50°8’7”W; 22.VIII.2010; ISLA 6292 1 ♂, 1 ♀; N5SM1_0020 cave; GEM_1193; 24.II.2011; ISLA 96763 • 1 ♀; N5SM1_0023 cave; GEM_1776; 6°6’32”S, 50°8’6”W; 8.II.2010; ISLA 6257 • 1 ♂, 3 ♀; N5SM1_0026 cave; GEM_1779; 6°6’29”S, 50°8’8”W; 25.II.2011; ISLA 96762 • 1 ♀; N5SM1_0027 cave; GEM_1184; 6°6’22”S, 50°8’20”W; 27.II.2011; ISLA 6271 1 ♀; N5SM1_0027 cave; GEM_1195; 01.IX.2010; ISLA 96757 1 ♂; N5SM1_0028 cave; GEM_1782; 6°6’19”S, 50°8’18”W; 22.IX.2010; ISLA 6276 • 1 juv.; N5SM1_0029 cave; GEM_1783; 6°6’32”S, 50°8’6”W; 19.II.2011; ISLA 96761 • 2 ♂; N5SM1_0030 cave; GEM_1784; 6°6’19”S, 50°8’19”W; 19.II.2010; ISLA 6280 1 ♀; N5SM1_0031 cave; GEM_1785; 6°6’19”S, 50°8’18”W; 27.VIII.2010; ISLA 6226 • 2 ♂, 3 ♀; N5SM1_0031 cave; GEM_1785; 21.II.2011; ISLA 6254 • 2 ♂; N5SM1_0032 cave; GEM_1786; 6°6’22”S, 50°8’11”W; 27.VIII.2010; ISLA 6282 • 1 ♀; N5SM1_0033 cave; GEM_1787; 6°6’19”S, 50°8’19”W; 19.VIII.2010; ISLA 6274 1 ♀; N5SM1_0034 cave; GEM_1788; 6°6’22”S, 50°8’7”W; 8.II.2010; ISLA 6239 • 1 juv.; N5SM1_0035 cave; GEM_1789; 6°6’42”S, 50°8’8”W; 25.II.2011; ISLA 96764 • 1 ♂, 2 ♀; N5SM1_0041 cave; GEM_1795; 6°6’30”S, 50°8’0”W; 25.II.2011; ISLA 6252 • 1 ♀; N5SM1_0044 cave; GEM_1798; 6°6’31”S, 50°8’3”W; 17.II.2011; ISLA 6248 • 4 ♀ ; N5SM1_0082 cave; GEM_1786; 6°6’17”S, 50°8’17”W; 7.II.2011; ISLA 6265 • 1 ♀; N5SM2_0001 cave; RESCUE; 6°8’32”S, 50°8’1”W; 21-31.X.2018; ISLA 61683 • 1 ♂, 1 ♀; N5SM2_0003 cave; GEM_1701; 6°8’23”S, 50°8’16”W; ISLA 15740 • 2 ♂, 3 ♀; N5SM2_0006 cave; GEM_1707; 6°8’27”S, 50°8’9”W; 25.XI.2010; ISLA 21143 • 2 ♂, 1 ♀; N5SM2_0007 cave; GEM_1708; 6°8’17”S, 50°8’17”W; 23.XI.2010; ISLA 15744 • 1 ♂, 1 ♀ ; N5SM2_0008 cave; GEM_1709; 6°8’16”S, 50°8’10”W; 26.X.2010; ISLA 6325 • 1 ♂, 1 ♀; N5SM2_0009 cave; GEM_1705; 6°8’18”S, 50°8’0”W; 23.XI.2010; ISLA 96747 • 1 ♂, 5 ♀; N5SM2_0010 cave; GEM_1699; 6°8’18”S, 50°8’1”W; 23.XI.2010; ISLA 6316 • 3 ♂, 6 ♀ ; N5SM2_0012 cave; GEM_1696; 6°7’58”S, 50°7’51”W; 29.XI.2010; ISLA 21144 • 2 ♂, 3 ♀; N5SM2_0013 cave; GEM_1703; 6°8’7”S, 50°8’6”W; 25.XI.2010; ISLA 6353 • 3 ♀; N5SM2_0015 cave; GEM_1735; 6°8’6”S, 50°8’5”W; 28.XI.2010; ISLA 6329 • 1 ♂, 1 ♀; N5SM2_0018 cave; GEM_1774; 6°8’7”S, 50°8’6”W; 28.X.2010; ISLA 21141 • 3 ♂, 1 ♀; N5SM2_0021 cave; GEM_1727; 6°8’8”S, 50°8’5”W; 27.X.2010; ISLA 21142 • 2 ♂, 2 ♀; N5SM2_0022 cave; GEM_1721; 6°8’4”S, 50°8’15”W; 19.IX.2010; ISLA 6352 • 3 ♀; N5SM2_0023 cave; GEM_1722; 6°8’4”S, 50°8’9”W; 18.X.2010; ISLA 6336 • 1 ♀ ; N5SM2_0024 cave; GEM_1723; 6°8’31”S, 50°8’5”W; 20.XI.2010; ISLA 6319 • 2 ♂, 3 ♀; N5SM2_0025 cave; GEM_1766; 6°8’1”S, 50°8’5”W; 18.XI.2010; ISLA 96745 • 3 ♀; N5SM2_0028 cave; GEM_1702; 6°7’59”S, 50°8’4”W; 20.XI.2010; ISLA 21138 • 1 ♀; N5SM2_0029 cave; GEM_1762; 6°7’58”S, 50°8’4”W; 18.XI.2010; ISLA 15750 • 2 ♂, 1 ♀; N5SM2_0029 cave; GEM_1726; 18.XI.2010; ISLA 96750 • 2 ♂, 4 ♀; N5SM2_0035 cave; GEM_1720; 6°7’57”S, 50°8’6”W; 26.X.2010; ISLA 6332 • 1 ♂, 2 ♀; N5SM2_0036 cave; GEM_1713; 6°7’58”S, 50°8’11”W; 26.X.2010; ISLA 6346 5 ♀; N5SM2_0038 cave; GEM_1715; 6°7’58”S, 50°8’12”W; 19.X.2010; ISLA 6322 • 1 ♀; N5SM2_0039 cave; GEM_1755; 6°7’56”S, 50°8’11”W; 19.X.2010; ISLA 6340 • 1 ♀; N5SM2_0040 cave; GEM_1756; 6°7’55”S, 50°8’10”W; 23.X.2010; ISLA 15751 7 ♀; N5SM2_0040 cave; GEM_1756; 23.X.2010; ISLA 96751 2 ♂, 2 ♀; N5SM2_0041 cave; GEM_1764; 6°7’54”S, 50°8’5”W; 25.X.2010; ISLA 6320 • 2 ♂, 2 ♀; N5SM2_0042 cave; GEM_1770; 6°7’54”S, 50°8’6”W; 21.X.2010; ISLA 6330 • 1 ♀; N5SM2_0043 cave; GEM_1757; 6°7’48”S, 50°8’3”W; 25.X.2010; ISLA 6350 • 2 ♂, 2 ♀; N5SM2_0045 cave; GEM_1717; 6°7’46”S, 50°8’4”W; 22.III.2011; ISLA 6341 • 2 ♂; N5SM2_0046 cave; GEM_1718; 6°7’46”S, 50°8’5”W; 20.X.2010; ISLA 15745 • 2 ♀; N5SM2_0054 cave; GEM_1694; 6°7’45”S, 50°8’5”W; 18.X.2010; ISLA 6345 • 1 ♂, 1 ♀; N5SM2_0056 cave; GEM_1626; 6°8’27”S, 50°8’9”W; 18.X.2010; ISLA 6343 • 3 ♂; N5SM2_0057 cave; GEM_1692; 6°7’41”S, 50°8’5”W; 16.X.2010; ISLA 6339 • 1 ♂; N5SM2_0059 cave; GEM_1690; 6°8’26”S, 50°8’11”W; 30.IX.2010; ISLA 6748 1 ♂; N5SM2_0063 cave; GEM_1688; 6°7’31”S, 50°7’54”W; 30.IX.2010; ISLA 15739 • 2 ♀; N5SM2_0075 cave; GEM_1743; 6°7’23”S, 50°7’48”W; 23.IX.2010; ISLA 21139 • 1 ♀; N5SM2_0078 cave; GEM_1761; 6°7’22”S, 50°7’49”W; 28.IX.2010; ISLA 6318 1 ♀; N5SM2_0079 cave; GEM_1745; 6°8’26”S, 50°8’9”W; 27.IX.2010; ISLA 6334 • 1 ♀; N5SM2_0081 cave; GEM_1752; 6°7’19”S, 50°7’43”W; 27.IX.2010; ISLA 15749 • 2 ♂, 1 ♀; N5SM2_0081 cave; GEM_1752; 27.IX.2010; ISLA 96749 • 2 ♀; N5SM2_0084 cave; GEM_1768; 6°7’19”S, 50°7’40”W; 29.IX.2010; ISLA 6311 • 10 ♀; N5SM2_0088 cave; GEM_1760; 6°7’14”S, 50°7’44”W; 24.XI.2010; ISLA 21140 • 2 ♂, 1 ♀; N5SM2_0093 cave; GEM_1731; 6°8’29”S, 50°8’14”W; 24.IX.2010; ISLA 6348 1 ♀; N5SM2_0094 cave; GEM_1729; 6°7’17”S, 50°7’55”W; 24.IX.2010; ISLA 15741 • 1 ♂; N5SM2_0096 cave; GEM_1698; 6°7’9”S, 50°7’54”W; 29.XI.2010; ISLA 21145 • 1 ♂; N8_0003 cave; GEM_541; 6°10’10”S, 50°9’34”W; 2-29.IV.2015; ISLA 30385 1 ♂; N8_0003 cave; GEM_923; 4.IX-6.X.2014; ISLA 30743 • 2 ♀; N8_0004 cave; GEM_562; 6°10’7”S, 50°9’29”W; 24.II-13.III.2015; ISLA 30406 • 1 ♂; N8_0004 cave; GEM_579; 24.II-13.III.2015; ISLA 30423 • 1 ♂, 1 ♀; N8_0004 cave; GEM_912; 4.IX-6.X.2014; ISLA 30732 • 1 ♀; N8_0004 cave; GEM_934; 4.IX-6.X.2014; ISLA 30754 • 1 ♂; N8_0007 cave; GEM_542; 6°10’5”S, 50°9’30”W; 2-29.IV.2015; ISLA 30386 • 1 ♂; N8_0007 cave; GEM_780; 17.VII-4.VIII.2014; ISLA 30611 • 1 ♂; N8_0007 cave; GEM_794; 17.VII-4.VIII.2014; ISLA 30625 • 1 ♂, 1 ♀; N8_0007 cave; GEM_827; 17.VII-4.VIII.2014; ISLA 30652 • 1 ♂; N8_0008 cave; GEM_552; 6°10’6”S, 50°9’33”W; 2-29.IV.2015; ISLA 30396 • 2 ♂; N8_0008 cave; GEM_583; 2-29.IV.2015; ISLA 30427 • 1 ♂, 1 ♀; N8_0009 cave; GEM_779; 6°10’6”S, 50°9’31”W; 17.VII-4.VIII.2014; ISLA 30610 • 1 ♂, 1 ♀; N8_0010 cave; 6°10’10”S, 50°9’28”W; 02-29.IV.2015; ISLA 37887 • 1 ♂; N8_0011 cave; GEM_916; 6°10’7”S, 50°9’27”W; 4.IX-6.X.2014; ISLA 30736 1 juv.; N8_0013 cave; GEM_; 6°10’8”S, 50°9’28”W; ISLA 30390 1 ♀; N8_0013 cave; GEM_572; 2-29.IV.2015; ISLA 30416 • 1 ♂; N8_0013 cave; GEM_914; 4.IX-6.X.2014; ISLA 30734 • 1 ♂, 2 ♀; N8_0013 cave; GEM_925; 4.IX-6.X.2014; ISLA 30745 1 ♀; N8_0013 cave; GEM_949; 4.IX-6.X.2014; ISLA 30764 • 1 ♂, 1 ♀; N8_0014 cave; GEM_913; 6°10’11”S, 50°9’26”W; 4. IX-6.X.2014; ISLA 30733 • 1 juv.; N8_0015 cave; GEM_560; 6°10’9”S, 50°9’26”W; 2-29.IV.2015; ISLA 30404 • 1 ♂, 2 ♀; N8_0017 cave; GEM_574; 6°10’6”S, 50°9’29”W; 2-29.IV.2015; ISLA 30418 • 3 ♂; N8_0017 cave; GEM_929; 4.IX-6.X.2014; ISLA 30749 • 1 ♀; N8_0017 cave; GEM_943; 4.IX-6.X.2014; ISLA 30758 • 1 ♀; N8_0018 cave; GEM_539; 6°10’7”S, 50°9’30”W; 2-29.IV.2015; ISLA 30383 • 1 ♀; N8_0018 cave; GEM_540; 2-29.IV.2015; ISLA 30384 • 1 ♂; N8_0018 cave; GEM_567; 2-29.IV.2015; ISLA 30411 • 1 ♀; N8_0019 cave; GEM_804; 6°10’30”S,

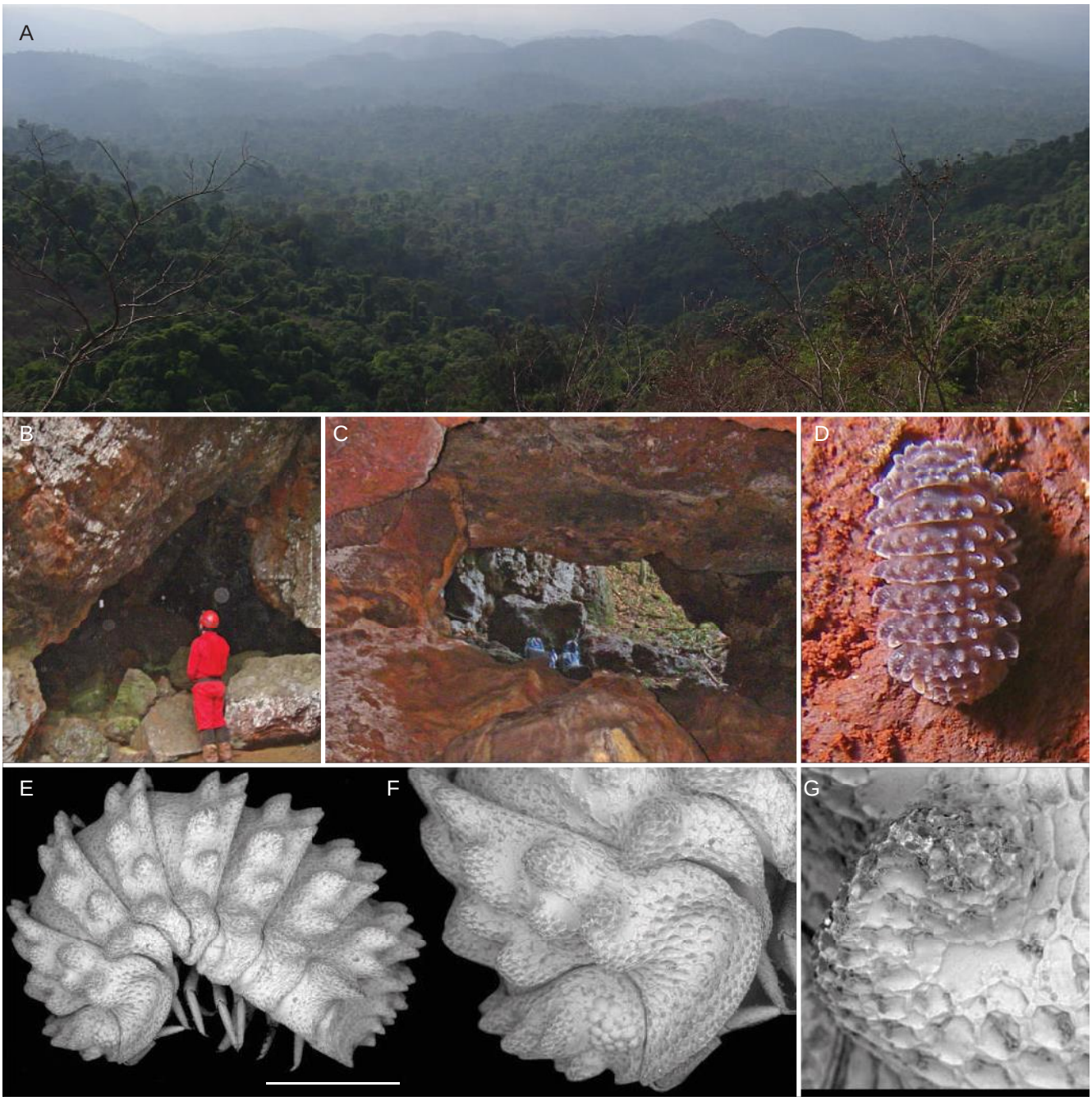


Fig. 1.— *Ctenorillo ferrarai* Campos-Filho, Araujo & Taiti, 2014: **A**, Serra Norte Mountain range in the Carajás National Forest; **B**, entrance of an iron ore cave in the Serra Norte region where specimens are found; **C**, inner portion of an iron ore cave where specimens are found; **D**, habitus in natural condition; **E**, lateral view; **F**, cephalon and epimeron 1, lateral view; **G**, dorsal tubercle with nodulus lateralis. Scale bar: 1 mm.

50°9’5”W; 17.VII-4.VIII.2014; ISLA 30635 • 1 ♀; N8_0020 cave; GEM_549; 6°10’16”S, 50°9’30”W; 24.II-13.III.2015; ISLA 30393 1 ♂; N8_0020 cave; GEM_830; 17.VII-4.VIII.2014; ISLA 30655 1 ♂, 2 ♀; N8_0022 cave; GEM_545; 6°10’32”S, 50°9’28”W; 2-29.IV.2015; ISLA 30389 • 1 ♂, 2 ♀; N8_0022 cave; GEM_545; 2-29.IV.2015; ISLA 30405 • 1 ♂; N8_0022 cave; GEM_775; 17.VII-4.VIII.2014; ISLA 30606 • 1 ♂; N8_0022 cave; GEM_814; 17.VII-4.VIII.2015; ISLA 30640 • 1 ♀; N8_0023 cave; GEM_553; 6°10’31”S, 50°9’3”W; 2-29.IV.2015; ISLA 30397 • 1 ♂, 1 ♀; N8_0023 cave; GEM_553; 2-29.IV.2015; ISLA 30412 • 1 juv.; N8_0023 cave; GEM_573; 2-29.IV.2015; ISLA 30417 • 1 ♀; N8_0023 cave; GEM_585; 2-29.IV.2015; ISLA 30429 • 1 ♀; N8_0023 cave; GEM_917; 4.IX-6.X.2014; ISLA 30737 • 1 ♀; N8_0023 cave; GEM_940; 4.IX-6.X.2014; ISLA 30755 • 1 ♀; N8_0025 cave; GEM_582; 6°10’6”S, 50°9’31”W; 2-29.IV.2015; ISLA 30426 • 1 ♂; N8_0026 cave; GEM_797; 6°10’25”S, 50°8’50”W; 17.VII-4.VIII.2016; ISLA 30628 • 1 ♂; N8_0026 cave; GEM_815; 17.VII-4.VIII.2016; ISLA 30641 • 1 ♂, 2 ♀; N8_0028 cave; GEM_580; 6°10’7”S, 50°9’28”W; 2-29.IV.2015; ISLA 30424 • 1 ♂; N8_0029 cave; GEM_802; 6°10’6”S, 50°9’35”W; 17.VII-4.VIII.2014; ISLA 30633 • 1 ♀; N8_0038 cave; GEM_554; 6°10’6”S, 50°9’33”W; 2-29.IV.2015; ISLA 30398 • 1 ♀; N8_0038 cave; GEM_799; 17.VII-4.VIII.2014; ISLA 30630 • 3 juv.; N8_0038 cave; GEM_825; 17.VII-4.VIII.2014; ISLA 30650 • 1 ♀; N8_0038

cave; GEM_839; 17.VII-4.VIII.2014; ISLA 30664 • 1 ♂, 2 ♀; N4E_016; RESCUE; 6°2’7”S, 50°9’38”W; 16.I.2018; ISLA 48892 1 ♀; N4E_018; RESCUE; 6°2’5”S, 50°9’38”W; 5.II.2018; ISLA 48895 • 1 ♀; N4E_027; 6°2’15”S, 50°10’4”W; 10-17.IV.2018; ISLA 95922 • 1 ♀; N4E_027; 10-17.IV.2018; ISLA 95926 • 1 ♀; N4E_027; 10-17.IV.2018; ISLA 95933 • 1 ♀; N4E_036; 6°2’9”S, 50°9’36”W; 14.II.2014; ISLA 40735 • 1 ♀; N4E_039; 6°1’59”S, 50°9’40”W; 21-30.VII.2018; ISLA 61310 • 1 ♀; N4E_043; 6°1’56”S, 50°9’51”W; 21-30.VII.2022; ISLA 61314 • 1 ♀; N4E_044; 6°1’56”S, 50°9’51”W; 21-30.VII.2019; ISLA 61306 • 1 juv.; N4W_023; RESCUE; 6°2’2”S, 50°10’8”W; 15.I.2018; ISLA 48884 • 1 ♀; N4WS_010; RESCUE; 6°5’22”S, 50°11’42”W; 21-31.X.2018; ISLA 61679 • 1 ♂; N4WS_018; 6°4’34”S, 50°11’37”W; 21-30.VII.2020; ISLA 61308 • 1 juv.; N4WS_036; 6°5’50”S, 50°11’8”W; 10-17.IV.2017; ISLA 95917 • 1 ♂; N4WS_036; 10-17.IV.2017; ISLA 95920 • 1 ♂; N4WS_036; 10-17.IV.2017; ISLA 95924 • 1 ♂; N4WS_036; 10-17.IV.2017; ISLA 95928 • 1 ♂, 4 ♀; N4WS_039; RESCUE; 6°3’59”S, 50°11’36”W; 21-31.X.2020; ISLA 61681 • 1 ♂, 1 ♀; N4WS_055; 6°4’51”S, 50°11’46”W; 21-30.VII.2018; ISLA 61316 • 1 ♀; N4WS_064; 6°4’53”S, 50°11’44”W; 21-30.VII.2021; ISLA 61312 • 1 ♂, 1 ♀; N4WS_064; 21-30.VII.2021; ISLA 61313.

Brazil. Pará state, Parauapebas municipality, Serra do Tarzan plateau, F.M.B. Silva leg. • 1 ♂; ST_0002 cave; 6°19’32”S, 50°7’7”W; 21.I.2016; ISLA44232 • 1 ♀; ST_0003 cave; 6°19’38”S, 50°6’50”W; 2.II.2016; ISLA44233 • 1 ♂; ST_0026, 21.I.2016; ISLA44234 • 1 ♀; ST_0022 cave; 6°19’11”S, 50°7’55”W; 2.II.2016; ISLA43714 • 1 ♀; ST_0045 cave; 6°19’4”S, 50°7’35”W; 3.VIII.2016; ISLA96369 2 ♀; ST_0018 cave; 6°19’49”S, 50°7’21”W; 4.VIII.2016; ISLA96374 • 1 ♂, 4 ♀; ST_0020 cave; 6°18’59”S, 50°7’13”W; 4.II.2016; ISLA96373 • 1 ♀; ST_0017 cave; 6°18’54”S, 50°6’20”W; 3.II.2016; ISLA96378 • 1 ♀; ST_0030 cave; 6°18’59”S, 50°7’13”W; 21.VII.2016; ISLA96752 • 1 ♀; ST_0031 cave; 6°18’37”S, 50°5’58”W; 13.VII.2016; ISLA96753 • 2 ♀, 1 juv.; ST_0030 cave; 6°18’59”S, 50°7’13”W; 21.VII.2016; ISLA96388 • 1 ♀; ST_0044 cave; 6°18’59”S, 50°7’39”W; 2.II.2016; ISLA96399 • 3 ♀; ST_0048 cave; 6°19’5”S, 50°7’39”W; 26.I.2016; ISLA96400 • 1 ♀; ST_0054 cave; 6°19’16”S, 50°8’21”W; 29.I.2016; ISLA96754 • 1 ♀; ST_0040 cave; 6°19’46”S, 50°9’51”W; 25.I.2016; ISLA96405 • 1 ♂, 1 ♀; ST_0020 cave; 6°18’57”S, 50°7’22”W; 21.I.2016; ISLA96410 • 2 ♀; ST_0016 cave; 6°19’10”S, 50°7’33”W; 4.III.2016; ISLA96413 • 1 ♀; ST_0026 cave; 6°19’32”S, 50°7’13”W; 18.VII.2016; ISLA96415 • 1 ♂; ST_0010 cave; 6°12’51”S, 50°6’32”W; 12.VII.2016; ISLA96412 1 ♀; ST_0030 cave; 6°18’59”S, 50°7’13”W; 4.II.2016; ISLA96419 1 ♂, 2 ♀; ST_0064 cave; 6°18’43”S, 50°8’35”W; 7.I.2016; ISLA96420 • 1 ♂; ST_0053 cave; 6°19’16”S, 50°8’21”W; 29.I.2016; ISLA96424 • 2 ♂, 1 ♀; ST_0049 cave; 6°19’10”S, 50°7’38”W; 26.I.2016; ISLA96425 • 1 ♂, 1 ♀; ST_0061 cave; 6°18’46”S, 50°8’30”W; 27.I.2016; ISLA96426 • 1 ♂, 1 ♀; ST_0013 cave; 6°19’1”S, 50°6’24”W; 3.II.2016; ISLA96427 • 1 ♂; ST_0070 cave; 6°19’0”S, 50°7’16”W; 2.VIII.2016; ISLA96431 • 1 ♀; ST_0017 cave; 6°18’54”S, 50°6’20”W; 14.VII.2016; ISLA96433 • 1 ♀; ST_0016 cave; 6°19’10”S, 50°7’33”W; 4.VIII.2016; ISLA96435 3 ♂, 5 ♀; ST_0030 cave; 6°18’59”S, 50°7’13”W; 4.II.2016; ISLA96436 • 2 ♂, 2 ♀; ST_0026 cave; 6°19’32”S, 50°7’13”W; 21.I.2016; ISLA96437 • 2 ♀; ST_0056 cave; 6°19’39”S, 50°8’23”W; 20.VII.2016; ISLA96438 • 1 ♀; ST_0009 cave; 6°19’28”S, 50°6’32”W; 12.VII.2016; ISLA96440 • 1 ♂; ST_0038 cave; 6°18’47”S, 50°5’50”W; 3.II.2016; ISLA96755 • 4 ♀; ST_0030 cave; 6°18’59”S, 50°7’13”W; 21.VII.2016; ISLA96756.

DISTRIBUTION. — Carajás National Forest, Pará State.

HABITAT

Ctenorillo ferrarai were originally found in two caves in the Carajás region, located in eastern Pará state, in the Amazon Forest. Unfortunately, data on their habitats were not provided in the original description (Campos-Filho *et al.* 2014). Herein we add additional occurrences for this species and some notes on their habitats, along with the first photographs of living specimens (Fig. 1). The Carajás region presents massive iron ore reserves (among other metals) thus being strategically important for the Brazilian economy. However, due to the accelerated growth of iron ore exploitation, the natural landscapes, including both external (forests) and subterranean (caves) components are under unprecedented threat. A considerable part of the iron ore plateaus in the Carajás region is located in the conservation unit of the Carajás National Forest. This National Forest embraces parts of the municipalities of Parauapebas, Canaã dos Carajás, and Água Azul do Norte and is composed by a mosaic of protected areas that adds up to 1.31 million hectares of preserved forests (Rolim *et al.* 2006) surrounded by severely impacted areas especially covered by pastures (Campos & Castilho 2012; Martins *et al.* 2012). This conservation unit preserves ombrophilous or seasonal forest formations (Fig. 1A), with 5% consisting of laterite plateaus, which outcrops on the high areas of the region (Campos & Castilho 2012). Despite the status of a conservation unit, the Carajás National Forest, is highly altered by mining, farming and illegal deforestation (Mertens *et al.* 2002; Souza-Filho *et al.* 2016; Oliveira *et al.* 2020; Rizzo *et al.* 2020). The current climate classification of the region is Aw according to Köppen’s system (Alvares *et al.* 2013). It is characterized by a high annual precipita- tion, which follows a unimodal pattern, with the rainy season peaking between January and March. The region receives an annual total precipitation of approximately 2.033 millimeters, with three-quarters of this occurring during the three wettest months. Monthly average temperatures range from 25.1°C to 26.3°C, with minimums between 15.6°C and 18.3°C (from July to October) and maximums between 34.3°C and 38.1°C, in the remaining months. The region maintains consistently high humidity levels throughout the year, with monthly average relative air humidity varying between 76.8% and 88.5%.

In Serra Norte Mountain Range samples were made in around 900 iron ore caves. Specimens of *C. ferrarai* (Fig. 1D) were found in 114 caves (which corresponds to approximately 12.7% of the caves in the area). Additionally, specimens were also found in 34 caves in the Serra do Tarzan region, in an area close to the Serra Sul complex (Fig. 1B, C). Hence, its wide distribution in caves located at different iron ore plateaus indicates that this species certainly occurs outside caves, and is considered a troglophilic species. The caves where the specimens were found are extremely variable in their geological traits, such as the number and size of their entrances, the total length, and the position on the plateaus, among other characteristics, thus indicating that the species seems to be a generalist cave inhabitant, apparently not demanding specific habitat traits. It is important to mention, however, that the quarries expansion in the last years may represent a significant threat, thus monitoring plans should include this species to evaluate any changes in its distributional patterns and population attributes.

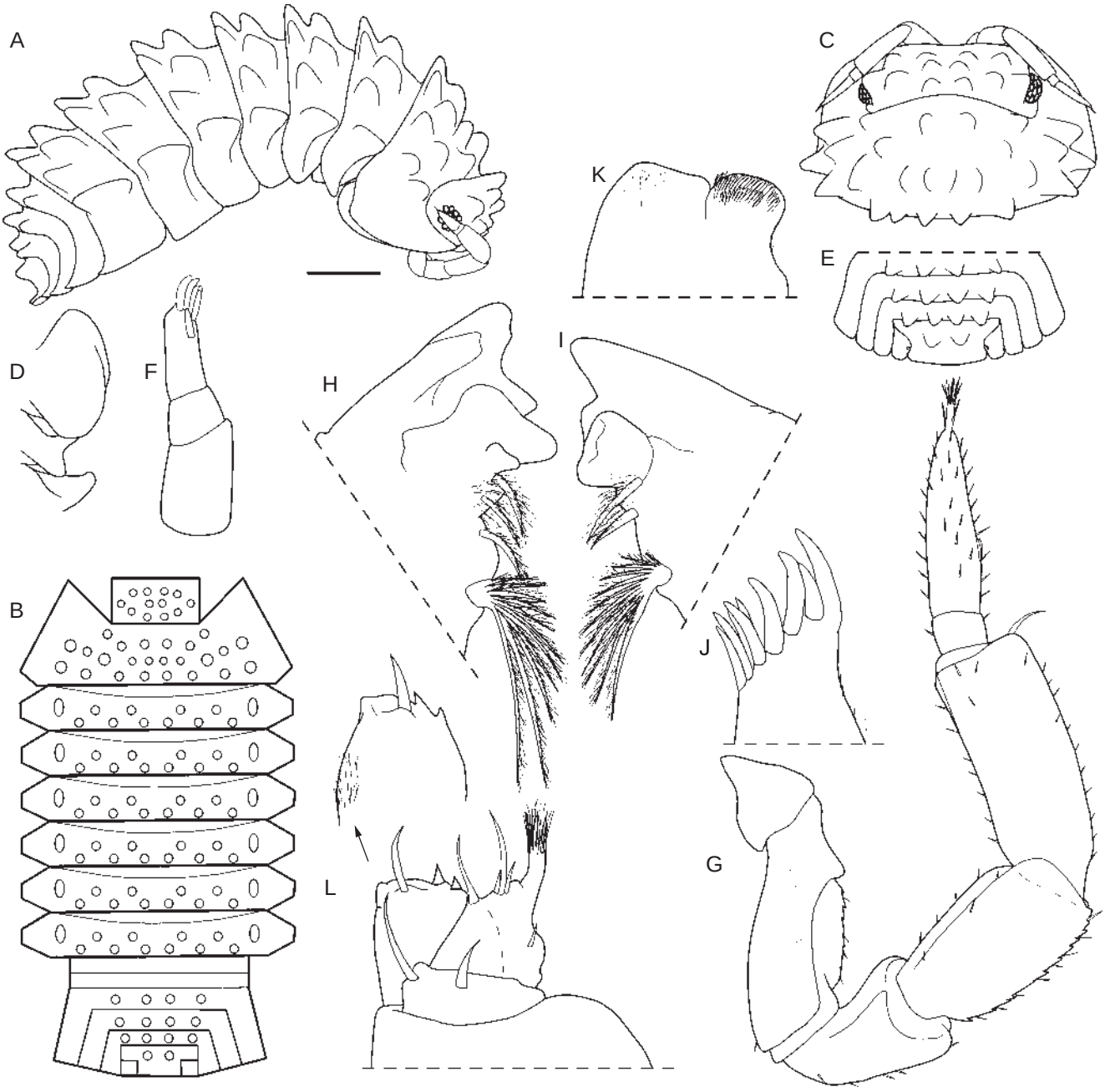


Fig. 2. — *Ctenorillo pelado* Cardoso & Ferreira, n. sp. paratype (male, 5 mm, ISLA96774): **A**, habitus, lateral view; **B**, disposition of dorsal tubercles; **C**, cephalon and pereonite 1, dorsal view; **D**, epimera 1-3 ventral view; **E**, pleonites 3-5, uropods and telson, dorsal view; **F**, antennula; **G**, antenna; **H**, right mandible; **I**, left mandible; **J**, maxillula; **K**, maxilla; **L**, maxilliped. Scale bar: 0.5 mm.

REMARKS

Ctenorillo ferrarai was initially documented in two distinct locations of Serra Norte within the Carajás National Forest. Additional surveys conducted in both Serra Norte and Serra do Tarzan provided evidence of similar configurations of dorsal tubercles, which suggests that these specimens are conspecific with the initial discovery. *Ctenorillo ferrarai* is distinguished by its well-defined tubercles present on both the pereon and pleon segments, as well as a singular rib comprising the first lateral tubercle on epimeron 1 (Fig. 1D-G). This trait is of particular interest and will be further examined in other species within this genus.

Ctenorillo pelado Cardoso & Ferreira, n. sp. (Figs 2-4; 27B; 28A-D)

urn:lsid:zoobank.org:act:B55B71C4-84ED-4DF5-AF0E-6B8356376022

nec *Ctenorillo ferrarai* – Campos-Filho *et al.* 2023: 560, figs 22, 23.

TYPE MATERIAL. — **Holotype. Brazil.** Pará state; Curionópolis municipality; Serra Leste plateau • ♂ (4.5 mm); SL_0001 cave; 5°57'58"S, 49°38'57"W; 14.I.2011; ISLA96773.
Paratypes. Brazil • 1 ♂ (parts in slide); same data as holotype; ISLA96774 • 4 ♂, 3 ♀; SL_0001 cave; same data as holotype; ISLA15135 • 2 juv.; same data as holotype; 4.VII.2010; ISLA15926 5 ♂, 5 ♀; same data as holotype; 4.VII.2010; ISLA15969.

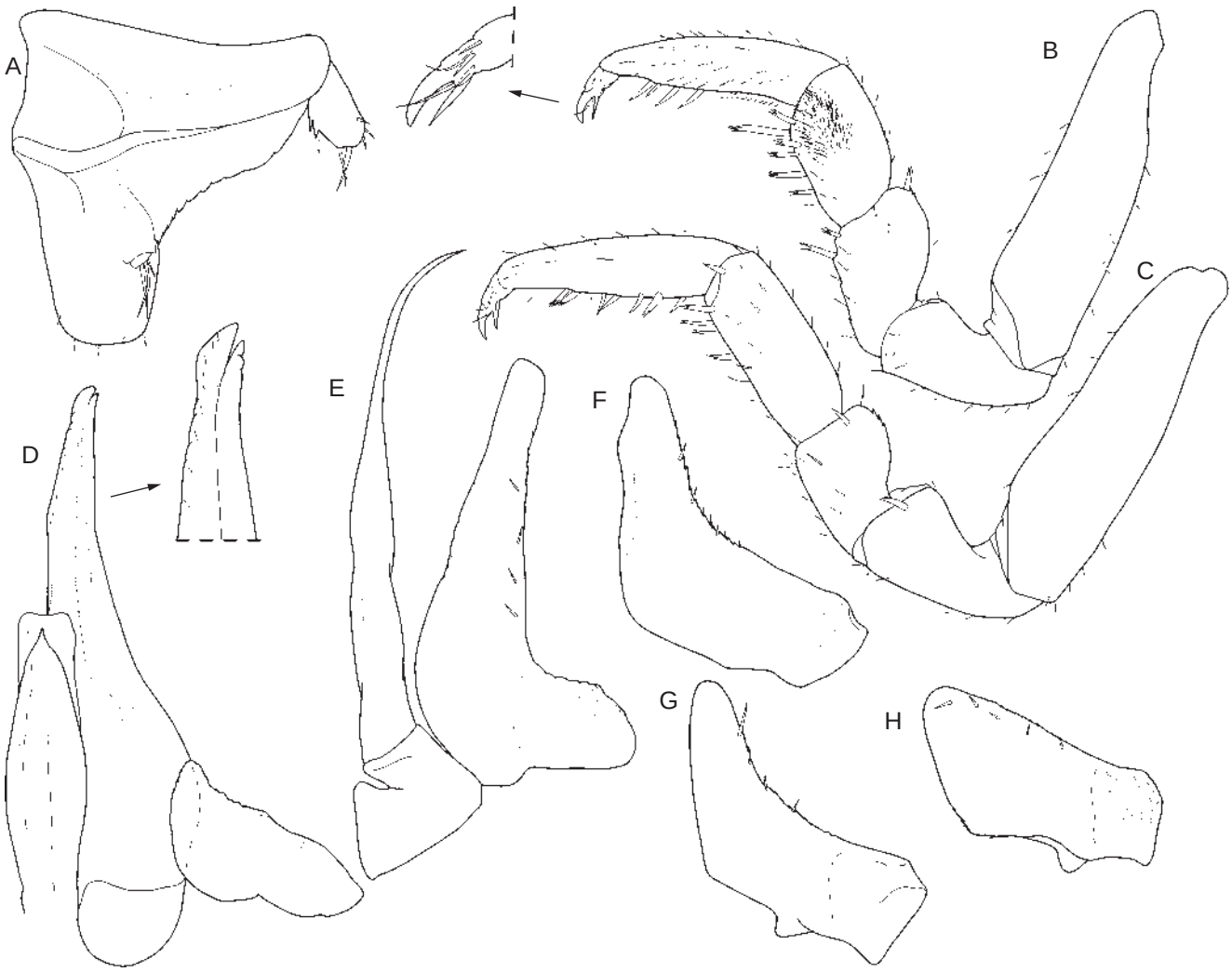


Fig. 3. — *Ctenorillo pelado* Cardoso & Ferreira, n. sp. paratype (male, 5 mm, ISLA96774): **A**, uropod, **B**, pereopod 1; **C**, pereopod 7; **D**, pleopod 1 and genital papilla; **E**, pleopod 2; **F**, pleopod 3 exopod; **G**, pleopod 4 exopod; **H**, pleopod 5 exopod.

Other material. — **Brazil**. Pará; Curionópolis municipality; Serra Leste plateau • 4 ♂, 5 ♀; SL_0002 cave; 5°52'57"S, 49°38'57"W; 13.I.2011; ISLA15136 • 8 ♂, 2 ♀; SL_0002 cave; 3.VII.2010; ISLA15970 • 2 ♂; SL_0003 cave; 3.VII.2010; ISLA15971 • 2 ♂, 5 ♀; SL_0004 cave; 5°57'49"S, 49°38'59"W; 13.I.2011; ISLA15137 2 ♂, 2 ♀; SL_0004 cave; 3.VII.2010; ISLA15972 • 1 ♂, 2 ♀; SL_0006 cave; 5°57'48"S, 49°38'59"W; 13.I.2011; ISLA15138 • 3 ♀; SL_0006 cave; 28.VI.2010; ISLA15902 • 1 ♂, 6 ♀; SL_0007 cave; 5°57'58"S, 49°38'58"W; 3.XII.-2011; ISLA15872 • 1 ♂, 2 ♀; SL_0007 cave; 4.VII.2010; ISLA15939 • 3 ♀, 3 juv.; SL_0008 cave; 5°58'3"S, 49°38'58"W; 14.I.2012; ISLA15139 • 4 ♂, 3 ♀; SL_0008 cave; 5.VII.2010; ISLA15973 • 1 ♀, 1 juv.; SL_0011 cave; 5°58'4"S, 49°38'59"W; 14.I.2011; ISLA15140 • 1 ♀; SL_0012 cave; 5°57'52"S, 49°38'59"W; 4.VII.2016; ISLA15974 • 2 ♀; SL_0013 cave; 5°57'47"S, 49°38'59"W; 13.I.2011; ISLA15141 • 1 ♀; SL_0014 cave; 5°57'46"S, 49°39'0"W; 13.I.2011; ISLA15878 • 1 ♀; SL_0015 cave; 5°57'44"S, 49°39'0"W; 2.II.2011; ISLA15142 • 1 ♂; SL_0016 cave; 5°58'12"S, 49°38'51"W; 12.I.2011; ISLA6211 2 ♂, 6 ♀; SL_0016 cave; 12.I.2011; ISLA15143 • 1 ♀; SL_0016 cave; 6.VI.2010; ISLA16588 • 1 ♂; SL_0017 cave; 5°58'16"S, 49°38'48"W; 8.I.2011; ISLA15144 • 3 ♀; SL_0019 cave; 5°58'15"S, 49°38'47"W; 12.I.2011; ISLA15145 • 1 juv.; SL_0020 cave; 5°58'15"S, 49°38'47"W; 12.I.2011; ISLA15146 • 2 ♀; SL_0022 cave; 5°58'17"S, 49°38'46"W; 29.I.2011; ISLA15147 • 1 ♀, 3 juv.; SL_0023 cave; 5°58'18"S, 49°38'46"W; 12.I.2011; ISLA15985 3 ♂, 6 ♀; SL_0024 cave; 5°58'19"S, 49°38'41"W; 9.VI.2010; ISLA15929 • 2 ♂, 4 ♀; SL_0026 cave; 5°58'21"S, 49°38'41"W; 12.I.2011; ISLA15976 • 2 ♂, 1 ♀; SL_0026 cave; 9.VI.2010; ISLA16589 • 2 ♂; SL_0030 cave; 5°58'20"S, 49°38'37"W; 8.VI.2010; ISLA15954 • 1 ♀; SL_0032 cave; 5°58'7"S, 49°38'40"W; 27.VII.2010; ISLA15942 • 1 ♂, 3 ♀; SL_0035 cave; 5°58'32"S, 49°38'16"W; 31.I.2011; ISLA15148 • 1 ♂, 2 ♀; SL_0036 cave; 5°58'31"S, 49°38'15"W; 23.VII.2010; ISLA15931 • 1 ♀; SL_0037 cave; 5°58'40"S, 49°37'54"W; 27.I.2011; ISLA15855 • 1 ♀; SL_0037 cave; 8.VII.2010; ISLA15935 • 1 ♂; SL_0042 cave; 5°58'14"S, 49°38'47"W; 2.II.2011; ISLA15149 • 2 ♂; SL_0042 cave; 8.VII.2010; ISLA16590 • 1 ♀; SL_0047; 30.VI.2010; ISLA16591 • 1 ♀; SL_0048 cave; 5°58'58"S, 49°37'52"W; 29.I.2011; ISLA15860 • 2 ♂, 1 ♀; SL_0049 cave; 5°58'58"S, 49°37'51"W; 29.I.2011; ISLA15980 • 2 ♂, 1 ♀; SL_0049; 27.VI.2010; ISLA16592 • 1 ♂, 2 ♀; SL_0057 cave; 5°58'36"S, 49°37'32"W; 11.I.2011; ISLA15151 • 1 ♀; SL_0058 cave; 5°58'34"S, 49°37'28"W; 29.I.2011; ISLA15150 • 1 ♂, 3 ♀; SL_0058 cave; 27.VI.2010; ISLA16593 • 3 ♂, 5 ♀; SL_0060 cave; 5°58'46"S, 49°37'22"W; 10.I.2011; ISLA15152 • 4 ♂, 5 ♀; SL_0060 cave; 10.VI.2010; ISLA16594 • 1 ♂; SL_0064 cave; 5°58'44"S, 49°37'17"W; 10.VI.2010; ISLA15924 •1 ♀; SL_0065 cave; 5°58'53"S, 49°37'11"W; 2.XII.-2011; ISLA15154 • 2 ♂, 1 ♀; SL_0065; 2.XII.-2011; ISLA15155 • 2 ♂, 8 ♀; SL_0065 cave;



Fig. 4. — *Ctenorillo pelado* Cardoso & Ferreira, n. sp.: **A**, Serra Leste Mountain range; **B**, habitus in natural condition; **C**, inner portion of an iron ore cave where specimens are found; **D**, entrance of an iron ore cave in the Serra Norte region where specimens are found.

5.VI.2010; ISLA16595 • 1 ♀; SL_0066 cave; 5°58’52”S, 49°37’12”W; 2.XII.-2011; ISLA15153 • 1 ♀; SL_0066; 8.VII.2010; ISLA16596 1 ♂, 1 ♀; SL_0067 cave; 5°58’51”S, 49°37’12”W; 5.VI.2010; ISLA16597 • 1 ♂, 3 ♀; SL_0067 cave; 3.III.2011; ISLA15156 3 ♂, 5 ♀; SL_0069 cave; 5°59’2”S, 49°37’14”W; 3.XII.-2011; ISLA15157 • 1 ♂, 3 ♀; SL_0069 cave; 11.VI.2010; ISLA16598 • 1 juv.; SL_0072 cave; 7.I.2011; ISLA15158 • 2 ♂, 1 ♀; SL_0072 cave; 5°58’21”S, 49°37’28”W; 23.VII.2010; ISLA15909 • 3 ♂, 2 ♀; SL_0074 cave; 5°57’57”S, 49°37’55”W; 11.I.2010; ISLA15965 • 4 ♀; SL_0074 cave; 24.VI.2010; ISLA16599 • 1 ♂, 1 ♀; SL_0075 cave; 5°57’55”S, 49°37’56”W; 12.I.2011; ISLA15966 • 2 ♂, 1 ♀; SL_0076 cave; 5°58’0”S, 49°38’32”W; 31.I.2011; ISLA15110 • 2 ♀; SL_0077 cave; 5°58’0”S, 49°38’33”W; 29.VI.2010; ISLA16600 • 1 ♂, 1 ♀; SL_0082 cave; 5°57’30”S, 49°38’15”W; 7.VII.2010; ISLA15911 • 1 ♀; SL_0083 cave; 5°57’29”S, 49°38’11”W; 7.VII.2010; ISLA15945 2 ♀; SL_0085 cave; 5°57’30”S, 49°38’10”W; 18.I.2011; ISLA15099 1 ♀; SL_0085 cave; 21.VII.2010; ISLA15894 • 1 juv.; SL_0086 cave; 5°57’31”S, 49°38’10”W; 18.I.2011; ISLA15990 • 2 ♂, 2 ♀; SL_0087 cave; 5°57’31”S, 49°38’9”W; 2.II.2011; ISLA15111 • 5 ♂, 8 ♀; SL_0087 cave; 21.VII.2010; ISLA15913 • 1 ♀; SL_0088 cave; 5°57’31”S, 49°38’9”W; 22.VII.2010; ISLA21127 • 1 ♀; SL_0089 cave; 5°57’31”S, 49°38’8”W; 2.II.2011; ISLA15967 • 2 ♂; SL_0089 cave; 2.II.2011; ISLA21128 • 1 ♀; SL_0091 cave; 5°57’32”S, 49°38’7”W; 2.II.2011; ISLA15906 • 1 ♀; SL_0092 cave; 5°57’33”S, 49°38’7”W; 2.II.2011; ISLA15885 • 1 ♀; SL_0092 cave; ISLA15904 1 ♂, 2 ♀; SL_0099 cave; 5°58’33”S, 49°37’28”W; 7.I.2011; ISLA15968 • 2 ♂, 5 ♀; SL_0100 cave; 5°58’45”S, 49°37’21”W; 10.I.2011; ISLA15964 • 3 ♂, 2 ♀; SL_0100 cave; ISLA21129 • 3 ♂, 10 ♀; SL_0101 cave; ISLA6178 • 1 ♀; SL_0102; ISLA6182 • 1 ♀; SL_cm-t4b; 5°58’36”S, 49°37’33”W; 17.IV.2018; ISLA21130 • 1 ♂, 3 ♀; SL_cm-t4c; 5°58’35”S, 49°37’35”W; 17.IV.2017; ISLA21131 1 ♂, 1 ♀; SL_as-t4d; 5°58’34”S, 49°37’37”W; 26.IV.2018; ISLA21132 • 1 ♀; SL_as-t4b; 5°58’36”S, 49°37’33”W; 26.IV.2017; ISLA21133 • 1 ♀; SL_as-t4c; 5°58’35”S, 49°37’35”W; 26.IV.2017; ISLA21134 • 1 ♂; SL_as-t1b; 5°58’23”S, 49°38’32”W; 29.IV.2017; ISLA21135 • 1 ♀; SL_cm-t4d; 5°58’34”S, 49°37’37”W; 17.II.2017; ISLA21136 • 1 ♂, 1 ♀; SL_apl-t4c; 5°58’35”S, 49°37’35”W; 17.II.2017; ISLA21137.

Etymology. — The new species name is a noun in apposition that refers to the region where the species was collected, also known as “Serra Pelada”, which means “naked mountains”, in reference to the presence of the metallophilic vegetation, that is considerably reduced (in size) when compared to the surrounding Amazon Forest.

Diagnosis. — Dorsum covered with conical tubercles and lateral ribs with three rows on cephalon (4, 2, 6); three rows on pereonite 1 (6, 10, 8); two rows on pereonites 2-7 (6 + 6); one row of four tuber- cles on pleonites 3-5; two paramedian tubercles on telson. Pleopod 1 exopod wider than long, triangular with protruding distal portion, outer margin concave and crenulate; endopod with distal portion straight, slightly swollen, four times longer than exopod.

Distribution. — Carajás National Forest, Pará State.

Description

Maximum size: ♂, 4.5 mm, ♀, 6 mm. Color grey in nature, brownish in ethanol (Figs 4B; 27B). Dorsum covered with conical tubercles and lateral ribs (Figs 2A-C; 28A, B): cephalon with three rows (4, 2, and 6 from front to back of vertex); pereonite 1 with 24 in three rows (6, 10 and 8); pereonites 2-7 with 12 (6 + 6); pleonites 3-5 with one row of four tubercles; telson with two paramedian tubercles. Dorsal cuti- cle (Fig. 28B) with short triangular scale setae; pereonites 1-7 bearing one line of *noduli lateralis* per side on outer surface of posterior tubercle of second line of tubercles. Cephalon with frontal shield slightly protruding above vertex; eye consisting of 11 ommatidia (Figs 2C; 28A). Pereonite 1 with posterior

margin distinctly sinuous at sides; inner lobe of schisma rounded, extending beyond posterior margin of outer lobe; pereonite 2 with triangular ventral tooth reaching epimeron posterior margin (Figs 2A, D; 28D). Pereonites 2-7 (Figs 2A; 28B) with wide quadrangular epimera slightly bent outwards. Telson (Fig. 2E) hourglass-shaped, proximal portion broader than distal portion. Antennula (Fig. 2F) of three articles, second article much shorter than first and third, third article with two apical and four subapical aesthetascs. Antenna (Fig. 2G) short and stout, flagellum shorter than fifth article of peduncle; second article of flagellum about three times as long as first. Mandibles (Fig. 2H, I) with molar penicil semidichotomised, consisting of several plumose setae from common stem; right mandible with 1 + 1 and left mandible with 2 + 1 free penicils. Maxillula (Fig. 2J) with outer branch bearing 4 + 5 simple teeth. Maxilla (Fig. 2K) distally setose and bilobate, with inner lobe narrower than outer lobe. Maxilliped (Fig. 2L) endite with subapical large seta and two triangular setae on apical margin; palp with two setae on basal article. All pleopod exopods with monospiracular covered lungs (Fig. 28C). Uropod (Fig. 3A) protopod flattened, enlarged on basal portion; exopod very short, inserted dorsally close to medial margin of protopod.

Male

Pereopods without particular modifications (Fig. 3B, C). Pleopod 1 exopod (Fig. 3D) wider than long, triangular with protruding distal portion, outer margin concave and crenulate; endopod four times longer than exopod, distal portion straight, slightly swollen. Pleopod 2 endopod longer than exopod (Fig. 3E). Pleopods 3-5 exopods as in Figure 3F-H.

HABITAT

Specimens of *C. pelado* Cardoso & Ferreira, n. sp. were found in several caves in the Serra Leste Mountain Range (also known as Serra Pelada) which is part of the geological complex of the Carajás region, in the Carajás National Forest (Fig. 4A). The specimens were found in caves, and also in the external habitats, during external surveys (Fig. 4B). The regional climate is also classified as Aw according to the Köppen system, characterized by the same patterns of precipitation and temperature as described for the previous species (*C. ferrarai*). Nevertheless, given the regularity with which specimens have been observed within cave systems, it is plausible to classify this species as troglophilic. Of the approximately 120 iron ore caves surveyed in the region, *C. pelado* Cardoso & Ferreira, n. sp. was identified in 63 of these caves (roughly 52.5% of the total caves in the area), indicating an even broader distribution within Serra Leste than *C. ferrarai* within the Serra Norte complex (Fig. 4C, D). It should be noted that Serra Leste is primarily comprised of a single, extensive plateau, as opposed to the multiple plateaus present in the Serra Norte complex. As with *C. ferrarai*, the geological characteristics of caves inhabited by *C. pelado* Cardoso & Ferreira, n. sp. vary significantly, suggesting that this species is not strongly reliant on specific habitat traits. Despite the wide distribution of this species in the caves of the area, a large quarry is rapidly expanding in the region, posing a significant threat to the species. Therefore, monitoring plans should include *C. pelado* Cardoso & Ferreira, n. sp. to assess any potential changes to its distributional patterns and population characteristics.

REMARKS

As mentioned previously, the *Ctenorillo* species are distinguished mainly by the shape, number, and disposition of dorsal tubercles. The morphology of *C. pelado* Cardoso & Ferreira, n. sp. and *C. ferrarai* is very similar, the species differ in the number of tubercles on pereonite 1 with *C. pelado* Cardoso & Ferreira, n. sp. presenting 24 tubercles and *C. ferrarai* presenting 22; this seems to be related to the prominent lateral rib in *C. ferrarai* while in *C. pelado* Cardoso & Ferreira, n. sp. the lateral rib is present from pereonite 2 to 7 with two tubercules (instead of one rib) on pereonite 1. The disposition of tubercles on pereonite 1 differ with 6 + 10 + 8 on *C. pelado* Cardoso & Ferreira, n. sp. and 4 + 12 + 6 on *C. ferrarai*. The specimen presented by Campos-Filho *et al.* (2023) were also collected in the Serra Leste plateau and resembles the morphology of *C. pelado* Cardoso & Ferreira, n. sp. presented here; therefore, we can consider them as the same species.

Comparing *C. pelado* Cardoso & Ferreira, n. sp. with other *Ctenorillo* species, on pleon, the presence of four tubercles on pleonites 3-5 is similar to *C. guinensis* (Schmalfuss & Ferrara, 1983), *C. legai* (Arcangeli, 1941), *C. mineri* and *C. ferrarai* from which it differs by the shape of male pleopod 1 exopod.

Ctenorillo araguaia Cardoso & Ferreira, n. sp. (Figs 5-7; 27C; 28E)

urn:lsid:zoobank.org:act:4F19B81C-879D-43EC-A3BF-0AFBB1D908EF

TYPE MATERIAL. — **Holotype**. **Brazil** • 1 ♂ (5 mm); Pará state; São Geraldo do Araguaia municipality; Serra das Andorinhas cave; 6°16'55"S, 48°32'34"W; sector 4; 17-20.II.2018; V.F. Sperandei leg.; ISLA96775.

Paratypes. Brazil • 1 ♂ in slide; same data as holotype; ISLA96784 • 6 ♀; sector 1; same data as holotype; ISLA96776 • 1 ♀; sector 1; same data as holotype; ISLA96777 • 1 ♀; sector 3; same data as holotype; ISLA96778 • 3 ♂, 8 ♀; sector 4; same data as holotype; ISLA96779 5 ♂; sector 5; same data as holotype; ISLA96780 • 3 ♂, 5 ♀ sector 6; same data as holotype; ISLA96781 •1 ♂; sector 7; same data as holotype; ISLA96782 • 1 ♂, 3 ♀; same data as holotype; ISLA96783.

OTHER MATERIAL. — **Brazil** • 4 ♂; Pará state; São Geraldo do Araguaia municipality; Remanso dos Botos cave; 6°22'6"S, 48°23'38"W; V. F. Sperandei leg.; 20.II.2018; ISLA96785.

ETYMOLOGY. — The new species name is a noun in apposition that refers to the Araguaia River, a Brazilian environmental heritage: the type locality is within the hydrographic basin of the Araguaia river. The word Araguaia comes from the indigenous Amazonian language term arauay (or araguaí), which designates a type of macaw species.

DIAGNOSIS. — Dorsum covered with conical tubercles and lateral ribs with three rows on cephalon (6, 2, 6); four rows on pereonite 1 (4, 7, 10, 6); two rows on pereonites 2-6 (10 + 8) and on pereonite 7 (6 + 8); one row of four tubercles on pleonites 3-5; and two parame- dian tubercles on telson. Pleopod 1 exopod distal portion round, outer margin straight; endopod with distal portion slightly bent outward, slightly swollen, four times longer than exopod.

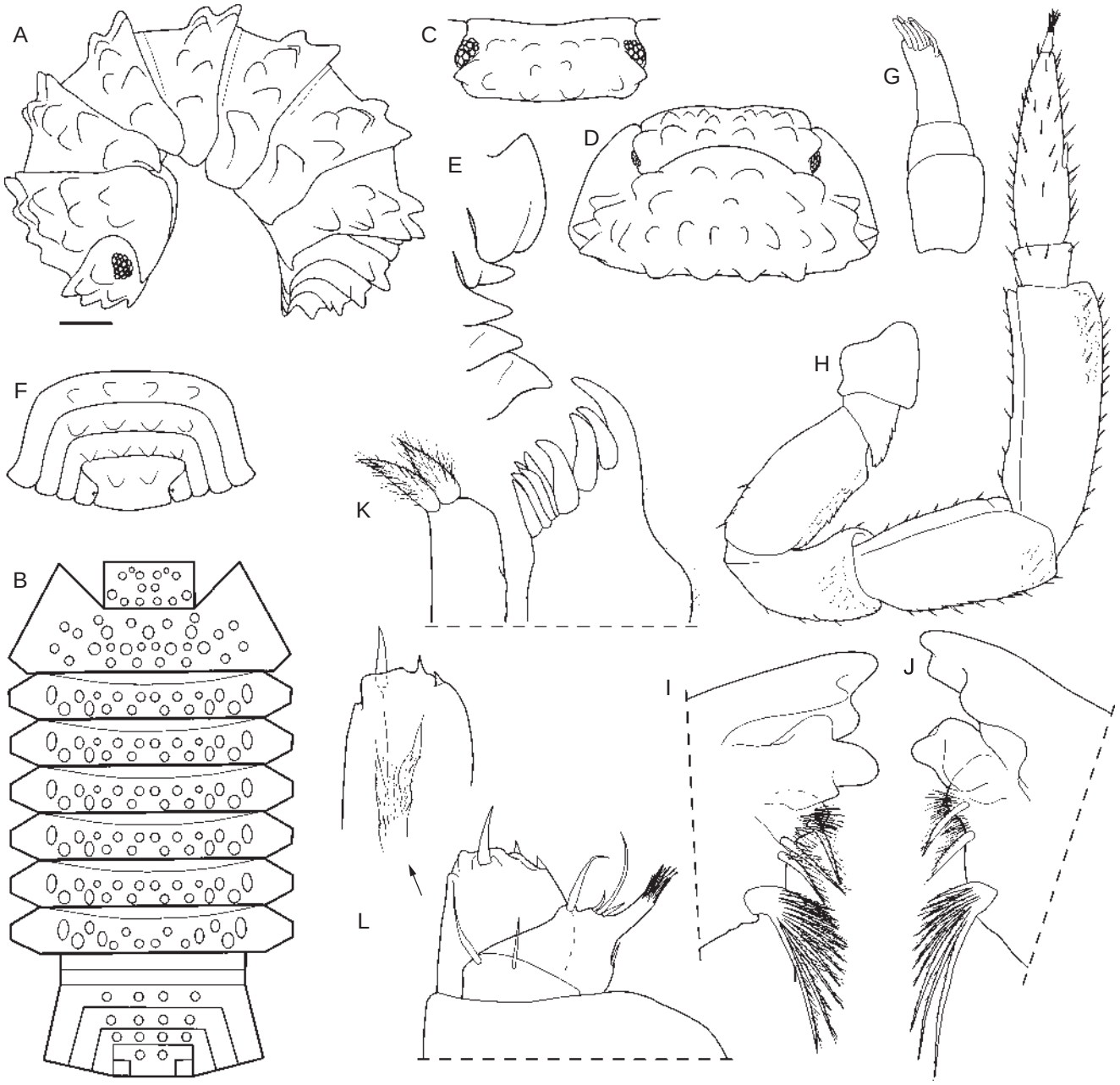


Fig. 5. — *Ctenorillo araguaia* Cardoso & Ferreira, n. sp. paratype (male, 5 mm, ISLA96784): **A**, habitus, lateral view; **B**, disposition of dorsal tubercles; **C**, cephalon, dorsal view; **D**, cephalon and pereonite 1, dorsal view; **E**, epimera 1-5 ventral view; **F**, pleonites 3-5, uropods and telson, dorsal view; **G**, antennula; **H**, antenna; **I**, right mandible; **J**, left mandible; **K**, maxillula; **L**, maxilliped. Scale bar: 0.5 mm.

DISTRIBUTION.— Serra dos Martírios/Andorinhas State Park in São Geraldo do Araguaia municipality, Pará state.

DESCRIPTION

Maximum size: ♂, 5 mm, ♀, 6 mm. Color grey with lateral margins depigmented (Fig. 27C). Dorsum covered with conical tubercles and lateral ribs (Figs 5A, B; 28E): cephalon with three rows (6, 2, and 6 from front to back of vertex); pereonite 1 with 27 in four rows (4, 7, 10 and 6); pereonites 2-6 with 18 (10 + 8); pereonite 7 with 14 (6 + 8); pleonites 3-5 with one row of four tubercles; telson with two paramedian tubercles. Dorsal cuticle (Fig. 28E) with short triangular scale setae; pereonites 1-7 bearing one line of *noduli lateralis* per side on outer surface of posterior tubercle of second line of tubercle. Cephalon with frontal shield directed upward; eye consisting of 16 ommatidia (Fig. 5C, D). Pereonite 1 with posterior margin sinuous at sides; inner lobe of schisma rounded, extending beyond posterior margin of outer lobe; pereonite 2 with triangular ventral tooth reaching epimeron posterior margin (Fig. 5E). Pereonites 2-7 (Fig. 5A) with wide quadrangular epimera slightly bent outwards. Telson (Fig. 5F) hourglass-shaped, proximal portion broader than distal portion. Antennula (Fig. 5G) of three articles, second article

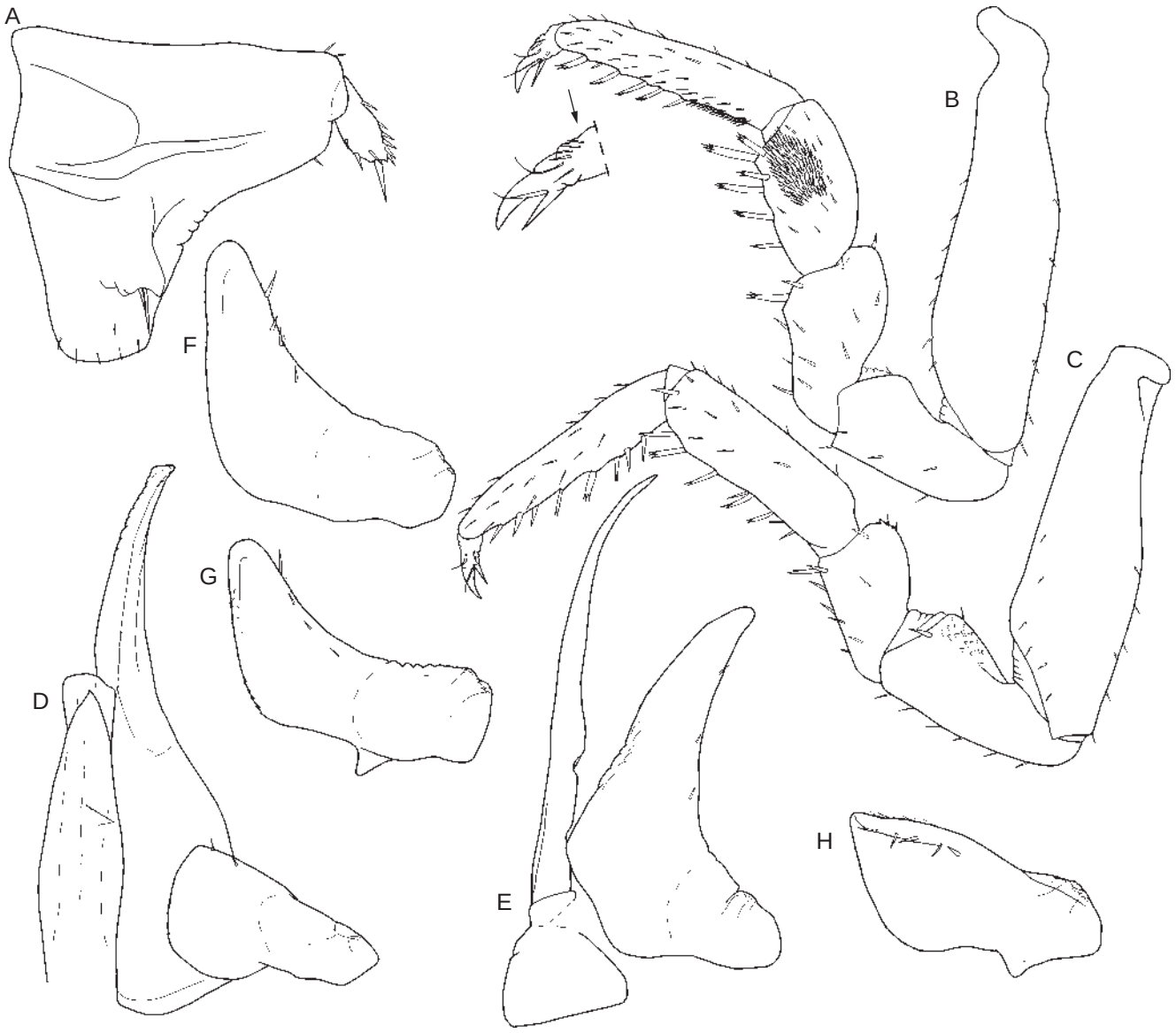


Fig. 6. — *Ctenorillo araguaia* Cardoso & Ferreira, n. sp. paratype (male, 5 mm, ISLA96784): **A**, uropod, **B**, pereopod 1; **C**, pereopod 7; **D**, pleopod 1 and genital papilla; **E**, pleopod 2; **F**, pleopod 3 exopod; **G**, pleopod 4 exopod; **H**, pleopod 5 exopod.

shorter than first and third, third article with six apical and one subapical aesthetascs. Antenna (Fig. 5H) short and stout, flagellum shorter than fifth article of peduncle; second article of flagellum about four times as long as first. Buccal pieces as *C. pelado* Cardoso & Ferreira, n. sp. (Fig. 5I-L). All pleopod exopods with monospiracular covered lungs. Uropod (Fig. 6A) protopod flattened, enlarged on basal portion; exopod very short, inserted dorsally close to medial margin of protopod.

Male

Pereopods without particular modifications (Fig. 6B, C). Pleopod 1 exopod (Fig. 6D) wider than long, distal portion round, outer margin straight; endopod four times longer than exopod, distal portion slightly bent outwards, slightly swollen. Pleopod 2 endopod longer than exopod (Fig. 6E). Pleopods 3-5 exopods as in Figure 6F-H.

HABITAT

Specimens of *C. araguaia* Cardoso & Ferreira, n. sp. were found in the Andorinhas cave and in Remanso dos Botos cave which are quartzite caves located in the Serra das Andorinhas Mountain Range (also known as Serra dos Martírios). The regional climate is classified, according to Köppen, as Aw5 (Tropical climate with dry season or Humid Equatorial), with annual rainfall between 1000 mm and 1500 mm and an average annual temperature of 26°C (22°-32°C). The rela- tive humidity is high and varies from 25% to 90% with an average of 78% (Alvares *et al.* 2013).

The Andorinhas cave is 1 km long, featuring entrances on both the side cliffs covered by Amazonian Forest and the mountaintop covered by savannah vegetation (Fig. 7A, B). During the rainy season, an intermittent drainage flows through the cave. A large colony of insectivorous bats (*Pter-*



Fig. 7. — *Ctenorillo araguaia* Cardoso & Ferreira, n. sp.: **A**, quartzite outcrops on the Serra das Andorinhas mountain range; **B**, entrance of the Andorinhas cave, where specimens are found; **C**, inner portion of the Andorinhas cave; **D**, habitus in natural condition.

onotus sp.) inhabits some inner and isolated parts of the cave, producing a massive guano piles that cover the floor of several conduits and chambers. In upper areas of the cave conduit (Fig. 7C) away from the bat colony, specimens of *C. araguaia* Cardoso & Ferreira, n. sp. were found under rocks (Fig. 7D). Given the lack of bat guano in that part of the cave, it is probable that the new species feeds on plant debris carried by floods and deposited along this conduit. In contrast, the Remanso dos Botos cave is smaller (125 m) and located at a lower altimetric level of the hill. The main organic deposits in this cave are guano produced by bats with distinct feeding habits, such as frugivory (*Carolia* sp.) and insectivory (*Peropteryx* sp. and *Natalus* sp.). Moreover, seeds transported by the bats germinate, resulting in sprouts that were also consumed by some invertebrates. Specimens of *C. araguaia* Cardoso & Ferreira, n. sp. were observed on the cave floor in deeper areas of the cave, as in the Andorinhas cave.

The caves are located in the Serra dos Martírios/Andorin- has State Park, which preserves the mountain top and cliffs. However, the surrounding landscape has been significantly impacted, particularly by deforestation for agriculture. The Andorinhas cave receives sporadic visitors, likely due to the difficult access to the cave. It is worth noting that the occurrence of *C. araguaia* Cardoso & Ferreira, n. sp. in these caves does not imply that the species is restricted to this habitat, especially considering the absence of any obvious troglomorphic traits. Therefore, further studies, including external samplings, are needed to better understand the distribution of the species.

Remark

Ctenorillo araguaia Cardoso & Ferreira, n. sp. is similar to *C. pelado* Cardoso & Ferreira, n. sp., presenting two tubercles on pereonite 1 and lateral ribs from pereonites 2 to 7, but differs in the number of tubercles on pereonite 1 (27 vs 24 in *C. pelado* Cardoso & Ferreira, n. sp.), in the number of tubercles on pereonites 2 to 7 (18 tubercles on pereonites 2 to 6 and 14 on pereonite 7 vs *C. pelado* Cardoso & Ferreira, n. sp. with 12 tubercles on pereonites 2 to 7).

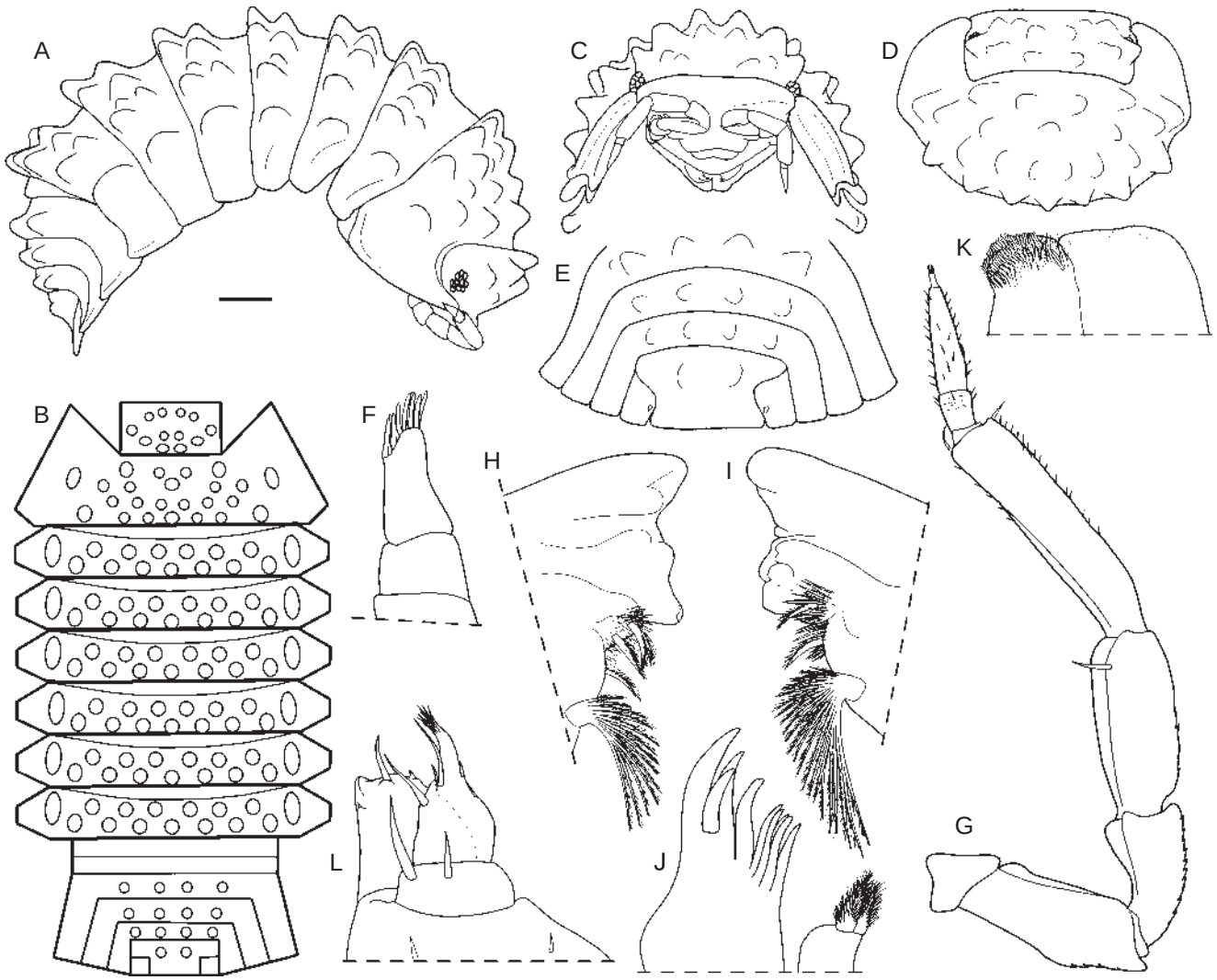


Fig. 8. — *Ctenorillo intertidalis* Cardoso & Ferreira, n. sp., paratype (male, 7.5 mm, ISLA96786): **A**, habitus, lateral view; **B**, disposition of dorsal tubercles; **C**, cepha- lon and pereonite 1, frontal view; **D**, cephalon and pereonite 1, dorsal view; **E**, pleonites 3-5, uropods and telson, dorsal view; **F**, antennula; **G**, antenna; **H**, right mandible; **I**, left mandible; **J**, maxillula; **K**, maxilla; **L**, maxilliped. Scale bar: 0.5 mm.

Ctenorillo intertidalis Cardoso & Ferreira, n. sp. (Figs 8-10; 27D; 28F, G)

urn:lsid:zoobank.org:act:B61E5142-E53A-4AD7-AF85-B24944928069

TYPE MATERIAL.— **Holotype. Brazil** • 1 ♂ (6 mm; parts in slide); Ceará state; Jijoca de Jericoacoara municipality; Jeri_10 cave; 2°47'12"S, 40°30'12"W; 25.IX.2019; R.L. Ferreira leg.; ISLA96786. **Paratypes. Brazil** • 2 ♂, 9 ♀; same data as holotype; ISLA96787.

OTHER MATERIAL. — **Brazil.** Ceará state; Jijoca de Jericoacoara municipality • 10 ♂, 12 ♀; Jeri_4 cave; 2°47'18"S, 40°30'42"W; 25.IX.2019; R.L. Ferreira leg.; ISLA96788 1 ♂ in slide. Jeri_4 cave; ISLA96789 • 10 ♂, 11 ♀; Jeri_7 cave; 2°47'16"S, 40°30'34"W; 24.IX.2019; R.L. Ferreira leg.; ISLA96790 • 11 ♂, 7 ♀; Jeri_8; 2°47'17"S, 40°30'32"W; 24.IX.2019; R.L. Ferreira leg.; ISLA96791 1 ♂ in slide; Jeri_8; 24.IX.2019; R.L. Ferreira leg.; ISLA96792 • 7 ♂, 1 ♀; Duas bocas cave; 2°47'16"S, 40°30'33"W; 24.IX.2019; R.L. Ferreira leg.; ISLA96793 • 1 juv.; Jeri Novo cave; 2°47'15"S, 40°30'33"W; 25.IX.2019; R.L. Ferreira leg.; ISLA 96800.

ETYMOLOGY. — The new species name is a noun in apposition that refers to area in where the caves are located, close to the beach, in an intertidal area.

DIAGNOSIS.— Dorsum covered with conical tubercles and lateral ribs with three rows on cephalon (4, 2, 6); four rows on pereonite 1 (4, 7, 6, 7); two rows on pereonites 2-7 (8 + 7); one row of four tubercles on pleonites 3-5; and two paramedian tubercles on telson. Pleopod 1 exopod distal portion round, sinuous outer margin; endopod with distal portion slightly bent outward, three times longer than exopod.

DISTRIBUTION. — Jericoacoara National Park, municipality of Jijoca de Jericoacoara, North of Ceará state.

DESCRIPTION

Maximum size: ♂ and ♀, 7.5 mm. Color grey with lateral margins depigmented. Dorsum covered with conical tubercles and lateral ribs (Figs 8A, B; 28F, G): cephalon with three rows (4, 2, and 6 from front to back of vertex); pereonite 1 with 24 in four rows (4, 7, 6 and 7); pereonites 2-7

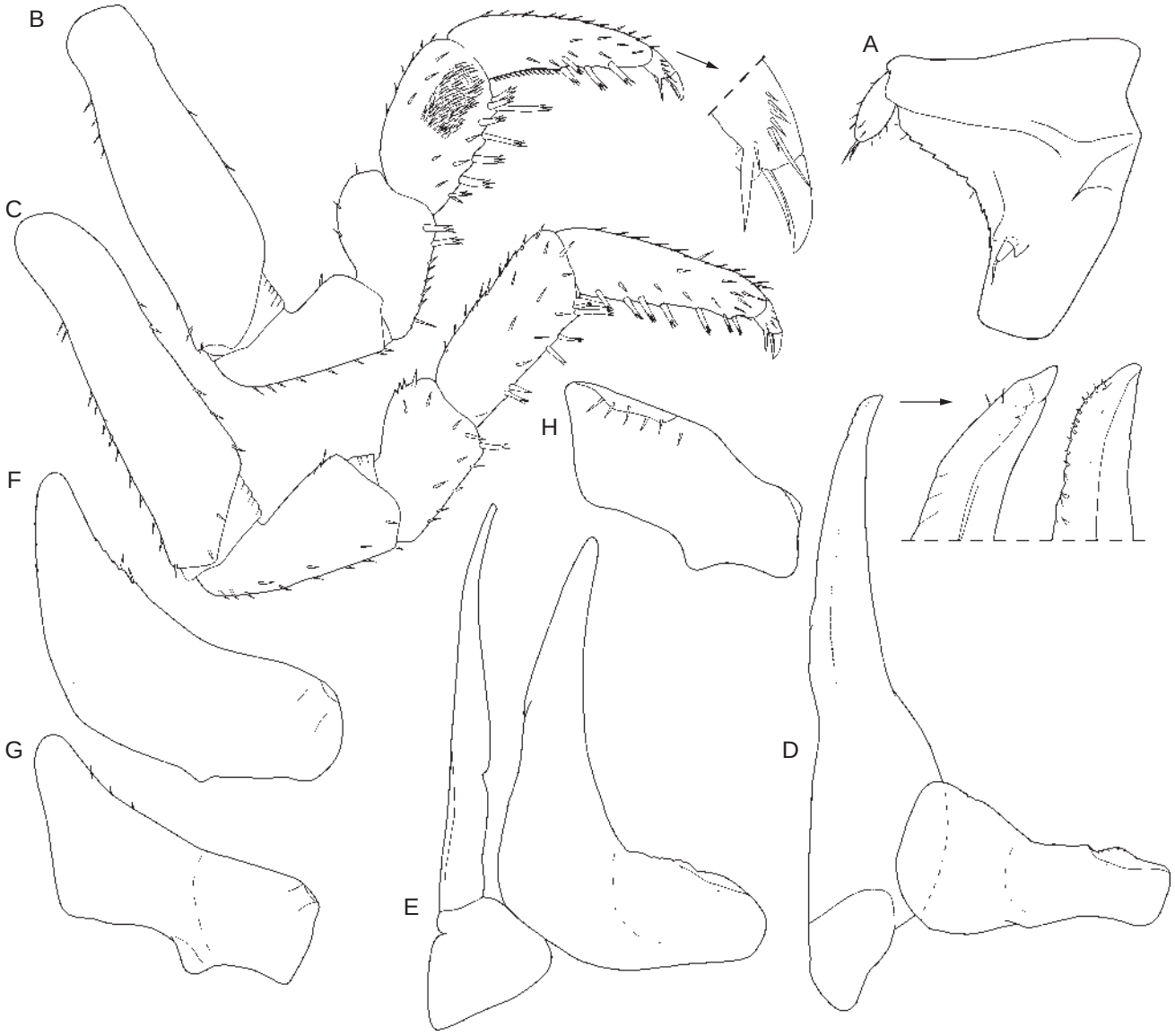


Fig. 9. — *Ctenorillo intertidalis* Cardoso & Ferreira, n. sp. paratype (male, 7.5 mm, ISLA96786): **A**, uropod, **B**, pereopod 1; **C**, pereopod 7; **D**, pleopod 1 and genital papilla; **E**, pleopod 2; **F**, pleopod 3 exopod; **G**, pleopod 4 exopod; **H**, pleopod 5 exopod.

with 15 (8 + 7); pleonites 3-5 with one row of four tubercles; telson with two paramedian tubercles. Dorsal cuticle (Fig. 28G) with short triangular scale setae, pereonites 1-7 bearing one line of *noduli lateralis* per side on outer surface of posterior tubercle of second tubercle. Cephalon with frontal shield protruding above vertex; eye consisting of 10 ommatidia (Figs 8A, C, D; 28F). Pereonite 1 with posterior margin sinuous at sides; inner lobe of schisma rounded, extending beyond posterior margin of outer lobe; pereonite 2 with triangular ventral tooth reaching epimeron posterior margin (Fig. 8C). Pereonites 2-7 (Fig. 8A) with wide quadrangular epimera slightly bent outwards. Telson (Fig. 8E) hourglass-shaped, proximal portion broader than distal portion. Antennula (Fig. 8F) of three articles, second article shorter than first and third, third article with four apical and five subapical aesthetascs. Antenna (Fig. 8G) short and stout, flagellum shorter than fifth article of peduncle; second article of flagellum about twice as long as first. Buccal pieces as *C. pelado* Cardoso & Ferreira, n. sp. (Fig. 8H-L), except maxillula (Fig. 8J) with 4 + 6 simple teeth. All pleopod exopods with monospiracular covered lungs. Uropod (Fig. 9A) protopod flattened, enlarged on basal portion; exopod outward, short, inserted dorsally close to medial margin of protopod.

Male

Pereopods without particular modifications (Fig. 9B, C). Pleopod 1 exopod (Fig. 9D) wider than long, distal portion round, sinuous outer margin; endopod three times longer than exopod, distal portion slightly bent outwards. Pleopod 2 endopod longer than exopod (Fig. 9E). Pleopods 3-5 exopods as in Figure 9F-H.



Fig. 10. — *Ctenorillo intertidalis* Cardoso & Ferreira, n. sp.: **A**, quartzite outcrops on the shoreline of Jericoacoara, with a cave entrance (**yellow star**); **B**, inner portion of a cave where specimens are found; **C**, *Ctenorillo intertidalis* Cardoso & Ferreira, n. sp. specimen; **D**, habitus in natural condition sharing the habitat (under rocks) with other isopods.

Habitat

Specimens of *C. intertidalis* Cardoso & Ferreira, n. sp. were found in six caves in quartzite outcrops on the shoreline (Fig. 10A, B), near the village of Jericoacoara, in the municipality of Jijoca de Jericoacoara. The climate is classified as hot and humid (Aw'sg. Köppen), with summer rains from January to July. Temperatures range from 25°C to 35°C, and the dry season lasts about six months and is often interrupted by heavy rains in October or September (Alvares *et al.* 2013).

The new species was found in six out of eight sampled caves in the area. The caves are quite small presenting, on average, 14.48 (± 7.48) meters of horizontal projection. Thus, most of them were devoid of aphotic zones. Specimens of *C. intertidalis* Cardoso & Ferreira, n. sp. were observed under rocks, sheltered from the wind off the coast (Fig. 10C). The organic matter inside the caves consisted of plant debris (brought by the wind or the tides, in caves closer to the sea) and bat guano in some caves (produced by the piscivorous *Noctilio leporinus* (Linnaeus, 1758)). In some caves, individuals of *C. intertidalis* Cardoso & Ferreira, n. sp. were observed co-occurring with another isopod species (Fig. 10D). The external environment comprises a "restinga" ecosystem dominated by herbaceous vegetation, which grows along the dunes. Thus, there are few external shelters for these organisms. As the samplings that resulted in the discovery of this new species focused specifically on caves, the actual extent of *C. intertidalis* Cardoso & Ferreira, n. sp. habitat is currently unknown, but their distribution may be much wider than that observed in this work, especially considering the lack of troglomorphic traits in this species.

The region is inserted in the Jericoacoara National Park, so the area and the caves are currently protected. Nonetheless, it is noteworthy that there is no regulation of visitor access to these caves, and due to the region's popularity as a tourist destination, uncontrolled foot traffic may inadvertently pose a threat to the invertebrate populations, including those of the newly discovered species.

Remark

Ctenorillo intertidalis Cardoso & Ferreira, n. sp. resembles *C. pelado* Cardoso & Ferreira, n. sp. in the number of tubercles on pereonite 1 (24), however the disposition with the presence of a lateral rib is similar to *C. ferrarai*, differing from both by the number of tubercles on pereonites 2 to 7 (15).

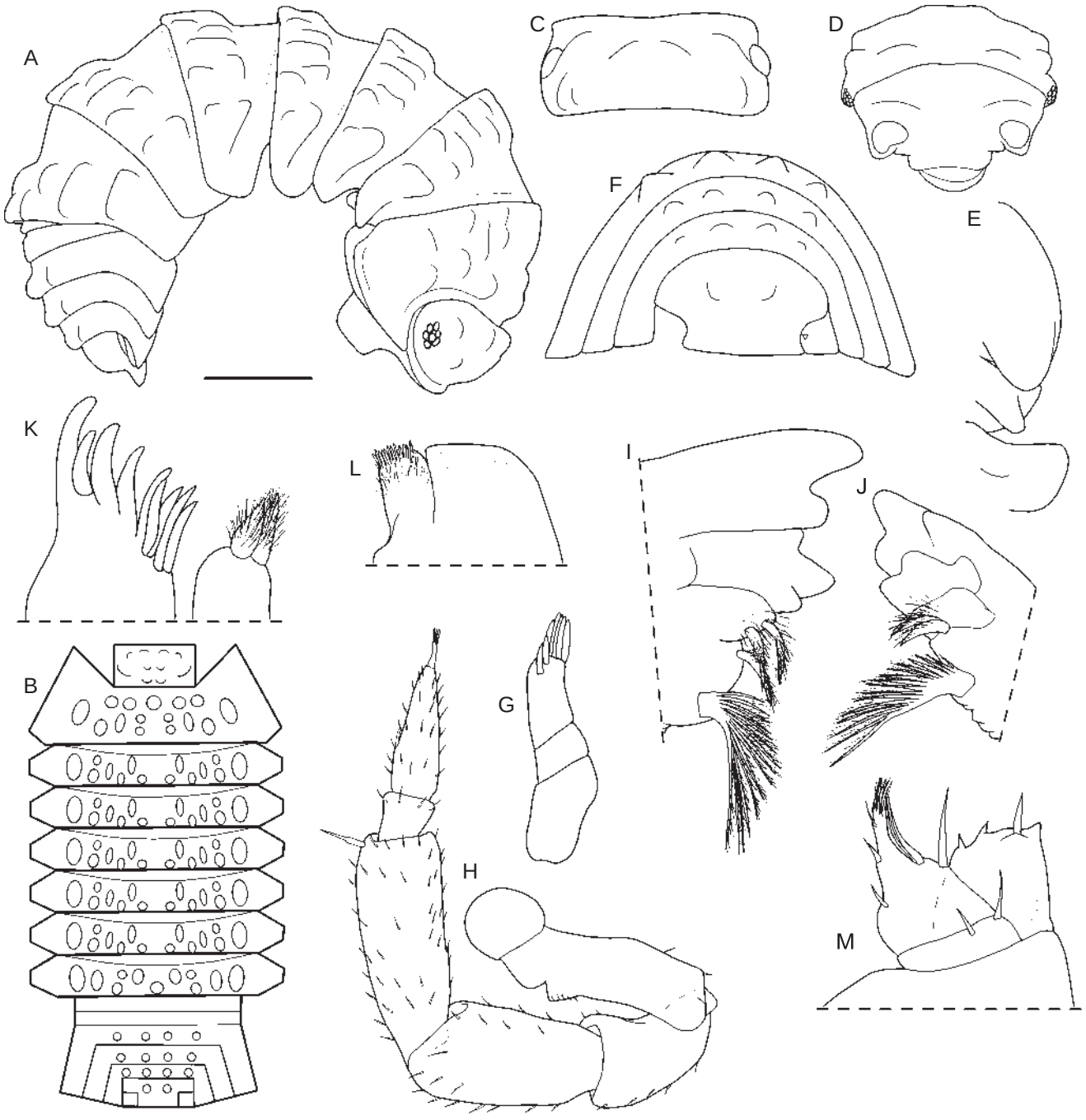


Fig. 11. — *Ctenorillo ubajarensis* Cardoso & Ferreira, n. sp., paratype (male, 6.5 mm, ISLA96794): **A**, habitus, lateral view; **B**, disposition of dorsal tubercles; **C**, cephalon, dorsal view; **D**, cephalon, frontal view; **E**, epimera 1-3 ventral view; **F**, pleonites 3-5, uropod and telson, dorsal view; **G**, antennula; **H**, antenna; **I**, right mandible; **J**, left mandible; **K**, maxillula; **L**, maxilla; **M**, maxilliped. Scale bar: 0.5 mm.

Ctenorillo ubajarensis Cardoso & Ferreira, n. sp. (Figs 11-13; 27E; 28H)

urn:lsid:zoobank.org:act:4C100618-9E25-499A-8078-F462716289C2

TYPE MATERIAL. — **Holotype. Brazil** • 1 ♂ (4 mm); Ceará state; Ubajara municipality; Urso Fóssil cave; 3°49'59"S, 40°53'32"W; 22.I.2019; R.L. Ferreira leg.; ISLA96794.
Paratypes. Brazil • 4 ♂, 5 ♀; same data as holotype; ISLA96795.

OTHER MATERIAL. — **Brazil** • 1 ♀; Ceará state; Ubajara municipality; Macaco Fóssil cave; 3°49'45"S, 40°54'6"W; 24.I.2019; R.L. Ferreira leg.; ISLA96796 • 1 ♀; Ubajara municipality; Pendurado cave; 3°50'4"S, 40°53'35"W; 25.I.2019; R.L. Ferreira leg.; ISLA96797.

ETYMOLOGY. — The new species name is a noun that refers to the type locality (the Ubajara National Park).

DIAGNOSIS. — Dorsum covered by bosses, more developed posteriorly with three rows on cephalon (4, 2, 4); three rows on pereonite 1 (5, 2, 8); two rows on pereonites 2-6 (6 + 6) and on pereonite 7 (6 + 5);



Fig. 12. — *Ctenorillo ubajarensis* Cardoso & Ferreira, n. sp., paratype (male, 6.5 mm, ISLA96794): **A**, uropod, **B**, pereopod 1; **C**, pereopod 7; **D**, pleopod 1 and genital papilla; **E**, pleopod 2; **F**, pleopod 3 exopod; **G**, pleopod 4 exopod; **H**, pleopod 5 exopod.

one row of four tubercles on pleonites 3-5; and two paramedian tubercles on telson. Pleopod 1 exopod with protruding distal portion, triangular, outer margin concave and crenulate; endopod with distal portion straight, slightly swollen, five times longer than exopod.

Distribution. — Ubajara National Park, Ubajara municipality, Ceará state.

Description

Maximum size: ♂, 5 mm, ♀, 6.5 mm. Color brown in nature (Figs 13C; 27E). Dorsum covered by bosses, more developed posteriorly (Figs 11A, B; 28H): cephalon with three rows (4, 2, and 4 from front to back of vertex); pereonite 1 with 15 in three rows (5, 2 and 8); pereonites 2-6 with 14 (6 + 6); pereonite 7 with 11 (6 + 5); pleonites 3-5 with one row of four tubercles; telson with two paramedian tubercles. Dorsal cuticle with short triangular scale setae; pereonites 1-7 bearing one line of *noduli lateralis* per side on the outer surface of posterior boss of second line (Fig. 28H). Cephalon with frontal shield protruding above vertex; eye consisting of eight ommatidia (Figs 11C; 28H). Pereonite 1 inner lobe of schisma rounded, extending beyond posterior margin of outer lobe; pereonite 2 with triangular ventral tooth reaching epimeron posterior margin (Fig. 11E); pereonites 2-7 with wide quadrangular epimera (Fig. 11A). Telson (Fig. 11F) hourglass-shaped, proximal portion broader than distal portion. Antennula (Fig. 11G) of three articles, second article shorter than first and third, third article with five apical and two subapical aesthetascs. Antenna (Fig. 11H) short and stout, flagellum shorter than fifth article of peduncle; second article of flagellum about twice as long as first. Buccal



Fig. 13. — *Ctenorillo ubajarensis* Cardoso & Ferreira, n. sp.: **A**, limestone outcrops at the Ubajara National Park; **B**, entrance of the Urso Fóssil cave, where specimens are found; **C**, habitus in natural condition.

pieces as *C. pelado* Cardoso & Ferreira, n. sp. (Fig. 11I-M). All pleopod exopods with monospiracular covered lungs. Uropod (Fig. 12A) protopod flattened, enlarged on basal portion; exopod outward, short, inserted dorsally close to medial margin of protopod.

Male

Pereopods without particular modifications (Fig. 12B, C). Pleopod 1 exopod (Fig. 12D) wider than long, protruding distal portion, triangular, outer margin concave and crenulate; endopod with distal portion straight, slightly swollen, five times longer than exopod. Pleopod 2 endopod longer than exopod (Fig. 12E). Pleopods 3-5 exopods as in Figure 12F-H.

HABITAT

Specimens of *C. ubajarensis* Cardoso & Ferreira, n. sp. were found in three caves located at the Ubajara National Park (Fig. 13A). These caves are associated with limestones from the Frecheirinha Formation, Ubajara karst Group (Neoproterozoic). This region experiences two distinct climatic seasons: the rainy period when 94% of rainfall occurs (from January to June), and the dry period that is practically without rain (from July to December). The average annual temperature ranges from 20°C to 22°C in Serra da Ibiapaba and around 24°C to 26°C in the peripheral depression. June and July are typically the warmest months, while October and November are the hottest (Alvares *et al.* 2013).

The Urso Fóssil cave, in which most of the specimens were found, extends up to 195 meters in length and has four entrances located along the cave main conduit (Fig. 13B). Most parts of the cave receive some light from the external environment, and aphotic areas are relatively few. Although this cave is located within the limits of the National Park, in which caves are important touristic attractions, tourists do not regularly visit this cave. However, it has been the target of several paleontological excavations in recent decades, which, on the one hand, revealed the great fossiliferous importance of this cave but, on the other hand, ended up altering several of its microhabitats. Most specimens of *C. ubajarensis* Cardoso & Ferreira, n. sp. (Fig. 13C) were found in Urso Fóssil cave, beneath fallen rocks or blocks on the cave floor. Additional specimens were observed in two other nearby caves (Pendurado and Macaco caves), with only one specimen found in each of these caves. Since external inventories were not conducted during our visit to the area, it is not possible to determine the actual distribution of this species, but it certainly occurs in external habitats in the caves' surroundings. Since the area is legally protected, the species is apparently not under any threat.

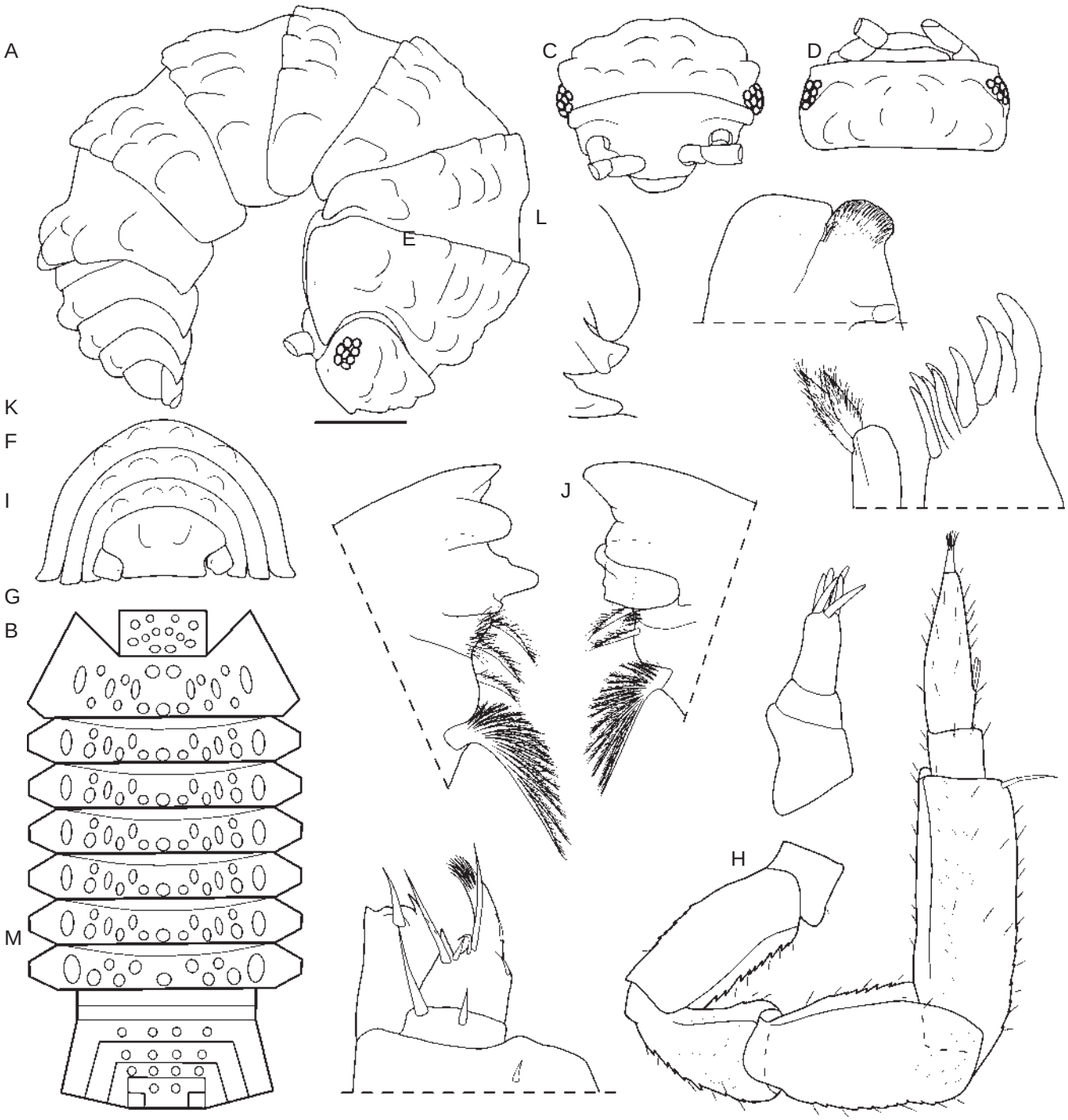


Fig. 14. — *Ctenorillo cearensis* Cardoso & Ferreira, n. sp., holotype (male, 4 mm, ISLA96021): **A**, habitus, lateral view; **B**, disposition of dorsal tubercles; **C**, cephalon, frontal view; **D**, cephalon, dorsal view; **E**, epimera 1-3 ventral view; **F**, pleonites 3-5, uropods and telson, dorsal view; **G**, antennula; **H**, antenna; **I**, right mandible; **J**, left mandible; **K**, maxillula; **L**, maxilla; **M**, maxilliped. Scale bar: 0.5 mm.

REMARK

Ctenorillo ubajarensis Cardoso & Ferreira, n. sp., like *C. kenyensis* Schmölzer, 1974, differ from the congeneric species by the less developed tubercles, however in *C. ubajarensis* Cardoso & Ferreira, n. sp. the tubercles are more like bosses and are slightly more developed on pereonite 7, while on *C. kenyensis* they are granulated and densely distributed dorsally.

Ctenorillo cearensis Cardoso & Ferreira, n. sp.
(Figs 14; 15; 27F)

urn:lsid:zoobank.org:act:29FFBB09-6896-4C9B-97BE-E50E44C7C180

TYPE MATERIAL. — **Holotype. Brazil** • 1 ♂ (4 mm; parts in slide); Ceará state; Santa Quitéria municipality; W_04 cave; 4°33'53"S, 39°46'36"W; Carste leg.; 10-18.III.2021; ISLA96021.

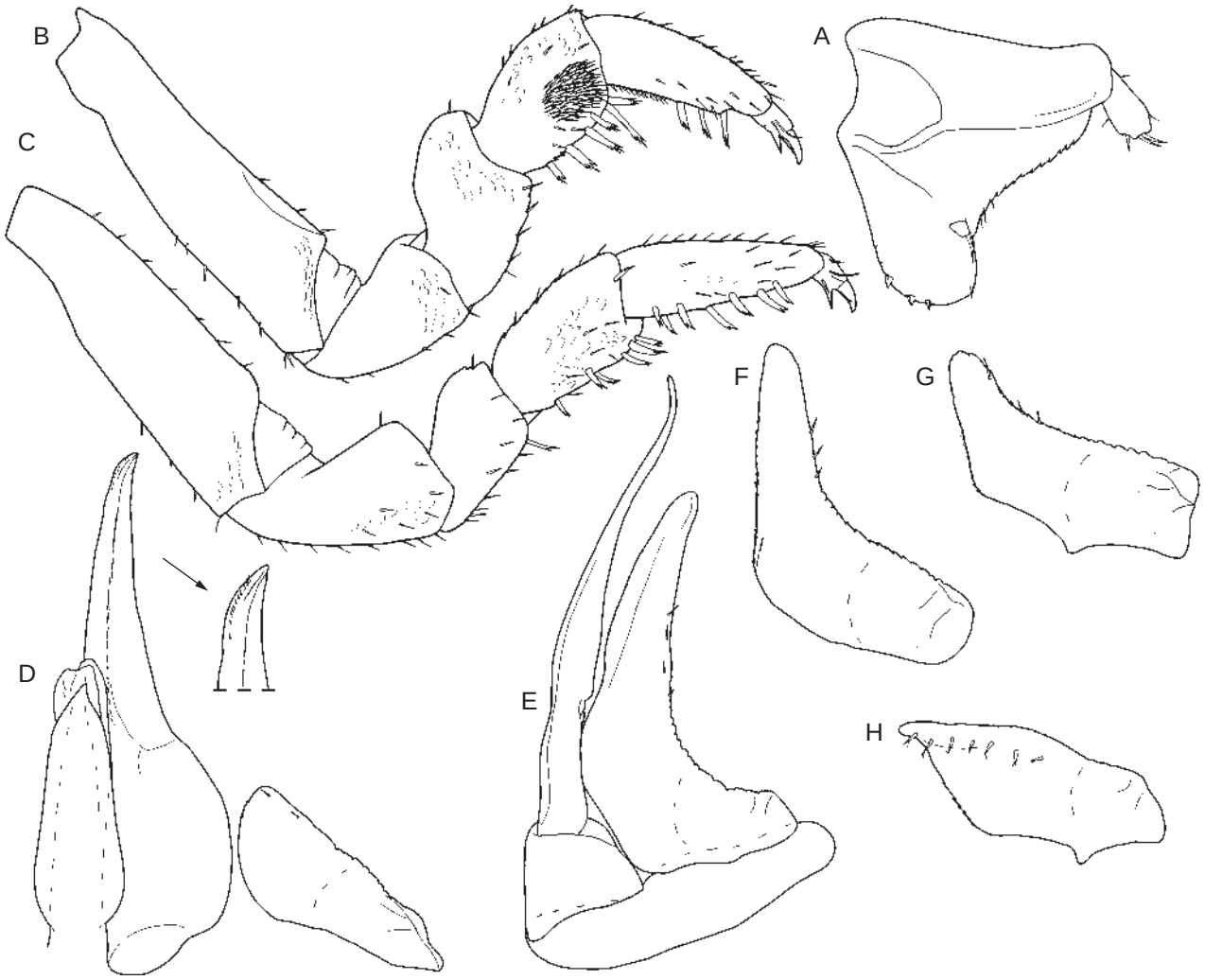


Fig. 15. – *Ctenorillo cearensis* Cardoso & Ferreira, n. sp., paratype (male, 4 mm, ISLA96021): **A**, uropod, **B**, pereopod 1; **C**, pereopod 7; **D**, pleopod 1 and genital papilla; **E**, pleopod 2; **F**, pleopod 3 exopod; **G**, pleopod 4 exopod; **H**, pleopod 5 exopod.

OTHER MATERIAL. — **Brazil** • 1 ♂; SQ_26 cave; 4°33'38"S, 39°46'51"W; Carste leg.; 10-18.III.2021; ISLA96020 • 1 ♀; W_16 cave; 4°33'43"S, 39°46'44"W; Carste leg.; 10-18.III.2021; ISLA96026 • 1 ♀; SQ_03 cave; 4°33'53"S, 39°46'40"W; Carste leg.; 10-18.III.2021; ISLA96033 • 2 ♂; SQ_P2 cave; 4°33'37"S, 39°45'57"W; Carste leg.; 10-18.III.2021; ISLA96962 • 3 ♀; SQ_03 cave; 4°34'4"S, 39°47'0"W; Carste leg.; 10-18.III.2021; ISLA96025.

ETYMOLOGY. — The new species name, "cearensis", refers to the people who are born in the State of Ceará, Brazil. The word Ceará comes from the tupy language that means the macaw's singing (o canto dajanaia in Portuguese).

DIAGNOSIS.— Dorsum covered by weakly developed tubercles and ribs with three rows on cephalon (4, 4, 4); three rows on pereonite 1 (2, 8, 9); two rows on pereonites 2-6 (4 + 11) and on pereonite 7 (4 + 7); one row of four tubercles on pleonites 3-5; and two paramedian tubercles on telson. Pleopod 1 exopod with round distal portion, outer margin straight; endopod with distal portion straight, four times longer than exopod.

DISTRIBUTION. — Santa Quitéria municipality, Ceará state.

DESCRIPTION

Maximum size: ♂ and ♀, 4 mm. Color grey (Fig. 27F). Dorsum covered by weakly developed tubercles and ribs (Fig. 14A, B): cephalon with three rows (4, 4, and 4 from front to back of vertex); pereonite 1 with 15 in three rows (2, 8 and 9); pereonites 2-6 with 15 (4 + 11); pereonite 7 with 11 (4 + 7); pleonites 3-5 with one row of four tubercles; telson with two paramedian tubercles. Dorsal cuticle with short triangular scale setae; pereonites 1-7 bearing one line of *noduli lateralis* per side on outer surface of posterior tubercle of second line of tubercle. Cephalon with frontal shield protruding above vertex; eye consisting of eight ommatidia (Fig. 14C, D). Pereonite 1 inner lobe of schisma rounded, extending beyond posterior margin of outer lobe; pereonite 2 with triangular ventral tooth reaching posterior margin of epimera (Fig. 14E); pereonites 2-7 with wide quadrangular epimera (Fig. 14A). Telson (Fig. 14F) hourglass-shaped, proximal portion broader than distal portion. Antennula (Fig. 14G) of three articles, second article shorter than first and third, third article with six apical aesthetascs. Antenna (Fig. 14H) short and stout,

flagellum shorter than fifth article of peduncle; second article of flagellum about three times as long as first. Buccal pieces as *C. pelado* Cardoso & Ferreira, n. sp. (Fig. 14I-M). All pleopod exopods with monospiracular covered lungs. Uropod (Fig. 15A) protopod flattened, enlarged on basal portion; exopod outward, short, inserted dorsally close to medial margin of protopod.

Male

Pereopods without particular modifications (Fig. 15B, C). Pleopod 1 exopod (Fig. 15D) wider than long, round distal portion, outer margin straight; endopod with distal portion straight, four times longer than exopod. Pleopod 2 endopod longer than exopod (Fig. 15E). Pleopods 3-5 exopods as in Figure 15F-H.

HABITAT

Specimens of *C. cearensis* Cardoso & Ferreira, n. sp. were found in six limestone caves inserted in the caatinga biome in northern Ceará state. The region experiences a Tropical Hot Semi-arid climate (BSh according to Koppen), with an average annual rainfall of 799.8 mm concentrated between February and April (Álvares *et al.* 2013). Average temperatures in the region hover around 27°C, with approximately 3°C of thermal amplitude (IPECE 2011). The area features three types of vegetation: Tropical Steppe, located in both the residual massifs and dissected areas of the Sertaneja Depression; Thorny Deciduous Forest and Tropical Rainforest. Unfortunately, the biologists who collected the specimens did not provide any data on the caves or the conservation status of the surrounding region. However, at least 74 caves were inventoried in the region, and specimens of *C. cearensis* Cardoso & Ferreira, n. sp. were found only in six of them. As mentioned for other species herein described, external inventories were not conducted, hence it is not possible to determine the actual distribution of this species. Nonetheless, the species does not present any troglomorphic traits, which would suggest its restriction to subterranean habitats. Importantly, the cave inventories were conducted to rank the importance of the caves in the area, as required by Brazilian environmental agencies for evaluating projects that may impact the environment. The potential installation of quarries in the area is a cause for concern since the limestone caves in the region are located close to uranium deposits (Júnior & de Souza 2012), and such enterprises could destroy the caves where the species occurs and severely alter the surrounding external habitats.

REMARKS

As *C. ubajarensis* Cardoso & Ferreira, n. sp., *C. cearensis* Cardoso & Ferreira, n. sp. presents the less developed tubercles, however the tubercles are more prominent than in *C. cearensis* Cardoso & Ferreira, n. sp. As the other Brazilian species, *C. cearensis* Cardoso & Ferreira, n. sp. presents the pleonites 3-5 with four tubercles each and differs from them by the number of tubercles on pereon, with 19 tubercles on pereonite 1, 15 on pereonites 2-6, and 11 on pereonite 7.

Ctenorillo quiteriensis Cardoso & Ferreira, n. sp.
(Figs 16; 17; 27G)

urn:lsid:zoobank.org:act:660D19DD-C840-4D69-A90B-F85FA9E916E8

TYPE MATERIAL. — **Holotype. Brazil** • 1 ♂ (7 mm) (part in slide); Ceará state; Santa Quitéria municipality; SQ_39; 4°33'42"S, 39°46'46"W; 10-18.III.2021; Carste leg.; ISLA96038.

OTHER MATERIAL. — **Brazil** • 1 ♀; Ceará state; Santa Quitéria municipality; SQ_P12; 4°33'39"S, 39°45'48"W; 10-18.III.2021; Carste leg.; ISLA96059.

ETYMOLOGY. — The new species name is a noun in apposition that refers to the people who are born in the municipality where the specimens were found (Santa Quitéria).

DIAGNOSIS. — Dorsum covered with conical tubercles and lateral ribs with three rows on cephalon (4, 2, 6); four rows on pereonite 1 (4, 5, 10, 7); two rows on pereonites 2-4 (8 + 7) and on pereonites 5-7 (10 + 7); one row of four tubercles on pleonites 3-5; and two paramedian tubercles telson. Pleopod 1 exopod with protruding distal portion, triangular, outer margin straight; endopod with distal portion straight, slightly swollen, three times longer than exopod.

DISTRIBUTION. — Santa Quitéria municipality, Ceará state.

DESCRIPTION

Maximum size: ♂ and ♀, 7 mm. Color brown with lateral margin depigmented (Fig. 27G). Dorsum covered with conical tubercles and lateral ribs (Fig. 16A-C): cephalon with three rows (4, 2, and 6 from front to back of vertex); pereonite 1 with 26 in four rows (4, 5, 10 and 7); pereonites 2-4 with 15 (8 + 7); pereonites 5-7 with 17 (10 + 7); pleonites 3-5 with one row of four tubercles; telson with two paramedian tubercles. Dorsal cuticle with short triangular scale setae; pereonites 1-7 bearing one line of *noduli lateralis* per side on outer surface of posterior tubercle of second line of tubercles. Cephalon with frontal shield protruding above vertex; eye consisting of eight ommatidia (Fig. 16A, D). Pereonite 1 with poste- rior margin distinctly sinuous at sides; inner lobe of schisma rounded, extending beyond posterior margin of outer lobe; pereonite 2 with triangular ventral tooth reaching posterior margin of epimera (Fig. 16E). Pereonites 2-7 (Fig. 16A) with wide quadrangular epimera slightly bent outwards. Telson (Fig. 16F) hourglass-shaped, proximal portion broader than distal portion. Antennula (Fig. 16G) of three articles, second article shorter than first and third, third article with three apical and five subapical aesthetascs. Antenna (Fig. 16H) short and stout, flagellum shorter than fifth article of peduncle; second article of flagellum about three times as long as first. Buccal pieces as *C. pelado* Cardoso & Ferreira, n. sp. (Fig. 16I-K). All pleopod exopods with monospiracular covered lungs. Uropod (Fig. 17A) protopod flattened, enlarged on basal portion; exopod very short, inserted dorsally close to medial margin of protopod.

Male

Pereopods without particular modifications (Fig. 17B, C). Pleopod 1 exopod (Fig. 17D) wider than long, protruding distal portion, triangular, outer margin straight; endopod with

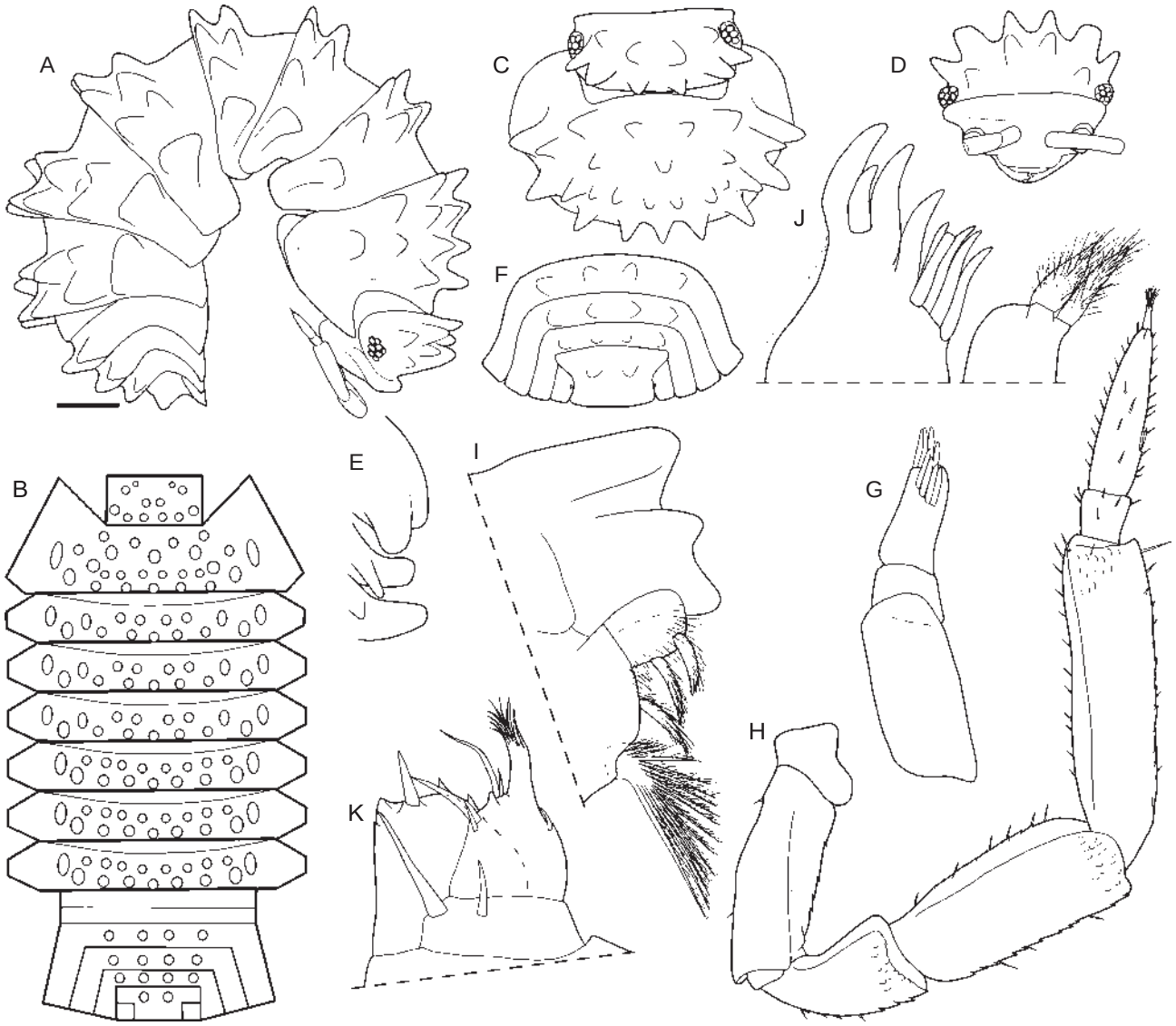


Fig. 16. — *Ctenorillo quiteriensis* Cardoso & Ferreira, n. sp., holotype (male, 7 mm, ISLA96038): **A**, habitus, lateral view; **B**, disposition of dorsal tubercles; **C**, cephalon and epimeron 1, dorsal view; **D**, cephalon, frontal view; **E**, epimera 1-3 ventral view; **F**, pleonites 3-5, uropods and telson, dorsal view; **G**, antennula; **H**, antenna; **I**, right mandible; **J**, maxillula; **K**, maxilliped. Scale bar: 0.5 mm.

distal portion straight, slightly swollen, three times longer than exopod. Pleopod 2 endopod longer than exopod (Fig. 17E). Pleopods 3-5 exopods as in Figure 17F-H.

Habitat

Specimens of *C. quiteriensis* Cardoso & Ferreira, n. sp. were found in two limestone caves inserted in the caatinga biome in northern Ceará state. The regional climate is also classified as BSh according to the Köppen system, characterized by the same patterns of precipitation and temperature as described for *C. cearensis* Cardoso & Ferreira, n. sp. Also, no data were available about the caves or the conservation status of the surrounding region. Regrettably, external inventories were not conducted during the sampling process in the area, making it difficult to determine the precise distribution of this species. It is likely that *C. quiteriensis* Cardoso & Ferreira, n. sp. occurs in external habitats surrounding the caves, as observed in other species described here. As with *C. cearensis* Cardoso & Ferreira, n. sp., the establishment of quarries for uranium extraction in the future could pose a significant threat to the habitats of this newly discovered species. It is essential to undertake further studies to determine the extent of its distribution and the potential impacts of anthropogenic activities in the region to develop conservation strategies to safeguard this species.

Remarks

Ctenorillo quiteriensis Cardoso & Ferreira, n. sp. occur in the same region as *C. cearensis* Cardoso & Ferreira, n. sp. and they clearly differ in the shape and number of tubercles, being more developed in *C. quiteriensis* Cardoso & Ferreira, n. sp. On pereonite 1, *C. quiteriensis* Cardoso & Ferreira, n. sp. presents 26 tubercles, resembling *C. ferrarai* in the presence of a lateral rib on the pereonites that are more developed posteriorly.



Fig. 17. — *Ctenorillo quiteriensis* Cardoso & Ferreira, n. sp., holotype (male, 7 mm, ISLA96038): **A**, uropod, **B**, pereopod 1; **C**, pereopod 7; **D**, pleopod 1 and genital papilla; **E**, pleopod 2; **F**, pleopod 3 exopod; **G**, pleopod 4 exopod; **H**, pleopod 5 exopod.

Ctenorillo potiguar Cardoso & Ferreira, n. sp. (Figs 18-20; 27H; 28I)

urn:lsid:zoobank.org:act:53D58AC8-70BA-48E8-A228-4F455E72B475

TYPE MATERIAL. — **Holotype**. **Brazil** • 1 ♂ (3 mm, parts in slide); Rio Grande do Norte state; Baraúna municipality; Furna Nova cave; 5°2'3"S, 37°34'16"W; 12.VI.2008; D.M. Bento leg.; ISLA96798. **Paratypes. Brazil** • 2 ♀; same data as holotype; ISLA96799.

OTHER MATERIAL. — **Brazil.** Rio Grande do Norte; Baraúna municipality • 1 ♂, 2 ♀; Furna Feia cave; 5°2'12"S, 37°33'36"W; 31.VII.2010; D.M. Bento leg.; ISLA59267 • 2 ♂; Esquecida cave; 5°2'16"S, 37°33'40"W; 12.VI.2010; D.M. Bento leg.; ISLA59283 1 ♀; same collection data as for preceding; ISLA59333 • 1 ♀; Britador cave; 11.VI.2010; D.M. Bento leg.; ISLA59263.

Brazil. Rio Grande do Norte; Felipe Guerra municipality • 1 ♂, 1 ♀; Crotes cave; 5°33'37"S, 37°39'30"W; 4.VI.2010; D.M. Bento leg.; ISLA59330 • 2 ♀; same collection data as for preceding; ISLA59282 1 ♂; Trapiá cave; 5°33'45"S, 37°37'15"W; 4.VIII.2010; D.M. Bento leg.; ISLA59270.

ETYMOLOGY. — The new species name is a noun in reference to people who are born in the State of Rio Grande do Norte, Brazil.

DIAGNOSIS. — Dorsum covered with round tubercles and ribs with three rows on cephalon (4, 4, 6); four rows on pereonite 1 (4, 5, 8, 9); two rows on pereonites 2-7 (8 + 7); one row of four tubercles on pleonites 3-5 with; two paramedian tubercles on telson. Pleopod 1 exopod with round distal portion, outer margin straight; endopod with distal portion bent outward, four times longer than exopod.

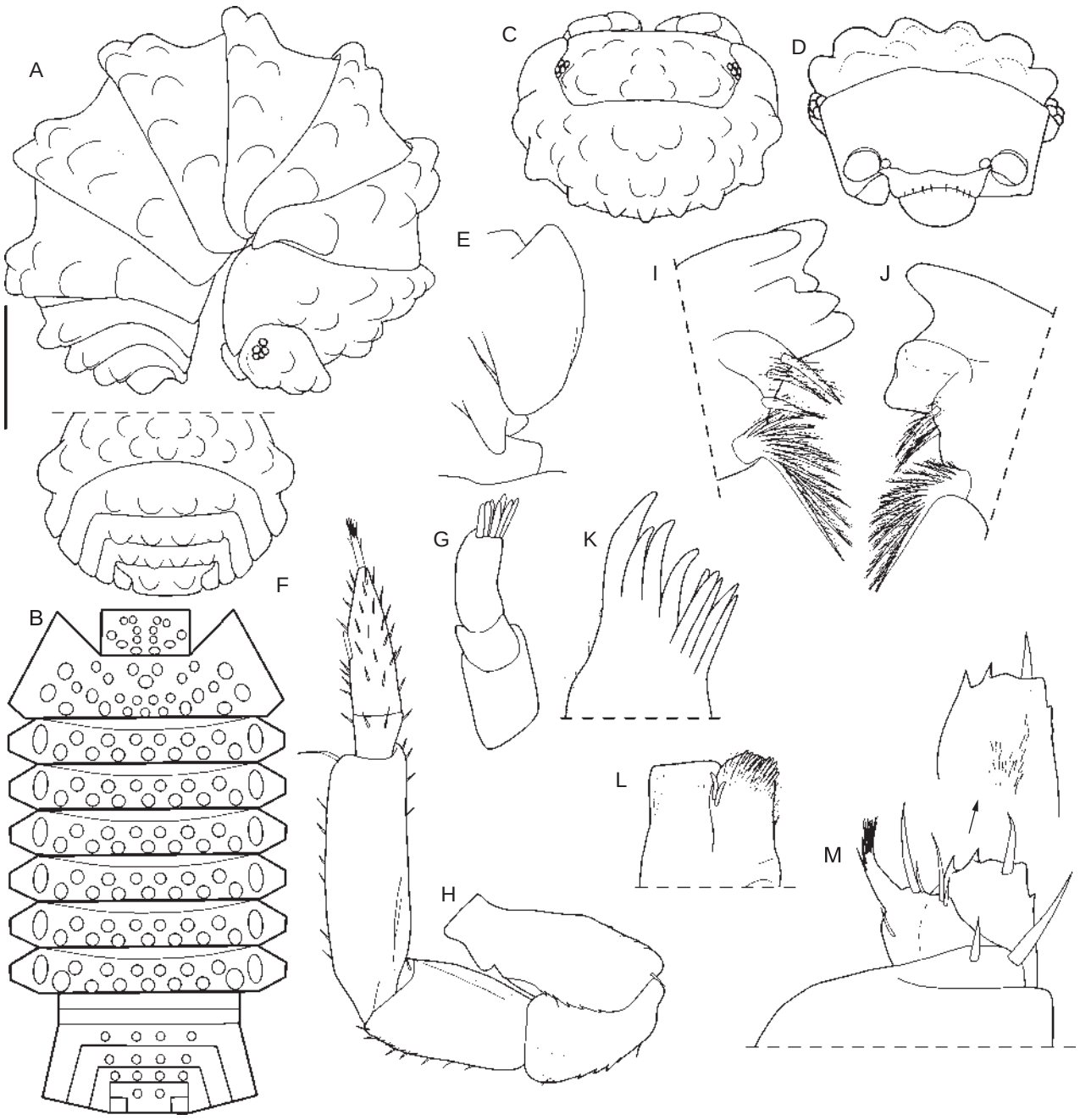


Fig. 18. — *Ctenorillo potiguar* Cardoso & Ferreira, n. sp., paratype (male, 3 mm, ISLA96798): **A**, habitus, lateral view; **B**, disposition of dorsal tubercles; **C**, cephalon and epimeron 1, dorsal view; **D**, cephalon, frontal view; **E**, epimera 1-3, ventral view; **F**, epimeron 7, pleonites 3-5, uropods and telson, dorsal view; **G**, antennula; **H**, antenna; **I**, right mandible; **J**, left mandible; **K**, maxillula; **L**, maxilla; **M**, maxilliped. Scale bar: 0.5 mm.

DISTRIBUTION. — Baraúna and Felipe Guerra municipalities, west of the Rio Grande do Norte state.

DESCRIPTION

Maximum size: ♂, 3 mm, ♀, 4 mm. Color brown with lateral margins depigmented in nature (Figs 20D; 27H). Dorsum covered with round tubercles and ribs (Fig. 18A, B): cephalon with three rows (4, 4, and 6 from front to back of vertex); pereonite 1 with 26 in four rows (4, 5, 8 and 9); pereonites 2-7 with 15 (8 + 7); pleonites 3-5 with one row of four tubercles; telson with two paramedian tubercles. Dorsal cuticle with short triangular scale setae; pereonites 1-7 bearing one line of *noduli lateralis* per side on outer surface of posterior tubercle of second tubercles (Fig. 28I). Cephalon with frontal shield protruding above vertex; eye consisting of five ommatidia (Figs 18C, D; 28I). Pereonite 1 with posterior margin sinuous at sides; inner lobe of schisma rounded, extending beyond posterior margin of outer lobe; pereonite 2 with triangular ventral tooth reaching posterior margin of epimera (Fig. 18E). Pereonites 2-7 (Fig. 18A) with wide quadrangular epimera slightly bent outwards. Telson (Fig. 18F) hourglass-shaped, proximal portion broader than

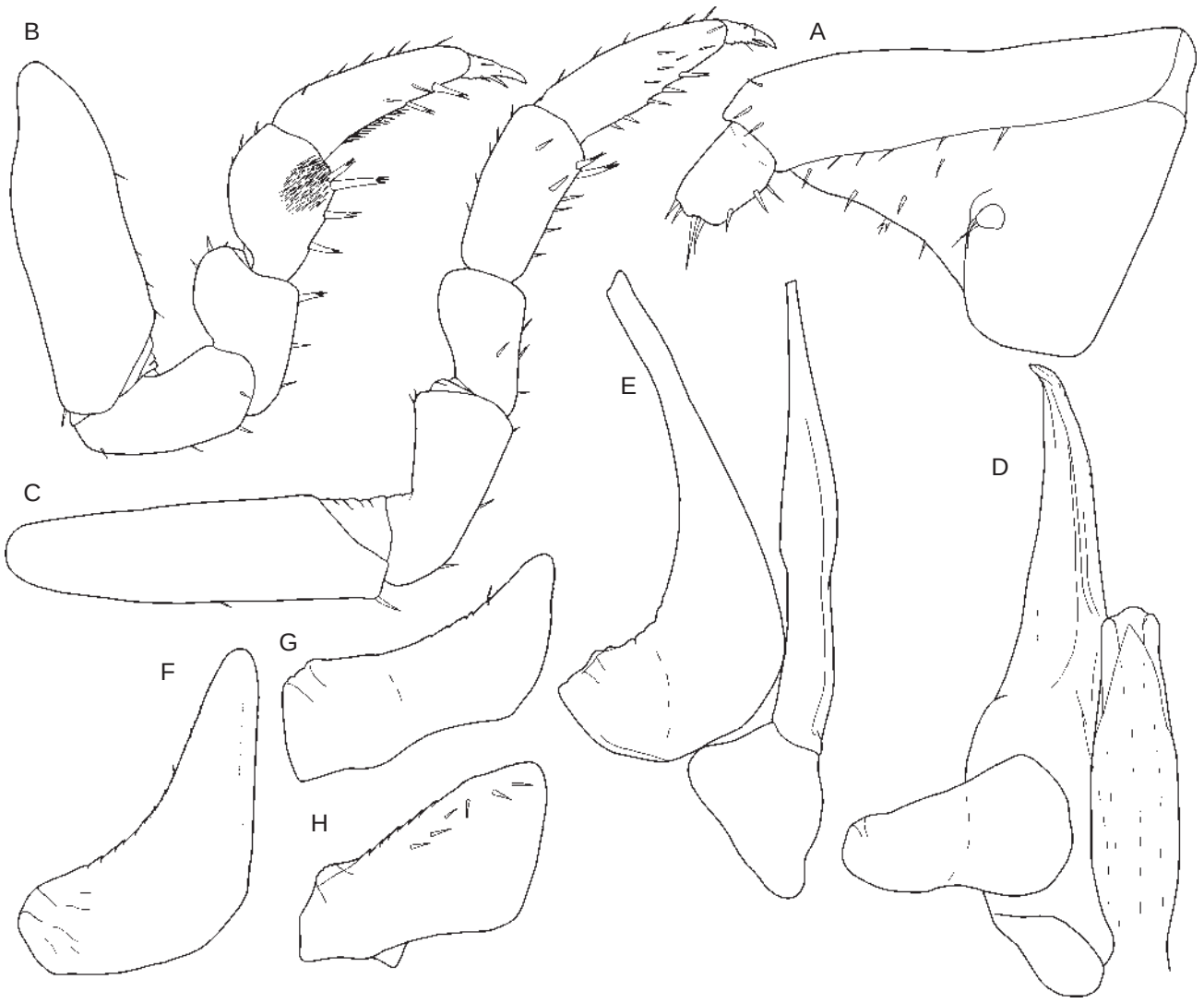


Fig. 19. — *Ctenorillo potiguar* Cardoso & Ferreira, n. sp., paratype (male, 3 mm, ISLA96798): **A**, uropod, **B**, pereopod 1; **C**, pereopod 7; **D**, pleopod 1 and genital papilla; **E**, pleopod 2; **F**, pleopod 3 exopod; **G**, pleopod 4 exopod; **H**, pleopod 5 exopod.

distal portion. Antennula (Fig. 18G) of three articles, second article shorter than first and third, third article with seven apical aesthetascs. Antenna (Fig. 18H) short and stout, flagellum shorter than fifth article of peduncle; second article of flagellum about three times as long as first. Buccal pieces as *C. pelado* Cardoso & Ferreira, n. sp. (Fig. 18I-M). All pleopod exopods with monospiracular covered lungs. Uropod (Fig. 19A) protopod flattened, enlarged on basal portion; exopod outward, short, inserted dorsally close to medial margin of protopod.

Male

Pereopods without particular modifications (Fig. 19B, C). Pleopod 1 exopod (Fig. 19D) wider than long, round distal portion, outer margin straight; endopod with distal portion bent outward, four times longer than exopod. Pleopod 2 endopod longer than exopod (Fig. 19E). Pleopods 3-5 exopods as in Figure 19F-H.

HABITAT

Specimens of *Ctenorillo potiguar* Cardoso & Ferreira, n. sp. were found in six caves located in the west of the Rio Grande do Norte state. This region has more than 1000 currently known caves (CANIE/CECAV 2022), but only about 48 have been inventoried (Ferreira *et al.* 2010; Bento *et al.* 2021). The caves are inserted in the limestones of the Janaíra Formation, deposited during the Upper Cretaceous, which corresponds to a carbonate ramp that emerged along the emersed portion of the Potiguar Basin (Bezerra *et al.* 2007). The region is in the Caatinga Biome, with a hot and semiarid climate (BSh on the Köppen climate classification) (Alvares *et al.* 2013). The average temperature is constant over the year, ranging from 25° to 30°C, with average annual precipitation around 800 mm (concentrated from February to June, but 70% can fall in a single month) (Silva *et al.* 2017).

Three caves, Furna Feia (Fig. 20A, B), Furna Nova (Fig. 20C) and Macacos/Esquecida, are located in the Furna Feia Na-

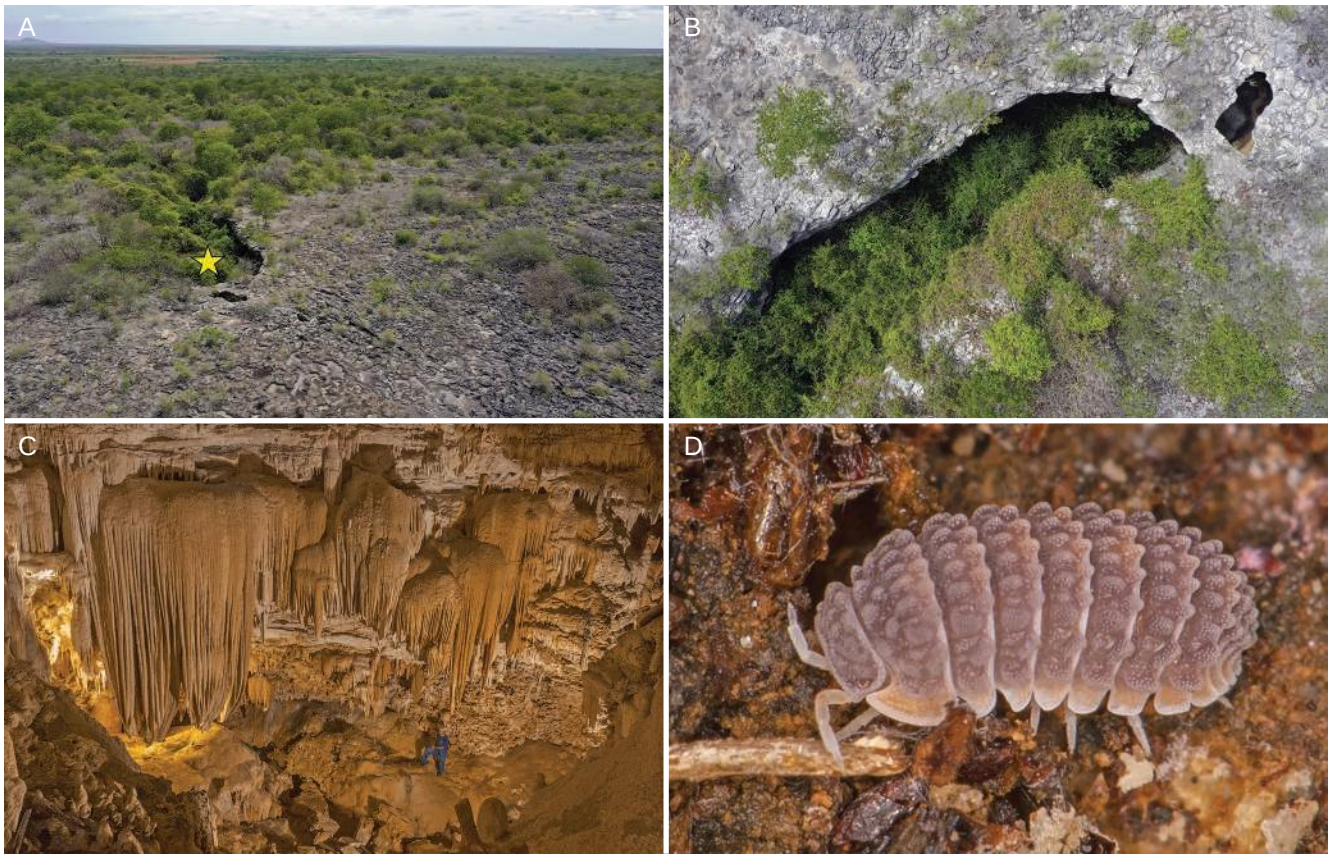


Fig. 20. — *Ctenorillo potiguar* Cardoso & Ferreira, n. sp.: **A**, limestone outcrops at the Furna Feia National Park, with the entrance of the Furna Feia cave (**yellow star**); **B**, detail of the Furna Feia cave entrance; **C**, inner portion of the Furna Nova cave, where specimens are found; **D**, habitus in natural condition.

tional Park (FFNP) in the municipality of Baraúna. Specimens were also found in the Britador cave, near FFNP, in Baraúna. Other specimens were found in Trapiá and Crotes caves, in the municipality of Felipe Guerra (RN), 60 km from the first ones. These caves exhibit varied morphology, dimensions, and environmental conditions, ranging from small photic caves spanning a few tens of meters (e.g. Britador cave) to large aphotic caves covering hundreds of meters and characterized by more stable climatic conditions (e.g. Furna Feia, Furna Nova, and Trapiá caves). Despite this distribution, individuals (Fig. 20D) were mainly found in aphotic and humid areas within the caves, often sheltered under rocks. This observation suggests that the species may have a specific habitat preference.

No samplings were conducted outside caves in the area, and it is likely that the species also occurs in surface habitats (espe- cially considering the absence of any obvious troglomorphic traits). Therefore, further studies including external samplings are needed to better understand the species distribution. Although only part of the distribution of the new species occurs within a conservation unit, the other caves are found in relatively conserved areas, without direct anthropic impacts. Three caves (Furna Feia, Furna Nova, and Crotes Caves) are visited by tourists in an orderly manner. Thus, the conservation status of the species can be considered of less concern.

REMARK

Ctenorillo potiguar Cardoso & Ferreira, n. sp. resembles *C. ubajarensis* Cardoso & Ferreira, n. sp. by the less developed tubercles, however they are more prominent on *Ctenorillo potiguar* Cardoso & Ferreira, n. sp. By the number of tubercles on pereonite 1, *Ctenorillo potiguar* Cardoso & Ferreira, n. sp. resembles *C. quiteriensis* Cardoso & Ferreira, n. sp. with 26 tubercles, differing by the shape.

Ctenorillo iuiuensis Cardoso & Ferreira, n. sp. (Figs 21-23; 27I)

urn:lsid:zoobank.org:act:0E0AFF4F-6924-438E-82A7-970FF1D1FD76

TYPE MATERIAL. — **Holotype. Brazil** • 1 ♂ (4 mm, parts in slide), Bahia state, Iuiu municipality, Lapa do Matias cave; 14°28'46"S, 43°36'50"W; R.L. Ferreira leg., 22.VII.2022; ISLA96802. **Paratypes. Brazil** • 2 ♀; same data as holotype; ISLA96803.

ETYMOLOGY. — The new species name "*iuiuensis*" refers to the municipality where the species inhabits.

DIAGNOSIS. — Dorsum covered with conical tubercles three rows on cephalon (2, 2, 2); three rows on pereonite 1 (4, 4, 11); two rows on pereonites 2-6 (6 + 7) and on pereonite 7 (6 + 5); and two paramedian tubercles on pleonites 3-5 and on telson. Pleopod 1 exopod with round distal portion, outer margin straight; endopod with distal portion slightly bent outward, five times longer than exopod.

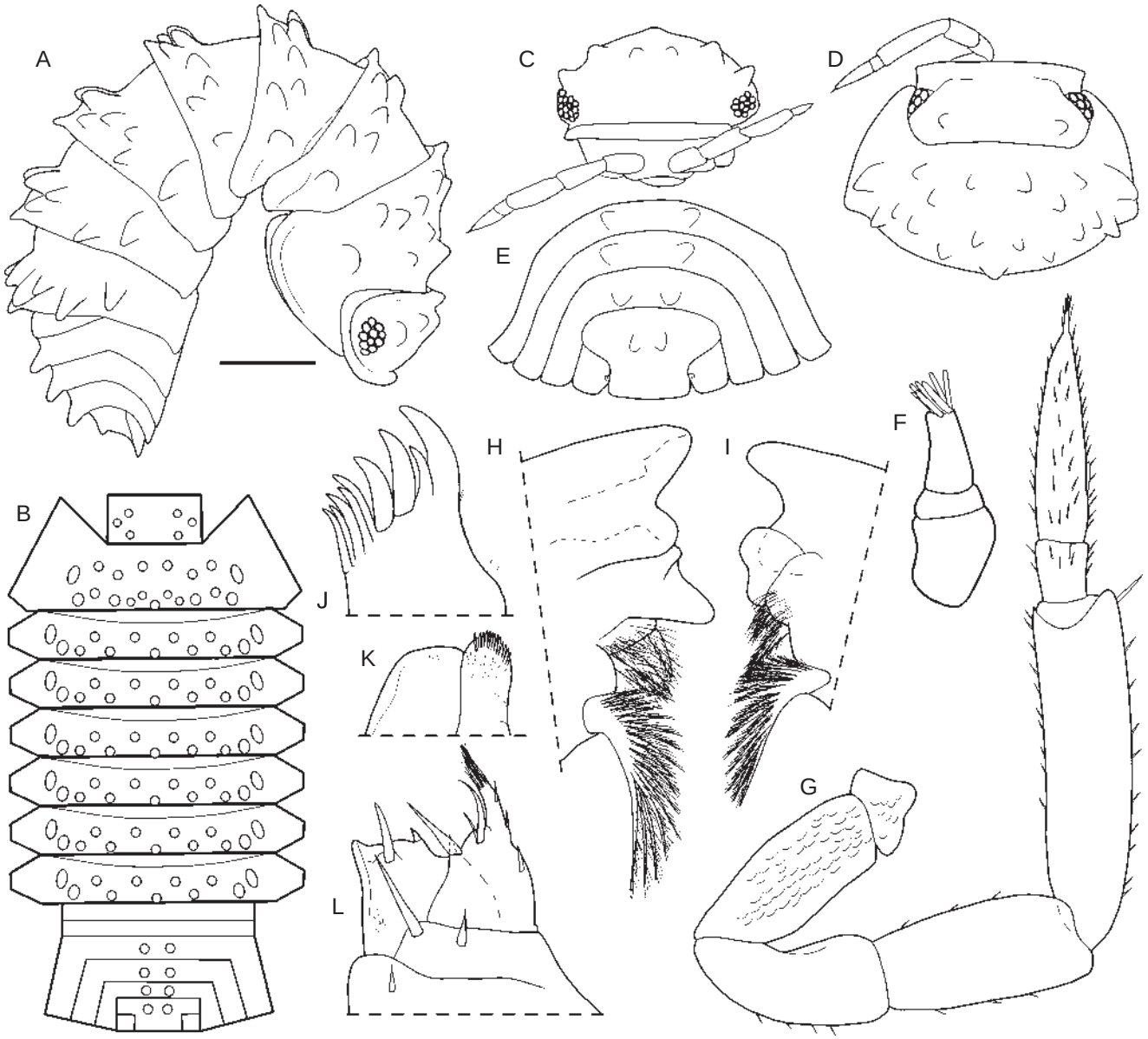


Fig. 21. — *Ctenorillo iuiuensis* Cardoso & Ferreira, n. sp., holotype (male, 4 mm, ISLA96802): **A**, habitus, lateral view; **B**, disposition of dorsal tubercles; **C**, cephalon, frontal view; **D**, cephalon and pereonite 1, dorsal view; **E**, pleonites 3-5, uropods and telson, dorsal view; **F**, antennula; **G**, antenna; **H**, right mandible; **I**, left mandible; **J**, maxillula; **K**, maxilla; **L**, maxilliped. Scale bar: 0.5 mm.

DISTRIBUTION. — Serra do Iuiu mountain range, Iuiu municipality, Bahia state.

DESCRIPTION

Maximum size: ♂ and ♀, 4 mm. Color pale (Fig. 27I). Dorsum covered with conical tubercles (Fig. 21A, B): cephalon with three rows (2, 2, and 2 from front to back of vertex); pereonite 1 with 19 in three rows (4, 4 and 11); pereonites 2-6 with 13 (6 + 7); pereonite 7 with 11 (6 + 5); pleonites 3-5 and telson with two paramedian tubercles. Cephalon with frontal shield protruding above vertex; eye consisting of 11 ommatidia (Fig. 21C, D). Pereonite 1 with posterior margin sinuous at sides; inner lobe of schisma rounded, extending beyond posterior margin of outer lobe; pereonite 2 with triangular ventral tooth reaching posterior margin epimera (Fig. 21A). Pereonites 2-7 (Fig. 21A) with wide quadrangular epimera slightly bent outwards. Telson (Fig. 21E) hourglass-shaped, proximal portion broader than distal portion. Antennula (Fig. 21F) of three articles, second article much shorter than first and third, third article with seven apical aesthetascs. Antenna (Fig. 21G) short and stout, flagellum shorter than fifth article of peduncle; second article of flagellum about three times as long as first. Buccal pieces as *C. pelado* Cardoso & Ferreira, n. sp. (Fig. 21H-L). All pleopod exopods with monospiracular covered lungs. Uropod (Fig. 22A) protopod flattened, enlarged on basal portion; exopod very short, inserted dorsally very close to medial margin of protopod.



Fig. 22. — *Ctenorillo iuiuensis* Cardoso & Ferreira, n. sp., holotype (male, 4 mm, ISLA96802): **A**, uropod, **B**, pereopod 1; **C**, pereopod 7; **D**, pleopod 1; **E**, pleo- pod 2; **F**, pleopod 3 exopod; **G**, pleopod 4 exopod; **H**, pleopod 5 exopod.

Male

Pereopods without particular modifications (Fig. 22B, C). Pleopod 1 exopod (Fig. 22D) wider than long, round distal portion, outer margin straight; endopod five times longer than exopod, distal portion slightly bent outward. Pleopod 2 endopod longer than exopod (Fig. 22E). Pleopods 3-5 exopods as in Figure 22F-H.

HABITAT

The Lapa do Matias cave, located in the Iuiú region, is the only place where specimens of *C. iuiuensis* Cardoso & Ferreira, n. sp. have been found, despite the extensive sampling of multiple caves in the region. The Iuiú region (northeastern Brazil) presents a significant karst area, known for its numerous caves and the occurrence of dozens of endemic species restricted to caves (Cardoso *et al.* 2021). This limestone formation is part of the Bambuí Group, the largest carbonate formation in South America. The landscape is situated within the Caatinga domain, with a seasonally dry tropical forest mostly found in the limestone outcrops due to past intensive land use. As per the Köppen-Geiger classification system, the climate in the area is semi-arid tropical (Bsh), with an annual precipitation of 788 mm and an average temperature of 24°C. The rainy season is from November to February while the dry season lasts from March to October.

The Lapa do Matias cave is located at the top of the outcrop at Serra do Iuiú, in a quite anthropized region (Fig. 23A). The cave is in a heavily human-impacted area with pastures and exposed soil, which increases erosion. Despite its small single entrance (Fig. 23B), the cave is voluminous and has two main conduits (Fig. 23C, D). A thorough search was carried out but only three specimens of *C. iuiuensis* Car- doso & Ferreira, n. sp. were found under limestone blocks in aphotic areas (Fig. 23E). It is worth noting that *C. iuiuensis*



Fig. 23. — *Ctenorillo iuiuensis* Cardoso & Ferreira, n. sp.: **A**, limestone outcrops at the surroundings of the Lapa do Matias cave (cave entrance indicated by the **yellow star**); **B**, detail of the Lapa do Matias cave entrance; **C**, inner portion of the Lapa do Matias cave, where specimens are found.

Cardoso & Ferreira, n. sp. displays some troglomorphic traits, including a lack of pigmentation in both the body integument and eyes. As this condition was observed in all collected specimens, and none of them appeared to have a soft exoskeleton (teneral aspect), it is likely that this species is troglobitic. However, as no samplings were conducted outside caves in the area, future research is needed to confirm or refute this diagnosis.

The Iuiú karst area has been facing severe threats, particularly due to changes in the surrounding environments, which have intensified over the last few decades. According to Cardoso *et al.* (2022), the land cover and land use practices surrounding the caves in this region have significantly influenced the subterranean environments, affecting both microhabitat features and terrestrial invertebrate communities. The authors have demonstrated that deforested areas have had adverse effects on subterranean invertebrate richness, mainly by altering the fauna composition and reducing subterranean microhabitat diversity. Additionally, this region is home to several endemic cave species (Ratton *et al.* 2012; Souza *et al.* 2015; Hoch & Ferreira 2016; Souza & Ferreira 2018; Cardoso *et al.* 2020), making it imperative for Brazilian environmental agencies to take urgent action to protect these caves in this important Brazilian karst area.

REMARK

Ctenorillo iuiuensis Cardoso & Ferreira, n. sp. differs from the Brazilian species by the presence of two paramedian tubercles on pleonites 3-5 and on telson.

Ctenorillo jequitinhonha Cardoso & Ferreira, n. sp. (Figs 24-26; 27J; 28J, K)

urn:lsid:zoobank.org:act:5CF8D003-88B7-465B-84EF-040FEC4FB7F2

TYPE MATERIAL. — **Holotype. Brazil** • 1 ♂ (7 mm, parts in slide), Minas Gerais state, Jequitinhonha municipality, Toca Juparanã cave; 16°25'3"S, 40°55'23"W; R.L. Ferreira leg., 7.IV.2017; ISLA96804. **Paratypes. Brazil** • 1 ♂ in slide; same data as holotype; ISLA96806 3 ♂, 8 ♀; same data as holotype; ISLA96805.

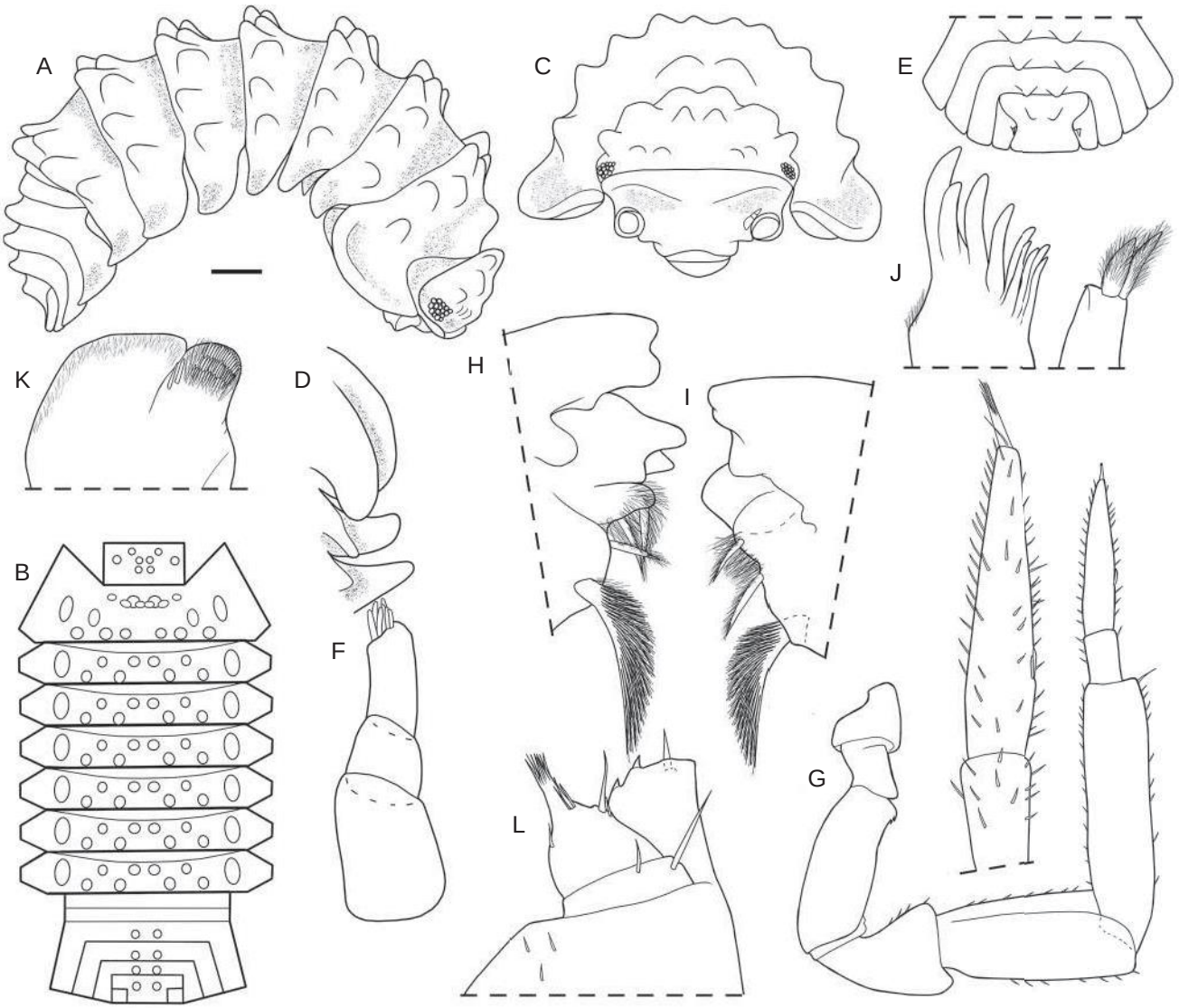


Fig. 24. — *Ctenorillo jequitinhonha* Cardoso & Ferreira, n. sp. paratype (male, 7 mm, ISLA96806): **A**, habitus, lateral view; **B**, disposition of dorsal tubercles; **C**, cephalon and epimeron 1, frontal view; **D**, epimera 1-3 ventral view; **E**, pleonites 3-5, uropods and telson, dorsal view; **F**, antennula; **G**, antenna; **H**, right man- dible; **I**, left mandible; **J**, maxillula; **K**, maxilla; **L**, maxilliped. Scale bar: 0.5 mm.

ETYMOLOGY. — The new species name is a noun in apposition that refers to the city and the Jequitinhonha River, one of the most important rivers in the north of Minas Gerais state; the type locality is within the drainage basin of the Jequitinhonha river. The word Jequitinhonha is of indigenous origin and means "wide river full of fish".

DIAGNOSIS.— Dorsum covered with round tubercles with three rows on cephalon (4, 4, 4); three rows on pereonite 1 (2, 4, 7); two rows on pereonites 2-7 (6 + 4); and two paramedian tubercles on pleonites 3-5 and on telson. Pleopod 1 exopod with protruding distal portion, triangular, outer margin sinuous; endopod distal portion straight, twice longer than exopod.

DISTRIBUTION. — Jequitinhonha municipality, Minas Gerais state.

DESCRIPTION

Maximum size: ♂, 7 mm, ♀, 9 mm. Color grey with lateral margins depigmented (Fig. 26C, D). Dorsum covered with round tubercles (Fig. 24A, B): cephalon with three rows (4, 4, and 4 from front to back of vertex); pereonite 1 with 13 in three rows (2, 4 and 7); pereonites 2-7 with 10 (6 + 4); pleonites 3-5 and telson with two paramedian tubercles. Dorsal cuticle (Fig. 28J, K) with short triangular scale setae, pereonites 1-7 bearing one line of *noduli lateralis* per side on outer surface of posterior tubercle of second tubercle. Cephalon with frontal shield protruding above vertex; eye consisting of 16 ommatidia (Figs 24C; 28J). Pereonite 1 with posterior margin sinuous at sides; inner lobe of schisma rounded, extending beyond posterior margin of outer lobe; pereonite 2 with triangular ventral tooth reaching epimeron posterior margin (Fig. 24D). Pereonites 2-7 (Fig. 24A) with wide quadrangular epimera slightly bent outwards. Telson (Fig. 24E) hourglass-shaped, proximal portion broader than distal portion. Antennula (Fig. 24F) of three articles, second article shorter than

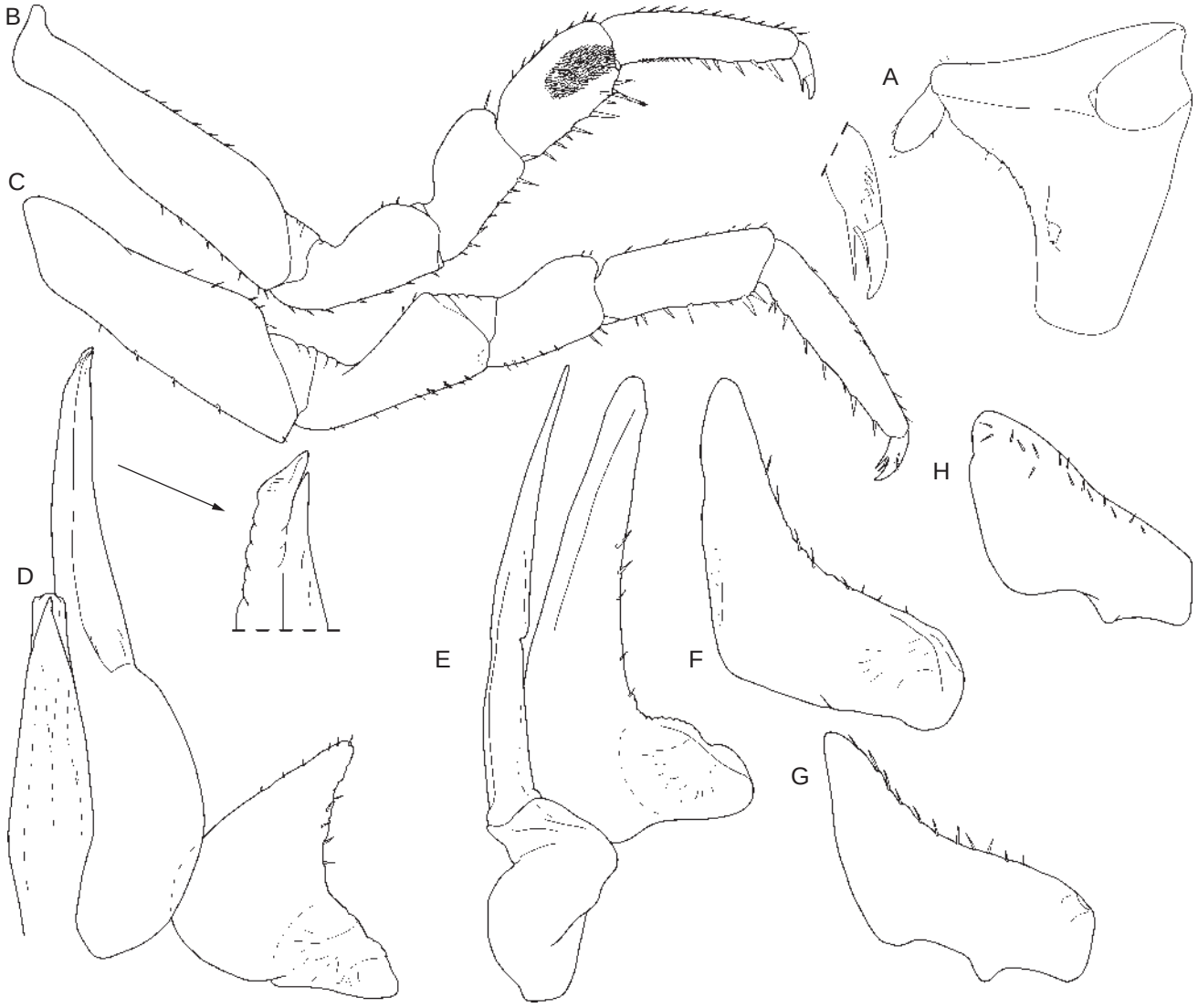


Fig. 25. — *Ctenorillo jequitinhonha* Cardoso & Ferreira, n. sp., paratype (male, 7 mm, ISLA96806): **A**, uropod, **B**, pereopod 1; **C**, pereopod 7; **D**, pleopod 1 and genital papilla; **E**, pleopod 2; **F**, pleopod 3 exopod; **G**, pleopod 4 exopod; **H**, pleopod 5 exopod.

first and third, third article with seven apical aesthetascs. Antenna (Fig. 24G) short and stout, flagellum shorter than fifth article of peduncle; second article of flagellum about three times as long as first. Buccal pieces as *C. pela- do* Cardoso & Ferreira, n. sp. (Fig. 24H-L). All pleopod exopods with monospiracular covered lungs. Uropod (Fig. 25A) protopod flattened, enlarged on basal portion; exopod outward, short, inserted dorsally close to medial margin of protopod.

Male

Pereopods without particular modifications (Fig. 25B, C). Pleopod 1 exopod (Fig. 25D) as wide as long, protruding distal portion, triangular, outer margin sinuous; endopod twice longer than exopod, distal portion straight. Pleopod 2 endopod as long as exopod (Fig. 25E). Pleopods 3-5 exopods as in Figure 25F-H.

HABITAT

Specimens of *C. jequitinhonha* Cardoso & Ferreira, n. sp. were found in Toca Juparanã, a granite cave located in Jequitinhonha municipality, in northeastern Minas Gerais state, Brazil. The average annual temperature is around 25°C, with the minimum temperature of approximately 15°C and the maximum of 38°C. The rainy season lasts from October to April, with December being the wettest month (140 mm of precipitation). The dry season lasts from May to September, with July being the driest month (average of 3 mm of precipitation) (Álvares *et al.* 2013).

The Toca Juparanã cave is a granitic talus cave that was formed by water removal of smaller sediments between large collapsed granitic blocks. The cave has two entrances of irregular shape, delineated by the contact of boulders (Fig. 26A). The main chamber of the cave has an irregular floor made up of collapsed boulders (Fig. 26B) and is euphotic/disphotic



Fig. 26. — *Ctenorillo jequitinhonha* Cardoso & Ferreira, n. sp.: **A**, detail of the Toca do Juparanã cave entrance; **B**, inner portion of the Toca do Juparanã cave; **C**, **D**, *Ctenorillo jequitinhonha* Cardoso & Ferreira, n. sp. habitus in natural habitat; **E**, landscape at the surroundings of the Toca do Juparanã cave, where the Jequitinhonha river can be seen.

due to the presence of two entrances located on either side of the chamber. There is a descending aphotic conduit from this chamber, which is crossed by a small hypogenic drainage. Specimens of *C. jequitinhonha* Cardoso & Ferreira, n. sp. were found under fallen rocks in this conduit trespassed by the small drainage, although the specimens were not observed close to the mainstream passage. The only visible organic resource in this area was plant debris brought by water, indicating that the isopods were likely feeding on this resource (Fig. 26 C, D). The vegetation surrounding the cave represents a well-preserved secondary forest, although many areas in the region are deforested for pastures and monocultures, especially near the Jequitinhonha River floodplain (Fig. 26E). The cave receives no visitors and is unknown to most of the local population. As for other *Ctenorillo* herein described, no samplings were conducted outside caves in the area, thus *C. jequitinhonha* Cardoso & Ferreira, n. sp. is likely to occur in external habitats. Therefore, it is advisable that further studies including external samplings be conducted to better understand the species distribution.

Remark

Ctenorillo jequitinhonha Cardoso & Ferreira, n. sp. differs from the Brazilian species by the round shape of tubercles, resembling *C. iuiuensis* Cardoso & Ferreira, n. sp. by the presence of two paramedian tubercles on pleonites 3-5 and on telson.



Fig. 27. — Habitus of the species of the genus *Ctenorillo* Verhoeff, 1942 discussed in the present paper: **A**, *Ctenorillo ferrarai* Campos-Filho, Araujo & Taiti, 2014; **B**, *Ctenorillo pelado* Cardoso & Ferreira, n. sp.; **C**, *Ctenorillo araguaia* Cardoso & Ferreira, n. sp.; **D**, *Ctenorillo intertidalis* Cardoso & Ferreira, n. sp.; **E**, *Ctenorillo ubajarensis* Cardoso & Ferreira, n. sp.; **F**, *Ctenorillo cearensis* Cardoso & Ferreira, n. sp.; **G**, *Ctenorillo quiteriensis* Cardoso & Ferreira, n. sp.; **H**, *Ctenorillo potiguar* Cardoso & Ferreira, n. sp.; **I**, *Ctenorillo iuiuensis* n. sp.; **J**, *Ctenorillo jequitinhonha* Cardoso & Ferreira, n. sp. Scale bars: 1 mm.

DISCUSSION

Taxonomy

Currently, the genus is composed by 22 species, 11 of which are from Africa, seven are from Colombia, three are from Brazil, and one is from the Democratic Republic of São Tomé and Príncipe (Taiti *et al.* 1998; Campos-Filho *et al.* 2014, 2017, 2018; Cifuentes & Da Silva 2023; Carpio-Díaz *et al.* 2023). Hence, the current manuscript contributes significantly to the knowledge of this genus, especially in Brazil, as nine new species are described, bringing the total number of species known in the country to 12 and the total number of species in the genus to 31.

As previously mentioned, *Ctenorillo* is typically identified by the shape, number, and arrangement of the dorsal tuber- cles. In this study, we have identified three distinct shapes of tubercles in the Brazilian species. The first group of species, including *C. ubajarensis* Cardoso & Ferreira, n. sp., *C. cearensis* Cardoso & Ferreira, n. sp. and *Ctenorillo potiguar* Cardoso & Ferreira, n. sp. display bosses or weakly developed tubercles. The second group of species, consisting of *C. pelado* Cardoso & Ferreira, n. sp., *C. araguaia* Cardoso & Ferreira, n. sp., *C. intertidalis* Cardoso & Ferreira, n. sp., *C. quiteriensis* Cardoso & Ferreira, n. sp., *C. iuiuensis* Cardoso & Ferreira, n. sp., *C. mineri* and *C. tuberosus*, possess conical tubercles. Finally, the third group, represented by *C. jequitinhonha* Cardoso & Ferreira, n. sp. exhibits round tubercles.

The number and arrangement of tubercles differed significantly among the species, and each species displayed a unique combination of these features. In most species, except for *C. jequitinhonha* Cardoso & Ferreira, n. sp., the tubercles developed in a lateral rib, which became increasingly prominent towards the posterior end of the last pereonites. In *C. ferrarai*, the first epimeron presented a single lateral rib that appeared to be the result of the fusion of two tubercles, which could be observed separately in *C. tuberosus*, *C. mineri*, *C. pelado* Cardoso & Ferreira, n. sp., and *C. araguaia* Cardoso & Ferreira, n. sp. With respect to the pleon, there was little variation among species, with most species displaying four tubercles on pleonites 3 to 5. However, *C. tuberosus* exhibits four tubercles on pleonites 3 and 4, and two on pleonite 5, while *C. iuiuensis* Cardoso & Ferreira, n. sp. and *C. jequitinhonha*

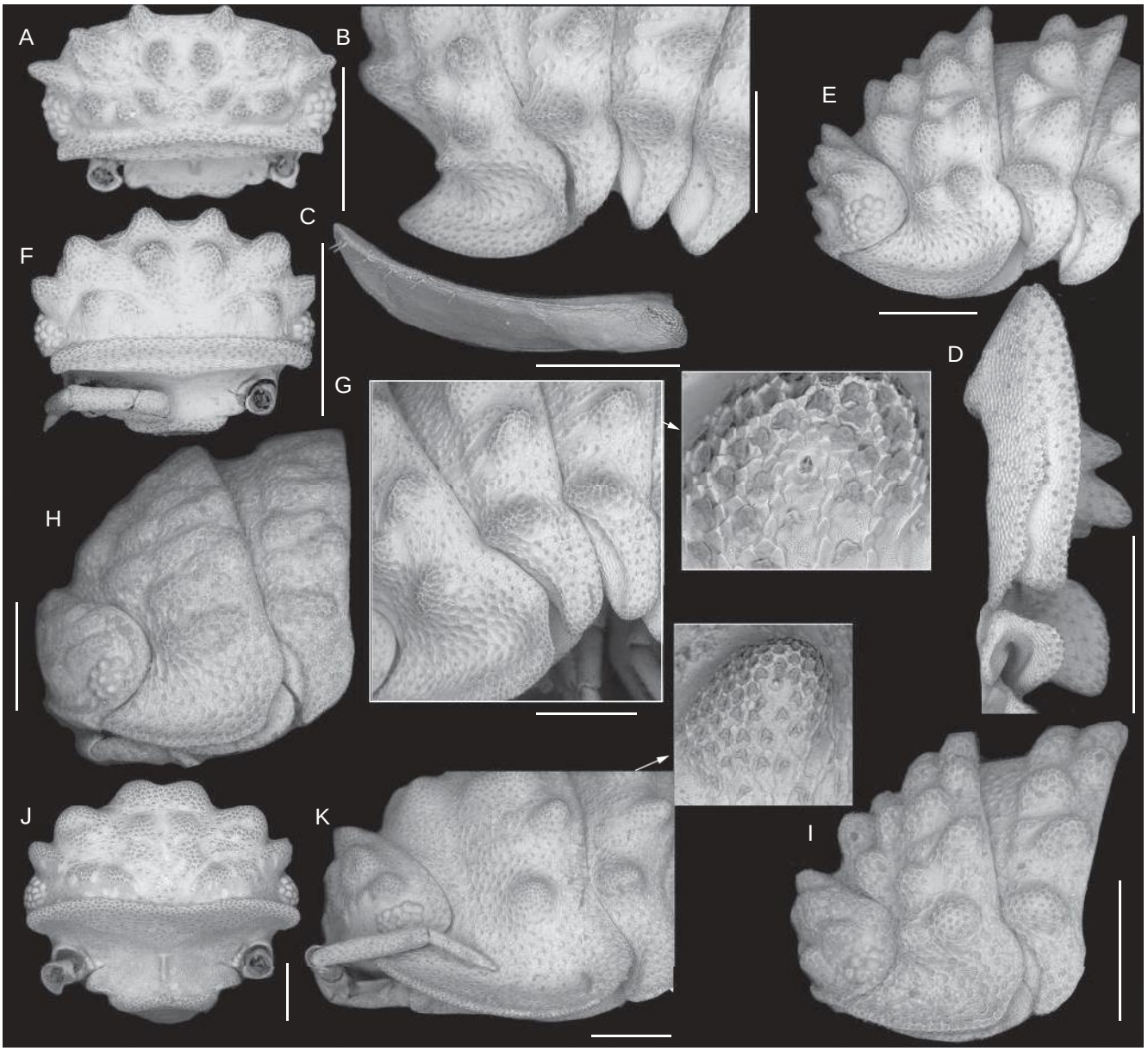


Fig. 28. — SEM images of *Ctenorillo* Verhoeff, 1942 new species: **A-D**, *Ctenorillo pelado* Cardoso & Ferreira, n. sp.: cephalon, dorsal view (**A**); epimera 1-3, lateral view (**B**); pleopod 3 exopod (**C**); epimera 1 and 2, ventral view (**D**); **E**, *Ctenorillo araguaia* Cardoso & Ferreira, n. sp.: , cephalon and epimera 1-3, lateral view; **F**, **G**, *Ctenorillo intertidalis* Cardoso & Ferreira, n. sp.: cephalon, frontal view (**F**); epimera 1-3, lateral view (**G**); **H**, *Ctenorillo ubajarensis* Cardoso & Ferreira, n. sp.: cephalon and epimera 1-3, lateral view; **I**, *Ctenorillo potiguar* Cardoso & Ferreira, n. sp.: cephalon and epimera 1 and 2, lateral view; **J**, **K**, *Ctenorillo jequitinhonha* Cardoso & Ferreira, n. sp.: cephalon, frontal view (**J**); cephalon and epimera 1 and 2, lateral view (**K**). Scale bars: A, B, D-K, 0.5 mm; C, 0.2 mm.

Cardoso & Ferreira, n. sp. presented only two tubercles on pleonites 3 to 5.

Regarding the shape of the male pleopod 1, variations were observed in the presence of a distal projection on exopod, which is present in *C. tuberosus*, *C. ferrarai*, *C. pelado* Cardoso & Ferreira, n. sp., *C. quiteriensis* Cardoso & Ferreira, n. sp. and *C. jequitinhonha* Cardoso & Ferreira, n. sp.

The morphological similarities among the species are generally consistent with their geographical distribution. The state of Pará, in northern Brazil, host *C. ferrarai*, *C. pelado* Cardoso & Ferreira, n. sp. and *C. araguaia* Cardoso & Ferreira, n. sp., which exhibit well-developed, conical-shaped tubercles. In contrast, the three species occurring in the northeast of Brazil, namely *C. ubajarensis* Cardoso & Ferreira, n. sp., *C. cearensis* Cardoso & Ferreira, n. sp. and *Ctenorillo potiguar* Cardoso & Ferreira, n. sp., display weakly developed tubercles. Notably, the most morphologically distinct species, *C. iuiuensis* Cardo- so & Ferreira, n. sp. and *C. jequitinhonha* Cardoso & Ferreira, n. sp., inhabit Bahia and Minas Gerais states, respectively, the former being troglobitic, as previously mentioned.

Conservation

The new species described here were found in highly heterogeneous regions, with some areas being well preserved while

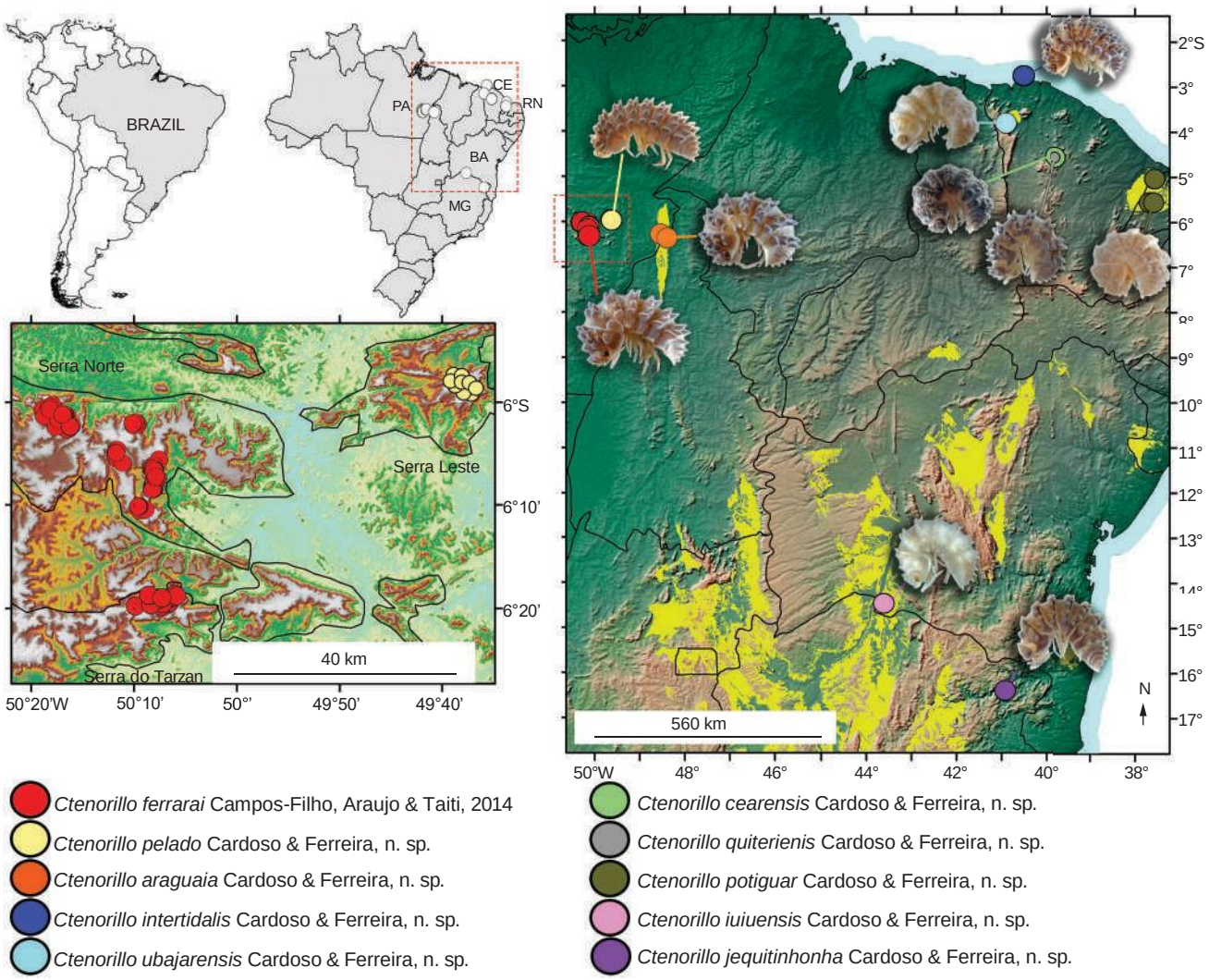


Fig. 29. — Distribution of *Ctenorillo* Verhoeff, 1942 species in Brazil, with the delimitation of the plateaus in Carajás Formation. Karstic areas marked in **yellow**. Abbreviations: **BA**, Bahia; **CE**, Ceará; **MG**, Minas Gerais; **PA**, Pará ; **RN**, Rio Grande do Norte.

others significantly altered, leading to increased threats to the species. Notably, five out of the nine new species were found in conservation units: Carajás National Forest (*C. pelado* Car- doso & Ferreira, n. sp.); Serra dos Martírios/Andorinhas State Park (*C. araguaia* Cardoso & Ferreira, n. sp.); Jericoacoara National Park (*C. intertidalis* Cardoso & Ferreira, n. sp.); Ubajara National Park (*C. ubajarensis* Cardoso & Ferreira, n. sp.) and the Furna Feia National Park (FFNP) (*Ctenorillo potiguar* Cardoso & Ferreira, n. sp.). As such, these species could be considered relatively well protected. However, it is important to note that some of these protected areas, particularly the national parks, feature caves as a key tourist attraction, which may pose a potential threat to the species in the event of unregulated tourist activity.

From a conservation standpoint, the primary concern centers around species inhabiting regions lacking legal protection. Among the newly described species are *C. cearensis* Cardoso & Ferreira, n. sp., *C. quiteriensis* Cardoso & Ferreira, n. sp., *C. iuiuensis* Cardoso & Ferreira, n. sp., and *C. jequitinhonha* Cardoso & Ferreira, n. sp. which are at a significant risk due to deforestation caused by agricultural and livestock expansion. Since these species are not entirely reliant on caves, the loss of forest cover can severely impact critical parts of these species habitat ranges, except for *C. iuiuensis* Cardoso & Ferreira, n. sp., which is exclusively found in one cave. Moreover, while the fact that these species inhabit caves suggests the possibility of shelter in these environments, the caves themselves are facing an unprecedented threat in Brazil (Ferreira *et al.* 2022; Cardoso *et al.* 2023).

Finally, of all the newly described species, particular attention must be given to *C. iuiuensis* Cardoso & Ferreira, n. sp. due to its unique ecological characteristics. This species is not only troglobitic but also confined to a single cave, making it especially vulnerable to habitat destruction. Furthermore, as previously mentioned, the landscape surrounding the cave where *C. iuiuensis* Cardoso & Ferreira, n. sp. is found has been significantly modified. Consequently, it is imperative that competent environmental agencies implement protective measures to guarantee the survival of this species.

Acknowledgements
The authors would like to thank the Centro Nacional de Pesquisa e Conservação de Cavernas – CECAV and Instituto Brasileiro de Desenvolvimento e Sustentabilidade – IABS for the financial support and scholarship provided to GMC (grant no. 006/2021. TCCE ICMBio/Vale 01/2018); CNPq (National Council for Scientific and Technological Development, grant n. 302925/2022-8) for the productivity scholarship provided to RLF; and the team from the Center of Studies in Subterranean Biology (CEBS/UFLA) for the support in the field trips; and reviewers for their valuable contribution to this manuscript.

Authors' contributions
GMC performed the morphological description. All authors drafted the manuscript, read, and approved the final manuscript.

REFERENCES

ALVARES C. A., STAPE J. L., SENTELHAS P. C., MORAES G. DE, LEONARDO J. & SPAROVEK G. 2013. — Köppen's climate classifica- tion map for Brazil. *Meteorologische Zeitschrift* 22 (6): 711-728. https://doi.org/10.1127/0941-2948/2013/0507

ARCANGELI A. 1941. — Crustacea, Isopoda, *in* Missione biologica Sagan-Omo 12. *Zoologia 6*: 5-18.

BENTO D. DE M., SOUZA-SILVA M., VASCONCELLOS A., BELLINI B. C., PROUS X. & FERREIRA R. L. 2021. — Subterranean "oasis" in the Brazilian semiarid region: neglected sources of biodiver- sity. *Biodiversity and Conservation* 30: 3837-3857. https://doi.org/10.1007/s10531-021-02277-6.

BEZERRA F. H. R., TAKEYA M. K., SOUSA M. O. L. & NASCIMENTO A. F. 2007. — Coseismic reactivation of the Samambaia fault, Brazil. *Tectonophysics* 430: 27-39. https://doi.org/10.1016/j.tecto.2006.10.007

BOYKO C. B., BRUCE N. L., HADFIELD K. A., MERRIN K. L., OTA Y., POORE G. C. B. & TAITI S. (eds) 2008 onwards. — World Marine, Freshwater and Terrestrial Isopod Crustaceans database. *Ctenorillo* Verhoeff, 1942. through: World Register of Marine Species at: https://www.marinespecies.org/aphia.php?p=taxdetails&id=248659 (accessed on 2023-03-31).

BUDDE-LUND G. 1904. — A Revision of Crustacea Isopoda Terrestria, with Additions and Illustrations. Pt 1 *Eubelum*, Pt 2 Spherilloninae, Pt 3 *Armadillo*. H. Hagerup, Copenhagen, Denmark, 144 p. https://doi.org/10.5962/bhl.title.9883

CAMPOS J. F. & CASTILHO A. 2012. — Uma visão geográfica da Região da Flona de Carajás, *in* MARTINS F. D., CASTILHO A. F., CAMPOS J. F., HATANO F. M. & ROLIM S. G. (eds) *Floresta Nacional de Carajás: estudos sobre vertebrados terrestres*. Nitro Imagens, São Paulo: 28-63.

CAMPOS-FILHO I. S., ARAUJO P. B., BICHUETTE M. E., TRAJANO E. & TAITI S. 2014. — Terrestrial isopods (Crustacea: Isopoda: Oniscidea) from Brazilian caves. *Zoological Journal of the Linnean Society* 172 (2): 360-425. https://doi.org/10.1111/zoj.12172

CAMPOS-FILHO I. S., MONTESANTO G., ARAUJO P. B. & TAITI S. 2017. — New species and new records of terrestrial isopods (Crustacea, Isopoda, Oniscidea) from Brazil. *Iheringia* Série Zoologia 107: 1-30. https://www.doi.org/10.1590/1678-4766e2017034

CAMPOS-FILHO I. S., CARDOSO G. M. & AGUIAR J. O. 2018. — Catalogue of terrestrial isopods (Crustacea, Isopoda, Oniscidea) from Brazil: an update with some considerations. *Nauplius* 26: 1-40. https://www.doi.org/10.1590/2358-2936e2018038

CAMPOS-FILHO I. S., GALLO J. S., GALLãO J. E., TORRES D. F., CHAGAS-JR A., HORTA L., CARPIO-DÍAZ Y. M., LÓPEZ-OROZCO C. M., BORJA-ARRIETA R., ARAUJO P. B., TAITI S. & BICHUETTE M. E. 2023. — Shedding light into Brazilian subterranean isopods (Isopoda, Oniscidea): expanding distribution data and describing new taxa. *Zoosystema* 45 (19): 531-599. https://doi.org/10.5252/zoosystema2023v45a19. http://zoosystema.com/45/19

CANIE/CECAV. CADASTRO NACIONAL DE INFORMAÇÕES ESPELEOLÓGICAS – CENTRO NACIONAL DE PESQUISA E CONSERVAÇãO DE CAVERNAS 2022. — Disponible at: https://www.gov.br/icmbio/ pt-br/assuntos/centros-de-pesquisa/cecav/cadastro-nacional-de-informacoes-espeleologicas (accessed 28 Apr. 2023).

CARDOSO G. M., BASTOS-PEREIRA R., SOUZA L. A. & FERREIRA R. L. 2020. — New cave species of *Pectenoniscus* Andersson, 1960 (Isopoda: Oniscidea: Styloniscidae) and an identification key for the genus. *Nauplius* 28. https://doi.org/10.1590/2358-2936e2020039

CARDOSO G. M., BASTOS-PEREIRA R. & FERREIRA R. L. 2023. — Cave-dwellers *Diploexochus* (Isopoda, Armadillidae): new species and new records of the genus from Brazil. *Nauplius* 31: 1-15. https://doi.org/10.1590/2358-2936e2023008

CARDOSO R. C., FERREIRA R. L. & SOUZA-SILVA M. 2021. — Priorities for cave fauna conservation in the Iuiú karst landscape, northeastern Brazil: a threatened spot of troglobitic species diver- sity. *Biodiversity and Conservation* 30 (5): 1433-1455. https://doi.org/10.1007/s10531-021-02151-5

CARDOSO R. C., FERREIRA R. L. & SOUZA-SILVA M. 2022. — Multi-spatial analysis on cave ecosystems to predict the diversity of subterranean invertebrates. *Basic and Applied Ecology* 65: 111-122. https://doi.org/10.1016/j.baae.2022.11.007

CARPIO-DÍAZ Y. M., LÓPEZ-OROZCO C. M., CAMPOS-FILHO I. S. & NAVAS G. R. 2018. — Terrestrial isopods (Isopoda: Oniscidea) of the Botanical Garden of Cartagena "Guillermo Piñeres", Colombia, with the description of three new species. *Arthropoda Selecta* 27 (4): 301-318. https://doi.org/10.15298/arthsel.27.4.05

CARPIO-DÍAZ Y. M., LÓPEZ-OROZCO C. M., BORJA-ARRIETA R., GUTIERREZ-ESTRADA M., CAMPOS-FILHO I. S., SFENTHOURAKIS S., TAITI S., MORENO J. C. N., BERMÚDEZ A., NAVAS-S. G. R. & BICHUETTE M. E. 2023. — The genus *Ctenorillo* Verhoeff, 1942 (Oniscidea, Armadillidae) from Colombia: new records, new species, and conservation comments. *Tropical Zoology* 36 (3-4): 53-84. https://doi.org/10.4081/tz.2023.141

CIFUENTES J. & DA SILVA L. P. 2023. — Terrestrial isopods (Isopoda, Oniscidea) of São Tomé Island, with the description of two new Armadillidae Brandt, 1831 species. *Zoosystema* 45 (21): 635-652. https://doi.org/10.5252/zoosystema2023v45a21. http://zoosystema.com/45/21

FERNANDES C. S., CAMPOS-FILHO I. S., ARAUJO P. B. & BICHUETTE M. E. 2019. — Synopsis of terrestrial isopods (Crustacea: Isopoda: Oniscidea) from Brazilian caves, with emphasis on new records from north, midwest, northeast and southeast regions. *Journal of Natural History* 53 (17-18): 1095-1129. https://doi.org/10.1080/00222933.2019.1634225

FERREIRA R. L., PROUS X., BERNARDI L. F. O. & SOUZA-SILVA M. 2010. — Fauna subterrânea do Estado do Rio Grande do Norte: Caracterização e impactos. *Revista Brasileira de Espeleologia* 1: 25-51.

FERREIRA R. L., BERNARD E., DA CRUZ JÚNIOR F. W., PILÓ L. B., CALUX A., SOUZA-SILVA M., BARLOW J., POMPEU P. S., CARDOSO P., MAMMOLA S., GARCÍA A. M., JEFFERY W. R., SHEAR W., MEDELLÍN R. A., WYNNE J. J., BORGES P. A. V., KAMIMURA Y., PIPAN T., HAJNA N. Z., SENDRA A., PECK S., ONAC B. P., CULVER D. C., HOCH H., FLOT J.-F., STOCH F., PAVLEK M., NIEMILLER M. L., MANCHI S., DEHARVENG L., FENOLIO D., CALAFORRA J.-M., YAGER J., GRIEBLER C., NADER F. H., HUMPHREYS W. F., HUGHES A. C., FENTON B., FORTI P., SAURO F., VENI G., FRUMKIN A., GAVISH-REGEV E., FIŠER C., TRONTELJ P., ZAGMA- JSTER M., DELIC T., GALASSI D. M. P., VACCARELLI I., KOMNENOV M., GAINETT G., TAVARES V. C., KOVÁČ Ľ., MILLER A. Z., YOSHIZAWA K., LORENZO T. DI, MOLDOVAN O. T., SÁNCHEZ- FERNÁNDEZ D., MOUTAOUAKIL S., HOWARTH F., BILANDŽIJA H.,

Drażina T., Kuharić N., Butorac V., Lienhard C., Cooper S. J. B., Eme D., Strauss A. M., Saccò M., Zhao Y., Wil- liams P., Tian M., Tanalgo K., Woo K.-S., Barjakovic M., Mccracken G. F., Simmons N. B., Racey P. A., Ford D., Labegalini J. A., Colzato N., Pereira M. J. R., Aguiar L. M. S., Moratelli R., Preez G. Du, Pérez-González A., Reb- oleira A. S. P. S., Gunn J., Mc Cartney A., Bobrowiec P. E. D., Milko D., Kinuthia W., Fischer E., Meierhofer M. B. & W. F. Frick 2022. — Brazilian cave heritage under siege. *Science* 375 (6586): 1238-1239. https://doi.org/10.1126/science.abo1973 Hoch H. & Ferreira R. L. 2016. — *Iuiuia caeca* gen. n., n. sp., a new troglobitic planthopper in the family Kinnaridae (Hemiptera, Fulgoromorpha) from Brazil. *Deutsche Entomologische Zeitschrift* 63: 171-181. https://doi.org/10.3897/dez.63.8432

Ipece 2011. — Instituto de Pesquisa e Estratégia Econômica no Estado do Ceará. http://www.ipece.ce.gov.br

Júnior J. T. G. & De Souza M. J. N. 2012. — Caracterização ambiental de Santa Quitéria, Ceará: a nova cidade uranífera do Brasil. *Revista GeoNorte* 3 (5): 1368-1377.

Linnaeus C. 1758. — *Systema naturæ per regna tria naturæ, secundum classes, ordines, genera, species, cum characteribus, differentiis, syn- onymis, locis.* Holmiae, Stockholm, ed. 10, vol. 1:1-824. https:// doi.org/10.5962/bhl.title.542

Martins F. D., Esteves E., Reis M. L. & Costa F. G. 2012. — Ações para conservação, *in* Martins F. D., Castilho A. F., Campos J. F., Hatano F. M. & Rolim S. (eds) *Floresta Nacional de Carajás: estudos sobre vertebrados terrestres*. Nitro Imagens, São Paulo: 198-229. Mertens B., Poccard-Chapuis R., Piketty M. G., Lacques A. E. & Venturieri A. 2002. — Crossing spatial analyses and live- stock economics to understand deforestation processes in the Brazilian Amazon: the case of Sao Felix do Xingu in South Para. *Agricultural Economics* 27 (3): 269-294. https://doi. org/10.1111/j.1574-0862.2002.tb00121.x

Montesanto G. 2015. — A fast GNU method to draw accurate scientific illustrations for taxonomy. *ZooKeys* 515: 191-206. https://doi.org/10.3897/zookeys.515.9459

Montesanto G. 2016. — Drawing setae: a GNU way for digital scientific illustrations. *Nauplius* 24 (1-6): e2016017. https://doi. org/10.1590/2358-2936e2016017

Oliveira G., Chen J. M., Mataveli G. A. V., Chaves M. E. D., Seixas H. T., Cardozo F. S., Shimabukuro Y. E., He L., Stark S. C. & Santos C. A. C. 2020. — Rapid recent deforesta- tion incursion in a vulnerable indigenous land in the Brazilian Amazon and fire-driven emissions of fine particulate aerosol pol- lutants. *Forests* 11 (8): 1-18. https://doi.org/10.3390/f11080829 Ratton P., Mahnert V. & Ferreira R. L. 2012. — A new cave-dwelling species of *Spelaeobochica* (Pseudoscorpiones: Bochicidae) from Brazil. *The Journal of Arachnology* 40 (3): 274-280. https://doi.org/10.1636/Ha12-39.1

Rizzo R., Garcia A. S., Vilela V. M. F. N., Ballester M. V. R., Neill C., Victoria D. C., Rocha H. R. & COE M. T. 2020. — Land use changes in Southeastern Amazon and trends in rainfall and water yield of the Xingu River during 1976-2015. *Climatic Change* 162 (3): 1419-1436. https://doi.org/10.1007/s10584-020-02736-z

ROLIM S. G., COUTO H. T. Z., JESUS R. M. & FRANÇA J. T.
2006. — Modelos volumétricos para a Floresta Nacional do Tapirapé-Aquirí, Serra dos Carajás (PA). *Acta Amazonica* 36 (1): 107-114. https://doi.org/10.1590/S0044-59672006000100013
SCHMIDT C. 2003. — Contribution to the phylogenetic system of the Crinocheta (Crustacea, Isopoda). Part 2 (Oniscoidea to Armadillidiidae). Mitteilungen aus dem Zoologischen Museum in Berlin. *Zoologische Reihe* 79: 3-179. https://doi.org/10.1002/ mmnz.20030790102
SCHMALFUSS H. 2003. — World catalog of terres rial isopods (Isopoda: Oniscidea). *Stuttgarter Beiträge zur Naturkunde, Serie A* 654: 1-341.
SCHMALFUSS H. & FERRARA F. 1983. — Terrestrial Isopods from West Africa: Part 3: Family Armadillidae Verhoeff, 1917. *Moni- tore Zoologico Italiano, Supplemento* 18 (1): 111-157.
SCHMÖLZER K. 1974. — Landisopoden aus Zentral-und Ostaf- rika (Isopoda, Oniscoidea). *Sitzungsberichte der österreichischen Akademie der Wissenschaften, mathematischnaturwissenschaftliche Klasse* I (182): 147-200.
SILVA J. M. C., LEAL I. & TABARELLI M. 2017. — *Caatinga: the largest tropical dry forest region in South America*, first ed. Springer, New York, 482 p. https://doi.org/10.1007/978-3-319-68339-3 SKET B. 2008. — Can we agree on an ecological classification of subterranean animals? *Journal of Natural History* 42 (21-22): 1549-1563. https://doi.org/10.1080/00222930801995762
SOUZA L. A., FERREIRA R. L. & SENNA A. R. 2015. — Amphibious shelter-builder Oniscidea species from the New World with description of a new subfamily, a new genus and a new species from Brazilian Cave (Isopoda, Synocheta, Stylonisci- dae). *PLoS ONE* 10 (5): 1-18. https://www.doi.org/10.1371/ journal.pone.0115021
SOUZA M. F. & FERREIRA R. L. 2018. — A new highly troglomorphic *Loxosceles* (Araneae: Sicariidae) from Brazil. *Zootaxa* 4438 (3): 575-587. https://doi.org/10.11646/zootaxa.4438.3.9
SOUZA-FILHO P. W. M., SOUZA E. B., SILVA JÚNIOR R. O., NAS- CIMENTO JR W. R., MENDONÇA B. R. V., GUIMARÃES J. T. F., DALL'AGNOL R. & SIQUEIRA J. O. 2016. — Four decades of land-cover, land-use and hydroclimatology changes in the Ita- caiúnas River watershed, southeastern Amazon. *Journal of Envi- ronmental Management* 167: 175-184. https://doi.org/10.1016/j. jenvman.2015.11.039
TAITI S. 2018. — A new termitophilous species of Armadillidae from South Africa (Isopoda: Oniscidea). *Onychium* 14: 9-15. https://doi.org/10.5281/zenodo.1218897
TAITI S., PAOLI P. & FERRARA F. 1998. — Morphology, bioge- ography, and ecology of the family Armadillidae (Crustacea, Oniscidea). *Israel Journal of Zoology* 44: 291-301.
VAN NAME W. G. 1936. — The American land and freshwater isopod Crustacea. *Bulletin of the American Museum of Natural History* 71: 1-535.
VERHOEFF K. W. 1942. — Äthiopische Isopoda terrestria der Hamburger *Zoologischen Museums. Zoologischer Anzeiger* 140: 1-163.

Submitted on 28 April 2023;
accepted on 25 October 2023;
published on 5 March 2024.

ORTHOPTERA



Zootaxa 5263 (1): 001–039
https://www.mapress.com/zt/
Copyright © 2023 Magnolia Press

Article

https://doi.org/10.11646/zootaxa.5263.1.1

ISSN 1175-5326 (print edition)
ZOOTAXA
ISSN 1175-5334 (online edition)

http://zoobank.org/urn:lsid:zoobank.org:pub:3386FD59-2075-4F6A-8B21-B36C7F463EA9

Three new cricket species and a new subgenus of *Endecous* Saussure, 1878 (Grylloidea: Phalangopsidae) from caves in northeastern Brazil

PEDRO HENRIQUE MENDES CARVALHO[1], VITOR GABRIEL PEREIRA JUNTA[1], RODRIGO ANTÔNIO CASTRO-SOUZA[2] & RODRIGO LOPES FERREIRA[1*]

[1]*Centro de Estudos em Biologia Subterrânea (www.biologiasubterranea.com.br), Setor de Biodiversidade Subterrânea, Departamento de Ecologia e Conservação, Universidade Federal de Lavras, Cx Postal 3037, Campus Universitário, CEP 37200-000, Lavras, Minas Gerais, Brazil.*

[2]*Programa de Pós-Graduação em Ecologia e Conservação da Biodiversidade, Departamento de Botânica e Ecologia, Universidade Federal do Mato Grosso, Rua Fernando Corrêa da Costa 2367, Cuiabá, 78060-900, Brazil.*

rodrigodesouzaac@gmail.com; https://orcid.org/0000-0002-3439-9991

carvalhopedrohm@gmail.com; https://orcid.org/0000-0003-0859-0255

vitor.junta@outlook.com; https://orcid.org/0000-0001-8579-955X

[*]*Corresponding author. drops@ufla.br; https://orcid.org/0000-0003-3288-4405*

Abstract

The genus *Endecous* (Orthoptera, Grylloidea, Phalangopsidae), commonly found in caves, comprises more than 20 species, grouped into three subgenera: *E.* (*Endecous*), *E.* (*Pedroecous)* and *E.* (*Notendecous*). In this study, from differences observed mainly in the male genitalia, we describe a new subgenus—*Endecous* (*Ramalhoecous*) **n. sp.**—as well as three new species—*E.* (*R.*) *infernalis* **n. sp.**, *E.* (*E.*) *zin* **n. sp.** and *E.* (*E.*) *zaum* **n. sp.**—all of them collected in caves in the Serra do Ramalho region, Northeastern, Brazil. We also briefly discuss some troglomorphisms verified in one of the new species: *E.* (*R.*) *infernalis* **n. sp.**

Key words: Orthoptera, taxonomy, troglomorphisms, phallic complex

Resumo

O gênero *Endecous* (Orthoptera, Grylloidea, Phalangopsidae), comumente encontrado em cavernas, compreende mais de 20 espécies, agrupadas em três subgêneros: *E.* (*Endecous*), *E.* (*Pedroecous)* e *E.* (*Notendecous*). Neste estudo, a partir de diferenças observadas principalmente na genitália masculina, descrevemos um novo subgênero—*Endecous* (*Ramalhoecous*) **n. subg.**—bem como três novas espécies de *Endecous*—*E.* (*R.*) *infernalis* **n. sp.**, *E.* (*E.*) *zin* **n. sp.** and *E.* (*E.*) *zaum* **n. sp.**—todas elas coletadas em cavernas da região de Serra do Ramalho, Nordeste, Brasil. Além disso, discutimos brevemente troglomorfismos verificados em uma das novas espécies: *E.* (*R.*) *infernalis* **n. sp.**

Palavras-chave: Orthoptera, taxonomia, troglomorfismos, complexo fálico

Introduction

The Phalangopsidae Blanchard, 1845 (Orthoptera, Grylloidea) are known for their spider-like appearance, long legs and developed antennal scapes (Souza-Dias 2015). These crickets are commonly found in tropical and subtropical environments all around the globe (Cigliano *et al.* 2022). The diversification center of the family, however, is the neotropical region (Desutter-Grandcolas 1995; Souza-Dias 2015), home to the most biodiverse ecosystems in the entire planet (Magrin *et al.* 2014).

The genus *Endecous* Saussure, 1878 (Phalangopsidae, Luzarinae), endemic to the South American continent, currently comprises 21 species, grouped in three subgenera: *E.* (*Endecous*), *E.* (*Pedroecous)* and *E.* (*Notendecous*) (Cigliano *et al.* 2022). These subgenera are distinguished based on observed differences in the male phallic complex

Accepted by D. Rentz: 13 Jan. 2023; published: 4 Apr. 2023

(Gorochov 2014; Castro-Souza *et al.* 2020a). Variations in the morphology of the male genitalia are also applied in the description of new species (Mews & Sperber 2008; Zefa *et al.* 2010; Bolfarini & Bichuette 2015; Souza-Dias 2015; Souza-Dias *et al.* 2017; Castro-Souza *et al.* 2017; Castro-Souza *et al.* 2020a; Castro-Souza *et al.* 2020b).

In Brazil, 17 species of *Endecous* have been identified in the Northeast, Southeast, Central-West and South regions (Cigliano *et al.* 2022). *E.* (*E.*) *naipi* Souza-Dias *et al.*, 2017 and *E.* (*E.*) *chape* Souza-Dias *et al.*, 2017, for example, inhabit the leaf litter of forests of the Iguaçu National Park (Souza-Dias *et al.* 2017). *E.* (*N.*) *onthophagus* (Berg, 1891) and *E.* (*E.*) *alejomesai* Zefa *et al.*, 2010, on the other hand, were found in both epigean and hypogean environments, and have caves as their type locality (Mesa & Garcia-Novo 1997; Cigliano *et al.* 2022). *E.* (*E.*) *betariensis* Mello & Pellegatti-Franco, 1998, *E.* (*E.*) *ubajarensis* Zefa *et al.*, 2014, *E.* (*N.*) *bahiensis* Castro-Souza *et al.*, 2017 and *E.* (*N.*) *potiguar* Castro-Souza *et al.*, 2017 also have caves as their type locality, but were not recorded anywhere else (Cigliano *et al.* 2022). Nevertheless, they likely also occur in external environments close to the subterranean cavities where they were originally found (Castro-Souza *et al.* 2020a), as the samplings performed on those regions only focused on subterranean environments.

In the last couple years, three new species of *Endecous*—*E.* (*P.*) *didymus* Castro-Souza *et al.*, 2020a, *E.* (*P.*) *troglobius* Castro-Souza *et al.*, 2020a and *E.* (*E.*) *painensis* Castro-Souza *et al.*, 2020b—were described based on individuals from caves in Minas Gerais State, Brazil (Cigliano *et al.* 2022). Amongst those species, *E.* (*P.*) *troglobius* stands out for its completely depigmented ommatidia (Castro-Souza *et al.* 2020a), feature typically associated with organisms that have evolved in subterranean environments (Christiansen 1962; Desutter-Grandcolas 1998b). Elongation of appendages and tegument depigmentation are also characterized as morphological modifications linked to a subterranean lifestyle, and can be observed not only in *Endecous*, but also in many other Orthoptera (Desutter-Grandcolas 1998b).

Other two species, *E.* (*P.*) *apterus* Souza-Dias *et al.*, 2014 and *E.* (*E.*) *peruassuensis* Bolfarini & Bichuette, 2015, were also regarded as being troglobitic, i.e., strictly subterranean organisms (Souza-Dias *et al.* 2014; Bolfarini & Bichuette 2015). However, it is worth pointing out that, although Souza-Dias *et al.* (2014) considered the apterism observed in *E.* (*P.*) *apterus* as an adaptation to a life cycle restricted to caves, it should not be acknowledged as a troglomorphic trait since many epigean Phalangopsidae, such as *Eidmanacris* Chopard, 1956, *Ottedana* de Mello & de Andrade, 2003 and *Sishiniheia* Souza-Dias & Mello, 2016, also have reduced wings or no wings at all (de Mello & de Andrade, 2003; de Mello & Souza-Dias, 2016; Campos *et al.* 2017; Castro-Souza *et al.* 2020a). Similarly, *E.* (*E.*) *peruassuensis* was classified as a troglobitic species based partially on observations of reduced cryptobiotic behavior, which was not verified by R.L. Ferreira during expeditions to Olhos d'Água cave, where the species was originally found. Regardless, *Endecous* must be recognized for its intimate relationship to the subterranean environment (Bolfarini & Bichuette 2015).

In this study, we describe three new species of *Endecous* from caves of the southwestern portion of Bahia State, Brazil. Furthermore, we discuss the troglomorphisms observed in one of the new species and propose a new subgenus to accommodate it. Finally, we provide some notes on these species' habitats, as well as how they are threatened by the expansion of human activities in the region.

Material and methods

Study area. The new species herein described were found in caves located in a region known as "Serra do Ramalho", located in southwestern Bahia State, northeastern Brazil. This region has several subterranean river systems, some of which presenting dozens of kilometers. Most of these systems are hydrologically dynamic, presenting high-water energy that results in great sedimentary movement in both surface and subterranean environments (Silva *et al.* 2019). According to Köppen's climate classification system, the local climate is "Aw", characterized by dry winters and an average annual rainfall of 640 mm3 (Alvares *et al.* 2013). The region is inserted in the Caatinga domain (the only Brazilian semiarid biome), with transitional areas to the Cerrado (Brazilian Savanna) (Cole 1960). Detailed description of the habitats of each species will be provided further on (see the sections "Ecological remarks" of each species).

Collection and examination. Specimens were found through active search, collected, fixed and stored in 70% ethanol. Individuals of *E.* (*R.*) *infernalis* **n. sp.** were captured during three expeditions (October 2017; September 14th to September 25th 2021; August 19th to September 1st 2022) to Lapa dos Peixes I (43°57′25.2″W, 13°49′22.08″S),

Gruna da Água Clara (43°57′6.24″W, 13°48′4.25″S) and Gruna do Pedro Cassiano I (43°54′50.4″W, 13°47′52.8″S) caves, located in the municipality of Carinhanha. *E.* (*R.*) *infernalis* **n. sp.** was also found in Baixão da Canoa cave (44° 9′50.35″W, 13°51′27.69″S), located in the municipality of Coribe. Specimens of *E.* (*E.*) *zin* **n. sp.** were collected during the second and third field trips to Serra do Ramalho region and were found in several caves: Gruna das Três Cobras cave (43°45′9.87″W, 13°37′6.62″S) and Gruna Serra Solta II cave (43°45′7.48″W, 13°30′38.16″S), both located in the municipality of Serra do Ramalho, and Gruna Grande cave (43°45′18.19″W, 13°36′8.9″S) and Gruna do Google cave (43°48′49.04″W, 13°37′41.93″S), both located in the municipality of Carinhanha. *E.* (*E.*) *zaum* **n. sp.** were captured in Serra Verde cave (44°19′26.85″W, 13°43′28.04″S), located in the municipality of Coribe, Bahia State, Brazil, during the second expedition (September 14th to September 25th 2021), and in Gruna do Enfurnado (44°12′7.99″W, 13°38′45.69″S) and Gruna do Zeferini (44°14′4.52″W, 13°46′15.55″S) caves, also located in the municipality of Coribe, during the third expedition (August 19th to September 1st 2022).

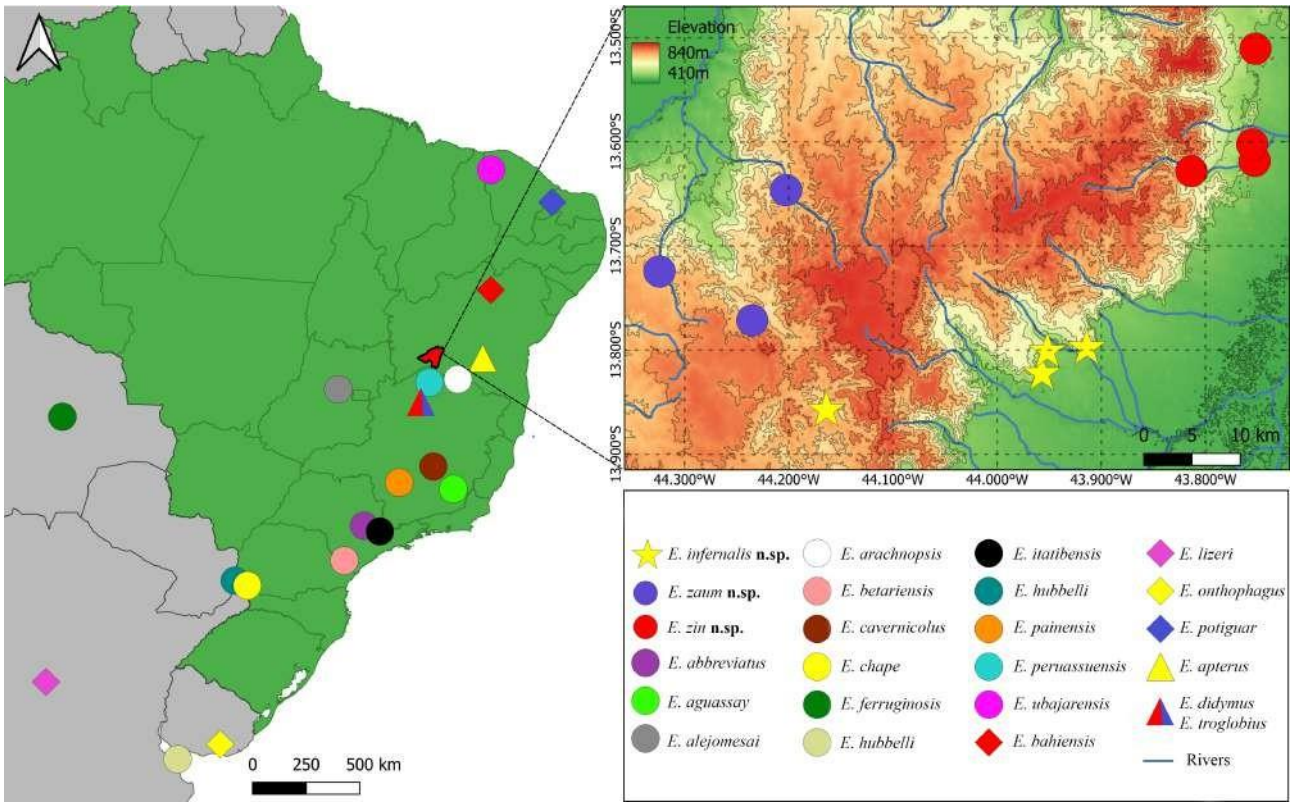


FIGURE 1. Distribution map of *Endecous* Saussure, 1878 (Brazilian territory in green). Serra do Ramalho region, where *E.* (*R.*) *infernalis* **n. sp.**, *E.* (*E.*) *zin* **n. sp.** and *E.* (*E.*) *zaum* **n. sp.** were found, is highlighted. Different symbols represent the four subgenera within *Endecous*. (*)

One adult female from Gruna das Três Cobras cave and male adults of the three new species were dissected and the phallic complexes and copulatory papilla digested by a pancreatin enzymatic solution (Álvarez-Padilla & Hormiga 2007) for about 24 hours to remove muscle tissue that hinders the visualization of structures of taxonomic relevance. The phallic complexes and copulatory papilla were further arranged in Petri dishes containing 70% ethanol and photographed using Axio Zoom V16 (ZEISS) and M205 A (Leica) stereomicroscopes.

The male phallic terminology proposed by Desutter (1987, 1998b) and Desutter-Grandcolas (2003) was applied in the description of the phallic complex of the three new species—*E.* (*E.*) *zin* **n. sp.**, *E.* (*E.*) *zaum* **n. sp.** and *E.* (*R.*) *infernalis* **n. sp.**—as well as the new subgenus. *Endecous* (*Ramalhoecous*) **n. subg**.

Species general morphology was examined and compared under a Stemi 508 (ZEISS) stereomicroscope. The right tegmen of male adults was removed from the body, placed on a microscope slide and analyzed through an Axio Lab.A1 (ZEISS) microscope. The number of teeth on the stridulatory file of each right tegmen was quantified using a mechanical counter. Measurements and photographs of the general morphology and right tegmen were taken under Axio Zoom V16 (ZEISS) and M205 A (Leica) stereomicroscopes. The internal morphology of the proventriculus was analyzed under the scanning electron microscope Hitachi TM4000.

Morphometric and statiscal analysis. The morphometric variables considered during morphometric and statiscal analysis were: head length (HL) and width, intraocular distance, compound eye length (CEL) and width, maxillary palpomeres length (MPL), pronotum length (PL) and width, right tegmen length (RTL) and width, leg I length (L1L), leg II length (L2L), femur III length, tibia III length, body length, number of teeth of the *pars stridens*, as well as the morphometric indices CEL/HL, MPL/HL, RTL/PL, L1L/PL, and L2L/PL.

Shapiro-Wilk test ($\alpha = 0.05$) was applied to determine whether the morphometric variables of *E.* (*R.*) *infernalis* **n. sp.**, *E.* (*E.*) *zin* **n. sp.** and *E.* (*E.*) *zaum* **n. sp.** are normally distributed. In order to verify if there are significant differences between the species, parametric data, i. e., normally distributed data, were submitted to analysis of variance (ANOVA). Tukey test was then applied to determine which species differed significantly from the others. The nonparametric data, on the other hand, were submitted to the Kruskal-Wallis test. Dunn test of multiple comparisons was used as *post-hoc* procedure to determine which species differed significantly from the others. The Shapiro-Wilk, ANOVA and Kruskal-Wallis tests were performed with the help of the *stats* R Package.

Morphometric variables of the three new species of *Endecous* were also submitted to Principal Component Analysis (PCA) through the *factoextra* R Package (Kassambara & Mundt 2020). All statistical analyses and tests were performed in the Software R 4.2.2 (R Core Development Team 2022).

Depository. Holotype and paratypes of *Endecous* (*Endecous*) *zin* **n. sp.** (6 ♂♂ and 1 ♀), *Endecous* (*Endecous*) *zaum* **n. sp.** (10 ♂♂) and *Endecous* (*Ramalhoecous*) *infernalis* **n. sp.** (8 ♂♂) were identified and deposited in the Collection of Subterranean Invertebrates of Lavras (ISLA), from the Center of Studies on Subterranean Biology (CEBS) at the Federal University of Lavras (UFLA), Minas Gerais State, Brazil.

Abbreviations. *Phallic complex*: **A**, pseudepiphallic ventral branch (or "A" sclerite); **Ps.arm**, pseudepiphallic arm; **Ps.db**, pseudepiphallic dorsal branch; **Ps.ib**, pseudepiphallic inner bars; **R**, pseudepiphallic rami (or pseudepiphallic membranous shield); **Ps.p**, pseudepiphallic paramere; **Ect.ap**, ectophallic apodeme; **Ect.arc**, ectophallic arc; **Ect.lb**, ectophallic lateral bar; **Ect.mp**, ectophallic median projection; **End.sc.a**, endophallic sclerite anterior portion; **End.sc.d**, endophallic sclerite duct; **End.sc.p**, endophallic sclerite posterior portion. *Proventriculus*: **mt**, median tooth; **md**, median denticles; **lt**, lateral tooth; **ld**, lateral denticles; **sl**, sclerotized lobe.

Results

Family Phalangopsidae Blanchard, 1845

Subfamily Luzarinae Hebard, 1928 Genus

Endecous Saussure, 1878 *Endecous*

(*Ramalhoecous*) n. subg.

Diagnosis. Combination of the following characteristics: uniformly broadened phallic complex, of intermediate length and almost quadrangular contour; pseudepiphallic inner bars (Ps.ib) deeply concave; tergites III to VII bearing centrally positioned protuberances in their anterior margins; cerci short in relation to body length, and dilated at the base.

Endecous (*Ramalhoecous*) *infernalis* n. sp.

(Figures 2–6, 7–15, 16–17, 18–21, 22–27, 28–31; Table 1)

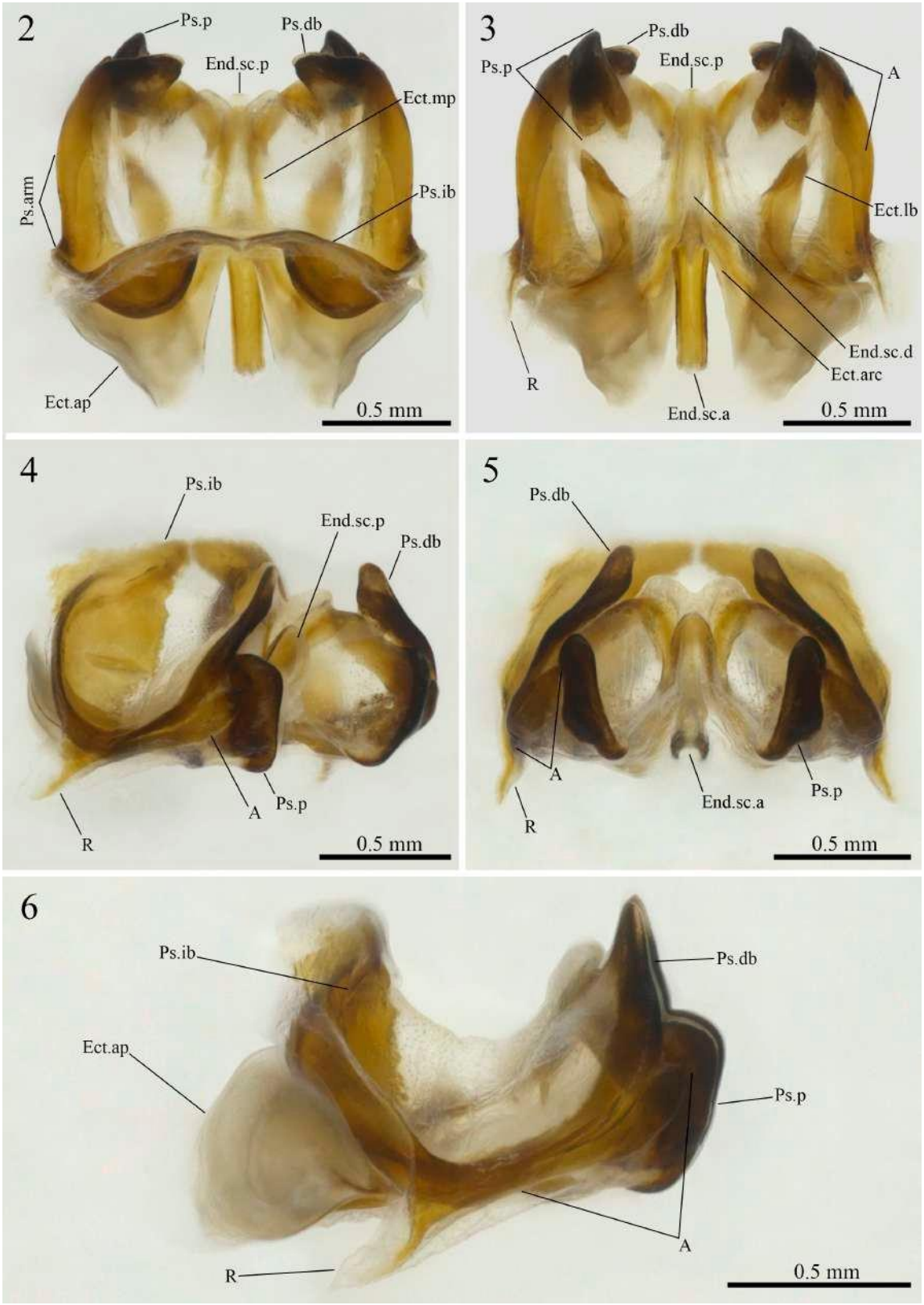
Material examined– *Holotype*, ♂, code ISLA 104838, Brazil, Bahia, municipality of Carinhanha, Água Clara cave (43°57′6.24″W, 13°48′4.25″S), 11.x.2017, R.L. Ferreira; condition: right tegmen and left legs I and II were detached and stored alongside the holotype. *Paratypes*, 7 ♂♂, ISLA 104839, municipality of Carinhanha, Água Clara cave (43°57′6.24″W, 13°48′4.25″S), 11.x.2017, R.L. Ferreira; ISLA 104840, 104841, 104842, municipality of Carinhanha, Água Clara cave (43°57′6.24″W, 13°48′4.25″S), 1.ix.2022, R.L. Ferreira; ISLA 104843, municipality of Carinhanha, Lapa dos Peixes I cave (43°57′25.2″W, 13°49′22.08″S), 10.x.2017, R.L. Ferreira; ISLA 104844, municipality of Coribe, Baixão da Canoa cave (44° 9′50.35″W, 13°51′27.69″S), 20.viii.2022, R.L. Ferreira; ISLA 104837, municipality of Carinhanha, Gruna do Pedro Cassiano I cave (43°54′50.4″W, 13°47′52.8″S), 14.ix.2021, R.L. Ferreira.

Etymology. The epithet "infernalis" is a Latin noun referring to those belonging to hell, or to the lower regions, thus being a reference to the subterranean habitat of the species.

Combination of the following characteristics: pseudepiphallic dorsal branches (Ps.db) dorsally projected and inclined inwards, apex broad and subtriangular in shape, with a less sclerotized tip; pseudepiphallic ventral branches (A) elongated, almost fused to the pseudepiphallic dorsal branches, apex broad and triangular in shape; pseudepiphallic rami (R) underdeveloped and falciform; ectophallic arch (Ect.arc) narrow and conical; ectophallic lateral bars (Ect.lb) short and contorted on themselves, apex acute; endophallic sclerite anterior portion (End.sc.a) elongated and lacking a crest opposite to its central groove.

Morphology (paratype ISLA 104837, Figs. 7–15). **Body color:** dorsal head yellowish brown, with irregular brown patches reaching the occiput; pronotum yellowish brown; abdomen yellowish brown dorsally and light yellowish brown ventrally (Figs. 7, 9–15); entire legs yellowish brown, whitish at their proximal portion (Figs. 18–21), cerci yellowish brown at the base (Fig. 13) and brownish towards the apex. **Head**: slightly pubescent, elongated in frontal view; front and gena yellowish brown; fastigium with long bristles, extending the vertex in an inclined plane pointing downwards; clypeus and labrum whitish with yellowish spots; mandibles yellowish brown and more sclerotized at the apex and margins; maxiles whitish and more sclerotized at the apex (Fig. 10); all maxillary palpomeres light yellowish brown and pubescent, the first two short and same-sized, the other three are longer, the palpomere V (2.21 mm) is claviform and whitish at the apex (Fig. 11); all labial palpomeres light yellowish brown, pubescent and increasing in size, the third one dilated from base to apex, which is whitish (Fig. 11); scape, pedicel and flagellomeres yellowish brown, distal portion whitish; compound eyes reduced, ommatidia black, ocelli absent (Figs**.** 9–11). **Thorax:** pronotum slightly pubescent, dorsal disk broader than long (2.38 and 3.86 mm in length and width respectively), lateral lobes subtriangular and leaning towards the anterior portion of the body, anterior and posterior margins arched and uneven, posterior margin with two laterally oriented small humps (Fig. 7). **Legs:** femur, tibia and tarsus pubescent. *Leg I* (Figs. 20 and 21): tibia slightly longer than the femur, with an oval tympanum on its inner side and two same-sized ventral apical spurs; first tarsomere ventrally serrated and longer than the second and third together. *Leg II* (Figs. 20 and 21): tibia slightly longer than the femur, with two same-sized ventral apical spurs; first tarsomere ventrally serrated and longer than the second and third together. *Leg III* (Figs. 18 and 19): femur developed; tibia slightly longer than the femur (11.44 and 11.11 mm, respectively); tibia armed with four subapical spurs on the outer side, the distal being the shortest, and three on the inner side (four subapical spurs on the inner side of the right leg), the proximal being the shortest, three apical spurs on the outer side (Fig. 19; a, b, c), spur "a" being the longest and "c" the shortest, and four on the inner side (Fig. 18; d, e, f, g), spurs "e" and "f" longer the "d" and "g" (three apical spurs on the inner side of the left leg, "d" probably lost during capture); first tarsomere longer than the second and third together, with two apical spurs, the inner being the longest. **Right tegmen**: slightly sclerotized; covering the first two urotergites (6.31 and 4.80 mm in length and width, respectively); *harp* with three well-marked crossveins and four cells; *mirror* subtriangular, with one well-marked crossvein and two cells, distal cell with a short and incomplete vertical vein; *basal field* with three secondary veins connecting Cu2 to 2A, secondary veins 2 and 3 connected by a crossvein, secondary vein 1 anteriorly bifurcated, 2A well-marked and proximally bifurcated, 1A absent; *lateral field* with two longitudinal veins and many irregular weakly marked secondary veins (Fig. 8); *stridulatory file* with 115 teeth. **Abdomen**: tergite III with an anterior semi-halved protuberance (Fig. 12), tergites IV, V, VI and VII with small and less conspicuous anterior humps; cerci short in comparison to body lenght, pubescent, with globose setae at the base, mainly on the inner side, and long bristles throughout all their extension, proximal portion dilated; sub-genital plate light yellowish brown, longer than wide, lateral margins slightly curved towards the outer side, distal margin rounded, with a small V-shaped dent in the center (Fig. 14); supra-anal plate whitish brown, distal margin rounded, shorter than the sub-genital plate, lateral projections rounded and pointing outwards, paraprocts as long as the supra-anal plate and barely visible in dorsal view (Fig. 15).

Proventriculus (paratype ISLA 104843, Figs. 16–17). Proventriculus internally organized in six rows of 12 overlaid sclerotized appendices (sa); sclerotized lobes (sl) bearing a cluster of bristles are visible on each side of the sclerotized appendices; sclerotized appendices formed by a median tooth (mt), with at least four, but up to nine median denticles (md), and two lateral teeth (lt), with several lateral denticles (ld); median denticles elongated and rounded at the tip; lateral denticles also elongated and rounded at the tip; the most posterior sclerotized appendix does not have a median tooth.



FIGURES 2–6. *Endecous* (*Ramalhoecous*) *infernalis* **n. sp. (**ISLA 104837) phallic complex. (2) dorsal view, (3) ventral view, (4) laterofrontal view, (5) frontal view, (6) lateral view. Abbreviations: **A**, pseudepiphallic ventral branch (or "A" sclerite); **Ps.arm**, pseudepiphallic arm; **Ps.db**, pseudepiphallic dorsal branch; **Ps.ib**, pseudepiphallic inner bars; **R**, pseudepiphallic rami (or pseudepiphallic membranous shield); **Ps.p**, pseudepiphallic paramere; **Ect.ap**, ectophallic apodeme; **Ect.arc**, ectophallic arc; **Ect.lb**, ectophallic lateral bar; **Ect.mp**, ectophallic median projection; **End.sc.a**, endophallic sclerite anterior portion; **End. sc.d**, endophallic sclerite duct; **End.sc.p**, endophallic sclerite posterior portion.

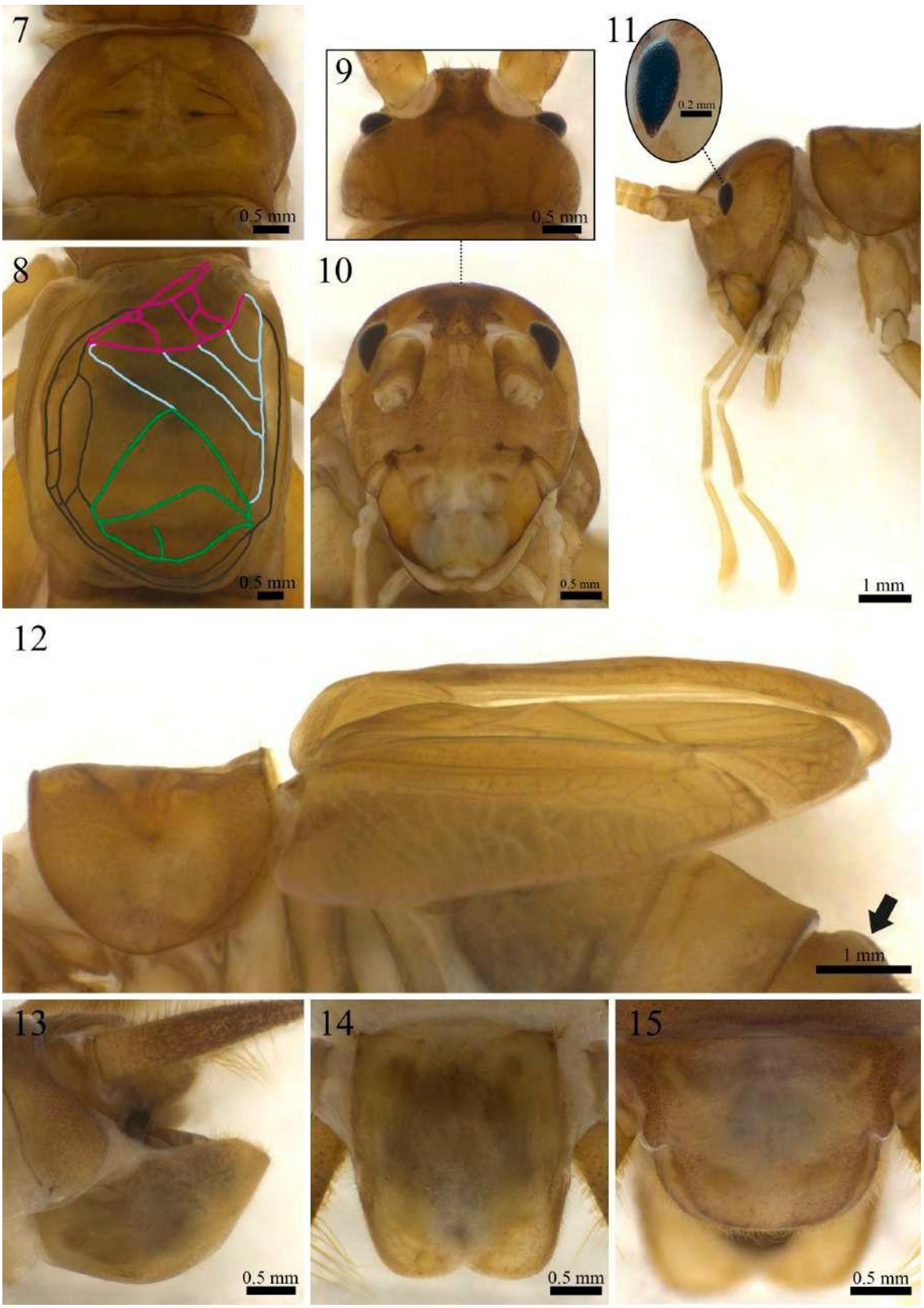
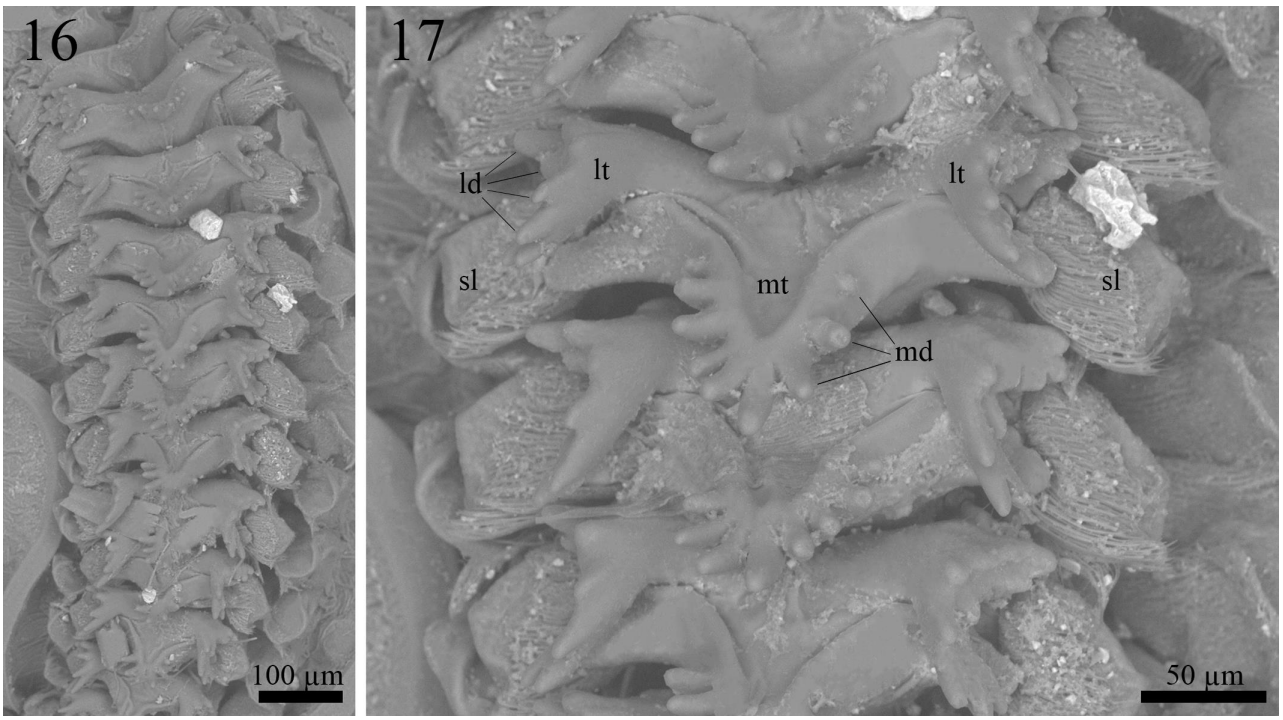


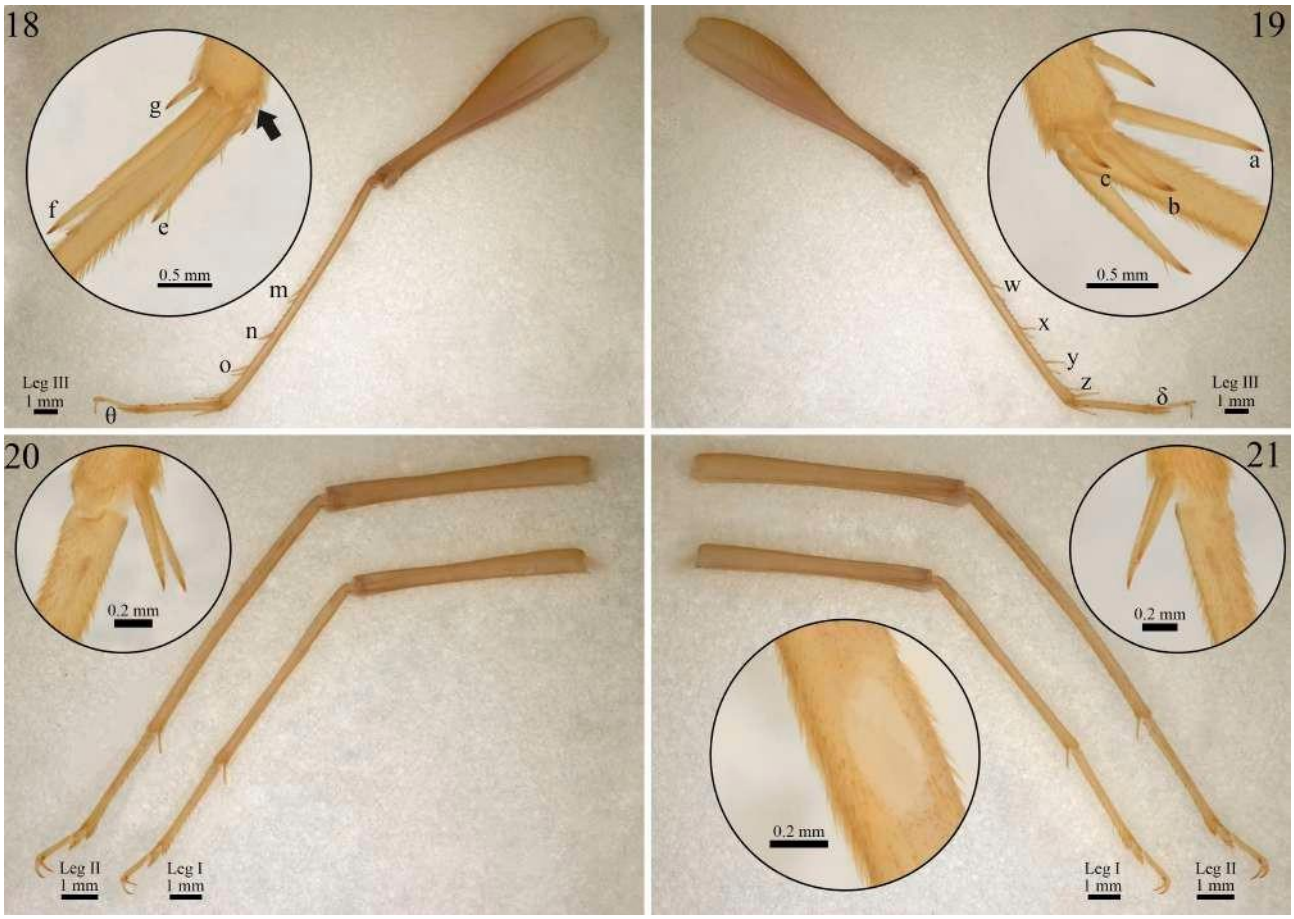
FIGURE 7–15. *Endecous* (*Ramalhoecous*) *infernalis* **n. sp. (**ISLA 104837) male general morphology. (7) pronotum in dorsal view; (8) right tegmen in dorsal view, harp highlighted in light blue, mirror highlighted in green, basal field highlighted in pink; (9) head in dorsal view; (10) head in frontal view; (11) head and palpi in lateral view, compound eye highlighted; (12) pronotum and tegmen in lateral view, black arrow indicates the central protuberance in tergite III; (13) supra-anal and sub-genital plates in lateral view; (14) sub-genital plate in ventral view; (15) supra-anal plate in dorsal view.



FIGURES 16–17. *Endecous* (*Ramalhoecous*) *infernalis* **n. sp. (**ISLA 104843) proventriculus. (16) row of sclerotized appendices; (17) sclerotized appendix. Abbreviations: **mt**, median tooth; **md**, median denticles; **lt**, lateral tooth; **ld**, lateral denticles; **sl**, sclerotized lobe.

Male phallic sclerites (paratype ISLA 104837, Figs. 2–6). Phallic complex uniformly broadened, of intermediate length and almost quadrangular contour in dorsal and ventral views. **Pseudepiphallus:** arms short and slightly inclined outwards in dorsal view (Fig. 2, Ps.arm); dorsal branches dorsally projected, apexes broad, subtriangular in shape, with an undeveloped and less sclerotized tip, and inclined towards the interior of the phallic complex in frontal view (Figs. 2 and 5, Ps.db); "A" sclerite well-developed, elongated, almost fused to the dorsal branch, apex broad and triangular shaped, reaching the dorsolateral central region of the parameres in lateral view (Fig. 4 and 6, A); paramere 1 and 2 fused in a single circular and concave structure, slightly projected past dorsal branches in dorsal view, ventral portion bifurcated, distal region highly sclerotized, dorsal portion sclerotized, forming a scythe-like edge that partially covers the posterior portion of the ectophallic median projections in dorsal view (Fig. 2, Ps.p); inner bars broad in frontal view, central region deeply concave, forming a basket-like structure, dorsal portion arranged in arc in dorsal view (Fig. 2, Ps.ib); rami underdeveloped, reduced to a short, scythe-shaped ventral projection in lateral view (Fig. 6, R). **Ectophallic invagination:** arc well-developed, expanding itself longitudinally rather than laterally, anterior and posterior central parts conical in dorsal view, posterior margin more sclerotized than the anterior margin (Fig. 3, Ect.arc); apodeme developed, ventrally positioned and inclined towards the interior of the sclerite in dorsal view (Fig. 2, Ect.ap); lateral bar developed, broad, shorter than the ectophallic median projections, slightly curved towards the exterior of the sclerite, apex acute and contorted on itself in ventral view (Fig. 3, Ect.lb); median projection long, slender and inclined inwards, reaching the parameres and fusing at the apex (Fig. 2, Ect.mp). **Endophallus:** anterior portion well-developed and sclerotized, elongated, rectangular in shape, with a central groove, but no crest opposite to the groove (Fig. 3, End.sc.a); duct short and mostly membranous, reaching the distal portion of the ectophallic median projections in ventral view (Fig. 3, End.sc.d); posterior portion conical, slightly sclerotized at the apex and barely exceeding the length of the ectophallic median projections in dorsal view (Fig. 2, End.sc.p).
Variations in phallic sclerites (holotype and paratypes, n = 7, ISLA 104838, 104839, 104840, 104841, 104842, 104843, 104844)**.** Phallic complexes vary slightly in size and degree of sclerotization; pseudepiphallic dorsal branches (Ps.db) vary subtly in degree of inclination towards the center of the sclerite; furthermore, its external contour and curvature also vary, ranging from less acute to more acute, with or without evident vertices; pseudepiphallic ventral branch (A) may be more or less fused to the dorsal branch; bifurcated ventral portion

of the pseudepiphallic parameres (Ps.p) may be evident or slightly evident; dorsal portion of the pseudepiphallic parameres in the form of a short or long scythe, covering only the apexes of the ectophallic median projections (Ect. mp) or, at most, half of their length; pseudepiphallic inner bars (Ps.ib) perpendicular or not to the longitudinal axis of the sclerite; ectophallic lateral bar (Ect.lb) contorted on itself only at the apex, throughout all of its extension or, at least, half of its length; ectophallic median projections sinuous or almost linear, but always merging at the apex; endophallic sclerite anterior portion (End.sc.a) rectangular or narrowed at the apex; endophallic sclerite posterior portion (End.sc.p) of conical or trapezoidal shape.



FIGURES 18–21. *Endecous* (*Ramalhoecous*) *infernalis* **n. sp.** (ISLA 104837) left legs. (18) leg III, subapical and apical spurs, black arrow indicates the absence of one of the apical spurs, inner view (19) leg III, subapical and apical spurs, outer view (20) legs I and II, apical spurs, outer view (21) legs I and II, apical spurs and tympanum, inner view.

Variations in male right tegmen (Figs. 22–27). **Stridulatory file** with 122 ± 7.31 teeth (n° = 8, holotype and paratypes). **Harp** outline conserved; two or three diagonal crossveins; three or four cells; a short and incomplete diagonal crossvein may be present (Fig. 23); one of the main crossveins may have a few knob-like projections throughout its extension (Fig. 26). **Mirror** outline always subtriangular; one or two crossveins, the proximal one being V-shaped; a short vertical or horizontal incomplete crossvein may be observed (Figs. 22 and 27); the distal crossvein may branch out into two crossveins, one short and one long, yet both reach the distal margin of the mirror (Fig. 25). **Basal field** outline conserved; 1A may be absent (Fig. 22); secondary veins may branch out from 1A, reaching the Cu2 or the 2A, and forming small cells (Figs. 23, 25 and 26); secondary crossveins may connect Cu2 to 2A directly (Fig. 22). **Lateral field** with two longitudinal veins that may or may not converge, but are usually connected through secondary veins and rarely completely parallel and isolated from one another throughout their extension.

Ecological remarks. Specimens of *Endecous infernalis* **n. sp.** were found in Baixão da Canoa cave, located in the municipality of Coribe, and in other two cave systems: the Gruna da Água Clara cave system (ACCS) and Gruna do Pedro Cassiano I cave (Fig. 29), both located in the municipality of Carinhanha, southwestern Bahia state, Brazil. The Água Clara cave system represents a set of functionally interconnected caves of approximately 24 km

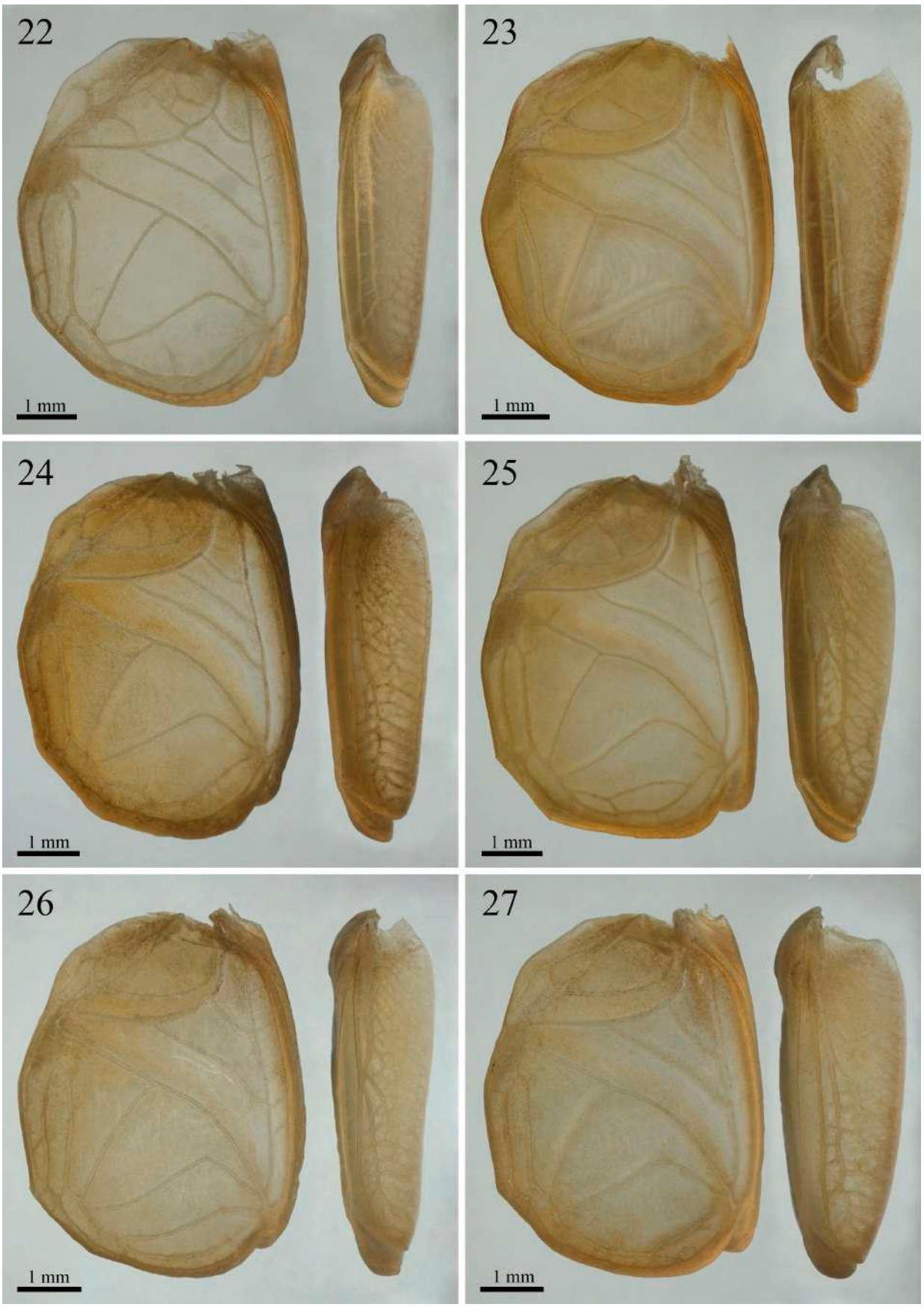
of extension. It is composed of four limestone caves trespassed by an intermittent stream, active during the austral summer (October until March) (Souza-Silva *et al.* 2021). The Gruna do Pedro Cassiano I cave (Fig. 29), in turn, is a single 2.660-meter-long cave that does not belong to the ACCS, but it is located near that system (approximately 4 km in a straight line). The Baixão da Canoa cave was only recently discovered, so it was not yet properly explored. It is safe to say, however, that the surveyed conduits have at least 1.5 km of extension. This cave has a single known entrance, which leads to a crawling conduit that connects to a wide main chamber, representing the main cave conduit, which has an intermittent drainage active during rainy periods.

Differently from what is usually observed for most of the *Endecous* species occurring in Brazilian caves, the caves aforementioned had a very low population density of *Endecous infernalis* **n. sp.** Hence, it was relatively hard to find specimens (especially adults) in all the caves in which it occurs. Although practically the entire ACCS has been inventoried for cave invertebrates in a study carried out in 2017 (Souza-Silva *et al.* 2021), only few specimens were found, mainly in deep and moistened areas within the system. It is noteworthy that the two caves located at the intermediate portion of the ACCS (Gruna dos Índios and Lapa dos Peixes caves) have a quite dry main conduit due to the airflow that comes from the entrances in both sides of their main conduits and trespasses both caves. Because of that, individuals of *E. infernalis* **n. sp.** were seldom observed in this intermediate portion of the ACCS, probably due to the unstable climatic conditions of the caves. A second population was observed in the Gruna do Pedro Cassiano I cave in deeper areas within the cave, far from the entrance. Most specimens found in both cave systems were observed freely walking on the cave floor or in the caves' walls (Figs. 30 and 31). Finally, a third population was recently discovered in the Baixão da Canoa cave. Again, specimens were only observed in deeper and moistened areas, and, as a result of the low-density population, the individuals were thinly dispersed. A single adult male was collected, despite the sampling efforts employed along the cave.

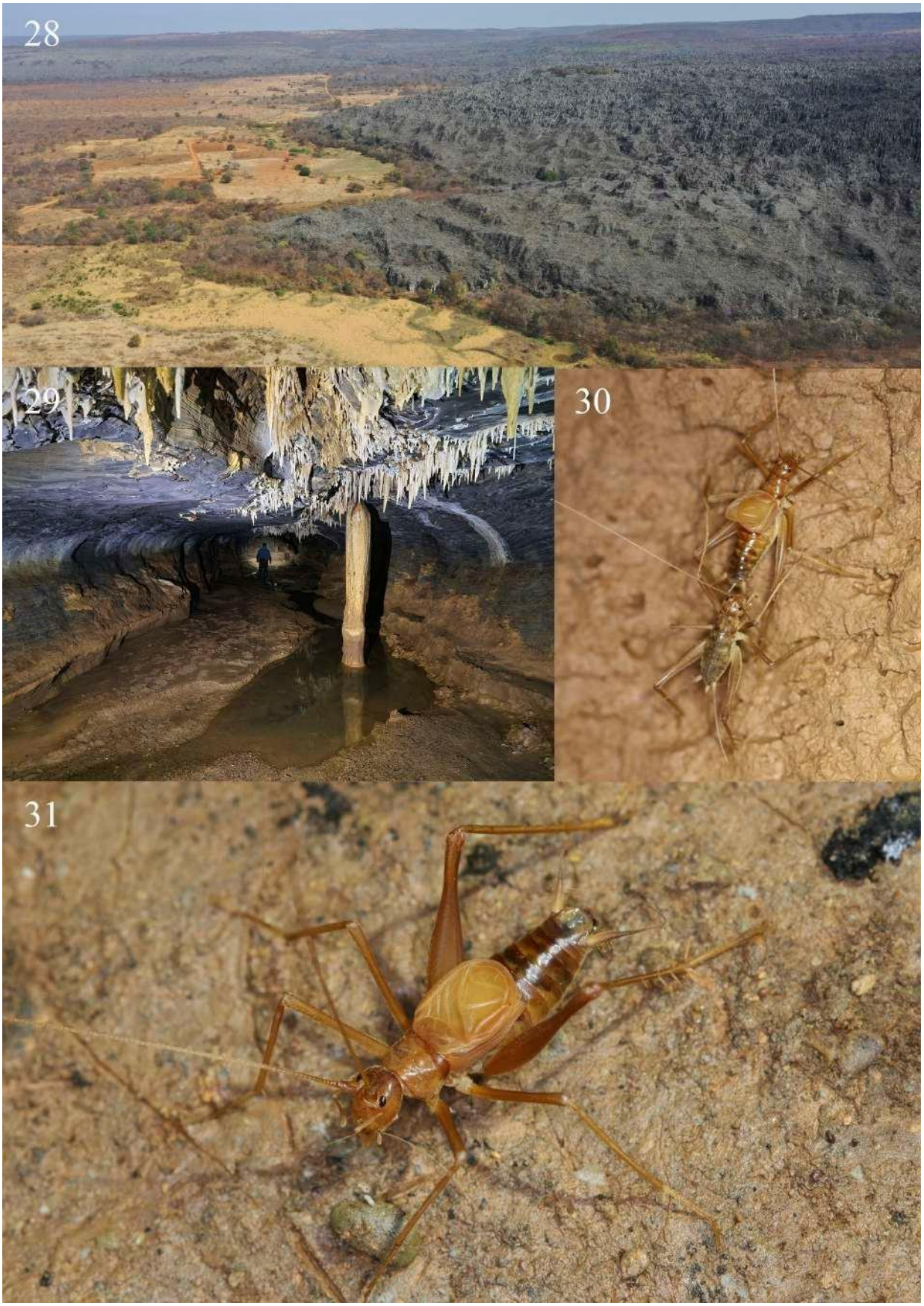
It is important to mention the distance among the Gruna da Água Clara cave system (ACCS), Gruna do Pedro Cassiano I and Baixão da Canoa cave. While ACCS and Gruna do Pedro Cassiano I cave comprise close systems (entrances located approximately 4 km in a straight line from each other), the Baixão da Canoa cave is located far from the first two cave systems (22 km in a straight line). All these caves are associated with the main massif of the Serra do Ramalho mountain range, which comprises a large continuous carbonate outcrop that runs from southwest to northeast. Furthermore, the Baixão da Canoa cave is located at a higher altitude, being associated with a hydrological recharge zone in the landscape, while the ACCS and the Gruna de Pedro Cassiano caves are located at lower altitudes, being associated with the base of the outcrops in hydrological discharge zone. Thus, it is plausible to assume the existence of subterranean connectivity between those systems.

An interesting observation was made in a deeper area of the Gruna da Água Clara cave (Part of the ACCS) during an expedition in 2017: an adult male was stridulating while a juvenile female was interacting with its cerci (Fig. 30). Although it was not possible to observe in detail, it seemed that the female was touching the basal region of the male's cerci, where modified setae (globose setae) can be found, with her mouthparts. In both Grylloidea and Blattodea, club-shaped and globose setae are hypothesized to act as gravity receptors (Nicklaus 1969; Bischof 1975; Horn 1985; Hartman *et al.* 1987), but, as pointed out by Desutter-Grandcolas (1998a), further neuroethological studies of these insects are necessary to confirm or refute this function. Given the observed behavior, one can hypothesize that such setae may also attract females for mating, functioning eventually as a nuptial gift. Although the SEM images of such setae usually show them flattened, they are, in their natural state, swollen, due to being filled with fluid. Considering that the observed female was immature (the ovipositor was still short and not sclerotized), this behavior could represent an advantage in the case of oligotrophic environments and low-density populations, in which the encounter among specimens may be more infrequent, especially in extensive cave systems such as the ACCS. Nevertheless, such hypotheses deserve further studies in order to confirm or refute it.

It is important to mention the troglomorphic traits observed in this species, which will be discussed further on. When compared to other *Endecous* species (most of which are troglophilic), *E. infernalis* **n. sp.** presents reduced eyes and longer legs. Other *Endecous* species previously considered troglobitic, as *E. peruassuensis* and *E. apterus*, presents much less regressive morphological traits than those observed in the species herein described. Bearing in mind the species distribution within the caves it inhabits (always in deeper moist regions) and the quite severe external dry habitat surrounding the caves, it is plausible to assume it is, in fact, a troglobitic (cave-restricted) species.



FIGURES 22–27. *Endecous* (*Ramalhoecous*) *infernalis* **n. sp.** right tegmen, dorsal and lateral view. (22) paratype, ISLA 104837; (23) paratype, ISLA 104844; (24) paratype, ISLA 104840; (25) paratype, ISLA 104842; (26) holotype, ISLA 104838; (27) paratype, ISLA 104839.



FIGURES 28–31. *Endecous* (*Ramalhoecous*) *infernalis* **n. sp.** habitat. (28) Gruna do Pedro Cassiano I cave, external environment; (29) Gruna do Pedro Cassiano I cave, internal environment; (30) adult male and immature female of *E.* (*R.*) *infernalis* **n. sp.** interacting; (31) adult male of *E.* (*R.*) *infernalis* **n. sp.**

TABLE 1. *Endecous* (*Ramalhoecous*) *infernalis* **n. sp.**, morphological measurements (mm), mean (M) and standard deviation (SD) of eight male adult specimens; *pars stridens* refers to the number of teeth of the stridulatory file.

♂	104837	104838	104839	104840	104841	104842	104843	104844	M	SD
Head width	2.925	2.788	3.013	2.982	3.064	3.075	2.795	2.921	2.945	0.103
Head length	1.946	1.897	2.089	1.933	1.776	1.943	1.737	1.947	1.909	0.103
Intraocular distance	1.670	1.541	1.722	1.683	1.755	1.744	1.546	1.614	1.659	0.079
Compound eye width	0.271	0.293	0.322	0.336	0.310	0.375	0.324	0.329	0.320	0.029
Compound eye length	0.659	0.685	0.785	0.763	0.788	0.788	0.691	0.766	0.741	0.050
Maxillary palpomere III	1.572	1.426	1.487	1.606	1.554	1.655	1.559	1.463	1.540	0.071
Maxillary palpomere IV	1.747	1.428	1.502	1.621	1.540	1.630	1.595	1.576	1.580	0.089
Maxillary palpomere V	2.215	1.955	2.000	2.149	2.204	2.327	2.044	2.213	2.138	0.119
Pronotum width	3.857	3.608	3.918	4.027	3.920	4.101	3.518	3.862	3.851	0.185
Pronotum length	2.376	2.229	2.506	2.434	2.431	2.285	2.138	2.562	2.370	0.134
Right tegmen width	4.802	4.760	4.525	4.520	4.461	4.421	4.663	4.322	4.559	0.157
Right tegmen length	6.310	5.595	5.992	5.816	5.908	5.921	6.192	5.399	5.892	0.277
Leg I length	18.433	17.891	19.243	19.396	19.796	20.482	18.914	19.648	19.225	0.760
Leg II length	19.687	18.843	20.359	20.122	20.533	21.366	20.040	20.622	20.197	0.690
Femur III length	11.109	10.253	10.995	11.352	11.981	11.157	10.924	11.578	11.169	0.473
Tibia III length	11.440	11.242	11.656	12.044	12.642	11.937	11.478	12.485	11.866	0.473
Body length	23.054	22.507	21.114	22.978	19.410	22.400	20.212	21.590	21.658	1.245
Pars stridens	115	112	120	114	129	126	127	133	122	7.314

Although Gruna do Pedro Cassiano cave receives local visitors sporadically, such visitors do not reach the cave deepest regions, where the specimens occur. The Gruna da Água Clara cave system, on the other hand, is only visited by speleologists during technical/scientific expeditions, which seldom occur. Such activities apparently do not represent a threat for the species. The Baixão da Canoa cave was only visited once by the researchers who sampled the cave, thus it is pristinely preserved. The external environment surrounding the caves, however, is severely altered (Fig. 28). Most of the original forests were replaced by pastures or other monocultures. The forests remain only in the top and border of the limestone outcrops, in randomly dispersed patches of vegetation or alongside intermittent drainages. Such impacts may reduce the organic input to the cave ecosystems and increase the silting in all those caves, thus altering several microhabitats of this species.

***Endecous* (*Endecous*) *zin* n. sp.**
(Figures 32–36, 37–45, 46–47, 48–51, 52–57, 58–63, 64–66; Table 2)

Material examined. *Holotype*, ♂, code ISLA 104845, Brazil, Bahia, municipality of Serra do Ramalho, Gruna das Três Cobras cave (43°45′9.87″W, 13°37′6.62″S), 15.ix.2021, R.L. Ferreira; condition: right tegmen, left legs and phallic complex were detached/dissected and stored alongside the holotype. *Paratypes*, 1 ♀, ISLA 104846, municipality of Serra do Ramalho, Gruna das Três Cobras cave (43°45′9.87″W, 13°37′6.62″S), 26.viii.2022, R.L. Ferreira; 5 ♂♂, ISLA 104847, 104848, 104849, municipality of Carinhanha, Gruna Grande cave (43°45′18.19″W, 13°36′8.9″S), 21.ix.2021, R.L. Ferreira; ISLA 104850, municipality of Carinhanha, Gruna do Google cave (43°48′49.04″W, 13°37′41.93″S), 22.ix.2021, R.L. Ferreira; ISLA 104851, municipality of Serra do Ramalho, Gruna da Serra Solta II cave (43°45′7.48″W, 13°30′38.16″S), 18.ix.2021, R.L. Ferreira.
Etymology. The epithet "zin" refers to a figure of speech often used in Brazil to refer to a friend. It is actually a shortening of "Zezin", which is a nickname for "José", a very common name in Brazil.
Diagnosis. Combination of the following characteristics: pseudepiphallic dorsal branches (Ps.db) elongated, inclined towards the parameres, projected towards the dorsal portion of phallic complex, apex tapered and acute; pseudepiphallic ventral branches (A) elongated and dilated at the apex; pseudepiphallic inner bars (Ps.ib) concave; pseudepiphallic rami (R) developed, forming a membranous shield that partially covers the ectophallic apodeme laterally; ectophallic arc (Ect.arc) broad and trapezoidal in general shape; ectophallic lateral bars (Ect.lb) elongated, meandering, slightly inclined towards the interior of the phallic complex, apex resembling a hook; endophallic sclerite anterior portion (End.sc.a) with a crest on the opposite side of its central groove.
Morphology (holotype ISLA 104845, Figs. 37–45). **Body color:** dorsal head yellowish brown; pronotum yellowish brown; abdomen whitish at its anterior portion and brownish at its posterior portion, and whitish ventrally (Figs. 37,39–45); entire legs yellowish brown, whitish at their proximal portion (Figs. 48–51); cerci yellowish brown throughout all their extension (Fig. 43). **Head**: slightly pubescent, elongated in frontal view; front yellowish brown; gena whitish brown; fastigium with long bristles, extending the vertex in an inclined plane pointing downwards; clypeus and labrum whitish with yellowish spots; mandibles yellowish brown and more sclerotized at the apex and margins; maxiles whitish and more sclerotized at the apex (Fig. 40); all maxillary palpomeres pubescent, the first two are whitish, short and same-sized, the other three palpomeres are longer and light yellowish brown, palpomere V (1.77 mm) is claviform and whitish at the apex (right maxillary palp missing) (Fig. 41); all labial palpomeres pubescent, increasing in size, palpomeres I and II are whitish, palpomere III is light yellowish brown and dilated from base to apex, which is whitish (Fig. 41); scape, pedicel and flagellomeres yellowish brown, distal portion whitish (Fig. 41); compound eyes reduced, ommatidia black; ocelli absent (Fig. 41). **Thorax**: pronotum lateroanterior and lateroposterior regions with long bristles; dorsal disk broader than long (1.94 and 2.86 mm in length and width, respectively), lateral lobes rounded and leaning towards the anterior portion of the body, anterior and posterior margins arched and sub-straight (Fig. 37). **Legs**: femur, tibia and tarsus pubescent (Figs. 48–51). *Leg I* (Figs. 50 and 51): tibia slightly longer than the femur, with an oval tympanum on its inner side and two same-sized ventral apical spurs, first tarsomere ventrally serrated and longer than the second and third tarsomeres together. *Leg II* (Figs. 50 and 51): tibia slightly longer than the femur, with two same-sized ventral apical spurs, first tarsomere ventrally serrated and longer than the second and third tarsomeres together. *Leg III* (Figs. 48 and 49): femur developed; tibia slightly longer than the femur (8.75 and 8.17 mm, respectively); tibia armed with four subapical spurs on the outer side, the distal being the shortest, and three on the inner side, the proximal being the shortest, three apical

spurs on the outer side (Fig. 49; a, b, c), spur "a" being the longest and "c" the shortest, and four on the inner side (Fig. 48; d, e, f, g), spurs "e" and "f" longer than the "d" and "g"; first tarsomere longer than the second and third tarsomeres together, with two apical spurs, the inner one being the longest (right leg missing). **Right tegmen**: slightly sclerotized; covering the first four urotergites (5.12 and 3.39 mm in length and width, respectively); *harp* with four well-marked crossveins and five cells, a fifth transversal crossvein is visible, but short, and does not reach the opposite margin of the harp, one of the main crossveins derives from two converging crossveins; *mirror* subtriangular, with three well-marked crossveins and three cells, the most anterior vein does not reach the opposite margin of the mirror; *basal field* with a single bifurcated secondary vein connecting Cu2 to 2A, 1A absent; *lateral field* with two connected longitudinal veins and several irregular and weakly marked secondary veins (Fig. 38); *stridulatory file* with 54 teeth. **Abdomen**: cerci pubescent, with globose setae at the base, mainly on the inner side, and long bristles throughout all their extension (right cerci broken); sub-genital plate whitish brown, distal margin rounded, with a small dent in the center (Fig. 44); supra-anal plate yellowish brown, shorter than the sub-genital plate, subtriangular, distal margin rounded, lateral projections short and curved outwards (Fig. 45); paraprocts as long as the supra-anal plate and barely visible in dorsal view (Fig. 45).

Proventriculus (paratype ISLA 104848, Figs. 46–47). Proventriculus internally organized in six rows of 13 overlaid sclerotized appendices (sa); sclerotized lobes (sl) bearing a cluster of bristles are visible on each side of the sclerotized appendices; sclerotized appendices formed by a median tooth (mt), with at least five, but up to seven median denticles (md), and two lateral teeth (lt), with several lateral denticles (ld); a single median tooth showed eight median denticles; median denticles elongated, tapered and acute at the tip; lateral denticles also elongated, tapered and acute at the tip; the most posterior sclerotized appendix does not have a median tooth.

Male phallic sclerites (holotype ISLA 104845, Figs. 32–36). Phallic complex broadened at the proximal and central portions, with an almost trapezoidal contour in dorsal and ventral views (Figs. 32 and 33). **Pseudepiphallus:** arms short and slightly inclined inwards in dorsal view (Fig. 32, Ps.arm); dorsal branches long, dorsally projected, tapered and acute at the apex, which is slightly inclined towards the interior of the phallic complex in frontal view (Fig. 35, Ps.db); "A" sclerite well-developed, elongated and dilated at the apex (Figs. 34 and 36, A); paramere 1 and 2 fused in a single circular and concave structure that does not extend itself past the dorsal branches in dorsal view, half-moon-shaped in frontal view, distal region highly sclerotized, dorsal portion sclerotized, forming a circular edge that reaches the tip of the posterior portion of the ectophallic median projections in dorsal view (Fig. 32, Ps.p); inner bars concave and slightly curved downwards in dorsal view (Fig. 32, Ps.ib); rami developed, forming a membranous shield that partially covers the ectophallic apodeme in lateral view (Fig. 36, R). **Ectophallic invagination:** arc well-developed, wide and trapeze-like in ventral view (Fig. 33, Ect.arc); apodeme developed and slightly inclined towards the interior of the sclerite in dorsal view (Fig. 32, Ect.ap); lateral bars developed, sinuous, longer than the ectophallic median projections, slightly inclined inwards, with a hook-shaped apex in ventral view (Fig. 33, Ect.lb); median projections long, slender, slightly curved towards the exterior of the sclerite and reaching the parameres in dorsal view (Fig. 32, Ect.mp). **Endophallus:** anterior portion well-developed and sclerotized, with a central groove and a crest opposite to the groove in lateral view (Fig. 36, End.sc.a.); duct short, membranous, barely exceeding the length of the ectophallic arc in ventral view (Fig. 33, End.sc.d); posterior portion membranous, trapezoidal at the apex, exceeding the length of the ectophallic median projections considerably and almost reaching the pseudepiphallic dorsal branches at their apexes in dorsal view (Fig. 32, End.sc.p).

Variations in phallic sclerites (paratypes, n = 5, ISLA 104847, 104848, 104849, 104850, 104851)**.** Phallic complexes vary slightly in size and degree of sclerotization; pseudepiphallic arms (Ps.arm), although always inclined to the interior of the sclerite, may vary slightly in the degree of inclination; right and left pseudepiphallic dorsal branches (Ps.db) with misaligned apexes as they extend dorsally and point to the center of the phallic complex; pseudepiphallic inner bars (Ps.ib) may be more or less concave, inclined or not towards the anterior and central part of the sclerite; ectophallic apodeme (Ect.ap) may or may not be inclined to the interior of the phallic complex; the distance between the endophallic sclerite posterior portion (End.sc.p) and the apex of the pseudepiphallic dorsal branches differs; in addition to that, the shape of the endophallic sclerite posterior portion also varies slightly, but still maintains the trapezoidal outline.

Variations in male right tegmen (Figs. 52–57). **Stridulatory file** with 56.17 ± 1.95 teeth (n° = 6, holotype and paratypes). **Harp** outline conserved; three to five diagonal crossveins; four to six cells; a short and incomplete diagonal crossvein may be present (Figs. 55–57). **Mirror** outline varies from subtriangular to almost arch-like; two or three arched crossveins; three or four cells; incomplete crossveins may be present (Fig. 52); irregular and poorly

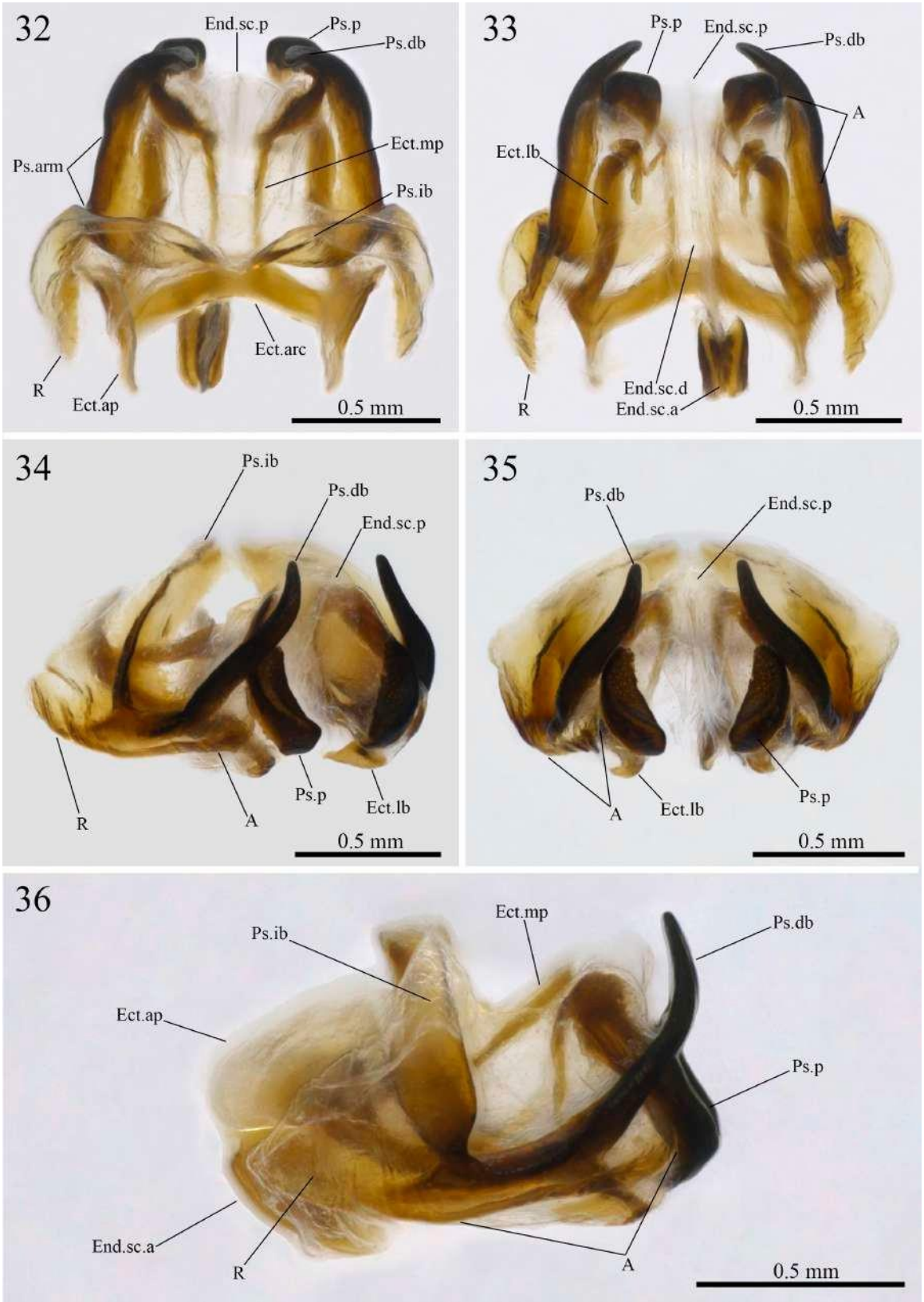
marked veins may also be present (Fig. 57); two main crossveins may be derived from a single bifurcated crossvein (Fig. 54). **Basal field** outline conserved; 1A may be poorly marked, incomplete (Fig. 52) or absent (Fig. 53). **Lateral field** with two parallel longitudinal veins that may or may not be connected.

Female (paratype ISLA 104846, Figs. 58–63). Same coloration of the male, except for the dorsal side of the abdomen, which is, in this case, yellowish brown; apterous; bigger than the male (17.03 and 13.47 mm ± 1.02 mm in length, respectively); supra-anal plate yellowish brown, pubescent, elongated, conical in shape, with two small lateral projections, distal margin rounded and covered by long bristles (Fig. 59); sub-genital plate brown, pubescent, short, but broad, distal margin rounded, with a large V-shaped dent in the center (Fig. 58); ovipositor shorter than the cerci (7.5 mm), with a dorsoventral constriction near the apex, shaped like a curved sword (Figs**.** 60 and 62). **Copulatory papilla** sclerotized and short, anterior portion membranous, with an almost rectangular contour in dorsal and ventral views; distal portion widened, chalice-like, V-shaped ventral end longer than the also V-shaped dorsal end in lateral and dorsal views (Fig. 63).

Ecological remarks. Specimens of *Endecous zin* **n. sp.** were found in four caves located in the municipalities of Carinhanha and Serra do Ramalho, southwestern Bahia State, Brazil. The Gruna das Três Cobras cave was defined as the type locality. This cave has 5,620 meters of horizontal projection (Silva *et al.* 2019), presenting internal conduits and chambers of labyrinthic aspect (Fig. 64). The cave has many entrances, most of them located at the base of the limestone outcrop. The cave atmosphere is constantly influenced by the airflow coming from those entrances and, as a consequence, several conduits dry out during the dry season (Fig. 65). However, due to the cave extension, there are moistened inner chambers located far from the entrances that remain humid even during the dry season. Specimens of *Endecous zin* **n. sp**. were observed in several areas along the cave, but never close to the entrances. They were usually walking on the cave floor or walls (Fig. 66). It is important to mention that this cave is partially flooded during the rainy season. Hence, the habitat of this species seems to be seasonally altered, thus, the crickets likely need to migrate to distinct areas in each season. The main organic resources occurring in the cave are plant debris from the epigean vegetation, and bat guano, the latter being more common in deeper regions of the cave. Such guano piles certainly represent an important food resource for this species, along with other decaying material, considering its generalist detritivore nature. This cave receives no human visitors, with the exception of few speleologists who sporadically explore it. Consequently, the cave is relatively well preserved. Nonetheless, the external area is highly degraded, with drone images revealing the extension of the logging activity in the cave surroundings (Fig. 64). Most areas were converted to pastures or had the vegetation removed and burned, maybe for future expansion of the grazing areas. As previously mentioned, such practices influence the organic input to the cave environment directly and, at the same time, contribute to the silting of many conduits and chambers inside the cave. Because of that, several microhabitats that might be important to this new species (among others) may be being severely altered by the external deforestation. In that sense, urgent actions are needed in order to prevent further negative impacts in the cave surroundings.

Endecous zin **n. sp**. was also observed in other three caves located not far from the Gruna das Três Cobras cave (Gruna do Google, Gruna Grande and Gruna da Serra Solta II caves). Such caves are considerably long (more than 1km of horizontal projection) and have intermittent drainages along their main conduit. The Gruna do Google and Gruna Grande caves were only visited by speleologists since its discovery, due to the difficulty in accessing their inner portions. Hence, its interior is quite preserved. The Gruna da Serra Solta II cave, on the other hand, is partially impacted, especially at the entrance area, where locals pump water from a cistern using a diesel engine. However, since the cave is quite long, most of its extension is devoid of visible impacts caused by humans. It is worth noting that there are many other caves in that area that were not sampled, so it is quite plausible to assume that *E. zin* **n. sp.** is more widely distributed in the region.

Similar to the Gruna das Três Cobras cave surroundings, the external landscape of Gruna do Google, Gruna Grande and Gruna da Serra Solta II caves is also altered, due to replacement of the original vegetation by pastures and crops. In that sense, it is important to highlight that the region is under risk, especially considering agriculture expansion and the growing threats of limestone extraction, which may impact the entire Serra do Ramalho region, affecting several caves, including those previously described.



FIGURES 32–36. *Endecous* (*Endecous*) *zin* **n. sp.** (ISLA 104845) phallic complex. (32) dorsal view, (33) ventral view, (34) laterofrontal view, (35) frontal view, (36) lateral view. Abbreviations: **A**, pseudepiphallic ventral branch (or "A" sclerite); **Ps.arm**, pseudepiphallic arm; **Ps.db**, pseudepiphallic dorsal branch; **Ps.ib**, pseudepiphallic inner bars; **R**, pseudepiphallic rami (or pseudepiphallic membranous shield); **Ps.P**, pseudepiphallic paramere; **Ect.ap**, ectophallic apodeme; **Ect.arc**, ectophallic arc; **Ect.lb**, ectophallic lateral bar; **Ect.mp**, ectophallic median projection; **End.sc.a**, endophallic sclerite anterior portion; **End. sc.d**, endophallic sclerite duct; **End.sc.p**, endophallic sclerite posterior portion.

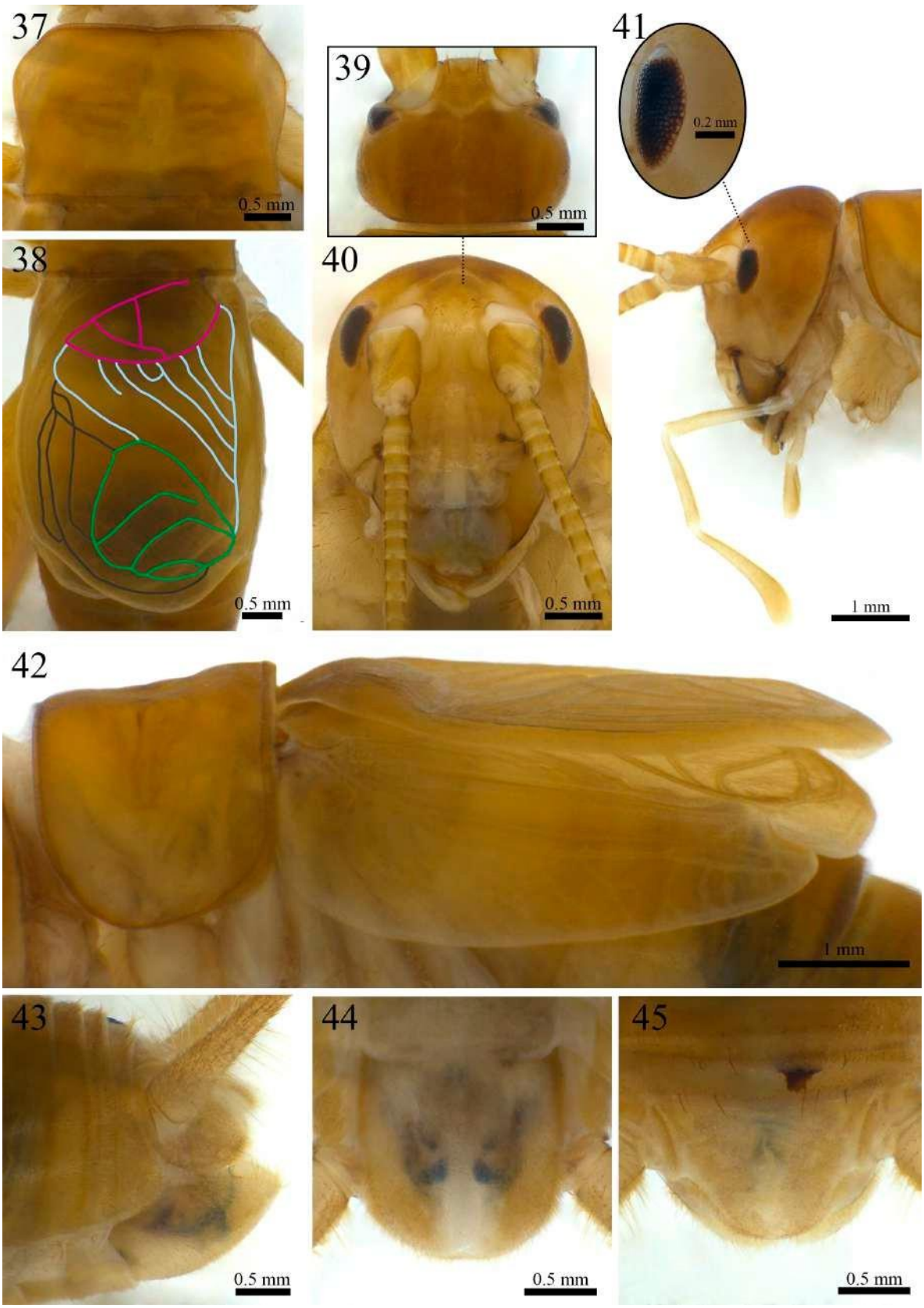
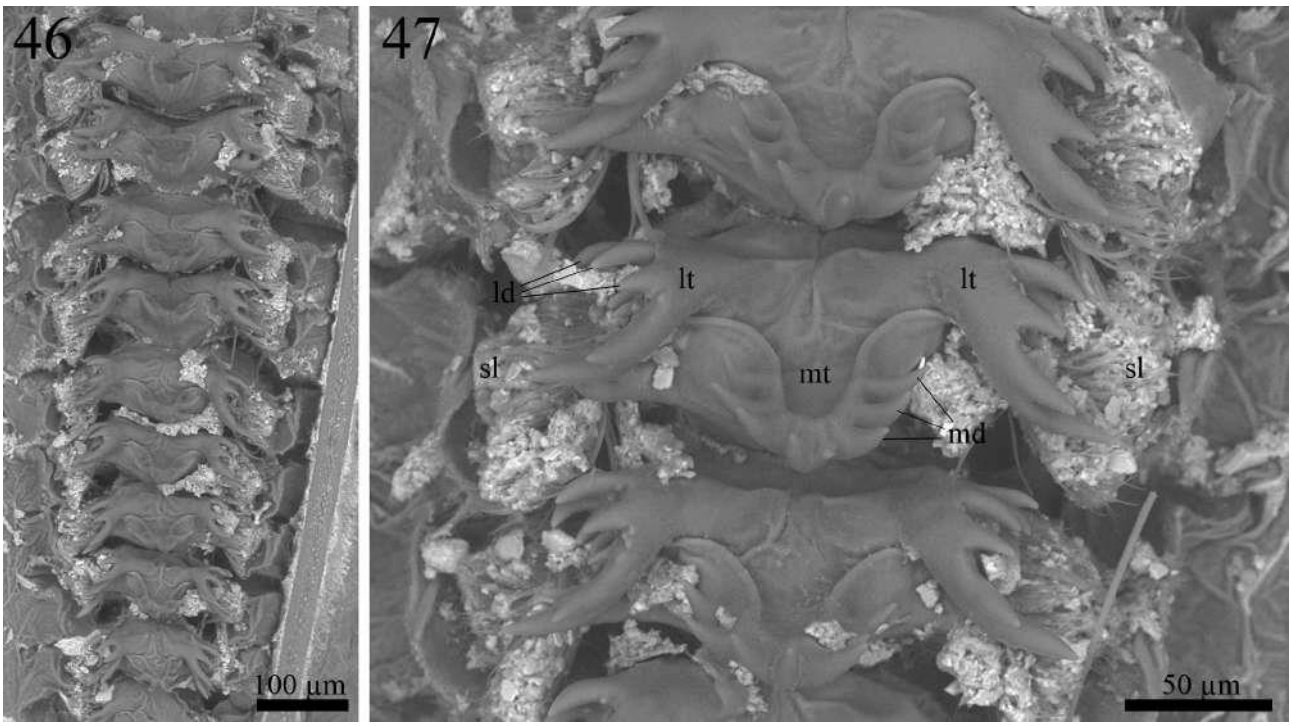
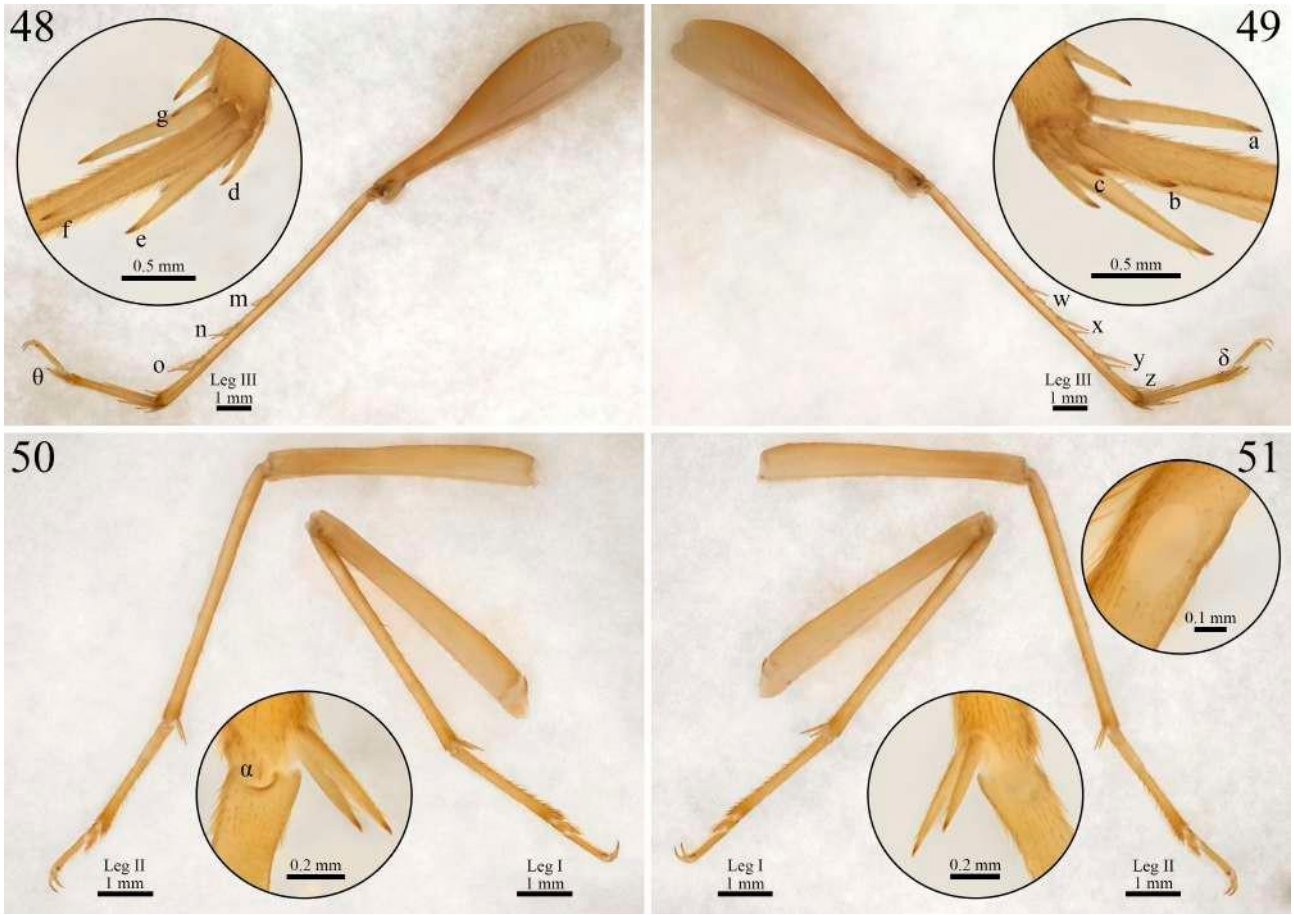


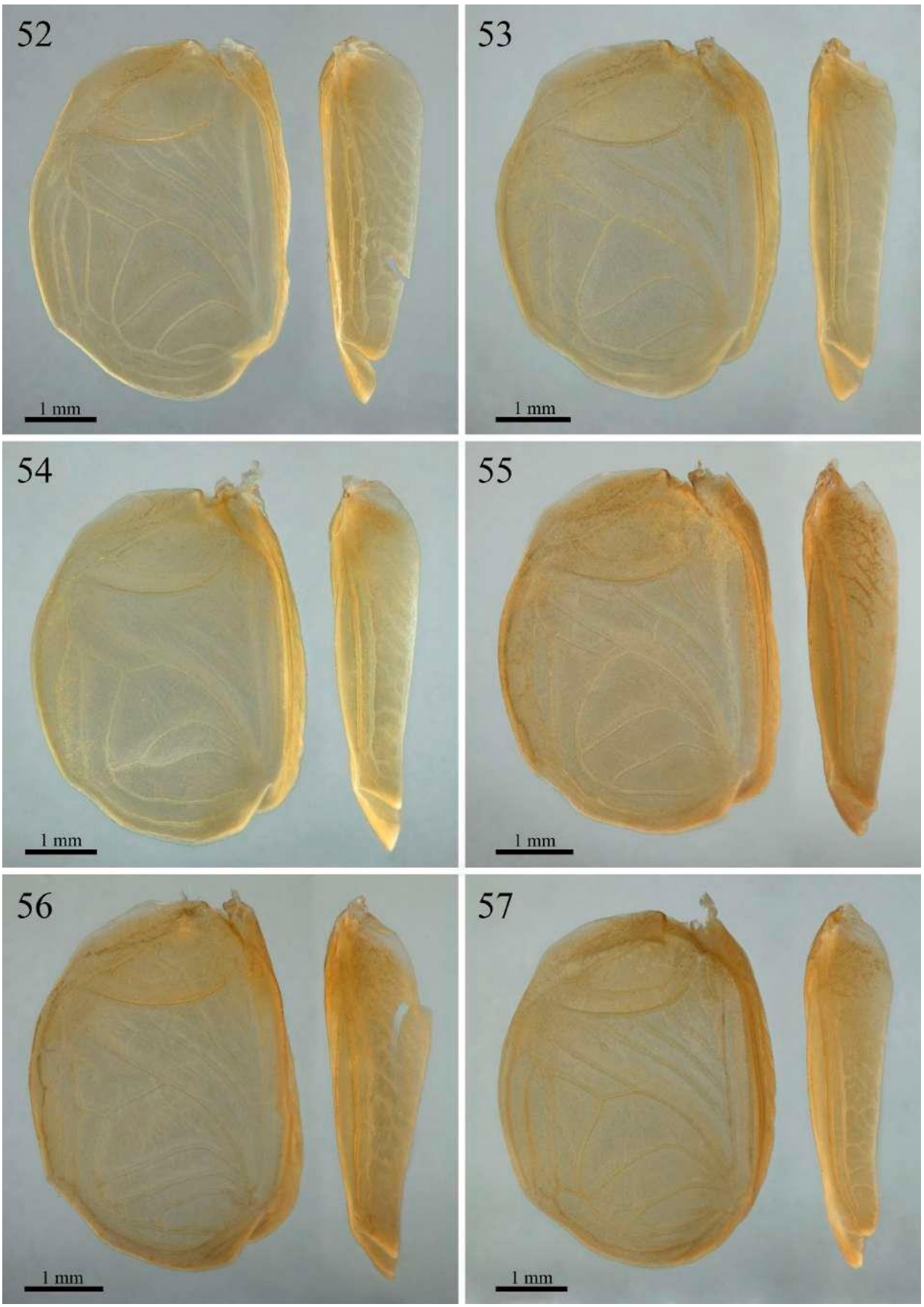
FIGURE 37–45. *Endecous* (*Endecous*) *zin* **n. sp.** (ISLA 104845) male general morphology. (37) pronotum in dorsal view; (38) right tegmen in dorsal view, harp highlighted in light blue, mirror highlighted in green, basal field highlighted in pink; (39) head in dorsal view; (40) head in frontal view; (41) head and palpi in lateral view, compound eye highlighted; (42) pronotum and tegmen in lateral view; (43) supra-anal and sub-genital plates in lateral view; (44) sub-genital plate in ventral view; (45) supra- anal plate in dorsal view.



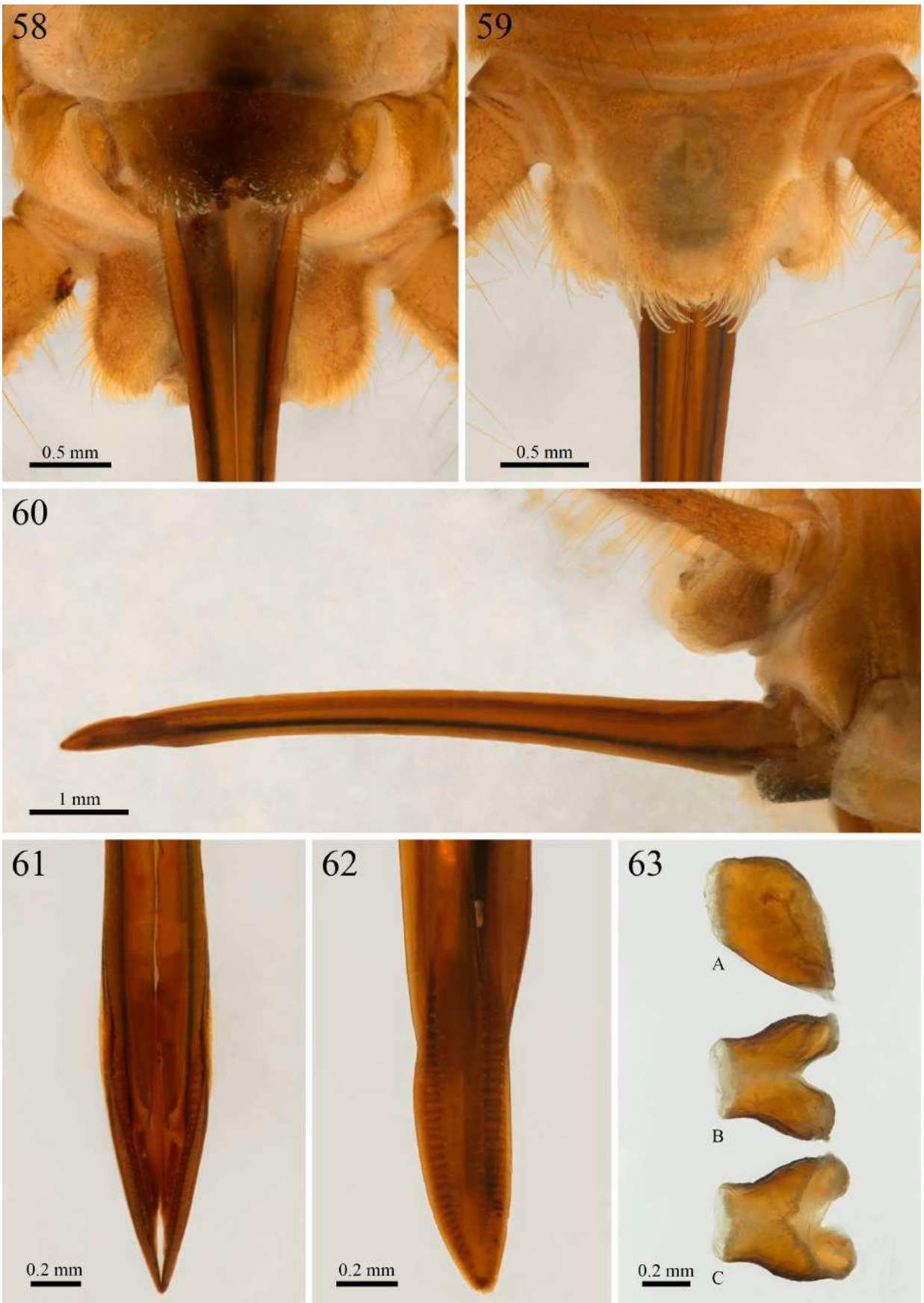
FIGURES 46–47. *Endecous* (*Endecous*) zin **n. sp. (**ISLA 104848) proventriculus. (46) row of sclerotized appendices; (47) sclerotized appendix. Abbreviations: **mt**, median tooth; **md**, median denticles; **lt**, lateral tooth; **ld**, lateral denticles; **sl**, sclerotized lobe



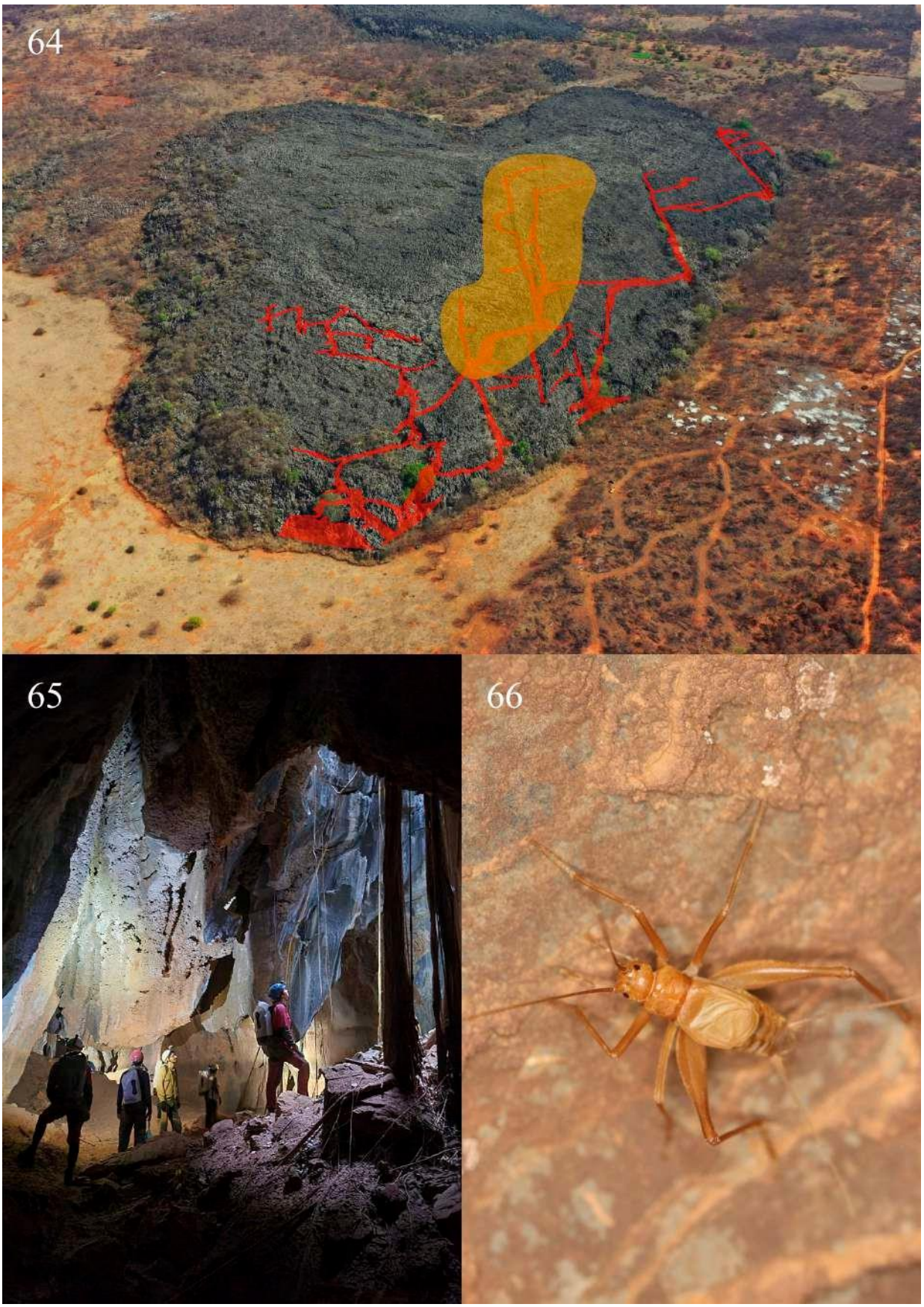
FIGURES 48–51. *Endecous* (*Endecous*) *zin* **n. sp.** (ISLA 104845) left legs. (48) leg III, subapical and apical spurs, inner view (49) leg III, subapical and apical spurs, outer view (50) legs I and II, apical spurs, third small spur (α) at the apex of the tibia, outer view (51) legs I and II, apical spurs and tympanum, inner view.



FIGURES 52–57. *Endecous* (*Endecous*) *zin* **n. sp.** right tegmen, dorsal and lateral view. (52) holotype, ISLA 104845; (53) paratype, ISLA 104847; (54) paratype, ISLA 104848; (55) paratype, ISLA 104849; (56) paratype, ISLA 104851; (57) paratype, ISLA 104850.



FIGURES 58–63. *Endecous* (*Endecous*) *zin* **n. sp.** (ISLA 104846) ovipositor and copulatory papilla. (58) sub-genital plate; (59) supra-anal plate; (60) ovipositor, lateral view; (61) ovipositor apex, dorsal view; (62) ovipositor apex, lateral view; (63) copulatory papilla, A—lateral view, B—ventral view, C—dorsal view.



FIGURES 64–66. *Endecous* (*Endecous*) *zin* **n. sp.** habitat. (64) Gruna das Três Cobras cave, external environment, highlighted in red: horizontal progression of the cave, highlighted in yellow: area where *E.* (*E.*) *zin* **n. sp.** were more commonly found; (65) Gruna das Três Cobras cave, internal environment; (66) adult male of *E.* (*R.*) *zin* **n. sp.**

TABLE 2. *Endecous* (*Endecous*) *zin* **n. sp.**, morphological measurements (mm), mean (M) and standard deviation (SD) of six male and one female adult specimens; *pars stridens* refers to the number of teeth of the stridulatory file.

♂	104845	104847	104848	104849	104850	104851	M	SD
Head width	2.308	2.206	2.278	2.239	2.398	2.201	2.272	0.068
Head length	1.742	1.342	1.390	1.462	1.542	1.573	1.509	0.131
Intraocular distance	1.316	1.311	1.308	1.326	1.284	1.308	1.309	0.013
Compound eye width	0.301	0.335	0.332	0.288	0.270	0.301	0.305	0.023
Compound eye length	0.685	0.673	0.665	0.649	0.714	0.704	0.682	0.022
Maxillary palpomere III	1.286	1.292	1.246	1.263	1.235	1.079	1.234	0.072
Maxillary palpomere IV	1.343	1.308	1.352	1.303	1.259	1.002	1.261	0.120
Maxillary palpomere V	1.772	1.710	1.775	1.830	1.727	1.212	1.671	0.209
Pronotum width	2.857	3.105	3.012	2.961	2.972	2.826	2.956	0.093
Pronotum length	1.945	1.969	1.919	1.990	2.035	1.848	1.951	0.059
Right tegmen width	3.391	3.573	3.714	3.467	3.567	3.401	3.519	0.113
Right tegmen length	5.120	4.729	5.027	4.491	4.942	4.774	4.847	0.209
Leg I length	12.226	13.091	13.066	13.242	13.585	12.721	12.989	0.426
Leg II length	12.764	13.463	13.316	13.524	13.777	13.083	13.321	0.326
Femur III length	8.170	8.301	8.531	8.469	8.706	8.770	8.491	0.210
Tibia III length	8.751	8.830	9.256	9.244	9.365	9.044	9.082	0.228
Body length	12.345	13.982	15.204	13.817	12.211	13.272	13.472	1.023
Pars stridens	54	59	57	54	58	55	56.167	1.951

Continued.

♀	104846
Head width	2.939
Head length	1.984
Intraocular distance	1.618
Compound eye width	0.402
Compound eye length	0.806
Maxillary palpomere III	1.540
Maxillary palpomere IV	1.587
Maxillary palpomere V	1.990
Pronotum width	3.843
Pronotum length	2.582
Femur III length	10.748
Tibia III length	12.290
Body length	17.033
Ovipositor length	7.501

***Endecous* (*Endecous*) *zaum* n. sp.**
(Figures 67–71, 72–80, 81–82, 83–86, 87–92, 93–97; Table 3)

Material examined. *Holotype*, ♂, code ISL 104855, Brazil, Bahia, municipality of Coribe, Serra Verde cave (44°19′26.85″W, 13°43′28.04″S), 20.ix.2021, R.L. Ferreira; condition: right tegmen, left legs and phallic complex were detached/dissected and stored alongside the holotype. *Paratypes*, 9 ♂♂, ISLA 104852, 104853, 104854, municipality of Coribe, Serra Verde cave (44°19′26.85″W, 13°43′28.04″S), 20.ix.2021, R.L. Ferreira; ISLA 104856, 104857, municipality of Coribe, Gruna do Enfurnado cave (44°12′7.99″W, 13°38′45.69″S), 25.viii.2022, R.L.

Ferreira; ISLA 104858, 104859, 104860, 104861, municipality of Coribe, Gruna do Zeferini cave (44°14′4.52″W, 13°46′15.55″S), 24.viii.2022, R.L. Ferreira.

Etymology. The epithet "zaum" is a Russian term composed by the prefix *за* (beyond) and *ум* (mind, knowledge). Hence, it literally means "beyond knowledge". This term should be treated as a noun in apposition.

Diagnosis. Combination of the following characteristics: pseudepiphallic dorsal branches (Ps.db) elongated, dorsally projected and pointing to the center of the phallic complex, distal portion turning inwards abruptly in relation to the proximal portion; pseudepiphallic ventral branches (A) elongated, apex dilated and rounded; pseudepiphallic inner bars (Ps.ib) flat and inclined inwards; pseudepiphallic rami (R) developed, forming a membranous shield that covers the most proximal portion of the ectophallic apodeme; ectophallic arc (Ect.arc) rounded at the posterior and anterior middle portions; ectophallic lateral bars (Ect.lb) elongated, sinuous and rounded at the apex; endophallic sclerite anterior portion (End.sc.a) with a crest on the opposite side of its central groove.

Morphology (paratype ISLA 104854, Figs. 72–80). **Body color:** dorsal head yellowish brown with irregular brown patches; pronotum yellowish brown; abdomen brown dorsally and whitish ventrally (Figs. 72,74–80); entire legs yellowish brown, whitish at their proximal portion (Figs. 83–86); cerci brown at the base and yellowish brown towards the apex (Fig. 78). **Head**: slightly pubescent, elongated in frontal view; front brown; gena yellowish brown; fastigium with long bristles, extending the vertex in an inclined plane pointing downwards; clypeus and labrum whitish; mandibles yellowish brown and more sclerotized at the apex and margins; maxiles whitish and more sclerotized at the apex (Fig. 75); all maxillary palpomeres pubescent, the first two whitish, short and same-sized, the other three palpomeres yellowish brown and longer, the palpomere V (1.81 mm) is claviform and whitish at the apex (Fig. 76); all labial palpomeres light yellowish brown, pubescent, increasing in size, the third one dilated from base to apex, which is whitish (Fig. 76); scape, pedicel and flagellomeres yellowish brown, distal portion whitish (Fig. 76); compound eyes reduced, ommatidia black; ocelli absent (Fig. 46). **Thorax**: pronotum lateroanterior and lateroposterior regions with long bristles; dorsal disk broader than long (2.55 and 3.51 mm in length and width, respectively), lateral lobes rounded and leaning towards the anterior portion of the body, anterior and posterior margins arched and sub-straight (Figs. 72 and 77). **Legs**: femur, tibia and tarsus pubescent (Figs. 83–86). *Leg I* (Figs. 85 and 86): tibia slightly longer than the femur, with an oval tympanum on its inner side and two same-sized ventral apical spurs, first tarsomere ventrally serrated and longer than the second and third tarsomeres together. *Leg II* (Figs. 85 and 86): tibia slightly longer than the femur, with two same-sized ventral apical spurs, first tarsomere ventrally serrated and longer than the second and third tarsomeres together. *Leg III* (Figs. 83 and 84): femur developed; tibia longer than the femur (12.49 and 10.99 mm respectively); tibia armed with four subapical spurs on the outer side, the distal being the shortest, and three on the inner side, the proximal being the shortest, three apical spurs on the outer side (Fig. 84; a, b, c), spur "a" being the longest and "c" the shortest, and four on the inner side (Fig. 83; d, e, f, g), spurs "e" and "f" longer than the "d" and "g"; first tarsomere longer than the second and third tarsomeres together, with two apical spurs, the inner one being the longest. **Right tegmen**: slightly sclerotized; covering the first three urotergites (5.22 and 4.17 mm in length and width, respectively); *harp* with five cells and four well-marked crossveins, the two most proximal ones share the same origin point, a fifth crossvein is visible, but short and does not reach the opposite margin of the harp; *mirror* with two distinct crossveins and three cells; *basal field* with a single and short secondary vein connecting Cu2 to 1A; *lateral field* with two longitudinal veins and several irregular and weakly marked veins (Fig. 73); *stridulatory file* with 95 teeth. **Abdomen**: cerci pubescent, with globose setae at the base, mainly on the inner side, and long bristles throughout all their extension; sub-genital plate whitish brown, U-shaped, proximal margin broader than the distal margin, which is rounded (Fig. 79); supra-anal plate yellowish-brown, subtriangular, distal margin rounded lateral projections short and slightly curved outwards (Fig. 80); paraprocts as long as the supra-anal plate, projecting themselves laterally and, therefore, visible in dorsal view (Figs. 78 and 80).

Proventriculus (paratype ISLA 104852, Figs. 81–82). Proventriculus internally organized in six rows of 11 or 12 overlaid sclerotized appendices (sa); sclerotized lobes (sl) bearing a cluster of bristles are visible on each side of the sclerotized appendices; sclerotized appendices formed by a median tooth (mt), with at least five, but up to nine median denticles (md), and two lateral teeth (lt), with several lateral denticles (ld); median denticles short and rounded at the tip; lateral denticles also short and rounded at the tip; the most posterior median tooth bears two or three short median denticles; the most posterior sclerotized appendix does not have a median tooth.

Male phallic sclerites (holotype ISLA 104855, Figs. 67–71). Phallic complex broadened at the proximal and central portions, with an almost trapezoidal contour in dorsal and ventral views (Figs. 67 and 68). **Pseudepiphallus:**

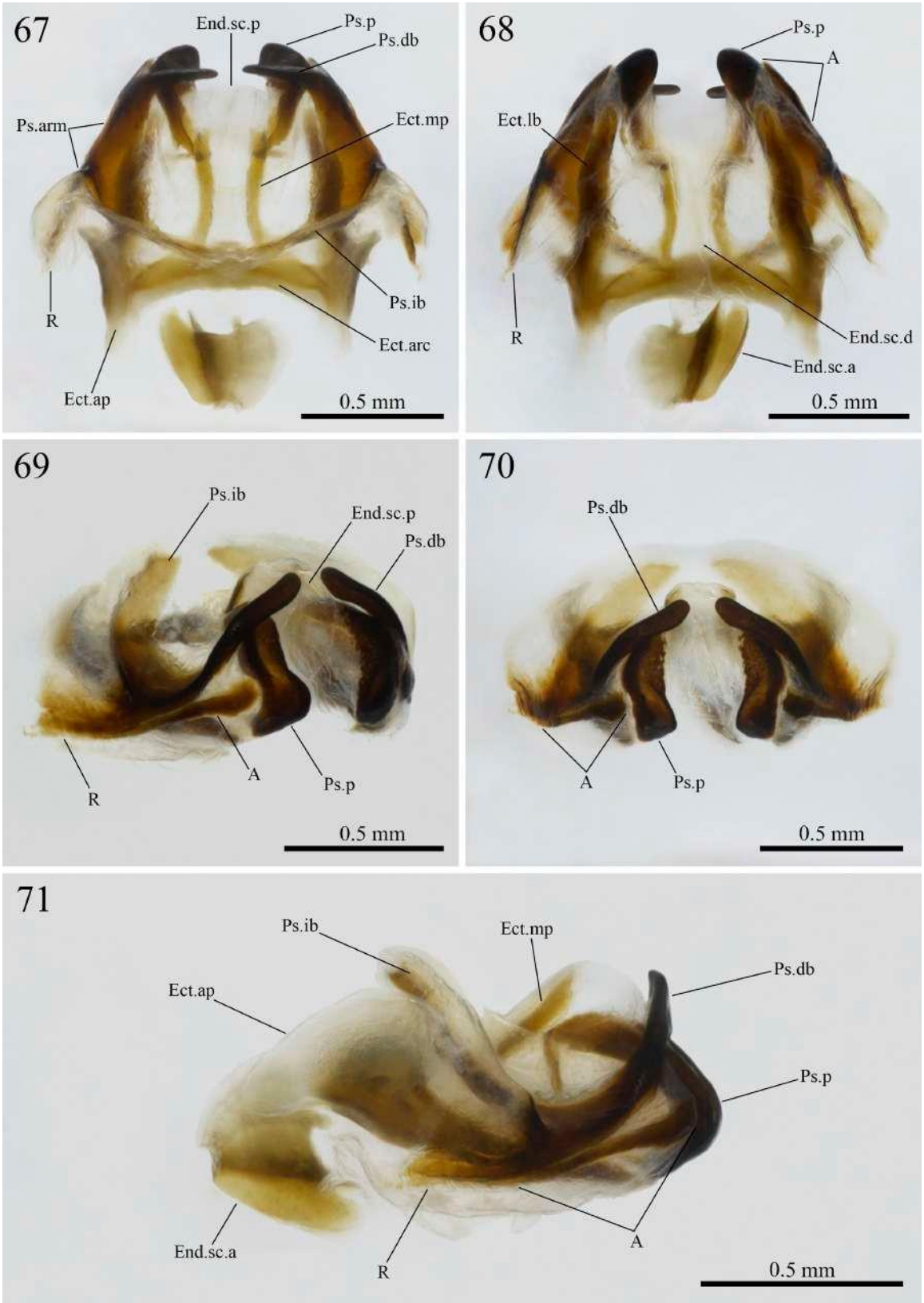
arms short and inclined inwards in dorsal view (Fig. 67, Ps.arm); dorsal branches long, projecting dorsally towards the center of the phallic complex, with the distal half virtually perpendicular to the proximal half in dorsal view, apexes slightly dilated, rounded at the tip and almost touching each other in frontal view (Fig. 70, Ps.db); "A" sclerite well-developed, elongated and dilated at the apex, with a rounded tip (Figs. 69–71, A); paramere 1 and 2 fused in a single circular and concave structure, bean-shaped in frontal view, distal region highly sclerotized, ventral region exceeding the length of the dorsal branches in both dorsal and ventral views, dorsal portion sclerotized, forming a scythe-like edge that reaches the ventral side of the posterior portion of the ectophallic median projections (Fig. 67, Ps.p); inner bars flat and slightly inclined downwards in dorsal view (Fig. 67, Ps.ib); rami developed, forming a membranous shield that covers only the proximal portion of the ectophallic apodeme in lateral view (Fig. 71, R). **Ectophallic invagination:** arc well-developed, wide, dome-shaped at both posterior and anterior central parts in ventral view (Fig. 68, Ect.arc); apodeme developed and slightly curved inwards in dorsal view (Fig. 67, Ect.ap); lateral bars well-developed, sinuous, slightly inclined inwards, longer than the ectophallic median projections, with a rounded apex and almost touching the parameres in ventral view (Fig. 68, Ect.lb); median projections slender, elongated, reaching the parameres, slender and slightly curved outwards in dorsal view (Fig. 67, Ect.mp). **Endophallus:** anterior portion well-developed and sclerotized, with a central groove and a dorsal crest, opposite to the groove in lateral view (Fig. 71, End.sc.a); duct short, membranous throughout all its extension, which subceeds the length of the ectophallic apodeme in ventral view (Fig. 68, End.sc.d); posterior portion membranous, trapeze-shaped, exceeding the length of the ectophallic median projections considerably and almost reaching the pseudepiphallic dorsal branches at their apexes in dorsal view (Fig. 67, End.sc.p).

Variations in phallic sclerites (paratypes, n = 6, ISLA 104852, 104853, 104854, 104856, 104860, 104861)**.** Phallic complexes vary slightly in degree of sclerotization; pseudepiphallic arms (Ps.arm) vary subtly in degree of inclination towards the center of the sclerite; pseudepiphallic dorsal branches (Ps.db) always bent abruptly towards the interior of the sclerite, but may not be perpendicular to the pseudepiphallic arms; pseudepiphallic inner bars (Ps. ib) may be more or less inclined to the anterior portion of the phallic complex; anterior margin of the ectophallic arch (Ect.arc) may be more or less curved; ectophallic apodeme (Ect.ap) may be more or less inclined towards the interior of the sclerite; endophallic sclerite posterior portion (End.sc.p) shape varies slightly, yet retains the trapezoidal outline.

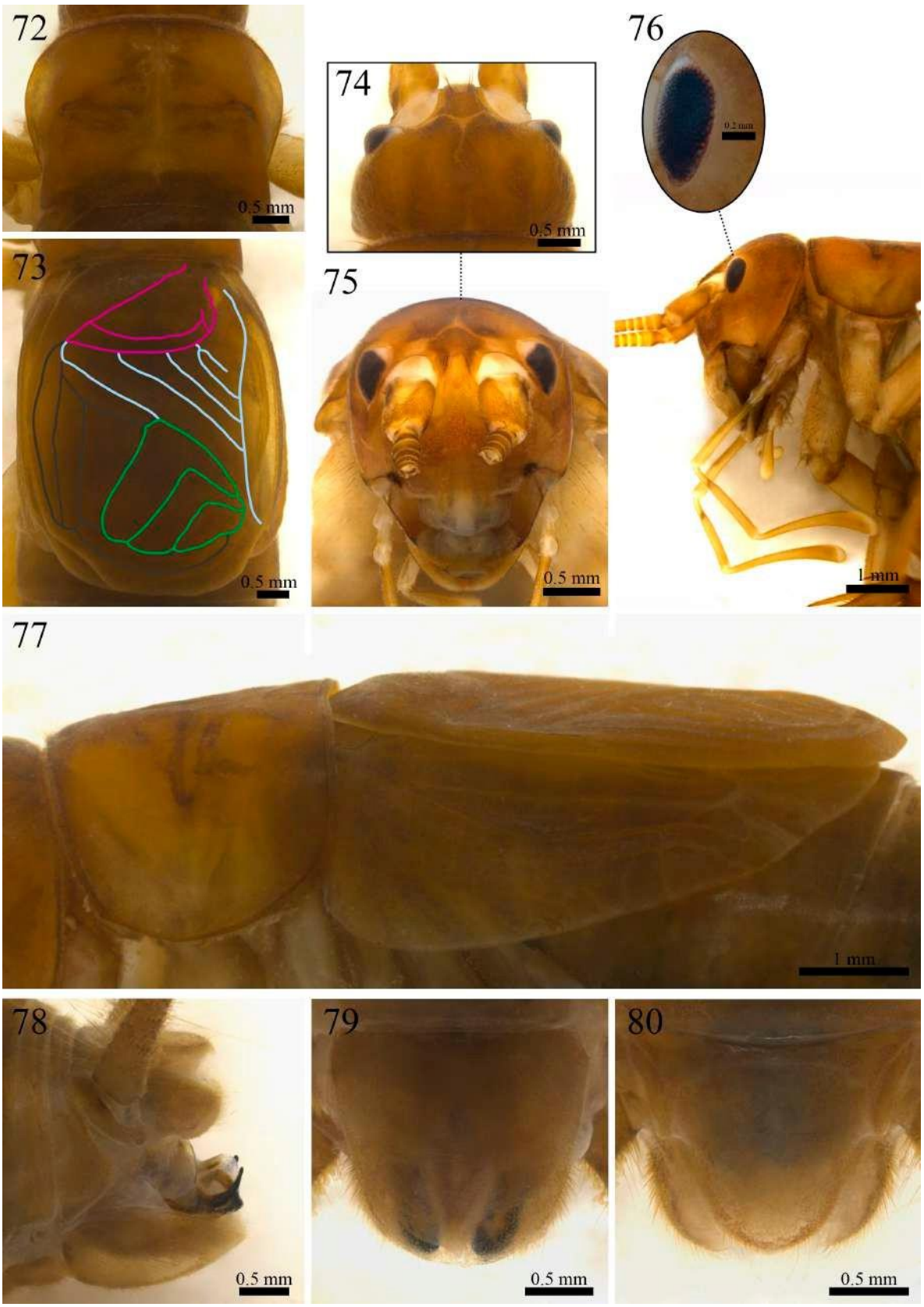
Variations in male right tegmen (Figs. 87–92). **Stridulatory file** with 87.10 ± 5.17 teeth (n° = 10, holotype and paratypes). **Harp** outline conserved; four or five diagonal crossveins and five or six cells; a short and irregular crossvein may be present (Figs. 87, 89 and 92). **Mirror** outline always triangular, with a trapezoidal apex; two complete, V-shaped crossveins (Figs. 87, 89 and 92), two incomplete veins (Fig. 88) one complete vein (Fig. 91) or one incomplete vein (Fig. 90); a third short, diagonal vein may be present (Fig. 88). **Basal field** outline conserved; 1A may branch out into several irregular and poorly marked veins (Fig. 88). **Lateral field** with two parallel longitudinal veins, which may be curved outwards.

Ecological remarks. Specimens of *Endecous zaum* **n. sp.** were observed in the Serra Verde, Gruna do Enfurnado and Gruna do Zeferini caves. However, many other caves exist in the area (most of them not biologically studied), so it is likely that other populations of *E. zaum* **n. sp.** may be found in the future.

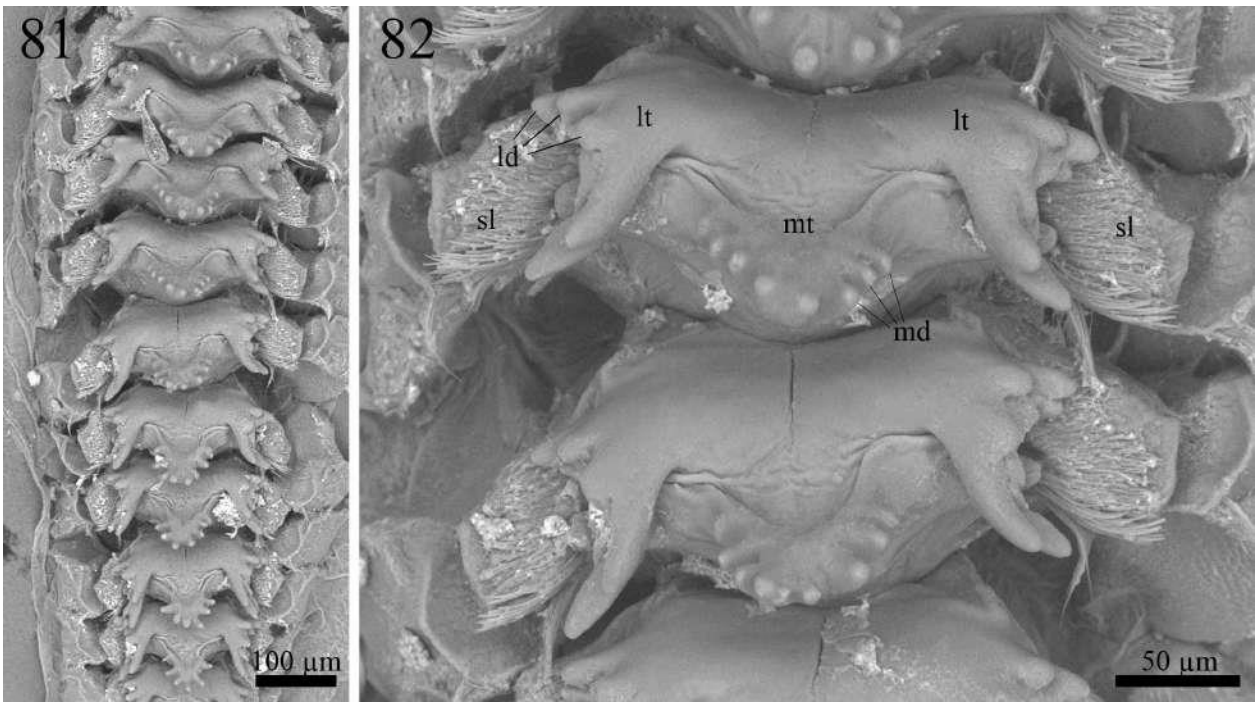
Serra Verde cave (the type locality) has at least 1,730 meters of horizontal projection, but it is still under exploration, so it might be longer than currently known. Even though the cave has a relatively wide entrance (Fig. 94), there is a constriction in the main conduit around 20 meters from the entrance, which prevents the locals from accessing the cave interior. The conduit that follows this constriction is relatively dry. Nevertheless, there are signs that the runoff water penetrates the cave in rainy periods. Our team visited the cave during the dry season, hence, the substrates were predominantly dry near the entrance. Nonetheless, it is important to mention that galleries became progressively wetter as depth increased, the conduits at the final portion of the cave being drenched in water (Fig. 95). Specimens of *E. zaum* **n. sp**. were observed in the humid galleries, far from the entrance, being more frequent in deeper regions of the cave. Individuals were most often seen on the cave floor (Fig. 96). The predominant organic resources were bat guano (especially produced by vampire bats—*Desmodus rotundus*) and plant debris brought by the water. In previous expeditions, speleologists discovered that the inner conduits partially flood during the rainy season, thus indicating that the water table varies greatly throughout the year. For that reason, it is fair to assume that these crickets probably migrate during rainy seasons to regions closer to the entrance that are not flooded.



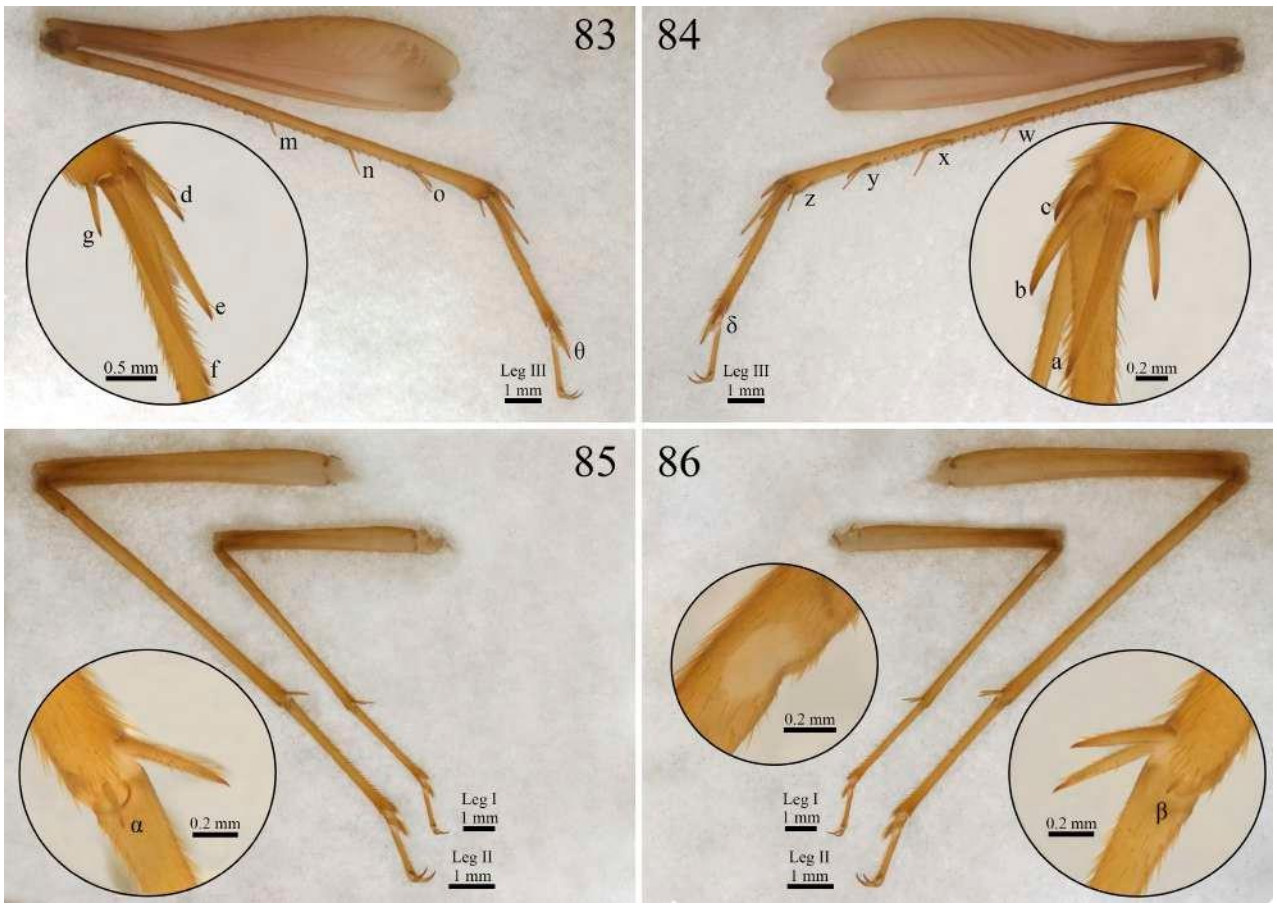
FIGURES 67–71. *Endecous* (*Endecous*) *zaum* **n. sp.** (ISLA 104855) phallic complex. (67) dorsal view, (68) ventral view, (69) laterofrontal view, (70) frontal view, (71) lateral view. Abbreviations: **A**, pseudepiphallic ventral branch (or "A" sclerite); **Ps.arm**, pseudepiphallic arm; **Ps.db**, pseudepiphallic dorsal branch; **Ps.ib**, pseudepiphallic inner bars; **R**, pseudepiphallic rami (or pseudepiphallic membranous shield); **Ps.P**, pseudepiphallic paramere; **Ect.ap**, ectophallic apodeme; **Ect.arc**, ectophallic arc; **Ect.lb**, ectophallic lateral bar; **Ect.mp**, ectophallic median projection; **End.sc.a**, endophallic sclerite anterior portion; **End. sc.d**, endophallic sclerite duct; **End.sc.p**, endophallic sclerite posterior portion.



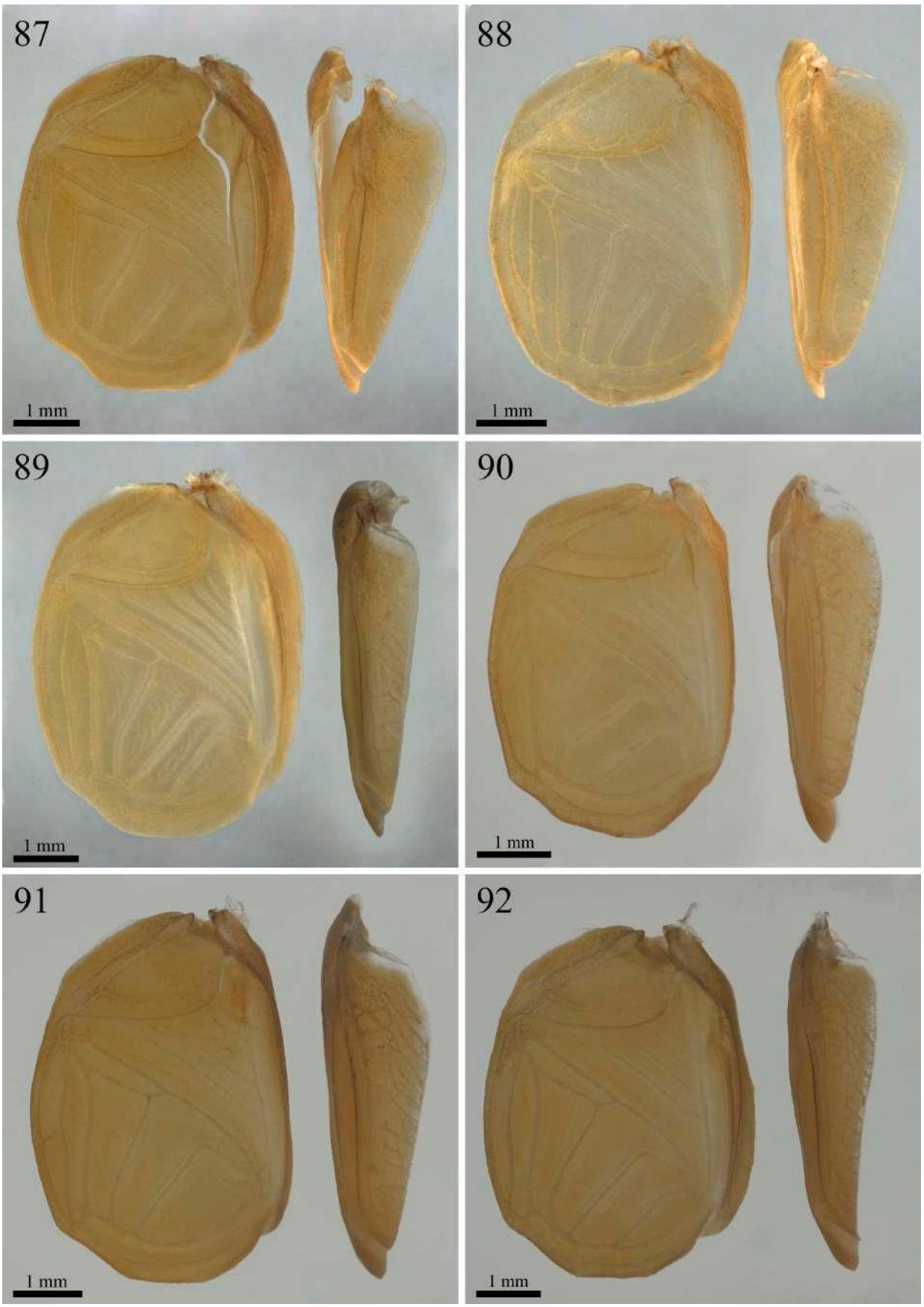
FIGURES 72–80. *Endecous* (*Endecous*) *zaum* **n. sp.** (ISLA 104854) male general morphology. (72) pronotum in dorsal view; (73) right tegmen in dorsal view, harp highlighted in light blue, mirror highlighted in green, basal field highlighted in pink; (74) head in dorsal view; (75) head in frontal view; (76) head and palpi in lateral view, compound eye highlighted; (77) pronotum and tegmen in lateral view; (78) supra-anal and sub-genital plates in lateral view; (79) sub-genital plate in ventral view; (80) supra-anal plate in dorsal view.



FIGURES 81–82. *Endecous* (*Endecous*) *zaum* **n. sp. (**ISLA 104852) proventriculus. (81) row of sclerotized appendices; (82) sclerotized appendix. Abbreviations: **mt**, median tooth; **md**, median denticles; **lt**, lateral tooth; **ld**, lateral denticles; **sl**, sclerotized lobe.



FIGURES 83–86. *Endecous* (*Endecous*) *zaum* **n. sp.** (ISLA 104854) left legs. (83) leg III, subapical and apical spurs, inner view (84) leg III, subapical and apical spurs, outer view (85) legs I and II, apical spurs, third small spur (α) at the apex of the tibia, outer view (86) legs I and II, apical spurs and tympanum, third small spur (β) at the apex of the tibia inner view.



FIGURES 87–92. *Endecous* (*Endecous*) *zaum* **n. sp.** right tegmen, dorsal and lateral view. (87) paratype, ISLA 104854; (88) paratype, ISLA 104853; (89) holotype, ISLA 104855; (90) paratype, ISLA104856 ; (91) paratype, ISLA 104858; (92) paratype, ISLA 104859.



FIGURES 93–97. *Endecous* (*Endecous*) *zaum* **n. sp.** habitat. (93) Serra Verde cave, external environment; (94) Serra Verde cave, entrance; (95) Serra Verde cave, internal environment; (96) adult male of *E.* (*E.*) *zaum* **n. sp.**; (97) cattle in the cave surroundings.

TABLE 3. *Endecous* (*Endecous*) *zaum* **n. sp.**, morphological measurements (mm), mean (M) and standard deviation (SD) of four male adult specimens; (*) unable to measure due to head being damaged; (#) leg III missing; *pars stridens* refers to the number of teeth of the stridulatory file.

♂	104852	104853	104854	104855	104856	104857	104858	104859	104860	104861	M	SD
Head width	2.522	2.501	2.661	2.607	2.601	2.623	2.881	*	2.862	2.586	2.649	0.127
Head length	1.914	1.863	1.724	1.658	1.730	1.592	1.939	*	1.936	1.839	1.799	0.120
Intraocular distance	1.378	1.378	1.407	1.428	1.343	1.370	1.471	*	1.523	1.347	1.405	0.056
Compound eye width	0.355	0.406	0.387	0.379	0.388	0.398	0.394	*	0.431	0.729	0.430	0.108
Compound eye length	0.736	0.767	0.837	0.787	0.764	0.720	0.814	*	0.782	0.384	0.732	0.128
Maxillary palpomere III	1.439	1.567	1.421	1.470	1.460	1.572	1.617	1.718	1.769	1.529	1.556	0.112
Maxillary palpomere IV	1.505	1.490	1.656	1.600	1.510	1.648	1.761	1.713	1.846	1.578	1.631	0.112
Maxillary palpomere V	1.950	1.987	2.167	1.677	2.018	1.970	2.211	2.085	2.210	2.014	2.029	0.150
Pronotum width	3.340	3.315	3.515	3.525	3.342	3.485	3.600	3.595	3.486	3.256	3.446	0.116
Pronotum length	2.303	2.238	2.552	2.359	2.455	2.471	2.565	2.449	2.560	2.334	2.429	0.110
Right tegmen width	3.114	3.722	4.169	4.065	3.668	4.078	3.979	4.105	4.249	3.606	3.876	0.329
Right tegmen length	4.725	5.214	5.225	5.542	5.248	5.475	5.679	5.789	5.774	5.160	5.383	0.315
Leg I length	16.291	16.640	18.173	17.447	16.753	17.656	17.983	17.688	17.953	16.777	17.336	0.630
Leg II length	16.654	16.929	18.433	17.823	17.342	18.387	18.448	18.190	18.053	16.949	17.721	0.658
Femur III length	10.096	10.302	10.994	10.519	10.303	10.564	11.335	10.761	#	10.186	10.562	0.383
Tibia III length	11.417	11.546	12.495	11.711	11.563	12.017	12.874	12.035	#	11.432	11.899	0.479
Body length	15.566	16.152	16.710	18.369	14.227	15.599	16.381	*	17.715	17.624	16.483	1.214
Pars stridens	82	84	95	90	83	93	88	92	86	78	87.1	5.166

As aforementioned, the constriction on the conduit close to the entrance of the cave hinders the access of locals to its interior, which in turn guarantees the preservation of the cave's inner environment. The external landscape, however, is severely altered, especially close to the limestone outcrops, where only a few remnants of the original vegetation can be verified (Fig. 93). Pastures replaced most of the native forests and cattle were observed in the cave surroundings (Fig. 97), compacting the exposed soil, which is highly vulnerable to erosive processes. Additionally, since the cave entrance is located at the bottom of a valley, the external topography ends up contributing to the input of sediments to the cave during rainy periods. The soil denudation in the external landscape can, therefore, intensify erosive processes, increasing the sediment input to the cave, and, consequently, silting up important microhabitats. Accordingly, it is highly recommendable to protect the cave surroundings, especially through the reforestation of the immediate external landscape, to preserve the cave and the species that it harbors.

The other two caves where specimens were found (Gruna do Enfurnado and Gruna do Zeferini caves) are quite distinct from each other and from Serra Verde cave, thus indicating the species is quite versatile in occupying different caves. Whilst Zeferini cave is mostly dry (there is only one pond on the cave), the Enfurnado cave is trespassed by a stream. The cave´s sizes are also very distinct: Zeferini cave has around 300 meters, while Enfurnado cave has more than 7.5 km in extension. As observed for the Serra Verde cave, the external surroundings of both the Zeferini and Enfurnado caves are also altered by human activities, especially farming (crops and pastures).

Morphometric and statiscal analysis

The Principal Component Analysis (PCA) demonstrated that *E.* (*R.*) *infernalis* **n. sp.**, *E.* (*E.*) *zin* **n. sp.** and *E.* (*E.*) *zaum* **n. sp.** form distinct groups (Fig. 98), thus indicating that the three species are morphometrically different from one another. Principal Component 1 (PC1) explained 72.3% of all variation found between the species, while (PC2) explained 13.5%. Leg I length (Leg I), leg II length (Leg II), head width, pronotum width, number of teeth of the stridulatory file (Stridens), intraocular distance (Intraocular dist.) and body length (Body) are the measurements that most contributed to the differentiation of *E.* (*R.*) *infernalis* **n. sp.** from the other species. It is also worth pointing out that *E.* (*R.*) *infernalis* **n. sp.** is more distinct from *E.* (*E.*) *zin* **n. sp.** than from *E.* (*E.*) *zaum* **n. sp.**

ANOVA and Kruskal-Wallis tests retrieved significant differences between *E.* (*R.*) *infernalis* **n. sp.**, *E.* (*E.*) *zin* **n. sp.** and *E.* (*E.*) *zaum* **n. sp.** for the following morphometric indices: L1L/PL (F: 35.45; p: 2.66×10^{-7}), L2L/PL (F: 48.85; p: 2.01×10^{-8}), RTL/PL (F: 8.06; p: 2.71×10^{-3}) and CEL/HL (X^2: 7.01; p: 2.87×10^{-2}). Using Tukey test and Dunn test of multiple comparison, we determined how the species differed from one another. The construction of Box Plots (Figs. 99–102) allowed the visualization of the results.

E. (*R.*) *infernalis* **n. sp.** stands out for having relatively longer legs (legs I and II) than *E.* (*E.*) *zin* **n. sp.** and *E.* (*E.*) *zaum* **n. sp.** (Figs. 99 and 100). The statiscal analysis also demonstrated that *E.* (*R.*) *infernalis* **n. sp.** have eyes of reduced size when compared to the eyes of *E.* (*E.*) *zin* **n. sp.** (Fig. 102). Furthermore, it was found that *E.* (*E.*) *zaum* **n. sp.** have reduced tegmen when compared to *E.* (*R.*) *infernalis* **n. sp.** and *E.* (*E.*) *zin* **n. sp.** (Fig. 101).

Discussion

Phallic complex comparisons

The phallic complex of *Endecous* (*Ramalhoecous*) *infernalis* **n. sp.** has a set of unique traits that makes it distinct from all the other species of the genus *Endecous*. Hence, in order to accommodate this new species in an appropriate subgroup, a fourth subgenus was established: *E.* (*Ramalhoecous*) **n. subg.**

Endecous (*Ramalhoecous*) **n. subg.** has, unlike the three subgenera established by Gorochov (2014), an almost square-shaped phallic complex. *E.* (*Ramalhoecous*) **n. subg.** is also characterized by ventrally partitioned pseudepiphallic parameres (Ps.p) and deeply excavated, shaped like baskets pseudepiphallic inner bars (Ps.ib), as well as enlarged, ventrally positioned ectophallic apodemes (Ect.ap). Besides that, the posterior portion of the endophallic sclerite of *E.* (*Ramalhoecous*) **n. subg.** is elongated and grooved, but devoid of dorsal crest.

E. (*R.*) *infernalis* **n. sp.**, in turn, is characterized by pseudepiphallic arms (Ps.arm) that are slightly inclined outwards, almost parallel to the longitudinal axis of the phallic complex, similar to *E.* (*N.*) *bahiensis* and *E.* (*N.*) *potiguar*. It also has enlarged and curved inwards pseudepiphallic dorsal branches (Ps.db), such as those of *E.* (*E.*) *betariensis* and *E.* (*E.*) *itatibensis*. The "A" sclerite (A) of *E.* (*R.*) *infernalis* **n. sp.** differs from the "A" sclerite of

E. aguassay, *E. alejomesai*, *E. betariensis*, *E. peruassuensis*, *E. zaum* **n. sp.** and *E. zin* **n. sp.** due to being short and almost fused to the pseudepiphallic dorsal branches.

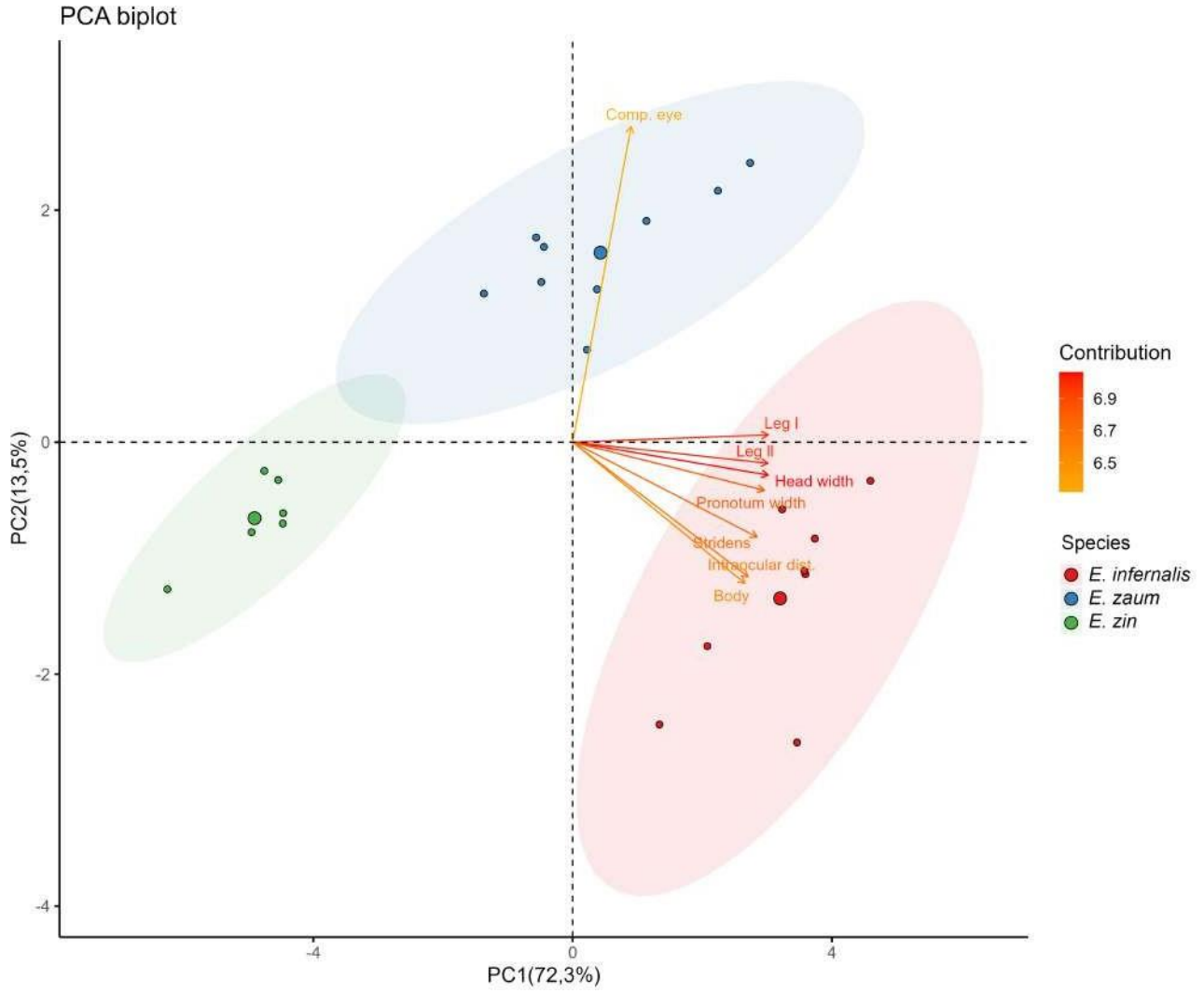


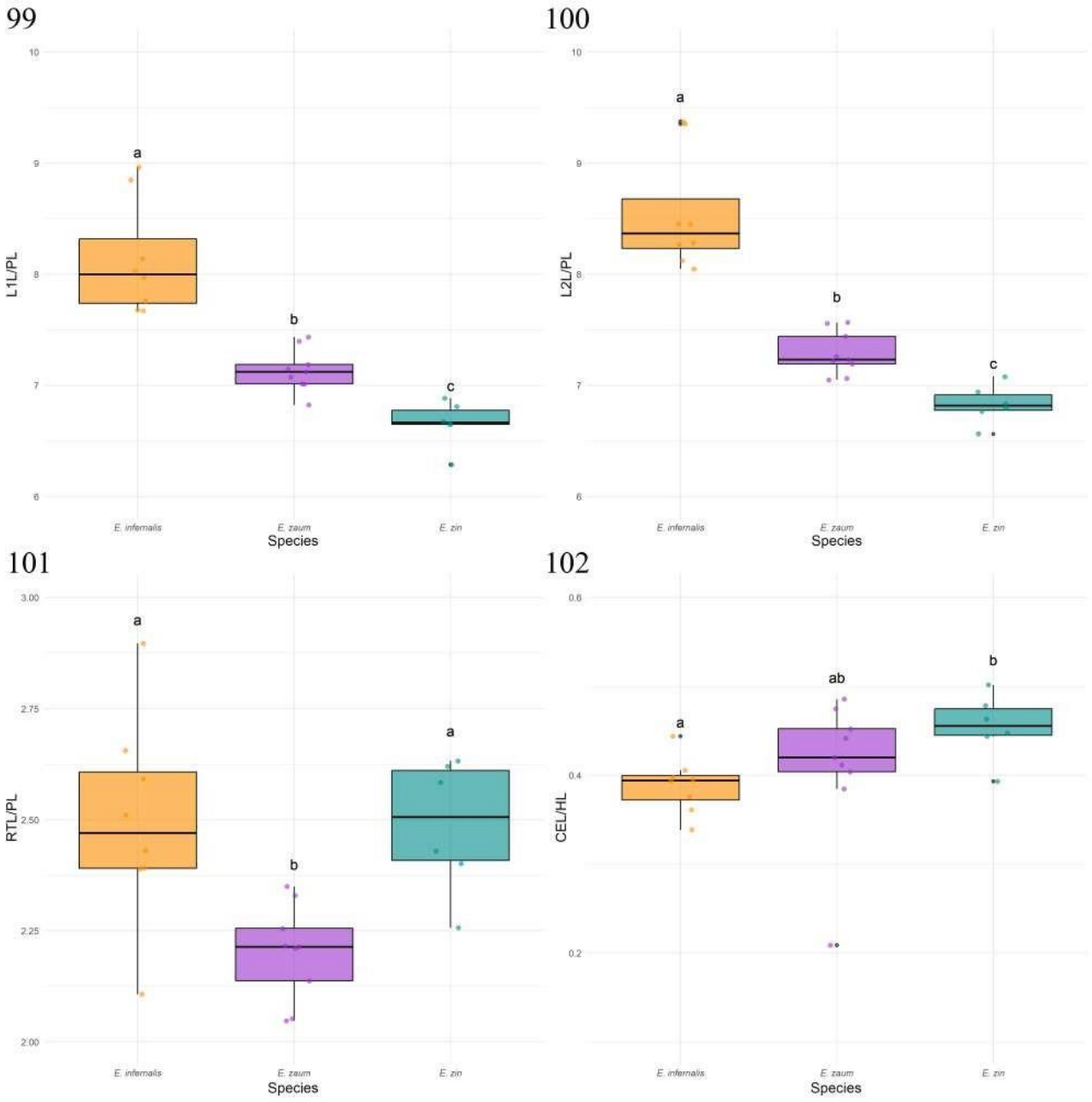
FIGURE 98. PCA Biplot. Principle Component 1 (PC1); principle Component 2 (PC2); main variables: leg I length (**Leg I**), leg II length (**Leg II**), head width, pronotum width, number of teeth of the stridulatory file (**Stridens**), intraocular distance (**Intraocular dist.**), body length (**Body**), compound eye length (**Comp. eye**).

The ectophallic arch (Ect.arc) of *E.* (*R.*) *infernalis* **n. sp.** is conical, like the ectophallic arches of *E.* (*E.*) *arachnopsis*, *E.* (*E.*) *cavernicolus*, *E.* (*E.*) *chape*, *E.* (*E.*) *naipi*, *E.* (*E.*) *painensis*, *E.* (*N.*) *bahiensis*, *E.* (*N.*) *onthophagus* and *E.* (*N.*) *potiguar*. *E.* (*R.*) *infernalis* **n. sp.** has ectophallic lateral bars (Ect.lb) that are contorted on themselves, as well as a short endophallic sclerite duct (End.sc.d), comparable to the endophallic sclerite duct of *E.* (*E.*) *alejomesai*. Additionally, it is worth mentioning that the anterior portion of the endophallic sclerite (End.sc.a) of *E.* (*R.*) *infernalis* **n. sp.** is elongated and shaped like those of *E.* (*E.*) *arachnopsis* and *E.* (*E.*) *chape*.

The pseudepiphallus of *Endecous* (*Endecous*) *zin* **n. sp.** and *Endecous* (*Endecous*) *zaum* **n. sp.** is elongated, similar to those of *E.* (*E.*) *cavernicolus*, *E.* (*E.*) *aguassay*, *E.* (*E.*) *peruassuensis*, *E.* (*E.*) *betariensis*, *E.* (*E.*) *naipi*, *E.* (*E.*) *chape* and *E.* (*E.*) *painensis*. Additionally, their endophallic sclerite ducts (End.sc.d), as well as those of *E.* (*E.*) *aguassay*, *E.* (*E.*) *painensis* and *E.* (*E.*) *peruassuensis*, are short, not exceeding the length of the ectophallic apodeme (Ect.ap). Therefore, according to Gorochov (2014), these two new species should be included in the subgenus *E.* (*Endecous*).

E. zin **n. sp.** has dorsally projected, slender at the apex pseudepiphallic dorsal branches (Ps.db), similar to those of *E. peruassuensis*, *E. aguassay* and *E. alejomesai*. However, unlike *E. peruassuensis*, *E. aguassay* and *E. alejomesai*, *E. zin* **n. sp.** bears a pseudepiphallic arm (Ps.arm) that is, at most, slightly inclined towards the interior of the sclerite, which makes it seem elongated, resembling the pseudepiphallus portion of the phallic complex of

E. painensis, *E. chape*, *E. betariensis* and *E. cavernicolus.* The pseudepiphallic inner bars (Ps.ib) of *E. zin* **n. sp.** are concave, this being another characteristic that distinguishes *E. zin* **n. sp.** from *E. peruassuensis*, *E. aguassay* and *E. alejomesai*, as well as *E. painensis* and *E. chape*. The pseudepiphallic ventral branch (A) of *E. zin* **n. sp.** is elongated, dilated at the apex and comparable to those of *E. aguassay*, *E. alejomesai* and *E. peruassuensis*, but different from *E. betariensis*, which, aside from also being elongated, is slender at the posterior extremity.



FIGURES 99–102. Box Plots of the following morphometric indices: L1L/PL (99), L2L/PL (100), RTL/PL (101) and CEL/ HL (102). Different colors represent different species: orange, *E. infernalis* **n. sp.**; purple, *E. zaum* **n. sp.**; blue, *E. zin* **n. sp.** Abbreviations: **L1L**, leg I length; **L2L**, leg II length; **RTL**, right tegmen length; **CEL**; compound eye length; **PL**, pronotum length; **HL**, head length.

The ectophallic arch (Ect.arc) of *E. zin* **n. sp.** has a trapezoidal shape, like the ectophallic arch of *E. alejomesai*. The ectophallic lateral bars (Ect.lb) of *E. zin*. **n. sp.** have a hook-shaped apex, which differentiates them from the lateral bars of *E. zaum* **n. sp.**, *E. aguassay*, *E. alejomesai*, *E. arachnopsis*, *E. naipi*, *E. chape*, *E. cavernicolus*, *E. painensis* and *E. ubajarensis*. *E. zin* **n. sp.** lateral bars are actually similar to the lateral bars of *E. peruassuensis*, which also have a hook-like curved end, although not as evident as those of *E. zin* **n. sp.**

The endophallic sclerite anterior portion (End.sc.a) of *E. zin* **n. sp.** phallic complex is sclerotized, has a central

groove and a dorsal crest, just like *E. zaum* **n. sp.**, *E. painensis*, *E. ubajarensis*, *E. aguassay*, *E. alejomesai*, *E. peruassuensis* and *E. cavernicolus*. *E. zin* **n. sp.** also has an endophallic sclerite duct (End.sc.d) similar to the *E. ubajarensis* duct. Furthermore, it is worth pointing out that the *E. zin* **n. sp.** endophallic duct is longer than those of *E. chape*, *E. arachnopsis* and *E. alejomesai*, and shorter than those of *E. zaum* **n. sp.**, *E. aguassay*, *E. cavernicolus*, *E. painensis*, *E. peruassuensis* and *E. naipi*.

E. zaum **n. sp.** has pseudepiphallic arms inclined to the center of the phallic complex, characteristic that distinguishes it from *E. zin* **n. sp.**, *E. painensis*, *E. chape*, *E. betariensis* and *E. cavernicolus*. The proximal portion of the pseudepiphallic dorsal branch of *E. zaum* **n. sp.** extends itself in the same direction of the pseudepiphallic arm, whereas the distal portion turns itself towards the center of the sclerite, similar to the pseudepiphallic dorsal branches of *E. arachnopsis*, *E. chape*, *E. cavernicolus* and *E. naipi*. The pseudepiphallic arms and dorsal branches of *E. zaum* **n. sp.** are more elongated than those of *E. alejomesai* e *E. ubajarensis*. In addition to that, and akin to *E. peruassuensis*, *E. aguassay*, *E. alejomesai*, *E. painensis* e *E. chape*, *E. zaum* **n. sp.** has flat inner bars, this being another trait that differentiates it from *E. zin* **n. sp.** It is also worth mentioning the moderate inclination of the pseudepiphallic inner bars of *E. zaum* **n. sp.** and the aligned, more or less perpendicular to the longitudinal axis of the sclerite nature of the inner bars of *E. zin* **n. sp.**, *E. naipi*, *E. chape* and *E. painensis*, which distinguishes those species and, thus, may be considered a characteristic of taxonomic relevance.

The ectophallic arch of *E. zaum* **n. sp.** dome-shaped, comparable to those of *E. ubajarensis*, *E. itatibensis*, *E. betariensis*, *E. aguassay* and *E. peruassuensis*. *E. zaum* **n. sp.** also has ectophallic lateral bars similar to those of *E. alejomesai*, *E. painensis* and *E. cavernicolus*. Nonetheless, it is possible to discriminate the lateral bars of *E. zaum* **n. sp.** from the other species based on inclined and sinuous contour.

Copulatory papilla of *Endecous* (*Endecous*) *zin*

Unlike the copulatory papilla of *E. cavernicolus*, *E. betariensis*, *E. aguassay* and *E. painensis*, whose apex is rounded, the apex of the copulatory papilla of *E. zin* **n. sp.** is shaped like a rectangle. Additionally, the dorsal and ventral extremities of the posterior portion of the copulatory papilla of *E. zin* **n. sp.** are V-shaped, which makes it even more distinct from *E. cavernicolus*, *E. betariensis*, *E. aguassay* and *E. painensis*, considering that these species copulatory papillae have concave and dome-like posterior extremities. The copulatory papilla of *E. zin* **n. sp.**, on the other hand, resembles the papilla of *E. itatibensis*, which also has an enlarged and almost rectangular apex. It is necessary to emphasize, however, that only the dorsal end of the posterior portion of the copulatory papilla of *E. itatibensis* has a V-shaped contour, and that the ventral extremity is concave, like the other species mentioned above.

Comparative morphology

E. zin **n. sp.** and *E. zaum* **n. sp.** have similar morphologies. *E. infernalis* **n. sp.**, on the other hand, can be easily differentiated from the other *Endecous* species. It is possible to set them apart, for example, through their body sizes: *E. zin* **n. sp.** is the smallest species, having, on average, 13.47 mm ± 1.02 mm (n = 6) in length, *E. zaum* **n. sp.** has intermediate size (16.48 mm ± 1.21 mm; n = 9), and *E. infernalis* **n. sp.** is the largest species, with 21.66 mm ± 1.24 mm (n = 8) in length. Besides that, *E. infernalis* **n. sp.** stands out for having a highly distinct protuberance in the anterior portion of its tergite III, alongside smaller humps in tergites IV through VII.

In addition to body size and tergite morphology, other differences can be observed in the supra-anal and sub- genital plates, as well as in the cerci of these species.

The supra-anal plates of *E. zin* **n. sp.** e *E. zaum* **n. sp.** have a subtriangular shape, with the supra-anal plate of *E. zaum* **n. sp.** being more elongated than the supra-anal plate of *E. zin* **n. sp.** The supra-anal plate of *E. infernalis* **n. sp.**, on the other hand, has a broadened and rounded apex. In addition to this, *E. infernalis* **n. sp.** stands out from the other species for having an elongated sub-genital plate, with a notch in the central region of its apex, similar to the sub-genital plate of *E. aguassay*, along with cerci that are short and dilated at the base.

In regards to the male right tegmen, it was noticed both intra and interspecific variations in the number and arrangement of veins in the basal field, lateral field, mirror and harp of *E. zin* **n. sp.**, *E. zaum* **n. sp.** and *E. infernalis* **n. sp.** The same situation was verified for *E. alejomesai*, E. *bahiensis*, *E. didymus*, *E. painensis*, *E. potiguar* and *E. troglobius*. For this reason, it is not advisable to use these characters on the diagnosis of new species in the genus (Castro-Souza *et al.* 2017; Castro-Souza *et al.* 2020a). Zefa *et al.* (2010) stated that the number of teeth in the stridulatory file (Cu2) of the right tegmen of *Endecous* should also be used with caution in taxonomy studies due to

great intraspecific variation. The number of teeth in the stridulatory file of *E. zin* **n. sp.**, *E. zaum* **n. sp.** e *E. infernalis* **n. sp.**, however, are taxonomically relevant, since the three species have a distinct number of teeth, and can be easily differentiated by this character.

It is worth pointing out that the right tegmen of *E. zaum* **n. sp.** is reduced in size when compared to those of *E. infernalis* **n. sp** and *E. zin* **n. sp.** Reduced or absence of wings have already been used by researchers as an argument in favor of classifying cave crickets as troglobitic species (Souza-Dias *et al.* 2014; Bolfarini & Bichuette 2015). It should be noted, however, that several species of epigean Phalangopsidae lack tegmen (de Mello & de Andrade 2003; de Mello & Souza-Dias 2016; Campos *et al.* 2017). Thus, reduction of wings may be a pre-adaptation to an subterranean lifestyle, being selected *a priori* and fixated on crickets populations before the process of colonization of caves occur (Desutter-Grandcolas 1998b; Castro-Souza *et al.* 2020a). In that sense, apterism or reduced wings should not be considered troglomorphic traits (Castro-Souza *et al.* 2020a). Tegument depigmentation, observed, for example, in *E. apterus*, *E. peruassuensis* and *E. troglobius*, and reduction of ocular structures, observed in *E. troglobius*, nonetheless, represent troglomorphisms (Desutter-Grandcolas 1998b) and should be evaluated in studies about troglobitic species.

Proventriculus comparisons

Fontanetti *et al.* (2002) suggested that the median and lateral denticles of the proventriculus of cavernicolous species of *Endecous* are more rounded at the tip when compared to those of epigean species. They also pointed out that this difference can be verified between hypogean and epigean populations of the same species. This tendency, however, was not observed in *E. infernalis* **n. sp.**, *E. zin* **n. sp.** and *E. zaum* **n. sp.**: the three new species bear denticles with different shapes and lengths, even though all specimens were collected inside caves. *E. infernalis* **n. sp.** and *E. zaum* **n. sp.**, for example, have rounded median and lateral denticles. On the order hand, *E. zin* **n. sp.** has tapered and acute at the tip denticles. In addition, the denticles of *E. infernalis* **n. sp.** and *E. zin* **n. sp.** are more elongated than the denticles of *E. zaum* **n. sp.** The shape of the denticles of the *Endecous* proventriculus, therefore, is not a reliable indication of adaptation to hypogean or epigean environments. Thus, it is necessary to investigate whether environmental factors, such as diet composition and resource availability, affect the internal morphology of the proventriculus.

Is *Endecous* (*Ramalhoecous*) *infernalis* n. sp. a troglobitic species?

The length of the compound eyes of *E.* (*E.*) *zin* **n. sp.**, *E.* (*E.*) *zaum* **n. sp.** and *E.* (*R.*) *infernalis* **n. sp.** are similar, even though the three species have different body sizes. Through morphometric analyses, it was verified that the compound eyes of *E.* (*R.*) *infernalis* **n. sp.** are reduced when compared to the compound eyes of *E.* (*E.*) *zin* **n. sp.** Besides that, it was found that the legs I and II of *E.* (*R.*) *infernalis* **n. sp.** are elongated when compared to the legs I and II of *E.* (*E.*) *zin* **n. sp.** and *E.* (*E.*) *zaum* **n. sp.**

The reduction of ocular structures and elongation of ambulatory appendages are well known troglomorphisms (Desutter-Grandcolas 1998b) and have now been observed in *E.* (*R.*) *infernalis* **n. sp.** Those characteristics represent adaptations to a strictly subterranean lifestyle, and are, therefore, indicative of the troglobitic nature of this species. Nonetheless, conducting the inventory of the fauna in the surroundings of the caves where *E.* (*R.*) *infernalis* **n. sp.** were found may further validated this hypothesis.

Conservation

It is important to emphasize the urgency in preserving the integrity of the Brazilian karsts areas, which are severely threaten by recent controversial government policies (Ferreira *et al.* 2022) and the advance of anthropic activities, such as mining, logging and farming (Cavalcanti *et al.* 2011). In view of this, the creation of conservation units in karstic regions represents a viable way of safeguarding not only *Endecous* species, but also the immense diversity of species associated with those environments (Mammola *et al.* 2019).

The establishment of protected areas in karsts regions is, in fact, a well-known strategy that has been implemented in various countries (Watson *et al.* 1997). Karstic regions recognized as World Heritage Sites, for example, are, most of the time, preserved because they contain archeological or paleontological remains, along with scenic views and relevant geological formations (Williams 2008; Badman *et al.* 2008). On that account, it can be stated that biodiversity is generally overlooked during the process of creation of new conservation units in karst areas, serving only as a complementary criterion (Culver & Sket 2000; Badman *et al.* 2008; Williams 2008). The main reason

behind the neglecting of the subterranean communities is the lack of information about them (Rabelo *et al.* 2018). Thus, the identification of novel cave species of *Endecous*, such as those described in this study (especially the troglobitic one), may encourage and help the establishment of protected areas, which will, in turn, ensure that the caves where those crickets are found and the communities within them are preserved.

Acknowledgements

The authors would like to thank the Centro Nacional de Pesquisa e Conservação de Cavernas—CECAV and Instituto Brasileiro de Desenvolvimento e Sustentabilidade—IABS (n°. 006/2021. TCCE ICMBio/Vale (01/2018) for the financial support and scholarship provided to PHMC; CNPq (National Council for Scientific and Technological Development) for the productivity scholarship provided to RLF (CNPq n. 302925/2022-8); and the team from the Center of Studies in Subterranean Biology (CEBS/UFLA) for the support in the field trips. We would also like to thank Paulo César Reis Venâncio for the help with the statiscal analysis, and Daniela Hoyos Benjumea for the help with the M205 A (Leica) stereomicroscope.

References

Alvares, C.A., Stape, J.L., Sentelhas, P.C., Moraes-Gonçalves, J.L. & Sparovek, G. (2013) Köppen's climate classification map for Brazil. *Meteorologische Zeitschrif*, 22, 711–728.
https://doi.org/10.1127/0941-2948/2013/0507

Álvarez-Padilla, F. & Hormiga, G. (2007) A protocol for digesting internal soft tissues and mounting spiders for scanning electron microscopy. *The Journal of Arachnology*, 35 (3), 538–542.
https://doi.org/10.1636/Sh06-55.1

Badman, T., Bomhard, B., Fincke, A., Langley, J., Rosabal, P. & Sheppard, D. (2008) *Outstanding universal value: Standards for natural world heritage*. International Union for Conservation of Nature and Natural Resources (IUCN), Gland, 52 pp.

Bischof, H.J. (1975) Die keulenförmigen Sensillen auf den Cerci der Grille *Gryllus bimaculatus* als Schwererezeptoren. *Journal of Comparative Physiology*, 98, 277–288.
https://doi.org/10.1007/BF00656974

Bolfarini, M.P. & Bichuette, M.E. (2015) *Endecous peruassuensis* **n. sp.** (Orthoptera: Grylloidea: Phalangopsidae) from caves of Eastern Brazil: evidence of isolation in the subterranean realm and discussion about troglomorphisms. *Zootaxa*, 4032 (3), 297–308.
https://doi.org/10.11646/zootaxa.4032.3.5

Campos, L.D., Souza-Dias, P.G.B. & Nihei, S.S. (2017) Taxonomic review of *Eidmanacris* Chopard, 1956 (Orthoptera: Grylloidea: Phalangopsidae). *Zootaxa*, 4321 (1), 1–93.
https://doi.org/10.11646/zootaxa.4321.1.1

Castro-Souza, R.A., Zefa, E. & Ferreira, R.L. (2020a) New troglobitic and troglophilic syntopic species of *Endecous* (Orthoptera, Grylloidea, Phalangopsidae) from a Brazilian cave: a case of sympatric speciation?. *Zootaxa*, 4810 (2), 271–304.
https://doi.org/10.11646/zootaxa.4810.2.3

Castro-Souza, R.A., Junta, V.G.P. & Ferreira, R.L. (2020b) Description and ecology of a new species of the cricket genus *Endecous* (Orthoptera: Grylloidea: Phalangopsidae) in the speleological province of Arcos-Pains-Doresópolis, Southeastern Brazil. *Zootaxa*, 4821 (2), 305–332.
https://doi.org/10.11646/zootaxa.4821.2.4

Castro-Souza, R.A., Zefa, E. & Ferreira, R.L. (2017) Two new species of cave crickets *Endecous* (*Notoendecous*) Gorochov, 2014 (Orthoptera: Grylloidea: Phalangopsidae) from northeastern Brazil. *Zootaxa*, 4318 (3), 474–498.
https://doi.org/10.11646/zootaxa.4318.3.3

Cavalcanti, L.F., Lima, M.F.D., Medeiros, R.D.C.S. & Meguerditchian, I. (2012) s.n. *In*: *Plano de ação nacional para a conservação do patrimônio espeleológico nas áreas cársticas da Bacia do Rio São Francisco*. Instituto Chico Mendes de Conservação da Biodiversidade, Instituto Chico Mendes, Brasília, pp. 240–256.

Christiansen, K. (1962) Proposition pour la classification des animaux cavernicoles. *Spelunca*, 2, 75–78.

Cigliano, M.M., Braun, H., Eades, D.C. & Otte, D. (2022) Orthoptera Species File. Version 5.0/5.0. Available from: http://Orthoptera.SpeciesFile.org (accessed 30 October 2022)

Cole, M.M. (1960) Cerrado, Caatinga and Pantanal: The Distribution and Origin of the Savanna Vegetation of Brazil. *The Geographical Journal*, 126, 168–179.
https://doi.org/10.2307/1793957

Culver, D.C. & Sket, B. (2000) Hotspots of subterranean biodiversity in caves and wells. *Journal of cave and Karst studies*, 62 (1), 11–17. [https://digitalcommons.usf.edu/kip_articles/2593]

Desutter, L. (1987) Structure et évolution du complexe phallique des Gryllidea (Orthoptera) et classification des genres Nétropicaux de Grylloidea, Première Partie. *Annales de la Société Entomolologique de France*, 23 (3), 213–239.
Desutter-Grandcolas, L. (1995) Nouveaux grillons cavernicoles de la région néotropicale (Orthoptera, Grylloidea, Phalangopsidae). *Annales de la Société entomologique de France*, 17, 97–106.
Desutter-Grandcolas, L. (1998a) Comparative morphology of cercal structures in true crickets and their allies (Orthoptera, Ensifera): a phylogenetic perspective. *Zoomorphology*, 118 (4), 235–243.
Desutter-Grandcolas, L. (1998b) II—faune souterraine II. 4—Insecta, 56—Ortóptera, B—Grylloidea. *In*: Juberthie, C. & Decu, V. (Eds.), *Encyclopaedia Biospeologica. V. Tome II*. Société de Biospéologie, Moulis, pp. 989–1001.
Desutter-Grandcolas, L. (2003) Phylogeny and the evolution of acoustic communication in extant Ensifera (Insecta, Orthoptera). *Zoologica Scripta*, 32, 525–561.
https://doi.org/10.1046/j.1463-6409.2003.00142.x
Ferreira, R.L., Bernard, E., da Cruz Júnior, F.W., Piló, L.B., Calux, A., Souza-Silva, M. & Frick, W.F. (2022) Brazilian cave heritage under siege. *Science*, 375 (6586), 1238–1239.
https://doi.org/10.1126/science.abo1973
Fontanetti, C.S., Zefa, E., Passetti, F. & Mesa, A. (2002) Morphological characterization and comparative analysis of the proventriculus from three species of *Endecous* Saussure, 1878 (Orthoptera: Gryllidae: Phalangopsinae). *Entomotropica*, 17 (1), 15–23.
Gorochov, A.V. (2014) Classification of the Phalangopsinae subfamily group, and new taxa from the subfamilies Phalangopsinae and Phaloriinae (Orthoptera: Gryllidae). *Zoosystematica Rossica*, 23 (1), 7–88.
https://doi.org/10.31610/zsr/2014.23.1.7
Hartman, H.B., Bennett, L.P., Moulton, B.A. (1987) Anatomy of equilibrium receptors and cerci of the burrowing desert cockroach *Arenivaga* (Insecta, Blattodea). *Zoomorphology*, 107 (2), 81–87.
https://doi.org/10.1007/BF00312117
Horn, E. & Föller, W. (1985) Tonic and modulatory subsystems of the complex gravity receptor system in crickets, *Gryllus bimaculatus*. *Journal of insect physiology*, 31 (12), 937–946.
https://doi.org/10.1016/0022-1910(85)90028-9
Kassambara, A. & Mundt, F. (2020) factoextra: Extract and visualize the results of multivariate data analyses. R package. Version 1.0.7. Available from: https://cran.r-project.org/web/packages/factoextra/index.html (accessed 16 January 2023)
Magrin, G.O., Marengo, J.A., Boulanger, J.-P., Buckeridge, M.S., Castellanos, E., Poveda, G., Scarano, F.R. & Vicuña, S. (2014) Central and South America. *In*: Barros, V.R., Field, C.B., Dokken, D.J., Mastrandrea, M.D., Mach, K.J., Bilir, T.E.; Chatterjee, M., Ebi, K.L., Estrada, Y.O., Genova, R.C., Girma, B., Kissel, E.S., Levy, A.N., MacCracken, S., Mastrandrea,
P.R. & White, L.L. (Eds.), *Climate Change 2014: Impacts, Adaptation, and Vulnerability. Part B. Regional Aspects*. Cambridge University Press, Cambridge and New York, pp. 1499–1566.
Mammola, S., Cardoso, P., Culver, D.C., Deharveng, L., Ferreira, R.L., Fišer, C., Galassi, D.M.P., Griebler, C., Halse, S., Humphreys, W.F., Isaia, M., Malard, F., Martinez, A., Moldovan, O.T., Niemiller, M.L., Pavlek, M., Reboleira, A.S.P.S., Souza-Silva, M., Teeling, E.C., Wynne, J.J., Zagmajster, M. (2019) Scientists' warning on the conservation of subterranean ecosystems. *BioScience*, 69 (8), 641–650.
https://doi.org/10.1093/biosci/biz064
Mello, F.A.G. & Andrade, M.A.B.S. (2003) *Ottedana cercalis*: a new genus and species of phalangopsid cricket from the Mantiqueira Range of southeastern Brazil (Orthoptera: Grylloidea). *Journal of Orthoptera Research*, 12, 141–148. [https://www.jstor.org/stable/3503767]
Mello, F.A.G. & Pellegatti-Franco, F. (1998) A new cave cricket of the genus *Endecous* from southeastern Brazil and characterization of male and female genitalia of *E. itatibensis* Rehn, 1918 (Orthoptera: Grylloidea: Phalangopsinae: Luzarinae). *Journal of Orthoptera Research*, 7, 185–188.
https://doi.org/10.2307/3503517
Mesa, A. & Garcia-Novo, P. (1997) *Endecous onthophagus*: a new combination. Phallic sclerites and karyology of the species (Orthoptera: Grylloidea). *Journal of Orthoptera Research*, 6, 117–120.
https://doi.org/10.2307/3503544
Mews, C.M. & Sperber, C.F. (2008) A new species of *Endecous* Saussure, 1878 and redescription of *Endecous cavernicolus* Costa-Lima, 1940 (Orthoptera: Grylloidea: Phalangopsidae). *Studies on Neotropical Fauna and Environment*, 43 (2), 159– 167.
https://doi.org/10.1080/01650520701492389
Nicklaus, R. (1969) The function of the club-shaped sensilla on the cerci of crickets. *Zool Ges Verh*, 1969, 393–398.
Rabelo, L.M., Souza-Silva, M. & Ferreira, R.L. (2018) Priority caves for biodiversity conservation in a key karst area of Brazil: comparing the applicability of cave conservation indices. *Biodiversity and conservation*, 27 (9), 2097–2129.
https://doi.org/10.1007/s10531-018-1554-6
R Core Team (2022) R: A language and environment for statistical computing. R Foundation for Statistical Computing, Vienna. Available from: https://www.R-project.org/ (accessed 16 January 2023)
Silva, R.C., Berbert-Born, M., Bustamante, D.E., Santoro, T.N., Sedor, F. & dos Santos Avilla, L. (2019) Diversity and preservation of Pleistocene tetrapods from caves of southwestern Bahia, Brazil. *Journal of South American Earth Sciences*, 90, 233–254.

https://doi.org/10.1016/j.jsames.2018.12.004
Souza-Dias, P.G.B., Bolfarini M.P., Nihei, S.S. & Mello, F.A. (2014) *Endecous apterus*: A new species of cave cricket from northeast Brazil, with comments on the use of subterranean habitats by Luzarinae crickets (Orthoptera: Grylloidea: Phalangopsidae: Luzarinae). *Zootaxa*, 3784 (2), 120–130.
https://doi.org/10.11646/zootaxa.3784.2.2
Souza-Dias, P.G.B. (2015) *Análise cladística e morfologia do complexo fálico de Phalangopsidae, com ênfase em Luzarinae (Orthoptera, Ensifera, Grylloidea).* Doctoral thesis, Instituto de Biociências da Universidade de São Paulo, São Paulo, 183 pp.
Souza-Dias, P.G.B., Mello, F.A.G; Vieira, L.B. (2016) A new genus and species of cricket from the Chapada Diamantina National Park, northeastern Brazil (Grylloidea: Phalangopsidae; Luzarinae). *Zootaxa*, 4121 (3), 258–266.
http://doi.org/10.11646/zootaxa.4121.3.2
Souza-Dias, P.G.B., Szinwelski, N., Fianco M., De Oliveira, E.C., Mello, F.A.G. & Zefa, E. (2017) New species of *Endecous* (Grylloidea, Phalangopsidae, Luzarinae) from the Iguaçu National Park (Brazil), including bioacoustics, cytogenetic and distribution data. *Zootaxa*, 4237 (3), 454–470.
https://doi.org/10.11646/zootaxa.4237.3.2
Souza-Silva, M., Cerqueira, R.F.V., Pellegrini, T.G. & Ferreira, R.L. (2021) Habitat selection of cave-restricted fauna in a new hotspot of subterranean biodiversity in Neotropics. *Biodiversity and Conservation*, 30 (14), 4223–4250.
https://doi.org/10.1007/s10531-021-02302-8
Watson, J., Hamilton-Smith, E., Gillieson, D. & Kiernan, K. (1997) *Guidelines for cave and karst protection*. International Union for Conservation of Nature and Natural Resources (IUCN) Gland and Cambridge, 63 pp.
Williams, P. (2008) *World heritage caves and karst*. International Union for Conservation of Nature and Natural Resources (IUCN) World Heritage Studies, Gland, 57 pp.
Zefa, E., Mesa, A. & Martins, L.D.P. (2010) New Brazilian species of *Endecous* Saussure, 1878: Phallic sclerites, calling song and tegmen morphometry (Orthoptera: Grylloidea: Phalangopsinae). *Entomological science*, 13 (1), 150–155. https://doi.org/10.1111/j.1479-8298.2010.00371.x
Zefa, E., Redu, D.R., Costa, M.K.M., Gottschalk, M.S., Padilha, G.B., Silva, A.F. & Martins, L.P. (2014) A new species of *Endecous* Saussure, 1878 (Orthoptera, Gryllidae) from northeast Brazil with the first X^1X^20 chromosomal sex system in Gryllidae. *Zootaxa*, 3847 (1), 125–132.
https://doi.org/10.11646/zootaxa.3847.1.7

Zootaxa 5353 (3): 201–234
https://www.mapress.com/zt/
Copyright © 2023 Magnolia Press

Article

https://doi.org/10.11646/zootaxa.5353.3.1

ISSN 1175-5326 (print edition)
ZOOTAXA
ISSN 1175-5334 (online edition)

http://zoobank.org/urn:lsid:zoobank.org:pub:A8B27F7F-5E7E-4DD4-8E92-A52DD0072BD1

Two new species of *Endecous* Saussure, 1878 (Orthoptera: Grylloidea: Phalangopsidae) from caves in central-western Brazil, with the proposition of a new subgenus to accommodate *E. vitreus* Bolfarini & Campos, 2023

PEDRO HENRIQUE MENDES CARVALHO[1,3], RODRIGO ANTÔNIO CASTRO-SOUZA[2,4] & RODRIGO LOPES FERREIRA[1,*]

[1]*Centro de Estudos em Biologia Subterrânea (www.biologiasubterranea.com.br), Setor de Biodiversidade Subterrânea, Departamento de Ecologia e Conservação, Universidade Federal de Lavras, Cx Postal 3037, Campus Universitário, CEP 37200-000, Lavras, Minas Gerais, Brazil*

[2]*Laboratório de Macroecologia e Conservação da Biodiversidade, Departamento de Botânica e Ecologia, Instituto de Biociências, Universidade Federal de Mato Grosso, CEP 78060-900, Cuiabá, MT, Brazil*

[3] *carvalhopedrohm@gmail.com; https://orcid.org/0000-0003-0859-0255*

[4] *rodrigodesouzaac@gmail.com; https://orcid.org/0000-0002-3439-9991*

[*]*Corresponding author: drops@ufla.br; https://orcid.org/0000-0003-3288-4405*

Abstract

The genus *Endecous* (Orthoptera, Grylloidea, Phalangopsidae) encompasses over 20 species, grouped into four subgenera: *E*. (*Endecous*), *E*. (*Pedroecous*), *E*. (*Notendecous*), and *E*. (*Ramalhoecous*). In this study, we present the description of two novel species belonging to the subgenus *Endecous* (*Endecous*) Saussure, 1878 (Phalangopsidae) discovered in caves located within the Serra da Bodoquena region of Mato Grosso do Sul state, Brazil. The descriptions are based on the distinguishing male genitalia characteristics, among other traits. Furthermore, we introduce a new subgenus, namely *Endecous* (*Bodoquenaecous*), specifically created to accommodate the recently discovered species *E. vitreus*, also found in caves within the same area. Initially, *E. vitreus* was placed under the subgenus *Endecous*; however, due to its numerous distinct traits, the establishment of a new subgenus became justified. In this study, we also introduce the first pictorial key for the subgenera within the genus *Endecous*. Additionally, we briefly discuss observed troglomorphic adaptations in species belonging to this genus. Finally, comprehensive ecological observations and conservation status assessments are provided for both newly described species, as well as for *E. vitreus*.

Key words: Taxonomy, Cricket, Cave, Orthoptera

Resumo

O gênero *Endecous* (Orthoptera, Grylloidea, Phalangopsidae) engloba mais de 20 espécies, agrupadas em quatro subgêneros: *E*. (*Endecous*), *E*. (*Pedroecous*), *E*. (*Notendecous*) e *E*. (*Ramalhoecous*). Neste estudo, apresentamos a descrição de duas novas espécies pertencentes ao subgênero *Endecous* (*Endecous*) Saussure, 1878 (Phalangopsidae), descobertas em cavernas localizadas na região da Serra da Bodoquena, no estado de Mato Grosso do Sul, Brasil. As descrições são baseadas em características distintivas da genitália masculina, além de outras características morfológicas. Além disso, introduzimos um novo subgênero, denominado *Endecous* (*Bodoquenaecous*), criado especificamente para acomodar a espécie recentemente descoberta *E. vitreus*, também encontrada em cavernas da mesma área. Inicialmente, *E. vitreus* foi incluído no subgênero *Endecous*; no entanto, devido às suas numerosas características distintivas, justifica- se o estabelecimento de um novo subgênero. Neste estudo, também apresentamos a primeira chave pictórica para os subgêneros dentro do gênero *Endecous*. Adicionalmente, discutimos brevemente as adaptações troglomórficas observadas em espécies pertencentes a esse gênero. Por fim, são fornecidas observações e avaliações abrangentes sobre a ecologia e o status de conservação das duas espécies recém-descritas, bem como de *E. vitreus*.

Palavras-chave: taxonomia, grilo, caverna, Orthoptera

Accepted by D. Rentz: 23 Aug. 2023; published: 10 Oct. 2023

Introduction

Crickets belonging to the genus *Endecous* Saussure, 1878 (Orthoptera, Phalangopsidae) are exclusively found in South America (Castro-Souza *et al.* 2023; Cigliano *et al.* 2023). They are widely distributed across Brazil, with the exception of the Amazon region, and are commonly associated with subterranean environments (Cigliano *et al.* 2023). Currently, the genus is divided into four subgenera: *E.* (*Endecous*), *E.* (*Notendecous*), *E.* (*Pedroecous*), and *E.* (*Ramalhoecous*) (Cigliano *et al.* 2023; Carvalho *et al.* 2023). These subgenera are primarily differentiated by variations in the male phallic complex, although other characteristics have also been utilized for their classification (Gorochov 2014; Carvalho *et al.* 2023). For instance, *E.* (*Ramalhoecous*) can be identified by the centrally positioned protuberances present on the anterior margins of tergites III to VII (Carvalho *et al.* 2023), and *E.* (*Pedroecous*) by the absence of wings (Gorochov 2014; but see Castro-Souza *et al. 2*020a).

Among the 25 species currently described for the genus, 16 have caves as their type locality: *E.* (*E.*) *onthophagus* (Berg, 1891); *E.* (*E.*) *cavernicola* Costa-Lima, 1940; *E.* (*E.*) *betariensis* de Mello & Pellegatti-Franco, 1998; *E.* (*E.*) *alejomesai* Zefa, 2010; *E.* (*E.*) *ubajarensis* Zefa, 2014; *E.* (*P.*) *apterus* Bolfarini & Souza-Dias, 2014; *E.* (*E.*) *peruassuensis* Bolfarini, 2015; *E.* (*N.*) *bahiensis* Castro-Souza *et al.*, 2017; *E.* (*N.*) *potiguar* Castro-Souza *et al.*, 2017; *E.* (*E.*) *painensis* Castro-Souza *et al.*, 2020b; *E.* (*P.*) *didymus* Castro-Souza *et al.*, 2020a; *E.* (*P.*) *troglobius* Castro-Souza *et al.*, 2020a; *E.* (*E.*) *zaum* Carvalho *et al.*, 2023; *E.* (*E.*) *zin* Carvalho *et al.*, 2023; *E.* (*R.*) *infernalis* Carvalho *et al.*, 2023; *E.* (*E.*) *vitreus* Bolfarini & Campos, 2023 (Cigliano *et al.* 2023). Nonetheless, some of these species, namely *E. alejomesai, E. betariensis, E. painensis, E. ubajarensis, E. bahiensis, E. potiguar* and *E. onthophagus*, also occur in external environments (see Campos *et al*. 2023). They are, therefore, troglophiles, that is, capable of surviving and reproducing both inside and outside of caves. This ecological plasticity is one of the traits that differentiates them from species adapted to a strictly subterranean life cycle, such as *E. apterus, E. peruassuensis, E. troglobius, E. infernalis* and *E. vitreus*.

Organisms that are exclusively found in subterranean environments are referred to as troglobites. Typically, these organisms exhibit morphological adaptations known as troglomorphisms, which are the result of evolutionary processes occurring in complete darkness within subterranean environments (Christiansen 1962). In Orthoptera, and specially in the genus *Endecous*, integument and ommatidia depigmentation, eye reduction, and appendage elongation are among the primary morphological changes that have arisen through evolution in subterranean habitats (Desutter-Grandcolas 1998; Souza-Dias *et al*. 2014; Bolfarini & Bichuete 2015; Castro-Souza *et al*. 2020a; Carvalho *et al*. 2023; Campos *et al*. 2023). For example, *E. troglobius* displays depigmented ommatidia, rendering it, unlike other *Endecous* species, unresponsive to light stimuli (Castro-Souza *et al.* 2020a). Conversely, *E. infernalis* possesses relatively reduced compound eyes and elongated locomotor appendages (Carvalho *et al.* 2023).

In this study, we present the description of two newly discovered species belonging to the genus *Endecous* (*Endecous*) Saussure, 1878 (Phalangopsidae), which were found in caves located within the Serra da Bodoquena region of Mato Grosso do Sul state, Brazil. Additionally, we introduce a new subgenus, specifically established to accommodate the recently described species *E. vitreus*, also found in caves within the same area. Initially, this species was assigned to the subgenus *E.* (*Endecous*); however, due to its numerous distinct traits, justifying the creation of a new subgenus became necessary. Moreover, we provide a brief discussion of observed troglomorphic adaptations in species belonging to *Endecous*. Finally, we offer comprehensive ecological observations and assessments of the conservation status for both the newly described species and *E. vitreus*.

Material and methods

Study area. The Serra da Bodoquena karst is located in the Mato Grosso do Sul state, in central-western Brazil. It extends for 200 km in a north-south direction, reaching up to 800 m in altitude (Sallun-Filho *et al.* 2009). This region was influenced by the Andean Orogeny that uplifted the Pantanal area, and subsequently drawdown during the Plio-Pleistocene, leading to some remaining elevated areas, such as the Serra da Bodoquena (Sallun-Filho & Karmann 2007). Furthermore, shifts to a moister and warmer climate during the Quaternary has also been observed in this area (Assine & Soares 2004; Sallun Filho & Karmann 2007). The area present a humid tropical climate with dry winter and humid summer (Zavattini 1992) with an annual precipitation varying between 1200 and 1500mm and an average annual temperature of 23.9 °C. The region presents two well-defined seasons: a dry winter that

extends from April to September and a rainy summer from October to March (Sallun-Filho & Karmann 2007). The original vegetation comprises a transition from semi deciduous sub montane seasonal forest to the Cerrado (Brazilian Savanna) (Fig. 1, A, B and C).

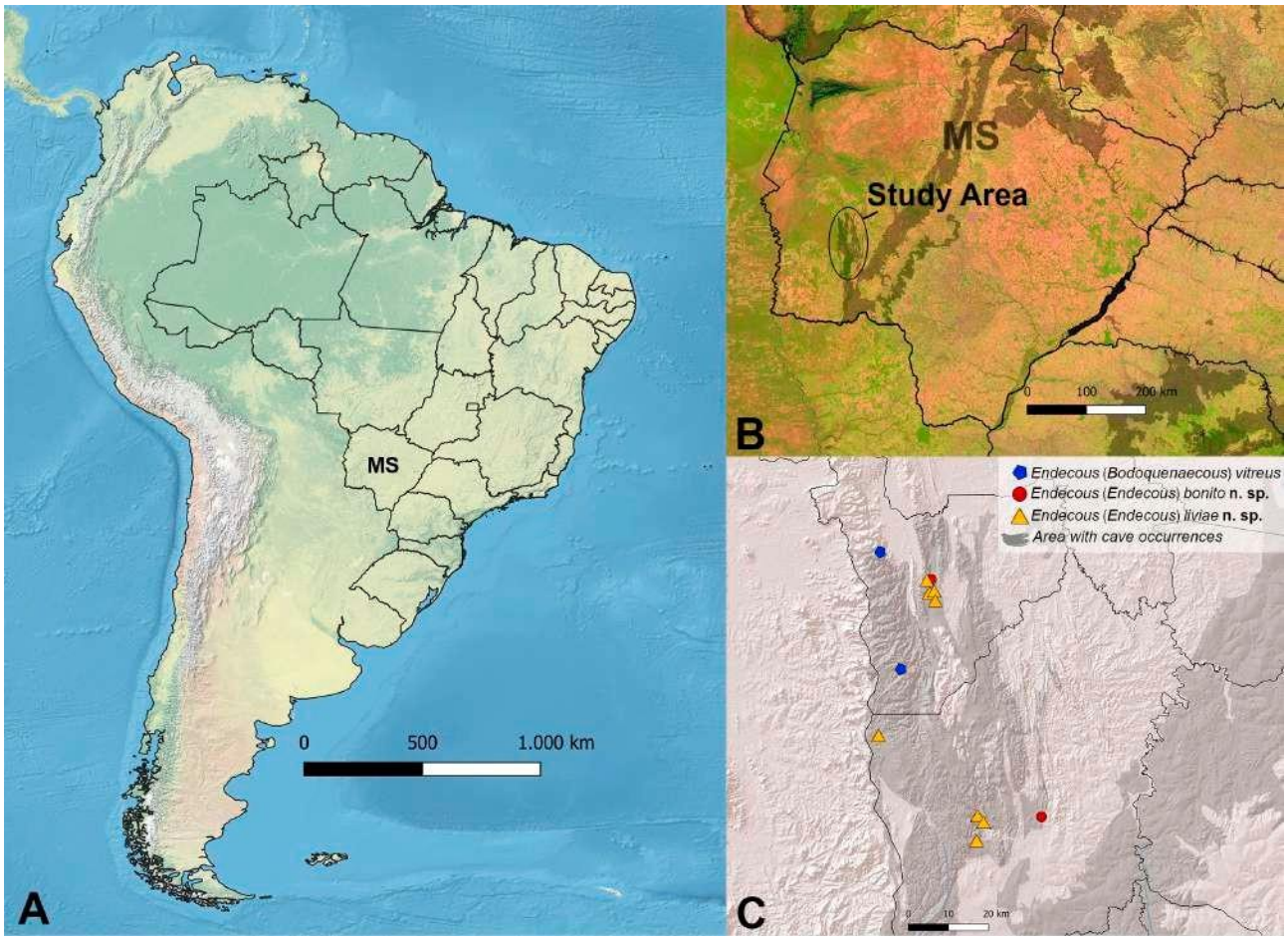


FIGURE 1. Distribution map of *Endecous* species in the Serra da Bodoquena region. (A) South America, Mato Grosso do Sul state—MS; (B) Landscape of Mato Grosso do Sul state, study area highlighted; (C) Elevation and borders of the Bodoquena and Bonito municipalities.

Collection and depository. Individuals were captured through active search, preserved in 70% ethanol and subsequently deposited in the Collection of Subterranean Invertebrates of Lavras (ISLA) at the Center of Studies on Subterranean Biology (CEBS), located at the Federal University of Lavras (UFLA) in Minas Gerais State, Brazil.
Holotype and paratypes of *Endecous* (*Endecous*) *liviae* **n. sp.** (18 ♂♂ and 12 ♀♀) were, through active search, found and captured during visits to Gruta do Alex II cave (56°42'35.06"w, 20°36'19.48"S), Gruta Dona Benedita cave (56°43'23.51"w, 20°34'0.55"S), Gruta Manoel Cardoso cave (56°43'23.39"w, 20°34'7.12"S), Gruta do Bel I cave (56°42'59.17" w, 20°35'20.53""S) and Bel II cave (56°43'0.48"w, 20°35'22.19"S), located in Bodoquena municipality, and Gruta América cave (56°36'39.01"w, 21°11'28.89"S), Gruta Terra Planetária cave (56°36'8.46"w, 21° 8'4.36"S), Gruta Catedral (56°50'46.90"w, 20°56'17.52"S) and Gruta do Lago Azul cave (56°35'28.91"w, 21°8'40.40"S), located in Bonito municipality, in September and October 2022.
Holotype and paratypes of *Endecous* (*Endecous*) *bonito* **n. sp.** (5 ♂♂ and 3 ♀♀) were captured using the same method during visits to Gruta São Mateus cave (56°27'17.25"w, 21° 8'1.26"S), located in Bonito municipality, and Gruta Dona Benedita cave (56°43'23.51"w, 20°34'0.55"S), located in Bodoquena municipality, in September 2022.
Additionally, topotypes of *Endecous* (*Bodoquenaecous*) *vitreus* (8 ♂♂ and 2 ♀♀) from Dente de Cão cave (20°44′47.88″W, 56°47′04.23″S), located in Bodoquena municipality, were collected in October 2022.
Finally, nymphs of *Endecous* were found within Vale do Prata I (56°29'26.44"w, 21°25'49.22"S), Gruta do Mimoso (56°33'31.84"w, 20°54'7.53"S), and Gruta São Miguel (56°34'53.21"w, 21°6'29.31"S) caves, located in Bonito municipality. It was not possible, however, to identify these specimens at species level.

Examination—The general morphology was examined using a Stemi 508 (ZEISS) stereomicroscope, and photographs were captured using a camera connected to an Axio Zoom V16 (ZEISS) stereomicroscope. Measurements were also taken under an Axio Zoom V16 (ZEISS) stereomicroscope. Subsequently, the right tegmen of the male adults was separated and mounted on a microscope slide. The number of teeth on the stridulatory file was quantified using an Axio Lab.A1 (ZEISS) microscope and a mechanical counter.

Adult males were dissected, and their phallic complexes were placed in eppendorf tubes filled with a pancreatin enzymatic solution (Álvarez-Padilla & Hormiga 2007) for a minimum period of 24 hours. This process enabled the digestion and removal of the soft tissue surrounding the sclerite. Subsequently, the phallic complexes were examined and compared using a Stemi 508 (ZEISS) stereomicroscope, and photographs were taken using an Axio Zoom V16 (ZEISS) stereomicroscope. The same procedure was conducted for females and their copulatory papillas.

The terminology used for describing the phallic complexes of both new species was originally proposed by Desutter (1987, 1998) and Desutter-Grandcolas (2003) and has been slightly adapted by Castro-Souza *et al.* (2020a, 2020b) and Carvalho *et al.* (2023).

Abbreviations—*Phallic complex*: **A**, pseudepiphallic ventral branch (or "A" sclerite); **Ps.arm**, pseudepiphallic arm; **Ps.db**, pseudepiphallic dorsal branch; **Ps.p**, pseudepiphallic paramere; **Ps.ib**, pseudepiphallic inner bars; **R**, pseudepiphallic rami; **Ect.ap**, ectophallic apodeme; **Ect.arc**, ectophallic arc; **Ect.fp**, ectophallic fold posterior portion; **Ect.lb**, ectophallic lateral bar; **Ect.mp**, ectophallic median projection; **End.sc.a**, endophallic sclerite anterior portion; **End.sc.d**, endophallic sclerite duct; **End.sc.p**, endophallic sclerite posterior portion.

Results

Family Phalangopsidae Blanchard, 1845

Subfamily Luzarinae Herbard, 1928

Genus *Endecous* Saussure, 1878 Subgenus

Endecous (*Endecous*) s. str.

Endecous (*Endecous*) *liviae* n. sp.

(Figures 2–6, 7–15, 16–19, 20–27, 28–32, 33–36, 37–39, 40–43; Table 1)

Etymology—The specific epithet of the species is dedicated to the biospeleologist Lívia Medeiros Cordeiro Borghezan, whose dedication to the study and preservation of caves in the Serra da Bodoquena karst region has been exceptional. The specific epithet is expressed as a Latinized adjective, paying homage to her significant contributions.

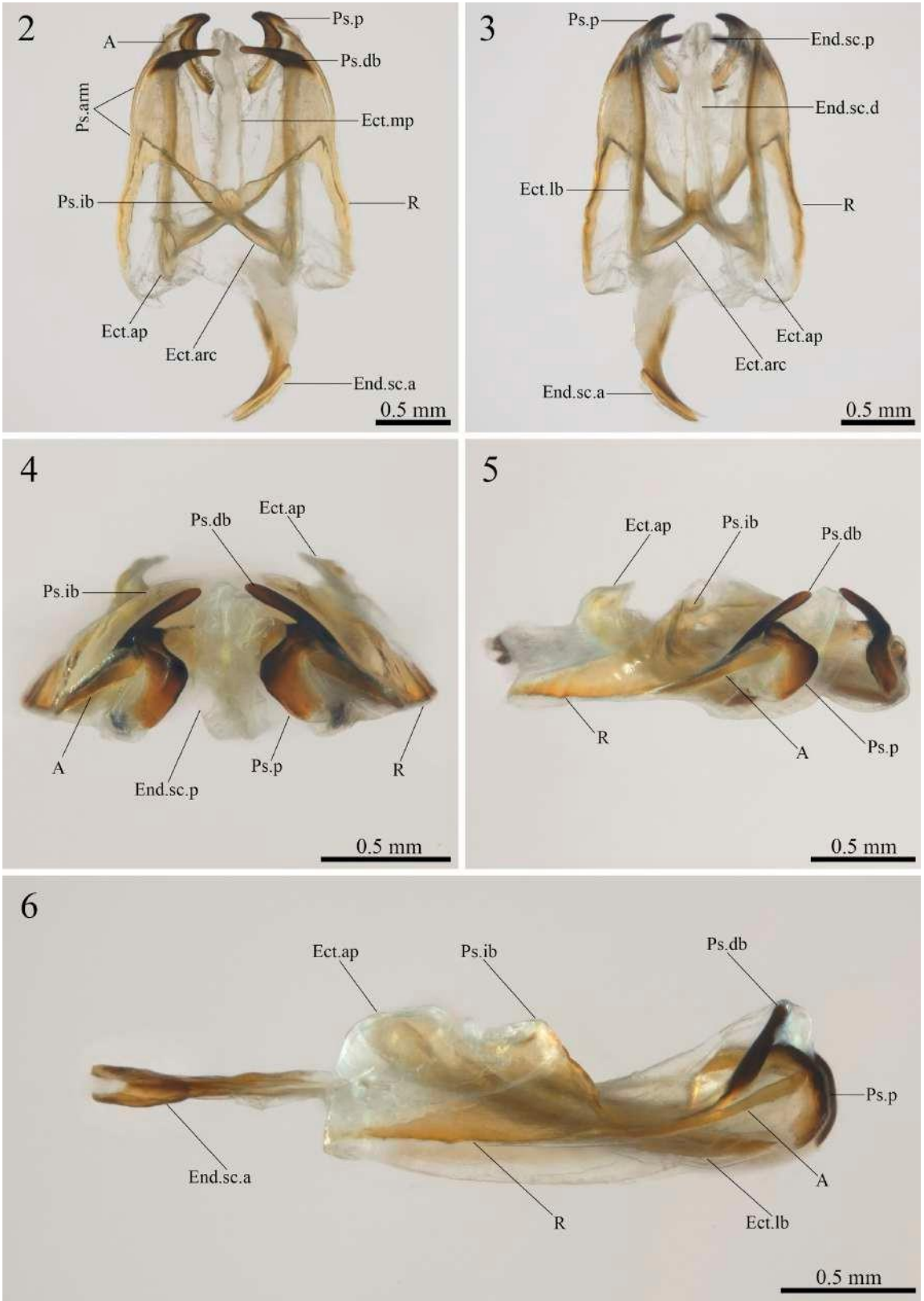
Material examined—*Holotype*, ♂, code ISLA 106153, Brazil, Mato Grosso do Sul, municipality of Bodoquena, Gruta do Alex II cave (56°42'35.06"w, 20°36'19.48"S), 02.X.2022, R.L. Ferreira; condition: head, right tegmen, legs I, II and III detached and stored alongside the holotype, phallic complex dissected and also stored alongside the holotype. *Allotype*: 1 ♀, ISLA 106154, same data as the holotype; condition: legs I, II and III detached and stored alongside the alotype, copulatory papilla dissected and also stored alongside the alotype. *Paratypes*: 1 ♂, ISLA 106152, 1 ♀, ISLA 106155, same locality and data as the holotype; 4 ♂♂, ISLA 106132, ISLA 106133, ISLA 106134, ISLA 106135, municipality of Bonito, Gruta América cave (56°36'39.01"w, 21°11'28.89"S), 29.IX.2022, R.L. Ferreira; 5 ♂♂, ISLA 106144, ISLA 106145, ISLA 106146, ISLA 106147, ISLA 106148, 3 ♀♀,
ISLA 106149, ISLA 106150, ISLA 106151, municipality of Bonito, Gruta Terra Planetária cave (56°36'8.46"w, 21° 8'4.36"S), 24.IX.2022, R.L. Ferreira; 1 ♂, ISLA 106156, 1 ♀, ISLA 106158, municipality of Bodoquena, Gruta Dona Benedita cave (56°43'23.51"W, 20°34'0.55"S), 26.IX.2022, R.L. Ferreira; 1 ♂, ISLA 106159, 1 ♀, ISLA 106160, municipality of Bodoquena, Gruta Manoel Cardoso cave (56°43'23.39"w, 20°34'7.12"S), 26.IX.2022, R.L. Ferreira; 2 ♂♂, ISLA 106171, ISLA 106172, 1 ♀, ISLA 106173, municipality of Bodoquena, Gruta do Bel I cave (56°42'59.17"W, 20°35'20.53"S), 03.X.2022, R.L. Ferreira; 1 ♀, ISLA 106174, municipality of Bodoquena, Gruta do Bel II cave (56°43'0.48"W, 20°35'22.19"S), 03.X.2022, R.L. Ferreira; 1 ♂, ISLA 106175, 1 ♀, ISLA 106176, municipality of Bonito, Gruta Catedral cave (56°50'46.90"w, 20°56'17.52"S), 05.X.2022, R.L. Ferreira; 2 ♂♂, ISLA 106177, ISLA 106178, 2 ♀♀ ISLA 106179, ISLA 106180, municipality of Bonito, Gruta do Lago

Azul cave (56°35’28.91”w, 21°8’40.40”S), 19.IX.2004, R.L. Ferreira; male paratypes condition: right tegmen and legs I, II and III detached and stored alongside the paratype, phallic complex dissected and also stored alongside the paratype; female paratypes condition: legs I, II and III detached and stored alongside the paratype, copulatory papilla dissected and also stored alongside the paratype.

TABLE 1. *Endecous (Endecous) liviae* **n. sp.**, morphological measurements (mm), mean (M) and standard deviation (SD) of 10 male and five female adult specimens; pars stridens refers to the number of teeth of the stridulatory file; # indicates that the right appendage, instead of the left one, was measured; * unable to measure due to damage in the structure.

♂	106133	106134	106145	106146	106152	106153	106156	106159	106171	106172	M	SD
Head width	3.372	3.054	2.887	2.778	2.772	2.733	2.830	2.995	2.827	2.757	2.901	0.196
Head length	2.440	2.313	2.159	2.225	2.007	1.989	2.143	2.295	1.950	2.075	2.160	0.159
Intraocular distance	1.831	1.624	1.578	1.496	1.502	1.552	1.561	1.605	1.533	1.501	1.578	0.099
Compound eye width	0.537	0.491	0.451	0.417	0.414	0.367	0.415	0.439	0.403	0.388	0.432	0.050
Compound eye length	1.005	0.958	0.914	0.879	0.894	0.789	0.866	0.896	0.877	0.826	0.890	0.061
Maxillary palpomere III	1.913	1.810	1.463	1.701	1.494	1.479	1.650	1.473	1.611	1.692	1.629	0.155
Maxillary palpomere IV	1.977	2.074	1.334	1.898	1.844	1.606	1.825	1.868	1.902	1.871	1.820	0.208
Maxillary palpomere V	2.571	2.554	1.768	2.360	2.068	1.953	2.251	2.202	2.459	2.276	2.246	0.260
Pronotum width	4.230	4.306	3.688	3.970	3.876	3.817	3.922	4.254	3.947	3.985	4.000	0.202
Pronotum length	2.896	2.619	2.482	2.478	2.522	2.376	2.417	2.610	2.506	2.568	2.547	0.145
Right tegmen width	4.206	3.999	3.810	3.588	3.487	3.588	3.635	3.958	3.619	3.600	3.749	0.234
Right tegmen length	4.927	4.941	4.495	4.435	4.496	4.435	4.395	4.859	4.685	4.582	4.625	0.213
Leg I length	20.878	18.772	17.465	17.181	16.355	15.353 #	16.088	17.601	16.536#	16.525#	17.763	1.631
Leg II length	21.614	19.187	18.069	17.876	16.359	15.725 #	16.413	17.806	16.839#	16.921	18.031	1.728
Femur III length	12.901	11.794	10.813	10.764	10.440	9.787#	10.080	11.404	10.277#	10.173	11.046	0.951
Tibia III length	13.732	13.110	11.600	11.586	10.962	10.293 #	10.763	11.787	10.888#	11.048	11.824	1.061
Body length	23.051	19.805	21.971	19.074	19.833	15.597	17.763	18.107	18.876	17.543	19.162	2.170
Pars stridens	75	72	58	60	62	64	63	66	71	72	66.300	5.832

♀	106149	106151	106154	106173	106158	M	SD
Head width	3.674	3.609	3.126	3.121	3.425	3.391	0.261
Head length	2.632	2.612	2.326	2.386	2.543	2.500	0.137
Intraocular distance	1.957	1.946	1.695	1.606	1.865	1.814	0.156
Compound eye width	0.609	0.526	0.513	0.462	0.537	0.532	0.074
Compound eye length	1.172	1.126	0.852	0.940	1.021	1.022	0.131
Maxillary palpomere III	2.199	2.221	1.652	1.777	1.844	1.939	0.257
Maxillary palpomere IV	2.193	2.587	1.898	2.025	2.118	2.164	0.261
Maxillary palpomere V	2.911	3.162	2.464	2.403	2.804	2.749	0.317
Pronotum width	4.987	4.882	4.527	4.214	4.645	4.651	0.305
Pronotum length	3.397	3.292	2.776	2.635	3.089	3.038	0.327
Femur III length	13.968	14.248	11.584	10.609	12.520	12.586	1.548
Tibia III length	14.854	15.138	12.346	11.525	13.076	13.388	1.570
Body length	24.936	25.694	21.027	18.915	24.040	22.922	2.856
Ovipositor length	13.831	14.262	10.887	10.462	*	12.361	1.962



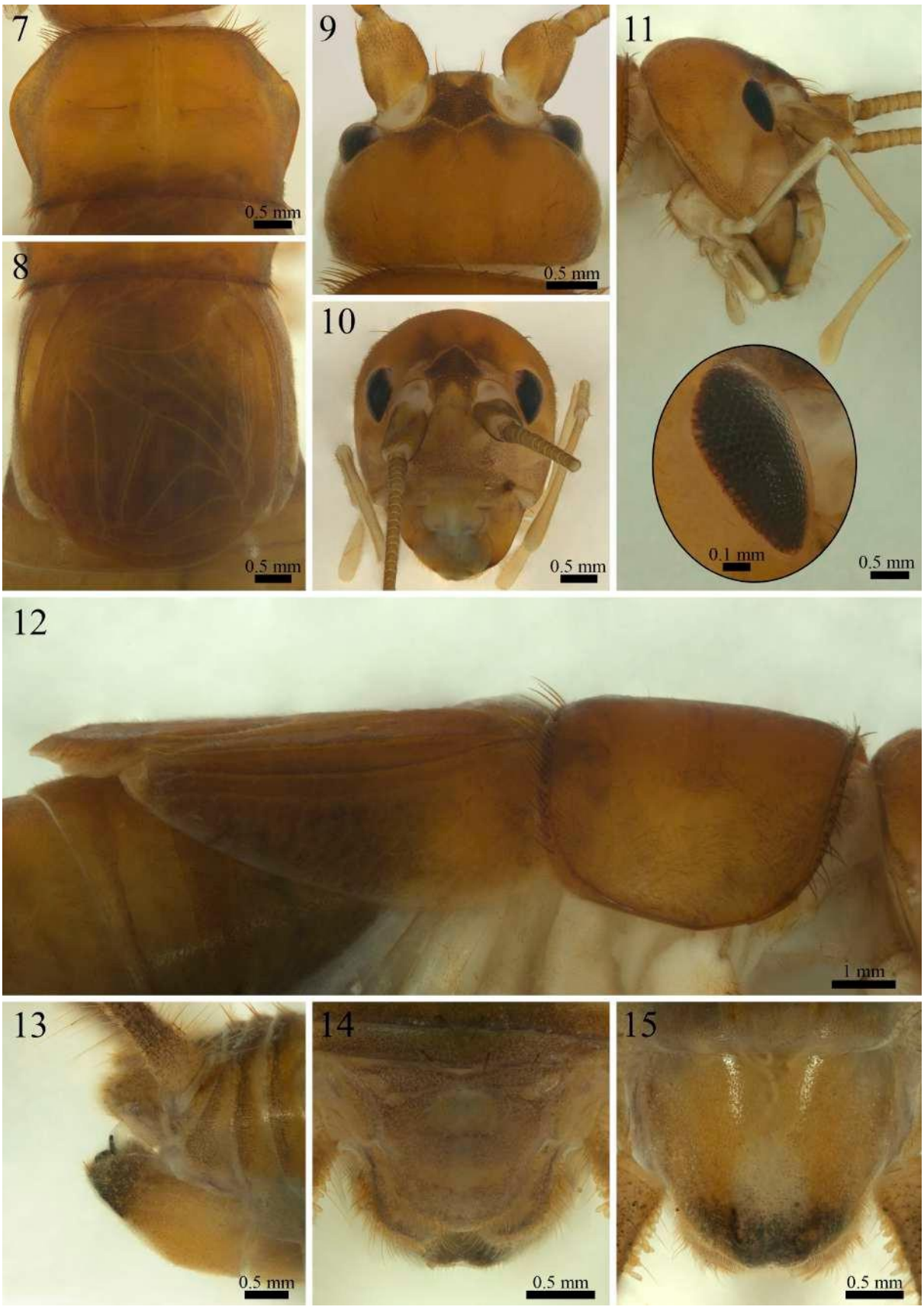
FIGURES 2–6. *Endecous* (*Endecous*) *liviae* **n. sp.** (ISLA 106153) phallic complex. (2) dorsal view, (3) ventral view, (4) frontal view, (5) laterofrontal view, (6) lateral view. Abbreviations: A, pseudepiphallic ventral branch (or "A" sclerite); Ps.arm, pseudepiphallic arm; Ps.db, pseudepiphallic dorsal branch; Ps.ib, pseudepiphallic inner bars; R, pseudepiphallic rami; Ps.p, pseudepiphallic paramere; Ect.ap, ectophallic apodeme; Ect.arc, ectophallic arc; Ect.lb, ectophallic lateral bar; Ect.mp, ectophallic median projection; End.sc.a, endophallic sclerite anterior portion; End.sc.d, endophallic sclerite duct; End.sc.p, endophallic sclerite posterior portion.

Diagnosis—Combination of the following characteristics: pseudepiphallic dorsal branches bending towards the center of the phallic complex, broadened at the base and tapered towards the apex, which is rounded (Figs. 2, 4–6, Ps.db); pseudepiphallic rami elongated and triangular in shape (Figs. 2–6, R); inner bars of the ectophallic invagination forming a V-shaped structure, with a less sclerotized, subtriangular in shape, dorsocentral projected extension (Figs. 2, 4–6, Ps.ib); ectophallic arc well-developed, conical and rounded, central portion bordering the base of the ectophallic median projections (Figs. 2 and 3, Ect.arc); anterior portion of the endophallus well-developed, sclerotized, with a long apodeme on the opposite side of the central groove (Figs. 2, 3 and 6, End.sc.a).

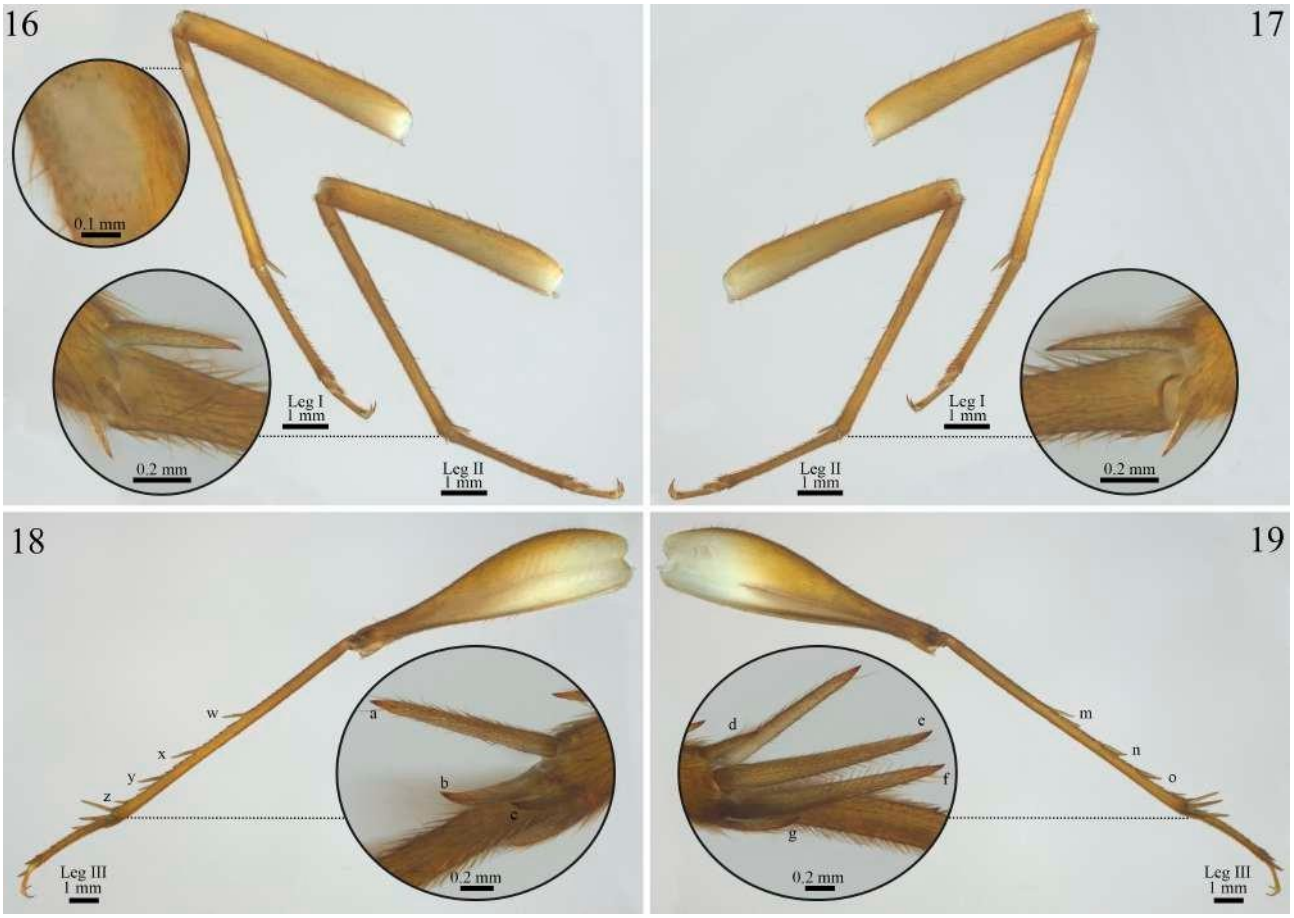
Male phallic sclerites (holotype ISLA 106153, Figs. 2–6)—Phallic complex longer than broad and dorsoventrally flattened. ***Pseudepiphallus***: arms slightly elongated and broadened laterally (Fig. 2, Ps.arm); dorsal branches sclerotized, bending towards the center of the phallic complex, broadened at the base and tapered towards the apex, which is rounded (Figs. 2 and 4, Ps.db); ventral branches elongated and sclerotized, reaching the dorsolateral portion of the pseudepiphallic parameres (Figs. 5 and 6, A); paramere 1 and 2 fused in a single sclerotized and concave structure, C-shaped in dorsal view, proximal end ventrally projected, bending and pointing outwards (Figs. 2 and 3, Ps.p); inner bars slightly concave, inclined, forming a V-shaped structure, with a less sclerotized, subtriangular in shape, dorsocentral projected extension in dorsal view (Fig. 2, Ps.ib); rami elongated, slightly longer than the ectophallic apodeme in dorsal and ventral views, broadened at the base, tapered at the end, triangular in shape in lateral view (Figs. 2, 3 and 6, R). ***Ectophallic invagination***: ectophallic arc well-developed, conical and rounded, central portion bordering the base of the ectophallic median projections (Fig. 3, Ect.arc); apodemes short and slightly sclerotized, distal end slightly curved inwards (Figs. 2, 3 and 6, Ect.ap); median projections thin, sinuous and barely sclerotized, reaching the pseudepiphallic parameres in dorsal view (Fig. 2, Ect.mp); lateral bars well-developed, elongated, curved outwards, tapered at the apex, reaching the outer ventral portion of the pseudepiphallic parameres (Figs. 3, 5 and 6, Ect.lb). ***Endophallus***: anterior portion well-developed, sclerotized, with a long apodeme on the opposite side of the central groove (Figs. 2, 3 and 6, End.sc.a); duct membranous, elongated, longer than the ectophallic apodeme and widened dorsoventrally at the connection to the sclerite anterior portion (Figs. 2, 3 and 6, End.sc.d); posterior portion membranous and well-developed, dorsally projected, almost touching the pseudepiphallic dorsal branches (Figs. 3 and 6, End.sc.p).

Variations in phallic sclerites (holotype and paratypes, n = 7, ISLA 106132, ISLA 106133, ISLA 106144, ISLA 106145, ISLA 106153, ISLA 106156, ISLA 106159)—Phallic complexes vary slightly in size and degree of sclerotization, being more or less flattened dorsoventrally; pseudepiphallic arms (Ps.arm) vary slightly in length; pseudepiphallic dorsal branches (Ps.db) vary slightly in degree of inclination towards the center of the phallic complex, the tips almost touching or slightly distant from one another, varying slightly in sinuosity; pseudepiphallic inner bars (Ps.ib) vary slightly in degree of inclination, dorsocentral extension varying in size and varying slightly in shape; ectophallic arcs (Ect.arc) central extension vary in length; ectophallic apodemes (Ect.ap) vary slightly in degree of sinuosity and sclerotization; endophallic sclerite posterior portion (End.sc.p) more or less projected dorsally.

Morphology (holotype ISLA 106153, Figs. 7–20)—***Body color***: vertex, scape, pedicel and flagellum yellowish brown; fastigium dark brown; front and gena varying from light yellow to white, partially covered by a dotted brown mark; clypeus and labrum also varying from light yellow to white; mandibles and maxiles yellowish brown, galea and labium white; ommatidia black, with a slightly depigmented area near the base of the antennal scapes (Figs. 9–11); maxillary palpomeres I and II whitish, maxillary palpomeres III, IV and V light yellow, palpomere V white at the tip; all labial palpomeres light yellowish brown, labial palpomere III white at the tip (Figs. 10 and 11); pronotum, tegmina and abdomen yellowish brown, tergites distal portion brown (Figs. 7, 8, 12 and 13); supra-anal plate yellowish brown, subgenital plate light yellow proximally, whitish in the central to distal region, and darkened towards the distal end (Figs. 13, 14 and 15); cerci yellowish brown, darker at first sight due to the presence of setae (Fig. 13); legs yellowish brown, white at their base (Figs. 16–19). ***Head***: slightly pubescent, elongated in frontal view; fastigium as a short and broad extension of the vertex, inclined and pointing downwards, with long bristles; mandibles sclerotized at the apex and lateral margins; maxiles sclerotized at the apex; maxillary palpomeres I and II short and same-sized, III–V longer, palpomere V claviform; labial palpomeres I–III increasing in size, palpomere III dilated at the apex; compound eyes reduced and elliptical, ocelli absent (Figs. 9–11). ***Thorax***: pronotum dorsal disk broader than long (3.82 mm and 2.38 mm in width and length, respectively), pubescent, anterior and posterior margins arched and covered in long bristles, lateral lobes subtriangular in shape and slightly shifted towards the head (Figs. 7 and 12). ***Right tegmen***: slightly sclerotized; covering the first two urotergites (3.59 mm and 4.43 mm in width and length, respectively); *harp* with one complete and four incomplete crossveins (two bifurcated proximally); *mirror* subtriangular, with one arched crossvein, and two cells; *basal field* with two secondary veins

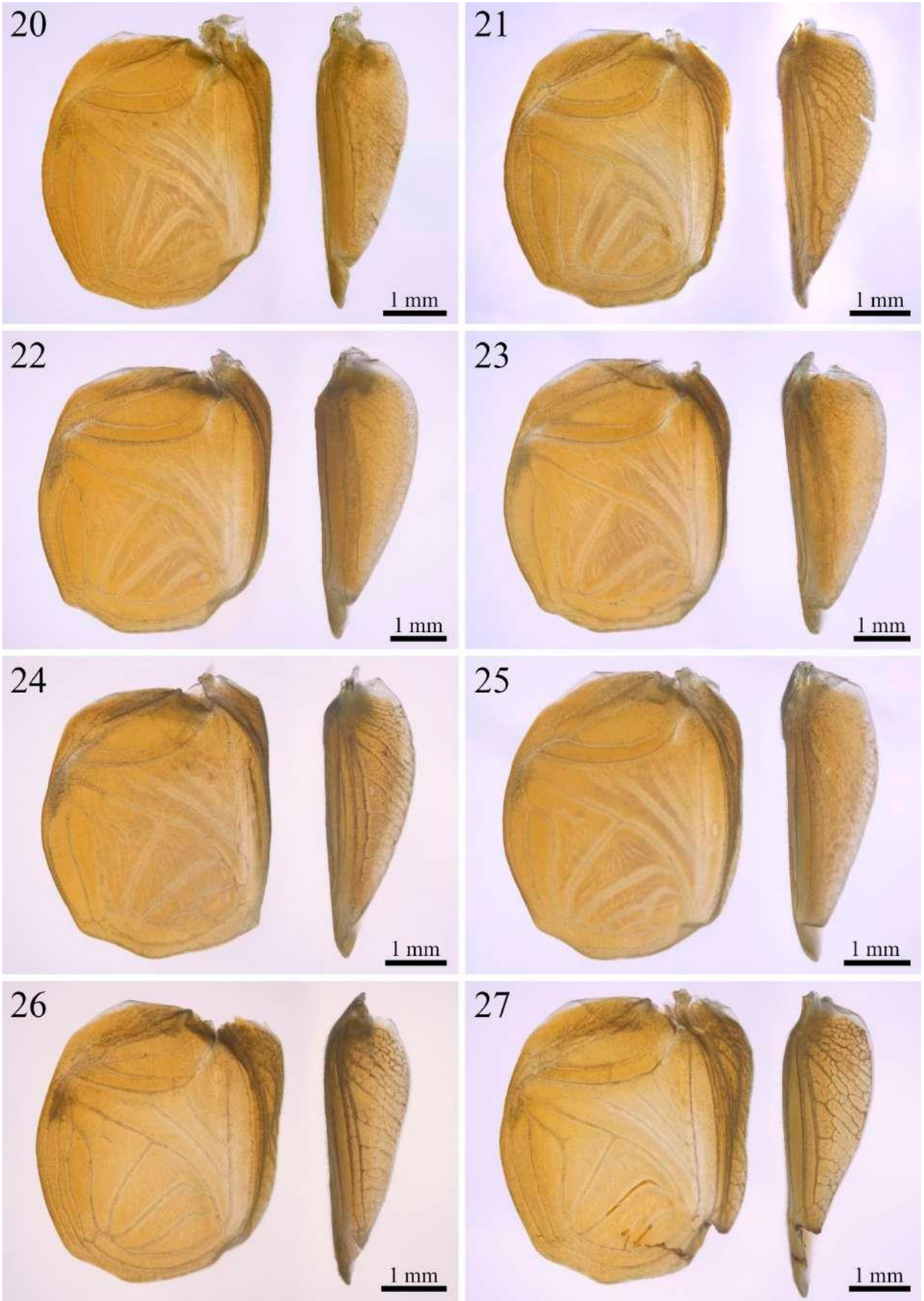


FIGURES 7–15. *Endecous* (*Endecous*) *liviae* **n. sp.** (ISLA 106153) male general morphology. (7) pronotum in dorsal view; (8) right tegmen in dorsal view (9) head in dorsal view; (10) head in frontal view; (11) head and palpi in lateral view, compound eye highlighted; (12) pronotum and tegmen in lateral view; (13) supra-anal and subgenital plates in lateral view; (14) supra-anal plate in dorsal view; (15) subgenital plate in ventral view.

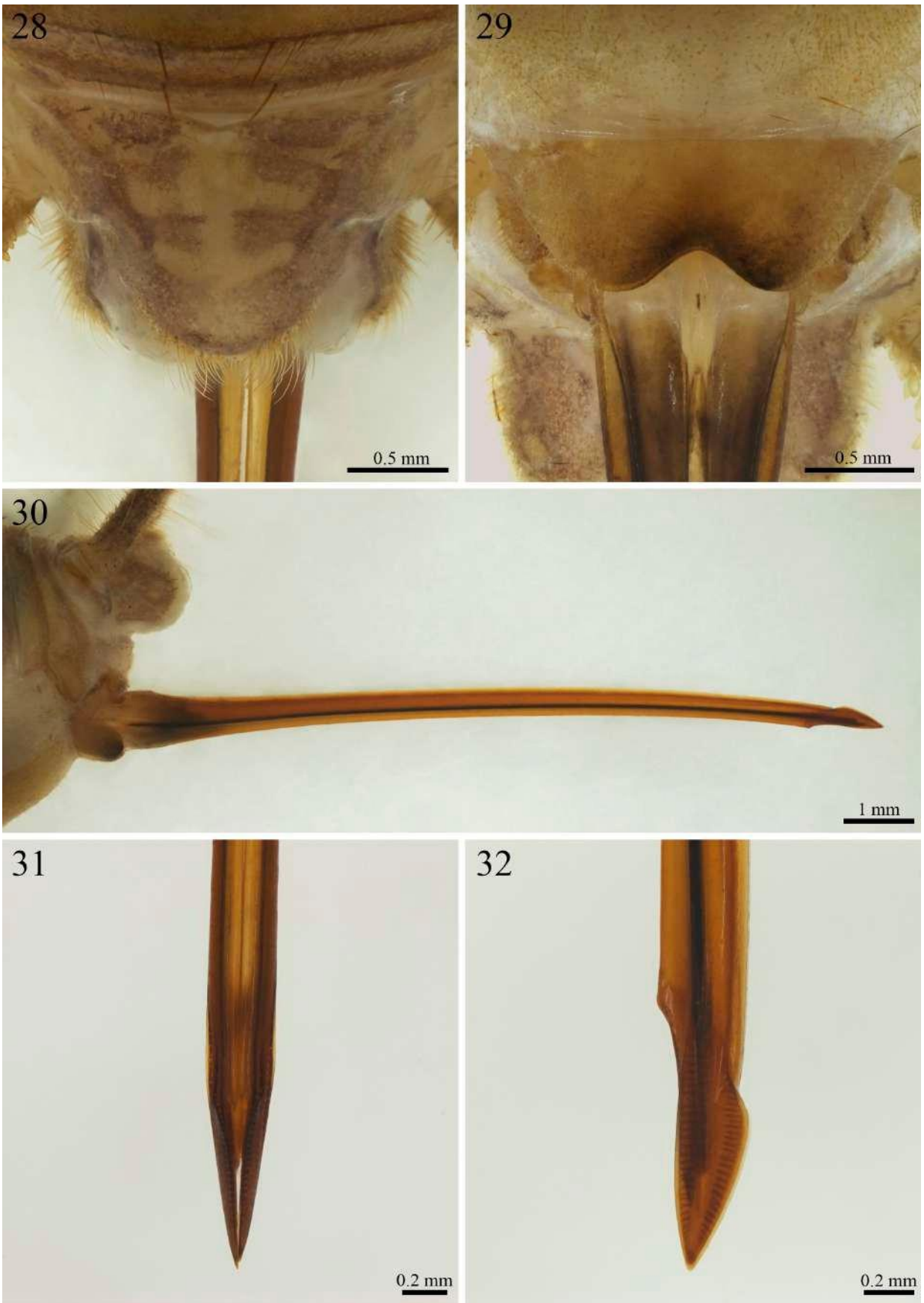


FIGURES 16–19. *Endecous* (*Endecous*) *liviae* **n. sp.** (ISLA 106153) right legs. (16) inner view: leg I, tympanum highlighted, and leg II, apical spurs highlighted; (17) outer view: leg I and leg II, apical spurs highlighted; (18) outer view: leg III, apical spurs highlighted; (19) inner view: leg III, apical spurs highlighted.

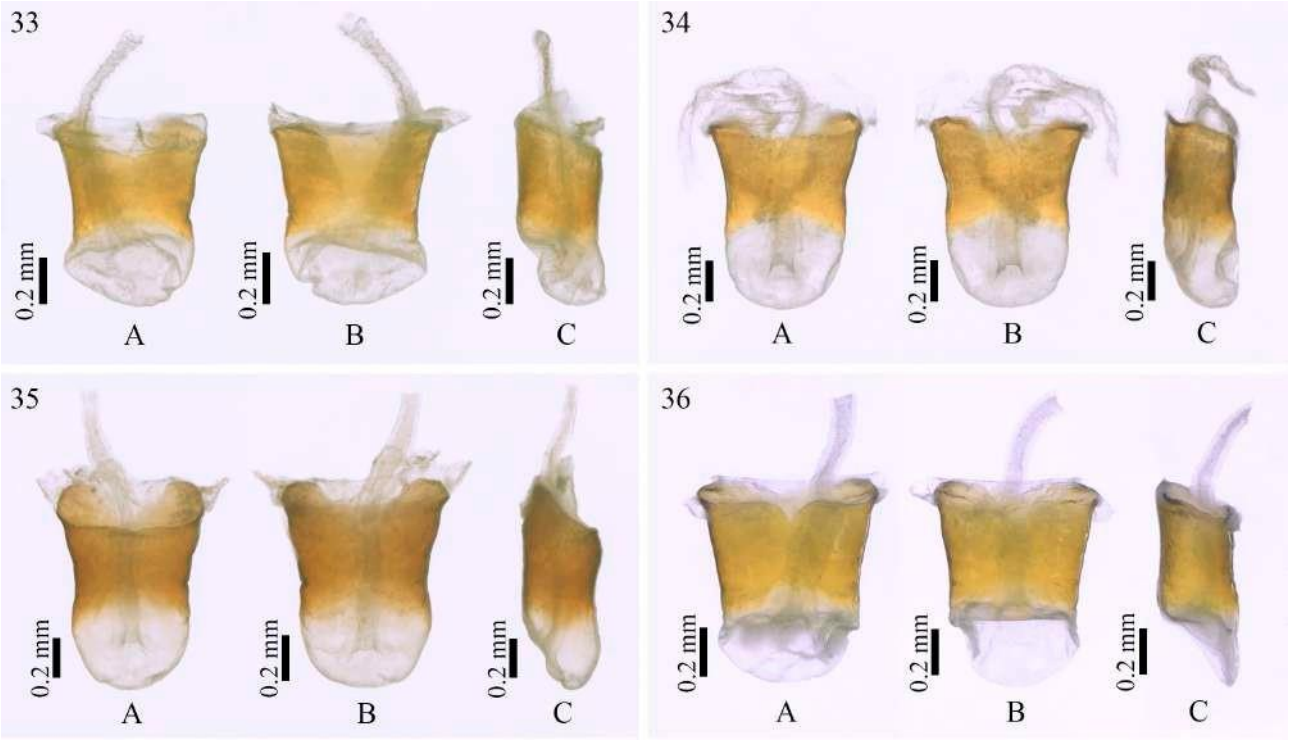
connecting Cu2 to 1A, 1A and 2A veins connected through a poorly-marked secondary vein; *lateral field* with two almost completely parallel longitudinal veins and several anastomotic poorly-marked secondary veins (Figs. 8, 12 and 20); *stridulatory file* with 64 teeth. ***Abdomen***: cerci pubescent, with long bristles throughout all their extension and globose setae at their base, mostly on the inner side (Figs. 13–15); supra-anal plate shorter than the subgenital plate, subtriangular, distal margin rounded and covered in long bristles, lateral projections short and rounded, paraprocts slightly longer than the supra-anal plate (Figs. 13 and 14); subgenital plate proximal margin substraight, distal margin rounded, with a small dent in the center and covered in bristles (Figs. 13–15). ***Legs***: pubescent. *Leg I* (Figs. 16 and 17): tibia with an oval tympanum on its inner side and two ventral apical spurs; tarsomere I ventrally serrated and longer than tarsomeres II and III together. *Leg II* (Figs. 16 and 17): tibia with two ventral apical spurs of equal size and two lateral short spurs, one on each side; tarsomere I ventrally serrated and longer than tarsomeres II and III together. *Leg III* (Figs. 18 and 19): femur developed; tibia longer than the femur (10.29 mm and 9.79 mm, respectively); tibia armed with three subapical spurs on the inner side (Fig. 19; m, n, o), four on the outer side (Fig. 18; w, x, y, z), the most distal one, "z", being the shortest, four apical spurs on the inner side (Fig. 19; d, e, f, g), spurs "e" and "f" longer the "d" and "g", and three on the outer side (Fig. 18; a, b, c), spur "a" being the longest and "c" the shortest; tarsomere I longer than tarsomeres II and III together, ventrally serrated, with two apical spurs, the inner one being the longest.



FIGURES 20–27. *Endecous* (*Endecous*) *liviae* **n. sp.** right tegmina, dorsal and lateral view. (20) holotype, ISLA 106153; (21) paratype, ISLA 106171; (22) paratype, ISLA 106133; (23) paratype, ISLA 106134; (24) paratype, ISLA 106145; (25) paratype, ISLA 106146, (26) paratype, ISLA 106156, (27) paratype, ISLA 106159.



FIGURES 28–32. *Endecous* (*Endecous*) *liviae* **n. sp.** (ISLA 106154) ovipositor. (28) supra-anal plate; (29) subgenital plate; (30) ovipositor, lateral view; (31) ovipositor apex, dorsal view; (32) ovipositor apex, lateral view.



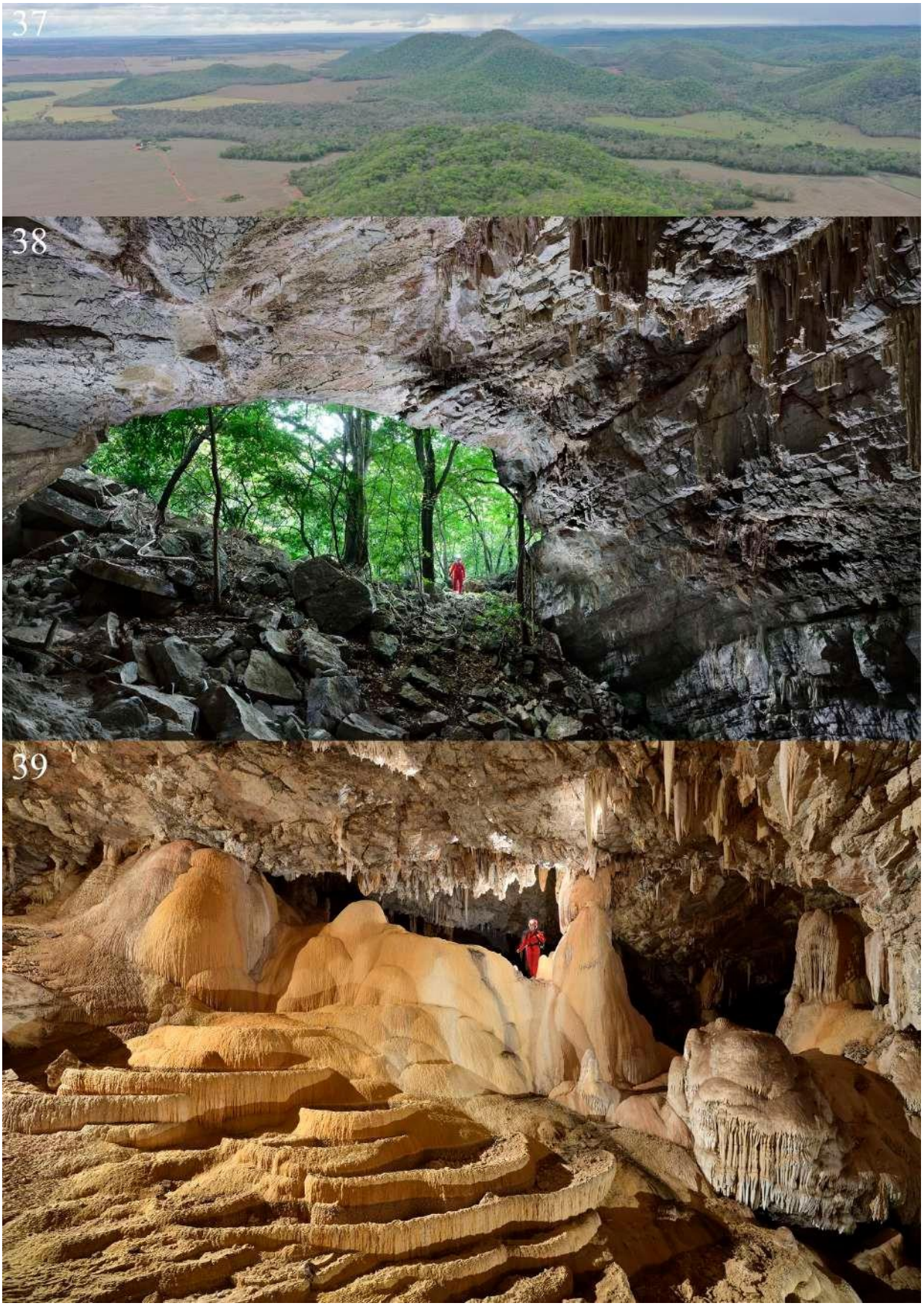
FIGURES 33–36. *Endecous* (*Endecous*) *liviae* **n. sp.** copulatory papillae. (33) allotype, ISLA 106154; (34) paratype, ISLA 106155; (35) paratype, ISLA 106149; (36) paratype, ISLA 106173; A—dorsal view; B—ventral view; C—lateral view.

Variations in right tegmina (holotype and paratypes, n = 8, ISLA 106133, ISLA 106134, ISLA 106145, ISLA 106146, ISLA 106153, ISLA 106156, ISLA 106159, ISLA 106171, Figs. 20–27)—***Stridulatory file*** with 65 ± 5.16 teeth (n = 10, holotype and paratypes). ***Harp*** with one (Figs. 20 and 23), two (Figs. 22, 24 and 26), three (Figs. 25 and 27) or four (Fig. 21) complete diagonal crossveins; incomplete crossveins may be present, some of them reaching a light-colored longitudinal striation (Figs. 20 and 23). ***Mirror*** with one (Fig. 20), two (Figs. 21–24, 26 and 27) or three (Fig. 25) complete crossveins, the second and third most distal ones are connected through a secondary vein; an incomplete crossvein may be present (Fig. 27); mirror outline inconsistent due to variations in the form of the distal margin. ***Basal field*** with poorly-marked secondary veins branching out of 1A and reaching Cu2; 1A may be directly connected to Cu2 (Fig. 26); 1A may also be fragmented in two and connected to the central portion of Cu2 (Fig. 24); 1A, 2A and 3A well-marked. ***Lateral field*** with two parallel longitudinal veins that may or may not be connected through short secondary veins; anastomosis of poorly-marked secondary veins branching out of the longitudinal veins; secondary veins reaching the right margin of the tegmina.

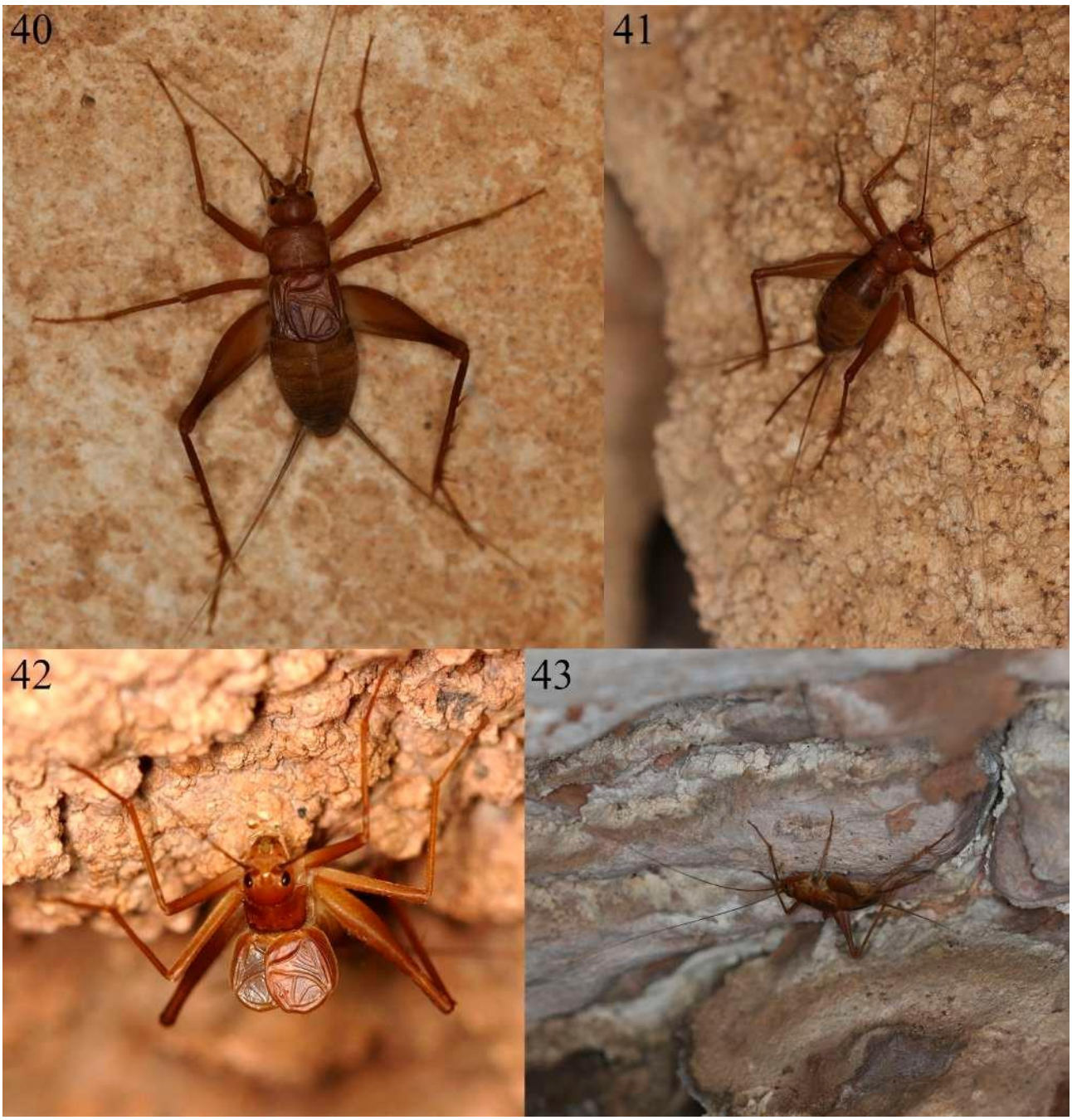
Female morphology (allotype ISLA 106154 Figs. 28–32)—same pattern of body coloration as the male, but slightly darker; bigger than the male (22.92 ± 2.86 mm and 19.16 ± 2.17 mm in length, respectively); apterous; supra-anal plate subtriangular in shape, pubescent, with long bristles covering the distal margin, which is rounded, lateral projections short and rounded (Fig. 28); subgenital plate pubescent, lateral margins angled inwards from the base, distal margin w-shaped (Fig. 29); ovipositor (10.89 mm in length) shorter than the cerci, shaped like a curved sword, with a dorsoventral constriction near the tip, apex acute like an arrow-head (Figs. 30–32).

Copulatory papilla (allotype ISLA 106154, Fig. 33)—sclerotized and chalice-like; anterior potion broadened, ventral side with a less sclerotized V-shaped region, like a deep indentation, ventral margin slightly longer than the dorsal margin; posterior portion membranous with a small circular opening on the ventral side.

Variations in copulatory papillae (allotype and paratypes, ISLA 106149, ISLA 106154, ISLA 106155, ISLA 106173, Figs. 33–36)—less sclerotized region on the ventral side may be reduced in size and U-shaped; a small V-shaped dent may be present in the center of the dorsal margin.



FIGURES 37–39. *Endecous* (*Endecous*) *liviae* **n. sp.** habitat. (37) Gruta América cave, external environment; (38) Gruta América cave, entrance; (39) Gruta América cave, internal environment. Photo credits: (37) Rodrigo Lopes Ferreira; (38) and (39) Philippe Crochet.



FIGURES 40–43. *Endecous* (*Endecous*) *liviae* **n. sp.** (40) adult male of *E.* (*E.*) *liviae* **n. sp.**, Gruta Alex II cave; (41) adult female of *E.* (*E.*) *liviae* **n. sp.**, Gruta Alex II cave; (42) adult male of *E.* (*E.*) *liviae* **n. sp.**, Gruta Terra Planetária cave; (43) adult female of *E.* (*E.*) *liviae* **n. sp.**, Gruta América. Photo credits: Rodrigo Lopes Ferreira.

Ecological remarks—Specimens of *Endecous* (*E.*) *liviae* **n. sp.** were found in nine caves located in the municipalities of Bodoquena (Gruta Dona Benedita, Gruta Manoel Cardoso, Gruta do Bel I, Gruta do Bel II and Gruta Alex II caves) and Bonito (Gruta América—Figs. 38 and 39, Gruta Catedral, Gruta do Lago Azul and Gruta Terra Planetária caves). Given the limited sampling of caves conducted by the authors, it is probable that the species has a widespread distribution in the region, potentially occurring in additional caves. Unfortunately, the once pristine vegetation in the area has undergone significant alterations over the past few decades due to extensive agricultural and pasture activities. Consequently, the landscape has become highly fragmented, with the remaining forests largely associated with the limestone outcrops (Fig. 37). This inference is supported by the abundance of caves in the area, coupled with the considerable distance between the caves where the three populations were found (68 km in a

straight line between the farthest caves). Most adult specimens were observed on the caves' walls (Figs. 40 and 41), while in several locations, they were found concealed within speleothems and rock crevices (Fig. 43). This behavior suggests a certain degree of photophobia, as the presence of researchers equipped with headlamps may disturb them, causing them to seek shelter. Nevertheless, adult specimens, particularly males, could be easily found while engaging in vocalizations as part of their courtship behavior aimed at attracting females (Fig. 42). Another noteworthy observation is that the majority of specimens found in all caves were in their immature stages. Consequently, locating adult individuals proved to be more challenging, potentially indicating the difficulty in reaching adulthood. This can be attributed to the presence of several predators within the caves that prey upon immature specimens. As a result, only a small proportion of the immature individuals are likely to successfully transition into adulthood due to the substantial predation pressure they face.

***Endecous* (*Endecous*) *bonito* n. sp.**

(Figures 44–49, 50–58, 59–62, 63–66, 67–71, 72–73, 74–78; Table 2)

Etymology—The specific epithet refers to the locality "Bonito", a municipality located in Mato Grosso do Sul state, Brazil, where the specimens were collected.

Material examined—*Holotype*, ♂, code ISLA 106137, Brazil, Mato Grosso do Sul, municipality of Bonito, Gruta São Mateus cave (56°27'17.25"w, 21° 8'1.26"S), 28.IX.2022, R.L. Ferreira; condition: head, right tegmen, legs I, II and III detached and stored alongside the holotype, phallic complex dissected and also stored alongside the holotype. *Allotype*: 1 ♀, ISLA 106142, same data as the holotype; condition: legs I, II and III detached and stored alongside the allotype, copulatory papilla dissected and also stored alongside the allotype. *Paratypes*, 3 ♂♂; ISLA 106138, ISLA 106139, ISLA 106140, 2 ♀♀ ISLA 106141, ISLA 106143, same data as the holotype; 1 ♂, ISLA 106157, municipality of Bodoquena, Gruta Dona Benedita cave (56°43'23.51"w, 20°34'0.55"S), 26.IX.2022, R.L. Ferreira; male paratypes condition: right tegmen and legs I, II and III detached and stored alongside the paratype, phallic complex dissected and also stored alongside the paratype; female paratypes condition: legs I, II and III detached and stored alongside the paratype, copulatory papilla dissected and also stored alongside the paratype.

Diagnosis—Combination of the following characteristics: pseudepiphallic dorsal branches elongated and abruptly curved inwards, outer margin more sclerotized than the inner margin, apex less sclerotized, dorsally projected after curving inwards, claviform with a rounded tip and bearing several setae on the distal inner surface (Figs. 44, 46–49, Ps.db); pseudepiphallic parameres 1 and 2 fused in a single sclerotized and concave structure, ventral portion bean-shaped, dorsal portion diamond-shaped and projected towards the center of the sclerite (Figs. 44–47, Ps.p); ectophallic arc well-developed, dome-shaped, central portion bordering the base of the ectophallic median projections (Fig. 45, Ect.arc); lateral bars well-developed, elongated, inclined inwards and broadened dorsoventrally (Figs. 45–47, Ect.lb); anterior portion of the endophallus well-developed, sclerotized, with a long apodeme on the opposite side of the central groove (Figs. 44, 45 and 49, End.sc.a).

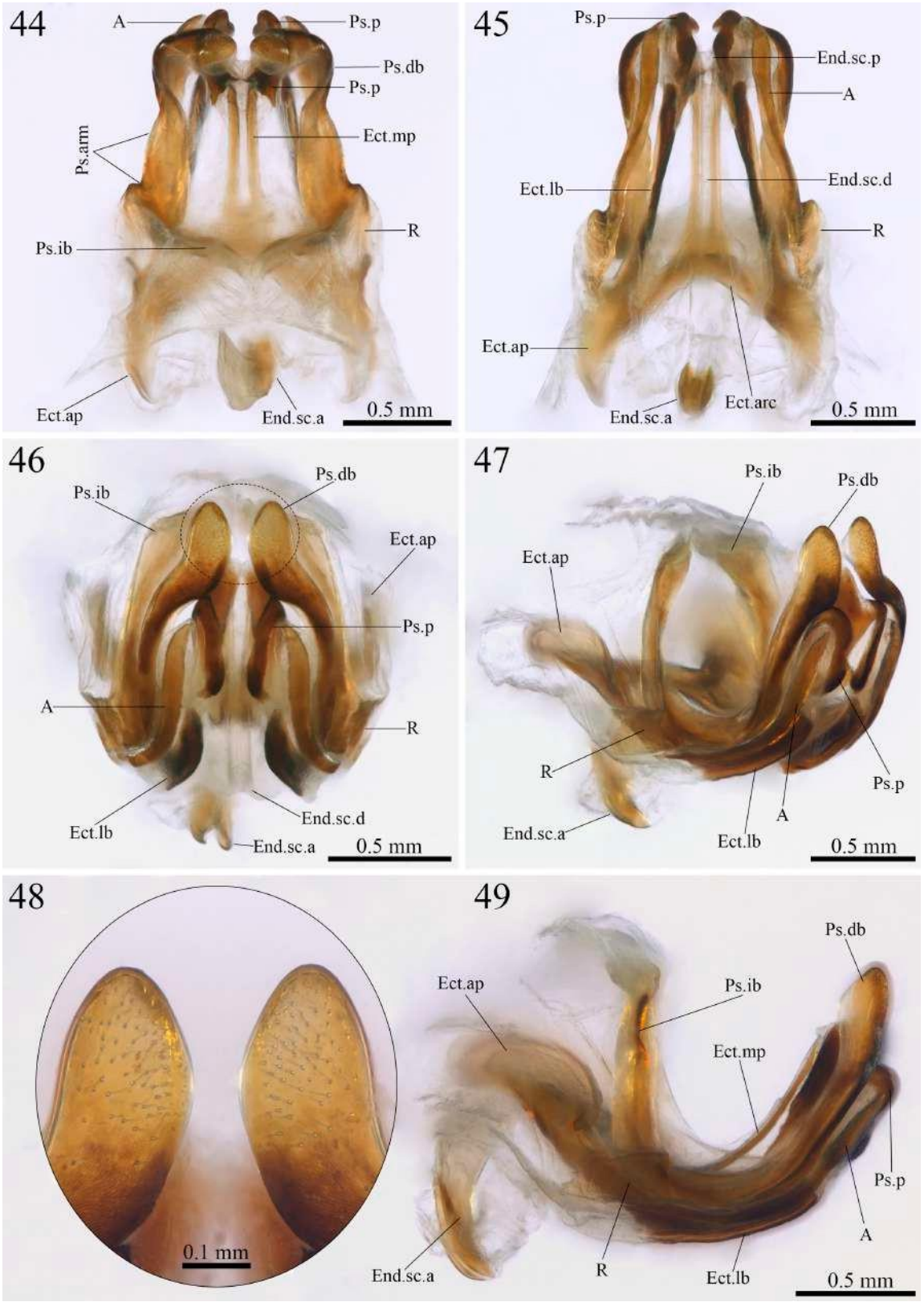
Male phallic sclerites (holotype ISLA 106137, Figs. 44–49)—Phallic complex longer than broad, and curved dorsoventrally. ***Pseudepiphallus***: arms short and broadened laterally, albeit to a lesser extent when compared to *E. liviae* **n. sp.** (Fig. 44, Ps.arm); dorsal branches elongated and abruptly curved inwards, outer margin more sclerotized than the inner margin, apex less sclerotized, dorsally projected after curving inwards, claviform with a rounded tip and bearing several setae on the distal inner surface (Figs. 44, 46–49, Ps.db); ventral branches sclerotized and elongated, almost reaching the tip of the pseudepiphallic parameres, distal half broader compared to that of *E. liviae* **n. sp.**, and with a tapered apex (Figs. 45–47, A); paramere 1 and 2 fused in a single sclerotized and concave structure, ventral portion bean-shaped, dorsal portion diamond-shaped and projected towards the center of the sclerite (Figs. 44–47, Ps.p); inner bars dorsally projected, slightly concave and inclined inwards, central portion pointing downwards in dorsal view (Figs. 44, 47 and 49, Ps.ib); rami short and shield-like, partially covering the proximal portion of the inner bars (Figs. 45, 47 and 49, R). ***Ectophallic invagination***: ectophallic arc well-developed, dome-shaped, central portion bordering the base of the ectophallic median projections (Fig. 45, Ect.arc); apodemes well-developed, distal end slightly curved inwards (Figs. 44, 45 and 49, Ect.ap); median projections sclerotized, broad and almost straight, reaching the pseudepiphallic parameres (Fig. 44, Ect.mp); lateral bars well-developed, elongated, inclined inwards and broadened dorsoventrally (Figs. 45–47, Ect.lb). ***Endophallus***: anterior portion of the endophallus well-developed, sclerotized, with a long apodeme on the opposite side of the central groove (Figs. 44, 45 and 49, End.sc.a); duct membranous, elongated, roughly the same length as the ectophallic apodemes (Figs. 45 and 49, End.sc.d); posterior portion membranous, tapered towards the apex and hidden between the pseudepiphallic parameres (Figs. 44 and 45, End.sc.p).

TABLE 2. *Endecous (Endecous) bonito* **n. sp.**, morphological measurements (mm), mean (M) and standard deviation (SD) of five male and three female adult specimens; pars stridens refers to the number of teeth of the stridulatory file; * unable to measure due to damage in the structure.

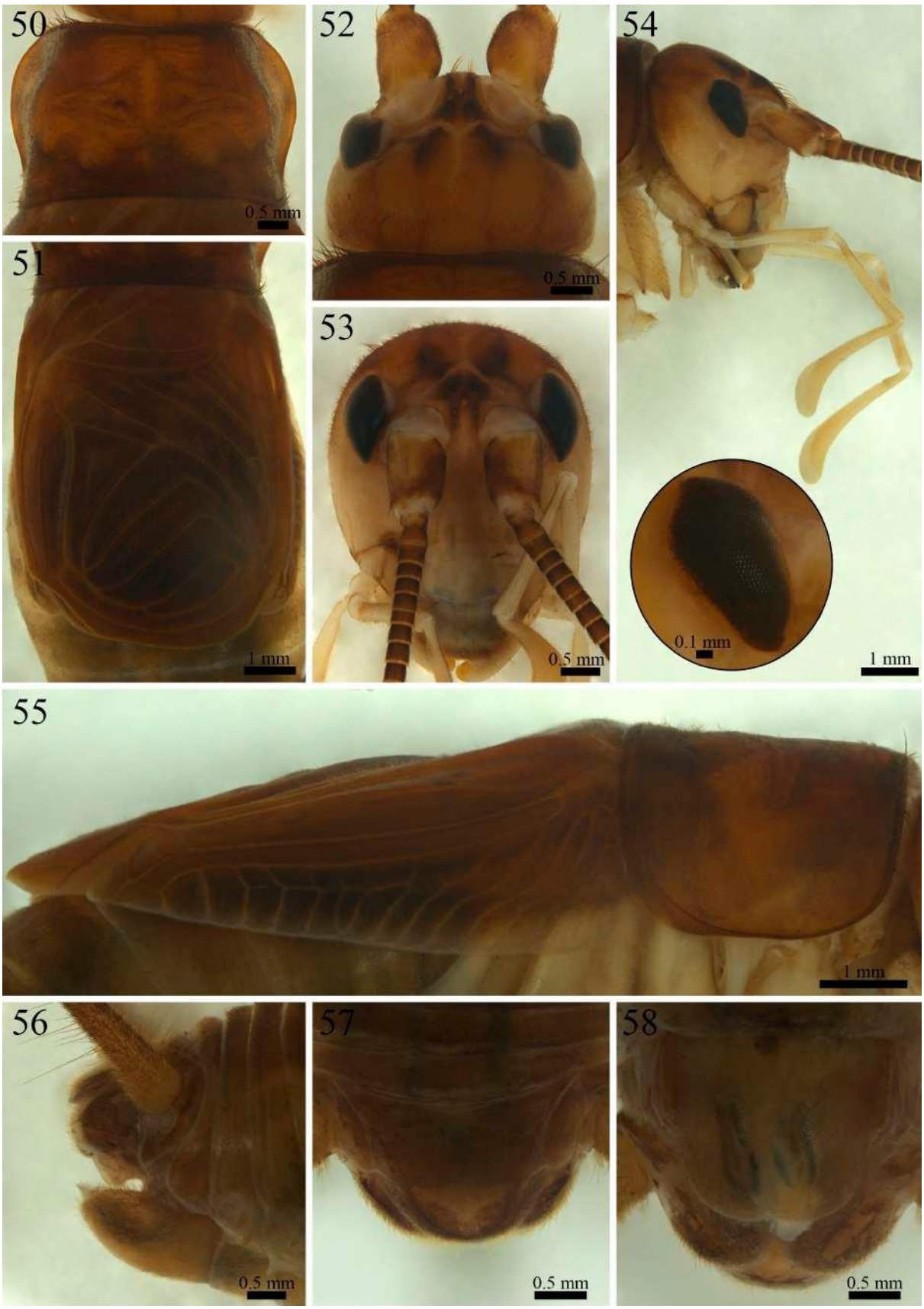
♂	106137	106138	106139	106140	106157	M	SD
Head width	3.320	3.285	3.259	3.196	3.155	3.243	0.067
Head length	1.921	2.202	2.065	2.393	2.028	2.122	0.182
Intraocular distance	1.535	1.640	1.518	1.484	1.481	1.532	0.065
Compound eye width	0.647	0.590	0.551	0.562	0.582	0.586	0.037
Compound eye length	1.236	1.188	1.171	1.176	1.251	1.204	0.037
Maxillary palpomere III	1.910	1.840	1.876	1.947	1.876	1.890	0.040
Maxillary palpomere IV	2.086	1.929	2.023	2.116	1.958	2.022	0.080
Maxillary palpomere V	2.746	2.392	2.900	2.640	2.455	2.627	0.208
Pronotum width	4.632	4.760	4.629	4.565	4.437	4.605	0.117
Pronotum length	3.112	3.072	2.949	3.022	3.079	3.047	0.063
Right tegmen width	5.474	5.587	5.767	5.395	5.355	5.516	0.166
Right tegmen length	7.587	7.876	7.725	7.458	7.731	7.675	0.159
Leg I length	19.982	19.133	19.156	20.700	19.833	19.761	0.651
Leg II length	20.091	19.208	19.513	20.654	20.041	19.901	0.560
Femur III length	13.380	12.456	12.933	13.170	12.776	12.943	0.356
Tibia III length	13.809	13.697	13.944	14.275	14.149	13.975	0.238
Body length	18.924	19.620	23.873	22.952	22.349	21.544	2.158
Pars stridens	81	72	79	79	83	78.800	4.147

♀	106141	106142	106143	M	D
Head width	3.485	4.166	3.811	3.821	0.341
Head length	2.422	2.513	2.645	2.527	0.112
Intraocular distance	1.591	1.983	1.788	1.787	0.196
Compound eye width	0.686	0.695	0.643	0.665	0.030
Compound eye length	1.269	1.353	1.316	1.313	0.042
Maxillary palpomere III	1.898	2.027	2.060	1.995	0.086
Maxillary palpomere IV	2.149	2.217	2.171	2.179	0.035
Maxillary palpomere V	2.761	2.870	3.052	2.894	0.147
Pronotum width	4.848	6.009	5.469	5.442	0.581
Pronotum length	3.352	3.940	3.671	3.654	0.294
Femur III length	13.647	16.057	*	14.852	1.704
Tibia III length	14.094	16.225	*	15.160	1.507
Body length	22.023	27.775	27.102	25.633	3.145
Ovipositor length	9.567	14.051	12.792	12.137	2.313

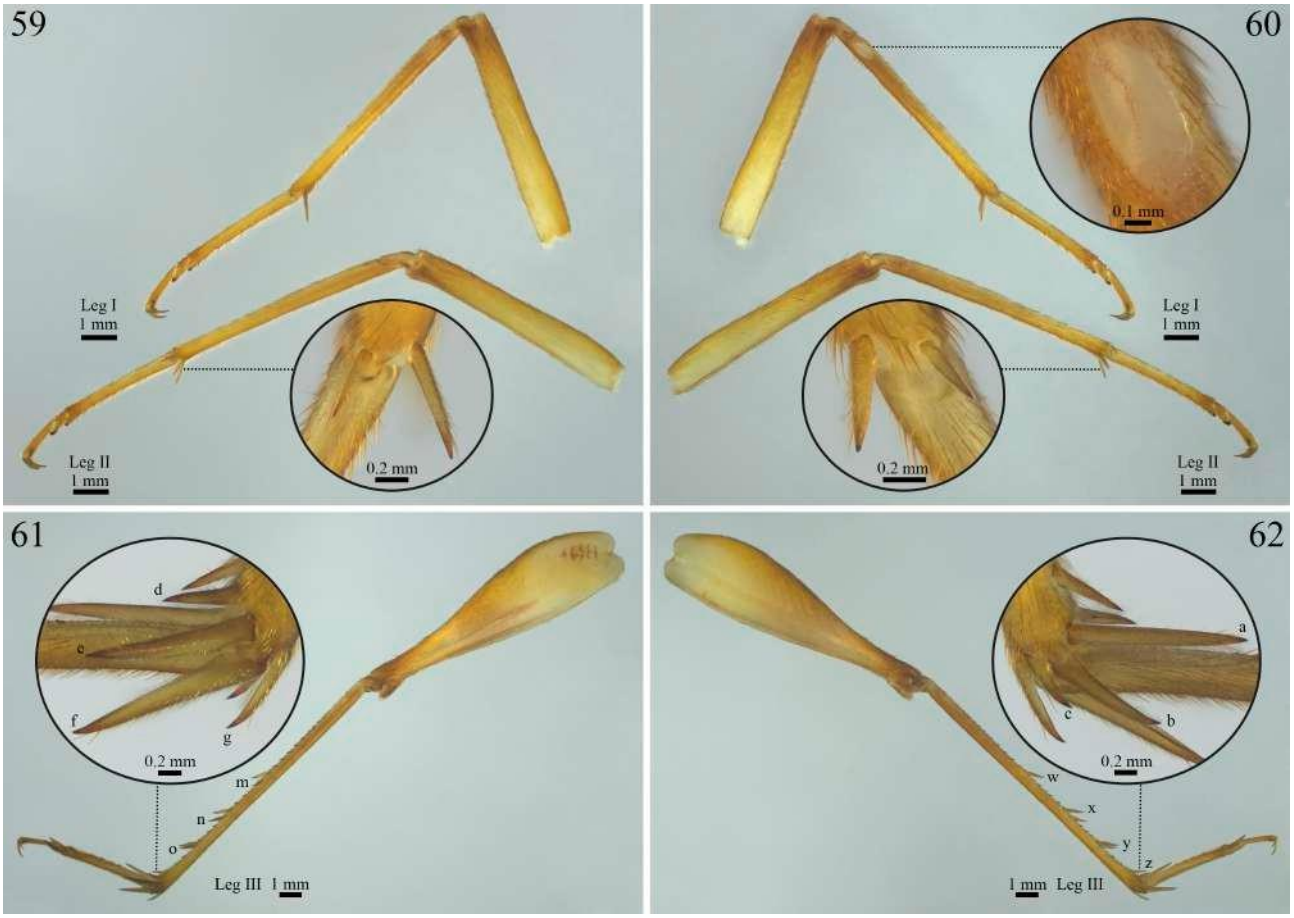
Variations in phallic sclerites (holotype and paratypes, n = 3, ISLA 106137, ISLA 106139, ISLA 106157)— Phallic complexes vary slightly in size and degree of sclerotization; pseudepiphallic arms (Ps.arm) and pseudepiphallic dorsal branches (Ps.db) vary slightly in degree of inclination and sinuosity, pseudepiphallic dorsal branches tips almost touching or slightly distant from one another; pseudepiphallic parameres (Ps.p) ventral portion also nearly touching or far from each other; pseudepiphallic inner bars (Ps.ib) vary slightly in degree of inclination, central portion straight or pointing downwards; ectophallic apodemes (Ect.ap) distal end vary slightly in degree of curvature and sclerotization; ectophallic median projections (Ect.mp) straight or inclined outwards.



FIGURES 44–49. *Endecous* (*Endecous*) *bonito* **n. sp.** (ISLA 106137) phallic complex. (44) dorsal view, (45) ventral view, (46) frontal view, (47) laterofrontal view, (48) highlight of the apex of the pseudepiphallic dorsal branches in frontal view, (49) lateral view. Abbreviations: A, pseudepiphallic ventral branch (or "A" sclerite); Ps.arm, pseudepiphallic arm; Ps.db, pseudepiphallic dorsal branch; Ps.ib, pseudepiphallic inner bars; R, pseudepiphallic rami; Ps.p, pseudepiphallic paramere; Ect.ap, ectophallic apodeme; Ect.arc, ectophallic arc; Ect.lb, ectophallic lateral bar; Ect.mp, ectophallic median projection; End.sc.a, endophallic sclerite anterior portion; End.sc.d, endophallic sclerite duct; End.sc.p, endophallic sclerite posterior portion.



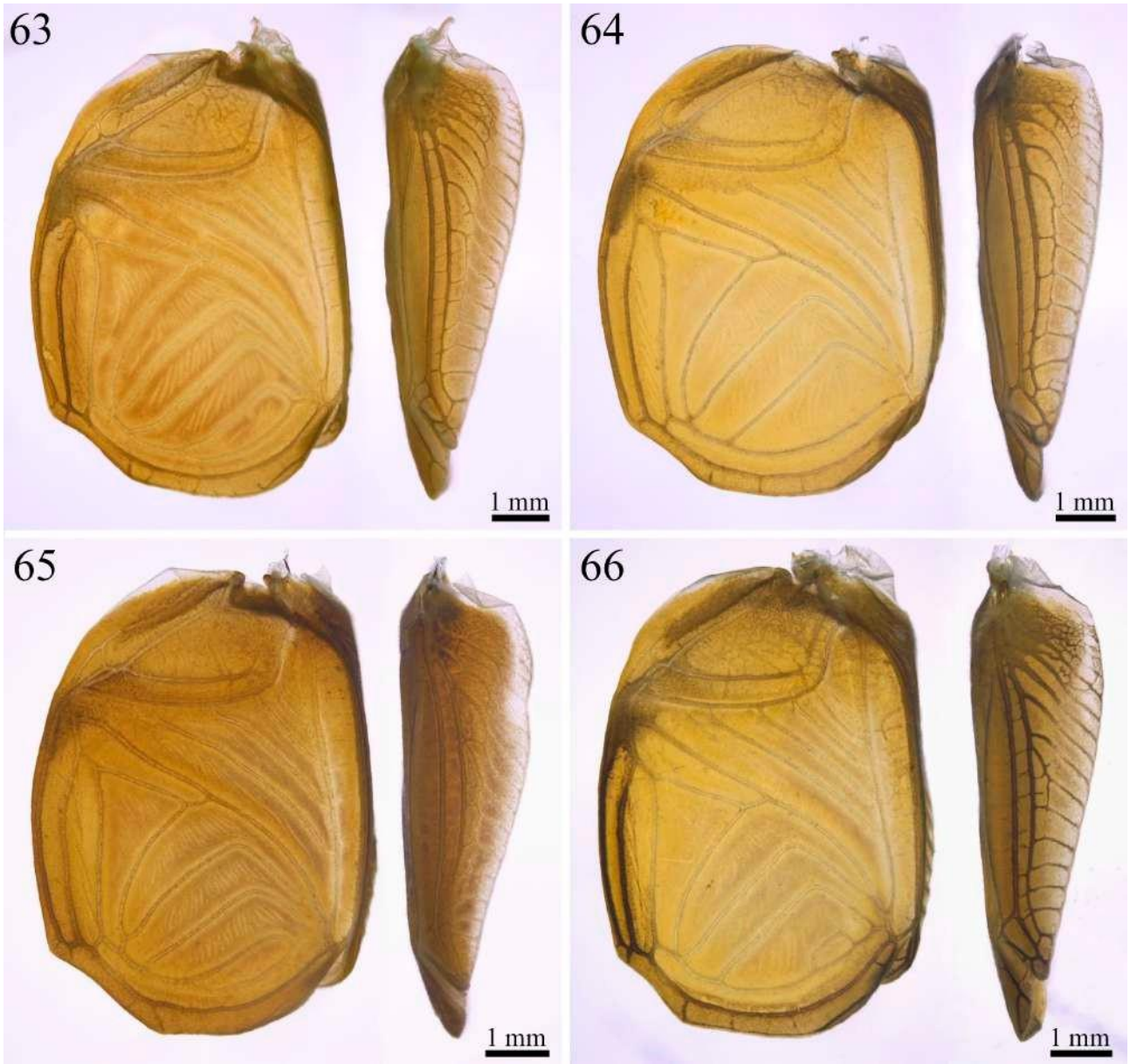
FIGURES 50–58. *Endecous* (*Endecous*) *bonito* **n. sp.** (ISLA 106138) male general morphology. (50) pronotum in dorsal view; (51) right tegmen in dorsal view (52) head in dorsal view; (53) head in frontal view; (54) head and palpi in lateral view, compound eye highlighted; (55) pronotum and tegmen in lateral view; (56) supra-anal and subgenital plates in lateral view; (57) supra-anal plate in dorsal view; (58) subgenital plate in ventral view.



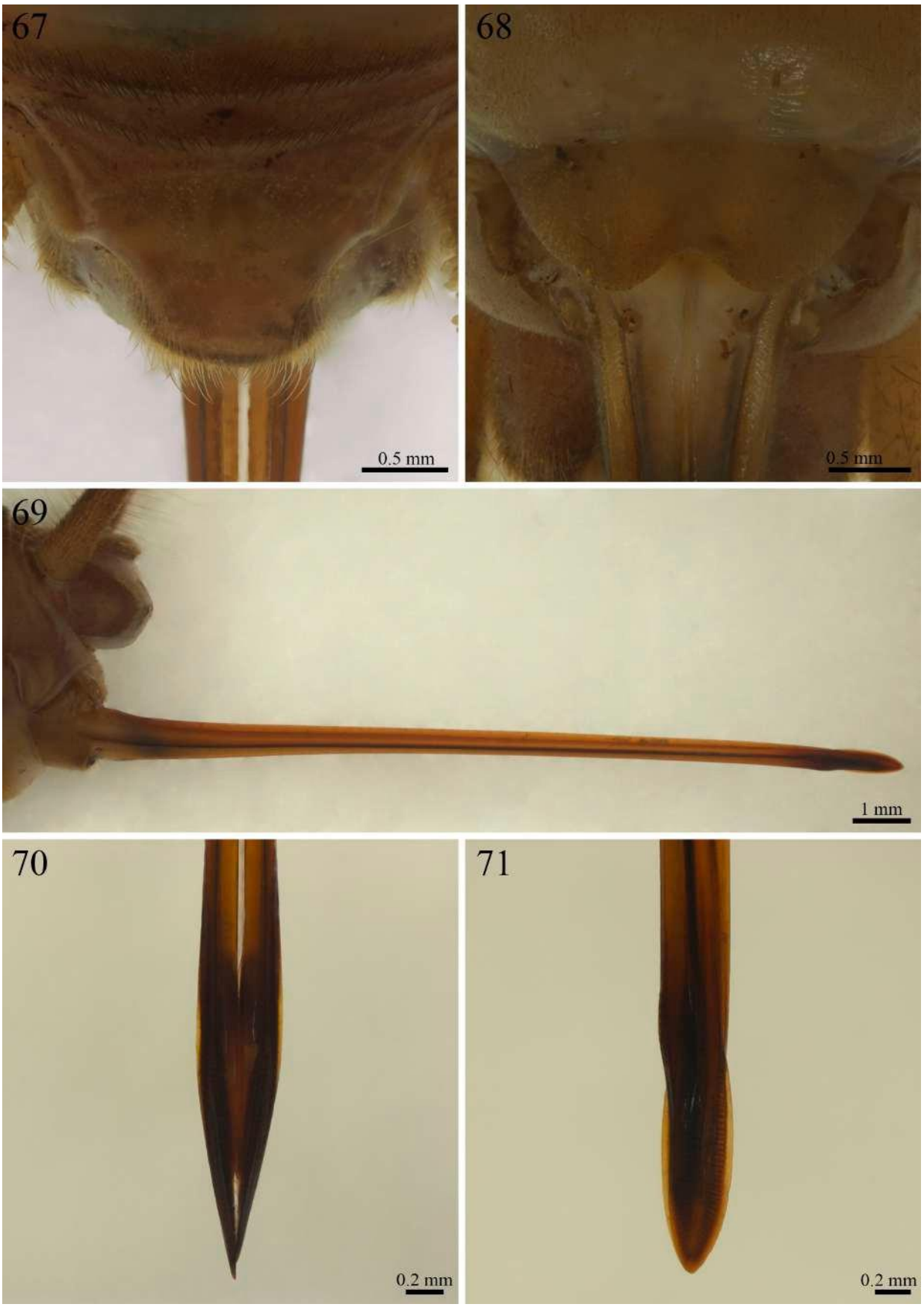
FIGURES 59–62. *Endecous* (*Endecous*) *bonito* **n. sp.** (ISLA 106138) right legs. (59) outer view: leg I and leg II, apical spurs highlighted; (60) inner view: leg I, tympanum highlighted, and leg II, apical spurs highlighted; (61) inner view: leg III, apical spurs highlighted; (62) outer view: leg III, apical spurs highlighted.

Morphology (paratype ISLA 106138, Figs. 50–63)—***Body color***: vertex, scape, pedicel and flagellum dark yellowish brown, vertex with four poorly-marked longitudinal stripes; fastigium dark brown; front and gena varying from light yellow to white; clypeus and labrum almost completely white; mandibles and maxiles yellowish brown, galea and labium light yellow; ommatidia black, with a slightly depigmented area near the base of the antennal scapes (Figs. 52–54); all maxillary and labial palpomeres light yellow, maxillary palpomere V and labial palpomere III whitish at the tip (Figs. 53 and 54); pronotum, tegmina and abdomen brown, pronotum with darker spots, mainly on the posterior margin, last portions of the latter tergites brown (Figs. 50, 51, 55 and 56); supra-anal plate and subgenital plate brown, slightly whitish distally (Figs. 56–58); cerci yellowish brown, darker at first sight due to the presence of setae (Fig. 56); legs yellowish brown, darker near the joints, white at their base (Figs. 59–62). ***Head***: slightly pubescent, elongated in frontal view; fastigium as a short and narrow extension of the vertex, inclined and pointing downwards, with long bristles; mandibles sclerotized at the apex and lateral margins; maxiles sclerotized at the apex; maxillary palpomeres I and II short and same-sized, III–V longer, palpomere V claviform; labial palpomeres I–III increasing in size, palpomere III dilated at the apex; compound eyes reduced and diamond- like in shape, more developed when compared to those of *E. liviae* **n. sp.**, ocelli absent (Figs. 52–54). ***Thorax***: pronotum dorsal disk broader than long (4.76 mm and 3.07 mm in width and length, respectively), pubescent, anterior and posterior margins arched and covered in long bristles, lateral lobes subtriangular in shape and slightly shifted towards the head (Figs. 50 and 55). ***Right tegmen***: slightly sclerotized, more developed when compared to that of *E. liviae* **n. sp.**, covering the first three urotergites (5.59 mm and 7.88 mm in width and length, respectively); *harp* with four crossveins, three complete (one bifurcated); *mirror* subtriangular, distal margin almost rounded, with three arched crossveins, and four cells; *basal field* with a poorly-marked secondary vein connecting Cu2 to 1A vein; *lateral field* with two almost completely parallel longitudinal veins connected by short poorly-marked

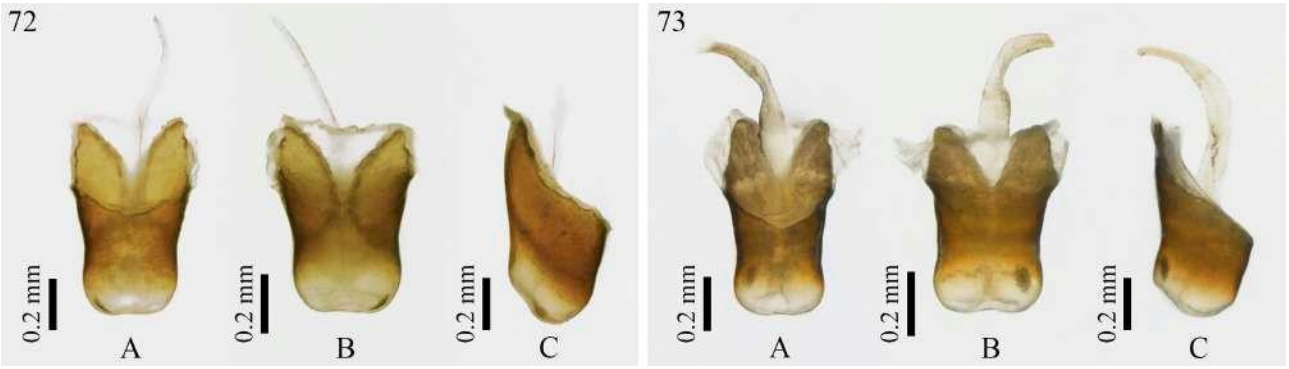
secondary veins, and more than ten anastomotic secondary veins leading to the right margin of the tegmina (Figs. 51, 55 and 63); *stridulatory file* with 72 teeth. ***Abdomen***: cerci pubescent, with long bristles throughout all their extension and globose setae at their base, mostly on the inner side (Figs. 56–58); supra-anal plate as long as the subgenital plate, subtriangular, distal margin rounded and covered in long bristles, lateral projections short and rounded, paraprocts as long as the supra-anal plate (Figs. 56 and 57); subgenital plate proximal margin substraight, distal margin rounded, with a small dent in the center and covered in bristles (Figs. 56–58). ***Legs***: pubescent. *Leg I* (Figs. 59 and 60): tibia with an oval tympanum on its inner side and two ventral apical spurs; tarsomere I ventrally serrated and longer than tarsomeres II and III together. *Leg II* (Figs. 59 and 60): tibia with two ventral apical spurs of equal size and two lateral short spurs, one on each side; tarsomere I ventrally serrated and longer than tarsomeres II and III together. *Leg III* (Figs. 61 and 62): femur developed; tibia longer than the femur (13.70 mm and 12.46 mm, respectively); tibia armed with three subapical spurs on the inner side (Fig. 61; m, n, o), four on the outer side (Fig. 62; w, x, y, z), the most distal one, "z", being the shortest, four apical spurs on the inner side (Fig. 61; d, e, f, g), spurs "e" and "f" longer the "d" and "g", and three on the outer side (Fig. 62; a, b, c), spur "a" being the longest and "c" the shortest; tarsomere I longer than tarsomeres II and III together, ventrally serrated, with two apical spurs, the inner one being the longest.



FIGURES 63–66. *Endecous* (*Endecous*) *bonito* **n. sp.** right tegmina, dorsal and lateral view. (63) paratype, ISLA 106138; (64) paratype, ISLA 106139; (65) paratype, ISLA 106140; (66) paratype, ISLA 106157.



FIGURES 67–71. *Endecous* (*Endecous*) *bonito* **n. sp.** (ISLA 106142) ovipositor. (67) supra-anal plate; (68) subgenital plate; (69) ovipositor, lateral view; (70) ovipositor apex, dorsal view; (71) ovipositor apex, lateral view.



FIGURES 72–73. *Endecous* (*Endecous*) *bonito* **n. sp.** copulatory papillae. (33) allotype, ISLA 106142; (34) paratype, ISLA 106143; A—dorsal view; B—ventral view; C—lateral view.

Variations in right tegmina (paratypes, n = 4, ISLA 106138, ISLA 106139, ISLA 106140, ISLA 106157, Figs. 63–66)—***Stridulatory file*** with 79 ± 4.15 teeth (n = 5, holotype and paratypes). ***Harp*** with three (Fig. 63), four (Figs. 64 and 65) or five (Fig. 66) complete diagonal crossveins, one of them may be bifurcated; incomplete crossveins may be present. ***Mirror*** with two (Fig. 64) or three (Figs. 63, 65 and 66) complete crossveins, the third most distal one may be very short (Fig. 66). ***Basal field*** with many anastomotic, poorly marked secondary veins; 1A, 2A and 3A well-marked. ***Lateral field*** with two parallel longitudinal veins that may or may not be connected through short secondary veins, and ten or more well-marked, sometimes anastomotic, secondary veins branching out of the longitudinal veins and reaching the right margin of the tegmina.

Female morphology (allotype ISLA 106142, Figs. 67–71)—same pattern of body coloration as the male, but with an abdomen slightly darker; bigger than the male (25.63 ± 3.14 mm and 21.54 ± 2.16 mm in length, respectively); apterous; supra-anal plate subtriangular in shape, pubescent, with long bristles covering the distal margin, which is rounded, lateral projections short and rounded (Fig. 67); subgenital plate pubescent, lateral margins angled inwards from the base, distal margin w-shaped (Fig. 68); ovipositor (12.14 mm in length) shorter than the cerci, shaped like a curved sword, with a dorsoventral constriction near the tip, apex tapered, but rounded when compared to that of *E. liviae* **n. sp.** (Figs. 69–71).

Copulatory papilla (allotype ISLA 106142, Fig. 72)—sclerotized and chalice-like; anterior potion broadened, ventral side with a M-shaped extension, making the ventral margin substantially longer than the dorsal margin; posterior portion membranous with a small circular opening on the ventral side.

Ecological remarks—Specimens of *Endecous* (*B.*) *bonito* **n. sp.** were found in two caves located in the municipalities of Bodoquena (Gruta Dona Benedita cave) and Bonito (Gruta São Mateus cave). The observed populations are not notably large, with immature specimens being more readily encountered than adults in all caves where the species is present. As mentioned for *E.* (*E.*) *liviae* **n. sp.**, this species is likely to have a wide distribution in the region, given the distances between the caves where specimens were found and the limited number of caves sampled in this study. It is noteworthy that both *E.* (*E.*) *bonito* **n. sp.** and *E.* (*E.*) *liviae* **n. sp.** can coexist in certain caves, indicating that they likely do not exclude each other through competitive exclusion. Notably, *E.* (*E.*) *bonito* **n. sp.** was observed in a show cave (Gruta São Mateus cave (Figs. 75 and 76), even within the tourist route of the cave (Figs. 77 and 78). This cave attracts numerous visitors, suggesting that this species exhibits considerable tolerance to anthropogenic impacts. Furthermore, the close proximity of this cave in relation to the city of Bonito (Fig. 74) also suggests a certain level of tolerance for anthropogenic conditions exhibited by this species.

Endecous (*Bodoquenaecous*) n. subg.

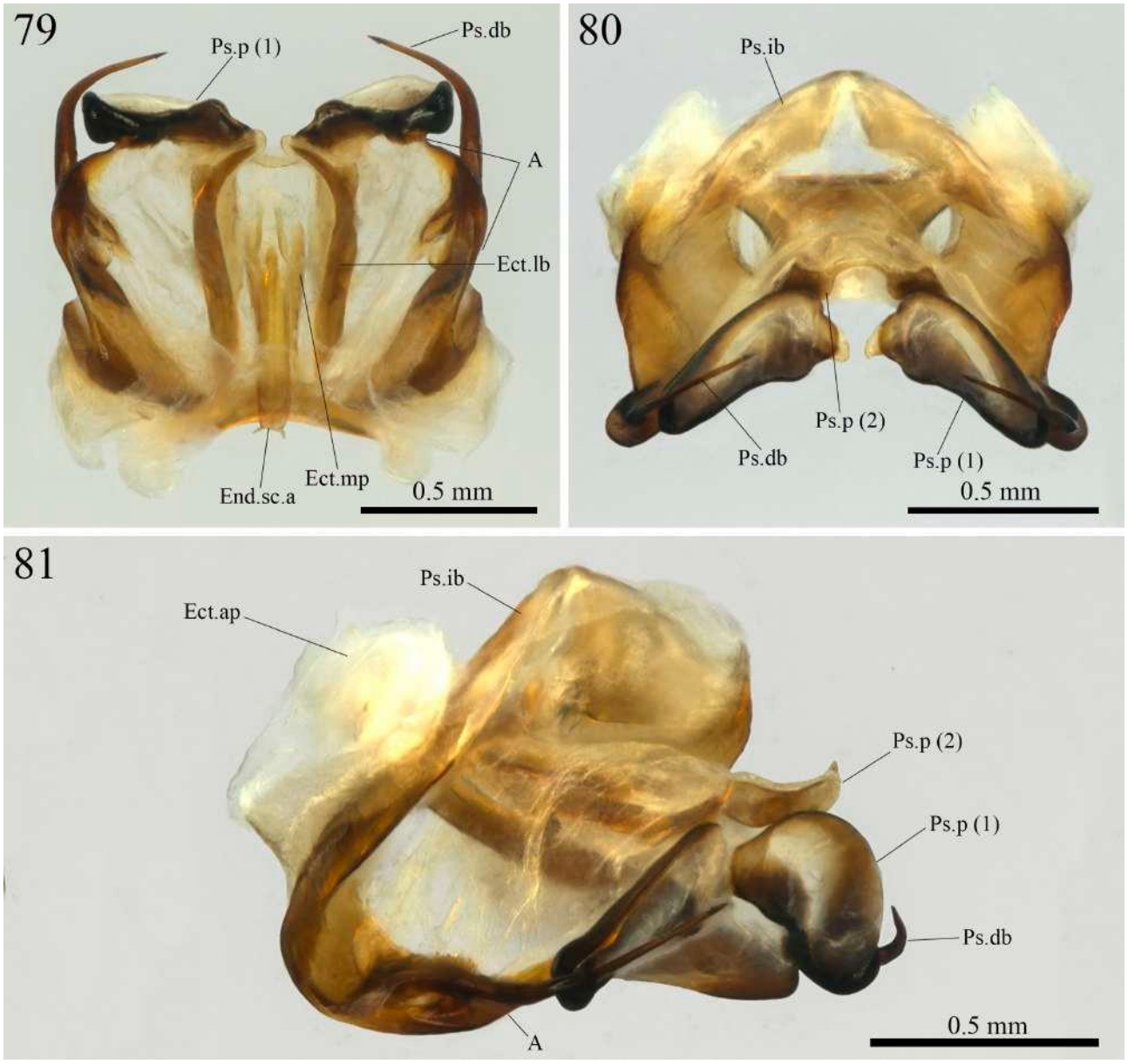
Diagnosis—Combination of the following characteristics: posterior margin of tergites I and II elevated, forming a dorsally projected edge (Fig. 98); pseudepiphallic parameres 1 and 2 not fused, paramere 1 (ventral) laterally oriented (Figs. 79–91, Ps.p).



FIGURES 74–78. *Endecous* (*Endecous*) *bonito* **n. sp.** habitat. (74) Gruta São Mateus cave, external environment; (75) Gruta São Mateus cave, entrance; (76) Gruta São Mateus cave, entrance and internal environment; (77) adult male of *E.* (*E.*) *bonito* **n. sp.**; (78) adult female of *E.* (*E.*) *bonito* **n. sp.** Photo credits: Rodrigo Lopes Ferreira.

Complementary description of *E.* (*B.*) *vitreus* Bolfarini & Campos, 2023
(Figures 79–81, 82–85, 86–91, 92–95, 96–97)

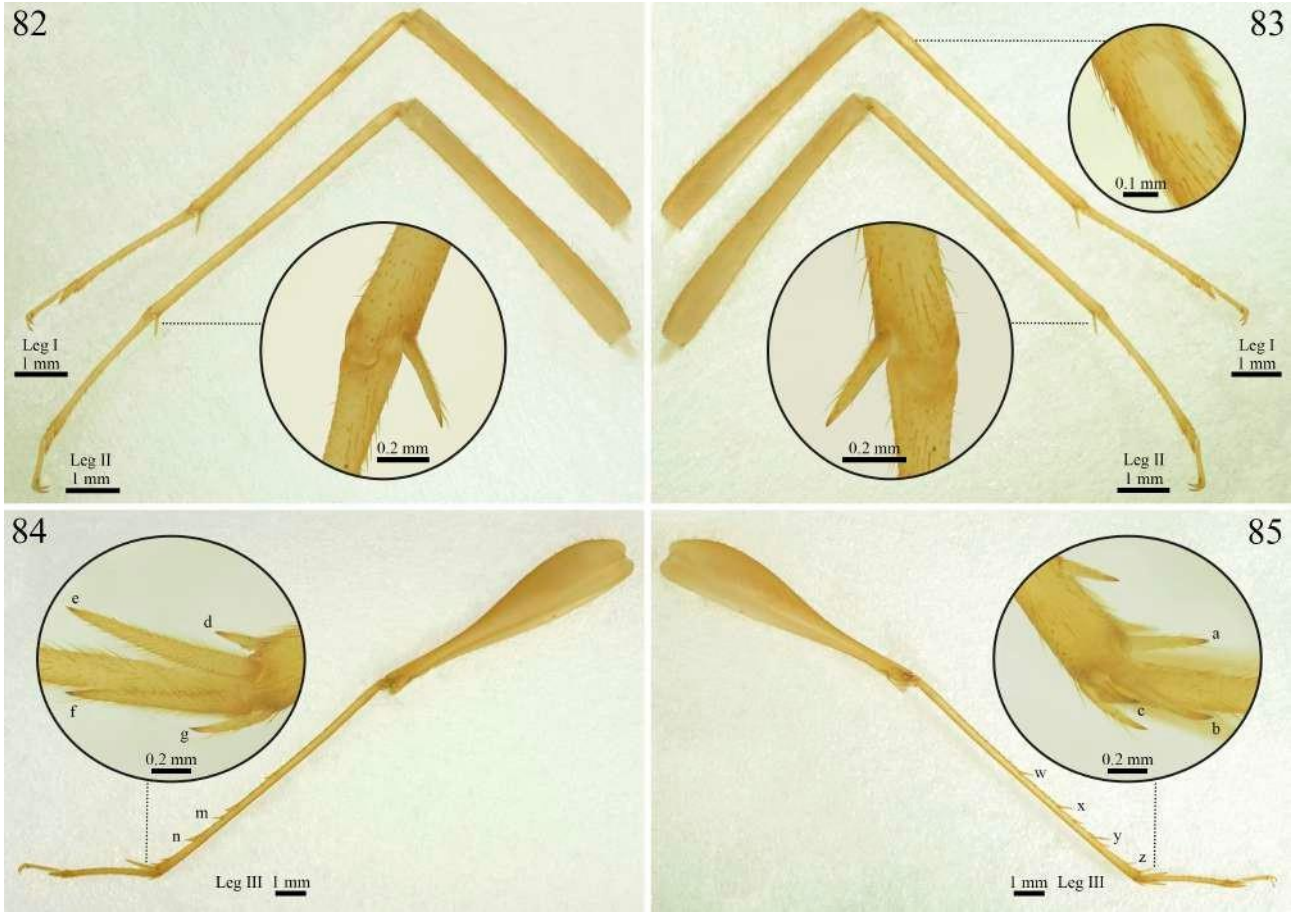
Material examined—*Topotypes*, 8 ♂♂, ISLA 106161, ISLA 106162, ISLA 106163, ISLA 106164, ISLA 106165, ISLA 106166, ISLA 106167, ISLA 106168, 3 ♀♀, ISLA 106169, ISLA 106170, Brazil, Mato Grosso do Sul, Bodoquena municipality, Dente de Cão cave (20°44′47.88″W, 56°47′04.23″S), 11.x.2022, R.L. Ferreira; condition: right tegmen and left legs I, II and III were detached and stored alongside the topotypes, phallic complexes and copulatory papillae were dissected and also stored alongside their respective topotypes.



FIGURES 79–81. *Endecous* (*Bodoquenaecous*) *vitreus* (ISLA 106162) phallic complex. (79) ventral view, (80) frontal view, (81) laterofrontall view. Abbreviations: A, pseudepiphallic ventral branch (or "A" sclerite); Ps.db, pseudepiphallic dorsal branch; Ps.ib, pseudepiphallic inner bars; Ps.p, pseudepiphallic paramere; Ect.ap, ectophallic apodeme; Ect.lb, ectophallic lateral bar; End.sc.a, endophallic sclerite anterior portion.

Male phallic sclerites (topotype ISLA 106162, Figs. 79–81)—***Pseudepiphallus***: dorsal branches elongated, apexes exceptionally acute and harpoon-like (Figs. 79–81, Ps.db); ventral branches sclerotized, elongated and broadened at the base, distal half bending abruptly inwards, reaching the base of the pseudepiphallic parameres 1 (Figs. 79 and 81, A); parameres 1 and 2 not fused, parameres 2 (dorsal) diamond-shaped and dorsally projected,

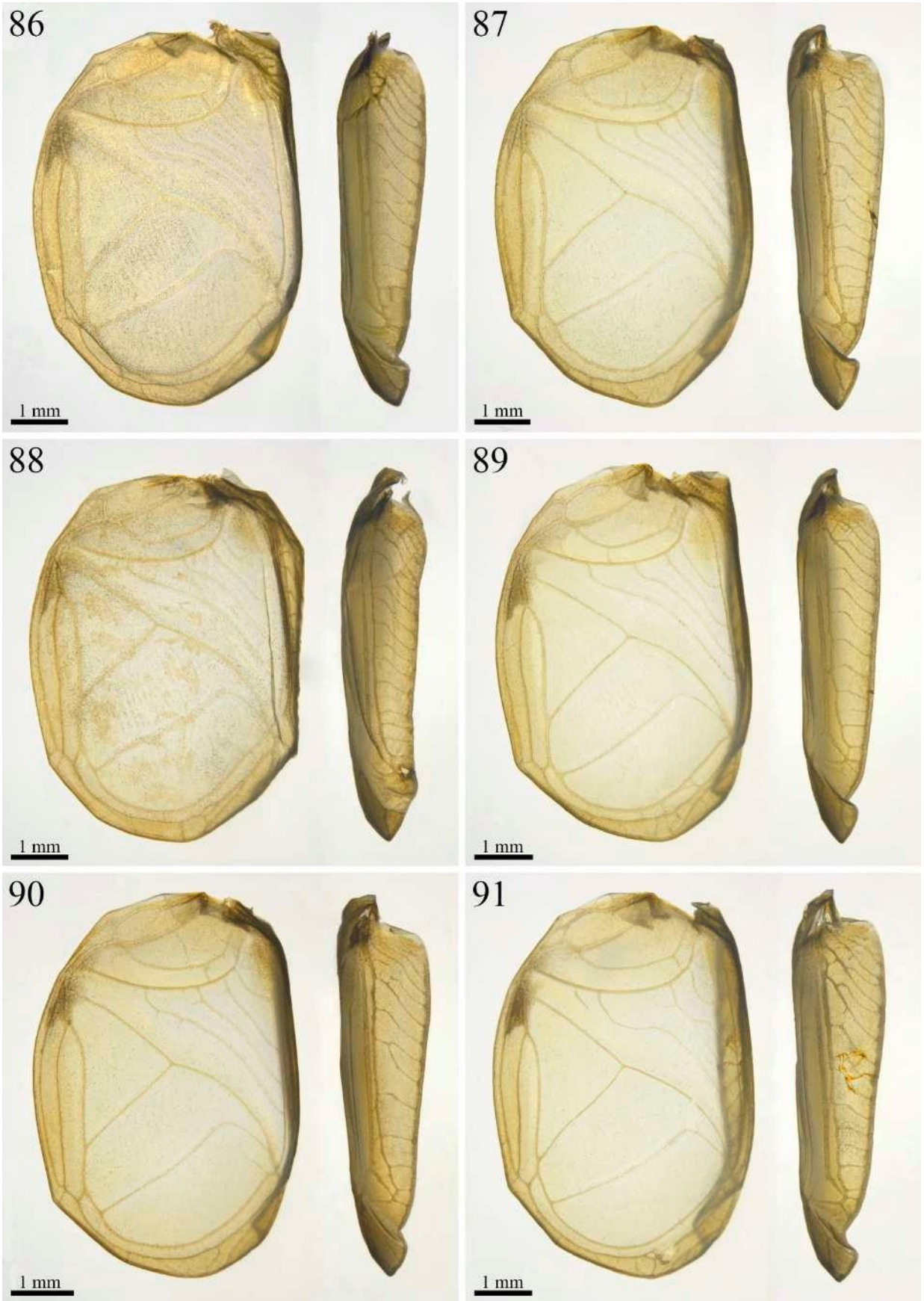
similar to the dorsal portion of *E. bonito* **n. sp.** parameres, pair of parameres 2 connected by a semicircular sclerotized bar, parameres 1 (ventral) laterally oriented (Figs. 79–81, Ps.p). ***Ectophallic invagination***: median projections almost as long as the endophallic sclerite posterior portion, slightly curved outwards, wider in the center when compared to its edges (Ect.mp); lateral bars well-developed, elongated, tapered and curved inwards near the apex, reaching the inner ventral portion of the pseudepiphallic parameres (Fig. 79, Ect.lb). ***Endophallus***: anterior portion well-developed, rectangular and sclerotized, lacking an apodeme opposite to the central groove, distal end with two short, acute and pointing-outwards processes (Fig. 79, End.sc.a).



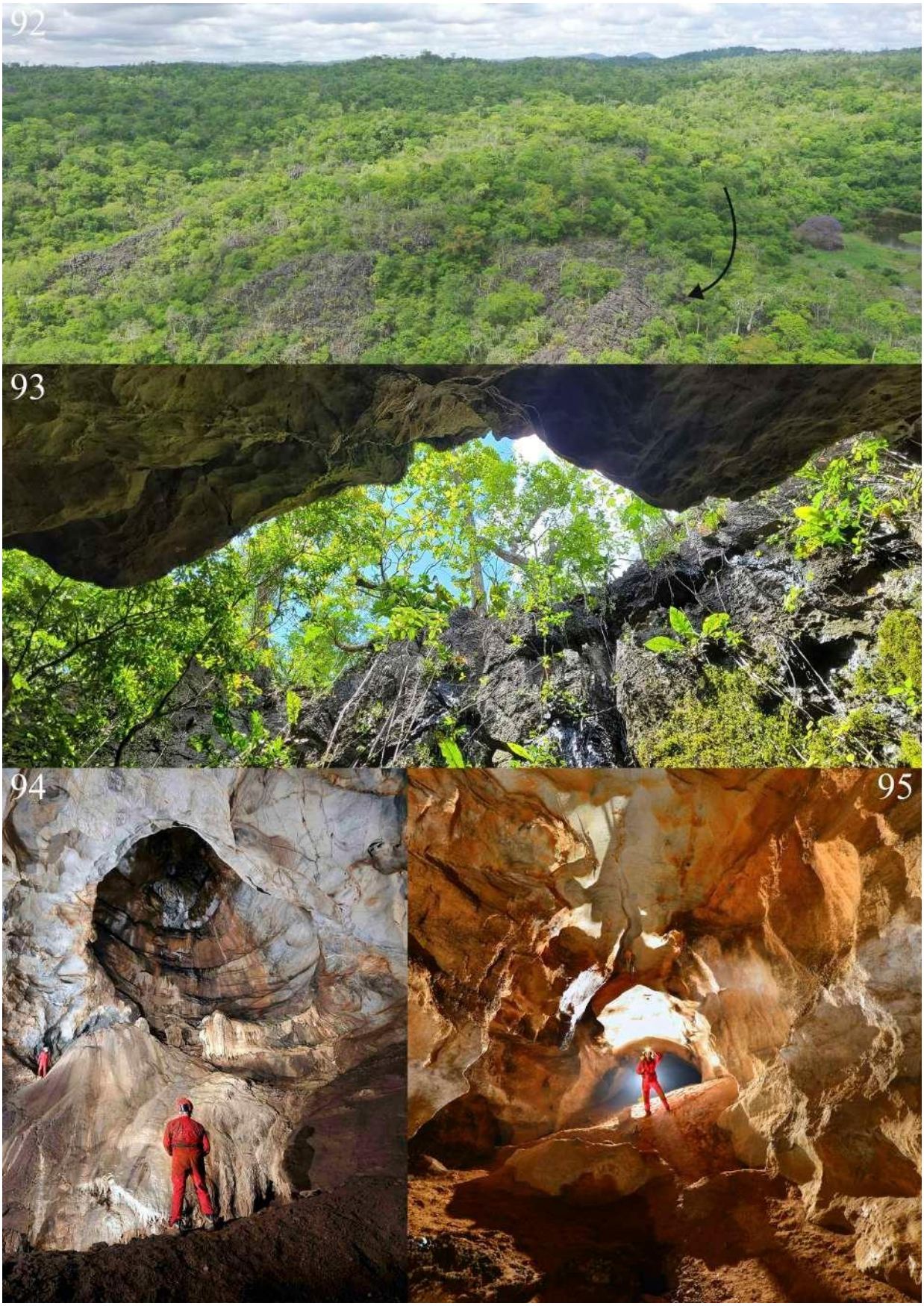
FIGURES 82–85. *Endecous* (*Bodoquenaecous*) *vitreus* (ISLA 106164) right legs. (59) outer view: leg I and leg II, apical spurs highlighted; (60) inner view: leg I, tympanum highlighted,and leg II, apical spurs highlighted; (61) inner view: leg III, apical spurs highlighted; (62) outer view: leg III, apical spurs highlighted.

Variations in phallic sclerites (topotypes, n = 8, ISLA 106161, ISLA 106162, ISLA 106163, ISLA 106164, ISLA 106165, ISLA 106166, ISLA 106167, ISLA 106168)—Phallic complexes vary slightly in size; pseudepiphallic dorsal branches (Ps.db) vary slightly in degree of inclination towards the center of the phallic complex; ectophallic lateral bars (Ect.lb) may have a small, nob-like extension projected outwards.

Variations in leg III morphology (topotypes ISLA 106161, ISLA 106162, ISLA 106163, ISLA 106164, ISLA 106165, ISLA 106166, ISLA 106167, ISLA 106168, ISLA 106169, ISLA 106170, Figs. 82–85)—ISLA 106161, ISLA 106162, ISLA 106163, ISLA 106164, ISLA 106166, ISLA 106167 and ISLA 106168 have only two subapical spurs on the inner side of both right and left legs; ISLA 106165 and ISLA 106169 have two subapical spurs on the inner side of the left leg and three on the inner side of the right leg; ISLA 106170 has three subapical spurs on the inner side of the right leg, left leg missing.



FIGURES 86–91. *Endecous* (*Bodoquenaecous*) *vitreus* right tegmina, dorsal and lateral view. (86) ISLA 106161; (87) ISLA 106162; (88) ISLA 106163; (89) ISLA 106164; (90) ISLA 106166; (91) ISLA 106168.



FIGURES 92–95. *Endecous* (*Bodoquenaecous*) *vitreus* habitat. (92) Dente de Cão cave, external environment; (93) Dente de Cão cave, entrance; (94) Dente de Cão cave, internal environment; (95) Dente de Cão cave, internal environment. Photo credits: (92) and (93) Rodrigo Lopes Ferreira; (94) Victor Ferrer; (95) Ataliba Coelho.





FIGURES 96–97. *Endecous* (*Bodoquenaecous*) *vitreus*. (96) adult male of *E.* (*B.*) *vitreus*, Dente de Cão cave; (97) adult female of *E.* (*B.*) *vitreus*, Dente de Cão cave. Photo credits: Rodrigo Lopes Ferreira.

Variations in right tegmen (topotypes, n = 6, ISLA 106161, ISLA 106162, ISLA 106163, ISLA 106164, ISLA 106166, ISLA 106168, Figs. 86–91)—***Stridulatory file*** with 178 ± 11.20 teeth (n = 8, topotypes). ***Harp*** outline conserved; with three (Fig. 91), four (Figs. 88–90) or five (Figs. 86 and 87) complete and diagonal crossveins, one of them might bifurcate (Fig. 91), a short and incomplete crossvein may be present (Fig. 86). ***Mirror*** outline conserved; always with one arched and complete crossvein. ***Basal field*** with one (Figs. 86, 88, 90 and 91), two (Fig. 87) or three (Fig. 89) secondary veins branching out of 1A vein and reaching Cu2; 1A and 3A veins converging to 2A roughly at the same point. ***Lateral field*** with two parallel longitudinal veins that may or may not be connected through short secondary veins; 11 to 14 secondary veins branching out and reaching the right margin of the tegmina.

Ecological remarks (Figs. 92–97)—The original description of *Endecous* (*Bodoquenaecous*) *vitreus* reported its occurrence in two caves, namely Dente de Cão and Urubu Rei caves, located in the municipality of Bodoquena, central western Mato Grosso do Sul state, Brazil. while Campos *et al.* (2023) provided some details regarding the species distribution, certain information in the description is inaccurate. For instance, the authors claimed that Dente de Cão cave lacks any connections with the surface. However, it should be noted that this cave actually has two small entrances, both associated with a crevice in the limestone massif (Figs. 92 and 93). These entrances are closely located to each other, and conduits from them lead to distinct levels within the cave. In this regard, we aim to provide additional information regarding the species distribution within Dente de Cão cave. It is crucial to emphasize that any details regarding the species' habitat, as presented in its description, can hold significant importance for conservation purposes. Particularly for species restricted to caves, such information will undoubtedly prove valuable in the assessment of extinction risk. Therefore, it is advisable to consistently include information on the habitat, ecology, conservation, or any relevant aspects of a species´ biology alongside its description.

Specimens of *E.* (*B.*) *vitreus* were observed in areas ranging from the cave entrances to the deeper regions of the cave. It is important to note that the cave entrances are small, resulting in a significant isolation from the external environment even in the proximity zones. In the areas closer to the entrances, specimens were more readily found compared to the deeper sections of the cave. This pattern is likely influenced by the accumulation of organic matter, such as vegetal debris and roots, which serve as potential food resources for the crickets and other detritivores. To access the inner portions of the cave, descent to the lower levels is required. Although water enters the cave during rainy periods, the irregular topography of the conduits in the lower level hampers the transport of organic matter to areas distant from the entrances. As a result, the majority of the cave exhibits oligotrophic conditions (Figs. 94 and 95). Close to the entrances, specimens of *E.* (*B.*) *vitreus* were predominantly observed on the cave walls, while in deeper regions, they were mostly found on the cave floor, albeit at much lower densities. These behavioral differences between the two cave zones may be attributable to a higher abundance of predators on the cave floor near the entrances compared to the deeper portions of the cave. However, further studies are required to verify this hypothesis. Lastly, it is worth noting that the photographs of living specimens presented in the original description, particularly those of male, appear to have been altered and appear lighter than their natural state. Living specimens, despite displaying weak pigmentation, are not as shiny as depicted in the original description (Figs. 96 and 97).

Pictorial key for *Endecous* subgenera (Fig. 98)

Gorochov (2014), using his terminology, proposed a dichotomous key that divided the genus *Endecous* into three subgenera (*Endecous, Pedroecous*, and *Notendecous*). However, due to the current terminology which has been used in most recent descriptions of *Endecous* (based on Desutter (1987, 1998) and Desutter-Grandcolas (2003)), we herein propose the first pictorial key for the subgenera of *Endecous*. Additionally, we introduce a new subgenus, *Endecous* (*Bodoquenaecous*), highlighting novel and important morphological characteristics for future studies.

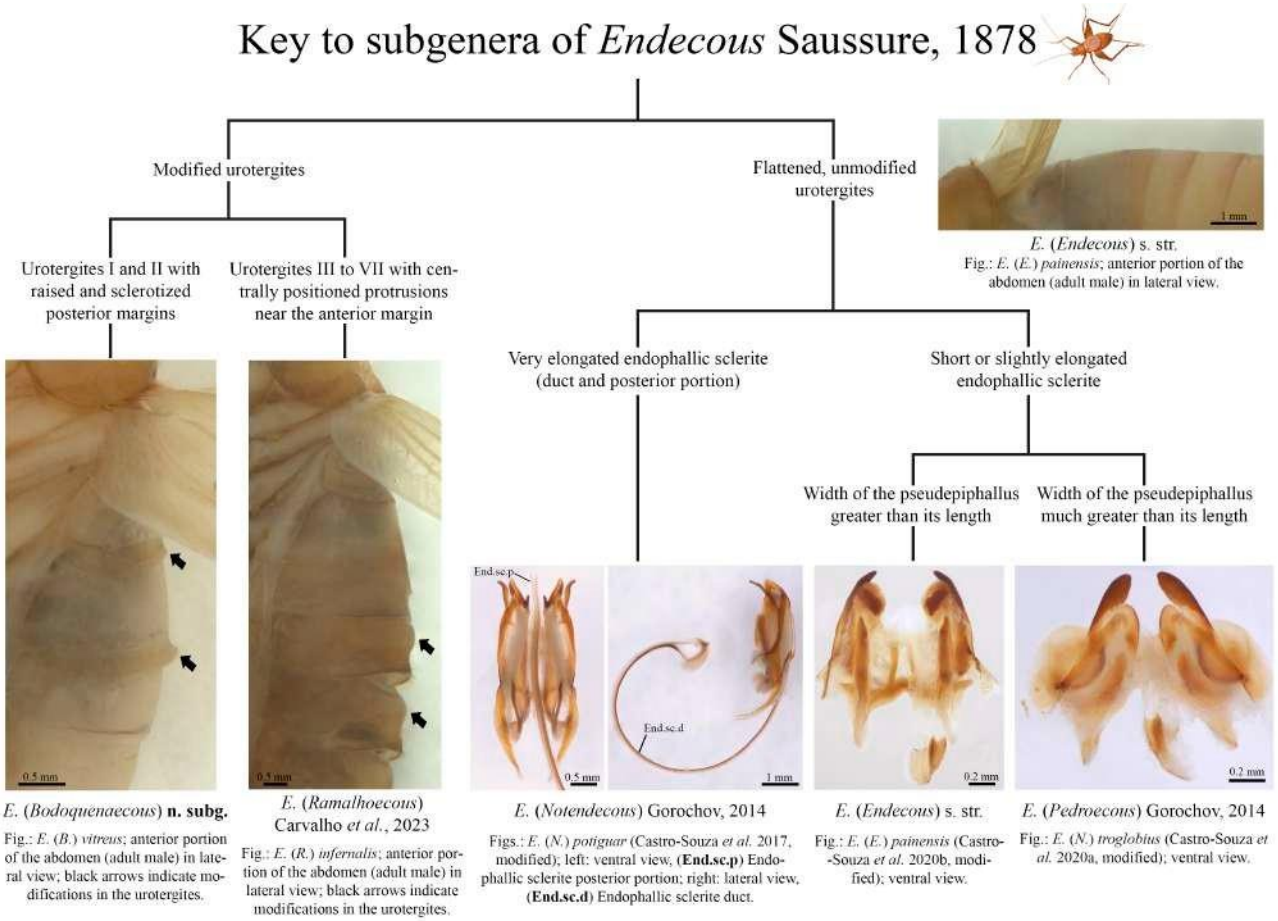


FIGURE 98. Pictorial key to subgenera of *Endecous* Saussure, 1878.

Discussion

Phallic complex comparisons

The genus *Endecous* exhibits a wide distribution and considerable diversity, encompassing species belonging to different subgenera. Therefore, it is pertinent to compare the newly described species with others within the same subgenus, *Endecous* (*Endecous*), in order to emphasize their distinctive characteristics as well as any similarities they may share.

The phallic complex of *E.* (*E.*) *liviae* **n. sp.** is dorsoventrally flattened, somewhat similar to the genitalia of *E.* (*E.*) *arachnopsis* Saussure, 1878. It is also elongated, just like the phallic complexes of *E.* (*E.*) *arachnopsis*, *E.* (*E.*) *betariensis* and *E.* (*E.*) *hubbelli* Liebermann, 1965. Its pseudepiphallic dorsal branches bend inwards, as seen in *E.* (*E.*) *arachnopsis*, *E.* (*E.*) *hubbelli* and *E.* (*E.*) *zaum*. However, their apexes are tapered and more acute, resembling those of *E.* (*E.*) *aguassay* Mews & Sperber, 2008, *E.* (*E.*) *alejomesai* and *E.* (*E.*) *zin*. It is worth mentioning the ectophallic arch of *E.* (*E.*) *liviae* **n. sp.**, which is characterized by a conical shape similar to that of *E.* (*E.*) *arachnopsis*. Furthermore, the endophallic sclerite duct of this new species is elongated, akin to that of *E.* (*E.*) *hubbelli*. The endophallic anterior portion is well-developed, featuring a large crest, larger than that found in *E.* (*E.*) *painensis*, *E.* (*E.*) *zin* and *E.* (*E.*) *zaum*, and similar to that of *E.* (*E.*) *bonito* **n. sp.**

The genitalia of *E.* (*E.*) *bonito* **n. sp.** are very similar to those of *E.* (*E.*) *naipi* Souza-Dias *et al.*, 2017. However, some differences can be observed. The pseudepiphallic dorsal branches of *E.* (*E.*) *bonito* **n. sp.** bend inwards and their outer margin has a rounded contour, whereas in *E.* (*E.*) *naipi*, the outer margin has an almost rectangular contour. Additionally, the inner side of the tip of the dorsal branches in *E.* (*E.*) *bonito* **n. sp.** has many setae, a feature that was not mentioned in the description of *E.* (*E.*) *naipi*. The ventral portion of the pseudepiphallic parameres in

E. (*E.*) *naipi* is broadened near the proximal end, whereas in *E*. (*E.*) *bonito* **n. sp.**, the proximal end of the ventral portion of the parameres is tapered and acute. The ectophallic apodemes of *E*. (*E.*) *bonito* **n. sp.** are more elongated and sinuous than those of *E*. (*E.*) *naipi*. The ectophallic median projections of the new species are straight or inclined outwards. The median projections of *E*. (*E.*) *naipi*, on the other hand, are inclined inwards and almost touch at the apex.

It is crucial to acknowledge, however, that the photos provided in the description of *E*. (*E.*) *naipi* are of low quality, and the genitalia seems to be deformed (Fig. 5, A–E, in Souza-Dias *et al*. 2017). These factors pose challenges and undermine the reliability of comparisons. Moreover, it is essential to take into account the substantial geographical distance between the type localities of the two species, which amounts to approximately 650 km, as well as the presence of geographical barriers like the Paraná River. These factors should be considered when evaluating the hypothesis that the two species, *E*. (*E.*) *bonito* **n. sp.** and *E*. (*E.*) *naipi*, are indeed distinct taxa.

E. vitreus, a troglobitic species, was recently described for the Serra da Bodoquena region, where *E*. (*E.*) *liviae* **n. sp.** and *E*. (*E.*) *bonito* **n. sp.** are also found. It is important to note that, although *E. vitreus* has been previously assigned to the subgenus *Endecous*, in this study, we have established a new subgenus to accommodate this species, which exhibits distinctive characteristics in its genitalia that set it apart from the other two species described in this study, as expected considering it belongs to a different subgenus. These distinguishing characteristics include parameres 1 and 2 not been fused, as well as laterally oriented parameres 1.

Troglomorphic traits in *Endecous* species

In recent years, several species of *Endecous* have been described, and some of them have been designated as troglobitic. However, it is crucial to undertake a critical evaluation of the troglomorphic traits described by different authors, as these traits may not always indicate genuine adaptations to cave environments. Therefore, caution should be exercised when attributing these characteristics as true troglomorphisms.

In comparison to other *Endecous* species, most of which are troglophilic, *E*. (*B.*) *vitreus* exhibits significantly reduced eyes and pigmentation, as well as elongated appendages. Similar characteristics can be observed in *E*. (*R.*) *infernalis* and *E*. (*P.*) *troglobius*, with the latter species being primarily characterized by the absence of pigmentation in both the integument and ommatidia. On the other hand, other *Endecous* species previously considered as troglobitic, such as *E*. (*P.*) *apterus* and *E*. (*E.*) *peruassuensis*, possess fewer regressive morphological traits (if any) compared to the species described herein.

It is important to note that *E*. (*P.*) *apterus*, which Souza-Dias *et al.* (2014) classified as a troglobitic species primarily based on the absence of tegmina, does not exhibit any other obvious troglomorphic traits. Therefore, tegmina reduction should not be considered a troglomorphic trait for this genus (or even the family), as suggested before, considering that other troglobitic species do not display such a condition (Castro-Souza *et al.*, 2020; Junta *et al.* 2020; de Mello & Ferreira 2021; Carvalho *et al.* 2023). As examples, several Phalangopsidae species from epigean habitats also exhibit reduced wings, such as *Eidmanacris suassunai* Souza-Dias *et al.*, 2015 and *Ottedana cercalis* de Mello & de Andrade, 2003, or are completely wingless, as seen in *Laranda uai* Mews *et al.*, 2008 (de Mello & de Andrade 2003; Mews *et al.* 2008; Souza-Dias *et al.* 2015; Castro-Souza *et al.* 2020a). Supporting this notion, *E*. (*B.*) *vitreus* has tegmina that practically cover the entire abdomen, which is uncommon for the genus. Thus, despite having several "classic" troglomorphic features such as eye and pigment reduction and elongated appendages, the tegmina of this species are among the largest within the genus, affirming that wing size is not indicative of troglomorphism in this genus.

Furthermore, it is crucial to take into account the extensive distribution of both *E*. (*P.*) *apterus* and *E*. (*E.*) *peruassuensis* when diagnosing these species, as their current distribution does not strongly support their troglobitic status. Populations of both species are found in caves located in fragmented outcrops within their respective occurrence areas, indicating limited opportunities for dispersal through subterranean voids. Additionally, comprehensive systematic surveys for invertebrates in the areas where these species are found are lacking, leaving open the possibility that they may also exist in external habitats.

For environmental licensing in Brazil, caves are classified based on their degree of relevance, and only those deemed highly relevant are afforded protection (Ferreira *et al.* 2022). Among the criteria used to determine a cave's relevance is the presence of troglobitic species. However, the inclusion of epigean species in the troglobitic category,

either mistakenly or without sufficient evidence, can undermine one of the primary tools for cave protection in Brazil. Addressing a non-troglobitic species as troglobitic creates a false impression that these species are not as endemic, rare, or specialized as previously believed. Such misconceptions can have detrimental effects on cave conservation efforts over time. This may provide a justification for increasing flexibility in environmental legislation. Therefore, it is crucial to ensure accurate diagnoses and classifications for the purpose of cave conservation, as misconceptions can lead to long-term negative consequences (Ferreira *et al.* 2023).

Accordingly, we here advocate that both *E.* (*P.*) *apterus* and *E.* (*E.*) *peruassuensis* should be reclassified as troglophilic species, rather than troglobitic. Our extensive observations provide evidence that these species exhibit ecological traits and behaviors that are more aligned with troglophilic organisms. Therefore, it is imperative to revise their taxonomic classification to accurately reflect their biological adaptations and affinity for cave habitats.

Conservation

The caves in both Bodoquena and Bonito municipalities are primarily visited by speleologists, although there are some show caves that attract a significant number of tourists annually. Regarding *E.* (*E.*) *bonito* **sp. n.** and *E.* (*E.*) *liviae* **sp. n.**, which are troglophilic species with a widespread distribution throughout the caves in the area, their conservation status is currently of low concern. This is mainly because caves are not their exclusive habitat, although they can play a crucial role in maintaining the species over time. However, it is essential to acknowledge that mining activities and deforestation pose potential impacts that could influence both species in the future. Fortunately, the National Park of Bodoquena currently ensures the preservation of numerous caves as well as the surrounding forests.

A more significant concern arises when considering *E.* (*B.*) *vitreus*, which is troglobitic and restricted to only two caves. Fortunately, these caves are visited only sporadically by speleologists. However, even these infrequent surveys can lead to disturbances, such as trampling on distinct sediments. Nevertheless, these alterations seem to be negligible given the extensive size of the caves, particularly in the case of Dente de Cão cave. It is crucial to emphasize that despite being the largest known cave in the Serra da Bodoquena area, the Dente de Cão cave is not recommended for any tourist activities. The complex topography and the presence of diverse troglomorphic fauna, including an onychophoran species and various arthropods such as spiders, harvestmen, and millipedes (Cordeiro *et al.* 2014), highlight the need for strict protection of this cave. Such measures are essential to preserve not only its geological heritage but also the unique and cave-restricted fauna it shelters.

Lastly, despite the current relatively low level of concern regarding conservation issues related to *Endecous* species in the Bodoquena karst area, recent models predicting the future distribution of this genus have raised significant concerns (Castro-Souza *et al.* 2023). Using species distribution modeling techniques, these authors have forecasted the biogeographic history of *Endecous* crickets to identify potential long-term environmental refuges for these species in South America. The predictions were based on paleoclimate scenarios, the current climate scenario, and a future global warming climate scenario (RCP8.5, 2080–2100). The future projections indicate a dramatic reduction in the spatial distribution of *Endecous* species, with an increased risk of isolation within subterranean ecosystems. Of particular concern is the potential disappearance of external suitable habitats for *Endecous* species in the near future in the Bodoquena region, leaving caves as the only refuge for all *Endecous* species in the area. In this scenario, coupled with the escalating deforestation in the region, it is likely that populations of all three species will become fragmented. Since no genetic studies have been conducted on these species, any interruption in gene flow may have detrimental consequences for their long-term survival.

Acknowledgements

The authors would like to thank the Centro Nacional de Pesquisa e Conservação de Cavernas—CECAV and Instituto Brasileiro de Desenvolvimento e Sustentabilidade—IABS (n°. 006/2021. TCCE ICMBio/Vale (01/2018) for the financial support and scholarship provided to PHMC; CNPq (National Council for Scientific and Technological Development) for the productivity scholarship provided to RLF (CNPq n. 302925/2022-8) and the team from the Center of Studies in Subterranean Biology (CEBS/UFLA) for the support in the field trips. we are also thankful to Livia Medeiros Cordeiro for her invaluable support during our expedition to the caves in the Serra da Bodoquena

region. Finally, we would like to express our gratitude to the photographers Victor Ferrer, Phillipe Crochet, and Ataliba Coelho for generously providing the photographs of the caves where the species described in this study were discovered. These photographs were captured as part of a significant project called “Luzes na Escuridão” (Lights in the Darkness), which involved several photographers from different countries united with the common objective of documenting important Brazilian caves.

References

Acosta, R.C., Timm, V.F., Szinwelski, N., da Costa, M.K.M. & Zefa, E. (2020) Mating behavior and acoustic communication of the long-legged cricket *Endecous* (*Notendecous*) *onthophagus* (Berg, 1891) from Southern Brazil (Orthoptera: Grylloidea: Phalangopsidae). *Zootaxa*, 4743 (3), 427–437.
https://doi.org/10.11646/zootaxa.4743.3.10

Álvarez-Padilla, F. & Hormiga, G. (2007) A protocol for digesting internal soft tissues and mounting spiders for scanning electron microscopy. *The Journal of Arachnology*, 35 (3), 538–542.
https://doi.org/10.1636/Sh06-55.1

Assine, M.A. & Soares, P.C. (2004) Quaternary of the Pantanal, west-central Brazil. *Quaternary International*, 114, 23–34.
https://doi.org/10.1016/S1040-6182(03)00039-9

Bolfarini, M.P. & Bichuette, M.E. (2015) *Endecous peruassuensis* n. sp**.** (Orthoptera: Grylloidea: Phalangopsidae) from caves of Eastern Brazil: evidence of isolation in the subterranean realm and discussion about troglomorphisms. *Zootaxa*, 4032 (3), 297–308.
https://doi.org/10.11646/zootaxa.4032.3.5

Carvalho, P.H.M., Junta, V.G.P., Castro-Souza, R.A. & Ferreira, R.L. (2023) Three new cricket species and a new subgenus of *Endecous* Saussure, 1878 (Grylloidea: Phalangopsidae) from caves in northeastern Brazil. *Zootaxa*, 5263 (1), 1–39.
https://doi.org/10.11646/zootaxa.5263.1.1

Castro-Souza, R.A., Zefa, E. & Ferreira, R.L. (2020a) New troglobitic and troglophilic syntopic species of *Endecous* (Orthoptera, Grylloidea, Phalangopsidae) from a Brazilian cave: a case of sympatric speciation?. *Zootaxa*, 4810 (2), 271–304.
https://doi.org/10.11646/zootaxa.4810.2.3

Castro-Souza, R.A., Junta, V.G.P. & Ferreira, R.L. (2020b) Description and ecology of a new species of the cricket genus *Endecous* (Orthoptera: Grylloidea: Phalangopsidae) in the speleological province of Arcos-Pains-Doresópolis, Southeastern Brazil. *Zootaxa*, 4821 (2), 305–332.
https://doi.org/10.11646/zootaxa.4821.2.4

Castro-Souza, R.A., Zefa, E. & Ferreira, R.L. (2017) Two new species of cave crickets *Endecous (Notoendecous*) Gorochov, 2014 (Orthoptera: Grylloidea: Phalangopsidae) from northeastern Brazil. *Zootaxa*, 4318 (3), 474–498.
https://doi.org/10.11646/zootaxa.4318.3.3

Castro-Souza, R.A., Sobral-Souza, T., Rabelo, L.M., Zefa, E. & Ferreira, R.L. (2023) Persisting while changing over time: modelling the historical biogeographic of cave crickets (Orthoptera, Grylloidea) in Neotropics. *Journal of Tropical Ecology*, 39, 310.
https://doi.org/10.1017/S0266467422000529

Christiansen, K. (1962) Proposition pour la classification des animaux cavernicoles. *Spelunca*, 2, 75–78.

Cigliano, M.M., Braun, H., Eades, D.C. & Otte, D. (2023) Orthoptera Species File. Version 5.0/5.0. Available from: http://Orthoptera.SpeciesFile.org (accessed 30 June 2023)

Cordeiro, L.M., Borghezan, R. & Trajano, E. (2014) Subterranean biodiversity in the Serra da Bodoquena karst area, Paraguay river basin, Mato Grosso do Sul, Southwestern Brazil. *Biota Neotropica*, 14 (3), 01–28.
https://doi.org/10.1590/1676-06032014011414

de Campos, L.D., Bolfarini, M.P., Suemitsu, M.M., Borghezan, L.M.C. & Souza-Dias, P.G. (2023) Living in the darkness: a new cave cricket species of the genus *Endecous* Saussure (Orthoptera, Grylloidea, Phalangopsidae) from Serra da Bodoquena in Mato Grosso do Sul state, Brazil. *Zootaxa*, 5285 (2), 325–336.
https://doi.org/10.11646/zootaxa.5285.2.6

Desutter, L. (1987) Structure et évolution du complexe phallique des Gryllidea (Orthoptera) et classification des genres Nétropicaux de Grylloidea, Première Partie. *Annales de la Société Entomolologique de France*, 23 (3), 213–239.
https://doi.org/10.1080/21686351.1987.12278443

Desutter-Grandcolas, L. (1998) II—faune souterraine II. 4—Insecta, 56—Ortóptera, B—Grylloidea. *In*: Juberthie, C. & Decu, V. (Eds.), *Encyclopaedia Biospeologica*. *V. Tome II*. Société de Biospéologie, Moulis, pp. 989–1001.

Desutter-Grandcolas, L. (2003) Phylogeny and the evolution of acoustic communication in extant Ensifera (Insecta, Orthoptera). *Zoologica Scripta*, 32, 525–561.
https://doi.org/10.1046/j.1463-6409.2003.00142.x

Ferreira, R.L., Bernard, E., da Cruz Júnior, F.w., Piló, L.B., Calux, A., Souza-Silva, M. & Frick, w.F. (2022) Brazilian cave heritage under siege. *Science*, 375 (6586), 1238–1239.
https://doi.org/10.1126/science.abo1973

Ferreira, R.L., Souza-Silva, M. & Zampaulo, R.A. (2023) Cave-dwelling gastropods (Mollusca: Gastropoda) of Brazil, state of the art and conservation: a critical review. *Zoologia* (*Curitiba*), 40, e22057.
https://doi.org/10.1590/S1984-4689.v40.e22057
Gorochov, A.V. (2014) Classification of the Phalangopsinae subfamily group, and new taxa from the subfamilies Phalangopsinae and Phaloriinae (Orthoptera: Gryllidae). *Zoosystematica Rossica*, 23 (1), 7–88.
https://doi.org/10.31610/zsr/2014.23.1.7
Junta, V.G.P., Castro-Souza, R.A. & Ferreira, R.L. (2020) Five new species of *Phalangopsis* Serville, 1831 (Orthoptera: Phalangopsidae) from Brazilian caves in the Amazon Forest. *Zootaxa*, 4859 (2), 151–194.
https://doi.org/10.11646/zootaxa.4859.2.1
Liebermann, J. (1965) El género *Endecous* Saussure, 1878, de la region neotropica con la descripción de una nueva especie argentina de habitat cavernícola (Ort., Grylloidea, Phalangopsidae). *Revista de la Sociedad Entomologica Argentina*, 28 (1–4), 33–43.
de Mello, F.A.G. & de Andrade, M.A.B.S. (2003) *Ottedana cercalis*: a new genus and species of phalangopsid cricket from the Mantiqueira Range of southeastern Brazil (Orthoptera: Grylloidea). *Journal of Orthoptera Research*, 12, 141–148. [https:// www.jstor.org/stable/3503767]
https://doi.org/10.1665/1082-6467(2003)012[0141:OCANGA]2.0.CO;2
de Mello, F.A.G. & Pellegatti-Franco, F. (1998) A new cave cricket of the genus *Endecous* from southeastern Brazil and characterization of male and female genitalia of *E. itatibensis* Rehn, 1918 (Orthoptera: Grylloidea: Phalangopsinae: Luzarinae). *Journal of Orthoptera Research*, 7, 185–188.
https://doi.org/10.2307/3503517
de Mello, F.A.G. & Ferreira, R.L. (2021) *Erebonyx catacumbae*, n. gen. *et* sp.: a blind, troglobitic cricket from Brazil (Orthoptera, Grylloidea, Phalangopsidae). *Zootaxa*, 4975 (2), 343–356.
https://doi.org/10.11646/zootaxa.4975.2.5
Mesa, A. & Garcia-Novo, P. (1997) *Endecous onthophagus*: a new combination. Phallic sclerites and karyology of the species (Orthoptera: Grylloidea). *Journal of Orthoptera Research*, 6, 117–120.
https://doi.org/10.2307/3503544
Mews, C.M., Lopes-Andrade, C. & Sperber, C.F. (2008) A new species of *Laranda* walker 1869 (Orthoptera: Grylloidea, Phalangopsidae) from remnant patches of the Brazilian Atlantic Forest. *Neotropical Entomology*, 37, 420–425. https://doi.org/10.1590/S1519-566X2008000400010
Mews, C.M. & Sperber, C.F. (2008) A new species of *Endecous* Saussure, 1878 and redescription of *Endecous cavernicolus* Costa-Lima, 1940 (Orthoptera: Grylloidea: Phalangopsidae). *Studies on Neotropical Fauna and Enironment*, 43 (2), 159– 167.
https://doi.org/10.1080/01650520701492389
Sallum-Filho, w. & Karmann, I. (2007) Geomorphological map of the Serra da Bodoquena karst, west-central Brazil. *Journal of maps*, 3 (1), 282–295.
https://doi.org/10.1080/jom.2007.9710845
Sallun-Filho, w., Karmann, I., Boggiani, P.C., Petri, S., Cristalli, P.S. & Utida, G. (2009) A Deposição de Tufas Quaternárias no Estado de Mato Grosso do Sul: Proposta de Definição da Formação Serra da Bodoquena. *Revista do Instituto de Geociência*, 9, 47–60.
https://doi.org/10.5327/Z1519-874X2009000300003
Saussure, H. (1878) Mélanges Orthoptérologiques. VI. fascicule Gryllides. *Mémoires de la Société de Physique et D' Histoire Naturelle de Geneve*, 25, 369–704.
Souza-Dias, P.G.B., Bolfarini M.P., Nihei, S.S. & Mello, F.A. (2014) *Endecous apterus*: A new species of cave cricket from northeast Brazil, with comments on the use of subterranean habitats by Luzarinae crickets (Orthoptera: Grylloidea: Phalangopsidae: Luzarinae). *Zootaxa*, 3784 (2), 120–130.
https://doi.org/10.11646/zootaxa.3784.2.2
Souza-Dias, P.G., De Campos, L.D. & Nihei, S.S (2015) Two new species of *Eidmanacris* (Orthoptera: Grylloidea: Phalangopsidae) from the Atlantic forest of São Paulo State, Brazil. *Florida Entomologist*, 98 (2), 547–555. https://doi.org/10.1653/024.098.0223
Souza-Dias, P.G.B., Szinwelski, N., Fianco M., De Oliveira, E.C., Mello, F.A.G. & Zefa, E. (2017) New species of *Endecous* (Grylloidea, Phalangopsidae, Luzarinae) from the Iguaçu National Park (Brazil), including bioacoustics, cytogenetic and distribution data. *Zootaxa*, 4237 (3), 454–470.
https://doi.org/10.11646/zootaxa.4237.3.2
Zefa, E., Mesa, A. & Martins, L.D.P. (2010) New Brazilian species of *Endecous* Saussure, 1878: Phallic sclerites, calling song and tegmen morphometry (Orthoptera: Grylloidea: Phalangopsinae). *Entomological science*, 13 (1), 150–155. https://doi.org/10.1111/j.1479-8298.2010.00371.x
Zefa, E., Redu, D.R., Costa, M.K.M., Gottschalk, M.S., Padilha, G.B., Silva, A.F. & Martins, L.P. (2014) A new species of *Endecous* Saussure, 1878 (Orthoptera, Gryllidae) from northeast Brazil with the first X^1X^20 chromosomal sex system in Gryllidae. *Zootaxa*, 3847 (1), 125–132.
https://doi.org/10.11646/zootaxa.3847.1.7

DIPLOPODA



Zootaxa 5428 (4): 571–588
https://www.mapress.com/zt/ Copyright © 2024 Magnolia Press

Article

https://doi.org/10.11646/zootaxa.5428.4.6

ISSN 1175-5326 (print edition)
ZOOTAXA
ISSN 1175-5334 (online edition)

Accepted by D. Antić: 29 Feb. 2024; published: 25 Mar.

http://zoobank.org/urn:lsid:zoobank.org:pub:01F1E185-5805-4814-9981-C912C4DB1E2A

Cayenniola albaserrata n. sp., a geographical relict from a Brazilian hotspot of subterranean biodiversity and the first troglobitic Priodesmini (Polydesmida: Chelodesmidae: Chelodesminae)

RODRIGO S. BOUZAN[1,2,*], JACKSON C. MEANS[3,5], KALOYAN IVANOV[3,6], RODRIGO L. FERREIRA[4,7], ANTONIO D. BRESCOVIT[1,8] & LUIZ F.M. INIESTA[1,9]

[1]*Laboratório de Coleções Zoológicas, Instituto Butantan, Av. Vital Brasil, 1500, Butantã, 05503-900 São Paulo, SP, Brazil*

[2]*Pós-Graduação em Zoologia, Instituto de Biociências, Universidade de São Paulo, Matão Street, Butantã, 05508-090 São Paulo, SP, Brazil; https://orcid.org/0000-0002-5331-7031*

[3]*Virginia Museum of Natural History, 21 Starling Avenue, Martinsville, Virginia 24112, USA*

[4]*Centro de Estudos em Biologia Subterrânea (www.biologiasubterranea.com.br), Departamento de Ecologia e Conservação, Universidade Federal de Lavras, 37200-000 Lavras, MG, Brazil*

[5] *jackson.means@vmnh.virginia.gov; https://orcid.org/0000-0001-7377-0696*

[6] *kal.ivanov@vmnh.virginia.gov;*

[7] *drops@ufla.br; https://orcid.org/0000-0003-3288-4405*

[8] *antonio.brescovit@butantan.gov.br; https://orcid.org/0000-0002-1511-5324*

[9] *luiz-moretti@hotmail.com; https://orcid.org/0000-0002-0529-4162*

**Corresponding author. rodrigobouzan@outlook.com*

Abstract

A new troglobitic species of Chelodesmidae, *Cayenniola albaserrata* **n. sp.**, from the Água Clara cave system, Caatinga Domain, Bahia, Brazil is described. The new species is only the sixth known troglobitic chelodesmid, the first troglobitic species in the Priodesmini, and the first member of the tribe recorded from the state of Bahia. Unique among the Priodesmini, male *C. albaserrata* **n. sp.** possess greatly elongated pre-gonopodal tarsal claws and differ from the only congener, *Cayenniola styliger* (Jeekel, 1963), by a combination of gonopodal and somatic characters including classical troglomorphic traits such as a nearly unpigmented body and remarkably long antennae, legs, and tarsal claws. *Cayenniola styliger* is only known from the type locality in the Amazon rainforest of coastal French Guiana, suggesting that *C. albaserrata* **n. sp.** may represent a relictual species from the Caatinga Domain of Brazil. We provide ecological notes and evaluate the potential threats to the habitat of *C. albaserrata* **n. sp.**, considering both the subterranean environment and the surrounding areas.

Key words: Bahia, caves, millipedes, Neotropics, taxonomy, troglomorphisms

Introduction

With nearly 800 described species in 176 genera, Chelodesmidae Cook in Cook & Collins, 1895 is one of the most diverse groups within the class Diplopoda (Hoffman 1980; Bouzan *et al.* 2019). Members of the family are commonly found in moist habitats, almost exclusively within the Neotropical and Afrotropical regions of the world, and exhibit an impressive degree of morphological variability including a wide range of color patterns, paranotal ornamentations, and gonopodal morphology (Schubart 1955; Hoffman 1969; Hoffman 1980; Pena-Barbosa *et al.* 2013; Bouzan *et al.* 2017, 2019). Chelodesmidae is divided into two subfamilies, Chelodesminae Cook in Cook & Collins, 1895 restricted to the Neotropical region, and Prepodesminae Cook, 1896 known from the Afrotropical and Palearctic regions (Hoffman 1980). Currently, 19 tribes are recognized within the Chelodesminae and two tribes in the Prepodesminae, with nearly half (43%) of the described species without a tribal assignment (Hoffman 1980; Pena-Barbosa *et al.* 2013; Bouzan *et al.* 2017; Shelley & Smith 2018).

Accepted by D. Antić: 29 Feb. 2024; published: 25 Mar.

According to Hoffman (1977), certain Chelodesminae (i.e., Batodesmini, Pandirodesmini, Priodesmini, andTrachelodesmini) in the sub-Caribbean region (including northern Brazil) may represent specialized members of ancestral lineages currently found only in Brazil and the Andes Mountains. These sub-Caribbean taxa exhibit distinct somatic characters such as the presence of tubercles on the body rings and legs, tergites partially or fully ornamented with tubercles and/or processes of different sizes, and a broader telson, which sets them apart from all other Chelodesminae tribes (Attems 1938; Hoffman 1977, 1980, 1982).

According to Hoffman (1977), the Priodesmini includes small to moderately sized species with broad and setose sterna, and granular metaterga with a transverse sulcus; robust antennae; long and slender legs with reduced tarsal claws, femora of anterior legs often swollen ventrally or with projecting adenostyles; telopodite straight, typically set at 90° from coxa, and without torsion. The tribe contains seven genera found in northern South America (Hoffman 1977), including three, *Cearodesmus* Schubart, 1945, *Brasiloschubartia* Jeekel, 1963, and *Parastenonia* Hoffman, 1977, which occur in Brazil. The monospecific genus *Cayenniola* Hoffman, 1977 was proposed to accommodate *Brasiloschubartia styliger* Jeekel, 1963, known only from the type series collected in Ilet Père, French Guiana in 1902.

Millipedes restricted to cave environments (i.e., troglobionts) are often morphologically distinct from their surface-dwelling counterparts based on a number of morphological adaptations (troglomorphisms) to life in darkness including a partial reduction, or loss, of both eyes and body pigmentation (Culver & Pipan 2014; Liu *et al.* 2017; Akkari *et al.* 2018). Additional troglomorphisms may include changes in body size, elongation or shortening of appendages, and thinning of the cuticle (Schubart 1946; Iniesta *et al.* 2012; Golovatch *et al.* 2022; for a review of Chelodesmidae troglomorphisms see Bouzan *et al.* 2022). Although 25 Chelodesmidae species and subspecies have been recorded from caves to date, only five of these, *Leodesmus yporangae* Schubart, 1946; *Platyurodesmus parallelus* Loomis, 1977; *Ricodesmus uniporus* (Loomis, 1977); *Strongylosomides troglobius* Golovatch, Bouzan & Gallo, 2022; and *Cantabrodesmus lorioli* Mauriès, 1971, are considered troglobitic (Bouzan *et al.* 2022). Of these, only *L. yporangae* and *S. troglobius* are known from Brazil, both recorded from carbonate caves in São Paulo and Bahia states, respectively (Bouzan *et al.* 2022; Golovatch *et al.* 2022).

We describe a sixth troglobitic chelodesmid, *Cayenniola albaserrata* **n. sp.**, from the Água Clara cave system, Caatinga Domain, Bahia, Brazil. The species is likely a representative of a relictual Priodesmini lineage, members of which are scattered across the Amazon rainforest of the Guiana Shield. The discovery of this unusual species suggests that subterranean environments may have acted as refugia in the past, and that additional Priodesmini may be expected in other cave systems of the Caatinga Domain. In addition, we provide ecological notes and evaluate the potential threats to this species' habitat, considering both the subterranean environment and the surrounding areas.

Material and

Methods

Study area

The Serra do Ramalho karst system is geographically delimited by the Carinhanha River to the south and the Corrente River to the north. These significant perennial tributaries, originating in the Urucuia plateaus of the Cerrado biome, traverse an expansive area of dissected karst landscapes known as the "Sanfranciscana depression", which plays a crucial role in maintaining the flow of the São Francisco River. A substantial portion of the Serra do Ramalho karst system corresponds to an elevated block representing an extensively incised extension of the Urucuia plateau. It is within this block that the prominent karst features characteristic of the local landscape can be found. The Água Clara Cave System (ACCS; Fig. 1) consists of a sequence of four interconnected large caves hydrologically linked through one of the numerous fluvial outlets situated along the eastern periphery of the Serra do Ramalho karst block. The system includes the Água Clara (13,880 m), Índios (510 m), Lapa dos Peixes I (9,320

Accepted by D. Antić: 29 Feb. 2024; published: 25 Mar.

m), and Lapa dos Peixes II (2,100 m) caves. The conduit system extends linearly for approximately 8 km stretching from the innermost end of the massif (upstream) to the final resurgence point (downstream) where it merges with the alluvial plain of the São Francisco River (Fig. 1A). Many entrances to the karst system also receive seasonal water inputs (Fig. 1B). Ferreira *et al.* (2023) provides a comprehensive review of the geological and hydrological characteristics of the ACCS.

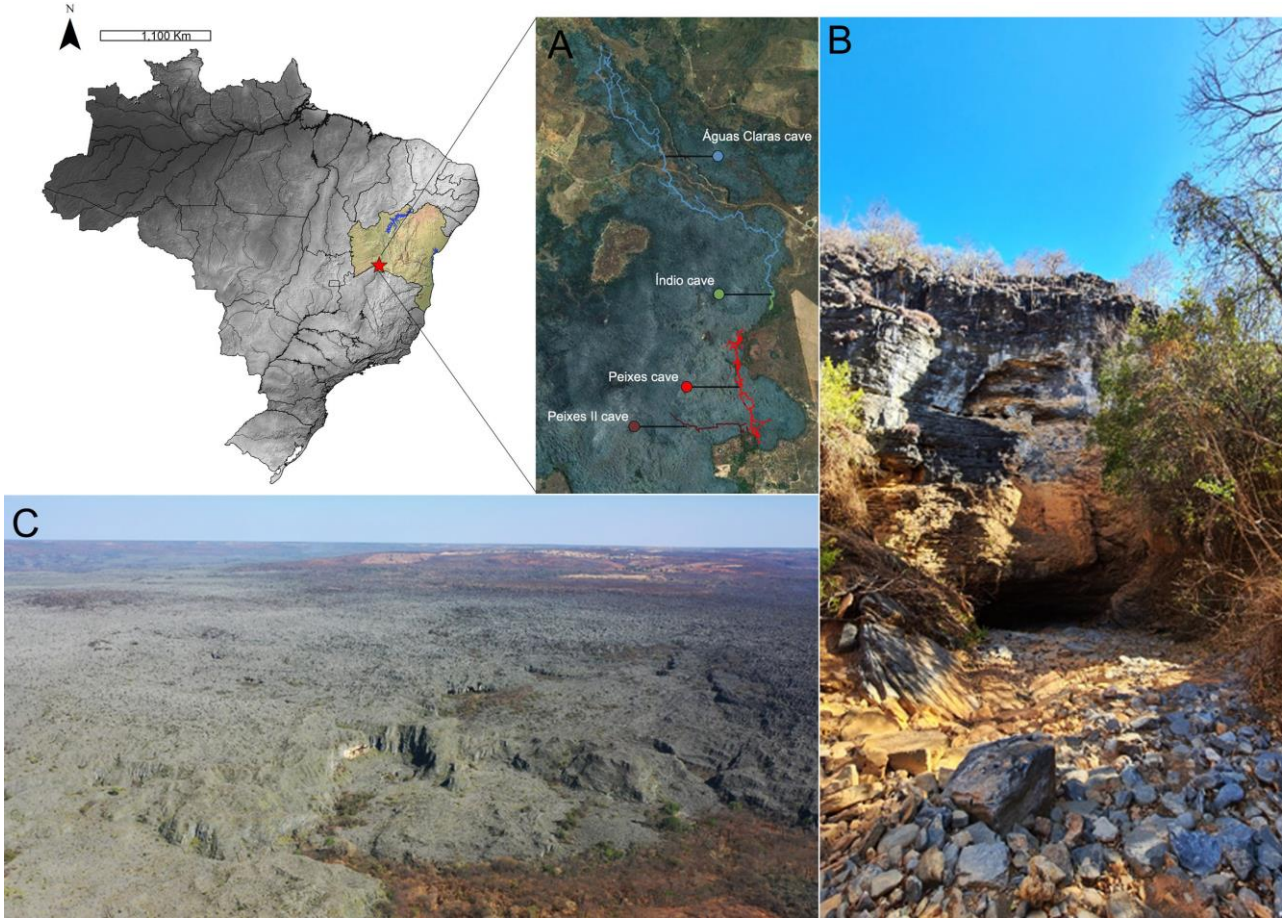


FIGURE 1. Serra do Ramalho karst and the Agua Clara Cave System (ACCS). **A.** Location of the Água Clara, Índios, and Lapa dos Peixes I and II caves. **B.** One of the entrances of the Água Clara cave, sink of the seasonal stream that drains sections of the ACCS. **C.** Aerial view of the exposed massif at the edge of the Serra do Ramalho block, where ACCS is located.

Methods

The examined material is deposited in the following institutions (curators in parentheses): **IBSP**, Instituto Butantan, São Paulo, Brazil (A.D. Brescovit); **ISLA**, Coleção de Invertebrados Subterrâneos de Lavras, Centro de Estudos de Biologia Subterrânea da Universidade Federal de Lavras, CEBS/UFLA, Minas Gerais, Brazil (R.L. Ferreira).

High-resolution photographs of relevant morphological features were captured with a Leica DFC 500 digital camera mounted on a Leica MZ16A stereomicroscope and extended focal range images were composed with Leica Application Suite version 2.5.0 (Leica Camera, Wetzler, Germany). Living specimens and habitats were photographed with a Canon EOS 50D digital camera. Illustrations of relevant morphological features were made by tracing the focus-stacked images in the vector graphics editor Inkscape ver. 1.3.1 (https://inkscape.org). All measurements were made at 20x magnification to the nearest 0.01 mm. Scanning electron micrographs were taken using a FEI Quanta 250 Scanning Electron Microscope (SEM) with an attached SLR digital camera (Thermo Fisher Scientific, Massachusetts, USA) at Instituto Butantan, São Paulo, Brazil. Specimens selected for SEM imaging were cleaned using brushes and an ultrasonic cleaner Q3.8 (Eco-Sonics, São Paulo, Brazil). The dissected material was dehydrated through an ascending series of ethanol dilutions (70, 80, 90 and 100%; 15 minutes at each step), critical-point dried, fixed on metal stubs,

Accepted by D. Antić: 29 Feb. 2024; published: 25 Mar.

and sputter coated with gold. Gonopodal terminology follows Pena-Barbosa *et al.* (2013), somatic terminology follows Attems (1898) and Brölemann (1900), and vulvar terminology follows Koch (2015).

Morphological abbreviations used in the text are as follows: (AP) acropodite process, (Ev) external valve, (Iv) internal valve, (Op) operculum, (PG) prostatic groove, (PfP) prefemoral process, (S) solenomere.

Geographic coordinates of the collection sites were obtained directly from the specimen labels and georeferenced in Google Earth Pro v. 7.1. (Alphabet Inc., Mountain View, California).Maps of the ACCS were provided by the Bambui Speleological group (https://bambuiespeleo.wordpress.com/).

Results

Taxonomy

Class Diplopoda de Blainville in Gervais, 1844

Order Polydesmida Pocock, 1887

Suborder Leptodesmidea Brölemann, 1916

Family Chelodesmidae Cook in Cook & Collins, 1895

Subfamily Chelodesminae Cook in Cook & Collins,

1895 Tribe Priodesmini Hoffman, 1977

Diagnosis. Small to moderately sized species with broad, setose sterna and granular metaterga with a transverse sulcus; robust antennae, with the 6th antennomere larger than the proceeding ones and the 7th antennomere often hemispherical; legs long and slender with reduced tarsal claws (except in *Cayenniola albaserrata* **n. sp.**), nearly concealed by an apical tuft of long setae, anterior femora often swollen ventrally or with projections; gonopod aperture oval to subtrapezoidal and large, gonocoxae lacking apophyses, telopodite straight, without torsion, and typically at 90° from coxa, with or without solenomere, and lacking enlarged setae beyond prefemur, prefemoral process variable.

Genus *Cayenniola* Hoffman, 1977

Diagnosis. Gonopods with the prostatic groove visible in mesal view for its entire length (vs prostatic groove ends in the middle of the acropodite region in *Cypraeogona* Hoffman, 1977), prefemoral process simple, slender, and acute (vs prefemoral process absent in *Cearodesmus* or stout in *Stenonia* Gray in Jones, 1843), without additional processes and reaching half the size of the acropodite (vs exceeding the size of the acropodite in *Brasiloschubartia* or reaching approximately the same size in *Parastenonia, Priodesmus* Cook, 1895 and *Stenonia*), acropodite with a slender digitiform solenomere, with or without an additional process, arising from a spoon-shaped subterminal laminate acropodite process (vs solenomere and acropodite process highly variable, in all other representatives of the tribe).

Cayenniola albaserrata Bouzan & Iniesta n. sp.

Figs 1–10

Diagnosis. Males of *C. albaserrata* **n. sp.** differ from those of *Cayenniola styliger* (Jeekel, 1963), based on the following combination of gonopodal characters: solenomere straight, apically acuminate, lacking projections (vs curved laterally, with a secondary process in *C. styliger*), longer than the acropodite and extending past margin of acropodite (Figs 7–9); prefemoral process smaller and arising at approximately midpoint of telopodite (vs larger and arising basally in *C. styliger*) (Figs 7A, 8A, C–D, 9A, C), medial region of telopodite thinner than in *C. styliger* (Figs 7A, 8A, 9). In addition to generic characters, males of *C. albaserrata* **n. sp.** differ from all other Priodesmini by the greatly elongated tarsal claws of the males' pre-gonopodal legs (2nd–7th pair; Fig. 6B–D), the more elongated tarsal claws of the post-gonopodal legs (Fig. 6E), prefemur lacking acute ventrodistal spine (c.f. *C. styliger*), the nearly

Accepted by D. Antić: 29 Feb. 2024; published: 25 Mar.

unpigmented body, and the remarkably long antennae and legs (Figs 2B–C, 6C–D).

Name. Derived from the Latin *alba* (white) plus *serrata* (saw-like) in reference to the body color and ornamentation of this species. Feminine adjective in the nominative singular form.

Material examined.

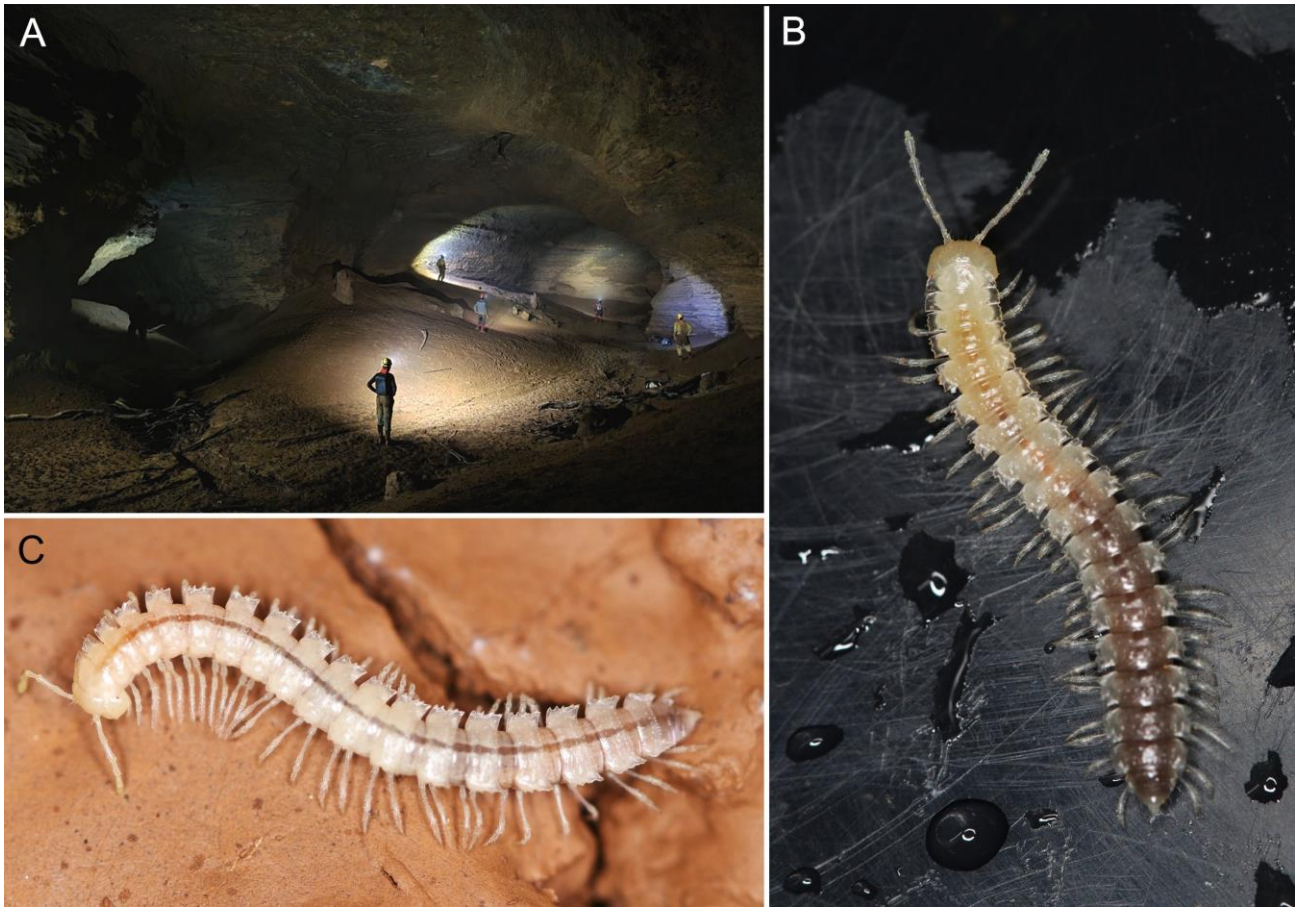


FIGURE 2. A. Inner conduit of the Água Clara cave. **B–C.** Habitus of living *Cayenniola albaserrata* **n. sp. Photos:** R.L. Ferreira.

Type material: **Holotype:** BRAZIL ● ♂; Bahia, Carinhanha, Serra do Ramalho, Água Clara cave (UTM 813350 8474058); 11 October 2017; R.L. Ferreira leg.; ISLA 120359.

Paratypes: ● 1 ♂; same data as for holotype; IBSP 15245; ● 4 ♀♀; same data as for holotype; ISLA 50593, ISLA 120360, ISLA 120361, IBSP 15246.

Other material: BRAZIL ● 1 juvenile; Bahia, Carinhanha, Serra do Ramalho, Água Clara cave (UTM 813350 8474058); 11 October 2017; R.L. Ferreira leg.; ISLA 50581; ● 1 ♂; ISLA 50579; ● 1 ♀; ISLA 50481; 12 October 2017; ● 1 ♀; ISLA 50582; 1 juvenile; ISLA 50580.

Description. Male (holotype, ISLA 120359). Coloration (preserved in 70% ethanol): head yellowish-white; antennae white; body white, with paranota margins translucent (Fig. 2B–C); legs whitish with tarsal claws yellowish; telson yellowish. Parts of the body of some individuals, including the terminal body rings of the holotype, with darker coloration due to the accretion of cave sediments. Head (Fig. 3A): labrum and clypeus covered with sparse setae; two (1+1) setae below the antennal sockets and two (1+1) setae between the antennae; vertex of head with two pairs (2+2) of setae; *incisura lateralis* subrounded. Antennae (Fig. 3B–E): covered with thin setae, becoming more densely setose on the lasts four antennomeres; nearly reaching the 7th body ring; 5th, 6th and 7th antennomeres with small clusters of basiconic sensilla on the distal, external margin (Fig. 3D–E). Gnathochilarium (Fig. 3F) without modifications, sparsely setose. Body with 17 podous rings + 2 apodous rings + telson. Body rings: metazonites with a slight transverse depression; cuticle with numerous small tubercles on the tergal and pleural regions, absent on the paranota (Figs 4, 5B–D); metaterga with three rows of large tubercles, one in the anterior region and two in the posterior region (last row with more numerous tubercles; Fig. 4); cuticle thin, nearly translucent on some body rings. Sternite of 4th body ring with a pair of small triangular projections (Fig. 5A, arrows); anterior portion of sternite of

Accepted by D. Antić: 29 Feb. 2024; published: 25 Mar.

5th body ring with a pair of less conspicuous triangular projections; remaining sternites without modifications (Fig. 5B). Paranota: collum without ornamentation or serration; remaining body rings, except for the 19th, divided into three

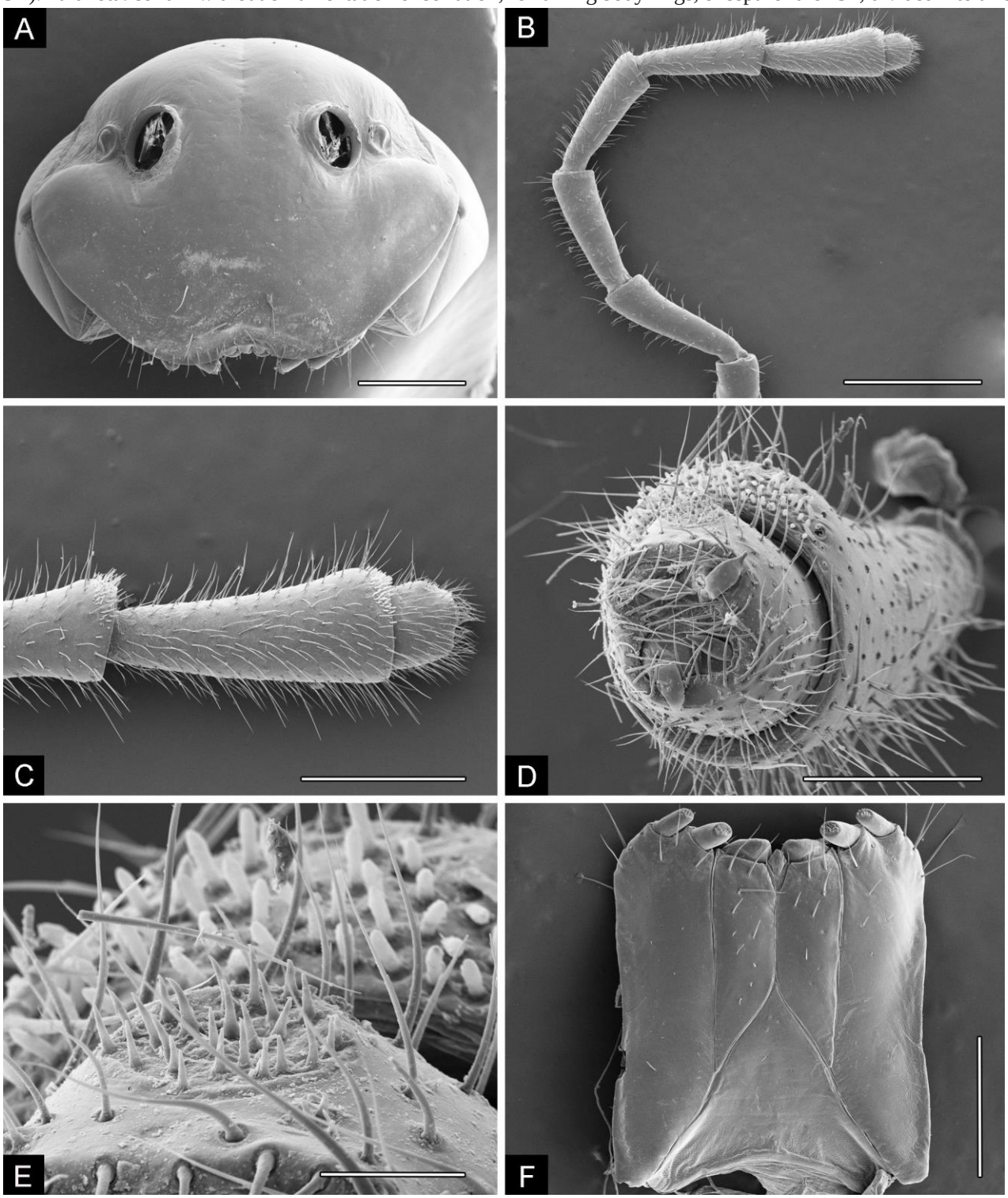


FIGURE 3. *Cayenniola albaserrata* **n. sp.** ♂ (ISLA 50579) somatic characters. **A.** Head. **B.** Right antenna, lateral view. **C.** Right antenommeres 5–7, lateral view. **D.** Left antennomeres 6, 7 and apical cones, distal view. **E.** Left antenommeres 6 and 7, sensilla basiconica. **F.** Gnathochilarium, ventral view. **Scale bars: A, C, F**. 0.5 mm; **B**. 1 mm; **D**. 0.2 mm; **E**. 0.04 mm.

(pro-, meso-, and meta-) lobes; 2nd body ring with only a small indentation on prolobe; 3rd body ring with a slight acute indentation on prolobe followed by a shallow indentation on mesolobe; 4th body ring with an acute indentation on prolobe as in the previous body ring, indentation on mesolobe more conspicuous, posterior margin of metalobe more pronounced; on all other paranota, pro- and mesolobes with two indentations

Accepted by D. Antić: 29 Feb. 2024; published: 25 Mar.

each,and metalobe with a single indentation on the posterior paranotal margin; the number of indentations can vary even within the same body ring (left vs right), but there are never more than five indentations to a margin (Figs 4, 5B–C). Ozopore arrangement typical for Polydesmida (5, 7, 9, 10, 12, 13, 15–19); ozopores surrounded by peritremata (Fig. 4B), centered between two indentations on mesolobe, except for 19th body ring; on posterior body rings the ozopore located closer to the metalobe; peritremata rounded. Gonopod aperture transversely oval, without modification (Fig. 5C). Legs: ventral portion of coxa and prefemur with a unique long seta (Fig. 6A); coxae of second leg pair with subrectangular gonopores (Fig. 6A, arrows); femur of anterior leg pairs densely setose; pre-gonopodal legs with greatly elongated tarsal claws (1st<2nd<3rd=4th=5th<6th=7th), those of 5th and 6th body rings with a sigmoid curvature (Fig. 6B–D); remaining leg pairs with tarsal claws elongated to a lesser degree. Telson triangular (Fig. 4D); epiproct with (5+5) macrosetae; two pairs of spinnerets; paraprocts with two pairs of macrosetae, dorsal pair of macrosetae closer to each other as compared to ventral pair; hypoproct subtriangular, with a pair of macrosetae. Gonopods (Figs 7–9): gonocoxae oval, equivalent to about half the length of the telopodite, without modification, with two macrosetae on dorsal side (Figs 7A, C, 8B); cannula hook-shaped (Figs 7A, 9A); prostatic groove visible along the entire length of telopodite in mesal view, running nearly straight and without a trace of torsion along the medial side of telopodite (Figs 7A, 8A, 9A); prefemoral region well-developed, approximately half the length of telopodite, densely setose at base, with only a few macrosetae apically (Figs 7A, C, 8A–B); prefemoral process (Figs 7A, 8A, C–D, 9A, C) acute and slender, separating from telopodite at midpoint; acropodite with slender digitiform solenomere arising from a spoon- shaped subterminal laminate acropodite process (Figs 7, 8, 9A–C).

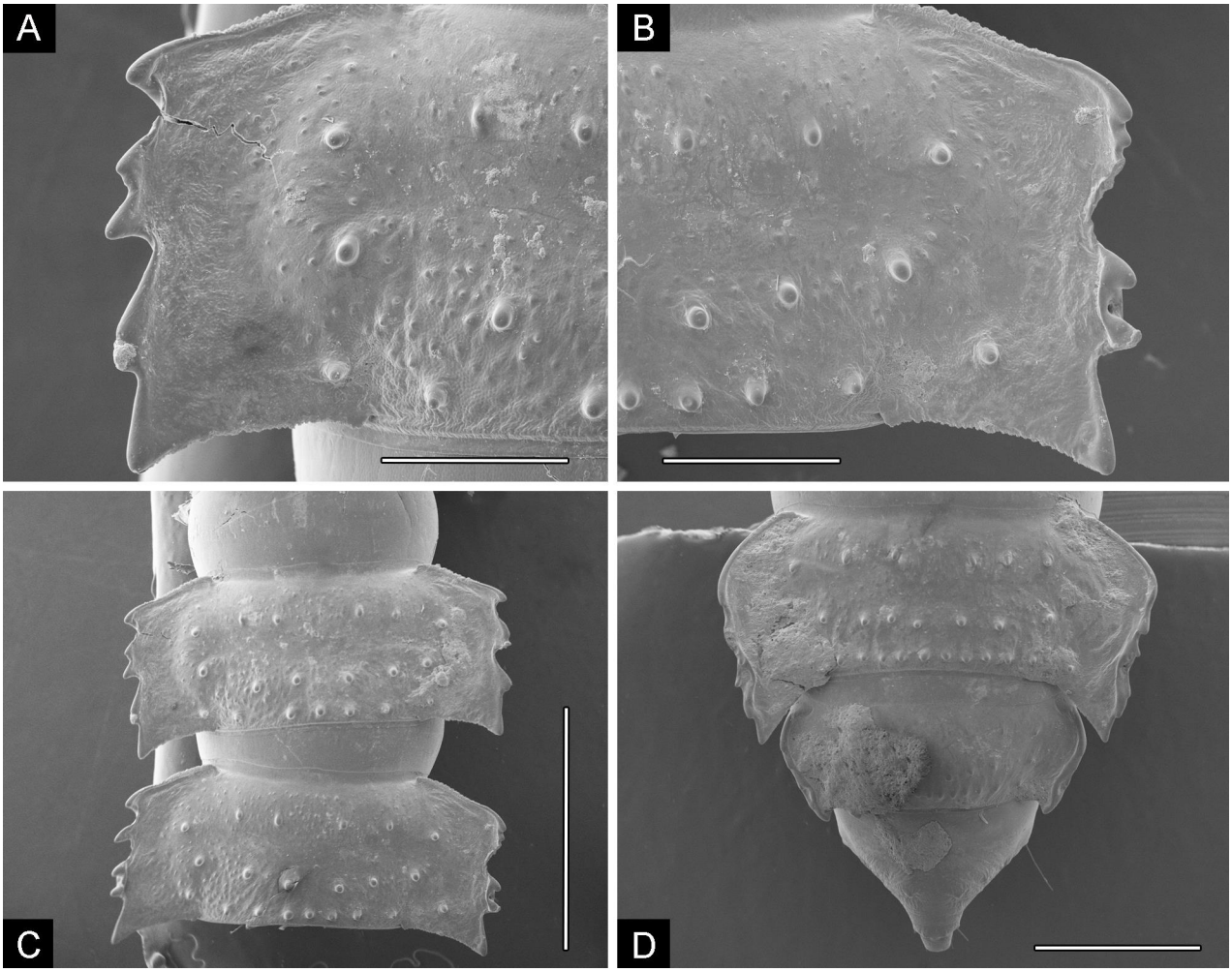


FIGURE 4. *Cayenniola albaserrata* **n. sp.** ♂ (ISLA 50579) somatic characters. **A.** Left part of metazonite 11, dorsal view. **B.** Right part of metazonite 12, dorsal view. **C.** Rings 11 and 12, dorsal view. **D.** Posterior part of body, dorsal view. **Scale bars: A, B**. 0.5 mm; **C**. 2 mm; **D**. 1 mm.

Accepted by D. Antić: 29 Feb. 2024; published: 25 Mar.

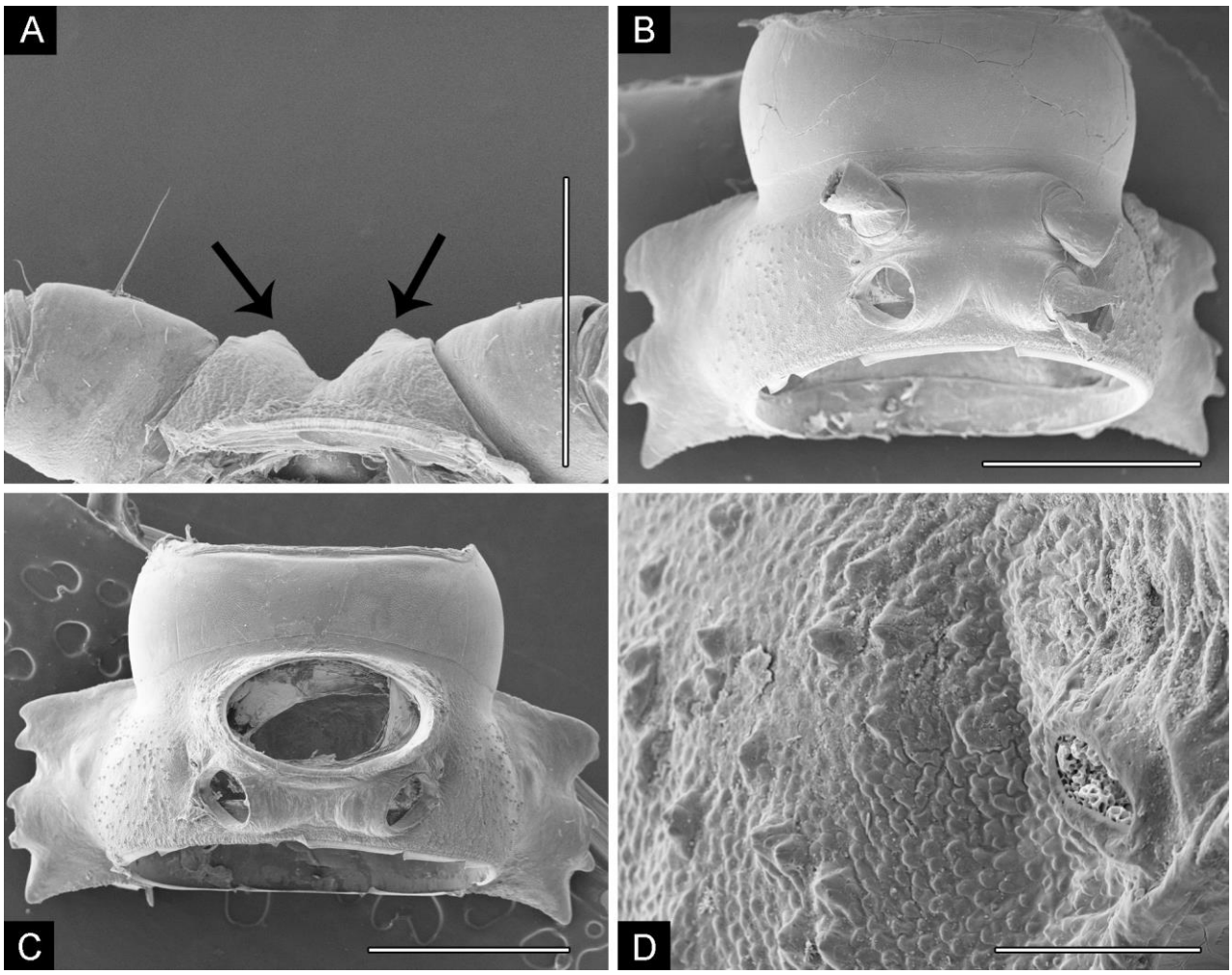


FIGURE 5. *Cayenniola albaserrata* **n. sp.** ♂ (ISLA 50579) somatic characters. **A.** Sternite of ring 4, anterior view. **B.** Ring 9, ventral view. **C.** Ring 7, ventral view. **D.** Tubercles and spiracle of ring 7 pleural region, ventral view. Arrows refer to the pair of triangular projections. **Scale bars: A**. 0.5 mm; **B, C**. 1 mm; **D**. 0.1 mm.

Measurements (in mm): Body: total length 26.6, width of 10th body ring 2.89. Antennomere lengths (1−7): 0.47; 1.16; 1.11; 0.98; 1.25; 1.02; 0.28. Podomere lengths of 6th leg (1−7): 0.48, 0.50, 1.12, 0.53, 0.70, 1.03, tarsal claw 0.87. Gonopod aperture: length 0.58, width 1.05. Telson length 0.85. Gonopod: length 1.39, width 0.65. Gonocoxae: length 0.46, width 0.44. Telopodite: length 1.39, width 0.29.

Female (Paratype, ISLA 120360). Coloration as in male. Antennae shorter than in males, nearly reaching the 5th body ring. Body with 17 podous rings + 2 apodous rings + telson. Sternite of fourth body ring with a pair of triangular projections as in males, other sternites without modifications. Paranota: collum without ornamentation or serration; remaining body rings, except for the 19th, divided into three (pro-, meso-, and meta-) lobes; 2nd body ring with only a small indentation on prolobe followed by a slight undulation of the lateral margin; 3rd body ring with a slight acute indentation on prolobe and a well-developed undulation on mesolobe; 4th body ring with an acute indentation on prolobe as in the previous body ring, indentation on mesolobe more conspicuous, posterior margin of metalobe more pronounced; prolobes with three indentations each, mesolobes with two indentations, and metalobes with a single indentation on the posterior margin; the number of indentations can vary even within the same body ring (left vs right) but there are never more than six to a margin (vs ≤ 5 in males). Coxae of second leg pair with an acute projection apically (Fig. 6F, arrow). Posterior margin of vulvae opening with a slightly rounded epigyne (Fig. 10A–B). Vulvae rounded in ventral (Fig. 10C) and lateral (Fig. 10D) views. External and internal valves subequal in size, densely setose; external valve with conspicuously longer and more numerous setae than internal valve (Fig. 10C). Interior region of valves slightly excavated and grooved in ventral view, lacking setae (Fig. 10C). Operculum setose, flattened, ~ 1/5 size of valves (Fig. 10D).

Accepted by D. Antić: 29 Feb. 2024; published: 25 Mar.

Measurements (in mm): Body: total length 28.3, width of 10th body ring 3.59. Width of posterior margin of vulvar aperture 1.01. Vulvae: length 0.40, width 0.39. External valve: length 0.38, width 0.36. Internal valve: length 0.38, width 0.36. Operculum: length 0.22, width 0.21.

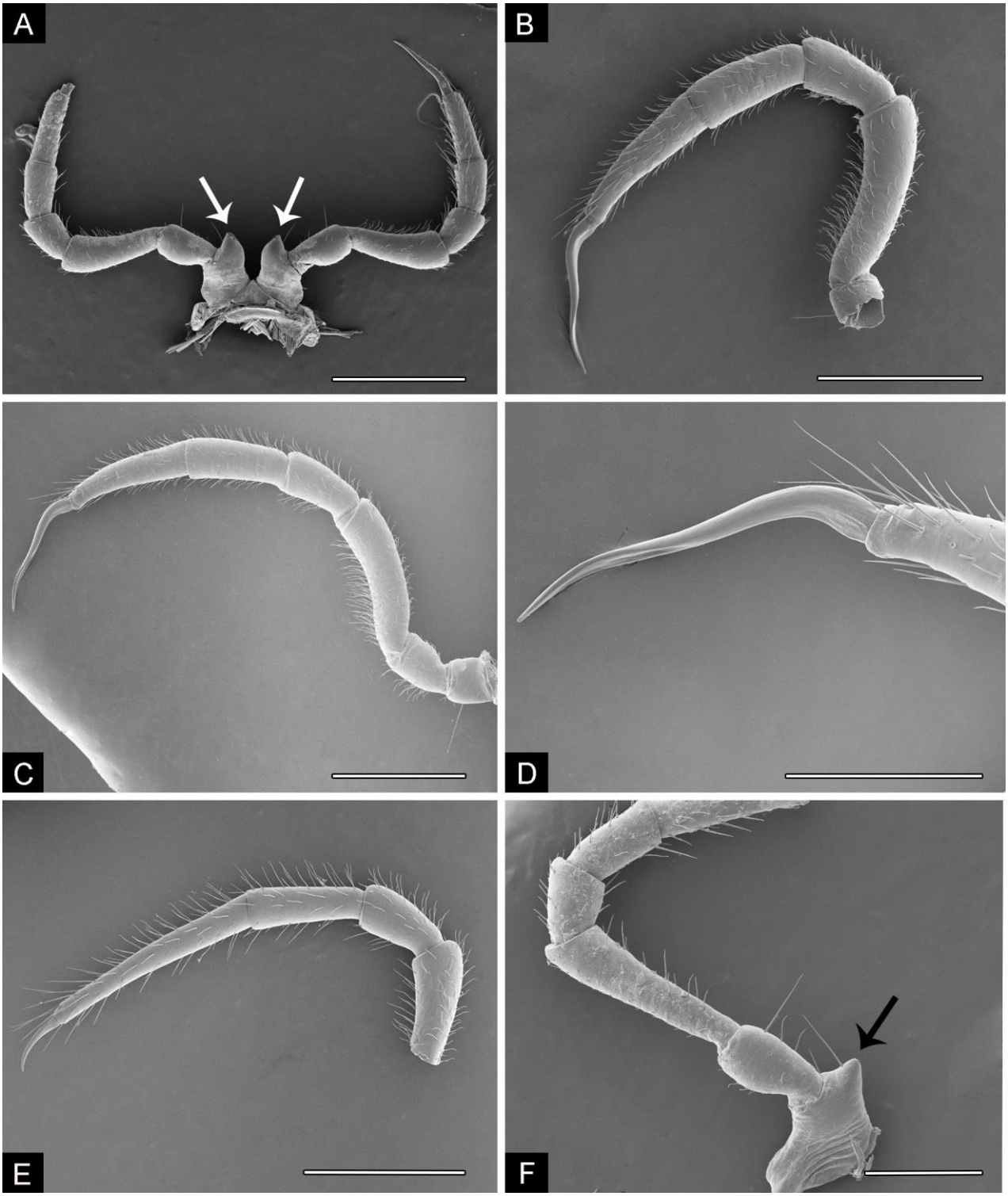


FIGURE 6. *Cayenniola albaserrata* **n. sp.**, somatic characters. **A–D.** ♂ (ISLA 50579), **E**–**F.** ♀ paratype (ISLA 50593). **A.** Leg pair 2, posterior view. **B.** Left leg of body ring 5, posterior view. **C.** Left leg of body ring 6, posterior view. **D.** Leg of 6th body ring, close-up of tarsal claw, posterior view. **E.** Left leg 9, posterior view. **F.** Right leg 2, posterior view. Arrows refer to the coxae of leg pair 2. **Scale bars: A, B, C, E**. 1 mm.; **D, F**. 0.5 mm.

Accepted by D. Antić: 29 Feb. 2024; published: 25 Mar.

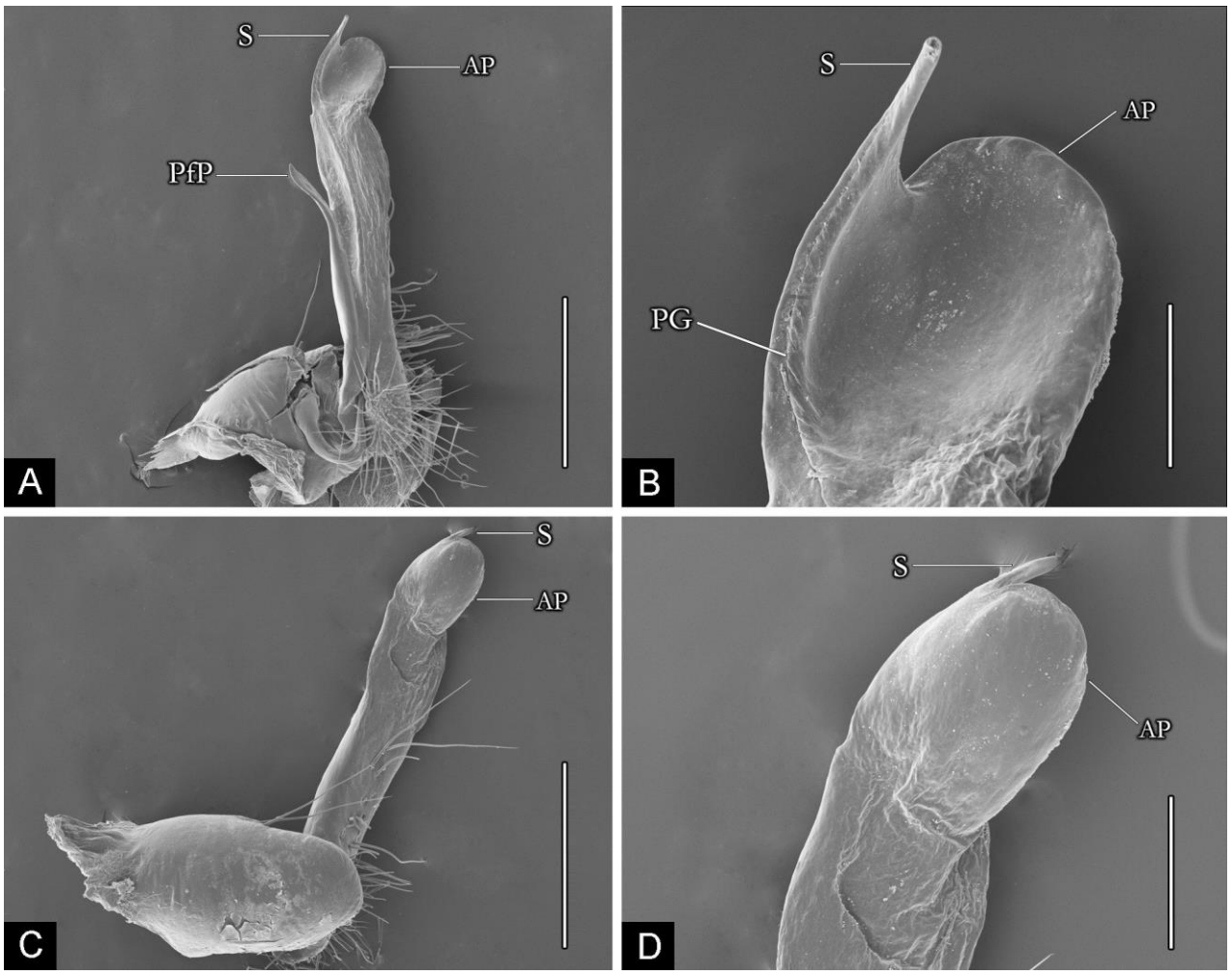


FIGURE 7. *Cayenniola albaserrata* **n. sp.** ♂ (ISLA 50579), gonopods. **A.** Left gonopod, mesal view. **B.** Distal region of acropodite, mesal view. **C.** Right gonopod, ectal view. **D.** Distal region of acropodite, ectal view. **Abbreviations**: **AP**: acropodite process; **PfP**: prefemoral process; **PG**: prostatic groove; **S**: solenomere. **Scale bars: A, C**. 0.5 mm; **B**. 0.1 mm; **D**. 0.2 mm.

Ecological notes. Specimens of *C. albaserrata* **n. sp.** (Supplementary Material) were found exclusively within the Água Clara Cave System (ACCS), situated in the municipality of Carinhanha in the southwestern region of Bahia, Brazil. The ACCS is located in the Serra do Ramalho karst system which houses numerous large caves. Specimens (Fig. 2B–C) were observed in all caves comprising the ACCS: in the Água Clara cave (Figs 1A–C, 2A), specimens were found at distances ranging from 450 m to 2,400 m from the nearest entrance; in the Índios cave, a single specimen was observed 280 m away from the closest cave entrance; in the Lapa dos Peixes I cave, a single specimen was observed ~ 350 m away from the closest cave entrance; and in the Lapa dos Peixes II cave, specimens were found between 600 m and 900 m from the nearest entrance.

It is worth noting that specimens were often found in close proximity to each other and, in general, finding of isolated specimens at significant distances from others was rare. Exceptions included the Indios and Lapa dos Peixes I caves, in which the substrates are drier and less suitable for this, and other, species. Most specimens were associated with decaying logs that had been washed into the caves during heavy rains. Many specimens were occasionally found on a single log, sheltered in the crevices beneath the bark, and likely feeding on decaying organic matter or fungi. Although most logs were located in the main cave conduit, especially in the Água Clara cave where the majority of the population occurs, most individuals were observed in logs located in higher areas, such as lateral chambers, rather than in those within the main conduit. The cave system experiences substantial water inflow, including flash floods, during the rainy season, and this behavior suggests that *C. albaserrata* **n. sp.** prefers higher areas, possibly to avoid being washed out during flood events. These observations suggest that despite this

species' generalist behavior, there are unknown factors leading to aggregations of individuals in various regions of the caves.

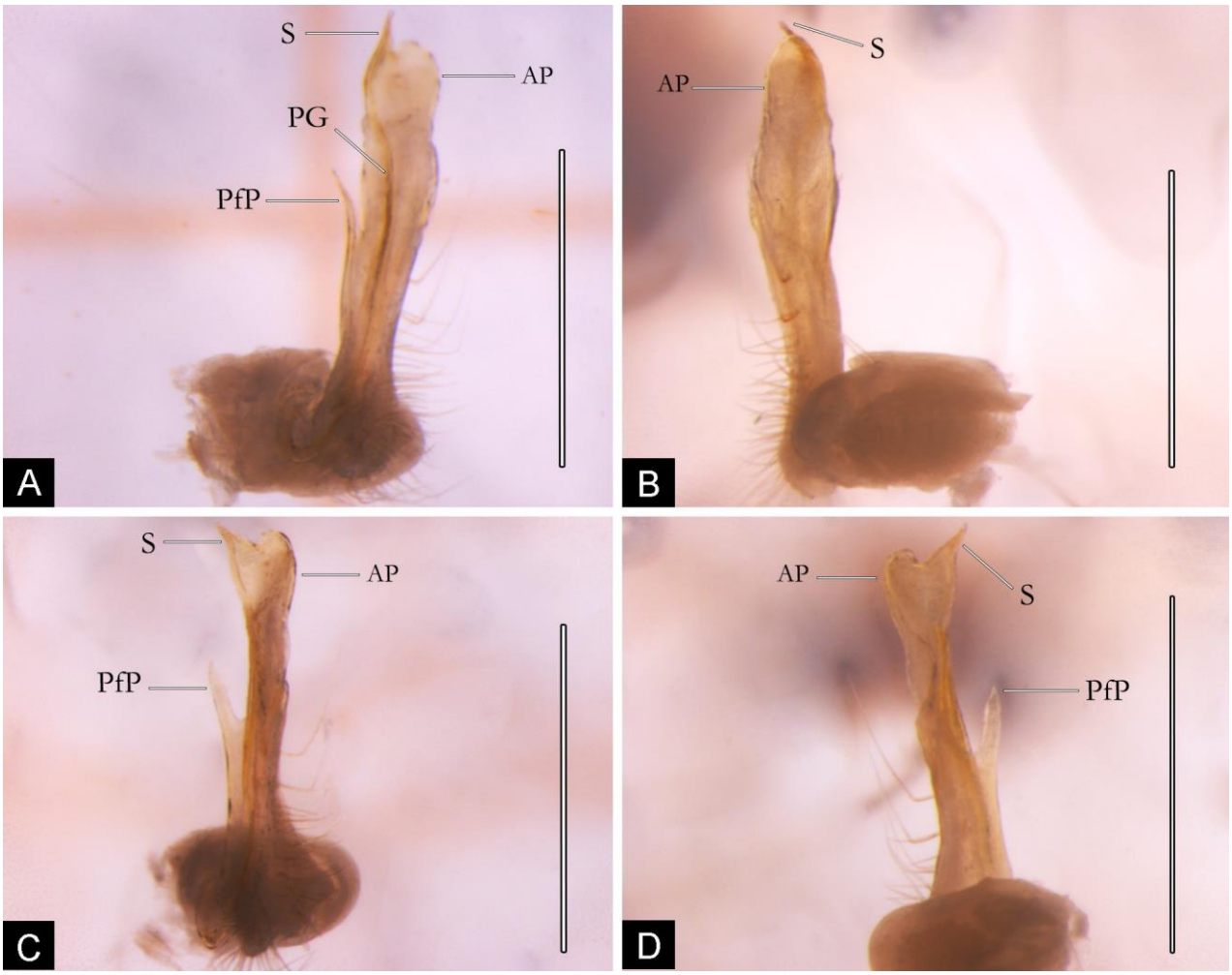


FIGURE 8. *Cayenniola albaserrata* **n. sp.**, ♂ holotype (ISLA 120359), left gonopod. **A.** Mesal view. **B.** Ectal view. **C.** Ventral view. **D.** Dorsal view. **Abbreviations**: **AP**: acropodite process; **PfP**: prefemoral process; **PG**: prostatic groove; **S**: solenomere. **Scale bars:** 1 mm.

Discussion

Climatic and other large-scale environmental changes can have fundamental impacts on species distribution patterns. Relicts are distinct, often species-poor, lineages with a severely restricted geographic range. Taxonomic (evolutionary) relicts are survivors of once diverse taxonomic assemblages, whereas geographic relicts are the descendants of once widespread taxa which now have a restricted distribution (Lomolino *et al.* 2006). Cave-restricted organisms are commonly regarded as relictual because they often represent taxa with no ancestral stock in the immediate area or because they have strikingly disjunct distributions (Barr 1985; Assmann *et al.* 2010).

At present, the Amazon rainforest and the Atlantic Forest are separated by a vast area composed of the Caatinga, Cerrado, and Chaco biomes referred to as the "diagonal of open formations" (Ab'Saber 1977). This formation of dry areas in central and northeastern Brazil acts as a barrier to faunistic and floristic exchange between the two forests (Raven & Axelrod 1974; Oliveira-Filho & Ratter 1995). Three hypothetical connections between the Amazon rainforest and the Atlantic Forest have been proposed regarding animal migrations during periods when these areas were still in contact, which occurred on multiple occasions during at least the last 120,000 years (Ledo & Colli 2017): *i*) the northeastern connection, now dominated by the semi-arid Caatinga biome (Andrade-Lima 1982;

Accepted by D. Antić: 29 Feb. 2024; published: 25 Mar.

Auler *et al.* 2004; Wang *et al.* 2004); *ii*) the central connection, which may have transected the Cerrado in central Brazil, either as a continuous forest corridor or as a series of forest patches (Por 1992; Oliveira-Filho & Ratter 1995; Costa 2003); and *iii*) the southern connection, which may have allowed for the passage of organisms between the Atlantic Forest and the Amazon Rainforest through the Paraná River Basin (Por 1992; Costa 2003; Batalha-Filho *et al.* 2013).

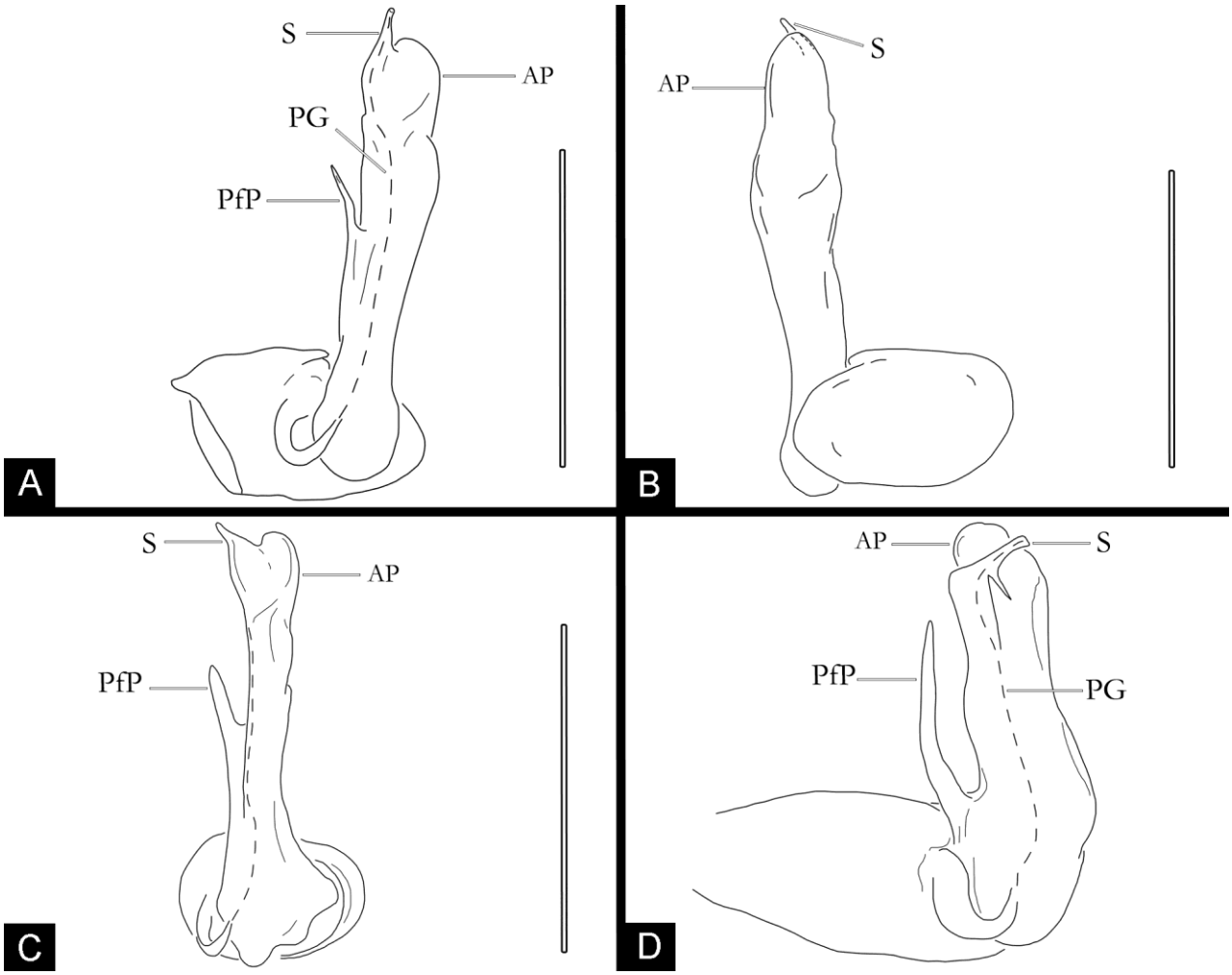


FIGURE 9. *Cayenniola* Hoffman, 1977 gonopods. **A**–**C.** *Cayenniola albaserrata* **n. sp.**, ♂ holotype (ISLA 120359), left gonopod in mesal, ectal and ventral views respectively. **D.** *C. styliger* (Jeekel, 1963), ♂ holotype, left gonopod, mesal view (redrawn from Jeekel (1963)). **Abbreviations**: **AP**: acropodite process; **PfP**: prefemoral process; **PG**: prostatic groove; **S**: solenomere. **Scale bars:** 1 mm.

The tribe Priodesmini was proposed to accommodate seven genera from northern South America, primarily distributed across the Guiana Shield: *Priodesmus* from the coast and central region of Suriname; *Stenonia* from the mountainous regions of Suriname, the coast and central region of French Guiana, and northern Brazil (Amapá state); *Cypraeogona* from northwestern French Guiana; *Brasiloschubartia*, and *Parastenonia* from northern Brazil (Pará state); *Cearodesmus* from northeastern Brazil (Ceará state); and *Cayenniola* from French Guiana and now, northeastern Brazil (Hoffman 1977).

With the exception of *Cearodesmus gomesi* Schubart, 1945, known from a single male specimen collected in Fortaleza, Ceará, Brazil, the greatest diversity of the Priodesmini is undoubtedly related to the Guiana Shield and the surrounding areas. *Cayenniola albaserrata* **n. sp.** indicates a putative relictual population that has survived in the ACCS, a restricted area surrounded by an arid region in the Brazilian tropical dry forest of the Caatinga Domain. In the past, members of Priodesmini were likely more widespread across the entire tropical rainforest of Brazil. Due to the historical transformations of the biome where the cave is located (Ferreira *et al.* 2023), ancestors of *C. albaserrata* **n. sp.** likely retreated to cave environments. During the Last Glacial Maximum, several areas of the Caatinga biome were covered with tropical rainforests, which may have served as habitats for the troglobitic

Accepted by D. Antić: 29 Feb. 2024; published: 25 Mar.

species' ancestors that were subsequently "trapped" inside caves following the retraction of the wet regions (Wang*et al.* 2004; Collevatti *et al.* 2013; Polhemus & Ferreira 2018). The finding of *C. albaserrata* **n. sp.** corroborates the hypothetical northeastern connection which took place during the Quaternary when mesic conditions may have favored the expansion of forested areas (Auler *et al.* 2004; Wang *et al.* 2004).

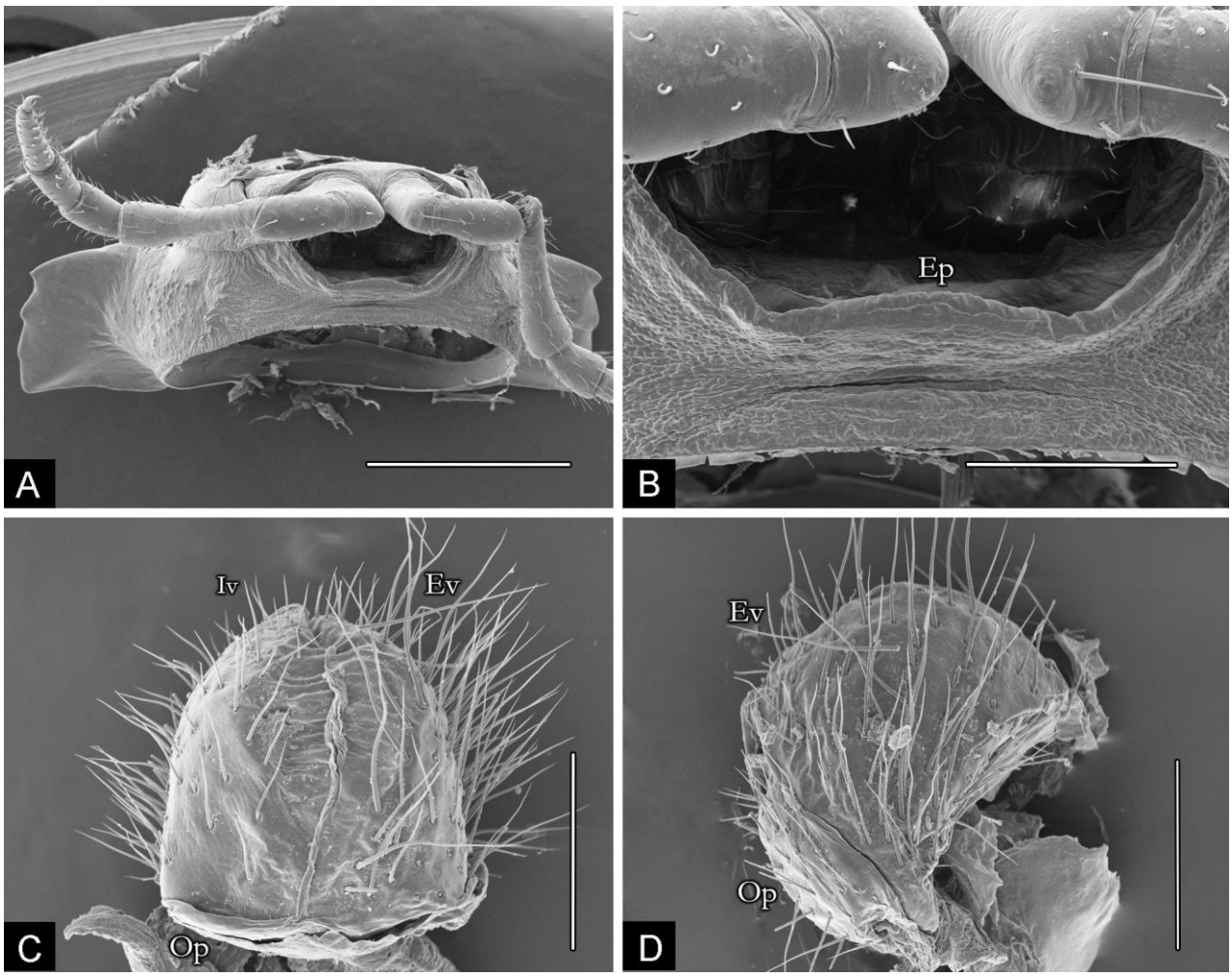


FIGURE 10. *Cayenniola albaserrata* **n. sp.**, females. **A**–**B.** (ISLA 50579), **C**–**D.** Paratype (ISLA 50593). **A.** Ring 3, ventral view. **B.** Epigynal region, ventral view. **C.** Left vulva, ventral view. **D.** Left vulva, ectal view. **Abbreviations**: **Ev**: external valve; **Iv**: internal valve; **Op**: operculum. **Scale bars: A**. 1 mm; **B**. 0.3 mm; **C, D**. 0.2 mm.

Relictual species possess high intrinsic value and hold significant potential as valuable sources of information about past diversity (Assmann *et al.* 2010; Pellens & Grandcolas 2015). Due to the ongoing extinction crisis, their significance is likely to grow in the future, emphasizing the need to conserve species not only for their ecological values but also as representatives of a valuable heritage intricately linked to the Tree of Life. Their distinctiveness makes relicts particularly valuable, and studying them can provide insights into regional and clade extinctions while serving as representatives of once large, now predominantly extinct groups (Grandcolas *et al.* 2014).

We agree with Hoffman (1977), who suggested that *C. styliger* is closely related to *Cypraeogona elisa* Hoffman, 1977 based on somatic characters, and that both genera appear more closely related to *Brasiloschubartia* than to other members of Priodesmini. While our placement of *C. albaserrata* **n. sp.** in *Cayenniola* is based on convincing morphological evidence, phylogenetic studies are needed to elucidate the relationship of this enigmatic species to other members of the Priodesmini. Due to the high degree of variability in gonopod morphology among members of the Priodesmini, Hoffman (1977) suggested that additional species of the tribe likely remain undiscovered in the Guianas and northern Brazil.

Troglomorphic traits in Chelodesmidae

Sket (2008) provided a comprehensive review of the different approaches used to define cave-restricted (troglobitic) taxa, and proposed a unified concept for all species restricted to hypogean environments. Determining whether a taxon is cave-restricted, however, remains one of the most difficult challenges faced by subterranean biologists because it requires demonstration of its absence aboveground (Ferreira *et al.* 2023). Given the high diversity of epigean environments, particularly in tropical areas, it is often impossible to determine (with any degree of certainty) whether a species is truly troglobitic. As a result, alternative approaches, such as the use of troglomorphic traits (troglomorphisms), have been proposed to identify potentially troglobitic taxa (Christiansen 1962). The presence of such traits serves as a valuable diagnostic tool for identifying troglobitic taxa, as they have presumably developed after isolation to subterranean environments. Some classical troglomorphisms, such as the absence of pigmentation, reduction or loss of eyes, and elongation of appendages, are easily recognizable, making them useful for identifying cave-restricted species. That said, some of these traits can also be observed in soil dwellers or taxa inhabiting endogenous/interstitial habitats, making it imperative to identify unique troglomorphic traits to aid in the determination of cave-restricted taxa.

Of the 25 Chelodesmidae species and subspecies reported from caves, only five are currently considered troglobitic (Bouzan *et al.* 2022). Because all species of the order Polydesmida lack eyes, the absence of eyes, a classic troglomorphic trait, cannot be used as evidence of restriction to subterranean environments in the Chelodesmidae. The few cave-restricted chelodesmid species were identified as troglobitic based on the reduction of integumental pigmentation, and thinning of the cuticle. Teneral or recently molted specimens, however, usually present such traits, and if only a single (or a few) specimen(s) have been collected, it is difficult to known whether the white body and soft cuticle are due to a recent molt or if they represent troglomorphisms. For example, despite the paucity of specimens, the recently described *Strongylosomides troglobius* from Brazil was considered a likely troglobiont due to its nearly unpigmented body and thin integument (Golovatch *et al.* 2022). The troglophilic *Obiricodesmus rupestris* Schubart, 1956 presents an interesting case with local populations exhibiting color dimorphism between cavernicolous and epigean subpopulations, with adult specimens collected from caves displaying nearly completely depigmented bodies and thin cuticles. There is, however, no indication that these are recently molted individuals (Schubart 1956; Bouzan *et al.* 2022). In fact, the determination of any chelodesmid species as one restricted to caves based solely on integumental modifications needs to be made with caution.

The relictual distribution of *C. albaserrata* **n. sp.** corroborates its restriction to caves, making it an excellent model for exploring troglomorphisms within the Chelodesmidae. In addition to the classical depigmented body, all collected adults had thin integuments, which is commonly associated with troglomorphism and further supports its classification as a troglomorphic trait. Based on our findings, the elongated antennae and legs of this species also seem to represent adaptations to a subterranean lifestyle. The enlargement of the tarsal claws of *C. albaserrata* **n. sp.** is a trait reported in only two other troglobitic chelodesmids, *Cantabrodesmus lorioli* and *L. yporangae*, although it is less pronounced in either of these taxa. Enlarged claws enable cave species to move more efficiently on moist substrates, a feature also observed in several other cave-restricted groups including spiders (Ribera *et al.* 1985), beetles (Perreau & Pavićević 2008), springtails (Ćurčić *et al.* 2007; Jantarit *et al.* 2009; Lukić *et al.* 2010; Vargovitsh 2019), and more recently, millipedes (Antić & Akkari 2023). Consequently, investigating this trait in *C. albaserrata*
n. sp. can provide a valuable insight into its adaptive value to cave life.

Accepted by D. Antić: 29 Feb. 2024; published: 25 Mar.

Conservation status

In order to investigate whether troglobitic species within the ACCS exhibit specialized niches, Souza-Silva *et al.* (2021) conducted an analysis utilizing the Outlying Marginality Index (OMI). The OMI measures the deviation between the mean values utilized by each species and the mean values available for each environmental condition, encompassing physical, trophic, and microclimatic variables. The study focused on ten troglobitic species, including arachnids, insects, and myriapods. *Cayenniola albaserrata* **n. sp.** (referred to as Chelodesmidae sp. 1) emerged as one of the most generalist species, displaying lower values of niche marginality and exhibiting a distribution closely aligned with the overall average habitat conditions, indicating a higher degree of environmental tolerance throughout the ACCS (Souza-Silva *et al.* 2021). As previously mentioned, it is important to note that individuals of

C. albaserrata **n. sp.** were frequently encountered in association with decaying logs which could be interpreted as a potential specialization to these substrates. Logs were prevalent across the majority of these caves and constituted a significant portion of the common substrate types on the cave floor.

Visitation to the ACCS caves by tourists is infrequent, resulting in minimal alteration to the cave system. However, the areas surrounding the caves have experienced significant anthropogenic impacts, which have become more pronounced in recent years (Ferreira *et al.* 2023). Consequently, concerns regarding these impacts have escalated, particularly in the light of prevailing deforestation in the region. Substantial areas of the original vegetation have been removed for the establishment of agricultural fields and for charcoal production (see Ferreira *et al.* 2023: fig. 5C, D). This practice not only diminishes the input of organic matter into the caves but also directly contributes to increased levels of siltation thereby reducing the heterogeneity of the cave microhabitats. Furthermore, pumps are frequently employed to extract water from the caves for irrigation purposes and for human and animal consumption. This practice not only contributes to a gradual decline in the water table but also poses a contamination risk, particularly when diesel pumps (the predominant type in the area) are utilized.

Ferreira *et al.* (2023) documented 31 species restricted to the ACCS, and recognized the system as the richest hotspot of subterranean biodiversity in South America. However, recent efforts (September 2023) have revealed 10 previously unknown species, raising the total count of cave-restricted taxa to 41 (Ferreira & Souza-Silva 2023). This incredible diversity makes it imperative to urgently implement conservation measures to safeguard the ACCS. We strongly advise the establishment of a conservation unit, incorporating not only the cave system but also its associated catchment micro-basins and the corresponding areas of influence. This unit should be accompanied by stringent regulations and restrictions to ensure the comprehensive protection of the entire ecosystem.

Acknowledgments

We thank Beatriz Mauricio (Laboratório de Biologia Celular of the Instituto Butantan) for her help with the SEM imaging. We would like to thank the reviewers, Dr. Henrik Enghoff and Dr. Derek Hennen, and the editor, Dr. Dragan Antić, for their valuable suggestions and corrections that significantly improved the manuscript. This study was financially supported by Coordenação de Aperfeiçoamento de Pessoal de Nível Superior (CAPES; 88887.510007/2020-00) grant to RSB; Conselho Nacional de Desenvolvimento Científico e Tecnológico (CNPq) grant to LFMI (162977/2020-4) and ADB by the grant from CNPq (303903/2019-8). The authors would like to thank the Centro Nacional de Pesquisa e Conservação de Cavernas—CECAV and Instituto Brasileiro de Desenvolvimento e Sustentabilidade—IABS for the financial support (TCCE ICMBio/Vale 01/2018). We are also thankful to the CNPq (National Council for Scientific and Technological Development, grant n. 302925/2022-8) for the productivity scholarship provided to R.L.F., and to the team from the Center of Studies in Subterranean Biology (CEBS/UFLA) for their support in the field.

Accepted by D. Antić: 29 Feb. 2024; published: 25 Mar.

References

Ab'Saber, A.N. (1977) Os domínios morfoclimáticos na América do Sul: primeira aproximação. *Geomorfologia*, 53, 1–23.

Andrade-Lima, D. (1982) Present-day forest refuges in northeastern Brazil. *In*: Prance, G.T. (Ed.), *Biological diversification in the Tropics.* Columbia University Press, New York, New York, pp. 245–251.

Antić, D. & Akkari, N. (2023) The genus *Inversotyphlus* Strasser, 1962, stat. nov. and *Inversotyphlus ammirandus* sp. nov., a new bizarre, highly modified troglobiotic millipede (Diplopoda, Julida, Julidae) from Albania, Balkan Peninsula. *ZooKeys*, 1184, 65–80. https://doi.org/10.3897/zookeys.1184.113498

Akkari, N., Gilgado, J.D., Ortuño, V. & Enghoff, H. (2018) Out of the dark void: *Ommatoiulus longicornis* n. sp., a new julid from Spain (Julida, Diplopoda) with notes on troglobiomorphic traits in millipedes. *Zootaxa*, 4420 (3), 415–429. https://doi.org/10.11646/zootaxa.4420.3.7

Assmann, T., Casale, A., Drees, C., Habel, J.C., Matern, A. & Schuldt, A. (2010) Review: The Dark Side of Relict Species Biology: Cave Animals as Ancient Lineages. *In:* Habel, J.C. & Assmann, T. (Eds.), *Relict Species.* Springer, Berlin, Heidelberg, pp. 91–103. https://doi.org/10.1007/978-3-540-92160-8_4

Attems, C.G. (1898) System der Polydesmiden. I. *Theil. Denkschriften der Kaiserlichen Akademie der Wissenchaften zu Wien, Mathematisch-Naturwissenschaftliche Classe*, 67, 221–482.

Attems, C.G. (1938) Myriapoda 3. Polydesmoidea II. Fam. Leptodesmidae, Platyrhachidae, Oxydesmidae, Gomphodesmidae.

Das Tierreich, 69, 1–487. https://doi.org/10.1515/97 83111430645

Auler, A.S., Wang, X., Edwards, R.L., Cheng, H., Cristalli, P.S., Smart, P.L. & Richards, D.A. (2004) Quarternary ecological and geomorphic changes associated with rainfall events in presently semi-arid northeastern Brazil. *Journal of Quaternary Science*, 19, 693–701. https://doi.org/10.1002/jqs.876

Barr, T.C. (1985) Pattern and process in speciation of trechine beetles in Eastern North America (Coleoptera: Carabidae: Trechinae). *In:* Ball, G.E. (Ed.), *Taxonomy, phylogeny and zoogeography of beetles and ants.* Dr. W. Junk Publishers, Dordrecht, pp. 350–407.

Batalha-filho, H., Fjeldsa, J., Fabre, P. & Miyaki, C.Y. (2013) Connections between the Atlantic and the Amazon forest avifaunas represent distinct historical events. *Journal of Ornithology*, 154, 41–50. https://doi.org/10.1007/s10336-012-0866-7

Bouzan, R.S., Pena-Barbosa, J.P.P. & Brescovit, A.D. (2017) Taxonomic review of the genus *Atlantodesmus* Hoffman, 2000 (Polydesmida: Chelodesmidae). *Zootaxa*, 4236 (2), 269–290. https://doi.org/10.11646/zootaxa.4236.2.3

Bouzan, R.S., Iniesta, L.F.M., Souza, C.A.R., Zampaulo, R.A. & Brescovit, A.D. (2019) Taxonomic review of the Amazonian millipede genus *Parastenonia* Hoffman, 1977 and description of a new species from iron-ore caves (Polydesmida: Chelodesmidae). *Journal of Natural History*, 53, 2781–2799. https://doi.org/10.1080/00222933.2020.1749956

Bouzan, R.S., Means, J.C., Ivanov, K., Ferreira, R.L., Brescovit, A.D. & Iniesta, L.F.M. (2022) Worldwide distribution of cave- dwelling Chelodesmidae (Diplopoda, Polydesmida). *International Journal of Speleology*, 51, 235–248. https://doi.org/10.5038/1827-806X.51.3.2448

Brölemann, H.W. (1900) Dous myriapodos notáveis do Brazil, Notas myriapodologicas. *Boletim do Museu Paraense de História Natural e Ethnographia*, 3, 65–71.

Brölemann, H.W. (1916) Essai de classification des Polydesmiens. *Annales de la Société Entomologique de France*, 84, 523– 608.

Cook, O.F. (1895) *Priodesmus*, a new genus of Diplopoda from Surinam. *Proceedings of the US National Museum*, 18, 53–57. https://doi.org/10.5479/si.00963801.18-1037.53

Cook, O.F. (1896) A new diplopod fauna in Liberia. *American Naturalist*, 30, 413–420. https://doi.org/10.1086/276402

Cook, O.F. & Collins, G.N. (1895) The Craspedosomatidae of North America. *Annals of the New York Academy of Sciences*, 9, 1–100. https://doi.org/10.1111/j.1749-6632.1896.tb55430.x

Accepted by D. Antić: 29 Feb. 2024; published: 25 Mar.

Collevatti, R.G., Terribile, L.C., de Oliveira, G., Lima-Ribeiro, M.S., Nabout, J.C., Rangel, T.F. & Diniz-Filho, J.A.F. (2013) Draw-backs to palaeodistribution modelling: The case of South American seasonally dry forests. *Journal of Biogeography*, 40, 345–358. https://doi.org/10.1111/jbi.12005

Costa, L.P. (2003) The historical bridge between the Amazonia and the Atlantic Forest of Brazil: a study of molecular phylogeography with small mammals. *Journal of Biogeography*, 30, 71–86. https://doi.org/10.1046/j.1365-2699.2003.00792.x

Christiansen, K.A. (1962) Proposition pour la classification des animaux cavernicoles. *Spelunca*, 2, 75–78.

Culver, D.C. & Pipan, T. (2014) *Shallow subterranean habitats: ecology, evolution, and conservation.* Oxford University Press, New York, New York, 258 pp. https://doi.org/10.1093/acprof:oso/9780199646173.001.0001

Ćurčić, P.M., Lučić, L.R., Tomić, V.T., Makarov, S.E. & Karaman, I.M. (2007) *Galeriella liciniana*, a new cave genus and species of springtails (Collembola, Sminthuridae) from Herzegovina. *Archives of Biological Sciences*, 59 (4), 63–64. https://doi.org/10.2298/ABS0704063C

Ferreira, R.L. & Souza-Silva, M. (2023) Beyond Expectations: Recent Discovery of New Cave-Restricted Species Elevates the Água Clara Cave System to the Richest Hotspot of Subterranean Biodiversity in the Neotropics. *Diversity*, 15, 1215 (1–8). https://doi.org/10.3390/d15121215

Ferreira, R.L., Berbert-Born, M., Souza-Silva, M. (2023) The Água Clara Cave System in Northeastern Brazil: The Richest Hotspot of Subterranean Biodiversity in South America. *Diversity*, 15, 761–784. https://doi.org/10.3390/d15060761

Grandcolas, P., Nattier, R. & Trewick, S.A. (2014) Relict species: a relict concept? *Trends in Ecology & Evolution*, 29 (12), 655–663. https://doi.org/10.1016/j.tree.2014.10.002

Gervais, P. (1844) Études sur les Myriapodes. *Annales des Sciences naturelles*, Série 3, 2, 51–80.

Golovatch, S.I., Bouzan, R.S., Gallo, J.S. & Bichuette, M.E. (2022) A new genus and two new species of the millipede family Chelodesmidae from Bahia state, northeastern Brazil, including a likely troglobiont (Diplopoda, Polydesmida). *Zootaxa*,5155 (1), 087–104. https://doi.org/10.11646/zootaxa.5155.1.4

Jones, T.R. (1847) Myriapoda. *In*: Todd, R.B. *The cyclopædia of anatomy and physiology. Vol.* 3. Sherwood, Gilbert, and Piper, London, pp. 544–560.

Hoffman, R.L. (1969) Chelodesmid studies. IV. A summary of the tribe Batodesmini, with the description of a new species of

Biporodesmus from northwestern Brazil. *Papéis Avulsos de Zoología*, 22 (25), 263–283.

Hoffman, R.L. (1977) Chelodesmid studies. X. A synopsis of the tribe Priodesmini (Diplopoda: Polydesmida). *Revue Suisse de Zoologie*, 84 (2), 349–359.

Hoffman, R.L. (1980) *Classification of the Diplopoda*. Múseum d'histoire naturelle, Genève, 237 pp.

Hoffman, R.L. (1982) Chelodesmid studies. XVIII. On some new or poorly-known taxa in the tribe Batodesmini (Polydesmida: Chelodesmidae). *Journal of Natural History*, 16, 633–654. https://doi.org/10.1080/00222938200770481

Iniesta, L.F.M., Ferreira, R.L. & Wesener, T. (2012) The first troglobitic *Glomeridesmus* from Brazil, and a template for a modern taxonomic description of Glomeridesmida (Diplopoda). *Zootaxa*, 3550 (1), 26–42. https://doi.org/10.11646/zootaxa.3550.1.2

Jantarit, S., Satasook, C. & Deharveng, L. (2019) *Coecobrya sirindhornae* sp. n., the most highly troglomorphic Collembola in Southeast Asia (Collembola, Entomobryidae). *ZooKeys*, 824, 21–44. https://doi.org/10.3897/zookeys.824.31635

Jeekel, C.A.W. (1963) Diplopoda of Guiana (1–5). *Studies on the Fauna of Suriname and Other Guyanas*, 4, 1–157.

Koch, M. (2015) General morphology. *In:* Minelli, A., editor. Treatise on Zoology - Anatomy, Taxonomy, Biology. *Vol. 2, The Myriapoda*. Brill, Leiden and Boston, pp. 7–68. https://doi.org/10.1163/9789004188273_003

Ledo, R.M.D. & Colli, G.R. (2017) The historical connections between the Amazonia and the Atlantic Forest revisited. *Journal of Biogeography*, 44 (11), 2551–2563. https://doi.org/10.1111/jbi.13049

Liu, W., Golovatch, S., Wesener, T. & Tian, M. (2017) Convergent Evolution of Unique Morphological Adaptations to a Subterranean Environment in Cave Millipedes (Diplopoda). *PLoS ONE*, 12 (2), e0170717. https://doi.org/10.1371/journal.pone.0170717

Accepted by D. Antić: 29 Feb. 2024; published: 25 Mar.

Loomis, H.F. (1977) Three new millipeds from West Indian caves. *Florida Entomologist*, 60 (1), 21–25. https://doi.org/10.2307/3494479

Lukić, M., Houssin, C. & Deharveng, L. (2010) A new relictual and highly troglomorphic species of Tomoceridae (Collembola) from a deep Croatian cave. *ZooKeys*, 69, 1–16. https://doi.org/10.3897/zookeys.69.739

Lomolino, M.V., Riddle, B.R. & Brown, J.H. (2006) *Biogeography*. Sinauer Associates, Sunderland, Massachusetts, 845 pp. Mauriès, J.-P. (1971) Diplopodes épigés et cavernicoles des Pyrénées espagnoles et des Monts Cantabriques. VI. Polydesmides. *Bulletin de la Sociétè d'histoire naturelle de Toulouse*, 107, 117–124.

Oliveira-Filho, A.T. & Ratter, J.A. (1995) A study of the origin of central Brazilian forests by the analysis of plant species distribution patterns. *Edinburgh Journal of Botany*, 52 (1), 141–194. https://doi.org/10.1017/S0960428600000949

Pellens, R. & Grandcolas, P. (2015) *Biodiversity Conservation and Phylogenetic Systematics: Protecting Species in a Major Extinction Crisis*, Springer, Paris, 395 pp. https://doi.org/10.1007/978-3-319-22461-9

Pena-Barbosa, J.P.P., Sierwald, P. & Brescovit, A.D. (2013) On the largest chelodesmid millipedes: taxonomic review and cladistic análisis of the genus *Odontopeltis* Pocock, 1894 (Diplopoda; Polydemsida; Diplopoda). *Zoological Journal of the Linnean Society*, 169 (4), 737–764. https://doi.org/10.1111/zoj.12086

Perreau, M. & Pavićević, D. (2008) The genus *Hadesia* Müller, 1911 and the phylogeny of Anthroherponina (Coleoptera, Leiodidae, Cholevinae, Leptodirini). Advances in the studies of the fauna of the Balkan Peninsula. *Papers dedicated to the memory of Guido Nonveiller. Institute for Nature Conservation of Serbia, monographs*, 22, 215–239.

Pocock, R.I. (1887) On the classification of the Diplopoda. *Annals and Magazine of Natural History*, 20, 283–295. https://doi.org/10.1080/00222938709460057

Polhemus, D.A. & Ferreira, R.L. (2018) Two unusual new genera of cavernicolous Hydrometridae (Insecta: Heteroptera) from eastern Brazil. *Tijdschrift voor Entomologie*, 161 (1), 25–38. https://doi.org/10.1163/22119434-00002072

Por, F.D. (1992) *Sooretama: the Atlantic rain forest of Brazil*. SPB Academic Publishing, The Hague, 130 pp.

Raven, P.H. & Axelrod, D.I. (1974) Angiosperm biogeography and past continental movements. *Annals of the Missouri Botanical Garden*, 61, 539–573. https://doi.org/10.2307/2395021

Ribera, C., Ferrandez, M.A. & Blasco, A. (1985) Araneidos cavernicolas de Canarias II. *Mémoires De Biospéologie*, 12, 51– 66.

Schubart, O. (1945) Alguns Diplópodos novos do Ceará colecionados por Alcides L. Gomes. *Revista Brasileira de Biologia*, 5 (2), 275–281.

Schubart, O. (1946) Primeira contribuição sôbre os Diplópodos cavernícolas do Brasil. *Livro de homenagem a R. F. d'Almeida*, 37, 307–314.

Schubart, O. (1955) Materiais para uma fauna do Estado de Sao Paulo - os Leptodesmidae. *Arquivos do Museu Nacional*, 42, 507–540.

Schubart, O. (1956) "Leptodesmidae" Brasileiras. III: Espécies de Minas Gerais (Diplopoda, Proterospermophora). *Revista Brasileira de Biologia*, 16, 355–367.

Shelley, R.M. & Smith, J.M. (2018) Expanded concept and revised taxonomy of the milliped family Xystodesmidae Cook, 1895 (Polydesmida: Leptodesmidea: Xystodesmoidea): incorporations of Euryuridae Pocock, 1909 and Eurymerodesmidae Causey, 1951, taxon revivals/proposals/transferrals, and a distributional update. *Insecta Mundi*, 0660, 1–41.

Sket, B. (2008) Can we agree on an ecological classification of subterranean animals? *Journal of Natural History*, 42 (21–22), 1549–1563. https://doi.org/10.1080/00222930801995762

Souza-Silva, M., Cerqueira, R.F.V., Pellegrini, T.G. & Ferreira, R.L. (2021) Habitat selection of cave-restricted fauna in a new hotspot of subterranean biodiversity in Neotropics. *Biodiversity and Conservation*, 30, 4223–4250. https://doi.org/10.1007/s10531-021-02302-8

Accepted by D. Antić: 29 Feb. 2024; published: 25 Mar.

Vargovitsh, R.S. (2019) Cave water walker: an extremely troglomorphic *Troglaphorura gladiator* gen. et sp. nov. (Collembola, Onychiuridae) from Snezhnaya Cave in the Caucasus. *Zootaxa*, 4619 (2), 267–284. https://doi.org/10.11646/zootaxa.4619.2.4

Wang, X., Auler, A.S., Edwards, R.L., Cheng, H., Cristalli, P.S., Smart, P.L., Richards, D.A. & Shen, C.C. (2004) Wet periods in northeastern Brazil over the past 210 kyr linked to distant climate anomalies. *Nature*, 432, 740–743. https://doi.org/10.1038/nature03067

Supplementary Material

Morphobank<https://morphobank.org/index.php/Projects/ProjectOverview/project_id/5120>

Accepted by D. Antić: 29 Feb. 2024; published: 25 Mar.

COLLEMBOLA



insects

MDPI

Article

A Highly Troglomorphic New Genus of Sminthuridae (Collembola, Symphypleona) from the Brazilian Semiarid Region †

Paolla Gabryelle Cavalcante de Souza [1], Gleyce da Silva Medeiros [1,*], Rodrigo Lopes Ferreira [2], Marconi Souza-Silva [2] and Bruno Cavalcante Bellini [1,*]

[1] Department of Botany and Zoology, Biosciences Center, Federal University of Rio Grande do Norte (UFRN), Highway BR-101, Lagoa Nova, Campus Universitario, Natal 59072-970, RN, Brazil; paollasouzac@gmail.com

[2] Centro de Estudos em Biologia Subterrânea, Departamento de Ecologia e Conservação, Instituto de Ciências Naturais, Universidade Federal de Lavras (UFLA), Lavras 37200-900, MG, Brazil; drops@ufla.br (R.L.F.); marconisilva@ufla.br (M.S.-S.)

* Correspondence: gleycemedeiros96@gmail.com (G.d.S.M.); entobellini@gmail.com (B.C.B.)

† This published work and the nomenclatural acts it contains have been registered in ZooBank, the online registration system for the ICZN (International Code of Zoological Nomenclature). The LSID (Life Science Identifier) for this publication is: urn:lsid:zoobank.org:pub:36547434-6C1B-45C3-A93E-EBF51E11D6FD.

Simple Summary: A new genus and species of cave springtail are herein described. The new species has a remarkable morphology, suggesting it evolved within caves, such as the appendages and chaetae elongation, loss of body pigments, and 5 + 5 eyes reduced in size. The new species may also be occasionally cannibalistic, as one of the analyzed females devoured another male from her species.

check for updates

Citation: de Souza, P.G.C.; Medeiros, G.d.S.; Ferreira, R.L.; Souza-Silva, M.; Bellini, B.C. A Highly Troglomorphic New Genus of Sminthuridae (Collembola, Symphypleona) from the Brazilian Semiarid Region. *Insects* **2022**, *13*, 650. https://doi.org/10.3390/insects13070650

Academic Editor: Marco Gebiola

Received: 10 June 2022
Accepted: 7 July 2022

Published: 19 July 2022

Publisher's Note: MDPI stays neutral with regard to jurisdictional claims in published maps and institutional affil- iations.

Copyright: © 2022 by the authors. Licensee MDPI, Basel, Switzerland. This article is an open access article distributed under the terms and conditions of the Creative Commons Attribution (CC BY) license (https://creativecommons.org/licenses/by/ 4.0/).

Abstract: Here, we describe the highly troglomorphic *Troglobentosminthurus* gen. nov. from Água Clara cave system, Caatinga domain, Bahia, Brazil. *Troglobentosminthurus luridus* gen. nov. sp. nov. has remarkably long antennae, legs and furca, and lacks body pigments, except for small orange eye patches which also show a reduction in the number of eyes (5 + 5) and lens sizes. The overall morphology of the genus, with long and highly sub-segmented antennae, resembles other Sminthurinae of the *Temeritas*-group, especially *Temeritas* Richards and *Galeriella* C´ urc˘ic´ and Luc˘ic´. However, it is unique, especially in the combination of the number of antennae IV subsegments and eyes, frontal head chaetotaxy and empodial complex morphology. Two type specimens have remnants of a mite and another specimen from the new species in their gut contents, supporting the species may be occasional predators and even cannibals. We also provide identification keys and comparative tables to the subfamilies of Sminthuridae and the *Temeritas*-group of genera.

Keywords: Neotropical Region; new species; Sminthurinae; Sminthuroidea; *Temeritas*-group

1. Introduction

The knowledge on the Brazilian Symphypleona strongly increased during the past two decades. In 2003, there were only 40 species recorded in the entire country, while in 2022, there are 73 nominal species recognized in Brazil [1,2]. Similarly to the Poduromorpha and Entomobryomorpha, this remarkable rise in the taxonomic understanding of the Symphypleona was mainly due to the description of new species rather than the register of previously described taxa from other countries [2]. In this context, the Brazilian fauna of Symphypleona is unique, with 57 endemic species (about 78% of its total), as well as some genera only found in Brazil, like *Arborianna* Bretfeld, 2002 [3] (Katiannidae), *Keratosminthurus* Zeppelini 2020 in [4], and *Varelasminthurus* Silva, Palacios-Vargas and Bellini, 2015 [5] (both Sminthuridae).

The cave fauna of Brazilian springtails is mainly represented by species of *Acherontides* Bonet, 1945 [6] (Poduromorpha); *Cyphoderus* Nicolet, 1842 [7], *Troglobius* Palacios-Vargas

and Wilson, 1990 [8], *Trogolaphysa* Mills, 1938 [9], *Pseudosinella* Schäffer, 1897 [10], *Coecobrya* Yosii, 1956 [11] (Entomobryomorpha); *Arrhopalites* Börner, 1906 [12], *Pararrhopalites* Bonet and Tellez, 1947 [13] and *Keratosminthurus* (Symphypleona), summing up more than 40 species [2,4,14–21]. Although many recent efforts aimed to describe the Brazilian cave fauna of Collembola, as in [4,15,16,18,19,21], it is noteworthy that most subterranean ecosys- tems in the country are undersampled for invertebrates in general (including the springtails fauna), especially in the semiarid landscapes. On the other hand, preliminary data supports that the Caatinga, a unique semiarid domain only found in Brazil, can host complex cave systems which shelter a high number of troglomorphic endemic invertebrates, many of them potentially troglobitic [22,23].

Sminthuridae Lubbock, 1862 is the largest and one of the most widely distributed families of Symphypleona [24]. Due to its species and genera richness, different attempts were made to break it into subfamilies [4,25–27]. Currently, this family is subdivided into: Sminthurinae Lubbock, 1862, with long antennae (mostly longer than the body), frequently lacking neosminthuroid chaetae on the parafurcal area and without cavities on the ungues, tibiotarsi with 8–9 chaetae on the distal (apical) whorl and 9–15 ventral (anterior) dental chaetae; Sphyrothecinae Betsch, 1980, with short antennae (smaller than the body), with a pair of neosminthuroid chaetae on the parafurcal area, tibiotarsi with 7 or

Sánchez-García and Engel, 2016, with antennal size and ventral dental chaetotaxy variable, more chaetae on the distal whorl, and dens with 6 or less ventral chaetae; and Songhaicinae parafurcal area with or without neosminthuroid chaetae, tibiotarsi with six or fewer chaetae on the distal whorl and, more importantly, ungues with cavity and tunica, or only with a peculiar filament-like tunica [4,26–28]. The variety of morphologies gathered within Songhaicinae, with overlapping features also observed in the other two subfamilies, raises doubts about its validity, similarly to some intersecting morphology shared by some genera of Sminthuridae [4,27,29].

genus of Symphypleona regarding appendages elongation, from the Água Clara cHere, we describe *Troglobentosminthurus* gen. nov., one of the most troglomorphic system, Caatinga domain, Bahia state, Brazil. We also compare it with other similar

genera and provide notes on its morphology and the boundaries of Sminthuridae and Bourletiellidae Börner, 1913. Finally, we provide information on the species' habitat, biology and threats.

2. Materials and Methods

dark zones of Água Clara cave system (more details in topic 3.3, habitat and threats), Specimens were collected manually with entomological brushes and ethanol in the preserved in 70% ethanol at 6 ˚C, cleared in Nesbitt's solution, washed in Arlé's liquid and mounted on glass slides in Hoyer medium, mixing [30,31] procedures. Ethanol-

fixed specimens were photographed in a Nikon SMZ1500 stereomicroscope with a DS-Ri1 camera, under NIS-Elements AR v.4.51 software. Morphological studies and first drawings were made under Leica DM750 phase-contrast microscope, with an attached drawing tube. Final drawings were vectorized in Adobe Illustrator 2020 software. The type series was deposited at the Collection of Subterranean Invertebrates of Lavras (ISLA), linked to the Center for Studies in Subterranean Biology from the Federal University of Lavras (biologiasubterranea.com.br (accessed on 10 June 2020)).

The terminology used in the text and figures follows [32] to labial palp papillae and guard-chaetae, [33] to the labral chaetotaxy, [34] to the head and anterior large abdomen chaetotaxy, Vargovitsh system [35–37] with adaptations for the posterior large abdomen chaetotaxy, [38] for the small abdomen chaetotaxy, and [39] to part of the tibiotarsal chaeto- taxy. Regarding the dens we considered the dorsal, dorso-internal and dorso-lateral rows summed as the dorsal chaetotaxy. Drawings and observations were made based on the entire type series.

The abbreviations used in the description and figures are: Abd.—abdominal seg- ment(s); Ant.—antennal segment(s); Th.—thoracic segment(s). In the drawings, structures

present or absent are marked with white arrows, and unpaired chaetae on the head and trunk are marked with a "*". Ant. IV subsegments are counted from the base to apex. Head, trunk (thorax + abdomen) and furca description of the chaetotaxy is given by half body. Chaetae and labial papillae labels are marked in bold in the text.

3. Results

3.1. Taxonomic Summary and Subfamily Diagnosis

Order Symphypleona Börner, 1901 [40] *sensu* Bretfeld, 1986 [41]
Suborder Appendiciphora Bretfeld, 1986 [41]
Superfamily Sminthuroidea Bretfeld, 1994 [42]
Family Sminthuridae Lubbock, 1862 [43]
Subfamily Sminthurinae Lubbock, 1862 [43] *sensu* Bretfeld, 1999 [26]

Diagnosis of the subfamily. Antennae long, subequal or longer than the body, Ant. IV with 9–46 subsegments, Ant. II with or without 1 ventrolateral sensillum. Neosminthuroid chaetae mostly absent in the parafurcal area, with the exception of *Keratosminthurus*. Tibiotarsi distal whorl with 8–9 chaetae, pretarsi mostly with 2 chaetae, rarely with only the anterior chaeta, ungues without cavity or filament-like tunica. Dens with 9–15 ventral chaetae, mucro apically symmetrical, rarely asymmetrical (updated from [4,25–27]).

Remarks. Here, we complement Zeppelini et al. [4] diagnosis of the Sminthurinae due to some findings concerning the new genus and species. Bretfeld [26] pointed out that the Sminthuridae always have one pair of pretarsal chaetae, contrarily to the Bourletiellidae, which only present a single chaeta—the anterior one. However, at least *Varelasminthurus potiguarus* Silva, Palacios-Vargas and Bellini, 2015 [5], *Disparrhopalites naasaveqw* Bernard and Wynne 2017 [27] (both Songhaicinae), and now *Troglobentosminthurus luridus* gen. nov. sp. nov. (Sminthurinae) may have only the anterior pretarsal chaeta. We also observed the new species presents one ventro-lateral sensillum at the apex of the Ant. II, similar to a bothriotrichum, a feature described as a synapomorphy of the Bourletiellidae by Bretfeld [26]. However, at least *Stenognathriopes* (*Tenentiella*) *janssensi* Zeppelini and Silva 2012 [44] (Bourletiellinae Börner, 1913) does not have such morphology. It is worth noting that, although the pretarsal and antennal morphology of *Troglobentosminthurus luridus* gen. nov. sp. nov. resembles the Bourletiellidae, the new species belongs to Sminthurinae due to the absence of the Abd. V bothriotrichum **E** and of spatulate tenent- hairs on the tibiotarsi, and large abdomen bothriotricha **A**–**C** misaligned. Due to these observations, we included the absence of one pretarsal chaeta and the presence of an apical bothriotrichum-like sensillum on Ant. II as possible features also observed within the Sminthuridae (Sminthurinae), and not exclusive of the Bourletiellidae. Table 1 and the key below summarizes the main differences between the Sminthuridae subfamilies.

Key to the subfamilies of Sminthuridae Lubbock, 1862 [43]

1. Ungues with cavity and/or a filament-like tunica, tibiotarsal distal whorl with six or fewer chaetae . . . . . Songhaicinae Sánchez-García and Engel, 2016 [28] *sensu* Bernard and Wynne, 2017 [27]
-. Ungues without cavity or a filament-like tunica, tibiotarsal distal whorl with 7–9 chaetae 2
2. Antennae shorter than the body, males' Abd. VI with a pair of spines similar to the subanal appendages of the females, dens ventrally with 0–6 chaetae ..... Sphyrothecinae Betsch, 1980 [25] *sensu* Bretfeld, 1999 [26]
-. Antennae subequal or longer than the body, males' Abd. VI without subanal appendages-like spines, dens ventrally with 9–15 chaetae Sminthurinae Lubbock, 1862 [43] *sensu* Bretfeld, 1999 [26]

Table 1. Comparison between the subfamilies of Sminthuridae.

Subfamilies/ Features	Antennae/Body Ratio	Ant. IV Subsegments	Distal Whorl of Chaetae on Tibiotarsi	Pretarsal Chaetae	Ungues with Cavity and/or a Filament-Like Tunica	Neosminthuroid Chaetae on the Parafurcal Area	Males' Abd. VI Ventrally with a Pair of Spines	Dens Ventral Chaetae	Mucronal Apex
Sminthurinae	=/(>)	9–46	8–(9)	1–(2)	–	+/(−)	–	9–15	(sym)/asym
Songhaicinae	variable	10–26	6 or less	1–(2)	+	+/(−)	–	5–13	sym
Sphyrothecinae	<	0–12 *	7–9	2	–	+	+	0–6	asym

Data based in: [4,5,25–27,29,45–50] and the new genus herein described. Only extant genera were considered. Legends: '+' present, '−' absent, '=' subequal; '>' longer than; '<' shorter than; 'sym' symmetrical; 'asym'; asymmet- rical; '( )' more commonly seen; '*' subsegments on the Ant. IV of the Sphyrothecinae may be somewhat vestigial.

3.2. Troglobentosminthurus gen. nov. Bellini, Medeiros and Souza

Diagnosis of the genus. Appendages remarkably elongated. Chaetae smooth and long, especially on antennae, tibiotarsi and posterior large abdomen, spine-like chaetae absent on head frontal area and dorsal large abdomen. Most chaetae alveoli slightly elongated, somewhat neosminthuroid-like, on the body and appendages. Ant. IV *Temeritas*-like, longer than the body combined with Ant. I–III, with 44 subsegments, Ant. II apically with one ventro-lateral bothriotrichum-like sensillum. Antennae and head chaetotaxy not sexually dimorphic. Mouthparts normal, not elongated, labial palp guard-chaeta **a1** laterally displaced and curved. Large abdomen without dorsal vesicles, small abdomen formed by Abd. V–VI. Bothriotricha **A**–**D** present and elongated, especially **D,** longer than the dens. Parafurcal area without sexually dimorphic or neosminthuroid chaetae. Trochanter III with a large spine in a rounded alveolus, tibiotarsi I–III distal whorls with 8/9/9 chaetae, respectively, pretarsi I–III with only a small anterior chaeta, ungues without cavity and tunica, but with underdeveloped pseudonychia, unguiculi without the apical filament. Ventral tube sacs warty, tenaculum with 1 + 1 distal chaetae. Dens ventral formula from the apex to the basis as 3, 2, 2, 1 . . . 1, mucro without chaeta, with the inner lamella serrated and the outer smooth, mucronal apex symmetric.

Etymology. The new genus honors our dear friend, the emergent skillful biospeleologist Dr. Diego de Medeiros Bento, nicknamed "Troglobento". Diego works at the National Center for Cave Research and Conservation (ICMBio/CECAV), tracking, mapping and studying caves and cave fauna in Brazil, mainly in the semiarid region of Rio Grande do Norte state, Brazil. His efforts, as well as those of many other professionals working for CE- CAV and other entities, helped to reveal and preserve several Brazilian caves. Contrary and irresponsibly, the Brazilian president signed in 2022 the federal decree 10,935, which enables the destruction of even the most relevant caves in Brazil for commercial purposes, putting at risk such efforts. Thus, the new genus honors not only Dr. Diego Bento but also many other Brazilian professionals committed to the conservation of underground environments. *Remarks.* The overall morphology of the new genus puts it within the *Temeritas*-group *sensu* Medeiros et al. [29], which gathers *Temeritas* Richards, 1963 in [51], *Richardsitas* Betsch, 1975 [52], *Galeriella* Ć urc˘ic´ and Luc˘ic´, 2007 in [53], and *Keratosminthurus*. This group of genera and *Troglobentosminthurus* gen. nov. share: antennae mostly longer than the body, Ant. IV with 18–46 subsegments, post-antennal chaeta absent and metatrochanteral spine present. The Ant. IV with 44 subsegments, presence of eyes, head without sexually di- morphic features, large abdomen lacking spines but with slender chaetae, parafurcal area without neosminthuroid chaetae and tibiotarsi without capitate tenent-hairs put the new

genus closer to *Temeritas stricto sensu* Medeiros and Bellini [54]. However, *Temeritas* differs from *Troglobentosminthurus* gen. nov. especially in the frontal area of the head with spines (vs. absent), unguiculi with the apical filament (vs. without), dens ventrally with 13 chaetae (vs. 9), specimens pigmented, mostly with complex color patterns (vs. lacking pigments), eyes 8 + 8 and normally developed (vs. 5 + 5 reduced eyes) [54]. The highly troglomorphic profile of *Troglobentosminthurus* gen. nov. strongly resembles that of *Galeriella*, a mono- typic cave genus only recorded from Bosnia and Herzegovina [53,55], but *Galeriella* differs from *Troglobentosminthurus* gen. nov. in Ant. IV with 32 subsegments (vs. 44), eyes ab- sent (vs. 5 + 5), ungues without teeth and pseudonychia (vs. present), tenaculum without chaetae (vs. 1 + 1) and mucro with both lamellae serrated (vs. only one). The distribution supports these genera emerged independently as well, since *Galeriella* was only found in the Balkan Peninsula, Palaearctic Region, and the new genus in the southern region of Caatinga Domain, Neotropical Region. *Galeriella* also presents a remarkably underdeveloped chaeto- taxy, different from most Sminthurinae, including the *Temeritas*-group, which suggests that the two type specimens, listed as males, may be juveniles, or at least that some chaetae at the proximal antennal articles, head, tibiotarsi and ventral dens may have been overlooked in the original description [53]. Such doubts prevent us from better comparing the genus with *Troglobentosminthurus* gen. nov. Further comparisons between the *Temeritas*-group genera are presented in Table 2 and the identification key below.

Although the antennal elongation of *Troglobentosminthurus* gen. nov. is supposedly linked to the cave life, it may also be the result, at least partially, of a shared ancestral with *Temeritas*, which also have long and subsegmented Ant. IV, but live in epigeic ecosys- tems [54]. Morphology, as previously discussed, and distribution support this hypothesis. There are currently 12 species of Neotropical *Temeritas*, with seven of them registered from Brazil, of which three were also found in the Caatinga domain [2,54]. Nevertheless, only a phylogenetic study could test if *Troglobentosminthurus* gen. nov. and *Temeritas* are closely related.

The elongation of the tibiotarsi in the new genus splits the chaetae on each whorl following Nayrolles [39], suggesting at first that the distal whorl is similar to the Songhaici- nae with only five or six chaetae. However, a more detailed study of the homology of the tibiotarsal chaetotaxy shows they fit the diagnosis of Sminthurinae, with 8/9/9 chaetae on tibiotarsi I–III, respectively, and three chaetae occur on the upper region of the distal tibiotarsi (see more details in the description of the new species). Other peculiar details on the morphology of the new genus are: the labial palp papillae similar to that of *Sminthurus* Latreille, 1802 [56] and *Disparrhopalites naasaveqw*, with the **a1** guard-chaeta large, api- cally curved and laterally displaced, almost or clearly external to the papilla **C** [27,32], a trait not reported to any *Temeritas*, *Richardsitas* or *Keratosminthurus* species (unknown to *Galeriella*) [4,29,54]; the absence of the posterior pretarsal chaeta, only recorded before within Sminthuridae to the Songhaicinae genera *Varelasminthurus* and *Disparrhopalites* Stach, 1956 [5,27,57]; and the Ant. II apically with one ventro-lateral bothriotrichum-like sensillum, a feature previously only observed in the Bourletiellidae [26].

Accepted by D. Antić: 29 Feb. 2024; published: 25 Mar.

Table 2. Comparison between the genera of the *Temeritas*-group (updated from [29]).

Genera/ Features	Ant. IV Subsegments	Eyes	Head Sexual Dimorphism	Antennae Sexual Dimorphism	Head Frontal Area Spines	Abdominal Dorso-Anterior Spines	Abdominal Dorso-Posterior Spines	Large Abdomen Sexual Dimorphism	Neosminthuroid Chaetae on Large Abdomen	Tibiotarsi distal Whorl Chaetae	Pretarsi Posterior Chaeta	Capitate Tenent-Hairs on Tibiotarsi II–III	Ungues Tunica	Ungues Pseudonychia	Ungues Inner teeth	Unguiculi Apical filament	Unguiculi Inner Teeth	Dens Ventral Chaetae	Mucronal Chaeta	Mucro Sexual Dimorphism
Galeriella	32	0 + 0	−?	—	−?	−?	−?	−?	−?	?	?	—	—	—	—	—	—	?	–	-?
Keratosminthurus	18–20	8 + 8	+	+	—	–	–	–	+	9	+	—	+/−	-	1	+	+/−	12–13	–	–
Richardsitas	28–30	8 + 8	—	—	+	+	+	+	—	9	+	+	—	+	1–2	+	+	13	+/−	–
Temeritas	18–46	8 + 8	—	—	+	+/−	—	+/−	—	9	+	—	+/−	+/−	1–2	+	+/−	13	+/−	–
Troglobentosminthurus gen. nov.	44	5 + 5	—	—	—	—	—	+	—	8–9	—	—	—	+	3–4	—	+	9	–	+

Data based in: [4,25,29,52–54,58] and the new genus herein described. Legends: '+' present, '−' absent, '?' unknown, unclear.

It is important to state we did not consider any chaetae on the parafurcal area as neosminthuroid because they all have similar slightly elongated alveoli, in accordance with most chaetae seen on the appendages and body. Further details on the chaetae which present different alveoli are detailed in the description of the new species.

Key to the genera of *Temeritas*-group *sensu* Medeiros et al. [29].

1. Eyes and ungual inner teeth absent ..... *Galeriella* Ć určić and Lučić, 2007 in [53]
-. Eyes and ungual inner teeth present 2
2. Clypeus and Ant. III with sexually dimorphic chaetae on males, parafurcal area with a pair of neosminthuroid chaetae ..... *Keratosminthurus* Zeppelini, 2020 in [4]
-. Clypeus and Ant. III without sexually dimorphic chaetae, parafurcal area lacking neosminthuroid chaetae 3
3. Specimens pale, eyes 5 + 5, head frontal area without spines, pretarsi posterior chaeta absent, dens ventrally with nine chaeta ..... *Troglobentosminthurus* gen. nov.
-. Specimens pigmented, eyes 8 + 8, head frontal area with spines, pretarsi posterior chaeta present, dens ventrally with 13 chaetae 4
4. Males with dimorphic short candle-shaped spines on the dorsal abdomen, capitate tenent-hairs present on tibiotarsi II–III ..... *Richardsitas* Betsch, 1975 [52]
-. Specimens without sexually dimorphic spines on the dorsal abdomen, tenent-hairs acuminate ..... *Temeritas* Richards, 1963 in [51]

3.3. Troglobentosminthurus luridus gen. nov. sp. nov. Souza, Medeiros and Bellini (Figures 1–10 and Table 2)

Type material. Holotype: female on slide, Serra do Ramalho, Água Clara cave system, Carinhanha municipality, Bahia state, Brazil (13°47′09.383" S, 42°06′07.667" W, Figure 1),

11/X/2017, R.L. Ferreira col (ISLA 79664). Paratypes: three males and one female, same data of the holotype, except for one male, collected on 16/X/2017 (ISLA 79664 and 79662). *Diagnosis of the species.* Specimens pale, without pigments, except for orange eye- patches. Dorso-frontal area with a cuticle crest on each side of the head posterior to the eyes, similar to a suture. Head chaetotaxy with only two medial unpaired chaetae, one frontal and one clypeal. Eyes 5 + 5, reduced in size. Trochanter III with five regular chaetae; tibiotarsi I–III with five oval organs each. Ungues with 3–4 inner teeth, unguiculi truncate with the inner lamella proximally serrated. Large abdomen of males with a dimorphic row of four chaetae upper to the parafurcal area (completely absent in females). Females' subanal appendage smooth and apically bent. Dens with 27 dorsal chaetae; mucro sexually dimorphic, with large crenulations on males in the serrated edge.

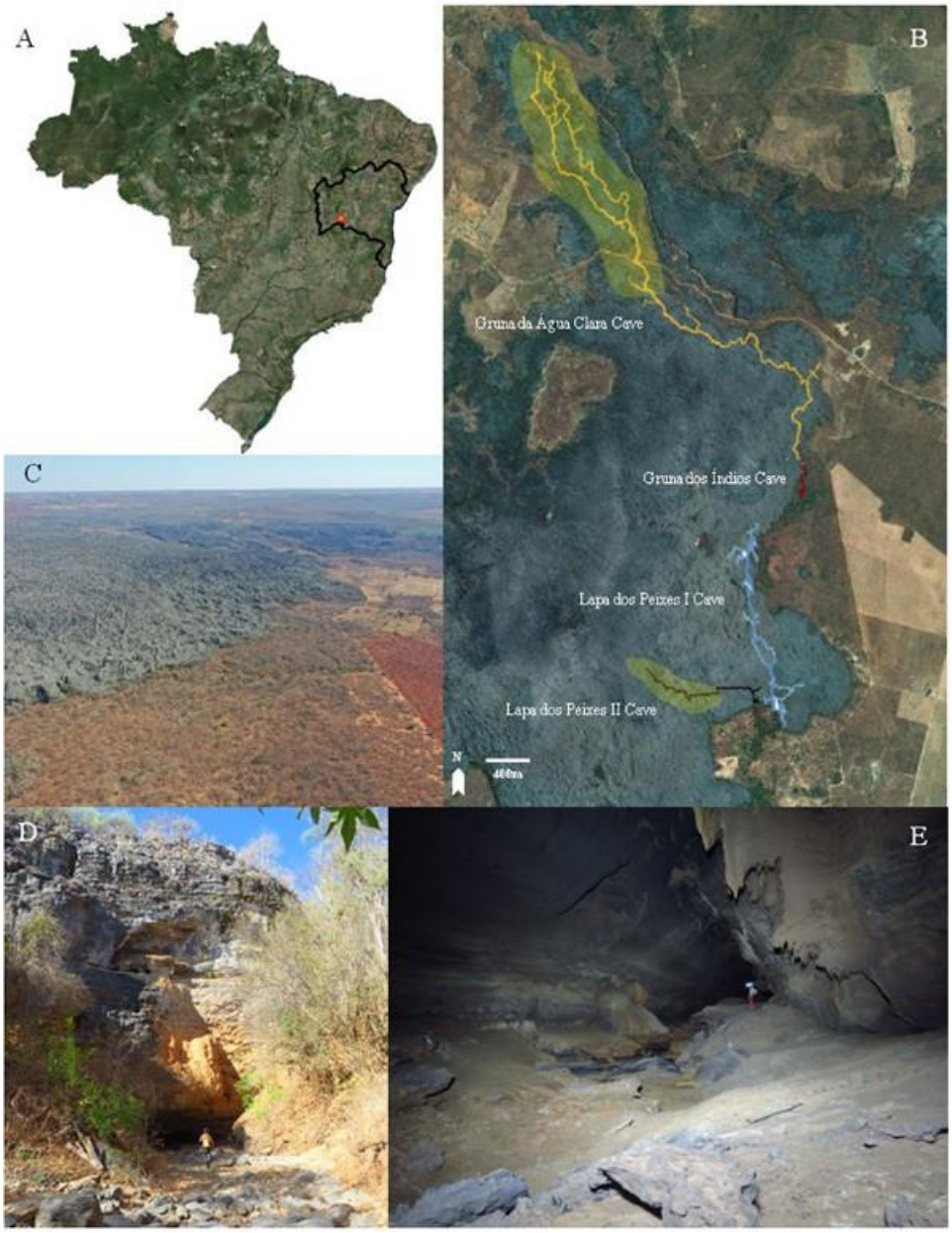


Figure 1. Type locality of *Troglobentosminthurus luridus* gen. nov. sp. nov.: (**A**) Água Clara cave system (ACCS) location, in the municipality of Carinhanha, Bahia state, Brazil; (**B**) spatial distribution of the caves within ACCS, the areas in translucent yellow correspond to the regions where the specimens of the new species were found; (**C**) aerial view from the surrounding region of the ACCS; (**D**) one of the entrances of the Gruna da Água Clara cave, which corresponds to a sink; (**E**) inner conduit of the Gruna da Água Clara cave.

Description. Body (head + trunk) length of the type series ranging between 1.15 and 1.68 mm, holotype with 1.68 mm, males average size 1.21 mm, females average size 1.63 mm, en- tire type series average size 1.38 mm. Body color of live specimens pale white, with a translucent yellowish dorsal large abdomen, pigments absent with the exception of small orange eyepatches (Figure 2). Fixed specimens also pale, with dark eyepatches (Figure 3A). Antennae, head, dorsal thorax and abdomen, legs and dorsal furca with long slender acuminate smooth chaetae inserted in slightly elongated alveoli (Figure 3B,C). Spines or spine-like chaetae absent, even on the head frontal area and dorsal large abdomen.

Accepted by D. Antić: 29 Feb. 2024; published: 25 Mar.



Figure 2. Living specimens of *Troglobentosminthurus luridus* gen. nov. sp. nov.: (**A**) one specimen apparently feeding on a bat guano pile in the Lapa dos Peixes II cave (another springtail specimen in the same pellet); (**B**) specimen walking around a dry bat guano pile in the Lapa dos Peixes II cave; (**C**,**D**) specimens freely walking on the cave muddy sediment in the deeper portion of the Gruna da Água Clara cave.

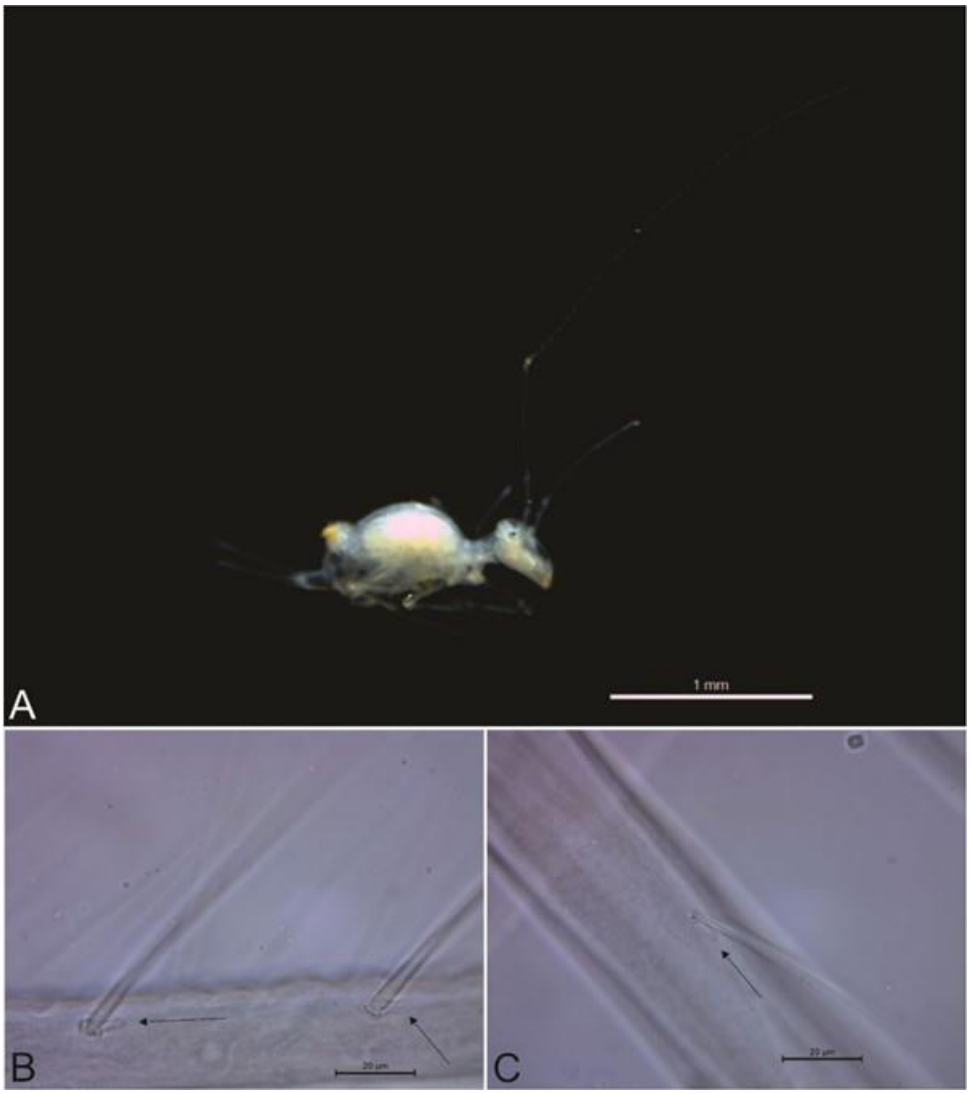


Figure 3. *Troglobentosminthurus luridus* gen. nov. sp. nov. morphology: (**A**) habitus of a fixed specimen in ethanol; (**B**) two chaetae elongate alveoli on the dorsal dens (marked with black arrows);
(**C**) one chaeta elongate alveolus on the tibiotarsus II (marked with a black arrow).

Head (Figures 4 and 5). Antennae more than twice the length of the body, with 3.65 mm in the holotype. Holotype antennal segments ratio I:II:III:IV as 1:2.6:10:37. Ant. IV longer than the Ant. I–III + body, with 44 subsegments (n = 1, only holotype with a complete antenna); subsegment 1 with at least nine chaetae (subsegment broken), two proximal reduced, subsegment 2 with eight chaetae, 3 with seven chaetae, 4 with eight chaetae, 5–7 with eight chaetae each, 8 with nine chaetae, 10–11 with 10 chaetae each, 12 with nine chaetae, 13–15 with 10 chaetae each, 16–17 with nine chaetae each, 18–43 with 10 chaetae each, and subsegment 44 with 20 chaetae (Figure 4A). Ant. III with 38–39 chaetae, apical organ sensory rods in two independent shallow invaginations, surrounding subapical microsensillum with rounded apex (Figure 4B). Ant. II with 18 chaetae, one of them as a ventro-lateral bothriotrichum-like sensillum (Figure 4B). Ant. I with seven chaetae (Figure 4B). Head length (eyes to mouth) of the holotype 0.55 mm. Eyes 5 + 5, reduced in size, apparently with an extra vestigial lens on each eyepatch. Clypeal area **a**–**g** series with 7/6–7/6/6(+1)/5/8/3 chaetae, respectively (Figure 5A,B). Interantennal area with only ***α*** and ***γ*** series with one and two chaetae, respectively, near to **g** series central field; frontal area **A**–**E** series with 1(+1)/2/1/2/3 chaetae, respectively; dorso-frontal area with a cuticle crest on each side of the head posterior to the eyes, similar to a suture; interocular

chaetae absent (Figure 5A). Ventral head with two **a** and one **b** chaetae on the post-labial region, labial basomedian field with four chaetae, one of them large, and basolateral field with five chaetae (Figure 5B). Six prelabral chaetae present (Figure 5A), labral **a**, **m**, **p** series with 2, 2(+1), 2(+1) chaetae respectively, **p1** smaller and thinner than the others, **m1** smaller than **m0**, **a2** reduced, and **p2** larger than the others (Figure 5C). Labial palp with five proximal chaetae, papillae formula of guard-chaetae for each papilla as **H**(2), **A**(0), **B**(5), **C**(0), **D**(4), **E**(4) + lateral process (**l**.**p**.) not reaching the papilla **E** base, papilla **H** guard- chaetae heterogeneous, papilla **B** guard-chaeta **a1** laterally displaced to **C**, large and curved anteriorly (Figure 5D). Maxilla with three lateral teeth and three central large lamellae (Figure 5E). Maxillary outer lobe developed, apical chaeta smooth with a proximo-internal barb (or toothlet), basal chaeta smaller than the apical one, oral fold with two chaetae, sublobal plate internally folded, without chaeta-like appendages (Figure 5F). Mandibles asymmetrical with 3 + 4–5 incisive apical teeth (Figure 5G).

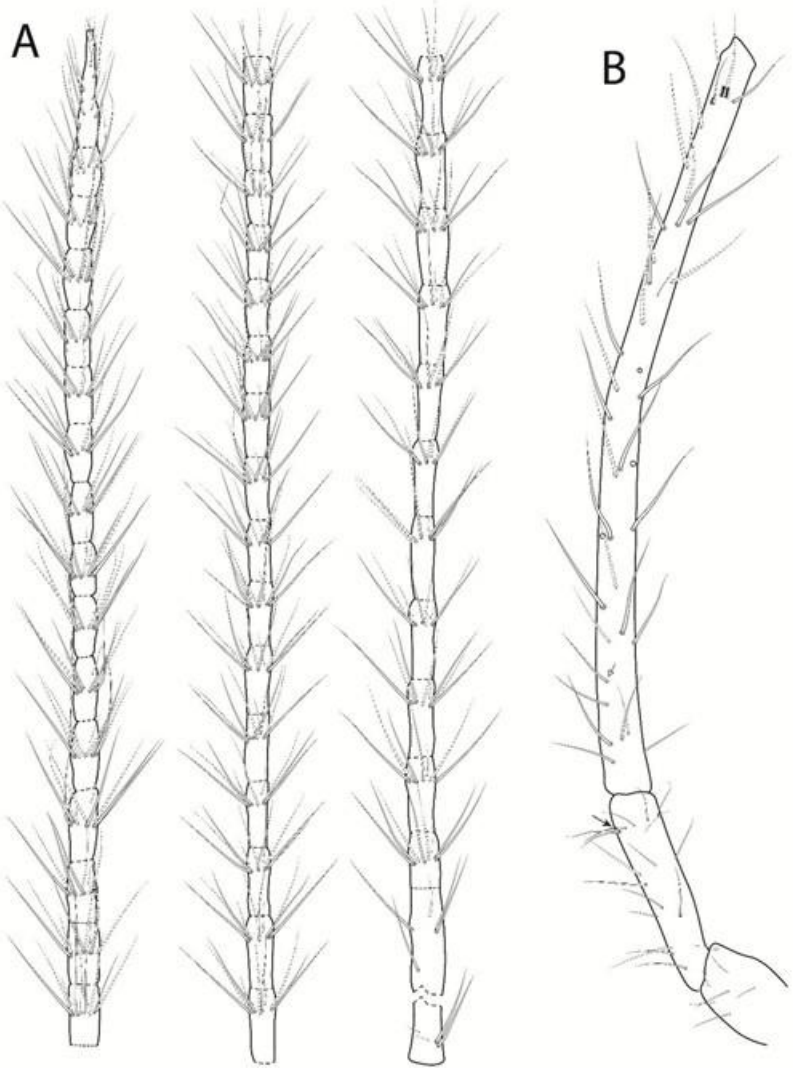


Figure 4. *Troglobentosminthurus luridus* gen. nov. sp. nov. left antenna: (**A**) Ant. IV subsegments, from left to right the more apical to the more proximal ones (**left**, 29–44 subsegments; **middle**, 13–28; **right** 1–12); (**B**) Ant. I–III, white arrow marks a chaeta present or absent, black arrow marks the ventro-lateral bothriotrichum-like sensillum.

Accepted by D. Antić: 29 Feb. 2024; published: 25 Mar.

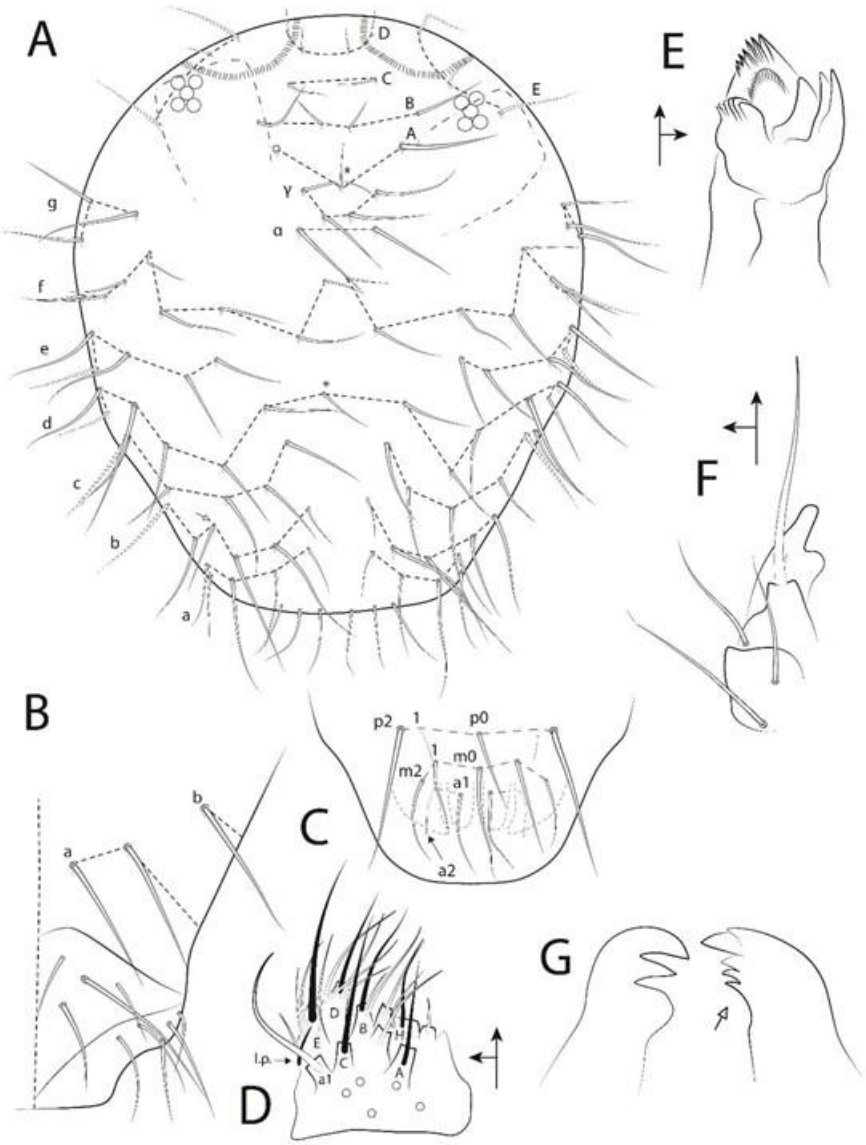


Figure 5. *Troglobentosminthurus luridus* gen. nov. sp. nov. head: (**A**) anterior head chaetotaxy, Ant. I marked in dotted lines, white arrow marks a chaeta present or absent, asterisks mark unpaired central chaetae; (**B**) right side of the posterior (ventral) head chaetotaxy, including post-labial, labial basomedial and basolateral chaetae; (**C**) labral chaetotaxy; (**D**) left labial palp; (**E**) right maxilla capitulum; (**F**) left maxillary outer lobe and sublobal plate; (**G**) incisive (apical) teeth of the mandibles, white arrow marks a tooth in the right mandible which can be absent.

Trunk (Figure 6). Trunk length of the holotype 1.13 mm. Large abdomen: thorax continuous with abdomen without any segmentation, constrictions or vesicles in both sexes. Sexual dimorphism on the large abdomen restricted to a row with four chaetae present only on males above the parafurcal area (Figure 6A, black arrow). Chaetotaxy as: Th. II with one **a** and one **m** chaetae; Th. III with one **a**, one **m** and one **p** chaetae; Abd. I with four **a**, three **m** and 0–1 **p** chaetae; bothriotricha **A**, **B** and **C** present and elongated on Abd. II and misaligned; bothriotrichia **A** with one (**a**), **B** with two (**m**) and **C** with one (**p**) accessory chaetae, respectively; Abd. III–IV with five main series of chaetae above the bothriotrichum **C**: **dI-1** with 3(+1), **dII-1** with 3–5, **dIII-1** with five, **dIV-1** and **dV-1** with three chaetae each, plus two ventro-lateral rows of chaetae under the bothriotrichum **C,** with four and eight chaetae, respectively. Parafurcal area with four rows of chaetae with two, four, four, four (total of 14) chaetae on males and females, all chaetae with the same type of elongate alveoli,

Accepted by D. Antić: 29 Feb. 2024; published: 25 Mar.

neosminthuroid chaetae absent (Figure 6A). Small abdomen: in both sexes including Abd. V and bothriotrichum **D**, the latter longer than the dens, **E** absent (Figure 6A,B,D). Female's dorsal anal valve with **as2–4**, **ams1**, **ms1**–**4**, **mps1–3** and **ps1–2** chaetae, **ams1**, **ms1** and **ps1** unpaired; each ventral anal valve with **aai6**, **ai1–6**, **mi1–5**, **mpi1–4** and **pi1–3** chaetae, **am1** as an oval organ and **mi5** as the subanal appendage, slender, smooth and curved toward the anus opening (Figure 6B). Genital plate of the female with 3 + 3 chaetae on the ventral field (Figure 6C). Male's dorsal anal valve with **as2–3**, **ams1**, **ms1**–**4**, **mps1–3** and **ps1–2** chaetae, **ams1**, **ms1** and **ps1** unpaired; each ventral anal valve with **aai6**, **ai1–6**, **mi1–5**, **mpi1–2, mpi4** (**mpi3** absent) and **pi1–3** chaetae, **am1** as an oval organ (Figure 6D). Genital plate of the male with about 13 + 1 + 13 chaetae (Figure 6A).

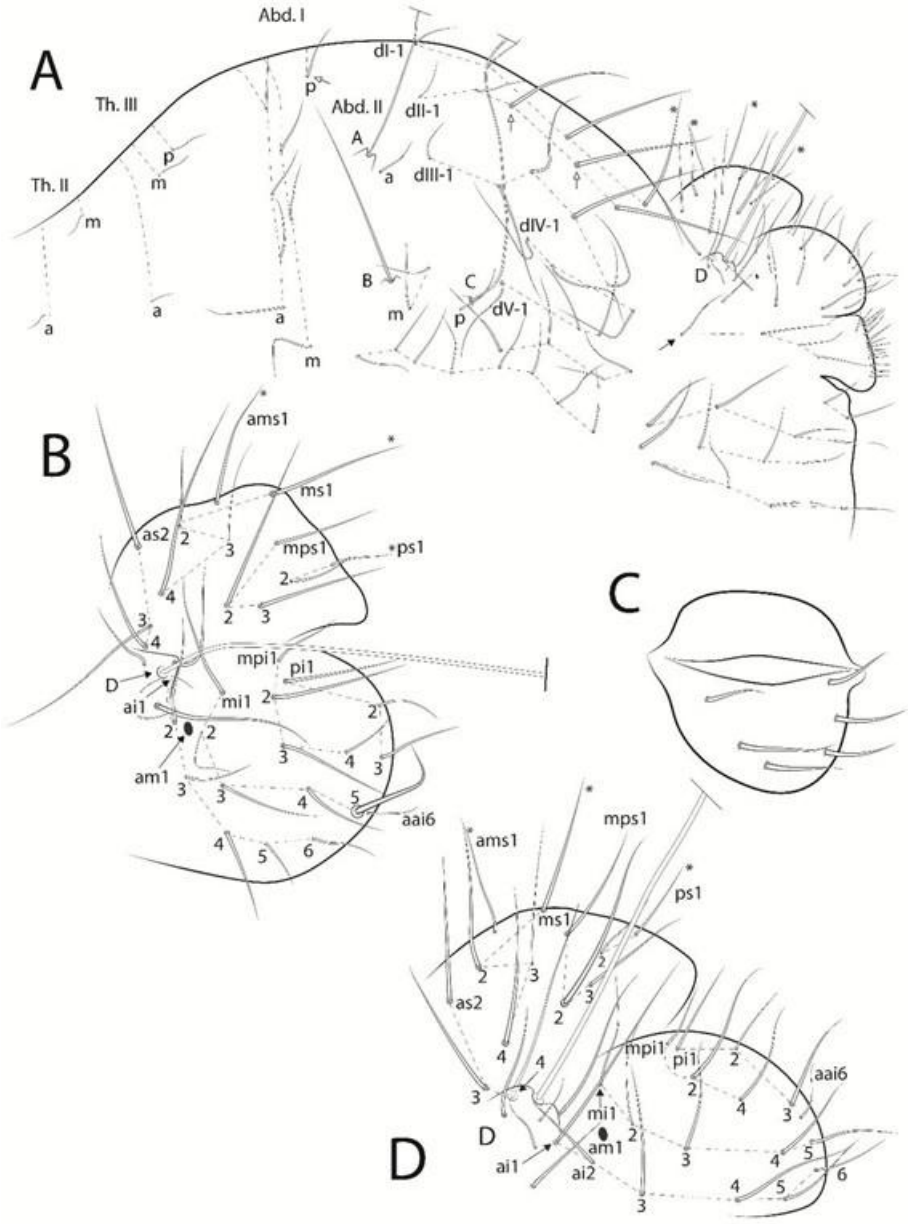


Figure 6. *Troglobentosminthurus luridus* gen. nov. sp. nov. trunk: (**A**) large and small abdomens of the male, white arrows mark chaetae present or absent, asterisks mark unpaired central chaetae, black arrow marks a row of chaetae only seen in males; (**B**) female's small abdomen, asterisks mark unpaired central chaetae; (**C**) female's genital plate; (**D**) male's small abdomen in detail, asterisks mark unpaired central chaetae.

Legs (Figures 7 and 8). Leg I: epicoxa, subcoxa and coxa with one chaeta each; trochanter with five chaetae, two of them reduced; femur with 18 chaetae, one of them reduced; tibiotarsus with 56 chaetae and five oval organs (**O1pe**, **O2pe**, **O3ae**, **O3pe**, **O4pe**) on the dorsal side, proximal group **F** with eight chaetae (**FPae**, **FPpe**, **FPe**, **FSae**, **FSpe**, **FSpi**, **FSp** and **FSai**), distal whorl with seven chaetae plus one long acuminate tenent-hair, tibiotarsal groups of chaetae and whorls spaced due to the elongation of the segment (Figures 7A and 8A); tibiotarsus I length in the holotype 0.76 mm. Leg II: epicoxa, subcoxa and coxa with one chaeta each; trochanter with seven chaetae, one of them reduced, plus one proximal oval organ; femur with 17 chaetae, one of them reduced; tibiotarsus with 57 chaetae and five oval organs (**O1pe**, **O2pe**, **O3ae**, **O3pe**, **O4pe**) on the dorsal side, proximal group **F** with seven chaetae (**FPae**, **FPpe**, **FPe**, **FSae**, **FSpe**, **FSp** and **FSai**), distal whorl with eight chaetae plus one long acuminate tenent-hair, tibiotarsal groups of chaetae and whorls spaced due to the elongation of the segment (Figures 7B and 8B); tibiotarsus II length in the holotype 0.69 mm. Leg III: epicoxa with one, subcoxa with two and coxa with four chaetae, respectively; trochanter with five regular chaetae and a thick trochanteral spine within a rounded alveolus, plus one proximal oval organ; femur with 19 chaetae; tibiotarsus with 62 chaetae and five oval organs (**O1pe**, **O2pe**, **O3ae**, **O3pe**, **O4pe**) on the dorsal side, proximal group **F** with seven chaetae (**FPae**, **FPpe**, **FPe**, **FSae**, **FSpe**, **FSp** and **FSai**), distal whorl with eight chaetae plus one regular-sized acuminate tenent-hair, tibiotarsal groups of chaetae and whorls spaced due to the elongation of the segment (Figures 7C and 8C); tibiotarsus III length in the holotype 0.85 mm. Foot complexes: pretarsi I–III with one discrete anterior chaeta each, posterior chaeta absent; ungues I–III with two pairs of lateral teeth, internal lamella with three proximal (2–3 on unguis I) and one apical smaller teeth, dorsal tooth absent, ungues without tunica but with partially developed pseudonychia; unguiculi I–III with proximally serrated antero-internal lamella, unguiculi I and III with about three serrations, II with about eight, postero-external lamella smooth, unguiculus filament absent in all legs (Figure 8D–F).

Abdominal appendages (Figure 9). Ventral tube with 1 + 1 chaetae on the corpus and 1 + 1 on the lateral flaps, sacs long and warty. Manubrium with nine, and dens with 27 dorsal chaetae, respectively (Figure 9A), dens ventrally (anteriorly) with nine chaetae inside rounded alveoli, following the formula from the apex to the basis: 3, 2, 2, 1 . . . 1 (Figure 9B). Mucro with the inner lamella slightly serrated with about 70 small teeth, outer lamella smooth; mucro sexually dimorphic, with large crenulations on males in the serrated edge; mucronal chaeta absent (Figure 9B–D). Ratio mucro:dens:manubrium of the holotype as 1:4.6:1.8. Tenaculum with three distal teeth plus one proximal basal tubercle on each ramus, corpus with 1 + 1 apical chaetae (Figure 9E).

Accepted by D. Antić: 29 Feb. 2024; published: 25 Mar.

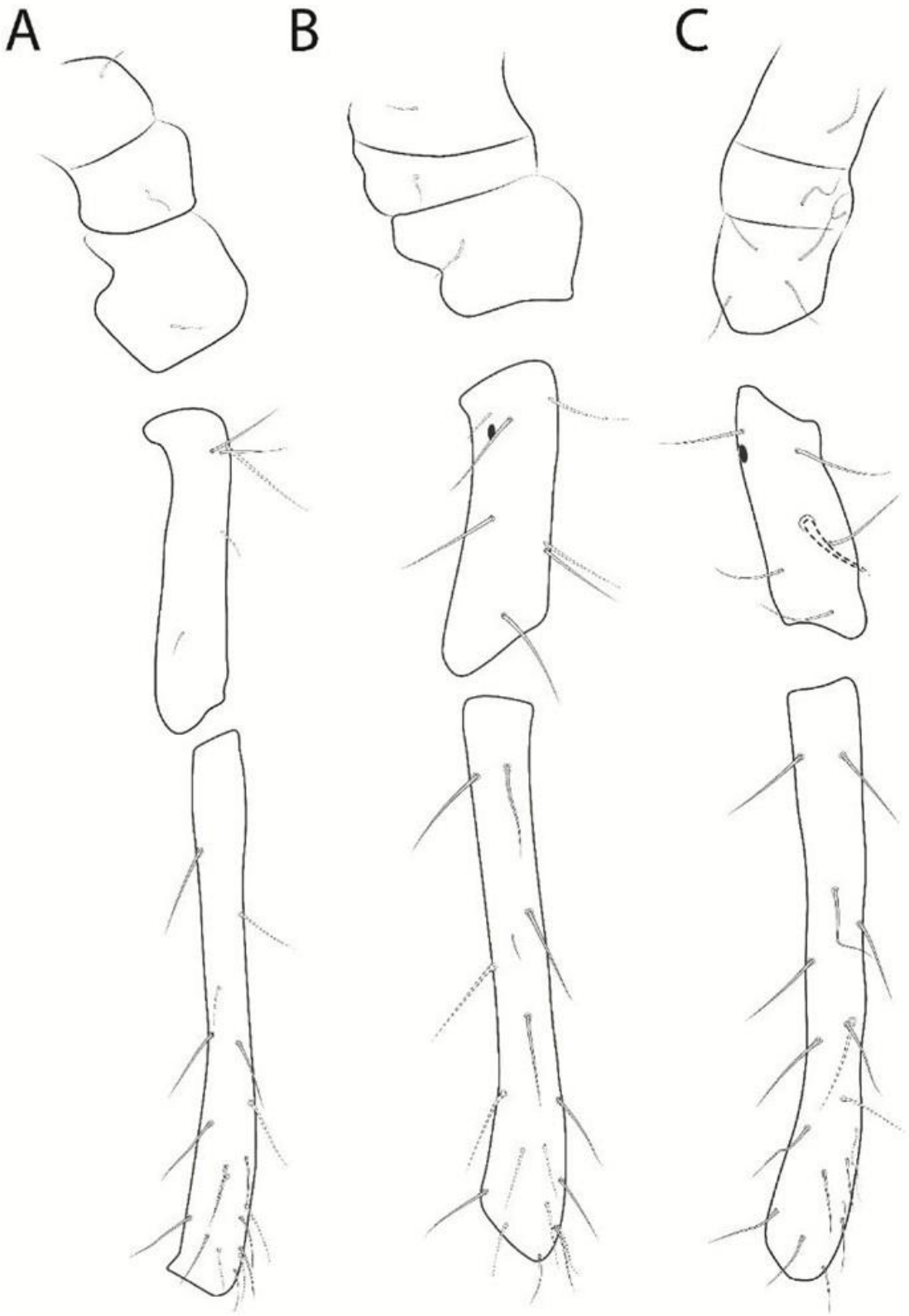


Figure 7. *Troglobentosminthurus luridus* gen. nov. sp. nov. legs: (**A**) epicoxa to femur of leg I; (B) epicoxa to femur of leg II; (**C**) epicoxa to femur of leg III.

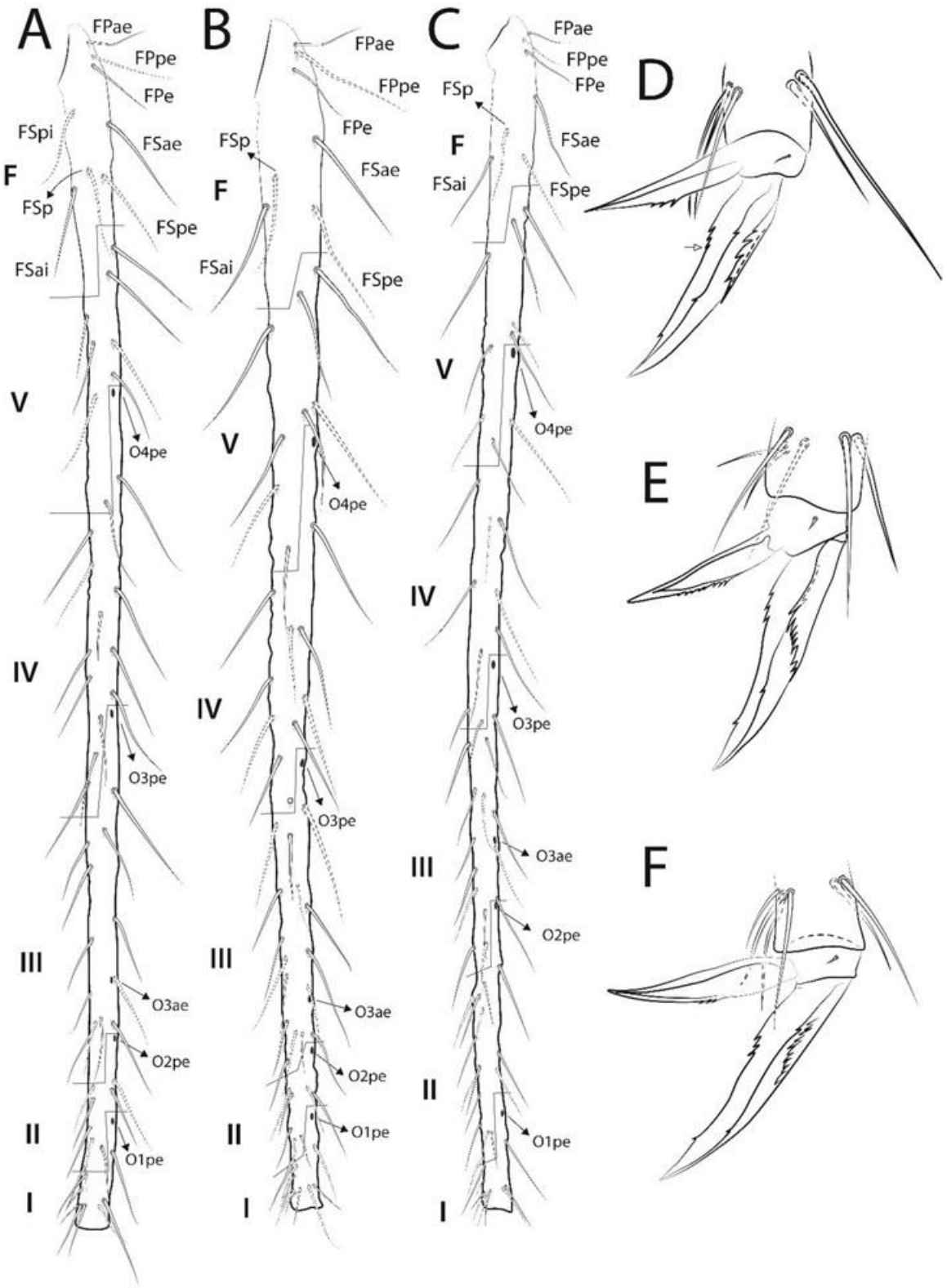


Figure 8. *Troglobentosminthurus luridus* gen. nov. sp. nov. legs: (**A**) tibiotarsus I; (**B**) tibiotarsus II; (C) tibiotarsus III; (**D**) empodial complex I, anterior view, white arrow marks a ungual tooth which can be absent; (**E**) empodial complex II, anterior view; (**F**) empodial complex III, anterior view.

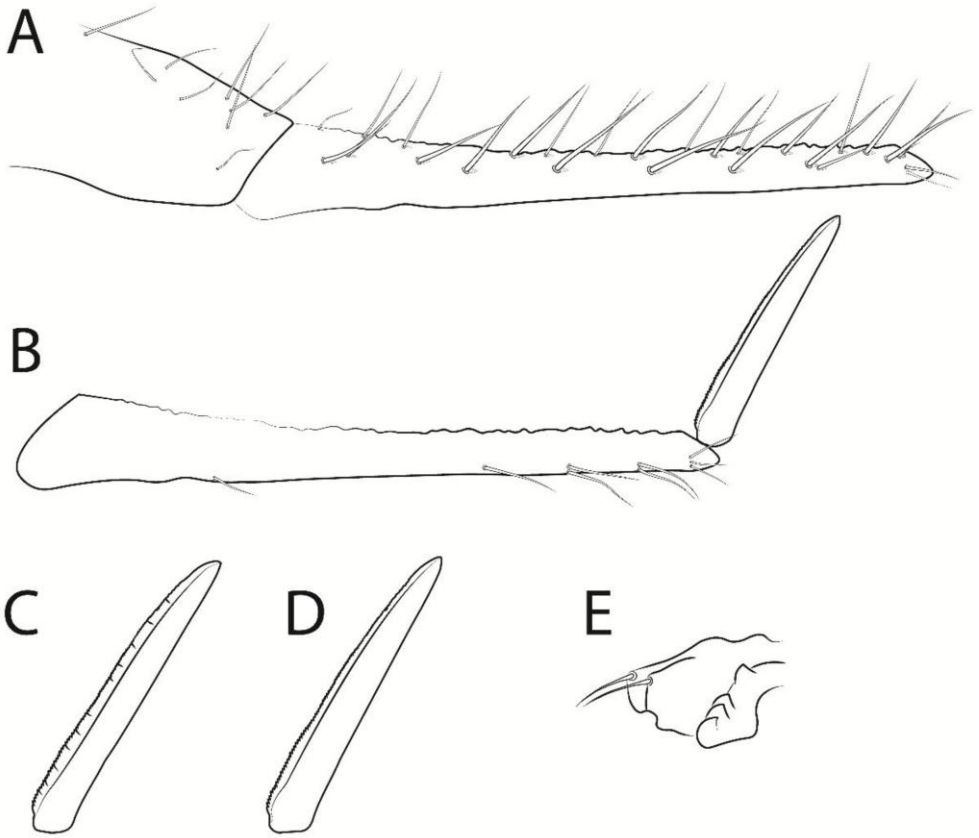


Figure 9. *Troglobentosminthurus luridus* gen. nov. sp. nov. furcula: (**A**) dorso-lateral view of the manubrium and dens; (**B**) ventro-lateral view of the left dens and mucro of a female; (**C**,**D**) sexual dimorphism regarding the mucro: (**C**) lateral view of the left mucro of a male; (**D**) lateral view of the left mucro of a female; (**E**) tenaculum.

Etymology. The new species was named *luridus* (from Latin: lurid or shockingly macabre) due to its pale, ghostly habitus, and due to one of the type-series females has remnants of a devoured male on its guts, suggesting the species can be cannibalistic or necrophile.

found in two caves from the Água Clara cave system (ACCS), located in the karst ar*Habitat and threats.* Specimens of *Troglobentosminthurus luridus* gen. nov. sp. nov. were is composed of four limestone caves (Gruna da Água Clara, Gruna dos Índios, Lapa dos of Serra do Ramalho, Carinhanha municipality, Bahia state, Brazil (Figure 1A). The ACCS Peixes I and Lapa dos Peixes II caves) which are trespassed by an intermittent stream, active

during the austral summer (October until March) (Figure 1B). The whole system presents around 24 km, but there are still unsurveyed galleries. According to Köppen's climate classification system, the local climate is "Aw", with dry winter and an average annual rainfall of 640 mm [59]. The Serra do Ramalho region is inserted in the Caatinga domain (an exclusive Brazilian semiarid biome), with transitional areas to the Cerrado (Brazilian Savanna) [60].

Specimens of *Troglobentosminthurus luridus* gen. nov. sp. nov. were only found in deep and moistened areas of the dark zone of the system, which have only horizontal caves. It is interesting noting that the two caves located at the intermediate portion of the ACCS (Gruna dos Índios and Lapa dos Peixes caves) have the main conduit quite dry (even with

the presence of some ponds) due to the wind, which trespasses both caves. Such caves

present entrances on both sides of their main conduit, thus favoring the airflow. Hence, individuals of *Troglobentosminthurus luridus* gen. nov. sp. nov. were not observed in this

intermediate portion of the ACCS, probably due to the unstable climatic conditions of the caves.
The individuals were found both associated with small bat guano pellets (especially in the Lapa dos Peixes II cave, Figure 2A,B) but also freely walking on the muddy sediment
in the deep areas of the Gruna da Água Clara cave (Figure 2C,D). In the latter, specimens
were often found in areas with no visible organic debris, so it is likely that they might be
feeding on some microbial content associated with the cave sediments. It is interesting to highlight that the caves of ACCS are seasonally flooded, as strong water flows trespass the caves during the rainy period, coming from several entrances along the ACCS (Figure 1D). Thus, individuals of *Troglobentosminthurus luridus* gen. nov. sp. nov. somehow overcome such floodings, probably by climbing up the cave's walls, which can be considerably high (Figure 1E), or entering rock cracks, but this subject certainly merits further research.
It is also noteworthy that in the deep regions where specimens are found, there are almost only troglobitic species [61], thus indicating that only highly specialized species can thrive under the restrictive conditions occurring in such areas (especially strong olig- otrophy). Among the 30 cave-restricted species observed in the ACCS, only 8 (~26%) are formally described [61]. Thus, it is of paramount importance to describe the remaining troglomorphic species in order to preserve the ACCS, since non-described species are often ignored in conservation actions [62].
The Serra do Ramalho region has been the target of increasing deforestation in the last decades, mainly due to charcoal production and the establishment of monocultures (Figure 1C). Forest removal in the areas that directly influence the caves can alter the organic sediments supply to the caves and negatively impacts bat communities as well, thus affecting the food resources available for the hypogean fauna [61]. Furthermore, species associated with systems with low availability of guano and carcasses, such as the ACCS, may be more dependent on allochthonous food resources [61].
Considering the recent setbacks in the Brazilian laws regarding cave protection [63], it is urgent to describe cave-restricted species from an important hotspot of subterranean biodiversity as the Agua Clara cave system. Since the caves are under serious threat, it is more urgent than ever to formally describe such endemic species, as they might become the only effective protection for the habitats they rely on.
Biology. The overall morphology of *Troglobentosminthurus luridus* gen. nov. sp. nov. with extraordinarily long appendages and chaetae, loss of pigments and part of the eyes, as well as the reduction of the eye lenses, support the species is a troglobite, especially com- pared to other species of the *Temeritas*-group. As discussed before, the limited distribution of the species within the ACSS, only found in deeper areas, reinforces this hypothesis.
The type specimens have soil particles in the guts mixed with some dark matter, suggesting the specimens may feed on bat guano, cave sediments with microbes or particles of organic matter (Figure 10A). However, the gut contents of two specimens were more unusual. One of the studied males has two mite legs in its contents (Figure 10A), while the holotype, a female, has the remains of one male of the same species in its digestive system (Figure 10B,C). In the case of the analyzed male paratype, we could not track any other clear part of the mite other than the legs, but in the case of the female, we could confirm the morphology of the six empodial complexes of the digested specimen as the ones described to *Troglobentosminthurus luridus* gen. nov. sp. nov. Although this devoured specimen was fragmented, we could also identify its testicles, both labial palps and many body chaetae on the remains found inside the holotype, supporting it is a male of her own species (Figure 10B,C). In this scenario *Troglobentosminthurus luridus* gen. nov. sp. nov. specimens may be occasional predators/cannibals, or even necrophiles and feed on dead arthropods. Such uncommon feeding habitats for springtails must be better studied to confirm which hypothesis fits best the biology of the new species. However, under extreme oligotrophic conditions, such as those observed in the areas where the specimens are found inside the ACCS, all raised behaviors (predation/cannibalism/necrophagy) are quite plausible.

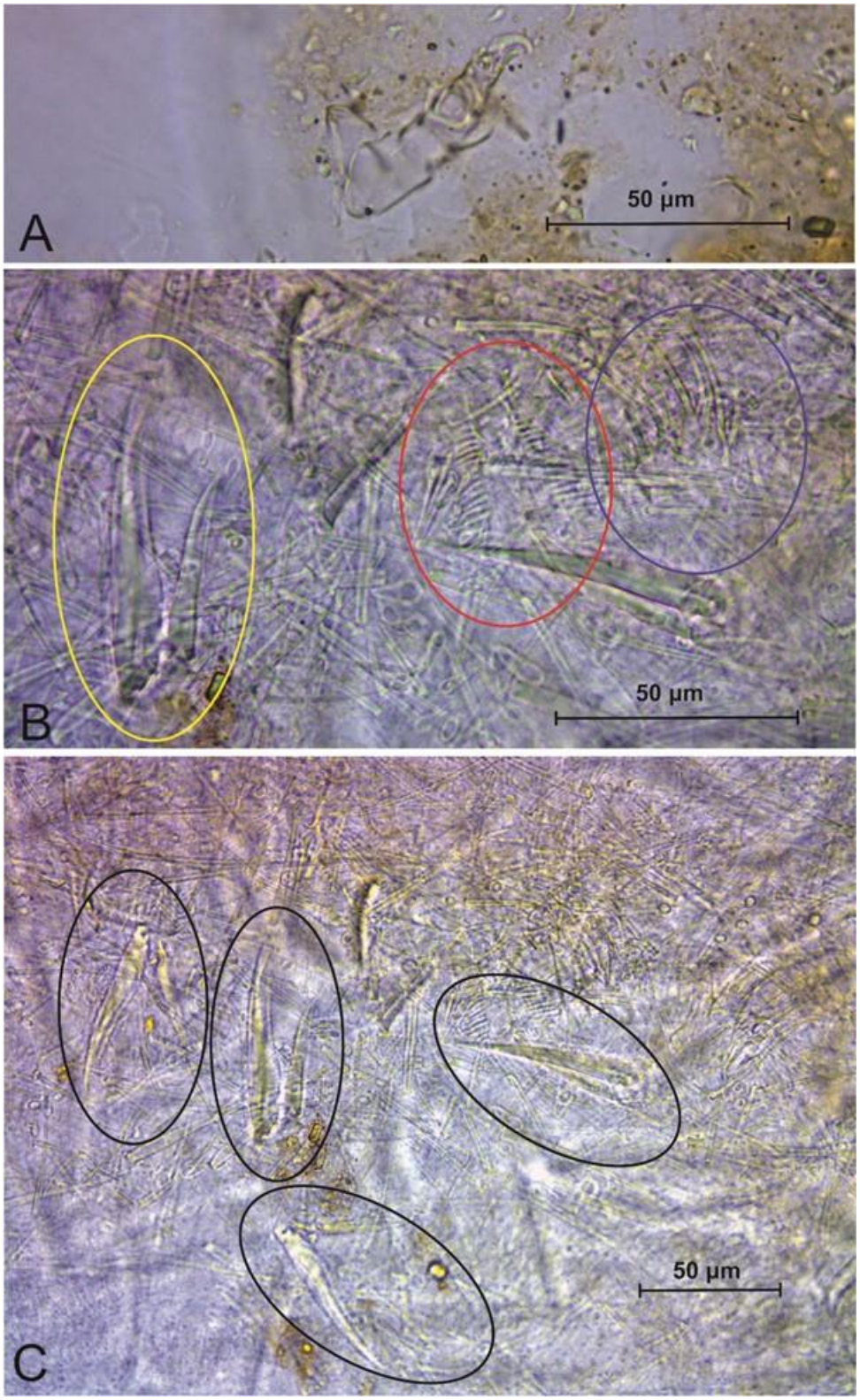


Figure 10. *Troglobentosminthurus luridus* gen. nov. sp. nov., gut contents: (**A**) a male's contents, with a mite leg at the center and dark matter mixed with soil particles at the right side; (**B**) holotype (female) contents, yellow circle marks an empodial complex, red marks the testicles, and blue marks one labial palp; (**C**) holotype (female) contents, black circles mark four devoured empodial complexes.

Accepted by D. Antić: 29 Feb. 2024; published: 25 Mar.

Remarks. Since the genus is monotypic, the species and genus diagnoses should be considered complementary. They also may have conflicting characters, as specific traits marked as diagnostic of the genus and vice-versa, which should be better understood with the description of further species of *Troglobentosminthurus* gen. nov. in the future, if any. For taxonomical comparisons, see the remarks of the new genus and Table 2.

4. Discussion

The description of *Troglobentosminthurus* gen. nov., as well as *Keratosminthurus* and the Songhaicinae, test the boundaries of the internal systematics of the Sminthuroidea. Until now, no representative molecular analysis aiming to resolve the internal relationships of the Symphypleona was published. Recent studies using different markers and phylogenetic methods only gathered a few taxa of the order, unable to clearly investigate the validity and affinities of its internal groups, as in [64–69]. In this scenario, arguably, the most reliable phylogenetic data available are based on morphology, as in [25,41,42,70]. However, it is im- portant to state that, even with limited sampling, molecular analyses do not clearly support important subdivisions of the Symphypleona. For instance, Schneider et al. [65] tree does not support the Dicyrtomidae as a family, Yu et al. [66] do not support the Sminthurididae, and Yu et al. [66], Sun et al. [68] and Cucini et al. [69] do not support the suborder Ap- pendiciphora. These are all well-delimited taxa based on morphology [26], and poor and uneven sample size and choice of markers could be blamed for such results. Nevertheless, more detailed phylogenetic analyses of the Symphypleona using modern tools are lacking, making its internal organization sometimes dubious and weakly supported in the light of the discovery of new taxa, as in the case of the Sminthuroidea. We hope in a near future more data on the systematics of the Symphypleona, as well as the Collembola as a whole, emerge to clarify its organization and to test different hypotheses concerning their evolution.

5. Conclusions

In this paper we described the highly troglomorphic *Troglobentosminthurus* gen. nov. from a cave system in the Brazilian semiarid region. The new genus shows a remarkable morphology, with troglomorphisms not recorded before in any Brazilian species of spring-tails and intermediate traits which made us revise the diagnosis of the Sminthurinae and discuss the exclusive morphology of the Bourletiellidae. *Troglobentosminthurus luridus* gen. nov. sp. nov. is discovered at the same time the Brazilian laws regarding cave protection be- come more flexible to favor commercial expansion, while the cave system where the species inhabits is developed in a karst already threatened by deforestation. Urgent conservation strategies are clearly in need to preserve this new taxon.

Author Contributions: Conceptualization, B.C.B., P.G.C.d.S., G.d.S.M. and R.L.F.; methodology, B.C.B., P.G.C.d.S., G.d.S.M. and R.L.F.; validation, P.G.C.d.S., G.d.S.M. and B.C.B.; formal analysis,
P.G.C.d.S., G.d.S.M. and B.C.B.; investigation, P.G.C.d.S., G.d.S.M. and B.C.B.; resources, R.L.F. and M.S.-S.; data curation, P.G.C.d.S., G.d.S.M. and B.C.B.; writing—original draft preparation, B.C.B., P.G.C.d.S., R.L.F. and G.d.S.M.; writing—review and editing, B.C.B., P.G.C.d.S., R.L.F., G.d.S.M. and
M.S.-S.; visualization, B.C.B., P.G.C.d.S., R.L.F., G.d.S.M. and M.S.-S.; supervision, B.C.B.; project administration, B.C.B. and R.L.F.; funding acquisition, B.C.B., R.L.F. and M.S.-S. All authors have read and agreed to the published version of the manuscript.

Funding: This research was funded by Centro Nacional de Pesquisa e Conservação de Cavernas— 006/2021. TCCE ICMBio/Vale (01/2018)); Fundação de Apoio à Pesquisa do Estado da Paraíba CECAV and Instituto Brasileiro de Desenvolvimento e Sustentabilidade—IABS (grant number (FAPESQ/PB, PhD scholarship, grant number #07/2021-SEECT); the Coordination for the Improve-
ment of Higher Education Personnel (CAPES, PhD scholarship, grant number #001); and the Na- tional Council for Scientific and Technological Development (CNPq, grant numbers #309114/2021-7, #308334/2018-3).

Institutional Review Board Statement: Ethical review and approval were waived for this study, due to Brazilian laws which do not require permission from an institutional ethics committee on the use of animals for taxonomical studies with microartropods.

Informed Consent Statement: Not applicable.

Data Availability Statement: All data is contained within the article. All biological material is deposited at ISLA (# 79662 and 79664) as previously stated.

Acknowledgments: The authors would like to thank the team from the Center of Studies in Subter- ranean Biology (CEBS/UFLA) for the support in the field trips.

Conflicts of Interest: The authors declare no conflict of interest.

References

1. Culik, M.P.; Zeppelini-Filho, D. Diversity and distribution of Collembola (Arthropoda: Hexapoda) of Brazil. *Biodivers. Conserv.* **2013**, *12*, 1119–1143. [CrossRef]
2. Zeppelini, D.; Queiroz, G.C.; Bellini, B.C. Symphypleona in Catálogo Taxonômico da Fauna do Brasil. PNUD. Available online: http://fauna.jbrj.gov.br/fauna/faunadobrasil/470 (accessed on 6 June 2022).
3. Bretfeld, G. Known and new genera and species of Symphypleona (Insecta, Collembola) obtained by canopy fogging in Central Amazonia, Brazil. *Amazoniana* **2002**, *17*, 109–137.
4. Zeppelini, D.; Brito, R.A.; Zampaulo, R.; Lima, E.C. A new highly dimorphic genus of Sminthuridae (Collembola: Symphypleona) from Brazil. *Zootaxa* **2020**, *4729*, 25–46. [CrossRef] [PubMed]
5. Silva, D.D.; Palacios-Vargas, J.G.; Bellini, B.C. A new genus and a new species of Sminthuridae (Collembola: Symphypleona) from Atlantic Forest of Brazil. *Zootaxa* **2015**, *3990*, 410–418. [CrossRef]
6. Bonet, F. Nuevos generous y species de hipogastrúridos de México (Collembola). *Rev. Soc. Mex. Hist. Nat.* **1945**, *6*, 13–45.
7. Nicolet, H. Recherches pour servir á l'Histoire des Podurelles. *Nouv. Mém. Soc. Helvet. Sci. Nat.* **1842**, *6*, 1–88.
8. Palacios-Vargas, J.G.; Wilson, J.M. *Troglobius coprophagus*, a new genus and species of cave Collembola from Madagascar, with notes on its ecology. *Int. J. Speleol.* **1990**, *19*, 67–73. [CrossRef]
9. Mills, H.B. Collembola from Yucatan Caves. *Carnegie Inst. Wash. Publ.* **1938**, *491*, 183–190.
10. Schäffer, C. Apterygoten. *Hamb. Magalh. Samm.* **1897**, *8*, 1–48.
11. Yosii, R. Höhlencollembola Japans II. *Jpn. J. Environ. Entomol. Zool.* **1956**, *11*, 609–627.
12. Börner, C. Das System der Collembolen nebst Beschreibung neuer Collembolen des Hamburger Naturhistorischen Museums. *Mitt. Aus Dem Nat. Mus. Hambg.* **1906**, *23*, 147–188.
13. Bonet, F.; Tellez, C. Un Nuevo Genero de Esminturidos (Collembola). *Rev. Soc. Mex. Hist. Nat.* **1947**, *8*, 193–203.
14. Palacios-Vargas, J.G.; Gnaspini-Netto, P. A new Brazilian species of *Acherontides* (Collembola: Hypogastruridae), with notes on its Ecology. *J. Kansas Entomol. Soc.* **1992**, *65*, 443–447.
15. Oliveira, J.V.L.C.; Brito, N.P.; Zeppelini, D. Two New *Cyphoderus* Nicolet (Collembola: Paronellidae) of the "bidenticulati-group" with Dental Plurichaetosis from Brazil. *Neotrop. Entomol.* **2021**, *50*, 579–592. [CrossRef]
16. Zeppelini, D.; Silva, D.D.; Palacios-Vargas, J.G. A new species of *Troglobius* (Collembola, Paronellidae, Cyphoderinae) from a Brazilian iron cave. *Subterr. Biol.* **2014**, *14*, 1–13. [CrossRef]
17. Yoshii, R. Paronellid Collembola from Caves of Central and South America collected by P. Strinati. *Rev. Suisse Zool.* **1988**, *95*, 449–459.
18. Cipola, N.G.; Oliveira, J.V.L.C.; Bellini, B.C.; Ferreira, A.S.; Lima, E.C.A.; Brito, R.A.; Stievano, L.C.; Souza, P.G.C.; Zeppelini, D. Review of Eyeless *Pseudosinella* Schäffer (Collembola, Entomobryidae, and Lepidocyrtinae) from Brazilian Caves. *Insects* **2020**, *11*, 194. [CrossRef]
19. Brito, R.A.; Lima, E.C.A.; Zeppelini, D. Three new species of Collembola (Arthropoda: Hexapoda) from Brazil. *Zootaxa* **2019**, *4700*, 401–430. [CrossRef]
20. Zeppelini-Filho, D.; Palacios-Vargas, J.G. A new troglomorphic species of *Arrhopalites* (Collembola: Arrhopalitidae) from Brazil. *J. N. Y. Entomol. Soc.* **1999**, *107*, 78–81.
21. Zeppelini, D.; Brito, R.A. Two new species of *Pararrhopalites* (Collembola: Symphypleona: Sminthuridae) in Brazil. *Fla. Entomol.* **2014**, *97*, 1733–1744. [CrossRef]
22. Bento, D.M.; Ferreira, R.L.; Prous, X.; Souza-Silva, M.; Bellini, B.C.; Vasconcellos, A. Seasonal variations in cave invertebrate communities in the semiarid Caatinga, Brazil. *J. Cave Karst Stud.* **2016**, *78*, 61–71. [CrossRef]
23. Bento, D.M.; Souza-Silva, M.; Vasconcellos, A.; Bellini, B.C.; Prous, X.; Ferreira, R.L. Subterranean "oasis" in the Brazilian semiarid region: Neglected sources of biodiversity. *Biodivers. Conserv.* **2021**, *30*, 3837–3857. [CrossRef]
24. Bellinger, P.F.; Christiansen, K.A.; Janssens, F. Checklist of the Collembola of the World. Available online: http://www.collembola. org (accessed on 6 June 2022).
25. Betsch, J.M. Éléments pour une monographie des Collemboles Symplyplêones (Hexapodes, Aptérygotes). *Mém. Mus. Natl. Hist. Nat. Sér. A, Zool.* **1980**, *116*, 1–227.
26. Bretfeld, G. Synopses on Palaeartic Collembola, Volume 2. *Symphypleona. Abh. Ber. Naturkundemus. Gorlitz* **1999**, *71*, 1–318.

Dietersminthurus Palacios-Vargas, Cuéllar & Vázquez, 1998 with *Disparrhopalites* Stach, 1956 and composition of Songhaicinae 27. Bernard, C.E.; Wynne, J.J. *Disparrhopalites naasaveqw* n. sp. from caves at Wupatki National Monument, Arizona, synonymy ȣ(Collembola: Sminthuridae). *Zootaxa* **2017**, *4319*, 77–90. [CrossRef]
28. Sánchez-García, A.; Engel, M.S. Long-term stasis in a diverse fauna of Early Cretaceous springtails (Collembola: Symphypleona). *J. Syst. Palaeontol.* **2016**, *15*, 513–537. [CrossRef]
29. Medeiros, G.S.; Greenslade, P.; Bellini, B.C. The Rare *Richardsitas* Betsch (Collembola, Symphypleona, Sminthuridae): A New Species from Australia with Comments on the Genus and on the Sminthurinae. *Insects* **2020**, *11*, 519. [CrossRef]
30. Arlé, R.; Mendonça, C. Estudo preliminar das espécies de *Dicranocentrus* Schött, 1893, ocorrentes no Parque Nacional da Tijuca, Rio de Janeiro (Collembola). *Rev. Brasil. Biol.* **1982**, *42*, 41–49.
31. Jordana, R.; Arbea, J.I.; Simón, C.; Luciáñez, M.J. *Fauna Iberica Volume 8: Collembola, Poduromorpha*, 1st ed.; Museo Nacional de Ciencias Naturales, Consejo Superior de Investigaciones Científicas: Madrid, Spain, 1997; pp. 1–807.
32. Fjellberg, A. The Labial Palp in Collembola. *Zool. Anz.* **1999**, *237*, 309–330.
33. Cipola, N.G.; Morais, J.W.; Bellini, B.C. A new species of *Seira* (Collembola: Entomobryidae: Seirini) from Northern Brazil, with the addition of new chaetotaxic characters. *Zoologia* **2014**, *31*, 489–495. [CrossRef]
34. Betsch, J.M.; Waller, A. Chaetotaxic nomenclature of the head, thorax and abdomen in Symphypleona (Insecta, Collembola). *Acta Zool. Fenn.* **1994**, *195*, 5–12.
35. Vargovitsh, R.S. New cave Arrhopalitidae (Collembola: Symphypleona) from the Crimea (Ukraine). *Zootaxa* **2009**, *2047*, 1–47. [CrossRef]
36. Vargovitsh, R.S. New troglomorphic Arrhopalitidae (Collembola: Symphypleona) from the Western Caucasus. *Zootaxa* **2012**, *3174*, 1–21. [CrossRef]
37. Vargovitsh, R.S. Cavernicolous *Arrhopalites abchasicus* sp. nov. (Collembola: Symphypleona: Arrhopalitidae) from the West Caucasus with a key to the World species of the genus. *Zootaxa* **2013**, *3666*, 16–30. [CrossRef]
38. Betsch, J.M. An ontogenetically focused chaetotaxial scheme in Symphypleona (collembolan): The 6th abdominal segment. *Pedobiologia* **1997**, *41*, 13–18.
39. Nayrolles, P. Chetotaxie tibiotarsale des collemboles symphyplèones. *Trav. Lab. Ecobiol. Arthr. édaph. Toulouse* **1988**, *5*, 1–19.
40. Börner, C. Neue Collembolenformen und zur Nomenclatur der Collembola Lubbock. *Zool. Anz.* **1901**, *24*, 696–712.
41. Bretfeld, G. Phylogenetic systematics of the higher taxa of Symphypleona Borner, 1901 (Insecta, Entognatha, Collembola). *Proc. 2nd Intern. Sem. Apterygota* **1986**, *1*, 302–311.
42. Bretfeld, G. *Sturmius epiphytus* n. gen. n. spec. from Colombia, a taxon of the Symphypleona (Insecta, Colembola) with an unexpected character combination. Description and position in non-Linnean and Linnean classifications of the Symphypleona. *Zoolog. Syst. Evol. Res.* **1994**, *32*, 264–281. [CrossRef]
43. Lubbock, J. Notes on the Thysanura. Part, I. *Trans. Linn. Soc. Lond.* **1862**, *23*, 429–448. [CrossRef]
44. Zeppelini, D.; Silva, D.D. A new *Stenognathriopes* (Collembola, Symphypleona, Bourletiellidae) from Brazilian coast. *Zootaxa* **2012**, *3540*, 51–58. [CrossRef]
45. Yosii, R. On some Collembola of Japan and adjacent countries. *Contrib. Biol. Lab. Kyoto Univ.* **1965**, *19*, 1–71.
46. Lawrence, P.N. South Pacific Symphypleona. *Pac. Insects* **1968**, *10*, 325–340.
47. Ellis, W.N. Some Collembola from Ibiza with descriptions of three new species, and a note on *Hypogastrura serrata* (Agren, 1904). *Bul. Zool. Mus. Univ. Amsterdam* **1974**, *3*, 125–141.
48. Snider, R.J. New species of Sminthuridae from North America (Collembola: Symphypleona). *Gt. Lakes Entomol.* **1978**, *11*, 217–241.
49. Betsch, J.M.; Weiner, W.M. *Sphyrotheca* Börner, 1906 and *Szeptyckitheca* gen. n. (Collembola, Symphypleona) from North Korea. *Acta Zool. Cracov.* **2009**, *52*, 35–44. [CrossRef]
50. Zeppelini, D.; Lopes, B.C.H.; Lima, E.C.A. A new species of *Szeptyckitheca* (Collembola, Symphypleona, Sphyrothecinae) from Brazil. *Neotrop. Entomol.* **2018**, *48*, 269–276. [CrossRef]
51. Delamare-Deboutteville, C.; Massoud, Z. Collemboles symphypléones. In *Biologie de L'Amérique Australe*, 1st ed.; Delamare-Deboutteville, C., Rapoport, E., Eds.; Éditions du CNRS: Paris, France, 1963; Volume 2, pp. 169–289.
52. Betsch, J.M. Étude des Collemboles de Madagascar IV—Deux nouveaux genres de Symphypléones à dimorphisme sexuel important: *Parabourletiella* et *Richardsitas*. *Rev. Ecol. Biol. Sol.* **1975**, *12*, 477–485.
53. C´ urc˘ic´, B.P.M.; Luc˘ic´, L.R.; Tomic´, V.T.; Makarov, S.E.; Karaman, I.M. *Galeriella liciniana*, a new cave genus and species of springtails (Collembola, Sminthuridae) from Herzegovina. *Arch. Biol. Sci.* **2007**, *59*, 63–64. [CrossRef]
54. Medeiros, G.S.; Bellini, B.C. Two new species of *Temeritas* Richards (Collembola, Symphypleona, Sminthuridae) from Neotropical Region, with coments on the genus. *Zootaxa* **2019**, *4586*, 536–552. [CrossRef]
55. Lukic´, M. Chapter 35–Collembola. In *Encyclopedia of Caves*, 3rd ed.; White, W.B., Culver, D.C., Pipan, T., Eds.; Academic Press: Cambridge, UK, 2019; Volume 1, pp. 308–319.
56. Latreille, P.A. Histoire naturelle, générale et particulière des Crustacés et des Insectes III. F. *Dufart Paris* **1802**, *15*, 69–83.
57. Stach, J. *The Apterygotan Fauna of Poland in Relation to the World-Fauna of This Group of Insects. Family: Sminthuridae*, 1st ed.; Polska Akademia Nauk, PWN: Krakow, Poland, 1956; pp. 1–287.
58. Betsch, J.M. Étude des Collemboles de Madagascar V—Sur deux Symphypléones de la forét séche en secteur bioclimatique subaride. *Bull. Soc. Entomol. Fr.* **1977**, *82*, 119–125. [CrossRef]

59. Alvares, C.A.; Stape, J.L.; Sentelhas, P.C.; Moraes-Gonçalves, J.L.; Sparovek, G. Köppen's climate classification map for Brazil.
Meteorol. Z. **2013**, *22*, 711–728. [CrossRef]
60. Cole, M.M. Cerrado, Caatinga and Pantanal: The Distribution and Origin of the Savanna Vegetation of Brazil. *Geog. J.* **1960**, *126*, 168–179. [CrossRef]
61. Souza-Silva, M.; Cerqueira, R.F.V.; Pellegrini, T.G.; Ferreira, R.L. Habitat selection of cave-restricted fauna in a new hotspot of subterranean biodiversity in Neotropics. *Biodivers. Conserv.* **2021**, *30*, 4223–4250. [CrossRef]
62. Cardoso, P.; Erwin, T.L.; Borges, P.A.; New, T.R. The seven impediments in invertebrate conservation and how to overcome them.
Biol. Conserv. **2011**, *144*, 2647–2655. [CrossRef]
63. Ferreira, R.L.; Bernard, E.; Cruz-Júnior, F.W.; Piló, L.B.; Calux, A.; Souza-Silva, M.; Barlow, J.; Pompeu, P.S.; Cardoso, P.; Mammola, S.; et al. Brazilian cave heritage under siege. *Science* **2022**, *375*, 1238–1239. [CrossRef]
64. Xiong, Y.; Gao, Y.; Yin, W.Y.; Luan, Y.X. Molecular phylogeny of Collembola inferred from ribosomal RNA genes. *Mol. Phylogenet. Evol.* **2008**, *49*, 728–735. [CrossRef]
65. Schneider, C.; Cruaud, C.; D'Haese, C.A.D. Unexpected diversity in Neelipleona revealed by molecular phylogeny approach (Hexapoda, Collembola). *Soil Org.* **2011**, *83*, 383–398.
66. Yu, D.; Zhang, F.; Stevens, M.I.; Yan, Q.; Liu, M.; Hu, F. New insight into the systematics of Tomoceridae (Hexapoda, Collembola) by integrating molecular and morphological evidence. *Zool. Scr.* **2015**, *45*, 286–299. [CrossRef]
67. Leo, C.; Carapelli, A.; Cicconardi, F.; Frati, F.; Nardi, F. Mitochondrial genome diversity in Collembola: Phylogeny, dating and gene order. *Diversity* **2019**, *11*, 169. [CrossRef]
68. Sun, X.; Yu, D.; Xie, Z.; Dong, J.; Ding, Y.; Yao, H.; Greenslade, P. Phylomitogenomic analyses on collembolan higher taxa with enhanced taxon sampling and discussion on method selection. *PLoS ONE* **2020**, *15*, e0230827. [CrossRef] [PubMed]
69. Cucini, C.; Fanciulli, P.P.; Frati, F.; Convey, P.; Nardi, F.; Carapelli, A. Re-evaluating the internal phylogenetic relationships of Collembola by means of Mitogenome Data. *Genes* **2021**, *12*, 44. [CrossRef] [PubMed]
70. D'Haese, C.A. Morphological appraisal of Collembola phylogeny with special emphasis on Poduromorpha and a test of the aquatic origin hypothesis. *Zool. Scr.* **2003**, *32*, 563–586. [CrossRef]

Accepted by D. Antić: 29 Feb. 2024; published: 25 Mar.

PRIORIDADES DE CONSERVAÇÃO



Áreas e cavernas prioritárias para a conservação

As três áreas abrangidas em nosso projeto possuíram cavernas que merecem ações imediatas de conservação, sendo, portanto prioritárias para ações que visem sua proteção.

Na região de Santana, indubitavelmente merece destaque o complexo hidrológico do qual faz parte a gruta do Padre. Esta caverna é agora o mais novo hotspot de biodiversidade subterrânea da América do Sul, passando a compor um seleto grupo de cavernas que possuem mais de 20 espécies estritamente subterrâneas. A gruta do Padre possui, até o momento, 25 espécies troglóbias conhecidas, boa parte delas descobertas ao longo deste projeto. Além disso, é uma caverna que compõe o mais extenso sistema hídrico subterrâneo do país. No entanto, mesmo com todo este destaque, o sistema do qual a gruta do Padre faz parte encontra-se desprotegido, já que não existem quaisquer unidades de conservação que abranjam este sistema ou parte dele. Assim, é de extrema urgência a criação de uma unidade de conservação que seja capaz de proteger este sistema, abrangendo preferencialmente a sua bacia de captação.

Na região da Serra do Ramalho, destaca-se o sistema de cavernas Água Clara, composto pelas cavernas Água Clara, Índio, Peixes e Peixes II. Atualmente este sistema é o mais rico em espécies troglóbias da região intertropical (em escala mundial), com impressionantes 41 espécies troglóbias (Ferreira & Souza-Silva, 2023). Além disso, outra caverna localizada muito próxima ao sistema Água Clara (3,5 Km em linha reta), conhecida como gruta do Pedro Cassiano, também possui uma fauna subterrânea de destaque, com 20 espécies troglóbias, 19 das quais compartilhadas com as cavernas do sistema Água Clara. Esse número elevado de espécies compartilhadas mostra a aparente conexão por mesocavernas entre estes dois conjuntos. Por fim, há também a gruta do Boqueirão, localizada nas imediações do sistema Água Clara (cerca de 8 Km em linha reta). A gruta do Boqueirão é a maior caverna conhecida na região da Serra do Ramalho, com mais de 15 km de condutos mapeados. Muito embora esta caverna não tenha sido amostrada neste projeto, é bastante provável que também contenha espécies compartilhadas com o sistema Água Clara, bem como outras espécies troglóbias exclusivas. Assim, o complexo formado pelas cavernas do sistema Água Clara, juntamente com a gruta do Boqueirão e a gruta Pedro Cassiano indubitavelmente formam o mais importante complexo subterrâneo da Serra do Ramalho, não somente pela extensão, como pela fauna troglóbia e endêmica extremamente rica e significativa. No entanto, assim como a gruta do Padre, este expressivo conjunto de cavernas encontra-se desprotegido, já que não existem quaisquer unidades de conservação que abranjam este sistema. Assim, é de extrema urgência a criação de uma unidade de conservação que seja capaz de proteger estas cavernas, abrangendo preferencialmente suas respectivas bacias de captação.

Finalmente, a região de Iuiú, muito embora possua diversas cavernas bastante expressivas, possui três cavernas que merecem destaque: a gruta do Baixão (com 16 espécies troglóbias), a gruta Tabocas (com 12 espécies troglóbias) e a gruta Tapera D'água (com 10 espécies troglóbias). Todas estas cavernas situam-se no maciço principal da serra de Iuiú,

Accepted by D. Antić: 29 Feb. 2024; published: 25 Mar.

muito embora em pontos diametralmente opostos (no caso das grutas Baixão e Tabocas). Além disso, há outras cavernas com espécies troglóbias situadas tanto no maciço principal quanto em macios periféricos. Assim, é bastante difícil traçar prioridades, especialmente considerando que as espécies presentes em maciços periféricos geralmente diferem daquelas que ocorrem no maciço principal. No entanto, considerando que as três cavernas com maior riqueza de espécies troglóbias se situam no maciço principal, é de extrema urgência a criação de uma unidade de conservação que seja capaz de proteger estas cavernas, abrangendo preferencialmente suas respectivas bacias de captação.

Por fim, é importante destacar os potenciais impactos futuros sobre cada uma destas áreas em decorr6encia do início de operações da Ferrovia de Integração Oeste-Leste (FIOL). Esta ferrovia, que tem trechos perpassando áreas muito próximas a cada uma destas regiões, passará a permitir o escoamento de produtos, dentre eles o calcário. Assim, muito em breve, é potencialmente esperado que polos minerários comecem a surgir e se expandir em cada uma destas áreas, já que vai existir meios de escoamento da produção mineral. Este cenário demonstra a urgência de se estabelecer unidades de conservação que assegurem a proteção pelo menos das cavernas mais expressivas de cada uma destas áreas. Somente por meio do estabelecimento de UCs, este patrimônio poderá ser assegurado ao longo do tempo.

Participação em eventos

Alguns dos trabalhos produzidos ao longo do projeto foram apresentados em diferentes eventos científicos, tanto nacionais como internacionais:

- 11th International Symposium on Terrestrial Isopod Biology "Facets of terrestrial isopod biology", ONLINE EDITION, Ghent-Belgium, 12-14 de Julho de 2021

- 36º Congresso Brasileiro de Espeleologia (36º CBE), 20/04/2022 – 23/04/2022 – realizado no Centro de Convenções Ulysses Guimarães - Brasília - Distrito Federal – Brasil

- 37º Congresso Brasileiro de Espeleologia (37º CBE), 20/07/2023 – 29/07/2023 – realizado em Curitiba - Paraná – Brasil

Accepted by D. Antić: 29 Feb. 2024; published: 25 Mar.

Equipe

Nome	Função	Instituição	Formação Acadêmica
Rodrigo Lopes Ferreira	Coordenador	UFLA	Doutor em Ecologia
Marconi Souza Silva	Sub-Coordenador	UFLA	Doutor em Ecologia
Giovanna Monticelli Cardoso	Pós-doutoranda	UFLA	Doutora em Biologia Animal
Lais Furtado Oliveira	Pós-doutoranda	UFLA	Doutora em Ecologia
Tássia Rayane F. Chagas	Pós-doutoranda	UFLA	Doutora em Ecologia
Vitor Gabriel Pereira Junta	Mestrando	UFLA	Bacharel em Biologia
Paulo César Reis Venâncio	Mestrando	UFLA	Bacharel em Biologia
Alicia Helena S. R. Ferreira	Mestranda	UFLA	Bacharel em Biologia
Guilherme Carvalho Prado	Bolsista IC	UFLA	Graduando em Biologia
Pedro Henrique M. Carvalho	Bolsista IC	UFLA	Graduando em Biologia

Formação de recursos humanos

O projeto contribuiu para a formação acadêmica, profissional e pessoal de diversas pessoas, que diretamente puderam contribuir para sua compleição. Destaca-se a formação de três pós-doc, três mestrandos e dois graduandos de iniciação científica. Todos estes pesquisadores, em diferentes momentos de sua formação acadêmica, contribuíram de forma intensa para o projeto, bem como puderam aprender muito sobre as cavernas e sua fauna. As contribuições deste projeto vão, no entanto, além das pessoas anteriormente cotadas (ver nomes no tópico "Equipe"). Muitos outros membros do Centro de Estudos em Biologia Subterrânea puderam também contribuir para estes trabalhos, participando ativamente das coletas de campo. Pelo menos outros 8 alunos deste centro auxiliaram nos trabalhos de campo. Por fim, destaca-se que diversos moradores das áreas abrangidas no projeto também foram beneficiados. Tivemos a preocupação de sempre informar à população local sobre os objetivos do projeto. Disponibilizamos cartilhas para os moradores locais e também, em algumas ocasiões, tivemos a oportunidade de levar conosco alguns moradores locais, para acompanharem de perto nossas atividades e também poderem aprender sobre este importante patrimônio.

Principais desafios enfrentados

Dentre os desafios encontrados ao longo da execução do projeto, podemos destacar alguns que foram recorrentes durante todas as expedições. É comum durante essa etapa nos depararmos com caminhos inacessíveis ou de difícil acesso, seja por aspectos da própria paisagem, como vegetação fechada e paredões rochosos, ou por dificuldades ligadas à autorização para entrada nessas áreas quando elas se encontram em propriedades particulares. Outra dificuldade está em encontrarmos a entrada de algumas cavernas, por conta do registro incorreto dos pontos de GPS. Além disso, algumas cavernas encontram-se distantes dos locais escolhidos como a base da expedição, demandando elevado tempo para

que a equipe chegue até o local e se realize o trabalho e, consequentemente, levando a uma diminuição no número de cavernas a serem trabalhadas durante o período determinado da expedição.

Nas regiões trabalhadas durante o projeto, algumas cavernas não estavam registradas no banco de dados do CANIE (Cadastro Nacional de Informações Espeleológicas) ou em artigos relacionados, tornando a participação dos moradores locais essencial, já que muitas vezes nos auxiliaram a encontrar diversas cavernas de difícil localização e até mesmo cavernas ainda desconhecidas e também não cadastradas no CANIE.

Por fim, merece menção uma situação extremamente desagradável ocorrida durante a realização do projeto, e que optamos por relatar neste documento a título de repúdio. Antes do início do projeto, fui informado pelo coordenador do CECAV, Sr. Jocy Cruz, sobre o andamento de um projeto coordenado pelo Grupo Bambuí de Pesquisas espeleológicas na região da Serra do Ramalho. O referido projeto, contava com amostragens biológicas em cavernas. Seguindo a recomendação do Sr. Jocy, contatei o coordenador do projeto, Sr. Ézio Rubbioli, para informar sobre nosso projeto. Na ocasião, me dispus a contribuir com o que fosse necessário, e ainda ofereci a futura base de dados biológicos que seria por nós gerada sobre a fauna de cavernas da região para que pudesse fortalecer o futuro relatório do projeto por ele coordenado. Cavernas que seriam importantes para serem amostradas em nosso projeto (como a Lapa do Boqueirão) deixaram de ser em função da insistência do Sr. Ézio para que não amostrássemos nesta caverna, sob alegação de que outra pesquisadora iria coletar nesta caverna. Vale ressaltar que esta é a maior caverna conhecida para a região, com mais de 16 km de extensão. Os métodos que utilizaríamos seriam complementares e a listagem final de fauna seria substancialmente incrementada pelo emprego de técnicas distintas de amostragem. Mesmo assim, ao final, optamos por não amostrar nesta importante caverna.

Durante diversas ocasiões, troquei mensagens com o Sr. Ézio que foi por mim informado sobre o andamento de nosso projeto (a parte referente à Serra do Ramalho). No entanto, para nossa surpresa, em meio ao nosso primeiro trabalho de campo na Serra do Ramalho, recebemos a solicitação de interrompermos nossas atividades de campo em função de uma denúncia, feita pelo Sr. Ézio (ele me confirmou isso) de que estaríamos sobrepondo nossas atividades às do projeto por ele coordenado. Isso nos surpreendeu bastante, já que desde o início informei a ele sobre nosso projeto e nos comunicamos diversas vezes. Além disso, tínhamos licenças de coletas para todas as cavernas que amostramos.

Na tentativa de resolver esta questão, o Sr. Jocy solicitou ao Grupo Bambuí que informasse em quais cavernas estavam sendo realizadas as coletas referentes ao projeto por eles coordenado. Para nossa surpresa, a listagem enviada perfazia 30% das cavernas conhecidas na região (um total de 56 cavernas das 186 conhecidas), além de incorporar praticamente **todas as cavernas de maior porte** e com a presença de corpos d'água (**21** das 26 cavernas com **mais de 1 km**). É importante enfatizar que o somatório das extensões das cavernas que eles informaram que realizariam coletas biológicas corresponde a inacreditáveis **98 km de condutos**, o que demonstra de forma inequívoca a completa impossibilidade de coletas em todas estas cavernas dentro do tempo do projeto. Pudemos constatar

imediatamente que a intenção do referido grupo era bastante clara: a de nos impedir de trabalhar nas cavernas da Serra do Ramalho. Um agravante desta situação é que o referido projeto coordenado pelo Grupo Bambuí de Pesquisas espeleológicas teve financiamento no mesmo TCCE que apoia nosso projeto. A compensação que deveria estar sendo utilizada de forma conjunta e sinergética para a geração de conhecimento em prol da proteção das cavernas da Serra do Ramalho estava sendo, em parte, "sabotada" por um grupo que passou a empreender tempo na tentativa de paralisar o trabalho de outro grupo de pesquisas.

Destaco que as cavernas brasileiras são bens da União, e não propriedades individuais ou de quaisquer grupos de espeleologia. A tentativa, felizmente frustrada, do Grupo Bambuí de Pesquisas Espeleológicas, de interromper ou pelo menos prejudicar nossos trabalhos, demonstra como certas áreas são equivocadamente consideradas "feudos" por algumas pessoas ou grupos, que aparentemente desconhecem a legislação nacional referente ao patrimônio espeleológico. Que se registre aqui nosso repúdio a este tipo de comportamento, a nosso ver inadmissível, e que somente vem a depor contra o desenvolvimento da espeleologia brasileira.

Referências bibliográficas

ALVARENGA, D. de A.; SOUZA-SILVA, M.; FERREIRA, R. L. Trogloregions: delimiting subterranean faunistic identities in Afrotropics and Neotropics. Communications Biology [submetido], [s. l.], [s. d.]. Available at: https://doi.org/10.21203/rs.3.rs-53597/v1

ANDERSON, M. J.; GORLEY, R. N.; CLARKE, K. R. Permanova+ for Primer: Guide to Software and Statistical Methods. 1st. ed. Plimouth: Primer-E Ltd, 2008.

BASELGA, A. Partitioning the turnover and nestedness components of beta diversity. Global Ecology and Biogeography, [s. l.], v. 19, n. 1, p. 134–143, 2010. Available at: https://doi.org/10.1111/j.1466-8238.2009.00490.x

BASELGA, A.; ORME, C. D. L. Betapart: An R package for the study of beta diversity. Methods in Ecology and Evolution, [s. l.], v. 3, n. 5, p. 808–812, 2012. Available at: https://doi.org/10.1111/j.2041-210X.2012.00224.x

BRESCOVIT, A. D. et al. Brasilomma gen. nov., a new prodidomid genus from Brazil (Araneae, Prodidomidae). Zootaxa, [s. l.], n. 3572, p. 23–32, 2012. Available at: https://doi.org/10.11646/zootaxa.3572.1.4

BRYSON, R. W. et al. Caves as microrefugia: Pleistocene phylogeography of the troglophilic North American scorpion Pseudouroctonus reddelli. BMC Evolutionary Biology, [s. l.], v. 14, n. 9, p. 16, 2014. Available at: https://doi.org/10.1111/j.1095-8312.1996.tb01434.x

DINERSTEIN, E. et al. An Ecoregion-Based Approach to Protecting Half the Terrestrial Realm. BioScience, [s. l.], v. 67, n. 6, p. 534–545, 2017. Available at: https://doi.org/10.1093/biosci/bix014

Accepted by D. Antić: 29 Feb. 2024; published: 25 Mar.

FERRIER, S. et al. Using generalized dissimilarity modelling to analyse and predict patterns of beta diversity in regional biodiversity assessment. Diversity and Distributions, [s. l.], v. 13, n. 3, p. 252–264, 2007. Available at: https://doi.org/10.1111/j.1472-4642.2007.00341.x

FICETOLA, G. F. et al. Differences between microhabitat and broad-scale patterns of niche evolution in terrestrial salamanders. Scientific Reports, [s. l.], v. 8, n. 1, p. 1–12, 2018. Available at: https://doi.org/10.1038/s41598-018-28796-x

FORD, D.; WILLIAMS, P. Speleogenesis: The Development of Cave Systems. In: FORD, D.; WILLIAMS, P. (org.). Karst Hydrogeology and Geomorphology. 2nd. ed. Chichester: John Wiley & Sons, 2007. p. 209–270.

GIBERT, J.; DEHARVENG, L. Subterranean Ecosystems: A Truncated Functional Biodiversity. BioScience, [s. l.], v. 52, n. 6, p. 473–481, 2002. Available at: https://doi.org/10.1641/0006-3568

GOLDSCHEIDER, N. et al. Global distribution of carbonate rocks and karst water resources. Hydrogeology Journal, [s. l.], 2020. Available at: https://doi.org/10.1007/s10040-020-02139-5

JUBERTHIE, C.; DELAY, B.; BOUILLON, M. Sur l'existence d'un milieu souterrain superficiel en zone non calcaire. C. R. Acad. Sc. Paris, [s. l.], v. 290, p. 49–52, 1980.

KONEC, M.; DELIĆ, T.; TRONTELJ, P. DNA barcoding sheds light on hidden subterranean boundary between Adriatic and Danubian drainage basins. Ecohydrology, [s. l.], v. 9, n. 7, p. 1304–1312, 2016. Available at: https://doi.org/10.1002/eco.1727

LEHNER, B.; VERDIN, K.; JARVIS, A. HydroSHEDS Technical Documentation. [s. l.], p. 1–27, 2006. Available at: http://hydrosheds.cr.usgs.gov/

LEHNER, B.; VERDIN, K.; JARVIS, A. New global hydrography derived from spaceborne elevation data. Eos, Transactions, American Geophysical Union. EOS, Transactions American Geophysical Union, [s. l.], v. 89, n. 10, p. 93–104., 2008.

MAMMOLA, S. et al. Ecology and sampling techniques of an understudied subterranean habitat: the Milieu Souterrain Superficiel (MSS). Die Naturwissenschaften, [s. l.], v. 103, n. 11–12, p. 88, 2016. Available at: https://doi.org/10.1007/s00114-016-1413-9

MENDES RABELO, L.; SOUZA-SILVA, M.; LOPES FERREIRA, R. Epigean and hypogean drivers of Neotropical subterranean communities. Journal of Biogeography, [s. l.], n. December, 2020. Available at: https://doi.org/10.1111/jbi.14031

MMA, M. do M. A. Instrução Normativa N°2Brazil: [s. n.], 2017. p. 1.

PACHECO, G. S. M. et al. Tourism effects on the subterranean fauna in a Central American cave. Insect Conservation and Diversity, [s. l.], 2020. Available at: https://doi.org/10.1111/icad.12451

PACIOGLU, O. et al. The multifaceted effects induced by floods on the macroinvertebrate communities inhabiting a sinking cave stream. International Journal of Speleology, [s. l.], v. 48, n. 2, p. 167–177, 2019. Available at: https://doi.org/10.5038/1827-806x.48.2.2239

PAVLEK, M.; MAMMOLA, S. Niche-based processes explaining the distributions of closely related subterranean spiders. Journal of Biogeography, [s. l.], v. 00, n. April, p. 1–16, 2020. Available at: https://doi.org/10.1111/jbi.13987

Accepted by D. Antić: 29 Feb. 2024; published: 25 Mar.

POULSON, T. L.; WHITE, W. B. The Cave Environment. Science, [s. l.], v. 165, n. 3897, p. 971–981, 1969.

RABELO, L. M.; SOUZA-SILVA, M.; FERREIRA, R. L. Priority caves for biodiversity conservation in a key karst area of Brazil: comparing the applicability of cave conservation indices. Biodiversity and Conservation, [s. l.], v. 27, n. 9, p. 2097–2129, 2018. Available at: https://doi.org/10.1007/s10531-018-1554-6

SMITH, J. R. et al. A global test of ecoregions. Nature Ecology and Evolution, [s. l.], v. 2, n. 12, p. 1889–1896, 2018. Available at: https://doi.org/10.1038/s41559-018-0709-x

SOBRAL-SOUZA, T.; LIMA-RIBEIRO, M. S.; SOLFERINI, V. N. Biogeography of Neotropical Rainforests: past connections between Amazon and Atlantic Forest detected by ecological niche modeling. Evolutionary Ecology, [s. l.], v. 29, n. 5, p. 643–655, 2015. Available at: https://doi.org/10.1007/s10682-015-9780-9

SOUZA-SILVA, M. et al. Transport and Consumption of Organic Detritus in a Neotropical Limestone Cave. Acta Carstologica, [s. l.], v. 41, n. 1, p. 139–150, 2012.

ZAGMAJSTER, M. et al. Subterranean Biodiversity Patterns from Global to Regional Scales. In: MOLDOVAN, O. T.; KOVÁČ, L.; HALSE, S. (org.). Cave Ecology. 1st. ed. Cham: Springer Nature Switzerland AG, 2018. p. 195–228.

ZUUR, A. F.; IENO, E. N.; ELPHICK, C. S. A protocol for data exploration to avoid common statistical problems. Methods in Ecology and Evolution, [s. l.], v. 1, n. 1, p. 3–14, 2010. Available at: https://doi.org/10.1111/j.2041-210x.2009.00001.x

Accepted by D. Antić: 29 Feb. 2024; published: 25 Mar.